VOLUME 68 • NUMBER 1 / WHOLE NUMBER 362

Culc-H02755-1-P024336

The American Journal of PATHOLOGY

JULY 1972

OFFICIAL PUBLICATION OF

E AMERICAN ASSOCIATION OF
IOLOGISTS AND BACTERIOLOGISTS

•

THE AMERICAN SOCIETY FOR
EXPERIMENTAL PATHOLOGY

1

BOARD OF EDITORS

Thomas D. Kinney, *Editor-in-Chief*
Donald B. Hackel, *Associate Editor*

Orville T. Bailey
Frederick F. Becker
Baruj Benacerraf
Kurt Benirschke
Kenneth M. Brinkhous
Joel G. Brunson
John R. Carter
Charles G. Cochrane
John M. Craig
Frank J. Dixon, Jr
John T. Ellis
Frank W. Fitch
Patrick J. Fitzgerald
David G. Freiman
Jack C. Geer
Gabriel Godman
John B. Hazard
Robert H. Heptinstall
Paul Kotin
Averill A. Liebow
Guido Majno
Donald G. McKay
Henry D. Moon
Councilman Morgan
Goetz W. Richter
David T. Rowlands, Jr
Edward A. Smuckler
Leon Sokoloff
Benjamin H. Spargo
Lewis Thomas
Jacinto J. Vazquez
F. Stephen Vogel

Editorial Assistant: Virginia Hotelling

EDICAL DEPARTMENT • HARPER & ROW, PUBLISHERS

Reichert Zetopan: A great microscope starts here.

The Reichert Zetopan is one of the most advanced research microscopes available today. And that's just the start of it.

The Zetopan can be extended to cover fluorescence, polarization, microphotometry and phase techniques. It will accept a variety of cameras—including the only automatic camera that features direct exposure read-out. The Zetopan can be used with transmitt incident, epi, or mixed illumination.

Learn more about this adaptable research microsco from Reichert. We'll be happy to arrange a convin demonstration with emphasis on your specific needs. Write American Optical Corporation, Reichert Products, Buffalo, New York 14215.

REICHERT
WIEN

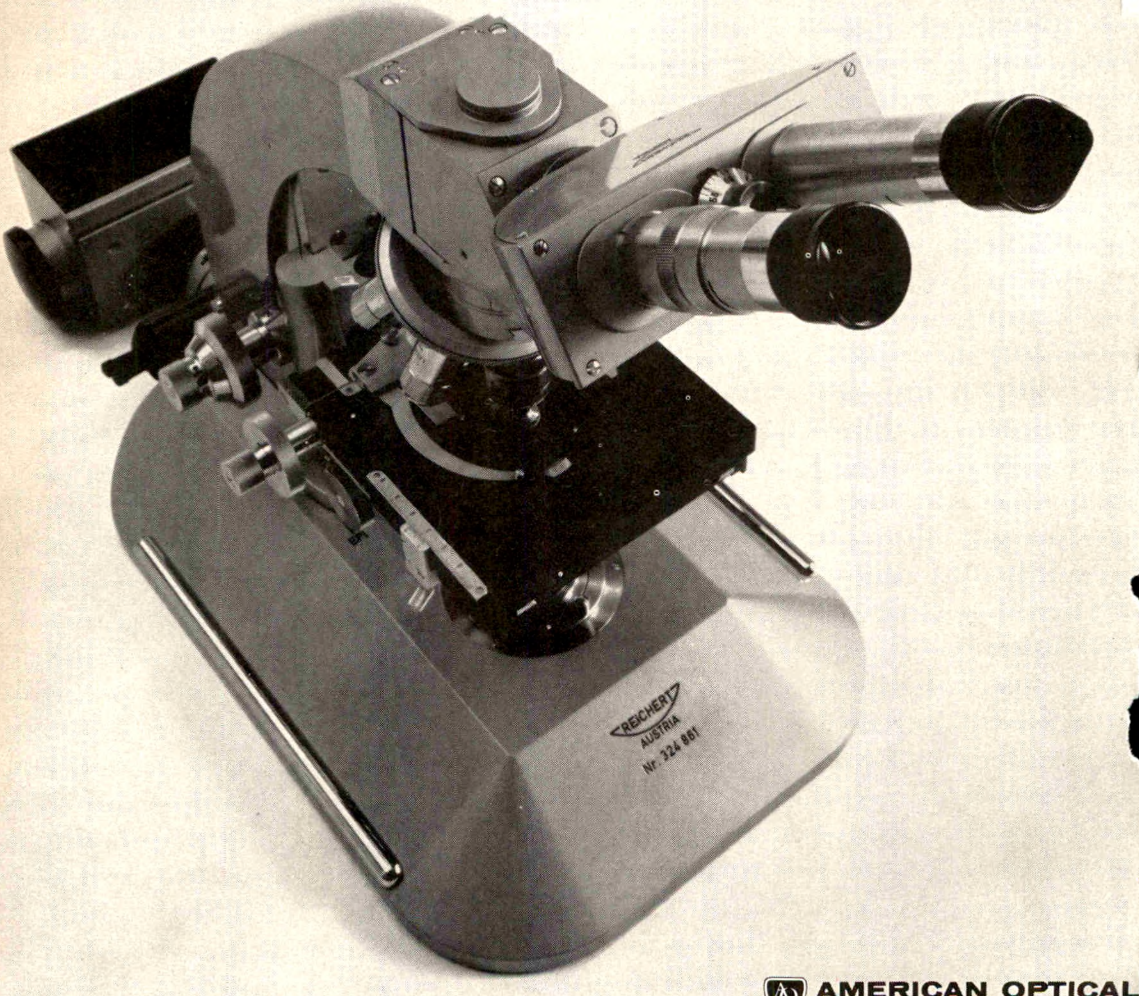

AMERICAN OPTICAL
CORPORATION
SCIENTIFIC INSTRUMENT DIVISION • BUFFALO, N.Y. 14215

P 24,336

A Closer Look At Thyroid Dysfunction With Thyroid Antibody Tests

Diagnostic tests for determination of thyroid autoantibodies can throw a new illumination on the nature of the patient's disease. The refined differential diagnosis afforded may provide additional insight for treatment and m[illegible]nt.

Clinical ap[illegible]cations include:

differential diagnosis between colloid goiter and Hashimoto's thyroiditis; differentiation between Hashimoto's disease and thyrotoxicosis; detection of mild thyroid disease in patients with pernicious anemia; investigation of other possible autoimmune disorders.

A complete thyroid panel should include thyroglobulin hemagglutination and complement fixation tests. We know of no other company which provides these materials.

We would like to fill your order, or would be happy to send information to your laboratory.

Wellcome Reagents Division
Wellcome
Burroughs Wellcome Co.
Research Triangle Park
North Carolina 27709

Quality Products of a Specialty Nature from: **Wellcome Reagents Division**
Wellcome
Burroughs Wellcome Co.
Research Triangle Park
North Carolina 27709

Please ship:

☐ KT 02
Thyroglobulin
Hemagglutination test kit
(50 tests) $27.50

☐ MR 22
Thyroid Complement
Fixing Antigen
(dried 1 ml) $5.75

Send information to:

Name of laboratory

Name of laboratory contact or purchaser

Title

Address

City State Zip code

Phone

An Important Contribution To Diagnosis In Certain Grave Conditions

1. Obstetrical Complications

abruptio placentae/eclampsia/"dead fetus" syndrome

2. Venous Thrombosis/ Pulmonary Embolism

3. Renal and Hepatic Disease

The Wellcome FDP Kit for assay of fibrinogen and its degradation products

Not all clinicians are aware of this diagnostic resource which can be of value also in myocardial infarction, coronary thrombosis, gram-negative septicemia, malignancies and other serious conditions.

The FDP Kit from Wellcome Reagents is complete; it provides a simplified technique for a convenient and sensitive assay of fibrinogen degradation products.

We know of no other source for this test.

Wellcome Reagents Division
Burroughs Wellcome Co
Research Triangle Park
North Carolina 27709

Quality Products of a Specialty Nature from: **Wellcome Reagents Division**
Burroughs Wellcome Co.
Research Triangle Park
North Carolina 27709

Please fill out coupon to order. Please also indicate if you would like a supply of reprints to provide for interested clinicians.

Please send_______FDP Kits (14 tests per kit) at $32.50 per kit.
_______Also, please send a supply of background reprints for clinicians.

Name ________________ Title ________________
Laboratory ________________
Address ________________
City ________ State ________ Zip Code ________
Phone ________________

THE YEAR OF PATHOLOGY
1971
1972

The American Journal of PATHOLOGY

JULY 1972 • Volume 68, Number 1

CONTENTS

1 Effects of Viral Infection on Nervous System Development. I. Pathogenesis of Bluetongue Virus Infection in Mice
Opendra Narayan and Richard T. Johnson

15 Effects of Viral Infection on Nervous System Development. II. Attempts to Modify Bluetongue-Virus-Induced Malformations with Cyclophosphamide and Antithymocyte Serum
Opendra Narayan, Henry F. McFarland and Richard T. Johnson

23 Histochemical Distribution of Carbonic Anhydrase After Ligation of the Pancreatic Duct
Andrew Churg and Ward R. Richter

31 Tissue Localization of Australia Antigen Immune Complexes in Acute and Chronic Hepatitis and Liver Cirrhosis
Adam Nowosławski, Krzysztof Krawczyński, Witold J. Brzosko and Kazimierz Madaliński

57 Effects of Normal and Aspirin Platelets on Defective Secondary Aggregation in the Hermansky-Pudlak Syndrome: A Test for Storage Pool Deficient Platelets
James G. White and Carl J. Witkop

67 Incidence and Significance of Muscle Capillary Basal Lamina Thickness in Juvenile Diabetes
Victoriano Pardo, Eliseo Perez-Stable, David B. Alzamora and William W. Cleveland

81 The Cellular Pathology of Experimental Hypertension. VI. Alterations in Retinal Vasculature
Filiberto Giacomelli, Kenneth B. Juechter and Joseph Wiener

97 Effects of Biliary Obstruction on Pulmonary Ultrastructure in the Rat
N. A. Popovic and J. F. Mullane

113 Lysosomes in the Pathogenesis of the Renal Necrosis of Choline-Deficient Rats
A. J. Monserrat, F. Hamilton, A. K. Ghoshal, E. A. Porta and W. S. Hartroft

147 Lymphocyte Depression Induced in Chickens on Diets Deficient in Vitamin A and Other Components
Betsy G. Bang, Frederik B. Bang and Marie A. Foard

163 Separation of Ascites Myeloma Cells, Lymphocytes and Macrophages by Zonal Centrifugation on an Isokinetic Gradient
M. J. Stewart, T. G. Pretlow II and Raymond Hiramoto

183 Mouse Cytomegalovirus: Necrosis of Infected and Morphologically Normal Submaxillary Gland Acinar Cells During Termination of Chronic Infection
Donald Henson and Alfonso J. Strano

203 **Animal Model for Human Disease:** Spinal Bifida, Sacral Dysgenesis and Myelocele
Hyram Kitchen, Ronald E. Murray and Beverly Y. Cockrell

© 1972 by The American Association of Pathologists and Bacteriologists

The seal commemorates The Year of Pathology, being celebrated from October 1971 to October 1972 by the major national pathology societies. Special educational events will emphasize the expanding role of pathology and the medical laboratory in modern health care.

Medical Department • HARPER & ROW, PUBLISHERS

The American Journal of PATHOLOGY

GENERAL INFORMATION

Editorial Communications: All correspondence concerning editorial matters should be addressed to the Editor-in-Chief, DR. THOMAS D. KINNEY, Department of Pathology, Duke University Medical Center, Durham, N.C. 27706.

Business Communications: All subscriptions and advertising inquiries should be addressed to: MEDICAL DEPARTMENT, HARPER & ROW, PUBLISHERS, 2350 Virginia Ave, Hagerstown, Md. 21740.

Rates: THE AMERICAN JOURNAL OF PATHOLOGY is issued monthly, four volumes per year. Regular (individual) subscriptions: $27.50 per year in the U.S. and Possessions; $30.00 per year in Canada and countries of the Pan-American Postal Union; and $31.00 elsewhere. Special rate for Interns and Residents: $16.00 per year ($1.50 extra postage in Canada and countries of the Pan-American Postal Union; $2.50 extra postage elsewhere). Regular (individual) subscriptions and Resident and Intern subscriptions must be in the names of, and billed to, individuals. Institutional subscriptions, available to all libraries, schools, clinics, and hospitals, to all government agencies, local or national, and to all private or public institutions and organizations: $35.00 per year in the U.S. and Possessions; $37.50 per year in Canada and countries of the Pan-American Postal Union; $38.50 per year elsewhere. All subscriptions are payable in advance. Single copies, when available, $4.00.

Back Issues: Single issues and complete volumes of THE JOURNAL published prior to 1961 may be purchased from Walter J. Johnson, Inc., 111 Fifth Ave., New York, N.Y. 10003.

INDEX TO ADVERTISERS

American Optical Corporation	2nd Cover
Grune & Stratton, Inc.	6
Hardco Scientific	12, 13
Harper & Row, Publishers	5, 11, 14, 16, 17
Ortho Diagnostics	9, 10, 18
Sigma Chemical Company	15
Sorvall, Inc., Ivan	7
Source Information Systems	4th Cover
Wellcome Reagents Division	1, 2

MOVING?

To avoid interruption in your receipt of this Journal, we need to know your new address—six weeks in advance.

When writing us, be sure to type or print clearly your name and your new address—complete with zip code. It is *essential* that you also list your old address.

IMPORTANT: We publish a number of medical and scientific periodicals. Therefore, please be sure to give the name of THIS Journal when you write us.

Thank you for cooperating!

MEDICAL DEPARTMENT
Harper & Row, Publishers, Inc.
2350 Virginia Ave,
Hagerstown, Md. 21740.

(see page 8)

Published monthly by the Medical Department, Harper & Row, Publishers, Inc., 2350 Virginia Ave., Hagerstown, Md. 21740, and at 2901 Byrdhill Road, Richmond, Va. 23205. Second Class Postage paid at Hagerstown, Md., and additional mailing offices. Regular (individual) Rates: $27.50 per year in U.S. and Possessions, $30.00 in Canada and Pan-American Postal Union; and $31.00 elsewhere. Special Rates: Interns and Residents, $16.00 per year ($1.50 extra postage in Canada and countries of Pan-American Postal Union; $2.50 elsewhere). Institutional subscriptions; $35.00 per year in U.S. and Possessions, $37.50 per year in Canada and Pan-American Postal Unions; $38.50 elsewhere. Single copies, $4.00. Printed in U.S.A.

A new panoramic presentation . . .

Freedman

Clinical Immunology

By **Samuel O. Freedman, M.D.,** *Professor of Medicine, McGill University; Director, Division of Clinical Immunology and Allergy, The Montreal General Hospital. With Chapters by* **Phil Gold, M.D., Ph.D., David Hawkins, M.D.,** *and* **Joseph Shuster, M.D., Ph.D.**

Clinical immunology is a relatively new and rapidly developing specialty in medicine. Consequently, as with any new field, there is an urgent need to provide both the information and the practical understanding of what this new field offers. This new book satisfies that need.

Written by a well-known authority and several contributors from his own department, **CLINICAL IMMUNOLOGY** offers the knowledgeable range of a multi-authored text without repeating the material or presenting conflicting opinions so often associated with multi-authored books.

Throughout the book, the clinical signfiance of the latest developments in research is emphasized. The clinical manifestations, diagnosis, and treatment of common immunologic disorders are related to current concepts of etiology and pathogenesis. In addition, the application of immunologic principles to the prevention of disease is stressed.

Following a comprehensive introduction to the fundamentals of modern immunology (*The Biology of the Immune Response*), the clinical chapters present a broad viewpoint of immunologic diseases. *This panoramic presentation* includes immune deficiency states, diseases associated with hypergammaglobulinemia, organ transplantation, cancer immunology, collagen-vascular diseases, atopic diseases, allergic drug reactions, common immunization procedures, hypersensitivity to infectious agents, and the immunologic aspects of rheumatology, dermatology, nephrology, and hematology.

There is no question that this book will benefit all who must understand and consider on a practical level the immunologic factors involved in patient care or clinical research.

704 Pages. 50 Illustrations. $20.00

HARPER & ROW, Publishers, Inc. *Medical Department*
Mail Order Dept. 2350 Virginia Avenue Hagerstown, Maryland 21740
Please send me on approval:
☐ Freedman: **CLINICAL IMMUNOLOGY** $20.00
☐ **Bill me.** ☐ Check enclosed. (*SAVE! We pay postage.*)

Name . . . .

Address . . . .

City . . . . State . . . . Zip . . . .
AJP-7

ELECTRON MICROSCOPIC ATLAS OF BRAIN TUMORS •

By Tung Pui Poon, M.D., Asao Hirano, M.D., and Harry M. Zimmerman, M.D.

What is the cell origin of the gigantocellular neoplasm? Is the cerebellar sarcoma different from the so-called medulloblastoma? What is the nature of the cerebellar hemangioblastoma?

Often only the high resolution microscopy of the electron microscope can elucidate these and many other unsolved problems of the cytogenesis of brain tumors.

This atlas, while still not definitive—the technique for preparing micrographs as well as the infrequent availability of the rare tumors preclude it—includes most of the gliomas, many meningiomas and neurilemomas, and a number of nongliomatous neoplasms.

144 pp. 94 illustrations $19.75

PROGRESS IN MEDICAL GENETICS • Volume VIII •

Edited by Arthur G. Steinberg, Ph.D. and Alexander G. Bearn, M.D.

Reflecting the broad spectrum of subjects which interest human geneticists, Volume VIII of this authoritative *Progress* series contains seven valuable articles.

The Contents include: Genetic Aspects of Viral Diseases in Animals; Genes Which Increase Chromosomal Instability in Somatic Cells and Predispose to Cancer; The Future of Human Population Genetics; Enzyme Defects; Prevention of RH Isoimmunization; Disorders of Ganglioside Metabolism; The Genetics of Short Stature.

"Highly recommended . . ."—*JAMA*, of earlier volumes.

320 pp. 45 illus. $19.00

CLINICAL HISTOPATHOLOGY OF THE LIVER • An Atlas •

By Wilhelm Wepler and Egmont Wildhirt • *Translated by Leo Lowbeer, M.D.*

The liver needle biopsy, together with chemical liver function tests, has become an indispensable tool in the diagnosis of hepatic disorders. The old knowledge gained from autopsy material has been enlarged and supplanted by new knowledge of the living organ.

In this new volume, appearing for the first time in English translation, clinical history, symptoms, signs, and function tests are intimately correlated with the microscopic appearance of the liver biopsy. A practical, relevant language for both pathologist and clinician is presented.

Since black and white photographs are adequate to describe tissue structure, but not the characteristic coloration or discoloration of the liver (a large part of pathologic changes of the histologic picture), over a third of the photomicrographs are in color.

160 pp. 210 illus. $25.00

Grune & Stratton
111 Fifth Avenue, New York, N.Y. 10003

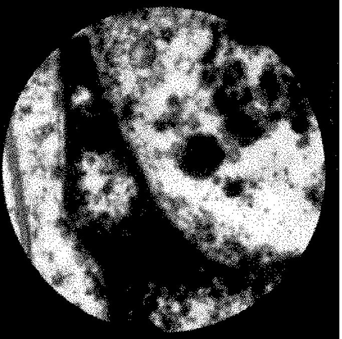

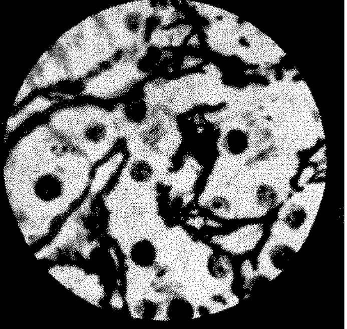

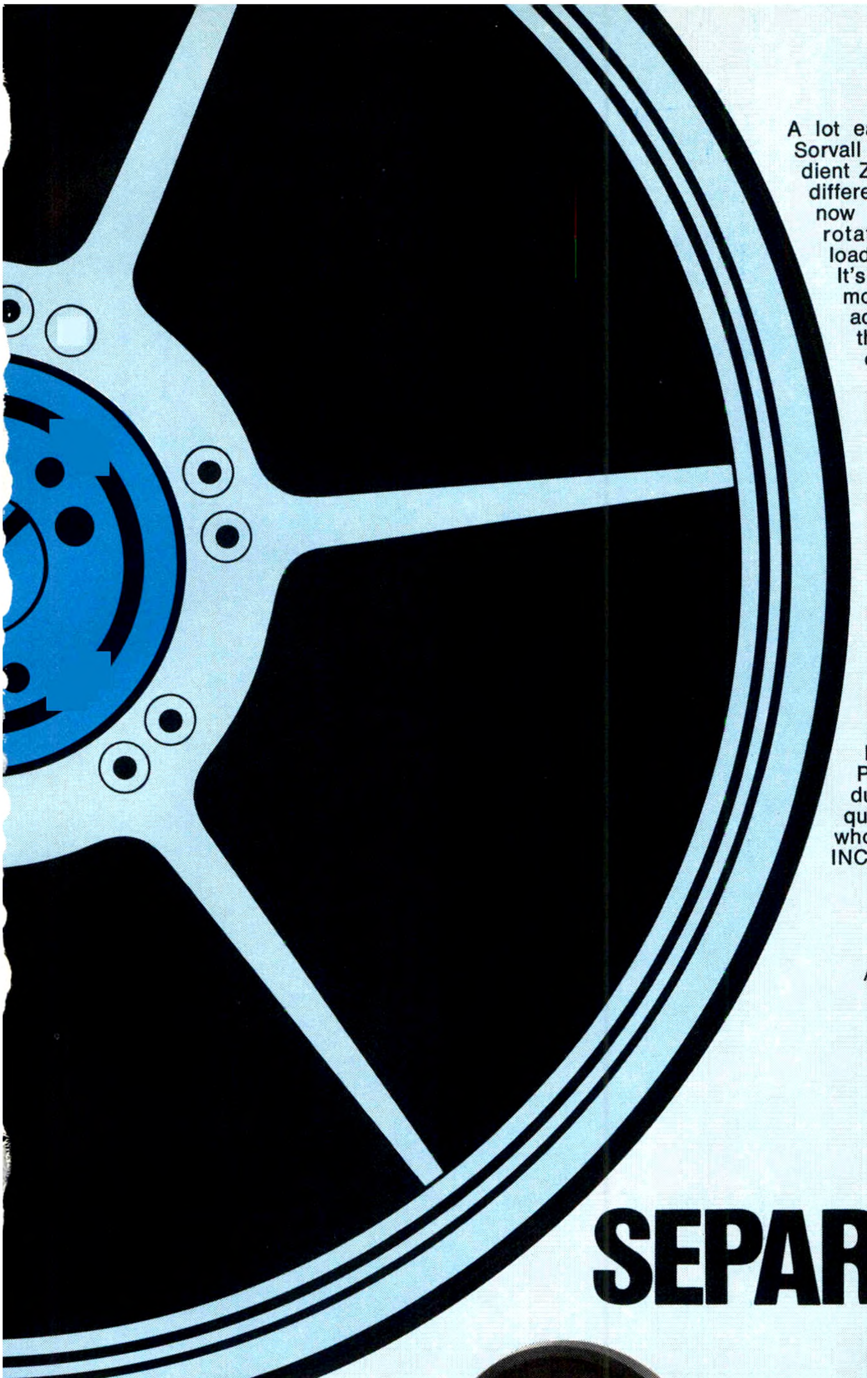

A lot easier — if you're using the new Sorvall SZ-14 Reorienting Density Gra- dient Zonal Rotor. The Sorvall SZ-14 is different from all other zonal rotors now available. It doesn't require a rotating-seal assembly. It can be loaded and unloaded *at rest.* Result? It's much simpler to operate. And more economical to maintain. The advantages don't stop there. With the SZ-14, you can perform zonal centrifugation at a fraction — literally—of yesterday's cost. The SZ-14 *and* a Sorvall RC2-B Auto- matic Superspeed Refrigerated Centrifuge together *cost little more than other zonal rotors alone.* If you already have a Sorvall RC2-B, RC-2, SS-3 or SS-4 Superspeed Centrifuge, (or an RC-3* General-Purpose Cen- trifuge) you can begin zonal cen- trifugation with the SZ-14 for about $2,000. A figure worth comparing. The performance is worth comparing, too. The SZ-14 accommodates up to 1,350 ml Operates at speeds up to 19,50 RPM (40,500 x G). Lets you sedi- ment most subcellular particles larger particles and whole cells Prevents particle sedimentatio during unloading. And doesn't re- quire any overlay solutions. Get the whole story. Write to: IVAN SORVALL INC., Norwalk, Conn. 06856.

*RC-3 requires slight modification in drive

SORVALL

Ask for Bulletin JP-7SZ-14

ZONAL SEPARATIONS CAN BE EASIER THAN YOU THINK

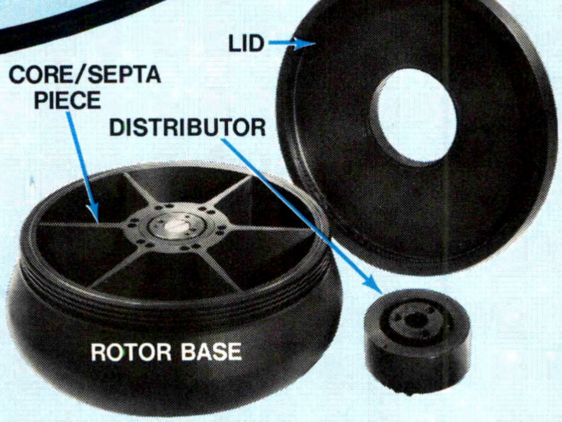

Professional Opportunities

PHYSICIANS WANTED

PATHOLOGIST. EXPERIENCED IN MODERN methods of diagnosis and research in kidney disease; for large private medical school on the east coast. Position and salary negotiable. Box No. 59.

EXPERIENCED EXPERIMENTAL IMMUNOLOGIST—oncologist. M.D. or Ph.D. for large private medical school on the east coast. Salary and position negotiable. Box No. 60.

CLASSIFIED ADVERTISING INFORMATION

RATES:

Non Display:	**1 Time**	**3 Times**	**6 Times or more**
20 words or less	$19.00	$16.00	$14.00
Each additional word	.50	.50	.50

Box Service—$2.00—First insertion only

Classified Display:	**1 Time**	**3 Times**	**6 Times or more**
	$35.00 per inch	$30.00 per inch	$25.00 per inch

Minimum Space—One (1) column inch

SEND ALL COPY,
AND BOX NUMBER INQUIRIES TO:

THE AMERICAN JOURNAL OF PATHOLOGY

Classified Dept.
131 Mineola Blvd.
Mineola, N. Y. 11501
(516) PI 6-0092

CHANGING YOUR ADDRESS?

In order to receive your journal without interruption, please complete this Change of Address notice and forward to the Publisher, 60 days in advance, if possible.

Old Address: (PLEASE PRINT)

NAME ________________________

____

STREET ________________________

____

CITY ________________________

STATE (or Country) ________________________

ZIP CODE ________________________

New Address: (PLEASE PRINT)

NAME ________________________

____

STREET ________________________

____

CITY ________________________

STATE (or Country) ________________________

ZIP CODE ________________________

Date New Address Effective: ________________

Name of Journal: ________________

NEW ADDRESS—MEDICAL DEPARTMENT

Harper & Row, Publishers, Inc.
Medical Department
2350 Virginia Avenue
Hagerstown, Maryland 21740

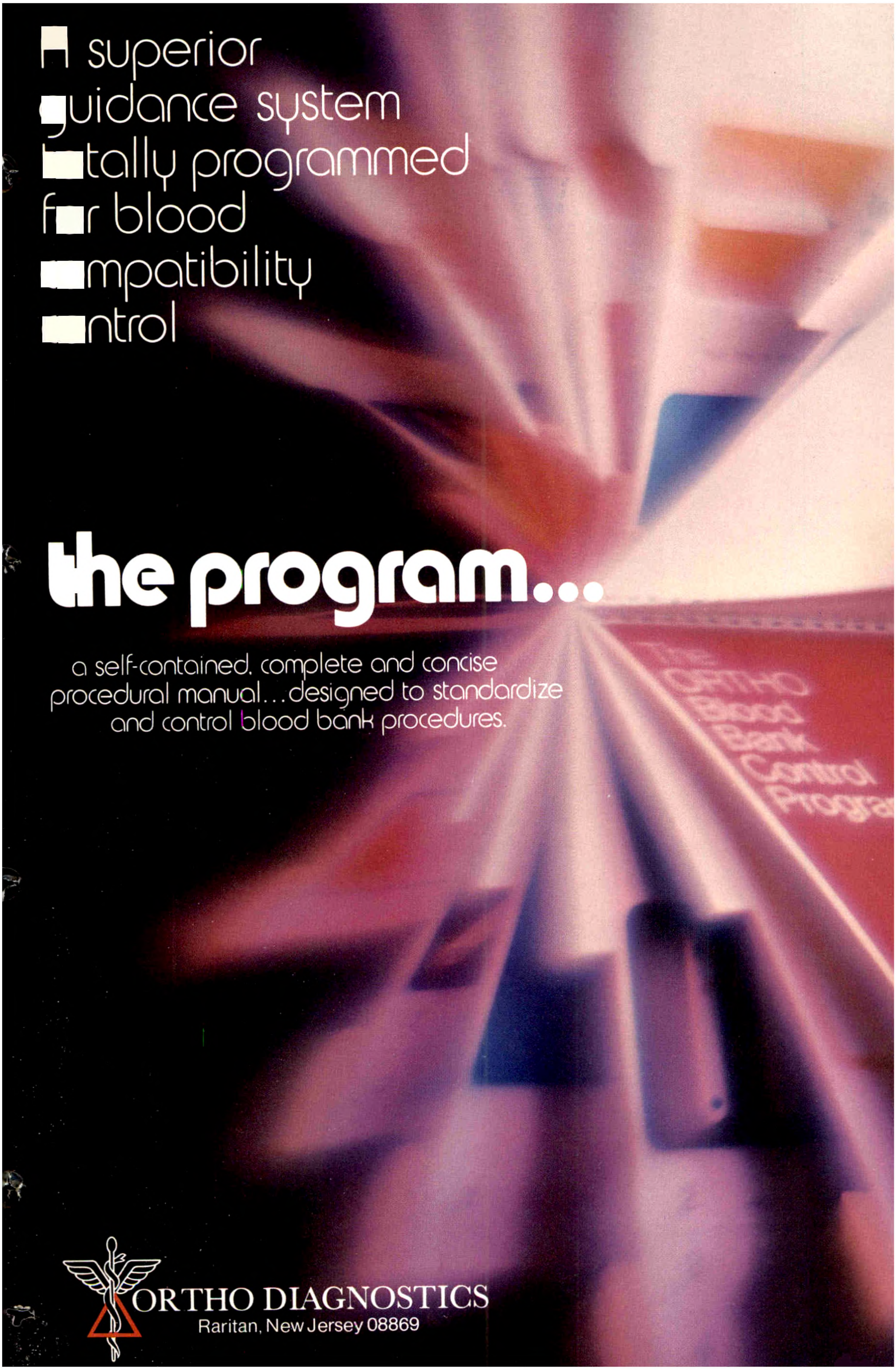
The
ORTHO
Blood
Bank
Control
Progra

A superior
guidance system
totally programmed
for blood
compatibility
control

the program...

a self-contained, complete and concise
procedural manual...designed to standardize
and control blood bank procedures.

ORTHO DIAGNOSTICS
Raritan, New Jersey 08869

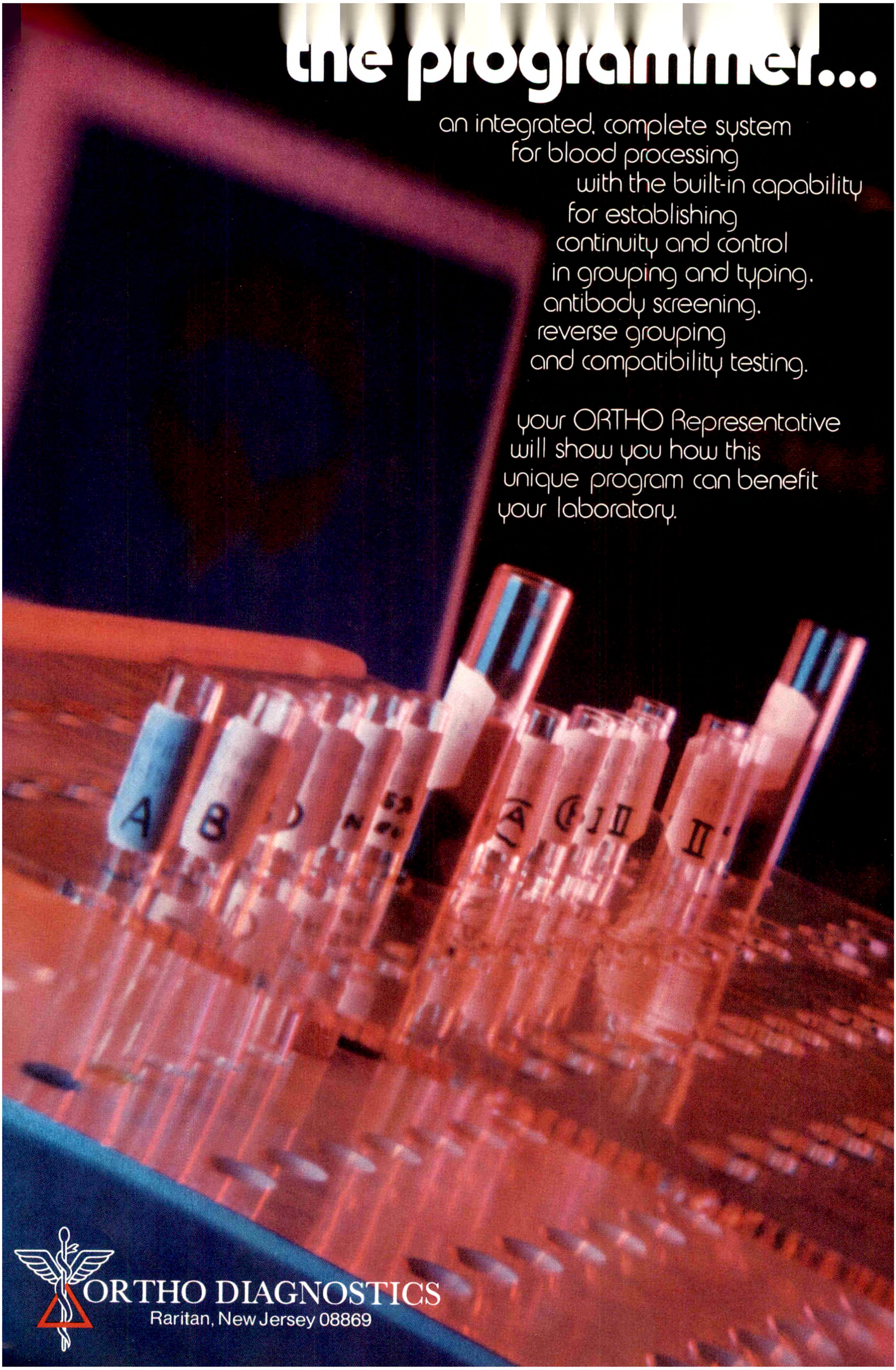

the programmer...

an integrated, complete system
for blood processing
with the built-in capability
for establishing
continuity and control
in grouping and typing,
antibody screening,
reverse grouping
and compatibility testing.

your ORTHO Representative
will show you how this
unique program can benefit
your laboratory.

ORTHO DIAGNOSTICS
Raritan, New Jersey 08869

DERMAL PATHOLOGY

This new work presents current concepts of dermal pathology including related embryology, anatomy, histology, electron microscopy and histochemistry. The highly illustrated text is divided into five sections, with the first section providing basic information and defining the special language of dermal pathology. The other four sections consist of: inflammatory dermatoses; granulomatous dermatoses; nevi and neoplasms; and reticuloendothelial and alternative dermatoses.

The diseases are arranged according to histopathologic features, with disorders presenting similar histopathologic changes grouped together. This approach stresses the differential diagnosis and emphasizes the differentiating features between diseases. The discussion of each disease includes a brief description of gross pathology or clinical morphology, histopathologic characteristics, pertinent histochemistry, the differential diagnosis, and a short clinical description. This book should enable the reader to improve his ability to diagnose skin lesions and to understand the pathogenesis of the diseases discussed.

With 17 Contributors. Edited by **James H. Graham, M.D.,** Professor of Medicine (Dermatology), Department of Medicine; Chairman, Division of Dermatology; Professor of Pathology, Department of Pathology; and Director, Section of Dermal Pathology, University of California, Irvin; **Waine C. Johnson, M.D.,** Professor of Dermatology, Department of Dermatology; Associate Professor of Pathology, Department of Pathology, Temple University School of Medicine; Director of Laboratories, the Skin and Cancer Hospital of Philadelphia, Philadelphia; and **Elson B. Helwig, MD.,** Chief, Department of Pathology and Branch of Dermal Pathology, Armed Forces Institute of Pathology, Washington, D.C.

1,155 Illustrations, 9 in color

Available in September. Advance orders now accepted.

HARPER & ROW, PUBLISHERS *Medical Department*

Mail Order Department, 2350 Virginia Avenue, Hagerstown, Maryland 21740

When published, please send me on approval: AJP7

GRAHAM, JOHNSON & HELWIG: Dermal Pathology ......About $40.00

NAME ____________________

____

ADDRESS ____________________

____

CITY ____________ STATE ____________ ZIP ________

5 ways you can convince your boss to make life easier for you.

(With automatic watering.)

First, memorize the "5 ways."

Then, after rehearsing your lines to perfection, march into the boss's office and impress him with your cool logic. Failing that, try threats. (He has relatives in the old country, perhaps?)

1. Your people spend a lot of time washing, filling, and changing water bottles. A three-handed caretaker you haven't discovered yet. Tell the boss that Hardco Automatic watering can free people to do more important work. And you can re-deploy your staff to meet the demands of expansion without increasing cost.
2. Water bottles breed contamination and cause accidental dehydration. Sometimes people tend to forget that when a rat works his stopper loose or jams something up the sipper tube, he doesn't only get a wet cage. He also gets no more water. But you have to put up with this kind of frustration all the time. So tell your leader that a Hardco Automatic Watering System guarantees every animal a constant source of clean, fresh water. (Which can't hurt your image when the U.S.D.A. or S.P.C.A. comes around.)
3. Bottles break, and you not only have to clean up the mess, but replace the bottles—something that's getting harder to do all the time. Deliveries are slower, and prices are higher. Pretty soon getting new bottles will be like trying to find a new front grill for a '58 Edsel. Also, bottles require all kinds of back up equipment like carts and racks and washers. You can tell your boss that Hardco eliminates all those problems. And boosts the morale of his employees who just happen to know that the other lab in town has already installed automatic watering.
4. About this morale thing. Nothing can get a man down like having to work with bottles. (Unless it's having to work in a pig room with a broken air conditioner.) Your boss already knows it's hard to get good people to do this work. And even harder to keep them. Tell him Hardco will make everybody happy.
5. You have made recommendations to the brass of your company before and have always come up against the same problem: money. Well, here's one time when they won't be able to fight you. Tell your money man Hardco Automatic Watering will save him 30% to 40% of his total labor costs. Tell him the cost of maintaining bottles for an average 5,000 cage facility runs about $20,000 a year. Every year. And then tell him that he will completely recover the cost of Hardco in about 17 months—and from then on it's all gravy.

It all adds up to this: your life is easier, your lab is more efficient, your animals are happier and healthier, and your boss is saving money.

If none of this works, Hardco has some very persuasive literature—not to mention some persuasive salesmen. For help, contact Hardco Scientific, 1705 Omni Drive, Cincinnati, Ohio 45245. Phone 513/752-0880.

hardco scientifi
division of fieldstone corporation

a new well-illustrated book for close-up study of the...

Fine Morphology of Mammalian Fertilization

By **Luciano Zamboni, M.D.,** *Professor of Pathology, University of California at Los Angeles School of Medicine and Department of Pathology, Los Angeles County Harbor General Hospital, Torrance, California.*

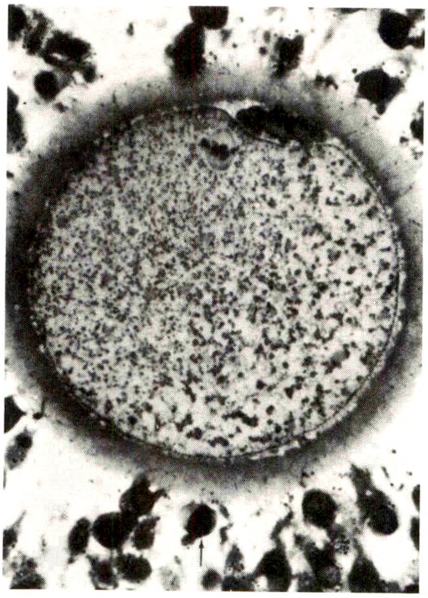

The purpose of this new book is to illustrate, by means of high resolution light microscopy and electron microscopy, the fundamental events which characterize fertilization in mammals, from the mitotic division of the spermatogonium and the stage of quiescence of the primary oocyte, through the development of a two-cell embryo. Of the species studied, emphasis has been given to the human, the relevant species and to the mouse, the animal which the author has used for his studies on uterine and tubal gametes. The book is divided into three sections: the first covers the differentiation and maturation of the spermatozoon in the testis and epididymis, the second considers the maturation of the oocyte in the ovarian follicle, and the third illustrates the various aspects of the interaction of male and female gametes. Of the 132 light and electron micrographs, 78 of them are from experimental animals (74 of which are from the mouse) and 54 micrographs are of human material. This atlas also includes an appendix which presents the technical procedures used for the preparation of the tissue.

250 Pages. 134 Illustrations. $15.00

HARPER & ROW, Publishers, Inc. *Medical Department*
Mail Order Dept. 2350 Virginia Avenue, Hagerstown, Maryland 21740

Please send me on approval:

☐ Zamboni: FINE MORPHOLOGY OF MAMMALIAN FERTILIZATION $15.00

☐ Bill me ☐ Check enclosed *(SAVE! We pay postage.)*

Name...

Address...

City...................... State.............. Zip........... AJP7

Call SIGMA for

SINGLE and TWO-REAGENT SYSTEMS

For the Ultraviolet Determination of

SGOT/SGPT

(Glutamic-Oxalacetic + Glutamic-Pyruvic Transaminase)

in serum or other fluids at 340 mμ

"Stat", Manual, or Automated Kinetic Procedures

SINGLE REAGENT SYSTEM — Per Sigma Technical Bulletin No. 55-UV.
A rapid, convenient procedure for routine or "stat" determinations — Manual or single reagent automated systems such as GEMSAEC, Centrifichem, Rotochem, etc. All you do is add water and serum — then read your O.D. One, five or ten assay vials - to fit your need.

Ask for free Sigma Technical Bulletin No. 55-UV or order:

Stock No.	For SGOT		Max. Assays*	Price
55-1	Single Assay Vial	10 vials	10	$5.00
55-5	5 Assay Vial	5 vials	5 x 5	7.50
		10 vials	10 x 5	14.85
55-10	10 Assay Vial	5 vials	5 x 10	12.50
		10 vials	10 x 10	24.85

Stock No.	For SGPT		Max. Assays*	Price
55-1P	Single Assay Vial	10 vials	10	$5.00
55-5P	5 Assay Vial	5 vials	5 x 5	8.00
		10 vials	10 x 5	15.50
55-10P	10 Assay Vial	5 vials	5 x 10	14.00
		10 vials	10 x 10	27.00

**Although vials for the above procedures are designed for a 3 ml Reaction Volume, many instruments can use much less. If so, the number of assays per vial can be increased proportionately and cost per test greatly reduced.*

TWO REAGENT SYSTEMS — Per Sigma Technical Bulletin No. 155-UV.
For Automated analyzers designed for two-reagent systems such as the LKB Reaction Rate Analyzer and the Beckman DSA-560 and 564-B.
Can also be used in single reagent automated analyzers and for manual procedures.

Ask for free Sigma Technical Bulletin No. 155-UV or order:

Kit No.	For	Max. Assays*	Price
155-A	SGOT	100	$22.50
155-B	SGPT	100	24.50

See above comment re: number of assays

Of course we still offer the **Original** Colorimetric Procedure — proven the world over — imitated everywhere, but still unequaled.

No. 505 — Sigma-Frankel Colorimetric at 490-530 mμ

Kit No.	For	Assays	Price
505	SGOT	100	$10.00
505-M	SGOT	25	5.50
505-P	SGPT	100	10.00
505-PM	SGPT	25	5.50
505-OP	SGOT/SGPT Combination	100	15.00

Also available:
No. 410-UV — Ultraviolet at 340 mμ

Kit No.	For	Assays	Price
410-50	SGOT	50	$11.55
410-100	SGOT	100	22.45
410-50P	SGPT	50	14.75
410-0P	SGOT/SGPT Combination	50 each	26.30

Free Sigma Technical Bulletins for the above methods are available upon request.
All prices **include** normal postage to you anywhere in the world.

It's a pleasure doing business with Sigma

ORDER DIRECT – TELEPHONE COLLECT from ANYWHERE in the WORLD
Day, Station to Station, 314-771-5750
Night, Person to Person, Dan Broida, 314-993-6418
TWX [Teletype] Day or Night: COLLECT 910-761-0593
TELEGRAM: SIGMACHEM, Saint Louis, Missouri

The Research Laboratories of
SIGMA® CHEMICAL COMPANY
P.O. BOX 14508 • SAINT LOUIS, MISSOURI 63178 U.S.A.
MANUFACTURERS OF THE FINEST BIOCHEMICALS AVAILABLE

Distributed through:
SIGMA LONDON Chem. Co. Ltd. • 12, Lettice St., London, S.W.6., England • Telephone: 01-736-5823 (Reverse Charges)
SIGMA ISRAEL Chem. Co. Ltd. • 28 Kaf-Gimel St., Givataim, Israel • Telephone: 03 760654 (Reverse Charges)

Laboratory

it's brand new now...
and
for years to come,
it will stay that way...

Medicine

Editor: George J. Race, M.D., M.S.P.H., Ph.D., Pathologist-in-Chief and Director of Laboratories, Baylor University Medical Center, Dallas, Texas.

Associate Editors: Clinical Pathology—Samih Y. Alami, M.D., Ph.D. Hematology—Eugene P. Frenkel, M.D. Chemistry—Robert J. Speer, Ph.D., Harold H. Varon, M.D., and Joel E. Young, Ph.D. Microbiology—Ralph Tompsett, M.D. With 100 Contributors.

In Three Volumes. **Here is a new exhaustive coverage presented for the first time as a loose-leaf reference. The dynamic loose-leaf concept means that your three volumes will always be new and updated through the ANNUAL SERVICE. *Volume 1* is entirely devoted to Clinical Chemistry, including the most modern automated techniques in use. *Volume 2* concerns Hematology, Blood Banking, Medical Microbiology, Virology, Serology, and Immunology. *Volume 3* covers Body Fluids including Urine, Cytology and Cytogenetics, Special Techniques (with modern methods and approaches to forensic pathology), and Laboratory Management and Function. A separate annually revised index is included. *For all the future information coming out in the various fields covered in these volumes, it is a worthwhile investment for knowledge and practice.***

ANNUAL SERVICE includes:

"*New pages for old.*" Partially or completely rewritten monographs, addenda and chapters on new subjects supplied annually along with a completely revised index.

HARPER & ROW, Publishers, Inc. *Medical Department*
2350 Virginia Avenue Hagerstown, Maryland 21740

☐ **Please send more information on LABORATORY MEDICINE**

LABORATORY MEDICINE (3 vols. & 1st yr. Annual Service): About $200.00.

About $30.00 a year thereafter for Annual Service. (Terms Available)

☐ **Bill me @ full price.** ☐ **Bill me @ $______ a month *(minimum $10.00 a month)***

Name . . . .

Address . . . .

City . . . . **State** . . . . **Zip** AJP-7

THROMBIN
THROMBIN
Fibrindex*
Thrombofax* Reagent
1.5 ml size
Ortho Plasma
Coagulation Control
THROMBIN
Fibrindex*
determination size
Ortho*
Brain Thromboplastin
ORTHO DIAGNOSTICS
Raritan, New Jersey

ORTHO coagulation reagents

reflect the standard of excellence in laboratory medicine

ACTIVATED THROMBOFAX* REAGENT
(Partial Thromboplastin with Activator)

THROMBOFAX* REAGENT
(Partial Thromboplastin)

ORTHO* BRAIN THROMBOPLASTIN

ORTHO* PLASMA COAGULATION CONTROL
(Human Plasma)

ORTHO DIAGNOSTICS

The American Journal of
PATHOLOGY

JULY 1972 • Volume 68, Number 1

Effects of Viral Infection on Nervous System Development

I. Pathogenesis of Bluetongue Virus Infection in Mice

Opendra Narayan, DVM, PhD and Richard T. Johnson, MD

Bluetongue vaccine virus was adapted to mice by serial intracerebral passage. The adapted virus was found to multiply selectively in immature cells of the subventricular zone of the forebrain and spread along cell migratory pathways to the olfactory bulbs, caudate/putamen, hippocampus and areas of cerebral cortex. Symmetrical, mineralized, partially cavitated lesions developed in these areas as a sequela of the infection. Infection of fetal mice led to more severe cerebral malformation, and infection of 2-week-old mice resulted in very limited multiplication without sequelae. The pattern of infection correlated with the maturation and migration of cells within the developing telencephalon (Am J Pathol 68:1–14, 1972).

VIRAL INFECTIONS have diverse effects on the developing nervous system. In addition to the destructive inflammatory lesions long associated with infection of the human fetal or newborn brain, several experimental viral infections have been found to induce pathologic sequelae resembling primary defects in neuroembryogenesis. These malformations, including nonclosure of the chick neural tube produced by myxoviruses,[1-3] granuloprival cerebellar hypoplasia caused by parvoviruses [4,5] and aqueductal stenosis with hydrocephalus following myxovirus and reovirus infections,[6-8] lack inflammation or other stigmata suggestive of an antecedent infectious process. Similarly,

---

From the Department of Neurology, The Johns Hopkins University School of Medicine, Baltimore, Md.

Supported by Grant NS08963 from the US Public Health Service and Grant R230-70 from the United Cerebral Palsy Research and Educational Foundation.

Accepted for publication Feb 23, 1972.

Address reprint requests to Dr. Richard T. Johnson, Johns Hopkins University School of Medicine, Department of Neurology, Traylor Bldg 709, Baltimore, Md 21205.

hydranencephaly and porencephaly were recently described in lambs infected *in utero* with the vaccine strains of bluetongue virus.[9-14] Although these viruses cause an acute inflammatory encephalitis in the fetal brain, the brains at birth show noninflammatory cavitary malformations resembling analogous defects of unknown etiology in the human newborn.[13]

Bluetongue virus is an arthropod-borne, double-stranded RNA virus, which causes epizootic disease of sheep manifest by acute inflammation of the gastrointestinal tract, respiratory tract, and muscle, but without evidence of nervous system infection.[15] An attentuated live virus vaccine was developed to protect against ovine epizootics,[16] and following its initial widespread use, many lambs with cerebral malformations were born from ewes immunized during pregnancy.[9] Subsequent experimental studies showed that infection of the ovine fetus at the end of the first trimester (50 days gestation) resulted in hydranencephaly, with the cerebral hemispheres reduced to membranous fluid filled sacs; infection at 75 days of gestation resulted in multiple porous cavities (porencephaly), and infection at 100 days of gestation caused no gross malformation.[13]

To further study the pathogenesis of this infection and the age-dependency of the lesions a more practical laboratory model was needed. Strains of bluetongue virus had previously been adapted to suckling mice, causing an acute fatal encephalitis.[12,17,18] In hopes of producing a model for the ovine malformations we have adapted the bluetongue vaccine virus to newborn mice to cause a nonfatal encephalitis. This report describes the pathogenesis and resultant pathology of this infection in fetal, newborn and 2-week-old mice.

Materials and Methods

Bluetongue live virus vaccine (Bluecine®), prepared by multiple passages in chick embryos, was adapted to mice by serial intracerebral inoculation of 1-day-old Swiss outbred mice. After the eighth passage, a fatal encephalitis was produced; therefore, the seventh passage, the highest passage not causing acute disease, was used. Stock virus was prepared as a 10% suspension of suckling mouse brains in Hanks' solution and titered 10^5 50% tissue culture infectious units (TCD_{50})/per ml.[19]

Animal Inoculations

Replicate experiments using at least 100 newborn and 2-week-old Swiss outbred mice were inoculated intracerebrally with 0.01 ml of Hanks' solution containing 10^3 TCD_{50} of virus. In one experiment, 4 newborn litters (approximately 40 mice) were inoculated intraperitoneally with 0.05 ml of the same inoculum. Fifty 4-week-old mice were inoculated intracerebrally with 0.02 ml of the virus material. Fetal mice were inoculated through the uterine wall with 0.001 ml of Hanks' solution containing 10^2 TCD_{50} of virus via laporatomies performed on 20

P 24,000

mice with timed gestations, using a 31 gauge needle and Hamilton micro-syringe. Groups of mice were killed at intervals after inoculation, and tissues were processed for virus assay, fluorescent antibody staining and histologic examination. Other groups were held for long term observation and histologic studies.

Virus Assays

Organs of 3 animals were pooled, ground in chilled mortars, and prepared as 10% suspensions in Hanks' solution containing 2% fetal calf serum. Tenfold or 0.5 log dilutions of suspensions in 0.2 ml aliquots were inoculated into 4 stationary tube cultures of mouse fibroblast cell line strain L929.[20] Cultures were observed for cytopathic effects 6 to 10 days after inoculation, and titers were expressed as TCD_{50}/0.02 g tissue.

Fluorescent Antibody Staining

Serum (obtained from Dr. F. C. Thomas, Madison, Wisconsin) was prepared by hyperimmunization of calves with tissue culture-derived BT8 strain of bluetongue virus. Gamma globulin was precipitated with NH_4SO_4 and conjugated with fluorescein isothiocyanate.[21] Brains were frozen rapidly in tubes immersed in a dry ice-alcohol mixture and stored at −70 C. Sections at multiple levels of brains in the horizontal or sagittal planes were cut at 7μ in a cryostat. Sections were air-dried, fixed in acetone for 10 minutes and stained for 30 minutes.

Histologic Studies

Mice were perfused with 10% buffered formalin, and brains were removed for further fixation and paraffin embedding. Brains were cut either horizontally or sagittally, and sections stained with hematoxylin and eosin.

Results

Infection of Newborn Mice

Newborn mice did not develop signs of illness for at last 10 days following intracerebral inoculation. During the subsequent 14 days about half showed retarded growth, and many of these died or were cannibalized. The remainder, including some runts, appeared healthy up to the conclusion of the experiment at 120 days.

Virus Growth

Virus multiplication in brains following intracerebral inoculation is shown in Text-figure 1. No virus was detected in blood or viscera following intracerebral inoculation. No virus multiplication was detected in viscera or brain following intraperitoneal inoculation.

Fluorescent Antibody Staining

Viral antigen was first seen in the brains 2 days after inoculation and was localized to the cytoplasm of cells of the lateral ventricular and subventricular zone (subependymal plate or germinal zone).[22] Four days after inoculation large numbers of cells contained antigen (Figure 1), but their distribution was still limited largely to the sub-

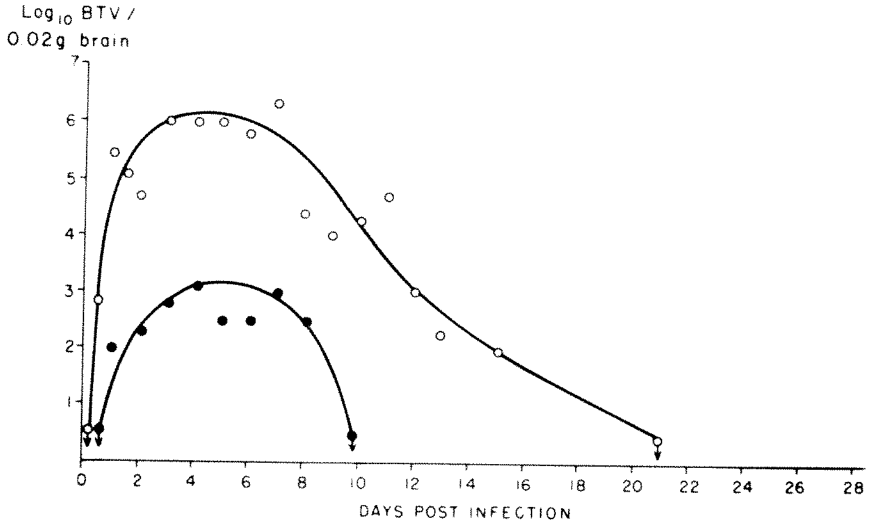

TEXT-FIG 1—Growth of bluetongue virus in brains of suckling mice inoculated intracerebrally at 1 day (*open circles*) and at 2 weeks (*closed circles*) of age.

ventricular zone, extending from the internal granular cells of the olfactory bulbs to the posterior extremity of the ventricle, and the dentate gyrus of the hippocampal formation (Text-figure 2). A few antigen-containing cells in the ventricular recess of the posterior colliculi were the only evidence of infection outside the telencephalon.

During the next 4 days viral antigen developed in cells of the caudate/putamen, and by 8 days cells of the anterior and occipital cortex were involved (Figure 2, Text-figure 2). Fluorescence faded after 8 days and was absent by 14 days.

Viral antigen was not seen in the ependyma, choroid plexus or vascular endothelium. Regions medial to the ventricles (including septal nuclei and thalamus), midbrain, cerebellum, and retina contained no viral antigen at any time during the infection.

Morphologic Changes

One to 10 days after inoculation brains were grossly normal. Between 11 and 14 days gross necrosis was seen in bilateral areas of the cerebral hemispheres and after 14 days white mineralization on the surface of the hemispheres, olfactory bulbs and occipital areas was often present. Brains of animals surviving beyond 10 days were usually small, and by 6 weeks marked reduction in the size of the telencephalon was apparent (Figure 3).

The first histologic abnormalities, found 4 days after inoculation, were focal areas of cell necrosis in the subventricular zone. By 6 days a

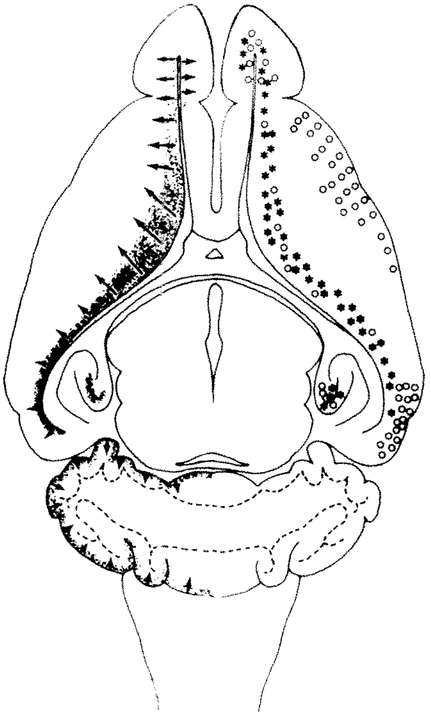

TEXT-FIG 2—Schematic horizontal section of a newborn mouse brain. On the left, stippled areas indicate normal position of immature cells of the brain at birth (subventricular cells anteriorly and external granular cells of the cerebellum posteriorly). *Arrows* indicate direction of subsequent migration of these cells. On the right the localization of cells infected with bluetongue virus 4 days (*stars*) and 8 days (*circles*) after inoculation are shown.

perivascular inflammatory reaction of mononuclear cells accompanied by parenchymal cell necrosis developed in the internal granular layer of the olfactory bulbs, subventricular zone, (Figure 4) and the caudate/putamen. In the hippocampal formation 10 to 50% of the granule cell neurones of the dentate gyrus were necrotic, while only rare pyramidal neurones of the hippocampus were abnormal. Lateral to the hippocampus, bilateral foci of necrosis, extending from the ventricle to the meninges, were consistently present in the occipital cortex. In contrast, the diencephalon, brainstem, cerebellum and the retina were normal.

Eight to ten days after inoculation more extensive necrosis was found in the same selective areas, and in more than 50% of animals additional foci of necrosis were found in the frontal cortex and around the ventricular recess of the posterior colliculi. Between 11 and 14 days basophilic mineralization of the necrotic areas was found, and this was more severe by 20 days. The perivascular inflammatory response resolved between 14 to 20 days.

Variation in the extent of lesions was noted in brains examined after 20 days. Runted mice surviving up to 45 days had subtotal necrosis and mineralization of the basal ganglia and internal granular cells of the olfactory bulbs, and extensive areas of mineralization in the cortex, yet abnormalities were confined to the telencephalon (Figure 5). Brains of apparently healthy mice killed 40 to 60 days after inoculation were less extensively affected. Lesions were still confined to the telencephalon and consisted of circumscribed, necrotic, mineralized foci in basal ganglia, cortex and centers of the olfactory bulbs (Figure 6). During the next two months these lesions became partially cavitated (Figure 7).

Infection of Fetal Mice

Intracerebral inoculations of either virus or diluent into fetuses before the 16th day of gestation (4 days prepartum) resulted in death and resorption. Fetal mice inoculated 4 and 3 days prepartum usually survived. Those inoculated with virus were pale and dehydrated at birth, and the majority died or were cannibalized during the first week postpartum.

In brains of mice infected 4 days before birth and killed 1 to 4 days postpartum, fluorescent antibody staining showed a similar sequence of infection to that in newborn mice. However, there was greater involvement of pyramidal cells of the hippocampus and cells in the region of the posterior colliculi.

Two mice inoculated 4 days prepartum survived 14 days after birth. Their brains were small, and most of the basal ganglia and neocortex was necrotic. The cortical layer was greatly reduced in thickness, and almost all neurons in dentate gyrus of the hippocampal formation and several in the pyramidal gyrus were necrotic (Figure 8). However, the diencephalon, midbrain, cerebellum, medulla and retina were normal.

Infection of Two-Week-Old Mice

No clinical disease was observed after intracerebral inoculation of 2-week-old mice. Virus replication in the brains was much more limited than in newborns (Text-figure 1). Fluorescent antibody staining showed limitation of infection to the population of subventricular cells at the rostral extension of the lateral ventricle and the internal granular cell layer of the olfactory bulbs.

Between 6 and 14 days a perivascular inflammatory response developed confined to these areas, but no other pathologic changes were evident. Brains examined after 14 days appeared normal.

Infection of Four-Week-Old Mice

Following intracerebral inoculation no clinical disease was seen, no viral multiplication was detected, fluorescent antibody staining showed no viral antigen, and, except for the stab wound of inoculation, no pathologic changes were found.

Discussion

The vaccine strain of bluetongue virus adapted to mice demonstrated an extraordinary selectivity, infecting almost exclusively the cells of subventricular origin within the forebrain. Nonfatal infection of the newborn mouse brain led to unique pathologic sequelae consisting of symmetrical, partially cavitated, mineralized lesions of predictable distribution in basal ganglia, olfactory bulbs, hippocampal formation and cerebral cortex.

As Sidman had aptly said, "the developing central nervous system is a different organ from its adult counterpart."[23] In the present model these differences are relevant both in terms of the susceptible cell populations and the pathologic reactions to infection. The brain of the mouse at birth is immature. The cell populations of ontogenetically older areas such as the thalamus, hypothalamus and brainstem are established early in gestation; however, the telencephalon and cerebellum continue to develop in the neonatal period.[24–27] In the forebrain this development is centered in the ventricular and subventricular zones composed of the densely staining immature cells lying dorsal and lateral to the lateral ventricles. In the neonatal period these cells migrate laterally into the caudate/putamen and neocortex, rostrally in the granular layer of the olfactory bulbs, and caudally in the dentate gyrus of the hippocampal formation.[28]

Fluorescent antibody staining 2 to 4 days after inoculation of newborn mice showed the bluetongue virus infection limited to the subventricular zone. The subsequent spread of infection over the next 4 days followed the migratory paths of these cells into the basal ganglia, cortex, olfactory bulbs and hippocampal formation. It was not determined whether infection was carried by migrating, infected cells or whether infection spread cell to cell through a susceptible population of the migrating, immature cells. The lack of spread of infection medial to the ventricles into the diencephalon and brainstem is consistent with either explanation.

Studies in late gestation and in 2- and 4-week-old mice further confirmed these findings. Prenatally, the subventricular zone is wider than after birth, and during late gestation pyramidal cells of the hippocampus are still forming.[28] Inoculation of fetal mice resulted in more extensive infection of the subventricular zone and greater involvement of the hippocampal pyramidal cells.

Postnatally, the subventricular zone is rapidly depleted. By 2 weeks of age, mitotic activity and migration is limited largely to a cluster of cells at the rostral extent of the lateral ventricles, which extend into the olfactory bulbs forming the internal granular layer. This remnant of the subventricular zone proved to be the sole susceptible cell population in the 2-week-old mouse. Four-week-old mice, with a very limited subventricular zone, showed no evidence of infection.

The selective vulnerability of the subventricular cells cannot be explained solely by immaturity of mitotic activity. The external granular layer of the cerebellum and layers of the retina are also developing in the neonatal period,[27,29] but neither showed evidence of infection. *In vivo* and *in vitro* studies have recently suggested that parvoviruses have a selective affinity for cells in mitosis.[30-33] Newborn animals infected with rat virus or feline panleukopenia virus show destruction of the extrenal granular cells of the cerebellum and only limited pathologic changes in the subventricular zone of the telencephalon. This results in granuloprival cerebellar hypoplasia but no significant abnormality of the cerebral hemispheres. In contrast, the bluetongue virus lesions were confined to the telencephalon.

In the majority of viral infections immature animals show greater susceptibility, and, on theoretical grounds, it seems reasonable that undifferentiated cells would be more susceptible to viral infection. Such cells are presumably multipotential, and this may include the potential to adsorb or replicate virus. When the cell reaches its ultimate anatomic destination and differentiates, it becomes committed to more specific functions. For example, specialization of cytoplasmic membranes of neural cells may lead to loss of virus receptor sites or specialization of metabolic function might lead to the repression of enzyme systems or synthetic mechanisms needed to render the cells susceptible to infection.

Bluetongue vaccine virus infections of mice provide a new model for the study of cavitary malformations of the developing nervous system and the unexplained mineralization which often develops after infections of the fetal brain. The sequelae of bluetongue infection in newborn mice resembled the porencephalic lesions following midterm fetal infection of sheep; but since intracerebral inoculations of the early mouse fetuses resulted in nonspecific deaths, a murine model for the hydranencephalic lesion produced by infection of the first trimester ovine fetus could not be sought. However, in this study the limitation of the infection to germinal cells of the telencephalon provides a unique example of the selective vulnerability of different populations of immature brain cells to viral infection, and the novel pathologic sequelae further demonstrate the variety of lesions that may be consequent to such infections.

References

1. Hamburger V, Habel K: Teratogenetic and lethal effects of influenza-A and mumps viruses on early chick embryos. Proc Soc Exp Biol Med 66:608–617, 1947
2. Blattner RJ, Heys RM: Role of viruses in the etiology of congenital malformations. Progr Med Virol 3:311–362, 1961
3. Johnson KP, Klasnja R, Johnson RT: Neural tube defects of chick embryos: an indirect result of influenza A virus infection. J Neuropathol Exp Neurol 30:68–74, 1971
4. Kilham L, Margolis G: Cerebellar ataxia in hamsters inoculated with rat virus. Science 143:1047–1048, 1964
5. Idem: Viral etiology of spontaneous ataxia of cats. Am J Pathol 48:991–1011, 1966
6. Johnson RT, Johnson KP, Edmonds CJ: Virus-induced hydrocephalus: development of aqueductal stenosis in hamsters after mumps infection. Science 157:1066–1067, 1967
7. Johnson RT, Johnson KP: Hydrocephalus as a sequela of experimental myxovirus infections. Exp Mol Pathol 10:68–80, 1969
8. Margolis G, Kilham L: Hydrocephalus in hamsters, ferrets, rats, and mice following inoculations with reovirus type 1. II. Pathologic studies. Lab Invest 21:189–198, 1969
9. Schultz G, DeLay PD: Losses in newborn lambs associated with bluetongue vaccination of pregnant ewes. J Am Vet Med Assoc 127:224–226, 1955
10. Cordy DR, Schultz G: Congenital subcortical encephalopathies in lambs. J Neuropathol Exp Neurol 20:554–562, 1961
11. Young S, Cordy DR: An ovine fetal encephalopathy caused by bluetongue vaccine virus. J Neuropathol Exp Neurol 23:635–659, 1964
12. Richards WPC, Cordy DR: Bluetongue virus infection: pathologic responses of nervous systems in sheep and mice. Science 156:530–531, 1967
13. Osburn BI, Silverstein AM, Prendergast RA, Johnson RT, Parshall CJ: Experimental viral-induced congenital encephalopathies. I. Pathology of hydranencephaly and porencephaly caused by bluetongue vaccine virus. Lab Invest 25:197–205, 1971
14. Osburn BI, Johnson RT, Silverstein AM, Prendergast RA, Jochim MM, Levy SE: Experimental viral-induced congenital encephalopathies. II. The pathogenesis of bluetongue vaccine virus infection in fetal lambs. Lab Invest 25:206–210, 1971
15. Howell PG, Verwoerd DW: Bluetongue virus. Virology Monographs 9:35–74, 1971
16. McKercher DG, McGowan B, Cabasso VJ, Roberts GI, Saito JK: Studies on bluetongue. III. The development of a modified live virus vaccine employing American strains of bluetongue virus. Am J Vet Res 18:310–316, 1957

17. Van den Ende M, Linder A, Kaschula VR: Experiments with the Cyprus strain of bluetongue virus: multiplication in the central nervous system of mice and complement fixation. J Hyg (Camb) 52:155-164, 1954
18. Svehag SE: Quantitative studies of bluetongue virus in mice. Arch Gesamte Virusforsch 12:363-386, 1962
19. Reed LJ, Muench HA: A simple method of estimating fifty per cent endpoints. Am J Hyg 27:493-497, 1938
20. Thomas FC, Trainer DO: Bluetongue virus in white-tailed deer. Am J Vet Res 31:271-278, 1970
21. Cherry WB, Goldman M, Carski TR: Fluorescent antibody techniques in the diagnosis of communicable diseases. US Public Health Service Publication 729, 1960
22. Boulder Committee: Embryonic vertebrate central nervous system: revised terminology. Anat Rec 166:257-261, 1970
23. Sidman RL: Cell proliferation, migration, and interaction in the developing mammalian central nervous system. The Neurosciences, Second Study Program. Edited by FO Schmitt. New York, Rockefeller University Press, 1970, pp 100-107
24. Hinds JW: Autoradiographic study of histogenesis in the mouse olfactory bulb. I. Time of origin of neurons and neuroglia. J Comp Neurol 134:287-304, 1968
25. Idem: Autoradiographic study of histogenesis in the mouse olfactory bulb. II. Cell proliferation and migration. J Comp Neurol 134:305-322, 1968
26. Smart I: The subependymal layer of the mouse brain and its cell production as shown by radioautography after thymidine-H^3 injection. J Comp Neurol 116:325-347, 1961
27. Miale IL, Sidman RL: An autoradiographic analysis of histogenesis in the mouse cerebellum. Exp Neurol 4:277-296, 1961
28. Angevine JB: Time of neuron origin in the hippocampal region: an autoradiographic study in the mouse. Exp Neurol Suppl 2:1-70, 1965
29. Sidman RL: Histogenesis of the mouse retina studied with tritiated thymidine. The Structure of the Eye. Edited by GK Smelser. New York, Academic Press, Inc, 1961, pp 487-505
30. Ruffolo PR, Margolis G, Kilham L: The induction of hepatitis by prior partial hepatectomy in resistant adult rats injected with H-1 virus. Am J Pathol 49:795-824, 1966
31. Margolis G, Kilham L: Rat virus, an agent with an affinity for the dividing cell. NINDB Monograph No. 2, Slow Latent and Temperate Virus Infections. Edited by DC Gajdusek, CJ Gibbs, M Alpers. Washington, DC, US Government Printing Office, 1965, pp 361-367
32. Tennant RW, Layman KR, Hand RE: Effect of cell physiological state on infection by rat virus. J Virol 4:872-878, 1969
33. Tennant RW, Hand RE: Requirement of cellular synthesis for Kilham rat virus replication. Virology 42:1054-1063, 1970

Acknowledgments

The authors wish to acknowledge the advice of Drs. Richard Sidman, Arthur Silverstein and Mark Molliver and the technical assistance of Susan Levy and Kathleen Kuehl.

Dr. Narayan is a recipient of a Canadian Medical Research Council Fellowship.

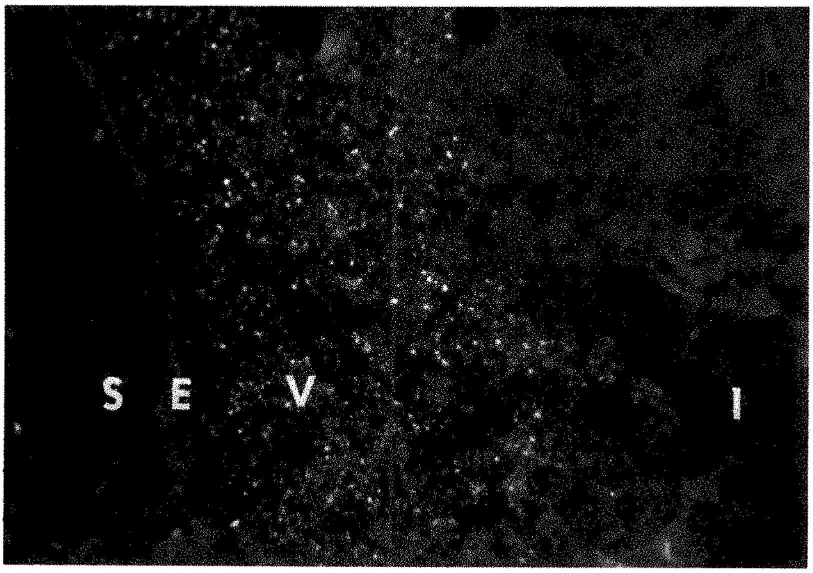

1

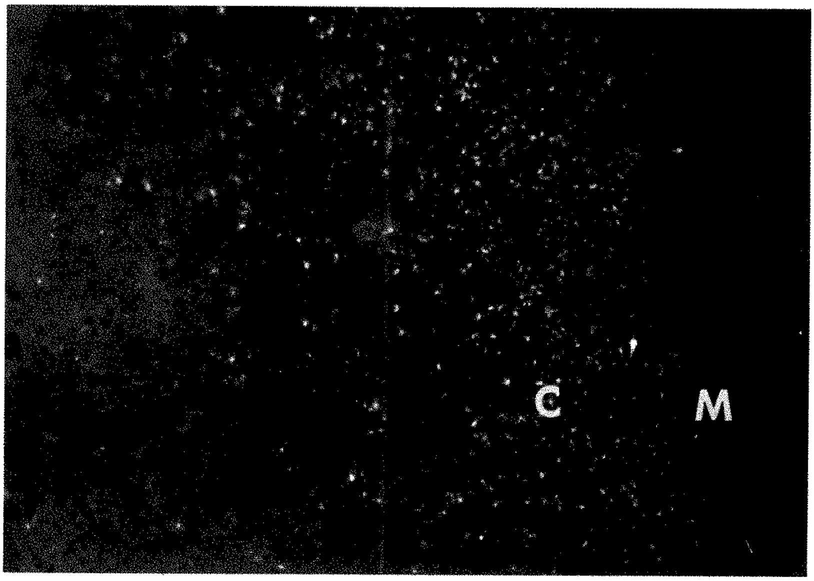

2

Fig 1—Localization of bluetongue virus in newborn mouse brain 4 days after intracerebral inoculation. Horizontal section stained with fluorescent antibody shows viral antigen localized to subventricular zone (*V*). The septal nucleus (*S*), ependyma (*E*), intermediate zone (*I*) and vascular endothelial cells contain no viral antigen (× 100). **Fig 2**—Localization of bluetongue virus in occipital cortex of newborn mouse 8 days after intracerebral inoculation. Horizontal section stained with fluorescent antibody shows no antigen in meninges and marginal zone (*M*), but many cells with viral antigen in the cortical plate (*C*) (× 100).

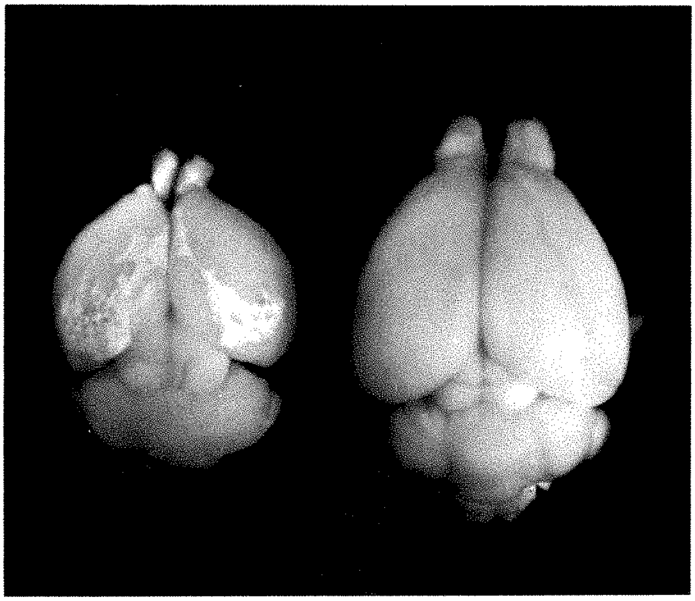

Fig 3—Brains of control (*right*) and bluetongue virus infected (*left*) mice 6 weeks after neonatal inoculation. Gross sequelae of infection include smallness of the cerebral hemispheres and mineralization extending from the olfactory bulbs to the occipital cortex (× 6).

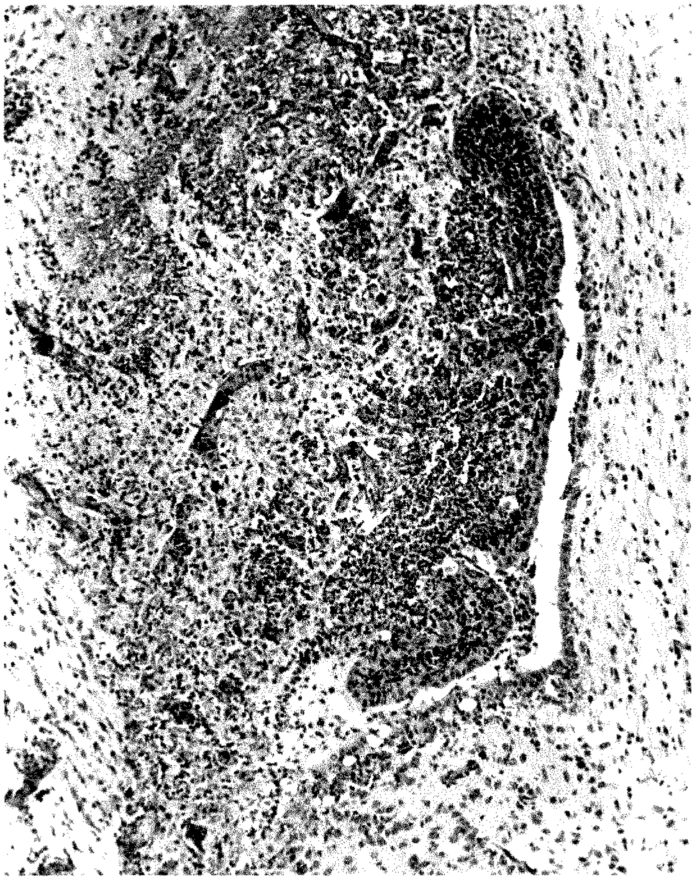

Fig 4—Horizontal section of the brain of a mouse inoculated neonatally with bluetongue virus and killed 7 days later. Necrosis of cells in the ventricular and subventricular zone of the lateral ventricle and a marked perivascular inflammatory response are shown (H&E, × 100).

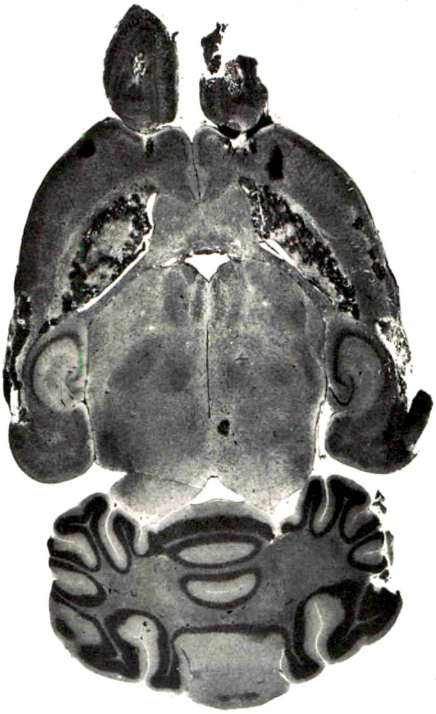

Fig 5—Horizontal section of the brain of a mouse inoculated neonatally with bluetongue virus and killed 3 weeks later. Bilateral necrosis and mineralization are present in the olfactory bulbs, caudate/putamen and the occipital cortex. The diencephalon and cerebellum appear normal (H&E, × 6).

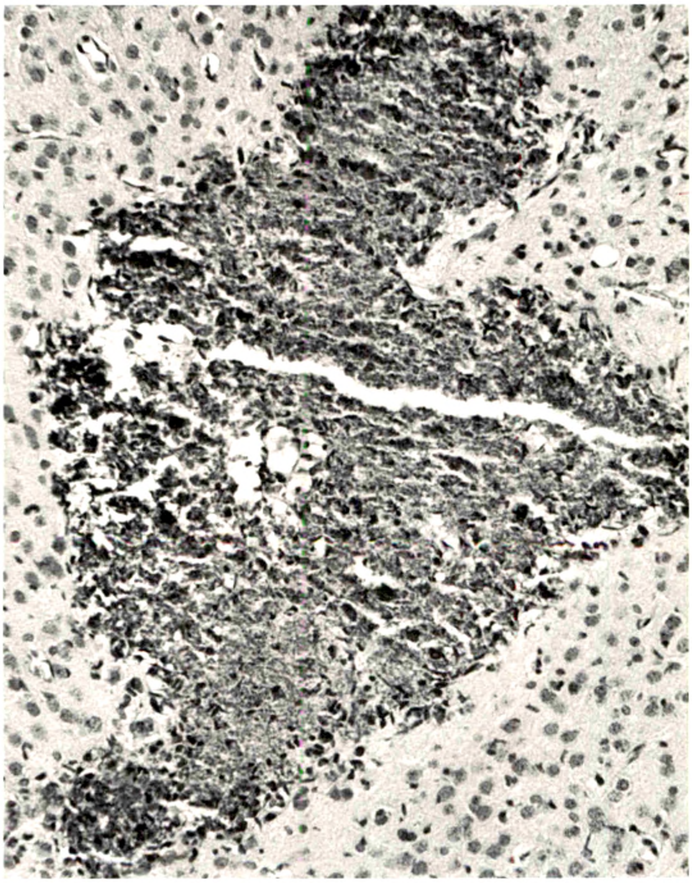

Fig 6—Section of the brain of a mouse inoculated neonatally with bluetongue virus and killed 42 days later. A circumscribed area of necrosis in the occipital cortex shows mineralization and a lack of inflammation (H&E, × 200).

7

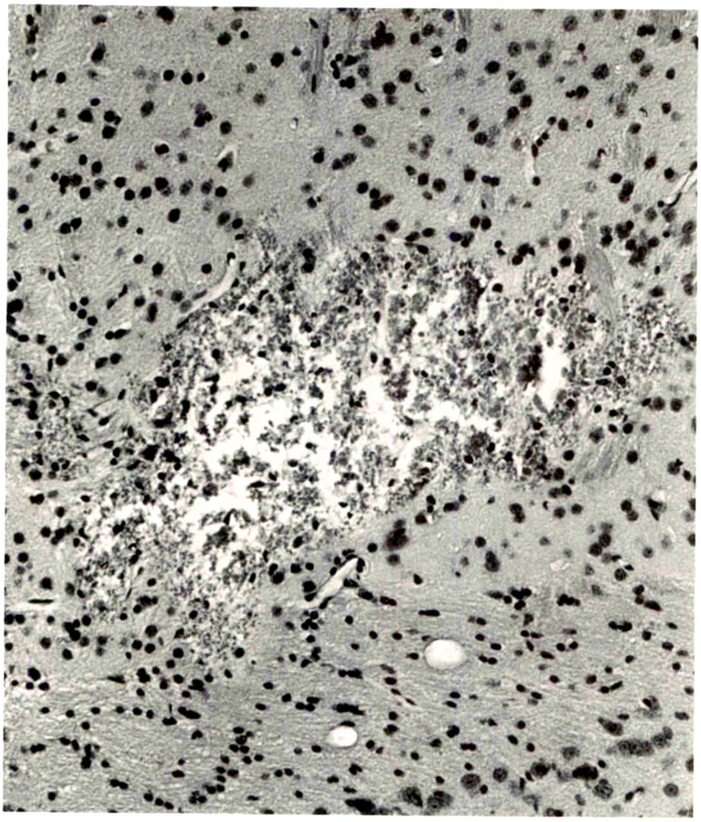

8

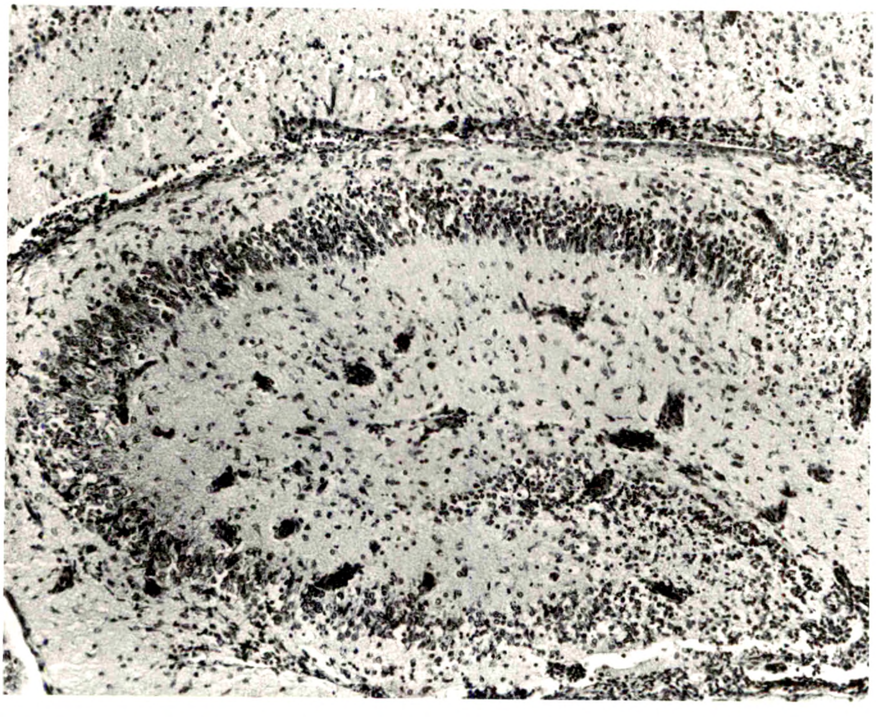

Fig 7—Section of the brain of a mouse inoculated neonatally and killed 120 days later. Focal area in basal ganglia shows mineralization and partial cavitation (H&E, × 200). **Fig 8**—Horizontal section of the brain of a mouse inoculated 4 days prepartum and killed 14 days after birth. Within the hippocampal formation the dentate gyrus (*lower right*) is almost totally destroyed and, unlike neonatally inoculated mice, pyramidal cells are also involved (H&E, × 100).

Effects of Viral Infection on Nervous System Development

II. Attempts to Modify Bluetongue-Virus-Induced Malformations with Cyclophosphamide and Antithymocyte Serum

Opendra Narayan, DVM, PhD, Henry F. McFarland, MD and Richard T. Johnson, MD

Treatment with cyclophosphamide and antithymocyte serum (ATS) did not significantly increase the susceptibility of mice to bluetongue virus infections of the nervous system. Cyclophosphamide actually inhibited virus growth in newborn and 2-week-old mice and, in newborn mice, diminished the severity of virus-induced pathologic sequelae. Autoradiographic studies suggested this inhibition resulted from the effect of cyclophosphamide on the immature cells of the subventricular zone which were the cell population selectively infected by bluetongue virus. In newborn mice ATS inhibited the inflammatory reaction and development of antibody, but did not result in alterations in mortality, initial virus growth and localization or early necrosis of cells in the subventricular zone. Antithymocyte serum only caused longer persistence of virus and slight extension of late pathologic lesions. The failure of cyclophosphamide and ATS treatment to induce more extensive lesions in older mice show that the age-dependency of bluetongue lesions is not determined by the immaturity of immune responses (Am J Pathol 68:15–22, 1972).

THE USUAL SUSCEPTIBILITY of the developing nervous system to viral infection has been explained both by the immunologic incompetence of the fetus or newborn and by the possibly greater vulnerability of immature neuroepithelial cells. The age dependency of nervous system lesions caused by bluetongue vaccine virus was initially thought to be determined by the stage of immunologic maturity of the infected sheep or mouse.[1] Subsequent work in fetal sheep showed that bluetongue vaccine virus selectively infected undifferentiated cells of the ventricular and subventricular zone of the forebrain. This suggested that early fetal infection leading to hydranencephaly, midterm infection leading to porencephaly and lack of mal-

---

From the Department of Neurology, The Johns Hopkins University School of Medicine, Baltimore, Md.

Supported by Grant R230-70 from the United Cerebral Palsy Research and Educational Foundation and Grant NS08963 from the US Public Health Service.

Accepted for publication Feb 23, 1972.

Address reprint requests to Dr. Richard T. Johnson, Johns Hopkins University School of Medicine, Department of Neurology, Traylor Bldg 709, Baltimore, Md 21205.

formation after late gestational infection might be determined by target cell maturation. However, the fetal sheep's capacity to produce neutralizing antibody against bluetongue virus also developed at the end of the second trimester, so the relative roles of immunologic immaturity and susceptibility of immature cells could not readily be resolved.[2] The production of analogous cavitary lesions in newborn mice with adapted bluetongue vaccine virus provided a model in which the determinants of these age-dependent malformations could be investigated.[3]

Materials and Methods

The adapted virus and methods of intracerebral virus inoculations, tissue sampling, virus assays and fluorescent antibody staining were those previously described.[3]

Cyclophosphamide Treatment

Cyclophosphamide in saline was given subcutaneously in a total dose of 150 mg/kg, in 3 divided doses to newborns and 2 divided doses in 2- and 4-week-old mice. The initial injection was given 6 hours before virus inoculation and subsequent injections at 24-hour intervals thereafter. Controls included mice receiving cyclophosphamide alone and mice given virus and saline injections.

Antithymocyte Serum (ATS) Treatment

Rabbits were injected intravenously with 1 ml suspensions of 10^6 mouse thymocytes at weekly intervals for 6 weeks and bled for serum 2 weeks after the final injection. Sera were adsorbed with mouse red blood cells and heat inactivated at 56 C for 30 minutes. A cytotoxicity titer of greater than 1:256 was determined with mouse thymocyte suspensions.[4] Groups of 5-day-old mice were given ATS diluted 1:4 in 0.1 ml volumes subcutaneously or intraperitoneally on the day of virus inoculation and on days 3, 6, 10, 15 and 20 thereafter. The efficacy of this dosage of ATS was confirmed by preventing the immunopathologic disease of mice infected intracerebrally with 100 LD_{50} of lymphocytic choriomenigitis virus [5] (tested by Dr. Gerald Cole, Johns Hopkins University School of Hygiene and Public Health).

Autoradiography

Uninfected mice were given cyclophosphamide, 150 mg/kg in 3 divided doses 12 hours after birth, and 24 and 48 hours later. At 7 days of age tritiated thymidine with a specific activity of 6.7 Ci/mM at 5 μCi/g was given intraperitoneally. Control mice were given saline before being pulse labeled. Mice were perfused with Bouin's solution 1, 2, 4 and 20 hours later, and brains were fixed for a further 24 hours in Bouin's solution before processing for autoradiography.[6]

Neutralizing Antibody Assays

Twofold dilutions of serum inactivated at 56 C for 30 minutes were mixed with equal volumes of diluent containing 100 TCD_{50} of virus. After incubation at room temperature for 1 hour, monolayer cultures of L cells were inoculated using 4 tubes per dilution.

Results

Effect of Cyclophosphamide Treatment

Cyclophosphamide was initially given to 2- and 4-week-old mice to determine whether suppression of immune responses would result in augmented virus growth and the production of cavitary lesions similar to those observed in newborns; it was given to newborns to determine whether more extensive cavitary lesions could be produced analogous to the hydranencephalic lesion resulting from infection of the 50-day-gestation fetal sheep. Instead of the anticipated lack of effect or augmentation of virus growth, no virus growth was detectable in 4-week-old mice and virus growth was inhibited in 2-week-old and newborn mouse brains during initial period after cyclophosphamide (Figures 1, 2); after this inhibition, infection was prolonged. Cyclophosphamide-treated 2-week-old mice had no detectable serum neutralizing antibody at 1:8 dilutions 14 or 21 days after infection, whereas virus control mice had antibody at dilutions of > 1:64 on these days.

Cyclophosphamide treatment of 2- and 4-week-old mice caused no clinical signs except alopecia. In newborns treatment resulted in

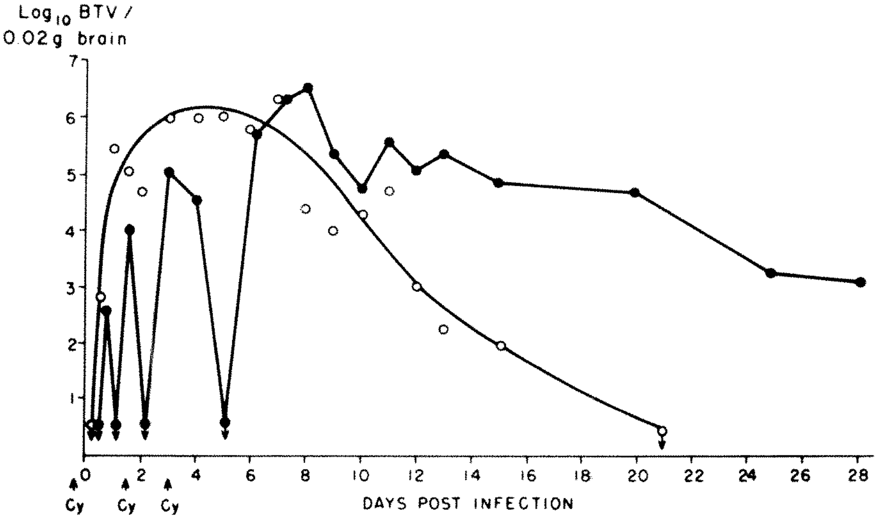

TEXT-FIG 1—Growth of bluetongue virus in brains of normal (*open circles*) and cyclophosphamide treated (*closed circles*) mice infected at 1 day of age. Each point represents a pool of 3 brains. The apparent variability in virus content in brain pools of mice during the first 5 days of cyclophosphamide treatment can be explained by viral replication in occasional brains.

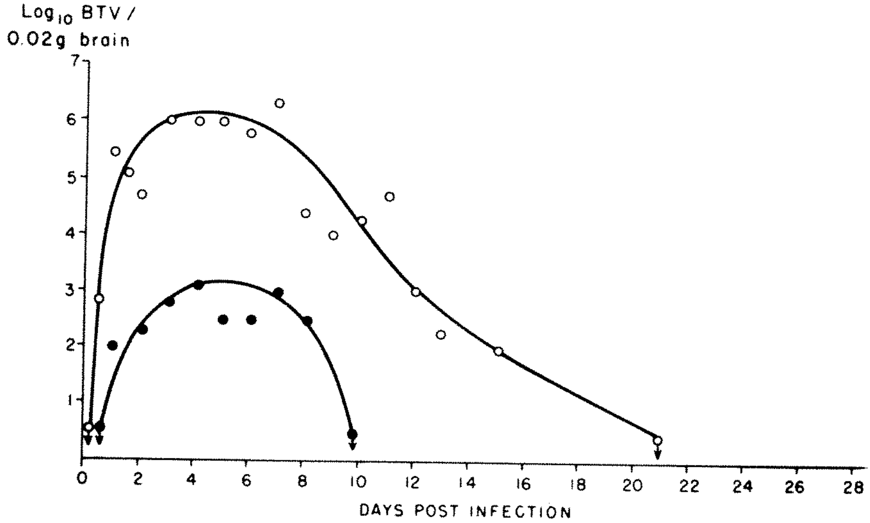

TEXT-FIG 2—Growth of bluetongue virus in brains of normal (*open circles*) and cyclophosphamide treated (*closed circles*) mice infected at 2 weeks of age. Each point represents a pool of 3 brains.

growth arrest and death of 50% by 8 days and 80% by 14 days. Surprisingly, virus infection in addition to treatment with cyclophosphamide did not alter this mortality.

Fluorescent antibody staining of infected brains of 2-week-old mice treated with cyclophosphamide showed viral antigen confined to the group of rostral subventricular cells and granular cells of the olfactory bulbs. This localization of antigen was identical to that found in 2-week-old mice receiving virus alone. Newborn mice treated with cyclophosphamide showed some antigen confined to the subventricular zone and olfactory bulbs 4 days after infection. However, unlike virus control mice in which infection spread laterally to involve the caudate/putamen and cortical areas 6 to 8 days after inoculation, cyclophosphamide-treated newborns showed viral antigen largely confined to the subventricular zone throughout the infection. In both 2-week-old and newborn mice, cyclophosphamide treatment resulted in the persistence of viral antigen for 14 days, in contrast to the disappearance of fluorescence after 8 days in virus controls.

Cyclophosphamide treatment led to little alteration in the histologic correlates of infection in 2-week-old mice. The maximal perivascular inflammatory response in the areas of infection was found 10 days after infection in contrast to 5 days in virus control mice. No pathologic sequelae were found in either group.

The effect of cyclophosphamide on infection was more evident in newborn mice. Necrosis developed in the subventricular zone 6 days after infection in cyclophosphamide-treated mice, as it did in virus control mice, but this necrosis did not evoke an inflammatory reaction. In cyclophosphamide-treated newborns this necrotic reaction did not spread into the caudate/putamen and cortex as it did in virus control mice. Newborn mice surviving cyclophosphamide treatment longer than 14 days showed occasional focal areas of necrosis in caudate/putamen and cortex as well as the subventricular lesions, but they did not develop the large, necrotic, partially cavitated lesions seen in virus control animals.

In addition, newborn animals treated with cyclophosphamide, whether inoculated with bluetongue virus or not, had small brains and disruption of the granular layer of the cerebellum, showing destruction of immature granular cells as well as migratory arrest.[7] However, effects of cyclophosphamide on the immature cells in the forebrain was not evident histologically. Thus, cyclophosphamide alone resulted in obvious histologic abnormalities limited to the cerebellum, whereas bluetongue virus infection resulted in abnormalities limited to the telencephalon. The combination of cyclophosphamide and virus caused a reduction of the pathologic changes in the telencephalon.

Autoradiographic studies of normal brains 7 days after birth showed labeling of the majority of granular cells of the cerebellum, 20 to 30% of cells in the subventricular zone, and rare cells in caudate/putamen and neocortex. Cyclophosphamide treatment caused almost total inhibition of the thymidine uptake in cerebellar granular cells and marked reduction in uptake in the subventricular zone. The labeled cells in the forebrain were not distributed throughout the zone, as they were in normal mice, but were confined to the area adjacent to the ventricular surface. There was less thymidine incorporation in the subventricular zone, and no evidence of migration of postmitotic cells during the 20-hour period after labeling.

Effect of Antithymocyte Serum

Newborn mice infected with bluetongue virus and treated for 20 days with ATS showed no increased mortality. Virus assays of brains showed that ATS prolonged infection but did not significantly increase maximal virus growth (Text-figure 3). Neutralizing antibody was not detectable in serum at 1:8 dilutions 15 days after inoculation, in contrast to antibody at 1:80 dilutions in virus control mice. Fluorescent antibody staining showed no difference in the sequence of infection in ATS-treated and virus control mice during the first 8 days. Beyond this time virus antigen disappeared in controls but persisted up to 20

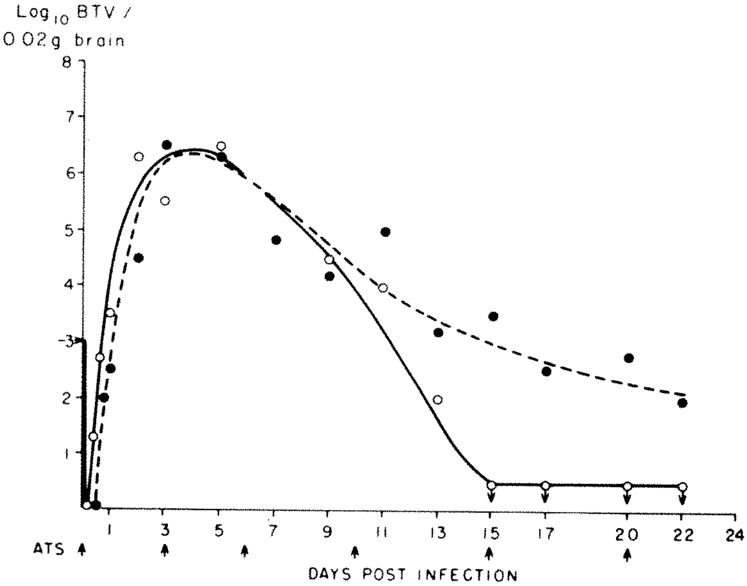

TEXT-FIG 3—Growth of bluetongue virus in brains of normal (*open circles*) and ATS-treated (*closed circles*) mice infected at 1 day of age. Each point represents a pool of 3 brains.

days in ATS-treated mice. The inflammatory reaction, observed between 6 and 20 days in the virus control mice, was completely abolished in the ATS-treated animals. However, the intensity and localization of acute necrosis were unaltered in ATS-treated mice. The resultant symmetrical, partially cavitated lesions seen 30 days after infection were similar in ATS-treated and control mice, although slightly more extensive in the former group.

Mice infected at 5 days of age did not develop the characteristic lesions induced by bluetongue virus in the newborn. Infection of these mice led only to small focal necrotic lesions in the subventricular zone. A study limited to late histologic sequelae of infection of 5-day-old mice showed no difference between lesions in ATS-treated and virus control mice.

Discussion

The effects of cyclophosphamide and ATS on bluetongue virus infections in mice of various ages indicate that the age dependency of the lesions is determined by the availability of susceptible immature cell populations and not by the immunologic immaturity of the young mouse. Suppression of immune responses by either method did not cause mice of a particular age to develop the type of infection and pathologic sequelae seen in more immature animals.

Antithymocyte serum affected the clearance of infection but did not significantly affect the localization of infection or the pathologic sequelae. In contrast, treatment with cyclophosphamide actually inhibited infection and, in newborn mice, reduced the extent of the resulting pathologic lesions. This was apparently due to the antimetabolic effect of cyclophosphamide on the dividing and migrating undifferentiated subventricular cells, which in immature mice were selectively vulnerable to bluetongue vaccine virus infection.

Cyclophosphamide has been widely used recently to evaluate the role of immune responses in acute and chronic viral infections.[8,9] An inhibitory effect of cyclophosphamide on viral replication has not previously been reported. However, had the appropriate parameters not been studied, the sparing effects of this "immunosuppression" on the lesions of bluetongue virus infection in the newborn mouse might have been erroneously interpreted as evidence for an immunopathologic pathogenesis.

References

1. Richards WPC, Cordy DR: Bluetongue virus infection: pathologic responses of nervous systems in sheep and mice. Science 156:530–531, 1967
2. Osburn BI, Johnson RT, Silverstein AM, Prendergast RA, Jochim MM, Levy SE: Experimental viral-induced congenital encephalopathies. II. The pathogenesis of bluetongue vaccine virus in fetal lambs. Lab Invest 25:206–210, 1971
3. Narayan O, Johnson RT: Effects of viral infection on nervous system development. I. Pathogenesis of bluetongue virus infection in mice. Am J Pathol 68:1–14, 1972
4. Gorer PA, O'Gorman PO: The cytotoxic activity of isoantibodies in mice. Transplantation Bull 3:142–143, 1956
5. Hirsch MS, Murphy FA, Hicklin MD: Immunopathology of lymphocytic choriomeningitis virus infection of newborn mice. Antithymocyte serum effects on glomerulonephritis and wasting disease. J Exp Med 127:757–766, 1968
6. Goldschneider I, McGregor DD: Migration of lymphocytes and thymocytes in the rat. I. The route of migration from blood to spleen and lymph nodes. J Exp Med 127:155–168, 1968
7. Nathanson N, Cole GA, van der Loos H: Heterotopic cerebellar granule cells following administration of cyclophosphamide to suckling rats. Brain Res 15:532–536, 1969
8. Nathanson N, Cole GA: Immunosuppression and experimental virus infection of the nervous system. Adv Virus Res 16: 397–448, 1970
9. Idem: Immunosuppression: a means to assess the role of the immune response in acute virus infections. Fed Proc 30:1822–1830, 1971

Acknowledgments

The technical assistance of Susan Levy and Kathleen Kuehl is gratefully acknowledged.

Dr. Narayan is a recipient of a Canadian Medical Research Council Fellowship; Dr. McFarland is the recipient of Special Fellowship NS2286 from the US Public Health Service.

[End of Article]

Histochemical Distribution of Carbonic Anhydrase After Ligation of the Pancreatic Duct

Andrew Churg, PhD and Ward R. Richter, DVM

The distribution of carbonic anhydrase in the exocrine pancreas of the rat has been examined during the first 3 weeks after duct ligation. The normal pattern of positive reaction in ducts, centroacinar cells and capillaries changed, by the end of the first week, to one in which all the cells in the dilated ducts showed the enzyme. This situation persisted through the third week. By electron microscopy, the enzyme was found on the apical membranes of ductular, centroacinar and acinar cells, as well as on the surface membranes of the modified cells seen at 1 week. The significance of these findings with respect to function and cell origin is discussed (Am J Pathol 68:23–30, 1972).

LIGATION OF THE PANCREATIC DUCT produces atrophy of exocrine acinar cells and their replacement by dilated ducts.[1–5] A recent study [5] has shown that these ducts are lined by a cell type intermediate in ultrastructure between normal acinar and ductal cells. Since normal pancreatic ductal cells secrete fluid and contain the enzyme carbonic anhydrase (CA), we have examined the distribution of this enzyme at various intervals after duct ligation in order to obtain some idea of the physiologic state of the tissue and of the origin of its morphologic components.

Materials and Methods

Male Sprague-Dawley rats weighing 100 to 200 g were used in these experiments. The method of ligation has been previously described.[5] Animals were sacrificed at 0 (control), 1, 2, 3, 5, 7 and 21 days after ligation, using pentobarbital anesthesia. Additional controls were sham-operated and sacrificed as above. Small pieces of pancreas were fixed in cold formalin (light microscopy only) or 4% paraformaldehyde for 24 hours, or 2% paraformaldehyde + 2.3% glutaraldehyde for 4 hours. All fixatives contained 0.1 M phosphate or cacodylate buffer. After fixation, tissues were briefly rinsed in cold buffer, quick frozen, cut and incubated in Hansson's medium [6] for the demonstration of carbonic anhydrase. For light microscopy the medium was made up with 5.85×10^{-3}M KH_2PO_4, and incubated for 10 to 20 minutes at 20 C. Sections were cut at 6 μ, floated on saline, incubated, washed, visualized with $(NH_4)_2S$, briefly counterstained with nuclear fast red, dehydrated and mounted in Permount. For electron microscopy, section thickness was 15 μ and incubation was 8 to 15 minutes at 37 C in a medium containing 5.85

From the Department of Pathology and the A. J. Carlson Animal Research Facility, The University of Chicago, Chicago, Ill.

Supported in part by a grant from the Chicago Chapter of the National Cystic Fibrosis Foundation, and by Grant FR-00409-02 from the US Public Health Service. Dr. Churg is supported by a grant from the University of Chicago Pritzker School of Medicine.

Accepted for publication Mar 6, 1972.

Address reprint requests to Dr. Andrew Churg, Department of Pathology, University of Chicago, 950 East 59th Street, Chicago, Ill 60637.

$\times$ 10^{-3}M KH_2PO_4 and 5.3 $\times$ 10^{-3} M H_2SO_4. This medium produces better penetration of the reaction through the tissue.[7] After incubation, sections were washed, visualized, postfixed 5 minutes in collidine-buffered osmium,[8] dehydrated in ethanol and embedded in Epon. Preparations were stained with uranyl acetate and lead citrate.

For inhibitor controls, acetazolamide (Diamox) was added to the incubation medium in a final concentration of 10^{-5}M for light microscopy and 10^{-4}M for electron microscopy, and the tissues were incubated and treated as above.

Results

Light microscopy

Normal and sham-operated control animals showed positive reactions (brown-black precipitate of CoS) in centroacinar cells, all ducts,[6,9] and red blood cells. Occasionally staining of capillary walls and of intercellular junctions in the acinus was observed, the latter when incubation times were long. Figures 1 and 2 show the regularity of the normal staining pattern.

By the third day after ligation this regularity was entirely lost. Heavily staining ducts were prominent. The parenchyma consisted of dilated circular structures in which one or several cells were positive for CA (Figures 3,4). It was not often possible to be sure whether acini or ducts were contributing to this reaction. At the end of 1 week the exocrine gland was made up entirely of dilated ducts, all of which were entirely positive (Figures 5, 6). The pattern was exactly the same after 21 days.

Electron microscopy

A positive reaction, in the form of distinct dots of precipitate, was found along the apical surface and microvilli of normal ductal and centroacinar cells and, also, along the apical surfaces of the modified cells in the dilated ducts (Figure 7). Often the apical acinar surfaces showed a similar but weaker staining. Nuclei were sometimes diffusely stained, and if the incubation time was overextended, a random pattern of deposit was seen in centroacinar and ductal cells. These last findings were probably artifacts of overstaining.

Controls

Red blood cells served as the positive controls. They stained very strongly in light microscopic sections; by electron microscopy the precipitate was localized as a heavy coat on the outside of the membrane. With long incubation the whole cell became electron dense. Acetazolamide, a specific inhibitor of CA, removed all differential staining in light microscopic sections. In the electron microscope the inhibitor abolished staining of ductal, centroacinar and acinar cells, and largely (but not entirely) eliminated the red cell reaction.

Discussion

In our previous paper on the morphology of duct ligation,[5] we concluded that the often held view of ductular dilatation as a result of accumulated protein secretion was probably incorrect, because a) there seemed to be little initial inspissation of secretion and b) the protein-producing acinar cells had largely disappeared by the third or fourth day of the experiment. We speculated at that time that distention was largely due to fluid secretion by the cells lining the dilated ducts, and our finding of strong CA activity (usually seen in H^+ or HCO_3^--rich fluid-secreting cells) [10,11] reinforces this idea. Presumably, distention continues until an equilibrium is reached between fluid secretion and filtration back through the duct wall. This process requires about one week; thereafter the duct size is constant.

The localization of CA to the apical cellular membrane is consistent with the few other studies on the fine structure distribution of the enzyme that have been published. Cross found CA along the membranes of intracellular canaliculi in gastric parietal cells,[7] and Yokota demonstrated it on the membranes surrounding bile canaliculi.[12] It seems that the ionic component of the secretion of all these cell types is produced right at the cell surface and immediately exported, rather than being created deep within the cell and transported to the surface in the manner of zymogen granules.

Our previous study also led us to conclude that good morphologic evidence was available for an acinar and/or ductular origin of the cells in the dilated ducts. Since CA is normally found in the ductular system, it would be easy to decide that these are the cells of origin; some support for this hypothesis is derived from the work of Wang *et al*,[13] who ligated rabbit pancreatic ducts and found that the dilated end structures were positive for alkaline phosphatase, an enzyme normally found in rabbit and dog pancreatic ducts.[13,14] However, as is true of CA, at the ultrastructural level alkaline phosphatase is distributed along the apical membranes of both centroacinar and acinar cells, although the latter reaction is weaker.[15] Certainly the ability of pancreatic acinar cells to manufacture even small amounts of CA and alkaline phosphatase implies that with a changed morphology and function the amount of enzyme produced could also be changed and that the cells in the dilated ducts might be of acinar origin. In this regard it is interesting to compare the somewhat analogous case of salivary gland duct ligation, a procedure which produces atrophy, but not loss, of acinar cells, and an end stage tissue with "resting" acini and nondilated ducts.[16] Tamarin [17,18] has recently shown that the ultrastructure of these ligated acinar cells changes from a clearly protein(actually sialoprotein)-secreting type to one which rather remarkably resembles the dilated duct cells in the pancreas; removing the ligature permits these same cells to return to the protein-producing form. It is conceivable that a similar process is occurring in the pancreas, and that the remaining "resting" cells could return to the acinar type under favorable conditions.

References

1. Bensley RR: Structure and relationships of the islets of Langerhans. Harvey Lect 10:250–289, 1914–1915
2. Opie EL: Cytology of the pancreas. Special Cytology, Vol I. Edited by EV Cowdry. New York, Paul Hoeber, Inc, 1928, pp 241–271
3. Boquist L, Edstrom C: Ultrastructure of pancreatic acinar and islet parenchyma in rat at various intervals after duct ligation. Virchows Arch [Pathol Anat] 349:69–79, 1970
4. Zelander T, Ekholm R, Edlund Y: The ultrastructure of rat exocrine pancreas after experimentally occluded outflow. J Ultrastruct Res 10:89–102, 1964
5. Churg A, Richter WR: Early changes in the exocrine pancreas of the dog and rat after ligation of the pancreatic duct: a light and electron microscopic study. Am J Pathol 63:521–546, 1970
6. Hansson HPJ: Histochemical demonstration of carbonic anhydrase activity. Histochemie 11:112–128, 1967
7. Cross SAM: Ultrastructural localization of carbonic anhydrase in rat stomach parietal cells. Histochemie 22:219–225, 1970
8. Bennett HS, Luft JH: s-Collidine as a basis for buffering fixatives. J. Biophys Biochem Cytol 6:113–114, 1959
9. Becker V: Histochemistry of the exocrine pancreas. The Exocrine Pancreas. Edited by AVS de Reuck. Boston, Little, Brown and Company, 1961, pp 56–64
10. Maren TH: Carbonic anhydrase: chemistry, physiology, and inhibitors. Physiol Rev 47:595–781, 1967
11. Maren TH: Carbonic anhydrase in the animal kingdom. Fed Proc 26: 1097–1103, 1967
12. Yokota S: Electron microscopic demonstration of carbonic anhydrase activity in mouse liver cells. Histochemie 19:255–261, 1969
13. Wang CC, Wang KJ, Grossman MI: Effects of ligation of the pancreatic duct upon the activity of secretin and pancreozymin in rabbits with a correlated histochemical study. Am J Physiol 160:116–121, 1950
14. Jacoby F: The pancreas and alkaline phosphatase. Nature 158:268, 1946
15. Churg A, Richter WR: Unpublished observation. We used the method of Mayahara H, Hirano H, Saito T, Ogawa K: The new lead citrate method for the demonstration of activity of non-specific alkaline phosphatase (orthophosphoric monoester phosphohydrolase). Histochemie 11:88–96, 1967
16. Junqueira LCU: Cytological, cytochemical and biochemical observations on secreting and resting salivary glands. Exp Cell Res 2:327–338, 1951
17. Tamarin A: Submaxillary gland recovery from obstruction. I. Overall changes and electron microscopic alteration of granular duct cells. J Ultrastruct Res 34:276–287, 1971
18. *Idem:* Submaxillary gland recovery from obstruction. II. Electron microscopic alteration of acinar cells. J Ultrastruct Res 34:288–302, 1971

[*Illustrations follow*]

Legends for Figures

Figures 1–6 are 6-μ frozen sections incubated for CA and counterstained with nuclear fast red.

Fig 1—Normal pancreas. Note the heavy staining of epithelium in ducts *(D)* and red blood cells *(R)*. The small black dots are single red blood cells in capillaries (× 160).

Fig 2—Normal pancreas. At high power the staining of red blood cells in capillaries and of centroacinar cells *(arrow)* is clearly seen. Note regularity of the staining pattern (× 500).

Fig 3—Pancreas, 3 days ligation. The normal reaction pattern is greatly modified. Some of the heavily staining structures are ducts, but dilated acini also show half positive circles (× 240).

Fig 4—Pancreas, 3 days ligation. Notice the staining of individual cells in the dilated structures *(arrows)* (× 500).

1

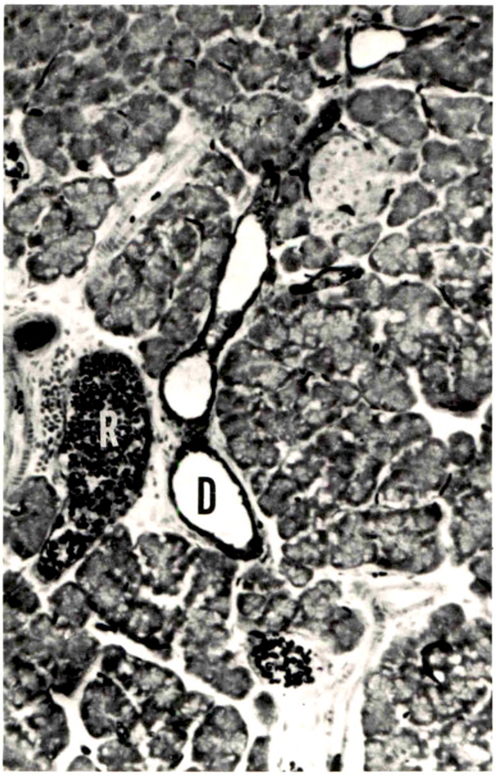

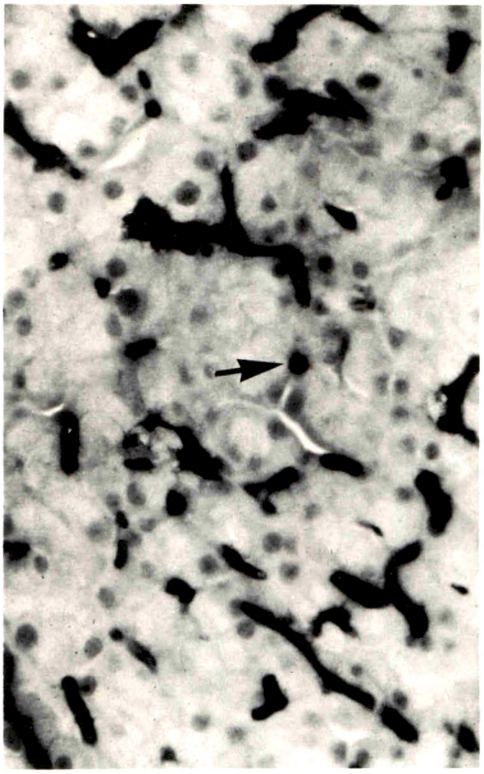

2

3

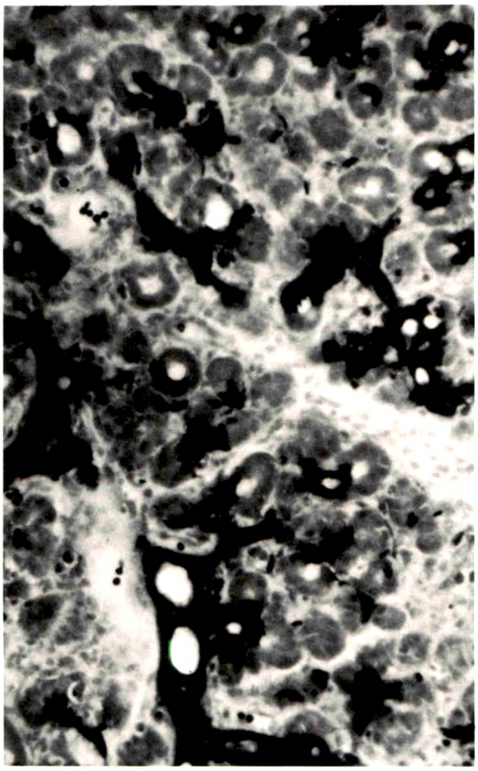

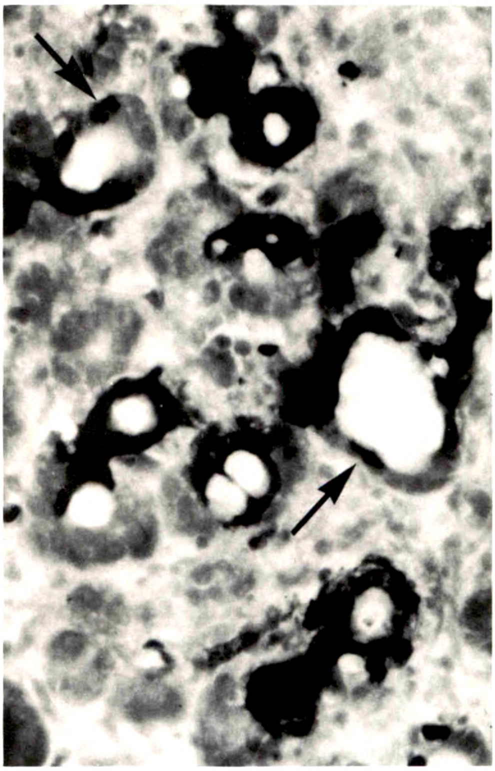

4

5

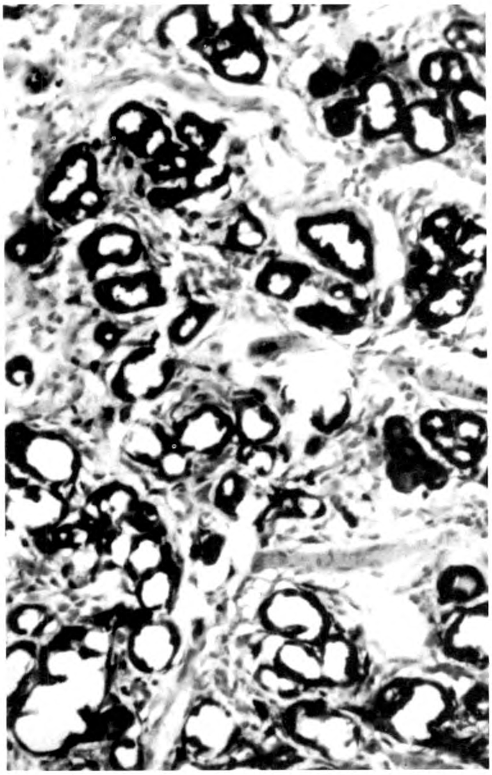

6

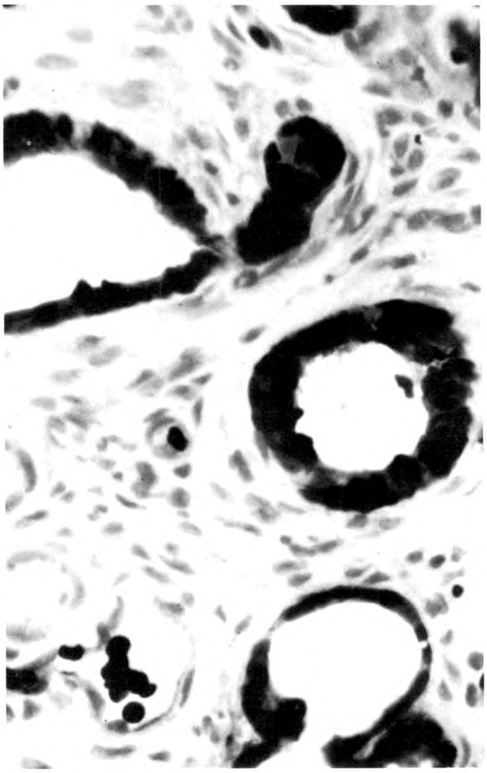

7

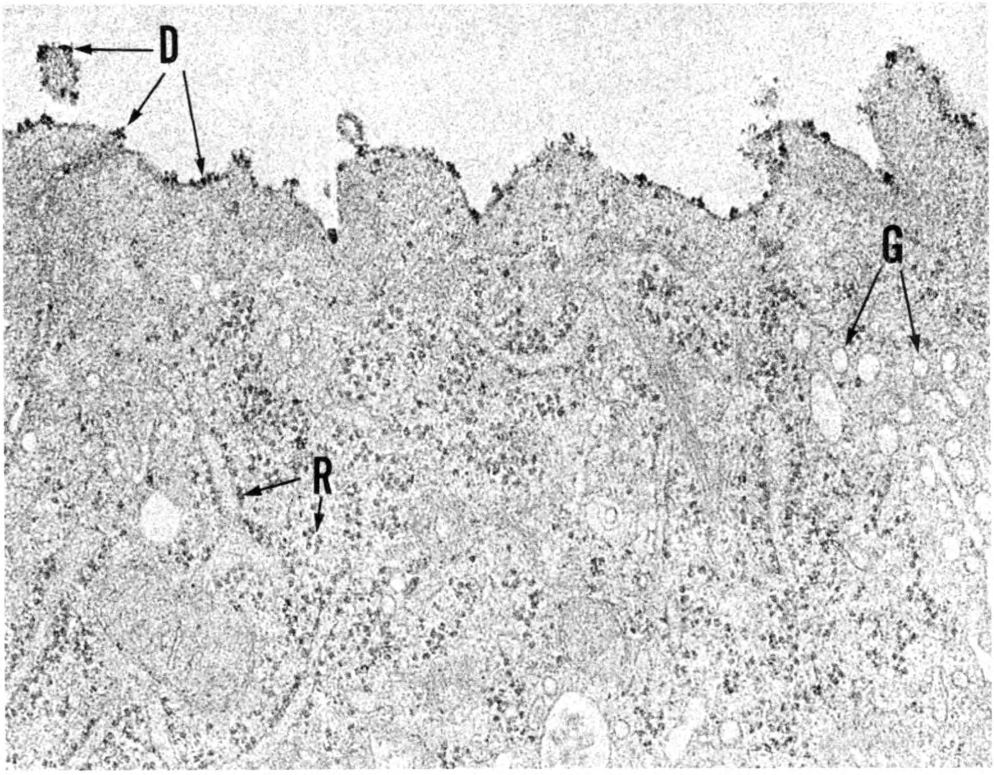

Fig 5—Pancreas, 7 days ligation. All the dilated ducts are positive for CA (× 260). **Fig 6**—Pancreas, 7 days ligation. A high-power view of the cell lining the dilated ducts. A small blood vessel contains individually staining red blood cells (× 650). **Fig 7**—Pancreas, 5 days ligation. Electron micrograph of the apical portion of two cells lining a dilated duct. The positive reaction is clearly seen as dense dots of precipitate (*D*) along the apical membrane and microvilli. The dots are of a greater density and generally larger size than the ribosomes (*R*), both free and along the RER in the cytoplasm. Golgi vacuoles are also visible (*G*). Frozen section, stained lightly with uranyl acetate and lead citrate (× 40,000).

Tissue Localization of Australia Antigen Immune Complexes in Acute and Chronic Hepatitis and Liver Cirrhosis

Adam Nowosławski, MD, Krzysztof Krawczyński, MD, Witold J. Brzosko, MD and Kazimierz Madaliński, MD

In a significant percentage of examined cases of fulminant hepatitis, subacute hepatitis, chronic aggressive hepatitis, liver cirrhosis and chronic persistent hepatitis, Australia (hepatitis-associated) antigen (Au/HAA) was identified in the liver and in extrahepatic locations. The several immunofluorescent patterns of Au/HAA localization in hepatocytes strongly suggested various stages of Au/HAA accumulation and release. Deposits of a mixture of immunoglobulins G and M and occasionally β1C-globulin were found in the cytoplasm of Au/HAA containing hepatocytes, on their plasma membranes, on or in the nuclei, in the cytoplasm of Kupffer cells and, rarely, in the sinusoids. The accompanying tissue changes were hepatocellular degeneration and necrosis. These intra- and extracellular complexes of Au/HAA and immunoglobulins displayed strong affinity for guinea pig complement in the immunohistochemical complement fixation reaction. When tested by immunodiffusion in agar, IgG dissociated from these complexes by potassium thiocyanate (KSCN) treatment showed anti-Au/HAA specificity. In fulminant hepatitis neither Au/HAA nor immunoglobulins and complement were found in the liver. In chronic aggressive hepatitis and subacute hepatitis the amount of the Au/HAA immune complexes identified in the liver was approximately inversely proportional to the extent and severity of the parenchymal lesions. In liver cirrhosis and chronic persistent hepatitis there was a positive correlation between the amount of the Au/HAA immune complexes found in the liver and the degree of hepatocellular damage. The deposits of Au/HAA, identified in extrahepatic locations including germinal centers of lymph nodes and spleen, kidney glomeruli and blood vessel walls, were as a rule accompanied by deposits of IgG, IgM, β1C-globulin and fibrin. All these deposits showed strong affinity for guinea pig complement in the immunohistochemical reaction of complement fixation. Germinal center activation, chronic membraneous glomerulonephritis, panarteritis and simple arteriolar hyalinosis were found at sites of localization of these deposits (Am J Pathol 68:31–56, 1972).

AUSTRALIA (HEPATITIS-ASSOCIATED) ANTIGEN (Au/HAA) has been found by various serologic methods in a significant percentage of patients with lymphoproliferative disorders and with a much higher frequency in patients with acute hepatitis, various forms of chronic

---

From the Department of Immunopathology and Laboratory of Electron Microscopy, State Institute of Hygiene, Warsaw, Poland.

Supported in part by Grant 0-5332-2 from the Center for Disease Control, Atlanta, Ga.

Presented in part at the First International Congress of Immunology, Washington, DC, August 1–6, 1971.

Accepted for publication Mar 1, 1972.

Address reprint requests to Dr. Adam Nowosławski, Department of Immunopathology, State Institute of Hygiene, Warsaw, Chocimska 24, Poland.

hepatitis and liver cirrhosis.[1-8] The most commonly encountered ultrastructural form of serum Au/HAA is a spherical particle measuring 180–210 Å in diameter, composed of several knob-like subunits.[9,10] This particle was shown to contain protein and lipids;[11-12] recently a small amount of RNA was detected in purified preparations of Au/HAA.[13] Au/HAA has been localized by immunofluorescence [14-17] and electron microscopy [16-19] in hepatocytes of patients with various forms of hepatitis and patients with lymphoproliferative disorders and protracted antigenemia.

The etiologic role of Au/HAA in hepatitis has not been proved and its exact pathogenic significance remains unknown. In the sera of a great majority of patients with hepatitis, Au/HAA occurs in the form of immune complexes.[4,20-22] It has been shown by electron microscopy that, depending on the amount of antibody, the appearance of these complexes varies in different forms of hepatitis, thus probably reflecting differences in the host immune response.[20] That the Au/HAA immune complexes in the serum of hepatitis patients may have phlogogenic properties has been deduced from experiments in animals.[23]

On the basis of these data it has been hypothesized that humoral response developed against Au/HAA plays a role in the pathogenesis of the liver lesions in acute and chronic hepatitis. The present study was undertaken to obtain evidence in support of this hypothesis. It was specifically aimed at the identification at the tissue level of Au/HAA immune complexes. Their presence, when established, was to be correlated with the type, severity and extent of the accompanying tissue changes.

Materials and Methods

Tissues

Tissue specimens were obtained at autopsy, within 6 to 14 hours after death, from 29 patients who died in the course of fulminant hepatitis (4 cases), subacute hepatitits (5 cases), chronic aggressive hepatitis (7 cases), postnecrotic liver cirrhosis (11 cases) and chronic persistent hepatitis (2 cases). All these cases were diagnosed on the basis of a morphologic examination supplemented by clinical and laboratory data. In cases of fulminant hepatitis microscopic examination revealed diffuse parenchymal necrosis and inflammatory infiltrations, mostly lymphocytic and plasmocytic. The basis for inclusion into the group of subacute hepatitis cases was focal parenchymal necrosis, disarrangement of lobular architecture, stromal collapse, intralobular bridging and postnecrotic scarring, bile ductular proliferation and stromal mononuclear infiltrations. The group of chronic aggressive hepatitis patients included cases showing features of widespread piecemeal necrosis, occasional patchy parenchymal necroses and progression to cirrhosis. Dense mononuclear infiltrations were encountered in the periportal stroma and also in the midzonal areas. In liver cirrhosis cases, chronic hepatitis was manifested by occasional foci of piecemeal necrosis and central necrosis and diffuse mononuclear infiltrations in the connective tissue septa. Persistent hepatitis was diagnosed on the basis of the presence of dense mononuclear infiltrations in the expanded portal areas, slight periportal fibrosis, occasional foci of piecemeal necrosis and midzonal or central hepatocellular degeneration and Kupffer cell hyperplasia.

In each case 6 specimens were taken from liver, 4 specimens from spleen and kidney and 2 specimens from myocardium (left ventricle with mitral valve). Portal and mediastinal lymph nodes were also taken in each case. Each specimen, a cube measuring approximately 10 mm on each side, was divided into two equal parts: one was rapidly frozen in petroleum ether precooled to about −80 C in a mixture of acetone and solid CO_2; the other was fixed in neutral buffered formalin, pH 7.2. The formalin-fixed tissue blocks were routinely processed and embedded in paraffin. The paraffin sections were stained with hematoxylin and eosin and periodic acid–Schiff methods.

Immunohistochemical Studies

Labeled Reagents

The following reagents were used for the detection of Au/HAA: a) Fluorescein isothiocyanate (FITC)-labeled immunoglobulin G, obtained from human serum containing antibodies against Au/HAA. The preparation and characterization of this reagent was described elsewhere.[16] b) FITC-labeled serum globulin of guinea pigs immunized with Au/HAA. The antigen used for immunization was prepared from sera of patients with Au/HAA antigenemia by a method previously described.[13] The immunization procedure followed the method employed by Henney and Ishizaka[24] for preparation of immunoglobulin-class-specific antisera in guinea pigs rendered tolerant to immunoglobulin-type-specific antigens. The guinea pigs used were injected intracardially with 0.15 ml of euglobulin fraction of human serum and simultaneously given 2 intramuscular injections of 0.25 ml of partially purified preparation of Au/HAA (3.6 mg protein/ml) emulsified with an equal volume of Freund's adjuvant. All animals were bled after 6 weeks. When tested by immunodiffusion in agar gel (IDA) against Au/HAA positive human sera, each guinea pig serum formed a single precipitin line identical with the line formed by human serum containing antibody against Au/HAA. The pool of guinea pig antisera was precipitated with half its volume of saturated ammonium sulphate solution and the crude globulin fraction was labeled with FITC according to the methods of procedure described elsewhere.[25] The labeled reagent was used at a protein concentration of 0.48 mg/ml after absorption with 50 mg/ml of acetone-dried mouse liver powder.

The immunohistochemical reagents used for the detection of plasma proteins were globulin fractions of goat or rabbit monospecific antisera against human IgG, IgM, IgA, IgD, β1C-globulin, fibrin, albumin, α2-macroglobulin, and guinea pig β1C-globulin labeled with FITC or lissamine rhodamine B (LRB). The preparation and characterization of these reagents was described elsewhere.[25-27]

Methods of Staining, Microscopy and Photography

Frozen sections cut at 4 μ in a cryostat at −18 C were air-dried and fixed in anesthetic ether for 3 minutes at room temperature. The sections were stained directly, either with a single reagent or a mixture of two reagents labeled in contrasting colors. The specificity of staining was ascertained by inhibition of fluorescence in serial sections first treated with unlabeled reagents, and in sections incubated with reagents absorbed with homologous antigens. The results of staining were evaluated in a Zetopan (Reichert) microscope equipped with HBO 200 light source and a dark-ground condenser. Microphotographs were taken on a Scopix G (Agfa-Gevaert) black and white 35-mm film.

Immunofluorescent Complement Fixation

The indirect procedure of heterologous (guinea pig) complement fixation was employed according to the method of Burkholder.[28] Frozen tissue sections were incubated with fresh guinea pig serum diluted 1:15 and subsequently stained with FITC-labeled anti-guinea pig β1C-globulin reagent. Control procedures consisted of directly staining the serial sections with anti-guinea pig β1C-globulin reagent and using heat-inactivated (56 C for 60 minutes) guinea pig serum as an intermediate layer.

Elution Procedures

These were performed on frozen sections of liver tissue from 2 cases of chronic aggressive hepatitis and consisted of 2 consecutive parts. First, the sections were mounted on slides and washed without preliminary fixation in phosphate-buffered 0.15 M NaCI, pH 7.6 (PBS) for 5, 10, 20 and 60 minutes at room temperature to remove unbound proteins. Serial sections from the same tissue blocks were similarly washed in 2.5 M KSCN.[29] All sections were then fixed in acetone and stained for the presence of immunoglobulins G and M, and Au/HAA. The amounts of these components in and/or on hepatocytes and sinusoid walls remained unchanged after 5 and 10 minutes and were only slightly diminished after 20 and 60 minutes washing in PBS. Both the 20 and 60 minute washing in PBS resulted in almost complete removal of immunoglobulins from the peri- and intralobular connective tissue and blood vessel walls. Serial sections from the same tissue blocks eluted for 20 minutes with 2.5 M potassium thiocyanate (KSCN) revealed a significant decrease of the amount of immunoglobulins and Au/HAA whereas only trace amounts of these components could be visualized after 60-minute elution. In the second part of the elution procedures, 10-μ liver sections were cut in a cryostat. The total amount of 0.35 g of liver tissue (wet weight) was thawed, homogenized with a glass rod and stirred for 20 minutes in 20-fold excess of PBS. The homogenized and PBS-washed tissue was centrifuged for 10 minutes at 3000 rpm. The sediment suspended in 20-fold excess of 2.5 M KSCN was eluted for 60 minutes at room temperature with constant agitation. The KSCN eluate was centrifuged at 80000 × *g* for 2 hours in a Spinco model L centrifuge (rotor 40.3). The pellet was resuspended in a few drops of distilled water and examined by electron microscopy for the presence of Au/HAA particles according to the method given by Almeida and Waterson.[20] The supernatant was dialysed against PBS for 40 hours, then concentrated sixfold by dialysis against 25% polyvinylpyrrolidone in PBS. The PBS and KSCN eluates were examined for protein content by the method of Lowry *et al*[30] and for the plasma proteins and individual immunoglobulins by immunoelectrophoresis[31] and immunodiffusion in agar (IDA). The eluates were also tested for the presence of Au/HAA and anti-Au/HAA antibodies by IDA and immunoelectroosmophoresis (IEOP).[32] The reactants employed in these tests were human sera containing either Au/HAA or anti-Au/HAA antibodies.

Electron Microscopy

Liver tissue was examined in 11 cases in which it could be obtained within 12 hours after death. The cases included subacute hepatitis (1 case), chronic aggresive hepatitis (5 cases), liver cirrhosis (4 cases) and chronic persistent hepatitis (1 case). Fragments of formalin-fixed or quick-frozen kidney cortex and spleen tissue were examined in cases in which abundant deposits of Au/HAA were disclosed by immunofluorescence in all glomeruli and in the intima of many blood vessels. Tissue fragments were fixed in 4% glutaraldehyde, postfixed in osmium tetroxide, dehydrated in graded alcohols and embedded in Epon. Ultrathin sections were cut on a Porter-Blum ultramicrotome, stained with lead citrate and uranyl acetate and examined in a JEM 6c electron microscope.

Results

Immunohistochemistry, Histopathology and Electron Microscopy

Immunohistochemistry disclosed the presence of Au/HAA in hepatic and/or extrahepatic locations in 17 of 29 examined cases (Table 1). In 8 of these 17 cases Au/HAA was found in extrahepatic locations. The data concerning the hepatic vs extrahepatic localization of Au/HAA in these 8 cases are given in Table 2.

Liver

The cells containing Au/HAA were most numerous in cases of chronic aggressive hepatitis, decidedly less numerous in subacute hepatitis and liver cirrhosis and the least numerous in chronic persistent hepatitis. In fulminant hepatitis Au/HAA was not found in the liver. In subacute hepatitis differing amounts of Au/HAA were encountered in hepatocytes in some of the foci of profound parenchymal damage (Figure 1). In chronic aggressive hepatitis and liver cirrhosis Au/HAA was localized mainly in cells at the periphery of the lobules and/or

Table 1—Hepatic vs Extrahepatic Localization of Au/HAA in Various Forms of Hepatitis and Liver Cirrhosis

Liver pathology (histopathological diagnosis)	No. of cases		
	Positive/ tested	With hepatic localization/ positive	With extrahepatic localization/ positive
Fulminant hepatitis	1/4	0/1	1/1
Subacute hepatitis	3/5	3/3	1/3
Chronic aggressive hepatitis	6/7	6/6	3/6
Liver cirrhosis	5/11	5/5	2/5
Chronic persistent hepatitis	2/2	2/2	1/2
Total	17/29	16/17	8/17

nodules (Figures 2, 3). In liver cirrhosis, however, nodules were encountered with nearly all the hepatocytes displaying cytoplasmic fluorescence of Au/HAA of approximately the same intensity. A distinctly focal distribution of cells containing Au/HAA was observed in all cases. In areas showing normal hepatic structure the amounts and distribution of the intracellular antigenic material were rather uniform. Varying amounts of Au/HAA were identified, both in apparently normal hepatocytes and in those undergoing degenerative changes in areas of distortion of lobular architecture (Figures 4–6). In rare instances, single hepatocytes containing trace amounts of Au/HAA could be disclosed in foci of parenchymal necrosis. Deposits of Au/HAA were also identified in occasional cells whose littoral position suggested that they were endothelial or Kupffer cells (Figure 6).

The following characteristic patterns of Au/HAA fluorescence were encountered in hepatocytes: linear fluorescence of shrunken nuclear membrane, homogenous fluorescence of enlarged nuclei and diffuse homogenous or granular cytoplasmic fluorescence (Figures 1–6). In chronic aggressive hepatitis and subacute hepatitis two other types of Au/HAA localization in hepatocytes were observed. One was characterized by a delicate honeycombed pattern of low intensity fluorescence tracing the outlines of individual hepatocytes in circumscribed foci. This pattern apparently resulted from the presence of granular and homogenous linear deposits of Au/HAA in and/or on the hepatocyte plasma membrane and, possibly, in its closest vicinity (Figure 7). The other type presented an intricate pattern of much higher intensity peripheral fluorescence of hepatic plates in limited areas of one or a few neighboring lobules. Continuous band-like and crescent-shaped masses of Au/HAA located at the periphery of several adjacent hepatocytes were encrouching upon the distended sinusoidal spaces (Figure 8). Patterns intermediate between these localization types were also encountered (Figure 9). In spite of rather poor preservation of cellular ultrastructure, Au/HAA particles were quite easily recognized by electron microscopy in the nuclei of hepatocytes in all the cases examined (Figure 10).

In chronic aggressive hepatitis and subacute hepatitis immunoglobulins G and M were found in the cytoplasm of several hepatocytes, and rarely on or in the nuclei, on plasma membranes, in and on the sinusoid walls, in their lumen and in the stromal connective tissue (Figures 11–13). Occasionally, trace amounts of β1C-globulin were found in the same locations (Figures 14, 15). In liver cirrhosis and chronic persistent hepatitis immunoglobulins were less frequently found in hepatocytes. They were, however, identified in endothelial or Kupffer cells and in the perinodular or perilobular connective tissue. In all cases examined, a delicate film of fibrin deposits was found in the sinusoids and on the intima of blood vessels except for areas of evident hepatocellular damage. No tissue-bound plasma protein deposits were found in the liver parenchyma in fulminant hepatitis.

Staining of serial sections with different reagents labeled in contrasting colors was employed to compare the approximate amounts and distribution of Au/HAA (FITC-labeled reagents), immunoglobulins and β1C-globulin (LRB-labeled reagents). Any or all of these components were seen either separately or as a more or less homogenous mixture in several locative, quantitative and qualitative combinations. In areas showing normal hepatic structure, pure apple green fluorescence of Au/HAA was observed both in intranuclear and intracytoplasmic locations. In areas of apparent hepatocellular damage, an orange-yellow fluorescence was seen indicative for the presence in several hepatocytes of a fairly homogenous mixture of Au/HAA and immunoglobulins G or M and occasionally β1C-globulin. A similar hue of fluorescence was observed in most of the pericytoplasmic and rare sinusoidal deposits and in the cytoplasm of endothelial or Kupffer cells. Trace amounts of a mixture of Au/HAA and immunoglobulins were rarely found in hepatocytes in the foci of evident parenchymal necrosis. In some of these foci, only immunoglobulins (predominantly IgM) were found in hepatocytes and amorphous masses in the sinusoids. Neither albumin nor α2-macroglobulin were identified in the material examined.

The majority of plasma cells in the inflammatory infiltrations of subacute and chronic aggressive hepatitis contained IgG. Cells containing IgM, IgA, and IgD were distinctly less numerous. In the cases of fulminant hepatitis the number of IgA containing plasma cells was higher than of those containing IgG and IgM.

Immunofluorescent Complement Fixation

There was complete overlap of the guinea pig complement fixation fluorescence pattern with that of localization of immunoglobulins G and M and Au/HAA in serial sections (Figure 16). There was no fluorescence in sections incubated in control heat-inactivated guinea pig serum or in sections stained directly with fluorescent anti-guinea pig β1C-globulin reagent.

Elution Procedures

From 0.35 and 0.25 g (wet weight) of homogenized liver tissue, 36.9 and 21.55 mg protein, respectively, was obtained by PBS elution. The immunoelectrophoretic examination of these eluates showed the presence of albumin and trace amounts of β- and γ-globulins. No anti-Au/HAA activity was found in the eluates either by IDA or IEOP; they were, however, positive for Au/HAA by the latter technic. The total protein content of the eluates obtained after treatment with 2.5 M KSCN, which followed initial PBS elution, amounted to 1.76 mg and 1.12 mg, respectively. In these eluates, shown by IDA to contain IgG only, the presence of anti-Au/HAA antibodies was disclosed by both IDA and IEOP (Figure 17). They were negative for Au/HAA when tested by the same methods. In the suspension prepared of pellets after ultracentrifugation of the eluates, several large clumps of Au/HAA particles were revealed by electron microscopy.

Spleen and Lymph Nodes

Au/HAA was found mainly in germinal centers of lymphoid follicles. The amount of antigenic material varied in different germinal centers from barely discernible granular deposits to large lumpy masses localized between reticular cells, on their plasma membranes and probably in their cytoplasm (Figure 18A).

On rare occasions granular deposits of Au/HAA were disclosed in macrophages on the periphery of lymphoid nodules. In serial sections from the same tissue blocks the distribution pattern of immunoglobulins IgG and IgM followed closely that of the Au/HAA deposits (Figure 18B). Small amounts of β1C-globulin were also disclosed in all the germinal centers containing Au/HAA and immunoglobulins. Eosinophilic, weakly PAS-positive masses located between reticu-

Table 2—Tissue Localization of Au/HAA, IgG, IgM and β1C-Globulin Deposits in Various Forms of Hepatitis and Liver Cirrhosis

	Au/HAA, IgG, IgM and β1C-globulin				
Liver pathology (histopathological diagnosis)	Liver	Spleen	Lymph nodes	Kidney	Blood vessels
Fulminant hepatitis	—	+	+	+*	+
Subacute hepatitis	+*	+	+	—	+
Chronic aggressive hepatitis	+	+	+	+*	+
Chronic aggressive hepatitis	+*	+	+	+*	+*
Chronic aggressive hepatitis	+*	—	—	+	+
Liver cirrhosis	+	+	—	—	—
Liver cirrhosis	+*	+	—	—	—
Chronic persistent hepatitis	+*	—	—	—	+

* Au/HAA particles identified by electron microscopy

lum cells of the activated germinal centers were seen in paraffin sections from corresponding duplicate blocks of spleen and lymph nodes.

Kidneys

Granular and lumpy deposits of Au/HAA were localized along the glomerular basement membrane in an irregular and discontinuous pattern (Figure 19). Immunoglobulins G (Figure 20) and M, and β1C-globulin (Figure 21) deposits were revealed in the same locations along with small amounts of fibrin. Immunoglobulin G was also occasionally found in the mesangia. Electron microscopic examination revealed dense aggregations of Au/HAA particles on the outer aspect of the glomerular basement membrane. They were apparently contained in the cytoplasm of epithelial cells (Figures 22, 23A). Smaller aggregations were found in deeper aspects of the basement membrane (Figure 23B). There was a striking symmetry in the incrustation pattern with Au/HAA particles of the basement membrane and the cytoplasm in that each particle was surrounded by a zone of low electron density (Figures 22, 23). In paraffin sections all these glomeruli showed mild diffuse thickening of the capillary basement membrane, slight focal increase in the mesangial and endothelial cellularity, and occasional intercapillary adhesions. Chronic membraneous glomerulonephritis was diagnosed in all these cases.

Blood vessels

Au/HAA deposits were found both in large arteries (aa arcuatae in kidneys, aa folliculares in the spleen) and in small arteries (interlobular arteries in kidneys, aa penicillares in the spleen, intramuscular branches of coronary arteries). In larger arteries, granular and lumpy deposits of Au/HAA were localized, chiefly subendothelially, in the hyperplastic intima (Figures 24–26). In small arteries homogenous Au/HAA deposits were localized diffusely throughout the intima which significantly narrowed or nearly occluded the lumen (Figures 28, 29A). In ultrathin sections, small aggregations of Au/HAA particles were found by electron microscopy in the amorphous masses of the hyalinized intima (Figure 29C). As a rule, Au/HAA deposits in blood vessel walls were accompanied by abundant deposits of immunoglobulins G and M, β1C-globulin, and fibrin. All displayed the same distribution pattern (Figures 27A, 27B, 29B). In routinely stained sections, two types of vascular lesions were associated with these deposits. One was a lesion complex comparable with that of panarteritis in the healing stage. The lesions included marked intimal proliferation with diffuse or circumscribed fibrinoid change, focal loss of elastic laminae, and mononuclear (mostly perivascular) inflammatory infiltrations. These infiltrations contained numerous plasma cells, both mature and immature, producing IgG, IgM and rarely IgA. The other was a typical hyaline lesion of the intima defined by the presence of homogenous eosinophilic and PAS positive masses.

In all the extrahepatic locations of Au/HAA a homogenous mixture of IgG, IgM, β1C-globulin and fibrin was found by the double staining procedure. In no instances were albumin and α2-macroglobulin disclosed in these locations.

All the extrahepatic deposits of Au/HAA and immunoglobulins were brilliantly stained in the immunofluorescent complement fixation reaction. The most intensive fluorescence was observed in the affected glomeruli, the least in hyaline vascular changes.

Discussion

The present findings provide considerable evidence for the presence of lesion-associated deposits of Au/HAA immune complexes both in the liver and extrahepatically in various forms of acute and chronic hepatitis. A wide spectrum of nuclear, intra- and pericytoplasmic localization patterns of Au/HAA in hepatocytes most probably reflects various stages of its intracellular development and liberation. The exact pathogenic significance of both these processes, however, remains unknown. The demonstration of immunoglobulin deposits bound to Au/HAA on or in the hepatocyte cytoplasm membrane, in the cytoplasm and in or on the nuclear membrane strongly suggests immune complex formation at the sites of antigen accumulation and/or release. This is supported by the results of elution procedures indicating that these intra- and extracellular immunoglobulin deposits represent, in part at least, the antibody component of Au/HAA immune complexes. That these complexes may bind complement could be inferred from their strong avidity for heterologous (guinea pig) complement and the occasional presence of homologous complement (β1C-globulin) in the same locations.[33] In the foci of profound hepatocellular damage immunoglobulins G and M were also found in hepatocytes in which Au/HAA could not be visualized. This fact could tentatively be explained by the formation of intracellular Au/HAA immune complexes in an antibody excess which made identification of antigen impossible[34] or by passive imbibition of the damaged hepatocytes by immunoglobulins.[35]

As evidence for a continuing presence of an etiologic agent was lacking, local autoimmune phenomena were proposed as the main pathogenic factor in chronic hepatitis and liver cirrhosis.[36] The present data offer strong presumptive evidence that the perpetuation mechanism of chronic hepatitis is primarily related to the continued intracellular accumulation and release of Au/HAA and subsequent immune complex formation. Following fixation of complement components by these complexes, hepatocyte damage may ensue by direct[37] or indirect immunologic insult, the latter resulting from chemotaxis and subsequent leukocyte lysosomal injury.[38] It is presumed that focal reactions of this nature may account for the development of the degenerative and inflammatory lesions in various forms of hepatitis and liver cirrhosis. The severity and extent of these lesions would then depend on several factors, such as the amount of Au/HAA and its homologous antibody present locally, their quantitative relation and ability to bind complement, the availability of complement components, the site of reaction and the ability of Kupffer cells to phagocytize immune complexes.[39,40] That the locally formed or circulating Au/HAA immune complexes may be phagocytized in the liver is apparent from their localization in Kupffer cells.

Experimental studies on allergic hepatitis (Arthus type) have shown that hepatic necrosis may develop rapidly after administration, via different routes, of either antigen in presensitized animals or preformed immune complexes.[39,44] In experimental Auer-type hepatitis accumulation of immune complexes in hepatocytes greatly magnified the preexisting mild liver injury.[40] In both types of this experimental, assumedly immunologic, liver damage, components of the immune complexes could be visualized in the areas of hepatic lesions for a very short period of time and in a limited number of animals.[43,44] These results were explained by the rapid degradation of immune complexes in the necrotic areas. The same explanation may be attributed to the trace amount of Au/HAA immune complexes found in the foci of profound hepatocellular damage in subacute hepatitis and the negative findings in fulminant hepatitis. In both instances, however, heavy deposits of Au/HAA, immunoglobulins and complement were found in extrahepatic locations. This implies that here the diffuse destruction of liver parenchyma may have occurred subsequent to the local formation of Au/HAA immune complexes and/or their deposition from circulation. This assumption would be supported by the recorded observations in fulminant hepatitis cases of immunoglobulin and complement deposits in the central veins.[45] The present findings, while allowing for emphasis on the pathogenic role of humoral immune phenomena, do not exclude the concomitant role of cell-mediated immune response. The latter, whether involving Au/HAA or autoimmune in origin [36] or both, may conceivably contribute to the development and/or perpetuation of at least some tissue lesions in chronic hepatitis.

Au/HAA localization in cells of organs other than liver (spleen, testis, lymph node, bone marrow) has been reported.[15] In the present study deposits compatible in composition with Au/HAA immune complexes and showing strong affinity for guinea pig complement were identified in germinal centers of lymph nodes and spleen, kidney glomeruli and the intima of blood vessels. Activation of germinal centers, chronic membraneous glomerulonephritis, panarteritis in the healing stage and simple arteriolar hyalinosis were found at these sites by histopathologic examination.

A mixture of immunoglobulins and β1C-globulin has been a frequent finding in activated germinal centers of human lymph nodes and spleen.[46] In immunized animals, evidence has been gained for the simultaneous presence in germinal centers of antigens and antibodies [46–49] and of immune complexes containing complement.[46] The overall immunomorphologic features of glomerular lesions associated with the presence of Au/HAA immune complexes were similar to those typical for experimental serum sickness.[50] Deposits of immunoglobulins and β1C-globulin have repeatedly been found in kidney glomeruli in a number of human glomerulonephritides.[51–53] Positive identification, however, of the presence of immune complexes has been achieved in a few instances only by characterization of respective antigens of intrinsic and extrinsic origin. Thus far, the presence of nuclear antigens, streptococcus Type 12 antigens and *Plasmodium malariae* antigens was demonstrated by various methods in glomerular deposits in lupus nephritis,[54] streptococcal nephritis,[55] and in nephritis of quartan malaria,[56] respectively. Typical lesions of panarteritis were observed in patients who died in the course of serum sickness [57] and similar lesions were produced experimentally in animals injected with foreign proteins.[58] In experimental serum sickness intraintimal deposits of antigen, antibody and complement were disclosed at sites of degenerative and inflammatory vascular lesions.[59] Vascular lesions of panarteritis were reported to contain gamma globulin,[51,60,61] fibrinogen and albumin.[61] Recently, deposits of immune complexes composed of Au/HAA, IgM and β1C-globulin were found in blood vessel walls in a case of panarteritis nodosa.[62] A large concentration of IgG, IgM and β1C-globulin found in arteriolar hyaline lesions in human spleen was interpreted as indicative for the presence of immune complexes.[27]

In light of these data, the lymph node and spleen germinal center reaction, and the kidney and vascular pathology in hepatitis cases included in this study all appear to be directly connected with the deposition of circulating Au/HAA immune complexes. These, owing to their antigenic component, would probably serve as immunogenic stimuli when trapped in germinal centers.[46,49] In kidney glomeruli and blood vessel intima their phlogogenic activity would largely depend on the antibody and not antigen component, independent of the probable pathogenicity of the latter.[63]

The occurrence in various forms of hepatitis of both circulating and lesion-associated Au/HAA immune complexes bears strong similarity to that in some of the chronic diseases of animals associated with persistent viral infections. Of these, the most extensively studied encompass lymphocytic choriomeningitis (LCM) virus infection in mice and viral plasmocytosis in mink both characterized by life-long persistence of virus in tissues, viremia, circulating viral antigen–antibody complexes and the development of characteristic tissue lesions, apparently subsequent to the deposition of these complexes. The tissue lesions include hepatocellular damage in mice infected with LCM virus, hyaline or fibrinoid vascular changes in mink with viral plasmocytosis and glomerular hyaline changes in both.[63-66] Immune complexes of viral antigen, antibody and complement were identified in nephritic lesions of mice infected with LCM virus [63,64] and of mink with viral plasmocytosis.[65,66] LCM-viral antigen, γ-globulin and complement were also disclosed in the foci of hepatocellular damage in mice infected with LCM virus. Here, the liver lesions were alternatively attributed to the local formation of immune complexes.[63] The development of all these lesions could not be related to the rather low intrinsic pathogenic potential of the respective infectious agents; it was postulated that they appear as the result of the interaction of the host immune response with the virus.[67] Host humoral immune response to viral antigens was also implicated in the pathogenesis of glomerulonephritis of mice chronically infected with leukemogenic and oncogenic viruses.[68-70] In glomerular lesions of NZB and (NZB × NZW) F_1 hybrid mice, which apparently carry Gross leukemia virus throughout life, antigens of this virus were detected together with homologous antibodies.[68,69] Immune complexes of viral antigens and antibodies were identified in similar lesions of Balb(c) mice neonatally infected with Moloney leukemia and sarcoma viruses.[70]

Direct pathogenicity of Au/HAA has not been proved; its indirect pathogenicity could, however, be tentatively assumed from finding circulating Au/HAA immune complexes in overt hepatitis cases and antigenemia alone in symptomless carriers.[4,20–22] This assumption is substantiated by observations in cases of lymphoproliferative disorders in which protracted antigenemia and abundant involvement of hepatocytes by Au/HAA were not accompanied by an apparent liver pathology.[16] The present findings strongly suggest that the humoral immune response against Au/HAA as manifested by Au/HAA immune complex formation both in situ and circulating could reasonably be incriminated as an important factor in the pathogenesis of hepatitis. Thus the several types of hepatitis studied (apparently closely related etiopathogenetically) would reflect various forms of this response, the extreme examples of which are fulminant hepatitis and chronic persistent hepatitis.

References

1. Blumberg BS, Gerstley BJS, Hungerford DA, London WT, Sutnick AI: A serum antigen (Australia antigen) in Down's syndrome, leukemia and hepatitis. Ann Intern Med 66:924–931, 1967
2. Blumberg BS, Sutnick AI, London WT: Hepatitis and leukemia. Their relation to Australia antigen. Bull NY Acad Med 44:1566–1586, 1968
3. Prince AM: An antigen detected in the blood during the incubation period of serum hepatitis. Proc Nat Acad Sci USA 60:814–821, 1968
4. Shulman NR, Barker LF: Virus-like antigen, antibody, and antigen-antibody complexes in hepatitis measured by complement fixation. Science 165:304–306, 1969
5. Giles JP, McCollum RW, Berndtson LW Jr: Viral hepatitis: relationship of Australia/SH antigen to the Willowbrook MS–2 strain. N Engl J Med 281:119–122, 1969
6. Wright R, McCollum RW, Klatskin G: Australia antigen in acute and chronic liver disease. Lancet 2:117–121, 1969
7. Gitnick GL, Gleich GJ, Schoenfield LJ, Baggenstoss AH, Sutnick AI, Blumberg BS, London WT, Summerskill WHJ: Australia antigen in chronic liver disease with cirrhosis. Lancet 2:285–288, 1969
8. Sherlock Sheila, Fox RA, Niazi SP, Scheuer PJ: Chronic liver disease and primary liver-cell cancer with hepatitis-associated (Australia) antigen in serum. Lancet 1:1243–1247, 1970
9. Bayer ME, Blumberg BS, Werner B: Particles associated with Australia antigen in the sera of patients with leukaemia, Down's syndrome, and hepatitis. Nature (Lond) 218:1057–1059, 1968
10. Almeida JD, Zuckerman AJ, Taylor PE, Waterson AP: Immune electron

microscopy of the Australia-SH (serum hepatitis) antigen. Microbios 2:117–123, 1969

11. Alter HJ, Blumberg BS: Studies on a "new" human isoprecipitin system (Australia antigen). Blood 27:297–309, 1966
12. Barker LF, Smith KO, Gehle WD, Shulman NR: Some antigenic and physical properties of virus-like particles in sera of hepatitis patients. J Immunol 102:1529–1532, 1969
13. Jożwiak W, Kościelak J, Madaliński K, Brzosko WJ, Nowosławski A, Kłoczewiak M: RNA of Australia antigen. Nature–New Biology (London) 229:92–94, 1971
14. Millman I, Zavatone VE, Gerstley BJS, Blumberg BS: Australia antigen detected in the nuclei of liver cells of patients with viral hepatitis by the fluorescent antibody technique. Nature (Lond) 222:181–184, 1969
15. Coyne V, Millman I, Cerda J, Gerstley BJS, London WT, Sutnick AI, Blumberg BS: The localization of Australia antigen by immunofluorescence. J Exp Med 131:307–319, 1970
16. Nowosławski A, Brzosko WJ, Madaliński K, Krawczyński K: Cellular localization of Australia antigen in the liver of patients with lymphoproliferative disorders. Lancet 1:494–497, 1970
17. Brzosko WJ, Krawczyński K, Madaliński K, Nowosławski A: Recherches sur l'antigene australien dans les affections du foie. Bull Acad Natl Med (Paris) 154:8–16, 1970
18. Nelson JM, Barker LF, Danovitch SH: Intranuclear aggregates in the liver of a patient with serum hepatitis. Lancet 2:773–774, 1970
19. Scotto J, Stralin H. Caroli J: Amas de particules viriformes dans le noyaux d'hepatocytes chez un sujet atteint d'hepatite virale. Compt Rend Acad Sci Ser D (Paris) 271:1603–1604, 1970
20. Almeida JD, Waterson AP: Immune complexes in hepatitis. Lancet 2:983–986, 1969
21. Millman I, London WT, Sutnick AI, Blumberg BS: Australia antigen-antibody complexes. Nature (Lond) 226:83–84, 1970
22. Brzosko WJ, Madaliński K, Krawczyński K, Skwarska H, Nowosławski A: Australia antigen immune complexes in patients with different forms of hepatitis. J Infect Dis 123:251–256, 1971
23. Nowosławski A, Swiderska H, Madaliński K, Krawczyński K, Brzosko WJ: Inflammatory effect of Au-antibody immune complexes. Lancet 1:598, 1971
24. Henney ChS, Ishizaka K: A simplified procedure for the preparation of immunoglobulin-class-specific antisera. J Immunol 103:56–61, 1969
25. Nowosławski A, Brzosko WJ: Immunopathology of rheumatoid arthritis. I. The rheumatoid synovitis. Pathol Eur 2:198–219, 1967
26. Nowosławski A, Brzosko WJ: Immunopathology of rheumatoid arthritis. II. The rheumatoid nodule (the rheumatoid granuloma). Pathol Eur 2:302–321, 1967
27. Krawczyński K: Immunohistochemical study of arteriolar (simple) hyalinosis in the spleen. Am J Pathol 62:253–264, 1971
28. Burkholder PM: Complement fixation in diseased tissues: I. Fixation of guinea pig complement in sections of kidney from humans with membraneous glomerulonephritis and rats injected with anti-rat kidney serum. J Exp Med 114:605–616, 1961

29. Edgington TS, Glassock RJ, Dixon FJ: Autologous immune-complex pathogenesis of experimental allergic glomerulonephritis. Science 155:1432–1434, 1967
30. Lowry OH, Rosebrough NJ, Farr L, Randall RJ: Protein measurement with the Folin phenol reagent. J Biol Chem 193:265–275, 1951
31. Scheidegger JJ: Une micromethode de l'immunoelectrophorese. Int Arch Allergy Appl Immunol 7:103–110, 1955
32. Prince AM, Burke K: Serum hepatitis antigen (SH): rapid detection by high voltage immunoelectroosmophoresis. Science 169:593–595, 1970
33. Lachman PJ, Müller-Eberhard HJ, Kunkel HG, Paronetto F: The localization of in vivo bound complement in tissue sections. J Exp Med 115:63–82, 1962
34. Prince AM, Fuji H, Gershon RK: Immunohistochemical studies on the etiology of anicteric hepatitis in Korea. Am J Hyg 79:365–381, 1964
35. Nairn RC, Chadwick CS, McEntegart MG: Fluorescent protein tracers in the study of experimental liver damage. J Pathol Bacteriol 76:143–153, 1958
36. Mackay IR, Weiden S, Hasker J: Autoimmune hepatitis. Autoimmunity—Experimental and Clinical Aspects, II. Ann NY Acad Sci 124:767–780, 1965
37. Müller-Eberhard HJ: Chemistry and reaction mechanisms of complement. Adv Immunol 8:1–80, 1968
38. Cochrane CG: Immunologic tissue injury mediated by neutrophilic leukocytes. Adv Immunol 9:97–162, 1968
39. Steiner JW: Investigations of allergic liver injury. I. Light, fluorescent and electron microscopic study of the effects of soluble immune aggregates. Am J Pathol 38:411–436, 1961
40. Paronetto F, Popper H: Aggravation of hepatic lesions in mice by in vivo localization of immune complexes (Auer hepatitis). Am J Pathol 47:549–563, 1965
41. Hartley G Jr, Luschbaugh CC: Experimental allergic necrosis of the liver. Am J Pathol 18:323–331, 1942
42. McKinnon GE, Andrews EC Jr, Heptinstall RH, Germuth FG Jr: An immunohistologic study on the occurence of intravascular antigen-antibody precipitation and its role in anaphylaxis in the rabbit. Bull Johns Hopkins Hosp 101:258–280, 1957
43. Fennel RH, Santamaria A: Anaphylaxis in the rat. Immunohistochemical and histochemical studies of the liver. Am J Pathol 41:521–534, 1962
44. Paronetto F, Woolf N, Koffler D, Popper H: Response of the liver to soluble antigen-antibody complexes. Gastroenterology 43:539–546, 1962
45. Paronetto F, Popper H: Hetero-iso- and autoimmune phenomena in the liver. Textbook of Immunopathology. Edited by PA Miescher and HJ Müller-Eberhard. New York, Grune and Stratton, Inc, p 569, 1968
46. Gail-Peczalska KJ, Fish AJ, Meuwissen HJ, Frommel D, Good RA: Localization of immunological complexes fixing β1C (C3) in germinal centers of lymph nodes. J Exp Med 130:1367–1393, 1969
47. McDevitt HO, Askonas BA, Humphrey JH, Schechter J, Sela M: The localization of antigen in relation to specific antibody producing cells. I. Use of a synthetic polypeptide [(T, G)-A-L] labeled with iodine-125. Immunology 11:337–351, 1966

48. Balfour BM, Humphrey JH: Localization of gamma globulin and labeled antigen in germinal centers in relation to the immune response. Germinal Centers in Immune Response, Edited by H Cottier, N Odartchenko, R Schindler, CC Congdon. New York, Springer Publishing Co, pp 80–85, 1967

49. White RG, French VJ, Stark JM: Germinal center formation and antigen localization in Malpighian bodies of the chicken spleen.[48] pp 131–142

50. Dixon FJ, Vazquez JJ, Weigle WO, Cochrane CG: Pathogenesis of serum sickness. Arch Pathol 65:18–28, 1958

51. Mellors RC, Ortega LG: Analytical pathology. III. New observations on the pathogenesis of glomerulonephritis, lipid nephrosis, periarteritis nodosa, and secondary amyloidosis in man. Am J Pathol 32:455–499, 1956

52. Mellors RC, Ortega LG, Holman HR: Role of gamma globulins in pathogenesis of renal lesions in systemic lupus erythematosus and chronic membraneous glomerulonephritis with an observation on the lupus erythematosus cell reaction. J Exp Med 106:191–202, 1957

53. Freedman P, Markowitz AS: Gamma globulin and complement in the diseased kidney. J Clin Invest 41:328–334, 1962

54. Koffler D, Schur PH, Kunkel HG: Immunological studies concerning the nephritis of systemic lupus erythematosus. J Exp Med 126:607–624, 1967

55. Andres GA, Accinni L, Hsu KC, Zabriskie JB, Seegal BC: Electron microscopic studies of human glomerulonephritis with ferritin-conjugated antibody. J Exp Med 123:399–412, 1966

56. Ward PA, Kibukamusoke JW: Evidence for soluble immune complexes in the pathogenesis of the glomerulonephritis of quartan malaria. Lancet 1:283–285, 1969

57. Rich AR: The role of hypersensitivity in periarteritis nodosa; as indicated by seven cases developing during serum sickness and sulfonamide therapy. Bull Johns Hopkins Hosp 71:123–140, 1942

58. Rich AR, Gregory JE: The experimental demonstration that periarteritis nodosa is a manifestation of hypersensitivity. Bull Johns Hopkins Hosp 72:65–88, 1943

59. Kniker WT, Cochrane CG: Pathogenetic factors in vascular lesions of experimental serum sickness. J Exp Med 122:83–98, 1965

60. Vazquez JJ, Dixon FJ: Immunohistochemical analysis of lesions associated with "fibrinoid change". AMA Arch Pathol 66:504–517, 1958

61. Paronetto F, Strauss L: Immunocytochemical oberservations in periarteritis nodosa. Ann Intern Med 56:289–296, 1962

62. Gocke DJ, Hsu K, Morgan C, Bombardieri S, Lockshin M, Christian CL: Association between polyarteritis and Australia antigen. Lancet 2:1149–1153, 1970

63. Oldstone MBA, Dixon FJ: Pathogenesis of chronic disease associated with persistent lymphocytic viral infection. I. Relationship of antibody production to disease in neonatally infected mice. J Exp Med 129:483–505, 1969

64. Oldstone M, Dixon F: Lymphocytic choriomeningitis: production of antibody by "tolerant" infected mice. Science 158:1193–1195, 1967

65. Porter DD, Larsen AE: Aleutian disease in mink: infectious virus-antibody complexes in the serum. Proc Soc Exp Biol Med 126:680–682, 1967

66. Porter DD, Larsen AE, Porter HG: The pathogenesis of Aleutian disease

of mink. I. In vivo viral replication and the host antibody response to viral antigen. J Exp Med 130:575–593, 1969

67. Oldstone MBA, Dixon FJ: Pathogenesis of chronic disease associated with persistent lymphocytic choriomeningitis viral infection. II. Relationship of the anti-lymphocytic choriomeningitis immune response to tissue injury in chronic lymphocytic choriomentingitis disease. J Exp Med 131:1–19, 1970
68. Mellors RC, Aoki T, Huebner RJ: Further implication of murine leukemia-like virus in the disorders of NZB mice. J Exp Med 129:1045–1062, 1969
69. Mellors RC, Shirai T, Aoki T, Huebner RJ, Krawczyński K: Wild-type Gross leukemia virus and the pathogenesis of the glomerulonephritis of New Zealand mice. J Exp Med 133:113–132, 1971
70. Hirsch MS, Allison AC, Harvey JJ: Immune complexes in mice infected neonatally with Moloney leukaemogenic and murine sarcoma viruses. Nature (Lond) 223:739–740, 1969

Acknowledgments

We are indebted to Professor Maria Kobuszewska-Faryna, MD and Dr. Maria Oczkowska from the Department of Pathologic Anatomy of the Postgraduate Medical Institute, Warsaw, and Dr. Maria Kaminska from the Pathologic Anatomy Division of the Infectious Diseases Clinic, Medical Academy, Warsaw for making available to us the autopsy material and case histories. We thank Magister biology Agata Sztachelska for assistance in the performance of elution procedures. The valuable technical assistance of Mrs. Hanna Pragert, Miss Anna Szwed and Miss Ewa Wojno is gratefully acknowledged.

[*Illustrations follow*]

Legends for Figures

Figures 1–9, 11–16, 18–21 are microphotographs of frozen sections stained with immunohistochemical reagents for identification of Au/HAA, IgG, IgM, β1C globulin and guinea pig complement. Figures 10, 22, 23 and 29C are electronmicrographs of ultra-thin sections double-stained with uranyl acetate and lead citrate.

Fig 1—Subacute hepatitis. Differing amounts of Au/HAA predominantly in the cytoplasm of hepatocytes in an area of profound parenchymal damage (×360).

Fig 2—Chronic aggressive hepatitis. Cytoplasmic localization of Au/HAA in hepatocytes at the periphery of a lobule (× 360).

Fig 3—Liver cirrhosis. Cytoplasmic localization of Au/HAA in hepatocytes at the periphery of a nodule (× 360).

Fig 4—Chronic persistent hepatitis. Nuclear and peripheral cytoplasmic localization of Au/HAA in a hepatocyte (× 360).

Fig 5—Chronic persistent hepatitis. Foamy appearance of the Au/HAA content in hepatocytes apparently undergoing degeneration (× 360).

Fig 6—Chronic aggressive hepatitis. Localization of Au/HAA in the nuclei and cytoplasm of hepatocytes. The hepatocyte in the right bottom corner is probably being extruded from the hepatic plate. Granular deposits of antigenic material in the sinusoid are seemingly contained in the cytoplasm of Kupffer cells (× 360).

Fig 7—Chronic aggressive hepatitis. Delicate, finely granular deposits of Au/HAA tracing the outlines of individual hepatocytes and groups of hepatocytes (× 360).

Fig 8—Chronic aggressive hepatitis. Band-like and crescent-shaped deposits of Au/HAA mostly in peripheral cytoplasmic localization (× 360).

Fig 9—Chronic aggressive hepatitis. Large masses of Au/HAA in the cytoplasm of several hepatocytes and occasional linear deposits at their periphery. Trace amounts of Au/HAA in a few hepatocyte nuclei and on nuclear membranes (× 360).

Fig 10—Au/HAA particles adjacent to the marginated remnants of nuclear chromatin of a hepatocyte (× 80,000).

Fig 11—Chronic aggressive hepatitis. IgG in the cytoplasm of hepatocytes, on and in the nuclei, and in the sinusoids (× 360).

Fig 12—Subacute hepatitis. IgM deposits in the cytoplasm and on or in the nuclear membranes of hepatocytes in an area of profound parenchymal damage (× 360).

Fig 13—Chronic aggressive hepatitis. Layer-like localization of IgG on hepatocyte plasma membranes and in the sinusoids (× 360).

Fig 14—A consecutive section from the same tissue block as in Fig 11. β1C localization pattern similar to that of IgG (× 360).

Fig 15—A consecutive section from the same tissue block as in Figure 13. β1C localization pattern similar to that of IgG (× 360).

Fig 16—A consecutive section from the same tissue block as in Figure 12. Immunofluorescent image of the guinea pig complement fixation reaction in an area of profound hepatocellular damage (× 360).

Fig 17—IEOP test showing the presence of anti-Au/HAA antibody in the KSCN eluate (anode well) from the liver in a case of chronic aggressive hepatitis. Cathode well contains 1:4 diluted Au/HAA positive serum. Test carried out at room temperature for 1.5 hours at 30 mA and 90 V/6.5 × 9 cm agar plate.

Fig 18—Fulminant hepatitis. Serial consecutive sections of a lymph node showing an active germinal center: **A**—Localization of Au/HAA deposits; **B**—Localization of IgG deposits (× 360).

Fig 19—Membraneous glomerulonephritis in a case of chronic aggressive hepatitis. Delicate granular deposits and large lumpy masses of Au/HAA localized along the capillary basement membrane of a glomerulus (× 360).

Fig 20—Consecutive section of the same kidney block. Localization of IgG (× 360).

Fig 21—Consecutive section from the same kidney block as in Figures 19 and 20. Localization of β1C (× 360).

Fig 22—Au/HAA particles in the cytoplasm of an epithelial cell closely adhering to the glomerular basement membrane. Regular interspacing suggests the presence of bound antibody (× 60,000).

Fig 23A—Aggregations of Au/HAA particles in the outer aspect of the glomerular basement membrane. **B**—Small aggregation of Au/HAA particles in the deeper aspect of the glomerular basement membrane (× 50,000).

Fig 24, 25 and 26—Panarteritis in a case of chronic persistent hepatitis. Granular and lumpy deposits of Au/HAA localized in the thickened intima of arcuate arteries in the kidney (× 255).

Fig 27—Consecutive sections of the same tissue block as in Fig 25. Granular and lumpy deposits of immunoglobulins showing a localization pattern similar to that of Au/HAA: **A**—Localization of IgG; **B**—Localization of IgM (× 255).

Fig 28—Arteriolar simple hyalinosis in a case of subacute hepatitis. Granular and lumpy masses of Au/HAA in the greatly thickened intima of a follicular splenic artery (× 255).

Fig 29—Arteriolar simple hyalinosis in a case of chronic aggressive hepatitis. **A**—Homogeneous deposits of Au/HAA in hyaline masses in the intima of a small artery in the kidney. **B**—Consecutive section of the same tissue block as in **A**. Homogeneous mixture of IgG and Au/HAA in the intimal hyaline masses (double staining procedure). **C**—Aggregation of Au/HAA particles in amorphous hyaline masses of the intima of small artery in the kidney (× 80,000).

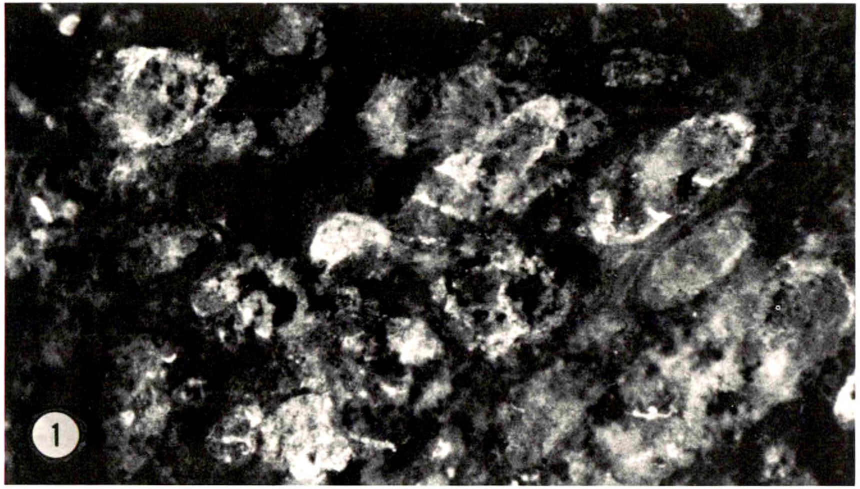
①

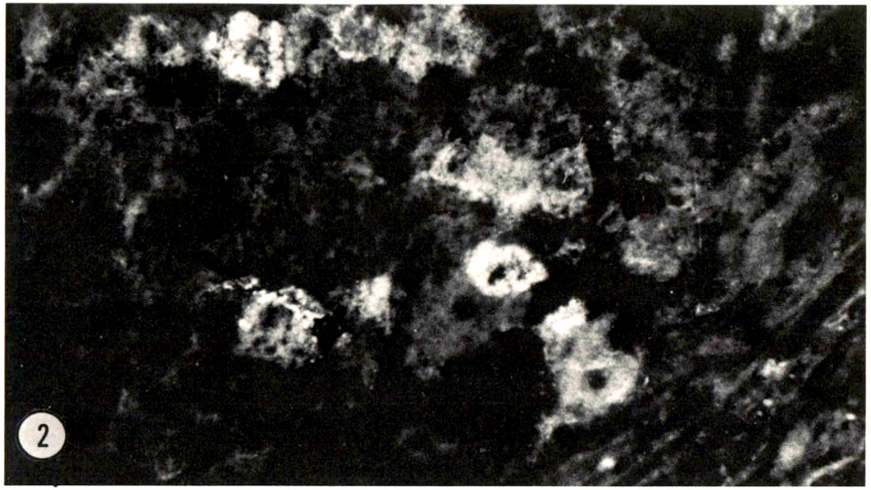
②

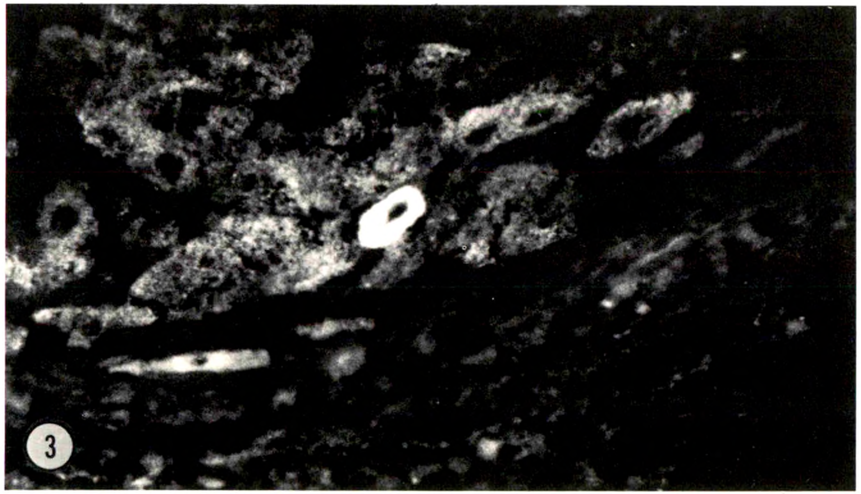
③

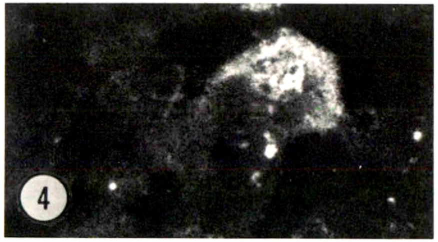
④

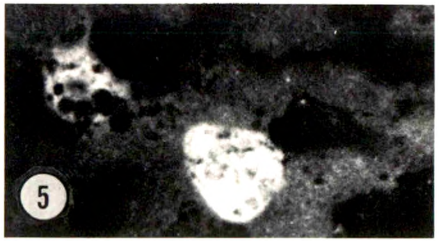
⑤

⑥

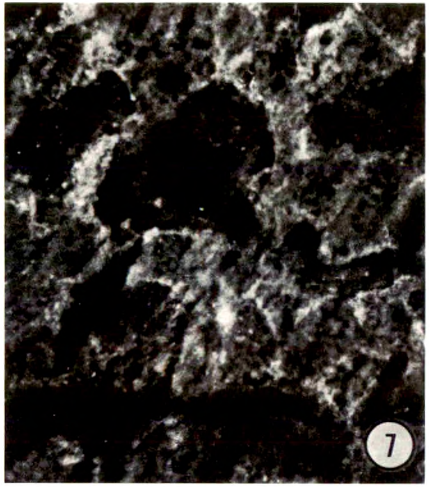
⑦

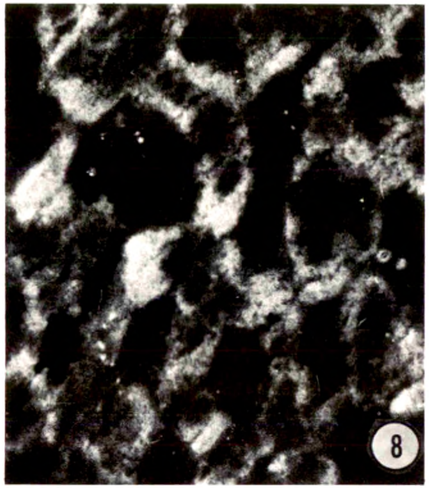
⑧

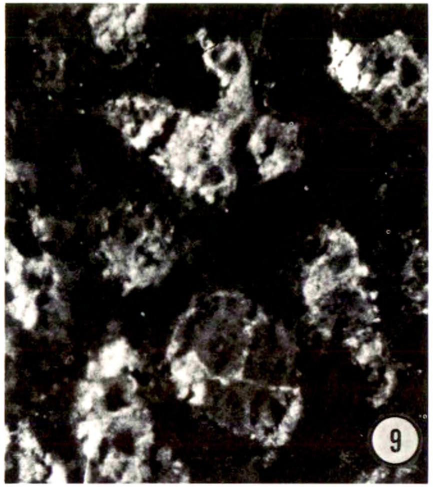
⑨

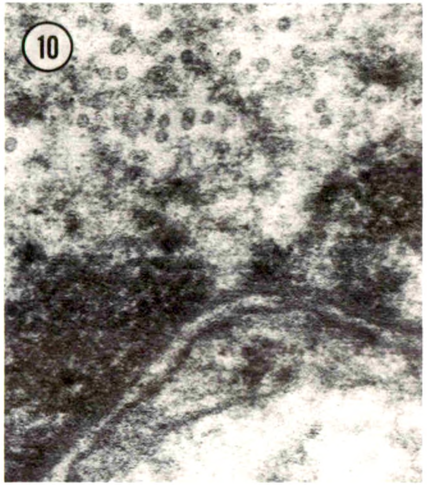
⑩

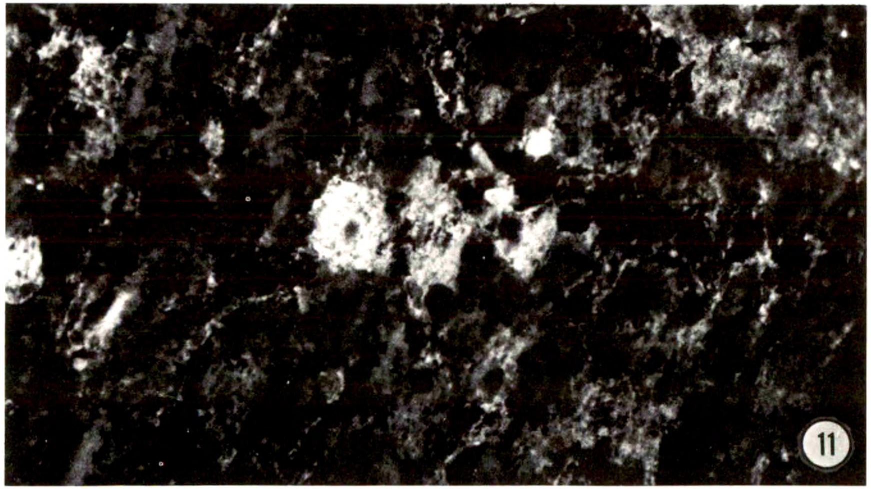
⑪

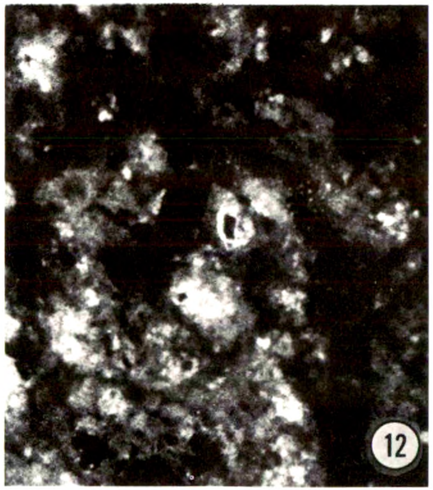
⑫

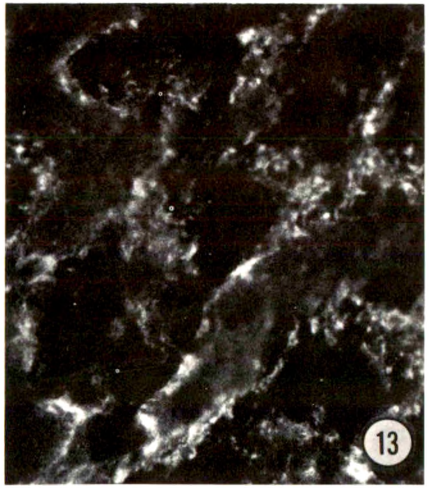
⑬

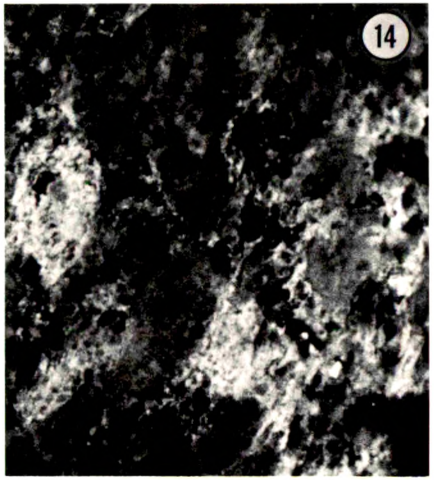
14

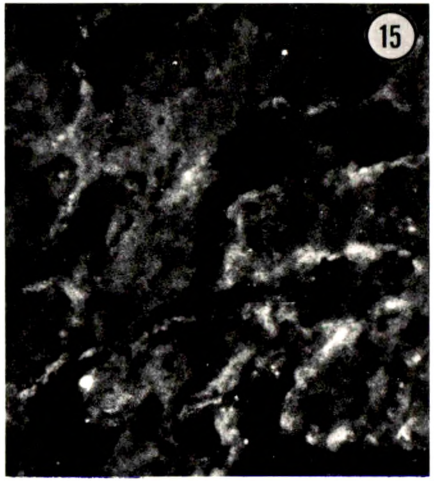
15

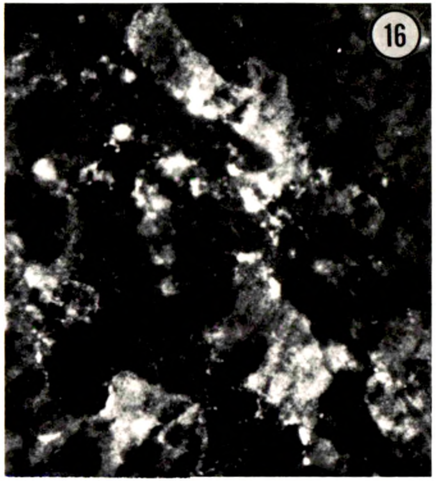
16

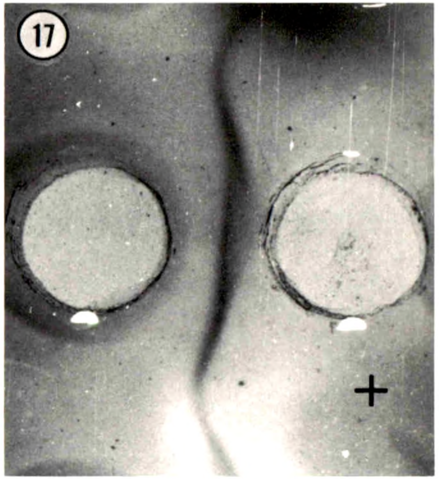
17

18A

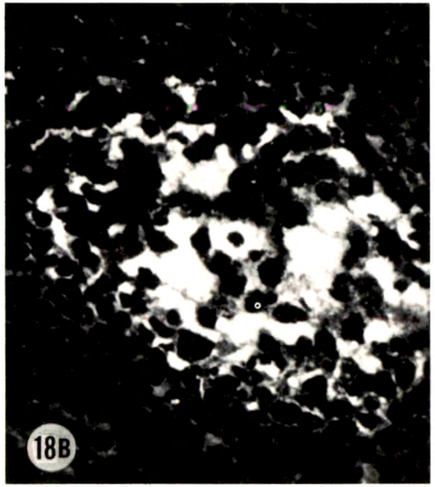
18B

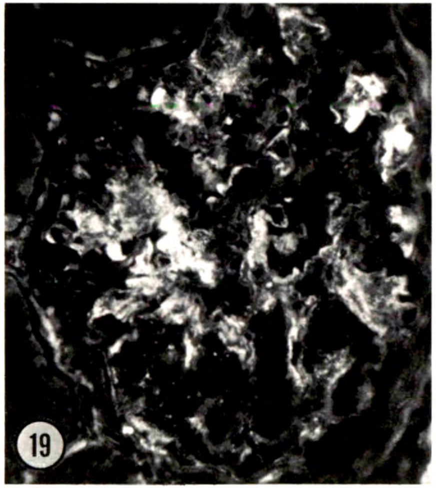
19

20

21

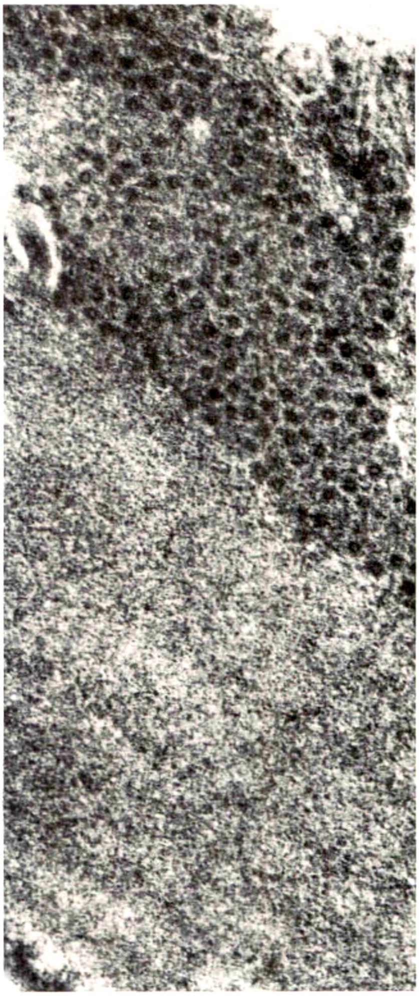

22

23 A

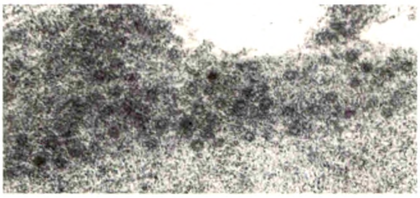

23B

24

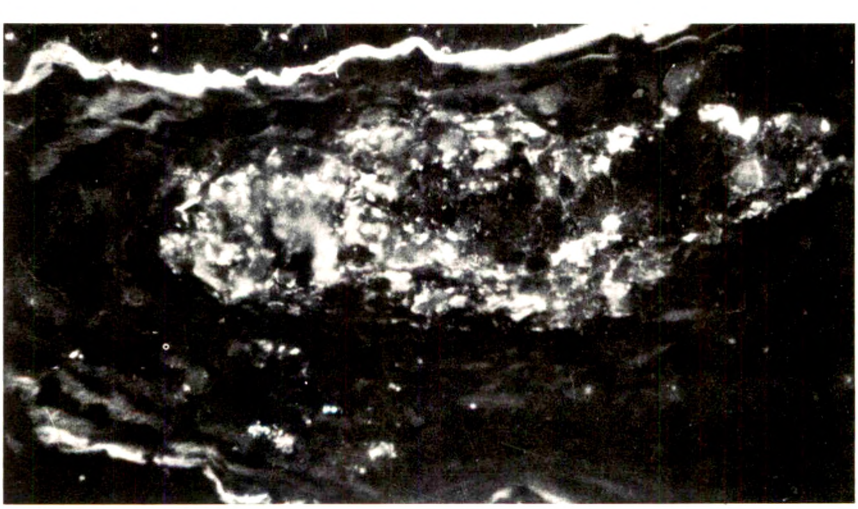

25

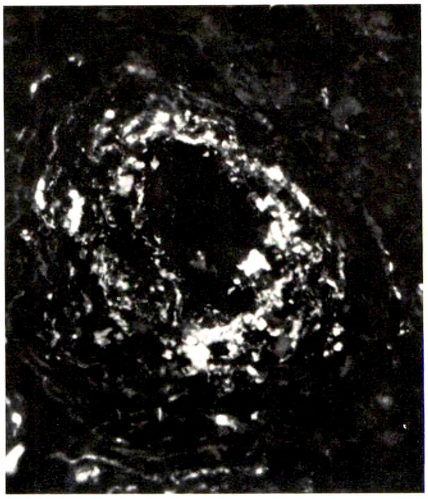

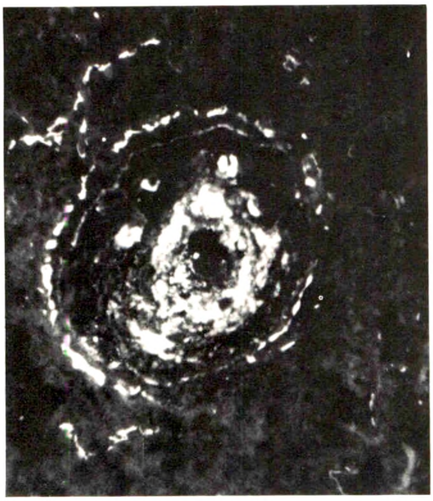

26

27A

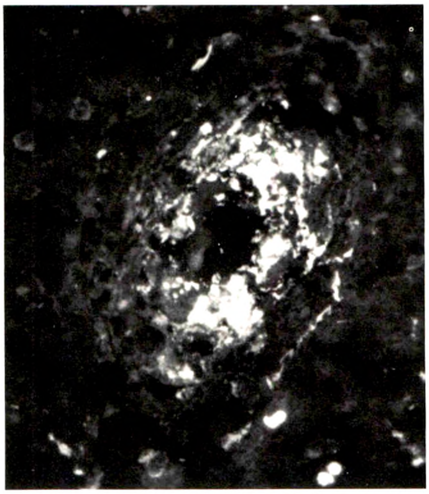

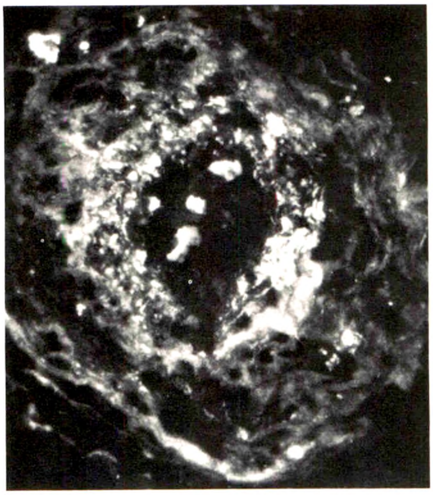

27B

28

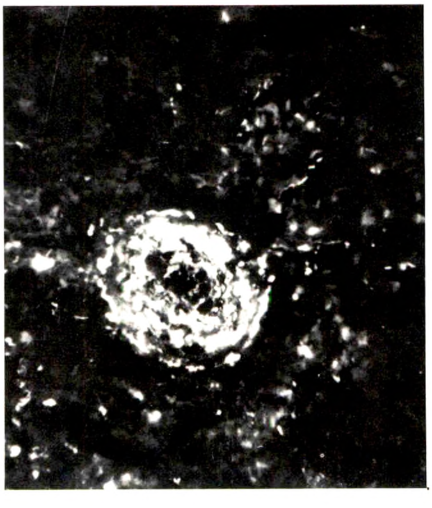

29A

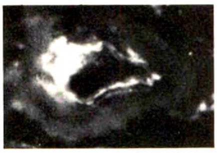

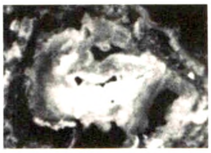

29B

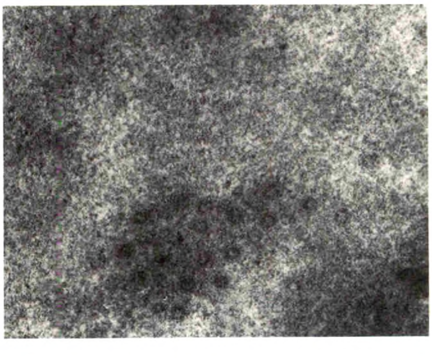

29C

[*End of Article*]

Effects of Normal and Aspirin Platelets on Defective Secondary Aggregation in the Hermansky-Pudlak Syndrome

A Test for Storage Pool Deficient Platelets

James G. White, MD and Carl J. Witkop, DDS

Platelets from patients with the Hermansky-Pudlak syndrome (albinism, accumulation of ceroid-like pigment in bone marrow macrophages and mild hemorrhagic symptoms) and aspirin-treated normal platelets fail to develop irreversible secondary waves of aggregation when exposed to aggregating agents on the platelet aggregometer. The present study demonstrates that equal volumes of Hermansky-Pudlak and aspirin-treated platelets, when mixed together, respond in a biphasic manner comparable to normal cells. Correction of the release defect of aspirin platelets by storage pool deficient Hermansky-Pudlak cells indicates that different mechanisms are involved in the failure of the release reaction in the two cell types. The simple test may serve to distinguish other patients with storage pool deficient platelets from individuals who have taken aspirin or other drugs with an aspirin-like effect on platelet function (Am J Pathol 68:57–66, 1972).

THE HERMANSKY-PUDLAK SYNDROME is characterized by the unusual association of albinism, storage of ceroid-like pigment in bone marrow macrophages and a mild hemorrhagic disorder.[1,2] Initially the bleeding symptoms were related to a vascular abnormality, but study of similar cases in several laboratories by advanced methods demonstrated that platelets from these patients are defective.[3-8] The cells are deficient in serotonin, a nonmetabolic pool of adenine nucleotides, and the inherently opaque organelles, referred to as dense bodies,[9] in which these chemical substances are stored. When potent aggregating agents are added to Hermansky-Pudlak (HP) platelets *in vitro,* the cells adhere normally, but fail to develop irreversible secondary aggregation, which depends entirely on secretion of the chemical compounds deficient in HP platelets.[10]

Ingestion of aspirin by normal subjects also causes a defect in the platelet release reaction characterized by failure of secondary aggre-

---

From the Departments of Pediatrics and Dentistry, University of Minnesota Medical Center, Minneapolis, Minnesota.

Supported by Grants HE-11880, AI-05153, CA-08832 and AM-15317 from the US Public Health Service and the Cardiovascular Clinical Research Program Project Grant, University of Minnesota.

Accepted for publication December 28, 1971.

Address reprint requests to Dr. James G. White, Department of Pediatrics, University of Minnesota, Box 284 Mayo Memorial Building, Minneapolis, Minn 55455.

gation *in vitro*.[11-14] Aspirin does not cause reduction of platelet serotonin or nonmetabolic adenine nucleotides, but interferes in an unknown manner with the extrusion of these chemicals after the cells are exposed to aggregating agents. As a result, the patterns of aggregation obtained by nephelometry are essentially identical to those observed in samples of HP platelet-rich plasma. The present investigation has evaluated the effects of normal platelets on the aggregation of HP platelets. Both normal and aspirin platelets corrected the defect in HP cells, resulting in a completely normal pattern of secondary response to aggregating agents.

Materials and Methods

General

This laboratory used the two syringe technic to collect blood; the sample was immediately combined with 3.8% trisodium citrate or citrate-citric acid anticoagulant in a ratio of 9 parts blood to one part citrate. The platelet-rich plasma (C-PRP) was separated by centrifugation at 100 × g for 20 minutes at room temperature.

Platelet-poor plasma (PPP) was prepared by sedimenting C-PRP at 250 × g for an additional 20 minutes. The platelet count of the C-PRP was adjusted to 300,000/cu mm by diluting with PPP. These methods have been described in recent publications.[7,15-17] A Chronolog platelet aggregometer, model S-201, coupled to a Bausch and Lomb VOM-5 recorder was used to follow platelet aggregation. The baseline of the recording was preset with C-PRP, and maximum upward deflection of the pen with PPP. Samples of C-PRP were placed in a 37 C water bath for at least 5 minutes before being placed on the aggregometer. The C-PRP was stirred magnetically at a constant rate of 1500 RPM at 37 C. Aggregating agents were either freshly prepared for each experiment, or stored in the frozen state between studies. The agents employed routinely in our studies of platelet aggregation include serotonin (1×10^{-4}M), epinephrine (5.5×10^{-6}M), adenosine diphosphate (1×10^{-6}M to 1×10^{-3}M), thrombin (0.1–0.2 U), collagen and bacteria. Each agent, dissolved in a volume of 0.1 ml of distilled water or buffered saline, was blown into 0.9 or 1 ml of C-PRP after the baseline has been recorded for at least 1 minute.

Specific

In the present study blood was obtained from a 26-year-old male with the Hermansky-Pudlak syndrome,[6] and from normal donors who had not taken any medications for at least ten days prior to the time of study. Blood was also obtained from a second group of normal donors who ingested 10 to 15 grains of aspirin 1 hour or more prior to venipuncture. Samples of patient platelet-rich plasma, normal platelet-rich plasma, and aspirin-affected normal platelet-rich plasma were tested independently for their response to the several aggregating agents. The corrective effect of normal C-PRP on C-PRP from the patient was examined by combining the samples in various ratios to a final volume of one ml. In this way the amount of normal C-PRP necessary to induce a biphasic response to aggregating agents in Hermansky-Pudlak C-PRP could be determined.

Various ratios of patient C-PRP and aspirin-treated C-PRP were also prepared and evaluated in a similar manner. The studies forming the basis of this report were repeated on three occasions with identical results.

Results

The patient selected for the present study has all of the features of the Hermansky-Pudlak (HP) syndrome,[6] and a complete description of his clinical, biochemical, and ultrastructural studies will appear in a separate report.[18] C-PRP from patients with this disorder manifests a normal primary response to aggregating agents.[4,5,7] Shortly after addition of epinephrine, ADP or thrombin to samples of HP C-PRP, upward deflection of the recording pen occurs, indicating an increase in light transmission due to platelet adhesion. In contrast to normal samples, however, the second wave of aggregation, which is entirely dependent on chemical products secreted by the cells, fails to occur. As a result the aggregated cells disassociate, and reassume their discoid form. This is indicated on the aggregometer by a return of the tracing toward the baseline, and recovery of the broad oscillations seen prior to addition of the aggregating agent. Platelets from the patient adhere to collagen, but do not aggregate. If the concentration of collagen is sufficiently high, or if the abnormal cells contain some stored products, a small increase in light transmission will occur. However, the rate of development is slower and the change in optical density far less than in normal C-PRP.

The addition of 10% normal C-PRP to C-PRP from the patient with the Hermansky-Pudlak syndrome corrected the defect due to the defective release reaction and produced normal biphasic responses to several agents on the aggregometer (Text-figure 1). Increased proportions of normal to patient cells did not appear to alter or improve the response observed when 10% normal C-PRP was present.

The results obtained with combinations of HP C-PRP and aspirin-treated normal C-PRP were of particular interest (Text-figures 2–4). Equal volumes of HP and aspirin platelets mixed together responded to all aggregating agents in the same manner as normal platelets. Second waves of aggregation occurred at the same time, developed at the same rate and reached the same maximal change in light transmission. The response of the samples containing equal volumes of HP cells and aspirin platelets to collagen was also identical to that of normal C-PRP. As the proportion of HP platelets combined with aspirin-treated platelets was increased, the tracings resembled those obtained from patients with an intermediate type of abnormal

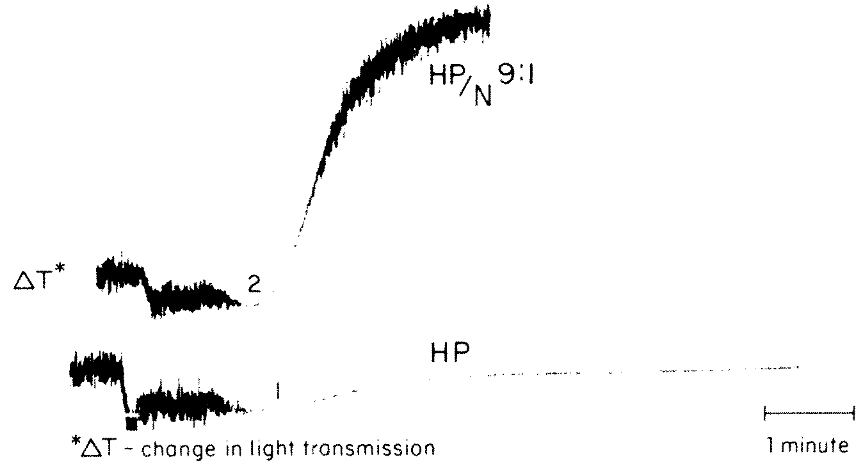

Text-fig 1—Effects of combining normal (N) citrate platelet-rich plasma (C-PRP) with Hermansky-Pudlak (HP) C-PRP on the defective secondary aggregation found in this disorder. Tracing 1 is typical of those obtained when collagen is added to C-PRP from the patient with HP syndrome. The oscillating character of the baseline indicates the presence of discoid platelets. Addition of collagen causes an increase in optical density, registered as a downward deflection of the recording pen. After a latent phase, the baseline narrows as platelet shape change develops. The narrowed baseline persists, but only a slight rise in light transmission occurs, suggesting formation of a few aggregates. Combining 10% normal C-PRP (N) with 90% patient C-PRP (HP) in Tracing 2 results in irreversible monophasic aggregation identical to the response of normal C-PRP alone after the addition of collagen.

release reaction[7]; the onset of the second wave of aggregation was delayed, the rate of aggregate formation slowed and the maximal change in optical density decreased. At a ratio of 9 parts HP to 1 part aspirin platelets, the tracing resembled the response obtained with HP platelets alone. A ratio of 2 parts HP and 8 parts aspirin platelets gave a result similar to that obtained with aspirin platelets alone.

Discussion

The ability of a small number of normal platelets to correct the defective secondary aggregation in samples of Hermansky-Pudlak platelets was not surprising. Only small amounts of adenine nucleotides are required for development of the second wave,[19] and most of the storage pool is extruded rapidly at the onset of secondary aggregation.[10,20] Even though HP platelets contain markedly reduced levels of nonmetabolic nucleotides and serotonin, the cells from most patients appear to store small amounts of these chemicals.[21] This small amount, together with the storage pool from 10% normal cells, appeared sufficient in the present study to correct the defective secondary response of HP platelets to various aggregating agents *in vitro*. Whether a similar volume of normal platelet-rich plasma will successfully correct the *in vivo* abnormality of platelets in Hermansky-Pudlak syndrome remains to be determined.

The decision to study the effect of aspirin-treated platelets on the defective secondary aggregation of HP cells was based on previous observations. Evaluation of platelet structure and function in a child with a variant of the Hermansky-Pudlak syndrome revealed that his cells underwent complete physical transformation despite failure to release endogenous chemical products.[7] The capacity of his cells to adhere in the presence of small amounts of aggregating agents, to form irreversible aggregates after addition of large amounts of ADP, to develop shape change, internal transformation and granule fusion consistent with complete viscous metamorphosis, and to retract clots indicated that two of the three basic mechanisms of platelet function,[22] adhesion and contraction, were intact in his cells. Secretion, the third basic mechanism, took place to a limited extent under maximum

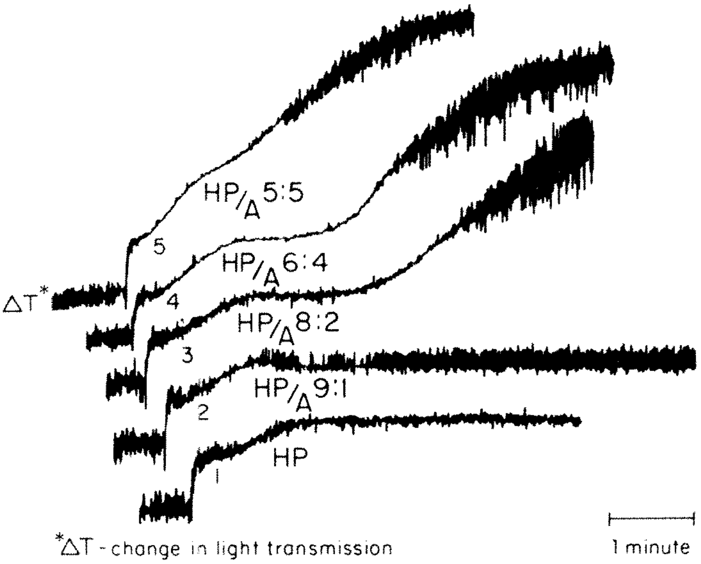

TEXT-FIG 2—Effects of C-PRP from a normal individual after the ingestion of aspirin on the defective secondary aggregation of a patient with HP syndrome to epinephrine (5.5×10^{-6} M). Tracing 1 of the patient's C-PRP alone is identical to the reaction of C-PRP from the aspirin-treated control, and the combination of 10% aspirin platelets (A) in Tracing 2 does not alter the defect in secondary aggregation. A mixture of 20% aspirin platelets and 80% HP cells develops a slightly delayed, but otherwise normal appearing second wave of aggregation in response to epinephrine in Tracing 3. Tracings 4 and 5 obtained from samples combined in ratios of 6HP:4A and 5HP:5A respectively are identical to biphasic responses observed in samples of normal C-PRP alone after the addition of epinephrine.

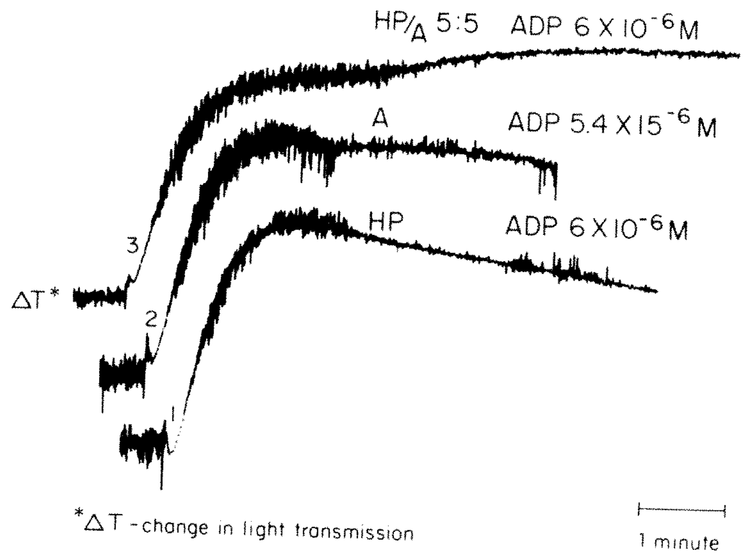

TEXT-FIG 3—Effects of aspirin-treated platelets on the defective secondary aggregation of HP platelets in response to ADP. The primary wave of aggregation is similar in all three tracings, but reverses in the samples of HP (Tracing 1) and aspirin (Tracing 2) platelets tested alone. A mixture of half HP platelets with half aspirin platelets (3) responds to ADP with a typical double wave of aggregation.

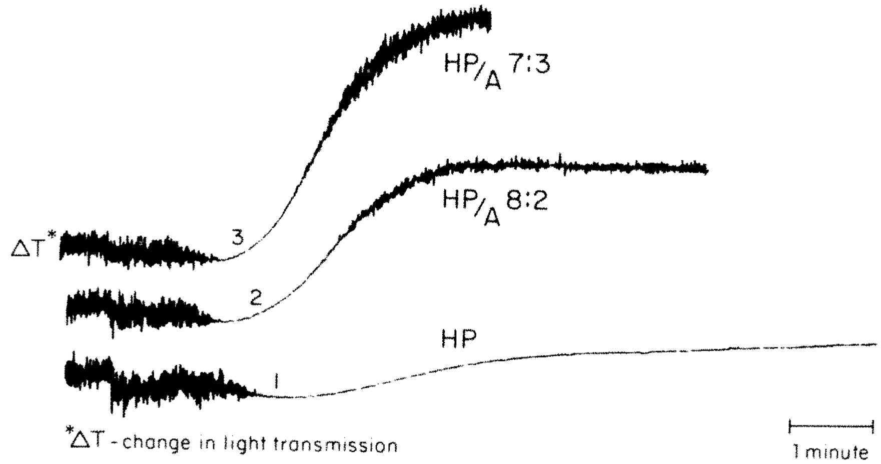

TEXT-FIG 4—Effects of aspirin platelets on the defective collagen-induced aggregation of HP platelets. Tracing 1 represents the typical reaction of the patient to collagen, and aspirin-treated normal platelets respond in a similar manner. Combining 20% aspirin platelets with 80% HP cells improves the response to collagen (Tracing 2), and 30% aspirin platelets mixed with 70% HP platelets yields Tracing 3 which is indistinguishable from the reaction of normal C-PRP to this agent.

stimulation, but failed after exposure of his platelets to small amounts of aggregating agents, due to the marked deficiency of serotonin and adenine nucleotides in the platelets. Thus, the mechanisms necessary for secretion were present and appeared to operate in a normal manner, but failed to generate irreversible secondary aggregation because of the reduced levels of secretory products available for release.

The impaired platelet release caused by aspirin is not due to reduction of serotonin or the nonmetabolic pool of adenine nucleotides.[11–14,23] Aspirin-treated platelets can adhere during the primary phase of response to aggregating agents, undergo shape change and internal transformation and retract clots. The impaired release reaction responsible for defective secondary aggregation is, therefore, not due to loss of adhesive properties, content of endogenous chemicals or complete destruction of contractile properties. However, electron microscopic studies have shown that the internal transformation of aspirin-treated platelets is limited following exposure to agents which stimulate release and secondary aggregation in normal platelets.[22–25] It is not known whether this effect of the drug is due to depression of the trigger mechanism for platelet contraction, interference with calcium flux necessary for activation of platelet contractile protein or interference with the contractile activity of thrombosthenin.[23,26,27] Interaction of these several components of the platelet contractile mechanism are essential for the internal transformation, granule fusion and emptying of dense bodies which characterize the platelet release reaction.[9,20,22,25] Failure of these physical alterations at the usual concentrations of aggregating agents indicates that defective release and absent secondary aggregation of aspirin-treated platelets are related to impairment of the platelet contractile mechanism.

The rationale for examining the influence of aspirin platelets on HP platelets was based on the inherent difference responsible for abnormal release in the two cell types. HP platelets have an intact, operating contractile mechanism, but fail to release because they lack the secretory products. Aspirin platelets contain secretory products but fail to secrete them due to an impaired response of the contractile mechanism to the usual concentrations of aggregating agents. Since the mechanisms responsible for defective release are different in HP and aspirin platelets, it was reasoned that combining them in various ratios might reveal a tendency for mutual correction.

The experimental results of this investigation support this hypothesis. Concentrations of aggregating agents which produced biphasic responses in samples of normal C-PRP, but only monophasic reactions in HP or aspirin C-PRP alone, caused typical double waves in samples formed from equal volumes of HP and aspirin cells. Increasing the proportion of patient platelets (8 HP:2A) or aspirin platelets (4HP:6A) resulted in intermediate secondary responses resembling tracings from the variant of Hermansky-Pudlak syndrome. When only 20 to 30% HP platelets were combined with aspirin platelets or 10% aspirin platelets with HP cells secondary aggregation failed to take place. Thus, aspirin platelets are less effective than normal platelets in correcting defective secondary aggregation of HP cells. Conversely, HP platelets are less potent than normal cells in correcting the defective release of aspirin platelets. The critical point, however, is the mutually corrective effect of HP and aspirin platelets on each other when approximately equal volumes of the two cell types are combined.

The findings suggest that the interaction of HP and aspirin platelets during the inital phase of adhesion establishes a relationship which facilitates the discharge of secretory products from the aspirin-treated platelets. Endogenous products must come from the aspirin platelets because they are nearly absent in HP cells, and the force for extrusion must develop from HP platelets, since aspirin platelets are unable to discharge the chemicals stored in dense bodies. The clumps of randomly associated HP and aspirin platelets formed during the first wave could provide the framework and proximity for the essential interaction. Whether the contraction of HP platelets forces the secretory products out of aspirin-treated cells, or overcomes the drug inhibition in some other manner, remains to be defined.

The findings of the present study may be helpful in the evaluation of other patients with bleeding due to platelet storage pool deficiency who lack the characteristic features of albinism and pigment accumulation in bone marrow.[28,29] Investigations of some of these patients have revealed platelet abnormalities nearly identical to those of patients with the HP syndrome.[30] However, the absence of identifying clinical features makes it more difficult to separate their platelet disorder from aspirin-like drug effects. Combination of their platelets with aspirin platelets may obviate the need for the complex technics required for specifically characterizing deficiencies in the platelet storage pool of serotonin and adenine nucleotides. If patient platelets and aspirin platelets together develop normal secondary aggregation not found with either type of cell alone, then it is probable the patient has a true storage pool deficiency rather than an acquired drug effect.

One exception would be the patient in whom defective release was due to an aberration of the contractile mechanism. In that case mutual correction would most likely fail to occur, suggesting that the patient's platelets were similar to aspirin-treated cells. However, defects in the contractile mechanism of platelets have not been defined as yet; if they exist other parameters of platelet function such as clot retraction would most likely be abnormal. Thus, the simple test system provided by combining equal volumes of patient and aspirin-treated platelets can be helpful in defining a probable storage pool deficiency and separating it from an aspirin-like drug effect on platelets. The test does not replace other technics necessary for identification of specific defects in platelet structure, biochemistry and physiology, but places a relatively easy method for identifying the probable presence of storage pool deficient platelets in the hands of clinicians and laboratories who are most likely to be exposed to such problems in practice.

References

1. Hermansky F, Pudlak P: Albinism associated with hemorrhagic diathesis and unusual pigmented reticular cells in the bone marrow: Report of two cases with histochemical studies. Blood 14:162–169, 1959
2. Bednar B, Hermansky F, Lojda Z: Vascular pseudohemophilia associated with ceroid pigmentophagia in albinos. Am J Pathol 45:283–294, 1964
3. Hardisty RM, Hutton RA: Bleeding tendency associated with "new" abnormality of platelet behavior. Lancet 1:983–985, 1967
4. Maurer JM, Buckingham S, McGilbray E, Spielvagel A, Wolff JA: Prolonged bleeding time, abnormal binding of platelet serotonin (5-HT), absent platelet dark body, defective platelet factor 3 activation, bone marrow inclusions and chromosome breaks in albinism. Proceedings of the Twelfth Congress, International Society of Hematology, New York, 1968, p 198 (abstr)
5. Mills DCB, Hardisty RM: The nature of the platelet defect in albinos with a bleeding tendency. Proceedings of the Thirteenth Congress, International Society of Hematology, Munich, 1970, p 31(abstr)
6. Muniz FJ, Fradera J, Moldonado N, Perez-Santiago E: Albinism, bleeding tendency, and abnormal pigmented cells in the bone marrow: a case report. Tex Rep Biol Med 28:167–173, 1970
7. White JG, Edson JR, Desnick SJ, Witkop CJ: Studies of platelets in a variant of the Hermansky-Pudlak syndrome. Am J Pathol 63:319–332, 1971
8. Logan LJ, Rapaport SI, Moher I: Albinism and abnormal platelet function. N Engl J Med 284:1340–1345, 1971.
9. White JG: Origin and function of platelet dense bodies. Ser Haematol 3:17–46, 1970
10. Holmsen H, Day HJ, Stormorken H: The blood platelet release reaction. Scand J Haematol Suppl 8:1–26, 1969
11. Weiss HJ, Aledort LM: Impaired platelet connective tissue reaction in man after aspirin ingestion. Lancet 2:495–497, 1967
12. Zucker MB, Peterson J: Inhibition of adenosine diphosphate-induced

secondary aggregation and other platelet functions by acetylsalicylic acid ingestion. Proc Soc Exp Biol Med 127:547–551, 1967

13. Obrien JR: Effects of salycilates on human platelets. Lancet 1:799–801, 1968
14. Evans G, Nishizawa EE, Packham MA, Mustard JF: The effect of acetylsalicylic acid (aspirin) on platelet function. Blood 30:550–563 1967
15. White JF: Effects of colchicine and vinca alkaloids on human platelets. III Influence on primary internal contraction and secondary aggregation. Am J Pathol 54:467–478, 1969
16. White JG: A biphasic response of platelets to serotonin. Scand J Haematol 7:145–151, 1970
17. Clawson CC, White JG: Platelet interaction with bacteria. I. Reaction phases and effects of inhibitors. Am J Pathol 65:367–380, 1971
18. Witkop CJ, White JG: Albinism, lipid storage by macrophages, and platelet dysfunction: A syndrome of defective membrane transport. Unpublished data
19. Born GVR: The platelet membrane and its functions. Metabolism and Membrane Permeability of Erythrocytes and Thrombocytes. Edited by E Deutsch, E Gerlach, K Moser. Stuttgart, Georg Thieme Verlag, 1968, pp 294–302
20. Day HJ, Holmsen H: Concepts of the blood platelet release reaction. Ser Haematol 4:1–27, 1970
21. Hardisty RM, Mills DCB: The platelet defect associated with albinism. Symposium on Platelets and Their Role in Hemostasis. NY Acad Sci 1971 (In press)
22. White JG: Platelet morphology. The Circulating Platelet. Edited by SA Johnson. New York, Academic Press, Inc, 1971, pp 45–121
23. Weiss HJ, Aledort LM, Kochwa S: The effect of salicylates on the hemostatic properties of platelets in man. J Clin Invest 47:2169–2180, 1968
24. Horowitz HI, Stein IM, Cohen BD, White JG: Further studies on the platelet inhibitory effect of guanadinosuccinic acid and its role in uremic bleeding. Am J Med 49:336–345, 1970
25. White JG: Platelet microtubules and microfilaments: Effects of cytochalasin B on structure and function. Platelet Aggregation. Paris, Masson et Cie, 1971, pp 15–52
26. Ball G, Fulwood M, Ireland DM, Yates P: Effect of some inhibitors of platelet aggregation on platelet nucleotides. Biochem J 144:669–671, 1969
27. Doery JCG, Hirsh J, deGrunchy GC: Aspirin: Its effect on platelet glycolysis and release of adenosine diphosphate. Science 165:65–67, 1969
28. Sahud MA, Aggeler PM: Platelet dysfunction-differentiation of a newly recognized primary type from that produced by aspirin. N Engl J Med 280:453–459, 1969
29. Weiss HJ, Chervenick PA, Zalusky R, Proctor A: A familial defect in platelet function associated with impaired release of adenosine diphosphate. N Engl J Med 281:1264–1270, 1969
30. Weiss HJ: Abnormalities in platelet function due to defects in the release reaction. Symposium on Platelets and Their Role in Hemostasis. NY Acad Sci (In press)

Incidence and Significance of Muscle Capillary Basal Lamina Thickness in Juvenile Diabetes

Victoriano Pardo, MD, Eliseo Perez-Stable, MD, David B. Alzamora and William W. Cleveland, MD

The mean minimal and average basal lamina thickness (MBLT and ABLT) of 17 to 20 muscle capillaries were measured in 26 overt juvenile diabetics and in 26 nondiabetic patients of similar age. The mean MBLT was significantly increased in diabetics although 17 of the individual values in diabetics overlapped those obtained in nondiabetics. Segmental and focal fluctuations in basement membrane width appeared to be the most important cause of variance, particularly in thick walled vessels, although multiple instrumental and technical sources of error were also present. As a result, in diabetics there was a mean variability of ±25% when measurements from two different sets of capillaries in the same subject were compared. Patients older than 12 years and diabetics with longer duration of the disease or abnormal findings on ophthalmoscopic examination exhibited a significant increase in capillary basal lamina. The mean ABLT averaged 1.8 times the mean MBLT, but the relative individual measurements as well as statistical correlations with clinical parameters were similar. Muscle capillary basement membrane hypertrophy, as quantitated by the present methods, does not seem to be an early, sensitive or consistent finding to identify individual diabetics (Am J Pathol 68:67–80, 1972).

ALTHOUGH CAPILLARY BASAL LAMINA THICKENING as a generalized phenomenon has been well established in patients with diabetes mellitus, ultrastructural studies concerning the incidence and significance of this finding have yielded conflicting results.

In a study of striated muscle capillaries, Siperstein *et al*[1] reported capillary basement membrane thickening in 98% of patients with overt diabetes mellitus and in 50% of the progeny of diabetic patients. The latter group was considered to be "genetically prediabetic," although these subjects did not present any demonstrable disturbance of carbohydrate metabolism. The lack of correlation between basal lamina hypertrophy and age or duration of disease in the overtly diabetic patients and the observation of vessel wall thickening in the genetically prediabetics suggested that diabetic microangiopathy was not related to the hyperglycemia of diabetes. This consideration is of great potential importance for our understanding of the pathogenesis

---

From the Electron Microscopy Laboratory, Veterans Administration Hospital, and the Departments of Pathology, Medicine and Pediatrics, University of Miami School of Medicine, Miami, Fla.

Supported in part by a Veterans Administration Research Grant.

Accepted for publication Jan 10, 1972.

Address reprint requests to Dr. Victoriano Pardo, Department of Pathology, Veterans Administration Hospital, 1201 NW 16th St, Miami, Fla 33125.

of the lesions and the value of control in the possible prevention of diabetic vascular disease.

Subsequent investigators have not been able to confirm Siperstein's observations. In fact, a considerable overlapping in capillary basal lamina thickness between adult overt diabetics and nondiabetics has been encountered in muscle as well as in other capillary beds.[2-5]

The present study in juvenile diabetes has attempted to clarify some of the divergent results reported in adult patients. The utilization of a younger population offers certain advantages. The effects of aging, associated diseases and prolonged periods of undetected carbohydrate intolerance would be minimized. In addition, the more explosive onset of juvenile diabetes would allow a more accurate estimation of the duration of hyperglycemia.

Materials and Methods

The patients were selected from the Diabetic and Orthopedic Clinics of Miami's Variety Children's Hospital and the Medical Wards of the Miami Veterans Administration Hospital.

The two groups consisted of: a) Twenty-six patients with juvenile diabetes mellitus: All the patients had frank clinical diabetes with onset in childhood and required insulin treatment. b) Twenty-eight nondiabetic patients: These subjects were in a similar age bracket as those in the previous group and had a variety of medical disorders. None had a family history of diabetes and fasting plasma glucose levels carried out in the SMA 12 Technicon Autoanalyzer (Tarrytown, NY) were under 110 mg/100 ml. A high-dose intravenous glucose tolerance test[6] was performed in 14 patients; the k values in all the tests were greater than 1.5 and thus considered normal.

Tissue was obtained from the vastus lateralis muscle at the anterolateral aspect of the upper third of the thigh, with a modified Vim-Silverman needle (Eisele & Co, Nashville, Tenn). Informed consent was obtained in each case previous to the procedure. Care was exercised to limit the infiltration of local anesthesic to the skin and subcutaneous tissue, far from the muscle mass to be sampled. Due to ethical limitations in obtaining muscle from nondiabetic children, autopsy material was used in 7 cases. This tissue was taken with similar technics less than 6 hours postmortem. The intact specimen was fixed in 1% osmium tetroxide in Millonig's phosphate buffer[7] at 4 C for 30 minutes, then minced into 1 mm cubes and immediately transferred to freshly prepared fixative for an additional period of 60 minutes. Dehydration and embedding in epon 812[8] were performed following a standard technic in all cases.

Semithin sections were cut in Porter-Blum MT2 ultramicrotome and stained with 1% alkaline toluidine blue to select areas containing capillaries in cross section. Thin sections were mounted on 300 mesh grids, stained with uranyl acetate and lead citrate[9] and examined in a Zeiss EM9A electron microscope (× 6000). For calibration of the instrument, a carbon replica grating, 28,800 lines per inch (EF Fullam, Inc, Schenectady, NY) was also photographed under the same conditions preceding each microscopy session. A Durst point light source enlarger (3.5 ×) was used for printing. This magnification was checked daily with a standard negative scale divided in millimeters.

Measurements of capillary basal lamina thickness were made on 17 to 20 capillaries from each patient with a 5× micrometer magnifier containing a field reticle calibrated in 0.1 mm.

The minimal basal lamina thickness (MBLT) was determined as described by Williamson *et al*;[10] 2 lines representing the minimal distance from the basal endothelial cell membrane to the outer surface of the basal lamina, at least 1 cm apart on the prints were taken for mensuration (Figure 1). Clearly tangentially cut capillaries and areas covered by pericytes were excluded. For each patient, the mean and coefficient of variation were calculated on the logarithms of the average of these two measurements and the antilogarithm of the mean designated as MBLT.

In addition, the same capillaries were also measured according to Siperstein's method[1] which utilizes a superimposed plastic sheet with 20 lines radiating from a central point (Figure 2) to measure an average basal lamina thickness (ABLT). For each patient, the mean and coefficient of variation were calculated on the logarithms of the average of 12 to 17 valid measurements in each capillary and the antilogarithm identified as ABLT.

Up to this point the biopsies had been labeled by number only; they were now identified and the clinical data tabulated. Two of the nondiabetic cases (27 and 28 in Table 2) were found to have a MBLT far outside the range of the remaining patients and were excluded from the subsequent calculations. Two additional nondiabetic patients (25 and 26 in Table 2) were added.

The following parameters were tabulated in each case: sex, age, height, duration of diabetes and insulin requirements. The presence of retinopathy was documented by microaneurysms, hemorrhages, exudates, new vessels, venous irregularities or retinitis proliferans on ophthalmoscopic examination which included fluorescein angiography.

Statistical evaluation of these results was performed by correlation analysis and analysis of variance.

A blind evaluation of the variability possibly resulting from the methodology applied to obtain individual measurements was also performed as follows: a) Estimations of MBLT were repeated at the same points of the capillary wall by the same observer at different times and by another observer at newly selected points. b) Estimations of MBLT were repeated in 10 diabetics and 10 nondiabetics, using a set of capillaries from blocks different from those previously evaluated. c) In 5 cases, MBLT measurements were compared from sets of 20 capillaries in successive serial thin sections showing silver and gold interference colors. d) Measurements were duplicated in 10 cases, estimating the MBLT with a caliper calibrated to 1/40000 inch instead of the micrometer magnifier.

Results

The individual mean values and coefficients of variation for MBLT and ABLT as well as some significant clinical parameters are presented in Tables 1 and 2. The results from the diabetic and nondiabetic groups as well as correlations with age and duration of diabetes appear in Table 3 and Text-figure 1.

Summary of Findings

Individual and group capillary basal lamina thickness (BLT) in diabetics and nondiabetics. The mean MBLT and ABLT were signif-

Table 1—Diabetics

			MBLT		ABLT			
Case	Sex	Age	Mean*	CV	Mean*	CV	Duration (yr—mo)	Eye
1	M	15	998	20.9	1599	29.1	8	
2	F	15	1310	35.3	2236	23.9	3—10	
3	M	13	872	34.1	1388	31.3	11	—
4	M	12	953	24.8	1777	44.2	2	
5	M	13	747	20.5	1276	22.2	3—4	
6	F	15	923	25.0	1434	26.2	3—6	
7	M	8	877	25.7	1988	28.5	4—6	—
8	M	7	878	15.9	1447	30.8	3	—
9	F	31	1499	59.7	2780	50.4	19	+
10	M	42	1368	36.0	2431	31.3	27	+
11	M	19	1596	35.7	3179	29.3	8	+
12	F	15	1063	30.6	1768	27.6	3—3	—
13	M	12	1304	35.9	2402	29.1	10	—
14	F	15	1389	32.2	2234	35.1	3—11	
15	M	16	1106	40.7	2311	36.6	8	+
16	M	27	1836	48.5	3712	44.3	12	
17	F	18	1190	46.5	1938	47.6	2	
18	M	23	1116	31.6	2152	42.7	20	+
19	F	24	2150	26.3	4142	27.9	21	+
20	M	42	3562	46.0	6821	22.5	26	+
21	M	27	1272	36.8	2317	35.1	15	+
22	F	16	1568	60.7	3052	40.5	4	+
23	F	10	786	37.5	1580	38.5	7	—
24	M	11	992	22.7	1607	15.3	2	—
25	M	6	972	25.4	1550	27.0	2	—
26	M	9	969	24.8	1511	19.2	2	—

Patients No. 2 and 12 are twins. Patient No. 24 is another sibling.
* Geometric means in Å.

icantly increased in diabetics in comparison to nondiabetics ($P < 0.001$), but we encountered a pronounced overlapping of individual values in the two groups. Only nine of the MBLT and six of the ABLT mensurations in diabetics were outside the nondiabetic range. There was still a significant difference between the two groups ($P < 0.002$ for MBLT and $P < 0.005$ for ABLT) if the two nondiabetic patients (27 and 28) excluded because of a markedly thick basal lamina were included in the statistical analysis.

Comparison of the results of MBLT and ABLT determinations. The mean absolute value for ABLT was higher by a factor of 1.8 than that for MBLT; nevertheless, relative results obtained with the two methods were similar and analysis of variance in respect to age, duration of diabetes and retinal changes was similar for the two methods.

Intercapillary variation. In the same subject variability in BLT between different capillaries and between segments of the capillary wall circumference in the same capillary was frequently seen and often substantial. This was particularly true for the diabetics in whom thickened vessels were occasionally encountered in juxtaposition to thin walled capillaries (Figures 1, 2). In agreement with these observations, the individual coefficients of variation were higher in diabetics than in nondiabetics ($P < 0.002$ for MBLT and $P < 0.0035$ for ABLT). This was also true of the coefficient of variation of the group of diabetics contrasted with the nondiabetics.

Effect of age on BLT in diabetic and nondiabetic patients. There was significant correlation between age and basal lamina thickness

Table 2—Nondiabetics

			MBLT		ABLT			
Case	Sex	Age	Mean*	CV	Mean*	CV	Diagnosis	GTT
1	F	4	705	23.1	1327	25.5	Pes equinus	
2	M	15	739	25.4	1291	24.2	Palsy secondary to trauma	
3	F	8	937	22.6	1662	19.1	Cystic fibrosis (a)	
4	F	2	834	18.0	1355	16.2	Dehydration (a)	
5	M	5	646	18.3	1268	26.8	Lactic acidosis	—
6	F	11	891	33.1	1723	46.8	Neisseria meningitis (a)	
7	F	2	699	19.7	1141	17.7	Hypophosphatasia	—
8	M	9	674	20.7	1172	20.7	Lipoid nephrosis	
9	F	15	1054	23.1	1682	28.6	Osteochondroma	
10	F	14	1292	26.6	2024	23.0	Mitral stenosis (a)	
11	M	12	1187	38.7	1877	23.5	Aortic & mitral lesions (a)	
12	F	5	643	12.8	1133	14.3	Lipoid nephrosis	
13	F	8	796	20.0	1380	23.1	Reye's syndrome	
14	M	13	923	25.5	1623	36.8	Sickle cell anemia (a)	—
15	F	9	733	26.2	1506	38.4	Cystic fibrosis (a)	
16	M	29	1095	31.9	1926	35.9	Astigmatism	
17	M	23	1095	25.2	1649	27.7	Astigmatism	
18	M	23	956	40.0	1926	35.4	Viral hepatitis	—
19	M	30	1070	31.9	1790	35.9	Drug addiction	—
20	M	22	1012	24.3	2202	26.4	Sarcoidosis	—
21	M	20	1051	33.1	1762	29.3	Drug addiction	—
22	M	25	904	18.8	1719	24.4	Epilepsy	—
23	M	22	854	24.8	1695	33.6	Viral hepatitis	—
24	M	23	1119	27.0	2309	16.8	Chronic hepatitis	—
25	M	29	766	26.0	1508	39.1	Malaria	—
26	M	49	1020	28.9	1966	31.2	Upper GI bleeding	—
27	M	27	1480	27.4	2750	26.1	Obesity, heart block	—
28	M	14	1981	25.2	3168	19.2	Kearns Sayre syndrome	—

* Geometric means in Å.

(Table 3). Upon examination of the scattergram of MBLT plotted against age in diabetics and nondiabetics, two subgroups became apparent if age 13 was taken as an arbitrary dividing line (Text-figure 1). The difference between the means of younger and older diabetics was significant ($P < 0.02$) as was the case between younger and older nondiabetics ($P < 0.001$). But, although the mean for the young diabetics was significantly higher than that for the young nondiabetics ($P < 0.02$), only 1 diabetic was outside the range for the nondiabetic group. There was no difference in mean thickness when the young diabetic subgroup was compared with the older nondiabetics.

Effect of duration of diabetes on BLT. There was a positive correlation of BLT and duration of disease (Table 3). In addition, the mean MBLT of patients with 5 or more years of diabetes was significantly higher ($P < 0.001$) than that of patients affected for less than 5 years.

Correlation between eyeground pathology and BLT. The mean BLT of diabetics who had any abnormality on ophthalmoscopic examination was significantly higher than that of nondiabetics ($P < 0.001$ for both MBLT and ABLT). Only one of the diabetics exhibiting normal eyeground findings had a MBLT outside the nondiabetic range.

There was no correlation of any of the remaining clinical parameters with capillary changes.

Evaluation of the Technical Reproducibility of Individual Measurements

Fluctuations in magnification of the electron microscope. Forty-five prints from replicas taken during each of the microscopy sessions

Table 3—Results from Diabetic and Nondiabetic Groups and Their Correlation coefficients

	MBLT		ABLT	
	Diabetics	Nondiabetics	Diabetics	Nondiabetics
Results (Å)				
Mean	1280	911	2332	1639
SD	±573	±168	±1170	±319
CV	44	18	50	19
Range	747–3562	643–1292	1276–6921	1133–2359
Correlation coefficient				
Age/thickness				
r =	.73	.50	.712	.623
P<	0.001	0.05	0.001	0.001
Duration diabetes/thickness				
r =	.659	—	.679	—
P<	0.001	—	0.001	—

of the study had a mean magnification of 21210 X (±660 SD). Thus, there was a mean variation in the precision of ±3.2%.

Comparison of measurements with a caliper and an ocular magnifier. The capillaries of 10 cases selected at random exhibited a mean MBLT difference of 50 Å between readings obtained with an ocular micrometer and those with a caliper.

Variation resulting from repeated measurements. A second set of measurements was performed a few days after the original ones by the same observer using the same reference points in all the capillaries. There was a mean MBLT difference between both readings of 53 Å (±112 SD) for the diabetics and 63 Å (±47 SD) for the nondiabetics. When another observer repeated the mensuration without reference to the previously selected points in the vessel circumference there was a mean MBLT difference of 137 Å (±67 SD) for the diabetics and 93 Å (±53 SD) for the nondiabetics.

Differences between the first set of 20 capillaries originally evaluated and a second set from different blocks on the same biopsy. Ten diabetics and ten nondiabetics were selected at random. The mean differences between both sets were 334 Å (±523 SD) for the diabetics and 131 Å (±109 SD) for the nondiabetics.

Comparison of thin sections with silver and gold interference colors. In five cases 20 capillaries from alternate serial silver and gold sections were evaluated. The mean MBLT was 5 Å higher in the thicker sections.

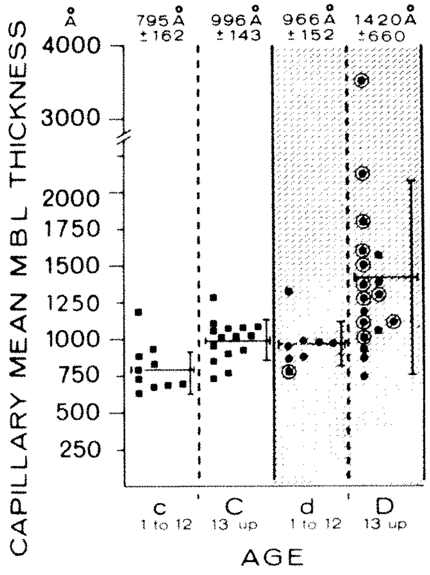

TEXT-FIG 1—Scattergram of mean minimal basal lamina thickness (MBLT) measurements in which nondiabetic (c-C) and diabetic (d-D) patients have been divided into two subgroups according to age. Diabetic patients with more than 5 years duration of the disease are represented by a circle. Values at the top of the columns correspond to mean and standard deviations for each subgroup.

Discussion

Any analysis of the significance of muscle capillary basal lamina thickness must take into consideration the technical factors which limit the precision of measurements. Yodaiken *et al*[2] reported a detailed study of this aspect of the problem. Through careful standardization, variability related to methods of tissue processing and sectioning, as well as conditions influencing instrument magnification, may be kept within a ± 10% range within the same laboratory.

The method used to estimate capillary basal lamina thickness in electron micrographs has been considered an important source of the divergent results obtained. The determination of an average basal lamina thickness based on multiple radial measurements of the capillary wall as proposed by Siperstein *et al*[1] includes false high readings resulting from tangentially cut areas. To avoid this artifact, Williamson *et al*[10] measured the two minimal basal lamina thickness values, a simpler method which produced a narrower coefficient of variation, with an apparent increase in sensitivity. In our hands, although the ABLT values were an average of 1.8 times higher than the MBLT readings, the clinicopathologic correlations and the analysis of variance were similar by either method. These findings suggest that other elements may play important roles in the observed differences.

Two unavoidable causes of error by either method are the segmental and local fluctuations in capillary basal lamina width, which were more obvious in the diabetic group. These were evidenced by the presence of thick- and thin-walled capillaries in the same section of some patients, the different estimates obtained from different sets of capillaries in the same muscle sample and the increased coefficient of variation of patients with thicker capillaries. The occurrence of such focal basement membrane lesions is well documented in glomerular and retinal vessels[11] in diabetes.

Furthermore, the observer bias in defining the limits of the basal lamina, the angle of the measured line in relation to the capillary wall or the points of the wall selected for mensuration, was reflected in a mean MBLT variation of 50 Å when measurements were repeated at different times, even by the same observer.

Finally, criteria for the selection of the "control" nondiabetic population are difficult to establish with precision. Family histories of diabetes may be unreliable and the interpretation of glucose tolerance tests equivocal. Also, thickening of the basal lamina has been recorded previously in several other diseases.[12,13] Thus, it is appreciated that the values for our nondiabetic group are probably higher than those which could be obtained from healthy control subjects. In this respect, it may be of interest that 2 nondiabetic patients exhibiting high capillary BLT had been in heart failure for prolonged periods of time, an observation which is consonant with the reported relation between the level of hydrostatic pressure and capillary wall width in muscle samples from different regions.[14]

Due to these cumulative errors, it seems reasonable to conclude that the reproducibility of individual mean vessel wall thickness has at least a ± 10 to 20% variability in many subjects and the ability of the present methods to distinguish small differences is limited. Therefore, our results, as well as those of others,[2,3] do not indicate that discrete changes in capillary basement membrane width are sufficient to establish the presence of early diabetic microangiopathy. Even in our group of 26 overt diabetics, we found that mean individual MBLT and ABLT values overlapped with those of nondiabetics in 17 and 20 patients respectively. Although the mean MBLT and ABLT of the diabetic group was significantly higher than that of the nondiabetic, basement membrane hypertrophy does not appear to be a sensitive and consistent finding in the identification of individual diabetics.

In contrast to those studies which failed to establish a relationship between age and basal lamina thickness (BLT),[1,2] our results are in agreement with reports of a significant positive correlation between age and BLT in both diabetics and nondiabetics.[3,15] The age-related differences were more apparent in our patients when age 13 was taken as an arbitrary dividing line. This age may distinguish prepuberal from adolescent subjects. An influence of the age of onset of diabetes on the incidence of retinopathy has been encountered in a long term study of children with puberal and prepuberal onset of the disease.[16]

If capillary BLT is influenced by age, it is conceivable that age-related thickening may be misinterpreted as early microangiopathy when this factor is not taken into consideration. This possibility is supported by the similar mean BLT encountered in our study for the older nondiabetics and young diabetics.

The statistically significant correlation of increased BLT and duration of diabetes, as well as the difference between the means of patients 5 or less years of duration and those with more than 5 years, favor the concept that identifiable vessel involvement is a late event which appears only after a prolonged period of disturbance in carbohydrate metabolism. Studies on kidney glomerular capillaries have also failed to uncover early lesions in diabetes.[17,18] Yet, the degree of control of the diabetes did not appear to influence the vascular changes and other genetic or metabolic factors may be responsible for suceptibility to diabetic microvascular abnormalities.

The close association between increased capillary BLT and diabetic retinopathy favors the assumption that the diabetic lesions are disseminated, although functional manifestations may be absent. A similar relationship has been encountered by Yanoff in a histologic study of retinal and glomerular capillaries.[19]

References

1. Siperstein MD, Unger RH, Madison LL: Studies of muscle capillary basement membranes in normal subjects, diabetic, and prediabetic patients. J Clin Invest 47:1973–1999, 1968
2. Yodaiken RE, Seftel HC, Kew MC, Lillestein M, Ipp E: Ultrastructure of capillaries in South African diabetics. II. Muscle capillaries. Diabetes 19:164–175, 1970
3. Williamson JR, Kilo C: Basement membrane thickening and the mystery of diabetes. Hosp Pract 6:109–117, 1971
4. Pardo V, Perez-Stable E, Fisher ER: Electron microscopic study of dermal capillaries in diabetes mellitus. Lab Invest 15:1994–2005, 1966
5. Yodaiken RE, Seftel HC, Rubenstein AN: Ultrastructure of dermal capillaries of Africans in South Africa. Diabetes 16:191–197, 1967
6. Dyck DR, Moorhouse JA: A high-dose intravenous glucose tolerance test. J Clin Endocrinol 26:1032–1038, 1966
7. Millonig G: Further observations on a phosphate buffer for osmium fixation. Proceedings of the Fifth International Congress for Electron Microscopy, Vol 2. Edited by SS Breese Jr. New York, Academic Press, Inc, 1962, p 8
8. Luft JH: Improvements in epoxy resin embedding methods. J Biophys Biochem Cytol 9:409–414, 1961
9. Venable JH, Coggeshall RA: A simplified lead citrate for use in electron microscopy. J Cell Biol 25:407–408, 1965
10. Williamson JR, Vogler NJ, Kilo C: Estimation of vascular basement membrane thickness: Theoretical and practical considerations. Diabetes 18:567–578, 1969
11. Bloodworth JMB: Ultrastructural aspects of human and canine diabetic retinopathy. Vascular Disorders of the Eye. Edited by JW Bettman. St Louis, CV Mosby Co, 1966, p 68
12. Gonzalez AA, Fraga A, Mintz G: Submicroscopic alterations in capillaries of skeletal muscles in polymyositis. Am J Med 45:873–879, 1968
13. Norton WL, Hurd E, Lewis D, Ziff M: Peripheral microvascular injury in scleroderma and systemic lupus erythematosus. Pan American Congress of Rheumatology, Vol 143, Excerpta Medica International Congress Series. p 154, Mexico, DF, 1967
14. Williamson JR, Vogler NJ, Kilo C: Regional variations in the width of the basement membrane of muscle capillaries in man and giraffe. Am J Pathol 63:359–367, 1971

15. Fuchs U, Scharnweber W: Elektronenmikroscopische Untersuchungen an Skeletmuskelcapillaren des Menschen bei Arteriosklerose und Diabetes Mellitus. Virchows Arch 343:276–285, 1968
16. Laws HW, Harpur ER, Belmonte MM, Adams KW: Long term study of retinal changes in the prepuberty and puberty onset of diabetes. Can J Ophthalmol 1:104–111, 1966
17. Fisher ER, Perez-Stable E, Amidi M, Sarver ME, Danowski TS: Ultrastructural renal changes in juvenile diabetes. JAMA 202:291–295, 1967
18. Hansen RO: Discussion on microangiopathy papers. Advances in Metabolic Disorders, Suppl 1, Early Diabetes. Edited by RA Camerini-Davalos, HS Cole. New York, Academic Press, Inc, 1970, p 288
19. Yanoff M: Diabetic retinopathy. N Engl J Med 274:1344–1349, 1966

Acknowledgments

The authors are grateful to Drs. Olga Ferrer and Edward W. D. Norton for the ophthalmologic examination of the patients included in this study. Excellent technical assistance was given by Mrs. Ceferina Amado, Mrs. Merle Arostegui and Mrs. Lutgarda Sanchez.

[*Illustrations follow*]

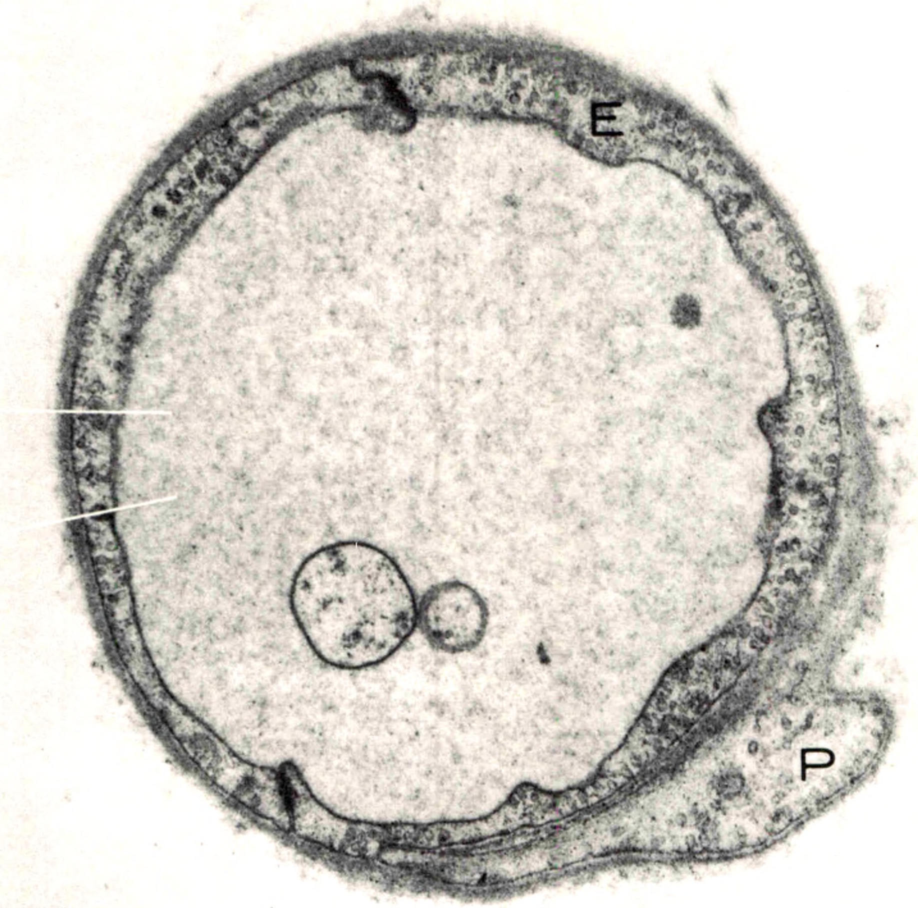

Fig 1—Thin walled capillary in diabetic patient No. 20. The portions of the white lines intersecting the basal lamina were measured for the minimal basal lamina thickness (MBLT). *E*, endothelium; *P*, pericyte (× 22,000).

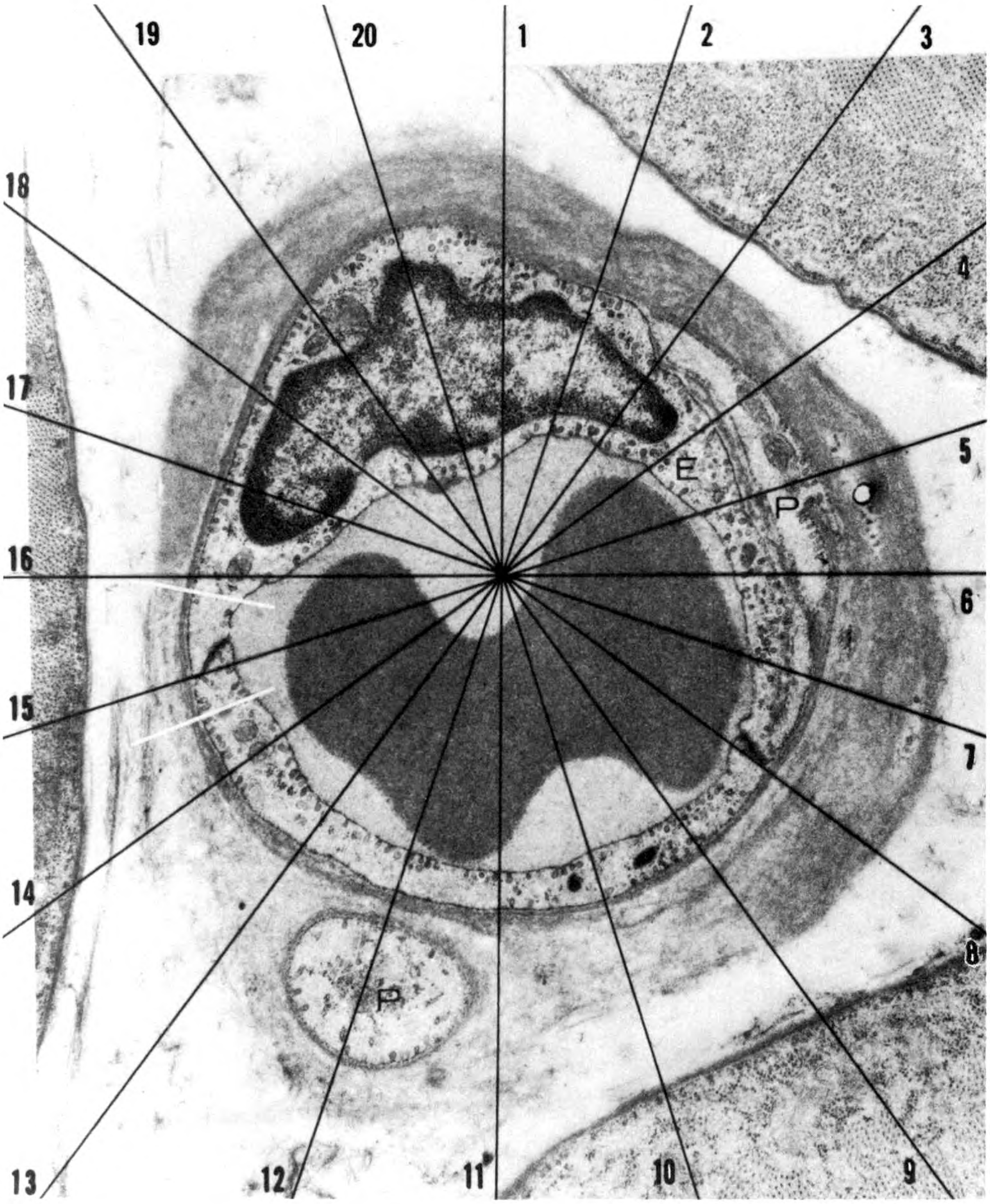

Fig 2—Capillary from the same thin section used for Figure 1. The two white lines represent the location of measurements for the MBLT. A plastic sheet with the lines on which average basal lamina thickness (ABLT) was determined has been superimposed on the picture. Notice the segmental variations of the thick basal lamina and the vague outer contours in some areas. *E*, endothelium; *P*, pericyte (× 14,700).

The Cellular Pathology of Experimental Hypertension

VI. Alterations in Retinal Vasculature

Filiberto Giacomelli, MD, Kenneth B. Juechter, MD and
Joseph Wiener, MD

The ultrastructure of retinal arterial vessels from rats with severe renal hypertension has been studied. The permeability of retinal vessels has also been examined by means of vascular labeling technics utilizing horseradish peroxidase and microperoxidase as tracer substances. Small retinal arteries and arterioles exhibit foci of smooth muscle necrosis characterized initially by fragmentation of medial smooth muscle cells, and subsequently by loss of myofilaments and release of free vesicles, vacuoles and other cytoplasmic organelles extracellularly. Evidence for increased permeability is observed occasionally in retinal capillaries and less frequently in arteries and arterioles. The enzymatic tracers penetrate the tight junctions of the endothelial cells and are found in the basement membranes adjacent to endothelial and smooth muscle cells, as well as in expanded extracellular spaces around the capillaries. The alterations in the ultrastructure and permeability of retinal vessels in experimental hypertension have been compared with that of visceral and cerebral cortical vessels (Am J Pathol 68:81–96, 1972).

PATHOLOGIC ALTERATIONS in the retinal vasculature[1] and an increase in its permeability, as demonstrated by fluorescein angiography,[2–4] are prominent features of severe hypertension in man. However, the literature concerning morphologic changes of the retinal vessels in animals with experimental hypertension is limited. Hyperplastic changes, characterized by the proliferation of smooth muscle cells, have been demonstrated in the retinal arterioles of rats with spontaneous hypertension.[5] Areas of constriction and dilatation have been observed opthalmoscopically in the retinal arteries of rats with renal hypertension.[6,7] Furthermore, the accumulation of PAS-positive material within dilated segments of the vasculature has also been described,[7] suggesting that these retinal vessels may be sites of increased permeability. Such a possibility is further supported by studies indicating that visceral and cerebral arterial vessels from animals with

---

From the Departments of Pathology and Ophthalmology, New York Medical College, New York, NY.

Supported in part by Grant HE 13742-01 from the National Institutes of Health of the US Public Health Service.

Accepted for publication Jan 19, 1972.

Address reprint requests to Dr. Filiberto Giacomelli, Department of Pathology, Laboratory of Experimental Pathology, New York Medical College, Flower and Fifth Avenue Hospitals, Fifth Ave at 106th St, New York, NY 10029.

experimental hypertension exhibit morphologic alterations that correlate with increased permeability.[8-11]

The ultrastructure and permeability of retinal vessels from rats with severe renal hypertension has been examined in the present study. Ultrastructural changes in the wall of these vessels are described. Vascular labeling technics applied at the cellular level disclose an increase in the permeability of the endothelial cell junctions of small arteries, arterioles and capillaries.

Materials and Methods

Hypertension was produced in 100-g male Columbia Sherman rats by partially constricting the left renal artery with a silver wire clip. Weekly measurements of systolic blood pressure were made on both hypertensive and control animals.[12] Only hypertensive rats with systolic pressures greater than 200 mmHg were utilized in this study. All of these animals exhibited weight loss and convulsive episodes.

Animals were sacrificed after periods of hypertension ranging from 2 to 8 weeks. Three control and five hypertensive animals were injected intravenously with horseradish peroxidase (HRP) Type II (Sigma Chemical Co, St Louis, Mo), dissolved in physiologic saline in the amount of 20 mg/100 g body weight. One control and one hypertensive rat received microperoxidase (MP) (courtesy of Dr. Ned Feder, National Institutes of Health) in the same dosage.[13]

Both eyes were enucleated, the right prior to the left, after intervals of 5 to 30 minutes. The lateral canthus was incised, Tenon's capsule grasped with forceps, and the eye elevated in its socket. The eye was then enucleated with a scalpel and immersed in a formaldehyde–gluteraldehyde mixture. The globe was opened coronally with iris scissors along the ora serrata under a dissecting microscope, and the posterior pole exposed to fresh fixative for 30 minutes. The retina was cut into 2-mm thick strips, parallel to the long axis of the vessels, and fixed for an additional 3 hours. The tissues were washed several times with buffer and stored overnight in the cold. The choroid was gently separated from the sclera and thin blocks incubated for 30 to 60 minutes in a Tris buffer (pH 7.6) containing 3, 3′-diaminobenzidine tetrahydrachloride and hydrogen peroxide.

The tissue was then postfixed in phosphate-buffered (pH 7.6) 2% osmium tetroxide, dehydrated in acetone and embedded in Araldite. Sections (2 μ thick) were cut from the plastic embedded material and examined by phase contrast microscopy in order to identify the vessels in the various layers of the retina. Thin sections of selected vessels were cut, stained with lead citrate and examined with a Philips EM 200 or Siemens Elmiskop IA electron microscope.

Results

Light Microscopic Observations

The different layers of the retina are readily discernible by phase contrast microscopy. Small arteries and arterioles are visible in the nerve fiber and ganglion cell layers (Figure 1). A capillary network is present between the inner nuclear and outer plexiform layers. Examination of the retinal vasculature in hypertensive animals discloses no apparent areas of constriction or dilatation; however, the walls of small arteries and arterioles are thickened (Figure 2) compared to the controls (Figure 1).

Electron Microscopic Observations

Control Animals

The retinal arterial vessels have an outer diameter of approximately 10 to 25 μ. The ultrastructure of retinal arterial vessels and capillaries is essentially similar to that previously described,[14-16] except for the presence of a barely discernible discontinuous layer of elastic tissue in the subendothelial space of small arteries (Figure 3). Up to 30 minutes after injection the reaction product in animals receiving HRP or MP is mainly confined to the lumens of small arteries and arterioles (Figures 3–5). The tracers penetrate the luminal portions of the clefts between endothelial cells only up to the region of the tight junction (Figure 5). A few pinocytotic vesicles at the luminal aspects of the endothelial cells also contain HRP or MP. A similar distribution of reaction product is seen in the capillaries and venules in the deeper layers of the retina.

Hypertensive Animals

Ultrastructural alterations in hypertensive animals are found primarily in small arteries, although similar but less extensive changes are occasionally found in arterioles. There is fragmentation of medial smooth muscle cells over distances measuring 5 to 20 μ in length (Figure 6). Occasionally, these regions of medial necrosis are very extensive and involve both sides of the vessel wall in longitudinal section (Figure 7). In these areas the media is composed of irregularly shaped smooth muscle cell fragments of variable size with the usual complement of cytoplasmic organelles (Figures 8–11). Some of the smooth muscle cells adjacent to these areas show invaginations of the plasma membrane that partially or almost entirely sever portions of cytoplasm from the bulk of the cell mass. Lying extracellularly near the fragments of smooth muscle cell cytoplasm are vesicles, vacuoles, electron-dense granules, multivesicular bodies, myelin figures and variable amounts of reduplicated basement membranes in the subendothelial space as well as media (Figures 9–11).

Many endothelial cells of arterial vessels have increased numbers of mitochondria and increased amounts of rough surfaced endoplasmic reticulum. The luminal portions of endothelial cells often contain sarcomere-like arrays[17] of filaments (Figure 12). These endothelial cell changes are observed in segments of arterial vessels both adjacent to and remote from foci of medial necrosis.

Rare arterioles and small arteries in the retinas of hypertensive animals exhibit reaction product in both the luminal and basal portions of the clefts between endothelial cells (Figures 13, 14). The peroxidase filling the basal portions of the clefts is sometimes continuous with that staining endothelial basement membranes. Where a cleft can be examined in a single plane of section from luminal to basal aspects, peroxidase penetrates the tight junctions and may be seen throughout its entire length (Figure 14). Dense deposits of reaction product are also visible in the subendothelial space and along the basement membranes surrounding smooth muscle cells. Penetration of the vessel walls by the tracers is seen in vessels with and without foci of medial necrosis.

Occasional capillaries in the deeper layers of the retina contain peroxidase reaction product not only in their lumina but also throughout the entire length of the intercellular endothelial clefts and along basement membranes adjacent to endothelial and perivascular cells. (Figures 15, 16). Furthermore, the enzymes penetrate between cellular processes of the outer plexiform and inner nuclear layers (Figure 15). In such areas there is a noticeable expansion of the extracellular spaces. The number and luminal distribution of pinocytotic vesicles containing HRP or MP in the endothelium lining small arteries, arterioles and capillaries in the retinas from hypertensive animals does not differ appreciably from that in the controls.

Discussion

In the present study small retinal arteries and arterioles of rats with severe renal hypertension exhibit areas of smooth muscle necrosis of varying extent. Portions of individual smooth muscle cells are separated from the remainder of the cytoplasm by progressive invagination of the plasma membrane, eventually resulting in detachment of cell fragments from the cell body. There is a subsequent loss of myofilaments and release of the vesicles, vacuoles and other organelles extracellularly. These changes are associated with the appearance in such areas of reduplicated basement membranes.

The foci of medial necrosis appear to constitute a pathologic entity distinct from vascular hyalinosis. The ultrastructural difference is great, for hyalin consists of granular electron-dense deposits of material that are formed by the fusion and confluence of reduplicated layers of basement membranes that replace smooth muscle cells to a variable extent.[18] Although reduplicated basement membranes are found in the foci of medial necrosis, their occurrence is not associated with retinal arteriolar hyalinosis. However, the occurrence of reduplicated basement membranes in these lesions does suggest a possible pathogenetic relationship between cell necrosis and basement membrane reduplication. Similar foci of medial necrosis have previously been seen in the middle cerebral arteries of rats with experimental renal hypertension,[19] in the renal, coronary and meningeal arterial vessels of rats with four different types of experimental hypertension (renal, adrenal regeneration, steroid-induced and salt),[20] as well as in renal biopsy material from patients with hypertension and chronic renal disease.[21] Capillary basal lamina thickening in skeletal muscle has been ascribed to endothelial cell death and replacement.[22]

Evidence for increased retinal vascular permeability in rats with severe hypertension is observed occasionally in capillaries and even less frequently in arteries and arterioles. Increased permeability is manifested by penetration of the tight junctions of the endothelial cells of such vessels by both HRP and MP, leading to the staining of basement membranes adjacent to the endothelial and smooth muscle cells, and the passage of both tracers into expanded extracellular spaces around the capillaries. Since the tight junctions of the endothelial cells of the retinal vasculature are impermeable to HRP and MP in the control animals, their penetration by the enzymatic tracers in the hypertensive state indicates that they are the sites of increased permeability. The vesicular mechanism for permeability does not appear to play a role in the retina, since there is no appreciable change in either the number or luminal location of the pinocytotic vesicles within the endothelium. This observation stands in contrast to the permeability properties of the aorta,[23] and visceral [9,11] and cerebral cortical [10] arterial vessels in hypertension, where both transendothelial and intercellular transport have been implicated. The increase in vascular permeability in retina also differs from that in other regions by being more limited in extent and involving capillaries as well as arterial vessels.

The mechanisms responsible for the medial degeneration and altered permeability of vessels in the hypertensive state are not known. Elevated hydrostatic pressure, perhaps mediated by the renin-angiotensin system, as well as nonpressor permeability factors of renal origin may be involved.[24–26] There is evidence that the vasoactive agent angiotensin acts directly on the vascular wall,[27] binding to the nuclei of endothelial and smooth muscle cells [28] or endothelial cell plasma membranes.[29] Treatment with vasodilator and/or vasoconstrictor agents can also produce necrosis of medial smooth muscle cells in arterial vessels.[30] The foci of medial necrosis represent potential or actual *loci minoris resistentiae.* Impaired contractility in conjunction with increased intraluminal pressure could expose precapillary–capillary vessels to abnormally high pressures, with a resultant breach of the blood–retinal barrier. A somewhat similar explanation has been offered for the occurrence of renal vascular lesions in steroid-induced hypertension.[31] The cross-striated arrays of filaments found in the endothelial cells of retinal arterial vessels are identical to arrays of filaments observed in the endothelium lining cerebral cortical arterial vessels.[17] It has previously been suggested that such filament arrays could represent the structural templates for endothelial contraction, and facilitate the passage of substances of low molecular weight.

The relationship between the retinal vascular lesions in the experimental animal and hypertensive retinopathy in man is speculative. Arteriolar necrosis [1] and increased permeability of retinal arterial and capillary vessels [2–4] are, however, prominent features of severe hypertension, and it is anticipated that further investigation of experimental retinopathy will lead to a better definition of the human disease.

References

1. Leishman R: The eye in general vascular disease. Br J Ophthalmol 41:641–701, 1957
2. Dollery CT, Hodge JV, Engel M: Studies of the retinal circulation with fluorescein. Br Med J 2:1210–1215, 1962
3. Hodge JV, Dollery CT: Retinal soft exudates. A clinical study by colour and fluorescence photography Q J Med 33: 177–131, 1964
4. Dollery CT, Ramalho PS, Paterson JW: Retinal vascular alterations in hypertension, antihypertensive therapy. Principles and Practice. An International Symposium. Edited by F Gross, SR Naegeli, AH Kirkwood. New York, Springer-Verlag, 1966, pp 152–163
5. Watanabe J: Ultrastructure of the retinal arterioles in spontaneously hypertensive rats. Acta Soc Ophthalmol Jap 74:999–1011, 1970
6. Byrom FB: The nature of malignancy in hypertensive disease. Evidence from the retina of the rat. Lancet 1:516–520, 1963
7. Nakazawa T: Studies on the changes in the retinal vessels of the rat with experimental renal hypertension. Acta Soc Ophthalmol Jap 73:417–432, 1969
8. Jellinek H, Nagy Z, Hüttner I, Bálint A, Kóczé A, Kerényi T: Investigations of the permeability changes of the vascular wall in experimental malignant hypertension by means of a colloidal iron preparation. Br J Exp Pathol 50:13–16, 1969

9. Wiener J, Lattes RG, Meltzer BG, Spiro D: The cellular pathology of experimental hypertension. IV. Evidence for increased vascular permeability. Am J Pathol 54:187–207, 1969
10. Giacomelli F, Wiener J, Spiro D: The cellular pathology of experimental hypertension. V. Increased permeability of cerebral arterial vessels. Am J Pathol 59:133–159, 1970
11. Suzuki K, Ookawara S, Ooneda G: Increased permeability of the arteries in hypertensive rats: an electron microscopic study. Exp Mol Pathol 15:198–208, 1971
12. Spiro D, Lattes RG, Wiener J: The cellular pathology of experimental hypertension. I. Hyperplastic arteriolarsclerosis. Am J Pathol 47:19–49, 1965
13. Feder N: Microperoxidase. An ultrastructural tracer of low molecular weight. J Cell Biol 51:339–343, 1971
14. Hogan MJ, Feeney L: The ultrastructure of the retinal blood vessels. I. The large vessels. J Ultrastruct Res 9:10–28, 1963
15. Hogan MJ, Feeney L: The ultrastructure of the retinal vessels. II. The small vessels. J. Ultrastruct Res 9:29–46, 1963
16. Hogan MJ, Feeney L: The ultrastructure of the retinal vessels. III. Vascular-glial relationships. J Ultrastruct Res 9:47–64, 1963
17. Giacomelli F, Wiener J, Spiro D: Cross-striated arrays of filaments in endothelium. J Cell Biol 45:188–192, 1970
18. Wiener J, Spiro D, Lattes RG: The cellular pathology of experimental hypertension. II. Arteriolar hyalinosis and fibrinoid change. Am J Pathol 47:457–485, 1965
19. Kojimahara M, Ooneda G: Electron microscopic study on the middle cerebral artery lesions in hypertensive rats. Acta Pathol Jap 20:309–408, 1970
20. Takebayashi S: Ultrastructural studies on arteriolar lesions in experimental hypertension. J Electron Microsc 19:17–31, 1970
21. Takebayashi S, Themann H, Manitz G, Giese W, Backwinkel K-P: Ultrastructural study of arteriolar lesions in human kidney: concerning the histogenesis of hyaline necrosis and other media-alterations. Beitr Pathol Bd 144:1–22, 1971
22. Vracko R, Benditt EP: Capillary basal lamina thickening. The relationship to endothelial cell death and replacement. J Cell Biol 47:281–285, 1970
23. Huttner I, More RH, Rona G: Fine structural evidence of specific mechanism for increased endothelial permeability in experimental hypertension. Am J Pathol 61:395–412, 1970
24. Asscher AW, Anson SG: A vascular permeability factor of renal origin. Nature (Lond) 198:1097–1098, 1963
25. Yasamura A: Experimental studies on the role of a vascular permeability factor of kidney cortex in the pathogenesis of vascular lesions. Jap Circ J 31:1457–1473, 1967
26. Murakami M, Sekimoto H, Yasuda Y, Masuda S, Yasumura A, Nagai T: On vasuclar permeability factor from the kidney cortex. Jap Heart J 9:461–472, 1968
27. Khairallah PA, Page IH, Bumpus FM, Türker RK: Angiotensin tachyphylaxis and its reversal. Circ Res 19:247–254, 1966
28. Robertson AL Jr, Khairallah PA: Angiotensin. II. Rapid localization in nuclei of smooth and cardiac muscle. Science 172:1138–1139, 1971

29. Richardson JB, Beaulnes A: The cellular site of action of angiotensin. J Cell Biol 51:419–432, 1971
30. Kóczé A, Bálint A, Nagy Z, Hintalin A, Jellinek H: The role and significance of vasodilatation in the development of small arterial lesions in the rat. Angiologica 7:374–380, 1970
31. Hill GS, Heptinstall RH: Steroid-induced hypertension in the rat. A microangiographic and histologic study on the pathogenesis of hypertensive vascular and glomerular lesions. Am J Pathol 52:1–40, 1968

Acknowledgments

The authors wish to acknowledge with thanks the critical evaluation of Dr. Alden V. Loud and Dr. Milton Best, as well as the contribution of Mr. James J. Rooney. The technical assistance of Mrs. Maria Demeri, Mr. Alfred E. Revzin and Mr. Osmay Yalis is greatly appreciated. Mrs. Elsa Morales typed the manuscript.

Legends for Figures

Fig 1 and 2—Phase contrast micrographs of approximately 2μ thick sections of retina from control and hypertensive animals, respectively, that were injected intravenously with HRP. Sections were incubated in a medium appropriate for producing a black reaction product at sites of peroxidase activity. The surface of the retina lies at the top. Small arterial vessels are present in the nerve fiber and ganglion cell layers. A capillary network is seen between the inner nuclear and outer plexiform layers. The walls of the arterial vessel in the retina of the hypertensive animal are thickened *(arrow)* (× 150).

Fig 3—Elastic tissue *(arrows)* is interposed between endothelial and medial smooth muscle cells. The pinocytotic vesicles in the endothelium are virtually devoid of MP (× 12,000).

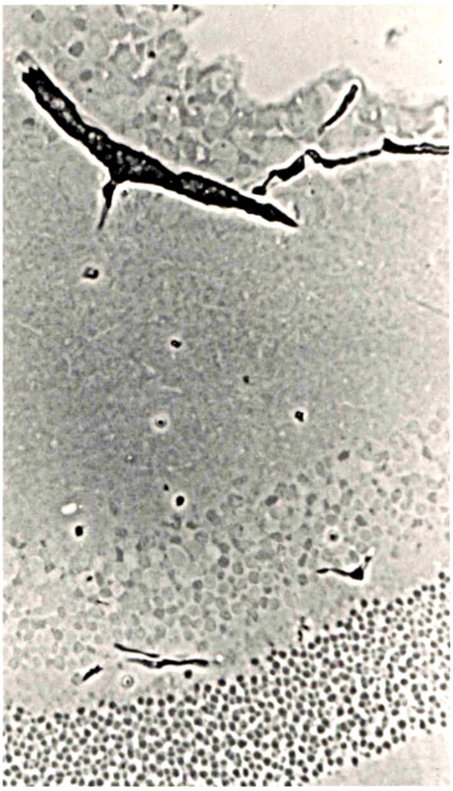

1

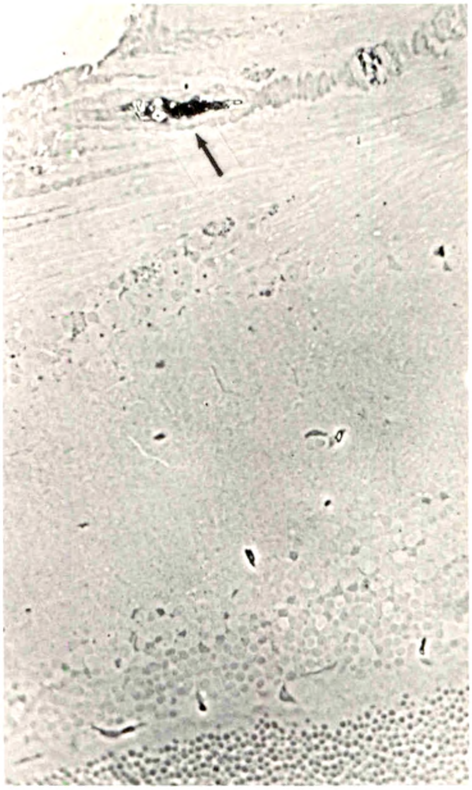

2

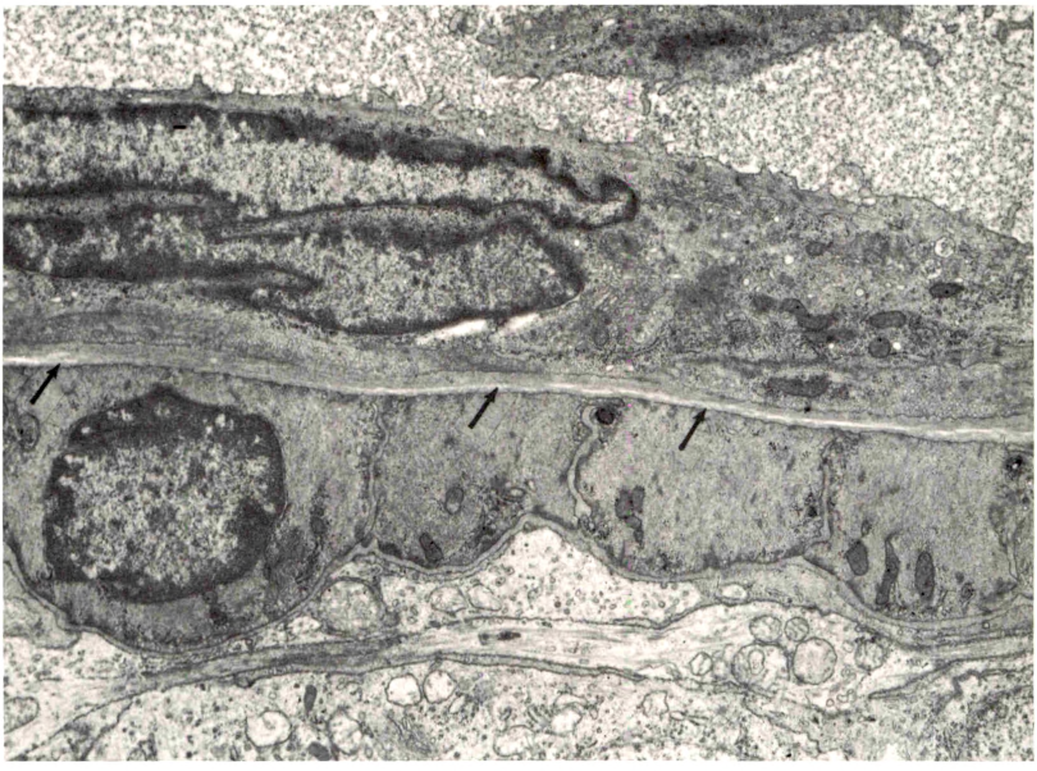

3

Fig 3–5 are electron micrographs from control animals injected intravenously with vascular tracers.

4

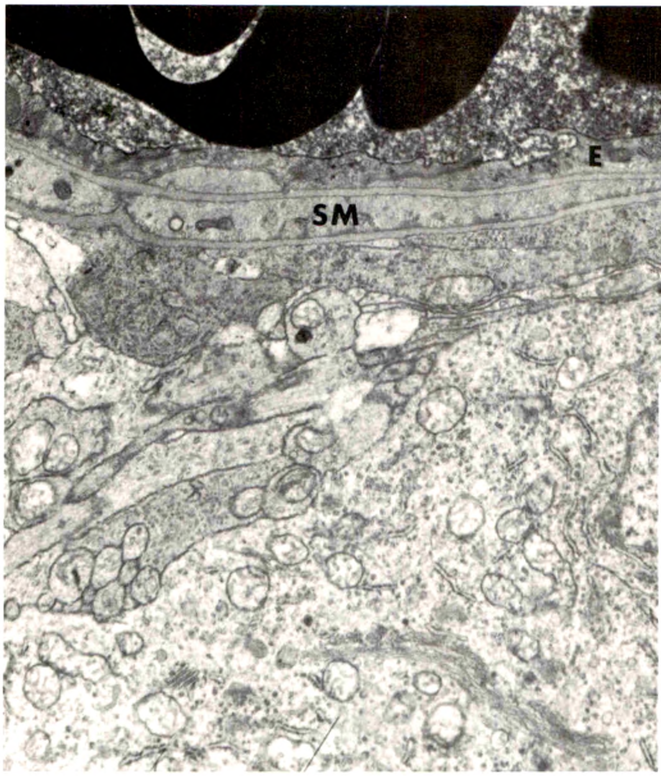

5

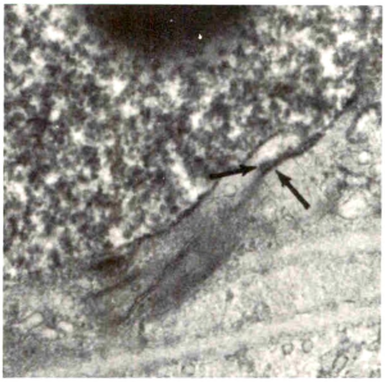

6

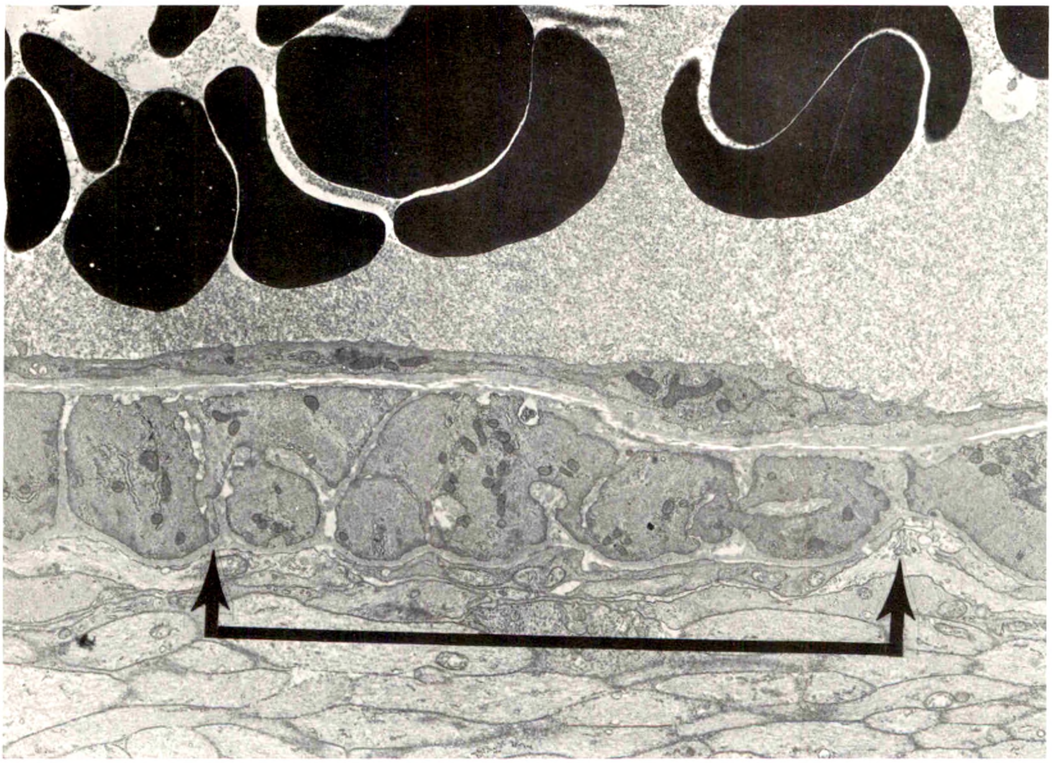

Fig 4—Micrograph of retinal arteriole. HRP is confined to the lumen of this vessel. No elastic tissue is discernible between the endothelium (*E*) and smooth muscle cells (*SM*) (× 10,000). **Fig 5**—Reaction product is visible in the lumen of this arteriole. HRP also penetrates the luminal portion of the cleft between endothelial cells up to the region of the tight junction (*arrows*) (× 37,000). **Fig 6**—Early stage of fragmentation of smooth muscle cells in the wall of a small artery is delimited by *arrows* (MP-injected, × 6000).

Fig 6–14 are electron micrographs of retinal arterial vessels from hypertensive animals.

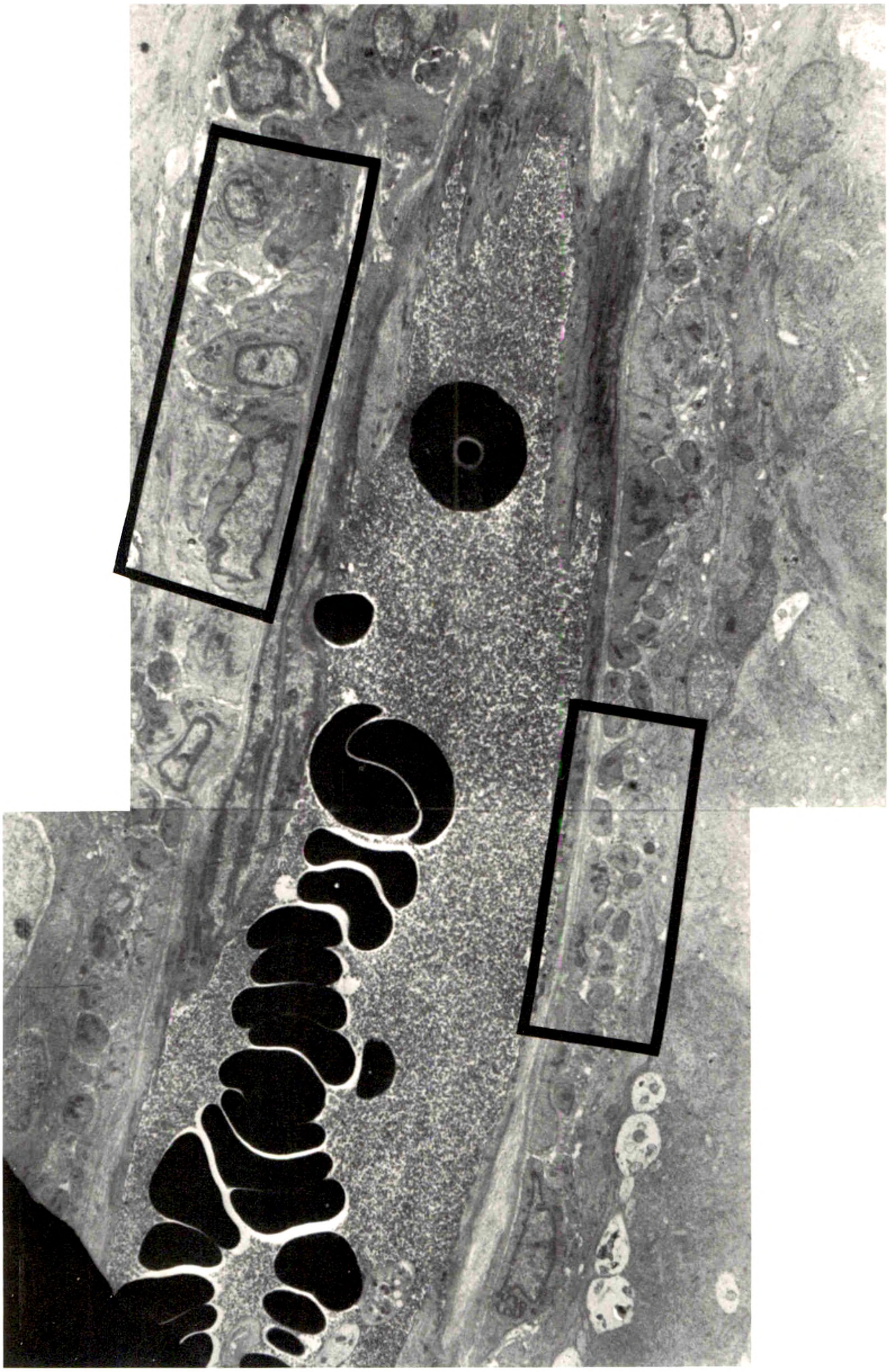

Fig 7—Composite micrograph of small artery showing extensive medial alterations. Fragmentation of smooth muscle cells is most apparent in the areas enclosed by rectangles (HRP-injected, × 3000).

8

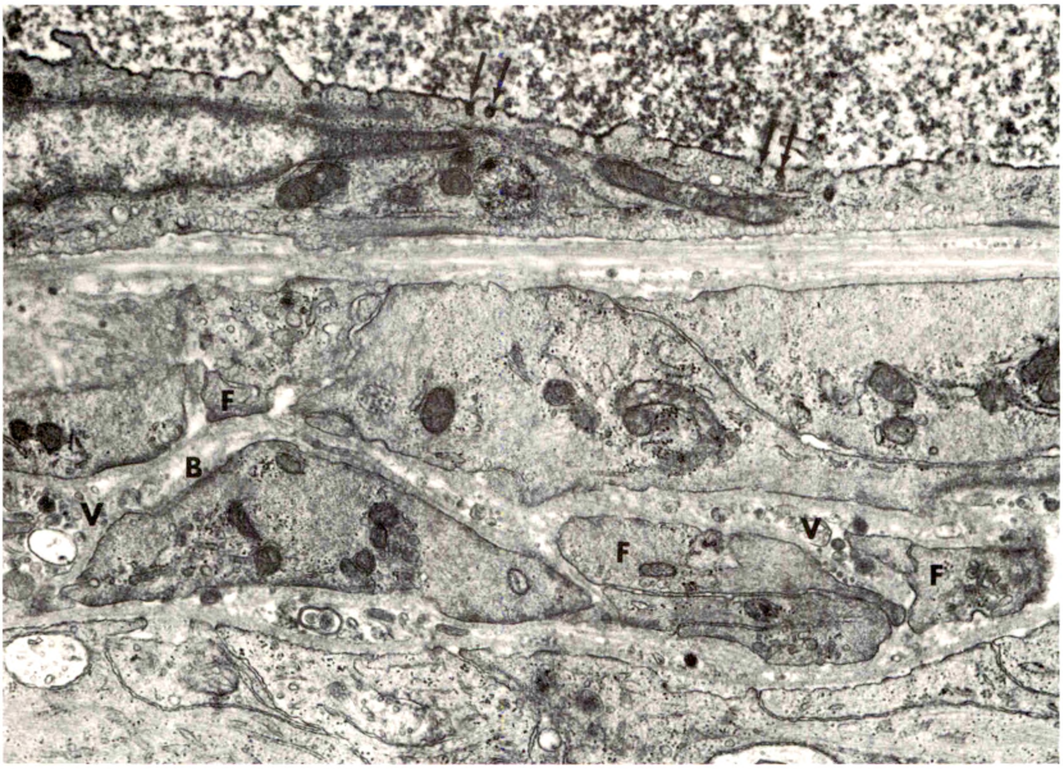

9

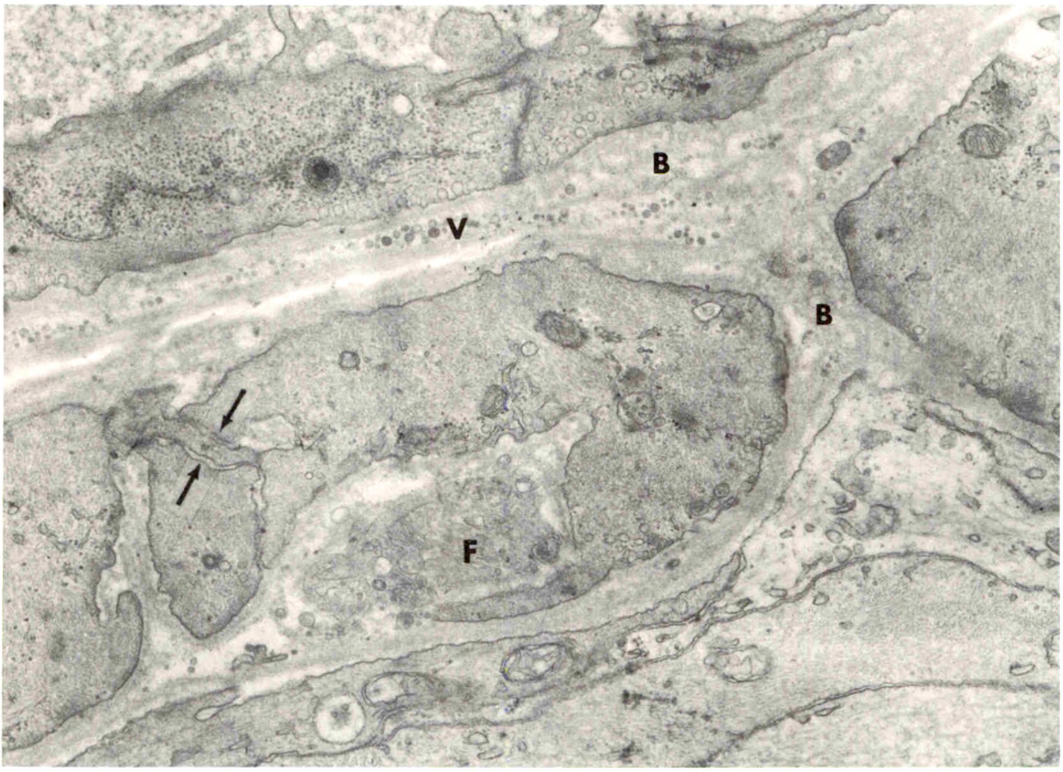

Fig 8—Smooth muscle cell fragments (*F*) of variable size are seen in the wall of a small artery. There are reduplicated basement membranes (*B*) in the media. Extracellular vesicles (*V*) lie adjacent to some of the muscle cell fragments. HRP-containing vesicles (*double arrows*) are seen only in the luminal aspects of the endothelium (× 19,000). **Fig 9**—Area of medial necrosis in small artery. Two muscle cell fragments are separated by an invagination of the plasma membrane (*arrows*). Another fragment (*F*) is devoid of filaments and contains various cytoplasmic organelles such as swollen mitochondria. Reduplicated basement membranes (*B*) are seen in both the subendothelial space and media. Extracytoplasmic vesicles (*V*) and vacuoles are also present (MP-injected, × 23,000).

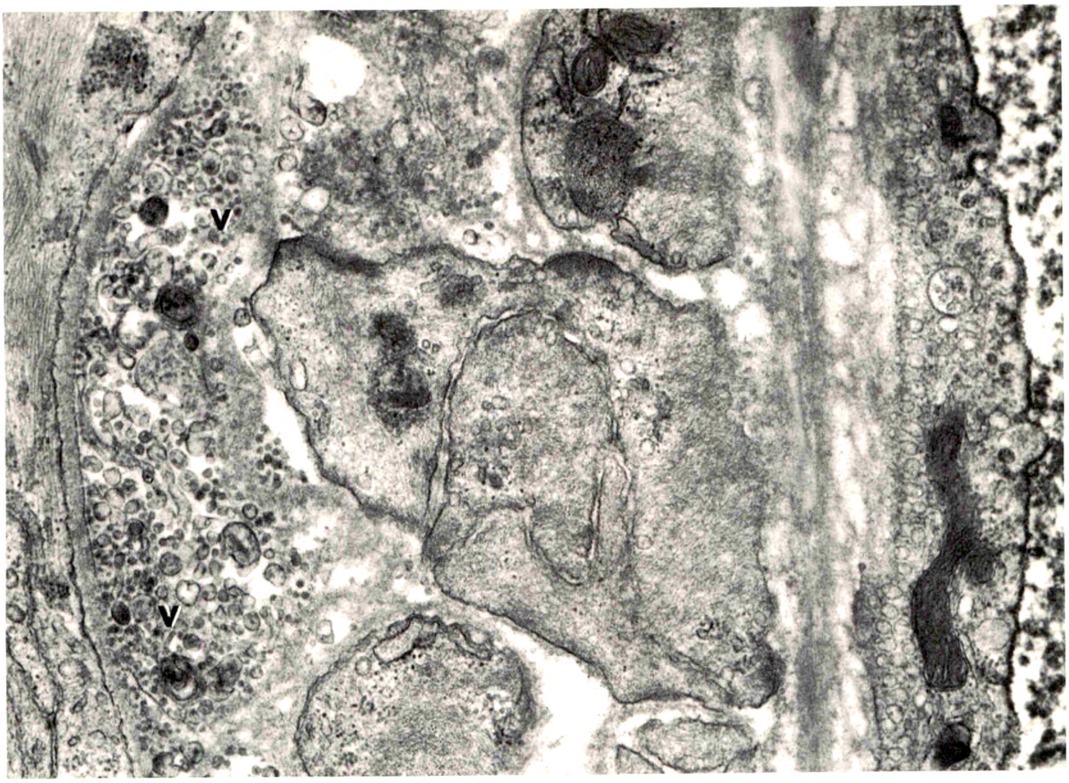

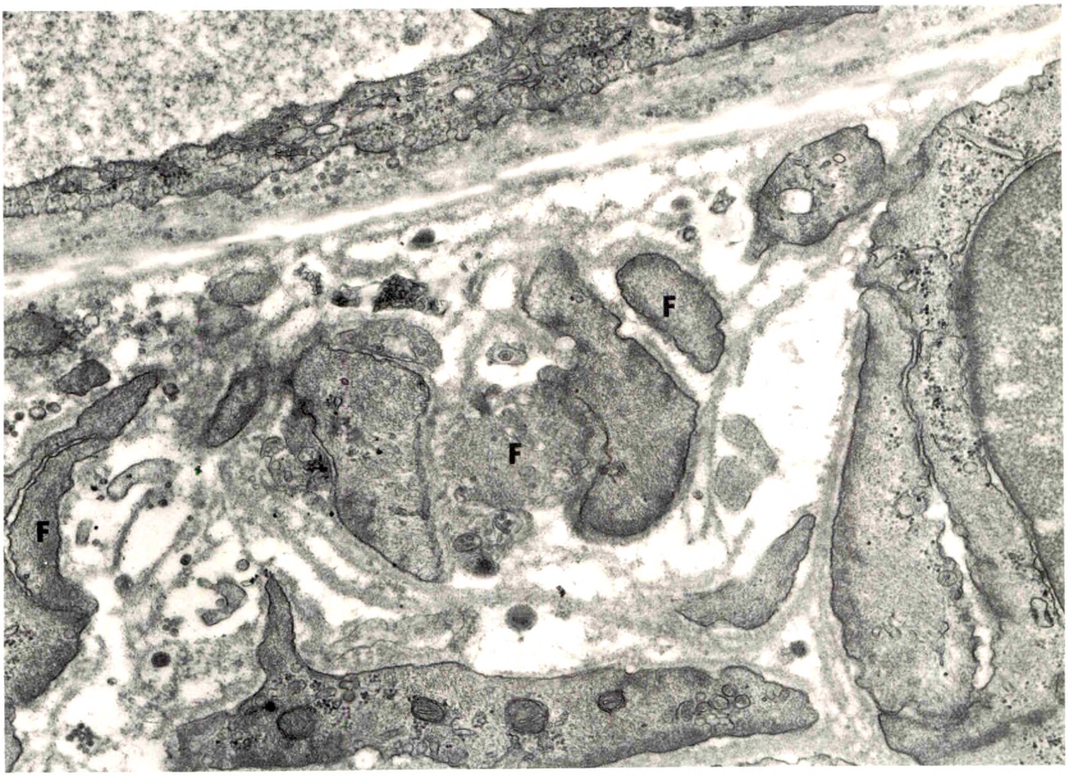

Fig 10—Similar to Figure 9. Note the large aggregate of extracytoplasmic vesicles (*V*), vacuoles, multivesicular bodies and other cell debris in the media. Only a few vesicles in the endothelium contain HRP (× 26,000). **Fig 11**—Area of medial degeneration in a small artery. The muscle cell fragments (*F*) exhibit varying degrees of necrosis (MP-injected, × 23,000).

Fig 12—Sarcomere-like arrays of filaments in endothelium of small artery. At least 3 electron-dense bands (*arrows*) are distributed along the long axis of the filament bundles at a spacing of about 0.5μ (HRP-injected, × 28,000).

Fig 13—Reaction product is seen in both the lumen (*L*) and basal portion of a cleft between endothelial cells (*arrows*) of a small artery. There is also some staining of the basement membranes (*B*) adjacent to the endothelial and smooth muscle cells. (Compare with electron density of basement membranes in Figures 3–5) (HRP-injected, × 34,000).

Fig 14—Small artery from animal injected with MP. Reaction product is present through the entire length of the intercellular endothelial cleft (*arrows*). There is heavy staining of the basement membranes (*B*) in the subendothelial space (× 70,000).

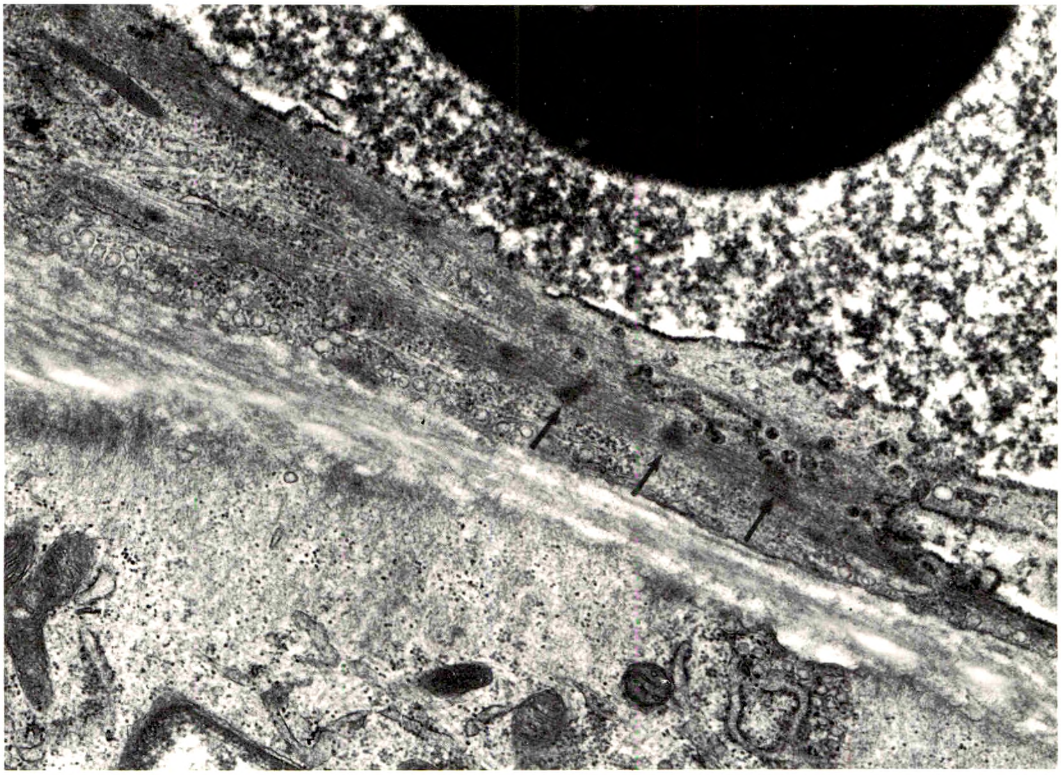

13

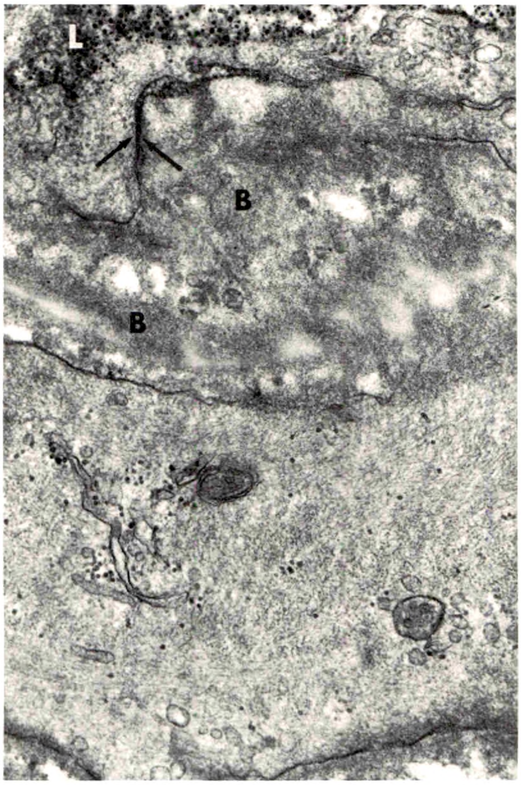

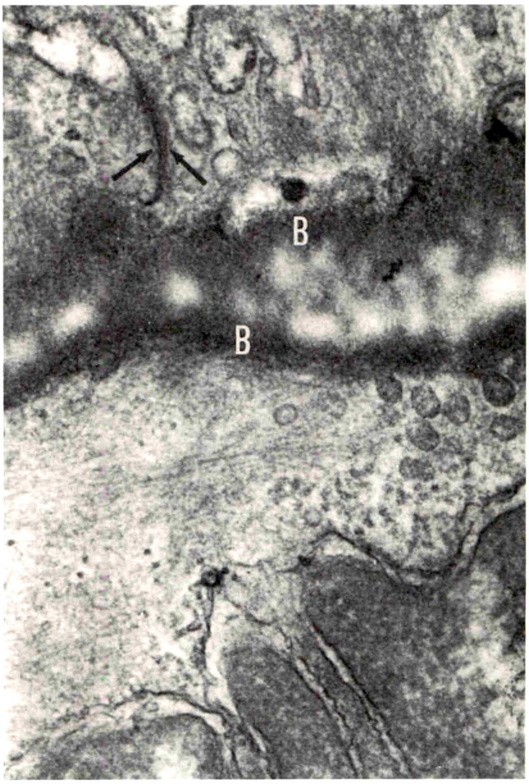

Fig 15 and 16 are electron micrographs of deeper layers of the retina.

5

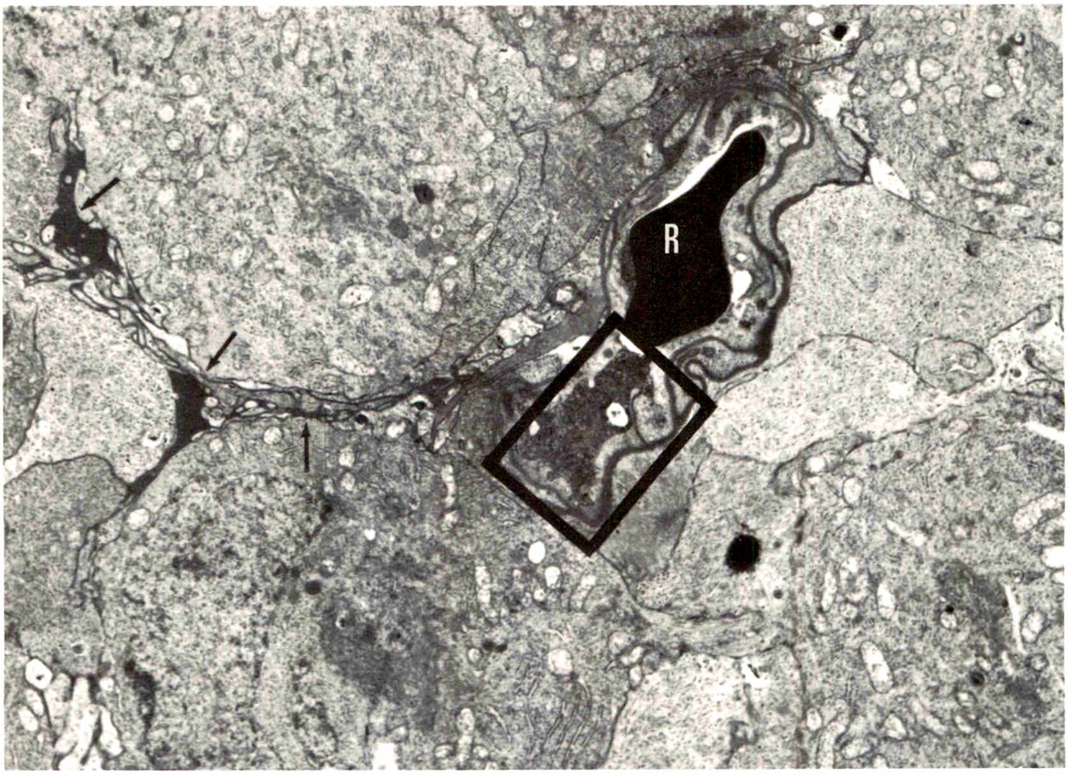

16

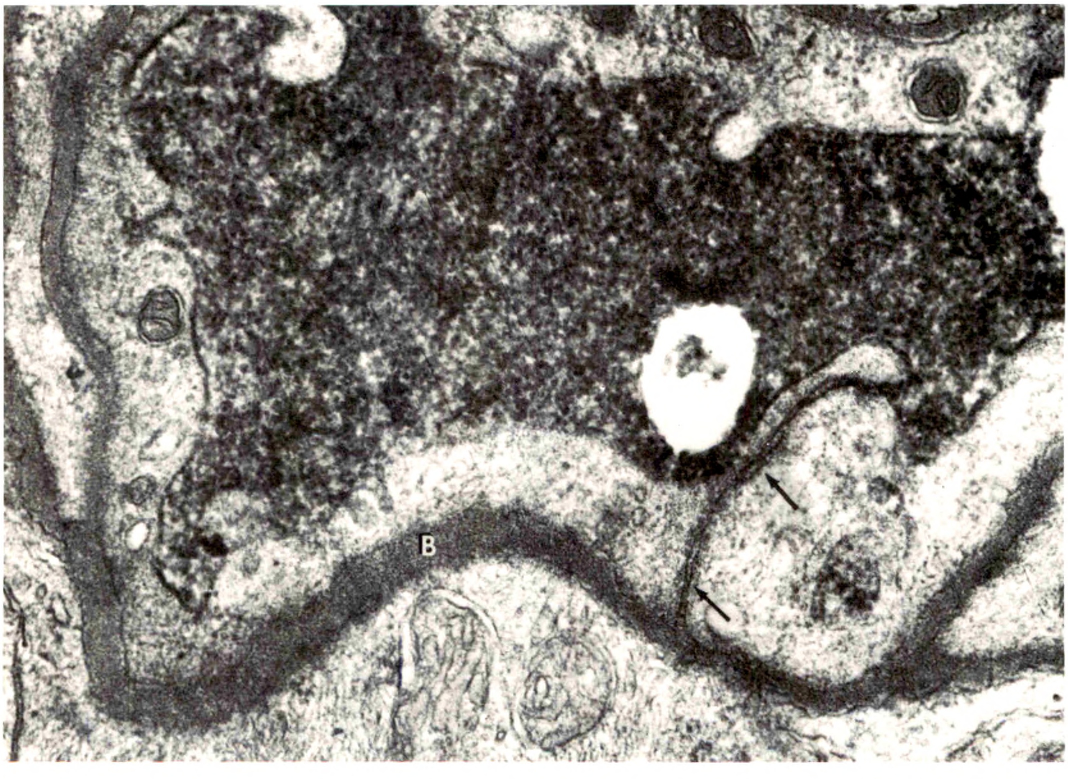

Fig 15—An erythrocyte (*R*) is present in the lumen of this capillary. Reaction product is seen in the lumen and basement membranes, and extends extravascularly between cell processes (*arrows*). The area enclosed in the rectangle is shown at higher magnification in the next figure (HRP-injected, × 6000). **Fig 16**—Reaction product fills both the lumen and entire length of the cleft between endothelial cells (*arrows*). There is also staining of the adjacent basement membranes (*B*) (× 46,000).

Effects of Biliary Obstruction on Pulmonary Ultrastructure in the Rat

N. A. Popovic, DVM, PhD and J. F. Mullane, MD, PhD

Hypoxemia and respiratory alkalosis have been described in patients with liver disease. Since no pulmonary parenchymal lesions have been related to the abnormal respiratory function, the effects of common bile duct ligation and division on pulmonary alveolar structure were studied in ninety-two 10- to 14-week-old male Wistar rats. In comparison with controls, the rats with ligated common bile ducts (CBD) developed progressive hepatic and pulmonary changes. The hepatic damage consisted of bile duct proliferation, loss of hepatocytes and generalized cirrhosis. Most pronounced pulmonary histologic differences between the CBD and sham-operated rats were thickening of interalveolar septa and generalized increase in cellularity of alveolar walls. With electron microscopy, frequently observed alterations included swelling and increased vacuolization of endothelial and epithelial (Type I) cells, proliferation of Type II alveolar pneumonocytes, and increase in amounts of collagen fibers and edema of the interstitium (Am J Pathol 68:97–112, 1972).

PHYSIOLOGIC EFFECTS of primary liver damage on the respiratory system include hyperventilatory alkalosis, hypoxemia, and arteriovenous shunting of blood.[1–3] Multiple small arteriovenous fistulae[4] and widespread pulmonary arterial changes[5] have also been described in affected lungs. The ultrastructural alterations of pulmonary parenchyma have been reported in cases of oxygen toxicity, carbon dioxide inhalation and many other conditions but they have not been described in cases of naturally occurring or experimentally caused hepatic damage.

The purpose of this study was to examine the light and electron microscopic changes in lungs of rats following experimental hepatic damage caused by the ligation and division of the common bile duct.

Methods

Ninety-two male Wistar rats* weighing 150 to 250 g were used in the study. All animals appeared normal and free of symptoms of disease. Control and

---

From the Division of Surgery, Walter Reed Army Institute of Research, Walter Reed Army Medical Center, Washington, DC.

Accepted for publication Feb 1, 1972.

Address reprint requests to Dr. Neven A. Popovic, Cpt, VC, Division of Surgery, Walter Reed Army Institute of Research, Walter Reed Army Medical Center, Washington, DC 20012.

* In conducting the research described in this report, the investigators adhered to the "Guide for Laboratory Animal Facilities and Care," as promulgated by the Committee on the Guide for Laboratory Animal Facilities and Care of the Institute of Laboratory Animal Resources, National Academy of Sciences–National Research Council.

experimental animals were studied simultaneously under the same environmental conditions. Common bile duct division and ligation (CBD) were performed under ether anesthesia. The sham surgery, performed under identical conditions, consisted of laparotomy and dissection but not ligation of the common bile duct.

Groups of rats were killed at various times after CBD or sham surgery (1 to 26 days) with the majority of necropsies at 26 days. Before death, under general barbiturate anesthesia, the trachea of each rat was clamped shut while the lungs were at the height of the normal inspiratory phase. The entire thoracic contents were removed and submerged in 10% buffered neutral formalin. In some cases, prior to formalin fixation small blocks of lung tissue were separated for preparation for electron microscopy. Liver samples were also fixed for light microscopy.

The paraffin sections were cut at 6 μ and stained with hematoxylin and eosin (H&E) and Masson's trichrome stain for connective tissue.[6] Light microscopic examination was performed on multiple sections of lung and liver of all 92 experimental and sham-operated rats.

The lung tissue to be prepared for electron microscopy was placed in cold 5% gluteraldehyde solution buffered at pH 7.6 with 0.1 M *s*-collidine. While in the fixative the tissue was further subdivided into smaller blocks approximately 1 mm in diameter. The fixation was continued under intermittent partial vacuum (down to 10 mmHg) until sufficient alveolar air was extracted to allow the lung blocks to sink. The entire time of aldehyde fixation was 4 to 5 hours. After fixation the blocks were washed with *s*-collidine for 30 minutes and postfixed in 1% osmium tetroxide in pH 7.6 *s*-collidine buffer for 2 hours. After a subsequent 5 minute rinse in *s*-collidine the tissues were dehydrated in increasing concentration of alcohol followed by propylene oxide. The tissue blocks were infiltrated with propylene oxide–Epon 812 mixture and embedded in Epon 812.[7]

Thick sections (0.5 to 1.0 μ) were stained with toluidine blue and viewed by light microscopy. Ultrathin sections were cut with a diamond knife on a Porter Bloom MT-2 ultramicrotome and stained with aqueous uranyl acetate followed by lead citrate. Sections of lungs of 4 experimental and 2 sham-operated rats killed 26 days after surgery were examined with the Hitachi 11C electron microscope.

Results

Light Microscopy

Pulmonary and hepatic changes, as observed with the light microscope, were progressive. Most prominent alterations were present at 26 days following the common bile duct ligation. The hepatic damage was observed in all CBD rats and consisted of bile duct proliferation, loss of hepatocytes and generalized cirrhosis as shown by deposition of connective tissue within portal triads and among the hepatocytes. Sham-operated rats had normal appearing livers.

Thickening of interalveolar septa and generalized increase in cellularity of alveolar walls, visible by the thirteenth postoperative day, were the most pronounced histologic differences between the CBD and sham-operated rats (Figure 1). Masson's trichrome stain revealed an increase in intraseptal connective tissue. Small patchy areas of atelectasis were occasionally observed in both CBD and sham animals and were not considered significant.

Electron Microscopy

Cuboidal cells with lamellated osmophilic bodies (Type II alveolar pneumonocytes) were predominant in CBD rats and in many cases were found close or even adjacent to each other (Figure 2). The osmophilic granules of these cells were of different sizes and most contained concentric layers of phospholipids (Figures 2, 3). In some cases (Figure 3) the granules appeared to discharge their contents into the alveolar space while other granules contained less osmophilic heterogeneous material suggestive of lamellae. The mitochondria within Type II cells were elongated and had increased matrix density. The microvilli characteristically found on Type II cells were blunt and in some cases completely missing (Figures 2, 3).

Occasionally, epithelial cells not resembling Type I or II pneumonocytes were observed in angular positions along alveolar walls of both sham and CBD rats (Figure 4). They did not have osmophilic granules but contained vacuoles of various sizes and shapes, and blunt microvilli. These cells appeared similar to alveolar brush cells previously described and designated as Type III pneumonocytes.[8]

The Type I pneumonocytes of CBD rats had irregular, thicker than usual, cytoplasm which contained multitudes of pinocytotic vesicles of various sizes (Figures 3–6). The epithelial and endothelial cells were separated in some areas only by the common basement membrane (Figures 4–6), which occasionally appeared irregular and edematous (Figure 5). In other areas the distance between epithelial cells and the endothelium of capillaries (air–blood barrier) contained accumulations of fibrin and collagen fibers intermixed with edema fluid (Figures 7, 8). Very rarely was the injury to Type I cells sufficient to cause the rupture of their cytoplasm (Figure 8). In general, the interstitial space contained connective tissue in greater amounts than observed in normal rats.

The cytoplasm of endothelial cells of CBD rats appeared in many instances, swollen and thickened (Figures 5, 6). It contained pinocytotic vesicles of various sizes, a few mitochondria and an occasional myelin body. The intercellular junctions were not disturbed and appeared to be maculae occludentes type.

Discussion

Biliary obstruction in the rat has a damaging influence on alveolar structures. Alveolar wall thickening, increase in collagen content and increased cellularity were observed with light microscopy. With electron microscopy, alterations of epithelial (Type I) and endothelial cells, edematous and collagenous widening of interstitial spaces, and an increase in numbers of Type II cells were the most frequently observed changes.

The pulmonary ultrastructure has been studied in several animal species and man.[9–11] Normal rat alveolar structure has been described adequately.[12,13] However, even at the present time there exists some confusion regarding the nomenclature and detailed ultrastructure of the alveolar wall. The fine structure of the lung can be greatly affected by methods of fixation and preparation, which may account for some of the observed variability.[14] Attempts were made to classify the cellular structure [15–18] and to standardize the nomenclature as early as 1965, but to date these efforts have not been completely successful. Therefore to clarify our data and nomenclature, several highlights of the normal rat lung structure will be mentioned.

The alveolar–capillary space (air–blood barrier) is composed in its narrowest portion of a thin layer of epithelial alveolar cells (Type I pneumonocytes), the basement membrane and the capillary endothelial cells. The basement membrane appears fused and forms a common structure between the epithelium and endothelium in thin areas while in the wider areas of the alveolar wall the basement membranes of epithelium and endothelium are separated thus enclosing an interstial space. This space may vary in width and it may contain fibroblasts, collagen and fine elastic fibers.[19] Both endothelial and epithelial cells are continuous and without pores.[11] Adjacent endothelial cells demonstrate junctions of maculae occludentes type while the epithelial cell junction appeared tight—*ie,* zonulae occludentes.[19,20] Tight junctions are normally found in epithelial linings of hollow organs.

In addition to large granular alveolar cells (Type II granular pneumonocyte) a third type of alveolar cell was recently described in the rat lung and named the alveolar brush cell.[8] It was reported to comprise 5 to 10% of all alveolar pneumonocytes. The function of alveolar brush cells is not known but it is speculated to be of a stretch or chemoreceptor nature.

The lung is an organ responsive to an array of noxious stimuli. Pulmonary epithelial and endothelial changes have been described in variety of experimental conditions such as oxygen toxicity,[13,21–27] carbon dioxide intoxication,[28] nickel carbonyl exposure,[29] irradiation,[30] vagotomy,[31] Freund's adjuvant administration [32,33] and asphyxiation.[34,35] While the changes observed in response to these stimuli are different in some respects, they have many similar features. Therefore our experimental findings of pulmonary changes following bile duct ligation can be compared with pulmonary alterations produced by some of the above conditions.

The swelling and vacuolization of endothelial cells observed in the lung of CBD rats was similar to, but not as extensive as, that observed in the pulmonary tissue following asphyxiation,[35] vagotomy [31] or nickel carbonyl poisoning.[29] Oxygen toxicity caused severe endothelial changes progressing to fragmentation and necrosis.[13]

The thickening of the air-blood barrier was reported in O_2 toxicity of rats; such thickening was observed, to a lesser degree, in our work in CBD rats. Increased collagen content and edema can diminish gas transport. Such septal thickening was observed to reduce gas diffusion by 50% in some cases of oxygen toxicity.[21]

The response of Type I cells to injury consists of increased numbers of pinocytotic vesicles, edema and in severe cases, fragmentation of epithelium. These changes were observed in CBD rats, following vagotomy [31] and injection of an irritant (Freund's adjuvant). Edema is considered to be an early reaction to injury and its presence in the interstitium and Type I cells 26 days following CBD ligation indicates continuous and persistent injury. Increase in pinocytotic activity and damage of Type I epithelial cells has also been associated with greater absorption of surfactant.[19,20] The reasons for increased absorption and later disappearance of surfactant, as observed in various types of lung injury, are not known. The increased pinocytotic activity of the Type I epithelial cells with CBD ligation might also be due to an impaired phagocytic activity of the alveolar macrophage since the intrapulmonary inactivation of bacteria is impaired with biliary obstruction in the rat.[36]

Alveolar Type II cells appear to be much more responsive to pulmonary irritants than Type I cells. Increase in Type II cell numbers and flattening and loss of microvilli were observed in our work with CBD rats as well as in rats with oxygen toxicity [13,21,22] and following injection of Freund's adjuvant.[29,33] The time for Type II cell to become predominant is approximately 7 days following pulmonary injury. However, as compared with changes following Freund's adjuvant, the number of lamellar granules of Type II cells was not increased in CBD rats.[32,33] The majority of literature [20,37–39] attributes surfactant production to Type II alveolar cells. In some type of pulmonary injury, such as that seen in cervical vagotomy, the lung surfactant levels are reduced.[31] Here, early decrease in the density of osmophilic granules (lamellar bodies) and their replacement with vacuoles was observed in Type II cells. While surfactant changes were not measured in the lungs of CBD rats the similar alteration of lamellar granules was noticed in the Type II cells.

In search for probable causes or stimuli responsible for proliferation of the Type II cells one cannot easily dismiss the possibility that these cells are under neurohumoral control. Some drugs such as pilocorpine exert a stimulating effect on the secretory activity of resting Type II cells.[40] Possibly some humoral factors of hepatic origin are responsible for changes observed in Type II cells of CBD rats.

Another possibility left for consideration is the effect of anoxia on Type II cells and their constituent osmophilic granules. It is possible that the relative anoxia observed in CBD rats [3] may be responsible for observed reduction of osmophilic granules. Such disappearances were also recorded in cases of carbon dioxide toxicity.[28]

References

1. Bashour FA, Cochran P: Alveolar-arterial oxygen tension gradients in the cirrhosis of the liver. Am Heart J 71:734–740, 1966
2. Bashour FA, McConnell T, Miller WF: Circulating and respiratory changes in patients with Laennec's cirrhosis of the liver. Am Hart J 74:569–577, 1967
3. Mullane JF, Popovic NA, Solis RT, Yhap EO: Effect of experimental biliary obstruction on respiratory function. Ann Surg (In press)
4. Hales RM: Multiple arteriovenous fistulae of the lungs. Am J Pathol 32: 927–937, 1956
5. Berthelot MD, Walker JG, Sherlock S, Reid L: Arterial changes in the lungs in cirrhosis of the liver—lung spider nevi. N Engl J Med 274:291–298, 1966
6. Luna LG: Manual of histologic staining methods of the Armed Forces Institute of Pathology. Edited by LE Luna. New York, McGraw-Hill Book Co, 1968, pp 92–94
7. Luft JH: Improvements in epoxy resin embedding methods. J Biophys Biochem Cytol 9:409–414, 1961
8. Meyrick B, Reid L: The alveolar brush cell in rat lung—a third pneumonocyte. J Ultrastruct Res 23:71–80, 1968
9. Low FN: The pulmonary alveolar epithelium of laboratory mammals and man. Anat Rec 117:241–263, 1953
10. Itaki K: Electron microscopic observations of pulmonary alveolar structure. Acta Tuberc Jap 122:34–45, 1955
11. Karrer HE: The ultrastructure of the mouse lung: General architecture of capillary and alveolar walls. J Biophys Biochem Cytol 2:241–252, 1956
12. Policard A, Collet A, Pregermain: Recherches au microscope electronique sur les cellules parietales alvelarires du poumon des manuniferes. Z Zellforsch Mikrosk Anat 50:561–568, 1959
13. Gonzague S, Ristler PB, Caldwell B, Weibel ER: Development of fine

structural damage to alveolar and capillary lining cells in oxygen-poisoned rat lungs. J Cell Biol 32:605–628, 1967

14. Kikkawa Y: Morphology of alveolar lining layer. Anat Rec 167: 389–400, 1970
15. Bertalanffy FD: Dynamics of cellular populations in the lung. The Lung. Edited by AA Liebow, DE Smith. Baltimore, The Williams & Wilkins Co, 1967, pp 19–30
16. Bertalanffy FD: Respiratory tissue: Structure, histophysiology, cytodynamics. Part I. Review and Basic Cytomorphology, International Review of Cytology. Edited by GH Bourne, JF Danielli. New York, Academic Press, Inc, 1964, pp 233–328
17. Brooks RE: Concerning the nomenclature of the cellular elements in respiratory tissue. Am Rev Resp Dis 94:112–113, 1966
18. Bertalanffy FD: On nomenclature of the cellular elements in respiratory tissue. Am Rev Resp Dis 94:605–609, 1965
19. Schneeberger-Keeley EE, Karnovsky MJ: The ultrastructural basis of alveolar–capillary membrane permeability to peroxidase used as a tracer. J Cell Biol 37:781–792, 1968
20. Dermer GB: The fixation of pulmonary surfactant for electron microscopy. II. Transport of surfactant through the air-blood barrier. J Ultrastruct Res 31:229–246, 1970
21. Kapanci Y, Weibel ER, Kaplan HP, Robinson FR: Pathogenesis and reversibility of the pulmonary lesions of oxygen toxicity in monkeys. Lab Invest 20:101–118, 1969
22. Cedergren B, Gyllensten L, Wersall J: Pulmonary damage caused by oxygen poisoning. An electron-microscopic study in mice. Acta Paediatrica 48:477–494, 1959
23. Ambrus CM, Pickren JW, Weintraub DH, Niswander KR, Ambrus JL, Rodbard D, Levy JC: Studies on hyaline membrane disease. V. Oxygen induced hyaline membrane disease in guinea pigs. Biol Neonate 12:246–260, 1968
24. Schaffner F, Felig P, Trachtenberg E: Structure of rat lung after protracted oxygen breathing. Arch Pathol 83:99–107, 1967
25. Kaplan HP, Robinson FR, Kapanci Y, Weibel ER: Pathogenesis and reversibiltiy of the pulmonary lesions of oxygen toxicity in monkey. I. Clinical and light microscope investigation. Lab Invest 20:94–118, 1969
26. Kistler GS, Caldwell PBR, Weibel ER: Development of fine structural damage to alveolar and capillary lining cells in oxygen poisoned rat lung. J Cell Biol 32:605–628, 1967
27. Nash G, Blennerhassett JB, Pontoppidan H: Pulmonary lesions associated with oxygen therapy and artificial ventilation. N Engl J Med 276:368–372, 1967
28. Schaefer KE, Avery ME, Bensch K: Time course of changes in surface tension and morphology of alveolar epithelial cells in CO_2—induced hyaline membrane disease. J Clin Invest 43:2080–2093, 1964
29. Hackett RL, Sunderman FW Jr: Pulmonary alveolar reaction to nickel carbonyl: Ultrastructural and histochemical studies. Arch Environ Health 16:349–362, 1968
30. Leroy EP, Liebner EJ, Jensik RJ: The ultrastructure of canine alveoli after

supervoltage irradiation of the thorax. I. Lesions of latent period. Lab Invest 15:1544–1558, 1966

31. Goldberg VE, Buckingham S, Sommers SC: Pulmonary alveolar lesions in vagotomized rats. Lab Invest 16:693–705, 1967
32. Galindo B, Imaeda T: Cellular response to Freund's adjuvant in the rabbit lung. An electron microscopic study. Lab Invest 15:1659–1681, 1966
33. Faulkner CS, Esterly JR: Ultrastructural changes in the alveolar epithelium in response to Freund's adjuvant. Am J Pathol 64:559–574, 1971
34. Seller, MJ, Spector RG: The effects of anoxia on the newborn and adult rat lung. J Pathol Bact 88:309–311, 1964
35. Reidbord HE, Spitz WU: Ultrastructural alterations in rat lung. Changes following asphyxiation. Arch Pathol 82:80–84, 1966
36. Mullane JF, LaForce FM, Huber GL: Effect of experimental liver injury on pulmonary anti-bacterial defense. Clin Res 19:723, 1971 (abstr)
37. Bensch K, Schaefer K, Avery ME: Granular pneumocytes: Electron microscopic evidence of their exocrinic function. Science 145:1318–1319, 1964
38. Buckingham S, Heinemann HO, Sommers SC, McNary WF Jr: Phospholipid synthesis in the large pulmonary alveolar cells: Its relation to lung surfactants. Am J Pathol 48:1027–1036, 1966
39. Askin FB, Juhn C: The cellular origin of pulmonary surfactant. Lab Invest 25:260–268, 1971
40. Goldenberg VE, Buckingham S, Sommers SC: Pilocarpine stimulation of granular pneumocyte secretion. Lab Invest 20:147–158, 1969

[*Illustrations follow*]

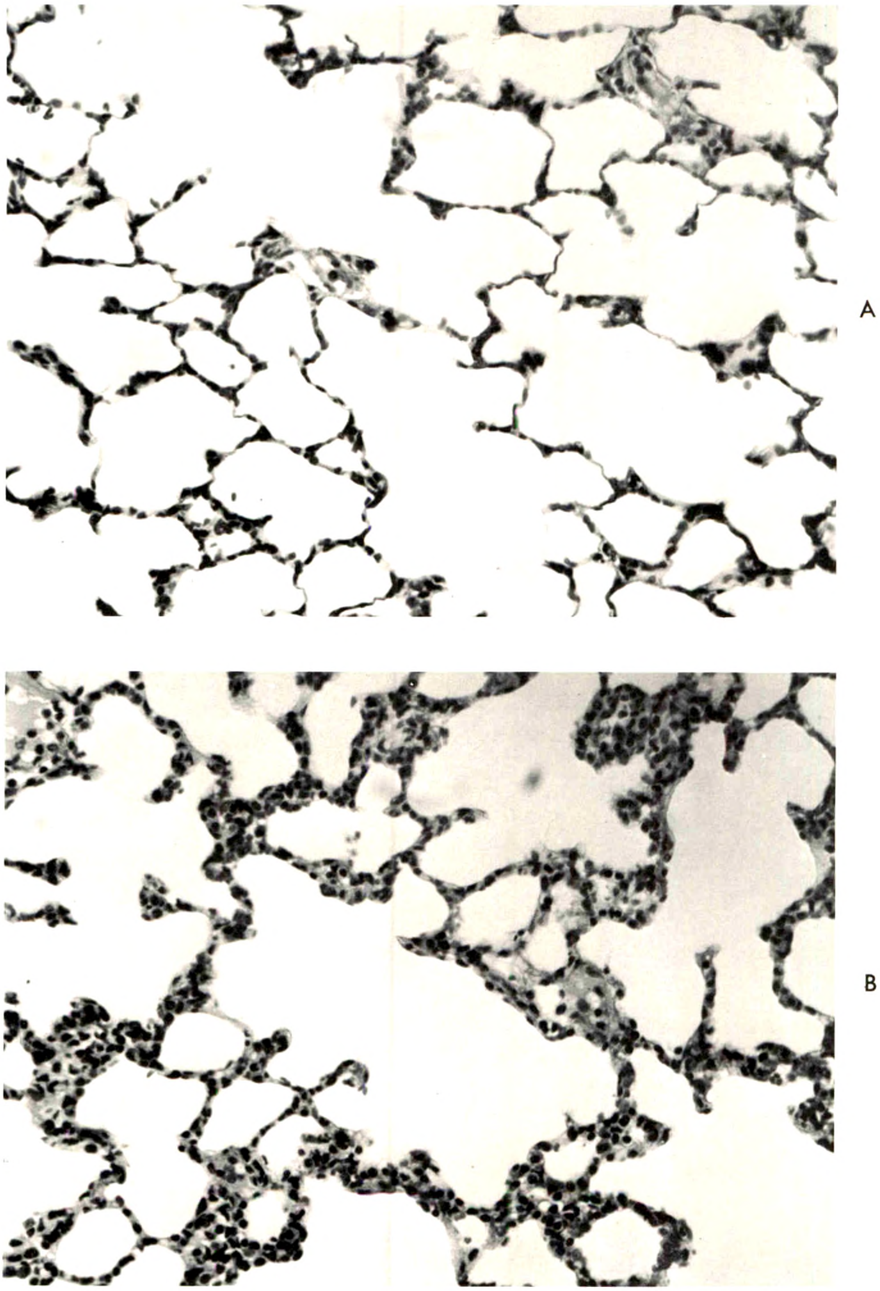

Fig 1A—Rat lung 26 days after sham operation. Thin alveolar septa with relatively few cells are shown. **B**—Rat lung 26 days after CBD ligation. Proliferation of alveolar cells and thickening of the septa are evident (H&E, approx. × 308).

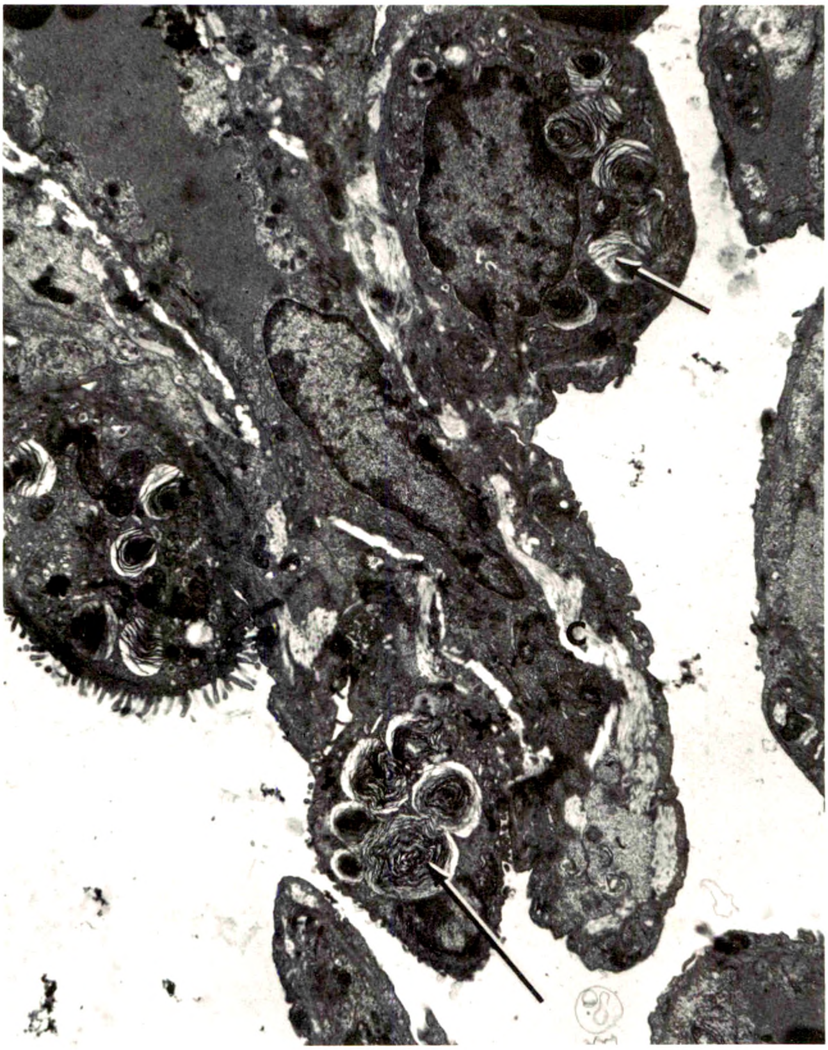

Fig 2—Rat lung 26 days after CBD ligation. Alveolar wall contains closely packed Type II cells with lamellar bodies of various sizes (*arrows*). Interstial space shows increase in collagen content (*C*) (approx. × 5000).

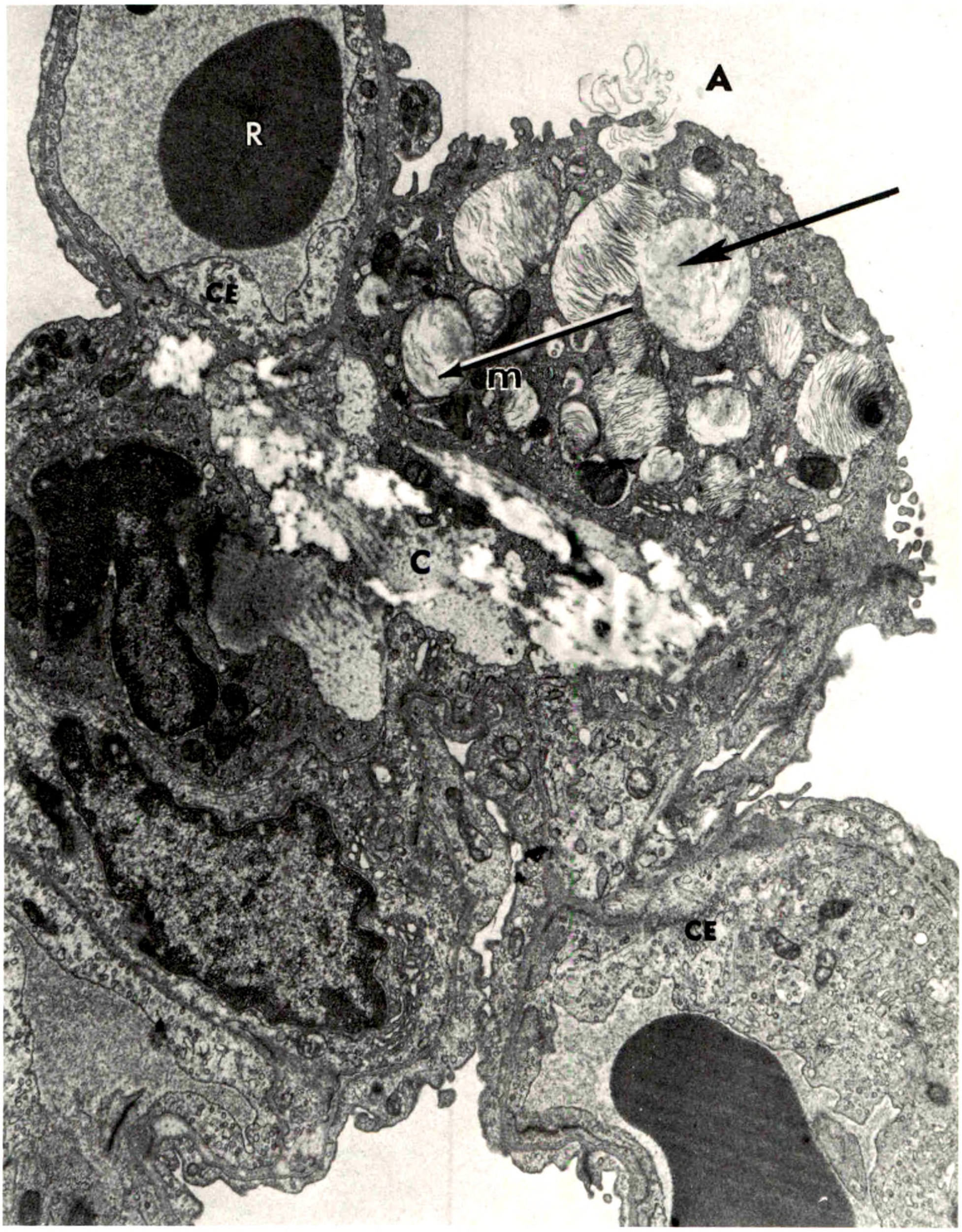

Fig 3—Type II alveolar cell with abnormally appearing lamellar bodies (*arrows*). One of the bodies is discharging its contents into the alveolar lumen (*A*). Mitochondria (*m*), collagen (*C*), capillary endothelium (*ce*), erythrocyte (*R*) within capillary lumen (approx. × 11,000).

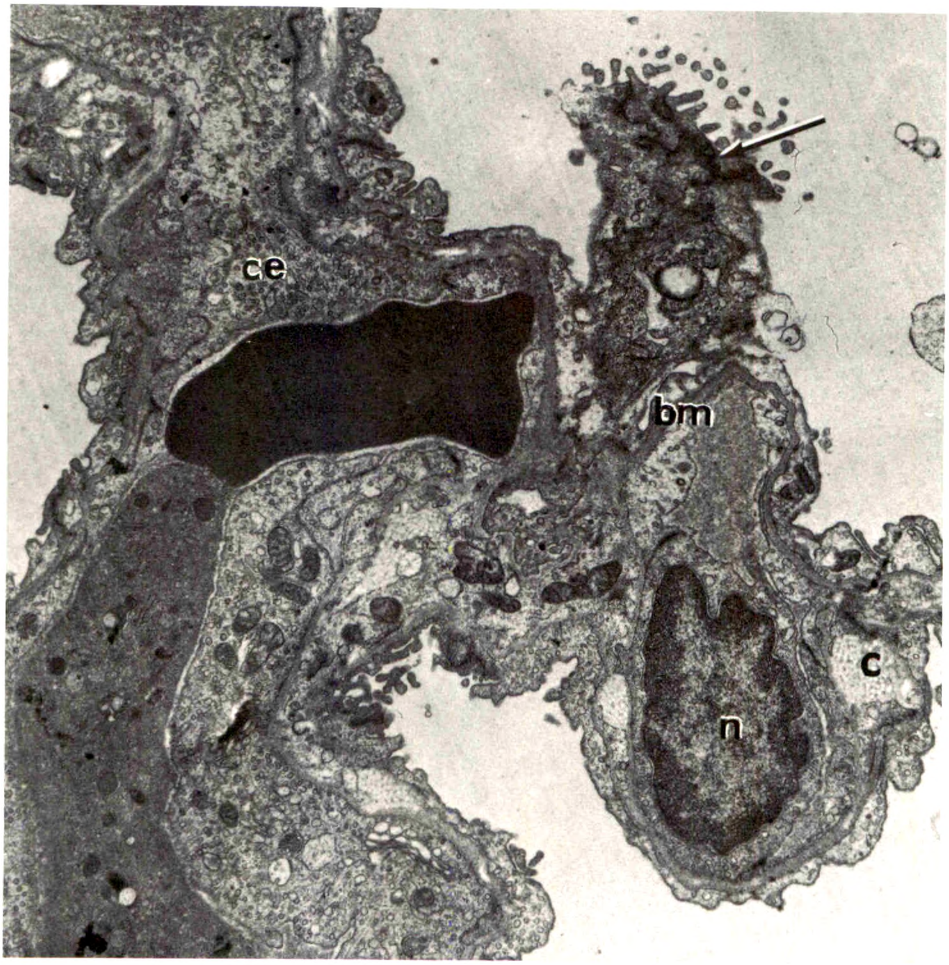

Fig 4—Alveolar epithelial cell resembling the alveolar brush cell (*arrow*). Capillary endothelium (*ce*), basement membrane (*bm*), nucleus of endothelial cell (*n*), and collagen (*c*) (approx. × 11,000).

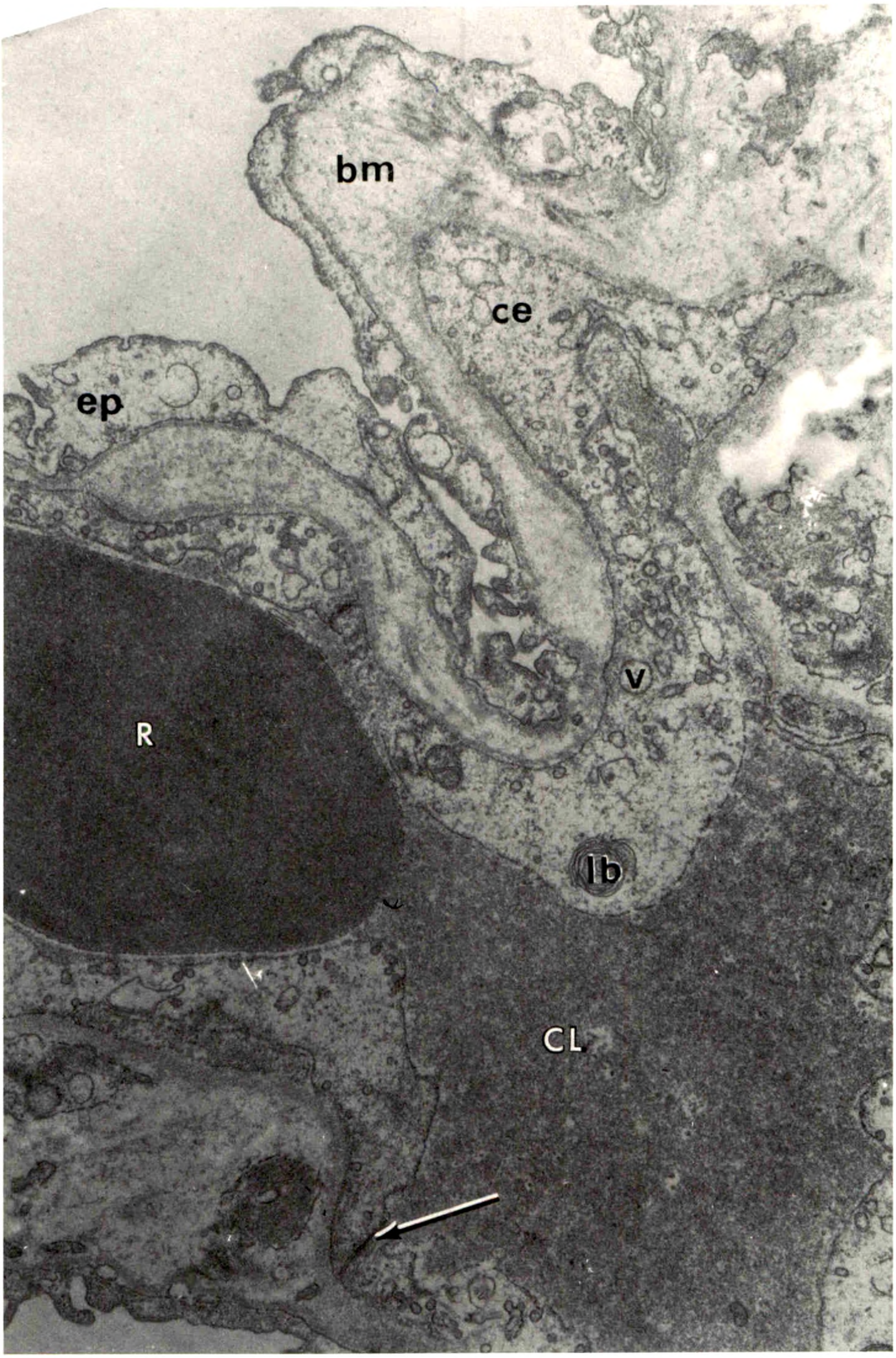

Fig 5—Irregular epithelium (*ep*) separated from the thickened capillary endothelium (*ce*) by a common basement membrane (*bm*). Vesicles (*v*) lamellated bodies (*lb*), capillary lumen (*CL*) enclosing an erythrocyte (*R*) and junction of two endothelial cells (*arrow*) (approx. × 23,000).

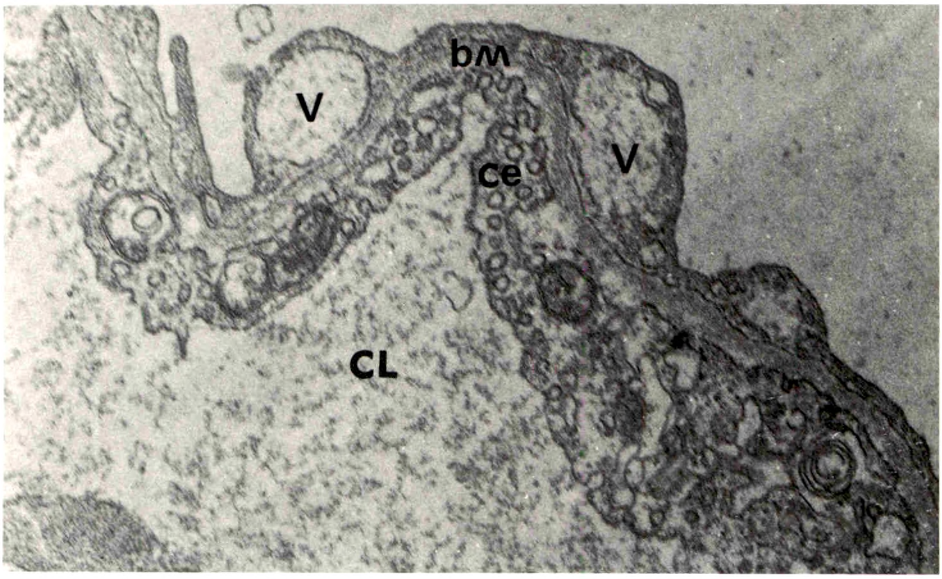

6

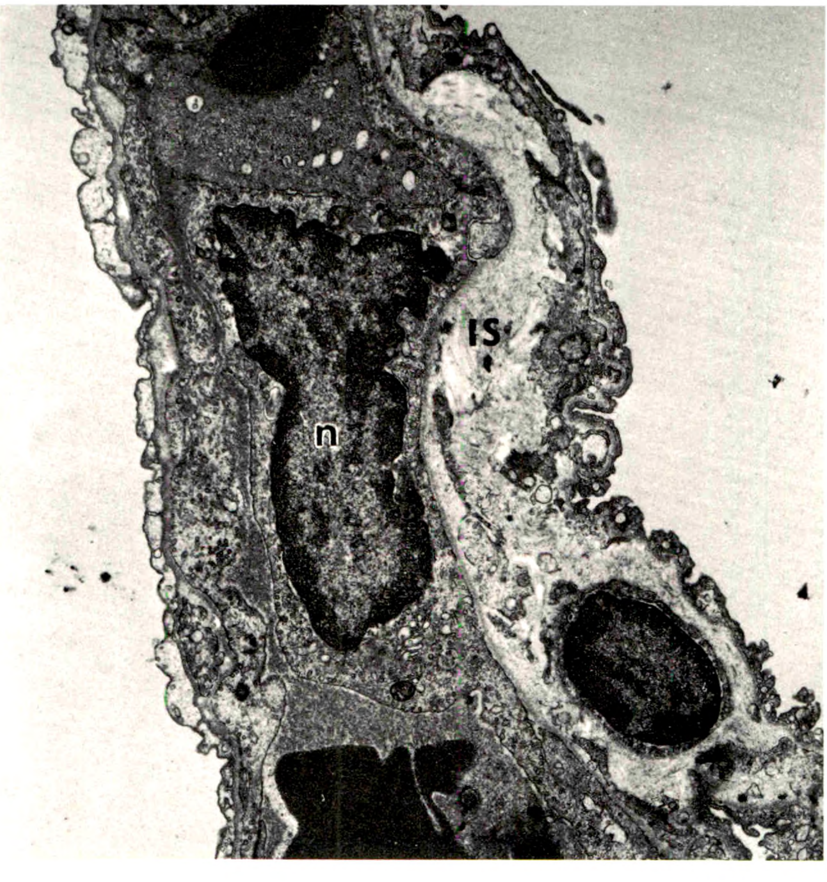

7

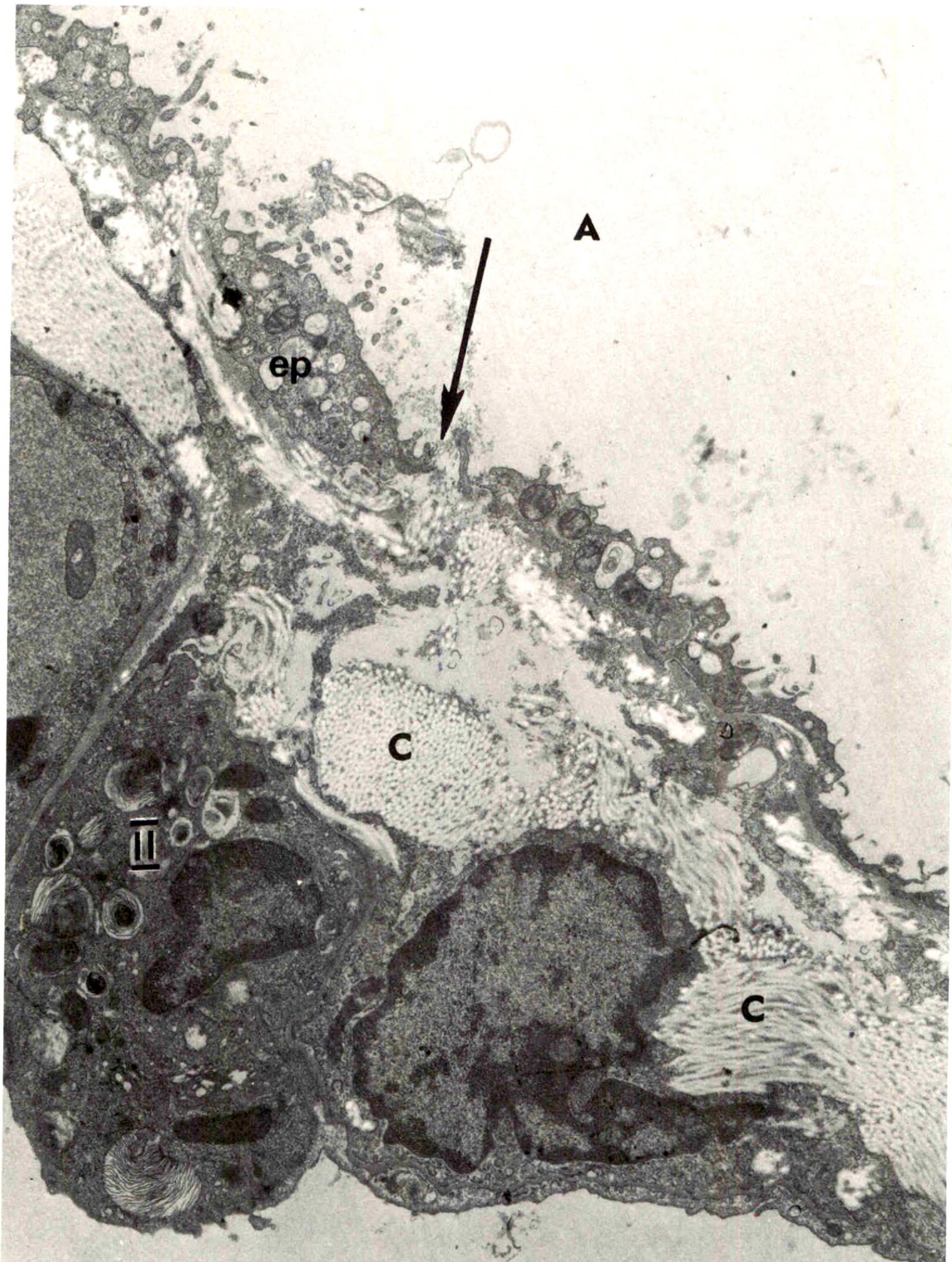

Fig 8—Thickened and adematous interstitium containing masses of collagen fibers (*c*). The epithelium (*ep*) appears ruptured (*arrow*) allowing cellular contents to escape into the air space (*A*). Type II cell (*II*) (approx. × 11,760).

Lysosomes in the Pathogenesis of the Renal Necrosis of Choline-Deficient Rats

A. J. Monserrat, MD, F. Hamilton, A. K. Ghoshal, PhD,
E. A. Porta, MD and W. S. Hartroft, MD, PhD

Previously published data from our laboratories led us to postulate that alterations in lysosomes may play a cardinal pathogenic role in the fatal renal necrosis of choline-deficient weanling rats. To explore this hypothesis further a series of five different experiments were carried out. In the first two experiments the effect of a "stabilizer" of the lysosomes, hydrocortisone, was studied; conversely, in the third and fourth experiments, the effect of a "labilizer," vitamin A, was studied. Finally, in the fifth experiment, the renal levels of a lysosomal enzyme, acid phosphatase, were evaluated biochemically. Results of the first two experiments revealed a protective effect of hydrocortisone while those of the third and fourth an aggravating effect of vitamin A. Results of the fifth experiment indicated lysosomal changes in the prenecrotic and early necrotic stages. These results along with those from our previous studies, support the concept that lysosomal alterations play an important pathogenic role in renal changes of choline-deficient weanling rats (Am J Pathol 68:113–146, 1972).

PREVIOUS EXPERIMENTS from our laboratories [1,2] have suggested that lysosomal alterations could play an important role in the pathogenesis of the renal necrosis which appears in weanling rats consuming a choline-deficient diet.[3]

Our hypothesis postulates that lipoperoxidative degeneration of the lysosomal membranes leads to the breakdown of these organelles with subsequent release of their hydrolytic enzymes. This concept was based in the following findings: a) Increase in number and size of lysosomes and their ultimate coalescence with eventual rupture were the most outstanding prenecrotic ultrastructural changes found in the epithelium of proximal convoluted tubules of the deficient animals. b) These lysosomal changes were paralleled by a corresponding increase in the prominence of lysosomes in suitable histochemical preparations (PAS, acid phosphatase, esterases) at the prenecrotic stage, and further diminution to the point of disappearance of this granular reaction at the onset of necrosis. c) The *in vivo* detection of conjugated dienes

---

From the Center of Experimental Pathology, University of Buenos Aires, Buenos Aires, Argentina, The Research Institute of The Hospital for Sick Children, Toronto, Ontario, Canada and the Department of Pathology, University of Hawaii, School of Medicine, Honolulu, Ha.

Supported by Grant MA-1904 from the Medical Research Council of Canada.

Accepted for publication Mar 17, 1972.

Address reprint requests to Dr. Eduardo A. Porta, Department of Pathology, University of Hawaii, School of Medicine, 1960 East-West Road, Honolulu, Ha 96822.

in the total renal lipids preceded the appearance of any morphologic evidence of necrosis. d) The *in vitro* malonaldehyde formation in renal homogenates after incubation was significantly less in necrotic than in nonnecrotic kidneys. e) The administration of the synthetic antioxidant DPPD (*N*-*N'*-diphenyl-*p*-phenylenediamine) consistently reduced the incidence and severity of the renal lesions.

To further study this working hypothesis we decided to explore, in weanling rats on a choline-deficient diet, the influence of drugs affecting the lysosomes ("stabilizers" and "labilizers") such as hydrocortisone and retynil acetate, as well as to evaluate biochemically the levels of acid phosphatase in renal homogenates in a series of several different experiments.

Materials and Methods

Experiment 1—Effects of Hydrocortisone on the Renal Lesions of Choline-Deficient Weanling Rats—Acute Experiment

Fifty-four weanling male Wistar rats (46 to 63 g initial body weight) were allotted to 5 groups (A, B, C, D and E) (Table 1). The 16 rats of Group A were

Table 1—Summary of Experimental Design in the Five Experiments

Exp	Group	No. rats	Diet	Injected intramuscularly with	Abbreviated	Day killed
1	A	16	CD **ad lib**	—	CD **ad lib**	8
	B	12	CS pf*	—	CS pf	8
	C	12	CD pf	Hydrocortisone†	CD pf + H	8
	D	6	CS pf	Hydrocortisone	CS pf + H	8
	E	8	Chow **ad lib**	—	Chow **ad lib**	8
2	F	12	CD **ad lib**	—	CD **ad lib**	—‖
	G	6	CS pf	—	CS pf	—
	H	12	CD **ad lib**	Hydrocortisone	CD **ad lib** + H	—
	I	6	CS pf	Hydrocortisone	CS pf + H	—
3	I	12	CD **ad lib**	Retynil acetate‡	CD **ad lib** + A	5
	II	12	CD pf	Vehicle (corn oil)§	CD pf + O	5
	III	12	CD **ad lib**	Vehicle (corn oil)	CD **ad lib** + O	5
	IV	12	CD pf	Retynil acetate	CD pf + A	5
4	V	12	CD **ad lib**	Retynil acetate	CD **ad lib** + A	6
	VI	12	CD pf	Vehicle (corn oil)	CD pf + O	6
	VII	12	CD **ad lib**	Vehicle (corn oil)	CD **ad lib** + O	6
	VIII	12	CD pf	Retynil acetate	CD pf + A	6
5	1	32	CD **ad lib**	—	CD **ad lib**	2,4,5
	2	17	CS pf	—	CS pf	2,4,5

* Pair-fed in a food weight basis

† 5 mg/100 g body weight

‡ 200,000 USP units/100 g body weight

§ 200 mg/100 g body weight

‖ See materials and methods

fed a choline-deficient basal diet[1,2] *ad libitum* (CD *ad lib*) of the following composition: 16% soya protein, 10% partially hydrogenated shortening, 4% corn oil, 39.7% sucrose, 19.8% dextrin, 4% vitamin mixture (without choline and B_{12}), 2% salt mixture, 4% cellulose and 0 5% L-cystine. The 12 rats of Group B received the basal diet supplemented with 0.35 g of choline chloride/100 g diet and were individually and daily pair-fed (food–weight basis) with those in Group A (CS pf). The 12 rats of Group C were pair-fed the choline deficient diet with Group A and were intramuscularly injected daily with 5 mg hydrocortisone (Solucortef, The Upjohn Co, Canada)/100 g body weight (CD pf + H). The 6 rats of Group D received the choline-supplemented diet and were similarly injected with hydrocortisone (CS pf + H). The 8 rats of Group E were fed a stock laboratory ration (Ralston Purina Co, Woodstock, Ont, Canada) *ad libitum* (Chow *ad lib*).

All rats were housed individually in air-conditioned quarters in wire-bottomed cages with free access to water. Body weights and food intakes were recorded daily.

At the eighth day, under light ether anesthesia, both kidneys were removed and weighed. Suitable selected portions of tissue were fixed in Dalton's solution[4] for electron microscopy and in formalin solution[5] for light microscopy. For light microscopic studies, paraffin sections were stained with hematoxylin and eosin[6] and frozen sections with oil red O[7] for the detection of fat.

Evaluation of the histologic extent of the renal necrosis was described by a classification system previously proposed by the authors.[2]

The material fixed in Dalton's was embedded in Epon 812[8] and thick sections (1 μ) were stained with toluidine blue[9] for histologic studies and topographic localizations. Adjacent thin sections were stained with lead[10] and photographed with a Philips 200 electron microscope.

For topographic localizations of different portions of the nephron a precise terminology was used.[11]

Experiment 2—Effects of Hydrocortisone on Duration of Survival up to 58 Days in Weanling Rats Consuming a Choline-Deficient Diet

Thirty-six weanling male Wistar rats (37 to 50 g initial body weight) were allotted to 4 groups (F, G, H and I) (Table 1). The 12 rats of Group F were fed the basal choline-deficient diet *ad libitum* (CD *ad lib*). The 6 rats of Group G were pair-fed with those of Group F and received the choline-supplemented diet (CS pf). The 12 rats of Group H were fed the choline-deficient diet *ad libitum* and were injected intramuscularly daily with 5 mg of hydrocortisone/100 g of body weight (CD *ad lib* + H). The 6 rats of Group I were pair-fed with those of Group H, received the choline-supplemented diet and were injected with hydrocortisone (CS pf + H).

The composition of the diet, housing and care of the animals was similar to that in Experiment 1.

To study the survival time of these groups, the rats fed the choline-deficient diet remained under these experimental conditions until they died, or if death did not occur, they were killed at the fifty-eighth day of the experiment. When leader rats died during the experiment, their corresponding choline-supplemented controls of the pair-fed groups were killed in order to provide matched control material for the morphologic studies.

In all rats dying spontaneously, autopsy was performed (average postmortem interval of about 4 to 5 hours), and suitable sections of the kidneys were fixed in formalin solution, embedded in paraffin and stained with hematoxylin and eosin (H&E),[6] Masson's trichrome,[12] oil red O[7] for the detection of ceroid, Perl's Prussian blue[13] and phosphotungstic acid–hematoxylin (PTAH).[14] Unstained section were studied with UV light for the detection of ceroid. Frozen sections were stained with oil red O[7] for the detection of fat.

The kidneys of the rats killed at the fifty-eighth day were removed, weighed and suitable sections processed for light microscopy as indicated previously. The kidneys were also studied by electron microscopy in a similar way to that used in Experiment 1; furthermore, sections were stained with phosphotungstic acid.[15]

Experiment 3—Effects of Retynil Acetate on the Kidneys of Choline-Deficient Weanling Rats—A 5-Day Experiment

Forty-eight weanling male Wistar rats (34 to 50 g initial body weight) were allotted to 4 groups (I, II, III, and IV) (Table 1). Rats of Group I were fed the choline-deficient diet *ad libitum* and injected intramuscularly daily starting from the 48 hours after the beginning of the experiment, with 200,000 USP units of vitamin A [Retinol acetate (Retynil Acetate) Type II, Sigma Chemical Co USA]/100 g of body weight (CD *ad lib* + A). Rats of Group II were pair-fed with those of Group I with the same choline-deficient diet and also injected daily from the third day of the beginning of the experiment with the vehicle alone (CD pf + O). Rats of Group III were fed the same choline-deficient diet *ad libitum* and injected from the third day with the vehicle alone (CD *ad lib* + O). Rats of Group IV were pair-fed with those of Group III with the choline-deficient diet and injected from the third day with vitamin A (CD pf + A).

Rats were kept and controlled in a similar way to those of Experiment 1.

At the fifth day of the experiment, under light ether anesthesia, blood was collected from the inferior vena cava in heparinized disposable syringes for evaluation of plasma urea nitrogen (PUN)[16] and plasma phospholipids.[17,18] Both kidneys were removed and weighed and suitable sections were fixed in formalin solution and then processed and studied in a similar way to those of Experiment 1.

Experiment 4—Effects of Retynil Acetate on the Kidneys of Choline-Deficient Weanling Rats—A 6-Day Experiment

Forty-eight weanling male Wistar rats (34 to 48 g initial body weight) were allotted to 4 groups (V, VI, VII and VIII) (Table 1).

Rats of Group V were fed the choline deficient diet *ad libitum* and injected intramuscularly daily from the third day of the experiment (48 hours after the beginning) with 200,000 USP units of vitamin A/100 g body weight (CD *ad lib* + A). Rats of Group VI were fed the same choline-deficient diet, pair-fed to those of Group V and injected daily from the third day with the vehicle alone (CD pf + O); rats of Group VII were fed the same choline-deficient diet *ad libitum* and injected daily from the third day with the vehicle alone (CD *ad lib* + O), and rats of Group VIII were fed the choline-deficient diet, pair-fed to those of Group VII and injected with vitamin A from the third day of the experiment (CD pf + A).

The rats were kept and studied in a similar way to those of Experiment 3, except that they were killed at the sixth day of the experiment.

Experiment 5—Biochemical Evaluation of Acid Phosphatase in the Kidneys of Choline-Deficient and Choline-Supplemented Weanling Rats

Forty-nine weanling male Wistar rats (30 to 58 g initial body weight) were allotted to 2 groups (1 and 2) (Table 1). The 32 rats of Group 1 were fed the choline-deficient diet *ad libitum*. The 17 rats of Group 2 were pair-fed with the choline-supplemented diet.

For preparation of whole kidney homogenates for the biochemical evaluation of acid phosphatase and total protein, the animals were decapitated in a cold room (4 C) and the kidneys of each rat were homogenized in a Potter and Elvehjen type homogenizer driven at about 1000 rpm, always with the same number (10) of strokes, in 0.25 M sucrose. Before homogenation both kidneys were carefully inspected grossly and weighed; a small biopsy was taken for histologic studies and the kidneys were weighed again.

The acid phosphatase (free and total) was evaluated according to the method proposed by Franklin.[19] Phosphorus was determined according to the method of Fiske and Subbarow [20] and protein by the method of Lowry *et al.*[21]

For the evaluation of acid phosphatase, from each rat 2 aliquots were used for blank controls, 3 aliquots for enzymatic assay of the free and 3 for the total acid phosphatase. In each aliquot (8/rat), phosphorus was determined once. Protein concentration was determined once in each of 2 aliquots of kidney homogenate per rat.

All the technical procedures up to the time of incubation were carried out in the cold room and the tubes kept in a box with a mixture of ice and water.

Six rats of the choline-deficient group were killed at 2 days, six at 4 days and twenty at 5 days; animals of the choline-supplemented group were also killed. five at 2 days, six at 4 days and six at 5 days.

Statistical Analyses

Experiments 1, 3 and 4. For every one of these experiments the number of rats developing necrosis in each of the two groups receiving a different treatment were compared by a χ^2-test; the means of renal weights of the rats were compared by a *t* test and the distributions of extent of histologic renal necrosis (which do not conform to the normal distribution) were compared performing Mann-Withney *U* test.[22]

Experiment 2. Mann-Withney *U* test [22] was used to compare the distribution of duration of survival up to 58 days in rats of Group F and H, since the assumptions of normality of distributions required by the *t* test did not hold in this case.

Experiment 5. The means of protein concentration and the percentages of increase of acid phosphatase (between free and total) in two different groups were compared by a *t* test (days 2 and 4). For the results of the fifth day, multiple comparisons between means of three different groups were performed by Scheffe's test.[23]

Results

Experiment 1—Effects of Hydrocortisone on the Renal Lesions of Choline-Deficient Weanling Rats—Acute Experiment

Food Intake

The average food intake–gross energy (expressed in kcal/100 g body weight) of the rats fed *ad libitum* the basal choline-deficient diet is represented in Text-figure 1 along with that of the rats fed the stock laboratory ration. Rats of Group A reduced their food intake on the fifth day and more sharply thereafter, correlating with the appearance

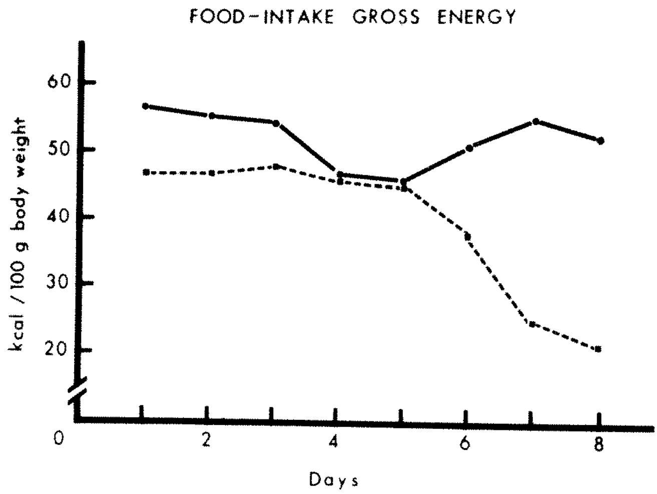

TEXT-FIG 1—Experiment 1. Averages of the daily food intake-gross energy in the 2 groups of rats fed *ad libitum*. (Basal diet *ad lib* – – –; Chow diet *ad lib* —)

of renal lesions. Of course, this reduction was not seen in the chow-fed rats. Although not represented in this text-figure, the type of curve of Group A was paralleled by the pair-fed groups, even though they did not eat all the food that was offered to them (Group B, 86%; Group C, 97%; Group D, 84%).

Body Weights

Changes in body weights of the different groups are represented in Text-figure 2 in the form of growth curves as percentages of the mean values at the beginning of the experiment.

Gross Changes

The gross changes in the necrotic kidneys were similar to those previously reported.[1,24]

The average weights of both kidneys (expressed as percentage of body weight) in the different groups are represented in Table 2. To aid in the interpretation of these values and the other parameters studied, those rats of Groups A and C with renal necrosis were specifically designated as being in subgroups Aa and Ca, thereby eliminating from the latter subgroups those rats without renal necrosis at the end of the experiment. Even in that case, rats of the group fed the choline-deficient diet and injected with hydrocortisone had smaller kidneys than those fed the choline-deficient diet and not injected with hydrocortisone. For statistical analysis of these results, see Table 4.

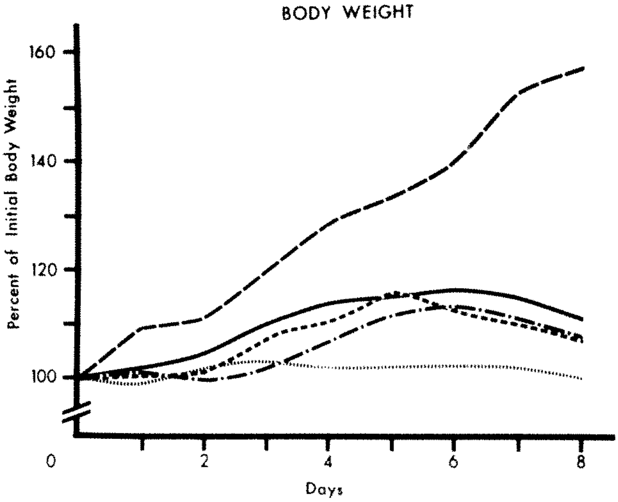

TEXT-FIG 2—Experiment 1. Growth curves in the different groups. (Chow *ad lib* ———; Basal diet *ad lib* —; Basal diet + Cholinesterase pair-fed ···; Basal diet + cholinesterase + hydrocortisone pair-fed — · —; Basal diet + hydrocortisone pair-fed – – –)

Light Microscopy

The renal lesions in the hemorrhagic kidneys of rats fed the choline-deficient diet (Groups A and C) were similar to those previously described.[1,25-27]

The incidence of histologic renal necrosis (Table 2), was lower in rats of Group C when compared to those of Group A. The histologic extent of the renal necrosis (Table 3) in the Groups A and C or in the subgroups Aa and Ca (only those rats with necrosis) was lower in rats

Table 2—Experiment 1. Renal Weights and Incidence of Renal Necrosis

Group	Abbreviated	No. rats	Renal weight* (g/100 g)	Incidence of necrosis No.	Incidence of necrosis %
A	CD **ad lib**	16	2.08 ± 0.12	15	93
Aa†		15	2.16 ± 0.11	15	100
B	CS pf	12	0.98 ± 0.03	0	0
C	CD pf + H	12	1.33 ± 0.08	5	42
Ca†		5	1.57 ± 0.13	5	100
D	CS pf	6	1.14 ± 0.04	0	0
E	Chow **ad lib**	8	0.94 ± 0.04	0	0

* Mean values ± SE
† Only those rats with renal necrosis (see results)

Table 3—Extent of the Renal Necrosis in Experiments 1, 3 and 4

Exp	Group	Abbreviated	No. rats	Grade 0		Grade I		Grade II		Grade III		Grade IV		Grade IV		Average (grade)
				No.*	%	No.	%	No.	%	No.	%	No.	%	No.	%	
1	A	CD **ad lib**	16	1	6.3	1	6.3	3	18.8	4	25.0	2	12.6	5	31.3	3.30
	Aa†		15	0	0.0	1	6.7	3	20.0	4	26.7	2	13.4	5	33.5	3.50
	C	CD pf + H	12	7	58.3	1	8.3	2	16.7	2	16.7	0	0.0	0	0.0	0.90
	Ca†		5	0	0.0	1	20.0	2	40.0	2	40.0	0	0.0	0	0.0	2.50
3	I	CD **ad lib** + A	12	5	41.7	0	0.0	4	33.3	3	25.0	0	0.0	0	0.0	1.42
	Ia†		7	0	0.0	0	0.0	4	57.1	3	42.9	0	0.0	0	0.0	2.43
	II	CD pf + O	12	11	91.7	1	8.3	0	0.0	0	0.0	0	0.0	0	0.0	0.08
	IIa†		1	0	0.0	1	100.0	0	0.0	0	0.0	0	0.0	0	0.0	1.00
	III	CD **ad lib** + O	12	7	58.3	3	25.0	1	8.3	1	8.3	0	0.0	0	0.0	0.67
	IIIa†		5	0	0.0	3	60.0	1	20.0	1	20.0	0	0.0	0	0.0	1.60
	IV	CD pf + A	12	7	58.3	2	16.7	2	16.7	1	8.3	0	0.0	0	0.0	0.75
	IVa†		5	0	0.0	2	40.0	2	40.0	1	20.0	0	0.0	0	0.0	1.80
4	V	CD **ad lib** + A	12	2	16.7	0	0.0	0	0.0	6	50.0	3	25.0	1	8.3	2.92
	Va†		10	0	0.0	0	0.0	0	0.0	6	60.0	3	30.0	1	10.0	3.50
	VI	CD pf + O	12	9	75.0	0	0.0	1	8.3	2	16.7	0	0.0	0	0.0	0.67
	VIa†		3	0	0.0	0	0.0	1	33.3	2	66.6	0	0.0	0	0.0	2.67
	VII	CD **ad lib** + O	12	1	8.3	2	16.7	4	33.3	5	41.7	0	0.0	0	0.0	2.08
	VIIa†		11	0	0.0	2	18.1	4	36.4	5	45.5	0	0.0	0	0.0	2.27
	VIII	CD pf + A	12	2	16.7	1	8.3	5	41.7	2	16.7	1	8.3	1	8.3	2.17
	VIIIa†		10		0.0	1	10.0	5	50.0	2	20.0	1	10.0	1	10.0	2.60

* Number of animals in each grade.

† Only those rats with renal necrosis.

injected with hydrocortisone than in those not injected. For statistical analysis of these results, see Table 4.

Table 4—Statistical Analyses of Experiments 1, 2, 3 and 4

Exp	Compared groups	Comparison	Statistical test	Difference*	**P** values
1	A vs C	Incidence of necrosis	χ^2	S	<0.01
	A vs C	Mean of renal weights	**t**	S	<0.01
	Aa vs Ca	Distribution of the grades of necrosis	Mann-Withney	S	<0.05
	Aa vs Ca	Mean of renal weights	**t**	S	<0.01
2	F vs H	Distribution of survival	Mann-Withney	S	<0.02
3	I vs II	Incidence of necrosis	χ^2	S	<0.05
	I vs II	Mean of renal weights	**t**	S	<0.05
	Ia vs IIa	Distribution of the grades of necrosis	Mann-Withney	NS	
	Ia vs IIa	Mean of renal weights	**t**	NS	
	III vs IV	Incidence of necrosis	χ^2	NS	
	III vs IV	Mean of renal weights	**t**	NS	
	IIIa vs IVa	Distribution of the grades of necrosis	Mann-Withney	NS	
	IIIa vs IVa	Mean of renal weights	**t**	NS	
4	V vs VI	Incidence of necrosis	χ^2	S	<0.02
	V vs VI	Mean of renal weights	**t**	S	<0.01
	Va vs VIa	Distribution of the grades of necrosis	Mann-Withney	NS	
	Va vs VIa	Mean of renal weights	**t**	S	<0.001
	VII vs VIII	Incidence of necrosis	χ^2	NS	
	VII vs VIII	Mean of renal weights	**t**	NS	
	VIIa vs VIIIa	Distribution of the grades of necrosis	Mann-Withney	NS	
	VIIa vs VIIIa	Mean of renal weights	**t**	NS	

* S = significant, NS = not significant

Except for the already noted decrease in incidence and extent of the renal lesions, no other differences which could be ascribed to the administration of hydrocortisone were found by light microscopy in the choline-deficient or in the choline-supplemented rats.

Electron Microscopy

The electron microscopic changes found in the "hemorrhagic" kidneys were similar to those previously described.[1] No differences were found between the sections examined from the hemorrhagic kidneys of rats of Group A and those of Group C. No obvious changes that could be attributed to the administration of hydrocortisone were observed in the nonnecrotic kidneys.

Experiment 2—Effects of Hydrocortisone on the Renal Lesions of Choline-Deficient Weanling Rats—A 58-Day Experiment

Food Intake

The average food intake–gross energy for each of the two groups of rats fed *ad lib* (Group F, CD *ad lib,* and Group H, CD *ad lib* +H), is represented in Text-figure 3. Rats of both groups sharply reduced their food intake after the sixth day, at which time many animals develop the acute renal lesions. The subsequent increase in food intake observed at the twelfth day in Group H and at the fourteenth day in Group F, could be attributed to the death of the more severely affected rats (with very poor food intake) as well as the recovery of renal damage in surviving animals. No substantial differences were found between the food intake of Groups F and H.

The food intakes of the pair-fed Groups (G and I), paralleled those of their respective leading Groups F and H, although they did not eat all the food offered to them (Group G, 87%; Group I, 98%).

Body Weights

The average body weights of rats fed *ad libitum* (Groups F and H) are represented in Text-figure 4. In relation to changes in food intake

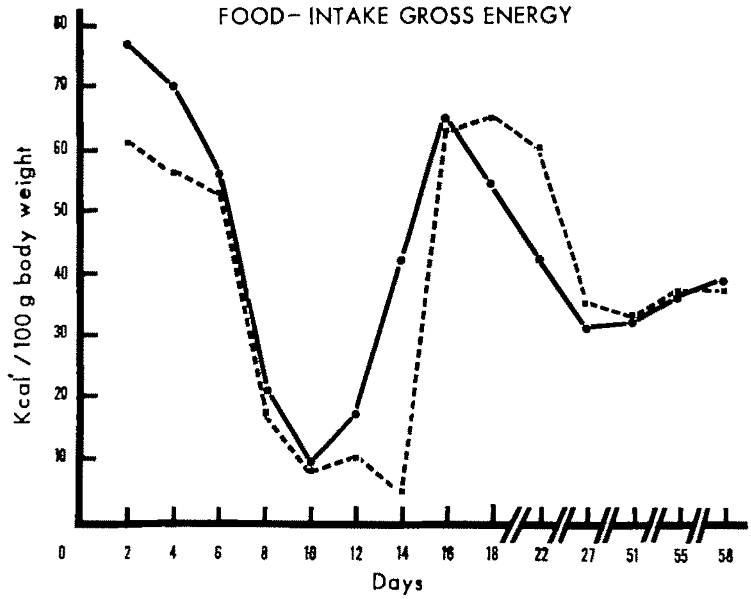

Text-fig 3—Experiment 2. Averages of the food intake-gross energy of the 2 groups of rats fed *ad libitum.* (Basal diet - - -; Basal diet + Hydrocortisone —)

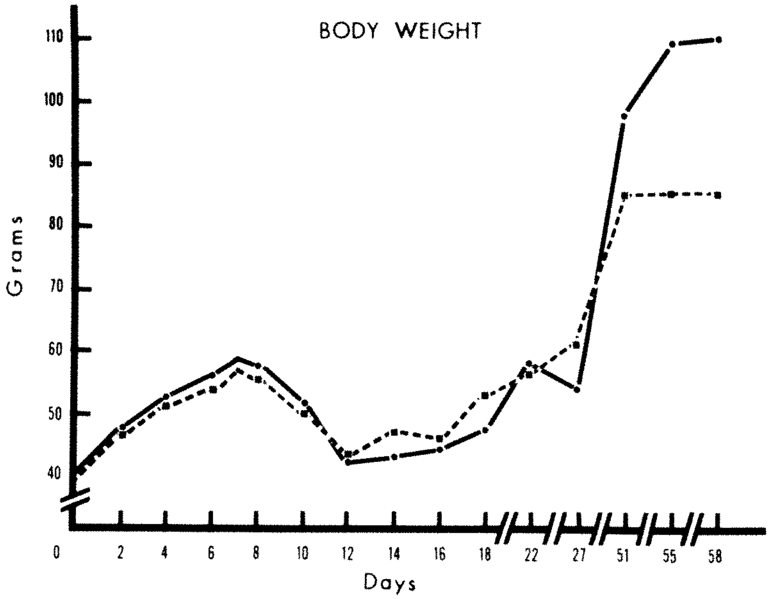

TEXT-FIG 4—Experiment 2. Growth curves in both groups of rats fed *ad libitum.* (Basal diet – – – –; Basal diet + hydrocortisone —)

there was a decrease in body weight from the seventh day and a subsequent increase at the twelfth day.

Survival

In the Text-figure 5, survival of animals from groups fed *ad lib* (H and F) is represented by a curve and expressed as a percentage of the total. The statistical analysis of these results is shown in Table 4.

It is of interest to note that more rats from Group F than from Group H died with renal lesions (11 vs 6) before the fifty-eighth day (when all the rats were killed); furthermore the life span of all animals dying before the fifty-eighth day was shorter in rats of Group F (12.3 ± 0.4, mean ± SE) than in those of Group H (28.7 ± 7.2).

Gross Changes

Rats of the choline-deficient groups that died during the first 2 weeks showed the typical aspect of the hemorrhagic kidney. All rats that died later had areas of variable degrees of "frosting"[24] in the surface of both kidneys.

Most of the rats sacrificed at the fifty-eighth day showed these types of lesions. None of the choline-supplemented rats developed renal lesions.

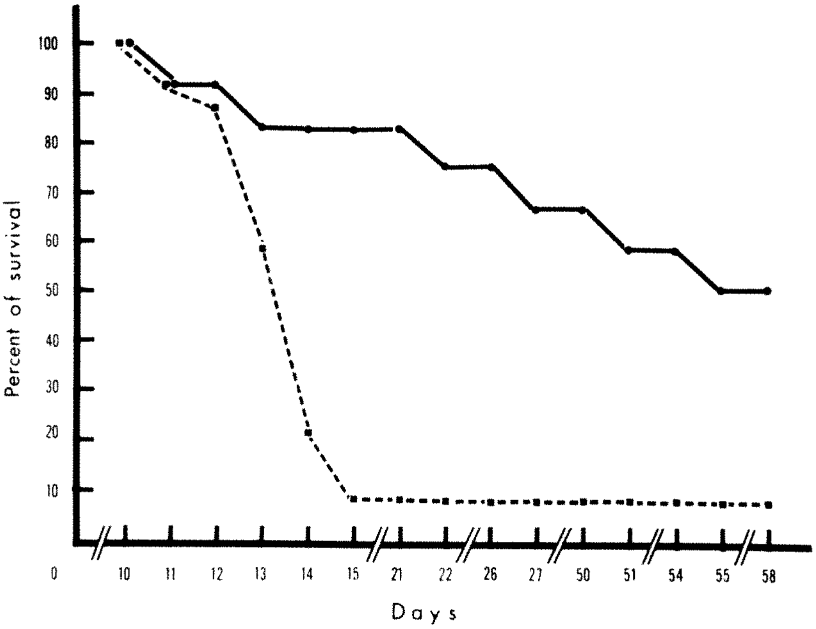

TEXT-FIG 5—Experiment 2. Percentages of survival in both groups of rats fed *ad libitum.* (Basal diet – – –; Basal diet + hydrocortisone —)

Light Microscopy

Rats of the choline-deficient groups (F and H) that died within the first 2 weeks showed, at the beginning, the typical lesions of the "hemorragic" kidney. By the end of the second week the changes consisted of proliferation and infiltration of inflammatory mesenchymal cells in the capsule and perirenal tissues, as well as proliferation of the interstitial cells of the renal cortex. In addition to the necrotic changes, in some tubules the epithelial cells were flattened and their nuclei elongated.

A progressive decrease in the degree of congestion was first observed in intertubular capillaries and later in glomeruli. Leukostasis was evident in some areas with diminution of the red cells.

Extensive fibrin deposits were observed beneath the capsule and focally within intertubular and glomerular capillaries and occasionally in arteries or afferent arterioles. Calcium and ferric deposits were demonstrated by suitable stains, specially beneath the capsule.

By the fifty-eighth day, in the kidneys of the sole survivor of Group F (Figure 1), large cortical areas of fibrosis with tubular atrophy and/or dilatation were present, as well as areas where the proximal tubules were enlarged. The cytoplasm of the latter type of tubules was acidophilic. In a few tubules hyalin casts containing epithelial cells were observed.

The outermost glomeruli were in contact with the renal capsule, the normal intervening zone of tubules having disappeared. Some of these glomeruli had atrophied, although most were normal. In a few glomeruli, slight periglomerular fibrosis and capsular thickening were found.

Calcium and ferric pigment deposits were again observed, especially beneath the capsule; no fibrin deposits were found.

In frozen sections stained with oil red O, fat deposits were found in many tubules, whether or not they were atrophic.

In the kidneys of the rats of Group H sacrificed at the fifty-eighth day (Figure 2), small areas of fibrosis with tubular atrophy and/or dilatation were found. Other changes were similar to those observed in the sole survivor of Group F. However, the renal lesions in these 6 rats were less severe than those found in the rat of Group F.

In rats dying between the fourteenth and fifty-eighth days, the different types of renal changes were related to the time of death, becoming progressively more similar to those found at the fifty-eighth day the longer the animals survived.

Electron Microscopy

Ultrastructural studies in rats of Group F were necessarily limited to the sole rat which survived the basal regimen for 58 days. The epithelium of many tubules was atrophic (Figure 3), as evidenced by diminished height of the cells, loss of brush borders and flattening of the basal portions of the plasma membranes. In some of these cells dilatation of the profiles of the endoplasmic reticulum and Golgi apparatus was also observed. Occasionally, cells of the atrophic tubules contained bodies which were interpreted to be huge cytosegresomes (Figure 4).

The basement membrane of the atrophic tubules displayed focal thickening (Figures 3, 4), and in the interstitial cells of contiguous intertubular areas the rough endoplasmic reticulum was well developed (Figure 3). Deposits of ferric pigment were also present. Excessive amounts of collagen fibers in intertubular spaces were clearly visualized in sections stained with PTA. Most glomerular tufts were normal.

Similar ultrastructural features were found in the less extensively damaged areas of the choline-deficient rats injected with hydrocortisone (Group H), but in the nonaffected areas tubular epithelium was normal.

No obvious changes were found in the kidneys of the choline-supplemented rats.

Experiment 3—Effects of Retynil Acetate on the Kidneys of Choline-Deficient Weanling Rats—A 5-Day Experiment

Food Intake

The average food intake-gross energy of the four different groups of rats expressed in kcal/100 g body weight, is represented in Text-figure 6. The early decrease in food intake in rats of Groups I (CD *ad lib* + A) and IV (CD pf + A) correlated with the administration of vitamin A (48 hours after the beginning of the experiment).

The pair-fed Groups II (CD pf + 0) and IV (CD pf + A) ate 95 and 83% of the food offered to them.

Body Weights

Changes in body weights are represented in Text-figure 7, in the form of growth curves as percentages of the values at the beginning of the experiment.

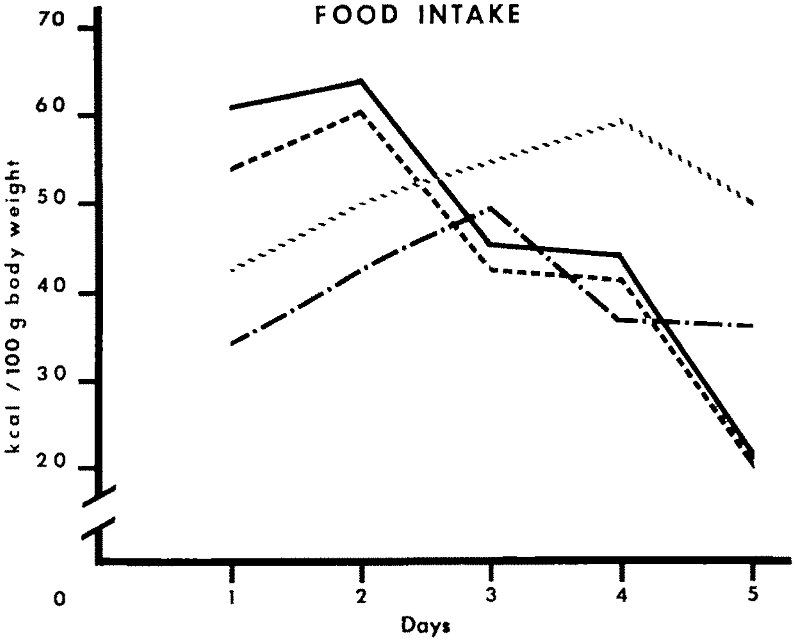

Text-fig 6—Experiment 3. Averages of the daily food intake-gross energy in the 4 groups. (Group I, CD *ad lib* + A —; Group II, CD pair-fed + 0 - - -; Group III, CD *ad lib* + 0 | | |; Group IV, CD pair-fed + A – · –)

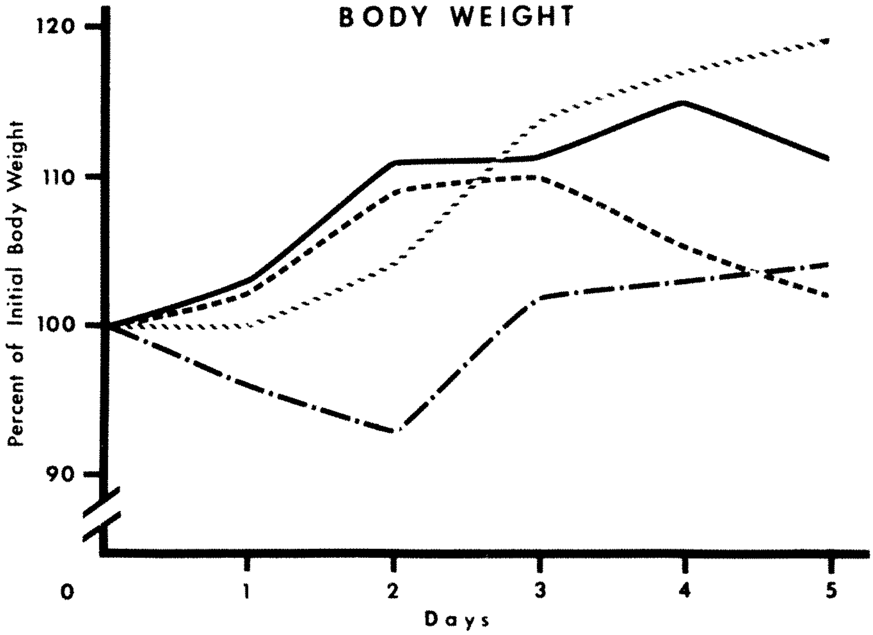

Text-fig 7—Experiment 3. Growth curves of the four different groups. (Group I, CD *ad lib* + A; —; Group II, CD pair-fed + 0 – – –; Group III, CD *ad lib* + 0 | | |; Group IV, CD pair-fed + A—·—·—)

Gross Changes

The gross changes in the necrotic kidneys essentially consisted of increase in size, congestion and patchy areas of subcapsular necrosis.

The average weights of both kidneys (expressed as percentage of body weight) in the different groups at the end of the experiment are represented in Table 5.

To aid in the interpretation of these values and the other parameters studied, those rats with histologic renal necrosis were specifically designated as being in Subgroups Ia, IIa, IIIa, and IVa, thereby eliminating from the latter subgroups the animals without renal necrosis. For statistical analyses of renal weights see Table 4.

Light Microscopy

The incidence of renal necrosis in the four different groups is shown in Table 5, and the extent of the necrosis in Table 3. The comparison of the different groups shows more renal damage in those rats given vitamin A. Statistical analyses of these results are shown in Table 4.

Except for the already noted differences in incidences and extents of

Table 5—Experiment 3. Renal Weights, Incidence of Renal Necrosis, Plasma Urea Nitrogen and Plasma Phospholipids

Group	Abbreviated	No. rats	Renal weights[*] (g/100 g body wt)	Incidence of renal necrosis No.	%	PUN[*] (mg/100 ml)	Plasma phospholipids[*] (mg/100 ml)
I	CD **ad lib** + A	12	1.34 ± 0.06	7	58	51 ± 12	133 ± 11[‡]
Ia[†]	CD **ad lib** + A		1.46 ± 0.08	7	100	74 ± 15	148 ± 9[§]
II	CD pf + O	12	1.18 ± 0.01	1	8	27 ± 2	95 ± 4[‖]
IIa[†]	CD pf + O	1	1.19	1	100	28	98
III	CD **ad lib** + O	12	1.20 ± 0.06	5	42	30 ± 7	91 ± 7
IIIa[†]	CD **ad lib** + O	5	1.24 ± 0.14	5	100	46 ± 15	94 ± 8[¶]
IV	CD pf + A	12	1.19 ± 0.07	5	42	35 ± 9	103 ± 60
IVa[†]	CD pf + A	5	1.55 ± 0.09	5	100	64 ± 14	115 ± 10

[*] Mean values ± SE
[†] Only those rats with renal necrosis
[‡] 9 rats
[§] 5 rats
[‖] 10 rats
[¶] 11 rats

the renal necrosis, no other changes that could be ascribed to the administration of vitamin A or corn oil, were observed.

Plasma Urea Nitrogen and Plasma Phospholipids

Levels of PUN and plasma phospholipids in the different groups at the end of the experiment are shown in Table 5. In correlation with the morphologic changes, rats injected with vitamin A had higher values than those not injected with the vitamin.

Experiment 4—Effects of Retynil Acetate on the Kidneys of Choline-Deficient Weanling Rats—A 6-Day Experiment

Food Intake

The average food intake–gross energy of the four different groups, expressed in kcal/100 g body weight, is represented in Text-figure 8. The early decreases in food intake in rats of Groups V and VIII correlate with the beginning of the administration of vitamin A (48 hours after the beginning of the experiment). The pair-fed groups (VI and VIII) ate 94 and 74% of the food offered.

Body Weights

Changes in body weights are represented in Text-figure 9 in the form of growth curves as percentages of the values at the beginning of the experiment. As in the end of Experiment 3 those rats fed *ad libitum*

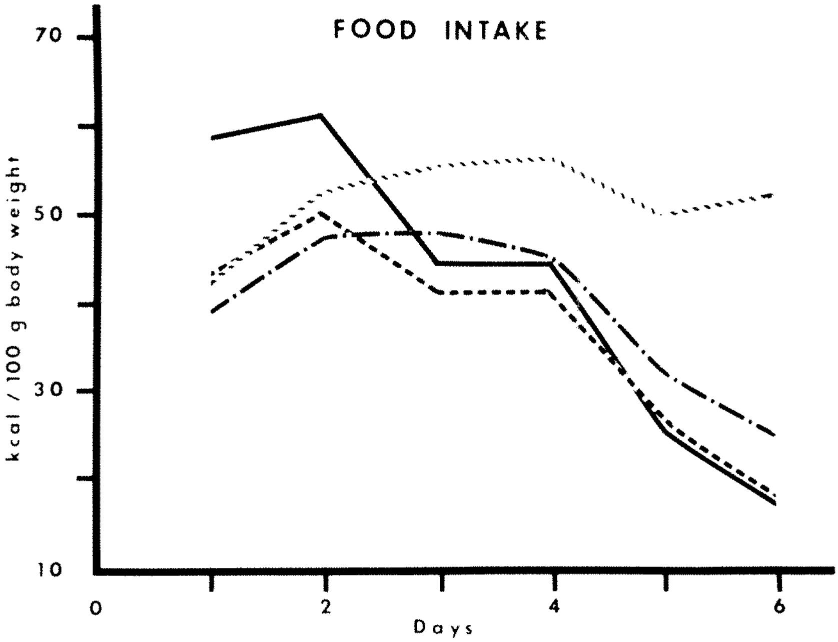

TEXT-FIG 8—Experiment 2. Averages of the daily food intake-gross energy of the four different groups. (Group V, CD *ad lib* + A —; Group VI, CD pair-fed + 0 – – –; Group VII, CD *ad lib* + 0 | | |; Group VIII, CD pair-fed + A)

and injected with the vehicle alone (Group VII), were heavier than those injected with vitamin A (Group V).

Gross Changes

Some of the kidneys had the typical hemorrhagic aspect, while others were similar to those found in Experiment 3; the remainder were normal.

The average weights of both kidneys (expressed as percentage of body weight) in the different groups are shown in Table 6, and the statistical analyses of these data are presented in Table 4.

To aid in the interpretation of these values and the other parameters studied, those rats with histologic renal necrosis were specifically designated as being in Subgroups Va, VIa, VIIa, and VIIIa, thereby eliminating from the latter subgroups the animals without renal necrosis.

Light Microscopy

Incidences of renal necrosis in the four different groups are shown in Table 6, and the extent of the necrosis in Table 3. The statistical analyses of these results are presented in Table 4.

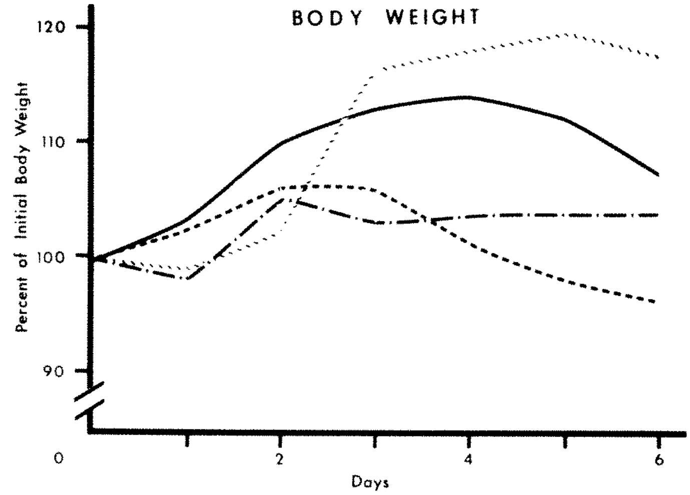

Text-fig 9—Experiment 4. Growth curves of the four different groups. (Group V, CD *ad lib* + A —; Group VI, CD pair-fed + 0 – – –; Group VII, CD *ad lib* + 0 | | |; Group VIII, CD pair-fed + A —·—)

Comparison of these results indicates that more renal damage had occurred in rats injected with vitamin A than in those injected with the vehicle alone. Except for these differences of extent and incidence of necrosis, no qualitative histologic differences were found between the vitamin A- and vehicle-alone-injected rats.

Table 6—Experiment 4. Renal Weights, Incidence of Renal Necrosis, Plasma Urea Nitrogen and Plasma Phospholipids

Group	Abbreviated	No. rats	Renal weights* (g/100 g body wt)	Incidence of renal necrosis		PUN (mg/100 ml)	Plasma phospholipids (mg/100 ml)
				No.	%		
V	CD **ad lib** + A	12	1.93 ± 0.10	10	83	114 ± 16‡	159 ± 16§
Va†	CD **ad lib** + A	10	2.07 ± 0.05	10	100	139 ± 9‖	172 ± 16¶
VI	CD pf + O	12	1.28 ± 0.08	3	25	—	—
VIa†	CD pf + O	3	1.65 ± 0.08	3	100	—	—
VII	CD **ad lib** + O	12	1.55 ± 0.11	11	92	75 ± 14	99 ± 8
VIIa†	CD **ad lib** + O	11	1.59 ± 0.11	11	100	80 ± 14	102 ± 9
VIII	CD pf + A	12	1.71 ± 0.11	10	83	99 ± 19	131 ± 8
VIIIa†	CD pf + A	10	1.80 ± 0.11	10	100	118 ± 17	131 ± 10

* Mean values ± SE

† Only those rats with renal necrosis

‡ 9 animals

§ 7 animals

‖ 7 animals

¶ 5 animals

Plasma Urea Nitrogen and Plasma Phospholipids

Levels of PUN and plasma phospholipids at the end of the experiment are stated in Table 6. Because of a technical problem no determinations were done on plasma of rats in Group VI. Higher values of both parameters were found in those rats injected with vitamin A when compared with similar values from those rats injected with the vehicle alone.

Experiment 5—Biochemical Evaluation of Acid Phosphatase in the Kidneys of Choline-Deficient and Choline-Supplemented Rats

Tables 7 and 8 include the results of the different parameters studied, such as body weight, renal weight, total renal protein and renal protein concentration, as well as free and total acid phosphatase expressed per mg of renal protein, per 100 mg of wet renal tissue and per total renal mass.

At the fifth day of the experiment, those rats fed the choline-deficient diet were separated into 2 groups according to whether or not they had evidence of renal necrosis by light microscopy in sections taken before the homogenation of the kidneys.

As usual, the kidneys of those rats with renal necrosis were heavier, whether expressed as absolute weights or as percentages of body weight.

No statistically significant differences were observed in renal protein concentrations throughout the experiment (Table 9). However, rats with renal necrosis had, at the fifth day, higher values of total renal protein and lower concentration than those supplemented with choline.

The results of the biochemical evaluation of free and total acid phosphatase are presented in Table 8. The percentages of increase at the fifth day were lower in the choline-deficient rats (with and without renal necrosis) than in the choline-supplemented rats. Moreover, the differences were statistically significant between the choline-deficient nonnecrotic and the choline-supplemented rats.

Discussion

For years the pathogenesis of the renal necrosis of choline-deficient weanling rats has been, and still is, a matter of debate.[2,28] In an experiment using histochemical and electron microscopic technics,[1] we found that changes in lysosomes were the most outstanding modifications in the prenecrotic stages. The results suggested the hypothesis that lysosomal alterations could play a fundamental role in the pathogenesis of this necrosis. We have also found [2] that antioxidants have a protective effect and that lipoperoxidation is present in the renal lipids before

Table 7—Experiment 5. Initial and Final Body Weights, Renal Weights and Renal Protein

Group	No. rats	Initial* body wt	Final* body wt	Both kidney* weights (mg)	Renal weights* (g/100 g body wt)	Renal protein* (mg/100mg tissue)	Total protein* both kidneys (mg)
At 2 days							
CD	6	39 ± 4	44 ± 3	479 ± 45	1.09 ± 0.03	13.9 ± 0.3	66.8 ± 6.7
CS	5	36 ± 1	43 ± 1	515 ± 20	1.21 ± 0.03	14.8 ± 0.4	76.4 ± 4.7
At 4 days							
CD	6	44 ± 3	55 ± 3	549 ± 41	1.09 ± 0.02	15.1 ± 0.3	82.7 ± 6.4
CS	6	50 ± 2	56 ± 1	604 ± 15	1.07 ± 0.02	15.2 ± 0.2	90.9 ± 2.5†
At 5 days							
CD necrotic	9	35 ± 2	49 ± 1	691 ± 28	1.42 ± 0.06	13.6 ± 0.3	94.9 ± 6.1
CD nonnecrotic	11	41 ± 2	51 ± 1	557 ± 15	1.09 ± 0.02	14.2 ± 0.2	79.1 ± 2.6
CS	6	36 ± 1	46 ± 3	462 ± 15	1.20 ± 0.04	14.9 ± 0.4	70.1 ± 2.0

* Mean values ± SE

† 5 animals

Table 8—Experiment 5. Renal Levels of Free and Total Phosphatase and Percentages of Increase

Group	No. rats	μgP/mg protein/10^{1}		Increase* (%)	μgP/100 mg tissue/10^{1}		μgP/whole kidneys/10^{1}	
		Free*	Total*		Free*	Total*	Free*	Total*
At 2 days								
CD	6	5.5 ± 0.3	10.1 ± 0.2	84 ± 7	76.9 ± 3.9	139.7 ± 2.0	364.4 ± 25.7	686.7 ± 59.3
CS	5	5.1 ± 0.1	9.3 ± 0.3	81 ± 6	75.9 ± 1.7	136.5 ± 3.0	389.8 ± 12.9	702.3 ± 29.7
At 4 days								
CD	6	5.3 ± 0.3	9.8 ± 1.0	89 ± 14	79.0 ± 4.5	145.9 ± 3.9	430.2 ± 31.4	806.0 ± 79.8†
CS	6	5.2 ± 0.2	9.7 ± 0.2	87 ± 5	79.3 ± 3.7	148.2 ± 3.2	457.8 ± 9.1†	882.7 ± 28.1†
At 5 days								
CD necrotic	9	5.5 ± 0.2	9.4 ± 0.2	72 ± 5	74.1 ± 2.1	138.7 ± 4.7	512.2 ± 24.2	957.7 ± 37.3
CD nonnecrotic	11	5.9 ± 0.1	9.9 ± 0.2	67 ± 4	84.5 ± 1.8	144.2 ± 2.2	470.7 ± 15.9	804.2 ± 26.0
CS	6	5.7 ± 0.4	10.5 ± 0.3	87 ± 6	84.7 ± 4.9	157.2 ± 5.1	406.1 ± 29.8†	746.4 ± 15.0†

* Mean values ± S E

† 5 animals

Table 9—Experiment 5. Statistical Analysis

Compared groups	Comparison	Statistical test used	Difference*	P Values
At 2 days				
CD vs CS	Mean renal protein concentration	t	NS	—
CD vs CS	Mean percentage increase of AcPase†	t	NS	—
At 4 days				
CD vs CS	Mean renal protein concentration	t	NS	—
CD vs CS	Mean percentage increase of AcPase	t	NS	—
At 5 days				
CD necrotic	Mean renal protein concentration	Scheffe	NS	—
vs				
CD nonnecrotic	Mean percentage increase of AcPase	Scheffe	NS	—
CD necrotic	Mean renal protein concentration	Scheffe	NS	—
vs				
CS	Mean percentage increase of AcPase	Scheffe	NS	—
CD nonnecrotic	Mean renal protein concentration	Scheffe	NS	—
vs				
CS	Mean percentage increase of AcPase	Scheffe	S	<0.05

* NS = Not Significant, S = Significant

† AcPase = acid phosphatase

the necrotic lesions developed. Since it is considered that lipoperoxidation damages subcellular structures, including lysosomes,[29,30] these results support our hypothesis.

The severe hypolipotropic diet used in our experiments induced renal lesions regularly within a short period (5 to 8 days) in a high percentage of animals (more than 90%), facilitating comparisons between choline-deficient groups of rats and their appropriate controls.

The evidence, previously presented by others in acute experiments,[31,32] that corticoids prevented to some extent the renal lesions induced by choline-deficient diets, appeared to substantiate the pathogenic implications of alterations in lysosomes, since these hormones have a stabilizing effect on these organelles *in vivo* as well as *in vitro*.[33,34]

In the first two experiments described in this paper we confirmed and explored further the previously reported preventive action of corticoids. Under our experimental conditions it was clearly evident that hydrocortisone significantly hindered the development of the renal lesions and diminished their extent while prolonging the survival of the animals.

In these two experiments the vehicle alone was not given to the rats of Groups A, B, E, F and G to avoid any "alarming" stimuli [35] that could interfere in the interpretation of the results.

Although individual pair-feeding *per se* induced a diminution of the incidence and severity of the renal lesions,[2] it was not as important as the one observed between Groups A and C of the first experiment reported in this paper. The results of this experiment indicate an undoubted protective effect of hydrocortisone.

Since rats of Group C (CD pf + H) grew similarly to those of Group A (CD *ad lib*), the lower incidence and extent of the renal lesions could not be attributed to a lesser increase in body weight than in the controls. In this regard it is interesting to note that in the experiment reported by Hall and Bieri[32] the group of rats injected with hydrocortisone had only grown by 0.5 g at the end of the experiment (6 days). Since the growth of rats is an important factor in the development of the renal lesions and the results obtained by Hall and Bieri might have been influenced by the poor growth of the animals, we considered it necessary to repeat and extend these investigations under more precisely controlled conditions. On the other hand, in the paper of Sellers *et al*[31] reporting the protective effect of cortisone in their experimental model, the precise incidence and extent of the renal lesions are not reported.

In addition, the administration of hydrocortisone to our animals did not induce any glomerular hyalinization as described by Hall and Bieri[32] in their treated animals, or the changes found by Selye[36] after administration of cortisone to normal rats. This apparent disagreement with Selye's results is quite likely explained by differences in doses and types of corticoids employed; we have no explanation however for the divergence of our results with those of Hall and Bieri.

In the chronic experiment (Experiment 2), the administration of hydrocortisone prolonged the survival of the choline-deficient animals by substantially reducing the incidence of fatal renal necrosis. As in the acute experiment (Experiment 1), the protective effect of hydrocortisone in the longer experiment could not be attributed to a decrease in food intake or ponderal growth of the animals since both were similar for rats of Group F (CD *ad lib*) and H (CD *ad lib* + H).

The six choline-deficient rats, treated with hydrocortisone and killed at the fifty-eighth day, developed varying degrees of renal damage which were always less than in kidneys of non-hydrocortisone-injected choline-deficient controls.

The renal histologic features of the hydrocortisone-treated rats killed at the fifty-eighth day, along with those found in similarly treated rats which died between the fourteenth and fifty-eighth day, indicated that the milder degree of the final lesions of the treated rats could be attributed to a less severe initial renal damage rather than to better recovery.

In Experiments 3 and 4, the effects of a well-known labilizer of the lysosomes such as vitamin A were studied. Since it is known that hypervitaminosis A, and perhaps hypovitaminosis A[37,38] are both labilizers of the lysosomes, we gave vitamin A by intramuscular injection to the rats of Groups I, IV, V and VIII and in addition we gave adequate amounts of vitamin A to every group in the diet. Therefore, some groups received normal dietary supplements of vitamin A and others extra amounts.

We killed the rats on the fifth and sixth day of the experiment in order to avoid an unduly high incidence of extensive renal necrosis as would have occurred otherwise on the eighth day thereby complicating interpretation of the results. In this way undesirable postmortem changes were also avoided.

The comparison of the various parameters studied in the different groups showed that the administration of vitamin A, produced an increase in the incidence and severity of renal lesions as evaluated by renal weight, extent of the renal necrosis and levels of PUN and plasma phospholipids. In comparing the results in the different groups, it is important and necessary to consider the protective effect of pair-feeding *per se*,[2] already described.

As we have previously reported,[39] the plasma phospholipids that usually decrease in uncomplicated choline-deficiency,[40,41] were elevated in those groups of rats with renal damage. We still cannot offer an explanation for this increase. Serum lipid changes have been reported by others in various types of renal abnormalities;[42–47] of particular interest in this regard is the recent work of Sneider and Shore[48] describing the role of the canine kidney in the kinetics of plasma-tissue phospholipids.

The possible part played by the release of the lysosomal enzymes in the pathogenesis of cellular necrosis is still not clear despite numerous studies on this aspect of cellular pathology.[49–52] On the other hand, it is still uncertain whether a diminution in the percentage of increase between free and total acid phosphatase (or an increase in the ratio free/total) is an indication of release of the lysosomal enzymes *in vivo*, or if the lysosomes are more fragile to technical manipulations.[53–55] Complicating these uncertainties is the fact that at present it is not known whether these changes represent alterations of the lysosomal membrane or matrix[55] or perhaps both. At any rate, these changes are accepted as an indication of lysosomal modifications and have been reported to be present under a variety of experimental conditions.[38,50,52,54,56] In Experiment 5 of this paper, we found a decrease in the percentage of increase between free and total acid phosphatase at the fifth day in the choline-deficient rats when compared to the choline-supplemented rats at the same period.

At first sight it is surprising that the difference in the percentage of increase is significantly different between the choline-deficient rats without renal necrosis but not in the choline-deficient with renal necrosis when compared to the results obtained in the choline-supplemented rats. This finding could be explained, perhaps, by the fact that in the necrotic kidneys there is congestion and that acid phosphatase from the red cells has modified the values due to the kidney cells.

To avoid confusion arising from possible variations of the reference base used, we have given the results expressed per milligram protein, per 100 mg wet tissue and per total renal mass.

The protein concentration did not change significantly throughout the experiment, but an increase was found in the total protein content of the necrotic kidneys at the fifth day. These results are in agreement with those previously reported by others.[57,58]

The possible pathogenic role of the changes in lipid composition which occur in kidneys of choline-deficient rats, in the development of the necrotic lesions, remains uncertain.[57–66] Since lipids are important in the structure and function of the lysosomes,[54,55,67,68] such changes could involve the lysosomes. Further studies are necessary to explore this correlation.

The results reported in this paper, give further support to our previous view that alterations of lysosomes could play an important role in the pathogenesis of the renal lesions of choline deficient weanling rats. Further, our results as well as those of others [2,69] have established that antioxidants have a protective effect in this experimental model because we have found direct evidence of lipoperoxidation in kidneys [2] but not in livers [70] at the fifth day of choline deficiency in weanling rats and before renal necrosis could be detected either grossly or microscopically. At the same stage of choline-deficiency, without detectable renal necrosis, we have now found significant changes in the ratio of free to total acid phosphatase. Since lipoperoxidation injures lysosomes,[29,30,52] it might be that these changes are interrelated.

References

1. Monserrat AJ, Porta EA, Hartroft WS: Sequential renal changes in choline-deficient weanling rats. Conventional and electron histochemistry. Arch Pathol 85:419–432, 1968

2. Monserrat AJ, Ghoshal AK, Hartroft WS, Porta EA: Lipoperoxidation in the pathogenesis of renal necrosis in choline-deficient rats. Am J Pathol 55:163–190, 1969
3. Griffith WH, Wade NJ: Some effects of low choline diets. Proc Soc Exp Biol Med 41:188–190, 1939
4. Dalton AJ: A chrome-osmium fixative for electron microscopy. Anat Rec 121:281, 1955 (abstr)
5. McManus JFA, Mowry RW: Staining Methods: Histological and Histochemical. New York, Paul B. Hoeber Inc, 1960, p 23
6. McManus JFA, Mowry RW: Staining Methods: Histological and Histochemical.[5] pp 57–59
7. Wilson W: Trichrome method for staining fat with oil red O in frozen sections. Bull Intern Assoc Med Mus 31:216–229, 1950
8. Luft JH: Improvements in epoxy resin embedding methods. J Biophys Biochem Cytol 9:409–414, 1961
9. Trump BF, Smuckler EA, Benditt EP: A method for staining epoxy sections for light microscopy. J Ultrastruct Res 5:345–348, 1961
10. Reynolds ES: The use of lead citrate at high pH as an electron-opaque stain in electron microscopy. J Cell Biol 17:208–212, 1963
11. Trump BF, Bulger RE: Morphology of the kidney. Structural Basis of Renal Disease. Edited by EL Becker. Paul B. Hoeber Inc, New York, 1968, pp 1–92
12. McManus JFA, Mowry RW: Staining Methods: Histologic and Histochemical.[5] pp 61–62
13. McManus JFA, Mowry RW: Staining Methods: Histologic and Histochemical.[5] pp 195–196
14. McManus JFA, Mowry RW: Staining Methods: Histologic and Histochemical.[5] pp 81–82
15. Watson ML: Staining of tissue sections for electron microscopy with heavy metals. J Biophys Biochem Cytol 4:475–478, 1958
16. Technicon Autoanalyzer Methodology. Method file Number 1–6, 1965
17. Kraml MA: Semiautomated determination of phospholipids. Clin Chim Acta 13:442–448, 1966
18. Hurst RO: The determination of nucleotide phosphorus with stannious chloride hydrozine sulphate reagent. Can J Biochem 12:287–292, 1964
19. Franklin TJ: The influence of age on the activities of some hydrolases in the rat liver and kidney. Biochem J 82:118–122, 1962
20. Fiske CH, Subbarow Y: The colorimetric determination of phosphorus. J Biol Chem 66:375–400, 1925
21. Lowry H, Rosenbrough NJ, Farr AL, Randall RJ: Protein measurement with the Folin phenol reagent. J Biol Chem 193:265–275, 1951
22. Sigel S: Nonparametric Statistics. New York, McGraw Hill Book Company, 1956, pp 116–117
23. Snedecor GW, Cochram WG: Statistical Methods, Sixth edition. Ames, Iowa, Iowa State University Press, 1967, pp 271
24. Griffith WH: The renal lesions in choline deficiency. Am J Clin Nutr 6:263–273, 1958
25. Christensen K: Renal changes in the albino rat on low choline and choline-deficient diets. Arch Pathol 34:633–646, 1942

26. Hartroft WS: Pathogenesis of renal lesions in weanling and young adult rats fed choline-deficient diets. Br J Exp Pathol 29:483–494, 1948
27. Moore HC: The acute renal lesions produced by choline-deficiency in the male weanling rat. J Pathol Bacteriol 74:171–184, 1957
28. Wells IC: Hemorrhagic kidney degeneration in choline deficiency. Fed Proc 30:151–154, 1971
29. Desai ID, Sawant PL, Tappel AL: Peroxidative and radiation damage to isolated lysosomes. Biochim Biophys Acta 86:277–285, 1964
30. Wills ED, Wilkinson AE: Release of enzymes from lysosomes by irradiation and the relation of lipid peroxide formation on enzyme release. Biochem J 99:657–666, 1966
31. Sellers EA, Ridout RW, Best CH: Partial protection by cortisone against renal lesions produced by hypolipotropic diets. Nature (Lond) 166:514, 1950
32. Hall CE, Bieri JG: Modifications of the choline deficiency syndrome in the rat by somatotropin and hydrocortisone. Endocrinology 53:661–666, 1953
33. Thomas L: A possible mechanism for the action of cortisone in reactions to tissue injury. International Symposium of Injury, Inflammation and Immunity. Edited by L Thomas, JW Uhr, L Grant. Baltimore, Williams and Wilkins Co, 1964, pp 312–319
34. Weissmann G: The effects of steroids and drugs on lysosomes. Lysosomes in Biology and Pathology. Edited by JT Dingle, HB Fell. Amsterdam, North Holland Publishing Co, 1969, pp 467–492
35. Baxter JH: Protective effect of thiouracil and dibenamine against renal injury due to choline deficiency: influence of endocrine and autonomic systems. J Pharmacol 107:394–408, 1953
36. Selye H: Stress. Montreal, Canada. Aeta, Inc Medical Pub, 1950, pp 623
37. Dingle JT, Lucy JA: Vitamin A, carotenoids and cell function. Biol Rev 40:422–461, 1965
38. Roels OA: The influence of vitamins A and E on lysosomes. Lysosomes in Biology and Pathology.[34] pp 254–275
39. Monserrat AJ, Porta EA, Hartroft WS: Orotic acid effects on the kidney. Changes in choline-deficient weanling rats. Arch Pathol 87:154–163, 1969
40. Lombardi B, Osler A: Choline deficiency fatty liver (protein synthesis and release). Lab Invest 17:308–321, 1967
41. Haines DSM, Mookerjea S: Impairment of triglyceride transport from the liver in choline deficiency. Can J Biochem 43:507–520, 1965
42. Ludewig S, Chanutin A: Experimental renal insufficiency produced by partial nephrectomy. X. Blood plasma cholesterol and phospholipid phosphorus values for control and partially nephrectomized rats fed diets containing dried extracted liver. Arch Intern Med 61:847–853, 1938
43. Heymann W: Renal hyperlipemia in dogs. Science 96:163–164, 1942
44. Winkler AW, Durlacher SH, Hoff HE, Man EB: Changes in lipid content of serum and of liver following bilateral renal ablation of ureteral ligation. J Exp Med 77:473–486, 1943
45. Schreiner GE: Acute renal failure. Renal Disease, Second edition. Edited by DAK Black. Oxford, England, Blackwell Scientific Publications, 1967, pp 309–326
46. Bierman EL: Abnormalities of carbohydrate and lipid metabolism in uremia. Arch Inter Med 7:790–792, 1970

47. Losowsky MS, Kenward DH: Lipid metabolism in acute and chronic renal failure. J Lab Clin Med 71:736–743, 1968

48. Sneider TW, Shore ML: Synthesis and utilization of plasma phospholipid by the isolated perfused dog kidney. Lab Invest 19:181–186, 1968

49. De Duve C: Lysosomes and cell injury. International Symposium of Injury. Edited by L Thomas, JW Uhr, L Grant. Baltimore, Williams and Wilkins Co. 1964, pp 283–311

50. Thomas L: The role of lyosomes in tissue injury. The Inflammatory Process. Edited by BW Zweifach, L Grant, RT McCluskey. New York, Academic Press, Inc, 1965, pp 449–463

51. Weissman G: The role of lysosomes in inflammation and disease. Annu Rev Med 18:97–112, 1967

52. Slater TF: Lysosomes and experimentally induced tissue injury. Lysosomes in Biology and Pathology,[34] pp 467–492

53. Chayen J, Bitensky L: Multiphase chemistry of cell injury. The Biological Basis of Medicine. Edited by EE Bittar, N. Bittar. London, Academic Press, 1968, pp 337–368.

54. Iqbal M, Dingle JT, Moore T, Sharman IM: Nutrition and lysosomal activity. The effect of dietary cod liver oil on the distribution of polyunsaturated fatty acids in the kidney lysosomes of rats receiving deficient or adequate intakes of vitamin E. Br J Nutr 23:31–39, 1969

55. Koening H: Lysosomes in the nervous system. Lysosomes in Biology and Pathology,[34] pp 111–162

56. Filkins JP: Lysosomes and hepatic regression during fasting. Am J Physiol 219:923–927, 1970

57. Patterson JM, McHenry EW: Choline and the prevention of hemorrhagic kidneys in the rat. III. Amounts of water, nitrogen, total lipid and choline in livers and kidneys. J Biol Chem 156:265–269, 1944

58. Parks PF, Smith RC: Chemical composition of kidneys from choline-supplemented and choline-deficient weanling rats. J Nutrition 96:263–268, 1968

59. Patterson JM, McHenry RW: Choline and the prevention of hemorrhagic kidneys in the rat. J Biol Chem 145:207–221, 1942

60. Patterson JM, Keevil NB, McHenry EW: Choline and the prevention of hemorrhagic kidneys in the rat. II. Phospholipid turnover determined with radioactive phosphorus. J Biol Chem 153:489–493, 1944

61. Baxter JH, Goodman H: Renal and hepatic lipid alterations in choline deficiency: relationship to renal necrosis. Lipids 89:682–687, 1955

62. Zaki G, Hoffbauer FW, Grande F: Prevention of renal necrosis by coconut oil in choline-deficient rats. Arch Pathol 81:8589, 1966

63. Fewster ME, Nye JF, Griffith WH: Renal lipid composition of choline-deficient rats. J Nutr 90:252–258, 1966

64. Fewster ME, Hall MO: The renal phospholipid composition of choline-deficient rats. Lipids 2:239–243, 1967

65. Simon JB, Scheig R, Klatskin G: Relationship of early lipid changes in kidneys and liver to the hemorrhagic renal necrosis of choline-deficient rats. Lab Invest 19:503–509, 1968

66. Parks PF, Smith RC: Synthesis of phospholipids and deoxyribonucleic

acid in choline-supplemented and choline-deficient weanling rats. J Nutr 97:481–488, 1969

67. Tappel AL: Lysosomal enzymes and other components.[34] pp 207–244
68. Goldstone A, Szabo E, Koenig H: Isolation and characterization of acidic lipoproteins in renal and hepatic lysosomes. Life Sci 9:607–616, 1970
69. Newbwerne PM, Brenahan MR, Kula N: Effects of two synthetic anti oxidants, vitamin E and ascorbic acid on the choline-deficient rat. J Nutr 97:212–231, 1969
70. Ghoshal AK, Monserrat AJ, Porta EA, Hartroft WS: Role of lipoperoxidation in early choline-deficiency. Exp Mol Pathol 12:31–35, 1970

Acknowledgments

We are greatly indebted to S. B. Hartman (Centro de Bioestadistica y Demografia, Facultad de Medicina, Universidad de Buenos Aires, Buenos Aires, Argentina) for the excellent technical assistance in the statistical analyses.

Dr. Monserrat's present address is II Catedra de Patologia, Facultad de Medicina, Universidad de Buenos Aires, Buenos Aires, Argentina. Drs. Hamilton and Ghoshal are with the Research Institute of The Hospital for Sick Children, Toronto, Ontario, Canada; Drs. Porta and Hartroft are with the Department of Pathology, University of Hawaii, School of Medicine, Honolulu, Hawaii.

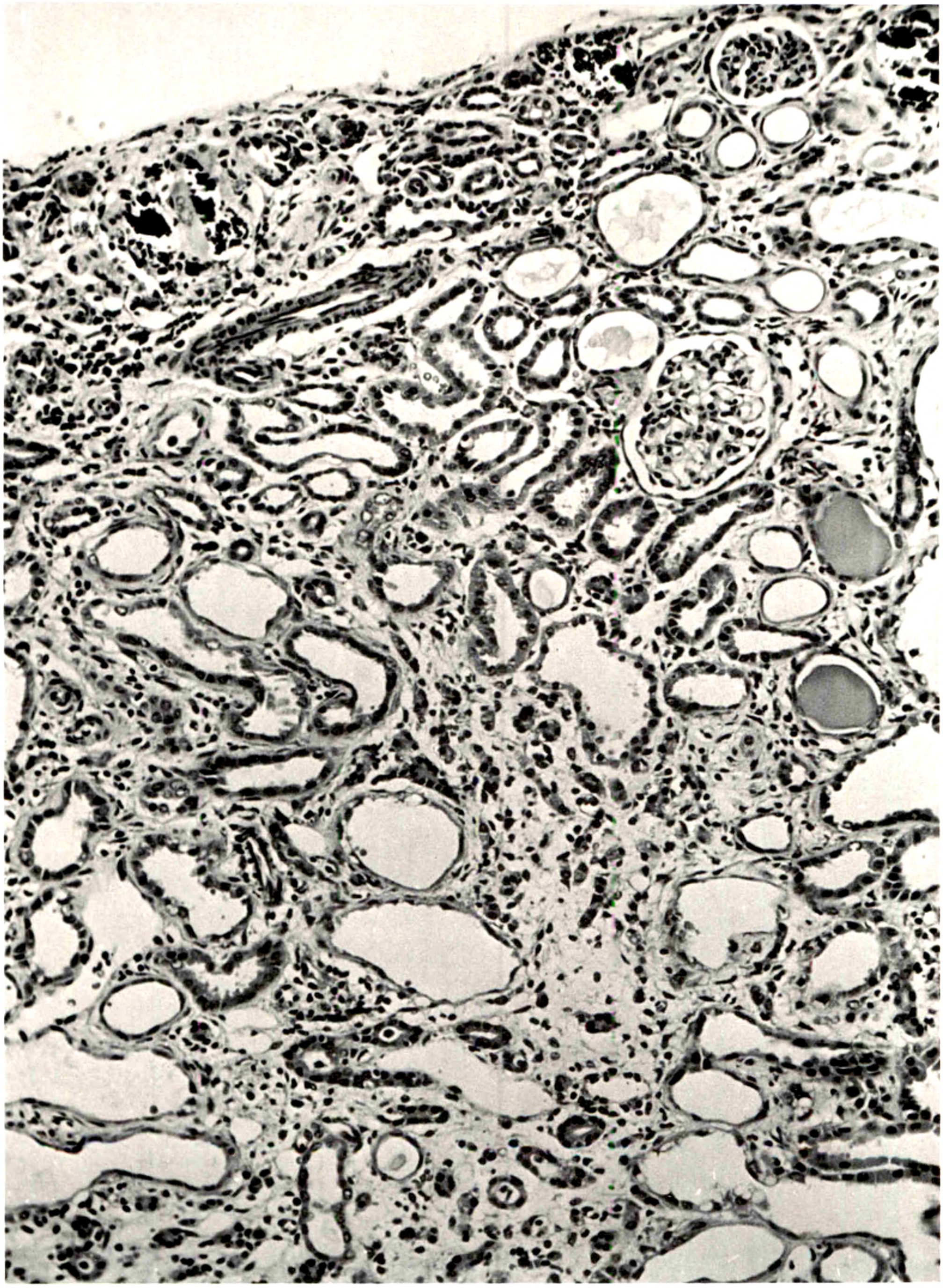

Fig 1—Experiment 2. Renal changes found in the sole survivor of Group F (CD *ad lib*) at the fifty-eighth day. Note the atrophy of some tubules, the dilatation of others and the hyalin casts present in some of them in one area of cortical fibrosis (compare with Figure 2) (H&E, × 240).

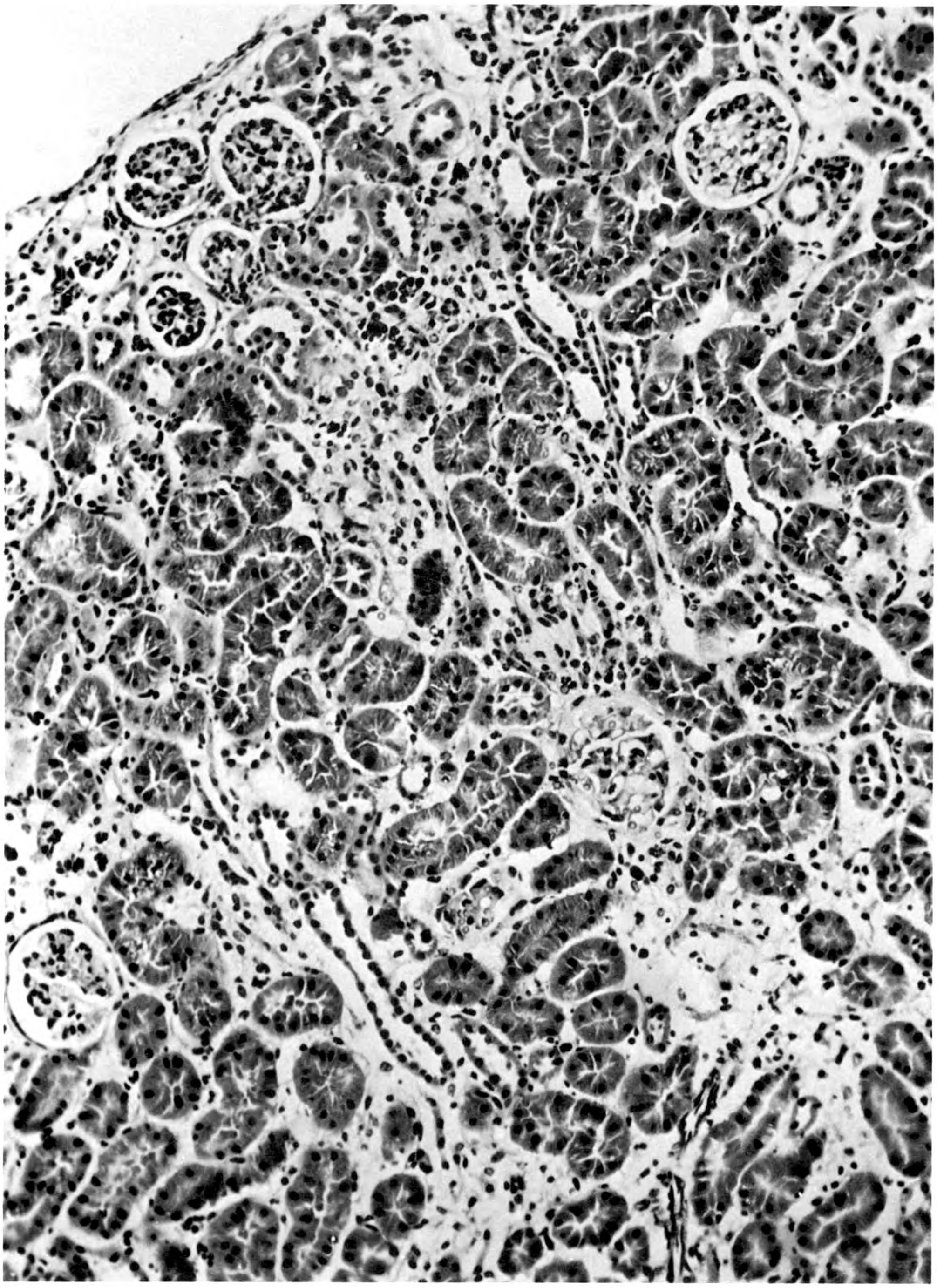

Fig 2—Experiment 2. Renal changes in rat of Group H (CD *ad lib* + H) at the fifty-eighth day are less severe than in rat of Group F (compare with Figure 1) (H&E, × 240).

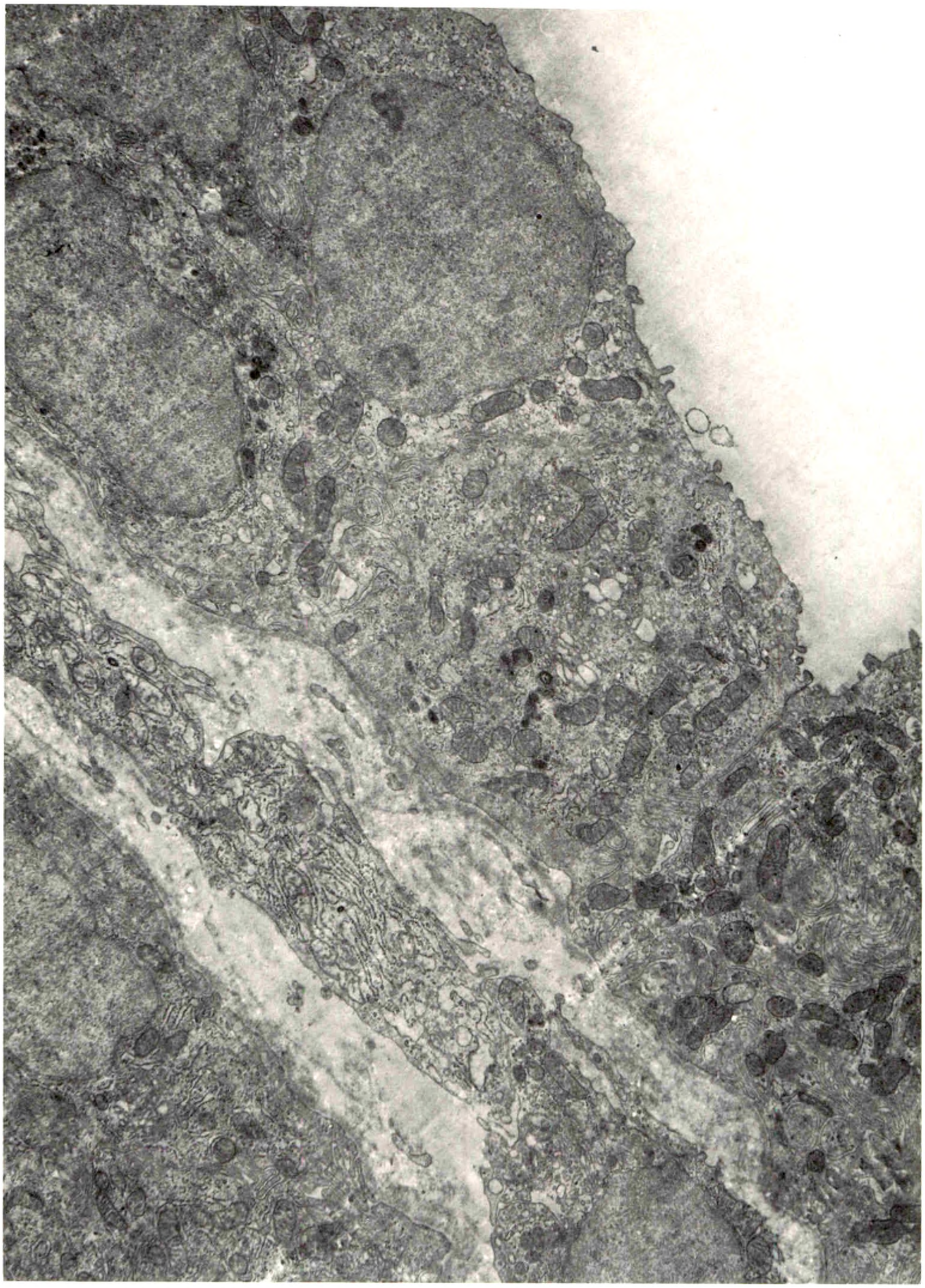

Fig 3—Experiment 2. The epithelial cells of this proximal convoluted tubule are atrophic; edema is present in the interstitium of the renal cortex of the sole rat which survived 58 days on the choline-deficient *ad libitum* regimen. (Lead stain, × 10,000).

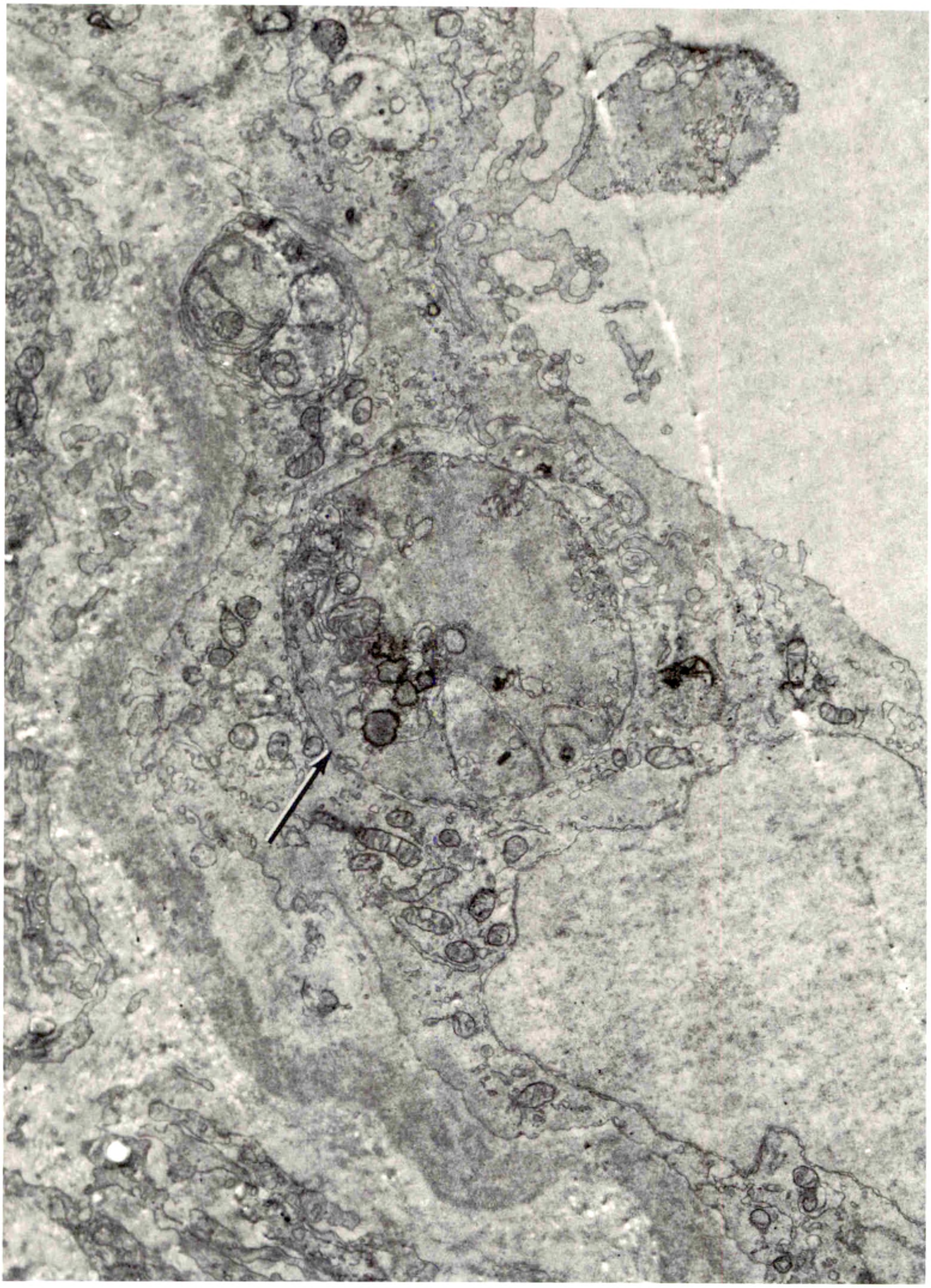

Fig 4—Experiment 2. Again the tubular cells are atrophic and the interstitium edematous in the cortex of the kidney of the same animal represented in Figure 3. The basement membrane is thickened. The body indicated by the arrow is interpreted as a huge cytosegresome in a tubular cell (Lead stain, × 11,700).

Lymphocyte Depression Induced in Chickens on Diets Deficient in Vitamin A and Other Components

Betsy G. Bang, BA, Frederik B. Bang, MD and Marie A. Foard, BS

Chickens maintained from time of hatching to age of 30 days on a diet lacking vitamin A, and on 2 diets lacking vitamin A and other nutritional components showed depletion of lymphocyte and plasma cell populations in nasal, paranasal and bursal lymphoepithelial tissues. Effects were significant with all diets but most severe with the most deprived diet. Infection of these birds with Newcastle disease virus showed further depletion of plasma cells, subnormal inflammatory response, keratinization of bursal epithelia and postsloughing metaplasia of nasal mucociliated epithelia. The bursae of infected chickens on the diet lacking only vitamin A were completely devoid of lymphocytes 6 days after virus inoculation. Infected chickens on the most deprived diet showed atrophy of areas of intranasal epithelia which indicated failure of basal cells to synthesize replacement cells (Am J Pathol 68:147–162, 1972).

SINCE SPICER[1] noted in 1892 that several childhood infectious diseases precipitated acute keratomalacia, many interactions between malnutrition and atrophy of tissus, and between malnutrition and disease have been reported in humans and experimental animals.[2-4] Recently the effects of protein calorie malnutrition (PCM) on depressing the cell-mediated immune (CMI) response in children have been highlighted, especially by Smythe *et al.*[5] Over the past three years we have observed effects of diets lacking either vitamin A alone or vitamin A and other dietary components on lymphoid and epithelial tissues in growing chickens. This report will summarize histologic findings on lymphoepithelial tissues associated with the upper respiratory tract and the bursa of Fabricius in chicks maintained on deprived diets from the time of hatching to 1 month of age.[6] Some chickens in each group were inoculated with the mesogenic strain of Newcastle disease virus (NDV) after 21 days on the respective diet; effects of the virus are compared with effects on birds maintained on normal mash and on a vitamin A-deficient diet supplemented with vitamin A palmitate.

From the Department of Pathobiology, The Johns Hopkins University, School of Hygiene and Public Health, Baltimore, Md.

Accepted for publication Feb 23, 1972.

Address reprint requests to Mrs. Frederik Bang, Department of Pathobiology, Johns Hopkins University, School of Hygiene and Public Health, 615 N Wolfe St, Baltimore, Md 21205.

Chickens have no cervical lymph nodes[7] nor do they normally have lymphoid nodules in the nasal submucosa, as do Japanese quails.[8] In healthy young stock chickens, however, there are 5 consistent loci of aggregate lymphoid cell expression associated with the oculonasal organ system:[8] in the fauces, lacrimal ducts, lateral nasal gland ducts and the nictitating-membrane glands of Harder and their ducts. Foci in fauces, lacrimal and Harderian ducts are invasive small-lymphocyte aggregations which often have germinal centers; those in nasal gland ducts are populations of plasmacytes which intrude among the basal and epithelial cells lining the ducts, and those in the Harderian glands are heavy concentrations of circulating plasma cells in the interlobular spaces. It was previously noted that: a) while the invasive foci meet Lucas' definition of abnormal or "ectopic" reactive sites,[9] the distinction between normal and abnormal may be academic in areas in which cells are constantly exposed to a sheet of mucus containing infectious agents; b) nasal gland ducts were possible shedding sites for plasmacytes or their products; and c) the heavy concentrations of plasma cells in the Harderian gland suggested a lymphocytopoietic function for this organ.[8] This latter possibility has since been explored by Glick,[10] who found that when sheep red blood cells were dropped onto the chick eyeball, plaque-forming cells were produced in the gland of Harder. He also found that 2 successive injections of cyclophosphamide into hatchling chicks apparently eliminated plasma cells from the Harderians within 16 days.[11] Leslie *et al*[12] have concluded that chickens have a secretory immunologic system wherein the secretory Ig is of the same class as the predominant serum Ig.

Another key lymphoid system in young chickens is the bursa of Fabricius, an organ essential for development of circulating antibody-producing cells and possibly for other aspects of the immune response. The discovery of Glick *et al*[13] of the role of the bursa of Fabricius in antibody production set off a variety of experiments in many laboratories; effects of bursectomy in chickens of various ages, with or without concomitant thymectomy or splenectomy, have been studied after subsequent challenge with various antigens. Results have not yet been sorted out in a way in which "the" function of the bursa at a given age in growing chicks can be fully specified.

Materials and Methods

Commercially obtained White Leghorn chickens were maintained from the time of hatching until the termination of the experiment on each of the following diets (25 to 35 chicks/group):

Diet I: Purina Chow's normal chick mash diet, "Growena";
Diet II: Diet III (below) supplemented daily with 3.2 mg of vitamin A palmitate/kg diet, in a sucrose base;[*]
Diet III: A specially formulated[*] vitamin-A-deprived diet for chickens,[†]

	g/kg
Soy assay protein	300.00
L-Cystine	3.00
DL-Methionine	2.00
Salt Mix Fox-Briggs [‡]	60.00
Cottonseed oil	40.00
Choline chloride	1.00
Corn starch	593.323
Sodium selenite (Na_2SeO_3)	0.002043
DL-α-Tocopherol acetate (1000 U/g)	0.200
Santoquin (Exthoxyquin)	0.040
Thiamine HCl	0.008
Riboflavin	0.008
Calcium pantothenate	0.020
Nicotinic acid	0.100
Pyridoxine HCl	0.008
Biotin	0.0003
Folic acid	0.003
Vitamin B_{12} in mannitol (0.1%)	0.020
Vitamin D_3 trituration (3000 U/g)	0.2667
Menadione	0.001

Diet IV: Nutritional Biochemical Chick Basal Ration, with cod liver oil USP 1.0% *deleted* to provide a vitamin A-deficient diet;
Diet V: Nutritional Biochemicals Vitamin A (Rat) Test Diet.

---

[*] We are indebted to Dr. J. G. Bieri of the Laboratory of Nutrition and Endocrinology, National Institute of Arthritis and Metabolic Diseases, National Institutes of Health, for his advice in the composition of Diet III and the regime of supplement in Diet II.

[†] General Biochemicals Diet TD-71122

[‡] General Biochemicals Catalogue No. 170740

After 21 days on the respective diets, 8 to 15 chickens in each diet group except Diet IV were inoculated intranasally with 1 drop/nostril of undiluted allantoic fluid stocks of the mesogenic (B) strain of Newcastle disease virus in which virus titers were between $10^{7.5}$ and $10^{9.0}$. Normally fed, deprived, uninfected and NDV-infected chickens (2 per category when possible) were sacrified at intervals of 7 hours approximately 3, 5, 7, 9 and 12 days after the time of inoculation. Blocks of nasal fossa including the area of the upper skull from the center of the nostril to the posterior limit of the eye, and the entire bursa of Fabricius from at least one of each pair were fixed in neutral formalin. Nasal blocks were decalcified in commercial "Decal." Four areas of nasal fossa selected to include the anterior mucocutaneous junctions, the lateral nasal gland and its ducts, the central portion of the maxillary turbinate and central portion of the nasolacrimal duct and the central portion of the gland of Harder were sectioned. Four to six sections/area were stained with hematoxylin and eosin, 2 to 4/area with alcian blue (1%)–periodic acid-Schiff (AB-PAS) stain. Methods of virus assay have been previously described.[14]

Results

This report is primarily concerned with the effects of the deficient diets on depression of lymphoid cell systems; however, the effects on epithelial cells lining the nasal fossa and bursa may be directly relevant and will be briefly noted.

A summary of the test diets follows for ready reference: Diet I: normal mash, Diet II: Diet III supplemented daily with vitamin A palmitate, Diet III: special chicken diet with complete nutrients lacking vitamin A, Diet IV: commercial chicken basal ration lacking vitamin A, Diet V: commercial vitamin-A-deprived diet for rats.

Epithelial Cells

After 25 days of vitamin A deprivation the mucociliated cells contiguous with mucocutaneous junctions of chickens on the 3 vitamin-A-deprived diets (III, IV, V) began to show keratinizing metaplasia which progressed posteriorly with time; by 30 days portions of some lacrimal ducts and lateral nasal gland ducts of chicks on Diets IV and V were keratinized (Table 1). Cell numbers in both ciliated and mucous components of the mucosa and in the mucous acini were reduced by about 50%, so that all mucosae were reduced in height. Mucus was conspicuously retained in the more anteriorly positioned acini and the surface sheet of mucus was thicker than normal.

The epithelial cells lining the lumen of the bursa of Fabricius were also affected. In normally fed birds this epithelium is a single row of regularly aligned secretory cells which stain faintly alcian blue, plus a less regular row of basal cells; there is a very fine sheet of alcian blue-positive surface secretion. After 30 days on Diet III, surface epithelia were disorganized, appeared pseudostratified and occasionally cystic; the tips of the rugae were metaplastic and heavily seeded with heterophils. On Diets IV and V the normally smooth surfaces of the rugae were indented and occasionally acinar; the cells were pseudostratified due to compression and some showed squamous metaplasia and heterophilia. On Diet IV the tips of many rugae were keratinized. In chickens on all three vitamin-A-deprived diets these bursal epithelial cells contained brilliant alcian blue-positive secretory material in the entire cytoplasm; there were quantities of alcian blue positive surface secretion and exudate in the lumen. There was no mucous metaplasia of the surface epithelial tuft cells at any stage of the diets.

Table 1—Effects of Each Diet on Oculonasal Epithelial and Lymphoid Cells

Diet	No. chicks	Days on diet	Degree of keratinization of mucociliated epithelial anterior fossa	Degree of plasmacyte abnormality, lateral nasal gland ducts	Degree of infiltration small lymphocytes in lacrimal ducts	Degree of infiltration small lymphocytes in tonsil area	Relative No. plasma cells in intralobular spaces in glands of Harder
I	1	24	0	0	+	+	+++
	1	26	0	0	++ GC	++ GC	+++
	1	31	0	0	+++	+++	+++
II	1	22	0	+	0	+ GC	+++
	1	24	0	+	++ GC	++ GC	+++
	1	26	0	0	+	++	+++
	1	29	0	±	++ GC	++ GC	+++
III	1	18	0	++	0	0	+
	1	21	+	++	0	+ GC	+
	1	24	+	+	±	+ GC	++
	1	29	+	+	0	0	++
IV	1	18	0	0	±	+	++
	2	25	+	+ M	M ++ GC	+ GC	+
	3	30	++	++ K	+ GC	+ GC	0
V	2	18	0	0	0	0	+
	2	25	++	+ M, K	±	+	+
	2	30	++	++ M, K	0 K	+	0

GC = germinal centers; M = metaplasia; K = keratinization

Lymphoid Cell Systems

Nasal and paranasal lymphocyte populations

Lacrimal Ducts and Fauces. There was significant depression in the amount of small lymphocyte infiltration on Diets III and IV; however, small germinal centers formed at both sites. In chickens on Diet V the infiltrations were essentially eliminated from lacrimal ducts and sharply reduced in fauces; germinal centers were not found. The effects are summarized in Table 1. Because of the volume of sectioning required for histologic review of the Harderian gland ducts, these were not included in the present survey.

Lateral Nasal Gland Duct. Populations of plasmacytes were also reduced after 30 days on all three vitamin-A-deprived diets. (Plasmacytes normally found associated with this duct epithelium are somewhat smaller than those found in the glands of Harder.) In the vitamin-A-deprived chickens nearly all of the cells found along the basal cell area were strongly eosinophilic agranular cells with dark compressed excentric nuclei; it could not be determined, when using the light microscope, whether they were abnormal plasmacytes or another cell type. As shown in Table 1, these changes were initially significant in Diet III but less significant at later stages; they were progressive over time in Diets IV and V. Heterophils were common in the loose areolar tissues adjacent to the ducts and were occasionally found in the duct walls.

The Harderian gland population of plasma cells showed the most remarkable depression in vitamin-A-deficient birds whose diets also lacked other components. In chickens on Diets IV and V, the rich populations of large clear plasma cells found in the Harderian gland of chickens on normal diets (Figures 1, 2) were apparently entirely eliminated at 30 days (Figure 3). Chickens on Diet III showed similar changes at 18 and 21 days, but at 25 and 30 days there were modest numbers of normal looking plasma cells in the intralobular spaces.

Thus it appears that each of the vitamin-A-deprived diets depressed or partly eliminated the infiltration of small lymphocytes into submucosal areas of the nasal fossa at sites most directly exposed to injurious particles carried in the mucous blanket (fauces and lacrimal ducts). Normal populations of plasma cells in the nictitating-membrane gland of Harder were reduced in number or were eliminated in all three deficient diets, but recovered partly in Diet III. Since the secretory flow from this gland is from gland body to eyeball via a long duct, airborne stimuli impinging on the eye must elicit response from the gland via information from circulating cells; it will be remembered that the long gland duct is lined with villi heavily infiltrated with small lymphocytes and germinal centers. Plasmacytes associated with the lateral nasal gland duct epithelia were reduced in number and were morphologically abnormal in all diets. Effects were less severe in birds on Diet III, and these seemed to improve in some respects with time. Depletion of lymphocytes was most severe in the most deprived diet, and the capacity to form germinal centers in normal conditions may have been abolished.

Bursa of Fabricius Lymphocyte Populations

While Diet II seemed to support normal development of epithelial tissues in the nasal fossa, it was evidently less adequate for fully normal development of the bursa. In contrast to Diet I at 30 days (Figure 4), there was less uniform development of follicles; follicles were less mature, very few were polygonal, and there was some subepithelial fibrosis and heterophilia.

Diet III produced follicles which were quite irregular in development (Figure 5), showed marked interfollicular fibrosis and degrees of fibrosis (rarely, granulocytosis) in the medullae; cortical development was uneven, and there were several sites in which cortical lymphocytes were replaced peripherally by heterophils. Changes in lining epithelial cells have been described above.

Diet IV produced widely spaced follicles which lacked small lymphocytes in the medullae. These latter consisted of loose networks of pale-nucleated epithelial cells which stained positively for alcian blue, a peripheral scatter of rounded dark nuclear remnants and a distinct margin of cuboidal epithelial cells adjacent to the often discontinuous vascular circlet of the cortex. The cortex varied in relative width and also contained numbers of nuclear remnants.

Diet V follicles were atrophic, entirely lacked the vascular circlet and lacked a cortex; medullae consisted of degenerate and degenerating cell nuclei in a disintegrating matrix of pale epithelial cells (Figure 6). Basal cells in surface epithelia, in the necks of tuft-cell areas and surrounding the medullae had swollen nuclei, were usually three or more layers thick and were disorganized in the medullae. There was marked interfollicular fibrosis and/or degeneration (Figure 7).

To summarize the bursal effects: Diet II caused moderate alteration (delay?) in bursal follicular development; Diet III induced retarded development or premature involution, irregular maturation of follicles and degrees of focal heterophilia. Diets IV and V seemed to have induced premature atrophy of lymphoid elements; Diet V seemed to have induced the most rapid attrition of cortical lymphocytes.

Effects of NDV Infection on Diet-Deprived Chickens

Nasal Fossa

Results of viral assays during the course of infection in chickens on Diets I and V have been reported.[15] For the present report selected results are summarized in order to compare results in uninfected and infected chickens on deprived diets. Chickens infected after 3 weeks on normal mash showed an initially strong submucosal inflammatory reaction and mild sloughing typical of response of nasal mucociliated areas to this strain of NDV. In addition there was a sharp initial drop in numbers of plasma cells from the Harderian gland; this was not fully restored until 10 days.

Chickens on Diet III (vitamin-A-deprived only) after infection showed delayed and depressed inflammatory response and increased keratinization of anterior nasal mucosae, persistent sloughing and/or squamous metaplasia of conchal mucociliated mucosae, abnormal plasmacytes in and occasional keratinization of lateral nasal gland ducts and *depletion* of plasma cells from the gland of Harder.

On Diet V, infected birds showed focalized *atrophy* in several epithelial cell areas in which there were no visible basal cells present to provide for synthesis of replacement cells. There was some inflammatory cell response in both lacrimal ducts and fauces, but in only 1 of 6 birds were there questionable small germinal centers. The Harderian plasma cells, depleted in uninfected chicks at the time of infection, remained absent.

Thus, in contrast to normally fed pairs, infected diet-deprived chickens showed increased oculonasal epithelial metaplasia or (Diet V) atrophy; inflammatory responses were depressed; and plasmacyte populations were either further altered morphologically, replaced by other types of cells or eliminated.

Bursa of Fabricius

Single specimens of bursae from chickens on Diets I and II at 4 intervals from 1 to 10 days after NDV infection showed no difference from bursae of uninfected birds at the same intervals. Those on Diet III after infection showed a rapid attrition of lymphocytes, atrophy of the vascular system, involution and progressive surface epithelial metaplasia, including marked keratinization. This effect was evident 3 days after NDV inoculation, was advanced by 5 days and by 6 days was indistinguishable from the situation seen in Figures 6 and 7, in comparison with the uninfected vitamin-A-deficient bursa the same age (Figure 4). Bursae of infected chickens on Diet V, already deprived of lymphocytes, showed significant advance over uninfected birds in bursal fibrosis, more epithelial metaplasia and greater basal cell proliferation, but no evident keratinization.

Discussion

With the wisdom of hindsight one can find clues in the literature on malnutrition and infection that the cell-mediated immune system is affected by malnutrition. Jackson [2] referred to several reports on intensive "migration or atrophy" of lymphocytes in the thymus and lymph nodes of starving or malnourished humans and experimental animals; Vint [15] in 1937 recognized that there was severe atrophy of the thymus in children who died of kwashiorkor; and Smythe and Campbell in 1959 noted that the bacteremia of kwashiorkor suggested a defect in the immune mechanism of the gut.[16] After Oomen [17] postulated that infection precipitated acute clinical hypo-A in persons with a latent deficiency, there were a number of accounts of precipitating effects of infections on clinical signs of vitamin A deficiency. These have been reviewed in Scrimshaw *et al*,[3] in DeSilva and Baptist,[4] and in a recent Ciba symposium on malnutrition and infection.[18] There has also been a highly pertinent observation by McLaren in 1963 that death rates were 65% higher in children who had PCM and showed xerophthalmia than in those who had PCM and no xerophthalmia.[19]

Yet it is Smythe *et al* [5] who have clearly highlighted the fact that the cell-mediated immune (CMI) response is profoundly depressed by PCM. McFarlane [20] has added that the degree of immunosuppression may depend on the degree of malnutrition plus the amount of concomitant infection.

Smythe's findings are germane to our present studies, which were prompted by observations that chickens which had been vitamin A-deprived in order to test the effects of hypo-A on the course of NDV infection [21] showed marked depletion of lymphoid tissues,[22] that 100 times more virus was recovered from throat swabs of vitamin A-deprived than from normally fed NDV-infected birds,[14] and that vitamin-A-deprived chicks were susceptible to influenza virus while normally fed were not.[14] Together these strongly suggested morphologic and functional suppression of lymphocytes in diet-deprived chickens. Since the diets used in these original experiments (Diets IV, V) lacked not only vitamin A but apparently other components necessary for optimal growth of chickens, a diet containing full nutritional requirements but specifically lacking vitamin A (Diet III) was added to the experimental design of the present series. Results with this diet were still significant but were less severe (except in the case of the bursa of infected birds). Which of the specific factors lacking in Diets IV and V were responsible for the more intensive lymphoid depression remains to be systematically investigated.

The chicken model may be an excellent analogue in which to study effects of specific dietary deficiencies on particular lymphoid cell systems involved in immune responses, since thymus-mediated and bursa-mediated cell systems are so clearly defined. It is obviously necessary in future studies with this model to use precisely designed diets; to include histologic data on thymus, spleen and cecal tonsils; to carry out tests for delayed hypersensitivity, lymphocyte transformation and antibody components; and to have parallel data on body and lymphoid organ weights in noninfected and infected deprived and control chicks.

The present study has suggested that in lymphoepithelial systems the primary lesion induced by vitamin A-deprivation in epithelial cells may interfere with normal information to the lymphocyte-line cells associated with them, especially in the presence of infection. This in turn, especially when concomitant with degrees of other nutritional deficiencies, could influence the differentiation of cells in the lymphocyte line. For example, in birds on Diet III incursions of heterophils into the cortex of the bursa and into the gland of Harder displaced or replaced lymphocytes; it is noteworthy that in pipping and newly hatched chicks the Harderians are filled with heterophils yet within one or two weeks after hatching these are replaced by a population of plasma cells.[8] The study also suggested that immune tolerance might be induced by infection in diet-deprived animals, since during early stages of postembryonic life the CMI response is presumably depressed; thus a gradual recovery of function of these cells might occur after the immune tolerant state had been established.

It is clear that there is a relationship between protein deficiency and vitamin A deficiency, but the manner in which they interact is not clear, nor are effects of these deficiencies on immune-cell mechanisms and mucous membranes.[23] As Follis [24] pointed out, the pathology of different deficiency states is traditionally expressed as the effect of a specific deficiency on the total growth of the organism. It remains to be seen whether the lymphoid regression described in this report, and the lymphoid regression described in the cited reports on human and experimental malnutrition and starvation, hinge on one or more specific dietary deficiencies, or on particular combinations of deficiencies. Axelrod's continuing studies[25,26] of specific states of vitamin deficiency have established the role of particular vitamins—especially in the vitamin B complex—in several aspects of immune responses.

A final important question is raised by the fact that the deficient diets, as well as infection, induce premature atrophy of the bursa. Since bursal involution normally begins at about 4½ months of age,[27] the possibility that the effects of malnutrition may be at least partly mediated through the hormonal system in these 1-month-old birds should not be overlooked.

References

1. Spicer H: Keratomalacia in young children. Lancet 2:1387–1388, 1892
2. Jackson CM: The Effects of Inanition and Malnutrition on Growth and Development. Philadelphia, P. Blackiston's Son & Co, 1925
3. Scrimshaw NS, Taylor CE, Gordon JE: Interactions of nutrition and infection. World Health Organization Monograph Series 57. Geneva, WHO, 1968
4. DeSilva CC, Baptist NG: Tropical Nutritional Disorders of Infants and Children. Springfield, Illinois, Charles C Thomas, Publisher, 1969
5. Smythe PM, Brereton-Stiles CG, Grace HJ, Mafoyane A, Schonland M, Coovadia HM, Loening WEK, Parent MA, Vos GH: Thymolymphatic deficiency and depression of cell-mediated immunity in protein-calorie malnutrition. Lancet 2:939–944, 1971
6. Jolly J: La bourse de Fabricius et les organes lympho-épitheliaux. Arch Anat Microsc Morphol Exp 16:363–547, 1915
7. Fürther H: Beiträge zur Kenntnis der Vögel-lymphknoten. Jena Z Naturwiss 50:359–410, 1913
8. Bang BG, Bang FB: Localized lymphoid tissues and plasma cells in paraocular and paranasal organ systems in chickens. Am J Pathol 53:735–751, 1968
9. Lucas AM, Oakberg EF: Lymphoid tissue and its relation to so-called normal lymphoid foci and to lymphomatosis. II. Quantitative analysis of lymphoid areas in the pancreas of laboratory and farm chickens. Am J Pathol 26:75–111, 1950
10. Glick B, Sato K, Mueller AP: The contribution of antibody producing cells by the chicken lacrimal gland, gland of Harder, spleen, cecal tonsil and accessory spleen. Fed Proc 30(2):291, 1971
11. Glick B: Morphological changes in humoral immunity in cyclophosphamide-treated chicks. Transplantation 11:433–439, 1971
12. Leslie GA, Wilson HR, Clem LW: Studies on the secretory immunologic system of fowl. I. Presence of immunoglobulins in chicken secretions. J Immunol 106:1441–1446, 1970
13. Glick B, Chang TS, Jaap RG: The bursa of Fabricius and antibody production. Poult Sci 35:224–225, 1956

14. Bang FB, Foard MA: The effect of acute vitamin A deficiency on the susceptibility of chicks to Newcastle disease and influenza virus. J Hopkins Med J 129:100–109, 1971
15. Vint FW: Post-mortem findings in natives in Kenya. East Afr Med J 13:332–340, 1937
16. Smythe PM, Campbell JAH: The significance of the bacteraemia of kwashiorkor. S Afr Med J 33:777, 1959
17. Oomen HACP: Clinical experience on hypovitaminosis A. Nutritional disease: Proceedings of the Conference on Beriberi, Endemic Goiter and Hypovitaminosis A. Princeton, New Jersey, June 1–5, 1958
18. Ciba Foundation Study Group No. 31: Nutrition and Infection. Edited by GEW Wolstenholme and M O'Connor. Boston, Little, Brown and Co, 1967
19. McLaren DS: Xerophthalmia: a neglected problem. Nutr Rev 22:289–291, 1964
20. McFarlane H: Cell-mediated immunity in protein-calorie malnutrition. Lancet 2:1146–1147, 1971
21. Bang BG, Bang FB: Replacement of virus-destroyed epithelium by keratinized squamous cells in vitamin A-deprived chickens. J Exp Biol Med 132:50–54, 1969
22. Bang FB, Foard M, Bang BG: Histology of vitamin A deficiency in chicks and susceptibility to influenza virus. Fed Proc 30:1224, 1971
23. DeLuca L, Wolf G: Vitamin A and protein synthesis in mucous membranes. International Symposium on the Metabolic Function of Vitamin A. Am J Clin Nutr, 1969
24. Follis RH: Deficiency Disease. Springfield, Illinois, Charles C. Thomas, Publisher, 1958
25. Axelrod AE: Nutrition in relation to acquired immunity. Modern Nutrition in Health and Disease. Fourth edition edited by MG Wohl and RS Goodhart. Philadelphia, Lea and Febiger, 1968
26. Axelrod AE: Immune processes in vitamin deficiency states. Am J Clin Nutr 24:265–271, 1971
27. Jolly J: L'involution physiologique de la bourse de Fabricius et ses relations avec l'apparition de la maturité sexuelle. C R Soc Biol (Paris) 75:638–640, 1913

Addendum

After submitting this paper, we found a recently published report which not only confirms our original observations[8] of early heterophil and late plasma cell populations in the gland, but also contains important quantitative data and growth curves: Wright PAL, Burns RB, Rothwell B, Mackenzie GM: The Harderian gland of the domestic fowl. J Anat 110:307–315, 1972

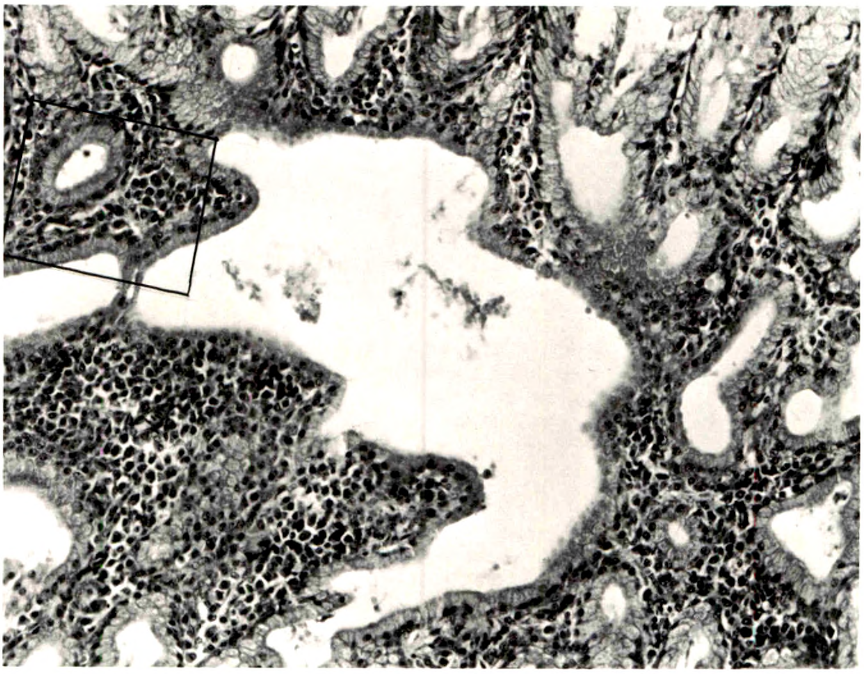

1

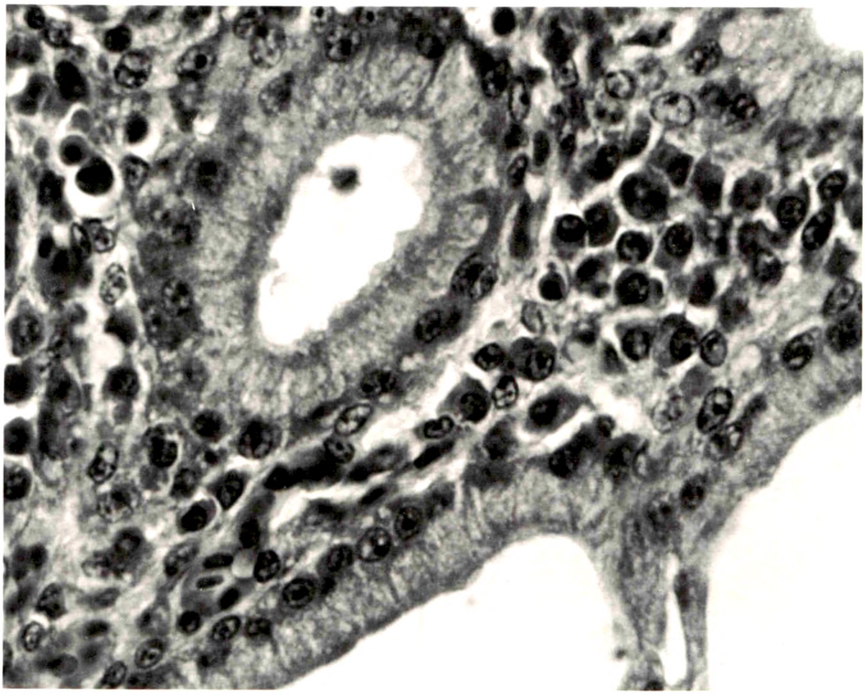

2

Fig 1—Portion of follicle of gland of Harder of normally fed 1-month-old chicken showing populations of plasma cells in the interfolicular spaces (H&E, × 250).
Fig 2—Area in Fig 1 enlarged to show plasma cells (H&E, × 1000).

3

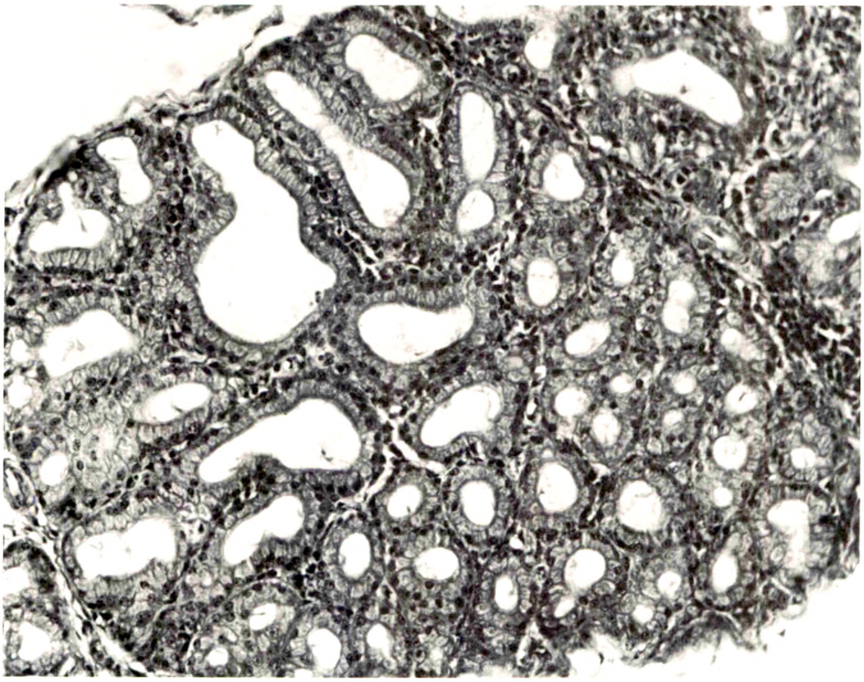

4

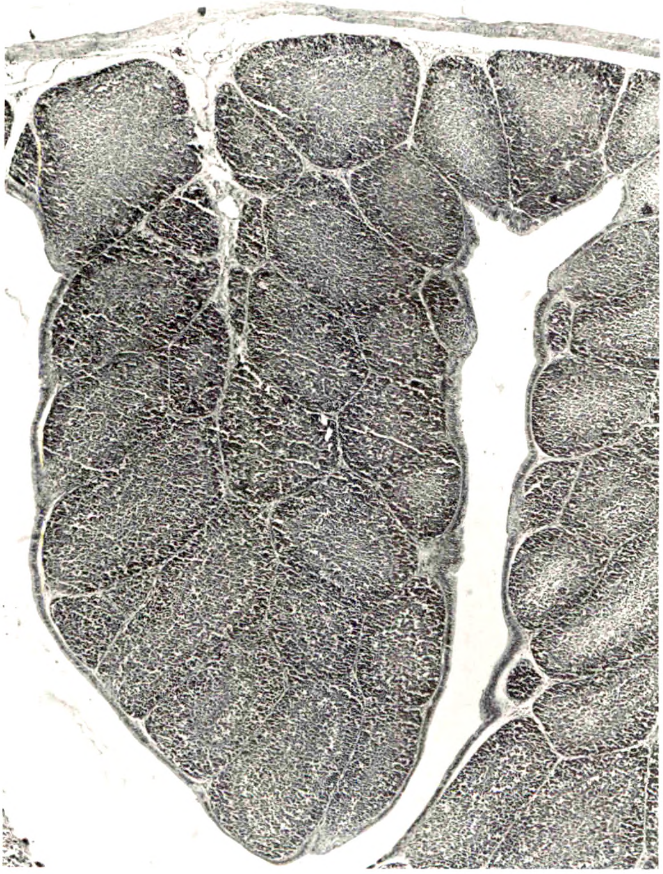

Fig 3—Gland of Harder of 1 month old chicken on Diet V since hatching, showing total lack of plasma cells (H&E, × 250). **Fig 4**—Rugal fold of bursa of normally fed 1-month-old chicken: regular, polygonal mature follicles; normal epithelium (H&E, × 45).

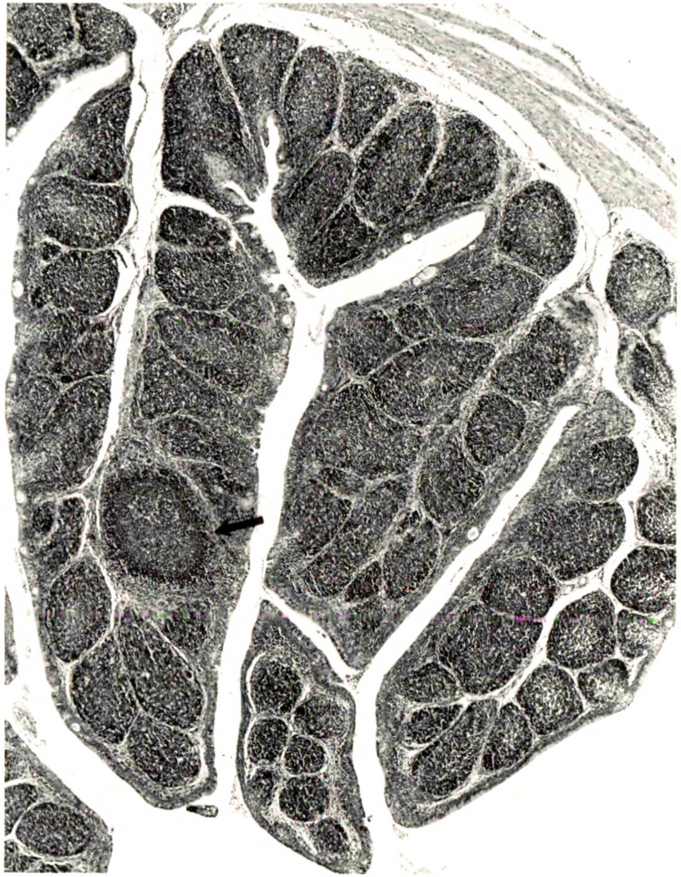

Fig 5—Comparable area of bursa of chicken on vitamin A-deprived Diet III: irregular follicular development, focal heterophil invasion (*arrow*) and disturbed epithelium (H&E, × 45).

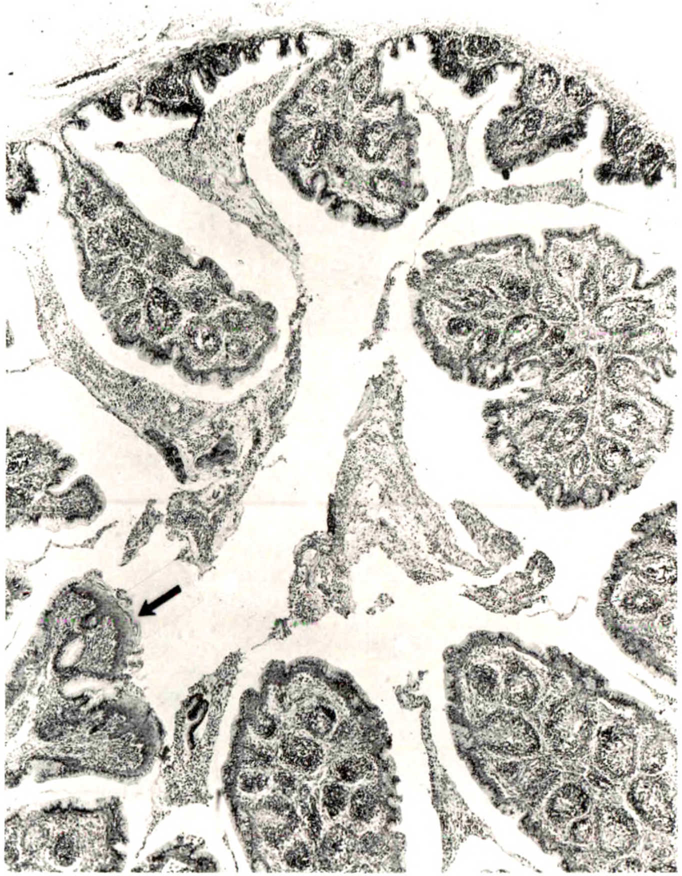

Fig 6—Comparable area in chicken on Diet V, lacking vitamin A and other components: atrophy of follicles, mucous and keratinizing (*arrow*) epithelial metaplasia, exudate in lumen (H&E, × 45).

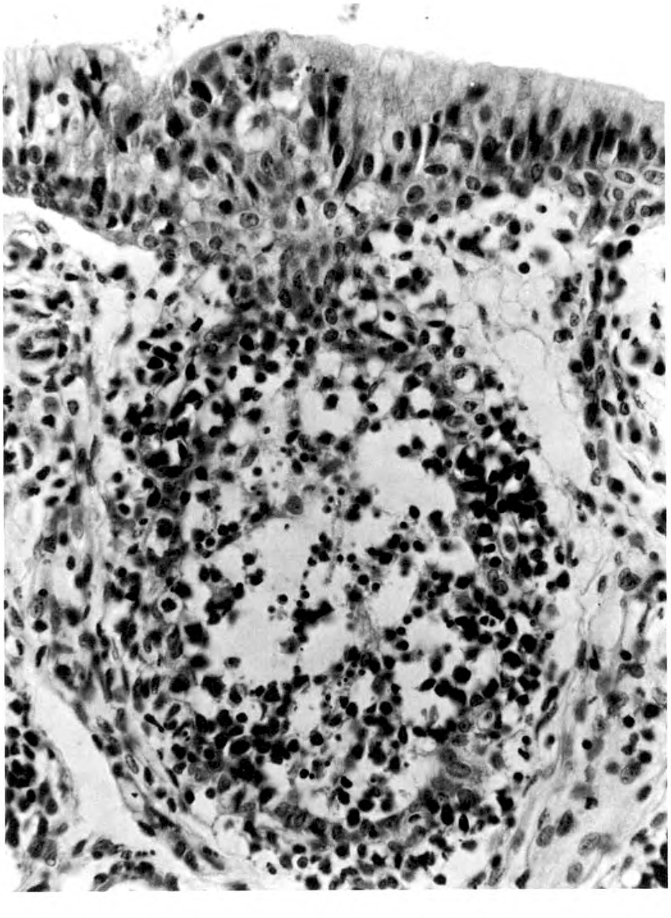

Fig 7—Enlarged follicle from Fig 6: loss of all normal lymphocytes and of the vascular circlet; disintegrating cell nuclei; basal cell hyperplasia (H&E, × 500).

Separation of Ascites Myeloma Cells, Lymphocytes and Macrophages by Zonal Centrifugation on an Isokinetic Gradient

M. J. Stewart, BS, T. G. Pretlow II, MD and Raymond Hiramoto, PhD

In attempting to quantitate immunoglobulin synthesis by ascites myeloma cells, we were surprised to note that malignant appearing cells never exceeded 35.9 ± 28.0% of ascitic cells and exceeded 22.4 ± 23.8% of ascitic cells on only one day between the transplantation of the tumor and the death of the host. The ascites tumor suspensions were separated primarily according to diameter, using a previously described isokinetic density gradient of Ficoll in tissue culture medium. This separation resulted in four modal populations of cells: red blood cells, lymphoid cells, macrophages and myeloma cells. The modal populations of macrophages and lymphoid cells always contained less than 0.2% myeloma cells. The purified cells were tested for tumorigenicity. The animal which received the largest number of cells from the macrophage zone received 296 times the number of cells which had been determined to be tumorigenic for myeloma cells. The animal which received the largest number of cells from the lymphoid zone received 1600 times the tumorigenic dose for myeloma cells. Neither of these animals has become ill 4 months after receiving the purified cells. We conclude that: a) Experimentalists who use ascites tumors are not justified in assuming that even easily detected quantitative differences between benign and malignant tissues would be reflected in analyses performed using unstandardized unexamined ascites tumor suspensions. b) In the case of the MOPC 104 mouse myeloma, cytologic criteria are adequate for distinguishing malignant cells from the inflammatory cells in the ascites suspension with a high degree of correspondence between cytologic appearance and biologic activity. c) Programmed gradient sedimentation in an isokinetic gradient of Ficoll in tissue culture medium is an effective means of separating malignant cells from benign cells in this particular ascites tumor (Am J Pathol 68:163–182, 1972).

THE TRANSPLANTABLE ASCITES TUMOR has been a widely used experimental model in the study of neoplasia. In the study of the biochemistry and immunology of cancer, the ascites tumor has proved to be particularly convenient and useful because of its relatively reproducible and constant rate of growth, because of the ease with which the tumor cells from the same animal can be repeatedly sampled and because of the homogeneous microenvironment of the neoplastic

---

From the Departments of Pathology, Engineering Biophysics and Microbiology, The School of Medicine and Dentistry, University of Alabama in Birmingham, Birmingham, Ala.

Supported by Grants CA-12870 and DE-2670 from the National Institutes of Health and Grant GB-13804 from the National Science Foundation.

Accepted for publication Mar 17, 1972.

Address reprint requests to Dr. Thomas G. Pretlow, II, Department of Pathology, University of Alabama in Birmingham, The Medical Center, 1919 Seventh Ave South, Birmingham, Ala 35233.

cells[1,2] in the suspension. In contrast to solid transplantable neoplasms, ascites tumors do not undergo focal necrosis and have been shown to be only slightly subject to change in mitotic rate as the disease progresses.[3] Since the development of Potter's method[4,5] for the induction of ascitic plasma cell tumors in mice, ascitic plasma cell tumors similar to the myeloma which is studied in this report have been used extensively in the study of immunoglobulins, protein synthesis, the biochemistry of cancer and tumor antigens.[6-9]

While studying immunoglobulin synthesis by an ascitic myeloma, we were surprised to find that the myeloma cells never constituted a majority of the nucleated cells in the ascitic fluid from the time of tumor transplantation until the death of the animal. This finding was independent of the number of tumor cells injected, the age and sex of the mice and the use of solid or ascitic myeloma as the source of cells for transplantation. In surveying more than 100 reports of biochemical and pharmacologic studies performed using ascites tumors, we found only three[1,10,11] which mentioned the presence of lymphocytes, monocytes or other benign nucleated cells in the ascitic tumor suspensions; most reports presented no evidence that cytologic examination of the ascitic tumor had ever been performed or that heterogeneity of the cellular composition had been considered in the interpretation of experimental data. In the study of cancer biochemistry, the characterization of tumor antigenicity, the evaluation of antineoplastic chemotherapy based on cell counts of ascitic tumor cell suspensions, etc, it would appear to be essential that the investigator be aware of the heterogeneity of the ascitic cells; it would seem desirable, in characterizing malignant cells, that most of the cells for analysis be malignant.

In this report, we present evidence—both cytologic and biologic—that the majority of the nucleated cells from at least one transplantable ascites myeloma are not malignant. A method is described for the separation of three modal populations of nucleated cells using sedimentation in a previously described isokinetic gradient[12] of Ficoll (polysucrose) in tissue culture medium. Cells from both the macrophage and lymphoid zones of the gradient failed to cause the development of ascites myeloma when injected intraperitoneally into isogeneic recipients, even when the number of injected cells exceeded the tumorigenic dose of myeloma cells by several orders of magnitude.

Materials and Methods

Previous publications have contained detailed descriptions of the theory[12-15] of gradient sedimentation as applied to mammalian cells and of the technic[12,16] used in this work. A detailed description of the theory and methods employed will therefore be omitted from this report.

Myeloma Cells

A mineral-oil-induced (MOPC 104) plasmacytoma was obtained originally from Dr. Michael Potter's laboratory, National Cancer Institute. The tumor was routinely carried as an ascitic tumor but was transplanted intramuscularly, rather than as an ascites tumor, for 2 generations in the thighs of Balb/c, female mice before use as a stock suspension for transplantation in the experiments reported here. Intramuscular growth of the stock tumor was desirable because of the characteristically very hemorrhagic ascitic fluid which is obtained from this particular ascitic plasmacytoma. The solid tumor was minced, digested according to the slightly modified method of Hilfer and Brown[17] with 1 mg/ml collagenase (Calbiochem, San Diego, Calif) in Joklik tissue culture medium containing 10% fetal calf serum (both from Grand Island Biological Company, Grand Island, NY), washed with 20% fetal calf serum in tissue culture medium, and resuspended in a solution of 7.5% dimethyl sulfoxide and 20% fetal calf serum in Joklik's modification of minimum essential medium. The cell suspension was then frozen in multiple duplicate vials at a rate of −1 C/min to −30 C and −10 C/min to −90 C and transferred to liquid nitrogen for storage. A similar method for the controlled rate freezing of transplantable tumors has been evaluated recently by Wodinsky *et al.*[18]

Mice

Strain Balb/c female mice (Laboratory Supply, Indianapolis, Indiana) were fed mouse pellets and watered *ad libitum*. The mice were used for tumor transplantation at the age of 7 to 8 weeks.

Natural History of Ascites Myeloma

Immediately upon removal from the liquid nitrogen freezer, the MOPC 104 cells were thawed in a 37 C water bath, cooled in an ice bath and washed 3 times with tissue culture medium containing 10% fetal calf serum by centrifuging at 200g for 7 minutes at 4.0 C. The cells were resuspended in tissue culture medium with 10% fetal calf serum and counted in hemocytometer chambers. Thirty million nucleated cells were injected intraperitoneally into each of 63 Balb/c female mice, 7 weeks of age. Eight mice were sacrificed by decapitation and exsanguination under ether anesthesia at 2, 5, 8, 9, 10, 11 and 14 days following tumor transplantation. The peritoneal cavities were irrigated with three successive 2-ml aliquots of Joklik tissue culture medium containing 10% fetal calf serum and heparin (4 units/ml). Cell counts were done using hemocytometer chambers; slides were prepared for microscopic examination using the Cytocentrifuge (Shandon Scientific Company, Sewickley, Pa). Differential counts of at least 200 nucleated cells were made from each Wright-stained preparation. Cells were classified as macrophages, tumor cells, lymphoid cells (including all lymphocyte types, blast cells and members of the plasma cell series), red blood cells, neutrophils, eosinophils and other (*eg*, lysed cells, mast cells, etc).

Density Gradients

Density gradients of Ficoll (polysucrose, average molecular weight 400,000; Pharmacia Fine Chemicals, Piscataway, NJ) in Joklik tissue culture medium were prepared using the technic and two-chambered gradient maker that were described and pictured previously.[16] The density gradients for both isopycnic and isokinetic velocity cell separation were constructed such that the Ficoll concentrations (w/v) and the densities varied as linear functions of the radial distances from the center of rotation. The density gradients used in isopycnic centrifugation varied from 4.1% (w/w) Ficoll at the sample–gradient interface, 14.2 cm from the center of revolution, to 43.0% (w/w) Ficoll at the gradient–cushion interface, 26.0 cm from the center of revolution. The isopycnic gradient was constructed on top of a 10-ml cushion of 45% (w/w) Ficoll in tissue culture medium. The density gradients for isokinetic velocity sedimentation were described in detail in a previous report from this laboratory; [12] they varied from 2.7% (w/w) Ficoll at the sample–gradient interface, 13.7 cm from the center of revolution, to 5.5% (w/w) Ficoll at the gradient–cushion interface 26.7 cm from the center of revolution. The isokinetic gradient was constructed on top of a 5.5-ml cushion of 45.0% (w/w) Ficoll. Both gradients were contained in 100-ml polycarbonate centrifuge tubes (No. 2806, International Equipment Company).

Starting Sample Suspensions of Ascites Cells

The peritoneal cells from 3 to 5 mice each of which had been inoculated with 30×10^6 ascites tumor cells 10 days previously were combined. Cell counts and slides were prepared as described above. For both isopycnic and isokinetic separation experiments, $21–35 \times 10^6$ cells were layered over the density gradients in a volume of 7 ml.

Centrifugation

The cell suspensions were centrifuged in an MSE Mistral 6L Centrifuge (Scott Instrument Company, Miama, Fla). Isopycnic centrifugation was performed at a centrifugal force of 850*g* (measured at the sample–gradient interface, 14.2 cm from the center of rotation) for 90 minutes at 4 C. Preliminary gradient centrifugation experiments were performed in order to determine a) how many modal populations of cells were present and b) the velocities of each modal population of cells on the isokinetic gradient at known centrifugal forces. The data from these experiments were used as described previously [12] in order to determine the optimal speed and duration of centrifugation for the separation of the individual kinds of cells in the starting sample suspension of ascites tumor cells. It was determined that optimal rate-zonal, one-step cell separation would be achieved by using a centrifugal force of 48.5*g* (measured at the sample–gradient interface, 13.7 cm from the center of rotation) for 20 minutes at 4 C; these conditions were employed in the experiments reported here.

Collection and Counting of Separated Cells

Following separation, the gradient fractions were collected by displacement with a dense sucrose solution using the gradient tapping cap which was described and illustrated previously.[16] The isopycnic gradient was collected in twenty-nine 3-ml fractions; the isokinetic gradient in twenty-four 4-ml fractions. The first gradient fraction of both gradients was the 7-ml starting sample suspension initially layered over the gradient.

After the fractions were collected, both isopycnic and isokinetic gradient fractions were treated identically. Refractive indices of all fractions were recorded in order to confirm the linearity of the gradients. Cell counts were performed using hemocytometer chambers. Slides for microscopic examination were prepared using the Cytocentrifuge and stained with Wright stain. Differential counts were made of at least 200 nucleated cells from each fraction.

Results

Natural History of Ascites Myeloma

The average number of cells recovered from each of the peritoneal cavities of the 8 mice sacrificed each day varied from 5.28 million cells on the second day to 2230 million cells on the fourteenth day following the intraperitoneal transplantation of the tumor (Table 1). Of the 63 mice which were inoculated originally with myeloma, 7 died spontaneously from advanced ascitic myeloma on days 11, 14, 15 (2 mice), 16 (2 mice), and 17.

Day 10 after inoculation was the only day on which the tumor cells were the most numerous (35.9 ± 28.0%) of the several kinds of peritoneal cells (Table 1); even on day 10 myeloma cells were less than a majority of nucleated cells. The composition of the ascitic suspension of cells is shown as a function of the day following tumor inoculation in Table 1. Characteristically, the ascites myeloma becomes very hemorrhagic a few days before the death of the mouse. When 30×10^6 cells are used as the inoculum for transplantation, hemorrhage begins late on day 10 or on day 11 and becomes progressively more severe. Subsequently, red blood cells are vastly more numerous than other kinds of cells.

As shown in Table 1, the cell suspensions from day 10 (*ie*, the cell suspensions from the day on which the starting sample suspensions for separations were obtained) consisted of 29.0 ± 21.6% lymphocytes, 25.7 ± 6.6% macrophages, 35.9 ± 28.0% myeloma cells, 8.19 ± 6.17% red blood cells, 0.88 ± 0.83% neutrophils and eosinophils, and 0.31 ± 0.68% other cells (lysed cells, mast cells, etc).

Isopycnic Cell Separation

Separation of the ascites myeloma cells by isopycnic sedimentation was considerably less effective than separation by velocity sedimentation. The densities of the individual kinds of cells varied as much as 0.01 g/ml in repeated experiments; this represents a slightly larger variation in density from one experiment to another than has usually been observed in our previous work with other kinds of cells and may reflect something about the unusual nature of the environment in which the ascitic cells grow. The individual kinds of cells from the ascites tumors exhibited broadly overlapping densities, the red blood cell density being 1.08 to 1.12 g/ml; the lymphocyte, 1.07 to 1.12 g/ml; the macrophage, 1.06 to 1.12 g/ml; and the myeloma cell, 1.08 to 1.13 g/ml. Following isopycnic centrifugation, the degree of cell

Table 1—Composition of Ascites Tumor*

Day†	2	5	8	9	10	11	14
Cells recovered (× 10^6)	5.28 ± 1.85 (3.25–8.57)	15.8 ± 6.7 (7.20–25.0)	31.6 ± 35.8 (5.80–104)	22.9 ± 23.8 (3.95–69.0)	55.8 ± 64.1 (10.7–167)	210 ± 460 (5.47–1150)	2230 ± 2340 (19.8–4980)
Composition (%)							
Lymphocytes	39.5 ± 10.5 (21.0–51.5)	40.3 ± 9.2 (23.5–53.5)	33.6 ± 19.8 (8.0–55.0)	31.1 ± 16.2 (8.5–55.5)	29.0 ± 21.6 (1.5–62.5)	22.9 ± 20.3 (0.0–48.0)	4.31 ± 9.57 (0.0–32.0)
Macrophages	39.4 ± 11.4 (26.5–59.5)	43.7 ± 8.8 (30.7–63.5)	37.6 ± 11.5 (8.5–54.5)	45.5 ± 15.1 (23.0–76.0)	25.7 ± 6.6 (14.3–35.0)	21.7 ± 19.2 (0.0–52.5)	8.3 ± 15.0 (0.0–50.0)
Ascites myeloma cells	1.20 ± 2.12 (0.0–7.0)	0.86 ± 1.51 (0.0–4.7)	7.66 ± 10.2 (0.0–31.5)	14.5 ± 17.9 (0.0–52.5)	35.9 ± 28.0 (0.0–76.5)	22.4 ± 23.8 (0.0–77.0)	21.8 ± 21.4 (0.0–58.0)
Red blood cells	3.33 ± 2.94 (0.0–11.5)	10.3 ± 9.1 (1.0–25.5)	14.5 ± 19.9 (1.0–66.0)	6.61 ± 9.11 (0.0–29.3)	8.19 ± 6.17 (1.5–20.5)	31.9 ± 34.7 (0.0–96.0)	65.0 ± 30.7 (15.0–100)
Neutrophils & eosinophils	15.9 ± 7.5 (0.5–27.0)	4.54 ± 2.28 (0.5–8.7)	6.5 ± 12.1 (0.0–40.5)	2.26 ± 1.76 (0.0–6.5)	0.88 ± 0.83 (0.0–2.5)	1.10 ± 1.24 (0.0–4.0)	0.31 ± 0.48 (0.0–1.5)
Other: (Lysed cells, mast cells, etc)	0.70 ± 0.80 (0.0–2.0)	0.28 ± 0.37 (0.0–1.0)	0.12 ± 0.22 (0.0–0.5)	0.03 ± 0.12 (0.0–0.5)	0.31 ± 0.68 (0.0–2.5)	0.12 ± 0.29 (0.0–1.0)	0.16 ± 0.35 (0.0–1.0)

* Ave ± SD; (min–max); N = 8

† Day 0 = injection day

purification was rather slight and highly variable from one experiment to another. In the purest fractions, lymphocytes represented 47.9 ± 33.1%, macrophages 72.5 ± 14.6% and myeloma cells 46.0 ± 41.0% of nucleated cells. A representative separation of the ascites myeloma cells by isopycnic centrifugation is shown in Text-figure 1.

Rate-Zonal Cell Separation on an Isokinetic Gradient

Sedimentation of the ascites myeloma cells using the previously described isokinetic gradient[12] resulted in the separation of modal populations of red blood cells, lymphocytes, macrophages and myeloma cells. In Fraction 6 (Figure 1) lymphocytes represented 98.9 ± 0.4% of the nucleated cells. In Fraction 10 (Figure 2) macrophages were 79.3 ± 12.1% of nucleated cells. Myeloma cells comprised 52.1 ± 6.9% of the nucleated cells in Fractions 15–17 (Figure 3). A photomicrograph of the starting sample suspension (Figure 4) is shown for comparison with the purified fractions from the gradient. The fractions of maximal purity for each kind of cell were the same (±1 fraction) in numerous repeated experiments. Myeloma cells were always less than

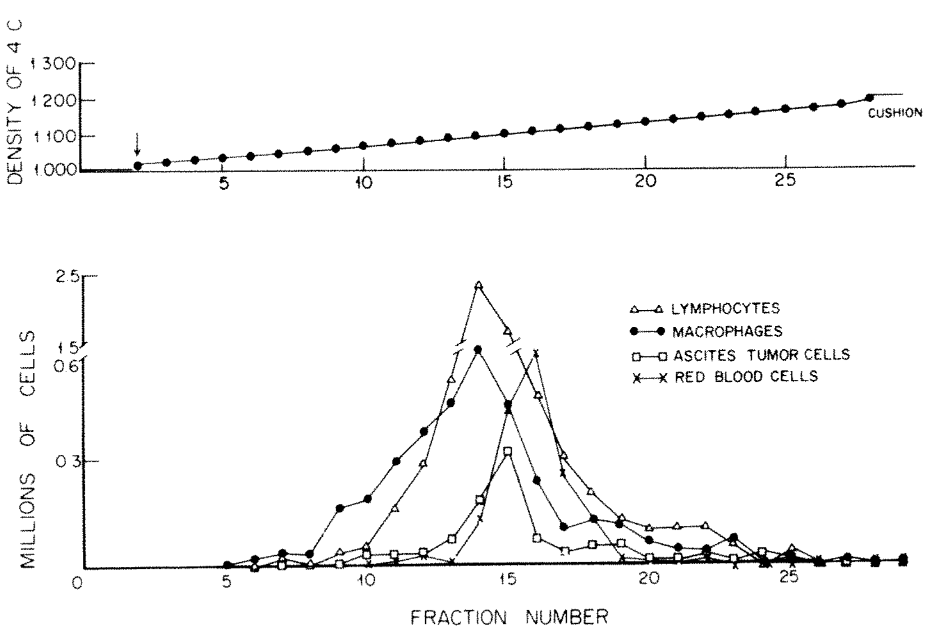

TEXT-FIG 1—Distribution of ascites cells in a density gradient following isopycnic centrifugation. The individual kinds of cells in the suspension of ascites tumor cells exhibit broadly overlapping densities and are not well separated by isopycnic sedimentation.

0.2% of the cells in both Fractions 6 and 10. A representative rate-zonal separation of the ascites myeloma cells on an isokinetic gradient is shown in Text-figure 2. More than 99.0% of the cells from Fractions 6, 10 and 15–17 excluded trypan blue. Preliminary experiments showed that lymphocyte purification could be more complete using the described isokinetic gradient if centrifugation were carried out for a longer period of time; however, our primary concern in these experiments was to separate malignant cells from the other cells in the ascites tumor suspensions. This end was accomplished by centrifugation on an isokinetic gradient resulting in less than 0.2% malignant cells in the purest fractions of macrophages and lymphoid cells (Table 2).

Injection of Purified Cells Into Mice

Two experiments were performed in which the separated lymphocytes (Fraction 6), separated macrophages (Fraction 10) and sep-

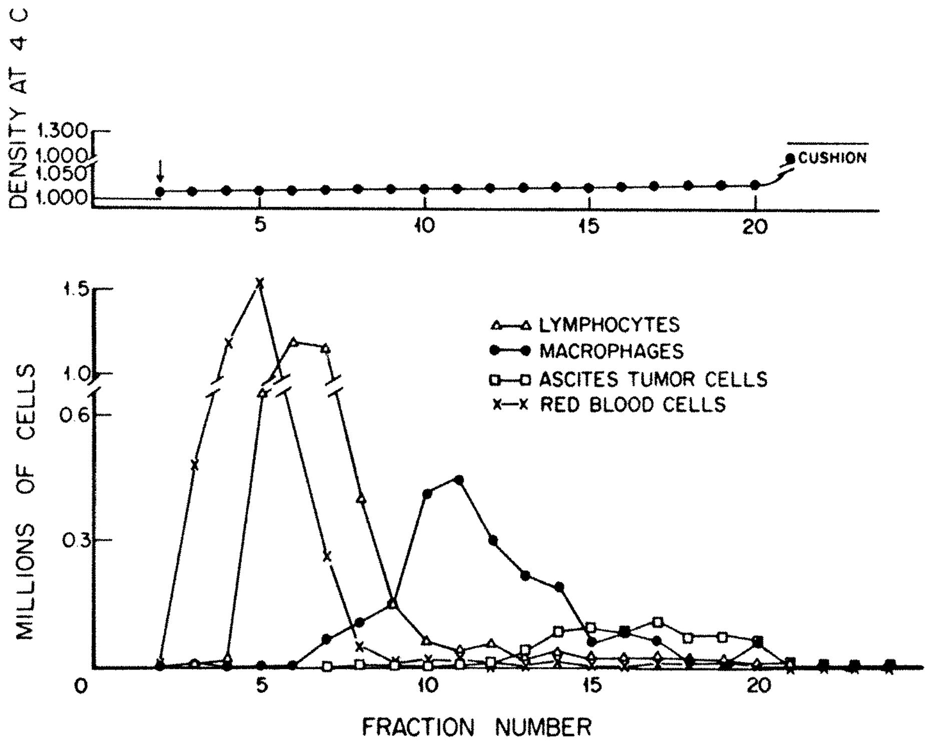

TEXT-FIG 2—Separation of ascites cells by velocity sedimentation in the isokinetic gradient. Additional experiments, not reported in detail here, demonstrated that red blood cells and lymphoid cells could be more widely separated, as would be expected, by continuing sedimentation until these two modal populations of cells have traveled farther on the gradient; in these experiments, the myeloma cells and the macrophage zone sediment all of the way through the gradient to the cushion.

Table 2—Cell Separation by Rate-Zonal and Isopycnic Centrifugation*

	Lymphocytes	Macrophages	Ascites myeloma cells	Red blood cells	Neutrophils & eosinophils	(Lysed cells, mast cells, etc)
Sample before separation (%)	29.0 ± 21.6	25.7 ± 6.6	35.9 ± 28.0	8.19 ± 6.17	0.88 ± 0.83	0.31 ± 0.68
Isokinetic centrifugation						
Purest fraction No.	6	10 ± 1	16 ± 1	4	—	—
Purity after separation (%)						
Inclusive of red blood cells	67.7 ± 10.6	77.8 ± 11.3	51.4 ± 7.2	97.4 ± 2.6	—	—
Exclusive of red blood cells	98.9 ± 0.4	79.3 ± 12.1	52.1 ± 6.9	—	—	—
Isopycnic centrifugation						
Purest fraction No.	12 ± 2	9 ± 1	14 ± 1	16 ± 2	—	—
Purity after separation (%)						
Inclusive of red blood cells	42.7 ± 30.7	70.3 ± 15.4	42.2 ± 42.4	49.8 ± 32.8	—	—
Exclusive of red blood cells	47.9 ± 33.1	72.5 ± 14.6	46.0 ± 41.0	—	—	—

* Ave ± SD; N = 4 (Rate); N = 3 (Isopycnic)

arated myeloma cells (combined Fractions 15–17) were injected intraperitoneally into mice. In these experiments, the cells from the gradient were washed in tissue culture medium containing 10% fetal calf serum, resuspended in 10% fetal calf serum in culture medium, and injected into individual mice in a geometric series of three-to-five fold dilutions depending on the number of cells available from the respective gradient fractions (Text-figure 3). The mice which received the various dilutions of lymphocytes, macrophages, and myeloma cells were observed for 4 months and the results of both experiments are shown in Text-figure 3.

In Experiment 1 the mouse which received the largest number of cells from the myeloma zone of the gradient (combined Fractions 15–17) received 9×10^5 cells intraperitoneally; 62.2% of these, or 5.6×10^5 cells, were considered to be myeloma cells after differential counts were performed (Table 3). The 6 animals in this experiment which received the largest numbers of cells (2.3×10^3 to 5.6×10^5 myeloma cells) died during the 5 weeks immediately following their inoculation. Each animal was autopsied as soon as possible following its death (animals were checked at least every 8 hours day and night) and was found to have 2 to 3 ml of grossly bloody ascitic fluid as well as plaques of tumor cells growing on the peritoneal surfaces. Microscopic examination of permanently stained preparations from the ascitic fluid revealed numerous myeloma cells among the more numerous red blood cells. Experiment 2 gave results which corresponded very closely to the results of Experiment 1. With respect to the animals which received the purified myeloma cells, the major difference between the two experiments was the death of 2 animals in Experiment 2 which received fewer than 2.3×10^3 myeloma cells. At autopsy, these 2 animals showed the above-described characteristic findings of animals dying of ascites myeloma. In both experiments, all animals which received 2.3×10^3 or more myeloma cells died from the tumor within 5 weeks. We shall therefore conservatively define 2.3×10^3 myeloma cells as the tumorigenic dose in comparing these animals with animals which received varying numbers of purified macrophages and lymphoid cells.

In Experiment 1, the mouse which received the largest number of cells from the macrophage zone (Fraction 10) received 3.6×10^5 cells intraperitoneally. The proportions of the various kinds of cells in Fraction 10 are given in Table 3; only 0.2% of the cells were myeloma cells. The animal which received the highest number of cells from the macrophage fraction (3.6×10^5 cells or 157 times the previously de-

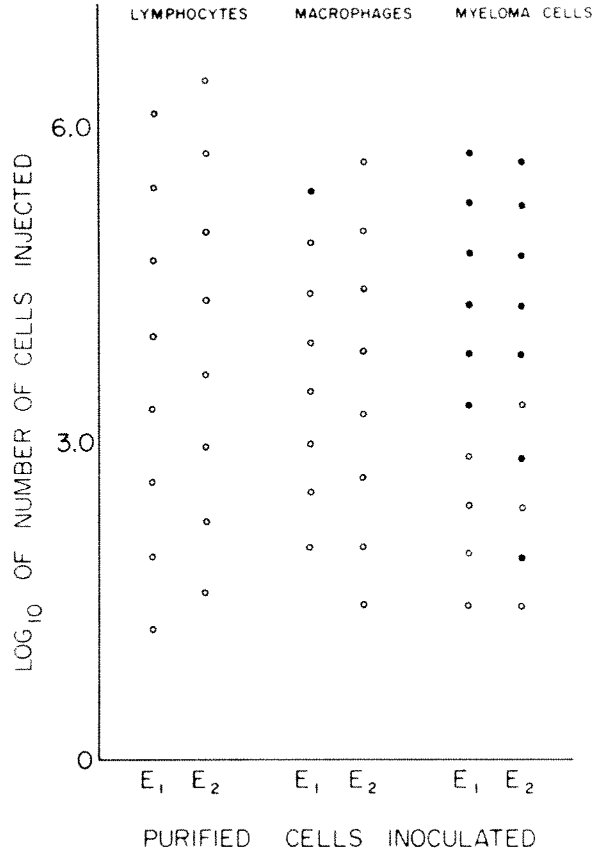

TEXT-FIG 3—Injection of purified cells into mice. Purified cells from Fraction 6 ("lymphocytes"), Fraction 10 ("macrophages"), and combined Fractions 15–17 (myeloma cells) were injected into individual mice in a geometric series of three- to fivefold dilutions depending upon the number of cells which were available for injection from the respective gradient fractions. Mice which were living 4 months after injection of the purified cells are depicted by open circles. All mice which died during a 4-month period of observation died during the 5 weeks immediately following the injection of the purified cells. The results of the Experiment 1 and the Experiment 2 are similar. All animals which received 2.3×10^3 or more myeloma cells died within 5 weeks with the characteristic gross and histologic findings for animals dying from ascites myeloma. No animals which received purified cells from Fraction 6 (lymphoid cells) died. Similarly, of the animals which received cells from Fraction 10, only one has died. An autopsy of this animal revealed a bilateral bronchopneumonia; however, a minute focus of myeloma cells was identified in one abdominal lymph node. There was no other evidence of myeloma. The plotted logarithms are the logarithms of the total number of cells injected multiplied by the per cent of lymphocytes, macrophages, and myeloma cells found in the respective fractions (Table 3). Neither Fraction 6 nor Fraction 10 ever contained more than 0.2% myeloma cells.

termined tumorigenic dose for myeloma cells) died 5½ weeks after receiving the cells. An autopsy revealed an advanced bronchopneumonia in both lungs; this was considered to be the cause of death.

Table 3—Injection of Purified Cells into Mice

	Experiment 1			Experiment 2		
	Fraction No.			Fraction No.		
Composition (%)	6	10	15–17	6	10	15–17
Lymphocytes	57.0	24.4	4.6	76.6	26.8	11.4
Macrophages	0.6	67.1	31.8	1.3	69.0	38.0
Acites myeloma cells	0.0	0.2	62.2	0.0	0.0	48.4
Red blood cells	42.4	3.0	0.0	22.1	0.8	0.8
Neutrophils	0.0	5.3	1.0	0.0	3.2	1.2

There was no ascites fluid and no tumor seen microscopically on the peritoneal surfaces; however, a minute focus of myeloma was seen microscopically in a mesenteric lymph node which was not grossly enlarged. Other abdominal nodes from the same mouse showed no myeloma, and there were no distant metastases.

In Experiment 2, the mouse which received the largest number of cells from the macrophage zone (Fraction 10) received 6.8 × 10^5 cells, or 296 times the previously determined tumorigenic dose of myeloma cells. The composition of Fraction 10 from Experiment 2 is shown in Table 3. None of these animals have appeared sick or died after being observed for 4 months. In both experiments, the macrophages were diluted in a geometric series of fourfold dilutions for the successive animals.

In Experiments 1 and 2, the animals which received the largest numbers of lymphoid cells (cells from Fraction 6) received 2.29 × 10^6 and 3.7 × 10^6 cells or 1000 and 1600 times the number of myeloma cells previously observed to be tumorigenic. None of these animals have become sick or died during the 4 months following inoculation.

Recovery of Cells

Following the separation of the cells by gradient centrifugation, calculations were performed to determine what proportions of the cells in the starting sample suspension were recovered from the gradients. Following isopycnic centrifugation, 66.1 ± 21.9% of the red blood cells, 62.4 ± 0.2% of the lymphocytes, 55.3 ± 21.4% of the macrophages and 28.3 ± 6.7% of the myeloma cells were recovered from the isopycnic density gradients. Following isokinetic centrifugation, 100.0% of the red blood cells, 60.9 ± 15.4% of the lymphocytes, 33.5 ± 5.5% of the macrophages and 15.6% of the myeloma cells were recovered from the isokinetic gradients. In accounting for a loss of cells, the wall-effect artifact is always present when gradient centrifugation is carried out in cylindrical centrifuge tubes. The proportion of each kind of cell recovered appears to decrease as a function of the distance traveled in the isokinetic gradient; this finding would be anticipated for cells which are lost because of the wall-effect artifact. The wall-effect artifact has been discussed by others.[14,19] In both isopycnic and isokinetic separation experiments, the myeloma cells appear to have been more fragile than the other cells as manifested by a disproportionately lower rate of recovery than was found for the other kinds of cells both in the experiments reported here and in previously reported experiments.

Discussion

A large body of experimental oncology–biochemical, immunochemical, virologic, etc–has involved the study of ascites tumors or whole solid neoplasms. There has been little quantitative study of the influence of stromal benign cells on the results of experiments which employ whole solid tumors or crude unpurified ascites tumors in the characterization of malignant neoplasia. The few studies which have been addressed to this problem have demonstrated an excess of stromal cells over malignant cells in solid tumors. In the ascites tumors which have been studied [10] malignant cells have, in some cases, been more numerous than benign cells in the very late stage of the disease; however, results have been highly variable, and the very few ascites tumors which have been studied [10] have shown a preponderance of benign cells during most of the course of the disease. In most cases, criteria for the recognition of malignant cells have been purely cytologic. While the criteria for the recognition of malignant cells in cytologic preparations from the uterine cervix, tracheobronchial tree, etc, are relatively well defined, such criteria are not as completely defined for ascites tumors, and in our experience, are even more difficult in the case of disaggregated solid tumors.

In the present communication, we employed cytologic methods in the identification of benign cells; however, the validity of this cytologic identification of malignant cells was confirmed by the demonstration that the intraperitoneal injection of cells from the macrophage and lymphoid zones of the gradient failed to result in the development of tumors. After determining that all animals which received 2.3×10^3 or more myeloma cells developed myeloma, it was possible to determine the relationship between the tumorigenic dose of myeloma cells and the number of purified lymphoid cells and macrophages which were administered to the animals receiving cells from the lymphoid and macrophage zones of the gradients. The largest number of cells from the macrophage zone which was administered to a single animal was 296 times the tumorigenic dose of myeloma cells; the largest number of cells from the lymphoid zone which was administered to a single animal was 1600 times the tumorigenic dose of myeloma cells. None of the animals which received purified lymphocytes or macrophages died of ascites myeloma. One animal which received macrophages (157 times the tumorigenic dose for myeloma cells) died 5½ weeks later of bilateral bronchopneumonia; a focal infiltrate of myeloma cells was found microscopically in one abdominal lymph node. One can only speculate about whether or not this animal might have developed ascites or metastatic myeloma if it had survived pneumonia.

The experiments reported here emphasize the need for quantitative microscopic study of the ascites tumors which are being used in many laboratories for the investigation of cancer biochemistry and immunochemistry. On all but one day during the natural course of this ascitic myeloma (Table 1), myeloma cells averaged less than 22.4% of the cells in the ascites tumor suspension. The variation in host response, which was observed in these inbred mice of the same age and sex, was enormous as represented by the standard deviations calculated for 8 mice on each of the 7 days during which the composition of the tumor was assessed. Since other nucleated cells were four times more numerous than myeloma cells on all but one day, it is not surprising that oncologists have encountered such difficulty in demonstrating biochemical characteristics which are unique for cancer using ascites tumors as their experimental models. If a virus is recovered from such a mixture, one does not know whether it came from a myeloma cell, a macrophage, a lymphocyte, or some other cell. If the investigator wishes to prepare a specific antibody against cancer cells, this already difficult task is enormously complicated by the presence in the ascites tumor of predominantly cells other than cancer cells.

References

1. Klein G: Use of the Ehrlich ascites tumor of mice for quantitative studies on the growth and biochemistry of neoplastic cells. Cancer 3:1052–1061, 1950

2. Sugiura K: Effect of various compounds on the Ehrlich ascites carcinoma. Cancer Res 13:431–440, 1953

3. Brodersen H: Mitosegifte und ionisierende Strahlung. Strahlentherapie 73:196–254, 1943

4. Potter M: The plasma cell tumors and myeloma proteins of mice. Methods Cancer Res 2:105–157, 1967
5. Potter M: Myeloma proteins (M-components) with antibody-like activity. N Engl J Med 284:831–838, 1971
6. Watanabe T, Yagi Y, Pressman D: Antibody against neoplastic plasma cells. I. Specific surface antigens on mouse myeloma cells. J Immunol 106:1213–1221, 1971
7. Wu TT, Kabat EA: An analysis of the sequences of the variable regions of Bence Jones proteins and myeloma light chains and their implications for antibody complementarity. J Exp Med 132:211–250, 1970
8. Melchers F: Biosynthesis of the carbohydrate portion of immunoglobulin. Radiochemical and chemical analysis of the carbohydrate moieties of two myeloma proteins purified from different subcellular fractions of plasma cells. Biochem 10:653–659, 1971
9. Choi YS, Knopf PM, Lennox ES: Subcellular fractionation of mouse myeloma cells. Biochem 10:659–667, 1971
10. Goldie H, Feelix MD: Growth characteristics of free tumor cells transferred serially in the peritoneal fluid of the mouse. Cancer Res 11:73–80, 1951
11. Hartveit F: The significance of the blood content of the Ehrlich ascites carcinoma. Br J Cancer 15:665–672, 1961
12. Pretlow TG: Estimation of experimental conditions that permit cell separations by velocity sedimentation on isokinetic gradients of Ficoll in tissue culture medium. Anal Biochem 41:248–255, 1971
13. Pretlow TG, Boone CW: Centrifugation of mammalian cells on gradients: a new rotor. Science 161:911–913, 1968
14. Boone CW, Harell GS, Bond HE: The resolution of mixtures of viable mammalian cells into homogeneous fractions by zonal centrifugation. J Cell Biol 36:369–378, 1968
15. Pretlow TG, Boone CW, Shrager RI, Weiss GH: Rate zonal centrifugation in a Ficoll gradient. Anal Biochem 29:230–237, 1969
16. Pretlow TG, Boone CW: Separation of mammalian cells using programmed gradient sedimentation. Exp Mol Pathol 11:139–152, 1969
17. Hilfer SR, Brown JM: Collagenase. Exp Cell Res 65:246–249, 1971
18. Wodinsky I, Meany KF, Kensler CJ: Viability of forty-two neoplasms after long-term storage in liquid nitrogen at −195° C. Cryobiology 8:84–90, 1971
19. Anderson NG: Studies on isolated cell components. VIII. High resolution gradient differential centrifugation. Exp Cell Res 9:446–459, 1955

Acknowledgments

We thank Mrs. Linda Hamilton for her expert technical assistance.

Miss Stewart is a candidate for a combined MS–MD degree, and is supported by Grant HD–00102 from the National Institutes of Health.

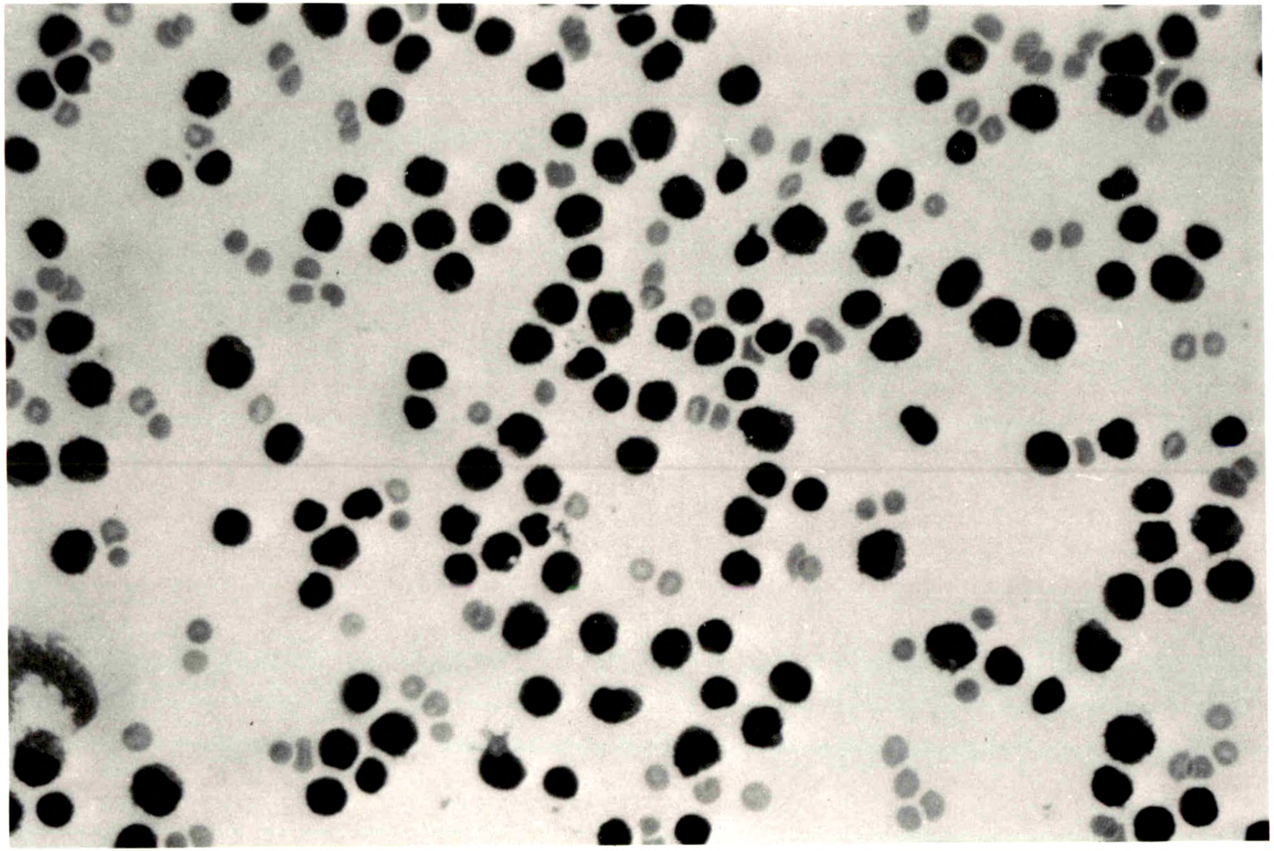

Fig 1—Cells from Fraction 6 after separation by velocity or rate-zonal sedimentation in the isokinetic gradient. The cells from this fraction are primarily lymphocytes and red blood cells. Lymphoid cells represent 98.9±0.4% of the nucleated cells from Fraction 6 (Wright stain, × 250).

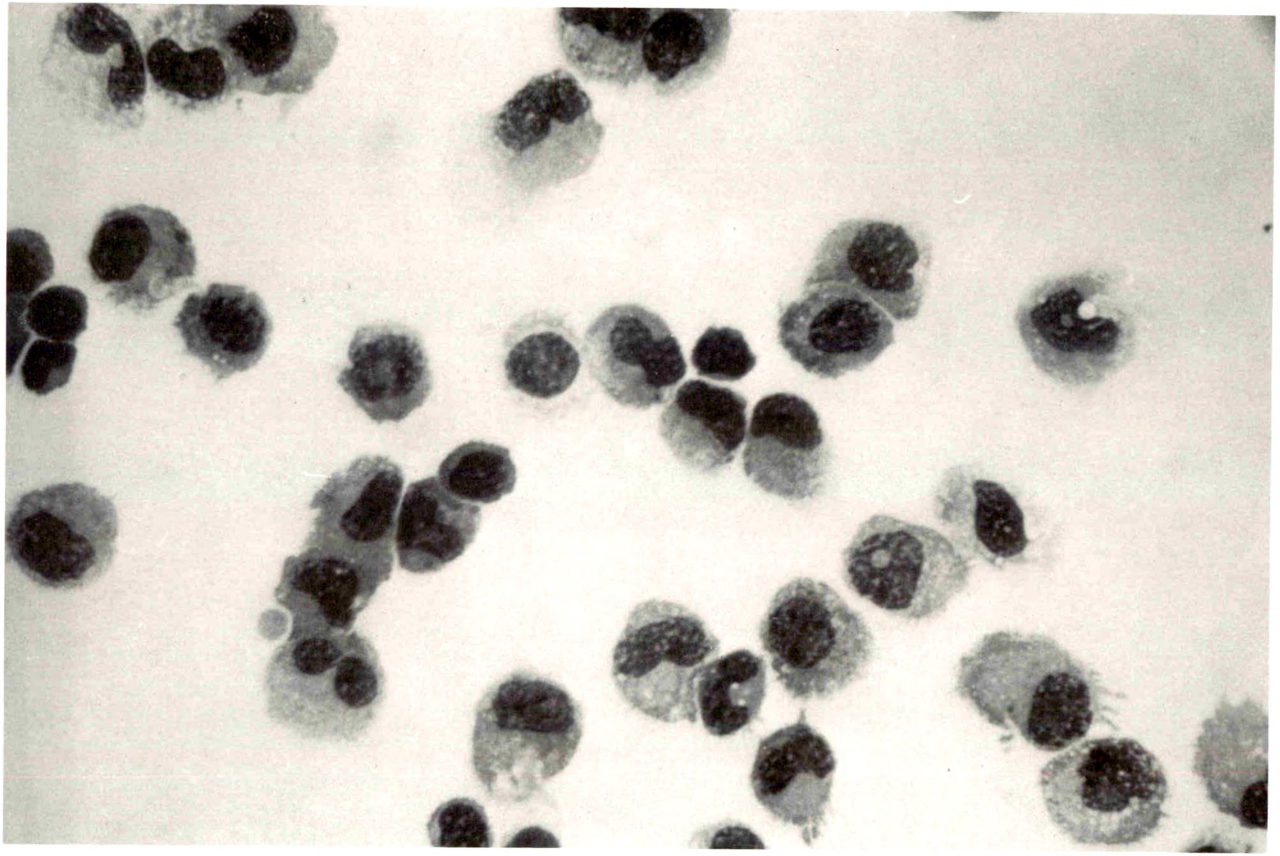

Fig 2—Cells from Fraction 10 after separation by velocity or rate-zontal sedimentation in the isokinetic gradient. The cells from this fraction are primarily benign inflammatory cells from the host's peritoneal reaction. The most frequent cell is the macrophage. Macrophages represent 79.3±12.1% of nucleated cells; myeloma cells, always less than 0.2% of nucleated cells (Wright stain, × 250).

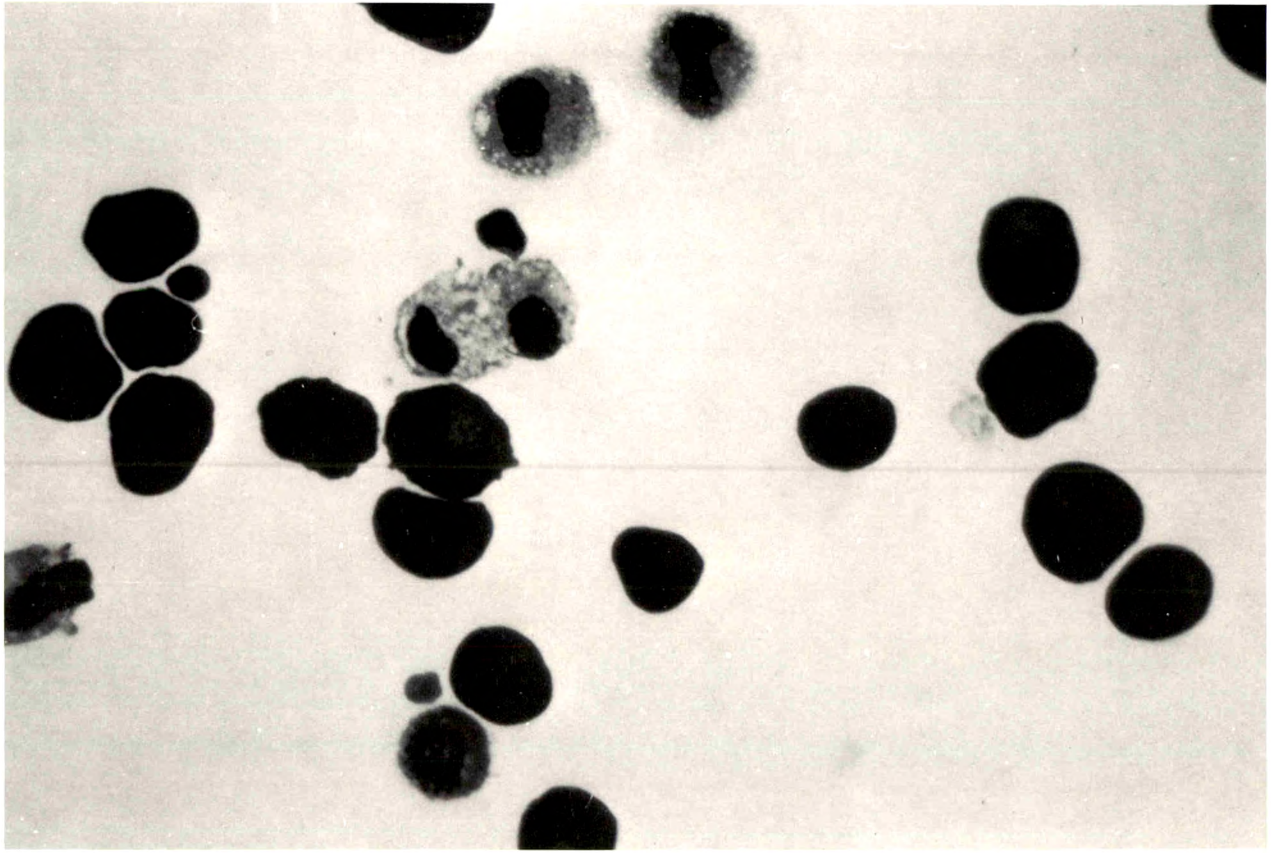

Fig 3—Combined Fractions 15–17 after separation by velocity or rate-zonal sedimentation in the isokinetic gradient. Fractions 15–17 always included the broad modal population of tumor cells which were 52.1±6.9% of nucleated cells. Each of these 3 fractions contained the highest proportion of tumor cells in at least one experiment, and the relative purities of these 3 fractions from any one experiment were quite similar (Wright stain, × 250).

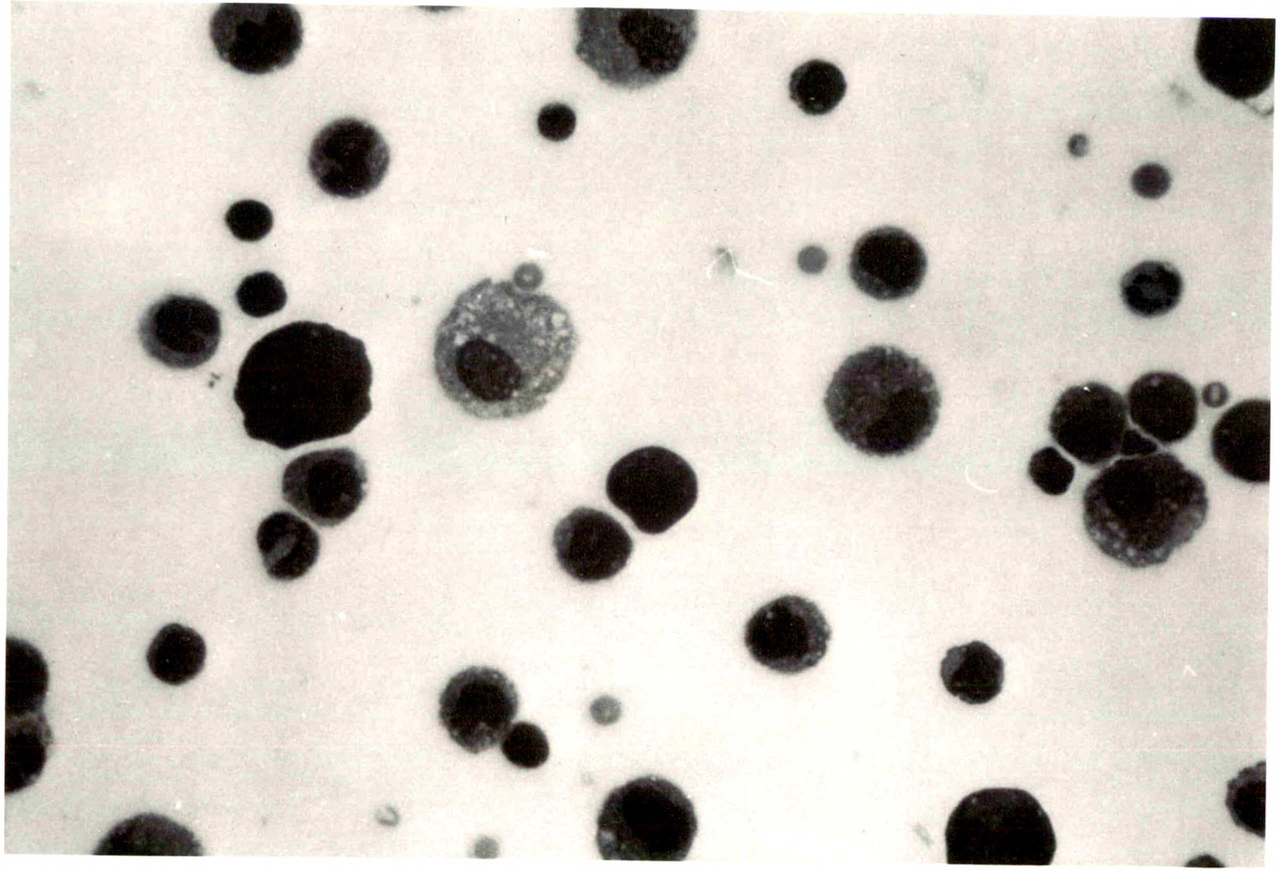

Fig 4—Starting sample suspension. The composition of the starting sample suspension (day 10) is given in Table 1. Myeloma cells were 35.9±28.0% of the starting sample suspension (Wright stain, × 250).

Mouse Cytomegalovirus

Necrosis of Infected and Morphologically Normal Submaxillary Gland Acinar Cells During Termination of Chronic Infection

Donald Henson, MD and Alfonso J. Strano, MD

The ultrastructural lesions in the submaxillary glands of C_3H mice chronically infected with the murine cytomegalovirus are reported. Virus was synthesized in the nucleus of acinar glandular cells. After passage into the cytoplasm, virus was located in large vesicles which were derived from the Golgi apparatus. These vesicles, which were periodic acid-Schiff positive, migrated to the apex of the cell and released virus into the acinar lumen or canaliculi. Eventually, lymphocytes infiltrated the interstitium and surrounded the basal lamina of acini which contained infected cells. In acini encompassed by lymphocytes, both infected cells and morphologically normal acinar cells simultaneously degenerated, producing a small focus of necrosis. Physical contact between lymphocytes and necrotic cells did not occur for an intact basal lamina was always found interposed between them. Degeneration of infected cells coincided with a decrease in virus titer in the salivary glands. Degeneration of infected and normal acinar cells also occurred in DBA/2 mice which lack the fifth component of complement. In mice conditioned with cortisone to suppress inflammation, neither infected nor normal acinar cells degenerated. We concluded from the electron microscope observations that lymphocytes terminate chronic MCMV infection, that MCMV infection of acinar epithelium is not cytolytic and that normal cells also undergo necrosis during termination of chronic MCMV infection. It is postulated that lymphocytes in responding to infection release a cytotoxic substance which diffuses into the acini and causes indiscriminate necrosis of acinar cells (Am J Pathol 68:183–202, 1972).

MANY VIRUSES BELONGING TO SEVERAL DIFFERENT GROUPS produce chronic infection either in their natural or in experimental hosts. With some of these viruses specific pathologic lesions develop during the course of chronic infection which differ from lesions produced during acute infection. For instance, in man, subacute scleros-

---

From the Laboratory of Pathology, National Cancer Institute, and Viro-Pathology Branch, Armed Forces Institute of Pathology, Washington, DC.

The opinions or assertions contained herein are the private views of the authors and are not to be construed as official or as reflecting the views of the Department of the Army or the Department of Defense.

Supported in part by a research contract, Project Number 3A061102B71Q, from the Medical Research and Development Command, US Army, Washington, DC.

Accepted for publication Mar 7, 1972.

Address reprint requests to Dr. Donald Henson, Laboratory of Pathology, National Cancer Institute, National Institutes of Health, Room 2A-29, Bldg 10, Bethesda, Md 20014.

ing panencephalitis has been associated with chronic measles virus infection of the central nervous system; [1-4] and, in mice, glomerulonephritis frequently occurs during chronic lymphocytic choriomeningitis virus infections.[5] The mechanisms of virus-induced tissue injury during chronic infection have not been elucidated, although there is a consentience that numerous mechanisms are involved.[6]

The cytomegaloviruses (CMV) belong to the herpesvirus family and cause chronic infection in many species of animals in which they occur. In newborn infants, congenital CMV infection causes cytomegalic inclusion disease. In older children and adults, CMV infections have been associated with pneumonitis,[7,8] fever with rash,[8] heterophil-negative infectious mononucleosis,[9,10] parotitis [11] and hepatitis.[12-14] As with other viruses causing persistent infection, disease apparently can occur during the course of chronic CMV infection.[8] One approach to understanding the pathogenesis of human CMV infection involves experimental studies with laboratory animal strains of CMV. In mice, the murine cytomegalovirus (MCMV) produces a hepatitis [15] and chronic infection in salivary glands,[16,17] kidneys [17] and lymphoid tissue.[18] The hepatic lesions and sites of virus persistence are similar to that found in humans infected with CMV. In this report, the ultrastructural cellular lesions that occur in the submaxillary glands during chronic MCMV infection are described. The results suggest that one mechanism of virus-induced tissue injury operates during the termination of chronic infection.

Materials and Methods

Mice

Male C_3H/He and DBA/2 mice 6 to 8 weeks of age were used. Mice were obtained from the NIH breeding colony and were free of MCMV infection.*

Experimental Procedure

Mice were inoculated intraperitoneally with 0.25 ml of virus suspension prepared by homogenizing the salivary glands of 3-week postinfected C_3H mice. Virus suspension was initially prepared as a 10% homogenate in saline and diluted 10^{-2} before injection. Following infection, submaxillary glands were removed twice a week for 9 weeks for electron and light microscopy. Generally, the left gland was fixed in Bouin's solution for light microscopy and the right gland was cut into 1-mm cubes and fixed in 0.1 M phosphate-buffered 4% glutaraldehyde at pH 7.2 for electron microscopy. In addition, mice were killed periodically after infection for assay of virus in the submaxillary glands. The methods of virus assay have been described.[16,19]

---

* In conducting the research described in this report, the investigators adhered to the "Guide for Laboratory Animal Facilities and Care," as promulgated by the Committee on the Guide for Laboratory Animal Facilities and Care of the Institute of Laboratory Animal Resources, National Academy of Sciences–National Research Council.

Cortisone Administration

Cortone® (Cortisone acetate, Merck, Sharpe and Dohme, West Point, Pa) was used. Mice were injected intraperitoneally 3 times a week with 0.5 mg cortisone beginning 10 days after MCMV infection.

Electron Microscopy

Glutaraldehyde-fixed tissue was washed in phosphate-buffered 5% sucrose solution pH 7.2, postfixed in 1% osmium tetroxide in water, dehydrated in alcohol and propylene oxide and embedded in Epon 812. Sections were cut on a Porter-Blum MT-2 Ultramicrotome, double stained with uranyl acetate and lead hydroxide and examined with a Siemens Elmskop I. Over 1600 sections were examined in the electron microscope.

Histology

Bouin's fixed tissues were embedded in paraffin and sections stained with hematoxylin and eosin or by the periodic acid-Schiff reaction. Reticulum stains were done by the Gridley method.

Results

The submaxillary glands of C_3H mice are trilobed, with each lobe containing only one type of secretory cell—serous, mucous or seromucous. During chronic infection, intranuclear inclusion bodies appear predominantly in seromucous secreting cells, occasionally in mucous secreting cells and rarely in serous secreting cells.

Ultrastructure of the Seromucous Secreting Cells

The ultrastructure of the seromucous secreting cells and acini is presented first as reference for describing changes in the infected cells. The acini consist of 8 to 10 pyramid-shaped cells with the apical regions forming the acinar lumen. The cytoplasm of these cells contains a well-developed Golgi apparatus, small amounts of rough and smooth endoplasmic reticulum, scattered small secretory granules, small vesicles near the Golgi region, occasional laminated myelin bodies and lysosomes. The nucleus is in the basilar half of the cell, oval in shape and has finely dispersed chromatin which is more dense along the nuclear membrane. The nucleolus is not prominent, but when present, it is located at the nuclear membrane. Laterally, the plasma membranes which interdigitate with adjacent cells are focally connected by desmosomes. Between adjacent cells are caniliculi formed by projecting microvilli. Surrounding the acini is a nonfenestrated basement lamina or membrane. Between the basal lamina and acinar cells lie the long, slender cytoplasmic processes of the myoepithelial cells. There are no desmosomes or interdigitating connections between acinar cells and myoepithelial cells. Interspersed between acini in the interstitium are collagen bundles, nerve fibers, capillaries and some fibroblasts.

Multiplication of MCMV in Submaxillary Glands

Virus appeared in the submaxillary glands 7 to 10 days after infection, reached maximum titers by days 16 to 21, then decreased in titer during the subsequent 3 to 4 weeks. Intranuclear inclusion bodies, which appeared 1 to 3 days after infectious virus was detected, increased in number to about day 21, then decreased as the virus titer declined. Concomitant with a decrease in number of inclusions was a progressive focal interstitial inflammatory reaction (Table 1).

Ultrastructure of Submaxillary Glands from Infected C_3H Mice

First Week

There were no changes evident. Although mature virus was seen in the hepatic sinusoids and vessels on days 4 to 7,[20] none was visible in arteries, capillaries or tissues of the salivary glands.

Second Week

The first indication of infection was not observed until the twelfth day. The nuclei of acinar cells became enlarged and rounded and the chromatin more uniformly dispersed. Within the region of the nucleolus, the first assembly of virus was seen. The nucleoli which remained along the nuclear membrane enlarged and exhibited feathering around the periphery (Figure 1). High-power magnification of the feathery edges revealed hollow fibrils identical to those of the virus

Table 1—Correlation of Virologic and Histologic Observations on Submaxillary Glands of C_3H Mice Infected with the Murine Cytomegalovirus

Days after infection	Virus titer*	Relative No. intranuclear inclusions	Relative amount inflammation
4	$<1.0 \times 10^1$†	—	—
16	2.9×10^6	+++	++
20	3.2×10^6	++++	+++
27	2.0×10^6	+++	++++
34	4.5×10^3	++	++++
43	7.5×10^1	—	++
55	1.8×10^2	—	—

* Plaque-forming units per milliliter of a 10% salivary gland homogenate.

† Titer for one mouse.

membrane. Irregular dense cores soon became associated with and surrounded by these hollow fibrils which seemed to form the capsid of the virus. Subsequently, cores, fibrils and virus were seen throughout the nucleoplasm. As virus passed into the cytoplasm it acquired a second membrane from the inner nuclear membrane.

The first change evident in the cytoplasm of infected cells was an increase in number and size of organelles. The mitochondria enlarged, the cisternae of the smooth and rough endoplasmic reticulum dilated and the number of vesicles greatly increased, especially in the area of the Golgi apparatus. After emerging from the nucleus, the virions were usually seen free within the cytoplasm. Eventually, they made contact with a unit membrane of a dilated vesicle, and by a process of invagination, passed into the vesicle (Figure 2). As the virus entered the vesicle, it acquired a third membrane, or envelope, from the invaginated part of the vesicular membrane. Although this process occurred most often in the Golgi region, we have seen virus enter vesicles derived from the endoplasmic reticulum. Initially, the vesicles contained only several complete viral particles, but as time progressed the vesicles enlarged, particularly when they approached the apex of the cell, and eventually contained as many as 100 virions visible on thin sections (Figure 3). Often individual infected cells contained as many as 10 large vesicles and numerous smaller ones. Inside the vesicles, the virions were randomly arranged in a poorly staining granular matix. With light microscopy, these large vesicles were periodic acid-Schiff positive and appeared as intracytoplasmic inclusion bodies. Eventually, these large vesicles reached the apical margin and ruptured releasing virus into the lumen or into the canaliculi (Figure 4).

As shown by multiple sections, the acini usually contained one, rarely two, infected cells. Occasionally, infected cells were binucleated with both nuclei producing virus.

At this stage, there were no changes in myoepithelial cells, basal lamina, or interstitial elements. The desmosome connections persisted between adjacent infected and uninfected cells.

Third Week

During this time, the number of infected cells increased, reaching maximum around day 21, which coincided with peak viral titers in the salivary gland. However, there were no significant changes in the infected cells. Although the number of viral particles within the acinar lumens, caniculi and ducts increased, virus was never seen in the interstitium, between or entering uninfected cells or in vascular channels. The morphology and development of MCMV in the submaxillary glands of inbred C_3H mice resembles that reported for random bred Swiss-Webster mice.[21]

After the sixteenth day, inflammatory cells began to appear in the interstitium. They progressively increased in number and surrounded acini in which there were infected cells, often dispersing periacinar fibroblasts and collagen (Figure 5). The early infiltrate consisted of small lymphocytes, and later, a combination of small lymphocytes, larger lymphocytes corresponding to the intermediate type,[22] and macrophages. The intermediate type predominated and were usually found aligned along the periphery of the basal lamina. The lymphocytes had a moderately developed rough endoplasmic reticulum, prominent Golgi apparatus and large nucleolus. At this time, silver-impregnated histologic sections showed displacement and fragmentation of the periacinar reticulum and severe distortion of acini by the inflammatory cells. However, the basal lamina remained intact, despite marked distortion of the acini. Penetration of inflammatory cells through the basal lamina was not observed. Polymorphonuclear leucocytes were never seen in the interstitial tissues of the salivary glands.

Fourth and Fifth Weeks

During this time, the number of inflammatory cells increased and the first evidence of necrosis was noted in acini encompassed by lymphocytes. Necrotic changes occurred simultaneously in infected and in uninfected acinar cells (Figure 6). The lysosomes enlarged, often coalesced and accumulated a dense osmophilic amorphous material. Organelles surrounding the lysosomes seemed to disintegrate and the ergastoplasm became disorganized. This was accompanied by an increase in number and size of laminated bodies within vesicles. In the infected cells, vesicles which still contained virus collapsed and the virions were dispersed in the cytoplasm. Nuclear changes occurred after the cytoplasmic changes were moderately advanced; they consisted of chromatin condensation and subsequent pyknosis.

The number of uninfected cells undergoing necrosis varied in the different acini. In some of the acini, only cells adjacent to infected cells became necrotic while in other acini, all visible cells except myoepithelial cells degenerated (Figure 7).

Degeneration of cells was visible only in acini surrounded by lymphocytes. Infected cells found in acini about which there were no inflammatory cells showed no evidence of necrosis, even though numerous virus containing vesicles were present in the cytoplasm. Furthermore, physical contact between lymphocytes and degenerating cells was not observed for an intact basal lamina was always found interposed between them. Necrosis was not recognized in acini adjacent to those acini with infected cells. Necrosis of acinar cells was maximal from days 25 to 35, corresponding to a progressive decline in the titer of infectious virus. Necrotic cells were extruded into the lumen and apparently were removed by passage out the ducts.

The myopithelial cells did not become infected nor did they degenerate with the acinar cells. Instead they enlarged and frequently extended their cytoplasmic processes toward the acinar lumen in between acinar cells (Figure 8).

Sixth to Ninth Weeks

This period was characterized by healing. Inflammatory cells migrated out of the submaxillary gland and the acini regenerated. The myoepithelial cells assumed their normal size and position. At the end of this period, the histology of the salivary gland was indistinguishable from that of uninfected mice.

Mucous Secreting Glands

In the lobe with mucous secreting cells there were fewer infected cells and correspondingly less inflammation. However, virus synthesis and the changes in the acini during termination of infection were virtually identical to that in the seromucous lobes.

Cortisone Conditioned Mice

In this group of mice the interstitial inflammatory reaction was completely suppressed through the entire period of observation. Compared to infected control mice, infected cells in this group exhibited greater cytomegaly, often compressing adjacent cells and severely distorting the acini. The cytoplasm of these cells also contained more vesicles filled with virus (Figure 9). However, we could not determine if this increase in number of vesicles resulted from greater virus production or delayed rupture at the apical plasma membrane. The assembly of virus, exodus of virus from the nucleus, and release from infected cells was the same as that in control mice. However, acini often contained 2 or 3 infected cells or, less frequently, multinucleated infected cells.

In the cortisone-conditioned mice there was no necrosis of infected or uninfected acinar cells. By day 39, when nearly all infected cells had degenerated in control mice, the infected cells were intact and showed no evidence of necrosis or focal degenerative changes. We concluded from these observations that lymphocytes are essential for terminating chronic MCMV infection.

DBA/2 Mice

The DBA/2 strain was selected because it reportedly lacks the fifth component of complement (C′5),[23] thus affording us the opportunity to test whether necrosis of acinar cells required complement.

The sequence of changes in the salivary glands of infected DBA/2 mice was similar to that seen in C_3H mice. Inflammatory cells appeared in the interstitium and surrounded acini which contained infected cells; subsequently, both infected and uninfected acinar cells degenerated. This suggests, therefore, that C′5 is not essential for necrosis of acinar cells and termination of MCMV infection.

Discussion

The results of this study support conclusions based on histologic observations that termination of chronic MCMV infection is associated with periacinar accumulation of lymphocytes.[16]In addition, the electron microscope revealed that, during termination of chronic infection, infected and morphologically normal acinar cells undergo simultaneous degeneration producing, in effect, a small focus of tissue necrosis. However, because of the dense inflammation and severe architectural distortion, these small focal lesions were not clearly evident in routine histologic sections. Interestingly, degeneration of acinar cells occurred while lymphocytes were aligned along the periphery of the basal lamina outside the acini. Lymphocytes were never seen within acini or in physical contact with necrotic cells. The basal lamina, which is considered to be a product of the overlying epithelium, remained intact and appeared to form an anatomical barrier between infected cells and lymphocytes.

Because acinar cells degenerated only in the presence of lymphocytes, we concluded that these inflammatory cells terminate chronic MCMV infection. This is consistent with other studies which suggest that cell-mediated immunologic mechanisms terminate certain viral infections. Mice infected with ectromelia virus and injected with antithymocyte serum to depress cellular immunity have a higher mortality than control mice.[24] Injections of spleen cells prepared from immune mice into marasmic mice infected with Coxsackie virus reduce mortality and extent of pathologic lesions.[25] Clinically, observations on human infants with primary immunologic deficiency diseases suggests that cell-mediated immune mechanisms are essential for recovery from vaccinia virus infection.[26]

Although mechanisms by which lymphocytes terminate viral infections are unknown, recent studies have indicated that *in vitro* lymphocytes elaborate several cytotoxic substances following specific or nonspecific mitogenic stimulation.[27-29] Released *in vivo*, these substances could diffuse and cause widespread tissue damage. Furthermore, lymphocytic choriomeningitis virus which also causes chronic infection in mice stimulates release *in vitro* of a cytotoxic factor from spleen cells of immune mice.[30] *In vitro*, this factor has a nonspecific effect, killing both infected and uninfected target cells.[30] Because of these data and the electron microscopic observations in this study, we suggest that lymphocytes, in responding to infection, released a cytotoxic substance which diffused into the acini and caused indiscriminate and simultaneous necrosis of acinar cells.

The possibility must be considered that uninfected cells either contained virus on their surface or were cryptically infected and were consequently treated as infected cells by the host. However, there was no morphologic evidence for these possibilities; uninfected cells appeared ultrastructurally normal, exhibited normal secretory activity prior to necrosis, did not contain intranuclear or intracytoplasmic virus and did not have virus visibly adsorbed on the surface. Furthermore, lymphocytes only surrounded acini in which there were infected cells. If acinar cells can become cryptically infected with MCMV, then one might expect that lymphocytes would also be found around acini in which no overt infected cells were seen. This, however, was not observed.

These morphologic studies suggest that MCMV infection of acinar epithelium is not cytolytic, in contrast to *in vitro* infection of mouse embryo cells [19] or macrophages.[31] Necrosis of acinar cells was seen only after inflammatory cells appeared in the periacinar interstitium and did not occur if cortisone was administered to suppress inflammation. These data are in accord with previously published histologic observations on MCMV chronically infected mice conditioned with cortisone.[16] Persistence of infected epithelial cells in the salivary glands and possibly in the renal tubules with periodic release of virus may be one mechanism of chronic intermittent excretion of virus in the saliva and in the urine.[8]

We do not know what attracts lymphocytes into the salivary glands of infected mice. It does not seem to be intact virions since they were never seen outside the acini. Necrotic cells were not visible until after the lymphocytes appeared. Most probably, an antigenic alteration on the surface of infected cells attracted the lymphocytes, perhaps in a manner analogous to that by which lymphocytes are attracted into the area of an allograft. Although surface changes on MCMV-infected cells have not been demonstrated as yet, cells infected with a related virus, herpes simplex, acquire new membrane antigens demonstrable by several immunologic technics.[32,33] In addition, some interesting relationships exist between salivary gland tissue and lymphoid tissue. The submandibular glands of male mice contain a saline extractable substance which induces generalized lymphoid atrophy in mice and prolongs survival of H-2 incompatible skin allografts.[34,35] Also, a protein has been isolated from mouse salivary glands which induces *in vivo* and *in vitro* transformation of thymic small lymphocytes into cells of the plasma series.[36] What role these substances play, if any, in the pathogenesis of chronic MCMV infection is unknown at present.

Results of this study have implications for diseases of suspected viral etiology which are characterized by focal lesions such as multiple sclerosis or focal myocardial fibrosis. The morphologic data indicate that focal lesions can develop during the termination of a chronic viral infection. Consequently, in searching for viruses that cause focal lesions, one should also look in uninvolved areas of tissue since, in the necrotic foci, the infection may have already been terminated and the virus no longer present. Furthermore, these data raise the question whether the cerebral lesions of congenital CMV infection or other pathologic lesions associated with this virus result from a lymphocytoxic substance.

Corticosteroids are considered to be contraindicated during CMV and many other viral infections. However, if pathologic lesions are caused by immunologic mechanisms, then corticosteroids or other immunosuppressive agents may be indicated. For instance, in adult mice infected with lymphocytic choriomeningitis virus, immunosuppression prevents manifestations of the disease.[37,38] In mice chronically infected with MCMV cortisone administration clearly suppresses the histologic lesions in the submaxillary glands [16] although it prolongs the infection. The beneficial effects of corticosteroid treatment on neonatal CMV infections have been reported.[39-41] Perhaps, in these cases, the corticosteroids were suppressing immunologically induced tissue injury.

From the morphologic data, we conclude that MCMV infection is not cytolytic in the salivary glands of mice, that lymphocytes are responsible for terminating chronic infection possibly by elaborating a cytotoxic substance which diffuses into the acini and that morphologcally normal acinar cells also degenerate during termination of chronic infection.

References

1. Connolly JH, Allen IV, Hurwitz LJ, Millar JHD: Measles-virus antibody and antigen in subacute sclerosing panencephalitis. Lancet 1:542–544, 1967
2. Horta-Barbosa L, Fuccillo DA, Sever J, Zeman W: Subacute sclerosing panencephalitis: Isolation of measles virus from a brain biopsy. Nature 221: 974, 1969 (abstr)
3. Payne, FE, Baublis, JV, Itabashi, HH: Isolation of measles virus from cell cultures of brain from a patient with subacute sclerosing panencephalitis. N Engl J Med 281:585–589, 1969
4. Parker, JC Jr, Klintworth GK, Graham DG, Griffith JF: Uncommon morphologic features in subacute sclerosing panencephalitis (SSPE). Am J Pathol 61:275–289, 1970
5. Kajima M, Pollard M: Ultrastructural pathology of glomerular lesions in gnotobiotic mice with congenital lymphocytic choriomeningitis (LCM) virus infection. Am J Pathol 61:117–140, 1970
6. Brody JA, Henle W, Koprowski H, editors: Chronic Infectious Neuropathic Agents (CHINA) and Other Slow Virus Infections, Vol 40, Current Topics in Microbiology and Immunology. New York, Springer-Verlag, 1967
7. Craighead JE: Pulmonary cytomegalovirus infection in the adult. Am J Pathol 63:487–504, 1971
8. Henson D, Siegel SE, Fuccillo DA, Matthew E, Levine AS: Cytomegalovirus infections during acute childhood leukemia. Submitted for publication.
9. Klemola E, Kääriäinen L: Cytomegalovirus as a possible cause of a disease resembling infectious mononucleosis. Br Med J 2:1099–1102, 1965
10. Klemola E, von Easen R, Wager O, Haltia K, Koivuniemi A, Salmi I: Cytomegalovirus mononucleosis in previously healthy individuals: Five new cases and follow-up of 13 previously published cases. Ann Int Med 71:11–19, 1969
11. Diosi P, Rosin N: Cytomegalic infection in the submaxillary glands of an adult. Pathol Microbiol 28:420–424, 1965
12. Hanshaw J: Acquired cytomegalovirus infection: Association with hepatomegaly and abnormal liver function tests. N Engl J Med 272:602–609, 1965
13. Carter AR: Cytomegalovirus disease presenting as hepatitis. Br Med J 3:786, 1968
14. Henson D: Cytomegalovirus hepatitis in an adult. An autopsy report. Arch Pathol 88:199–203, 1969
15. Henson D, Smith RD, Gehrke J: Non-fatal mouse cytomegalovirus hepatitis: Combined morphologic, virologic and immunologic observations. Am J Pathol 49:871–888, 1966
16. Henson D, Neapolitan C: Pathogenesis of chronic mouse cytomegalovirus infection in submaxillary glands of C_3H mice. Am J Pathol 58:255–267, 1970
17. Medearis DN Jr: Mouse cytomegalovirus infection. II. Observations during prolonged infections. Am J Hyg 80:103–112, 1964

18. Henson D, Strano A, Slotnik M, Goodheart C: Mouse cytomegalovirus: Isolation from lymphoid organs of chronically infected mice. (In press)
19. Henson D, Pinkerton H: Characteristics of a plaque method for the murine salivary gland virus. Proc Soc Exp Biol Med 114:130–133, 1963
20. Henson D, Strano A: Unpublished data
21. Reubner BH, Hirano T, Slusser R, Osborn J, Medearis DN Jr: Cytomegalovirus infection. Viral ultrastructure with particular reference to the relationship of lysosomes to cytoplasmic inclusions. Am J Pathol 48:971–989, 1966
22. Daniels JC, Ritzman SE, Levin WC: Lymphocytes. Morphological, developmental and functional characteristics in health, disease and experimental study. An analytical review. Tex Rep Biol Med 26:5–93, 1968
23. Nilsson UR, Müller-Eberhard HJ: Deficiency of the fifth component of complement in mice with an inherited complement defect. J Exp Med 125:1–16, 1967
24. Blanden RV: Mechanisms of recovery from a generalized viral infection: Mousepox I. The effects of antithymocyte serum. J Exp Med 132:1035–1054, 1970
25. Woodruff JF, Woodruff JJ: Modification of severe coxsackievirus B_3 infection in marasmic mice by transfer of immune lymphoid cells. Proc Nat Acad Sci USA 68:2108–2111, 1971
26. Fulginiti VA, Kempe CH, Hathaway WE, Pearlman DS, Sieber OF, Eller JJ, Joyner JJ, Robinson A: Progressive vaccinia in immunologically deficient individuals. Immunologic Deficiency Dis in Man 4:129, 1968
27. Granger GA, Kolb WP: Lymphocyte *in vitro* cytoxicity: Mechanisms of immune and non-immune small lymphocyte mediated target L Cell destruction. J Immunol 101:111–120, 1968
28. Williams TW, Granger GA: Lymphocyte *in vitro* cytotoxicity: Mechanism of lymphotoxin-induced target cell destruction. J Immunol 102:911–918, 1969
29. Granger GA, Moore GE, White JG, Matzinger P, Sundsmo JS, Shupe S, Kolb WP, Kramer J, Glade PR: Production of lymphotoxin and migration inhibitory factor by established human lymphocytic cell lines. J Immunol 104:1476–1485, 1970
30. Oldstone MBA, Dixon FJ: Tissue injury in lymphocytic choriomeningitis viral infection: Virus-induced immunologically specific release of a cytoxic factor from immune lymphoid cells. Virology 42:805–813, 1970
31. Tegtmeyer, PJ, Craighead JE: Infection of adult mouse macrophages *in vitro* with cytomegalovirus. Proc Soc Exp Biol Med 129:690–694, 1968
32. Nii S, Morgan C, Rose HM, Hsu KC: Electron microscopy of herpes simplex virus. IV. Studies with ferritin-conjugated antibodies. J Virol 2:1172–1184, 1968
33. Roizman B, Spear PG: Herpesvirus antigens on cell membranes detected by centrifugation of membrane–antibody complexes. Science 171:298–300, 1971
34. Takeda T, Yamasaki Y, Yamabe H, Suzuki Y, Haebara H, Irino T, Grollman A: Atrophy of the lymphoid tissues of mice induced by extracts of the submaxillary gland. Proc Soc Exp Biol Med 126:212–216, 1967
35. Kongshavn PAL, Bliss JQ: Effect of mouse submandibular gland extracts on survival of H-2 incompatible skin allografts. Immunol 19:363–367, 1970

36. Naughton MA, Koch J, Hoffman H, Bender V, Hagopian H, Hamilton E: Isolation and activity of a thymocyte-transforming factor from the mouse submaxillary gland. Exp Cell Res 57:95–103, 1969
37. Rowe W: Studies on pathogenesis and immunity in lymphocytic choriomeningitis infection of the mouse. Naval Med Res Inst Rep 12:167–219, 1954
38. Hotchin J, Weigand H: The effects of pre-treatment with X-rays on the pathogenesis of lymphocytic choriomeningitis in mice. I. Host survival, virus multiplication and leucocytosis. J Immunol 87:675–681, 1961
39. Margileth AM: Diagnosis and treatment of generalized cytomegalic inclusion disease of newborn. Pediatrics 15:270–283, 1955
40. Birdsong M, Smith DE, Mitchell FN, Corey JH Jr: Generalized cytomegalic inclusion disease in newborn infants. JAMA 162:1305–1308, 1956
41. Gelderen HH van: Successfully treated case of cytomegalic disease in a newborn infant. Acta Paediat 48:169–174, 1959

1

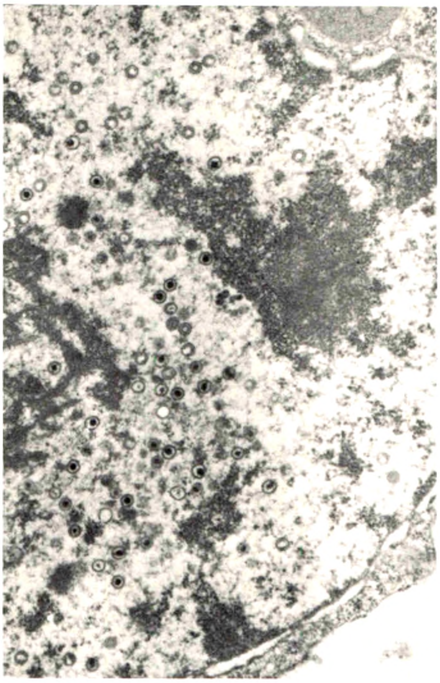

2

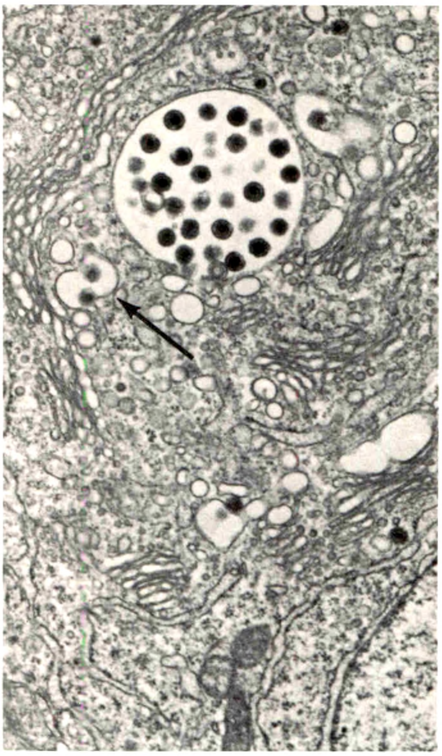

3

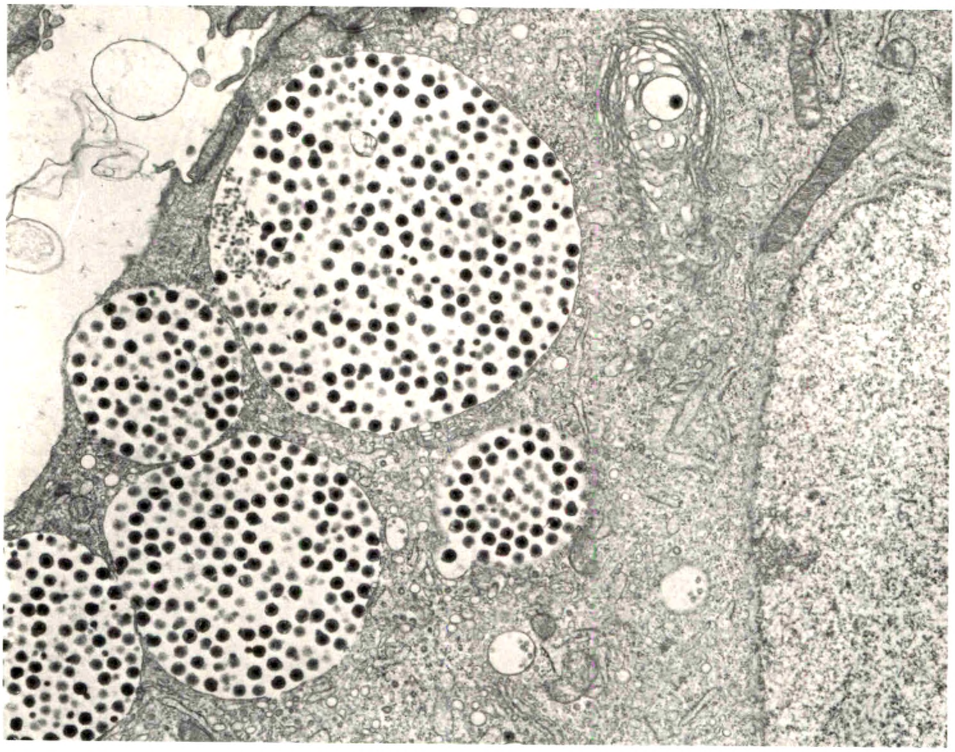

Fig 1—An enlarged nucleolus in an infected cell. The nucleolus is partly surrounded by filamentous structures which form the virus capsid (× 15,900). **Fig 2**—Virus (arrows) budding into small vesicle in region of Golgi. Adjacent is a large virus-filled vesicle. Other viral particles lie free within cytoplasm (× 14,000). **Fig 3**—Salivary gland from C_3H mouse 21 days after mouse cytomegaovirus infection. Large virus-filled vesicles are present in apical cytoplasm near acinar lumen (× 9600).

Fig 4—Mouse 23 days after infection. A virus-filled vesicle has ruptured releasing virus into a canaliculus. Nucleus of infected cell contains virus. Contiguous uninfected acinar cells are markedly compressed by the enlarged infected cell and the acinus distorted. *Arrows* indicate basal lamina (× 6750).

Fig 5—C_3H submaxillary gland 34 days after MCMV infection. To the right in the electron micrograph is part of an acinus surrounded by an intact basal lamina (*arrows*). Infected acinar cell is not included in the micrograph. Three lymphocytes are present to the left in the interstitium. Penetration of lymphocytes through basal lamina was never observed (× 4000).

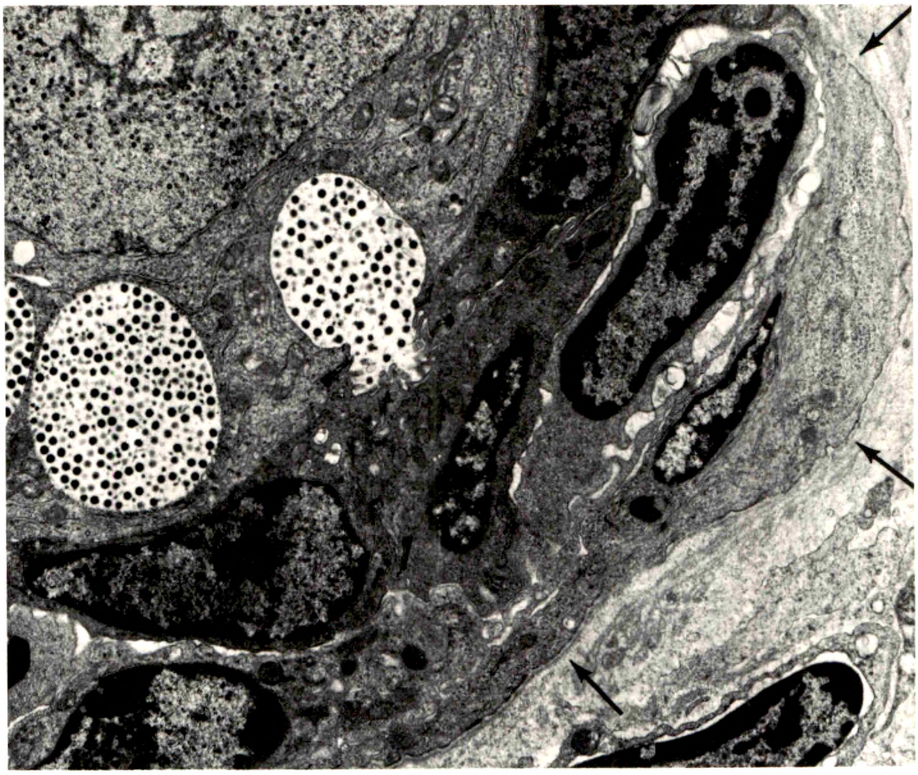

4

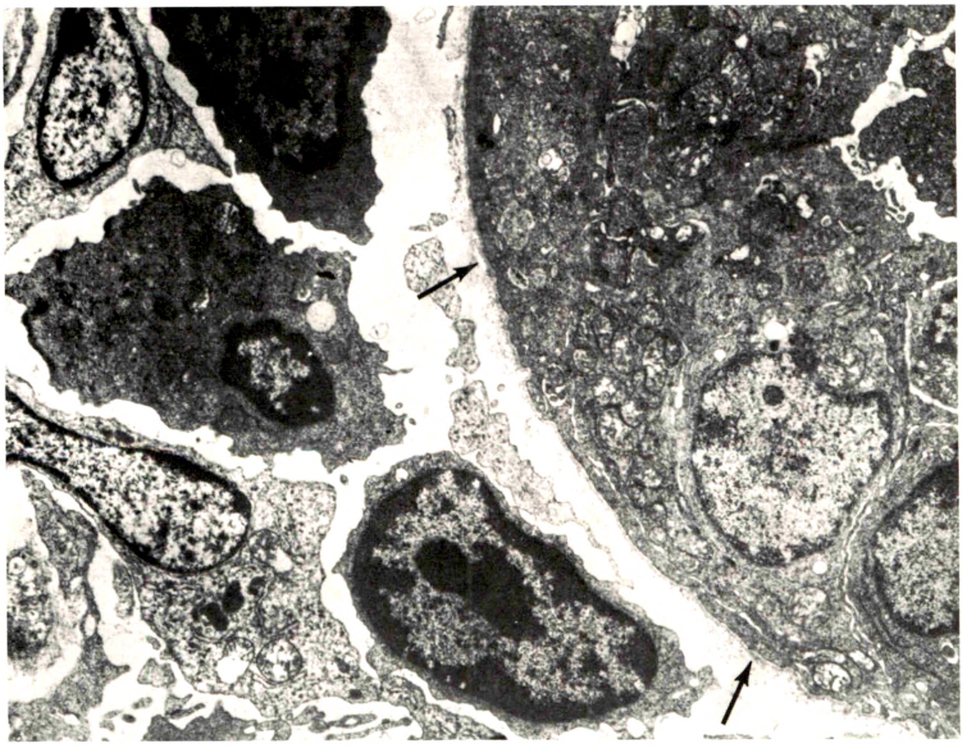

5

6

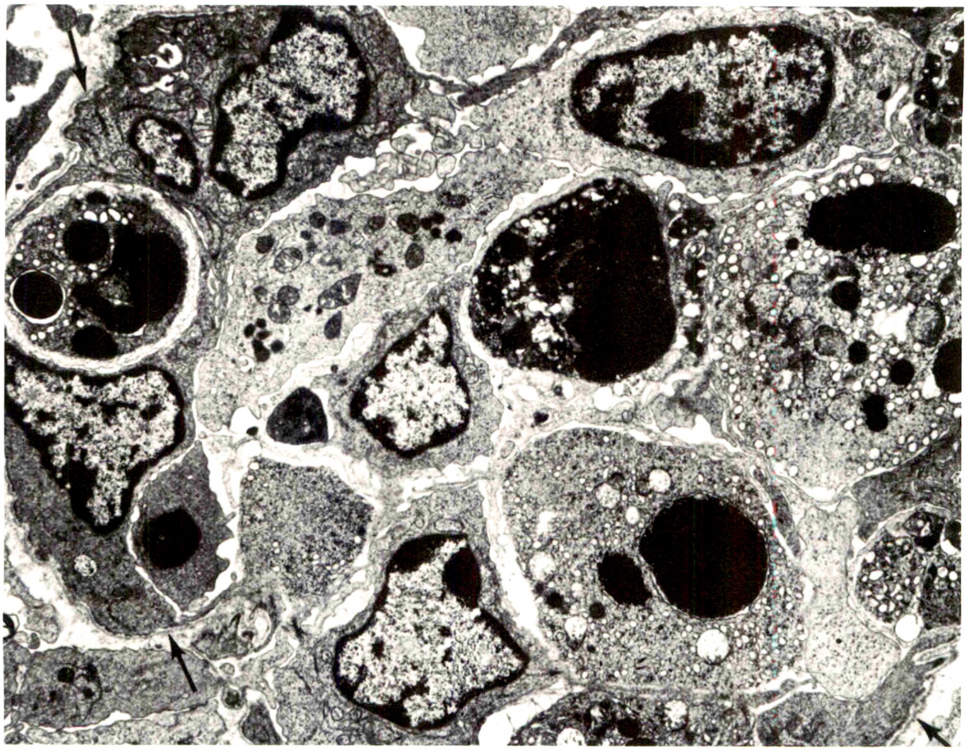

Fig 6—Section through acinus from submaxillary gland of C_3H mouse 34 days after MCMV infection. Many of the acinar cells are undergoing necrosis, characterized by an accumulation of dense osmophilic material within large cytoplasmic vesicles. At this advanced stage of degeneration, it was often difficult to determine which cell had been infected. An intact basal lamina is present around the periphery (*arrows*) (× 4800).

Fig 7—Necrosis of adjacent infected and non-infected acinar cells 34 days post infection. Basal lamina (*arrows*) is intact. Infected cell is recognized by remnants of virus-filled vesicles (*long arrow*) in cytoplasm. Part of a myoepithelial cell is situated between basal lamina and noninfected cell (× 10,600).

Fig 8—C_3H mouse salivary gland 39 days after infection. *Arrows* indicate intact basal lamina. In the center is a myoepithelial cell with its cytoplasm extending toward the acinar lumen. To the left is a degenerating infected cell recognizable by the presence of incomplete virions. To the right is degeneration of a noninfected acinar cell characterized by accumulation of dense osmophilic material. Inflammatory cells are present along the basal lamina outside the acinus (× 6000).

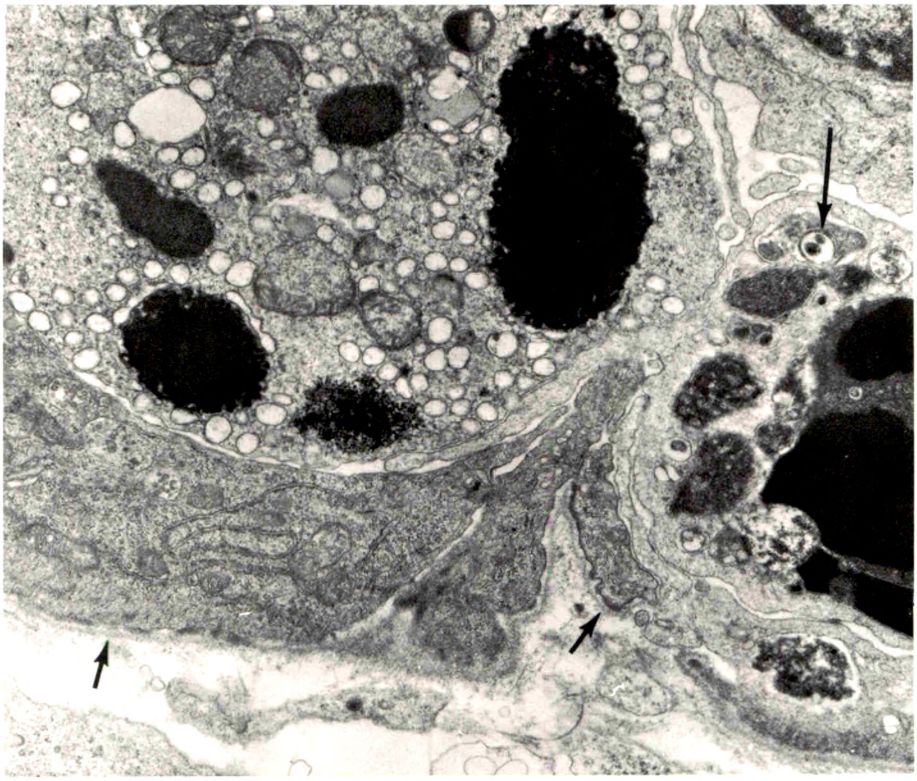

7

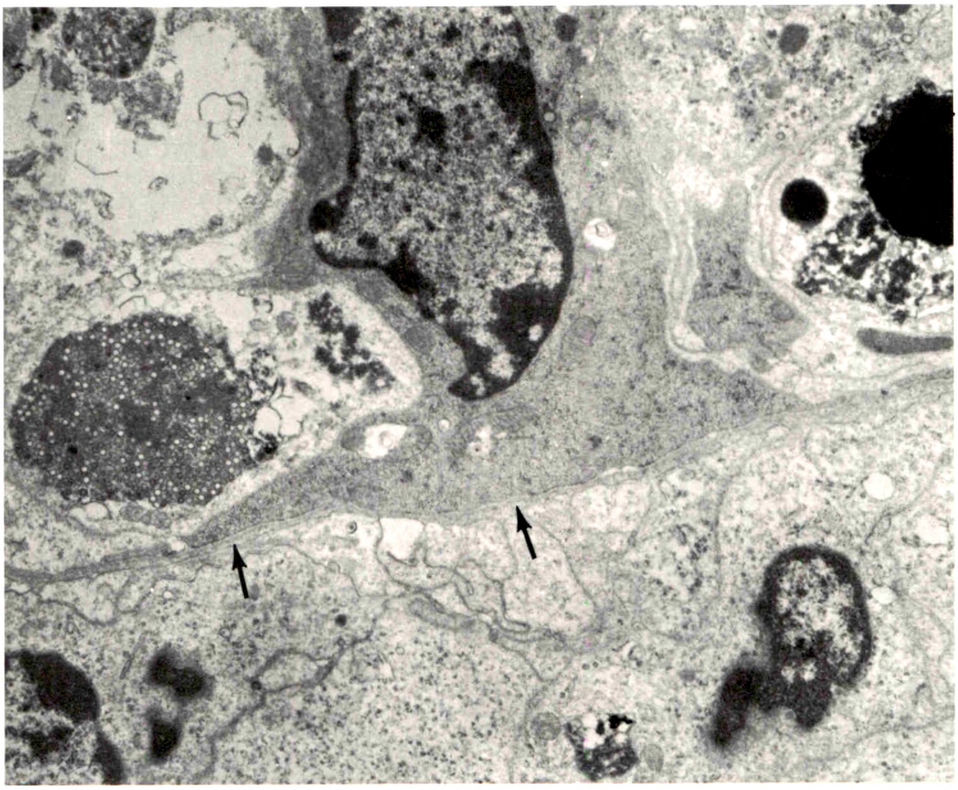

8

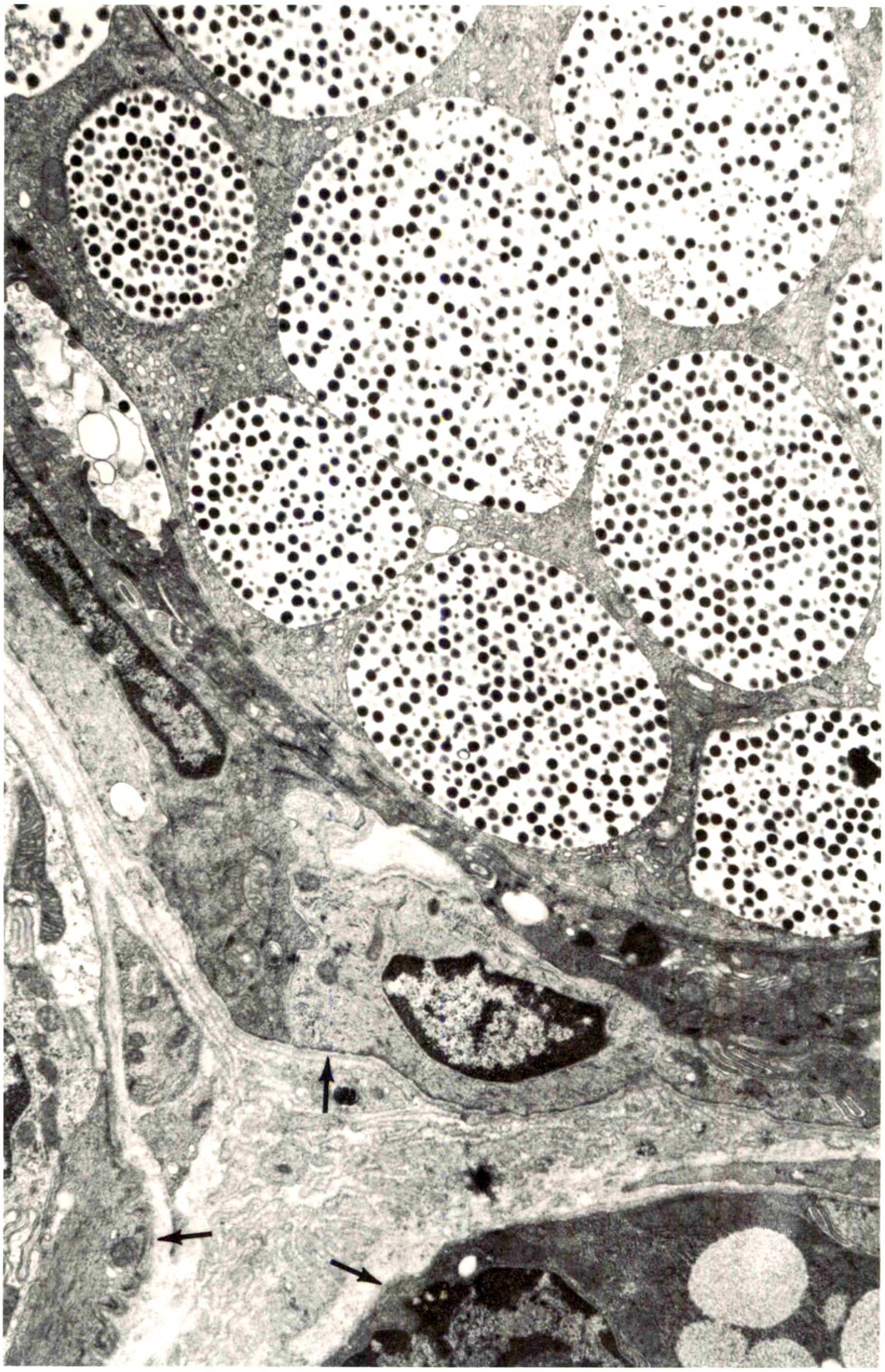

Fig 9—Submaxillary gland from cortisone-conditioned C_3H mouse 28 days after infection. Numerous large vesicles containing mature virions fill cytoplasm of an enlarged cell. There is no evidence of necrosis. Inflammatory cells are not present in the interstitium. *Arrows* indicate basal lamina of two adjacent acini and small duct (× 10,200).

ANIMAL MODEL FOR HUMAN DISEASE

Spina Bifida, Sacral Dysgenesis and Myelocele

Animal Model: Manx Cats

Contributed by: Hyram Kitchen, DVM, PhD, Ronald E. Murray, DVM, and Beverly Y. Cockrell, DVM, PhD, Center for Laboratory Animal Resources, Michigan State University, East Lansing, Mich.

Manx are a clownish breed of cat said to originate on the Isle of Man. Easily distinguishable by a variety of biologic and morphologic characteristics, they are most noted for their absence of a tail. However, a peculiar autosomal dominant trait[1] provides the genetic basis not only for taillessness and the related traits so prized by cat fanciers, but also for a number of associated anomalies. Few people realize that the unique appearance of the Manx actually constitutes the observable, relatively normal end of a spectrum of genetically controlled breed characteristics which include many serious deficiencies and potentially lethal abnormalities.

Biologic Features

Both the "normal" and "abnormal" characteristics express themselves in a wide variety of phenotypes.[2,3] This intraspecies variation is most readily evident with respect to tail length. Common Manx characteristics are disproportionately long hind legs, short back, large round head, round-shaped rump and a distinctive rabbity humpy gait. Manx cats of show quality must be completely tailless in addition to possessing these other traits, but Manx litters generally yield some kittens with normal tails, some with short tails ("stumpies"), and others with a mere remnant of cartilaginous material ("high-riser"), as well as the tailless "rumpies" who completely lack coccygeal vertebrae. The hollow at the base of the backbone in "rumpies" indicates total coccygeal agenesis.

Despite their unusual physique, many Manx cats grow to be successful show animals or delightful pets without signs of any other remarkable disorders. The Manx breeder, however, soon discovers that a considerable percentage of the kittens suffer from severe congenital abnormalities primarily related to spinal lesions. These abnormalities range from fecal and urinary incontinence to a variety of severe spinal lesions—everything from agenesis of the sacrum to agenesis of the coccygeal

---

Publication sponsored by the Registry of Comparative Pathology of the Armed Forces Institute of Pathology and supported by Public Health Service Grant RR 00301 from the Division of Research Resources, US Department of Health, Education and Welfare, under the auspices of Universities Associated for Research and Education in Pathology, Inc.

Published by Medical Department
HARPER & ROW, PUBLISHERS
© 1972 The American Association of Pathologists and Bacteriologists

vertebrae, absence of cauda equina, etc.[4] Such kittens generally must be euthanatized.

James *et al*[4] has reported that the monoplegic Manx cat demonstrates a medial rotation of the metatarsal homologous to the inversion and cavovarus associated with abnormalities of the human foot; this abnormality causes the distinctive hopping gait in affected Manx cats. The severely affected cat can travel quickly in a straight line but tends to fall over when changing direction. Whether the peculiar incoordination of the hind legs is due to the abnormal pelvic posture or to longer than normal length of the hind legs is not known.

Most frequently animals with the coccygeal agenesis but normal sacrum are free from any clinical disability; however, they can show a variety of abnormalities without severe hind-limb paralysis. Three cats who exhibited sacral dysgenesis were found by James *et al*[4] to be either monoplegic or incontinent in the urine or feces, or both. In one case where severe defect of the sacrum was associated with incomplete dorsal laminae (spina bifida), the lower cord of cauda equina was united with the meninges and covered only a subcutaneous fat and skin resembling a myelocele in man.[4] The abnormalities of the sacrum cauda equina explain the incontinence of urine and feces.

These reports have stimulated the development of a colony of Manx cats here at the Center for Laboratory Animal Resources. At the present time, the study has included 6 males and 2 females. Three of the animals have died during this period. Necropsy of these animals was performed. The predominant lesion in the first cat was obstruction of the pelvic urethra. The second cat had a history of urinary and fecal incontinence and was lacking its coccygeal vertebrae. Changes in the terminal urinary and intestinal tracts supposedly resulted from functional or anatomical deficiencies in innervation. The predominant lesion of the third cat was coccygeal agenesis; the spinal cord appeared somewhat shortened, the cauda equinae being found in the midsacral region. The cauda equinae was not fused with the meninges; hence, there was no strong resemblance to myelocele or spina bifida in man. Sections of spinal cord from the sacral, lumbar, thoracic and cervical areas were histiologically normal, and lacked the dorsal cord lesions associated with human dysraphism.

Of the remaining animals, 2 males exhibit no clinical abnormalities; 1 female has the very distinct hopping gait and previously had 3 litters of kittens—cesarean section was necessary with all but 1 litter. Only 2 kittens from the litters lived past 3 months of age. The need for cesarean section was a result of uterine inertia, which may represent lack of normal nerve innervation. One kittten developed severe clinical signs of abdominal distention and urinary and fecal incontinence.

Figure 1 demonstrates one of the more obvious clinical signs, the occurrence of abnormal distention of abdominal cavity and accumulation of fecal material and distinct intestine dilatation. Dysgenesis or sacrococcygeal agenesis is shown in Figure 2.

Comparison with Spina Bifida

Paraplegia and hind limb monoplegia in Manx cats are similar to the clinical syndrome in some cases of human spina bifida occulta. Spina bifida, a cleft in the spine, is a congenital abnormality attributed to the

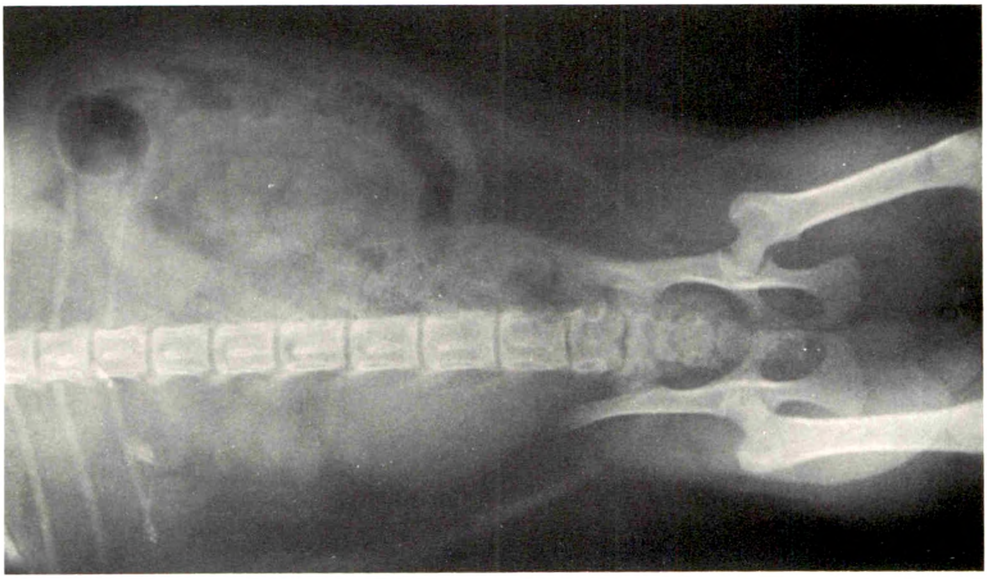

Fig 1—X-ray of a 4-month-old male Manx cat. Note the abnormal distention of the abdominal cavity due to the accumulation of fecal material and intestinal dilation.

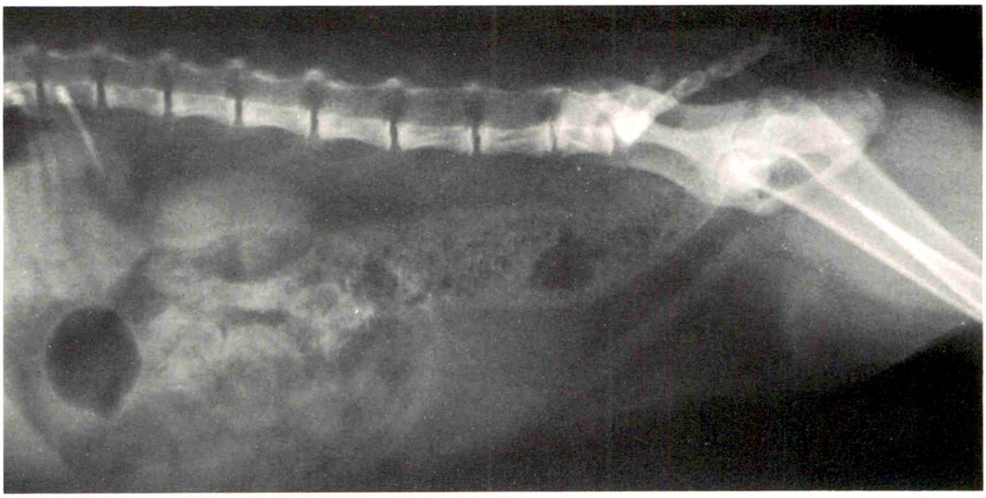

Fig 2—X-ray of a 6-month-old Manx cat. Note the agenesis of the coccygeal bones.

incomplete fusion of the laminae to form the vertebral arches. In man and in cats there may be a steady deterioration after birth; the organism becomes paraplegic or partially disabled and many remain stationary.[5]

Kerruish was the first to describe some of the pathologic characteristics of the Manx cat and compared them with spina bifida in man.[5] The Manx cat would seem to be a particularly valuable animal model not only for the study of spina bifida but also for understanding the variable expression of simple autosomal alleles. Further, there is the possibility of associating these various abnormalities with behavorial characteristics. These possibilities indicate the Manx to be a highly desirable biomedical model which merits further investigation.

Spina bifida and sacrococcygeal agenesis have been described in other cat breeds,[6, 7] as well as in Swiss mice, calves, dogs and sheep.[8, 9] Experimentally induced spina bifida using trypan blue has also been described.[10] The occurrence of spontaneous abnormalities with a predominant high frequency certainly underlines the logical use of the Manx cats for biomedical models.

Availability

Manx cats are uncommon but certainly not rare; breeders can be found in most areas of the United States. The spontaneous lesions, described here, are increased by breeding rumpy phenotypes to rumpy phenotypes.

Acknowledgments

This investigation was supported in part by National Science Foundation Research Grant GB-20947 and National Institutes of Health Grant 5-P06-RR00366-04. The authors gratefully thank Dr. U. V. Mostosky, Professor, Small Animal Surgery and Medicine and Dixie Middleton, x-ray Technician, College of Veterinary Medicine, Michigan State University.

References

1. Todd NB: The inheritance of taillessness in Manx cats. J Hered 52:228–232, 1961
2. Todd NB: The Manx factor in domestic cats. J Hered 55:225–230, 1964
3. Howell JM, Siegel PB: Phenotypic variability of taillessness in Manx cats. J Hered 54:165–169, 1963
4. James CCM, Lassman LP, Tomlinson BE: Spinal anomalies in Manx cats. J Pathol 97(2):269–276, 1969
5. Kerruish DW: The Manx cat and spina bifida. J Cat Genet 1:16–17, 1964
6. Frye FL, McFarland LZ: Spina bifida with rachischisis in a kitten. J Am Vet Med Assoc 146:481–482, 1965
7. Frye FL: Spina bifida occulta with sacro-coccygeal agenesis in a cat. Animal Hosp 3:238–242, 1967
8. Frye FL, McFarland LZ, Enright JB: Sacrococcygeal agenesis in Swiss mice. Cornell Vet 54:487–495, 1964
9. McFarland LZ: Spina bifida with myelomeningocele in a calf. J Am Vet Med Assoc 134:32–34, 1959
10. Gunberg DL: Spina bifida and the Arnold-Chiari malformation in the progeny of trypan blue injected rats. Anat Rec 126:343–359, 1956

The American Journal of PATHOLOGY

is published by the Medical Department of Harper & Row, Publishers, under the auspices of The American Association of Pathologists and Bacteriologists and The American Society for Experimental Pathology, and is edited by a Board appointed by the Councils of the two Societies. It is devoted to the prompt publication of original observations and investigations in the field of pathology and microbiology and is published monthly in four volumes per year.

Information for Authors

ORIGINAL PAPERS will be considered for publication on condition that they are contributed solely to THE AMERICAN JOURNAL OF PATHOLOGY. Address manuscripts to the Editor-in-Chief: THOMAS D. KINNEY, MD, Department of Pathology, Duke University Medical Center, Durham, NC 27706.

MANUSCRIPTS must be typed **double-spaced** (including tables, references, and legends for figures), and all material should be submitted in duplicate. The literature should be summarized as concisely as is consistent with establishing the necessary basis for new material, and original observations should be presented in a clear, well-organized manner. Papers should rarely exceed 20 printed pages. Tables should be planned to suit the page size of THE JOURNAL. Excess tabular matter must be paid for by the contributor.

REFERENCES to the literature should be numbered in the order of citation in the text and should conform to the following style: names of all authors, complete title of article (including subtitle), abbreviated name of periodical (use *Index Medicus* style abbreviations), volume in Arabic numerals, inclusive pagination, and year (*eg*, 14:111–120, 1938). Titles are to be in the original language when they can be reproduced in the English alphabet. Translated titles should be enclosed in square brackets.

ILLUSTRATIONS must be planned to suit the page size of THE JOURNAL (**maximum plate size is 5¼ × 8 inches**) and should be submitted **unmounted**, with figure number, top, and author's name marked lightly on the back in soft pencil. Oversize illustrations should be avoided because handling of these delays publication. To be accepted, illustrations must reach a certain standard of excellence technically, present an attractive appearance, and add significantly to the value of the presentation. Marking lines and letters, if essential, must be kept at least ¼ inch inside all margins. If two or more illustrations are to appear on a page, they should be so trimmed that the edges may be butted and the outer margins squared. The legends for photomicrographs should state the staining method and the degree of magnification. Black and white illustrations will be furnished in moderate numbers. Excess illustrations, when accepted, and the cost of illustrations in color, must be paid for by the contributor.

REPRINTS: An order blank for reprints is sent with the proof.

HE CARD REQUISITION ENTRY SYSTEM WITH POSITIVE PATIENT IDENTIFICATION

TEMPLAPUNCH®

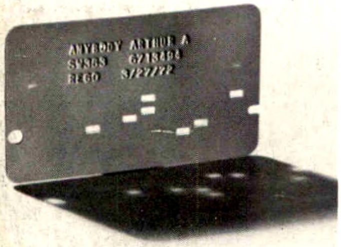

TEMPLAPUNCH® SYSTEM STARTS HERE

t, an ID plate is issued for each
ient. Punched in IBM code is the
ient's unique medical record. Em-
sed is man-readable information
reference to the patient. This
plifies the card requisition sys-
, assures positive patient identi-
tion, and initiates cost savings
ughout the system.

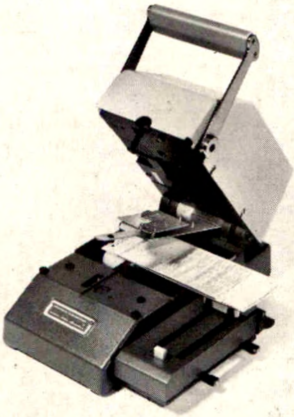

SERVICE REQUEST INITIATION IS SIMPLE—SELF-VERIFYING

ID plate and service request form are positively positioned by the TEMPLAPUNCH. In a single operation the request form is imprinted with the embossed information and punched with patient's unique medical record number and location. Positive patient identification is assured. No chance for patient ID errors to enter the computer.

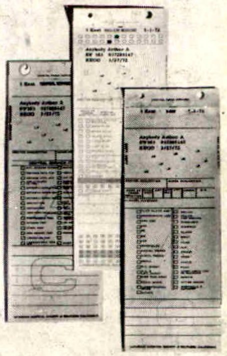

USES COMPUTER COMPATIBLE SERVICE REQUEST FORMS

Laboratory and all hospital service request forms are designed to meet the systems and procedures requirements of the individual departments and the total hospital.

e nurse checks off each item requested on the individual form. The form is then ready for mediate input to your hospital's laboratory and/or business computer via any optical mark ader. The TEMPLAPUNCH system is compatible with all laboratory and business computer stems. Card Requisition Entry is not a problem when you use TEMPLAPUNCH. TEMPLAPUNCH s solved this problem in numerous installations. Why not yours? Write for descriptive brochure.

OURCE INFORMATION SYSTEMS, INC.
OX 3088, SANTA MONICA, CALIFORNIA 90403 • (213) 451-1628

VOLUME 68 • NUMBER 2 / WHOLE NUMBER 363

The American Journal of PATHOLOGY

AUGUST 1972

OFFICIAL PUBLICATION OF

THE AMERICAN ASSOCIATION OF PATHOLOGISTS AND BACTERIOLOGISTS

•

THE AMERICAN SOCIETY FOR EXPERIMENTAL PATHOLOGY

BOARD OF EDITORS

Thomas D. Kinney, *Editor-in-Chief*
Donald B. Hackel, *Associate Editor*

Orville T. Bailey
Frederick F. Becker
Baruj Benacerraf
Kurt Benirschke
Kenneth M. Brinkhous
Joel G. Brunson
John R. Carter
Charles G. Cochrane
John M. Craig
Frank J. Dixon, Jr
John T. Ellis
Frank W. Fitch
Patrick J. Fitzgerald
David G. Freiman
Jack C. Geer
Gabriel Godman
John B. Hazard
Robert H. Heptinstall
Paul Kotin
Averill A. Liebow
Guido Majno
Donald G. McKay
Henry D. Moon
Councilman Morgan
Goetz W. Richter
David T. Rowlands, Jr
Edward A. Smuckler
Leon Sokoloff
Benjamin H. Spargo
Lewis Thomas
Jacinto J. Vazquez
F. Stephen Vogel

Editorial Assistant: Virginia Hotelling

MEDICAL DEPARTMENT • HARPER & ROW, PUBLISHERS

Sigma is pleased to offer

Stat CPK

Creatine Phosphokinase

A carefully standardized
SINGLE or MULTI
DETERMINATION VIAL

in serum or other fluids, at 340mμ
per Sigma Technical Bulletin No. 45-UV

Remarkably simple, convenient and fast!

1. Add water and 0.1 ml serum; "equilibrate".
2. Take Initial Reading.
3. Take Second Reading 5 minutes later.

THAT IS ALL!

Request Sigma Technical Bulletin No. 45-UV, or order:

Stock No. 45-1	Single Assay Vials	10 vials	10 Assays	$11.50
Stock No. 45-5	5 Assay Vials	10 vials	50 Assays	42.50

Includes Air Mail postage to any Destination in the World.

SIGMA CPK PROCEDURES

SIGMA has probably done more developmental work on CPK than any other firm. These studies, plus SIGMA'S unique position as the world's largest producer of Research Biochemicals, has resulted in several extremely dependable methods for almost any instrument. We offer:

No. 661 — Colorimetric procedure. Uses 0.6 ml serum.
ATP + Creatine → ADP + Phosphocreatine + Inorganic Phosphate. Measure the Inorganic Phosphate per Fiske and Subbarow.

With Fiske & Subbarow Reagents			Without Fiske & Subbarow Reagents (Use your own)		
Kit No. 661-PA	25 Assays	$13.00	Kit No. 661-A	25 Assays	$ 6.00
Kit No. 661-PB	100 Assays	32.25	Kit No. 661-B	100 Assays	19.00

No. 520 — Colorimetric procedure. Uses only 0.01 ml Serum.
ADP + Phosphocreatine → ATP + Creatine. Measure the Creatine released by reaction with Diacetyl and Naphthol. Very sensitive.

Kit No. 520 25 Assays $18.75 • Kit No. 520-C 100 Assays $44.75

No. 80-F — Fluorometric procedure. Uses only 0.01 ml serum.
ADP + Phosphocreatine → ATP + Creatine. Measure the fluorescence of the Creatine plus Ninhydrin.

Kit No. 80-F 20 Assays $17.75 • Kit No. 80F-C 100 Assays $49.50

No. 40-UV — Kinetic Ultraviolet procedure at 340 mμ. Uses 0.2 ml serum.
ATP + Creatine → ADP + Phosphocreatine. Couple this with Pyruvate Kinase, LDH and DPNH, and measure the rate of oxidation of the DPNH by the decrease in OD_{340}.

Kit No. 40-A 15 Assays $25.00 • Kit No. 40-B 45 Assays $70.00 • Kit No. 40-C 90 Assays $138.50

No. 45-UV — Stat Ultraviolet procedure at 340mμ.
All reagents pre-standardized into one Single or Multi-Assay vial. Simply add water and 0.1 ml serum; equilibrate. Take initial reading. Read OD (or %T) after only 5 minutes. Remarkably simple, convenient and **fast.**

Stock No. 45-1	Single Assay Vials	10 vials	10 Assays	$11.50
Stock No. 45-5	5 Assay Vials	10 vials	50 Assays	42.50

No. 910 — Automated Colorimetric procedure.
An automated version of our No. 520 procedure. Although this is probably the most accurate automatic procedure available to date, we are now field-testing our improved No. 911 procedure which eliminates the α-Naphthol reagent and substitutes the much more stable Orcinol. Prices are the same as the No. 910. Inquiries or orders are invited. Satisfaction is guaranteed, of course.

Kit No. 910-A 300 Assays $104.00 • Kit No. 910-B 1500 Assays $381.50

Also available: **CPK Enzyme Reference.** A carefully assayed preparation, which may be used as control or reference for various CPK procedures offered by Sigma. Available in two sizes for your convenience. Activity: 30-50 Sigma units per ml when reconstituted with water.

CPK-1 1 ml size vial 10 vials $8.75 • CPK-2 2 ml size vial 10 vials $12.50

We pay all normal shipping charges on these reagents — anywhere in the World.
Free Sigma Technical Bulletins for the above methods are available to eligible Laboratories.

It's a pleasure doing business with Sigma

ORDER DIRECT — TELEPHONE **COLLECT** from **ANYWHERE** in the **WORLD**
Day, **Station to Station, 314-771-5750** (Including Saturday and Sunday until 1 P.M.)
Night, **Person to Person,** Dan Broida, **314-993-6418**
TWX [Teletype] Day or Night: COLLECT 910-761-0593
TELEGRAM: SIGMACHEM, Saint Louis, Missouri

The Research Laboratories of
SIGMA CHEMICAL COMPANY
P.O. BOX 14508 • SAINT LOUIS, MISSOURI 63178 U.S.A.
MANUFACTURERS OF THE FINEST BIOCHEMICALS AVAILABLE

Distributed through:
SIGMA LONDON Chem. Co. Ltd. • 12, Lettice St., London, S.W.6., England • Telephone: 01-736-5823 (Reverse Charges)
SIGMA ISRAEL Chem. Co. Ltd. • 28 Kaf-Gimel St., Givataim, Israel • Telephone: 03 760654 (Reverse Charges)

A Closer Look At Thyroid Dysfunction With Thyroid Antibody Tests

Diagnostic tests for determination of thyroid autoantibodies can throw a new illumination on the nature of the patient's disease. The refined differential diagnosis afforded may provide additional insight for treatment and management.

Clinical applications include:

differential diagnosis between colloid goiter and Hashimoto's thyroiditis; differentiation between Hashimoto's disease and thyrotoxicosis; detection of mild thyroid disease in patients with pernicious anemia; investigation of other possible autoimmune disorders.

A complete thyroid panel should include thyroglobulin hemagglutination and complement fixation tests. We know of no other company which provides these materials.

We would like to fill your order, or would be happy to send information to your laboratory.

Wellcome Reagents Division
Wellcome
Burroughs Wellcome Co.
Research Triangle Park
North Carolina 27709

Quality Products of a Specialty Nature from: **Wellcome Reagents Division**
Wellcome
Burroughs Wellcome Co.
Research Triangle Park
North Carolina 27709

Please ship:

☐ KT 02
Thyroglobulin
Hemagglutination test kit
(50 tests) $27.50

☐ MR 22
Thyroid Complement
Fixing Antigen
(dried 1 ml) $5.75

Send information to:

Name of laboratory

Name of laboratory contact or purchaser

Title

Address

City State Zip code

Phone

An Important Contribution To Diagnosis In Certain Grave Conditions

1. Obstetrical Complications

abruptio placentae/eclampsia/"dead fetus" syndrome

2. Venous Thrombosis/ Pulmonary Embolism

3. Renal and Hepatic Disease

The Wellcome FDP Kit for assay of fibrinogen and its degradation products

Not all clinicians are aware of this diagnostic resource which can be of value also in myocardial infarction, coronary thrombosis, gram-negative septicemia, malignancies and other serious conditions.

The FDP Kit from Wellcome Reagents is complete; it provides a simplified technique for a convenient and sensitive assay of fibrinogen degradation products.

We know of no other source for this test.

Wellcome Reagents Division
Wellcome
Burroughs Wellcome Co
Research Triangle Park
North Carolina 27709

Quality Products of a Specialty Nature from: **Wellcome Reagents Division**
Wellcome
Burroughs Wellcome Co.
Research Triangle Park
North Carolina 27709

Please fill out coupon to order. Please also indicate if you would like a supply of reprints to provide for interested clinicians.

Please send________FDP Kits (14 tests per kit) at $32.50 per kit.

________Also, please send a supply of background reprints for clinicians.

Name ________ Title ________

Laboratory ________

Address ________

City ________ State ________ Zip Code ________

Phone ________

THE YEAR OF PATHOLOGY
1971
1972

The American Journal of PATHOLOGY

AUGUST 1972 • Volume 68, Number 2

CONTENTS

207 Presentation of The Gold Headed Cane to Esmond R. Long
Robert E. Stowell

213 Experimental Papillary Necrosis of the Kidney. II. Electron Microscopic and Histochemical Studies
G. S. Hill, R. G. Wyllie, M. Miller and R. H. Heptinstall

235 Experimental Papillary Necrosis of the Kidney. III. Effects of Reserpine and Other Pharmacologic Agents on the Lesion
R. G. Wyllie, G. S. Hill, G. Murray, P. W. Ramsden and R. H. Heptinstall

255 Lysosome and Phagosome Stability in Lethal Cell Injury: Morphologic Tracer Studies in Cell Injury Due to Inhibition of Energy Metabolism, Immune Cytolysis and Photosensitization
Hal K. Hawkins, Jan L. E. Ericsson, Peter Biberfeld and Benjamin F. Trump

289 Degranulation of Discoid Platelets
James G. White and Richard D. Estensen

303 Ultrastructural Characteristics of Freeze-Dried Human Blood Platelets
Richard B. Davis

317 Alterations in Cell Proliferation in Mouse Lung Following Urethane Exposure. III. Effects of Chronic Exposure on Type 2 Alveolar Epithelial Cell
Shirley L. Kauffman

327 *In Vivo* Quantitation of Local Anesthetic Suppression of Leukocyte Adherence
D. B. Giddon and J. Lindhe

339 Glomerulonephritis Associated With Sarcoidosis
Ralph C. McCoy and C. Craig Tisher

359 Cell Proliferation in Rat Kidneys After Prolonged Treatment With Lead
David D. Choie and Goetz W. Richter

371 Amyloidogenesis in Healing Wound: Electron Microscopic Studies of Biopsied Wounds in Macular Amyloidosis
Ken Hashimoto and Martin H. Brownstein

391 Chemical and Histochemical Studies of Glomerular Sialoprotein in Nephrotoxic Nephritis in Rats
Jane Chiu and Keith N. Drummond

407 Mucous Hypersecretion Induced in Isolated Mucociliated Epithelial Cells by a Factor in Heated Serum
B. G. Bang and F. B. Bang

423 The Variable Prevalence of Junctional-Complex-Associated Bodies in the Human Sweat Gland
S. S. Spicer, B. J. Martin and J. P. Reynolds

441 **Animal Model for Human Disease:** Spontaneous and Induced Amyloidosis
Alan S. Cohen and Tsuranobu Shirahama

© 1972 by The American Association of Pathologists and Bacteriologists

The seal commemorates The Year of Pathology, being celebrated from October 1971 to October 1972 by the major national pathology societies. Special educational events will emphasize the expanding role of pathology and the medical laboratory in modern health care.

Medical Department • HARPER & ROW, PUBLISHERS

The American Journal of PATHOLOGY

GENERAL INFORMATION

Editorial Communications: All correspondence concerning editorial matters should be addressed to the Editor-in-Chief, DR. THOMAS D. KINNEY, Department of Pathology, Duke University Medical Center, Durham, N.C. 27706.

Business Communications: All subscriptions and advertising inquiries should be addressed to: MEDICAL DEPARTMENT, HARPER & ROW, PUBLISHERS, 2350 Virginia Ave, Hagerstown, Md. 21740.

Rates: THE AMERICAN JOURNAL OF PATHOLOGY is issued monthly, four volumes per year. Regular (individual) subscriptions: $27.50 per year in the U.S. and Possessions; $30.00 per year in Canada and countries of the Pan-American Postal Union; and $31.00 elsewhere. Special rate for Interns and Residents: $16.00 per year ($1.50 extra postage in Canada and countries of the Pan-American Postal Union; $2.50 extra postage elsewhere). Regular (individual) subscriptions and Resident and Intern subscriptions must be in the names of, and billed to, individuals. Institutional subscriptions, available to all libraries, schools, clinics, and hospitals, to all government agencies, local or national, and to all private or public institutions and organizations: $35.00 per year in the U.S. and Possessions; $37.50 per year in Canada and countries of the Pan-American Postal Union; $38.50 per year elsewhere. All subscriptions are payable in advance. Single copies, when available, $4.00.

Back Issues: Single issues and complete volumes of THE JOURNAL published prior to 1961 may be purchased from Walter J. Johnson, Inc., 111 Fifth Ave., New York, N.Y. 10003.

INDEX TO ADVERTISERS

Amersham/Searle Corporation	14, 15
Dow Chemical Company, The	10, 11
Harper & Row, Publishers	6, 8, 12, 13
Leitz, Inc., E.	5
Ortho Diagnostics	16
Sigma Chemical Company	2nd Cover
Unitron Instrument Company	9
Wellcome Reagents Division	1, 2
Zeiss, Inc., Carl	4th Cover

MOVING?

To avoid interruption in your receipt of this Journal, we need to know your new address—six weeks in advance.

When writing us, be sure to type or print clearly your name and your new address—complete with zip code. It is *essential* that you also list your old address.

IMPORTANT: We publish a number of medical and scientific periodicals. Therefore, please be sure to give the name of THIS Journal when you write us.

Thank you for cooperating!

MEDICAL DEPARTMENT
Harper & Row, Publishers, Inc.
2350 Virginia Ave,
Hagerstown, Md. 21740.

(see page 7)

Published monthly by the Medical Department, Harper & Row, Publishers, Inc., 2350 Virginia Ave., Hagerstown, Md. 21740, and at 2901 Byrdhill Road, Richmond, Va. 23205. Second Class Postage paid at Hagerstown, Md., and additional mailing offices. Regular (individual) Rates: $27.50 per year in U.S. and Possessions, $30.00 in Canada and Pan-American Postal Union; and $31.00 elsewhere. Special Rates: Interns and Residents, $16.00 per year ($1.50 extra postage in Canada and countries of Pan-American Postal Union; $2.50 elsewhere). Institutional subscriptions; $35.00 per year in U.S. and Possessions, $37.50 per year in Canada and Pan-American Postal Unions; $38.50 elsewhere. Single copies, $4.00. Printed in U.S.A.

THE GENERATION LINK

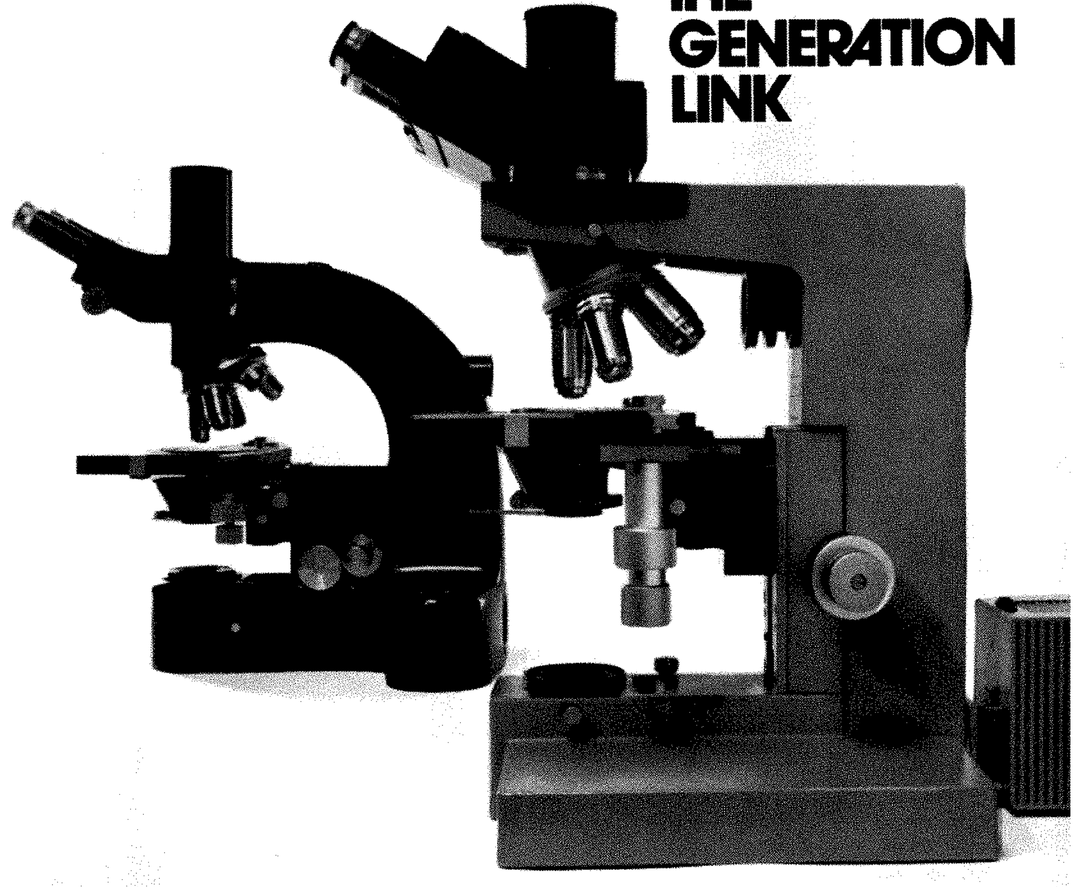

ORTHOLUX II

The introduction of the Leitz® Ortholux 35 years ago started a revolution in microscope design. Leitz scientists working in close rapport with every discipline of the scientific community developed a microscope so appreciably ahead of its time that new standards were set for the entire industry. Standards often copied but never matched.

Ortholux microscopes helped open exciting new areas of scientific inquiry. Areas that grew in complexity and sophistication to such proportions that a new instrument, as revolutionary in 1972 as was the original Ortholux in 1937, was clearly indicated. In tribute to its predecessor, we are calling our new microscope the Ortholux II.

The clean-cut modern lines, a new series of Plan Apochromatic objectives, new, more powerful light sources, a nosepiece that keeps conveniently out of the way, a mechanical perfection of optimum smoothness, an adaptability to a full assortment of modern accessories created for specific needs, all separate this microscope from any competition.

Yes, we are somewhat sorry to see the original Ortholux go, but the reputation it built and the trends it set are being reflected and magnified in the "new generation" Ortholux II, an instrument beyond comparison.

Please write for our detailed brochure describing this truly modern microscope. 125672

Leitz® E. Leitz, Inc.,
Leica® Rockleigh, N.J. 07647

Announcing for 1972!

infectious diseases

With over 80 contributors, edited by Dr. Paul D. Hoeprich, this major reference work considers diseases caused by viruses, chlamydia, rickettsia, mycoplasmas, bacteria, spirochetes, protozoa, helminths and some ectoparasites. Each disease is discussed as a discrete clinical entity and is presented from the point of view of the organ-system involved thus affording to its reader a clinical and practical approach to diagnosis and treatment. Epidemiology and pathogenesis are emphasized throughout as they are keys to understanding the interactions of host and parasite. With some 300 illustrations to complement the text, *this book offers a completeness previously unavailable in one volume!*

Advance orders now accepted!

HARPER & ROW, Publishers, Inc.
Medical Department Mail Order Dept.
2350 Virginia Avenue
Hagerstown, Maryland 21740

☐ Please send me *on approval,* when it is published:

INFECTIOUS DISEASES

Name ....
Address ....
City .... State .... Zip AJP-8

Professional Opportunities

PHYSICIAN WANTED

WANTED—PATHOLOGIST QUALIFIED TO assume full and sole responsibility in clinical and anatomic pathology for a small but enlarging department. Early partnership. Substantial fringe benefits with excellent noncontributory retirement program. Write or call Sam Packer, M.D., Medical Director, 11717 Euclid Avenue, Cleveland, Ohio 44106. Area Code 216, 795-4400.

CLASSIFIED ADVERTISING INFORMATION

RATES:

Non Display:	**1 Time**	**3 Times**	**6 Times or more**
20 words or less	$19.00	$16.00	$14.00
Each additional word	.50	.50	.50

Box Service—$2.00—First insertion only

Classified Display:	**1 Time**	**3 Times**	**6 Times or more**
	$35.00 per inch	$30.00 per inch	$25.00 per inch

Minimum Space—One (1) column inch

SEND ALL COPY,
AND BOX NUMBER INQUIRIES TO:

THE AMERICAN JOURNAL OF PATHOLOGY

Classified Dept.
131 Mineola Blvd.
Mineola, N. Y. 11501
(516) PI 6-0092

CHANGING YOUR ADDRESS?

In order to receive your journal without interruption, please complete this Change of Address notice and forward to the Publisher, 60 days in advance, if possible.

Old Address: (PLEASE PRINT)

NAME

STREET

CITY

STATE (or Country)

ZIP CODE

New Address: (PLEASE PRINT)

NAME

STREET

CITY

STATE (or Country)

ZIP CODE

Date New Address Effective:

Name of Journal:

NEW ADDRESS—MEDICAL DEPARTMENT

Harper & Row, Publishers, Inc.
Medical Department
2350 Virginia Avenue
Hagerstown, Maryland 21740

DERMAL PATHOLOGY

This new work presents current concepts of dermal pathology including related embryology, anatomy, histology, electron microscopy and histochemistry. The highly illustrated text is divided into five sections, with the first section providing basic information and defining the special language of dermal pathology. The other four sections consist of: inflammatory dermatoses; granulomatous dermatoses; nevi and neoplasms; and reticuloendothelial and alternative dermatoses.

The diseases are arranged according to histopathologic features, with disorders presenting similar histopathologic changes grouped together. This approach stresses the differential diagnosis and emphasizes the differentiating features between diseases. The discussion of each disease includes a brief description of gross pathology or clinical morphology, histopathologic characteristics, pertinent histochemistry, the differential diagnosis, and a short clinical description. This book should enable the reader to improve his ability to diagnose skin lesions and to understand the pathogenesis of the diseases discussed.

With 17 Contributors. Edited by **James H. Graham, M.D.,** Professor of Medicine (Dermatology), Department of Medicine; Chairman, Division of Dermatology; Professor of Pathology, Department of Pathology; and Director, Section of Dermal Pathology, University of California, Irvin; **Waine C. Johnson, M.D.,** Professor of Dermatology, Department of Dermatology; Associate Professor of Pathology, Department of Pathology, Temple University School of Medicine; Director of Laboratories, the Skin and Cancer Hospital of Philadelphia, Philadelphia; and **Elson B. Helwig, MD.,** Chief, Department of Pathology and Branch of Dermal Pathology, Armed Forces Institute of Pathology, Washington, D.C.

1,155 Illustrations, 9 in color

Available in September. Advance orders now accepted.

HARPER & ROW, PUBLISHERS *Medical Department*
Mail Order Department, 2350 Virginia Avenue, Hagerstown, Maryland 21740
When published, please send me on approval: AJP-8
GRAHAM, JOHNSON & HELWIG: Dermal Pathology .... About $45.00
NAME ______________________________
____
ADDRESS ______________________________
____
CITY ______________ STATE ______________ ZIP __________

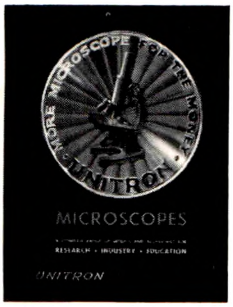
MORE MICROSCOPE FOR THE MONEY
UNITRON
MICROSCOPES
UNITRON

FREE MICROSCOPE BUYING GUIDE

Shown here in miniature are just some of the informative brochures which comprise the UNITRON Catalog . . . your buying guide to quality microscopes at prices within your budget. Whether your application is routine laboratory analysis, advanced biological research, or industrial quality control, you will find the instrument you need in UNITRON's complete line.

A UNITRON MICROSCOPE CATALOG is Yours for the Asking.

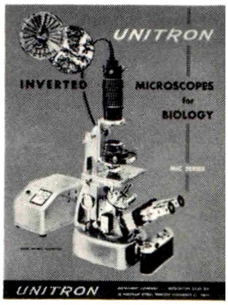
UNITRON
INVERTED MICROSCOPES for BIOLOGY
UNITRON

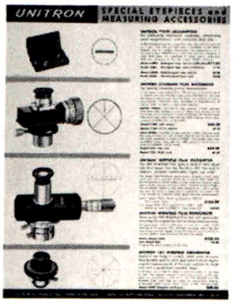
UNITRON
SPECIAL EYEPIECES and MEASURING ACCESSORIES

UNITRON
LABORATORY and MEDICAL
A Complete Line Offering ...

UNITRON
PHASE and BRIGHTFIELD CAMERA MICROSCOPES for BIOLOGICAL RESEARCH
New Series N

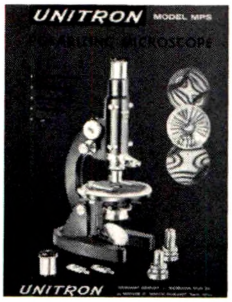
UNITRON MODEL MPS
POLARIZING MICROSCOPE
UNITRON

UNITRON
UNIVERSAL MEASURING MICROSCOPE

TRY ANY UNITRON MICROSCOPE FREE FOR 10 DAYS

A salesman's demonstration gives you only about 30 minutes to examine a microscope, hardly the best conditions for a critical appraisal. But UNITRON's Free 10 Day Trial gives you the opportunity to evaluate any model in your own laboratory and prove its value in your own application before you decide to purchase. See for yourself, as have thousands of other buyers, why . . .

UNITRON Means More Microscope for the Money.

UNITRON
PHASE MICROSCOPES

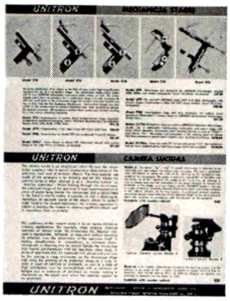
UNITRON
MECHANICAL STAGES
UNITRON
CAMERA LUCIDAS
UNITRON

UNITRON
STEREOSCOPIC MICROSCOPES
3-D, WIDEFIELD BINOCULAR MODELS
UNITRON

UNITRON
Photomicrography Set
UNITRON

UNITRON
STEREOSCOPIC MICROSCOPES
3-D, WIDEFIELD BINOCULAR MODELS
UNITRON

UNITRON
STEREOSCOPIC MICROSCOPES
3-D, WIDEFIELD BINOCULAR MODELS
UNITRON

UNITRON
METALLURGICAL MICROSCOPES
UNITRON

Please send UNITRON's Microscope Catalog No. U-16

Name ____________________

Company ____________________

Address ____________________

City ____________ State ____________ Zip ____________

UNITRON
INSTRUMENT COMPANY

MICROSCOPE SALES DIVISION
66 NEEDHAM STREET
NEWTON HIGHLANDS
MASSACHUSETTS 02161

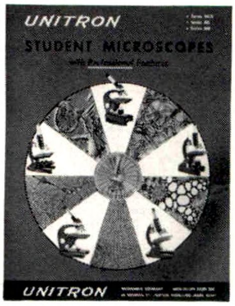
UNITRON
STUDENT MICROSCOPES
UNITRON

To protect her next baby…

Gamulin® Rh Rh$_0$(D) immune globulin (human)
...complete with a disposable syringe
in a compact, space-saving package.

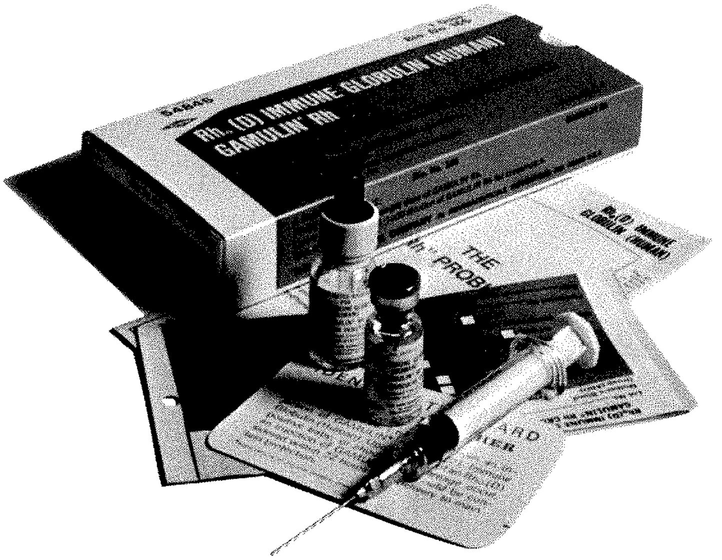

As a major producer of blood fractions, Dow now brings you a new source for Rh$_0$(D) immune globulin to protect the Rh negative mother's next baby from probability of hemolytic disease.

Studies to demonstrate its safety and effectiveness show that Gamulin Rh is effective in suppressing the production of Rh$_0$(D) antibodies.

And it comes in a space-saving, compact package that includes a vial, disposable syringe, lay literature, patient laboratory form, ID card, package insert and a crossmatch vial.

DESCRIPTION: GAMULIN Rh, Rh$_0$(D) Immune Globulin (Human), is a sterile concentrated solution of gamma globulin derived from blood of human donors known to have antibodies to Rh$_0$(D). It is standardized to contain 10.0 to 18.0 percent globulins with a level of antibody to Rh$_0$(D) equal to or greater than that of the NIH Reference Rh$_0$(D) Immune Globulin (Human). The final product contains 0.2 to 0.3 molar glycine as a stabilizer and 1:10,000 thimerosal as a preservative.

INDICATIONS: GAMULIN Rh suppresses the immune response of nonsensitized Rh$_0$(D) negative mothers following Rh incompatible pregnancies. The criteria for an Rh incompatible pregnancy are: That the mother shall be Rh$_0$(D) negative, D^u negative; and the infant shall be Rh$_0$(D) positive or D^u positive.

CONTRAINDICATIONS: Gamulin Rh must not be given to the infant. Gamulin Rh also should not be administered to an Rh$_0$(D) positive or D^u positive individual, to a recipient of an Rh$_0$(D) positive blood transfusion, or to an Rh$_0$(D) negative mother previously sensitized by an Rh incompatible pregnancy. Do not give intravenously.

PRECAUTIONS AND REACTIONS: It is essential that certain diagnostic and laboratory criteria be met before administering this product. (See package literature.) An occasional patient has shown a systemic reaction manifested by a low grade fever. Allergic reactions, although not expected, could occur.

ADMINISTRATION: Consult package insert for detailed instructions.

This product must be administered within 72 hours postpartum.

Gamulin® Rh
Rh$_0$(D) immune globulin (human)

DOW

THE DOW CHEMICAL COMPANY
Rx Pharmaceuticals
Indianapolis

Laboratory

it's brand new now...
and
for years to come,
it will stay that way...

Medicine

Editor: George J. Race, M.D., M.S.P.H., Ph.D., Pathologist-in-Chief and Director of Laboratories, Baylor University Medical Center, Dallas, Texas.

Associate Editors: Clinical Pathology—Samih Y. Alami, M.D., Ph.D. Hematology—Eugene P. Frenkel, M.D. Chemistry—Robert J. Speer, Ph.D., Harold H. Varon, M.D., and Joel E. Young, Ph.D. Microbiology—Ralph Tompsett, M.D. With 100 Contributors.

In Three Volumes. Here is a new exhaustive coverage presented for the first time as a loose-leaf reference. The dynamic loose-leaf concept means that your three volumes will always be new and updated through the ANNUAL SERVICE. *Volume 1* is entirely devoted to Clinical Chemistry, including the most modern automated techniques in use. *Volume 2* concerns Hematology, Blood Banking, Medical Microbiology, Virology, Serology, and Immunology. *Volume 3* covers Body Fluids including Urine, Cytology and Cytogenetics, Special Techniques (with modern methods and approaches to forensic pathology), and Laboratory Management and Function. A separate annually revised index is included. *For all the future information coming out in the various fields covered in these volumes, it is a worthwhile investment for knowledge and practice.*

ANNUAL SERVICE includes:

"New pages for old." Partially or completely rewritten monographs, addenda and chapters on new subjects supplied annually along with a completely revised index.

HARPER & ROW, Publishers, Inc. *Medical Department*
2350 Virginia Avenue Hagerstown, Maryland 21740

☐ Please send more information on LABORATORY MEDICINE

LABORATORY MEDICINE (3 vols. & 1st yr. Annual Service): About $200.00.

About $30.00 a year thereafter for Annual Service. (Terms Available)

☐ Bill me @ full price. ☐ Bill me @ $______a month *(minimum $10.00 a month)*

Name . . . .

Address . . . .

City . . . . State . . . . Zip AJP-8

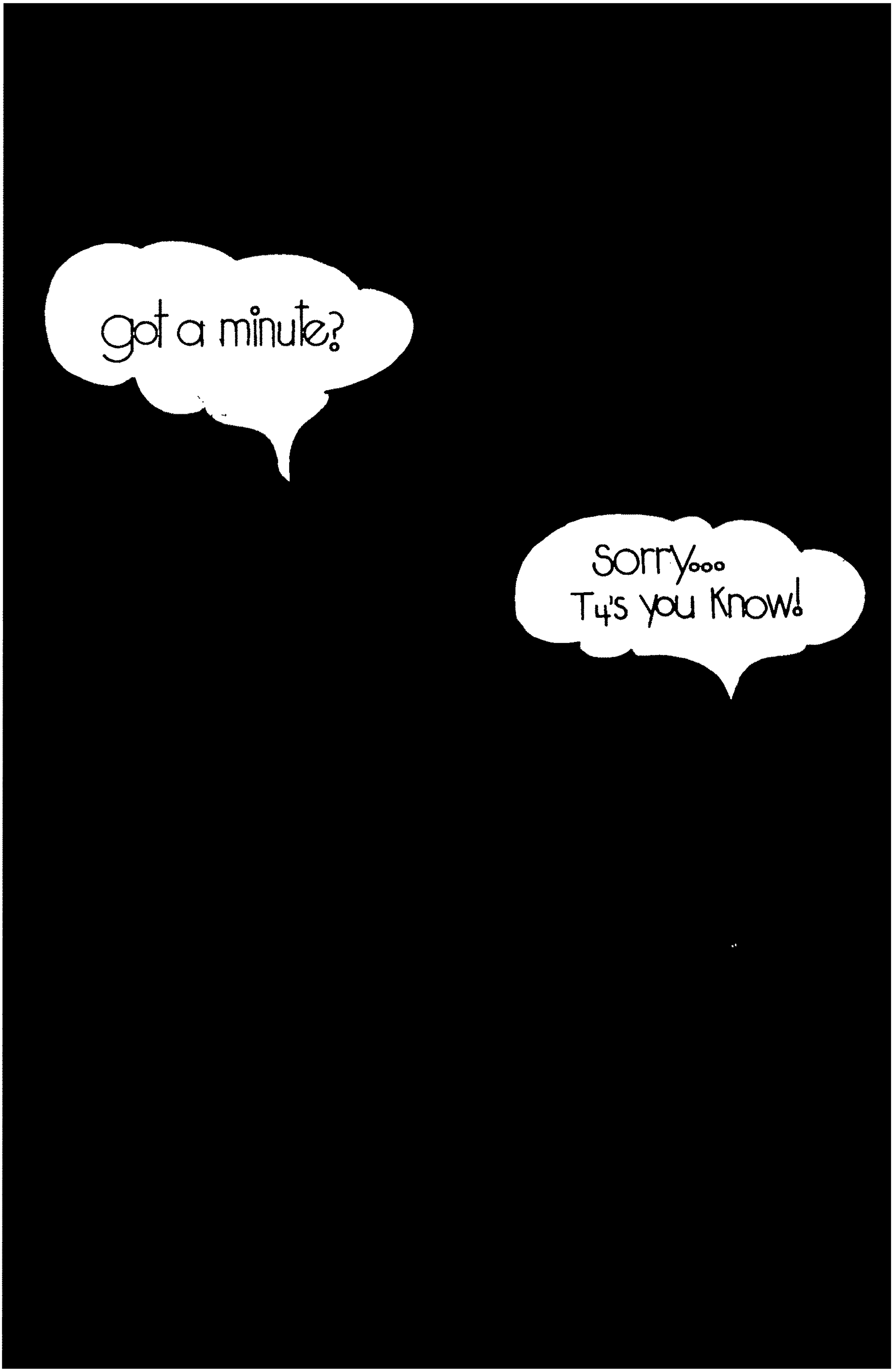
got a minute?
Sorry...
T4's you Know!

Now...T_3/T_4 Tests that don't mind interruptions.

(You won't have to control the temperature either.)

Thyopac-3
Thyopac-4

In vitro thyroid assays usually involve sampling a reaction **before** equilibrium is reached. Other T_3 and T_4 tests are of the "rate" reaction type and, therefore, control of both temperature and time is necessary, but with Thyopac™-3, T_3 uptake kit and Thyopac -4, T_4 assay kit, the reactions rapidly reach equilibrium. Since Thyopac-3 and Thyopac-4 are performed **at equilibrium,** exact control of time and temperature variables are not required.

Consider these advantages:

THYOPAC-4, T_4 assay kit
Independent of time
Independent of temperature
Small serum sample required (0.5 ml)
No extraction efficiency corrections
Speed (only 30 minutes mixing time)
Evaporation not required
No washing required

THYOPAC-3, T_3 uptake kit
Independent of time
Independent of temperature
Small serum sample required (0.1 ml)
Speed (only 10 minutes mixing time)
No washing required

Because Thyopac-3 and Thyopac-4 are performed at equilibrium, you can expect precise separation of normal/abnormal T_3/T_4 levels.

The combination of Thyopac-3 and Thyopac-4 into the Free Thyopac Index helps eliminate complicating factors such as raised or lowered TBG levels.

our specific activity is service

Amersham/Searle
AMERSHAM / SEARLE CORPORATION:
An Activity of G. D. Searle & Co. and the Radiochemical Centre
2636 S. Clearbrook Drive
Arlington Heights, Illinois 60005
Telephone: 312-593-6300—Telex: 28-2452

No TIME FOR VARIABLES

Your day is too busy...and you have too many important responsibilities to be concerned with variations in centrifugation and incubation time...or number of drops per test. ORTHO Reagents and Procedures consider both the test and the tester. They eliminate the variables with one standard procedure for ABO Grouping, Rh Typing, Screening and Crossmatching. They consistently ensure highly avid reactions. They complement your training and skills ...the key to successful transfusion therapy.

ORTHO DIAGNOSTICS
Raritan, New Jersey 08869

The Standard of Excellence in Laboratory Medicine

©O.D. 1971

GOLD
HEADED
CANE
AWARD

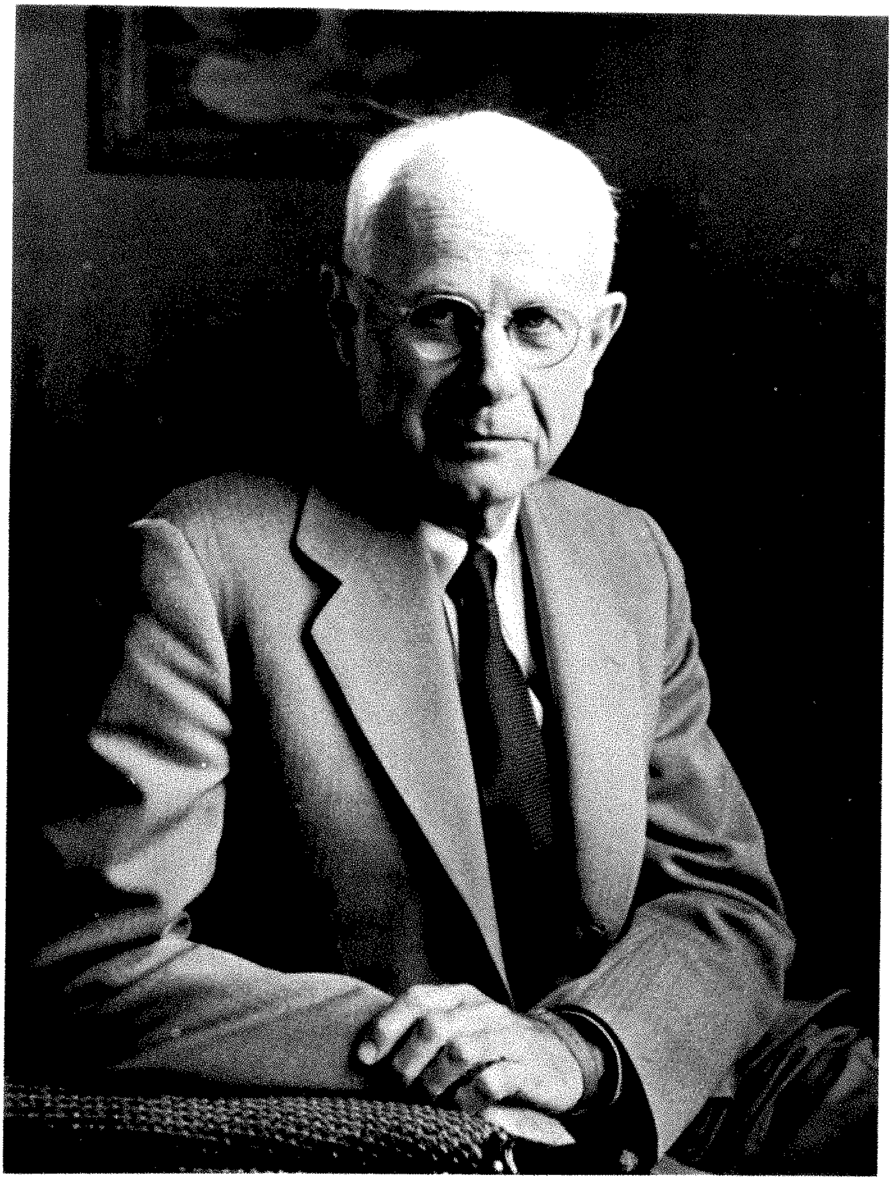

ESMOND R. LONG, MD

The photograph was taken by William Feldman and is part of the collection he presented to the National Library of Medicine.

The American Journal of
PATHOLOGY

August 1972 • Volume 68, Number 2

Presentation of The Gold Headed Cane to Esmond R. Long

March 8, 1971

For more than 50 years the Gold-Headed Cane of this Association has been the highest award conferred by colleagues on an American Pathologist who "represents the highest ideals in pathology and medicine." Patterned after the original Gold-Headed Cane in England, whose story began in 1689 with Radcliffe, it was originally kept for the lifetime of the recipient until in 1958 and since then awarded annually or biennially. At this time the Council of the American Association of Pathologists and Bacteriologists pays honor to another of the great leaders of American pathology. The name of Dr. Esmond R. Long, the nineteenth recipient of the Gold-Headed Cane, will join his distinguished predecessors Doctors Ernst, Welch, Smith, Mallory, Ewing, Hektoen, Karsner, Goodpasture, Opie, Whipple, Boyd, Rous, Cannon, Goldblatt, Oliver, Bayne-Jones, Warren and Moritz.

The 1970 awardee was born in Chicago 80 years ago and received his AB, PhD, and MD degrees from the University of Chicago and its constituent, Rush Medical College, in 1911, 1918 and 1926 respectively. The first four decades of his life, except for the years 1913 to 1919, were spent in Chicago. His colleague, Dr. Paul R. Cannon, has told me of his years in Chicago and how his long and distinguished career was interrupted in 1913 by his first serious encounter with the tubercle bacillus, which he diagnosed in his own laboratory, as a second-year medical student.

As you know, in the days before streptomycin and isoniazid, the therapy and curability of tuberculosis was quite different than today. For six frustrating years, Dr. Long sampled the changing varieties of tuberculosis therapy then in vogue, including dry-air treatments in a tent in Arizona, exercise under modified conditions, bed-rest in Seattle and superalimentation with a diet excessive in cholesterol and other presumably atherogenic materials. Fortunately, during this period he kept abreast of the scientific literature, did some laboratory work, and toward the end of his period of incapacitation, spent valuable time in Saranac Lake and the Trudeau Sanitorium, which provided him with definite intellectual rewards.

By 1919, he had recovered sufficiently to return to his laboratory in Chicago, and carry on his interrupted research under the guidance of Dr. H. Gideon Wells, the acknowledged leader of that era in the field of chemical pathology. He was soon able to take his examinations for the PhD degree in pathology and to resume, more systematically, his studies in pathology, tuberculosis and medical history. His accomplishments in these subjects during the next few decades led to his international acclaim.

Several months in Prague, in 1922, with Anton Ghon enabled Dr. Long to strengthen his postmortem dissection technic while devoting particular attention to varying aspects of tuberculosis, especially the pathologic lesions of primary infection, the so-called *Ghon nodules.* When he resumed his Chicago program, in 1923, his attack upon the problems of tuberculosis was definitely broadened, especially in the nature of the active principle of tuberculin. Soon he was occupied by the problems of differing inflammatory reactions to tuberculin in both normal and tuberculous subjects. The intensified responses in such tissues as the testis, kidney, cornea and skin created great interest because of the heightened effects of tuberculin sensitization upon a specific cell, the spermatocyte. This led to the development of the *spermatocyte test.* As a result of these studies, he was subsequently awarded the Trudeau Medal by the National Tuberculosis Association.

When Dr. Florence Seibert joined him as a chemical assistant, the work progressed rapidly. Together they soon demonstrated that the active principle of tuberculosis was protein in nature. Later, Dr. Seibert was able to crystallize the material and purify it. This material is now well know as Purified Protein Derivative (PPD), the standard for the US Public Health Service and for the World Health Organization.

In 1928, Dr. Long's *History of Pathology* was published. In the foreword Colonel F. H. Garrison remarked that "although intended primarily for students, this book can be cordially recommended to any physician who wishes to know the origins and evolution of the basic discipline of scientific medicine." A second book, *Selected Readings in Pathology from Hippocrates to Virchow*, appeared in 1929. It was designed to acquaint the reader more intimately with a few of the great masters of pathology by allowing them to tell their own stories. Through his books Dr. Long helped enrich the educational maturation of large numbers of students of medicine. A lesser known fact is that during these years when he was occupied so importantly, he was also serving as the editor in medicine for *Webster's International Dictionary*.

With such a record of accomplishments, it was not surprising that he applied his talents even more completely to tuberculosis research. Accordingly, in 1932 he accepted a professorship at the University of Pennsylvania, where he became Director of the laboratories at the Henry Phipps Institute for the Study, Treatment and Prevention of Tuberculosis. Although he became a retired professor in 1955, he has been remarkably active ever since.

In his active career he has had many special appointments, including Chairman of the Division of Medical Sciences of the National Research Council, President of Wistar Institute of Anatomy and Biology, and Director of Medical Research of the National Tuberculosis Association. He has been active in many societies, being elected president of at least six, including the American Association of Pathologists and Bacteriologists in 1937. His well-deserved honors are too numerous to delineate. He has given 20 special named lectures, written over 270 articles and editorials, 12 books and served as editor of three different journals.

This is just a brief historic account of one of our greatest living pathologists, our leading historian of pathology who even now is writing the histories of the American Society of Experimental Pathology and the American Association of Pathologists and Bacteriologists. On behalf of the Council of the American Association of Pathologists, it is my pleasure to present the Gold-Headed Cane to one of the United States' finest pathologists, scholars and gentlemen, Dr. Esmond R. Long.

The account of the original Gold-Headed Cane and its travels as it accompanied its owners on their rounds to see patients was published in a book, *The Gold-Headed Cane*, written as though the cane itself were telling the story. I believe this cane, when its story is written by Esmond Long, will make even better reading than the original.

ROBERT E. STOWELL

Experimental Papillary Necrosis of the Kidney

II. Electron Microscopic and Histochemical Studies

G. S. Hill, MD, R. G. Wyllie, MD, M. Miller, BA and
R. H. Heptinstall, MD

Renal papillary necrosis was induced in rats by bromoethylamine hydrobromide and studied electron microscopically and histochemically. Morphologic changes appear to develop in vessels and tubules simultaneously, rather than tubular lesions preceding and leading to vascular lesions, or vice versa. Abnormalities are recognized as early as 3 hours, but platelets do not make their appearance until 12 hours, eliminating primary vascular thrombosis as the source of papillary injury (Am J Pathol 68:213–234, 1972).

RENAL PAPILLARY NECROSIS may be produced experimentally in the rat by bromoethylamine hydrobromide (BEA).[1-3] A single injection of this drug in the appropriate dose will consistently produce papillary necrosis in approximately 95% of the normal animals to which it is administered.[3] The pathologic changes produced, particularly in their later stages, bear a striking resemblance to those seen in papillary necrosis in man.

The mechanism by which BEA and similar drugs produce their effects is not certain. On the basis of light microscopic studies, several different possible pathogenetic mechanisms have been proposed: generalized cytotoxic action,[2,3] direct damage to tubules,[4] or primary vascular abnormality, whether in the form of direct vascular damage with consequent thrombosis[5] or indirect damage secondary to vasoconstriction.[3] However, light microscopy has been of little help in separating out these possibilities. Relatively little histologic damage is evident before 12 to 24 hours, yet urinary output begins to increase dramatically shortly after injection of BEA, suggesting strongly that there is functional, and perhaps morphologic, damage early before changes can be identified with the light microscope. Therefore electron microscopic and histochemical studies of the early stages of

---

Department of Pathology, Johns Hopkins University School of Medicine and Hospital, Baltimore, Md.

Supported by Grants HE-07835 and GM-00415 from the US Public Health Service.
Accepted for publication Mar 17, 1972.

Address reprint requests to Dr. R. H. Heptinstall, Department of Pathology, The Johns Hopkins Hospital, Baltimore, Md 21205.

papillary necrosis were performed to attempt to elucidate which elements of the renal papilla, tubular or vascular, first show damage, (or whether both are affected concomitantly), in order to gain more insight into the pathogenesis of BEA-induced papillary necrosis.

Materials and Methods

Female Holtzman rats weighing 180 to 220 g were used. Sixteen normal animals were studied. Seventeen rats received a single intravenous injection of 50 mg of bromoethylamine hydrobromide (BEA), made up as a 10% aqueous solution. They were killed at the following intervals after BEA injection: 3 at 3 hours, 2 at 6 hours, 2 at 12 hours, 6 at 24 hours and 4 at 48 hours. At the time of killing, specimens were taken from the proximal, middle and distal thirds of the renal papilla. These were immediately fixed in a chilled solution of 3% glutaraldehyde in 0.1 M cacodylate buffer to which was added varying quantities of a sucrose solution to bring the osmolality of the solution to the desired level. In general it was found that fixation in a 600 to 650 mOsm solution produced the best results in normal animals with normally concentrated urine (see below). By contrast, the experimental animals in which BEA had induced a brisk diuresis, with presumed lowering of the tissue osmolality in the papilla, showed best results when the renal papillae were fixed in solutions in the range of 350 to 400 mOsm. After fixation, the tissue was postosmicated in 2% osmium tetroxide and embedded in Epon. Ultrathin sections were stained with lead citrate and/or uranyl acetate. They were examined in RCA EMU-3G and 3H electron microscopes.

For histochemical study, fresh unfixed kidney slices were snap-frozen in methylbutane and dry ice, and 4 μ sections cut on a cryostat. Sections were dehydrated for 10 minutes in a vacuum and then processed. Lactic dehydrogenase (LDH), a mitochondrial enzyme, was demonstrated by the method quoted by Barka and Anderson.[6] Adenosine triphosphatase (ATPase) was demonstrated by the method of Wachstein and Meisel.[7] All sections were counterstained with hematoxylin.

Results

Normal Anatomy

There have been a number of electron microscopic studies of the normal renal papilla in the rat,[8-11] rabbit[12,13] and in man.[14-16] The fine structure of the papilla is described beautifully in these papers, so that here it is only necessary to recapitulate the major points pertinent to the present study.

Collecting Ducts

Two types of cells have been described in the collecting duct, light cells and dark cells.[12,14,17] The light cells comprise the majority of the cell population. Dark cells are relatively few in number, being most frequent in the cortex and outer medulla and less abundant toward the papilla. Indeed, Bulger and Trump[8] were unable to recognize any dark cells in the rat papilla. However Hancox and Komender[17] have been able to identify them in that site, in a ratio of approximately 50 light to 1 dark cell, and we have seen dark cells in modest numbers in our material.

The light cells are cuboidal to columnar, becoming progressively taller toward the tip of the papilla. The luminal surface carries a number of irregularly disposed microvilli. The lateral borders show very considerable interdigitations, becoming progressively more prominent and elaborate from the surface of the cell toward its base. The upper portions of these cells are closely apposed with tight junctions at the apical surfaces, but as the interdigitations become more elaborate the margins become progressively more separated, leaving an apparently empty space between (Figure 1). The base of the cell is continuous with the lateral margins and shows prominent basal infoldings, so that a gap is formed between the cell basement membranes as well.

The nuclei of the cells have uniform, finely dispersed chromatin with little tendency to clump. Generally, the cytoplasm is finely granular with scanty organelles, including mitochondria, varying numbers of small clear vesicles, occasional cytosomes and lipid droplets.

The dark cells seen are similar to the light cells except that the cytoplasm is somewhat darker, primarily because of the presence of profiles of rough endoplasmic reticulum and increased numbers of mitochondria. These cells also have increased numbers of microvilli on their luminal surfaces and more elaborate basal infoldings along the basement membrane.

Thin limb of Henle's loop

Zimmerman[18] pointed out very early that the thin limb of Henle has complex interdigitations at its origin and these become progressively more simple along its length. Rhodin[16] confirmed that two types of thin limbs can be distinguished in the outer medulla. Descending limbs show numerous small basal interdigitations between cells and along the basement membrane, and occasional larger lateral interdigitations extending the full height of the cell (Figure 1). Ascending limbs are simpler, with relatively fewer basal processes and interdigitations between cells. These basal processes serve to distinguish thin limbs from vasa recta where such basal processes are quite uncommon and limited to the junctions between cells. Rhodin has stated that in the papilla the configuration of all thin limbs is relatively simple and descending and ascending limbs cannot be distinguished. Bulger and Trump,[8] on the other hand, maintain that they can distinguish between the two limbs. We find that, although it is often possible to recognize clearcut descending and ascending limbs in the outer papilla, distinctions in the inner papilla tend to blur and it is not fruitful to attempt to distinguish between the two limbs.

All cells tend to be of the same general height around the circumference of the tubules, except in the vicinity of nuclei. The luminal surface is provided with a few small microvilli. The cytoplasm is relatively pale, with only scanty endoplasmic reticulum, occasional mitochondria and other organelles. The nuclei show a uniform fine dispersion of chromatin through the nucleoplasm, with dense aggregates in the center and some clumping along the nuclear membrane.

Vasa Recta

Numerous authors have reported two distinct types of vasa recta, descending and ascending in the papilla.[8,11,15,19] With certain reservations, one can usually distinguish between descending and ascending vasa recta. The descending vas rectum is characterized by a continuous lining without fenestrations. The cytoplasm is moderately dense, with occasional mitochondria, free RNP particles and other organelles. The surface is provided with rare microvillous processes. Usually, but not invariably, invaginations and pinocytotic vesicles are discernible on and near both the luminal and basal surfaces. The nuclei, both in descending and ascending limbs, usually are relatively dark with dense, finely dispersed chromatin and some chromatin clumps, both centrally and along the nuclear membrane. Junctions between cells are relatively infrequent and true basal processes are limited to these regions. The ascending vasa recta (Figure 1) are characterized by very thin, fenestrated cytoplasm throughout most of their circumference, except in the vicinity of the nucleus. These fenestrated stretches of cytoplasm extend between the angles of the vessels in which are found postlike projections of cytoplasm, four to five such projections being distributed about the circumference of the vessel. Toward the tip of the papilla distinctions between descending and ascending vasa recta become blurred; the cytoplasm of the descending vessel becomes progressively lower and more scalloped. The attenuated areas blend gradually into the areas of fenestration. The higher areas come to resemble the domelike projections seen in the ascending vasa recta. Thus, particularly near the tip of the papilla, it is only possible to identify a structure as a vas rectum, without being able to specify whether it is descending or ascending. More important, and more difficult, is the distinction between vasa recta (particularly those without fenestrations), and thin limbs of Henle. Several features are of help in this distinction: in loops of Henle the cytoplasm tends to be relatively uniform in height about the circumference of the tubules whereas that in the vasa recta usually has a somewhat scalloped appearance even when not greatly attenuated. Basal processes and microvilli are characteristic of thin limbs and are rare or absent in vasa recta. By contrast, pinocytotic vesicles are a hallmark of vasa recta. However, there is no consistent difference between the two in other cytoplasmic constituents. Vasa recta tend to have darker cytoplasm than do loops of Henle, but this is not invariable.

Interstitial Cells and Interstitium

Interstitial cells were found at all levels of the renal papilla (Figure 1). They were of varying sizes and irregular shape, and were surrounded in part by a layer of basement membrane-like material, so closely applied that in some instances it appeared to originate within the cytoplasm. Strands and webs of this basement membrane-like material wended their way through the interstitium, connecting directly with the basement membranes of vasa recta and tubules. These basement membranes consisted of several delicate layers of this material. The rest of the interstitium was filled with a finely granular amorphous material through which coursed delicate collagen fibrils.

The interstitial cells often abutted directly on a tubule or blood vessel (more frequently the latter), being separated from it only by the basement membrane. The nuclei of these cells were relatively dark with prominent chromatin clumping on the nuclear membrane. The cytoplasm contained numerous organelles, including cytosomes with a variety of contents, including myelin figures. The most striking feature of these cells, however, was the presence of variable numbers of lipid droplets, which Tobian and others[20,21] believe to be the source of renomedullary vasodepressor lipid. In general, these granules were both larger and more numerous in the upper papilla than near its tip.

Histochemistry of Normal Papilla

The ordinary, or light, cells of the collecting ducts had moderate lactic dehydrogenase (LDH) activity, while the dark cells, located primarily in the upper third of the inner zone, had high levels of LDH activity. Collecting ducts were adenosine triphosphatase (ATPase) negative. Some of the collecting ducts were dilated, others collapsed;

in the middle reaches and tip they were predominantly partially collapsed. Thin limbs were weakly LDH positive and could only be identified with difficulty. The larger vasa recta were strongly ATPase positive, could be traced in straight lines through the outer third of the zone, were widely patent and had few anastomoses. The smaller capillaries contained small amounts of ATPase activity which progressively decreased towards the papillary tip. Some of these ran along thin limbs, while others were closely applied to collecting ducts and sent fine fingerlike processes between the ducts. Interstitial cells were weakly LDH positive and contained between 1 and 30 black granules. Most interstitial cells were oriented perpendicular to thin limbs and collecting ducts.

Fixation Artifacts

It is notoriously difficult to obtain adequate fixation of the renal papilla for electron microscopic study,[8,22] because under normal circumstances the normal renal papilla is markedly hyperosmolar compared to other tissues. Ordinary fixatives, particularly those with constituents that penetrate rapidly as opposed to glutaraldehyde which penetrates relatively slowly, cause a number of artifacts related to differences in osmolality between fixative and tissue. Thus, it is actually the osmolality of the sucrose moiety (which penetrates rapidly), rather than the osmolality of the complete fixative solution, which is crucial.[22]

Fixation in a solution hypoosmolar to the tissue causes a variety of swelling and ballooning artifacts. Mitochondria are usually the most sensitive to change, showing swelling and rupture of membranes. Other progressive changes include swelling of endoplasmic reticulum and nuclear envelopes, breaking of cell membranes and clefts in the cytoplasm. Perhaps most striking are cleared out areas in the cytoplasm which are devoid of organelles, these being pushed to the periphery of the cleared space, much as if a miniature explosion had occurred.

By contrast, tissue fixed in a hyperosmolar fixative shows contraction and shrinkage of the cells, with increased density of the cytoplasm and crowding of the cytoplasmic organelles. The cells tend to pull apart from one another at their lateral borders, particularly in the collecting ducts where the cleft between the interdigitating lateral margins of cells becomes much wider and the cell margins in some instances concave. Mitochondria become dark and shrunken, and it becomes difficult to make out the separate layers of the cristae and external membrane.

Fortunately in the present study, fixation artifacts were not so bothersome in the experimental animals as they were in normal controls, because administration of BEA induced a brisk diuresis, wiping out the medullary concentration gradient and reducing the osmolaltiy of the papilla to near that of plasma. Nonetheless, in evaluating early and subtle cytoplasmic changes, in order to definitely state that a given change was real and not an artifact, we required that at least some adjacent cells or tubules appear normal, without alterations which might be attributed to osmolal fixation artifact. As the process progressed and the papilla was more extensively involved, this was no longer possible, but by that point the changes were sufficiently gross to render it unnecessary to make this stipulation.

BEA Animals

Before detailing the specific observations made at the various time intervals, several general observations should be made. First, regardless of the overall severity of the lesions in a given animal or at a given time interval, changes were most advanced and most severe at the papillary tip and declined in severity as one passed upward in the papilla. Second, the thin limbs and vasa recta suffered the earliest and most consistent alterations, with the interstitial cells, and especially the collecting ducts, being more resistant and showing significant damage only in more advanced and/or severe lesions.

Three-Hour Animals

At 3 hours alterations were already apparent in all elements, particularly the vasa recta and the thin limbs. The most striking change was condensation of portions of the cytoplasm, which assumed a dark and finely granular appearance; the mitochondria also showed shrinkage and darkening (Figures 2, 3). This was not an artifact of fixation, for condensed and noncondensed areas appeared often in adjacent cells or cell processes, and occasionally both appearances coexisted in the same cell (Figure 2). Vacuoles often appeared in the cytoplasm of cells, both in relatively normal and in condensed areas. Nuclei in both vessels and loops of Henle showed early signs of injury, with a tendency for the finely distributed chromatin to aggregate on the nuclear membrane. In some instances there was slight wrinkling of the nucleus, with a tendency to retract from the outer nuclear membrane.

In the vessels focal separations of the cells from the basement membrane were infrequently seen, usually in the attenuated areas of the ascending vasa recta (Figure 3). Similar separations occurred in the thin limbs; often the space between the cell membrane and the basement membrane was filled by an amorphous granular material. No denuding of the basement membrane was seen at this stage, however, and platelets and fibrin were not seen either in the vessels or tubules.

It is difficult to compare the vasa recta and loops of Henle quantitatively, but it was our impression that the damage in the vasa recta was slightly greater than that in the loops of Henle.

Minor changes were also seen in the interstitial cells and the collecting ducts. These included modest chromatin clearing and clumping along the nuclear membranes, some cytoplasmic condensation (particularly in interstitial cells) and a tendency to increased separation of the lateral cell membranes in the collecting ducts. Also seen were increased numbers of autophagic vacuoles in the collecting ducts. These were dark membrane-bound structures containing dark osmiophilic material of cytoplasmic origin, often including mitochondrial and other lamellated profiles. These were the electron microscopic counterparts of the PAS-positive droplets seen histologically during the course of papillary necrosis.[3] They also bear a resemblance to the multivesicular bodies seen in the collecting duct cells during potassium depletion.[23] However, they differ in that these latter show no mitochondrial or other organelle profiles and do not undergo digestion with consequent homogenization.

Histochemical studies at this period revealed no constant alterations. There was a tendency to dilatation of the thin limbs, otherwise structures were relatively normal.

Six-Hour Animals

At 6 hours nuclear and cytoplasmic alterations were more generalized than at 3 hours. Condensation of cytoplasm, especially in the vasa recta and in the thin limbs of Henle, was more prominent (Figure 3). In the vasa recta, lifting of the cytoplasm from the basement membrane in attenuated areas was common; in rare areas rupture of the attenuated cytoplasm with denudation of the basement membrane was seen (Figure 4). At this stage, however, no platelets were seen adhering to the bare basement membrane.

The loops of Henle also showed separation between the basement and cell membranes, the space being filled with a coarsely granular material in which there were small vesicular structures. This appeared to represent the first stage of the microvesicular and microvillous degeneration which becomes so prominent later. The cytoplasm generally appeared somewhat condensed, finely granular and homogenous; occasional cells appeared markedly swollen.

Interstitial cells showed mild degenerative changes, but without alteration in the number of lipid droplets they contained. Collecting ducts by now showed significant damage: chromatin clumping and nuclear wrinkling, with condensation and granularity of the cytoplasm (particularly in the vicinity of the nucleus); the larger organelles were pushed toward the periphery (Figure 4). More striking was the increase in number and size of the cytosomes containing osmiophilic material, often in the form of myelin figures. As a function of the cytoplasmic condensation the lateral margins and basal processes tended to show greater than normal separation. However, an occasional cell, rather than being condensed, was markedly swollen, often with rupture of the cell membrane.

Histochemical Alterations: In the cortex and outer medulla there was widespread dilation of tubules and vasa recta, with some tendency for loss of ATPase activity in the vasa recta, together with some congestion. ATPase activity was increased in the distal tubules. There was some tendency to narrowing of the collecting ducts at the junction between outer and inner zones of the medulla, but they were dilated through the rest of their course through the papilla. At the base of the papilla, collecting duct LDH activity was normal but decreased progressively towards the tip. ATPase activity was diminishing in the vasa recta and capillaries, particularly in their finer ramifications; the enzyme was diffusing away. The granularity of the interstitial cells was reduced to less than half by histochemistry (although as mentioned above, there was little change in the number of lipid droplets seen by electron microscopy).

Twelve-Hour Animals

Whereas in the earlier stages cytoplasmic condensation had been the predominant evidence of cellular injury, at 12 hours substantial numbers of both vascular and tubular cells showed severe swelling, often in the same vessel or tubule with other cells showing condensation. The cytoplasm in these swollen cells was usually finely granular and homogenous, with few recognizable organelles.

The vasa recta showed even more pyknotic nuclei than previously and lifting of the cytoplasm in attenuated areas; rupture and denudation of the capillary basement membrane was quite common (Figure

4). Rare platelets were seen attaching themselves to this denuded basement membrane. In the thin limbs separation of the cytoplasm from the basement membrane was quite common, with early microvesicular transformation of the cytoplasm on the side of the cell away from the lumen. Microvesicular and microvillous transformation occurred not only at the cell membrane, but apparently in the cell cytoplasm as well. At this stage the tubular lumens contained only a granular amorphous debris.

The interstitial cells now quite often had a dark granular cytoplasm which was totally homogenous except for the characteristic lipid droplets. These latter seemed reatively unchanged in number and size. In the collecting ducts the cytosomes were more numerous than earlier and perhaps slightly larger.

Twenty-four Hour Animals

By 24 hours degenerative changes were sufficiently extensive and severe that it became difficult in some instances to identify structures specifically as vessels or thin limbs. The vast majority of vasa recta showed extensive denuding of the basement membrane and were lined wholly or in part by platelets (Figure 6), adherent not only in the bare regions but spread out over the adjacent cytoplasm as well. However, complete occlusion of the vessel lumen was quite uncommon; most simply showed a coating of platelets. Leukocytes were relatively uncommonly seen in association with these adherent platelets. Occasional vasa recta had ruptured, with extravasation of red cells into the interstitium. The endothelial cytoplasm was quite degenerated, usually condensed and homogenous, but occasionally containing some vacuoles and rarely appearing markedly swollen with cell rupture.

In the thin limbs the microvillous and microvesicular alterations of the cytoplasm, first seen at 12 hours, were now quite dramatic (Figures 5, 7). The cells were frequently lifted off of the basement membrane around the entire circumference of the tubule and pushed inward by the accumulation of these vesicular and villous structures, with the result that the residuum of the original cytoplasm formed a coiled and convoluted mass in the center of the tubule, with the original lumen reduced to a mere slit. In a few instances the entire tubule was filled with these microvesicular structures, with no vestige of the original cytoplasm or lumen remaining.

First noted at this time was the appearance of quantities of fibrillar, fibrin-like material (Figures 6–8). In the vast majority of cases this material was found in structures clearly identifiable as thin limbs. In only one instance was it found in a definitely recognizable vessel. This material varied considerably in its appearance, from accumulation of short, extremely delicate fibrils arranged in random array, to somewhat larger fibers with a definite periodicity arranged in interlacing bundles, to large tactoid-like fibers quite broad and dark in their appearance. Usually this material completely filled the lumen of the thin limb, but on occasion it was found beneath the epithelial cytoplasm in the space between the cell membrane and basement membrane, or in some instances in the cytoplasm of the epithelial cells. Often small vesicular structures were intermingled among the fibrils, but in no instance have red cells, leukocytes or platelets been seen in this fibrin-like material when it appears in tubules.

The interstitial cells appeared to have dissolved completely in many instances, leaving behind only their characteristic lipid droplets and a few vesicular and membranous structures (Figures 6, 7). The collecting ducts showed definite necrosis, but with rare exceptions the cells were still attached to one another and had not become dislodged from the basement membrane. The cytosomal or autophagic structures seen earlier were yet larger, but were now more uniformly dark and homogenous than earlier. It was no longer possible to recognize discrete structures within them in most instances.

Histocemical Alteration: There was widespread irregular dilatation of tubules, particularly distal tubules. Vessels showed irregular loss of ATPase activity, increasing as the boundary between the outer and inner zones was approached. At this level the larger vasa recta appeared contracted, with relatively normal ATPase activity, but in the papilla proper the vessels were dilated and showed increasing diffusional loss of enzyme. The collecting ducts had normal LDH activity at the inner zone junction. As the collapsed or barely patent ducts approached the mid-level of the papilla they became partially dilated with a decrease in LDH activity. This enzyme decrease progressed until near the tip duct cells became ghosts without LDH activity. Most of the thin limbs in the distal half of the papilla contained casts of granular material. All interstitial cells lacked granules by light microscopy, and only those in the outer portion of the papilla had any LDH activity.

Forty-eight-Hour Animals

At 48 hours cellular changes took two quite diverse directions. First, those elements which were totally necrotic went onward toward complete dissolution. The vasa recta showed complete thrombosis (Figure 9), with an admixture of platelets, fibrin and leukocytes. The thin limbs of Henle in most instances had undergone complete dissolution into microvesicular and microvillous structures with only rare larger remnants of cytoplasm. The fibrin-like material seen in their lumens was now predominantly of the tactoid variety. The interstitial cells were now almost completely dissolved, leaving behind only their granules and occasional fragments of other organelles. Severe damage was seen in the collecting ducts, which were lifted off their basement membranes and were lying free in the lumen. Their cytosomes were now extremely large and totally black and homogenous (Figure 9). Substantial accumulations of fibrin-like material, predominantly of the tactoid variety, were now present in the lumens; such material was not noted in this location at 24 hours.

By contrast, particularly in the upper levels of the papilla, there was evidence of regenerative activity. Regenerative cells appeared to occur predominantly in thin limbs. They lay beneath the necrotic cells, when these were still present. They showed considerable mitotic activity, and their cytoplasm was quite rich in free ribonucleoprotein granules.

Discussion

For the most part, the cytoplasmic alterations found in this study are not specific for papillary necrosis but are seen in a variety of other injuries to the renal tubules. The autophagic vacuoles in the collecting ducts have been described in glycerin-induced acute tubular necrosis,[24] acute renal failure due to methemoglobin-sodium ferrocyanide[25] and in flounder tubules damaged by cyanide.[26] These autophagic vacuoles are thought to represent a nonspecific response to a variety of cellular insults, and it is felt that they are derived from profiles of smooth endoplasmic reticulum which surround and incorporate portions of cytoplasm and organelles such as mitochondria, with subsequent digestion of this cytoplasm by acid hydrolases.[27] This would serve to explain in part the progressive increase in size and the progressively more homogenous appearance that the autophagic vacuoles in the present study displayed.

The microvesicular degeneration which was so prominent in the loops of Henle has been described previously in proximal tubules poisoned by mercuric chloride[28] and also in the nephropathy secondary to administration of uranyl nitrate.[29] Gritzka and Trump,[28] who studied the process in relation to mercuric chloride poisoning, felt that this microvesicular degeneration represented swelling and fragmentation of the smooth and rough endoplasmic reticulum, with shedding of ribonucleoprotein granules by the latter, and possibly some contribution resulting from dissolution of the cell membrane. The major difference between their observations and ours was that they noted microvesicular degeneration more or less uniformly throughout the cell, whereas in our study the changes occurred primarily in the cytoplasm on the basement membrane side of the cell. However, they examined proximal tubules, whereas the present study deals only with Henle's loops, a fact which may account for the difference in distribution of microvesicles.

Aggregation of fibrin in the thin limbs of Henle has previously been described in a light microscopic study of papillary necrosis induced by ethyleneimine, a drug similar to BEA.[5] However, such accumulations of fibrin-like material have not been previously described in electron microscopic studies. This material has all of the developmental and behavioral characteristics of fibrin, commencing as individual extremely delicate fibrils, progressing to interlacing bundles of fibrils and finally to broad, blunt tactoid-like structures. However, although an impression was gained of fibril periodicity in many regions, nowhere were we able to clearly demonstrate fibrils with the classical periodicity of fibrin. Assuming that this material is indeed fibrin, and this seems the most likely possibility, its presence in loops of Henle remains puzzling. It was always seen in pure form, without associated red cells, leukocytes, or platelets, essentially eliminating the possibility that it represented some form of hemorrhage into the tubules. And its presence in collecting ducts, in lesser amounts at 48 hours, would tend to indicate that the change, whatever its nature, was not specific for the loops of Henle, although the possibility cannot be ruled that the material in the collecting ducts simply represented material washed downstream over the course of time. One attractive explanation for the accumulations of fibrin is that they represent *in situ* coagulation of protein which filtered through a damaged glomerulus, possibly through release of tissue thromboplastin or by contact activation at sites of cellular necrosis in the thin limbs. However it is hard to envision why such a tendency to coagulation would not be as great in the vasa recta, where damage to cells was just as severe and the concentration of plasma proteins of course much higher. At present there is no adequate explanation for the fibrin in the thin limbs and collecting ducts.

The observations in this study serve to set the BEA model clearly apart from that of serum-induced papillary necrosis. Electron microscopic studies by both Ljungqvist *et al*[30] and Lee *et al*[31] have shown that by 30 minutes to 1 hour after injection of serum, necrosis of the endothelium of the vasa recta is complete. There are numerous platelets adherent to the wall, forming occasional occlusive thrombi. With BEA the time course is much more protracted, the first adherent platelets not appearing until 12 hours and rare vascular occlusions only after 24 hours. Also, in serum-induced papillary necrosis the epithelial alterations seem to occur after, and be consequent to, the vascular phenomena, rather than occur *pari passu* with endothelial lesions as in the BEA model. Both of these observations suggest that these two models have different pathogenetic mechanisms.

Perhaps the most important information in the present study related not specifically to the individual lesions, but rather to their chronology. From the earliest time of observation (3 hours) both the vasa recta and the thin limbs show damage of a progressive nature. Furthermore, although one has the impression that damage in the vasa recta may be slightly worse than in the thin limbs, the degree of severity of lesions in the two seems to be roughly the same. (This comparison may not be entirely fair as one is comparing two different types of cells.) At all events, the important point is that one does not see virtually total necrosis of the vasa recta at a time when tubular lesions are only minimal, or *vice versa*. Another observation of importance is that platelets are not seen in the vessels until endothelial necrosis is complete and the basement membrane denuded, as is the case at 12 hours. Thrombi became recognizable only at 24 hours. We consider, as did Ljungqvist[30] in the serum-induced model, that the adherent platelets represent a secondary response to vascular damage—particularly that baring the basement membrane—rather than a primary phenomenon. From these observations several tentative conclusions may be drawn. First, tubule damage is not the primary lesion, as Levaditi originally suggested,[4] with vascular damage as a secondary phenomenon. Rather the vascular and tubular lesions develop simultaneously. Second, by the same token, primary vascular endothelial damage with thrombosis and secondary ischemic damage to other structures does not seem to be implicated. By the time platelets are seen in significant numbers thin limb necrosis is quite advanced and collecting duct damage well established.

Two major pathogenetic possibilities thus remain: First BEA may exert a generalized cytotoxic effect, affecting all cellular elements more or less equally. Such an effect would tend to be expressed most vigorously in the papilla because of the countercurrent mechanism tending to concentrate substances in this region, but lesser degrees of damage might be anticipated elsewhere. (Indeed histologic evidence from our previous study[3] and histochemical data from the present study indicate that there is mild to moderate damage, both to tubules and to vessels, in the renal cortex and outer medulla.) The second possibility is that all of the changes in the papilla are ischemic in nature and consequent on severe vasoconstriction with the injection of BEA. The limitations of this study do not permit us to chose definitively between these two pathogenetic mechanisms. This problem will be approached in detail, using pharmacologic manipulation of the basic BEA model, in a subsequent communication.

References

1. Oka A: Zur Histologie der Vinylaminnephritis. Virchows Arch [Pathol Anat] 214:149–160, 1913
2. Fuwa M, Waugh D: Experimental renal papillary necrosis. Effects of diuresis and antidiuresis. Arch Pathol 85:404–409, 1968
3. Murray F, Wyllie RG, Hill GS, Ramsden PW, Heptinstall RH: Experimental papillary necrosis of the kidney. I. Morphologic and functional data. Am J Pathol 67:285–302, 1972
4. Levaditi C: Experimentelle Untersuchungen uber die Nekrose der Nierenpapille. Arch Int Pharmacodyn 8:45, 1901
5. Davies DJ: The structural changes in the kidney and urinary tract caused by ethyleneimine ("vinylamine"). J Pathol 97:695–703, 1969
6. Barka T, Anderson PJ: Oxidative enzymes in histochemistry. New York, Harper and Row, 1963, pp 296–333
7. Wachstein M, Meisel E: Histochemistry of hepatic phosphatases at a physiologic pH. Am J Clin Pathol 27:13–23, 1957
8. Bulger RE, Trump BF: The structure of the rat renal papilla. Am J Anat 118:685–722, 1966
9. Osvaldo L, Latta H: The thin limbs of the loop of Henle. J Ultrastruct Res 15:144–168, 1966
10. Osvaldo L, Latta H: Interstitial cells of the renal medulla. J Ultrastruct Res 15:589–613, 1966
11. Moffat DB: The fine structure of the blood vessels of the renal medulla with particular reference to the control of the medullary circulation. J Ultrastruct Res 19:532–545, 1967
12. Johnson FR, Darnton SJ: Ultrastructural observations on the renal papilla of the rabbit. Z Zellforsch 81:390–406, 1967
13. Gosling JA, Dixon JS: The fine structure of the vasa recta and associated nerves in the rabbit kidney. Anat Rec 165:503–514, 1969
14. Bulger RE, Tisher CC, Myers CH, Trump BF: Human renal ultrastructure. II. The thin limb of Henle's loop and the interstitum in healthy individuals. Lab Invest 16:124–141, 1967

15. Latta H, Maunsbach AB, Osvaldo L: The fine structure of renal tubules in cortex and medulla. Ultrastructure of the Kidney. Edited by AJ Dalton, and F Hageunau. New York, Academic Press, Inc. 1967, pp 2–56
16. Rhodin JAG: Electron microscopy of the kidney. Am J Med 24:661–667, 1958
17. Hancox NW, Lomender J: Quantitative and qualitative changes in the "dark" cells of the renal collecting tubules in rats deprived of water. Q Exp Physiol 48:346–354, 1963
18. Zimmerman KW: Zur Morphologie der Epithelzellen der Saugetierniere. Arch Mikr Anat 78:199–231, 1911
19. Longley JB, Bandfield WG, Brindley DC: Structure of the rete mirabile in the kidney of the rat as seen with the electron microscope. J Biophys Biochem Cytol 7:103–106, 1960
20. Tobian L, Ishii M, Duke MA: A study of the cytoplasmic granules in renal papillary interstitial cells in relation to hypertension. Trans Assoc Am Physicians 81:125–134, 1968
21. Tobian L, Ishii M: Interstitial cell granules and solutes in renal papilla in post-Goldblatt hypertension. Am J Physiol 207:1699–1702, 1969
22. Maunsbach AB: The influence of different fixatives and fixation methods on the ultrastructure of rat kidney proximal tubule cells. II. Effects of varying osmolality, ionic strength, buffer system and fixative concentration of glutaraldehyde solutions. J Ultrastruct Res 15:283–309, 1966
23. Wilson H, Spargo B, Penska R: An experimental system for the study of a specific pattern of cytoplasmic change. Meth Achievm Exp Pathol 4:92–120, 1969
24. Suzuki T, Mostofi FK: Electron microscopic studies of acute tubular necrosis. Early changes in lower tubules of rat kidney after subcutaneous injection of glycerin. Lab Invest 23:15–28, 1970
25. Rosen S, Mailloux LU, Lawson NL, Teschan PE: Acute renal failure in the rat. II. Light and electron microscropic observations. Lab Invest 18:444–459, 1968
26. Trump BF, Bulger RE: Studies of cellular injury in isolated flounder tubules. I. Correlation between morphology and function of control tubules and observations of autophagocytosis and mechanical cell damage. Lab Invest 16:453–482, 1967
27. Arstila AU, Trump BF: Studies on cellular autophagocytosis. The formation of autophagic vacuoles in the liver after glucagon administration. Am J Pathol 53:687–733, 1968
28. Gritzka TL, Trump BF: Renal tubular lesions caused by mercuric chloride. Electron microscopic observations: Degeneration of the pars recta. Am J Pathol 52:1225–1277, 1968
29. Stone RS, Bencosme SA, Latta H, Madden SC: Renal tubular fine structure studied during reaction to acute uranium injury. Arch Pathol 69:470–476, 1960
30. Ljungqvist A, Osvaldo-Decima L, Richardson, J: Studies on the pathogenesis of serum-induced renal papillary necrosis in the rat. Lab Invest 17:447–457, 1967
31. Lee JC, French SW, Wizgird JP, Hooper J Jr: Early morphologic changes in serum-induced renal papillary necrosis. Light and electron microscopic studies. Lab Invest 17:458–464, 1967

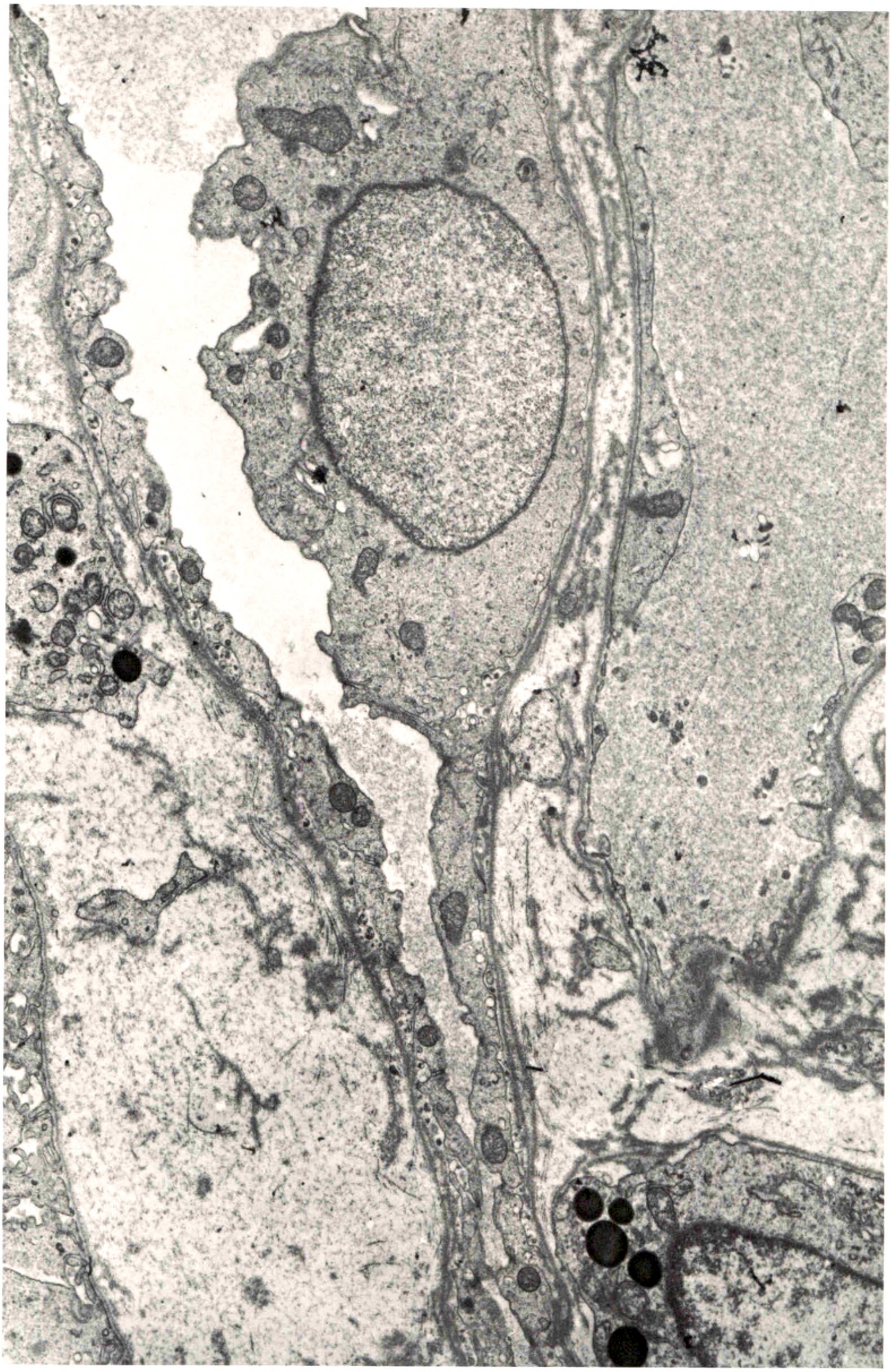

Fig 1—Electron micrograph of normal renal papilla. At right is a vas rectum, showing in its lower portion the attenuated, fenestrated cytoplasm typical of ascending vasa recta. At center is a thin limb of Henle showing, particularly on the left wall the complex interdigitating lateral and basal processes typical of thin limbs. At lower left are the bases of several collecting duct cells showing the prominent lateral processes and basal infoldings of these cells. At midleft and lower right are seen portions of two interstitial cells showing their characteristic lipid inclusions (× 9350).

2

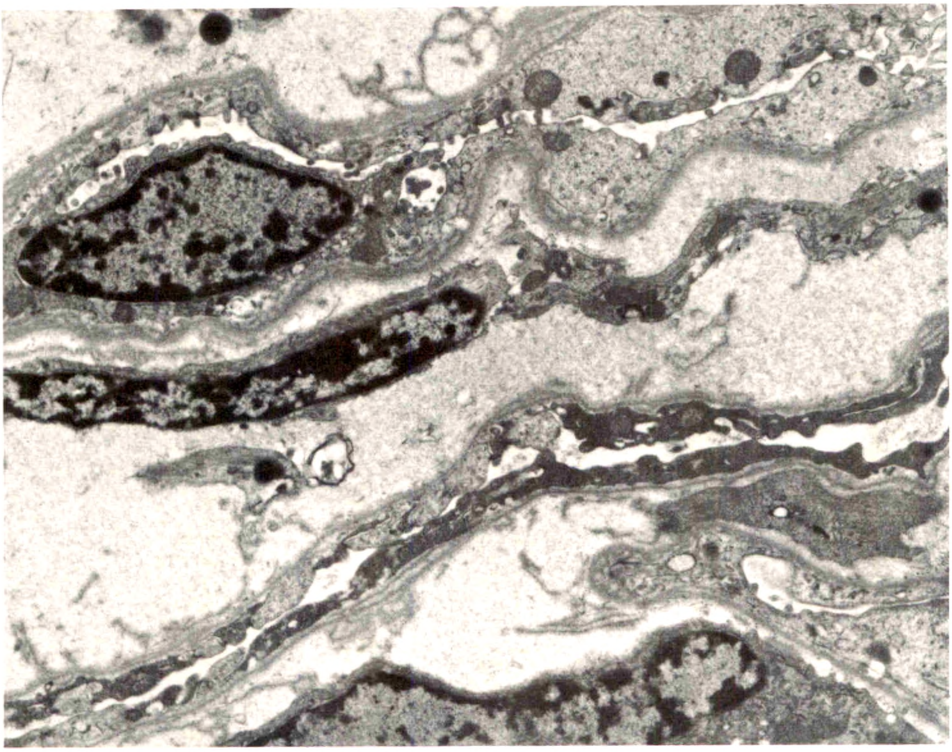

3

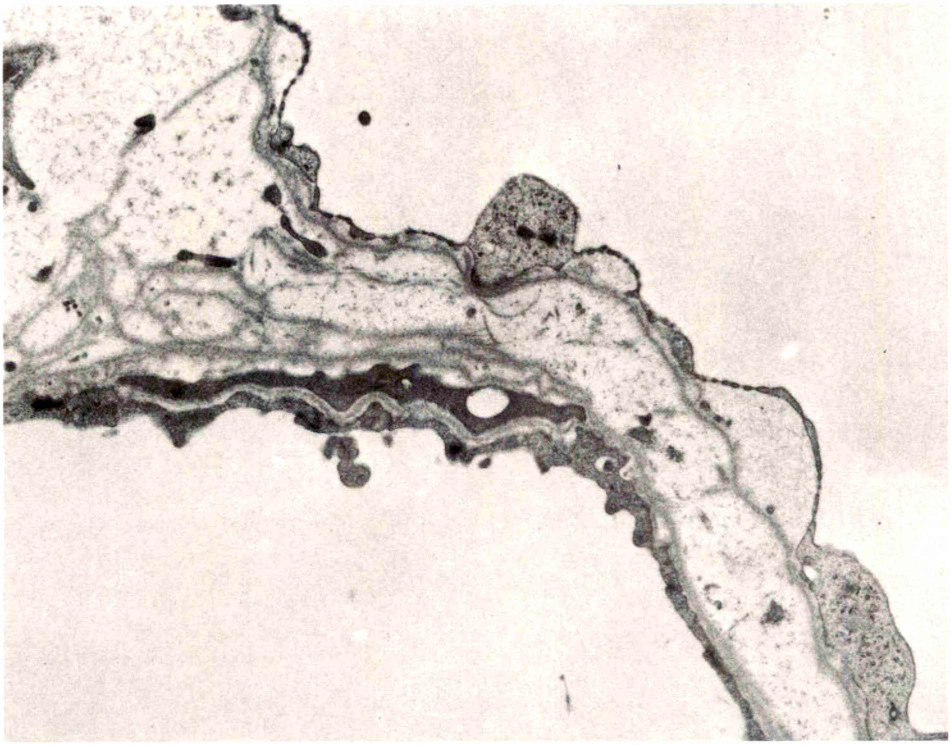

Fig 2—Limb of Henle showing early cytoplasmic condensation in some processes but not in others. Compare with the still-normal cytoplasm in the limbs above and below. Nuclei are also beginning to show slight increase of chromatin clumping on the nuclear membrane (× 9000). **Fig 3**—Ascending vasa recta, above, showing several foci in which the attenuated cytoplasm between the domelike projections at the corners of the vessel is lifted up with accumulation of a granular material between the cytoplasm and the basement membrane. The loop of Henle below shows extensive condensation of the cytoplasm as does the thin interstitial cell process immediately outside its basement membrane (× 11,950).

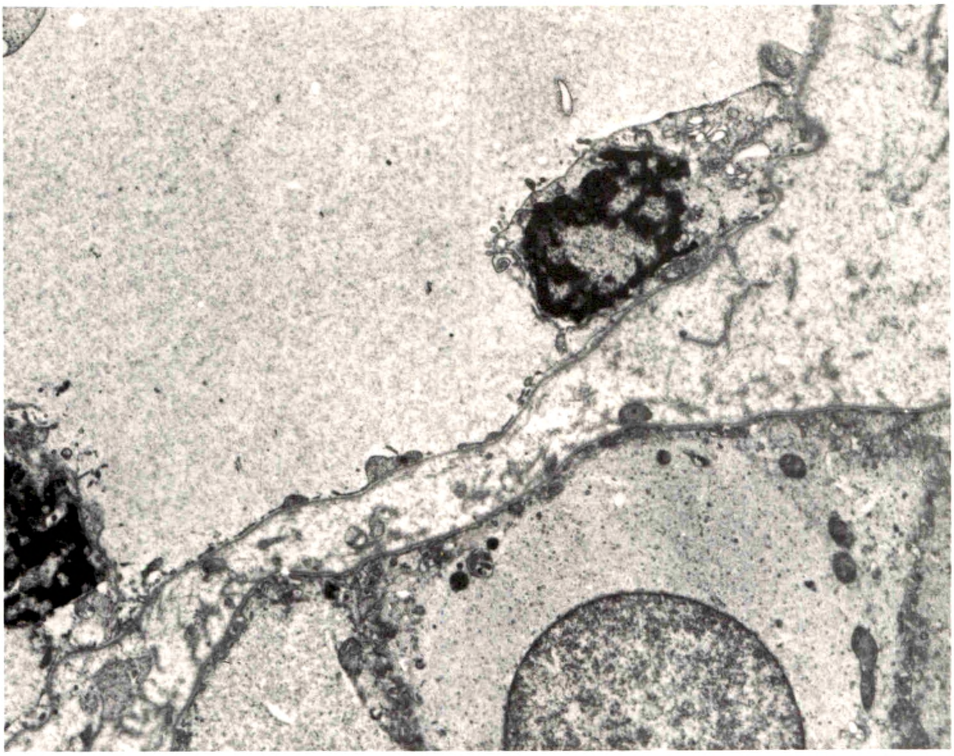

4

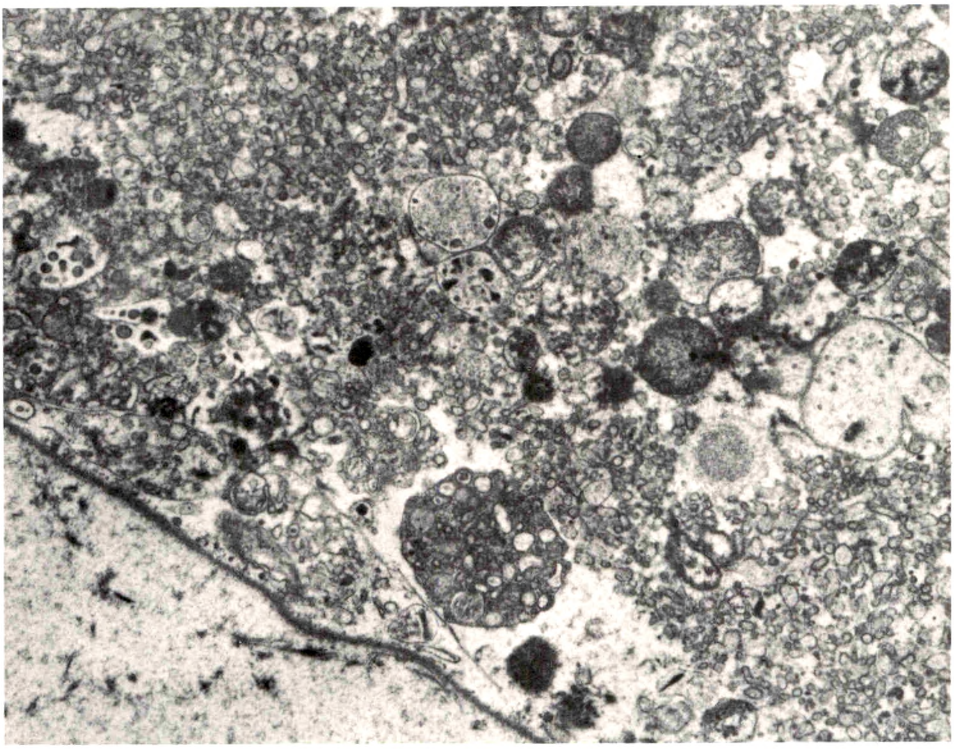

5

Fig 4—Ascending vessel showing extensive cytoplasmic damage with nuclear wrinkling and chromatin clumping. The cytoplasm in the attenuated portions shows multiple areas of rupture with denuding of the basement membrane, though without adherent platelets at this stage. The collecting duct cells below show regions of homogenous cytoplasm, the mitochondria and other organelles being pushed to the periphery of these regions (× 9350).
Fig 5—High power view of the structures remaining after a tubule has undergone microvesicular and microvillous degeneration. A variety of structures are recognized including mitochondria, cytosomes, microvillous structures, and vesicles (× 8600).

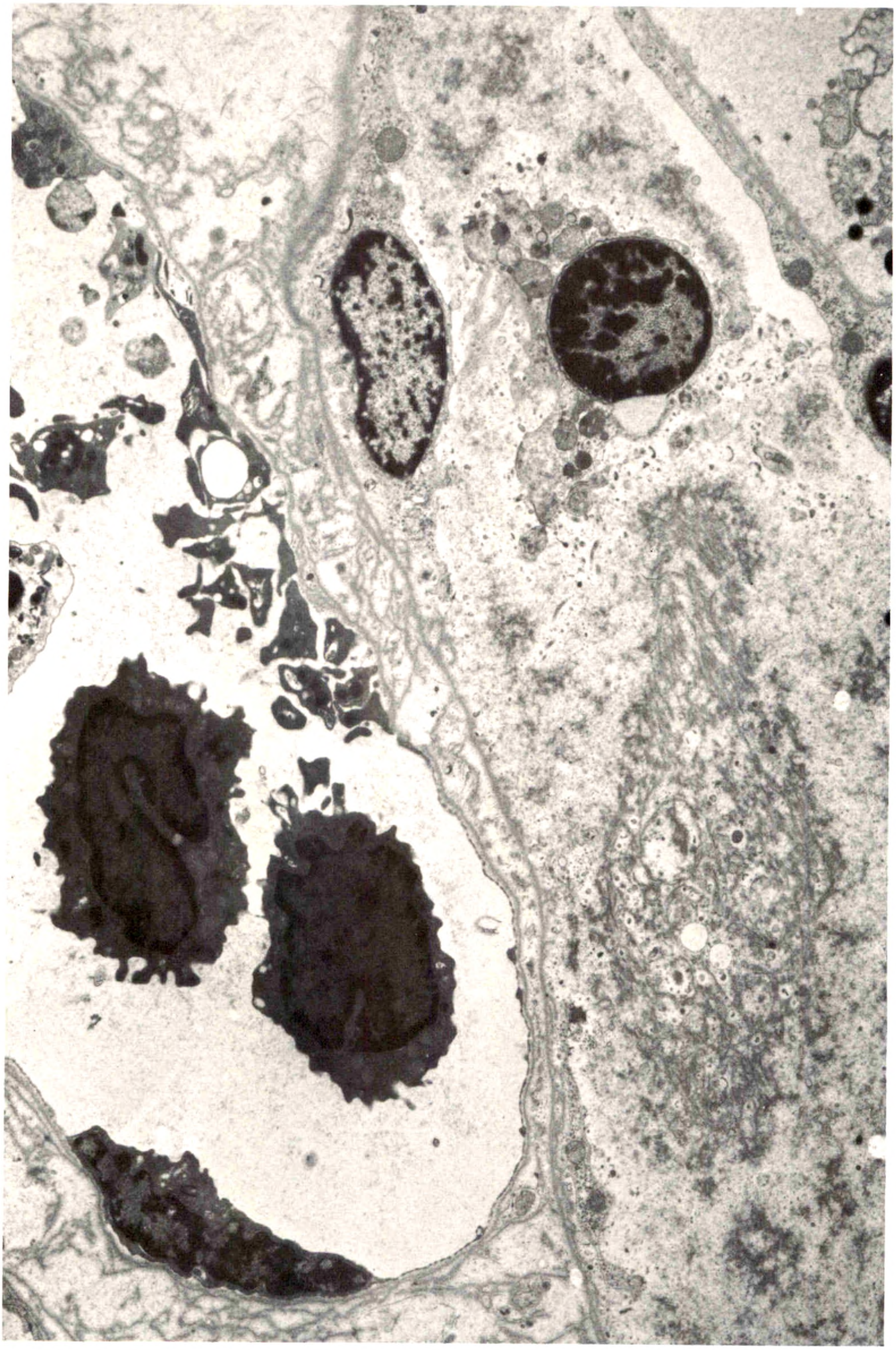

Fig 6—An ascending vessel, left, shows extensive cytoplasmic and nuclear degeneration in its lining cells. Platelets are adherent to the bare basement membrane but not where the cytoplasm is intact. At right is a thin limb which has undergone exensive degeneration. In its lumen are fine strands of a fibrin-like material. Transitions can be traced between these delicate strands and large tactoid-like structures seen later. Above right are the remnants of an interstitial cell which has undergone complete dissolution, leaving behind only the characteristic lipid droplets plus a few cytoplasmic organelles (× 6250).

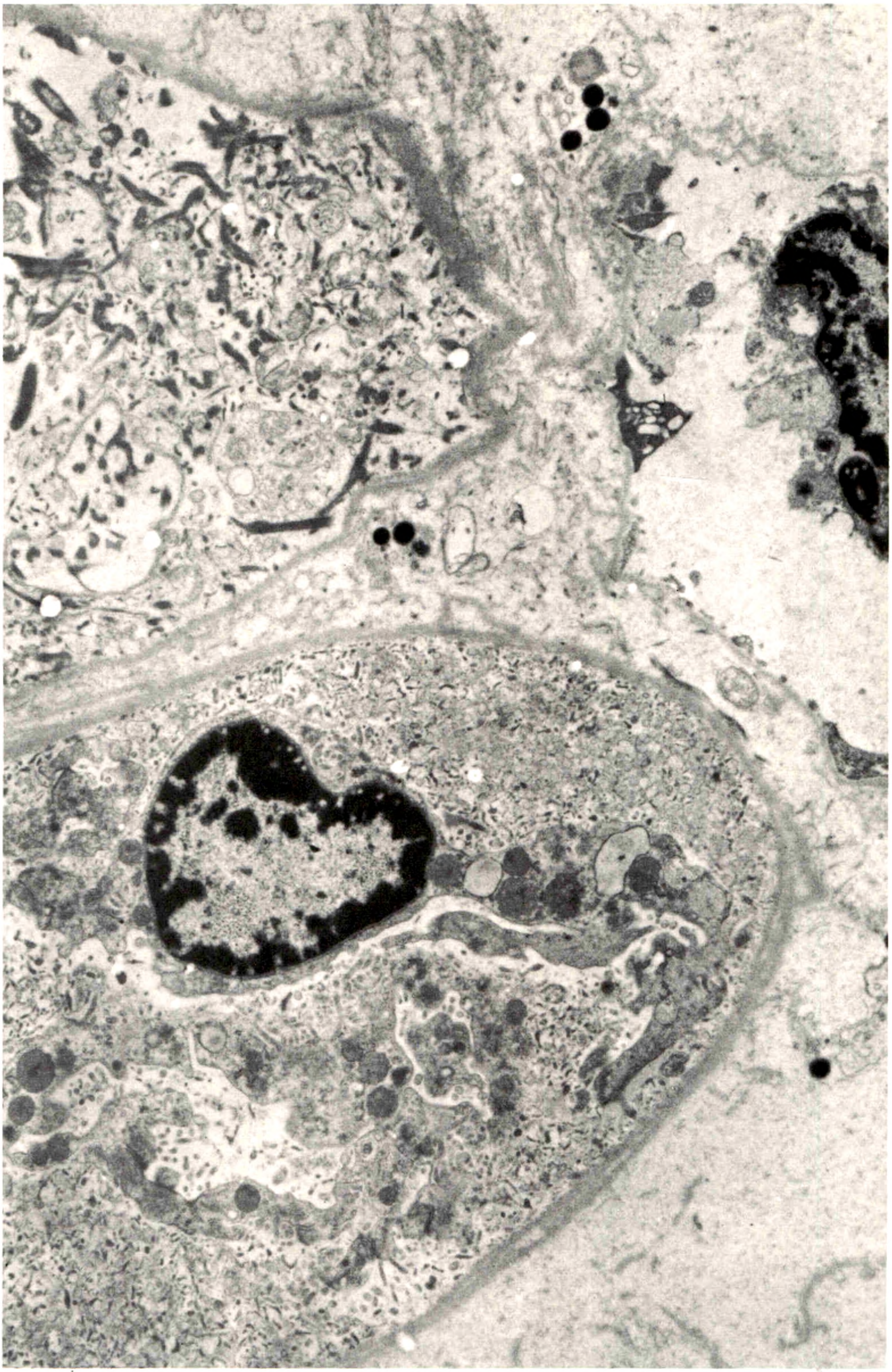

Fig 7—The thin limb below left shows extensive microvesicular and microvillous degeneration. The remaining intact cytoplasm has largely been displaced toward the center of the tubule, reducing the lumen to a mere slit. The thin limb above also shows some microvesicular degeneration but more prominently shows large tactoid-like structures of fibrillar material. The vessel at right shows extensive cytoplasmic disruption with a platelet adherent to the denuded basement membrane. Also seen in the interstitium are the remnants of three dissolved interstitial cells marked by the characteristic lipid droplets (× 8630).

8

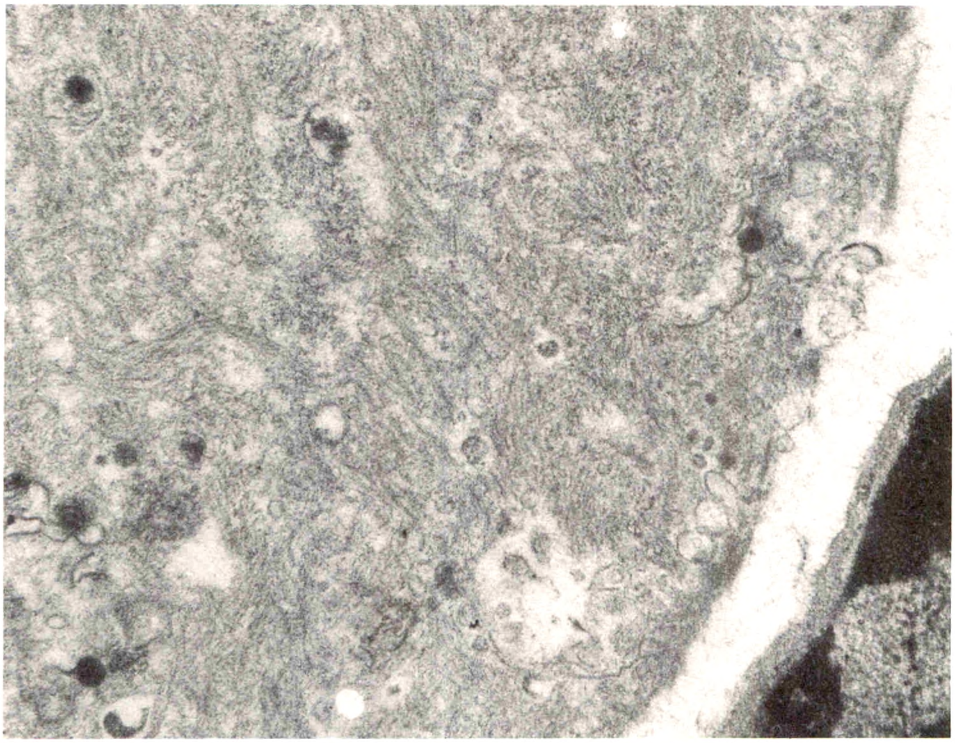

9

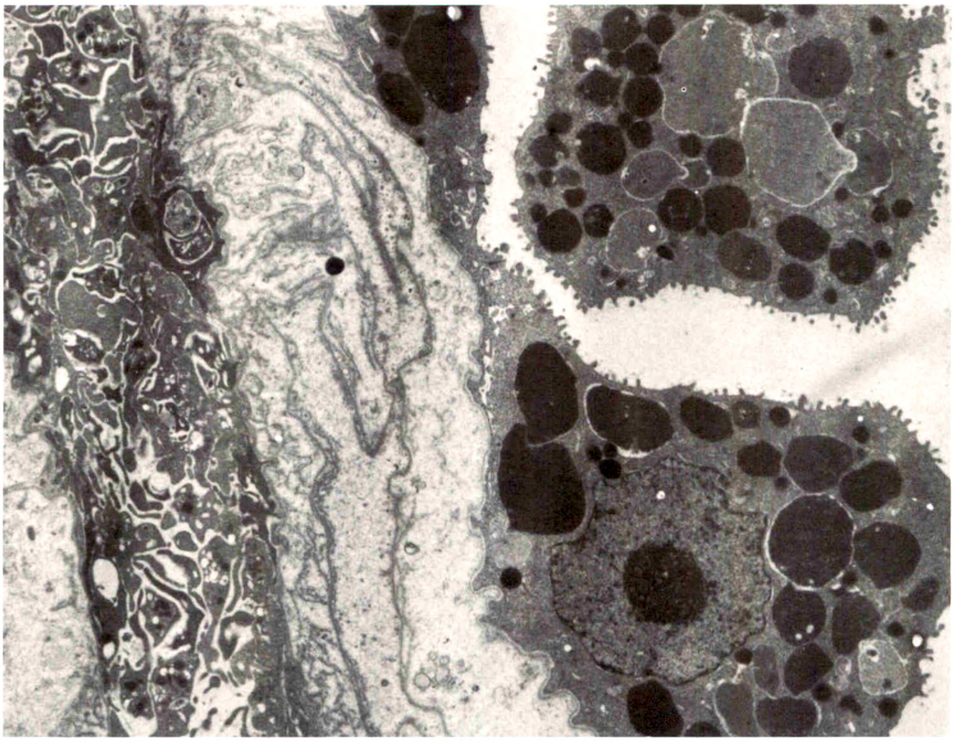

Fig 8—High magnification of the fibrin-like material found in the lumens of thin limbs. Although there was a definite impression of fibril periodicity, no accurate measurement could be made of this periodicity (× 32,600). **Fig 9**—In the later stages the collecting duct cells, right, show extensive alteration. The cytoplasm is sufficiently condensed that the lateral margins of the cells are completely pulled apart. The cytoplasm is filled with cytosegrosomes which by this stage have become quite large and electron dense and are almost totally homogenous. The vessel at left shows total thrombosis, predominantly by platelets (× 4100).

Experimental Papillary Necrosis of the Kidney

III. Effects of Reserpine and Other Pharmacologic Agents on the Lesion

R. G. Wyllie, MD, G. S. Hill, MD, G. Murray, MD, P. W. Ramsden and
R. H. Heptinstall, MD

Reserpine is able to exert a pronounced inhibitory effect on the development of papillary necrosis following the administration of bromoethylamine hydrobromide to the rat. This inhibitory effect has been observed using light microscopy, histochemistry, indigo carmine excretion and urine output. These observations suggest that vasoconstriction may play a significant role in the pathogenesis of papillary necrosis, but the evidence for this is incomplete (Am J Pathol 68:235–254, 1972).

A SINGLE INTRAVENOUS INJECTION of bromoethylamine hydrobromide (BEA) produces papillary necrosis of the kidney in over 95% of the rats so treated. In two previous papers[1,2] we have described the sequential pathologic changes using light and electron microscopy and histochemical methods. From these studies we were unable to demonstrate any organic blockage of the vasa recta or capillaries to account for the changes that developed in the papilla. The present experiments were designed to extend these studies and, in particular, to explore the possibility that vascular constriction of a nonorganic type may be the mechanism by which BEA produces papillary necrosis.

In the first experiment agents were used that prevent either aggregation of platelets or the formation of fibrin thrombi. In the second experiment various pharmacologic agents were employed to determine whether they could interfere with the action of BEA, which is a short chain aliphatic amine with pressor activity. The compounds used were chlorpromazine, phenoxybenzamine, 6-hydroxydopamine and reserpine. It was found that reserpine had a significant influence on the genesis of the lesion; the experiments to be described were designed to study further the effects of reserpine on BEA-induced necrosis.

From the Department of Pathology, Johns Hopkins University School of Medicine and Hospital, Baltimore, Md.

Supported by Grants HE—07835 and GM–00415 from the US Public Health Service.
Accepted for publication Mar 17, 1972.

Address reprint requests to Dr. R. H. Heptinstall, Department of Pathology, The Johns Hopkins Hospital, Baltimore, Md 21205.

Materials and Methods

General

Female Holtzman rats weighing 200 to 225 g were used in all of the experiments. They were fed Purina Chow and allowed unlimited amounts of water to drink. Urine output was measured over 24-hour periods, and serum urea nitrogen was measured by a modified Berthelot reaction. Blood pressures were measured under light Nembutal® anesthesia. A polythene cannula was introduced into the aorta and connected to a pressure transducer and a Sanborn model 301 Carrier recorder. Recordings were made for periods of up to 1 hour.

Drug dosages

The standard dose of BEA was a single intravenous injection of 50 mg, a dose known to produce papillary necrosis in 95% of the animals. Sulfinpyrazone was administered intramuscularly in a dose of 20 mg. Heparin was injected intramuscularly in amounts of 500 units. Either a single dose, or 3 doses, spaced out, with a 12-hour interval between each, was given. Chlorpromazine was injected intravenously in quantities of 0.625 mg. The dose of phenoxybenzamine was 1.6 mg, injected intravenously; that of 6-hydroxydopamine was 5 mg, intramuscularly, injected on each of 4 consecutive days. Reserpine was administered subcutaneously in two different ways: in the first, 0.75 mg was given in a single dose; in the second, 1.5 mg was injected in 2 divided doses.

Histochemistry

Fresh unfixed kidney slices were snap frozen in methylbutane and dry ice, and 4 μ sections cut on a cryostat. Sections were dehydrated for 10 minutes in a vacuum and then processed. Lactic dehydrogenase (LDH), being a mitochondrial enzyme, was demonstrated by the method quoted by Barka and Anderson.[3] Adenosine triphosphatase (ATPase) was demonstrated by the method of Wachstein and Meisel.[4] All sections were counterstained with hematoxylin.

Catecholamine demonstration

This was performed by formaldehyde-induced fluorescence using the method of Spriggs *et al.*[5]

Indigo carmine test

Each rat in which this test was performed received an intravenous injection of 0.5 ml of 0.8% solution of indigo carmine (soldium indigotendisulfonate USP). After 10 minutes the animal was killed by exsanguination from the heart after light ether anesthesia was induced. At autopsy the color of the bladder urine was recorded and the kidneys excised. The perihilar cortex was quickly removed to expose the papilla which was then examined under a dissecting microscope.

Histology and grading system

Animals were killed by exsanguination from the heart after light ether anesthesia. Coronal sections were prepared through the midpoint of the kidney after fixation in formal-saline. They were stained with hematoxylin and eosin, by the periodic acid-Schiff (PAS) method, and by Martius scarlet for fibrin. A 1 to 3 grading system was made based on the following principles. When rats receive a single injection of BEA 95% show a constant picture at each time interval at which they are studied. Thus at 24 hours the thin limbs and collecting ducts show characteristic changes, while at 7 days necrosis of all elements is complete. Intervening time periods show an orderly progression of changes; later time periods show separation of the papilla and secondary changes in the cortex. These changes are taken as the absolute standards against which the changes in the animals treated with various drugs are compared. Three grades were used: the first is that in which there were no changes or only trivial changes; the second showed definite abnormalities, but far short of those in rats receiving BEA alone; these are referred to as minor changes; the third group showed changes indistinguishable for those with BEA alone; this is referred to as the grade with necrosis. Because approximately 5% of rats receiving a single intravenous injection do not develop papillary necrosis, the same grading system was used for animals receiving BEA alone. Clearly in this circumstance only a few animals will show Grade 1 and Grade 2 changes, while the vast majority will fall in Grade 3, the necrotic grade.

Experiment 1

Because of its ability to prevent platelet aggregation, sulfinpyrazone was administered to 8 rats 1 hour before the injection of BEA. In order to prevent thrombus formation, 18 rats were treated with heparin 30 minutes before receiving BEA. The animals receiving sulfinpyrazone were killed at time intervals from 18 hours to 7 days, and those receiving heparin at intervals of 1 to 7 days. The kidneys were examined histologically.

Experiment 2

Various drugs were employed to study their effects on BEA-induced papillary necrosis. Thirteen rats received chlorpromazine 30 minutes to 2 hours before the injection of BEA, while 14 received phenoxybenzamine 4 hours before BEA. A further 8 rats received 4 daily injections of 6-hydroxydopamine, BEA being given on the fifth day. Twelve animals received the smaller dose of reserpine (0.75 mg) followed by BEA after 18 hours. The animals were killed at the time intervals shown in Table 1, and examined histologically.

Experiment 3

In this experiment the effects of reserpine in 2 dosage ranges were studied on BEA-induced necrosis. Group A was made up of 72 rats receiving 0.75 mg reserpine; BEA was injected 18 hours later. Group B contained 15 rats receiving 1.5 mg reserpine followed 18 hours later by BEA, and Group C consisted of 61 rats which received BEA only. Animals were killed 1 to 30 days after the injection of BEA in all groups.

Experiment 4

This was performed to study the histochemical changes during the first 24 hours after BEA, reserpine having been administered in 0.75 mg doses 18 hours previously. There were 50 animals so treated and these were compared with animals receiving BEA alone. A further 5 rats received reserpine alone.

Experiment 5

The indigo carmine pattern was studied in 9 normal rats, in 59 rats receiving BEA alone, in 55 rats receiving 0.75 mg reserpine followed by BEA 18 hours later and in 5 rats receiving 0.75 reserpine alone. These are designated Groups 5A, 5B, 5C and 5D respectively; the time intervals following BEA at which the tests were done are shown in Table 3.

Urine output was measured in 16 rats receiving 0.75 mg reserpine followed 18 hours later by BEA and compared with that in normal rats and rats receiving BEA alone.

Intraarterial blood pressure recordings were made on 10 rats receiving BEA alone and in 10 rats receiving 0.75 mg reserpine 18 hours before BEA.

Results

Experiment 1

Of the 8 rats receiving sulfinpyrazone all showed the type of change found when BEA is administered alone. There were no findings even suggestive that sulfinpyrazone can exert any protective action.

Of the 18 rats treated with heparin, 15 showed changes of papillary necrosis. Two rats killed at 2 days showed less well-marked changes in the papilla, and 1, killed at 9 days showed no abnormalities whatsoever.

Experiment 2

The results of this experiment are presented in Table 1. It will be seen that 6-hydroxydopamine gave no protection whatsoever against the effects of BEA in the dose range employed. The results with chlorpromazine and phenoxybenzamine showed some amelioration of lesions, but were not comparable with those receiving reserpine. With this drug only 4 out of 12 animals had the type of change that is the forerunner of papillary necrosis, or papillary necrosis

Table 1—Experiment 2; Severity of Papillary Lesion when BEA is Preceded by Various Drugs

			Severity of lesion		
Drug	Time after BEA (days)	No. animals	No change or trivial change	Minor changes	Necrosis
Chlorpromazine	1 & 2	9	2	0	7
	3	4	0	1	3
Phenoxybenzamine	1 & 2	5	0	1	4
	3	9	2	1	6
6-Hydroxydopamine	1 & 2	3	0	0	3
	6	5	0	0	5
Reserpine	1 & 2	5	3	1	1
	3 & 6	7	1	3	3

itself. Because of the better promise of reserpine, it was decided to concentrate on this drug for the other experiments.

Experiment 3

The results are summarized in Table 2. Of the 72 rats in Group 3A (0.75 mg reserpine plus BEA) 15 (21%) showed no change or only trivial changes in the papilla, 14 (19%) showed only minor changes and 43 (60%) showed changes no different from those in animals receiving BEA alone. Of the 15 rats in Group 3B (1.5 mg reserpine plus BEA) the comparable figures were 3 (20%), 1 (7%) and 11 (73%) respectively. Of the 61 rats receiving BEA alone (Group 3C) only 1 (1.6%) showed minimal changes, 2 (3.2%) showed minor changes, while no less than 58 (95.2%) showed necrotic changes.

Text-figure 1 is a histogram which shows the 3 grades of change according to the time at which the animals of Group 3A were killed. It will be noted that the two grades, no change or trivial change, and minor change, were relatively more frequent in animals killed at 1 or 2 days following BEA than at 3 to 8 days, which in turn showed relatively greater frequency of these less severe changes than rats killed between 10 and 30 days. This is shown more convincingly in Text-figure 2 where the two less severe grades are represented as one column. The same trend was noted in Group 3B, but this does not lend itself to illustration because the total pool of animals was only 15. In contrast is the histogram (Text-figure 3) for rats in Group 3C, where necrosis predominates at all time intervals. The two less severe grades are treated as one column.

Experiment 4

Lactic dehydrogenase is present as fine granules in the cells of the normal collecting duct in the papilla. There are particularly high

Table 2—Experiment 3; Severity of Papillary Lesion for Different Regimens (Figures Express Percentage of Animals in Each Grade of Severity)

		Severity of lesion (percent)		
Group and regimen	No. animals	No change or trivial change	Minor change	Necrosis
3A 0.75 mg reserpine BEA	72	21	19	60
3B 1.5 mg reserpine BEA	15	20	7	73
3C BEA alone	61	1.6	3.2	95.2

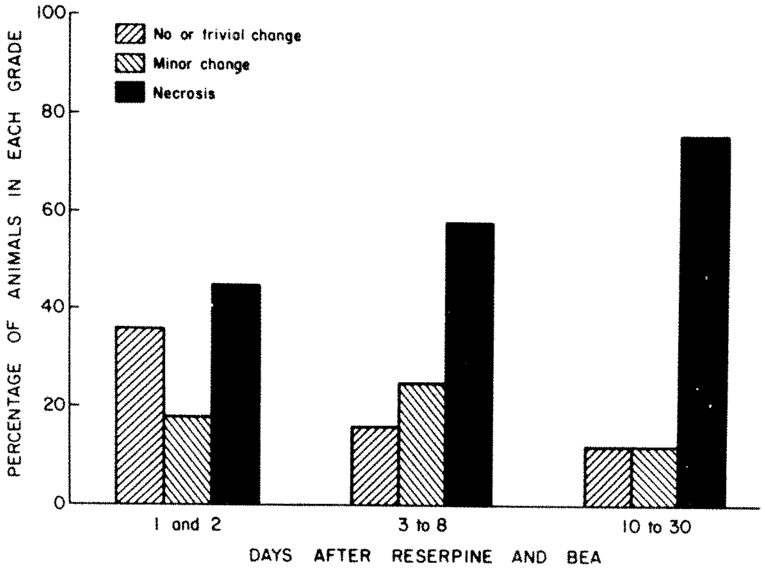

TEXT-FIG 1—Histogram showing 3 grades of change according to time at which animals are killed. Animals received 0.75 mg reserpine followed 18 hours later by BEA. (Group 3A).

levels in the dark cells. When BEA is injected there is a coarsening of the reduced tetrazolium granules—indicative of mitochondrial injury—in the collecting ducts, particularly towards the papillary tip, as early as 6 hours. By 24 hours activity is lost except for that part adjacent to the inner stripe of the outer zone. In animals pretreated with reserpine and then receiving BEA, there are no changes in the collecting ducts at 6 hours. At 24 hours there is a coarsening of the pattern in the distal one-third, but no loss. This enzyme is also present in small amounts in the thin limbs. Twenty-four hours after BEA injection there is loss of activity in these structures in the distal half of the papilla. In animals receiving reserpine and BEA there is no demonstrable loss of activity at 24 hours. Interstitial cells, which normally contain fine granules, show a decrease in activity at 6 hours and loss by 24 hours following BEA injection. In rats receiving reserpine and BEA, there is reduction in the number of granules, but no complete loss at 6 hours and 24 hours.

Adenosine triphosphatase staining shows a strongly positive reaction in the endothelium of the vasa recta and a mildly positive reaction in the capillaries of the normal papilla. Six hours after BEA injection there is little change in activity in the vasa recta but some loss in the capillaries. At 24 hours there is reduction and loss in both structures, particularly in the more distal part of the papilla. When BEA is preceded by reserpine there is no reduction or loss of activity in vasa recta at 6 hours and 24 hours. The capillaries retain activity in the proximal one-third of the papilla at 6 hours and 24 hours, but there is reduction at 24 hours in the remainder of the papilla.

Reserpine alone showed some reduced activity of LDH in the dark cells of the collecting ducts, and the granule content of interstitial cells was reduced for this enzyme. These kidneys were examined 24 hours after reserpine administration.

Experiment 5

Before proceeding to describe the changes in the papilla in the various groups following injection of indigo carmine, a brief account of the sequence of changes in the normal rat will be given. Within 3 minutes the ears, nose, paws and buccal mucosa become conspicuously blue. On opening the abdomen the mesenteric blood vessels are seen to be deep red in color. The kidneys are a dusky blue and the bladder is beginning to contain blue-colored urine. Urine passage is manifest as small blue segments some 2 mm in length travelling down the ureter every 3 or 4 seconds.

Group 5A (normal). On inspection of the papilla at the standard

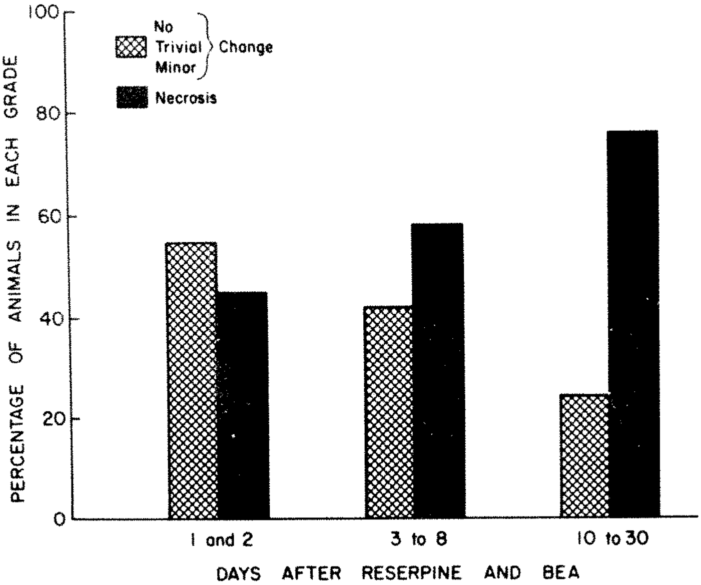

TEXT-FIG 2—Histogram showing 2 grades of change according to time at which animals are killed. This is the same as Text-figure 1 except that no-or-trivial grade has been combined with minor grade. (Group 3A).

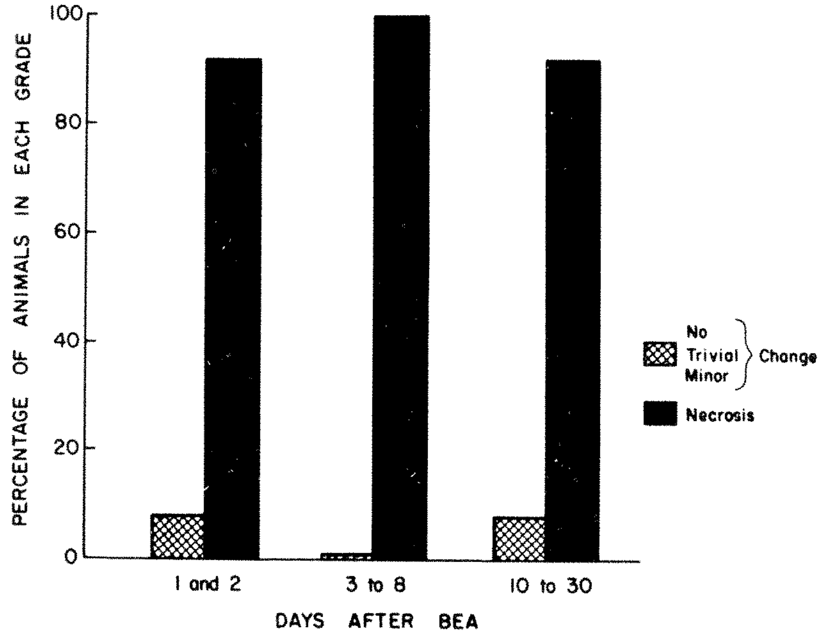

TEXT-FIG 3—Histogram showing the same 2 grades of change as in Text-figure 2, for rats receiving BEA alone. (Group 3C).

time of 10 minutes after indigo carmine injection, there was a characteristic pattern in the normal animal. The surface was glistening except for the area cribrosa at the tip which had a ground glass appearance; the papilla had a light blue color. Collecting ducts were stained an intense deep blue color and the branchings could be seen very clearly (Figures 1, 2). The intense coloration was brought about by the high concentration of indigo carmine in the tubular lumens. Vasa recta and capillaries could be seen as fine red lines, decreasing towards the tip. The substance of the papilla was relatively transparent. Thin limbs could not be identified.

Group 5B (BEA alone). Eleven rats received indigo carmine 1 hour after injection of BEA. At the standard time of 10 minutes after indigo carmine injection it was noted that only 1 animal had a papilla with a pattern similar to that of the normal animals in Group 3A. The other 10 showed sundry minor abnormalities. The collecting ducts, instead of having a continuous homogenous appearance, were made up of discontinuous blue segments or were not identifiable at all (Figure 3). Bladder urine was blue but sometimes of a paler hue. At 2 hours after BEA, 8 rats were studied. The color of the papilla was gray-blue and a band of vascular congestion was noted at the base of the region near the inner stripe of the outer zone. The collecting ducts contained only short lengths of blue staining urine but often were unidentifiable (Figure 4). Bladder urine was much paler than at 1 hour. The 9 rats studied 3 hours after BEA injection had a very pale blue papilla and the collecting ducts could only be discerned occasionally, containing a few isolated blue segments. Bladder urine was clear. At 4 hours (9 rats) and at 5 to 7 hours (9 rats) after BEA injection the papilla was a very pale blue color or, in some cases, white. Collecting ducts could not be identified and the bladder urine was colorless. Beyond this time (13 rats) the papilla was invariably white and no indigo carmine could be discerned. Opaque white segments of the same size as collecting ducts could be made out in the papilla of some animals. The urine was invariably colorless. The results are summarized in Table 3.

Group 5C (Reserpine–BEA). At 1 hour (12 rats) and 2 hours (10 rats) after BEA the indigo carmine pattern was entirely normal (Figure 5), and blue urine was present in the bladder. Of the 8 rats studied 3 hours after BEA, 6 showed a normal pattern (Figure 6), but 2 showed changes similar to the 3 hour animals receiving BEA alone. At 4 to 6 hours the 9 rats showed a normal pattern with blue urine in the bladder. Of the 9 animals studied 1 and 2 days after BEA, 3 showed a pale papilla with no indigo carmine in the collecting ducts and pale urine in the bladder. Six showed minor abnormalities in that the papilla was of a lighter blue color than in a normal animal, and the collecting ducts were only partially filled with indigo carmine; the bladder urine was blue. Animals studied at 3 to 8 days showed 2 to have a pale papilla with no indigo carmine and 5 to have minor abnormalities such as were present in the animals at 1 and 2 days. None of the opaque white lines, such as were seen at comparable times in animals with BEA only, were seen in these 5 rats. The results are summarized in Table 3.

Group 5D (Reserpine alone). A normal pattern was seen in all 5 animals.

Urine output

Text-figure 4 shows the mean 24-hour urine output of a group of 16 rats receiving reserpine (0.75 mg) followed after 18 hours by 50 mg BEA intravenously. This is compared with the mean output of rats receiving BEA alone and a group of control rats receiving no drugs at all. It will be seen that all these patterns are different. Whereas the rats receiving BEA alone show a considerable increase in the urinary output by the end of the first day, those receiving reserpine plus BEA show a gradual increase in output which does not

Table 3—Experiment 5; Indigo-Carmine Pattern in Papilla of Rats According to Regimen Used (Three Pattern Categories are Normal, Minor Changes and Gross Changes)

Group	Time after BEA injection*	No. animals	Normal pattern	Minor changes	Gross changes
5A					
(Normal rats)	—	9	9	0	0
5B					
(Rats receiving BEA alone)	1 h	11	1	10	0
	2 h	8	0	0	8
	3 h	9	0	0	9
	4 h	9	0	0	9
	5–7 h	9	0	0	9
	1–2 d	6	0	0	6
	3–8 d	7	0	0	7
5C					
(Rats receiving reserpine and BEA)	1 h	12	12	0	0
	2 h	10	10	0	0
	3 h	8	6	0	0
	4–6 h	9	9	0	0
	1–2 d	9	0	6	3
	3–8 d	7	0	5	2
5D					
(Rats receiving reserpine alone)	—	5	5	0	0

* h = hours; d = days

reach the levels of the animals with BEA alone until the end of the first week. From this time on the output continues at a steady level somewhat below the volumes for animals receiving BEA alone.

Blood pressure changes

It was found that when 50 mg BEA was injected intravenously into a lightly anesthetized rat with a cannula in the abdominal aorta, there was an immediate fall in blood pressure of 20 to 40 mm Hg. This was present for a very short time, up to 10 seconds, after which the pressure slowly rose to the original level and eventually exceeded this by up to 30 mm Hg. This elevated pressure was maintained for the duration of the recording which was of 1 hour's duration.

When 0.75 mg reserpine was injected 18 hours before BEA the pattern was different. In the first instance the basal intraarterial pressures were slightly lower—as a consequence of the reserpine—and following BEA the drop in pressure was of the order of 20 to 30 mm Hg. This was maintained for 10 to 15 seconds, after which, over the course of the next 2 minutes, the levels present before the injection of BEA were attained. This was not followed by any further rise in pressure as was the case with the rats receiving BEA only.

Catecholamine distribution

In the normal rat kidney it is possible to demonstrate, by their fluorescence, small nerves accompanying the vasa recta and tubules in the outer medulla. One hour after BEA administration the nerves were depleted of catecholamines, as indicated by a loss of fluorescence. There was no restoration for the following 6 hours. Reserpine causes a depletion when tissues are tested after 24 hours.

Discussion

Bromoethylamine hydrobromide has the unique property of producing necrosis of the renal papilla without, as a rule, at the same time producing any significant changes in the cortex. Changes that occur in the cortex are secondary to those that occur in the papilla and do not develop until the latter are severe. An occasional animal, however, does develop necrosis of the cortical tubules, but this change is exceptional.

The mechanism by which papillary necrosis is caused by this compound is unknown, but there are two main possibilities. First, it could be an interference with the blood supply to the papilla, either by organic blockage of the vasa recta or juxtamedullary arterioles, or by intense constriction of these vessels. Second, it could be a direct

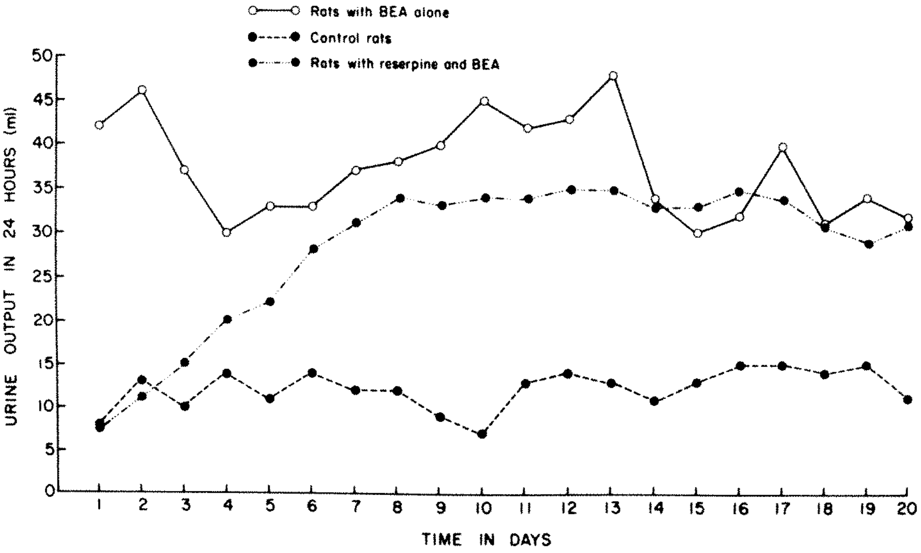

TEXT-FIG 4—Twenty four hour urinary output of rats receiving BEA alone, normal rats and rats receiving reserpine followed by BEA.

poisoning of the cells of the limbs of Henle and collecting ducts, with diffusion of the compound into the interstitial substance causing destruction of other structures such as the interstitial cells.

Our previous light and electron microscopic studies [1,2] have indicated that there is no organic blockage by platelets or fibrin during the early stages of developing papillary necrosis. Further evidence against this idea is provided by Experiment 1, in which sulfinpyrazone, a drug which prevents formation of platelet aggregates, has no protective effect against BEA. Similarly, in Experiment 1 it was not possible to prevent papillary necrosis in animals receiving heparin. It can therefore be reasonably assumed that organic blockage by platelets or fibrin plays no part in the early changes leading to papillary necrosis. Fuwa and Waugh [6] were also unable to detect any capillary thrombi using the same experimental model; Davies,[7] using a similar compound (vinylamine) in the rabbit, was of the opinion that organic blockage to blood vessels was not the pathogenetic mechanism. Likewise, Ljungqvist and Richardson [8] and Ljungqvist *et al* [9] were unable to demonstrate blockage of the vasta recta using microangiography and electron microscopy in the serum-induced papillary necrosis model in the rat. They were also unable to prevent the necrosis using anticoagulation. On the other hand it should be stated that organic blockage of the vasa recta by platelets in serum-induced papillary necrosis has been claimed by Wizgird *et al* [10] and Lee *et al.*[11] In the analgesic-induced papillary necrosis model in the rat, Kincaid-Smith *et al* [12,13] have described reduced numbers and dimensions of the vasa recta. In spite of the absence of organic vascular lesions in our studies, it would still be possible for vasoconstriction to be a factor, and the main part of this study explores this possibility.

Bromoethylamine hydrobromide was shown to have a certain amount of pressor activity when tested in the dosage used to produce papillary necrosis. It has been shown by several authors [14-16] that there is a tautomeric equilibrium in solution between bromoethylamine hydrobromide and ethylenimonium (azeridine) bromide:

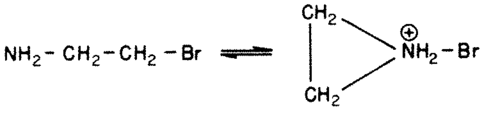

Bromoethylamine hydrobromide **Ethylenimonium (azeridine) bromide**

Larsen,[17] in a review of the chemical evidence, has shown that for α-adrenergic agonists, the characteristic catecholamine seems to be an azeridine.

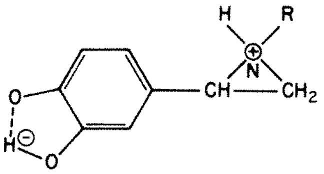

Azeridine form of norepinephrine

Since BEA and the receptor activating portion of the norepinephrine molecule have the same chemical conformation, the drug could function as a norepinephric sympathomimetic amine, mobilizing norepinephrine, or as a partial norepinephric agonist. In either case it could act with sufficient intensity to cause peripheral vasoconstriction. If α-receptor-induced vasoconstriction was the cause of BEA-mediated papillary necrosis then it should be possible to inhibit this action by blocking the α-receptors before giving the drug. Experiments were performed to test this. *Chlorpromazine*, a drug with some α-blocking activity gave partial protection against necrosis in 3 of 13 animals; *phenoxybenzamine* gave varying degrees of protection in 4 out of 14 animals. Although a definite effect was obtained with both drugs it was felt that the results were not as promising as those obtained with reserpine; therefore no further studies were made. The poorest results were obtained with *6-hydroxydopamine*, a rapid and potent depleter of endogenous norepinephrine; depletion was due mainly to destruction of adrenergic nerves.[18-21] All 8 rats treated with the drug showed papillary necrosis. Malmfors[22] has shown that the effects of 6-hydroxydopamine vary between different individual neurons, in different organs and when injected at different ages, which may account for its failure to protect. Therefore, no further investigation with this drug was made because of the large number of animals which would have been required to isolate the variables and define the optimum conditions for experimentation. On the other hand, *reserpine*, a compound which depletes nerve endings of most of their catecholamine, allowed BEA to produce papillary necrosis, or the changes we know precede papillary necrosis, in only 4 of the initial 12 animals studied earlier. It was felt that these results merited a more detailed investigation of the effects of this compound.

In Experiment 3, the effects of reserpine were studied histologically. In the total group of animals receiving 0.75 mg reserpine before injection of BEA, there was a 60% incidence of papillary necrosis compared with over 95% in animals receiving BEA alone. No less than 21% had either *no change* or only *trivial changes*, a figure that should be compared with 1.6% in animals treated with BEA alone.

Nineteen percent of animals pretreated with the same dose of reserpine had only *minor lesions*. These figures are more convincing during the early stages following BEA injection. The histograms in Text-figures 1, 2 show how reserpine has its most potent effect during the first 2 days after BEA administration, how it still exerts a similar effect in rats studied between 3 and 8 days, but how in long term animals it allows papillary necrosis to develop in 76% of rats. The larger dose of reserpine (1.5 mg) showed no improvement on these figures; in fact the results were less good. Before discussing the implications of these findings, evidence from the other experiments should be considered.

Histochemical studies were carried out only during the first 24 hours. There were decided differences between animals treated with reserpine and BEA, and animals receiving BEA only. The loss of LDH from collecting ducts and limbs of Henle was less in those receiving reserpine; the same held true for the LDH content of interstitial cells. The activity of ATPase in the vasa recta was little altered up to 24 hours in rats receiving reserpine; activity in the capillaries, although being reduced in the distal two-thirds of the papilla, was little affected in the proximal one-third. Thus there was substantial prevention of the renal changes of BEA during the first 24 hours.

The ability of a kidney to exhibit a normal indigo carmine pattern is probably related to the ability to concentrate urine, the dense staining of the collecting ducts representing the presence of concentrated indigo carmine in the tubular lumen. The indigo carmine pattern of the papilla deviated very significantly from that of normal animals during the first few hours following the administration of BEA; in fact, even at 1 hour, 10 out of 11 rats showed some degree of change and at 2 hours gross deviation was found in all 8 animals. This abnormal pattern was constant from this time onwards. Functional changes therefore occurred at a very early stage. When reserpine preceded BEA, a normal pattern was preserved in each of 39 animals until 6 hours following BEA injection. Changes occurred in animals at 1 to 2 days and at 3 to 8 days, but these were often not so severe as those seen with BEA alone.

Urine output was considerably increased even during the first day following BEA. Pretreatment with reserpine prevented this early rise in output, and although urinary outputs almost as high as those with BEA alone were eventually reached, several days were required before these levels were attained.

There is, therefore, good evidence from these studies that reserpine has a decided effect on the necrotizing action of BEA. It is also apparent that the effect is maximal during the early stages and decreases considerably in effectiveness in animals tested after several days. In fact, if only animals of over 9 days post-BEA are considered, it is found that reserpine gives protection in less than 25% of animals studied. The main action appears to be one of delaying the sequence of events leading up to necrosis, although certain animals seem to be absolutely protected. How, then, can these various observations be reconciled with the known actions of reserpine? Both reserpine and the norepinephric sympathomimetic amines release norepinephrine from stores in the tissues.[23-29] Reserpine also blocks the cellular synthesis and uptake of norepinephrine into storage vesicles for 24 hours after its administration. These functions are slowly recovered during the succeeding 48 hours and are completely restored by the eighth day.[30] After depletion of norepinephrine by reserpine, the α-receptors are supersensitive to the action of norepinephrine[24,31] and insensitive to the pressor action of the norepinephric sympathomimetic amines.[29] If BEA acts as a norepinephric sympathomimetic amine, and if the effects on the papilla are brought about by its action on the vessels supplying the papilla, then the known pharmacologic properties of reserpine would be expected to ameliorate the lesion during the early stages (but not at later ones); assuming that BEA persisted for several days, it would thus outlast the protective action of reserpine. This, in fact, was the general finding.

Our results appear consistent with the idea that BEA acts by producing a degree of ischemia sufficient to cause necrosis of the papilla. However, we cannot accept this with absolute certainty for the following reasons. First, such an explanation would require BEA to act more intensely on the vessels supplying the papilla than elsewhere in the kidney. Ljungqvist and Wagermark[32] have clearly shown that vessels supplying the papilla have demonstrable adrenergic fibers at their origin, although the cortex also has profuse innervation. We have shown that BEA depletes the medullary norepinephrine stores. If the arterioles supplying the papilla were to have a higher density of effective α-receptors than elsewhere in the kidney, then the norepinephrine released would produce a relatively greater degree of vasoconstriction at that site. It must be stressed, however, that in the absence of any knowledge on the distribution of α-receptors this postulate is only speculation. Second, the pressor activity of BEA is not great; the rise in blood pressure following its administration was only

30 mm Hg in the anesthetized rat. This suggests that vasoconstriction is not intense; it must be mentioned, however, that we have little information on the papillary circulation following Bea. Third, we have been unable to find any record of papillary necrosis in animals subjected to continuous injection of renin or norepinephrine. Fourth, Fuwa and Waugh[6] showed that the diuretic state affords some protection against necrosis; we have been able to demonstrate some degree of protection by chlorthiazide. It is difficult to reconcile these observations with a powerful vasoconstrictive action, although admittedly we lack adequate knowledge of the vascular responses in the diuretic state. The alternative pathogenesis is direct toxic effect on the papillary tubules and, secondarily, on the other structures in the papilla in concentrating urine. A high concentration of the compound would be achieved in the papilla, a fact that would explain the presence of necrosis in the papilla and a sparing of the cortex in most animals. This mechanism is difficult to reconcile with the known actions of reserpine. We know of no evidence to show that reserpine can protect against the direct action of toxic agents. Also, because of the rapidity with which the indigo carmine pattern is upset, it is necessary to suggest early damage to papillary structures. Cellular damage is not apparent in tubules either ultrastructurally or histochemically at a time when the indigo carmine pattern is first upset. It is appreciated that these technics may not be capable of detecting early changes. Again, a cellular exudate has not been found in the papilla with any frequency. Allowing for the fact that the papilla is slow to mobilize inflammatory cells, lack of an inflammatory response is not altogether in favor of a necrosis produced by poisoning of capillary constituents.

Thus, although we have good evidence for the ability of reserpine to modify the sequence of events brought about by BEA, we are in no position to make a categorical statement on the pathogenesis of the necrosis. Our failure to come to any definite conclusions is perhaps a reflection on the overall lack of knowledge of the hemodynamics and nervous innervations of the papilla.

References

1. Murray G, Wyllie RG, Hill GS, Ramsden PW, Heptinstall RH: Experimental papillary necrosis of the kidney. I. Morphologic and functional data. Am J Pathol 67:285–302, 1972
2. Hill GS, Wyllie RG, Miller M, Heptinstall RH: Experimental papillary necrosis of the kidney. II. Electron microscopic and histochemical studies. Am J Pathol 68:213–234, 1972

3. Barka T, Anderson PJ: Oxidative enzymes in histochemistry. New York, Harper and Row Publishers, Inc, 1963, pp 296–333
4. Wachstein M, Meisel E: Histochemistry of hepatic phosphatases at a physiologic pH. Am J Clin Pathol 27:13–23, 1957
5. Spriggs TLB, Lever JD, Rees PM, Graham JDP: Controlled formaldehyde-catecholamine condensation in cryostat sections to show adrenergic nerves by fluorescence. Stain Technol 41:323–327, 1966
6. Fuwa M, Waugh D: Experimental renal papillary necrosis. Arch Pathol 85:404–409, 1968
7. Davies DJ: The structural changes in the kidney and urinary tract caused by ethyleneimine ("vinylamine"). J Pathol 97:695–703, 1969
8. Ljungqvist A, Richardson J: Studies on the pathogenesis of serum-induced renal papillary necrosis in the rat. I. Stereo-microangiographic and histologic examination of the renal lesion in nonheparinized and heparinized animals and in animals given diuretic drugs. Lab Invest 15:1395–1401, 1966
9. Ljungqvist A, Osvaldo-Decima L, Richardson J: Studies on the pathogenesis of serum-induced renal papillary necrosis in the rat. III. The early morphologic changes studied by light and electron microscopy. Lab Invest 17:447–457, 1967
10. Wizgird JP, French SW, Coulson W: Pathogenesis of serum-induced papillary necrosis. Arch Pathol 79:57–64, 1965
11. Lee JC, French SW, Wizgird JP, Hopper J Jr: Early morphologic changes in serum-induced renal papillary necrosis. Light and electron microscopic studies. Lab Invest 17:458–464, 1967
12. Kincaid-Smith P, Saker BM, McKenzie IFC: Lesions in the vasa recta in experimental analgesic nephropathy. Lancet 1:24, 1968
13. Kincaid-Smith P, Saker BM, McKenzie IFC, Muriden KD: Lesions in the blood supply of the papilla in experimental analgesic nephropathy. Med J Aust 1:203–206, 1968
14. Howard CC, Marckwald W: Zur Constitution des Vinylamins. Ber Deut Chem Ges 32:2036–2038, 1899
15. Freundlich H, Neumann W: Über die Kinetik der Umwandlung von Halogenalkylaminen in heterocyklische Verbindungen. Z Physik Chem (Leipzig) 87; 69–86, 1914
16. Freundlich H, Salomon G: Über die Erhöhung der Lebensoauer des β-phenyl-β-chlorothylamins an Kohle. Z Physik Chem (Leipzig) 116:179–204, 1933
17. Larsen AA: Catecholamine chemical species at the adrenergic receptors. Nature 227:224–225, 1968
18. Porter CC, Totaro JA, Stone CA: Effects of 6-hydroxydopamine and some other component on the concentration of norepinephrine in the hearts of mice. J Pharmacol Exp Ther 140:308–316, 1963
19. Laverty R, Sharman DF, Vogt M: Action of 2, 4, 5-trihydroxyphenlyethylamine on the storage and release of noradrenaline. Br J Pharmacol 24:549–560, 1965
20. Tranzer JP, Thoenen H: Ultramorphologische Veränderingen der sympathischen Nervendigungen der Katze nach Vorbenhandlung mit 5-and 6-hydroxy-dopamin. Naunyn-Schmiedebergs Arch Exp Pathol Pharmakol 257:343–344, 1967

21. Thoenen H, Tranzer JP: Chemical sympathectomy by selective destruction of adrenergic nerve endings with 6-hydroxydopamine. Naunyn-Schmiedebergs Arch Exp Pathol Pharmakol 261:271–288, 1968
22. Malmfors T: The effects of 6-hydrovydopamine on the adrenergic nerves as revealed by the fluorescence histochemical method. 6-Hydroxydopamine and Catecholamine Neurones. Edited by T Malmfors, H Thoenen. Amsterdam, North Holland Publishing Co, 1971, pp 47–58
23. Burn JH, Rand MJ: Noradrenaline in artery walls and its dispersal by reserpine. Br Med J 1:903–908, 1958
24. Burn JH, Rand MJ: The action of sympathomimetic amines in animals treated with reserpine. J Physiol 144:314–336, 1958
25. Lockett MF, Eakins KE: The release of sympathetic amines by tyramine from the aortic walls of cats. J Pharm Pharmacol 12:720–727, 1960
26. Hertting G, Axelrod J, Patrick RW: Action of cocaine and tyramine on the uptake and release of ^{3}H-norepinephrine in the heart. Biochem Pharmacol 8:246–247, 1961
27. Lindmar R, Muschool E: Die Wirkung von Cocaine Guanethedine, Reserpine, Hexamethonium Tetracaine und Psicain auf die Noradrenaun freisetzung aus dem Herzen. Naunyn-Schmiedebergs Arch Exp Pathol Pharmarkol 242:214–217, 1961
28. Potter LT, Axelrod J, Kopin IJ: Differential binding and release of norepinephrine and tachyphylaxis. Biochem Pharmacol 11:254–256, 1962
29. Axelrod J, Gordon E, Hertting G, Kopin IJ, Potter LT: On the mechanism of tachyphylaxis to tyramine in the isolated rat heart. Br J Pharmacol 19:56–63, 1962
30. Viveros OH, Arqueros L, Connett RJ, Kirshner N: Mechanism of secretion from theadrenal medulla. IV. The fate of the storage vesicles following insulin and reserpine administration. Mol Pharmacol 5:69–81, 1969
31. Trendelenburg U: Supersensitivity and subsensitivity to sympathomimetic amines. Pharmacol Rev 15:225–276, 1963
32. Ljungqvist A, Wagermark J: The adrenergic innervation of intrarenal glomerular circulatory routes. Nephron 7:218–229, 1970

Acknowledgments

Dr. Murray is a Kellogg Fellow; his present address is Casilla-6539, Correo 4, Santiago, Chile.

1

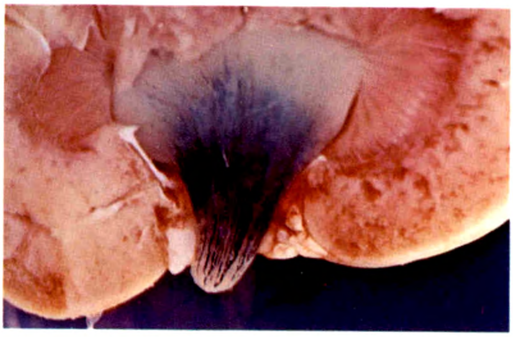

2

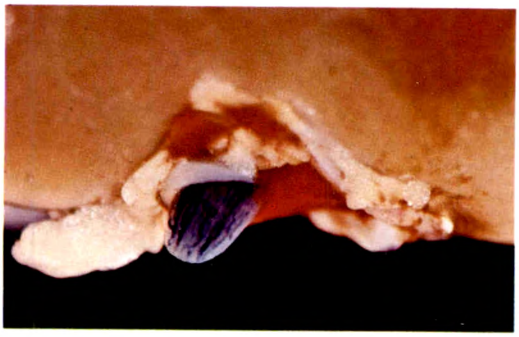

3

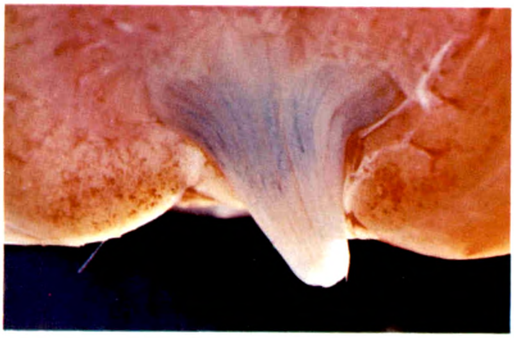

4

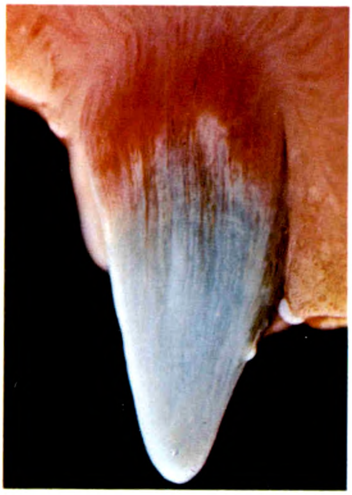

5

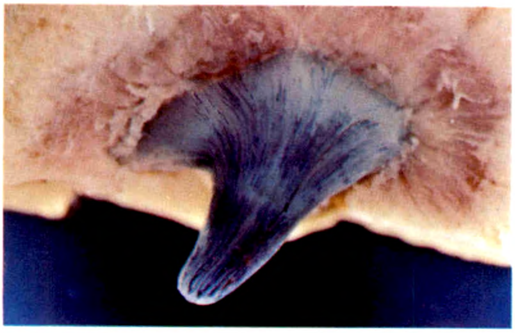

6

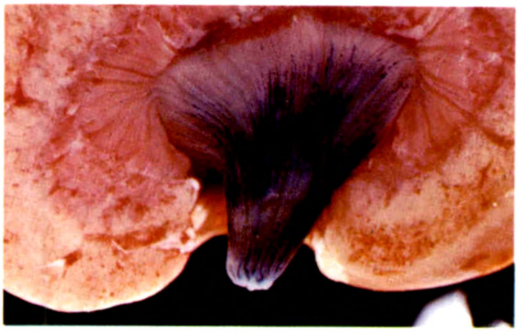

Fig 1—Normal indigo carmine pattern 10 minutes. In this and the other animals illustrated, the injection of indigo carmine was made 10 minutes before the animal was killed.

Fig 2—Normal indigo carmine pattern with well filled collecting ducts.

Fig 3—Indigo carmine pattern 1 hour after injection of BEA. The distal half of the papilla is pale and shows no filling of the collecting ducts.

Fig 4—Indigo carmine pattern 2 hours after BEA injection. The pale blue background is common in the early stages following BEA. The collecting ducts are not filled.

Fig 5—Indigo carmine pattern 2 hours after BEA injection, reserpine having been injected 18 hours previously. The pattern is normal with good filling of collecting ducts.

Fig 6—Indigo carmine pattern 3 hours after BEA injection, reserpine having been injected 18 hours previously. Pattern similar to Figure 5.

Lysosome and Phagosome Stability in Lethal Cell Injury

Morphologic Tracer Studies in Cell Injury Due to Inhibition of Energy Metabolism, Immune Cytolysis and Photosensitization

Hal K. Hawkins, MD, PhD, Jan L. E. Ericsson, MD, Peter Biberfeld, MD and Benjamin F. Trump, MD

In two types of cell injury in a tissue culture system, the possibility was tested that lysosome rupture may be a lethal cellular reaction to injury, and thus an important general cause of irreversibility of damage in injured tissue. Prior labeling of secondary lysosomes with the fluorochrome acridine orange, or with ferritin, was used to trace changes in lysosomes after applying an injury. The metabolic inhibitors iodoacetate and cyanide were used together to block the cell's energy supply, or attachment of antiserum and subsequent complement attack were used to damage the surface membrane, producing rapid loss of cell volume control. Living cells were studied by time-lapse phase-contrast cinemicrography and fluorescence microscopy, and samples were fixed at intervals for electron microscopy. The cytolytic action of complement was lethal to sensitized cells within 2 hours, but results showed that lysosomes did not rupture for approximately 4 hours and in fact did not release the fluorescent dye until after reaching the postmortem necrotic phase of injury. Cells treated with metabolic inhibitors also showed irreversible alterations, while lysosomes remained intact and retained the ferritin marker. The fluorochrome marker, acridine orange, escaped from lysosomes early after metabolic injury, but the significance of this observation is not clear. The results are interpreted as evidence against the concept that lysosome rupture threatens the survival of injured cells. The original *suicide bag* mechanism of cell damage thus is apparently not operative in the systems studied. Lysosomes appear to be relatively stable organelles which, following injury of the types studied, burst only after cell death, acting then as scavengers which help to clear cellular debris (Am J Pathol 68:255–288, 1972).

DURING THE PAST TEN YEARS, the concept has frequently been advanced that lysosomes may burst open within injured but still living cells, and that the subsequent release of hydrolytic enzymes into the cell sap and inappropriate self-digestion may be significant

---

From the Department of Pathology, Duke University Medical Center, Durham, NC and the Department of Pathology, Karolinska Institute, Sabbatsberg, Sjukhus, Stockholm, Sweden.

Supported by Grants AM-10698 and GM-01678 from the National Institutes of Health and Grant B71-12X-1006C-06C from the Sweden Medical Research Council.

Accepted for publication May 1, 1972.

Address reprint requests to Dr. Hal K. Hawkins, Department of Pathology, Box 3712, Duke University Medical Center, Durham, NC 27710.

factors in causing the death of the cell.[1-3] This hypothesis has two parts: first, that release of enzymes from lysosomes should occur, following a specific injury, prior to the time of cell death; and second, that this extent of antemortem enzyme release should be sufficient to cause the death of injured cells in some cases. Cell death is considered to occur when cell injury becomes irreversible—*ie*, the cell is dead at the time when it loses its ability to recover normal functions if the injury were removed. Events occurring after cell death comprise the phase of cellular necrosis.[4]

A great deal of biochemical evidence, taken from many different models of cell injury, has been presented in support of the concept of lysosomes as threats to the survival of injured cells. In most cases the data are insufficient to firmly establish this concept, however, since it is very difficult, if not impossible, to distinguish the enzyme release from lysosomes which might occur in intact injured cells from the enzyme solubilization which occurs during the processes of homogenizing the cells and preparing subcellular fractions. This induced solubilization may well be greater when injured cells are homogenized. Some histochemical studies have been interpreted as suggesting rupture of lysosomes before cell death,[5,6] and some have yielded evidence inconsistent with this interpretation.[7-9] Electron microscopic studies of well-controlled models of cell injury have generally failed to provide evidence for antemortem lysosome rupture,[8-10] but this negative evidence is inconclusive, because of the vagaries of fixation in injured cells and the uncertainty as to the expected appearance of cells whose lysosomes have discharged their enzymes. Previous studies have failed to disclose evidence of perilysosomal deterioration; however, even if lysosomal enzymes were released, it has been suggested that they would diffuse rapidly throughout the cell.[11]

The present study is an effort to estimate the time of bursting of lysosomal membranes relative to other changes of cell injury and necrosis in tissue culture cells derived from human liver (Chang, 1956). Before injury, the cells were induced to form many secondary lysosomes containing both enzymes and extraneous tracer substances which could be observed at will by morphologic technics. Cells were observed by fluorescence microscopy following labeling of lysosomes with acridine orange dye and during their subsequent reaction to injury. In parallel experiments, cells loaded with ferritin before injury were fixed at intervals and examined by electron microscopy. Two modes of rapidly lethal cell injury were applied. The first mode consisted of incubating cells with relatively high doses of sodium iodoacetate, potassium cyanide, or both, to inhibit the Embden-Meyerhof and oxidative routes of cellular energy metabolism. The other injury was applied by incubating cells with cell-directed antiserum without complement, then washing and exposing the cells to complement in order to produce rapid immunologic damage to the cell surface membrane. The results indicated release of acridine orange dye from lysosomes before irreversible changes were seen after metabolic injury. Release of dye occurred, however, only after apparent cell death following immune cytolysis. It is uncertain exactly what changes in the lysosomal membrane were indicated by this loss of acridine orange labeling. Following both modes of injury, ferritin was not released from within secondary lysosomes until the postmortem phase of cell necrosis, when irreversible structural alterations had already occurred.

Materials and Methods

Cells

Chang tissue culture cells, originally derived from human liver,[12] were maintained as monolayers in Parker's or Eagle's media supplemented with 10% fetal calf or horse serum, penicillin, streptomycin and glutamine. Chang cell suspension cultures were kindly provided by Dr. Eva Eliasson, Wenner-Gren Institute, Stockholm, Sweden; in later work a derivative of the Chang cell line of the American Type Culture Collection was used.

Observation Chambers

Cells were grown in sterile Sykes-Moore double-coverslip chambers,[13] or in a simple enclosed chamber fabricated from a microscope slide and cover slip, dental wax and Parafilm. For fluorescence studies in which a larger surface area of cells was needed, cells were grown on oversized coverslips (Carolina Biological Supply Co) in Falcon plastic petri dishes, and were inverted onto a shallow (1 mm) well in a Lucite sheet. Coverslips were held in place either by a spring clip or by another sheet of Lucite attached around the shallow well. All chambers were made to fit the mechanical stage of the microscope and included ports fitted with catheters so that the media could be changed at will. Although the first light-microscopic observations were made at room temperature, all results were confirmed using Sykes-Moore chambers maintained at 37 C by a homemade, thermistor-controlled, air-curtain incubator.[13]

Markers

Euchrysine 3R from E. Gurr Ltd, London (Michrome 1197; Color Index 46005), was stored as a 10^{-3} g/ml aqueous solution. Euchrysine is a commercial name for the dye usually called acridine orange. Cell monolayers were exposed to a 1:100 dilution of this dye solution in the standard medium (10^{-5} g/ml) for 15 minutes; they were then incubated in fresh medium without dye for at least 60 minutes before any further handling. This resulted in bright red fluorescent granular staining in the cytoplasm, with faint green nuclear fluorescence. Lower concentrations of dye were found to produce this pattern if larger volumes were used.

By light and electron microscopy, cells appeared unchanged after this treatment, and mitotic cells with granular fluorescence could be observed on the following day. Furthermore, specific activities of the four lysosomal enzymes assayed were normal in cells exposed to acridine orange.

Ferritin, 2X crystallized cadmium-free (Pentex), was passed through a column of Sephadex G-25 (coarse), centrifuged for 2 hours at 100,000g and redissolved in the standard medium at 15 to 25 mg/ml. Monolayers were exposed to this medium overnight (12 to 18 hours) and the medium was changed 1 hour before the start of the experiment.

Phase-Fluorescence Microscopy

Cells on coverslips were observed using either Reichert *Anoptral* or Leitz *Heine* phase-contrast optics, with a green filter. Fluorescence microscopy was done using an HBO-200 mercury arc source, Jena UG-1 source filter, Leitz 510 nm barrier filter, and a Leitz long-working-distance dark-field condenser. Photographs were taken on Kodak Ektachrome HS 35 mm film, daylight type, ASA 160. Time-lapse phase-contrast movies were taken of the cells' reactions to each type of injury, using a Sage time-lapse unit with shutter and a Bolex 16 mm camera, on Kodak Tri-X or Plus-X reversal film.

Electron Microscopy

Cells grown in Falcon plastic dishes were fixed in ice-cold 3% glutaraldehyde for 30 minutes, washed and postfixed overnight in sucrose-containing 1% osmium tetroxide. Alternatively, monolayers were fixed for 30 minutes on ice in a freshly prepared cacodylate-buffered mixture containing glutaraldehyde (4%) and osmium tetroxide (1%),[14,15] then stained in Veronal-buffered uranium acetate for 30 minutes.[16] After dehydration in graded alcohol solutions, 2 to 4 ml of propylene oxide were added to each dish. A few seconds after partial dissolution of the plastic substrate, the sheets of cells floated free; the released monolayer fragments were poured into vials of propylene oxide and washed several times to remove dissolved plastic.[17] The monolayers were then infiltrated with epoxy resin and embedded in Epon 812 according to Luft,[18] or in an Epon-Araldite mixture. Thin sections were stained with uranium acetate and alkaline lead hydroxide, or with uranium acetate alone, and examined in Siemens Elmiskop 1 or Hitachi HS-8 electron microscopes. Unless otherwise noted, all electron micrographs shown are of cells fixed in the glutaraldehyde-osmium mixture and stained only with uranium acetate.

Photosensitization

In order to demonstrate that lysosome rupture would cause release of the ferritin marker to the cell sap space, and that ferritin would remain in that space throughout processing for electron microscopy, a positive control experiment was carried out. Cells which had phagocytized ferritin overnight as described were also treated with acridine orange as above, and fluorescence observation revealed bright red granular fluorescence as usual. These cells were then placed on the microscope base and irradiated for 30 minutes with filtered (BG-12) blue-violet light from the HBO-200 mercury arc light source. The monolayer was fixed in the glutaraldehyde-osmium mixture and processed for electron microscopy as described. According to Allison,[19] such intense irradiation with light absorbed by the dye in lysosomes would be expected to cause photooxidative damage to the lysosomal membrane.

Enzyme Assays

Total activities of 4 lysosomal enzymes (acid phosphatase, aryl sulfatase, β-glucuronidase and cathepsin) were measured in homogenates of acridine orange-treated cells and compared with those in control cells. Two Falcon petri plates were inoculated with the same number of cells, and when both were confluent, one was treated with acridine orange as described. Cells were removed from each plate by scraping with a rubber policeman, frozen, suspended in deionized water, homogenized with 10 strokes of a Potter-type homogenizer and then frozen and thawed 10 times in deionized water containing 0.1% Triton X-100. Cathepsin D was assayed at pH 3.6 with acid denatured bovine hemoglobin (1.75 w/v) (Sigma) as the substrate.[20] Acid phosphatase was measured at pH 5.4 with β-glycerophosphate (63 mM) as the substrate.[21] Aryl sulphatase was determined at pH 5.7 according to the method of Roy [22] as modified by Bowers *et al.*[21] The activity of β-glucuronidase was estimated at pH 5.7 with phenolphthalein-glucuronic acid (1.25 mM) (Sigma) as the substrate.[21] Protein was determined by the method of Lowry *et al.*[23]

Histochemistry

In order to validate the use of ferritin as a tracer for secondary lysosomes in this system, acid phosphatase electron microscopic histochemical staining was performed on untreated and ferritin-loaded cells. Monolayers in 60 mm plastic Petri dishes were fixed for 10 minutes at room temperature in 4% glutaraldehyde buffered with 0.1 M sodium cacodylate. The monolayers were then washed for 1 hour in 0.1 M cacodylate buffer and incubated for acid phosphatase activity for 30 minutes, according to Gomori.[24] After incubation the monolayers were post-fixed for 1 hour in cacodylate-buffered 2% osmium tetroxide and processed for electron microscopy.

Cell Injury Protocols

Metabolic

Cells in the logarithmic phase of growth were washed twice in serum-free medium, and 30 minutes later were exposed to serum-free medium which was 10 mM in iodoacetic acid (IAA) and 5 mM in potassium cyanide (KCN). As controls, cells were incubated in serum-free medium or in medium containing only KCN or IAA. In other experiments IAA and/or KCN were present in complete medium (containing serum). The chemicals used were reagent grade, and all stock solutions were titrated to pH 7.0. The cells' responses were recorded continuously by time-lapse, phase-contrast microscopy, and in other experiments samples were fixed for electron microscopy 30, 60, 90, 120, 360 and 240 minutes after poisoning.

Cytolytic

Cells were exposed for 10 minutes to standard medium containing 5 or 10% immune rabbit serum. This antiserum was prepared by repeated injections of whole Chang cells in Freund's adjuvant, and was heat inactivated before use (56 C, 30 minutes). The titer of the antiserum was 6400 when tested by the mixed hemadsorption test.[25] The monolayer was then washed twice in standard medium, and 20 minutes later was exposed to medium containing 10% guinea pig serum as a source of complement. Controls consisted of treatment with immune serum or guinea pig serum alone.

Results

Definitions

The terminology used in this paper for the various parts of the lysosomal system was proposed by DeDuve and Wattiaux.[26] *Primary lysosomes* contain only enzymes and other components characteristic of all lysosomes of a tissue and have never participated in a digestive event. *Secondary lysosomes* are or have been involved in a digestive process and, in addition to the components of primary lysosomes, may contain additional material from within the cell (autolysosomes) or from outside the cell (heterolysosomes), in any stage of digestion. *Phagosomes* are considered to be either membranes with enclosed intracellular material (autophagosomes) or plasma membrane derivatives with enclosed extracellular material (heterophagosomes), but are devoid of lysosomal hydrolases. After fusion with primary or secondary lysosomes, phagosomes would become incorporated into new secondary lysosomes.

The terms *rupture, bursting,* and *breaking* of lysosomes are used synonymously in this paper and refer to the appearance, for any length of time, of a defect in the lysosomal membrane large enough to be easily demonstrable by electron microscopy if preservation and orientation of the tissue were ideal—ie, 100 Å or larger in its smallest dimension.

Increases in the permeability of the lysosomal membrane, or in the number of compounds which could cross the membrane freely, could conceivably occur without rupture.

Characteristics of Markers

Acridine orange was accumulated by living cells to give bright red lysosomal fluorescence under appropriate conditions, as previously reported[27,28] (Figure 5). The minimum concentration of dye which gave useful fluorescence was about 10^{-6} g/ml if adequate volumes were used. Concentrations above 10^{-4} g/ml at first gave extensive orange cytoplasmic staining which later disappeared in most cells as the fluorescent granules became larger and brighter. Acridine orange dye exhibits concentration-dependent metachromasia, so that concentrations of 10^{-3} g/ml or more in water show maximum fluorescence above a wavelength of 580 nm (red), and concentrations of 10^{-4} g/ml or less fluoresce maximally around 530 nm (green). Similarly, small amounts of dye bound to macromolecules such as DNA fluoresce green, whereas if more dye is bound, the fluorescence color changes to red. A detailed theory developed by Bradley[29] accounts for these fluorescence color changes on the basis of the self-association of single dye molecules (which fluoresce green) into dimers with a characteristic red fluorescence emission. Whenever a given amount of acridine orange is concentrated into a small enough volume or a small enough number of binding sites, the proportion of dimers increases and red fluorescence is observed. If this amount of dye gains access to a larger volume or many more binding sites, the dimers dissociate and the fluorescence color changes to green. When dye diffuses away from the lysosomes, therefore, the resultant cytoplasmic and nuclear staining should be bright green, and this was consistently observed. Since red and green are primary colors, this color shift is very striking to the eye and readily recorded on color film.

Assay of 4 lysosomal enzymes showed approximately the same activities in homogenates of cells treated with Euchrysine 3R as in homogenates of identical untreated cultures. Thus the fluorescent marker did not inhibit lysosomal enzymes in the doses used.

Overnight incubation of monolayers with ferritin resulted in accumulation of many well-filled heterophagosomes and heterolysosomes in all cells; several were visible in nearly all random sections (Figure 1). The ferritin-containing structures were predominantly multivesicular bodies. In cells loaded with ferritin and incubated for the ultrastructural demonstration of acid phosphatase, reaction product was regularly found within ferritin-containing multivesicular bodies (Figure 4). Reaction product was present in similar structures in cells which were not exposed to ferritin. With the procedure described ferritin does appear to mark sites of acid phosphatase activity, which must be (heterophagic) secondary lysosomes. Single ferritin molecules could easily be recognized in electron micrographs by the high electron density, characteristic size (60 Å) and irregular shape of the iron core. The cells continued to grow and divide quite well in the ferritin-containing medium.

The observed uptake of ferritin was in agreement with previous findings in this laboratory on phagocytic pathways in HeLa cells.[30] According to those studies and the present work, particulate tracers appear to be taken in by cells in small vesicles which rapidly fuse into larger phagocytic vesicles and then internalize part of the vesicle membrane to form multivesicular bodies. Concurrently, within about an hour, fusion occurs with small primary lysosomes or secondary lysosomes, forming new heterophagic secondary lysosomes, which are also multivesicular bodies morphologically. The membranes of these secondary lysosomes presumably include both material derived from the plasma membrane and other membrane derived from primary lysosomes. With extensive, rapid loading, it may be possible to incorporate most if not all of the cell's primary lysosomes into new secondary lysosomes. In rat liver loaded with Triton WR-1339, for example, the bulk of all acid hydrolases are found in vesicles (secondary lysosomes) which contain phagocytized Triton and thus have a lower than normal density.[1,31]

Phase-Contrast Cinemicrography and Fluorescence Studies

Continuous phase-contrast observation of cells spread on coverslips in a 37 C chamber revealed a characteristic, quite distinct pattern of reaction to each type of injury. The same sequence of changes was observed in each case whether or not the cells had been prelabeled with acridine orange.

Metabolic Injury

Cells treated with KCN and IAA in serum-free medium showed no changes at first, but after approximately 10 minutes, nuclear chromatin began to clump and marginate slowly. Fifteen to twenty minutes after adding the inhibitors, the normal surface ruffling and orderly spreading was lost, and long tubular extensions formed at the cell surface membranes; some of these formed vesicles at their tips, which later seemed to pinch off and float away. These tubular membrane extensions showed continuous disorderly, asynchronous writhing motions. Between 30 and 90 minutes of incubation the fibrillar network of organelles in the Golgi region changed to a pattern of many small round densities (Figure 8). By 1 hour after beginning the injury a few phase-lucent vacuoles appeared near the cell center and slowly enlarged in most cells. By 90 minutes, more and larger vesicles were present and many cells showed swollen, phase-lucent nuclear envelopes. Only about 2 hours after injury did cells appear to swell throughout, but after 3 hours of incubation most cells had swollen and become roughly spherical; nuclear chromatin was in the form of multiple dense clumps, and Brownian motion was extensive in the cytoplasm (Figure 9). No further changes were visible by light microscopy for at least 2 more hours.

In control experiments, cells treated with KCN and IAA in standard medium containing 10% serum showed no visible alterations by

24 hours. Nonspecific binding of IAA by serum proteins presumably accounts for this unexpected finding. Cells exposed to serum-free medium containing either KCN or IAA showed no changes within 4 hours, except for margination of nuclear chromatin in a few cells. In vital dye viability tests, cells treated for 4 hours with serum-free medium containing either KCN or IAA showed less than 5% staining with 0.1% Nigrosin. After being treated with both inhibitors in serum-free medium for 3 hours, most cells stained with Nigrosin and thus were considered nonviable.

By fluorescence microscopy, many cells began to show increasingly bright green nuclear fluorescence beginning about 30 minutes after adding KCN and IAA in serum-free medium, although they retained their red lysosomal fluorescence. By 1 hour this red granular lysosomal fluorescence had faded in most cells and become orange or yellow, and the green nuclear fluorescence appeared brighter than that of the lysosomal granules. After 2 hours of incubation the nucleus and cytoplasm of most cells were stained diffusely bright green, with no red cytoplasmic granules remaining visible (Figure 10). Control cells treated with either inhibitor alone continued to show red granular fluorescence for at least 4 hours.

Cytolytic Injury

Cells pretreated with rabbit antiserum showed no changes for 10 to 15 minutes after adding guinea pig complement, but then chromatin clumping occurred very rapidly; the cytoplasm became more coarsely granular in appearance and large portions of the cell membrane bulged and then ballooned out in most cells. The typical appearance 20 minutes after adding complement was that of a grossly swollen cell with one or two large round, phase-lucent outpouchings of its surface membrane (Figure 15). Within 30 minutes after addition of complement, one or several large phase-lucent cytoplasmic vacuoles appeared and slowly enlarged in most cells, and frequently a very large clear space developed around one side of the nucleus. As the cells became distended, many organelles were seen to enlarge and subsequently become invisible. By 60 to 90 minutes after addition of complement, all cells were extremely swollen, with very pale cytoplasm and densely clumped nuclear remains; the only activities observed in the next several hours were further organelle swelling and Brownian motion (Figure 16). Cells incubated for 4 hours in antiserum alone or complement alone were indistinguishable from untreated controls.

By fluorescence microscopy the red granular staining of lysosomes persisted during cytolytic injury, however, and even 2½ hours after adding complement nearly all cells showed bright red granular fluorescence of lysosomes and only faint green nuclear fluorescence, closely resembling the fluorescence pattern of control cells (Figure 17). Complement-damaged cells were very fragile, and occasional cells, whose surface membranes ruptured, released red-fluorescent granules into the medium. By 4 hours after injury, bright green nuclear staining had developed in most cells, but red-orange granules remained in most, indicating partial release of lysosomal dye.

Electron Microscopic Observations

Controls

Electron micrographs of untreated cells showed numerous elongated mitochondrial profiles, one or more Golgi complexes often containing 5 to 10 dictyosomes each, several multivesicular bodies, many small circular profiles of smooth membranes and long narrow profiles of rough endoplasmic reticulum (Figure 1). In cells fixed with the glutaraldehyde-osmium mixture, nuclear chromatin was finely granular and evenly dispersed, and prominent nucloli were visible (Figure 2). Cells which were incubated for 4 hours in medium containing antibody only, complement only, acridine orange, or in medium lacking serum, all appeared the same as untreated cells. Since cells loaded with ferritin showed the same changes following injury as unlabeled cells, they will be described together. In uninjured cells ferritin molecules could never be found in the cell sap (Figure 1).

Ferritin-loaded cells which were photosensitized by uptake of acridine orange dye (Figures 3, 5) and exposed for 30 minutes to intense blue-violet irradiation showed a number of interesting changes, including enlargement of endoplasmic reticulum profiles, mitochondrial swelling, and the presence of coarsely granular flocculent material in the cell sap (Figures 6, 7). Ferritin was present throughout the nuclear and cell sap spaces and frequently seemed to be bound to the exterior surfaces of organelles. It is not known, of course, whether the cellular damage observed was a consequence of the release of lysosomal hydrolases, of propagated lipid peroxidation, or of direct photodynamic damage by the dye to the cell membrane or other structures after its release from lysosomes. The results indicate, however, that photosensitization damaged the lysosomal membrane sufficiently to allow dispersion of the ferritin marker, and that this marker, once released, could easily be seen throughout the cell sap in electron micrographs.

Metabolic Injury

Thirty minutes after addition of KCN and IAA in serum-free medium, the only consistent difference from controls was the appearance of long, irregular extensions of the surface membrane resembling long microvilli or large folds. Slight dilatation of rough and smooth endoplasmic reticulum (ER) was commonly seen, and there was slight margination of nuclear chromatin.

By *1 hour* the surface membrane extensions were still present, and somewhat more extensive ER dilatation was seen. Many mitochondria showed matrix condensation with enlarged intracristal spaces. Most mitochondrial profiles were ovoid; elongated profiles were rare. Ferritin-laden multivesicular bodies (secondary lysosomes) resembled those in control cells.

By *90 minutes*, many mitochondrial profiles were large and circular, but no mitochondrial densities were seen. Swelling of ER was more pronounced than at the previous interval, but ribosomes were still attached and the Golgi apparatus still contained flat cisternae.

Cells *2 hours* after exposure to KCN and IAA still showed moderate swelling of ER and mitochondria. The surface extensions remained in most cells, but some appeared swollen, with rounded surface contours, pale cytoplasm and much more extensive swelling of organelles. Pronounced chromatin clumping was observed in many cells (Figure 11). Occasional ferritin-filled lysosomes appeared enlarged and less densely packed than those of controls. However, their membranes appeared intact, and except for a few cells clearly damaged in processing, no ferritin molecules could be found in the cell sap or on the exterior surfaces of organelles.

By *3 hours* all organelles were grossly swollen, and the cytoplasm was often very pale; all mitochondria showed pronounced swelling, disorganization and flocculent matrix densities, and no narrow profiles of ER cisternae nor any rough ER could be found; nuclear chromatin was densely clumped. Many lysosomes were apparently unchanged, but many appeared swollen; ferritin molecules could not be found in the cell sap nor adherent to the outer surfaces of mitochondria or smooth membrane profiles (Figure 12).

Four hours after adding KCN and IAA the ultrastructural appearance was much the same as at 3 hours; cells and organelles were grossly swollen and disorganized. Although all lysosomes of most cells appeared intact and retained their ferritin, a small amount of ferritin was sometimes present in the cell sap, indicating release from ruptured secondary lysosomes (Figures 13, 14).

Immune Cytolysis

Some cells fixed *15 minutes* after addition of complement showed no change from controls, but most showed indications of cell swelling, with moderate dilatation of most of the cell's smooth-surfaced vesicles or cisternae, and part of the Golgi apparatus. Mitochondria were mostly of normal shape, but showed matrix condensation, which was most pronounced in glutaraldehyde-fixed tissue. Mitochondria in altered cells also showed dark, granular circular densities in their matrices, and in some cells this peculiar mitochondrial change was the only visible alteration.

By *30 minutes* most cells showed dilatation of ER and margination of nuclear chromatin. Occasional mitochondria showed matrix condensation, forming very long, narrow profiles. Most mitochondria appeared circular and enlarged in section, however, and nearly all showed strikingly electron-dense, small circular densities (Figure 18). These were within the matrix space but very closely apposed to the mitochondrial inner membrane at the bases of the cristae; they were composed of very fine, dark granules and contained clear centers (Figure 21). These mitochondrial changes closely resemble those which have been reported to appear in a variety of circumstances all of which involve active accumulation of calcium by mitochondria. These circumstances include the *in vitro* experiments of Vasington and Greenawalt,[32] studies of toxic liver injury by Reynolds,[33] the model injuries in flounder tubules reported from this laboratory,[34-36] and the studies of heart muscle ischemia reported by Jennings *et al.*[37,38]

One hour after adding complement, various degrees of cellular swelling were observed. Most cells showed very extensive enlargement of all organelles, including the nuclear envelope, and pronounced chromatin clumping (Figure 19). Nearly all mitochondria showed the typical appearance of severe swelling, and fluffy, gray mitochondrial matrix densities were often seen. The great majority of mitochondria contained even more numerous (3 to 5 per organelle section) dark circular densities. Ferritin-containing secondary lysosomes frequently appeared markedly enlarged, with diluted contents, but intact surrounding membranes could be seen, and no ferritin molecules could be found in the cell sap.

After *two hours* the appearance was similar but with nearly all cells showing even more extensive organelle swelling; ferritin was still retained within multivesicular secondary lysosomes (Figure 20).

By *four hours* after complement treatment essentially all cells showed very pronounced swelling, irregularity and disorganization of all organelles; ferritin-containing organelles were still generally intact, but clear evidence of ferritin release could be obtained in some cells (Figures 22–27).

Nine hours after complement injury, swollen mitochondria with both flocculent and round granular densities and irregular smooth and rough-surfaced ER membranes were still present. Many intact ferritin-loaded lysosomes remained but some clearly had disintegrated, releasing their content of ferritin.

Discussion

The present findings of retention of macromolecular lysosomal contents until late in the course of cell injury are contrary to what one would expect on the basis of considering lysosome rupture as a universal mechanism leading to irreversibility of cell injury. Thus it may be important to reevaluate the evidence which does suggest a destructive role for lysosomes in injured cells.

Biochemical studies of injured cells have an inherent, well-recognized problem of interpretation since changes in the subcellular distribution of lysosomal enzymes can be evaluated only after grinding the cells in a homogenizer. As DeDuve has frequently emphasized, it is important not to misinterpret increases in unsedimentable or free enzyme activity which occur during homogenization as evidence for enzyme release in the intact injured cells. Lysosomes of injured cells should not be expected to behave exactly like those of control cells during drastic isolation procedures. Changes in lysosomes such as increased size, following heterophagy or autophagy, cause them to rupture more easily during homogenization but do not cause rupture in intact cells.[39–41] The most likely artifact in this situation would thus lead to overestimation of intracellular rupture of lysosomes, which actually might only be less stable. It would be possible and quite interesting, in this regard, to obtain estimates of the mean volume and osmotic behavior of intact lysosomes from injured tissue by means of centrifugation analyses.

Enzyme cytochemical studies must be interpreted cautiously for several reasons, of which structural and enzymatic artifacts of fixation are probably the most serious.[24] Lysosomal membranes clearly become more permeable to small molecules following fixation, and fixative damage might conceivably cause release of lysosomal enzymes in itself. However, the most likely artifact would seem to be more rapid inactivation by the fixative of any enzyme that was released to the cell sap than of lysosomally bound enzyme.[42] This would lead to an underestimate of lysosomal enzyme release. Lysosome histochemistry in unfixed tissue culture cells, although yielding interesting information, is again a type of stability test, since the incubation mixture is sufficiently toxic to give lysosomal staining (interpreted as partial activation of lysosomes or moderate damage) within a few minutes even in normal cells.[43] Indeed, the interpretations of lysosomal changes based on centrifugation of homogenates have often conflicted with interpretations based on histochemical studies of the same or similar systems.[8,44,45]

Ultrastructural observations of lysosomes in ischemic cells are also difficult to interpret. Artifacts of fixation, for example, may account for false images of breakage or fusion of membranes. In a previous study of mouse liver, it was noted that lysosomes in injured cells, though mostly intact, often showed points of membrane interruption in osmium-fixed tissues.[8] Such breaks were only rarely observed after fixation in glutaraldehyde, perhaps because of the better protein-stabilizing properties of the latter fixative. These findings are probably best interpreted as evidence of increased fragility of lysosomal membranes in injured cells—*ie*, increased likelihood of artifactual rupture during processing.

On the other hand, sizable gaps in lysosomal membranes could be missed by electron microscopy due to sectioning in planes where the membranes might appear normal. Furthermore, lysosomal rupture might involve rapid disintegration or collapse of the lysosomal membrane with rapid diffusion of lysosomal contents throughout the cell, leaving little or no morphologic evidence.[11]

It seemed that an independent method of estimation of lysosome stability would be helpful in approaching this elusive problem. Our efforts, therefore, have been directed toward developing technics by which the lysosomal space could be specifically labeled before a controlled cell injury was applied, and the fate of lysosomal contents could be followed after injury, with a minimum of experimental manipulation of the injured cells.

The original *suicide-bag* hypothesis in its broadest form, that lysosome rupture may be a final common pathway leading to death in most kinds of cell injury, is not now accepted widely or without reservation. However, for the reasons outlined above, it has not been possible to show unequivocally that it is not a common cause of cell death. In several specific types of cell injury, including photosensitization by dyes and prophyrins,[19] and silica and urate toxicity to phagocytes and polymorphs,[46-49] substantial cases have recently been made that lysosome rupture does kill cells. Lysosomes have also been implicated in viral cytotoxicity[3] and in the programmed cell death of insect metamorphosis.[50]

The purpose of the present study was to test, in a relatively direct and well-controlled way, the simple question of whether lysosomes of cultured cells burst open prior to cell death, either following inhibition of energy metabolism or following immunologic cell membrane damage. Another possibility, that lysosomal permeability to substrate or even to enzymes may increase during cell injury, was approached with the use of a low molecular weight fluorescent vital dye, but without yielding definitive results. The general question of interest was whether lysosomes are sensitive to the reversible changes of cellular reaction to injury, and thus threaten the survival of injured cells, or alternatively are stable organelles which are not altered until after cell death. This is significant not only in gaining an accurate understanding of cell injury and death, but also in rationally planning therapy to affect lysosomes.[47,51,52] The present work represents only a first approach to the problem, in which the presence or absence of secondary lysosome rupture was tested after 2 rapidly lethal cell injuries.

Types of Injury Applied

Metabolic

The two inhibitors, cyanide and iodoacetate, were used together in an effort to curtail the synthesis of ATP by the cells. Iodoacetate at low doses specifically inhibits 3-phosophoglyceraldehyde dehydrogenase,[53] thus effectively blocking the glycolytic pathway, which is well developed in most tissue culture cells. If, in the present study, the concentration of IAA in the cell interior reached that of the IAA applied, other effects would be expected; however, the fact that application of IAA alone caused no cytopathic effects by 4 hours suggests that any nonspecific effects must not severely compromise the cells' homeostatic ability. In the presence of a block in the Embden-Meyerhof glycolytic pathway, substrates such as acetate, pyruvate and succinate may be oxidized to provide ATP via the Krebs citric acid cycle in the mitochondria. When oxygen utilization is blocked by cyanide, this pathway becomes inoperative. It seems that Chang cells are able to survive, at least for several hours, with ATP synthesis proceeding either via substrate-level phosphorylation in the anaerobic glycolysis pathway (in the presence of cyanide), or via oxidative metabolism alone (in the presence of iodoacetate). The synergistic effect of these two inhibitors in causing cellular degeneration is interpreted as being due to inhibition of both the glycolytic and oxidative pathways for ATP synthesis. The use of both inhibitors simulates the effects of total ischemia, since in the absence of a blood supply both glucose and oxygen are lacking, whereas IAA and KCN together block the utilization of both glucose and oxygen.

Cytolytic

In the method used, exposure to antiserum produced against whole Chang cells should lead to binding of antibody at the cell surface. Antibodies against cell organelles, though possibly present, would not be expected to penetrate the cells' plasma membranes, and so could not bind internal cellular antigens.[54] A small amount of antiserum may, however, be taken up by pinocytosis during the 10 minutes of its exposure to cells or the 20 minutes of incubation of cells in fresh medium. During washing with two changes of medium, essentially all antibody not bound or enclosed by the cell membrane should be removed. Thus when complement is added, one would expect it to be activated by antigen-antibody complexes and to begin to cause damage only at the cell surface membrane. (The small amount of complement which could be taken up by pinocytosis before cessation of this process might also damage a few new phagocytic vacuoles which might contain membrane-bound antibody.) Surface membrane damage caused by activated complement has been shown in other systems to lead to an immediate efflux of potassium from cells, together with cell swelling, followed by loss of cytoplasmic enzymes and even ribosomal RNA.[55] Similar cellular responses are to be expected in the present system.

Interpretation of Fluorescence Changes

Acridine orange, an aminoacridine dye of molecular weight near 300, is apparently incorporated by living cells in the same way as many other basic vital dyes.[56] The distribution of acridine orange within living cells, under appropriate conditions, has been shown to be indistinguishable from that of acid phosphatase in HeLa cells by histochemistry and in rat muscle cells by rate-zonal centrifugation studies.[28,57] Acridine dyes can be shown to bind to isolated lysosomes and even to a purified lysosomal glycoprotein,[58] where, under appropriate conditions, red fluorescence is observed. Dye bound by intact isolated lysosomes can be displaced by adding protamine, and the same quantity of dye is bound whether the lysosomes are intact or disrupted.[58] Both findings suggest that the component which passively binds acridine dye is associated with the lysosomal membrane. Surprisingly, extensive studies of acridine orange staining in nonliving tissue culture cells have failed to show a significant amount of dye binding to lysosomes; in freeze-dried or acetone-ethanol-fixed cells the bulk of the acridine orange is bound to RNA and DNA, which can be quantitatively assayed by this technic.[59] In living cells with pronounced red-fluorescent acridine orange labeling of lysosomes, it was observed that exposure to buffered glutaraldehyde causes fading of lysosomal fluorescence within seconds and the simultaneous appearance of bright green nuclear and cytoplasmic staining.

Acridine orange labeling of lysosomes in living tissue culture cells has been studied carefully by Robbins, Marcus and Gonatas,[27,28] and this process is apparently much more complex than dye binding *in vitro*. These authors showed that even in cells deprived of glucose or incubated at 0 C lysosomes did accumulate enough acridine orange to fluoresce red; however, addition of more than a critical amount of dye resulted in additional diffuse red-orange cytoplasmic staining under these conditions. If the cells were warmed or provided with glucose, this cytoplasmic reddening disappeared as the lysosomes became brighter red and larger; if deprived of substrate, however, the cells degenerated.

By electron microscopy, lysosomes of acridine orange-labeled cells appeared to be enlarged; after several days of exposure to dye myelin figures appeared in lysosomes. Thus it seems that acridine orange staining of lysosomes in live cells occurs by at least two processes: passive binding by a lysosomal component, and a distinct energy-requiring process which can accumulate much more dye in lysosomes, perhaps by a membrane transport process. One attractive hypothesis is that only the nonionized form of the dye freely equilibrates across the lysosomal membrane, the concentration of the predominant cationic form depending upon the pH, and thus being much higher in the acid interior of the lysosome.[60] In this case, actively maintaining a low pH in lysosomes would allow protonation and trapping of larger amounts of dye, and the loss of a pH gradient across the membrane would lead to leakage of dye from lysosomes.

The observation that acridine diffuses out of lysosomes to the nucleus and cytoplasm early in the cell's reaction to metabolic inhibition could have several reasonable interpretations; therefore, its significance is not clear. Changes in the concentration of hydrogen or other ions or metabolites in the cell sap could interfere with passive binding of dye to the lysosomal glycoprotein or trapping of dye within lysosomes. Alternatively, the lack of metabolic energy could prevent the operation of whatever mechanism is normally capable of transferring dye from the cell sap to lysosomes. This would make apparent any slow diffusion of dye from lysosomes, even if it occurs continuously in normal cells. A third possibility is that the lysosomal membrane would normally retain most of the acridine orange within labeled lysosomes and that release of dye would reflect an increase in permeability of this membrane.

It is interesting to note that lysosomal staining persisted throughout immune cytolysis, by contrast, long after the composition of the cell sap was drastically altered by damage to the cell membrane and after subsequent equilibration with the external medium.

It was important to rule out the possibility that the fluorescent marker used might inhibit lysosomal enzymes. The finding that all four enzymes assayed did retain full activity in Euchrysine-treated cells indicates that the possibility of cell damage by lysosomal hydrolases was not affected by the use of the fluorescent dye.

Ultrastructural Findings

The progression of ultrastructural changes seen in each of these types of injury was quite similar to previously described patterns of many other forms of lethal injury in this and other cell types. Cytolytic complement attack led to a more rapid progression of cellular responses, in which early, extensive cell swelling and the appearance of small, circular, fine-grained densities in mitochondria were characteristic. Similar responses have been reported in other forms of primary plasma membrane injury in other systems.[35,36]

The presence of ultrastructural changes in mitochondria suggestive of calcification seems to indicate that the conditions necessary for mitochondrial calcification were present in complement-damaged cells. Isolated mitochondria require both calcium and a source of energy (either as ATP or as oxidizable substrate) to accumulate calcium from the medium. In complement-damaged cells, one would expect that the increased membrane permeability would allow extracellular calcium to enter the cells, and the supply of substrates, oxygen and even ATP to the cells need not be greatly decreased. In cells with inhibited energy metabolism, on the other hand, calcification could not proceed in the absence of ATP or usable oxygen, even if calcium were present in increased amounts in the cytoplasm.

The use of ferritin as a marker for secondary lysosomes is convenient, since individual molecules can be identified in thin sections and routine fixation and staining may be used in preparation of the tissue. The use of a tracer such as ferritin overcomes some of the problems of assessing the integrity of lysosomal membranes by electron microscopy. The presence of ferritin in the cell sap should clearly indicate the existence of any lysosomal membrane breaks 100 Å or more in diameter, even if these are transient, obscured by fixation artifacts or missed by the plane of section. A single ferritin-loaded lysosome, if it burst open, should spread evidence of its breakdown throughout the cell, and thus should be detected efficiently. The results of the photosensitization experiments lend support to this concept.

The finding that no ferritin could be observed in the cytoplasm outside single-membrane profiles for 3 hours after a rapidly lethal cell injury (immune cytolysis) clearly indicates that rupture of lysosomes was not an early, sublethal reaction to injury in this model system.

Ferritin could not be shown to escape from lysosomes for at least 3 hours following inhibition of energy metabolism in Chang cells. It is difficult to pinpoint the time of cell death in this system, however. Many cells by 2 hours, and most cells by 3 hours, showed very dense chromatin clumping and mitochondrial swelling with flocculent matrix densities, which are ultrastructural lesions typical of the irreversible or necrotic phase of cell injury.[10] As late as 4 hours after KCN–IAA poisoning, when irreversible structural changes were uniformly seen, it was clear that the great majority of lysosomes continued to retain the ferritin marker within a morphologically intact membrane although some release of ferritin to the cell sap was demonstrated.

In conclusion, the findings do not indicate that the suicide bag mechanism of lysosomal rupture prior to cell death was operative in the two systems studied. On the contrary, the lysosomes appeared to be relatively stable organelles which only burst in the postmortem phase of cellular necrosis. However, it is important to note that only the resistance of secondary lysosomes to membrane rupture was well evaluated. It will be of interest in the future to study the fate of lysosomal tracers smaller than ferritin to test for lysosomal permeability changes without rupture, and to study other more gradual modes of cell injury.

References

1. Wattiaux R: Biochemistry and function of lysosomes. Handbook of Molecular Cytology. Edited by A Lima-de-Faria. New York, John Wiley & Sons, Inc, 1960, pp 1159–1178
2. DeDuve C: Lysosomes and cell injury. Injury, Inflammation and Immunity. Edited by L Thomas, JW Uhr, and L Grant. Baltimore, Williams and Wilkins Co, 1964, pp 283–311
3. Allison AC, Sandelin K: Activation of lysosomal enzymes in virus-infected cells and its possible relationship to cytopathic effects. J Exp Med 117:879–887, 1963
4. Majno G, La Gattuta M, Thompson TE: Cellular death and necrosis: chemical, physical and morphological changes in rat liver. Virchows Arch [Pathol Anat] 333:421–465, 1960
5. Novikoff AB: Biochemical and staining reactions of cytoplasmic constituents. Developing Cell Systems and Their Control. Edited by D Rudnick. New York, The Ronald Press Company, 1960, pp 167–203
6. Allison AC, Mallucci L: Histochemical studies of lysosomes and lysosomal enzymes in virus-infected cell cultures. J Exp Med 121:463–476, 1965
7. Goldblatt PJ, Trump BF, Stowell RE: Studies on necrosis of mouse liver *in vitro*. Alterations in some histochemically demonstrable hepatocellular enzymes. Am J Pathol 47:183–208, 1965
8. Trump BF, Goldblatt PJ, Stowell RE: Studies of necrosis *in vitro* of mouse hepatic parenchymal cells; ultrastructural and cytochemical alterations of cytosomes, cytosegresomes, multivesicular bodies and microbodies and their relation to the lysosome concept. Lab Invest 14:1946–1968, 1965
9. Ericsson JLE, Biberfeld P, Seljelid R: Electron microscopic and cytochemical studies of acid phosphatase and aryl sulfatase during autolysis. Acta Pathol Microbiol Scand 70:215–228, 1967
10. Trump BF, Bulger RE: Studies of cellular injury in isolated flounder tubules. IV. Electron microscopic observations of changes during the phase of altered homeostasis in tubules treated with cyanide. Lab Invest 18:731–739, 1968
11. Danielli JF, Discussion. CIBA Symposium on Lysosomes. Edited by AVS DeRouck, MP Cameron. Boston, Little, Brown and Company, 1963, p 353
12. Chang RS: Continuous subcultivation of epithelial-like cells from normal human tissues. Proc Soc Exp Biol Med 87:440–443, 1954
13. Sykes JA, Moore EB: A new chamber for tissue culture. Proc Soc Exp Biol Med 100:125–127, 1959
14. Trump BF, Bulger RE: New ultrastructural characteristics of cells fixed in a glutaraldehyde-osmium tetroxide mixture. Lab Invest 15:368–379, 1966
15. Hirsch JG, Fedorko ME: Ultrastructure of human leukocytes after simultaneous fixation with glutaraldehyde and osmium tetroxide and "post-fixation" in uranyl acetate. J Cell Biol 38:615–627, 1968
16. Kellenberger E, Ryter A, Sechaud J: Electron microscope study of DNA-containing plasms. II. Vegetative and mature phage DNA as compared with normal bacterial nucleoids in different physiological states. J Biophys Biochem Cytol 4:671–678, 1958

17. Biberfeld P: A method for the study of monolayer cultures with preserved cell orientation and interrelationship. J Ultrastruct Res 25:158–159, 1968

18. Luft JH: Improvements in epoxy resin embedding methods. J Biophys Biochem Cytol 9:409–414, 1961

19. Allison AC, Magnus IA, Young MR: Role of lysosomes and of cell membranes in photosensitization. Nature (Lond) 209:874–878, 1966

20. Anson ML: The estimation of pepsin, trypsin, papain, and cathepsin with hemoglobin. J Gen Physiol 22:79–89, 1938

21. Bowers WE, DeDuve C: Lysosomes in lymphoid tissue. II. Intracellular distribution of acid hydrolases. J Cell Biol 32:339–348, 1967

22. Roy AB: The synthesis and hydrolysis of sulfate esters. Adv Enzymol 22:205–235, 1960

23. Lowry OH, Rosebrough NJ, Farr AL, Randall RJ: Protein measurement with the Folin phenol reagent. J Biol Chem 193:265–275, 1951

24. Ericsson JLE, Trump BF: Electron microscopic studies of the epithelium of the proximal tubule of the rat kidney. I. The intracellular localization of acid phosphatase. Lab Invest 13:1427–1456, 1964

25. Jonsson J, Fagraeus A, Biberfeld G: The mixed haemadsorption test as an aid to the diagnosis of thyroid autoimmune disease. Clin Exp Immunol 3:287–304, 1968

26. DeDuve C, Wattiaux R: Functions of lysosomes. Ann Rev Physiol 28:435–492, 1966

27. Robbins E, Marcus PI: Dynamics of acridine orange-cell interaction. I. Interrelationships of acridine orange particles and cytoplasmic reddening. J Cell Biol 18:237–250, 1963

28. Robbins E, Marcus PI, Gonatas NK: Dynamics of acridine orange-cell interaction. II. Dye-induced ultrastructural changes in multivesicular bodies (acridine orange particles). J Cell Biol 21:49–62, 1964

29. Bradley DF: Molecular biophysics of dye-polymer complexes. Trans NY Acad Sci 24:64–71, 1961

30. Arstila AU, Jauregui HO, Chang J, Trump BF: Studies on cellular autophagocytosis. Relationship between heterophagy and autophagy in HeLa cells. Lab Invest 24:162–174, 1971

31. Baudhuin P, Beaufay H, DeDuve C: Combined biochemical and morphological study of particulate fractions from rat liver. J Cell Biol 26:219–243, 1965

32. Vasington FD, Greenawalt JW: Osmotically lysed rat liver mitochondria. Biochemical and ultrastructural properties in relation to massive ion accumulation. J Cell Biol 39:661–675, 1968

33. Reynolds ES: Liver Parenchymal Cell Injury. III. The nature of calcium-associated electron-opaque masses in rat liver mitochondria following poisoning with carbon tetrachloride. J Cell Biol 25 (No. 3, part 2):53–75, 1965

34. Gritzka TL, Trump BF: Renal tubular lesions caused by mercuric chloride: electron microscopic observations: degeneration of the pars recta. Am J Pathol 52:1225–1277, 1968

35. Ginn FL, Shelburne JD, Trump BF: Disorders of cell volume regulation. I. Effects of inhibition of plasma membrane adenosine triphosphatase with ouabain. Am J Pathol 53:1041–1072, 1968

36. Sahaphong S, Mergner WJ: The effect of mercurials on mitochondria *in vivo* and *in vitro*. Fed Proc 30:637 1971 (Abstr)

37. Jennings RB, Herdson PB, Sommers HM: Structural and functional abnormalities in mitochondria isolated from ischemic dog myocardium. Lab Invest 20:548–557, 1969

38. Herdson PB, Sommers HM, Jennings RB: A comparative study of the fine structure of normal and ischemic dog myocardium with special reference to early changes following temporary occlusion of a coronary artery. Am J Pathol 46:367–386, 1965

39. Cohn RA, Hirsch JG: The influence of phagocytosis on the intracellular distribution of granule-associated components of polymorphonuclear leukocytes. J Exp Med 112:1015–1022, 1960

40. Zucker-Franklin D, Hirsch JG: Electron microscope observations on the degranulation of rabbit peritoneal leukocytes during phagocytosis. J Exp Med 120:569–576, 1964

41. Deter RL, DeDuve C: Influence of glucagon, an inducer of cellular autophagy, on some physical properties of rat liver lysosomes. J Cell Biol 33:437–449, 1967

42. Ericsson JLE, Biberfeld P: Studies on aldehyde fixation. Fixation rates and their relation to fine structure and some histochemical reactions in liver. Lab Invest 17:281–298, 1967

43. Bitensky L: The reversible activation of lysosomes in normal cells and the effects of pathological conditions.[11] pp 362–383

44. Beaufay H, DeDuve C: Tissue fractionation studies. IX. Enzymic release of bound hydrolases. Biochem J 73:604–609, 1959

45. Griffin CC, Waravdekar VS, Trump BF, Goldblatt PJ, Stowell RE: Studies on necrosis of mouse liver *in vitro*. Alterations in activities of succinoxidase, succinic dehydrogenase, glutamic dehydrogenase, acid phosphatase, uricase, glucose-6-phophatase and NAD-pyrophosphorylase. Am J Pathol 47:833–850, 1965

46. Allison AC, Harington JS, Birbeck M: An examination of the cytotoxic effects of silica on macrophages. J Exp Med 124:141–154, 1966.

47. Weissman G: Molecular basis of acute gout. Hosp Pract 6 (No. 7):43–52, 1971

48. Schumacher HR, Phelps P: Sequential changes in human polymorphonuclear leukocytes after urate crystal phagocytosis. An electron microscopic study. Arthritis Rheum 14:513–526, 1971

49. Weissman G, Rita G, Zurier RB: Molecular basis of gouty inflammation. J Clin Invest 50:97a, 1971

50. Lockshin R: Lysosomes in insect physiology. Biology and Pathology of Lysosomes. Edited by JT Dingle and HB Fell. New York, John Wiley & Sons, Inc, 1969, Chapter 13

51. Janoff A: Alterations in lysosomes (intracellular enzymes) during shock; effects of preconditioning (tolerance) and protective drugs. Shock. Edited by SG Hershey. Boston, Little, Brown and Co, 1964, pp 93–111

52. Barankay T, Horpacsy G, Nagy S, Petri G: Changes in the level of lysosomal enzymes in plasma and lymph in hemorrhagic shock. Med Exp 19:267–271, 1969

53. Webb JL: Enzyme and Metabolic Inhibitors. Vol III. New York, Academic Press, Inc 1966, pp 1–283

54. Hiramoto R, Goldstein MN, Pressman D: Limited fixation of antibody by viable cells. J Nat Cancer Inst 24:255–266, 1959

55. Green H, Fleischer RA, Barrow P, Goldberg B: The cytotoxic action of immune gamma globulin and complement on Krebs ascites tumor cells. II. Chemical studies. J Exp Med 109:511–521, 1959

56. Allison AC, Young MR: Uptake of dyes and drugs by living cells in culture. Life Sci 3:1407–1414, 1964

57. Canonico PG, Bird JWC: The use of acridine orange as a lysosomal marker in rat skeletal muscle. J Cell Biol 43:367–371, 1969

58. Barrett AJ, Dingle JT: A lysosomal component capable of binding cations and a carcinogen. Biochem J 105:20p, 1967

59. Rigler R: Microfluorometric characterization of intracellular nucleic acids and nucleoproteins by acridine orange. Acta Physiol Scand [Suppl] 267:1–122, 1966

60. Homewood CA, Warhurst DC, Peters W, Baggaley VC: Lysosomes, pH and the antimalarial action of chloroquine. Nature 235:50–52, 1972

Legends For Figures

Fig 1—A ferritin-loaded, otherwise untreated control Chang liver cell, fixed in the glutaraldehyde and osmium tetroxide solution, stained only with uranium acetate. *M* = mitochondria, *SL* = secondary lysosomes, *N* = nucleus (× 23,000).

Fig 2—An untreated Chang cell without ferritin. RER = long cisternae of rough endoplasmic reticulum, *N* = nucleus with dispersed chromatin (× 18,500).

Fig 3—Part of a cell exposed to ferritin overnight, washed, and treated for 15 minutes with acridine orange 1 hour prior to fixation (× 41,500).

Fig 4—A secondary lysosome in a cell exposed to ferritin overnight, then fixed in 4% glutaralydehyde, incubated for acid phosphatase, postfixed in 2% osmium tetroxide and stained only with uranium acetate. *Arrows* indicate histochemical reaction product (× 95,000).

Fig 5—The appearance by fluorescence microscopy of living Chang cells after labeling with acridine orange as described. The cytoplasmic granules (lysosomes) fluoresce brightly red, and nucleoli fluoresce faintly green (× 700).

Figs 6 and 7—A cell exposed to ferritin overnight, treated with acridine orange as in Figure 5, then irradiated with blue-violet light as described. Ferritin molecules, identifiable in Figure 6, are present throughout cell sap and nucleoplasm but have not penetrated other organelles. *FD* = fat droplet, *MvB* = multivesicular body (× 50,000 and × 20,000).

Fig 8—Phase-contrast photomicrography of a typical cell after 90 minutes of incubation with both KCN and IAA in serum-free medium. Filamentous processes (*F*), some resembling strings of beads, protrude from the surface of a poorly-spread cell (× 1100).

Fig 9—Cells after 2 hours of incubation with KCN and IAA in serum-free medium, illustrating rounding up and vacuolation of cells, and the ballooning out of local regions of the cell surface (*arrows*) (× 600).

Fig 10—The same cells as in Figure 9, by fluorescence microscopy.

Fig 11—Electron micrograph of a cell 2 hours after exposure to KCN and IAA in serum-free medium. Note enlarged, round mitochondrial profiles with flocculent matrix densities (*M*) and swollen endoplasmic reticulum profiles (*ER*) (× 23,000).

Fig 12—A cell pre-loaded with ferritin. Three hours in KCN and IAA, no serum. Note the clumping of nuclear chromatin (*N*), the narrow extension of cell surface membrane (*arrow*) and the intact second lysosomes (SL). G = Golgi region (× 16,000).

Figs 13 and 14—Four hours in KCN and IAA, no serum. Figure 13 shows the typical lysosomal retention of ferritin, Figure 14 documents its apparent release to the cell sap, observed occasionally ×25,000 and ×30,000.

Fig 15—Phase photomicrograph of a cell pretreated with heat-inactivated antiserum, washed and exposed to guinea-pig complement for 30 minutes. Cytoplasmic vacuolation and multiple outward bulges or "blebs" (B) of the surface membrane are apparent (× 1140).

Fig 16—Sensitized cells, prelabeled with acridine orange, two hours thirty minutes after addition of complement (× 800).

Fig 17—Same cells as in Figure 16, photographed by fluorescence immediately after Figure 16 was taken. The lysosomal granules fluoresce brightly red (× 800).

Fig 18—Mitochondria of a sensitized cell 30 minutes after adding complement (× 35,000).

Fig 19—Electron micrograph of a sensitized cell after one hour of exposure to complement. Extensive chromatin clumping is apparent in a pale nucleus (*N*); endoplasmic reticulum profiles are grossly dilated (*RER*), and mitochondria (*M*) contain multiple finely granular, peripheral densities (× 19,000).

Fig 20—Two hours after antibody-complement treatment. Mitochondrial changes (*M*), and dilatation of endoplasmic reticulum (*RER*) are apparent. Ferritin-filled secondary lysosomes seem intact, since ferritin cannot be found in the cell sap (× 24,000).

Fig 21—A mitochondrion (*M*) from a sensitized cell one hour after complement treatment, without ferritin preloading. The mitochondrial densities are finely granular, circular in profile and have clear centers (*GD*). They appear nearly surrounded by evaginations of the inner mitochondrial membrane into cristae (*CM*) (× 34,000).

Figs 22 and 23—Four hours after antibody-complement treatment. Nuclear chromatin is present (*N*) but is no longer surrounded by a nuclear envelope. Secondary lysosomes (*SL*) appear completely intact in this typical cell (× 40,000 and × 18,000).

Figs 24, 25, 26—A less common appearance four hours after antibody-complement treatment. Nuclear chromatin clumping (*N*), and mitochondrial changes (*M*) including the appearance of flocculent matrix densities, may be seen. Most ferritin-filled secondary lysosomes appear intact, but some ferritin may be found free in the cell sap × 28,000, × 75,000 and 200,000.

Fig 27—Enlargement of a mitochondrion four hours after antibody-complement treatment. Two types of densities may be seen: a finely granular membrane-associated density (*GD*) and a flocculent, coarsely granular matrix density (*FD*) (× 50,000).

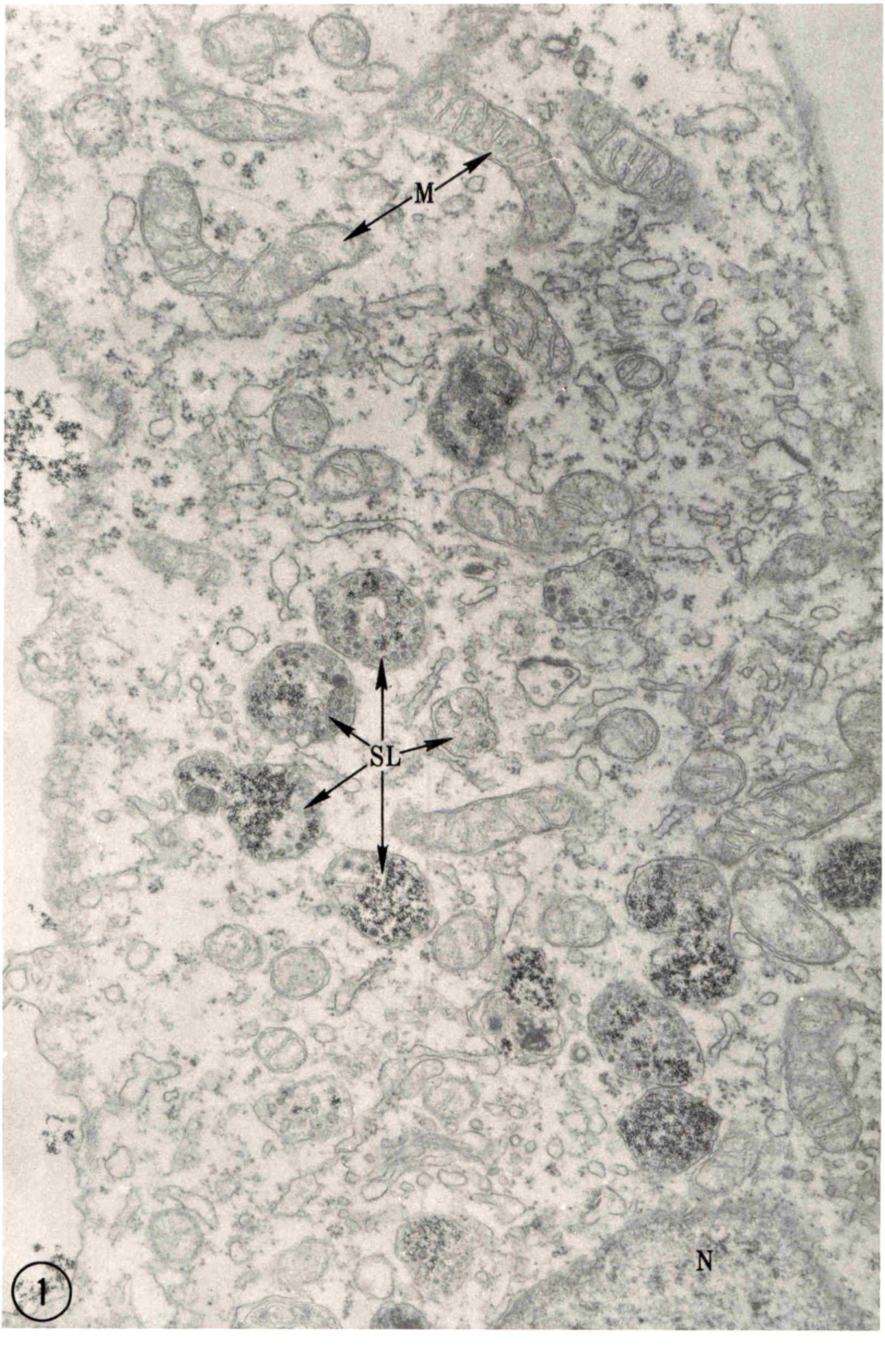
M
SL
N
1

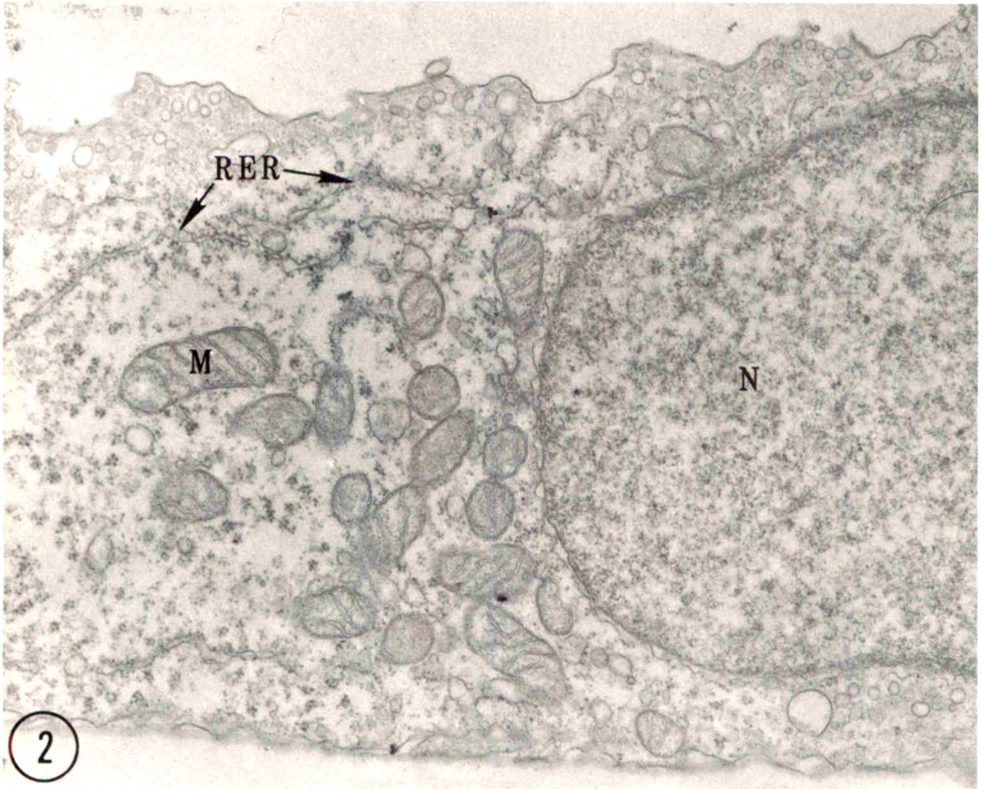

②

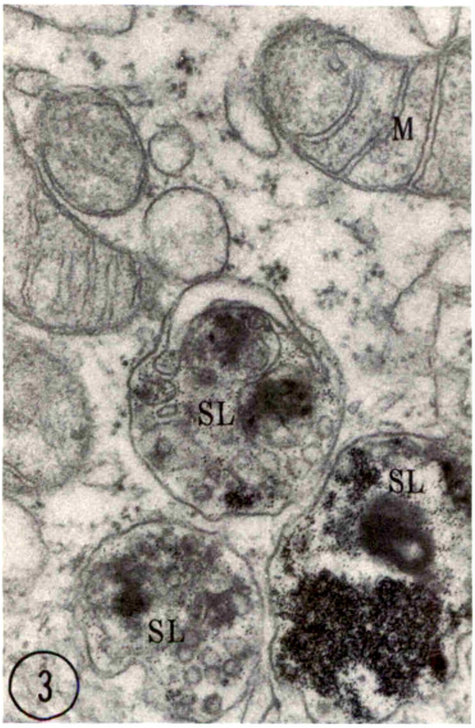

③

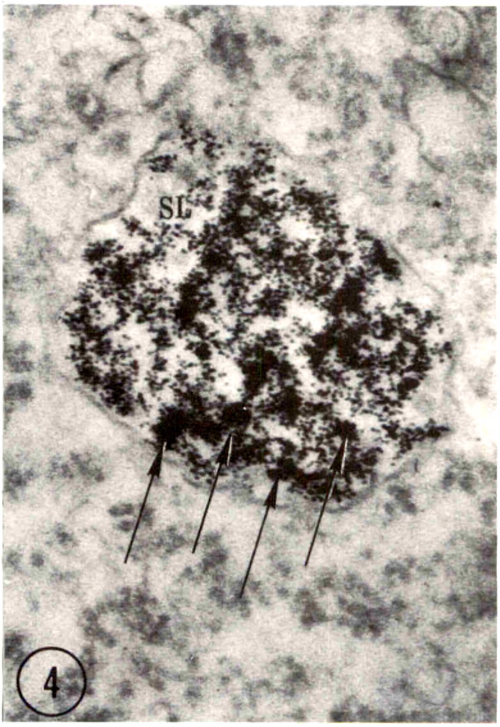

④

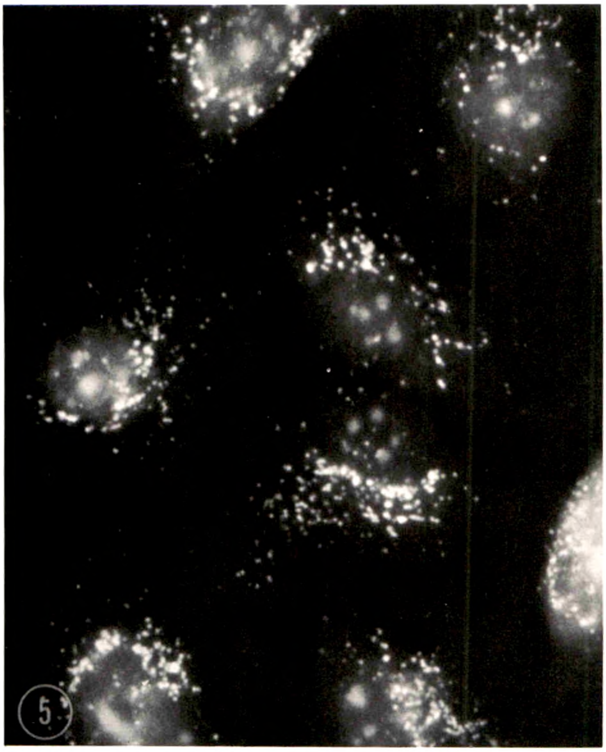
5

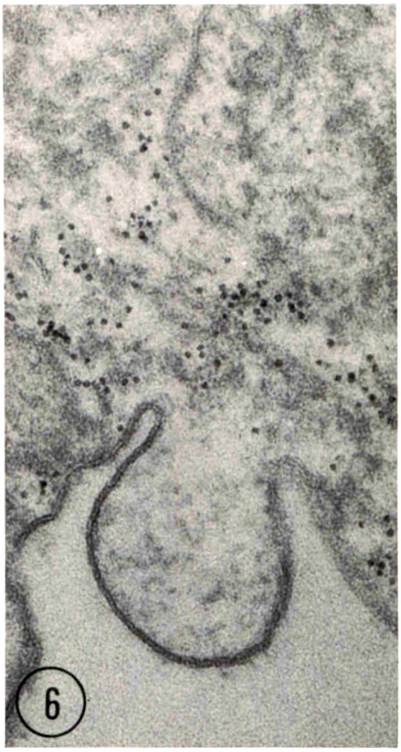
6

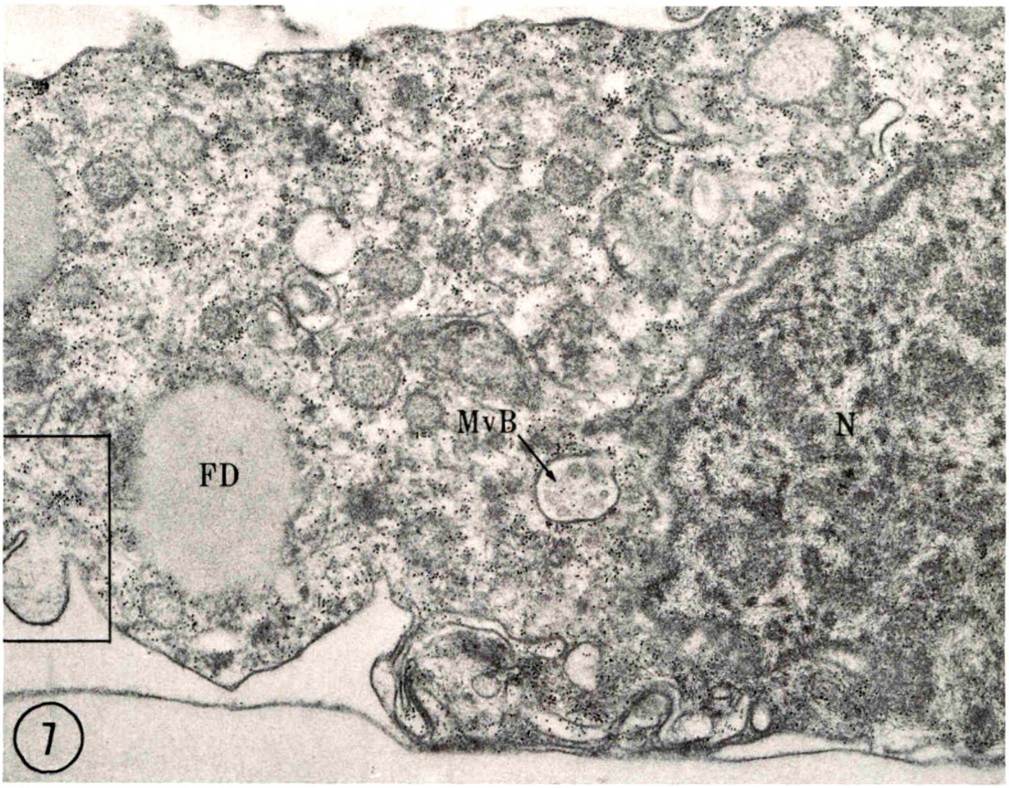
MvB
FD
N
7

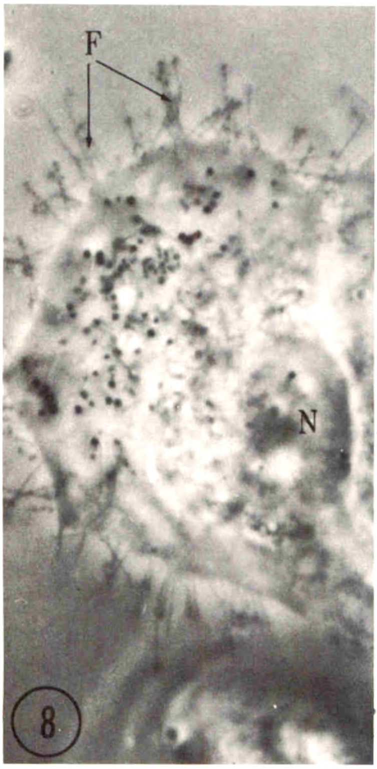
F
N
8

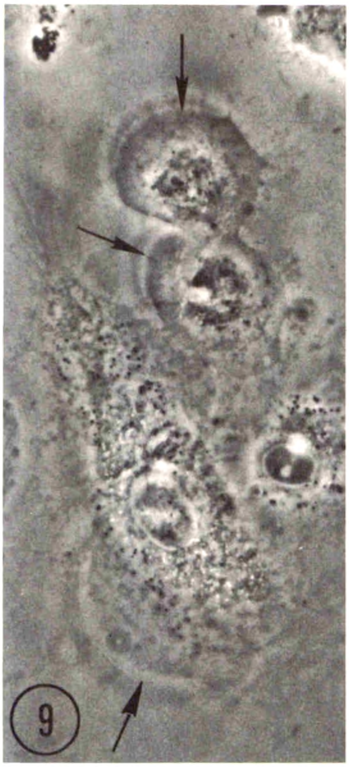
9

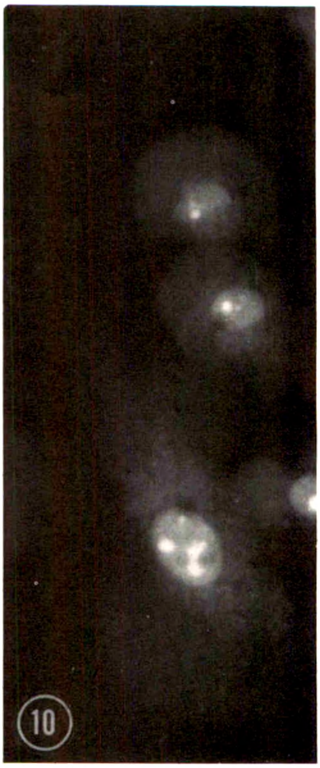
10

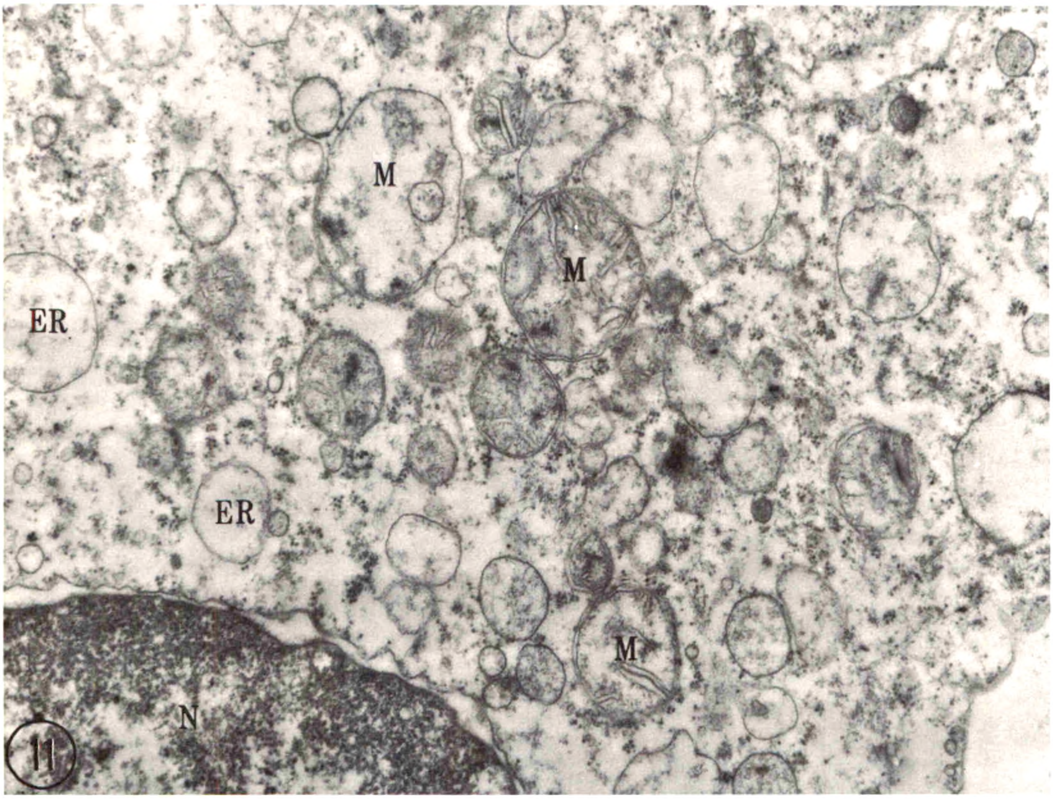
M
M
ER
ER
M
N
11

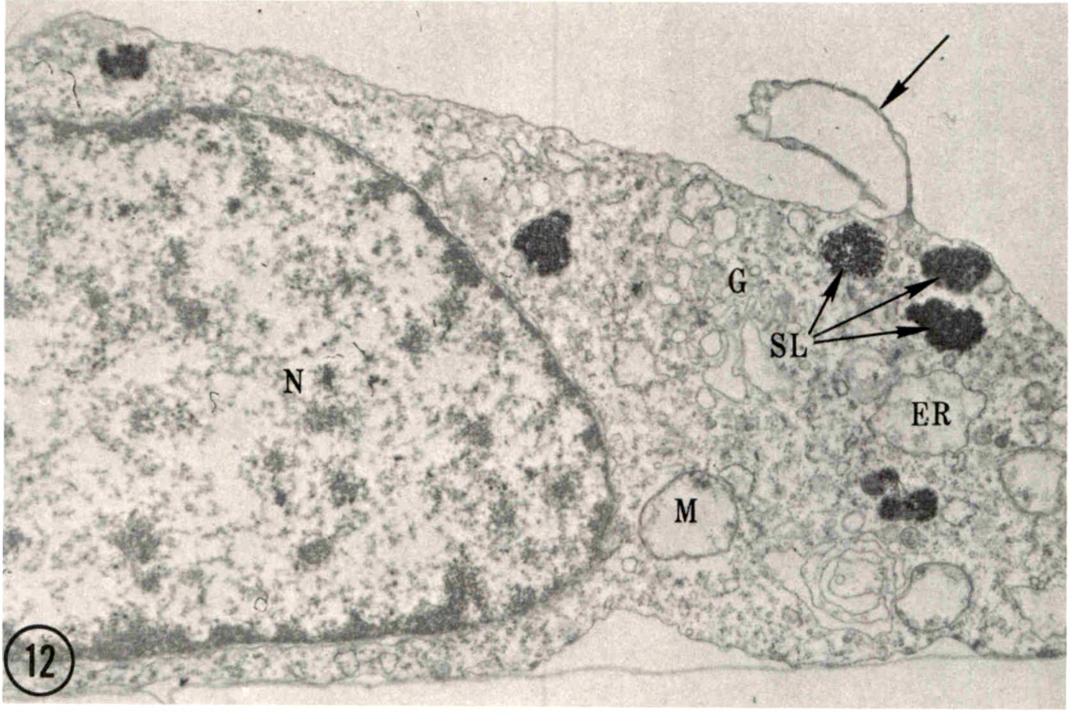

12

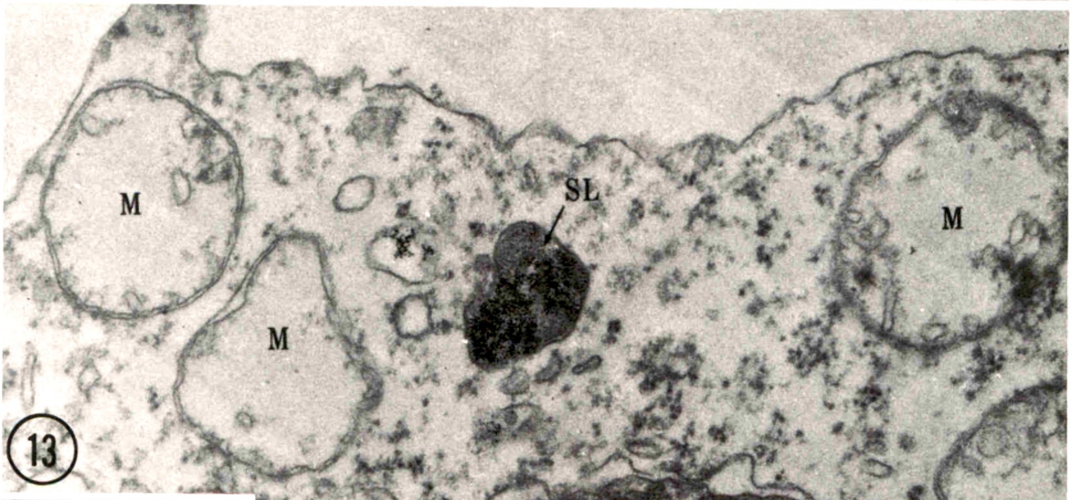

13

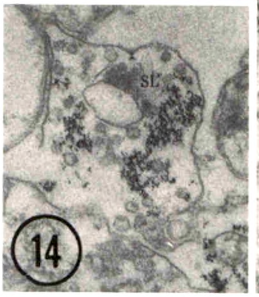

14

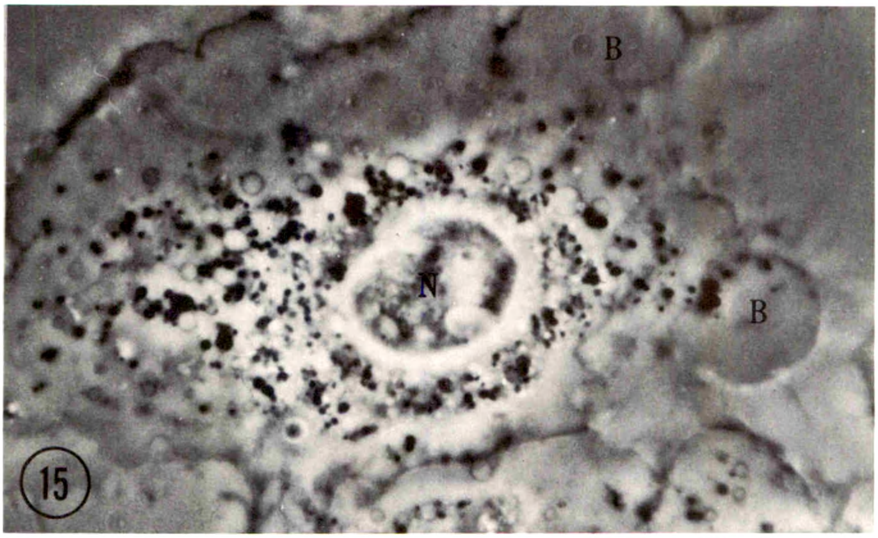

15

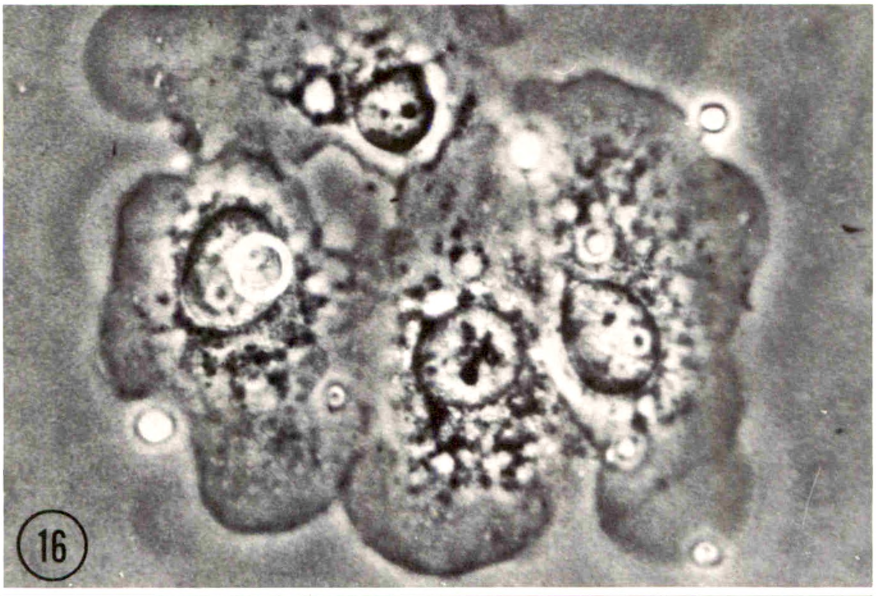

16

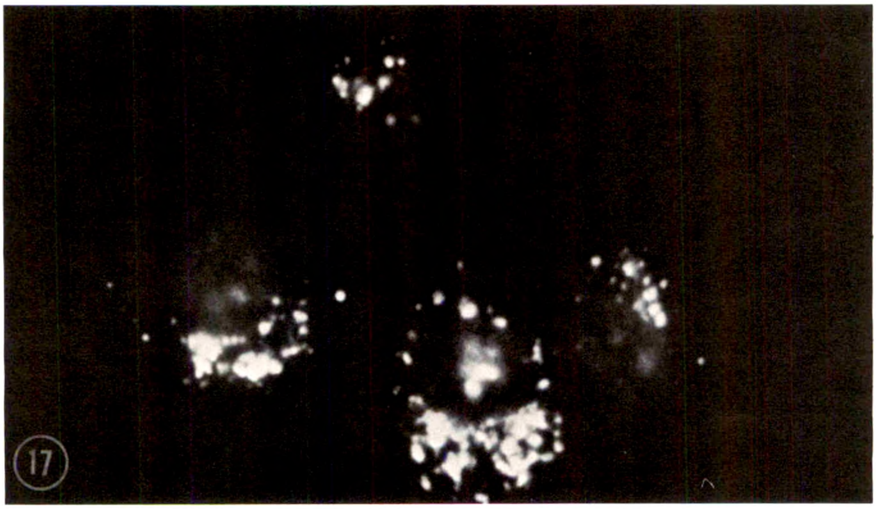

17

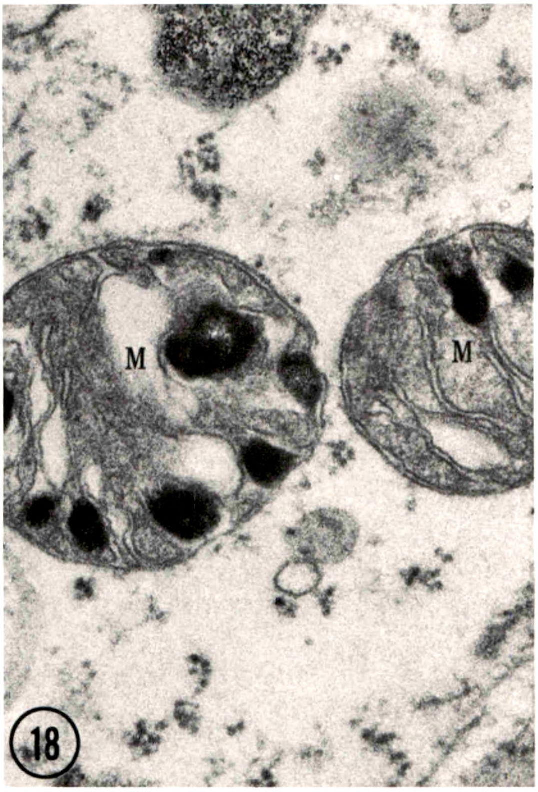
M
M
⑱

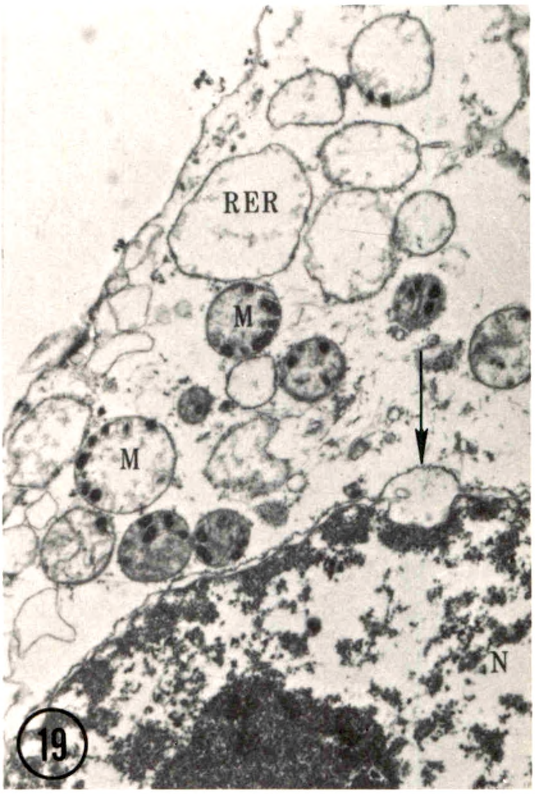
RER
M
M
N
⑲

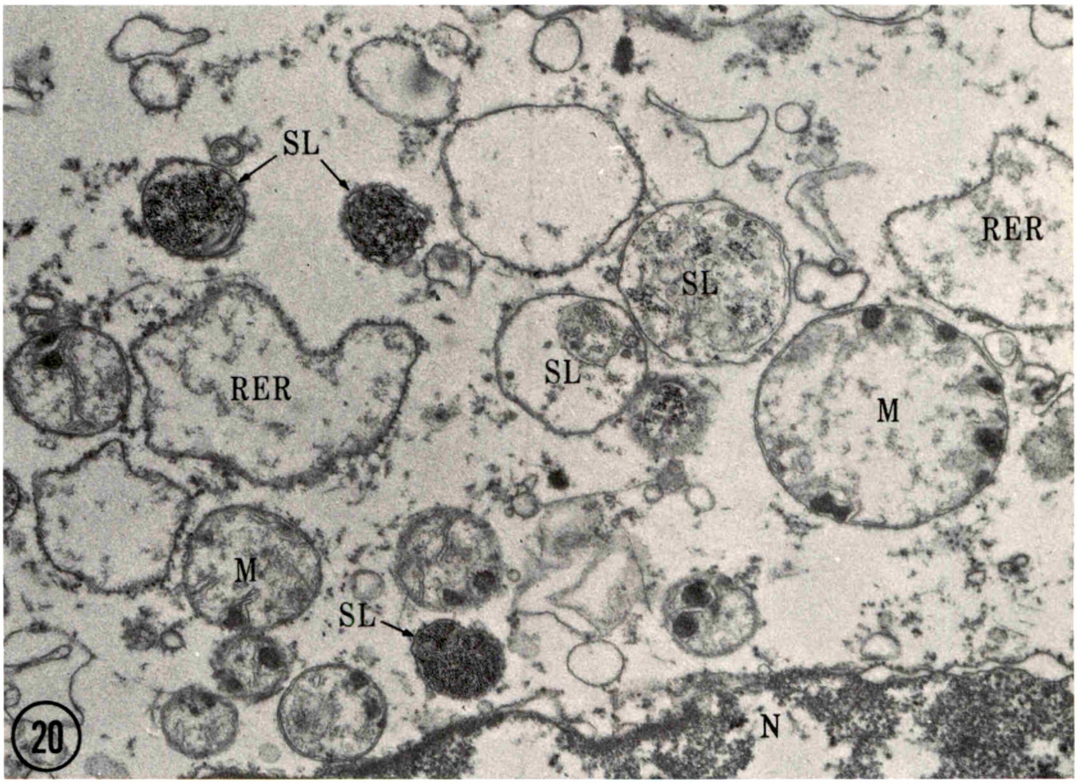
SL
RER
SL
SL
RER
M
M
SL
N
⑳

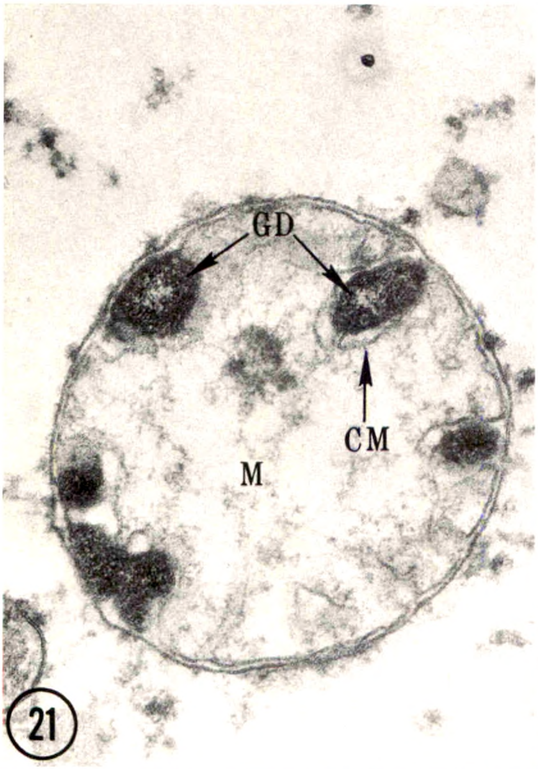
GD
CM
M
21

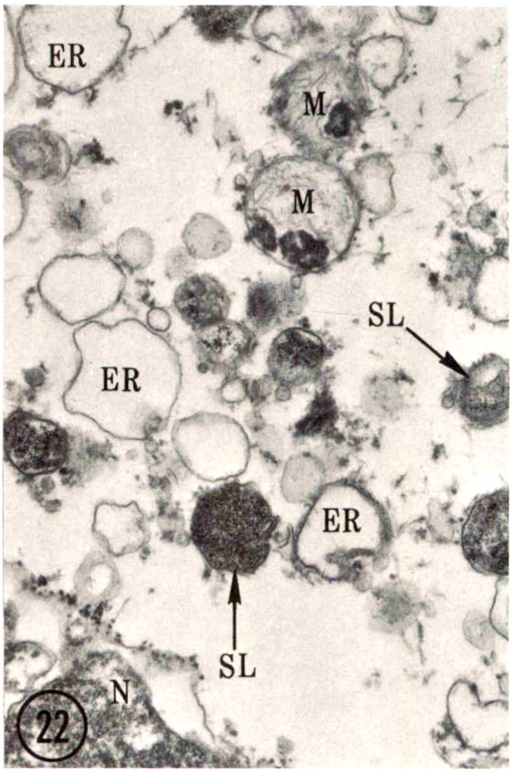
ER
M
M
SL
ER
ER
SL
N
22

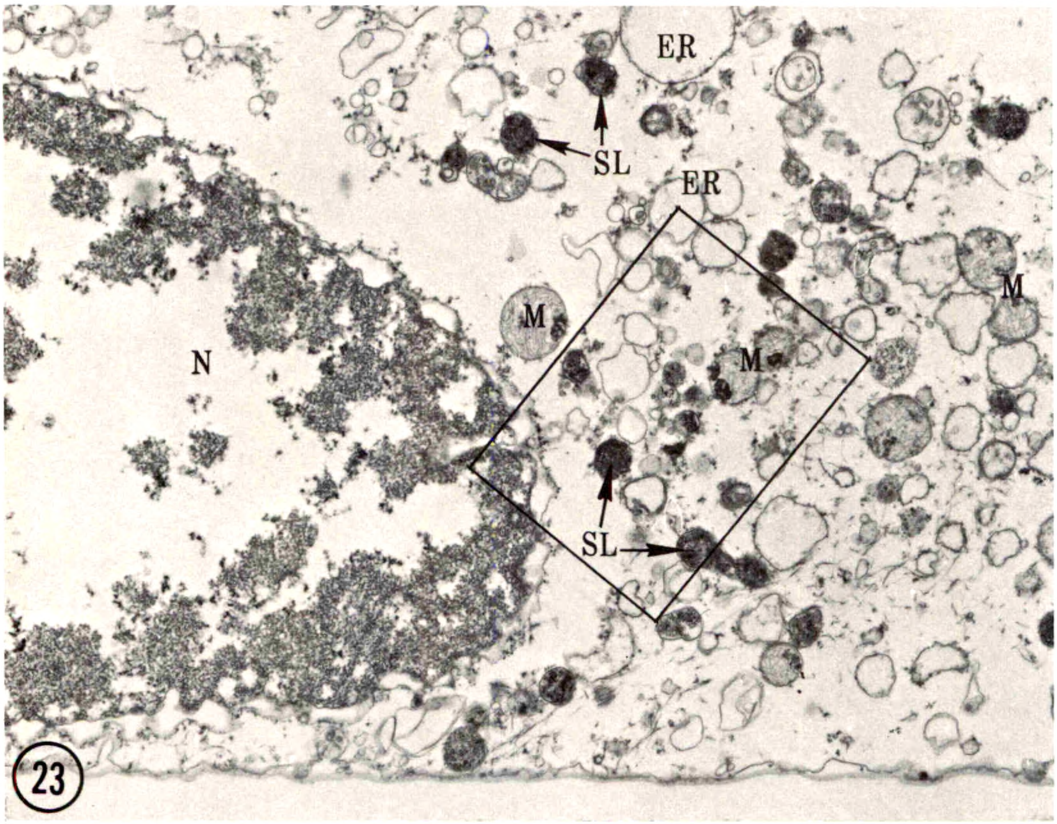
ER
SL
ER
M
N
M
M
SL
SL
23

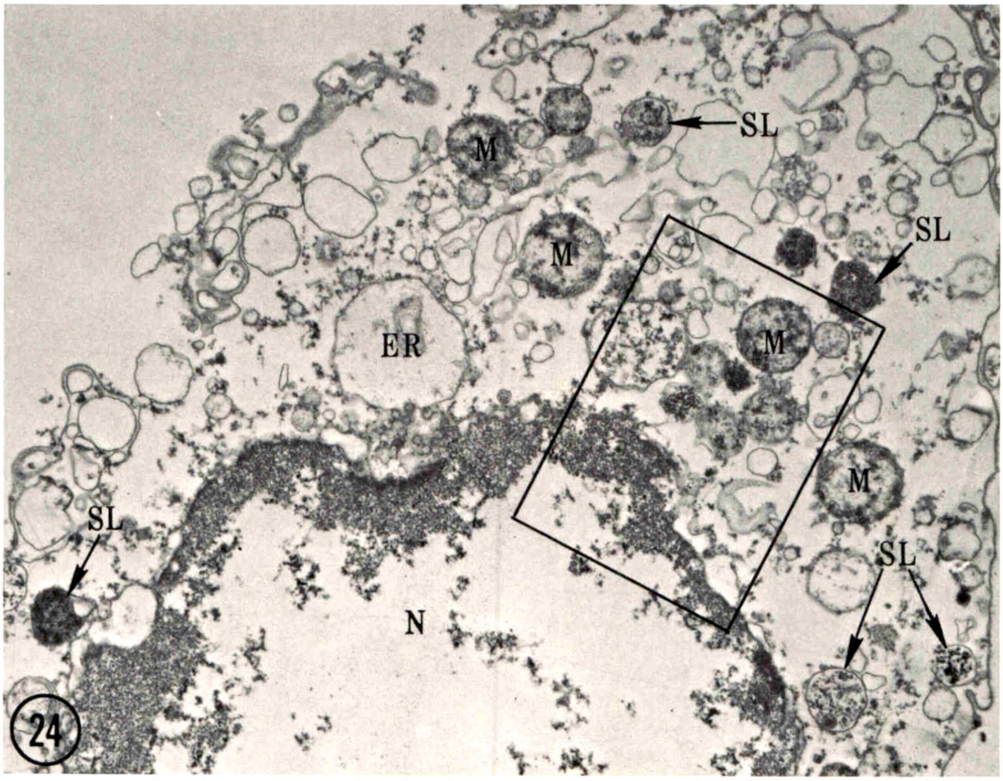
24

SL
SL
M
M
ER
M
M
SL
SL
N

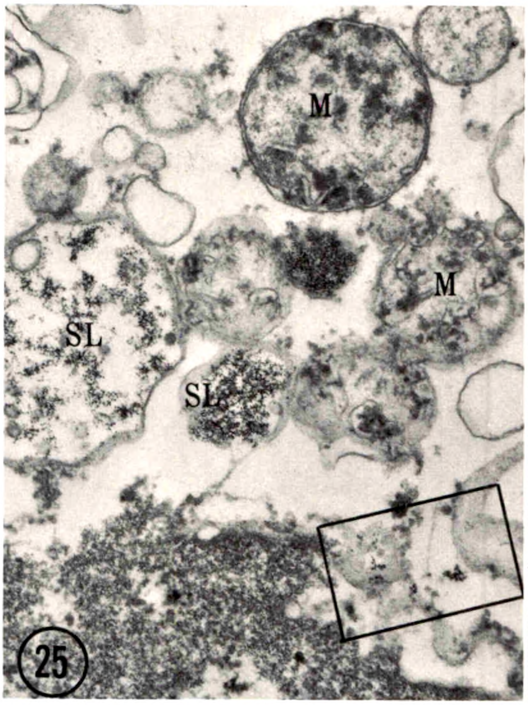
25

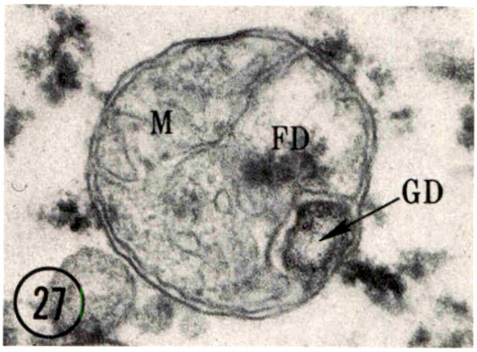
27

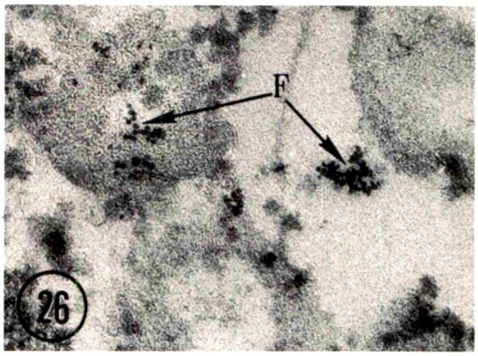
26

[*End of Article*]

Degranulation of Discoid Platelets

James G. White, MD and Richard D. Estensen, MD

Platelet degranulation is a characteristic feature of platelet response to aggregating agents, but the mechanism and route by which secretory organelles are transferred to plasma are still uncertain. In the present study, human platelets were incubated with cytochalasin B, an agent which stabilizes discoid shape, and trypsin, which is known to cause release reaction and degranulation. Platelets treated in this manner retained their disc form, but were nearly devoid of granules and dense bodies. Electron-dense tracers indicated that degranulation was accomplished by fusion of secretory organelles with channels of the open canalicular system. The degranulated discoid platelet appears to survive exposure to cytochalasin B and trypsin and may prove to be a useful model for *in vivo* and *in vitro* experimental studies (Am J Pathol 68:289–302, 1972).

THE PLATELET RELEASE REACTION is a characteristic feature of the maximum platelet response to aggregating agents *in vitro* and *in vivo*.[1] It involves the discharge in parallel of specific substances, including ADP, ATP, serotonin and calcium, stored inside platelets to the surrounding plasma without loss of chemical constituents suggestive of cell damage.[2] Many features of the platelet release reaction have been defined, but the mechanisms by which the intracellular organelles containing the products of secretion are transferred to the exterior environment remain uncertain.[3] One of the problems involved in clarifying the mechanism of platelet secretion is the difficulty in separating the degranulation process from other physical changes occurring in the cells during viscous metamorphosis.[4]

In the course of investigations into the effects of cytochalasin B on platelet structure and function, a new approach to this problem was found.[5] Cytochalasin B is a mold metabolite with a macrolide structure in which the lactone ring is joined to a bicyclic lactum.[6,7] This unusual chemical inhibits certain functions regarded as contractile in nature in many different cells,[8,9] including the platelet-dependent process of clot retraction.[10,11] Examination of the response of cytochalasin-B-treated platelets to potent aggregating agents suggested that the drug

---

From the Departments of Pediatrics and Pathology, University of Minnesota Medical Center, Minneapolis, Minn.

Supported by Grants HE-11880, AI-05153, CA-08832 from the US Public Health Service and the Cardiovascular Clinical Research Program Project.

Accepted for publication Feb. 23, 1972.

Address reprint requests to Dr. James G. White, Department of Pediatrics, University of Minnesota Medical Center, Box 284 Mayo Memorial Bldg, Minneapolis, Minn 5545.

stabilizes platelet discoid form and inhibits shape change, pseudopod formation and internal reorganization without affecting stickiness.[5]

The stabilizing influence of cytochalasin B on platelet discoid shape provided an opportunity to examine degranulation as an entity separate from other features of platelet viscous metamorphosis. Trypsin was chosen as a trigger agent because it is a powerful stimulus of platelet release and degranulation, but under appropriate conditions does not cause clotting or platelet aggregattion.[12] After incubation with cytochalasin B and trypsin, platelets retained their discoid form, circumferential microtubules, filamentous matrix, mitochondria and cytochemically detectable enzymes; nearly all granules and dense bodies were extracted from the cells.

Materials and Methods

The technics used in this laboratory to obtain blood from normal donors in citrate anticoagulant, separate platelet-rich plasma (C-PRP) and prepare samples for study in the electron microscope were described in detail in recent reports.[4,13,14] Cytochalasin B (CB) was dissolved in ethanol at 2 to 4 mg/ml and diluted in Hank's buffered salt solution to a concentration of 250 μg/ml. A 0.1 ml aliquot of this solution was added to 0.9 ml samples of C-PRP, and the tubes placed in a constant temperature water bath at 37 C for 15 minutes. Trypsin was then added to the samples at a final concentration of 1 to 3 mg/ml of C-PRP. The tubes were incubated at 37 C for intervals of 5 minutes to 1 hour, then fixed for study in the electron microscope. Horseradish peroxidase (HRP), 20 mg/ml, or a 0.1 ml aliquot of thorium dioxide were added 15 minutes before fixation to some samples of C-PRP incubated with CB and trypsin for 1 hour. [13,14] Samples containing HRP were processed by the method of Graham and Karnovsky.[15] Additional platelet samples exposed to CB and trypsin were fixed by a slight variation of our usual procedure, and incubated in a modification of the Graham and Karnovsky medium adapted by others for the localization of endogenous peroxidase and catalase.[16] Details of our method for demonstrating endogenous peroxidase have been reported.[17] The effects of trypsin alone, CB alone and trypsin added to C-PRP before CB under the conditions described above were also evaluated.

Results

Effects of Cytochalasin B (CB) Alone

In previous studies we have shown that concentrations of CB up to 30 μg/ml have a minimal effect on the morphology of blood platelets.[5] After exposure at 37 C for 1 hour, CB treated platelets retained their characteristic discoid form (Figure 1). Organelles inside the cells were generally unaltered in appearance and remained randomly dispersed in the cytoplasmic matrix. The circumferential band of microtubules was unaffected by CB. Channels of the open canalicular system were somewhat dilated after exposure to CB, and elements of the dense tubular system were occasionally grouped together in the cytoplasm.

The matrix developed a "ground glass" appearance in some cells, but otherwise appeared undamaged. Aside from the minor changes, morphology of CB treated platelets was indistinguishable from normal cells incubated for the same period of time.

Effects of Trypsin Alone

Hovig pointed out the effects of various concentrations of trypsin on platelet fine structure several years ago.[12] Our results are basically similar to those he described. The changes in fixation methods, however, produce a slightly different impression of the effects of trypsin. We used a concentration of 3 mg trypsin/ml C-PRP because it caused alterations similar to those produced by 1 mg/ml, yet avoided the problem of clot formation completely. Platelets incubated for a few minutes with 3 mg trypsin had the same appearance as those which had been exposed to the agent for 1 hour.

The platelets lost their discoid form and appeared irregular or spherical with few pseudopods (Figure 2). Granules and other organelles when still present were gathered toward cell centers. The curious change in internal membrane systems which Hovig noted [12] was also apparent in our material (Figures 3, 4). In some platelets the membranes were stacked in arc-like segments, and in others they were arranged in concentric layers. Hovig recognized the similarity of the internal membranes to the platelet surface, but suggested that they probably developed from endoplasmic reticulum. However, it appears more likely that the membranes are stretched out channels of the open canalicular system, the linings of which are in continuity with the platelet cell wall. The trypsin-treated cells resembled platelets exposed to thrombin and collagen except for two features: virtual absence of aggregation and the unusual transformation of channels belonging to the open canalicular system.

Effects of Cytochalasin B and Trypsin

The appearance of platelets exposed to trypsin after incubation with CB differed strikingly from cells treated with either agent alone (Figure 5A–C). Platelets were generally discoid, although swelling of the open channel system caused some distortion. The circumferential band of microtubules usually remained peripherally located in the equatorial plane of the platelets. Mitochondria were present, but nearly all platelets were completely devoid of dense bodies and granules. The cytoplasm of the platelets often contained concentric areas of dense filamentous material (Figure 6A). The contracted masses in the matrix resembled those seen in cells treated with trypsin alone. However, granules and microtubules were rarely associated with the filamentous zones. The appearance of these cells indicated that trypsin had caused degranulation and alterations in the cytoplasmic matrix without inducing aggregation of platelets or loss of the characteristic discoid form. Platelets incubated first with trypsin, then with CB, did not differ from platelets treated with trypsin alone.

Localization of Horse Radish Peroxidase and Thorium Dioxide in Platelets Treated with CB and Trypsin

It was important to know if an access route from the interior of the CB-trypsin-treated platelets to the surrounding plasma remained, since granules and dense bodies had apparently not emptied through the surface membrane. The electron-dense tracers, HRP and thorium dioxide, were employed to evaluate this question (Figure 6B–D). Both agents readily entered dilated channels of the open canalicular system. In some examples, thorium dioxide was present in channels which were in continuity with partially empty granules (Figure 6C).

Endogenous Peroxidase Activity of Platelets After Treatment with Cytochalasin B and Trypsin

The experiments with electron-dense tracers demonstrated that the open channel system was affected, but did not reveal whether the second system of canaliculi, the dense tubular system (DTS), was altered by the chemical treatment. Endogenous peroxidase activity resides exclusively in the DTS when platelets fixed in paraformaldehyde-glutaraldehyde are incubated at pH 6 in the medium modified from Graham and Karnovsky.[51-17] After treatment with CB and trypsin, enzyme reaction product was still detectable in channels of the DTS (Figure 6E, F). The channels were slightly dilated, in shorter segments and more dispersed than in control platelets, but the differences were minimal. Thus, the chemical treatment which radically modified the OCS had only a slight effect on the DTS and did not digest its content of enzyme with peroxidase activity.

Discussion

The terms "platelet release reaction", "platelet secretion", and "platelet degranulation" are essentially synonymous.[1-3,18] Secretion of specific chemical compounds by platelets after exposure to aggregating agents is the release reaction,[1] and the substances secreted during release are products stored in platelet granules and dense bodies.[2,3,18] Morphologic studies have indicated that the release reaction is closely related to physical changes in platelet shape and internal organization.[19] When platelets are exposed to aggregating agents capable of triggering release, they lose their discoid form and become roughly spherical with multiple pseudopods. The circumferential band of microtubules and masses of hyaloplasmic microfilaments shift toward the central region of the platelet where they encircle closely grouped organelles. During the phase of irreversible aggregation the granular and filamentous elements fuse together, leaving a dense mass inside the cells.

Apposition, fusion and loss of substance from closely grouped granules to elements of the open canalicular system appear to be important components of the platelet release reaction. Evidence that organelles move outward to the cell surface, fuse with it and empty to the outside is meager.[20,21] The concept that individual granules dissolve in the hyaloplasm permitting their contents to diffuse through the cell and surface membrane has been largely dispelled by observations on the specificity of the substances secreted.[1,18] Ultrastructural studies employing electron-dense tracers have suggested that the open channel system of the platelet serves as the conduit for products of the release reaction; portions of granules and dense bodies have been identified in channels after aggregation.[14] Yet, the mechanism of organelle transfer and the fate of the extruded products entering channels have not been clearly defined.

The present investigation has examined the influence of two chemical agents, Cytochalasin B and trypsin, on blood platelets in order to gain new insights into the process of degranulation. Trypsin at low concentrations causes platelet aggregation and stimulates release.[22] At higher concentrations the agent initiates the release reaction but renders platelets inaggregable.[1,2,12,18,22,23] Both high and low concentrations appear to produce similar effects on platelet morphology.[12] Alterations in platelet shape and internal organization are similar to those initiated by other potent aggregating agents, except for the changes noted in the open channel system. Conversion of the tortuous fenestrated channels into long, arc-like or circular tubes is peculiar to trypsin. Ethylenediaminetetracetic acid (EDTA) is the only other chemical agent with a somewhat similar effect on platelets.[24]

Cytochalasin B causes only minor changes in platelet morphology,[10] but strongly influences the capacity of the cells to undergo shape change and alters the pattern of internal reorganization induced by aggregating agents.[5] It does not affect the capacity of platelets to become sticky or secrete substances essential for development of irreversible aggregation, but delays the onset of the release reaction in a concentration dependent manner. The resistance of CB-treated cells to shape change, pseudopod formation, internal reorganization and onset of release appear to underlie the inhibitory effect of this agent on clot retraction.[5,10,11]

Examination of platelets treated with CB prior to trypsin confirmed the impression gained in previous studies.[5] Despite the potent effects of the proteolytic enzyme, most CB-treated platelets retained a relatively discoid shape. Circumferential bundles of microtubules remained in their usual location in the equatorial plane under cell surfaces. Channels of the open canalicular system were dilated and straightened after CB and trypsin, but were not converted into the concentric or arc-like arrangements seen in cells exposed to trypsin alone. Filamentous elements and mitochondria were well preserved in the hyaloplasmic matrix of treated cells. Granules and dense bodies, however, were virtually absent.

Thus, CB appeared to protect platelets from the drastic changes in form and internal reorganization usually caused by trypsin, but did not prevent contraction of the matrix, disappearance of the storage organelles or alterations in the open canalicular system. Previous investigations have indicated that trypsin acts on the outside surface of platelets and does not enter the hyaloplasm.[1,22,23,25] The excellent preservation of filaments and mitochondria, and the cytochemical demonstration of endogenous peroxidase activity in the dense tubular system after treatment with CB and the proteolytic enzyme indicate that trypsin did not seriously damage the interior of platelets observed in this study. The contraction of the matrix into dense spots is not an indication of platelet cytoplasmic injury, but a peculiar effect of CB on internal reorganization. An identical condensation of filamentous material occurs in CB treated platelets after exposure to all other aggregating agents tested.[5]

Trypsin might have caused granules to move to the platelet surface, fuse with it and empty to the exterior, but no evidence supporting this possibility was encountered. An unusual influence of trypsin on channels of the open canalicular system and interaction between the altered channels and organelles in CB-treated cells seemed more likely. Addition of electron-dense tracers to the treated cells verified this hypothesis. Neither horseradish peroxidase nor thorium dioxide entered the cytoplasm of CB-trypsin-treated platelets, indicating that the cell membrane was intact. Both agents, however, penetrated into channels of the open canalicular system. In some cells the channels containing thorium dioxide were in continuity with incompletely dissolved granules. These findings suggested that trypsin-induced degranulation of platelets is accomplished by fusion of granules and dense bodies with channels of the open canalicular system. The paucity of granular debris in the open channels may have been due to proteolysis of the extruded material by trypsin or to lysis of granules on contact with plasma.

In conclusion, the stabilizing influence of cytochalasin B on disc form and the capacity of trypsin to alter the open canalicular system and selectively remove dense bodies and granules from platelets have been employed in the present investigation to prepare discoid platelets without secretory organelles. Mitochondria, glycogen, elements of the dense tubular system, filaments, microtubules and the cell membrane appeared essentially unchanged after chemical dissection by the two agents; a specific enzyme activity, platelet peroxidase, could still be detected cytochemically in its usual location. Trypsin, in the concentration used, renders plasma incoagulable and causes such profound changes in the exterior coat that the platelets no longer aggregate. However, the platelets appear in excellent morphologic condition despite the loss of secretory organelles and susceptible components of the exterior surface, and it is possible that they survive the drastic treatment as intact, metabolically active cellular units. If so, the degranulated discoid platelet can serve as a useful model for a variety of biochemical, physiologic and immunologic studies *in vitro* and *in vivo*.

References

1. Grette K: Studies on the mechanism of thrombin-catalyzed hemostatic reactions in blood platelets. Thromb Diath Haemorrh 56 (Suppl 195):1–93, 1962
2. Holmsen H, Day HJ, Stormorken H: The blood platelet release reaction. Scand J Haematol (Suppl) 8:1–26, 1969
3. White JG: Origin and function of platelet dense bodies. Series Haematol 3:17–46, 1970
4. White JG: Fine structural alterations induced in platelets by adenosine diphosphate. Blood 31:604–622, 1968
5. White JG: Platelet microtubules and microfilaments: Effects of cytochalasin B on Structure and Function. Platelet Aggregation. Edited by J Caen. Paris, Masson et Cie, pp 15–52, 1971
6. Carter SB: Effects of cytochalasin B on mammalian cells. Nature (Lond.) 213:261–264, 1967
7. Aldridge DC, Armstrong JJ, Speake RN, Turner WB: The structure of cytochalasins A and B. Chem Com 1:26–27, 1967
8. Schroeder TE: The contractile ring. I. Fine structure of dividing mammalian (HeLa) cells and the effects of cytochalasin B. Z Zellforsch Mikroskop Anat 109:431–449, 1970

9. Estensen RD: Cytochalasin B. I. Effect on cytokenesis of Novikoff hepatoma cells. Proc Soc Exp Biol Med 136:1256–1260, 1971
10. Shepro D, Belamarich FA, Robblee L, Chao F: Antimotility effect of cytochalasin B observed in mammalian clot retraction. J Cell Biol 47:544–547, 1970
11. Wessells NK, Spooner BS, Ash JF, Bradley MO, Luduena MA, Taylor EL, Wrenn JT, Yamada KM: Microfilaments in cellular and developmental processes. Science 171:135–143, 1971
12. Hovig T: The effect of various enzymes on the ultrastructure aggregation and clot retraction ability of rabbit blood platelets. Thromb Diath Haemorrh 13:84–113, 1966
13. White JG: The interplatelet zone. Am J Pathol 58:19–29, 1970
14. White JG: A search for the platelet secretory pathway using electron dense tracers. Am J Pathol 58:31–49, 1970
15. Graham RC, Karnovsky MJ: The early stages of absorption of injected horse-radish peroxidase in the proximal tubules of kidney. Ultrastructural cytochemistry by a new technique. J Histochem Cytochem 17:675–680, 1969
16. Novikoff AB, Goldfischer S: Visualization of peroxisomes (microbodies) and mitochondria with diaminobenzidine. J Histochem Cytochem 17:675–680, 1969
17. White JG: Interaction of membrane systems in blood platelets. Am J Pathol 66:295–312, 1972
18. Day HJ, Holmsen J: Concepts of the blood platelet release reaction. Series Haematol 4:3–27, 1971
19. White JG: Platelet morphology. The Circulating Platelet. Edited by SA Johnson. New York, Academic Press, Inc, pp 45–121, 1971
20. White JG, Krivit W: The ultrastructural localization and release of platelet lipids. Blood 27:167–186, 1966
21. Weber AJ, Johnson AA: Platelet participation in blood coagulation: Aspects of Hemostasis. Am J Pathol 60:19–27, 1970
22. Haslam RJ: Role of adenosine diphosphate in the aggregation of human blood platelets by thrombin and by fatty acids. Nature 202 765–769, 1964
23. Schmid HJ, Jackson DP, Conley CL: Mechanism of action of thrombin on platelets. J Clin Invest 41:543–549, 1962
24. White JG: Effects of ethylenediaminetetracetic acid (EDTA) on platelet structure. Scand J Haematol 5:241–254, 1968
25. Markwardt F: Studies on the release of biogenic amines from blood platelets. Biochemistry of Blood Platelets. Edited by E Kowalski, S Niewiarowski. New York, Academic Press, Inc, pp 105–116, 1967

[Illustrations follow]

Fig 1—Cytochalasin B (*CB*)-treated platelet. The cell is from a sample of normal C-PRP incubated 30 minutes with CB at a concentration of 25 μg/ml. Platelet discoid shape is preserved, despite some dilatation of the open canalicular system (*OCS*). The circumferential bundle of microtubules (*MT*) remains intact and in its usual location under the cell surface. Granules (G), dense bodies (*DB*), and other cytoplasmic organelles appear relatively unaltered. The matrix of the platelet develops a "ground glass" appearance after exposure to CB. Aside from these mild changes, the morphology of CB-treated platelets did not differ significantly from normal cells (× 39,900).

Fig 2—Trypsin-treated platelets. The cells are from a sample fixed 60 minutes after addition of trypsin at 3 mg/ml C-PRP. After exposure to this concentration the sample does not clot, and the platelets no longer aggregate. Trypsin causes platelets to lose their discoid form and become irregular. Organelles are shifted toward the cell centers where they may fuse or disappear. In addition, to these alterations, which are similar to those produced by potent aggregating agents, trypsin causes striking changes in the open canalicular system. Several types of membrane alterations are apparent in the cells of this illustration (× 18,500).

Fig 3 and 4—Trypsin-treated platelets. The cells are from samples exposed to 3 mg trypsin/ml of C-PRP for 30 minutes. In Figure 3 the altered channels of the open canalicular system are arranged concentrically, while in Figure 4 the channels are stacked in an arc-like segment. The arrangement suggests a relationship between the altered channels and membranes enclosing granules (**3**, × 41,500; **4**, × 41,500).

Fig 5A, B, C—Platelets from samples of C-PRP incubated initially with cytochalasin B (25 μg/ml) for 15 minutes, then with trypsin (3 mg/ml) for 30 minutes at 37 C. After exposure to the two agents platelets are slightly irregular due to swelling of the open channel system, but most cells retain a relatively discoid form. The platelets in Figure 5A reveal normal mitochondria (*M*) and occasional lipid droplets (*L*), but are nearly devoid of granules and dense bodies. In some cells remnants of partially dissolved granules (G) can be identified. The platelets in Figure 5B and C are discoid and contain circumferential bundles of microtubules in cross section at opposite poles in each cell. Granules and dense bodies are entirely absent in this plane of the section (**A**, × 15,300; **B**, × 42,300; **C**, × 41,500).

Fig 6—The platelet in Fig 6A is from C-PRP exposed to CB and trypsin and demonstrates the contraction of cytoplasmic gel into a filamentous mass (arrow) without loss of disc form. A residual granule (G) remains in the treated cell. Platelets in Fig 6B and C are from C-PRP treated with CB and trypsin to which a small amount of thorium dioxide (*TD*) has been added. Particles of electron-dense TD appear in the open canalicular system of the platelets. In Fig 6C TD particles are also present in a partially dissolved granule (arrow) which appears to communicate with a channel of the OCS. The platelet in Fig 6D is from a sample incubated with CB and trypsin to which horseradish peroxidase has been added before fixation. After fixation the sample was incubated for peroxidase activity. Peroxidase is apparent covering the cell surface and lining the OCS. The platelets in Fig 6E and F were treated with CB and trypsin, and incubated for the demonstration of endogenous platelet peroxidase. The sections were not stained with uranyl acetate or lead citrate. At either pH 9 (Fig 6E) or pH 6 (Fig 6F) endogenous platelet peroxidase is demonstrable in the treated cells, and is confined to channels of the dense tubular system as it is in normal cells (**6A**, × 42,000; **6B**, × 37,300; **6C**, × 33,200; **6D**, × 37,000; **6E**, ×33,200; **6F**, × 41,500).

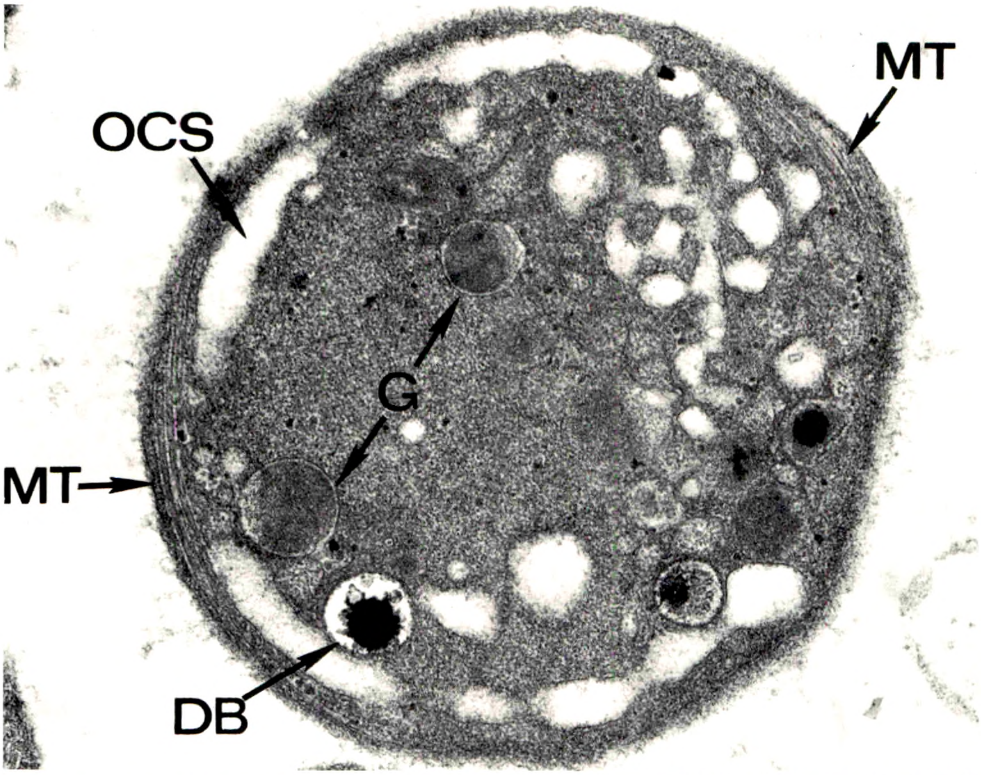
MT
OCS
G
MT
DB

1

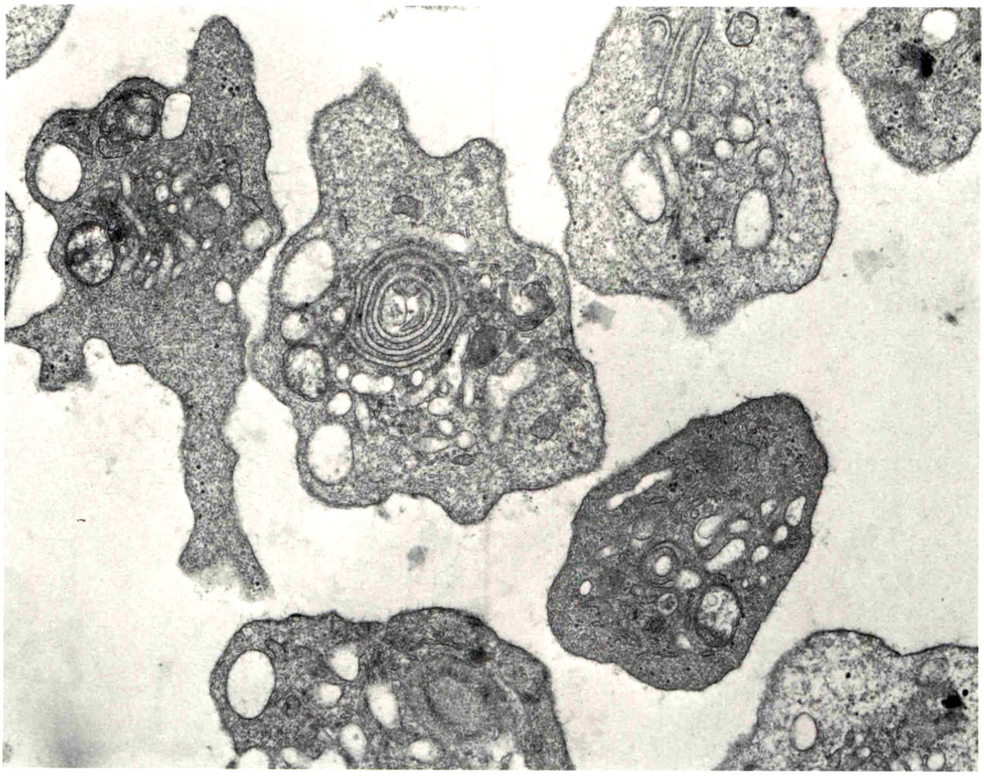

2

3

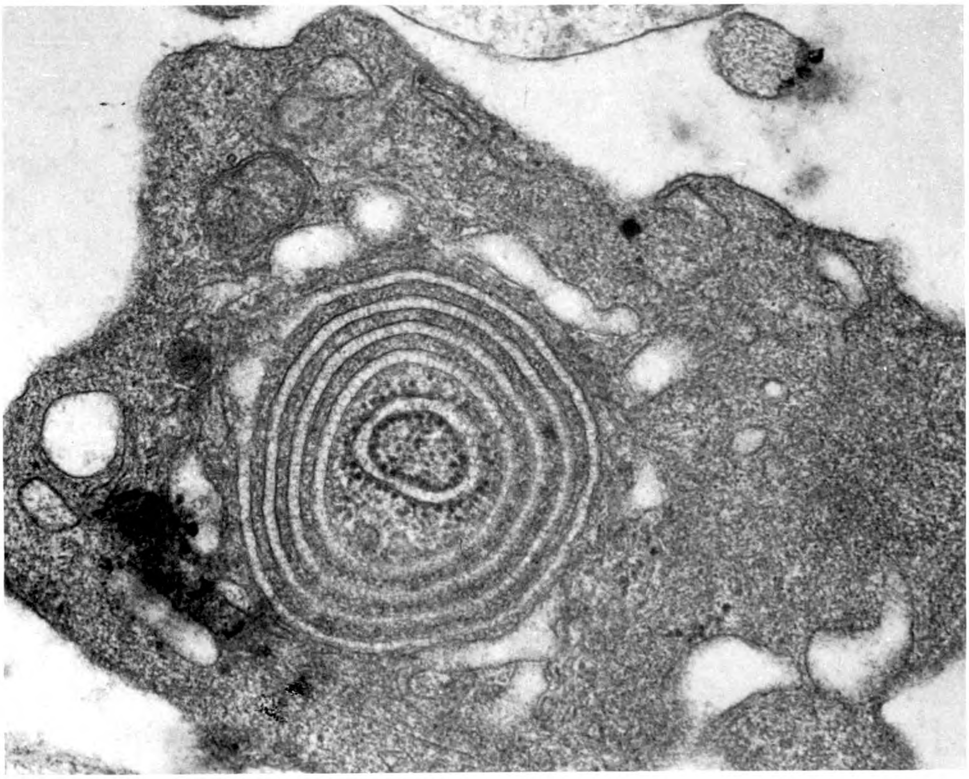

4

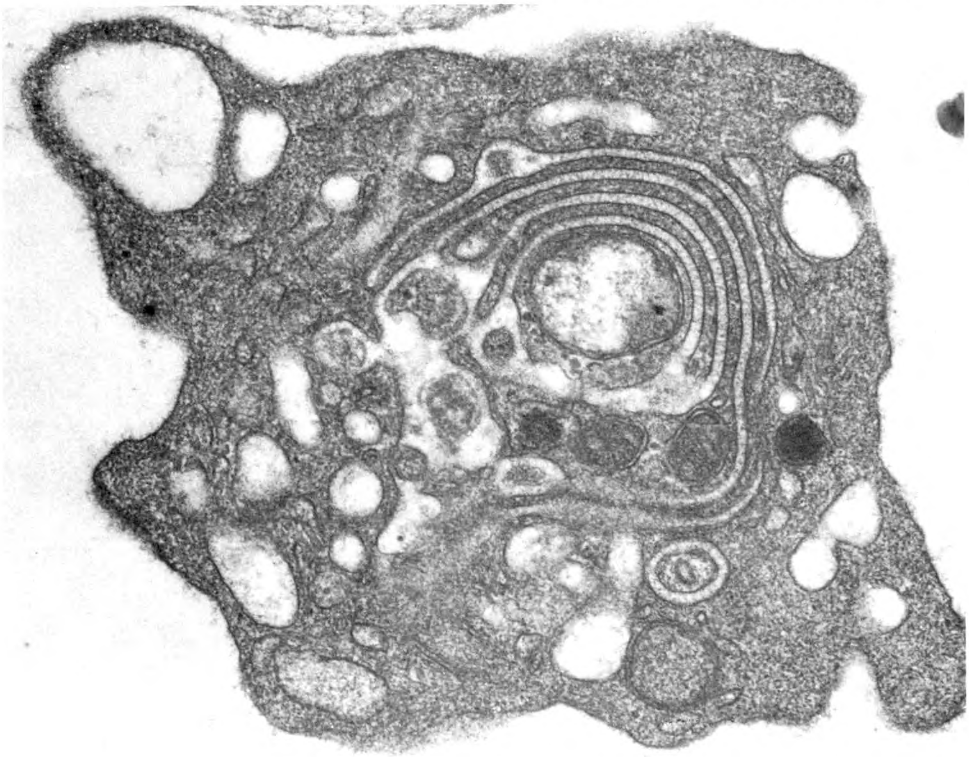

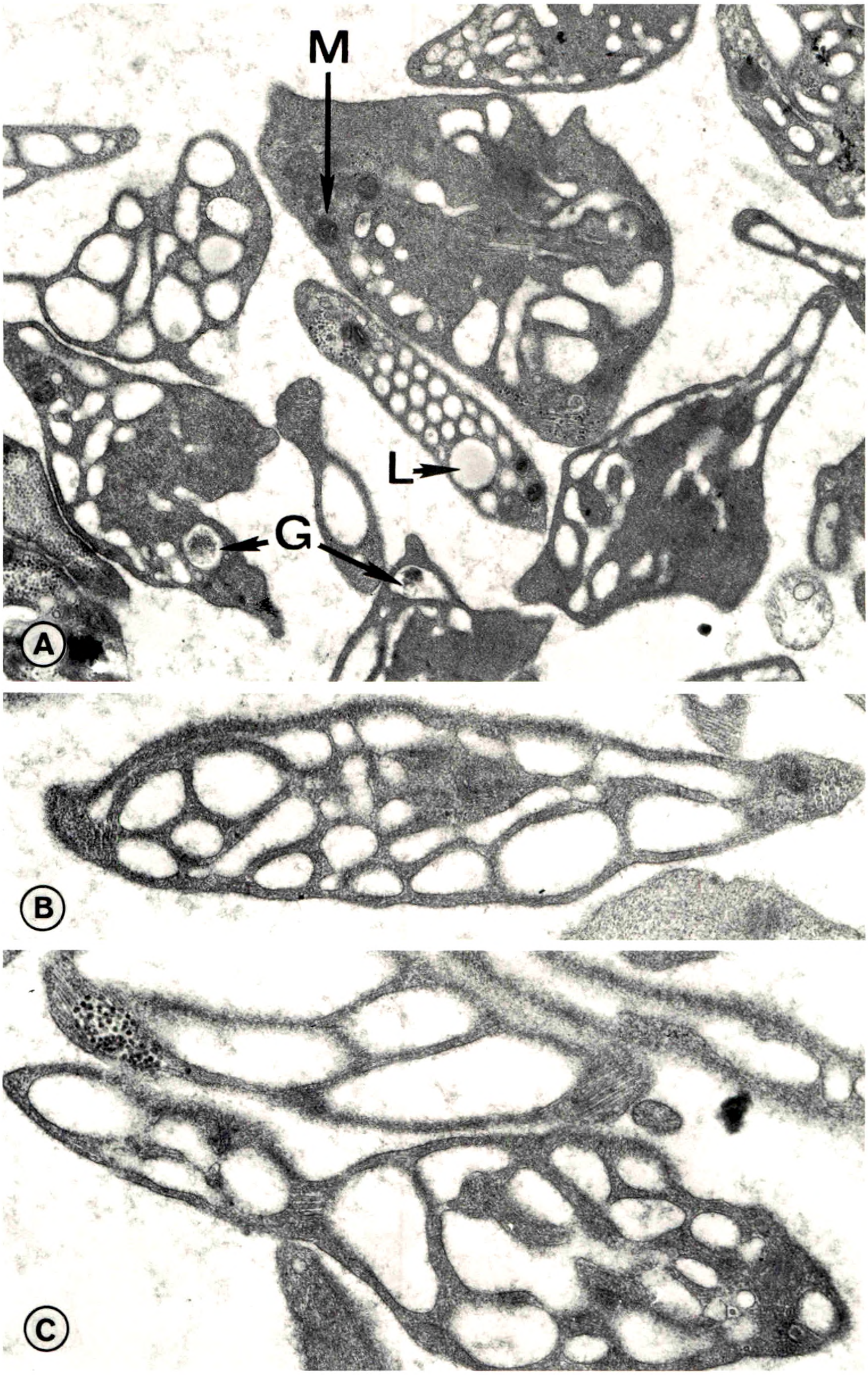

5

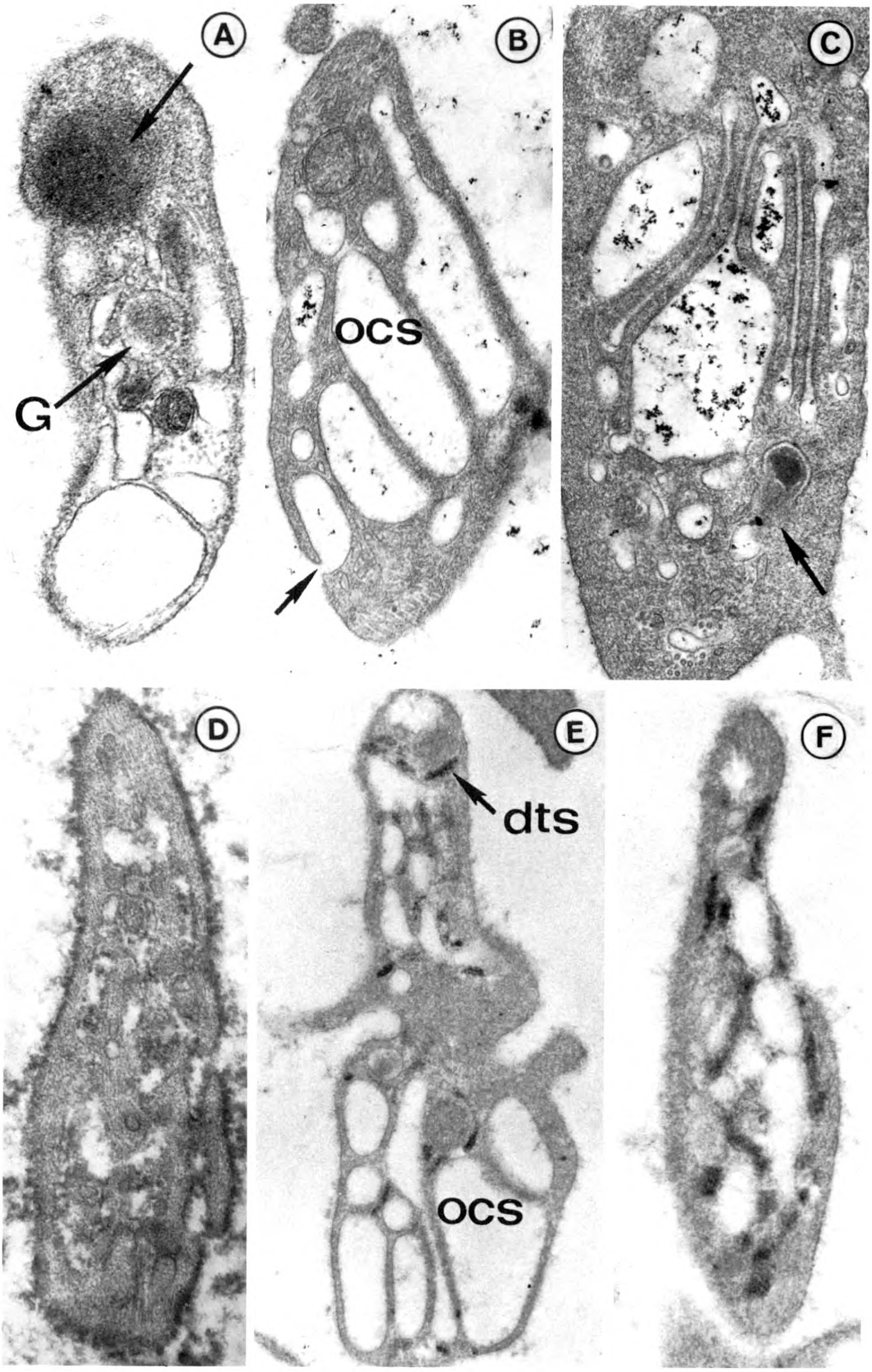
A
G
B
ocs
C
D
E
dts
ocs
F

6

Ultrastructural Characteristics of Freeze-Dried Human Blood Platelets

Richard B. Davis, MD, PhD

Ultrastructural characteristics of freeze-dried human blood platelets were investigated. Extensive ice crystal formation was found in platelets frozen in the absence of cryoprotective agents. Platelet preservation was much improved by the addition of dimethyl sulfoxide, or dimethyl acetamide, with glucose or 0.25 M sodium glycerophosphate, to platelet-rich plasma prior to the freeze drying process. Platelet membranes and organelles were generally well preserved, and many granules demonstrated eccentric areas of electron density. Microtubules were not clearly identified, but some platelets showed tubule-like structures within platelet hyaloplasm. Pseudopods were often observed at the platelet surface, and often contained membrane-bound granule-like structures. Some pseudopods contained electron-dense material which extended between adjacent platelets in interplatelet bridges and which was released to the surrounding medium. Interplatelet bridge formation was not prevented by chelation of calcium by ethylenediamine tetraacetic acid. The observations were consistent with the suggestion that contractile protein is present in interplatelet bridges and serves as a basis for clot retraction (Am J Pathol 68:303–316, 1972).

IN RECENT YEARS there has been much interest in the behavior of human blood platelets at temperatures below 37C, because of efforts to preserve platelets for transfusion purposes. Several methods of cooling and storage have been evaluated. These include the storage of platelets at room temperature [1-3] and the freezing of platelets in the presence of cryoprotective agents. Dimethyl sulfoxide (DMSO) and dextrose, dimethyl acetamide (DMAC) with dextrose, and DMSO with sodium glycerophosphate have been found to improve the preservation of frozen platelets.[4-10]

Zucker and Borrelli [11] showed that platelets washed at cold temperatures became spiny spheres, and platelet volume increased in the cold.[12] The spherical change was accompanied by depolymerization and disappearance of the marginal band of microtubules in platelets exposed to a temperature of 0 to 4 C, while platelet organelles were distributed in a random fashion.[13] Platelets frozen in the presence of DMSO-dextrose retained their morphologic integrity by phase

---

From the Division of Hematology and the Department of Internal Medicine, University of Nebraska Medical Center, Omaha, Neb.

Supported in part by the American Heart Association.

Accepted for publication Apr 24, 1972.

Address reprint requests to Dr. Richard B. Davis, Department of Internal Medicine, University Hospital, University of Nebraska Medical Center, 42nd and Dewey Ave, Omaha, Neb 68105.

microscopy, whereas vacuolization and other abnormalities occurred in platelets frozen in the absence of DMSO.[6] The findings reported in this study have evaluated ultrastructural changes in frozen human platelets, both freeze-dried in the absence of fixation and fixed after freezing.

Materials and Methods

Platelets were obtained from human venous blood which was collected in plastic syringes and 9 ml mixed with 1 ml acid citrate anticoagulant[14] in polycarbonate centrifuge tubes. Platelet-rich plasma (PRP) was obtained by centrifugation at 150g for 7 minutes at 21 C. Samples of PRP were processed without cryoprotective agents, or were mixed by inversion with: a) 5% DMSO plus 5% dextrose (final concentration) b) 5% DMAC plus 5% dextrose, c) 5 DMSO plus 0.25 M sodium glycerophosphate, and d) 5% DMAC plus 0.25 M sodium glycerophosphate. PRP, with or without cryoprotective agents, was frozen directly in a copper wire loop or was centrifuged at 3700g for 5 minutes to obtain a platelet button, which was subsequently frozen on small boats of aluminum foil. Samples were plunged into isopentane that had been precooled to −155 C in liquid nitrogen and then transferred into or occasionally frozen in liquid nitrogen. Slow freezing was accomplished by placing platelet buttons in an aluminum tray positioned on the cooling plate of an Edwards-Pearse tissue dryer (Model EPD-2). The temperature of the plate was reduced at an average rate of 1 degree/min, to −65 C.

All samples were dried in an Edwards-Pearse EPD-2 tissue dryer at −65 C (plate temperature) for 24 hours. Samples were warmed to 21 C in a period of 1 to 2 hours, infiltrated in vacuum for 1 hour, and for an additional 48 hours at atmospheric pressure, with shaking, on a rotating apparatus. Unaccelerated resin (Epon 812-Araldrite 502) then was replaced with accelerated (3% DMP-30) resin, and infiltration continued for 24 hours. All capsules were polymerized at 60 C.

Three modifications of the technic described above were employed. These included: a) blood collected and 9 ml mixed with 1 ml of 0.6% ethylene diamine tetraacetic acid (EDTA) and platelet buttons frozen in isopentane after the addition of 5% DMSO and 5% dextrose to PRP; b) washed platelets, prepared from blood collected in acid citrate, followed by centrifugation, gentle resuspension in 0.05 M Tris-buffered 0.154 M sodium chloride, containing 5% DMSO and 5% dextrose and platelet buttons frozen in isopentane; c) PRP frozen and fixed directly. Platelet buttons were transferred from liquid nitrogen directly to glutaraldehyde (3% in Earle's salt solution) and fixed for 1 hour at 21 C. After washing with Earle's salt solution at 21 C, platelets were fixed for 1 hour at 4 C with 1% osmium tetroxide, and dehydrated with graded ethanols. Sections were double stained using lead citrate and uranyl acetate, and examined in a Phillips 300 electron microscope.

Results

Platelets Freeze-Dried Without Cryoprotective Agents

Platelets frozen directly in isopentane and subsequently freeze-dried were poorly preserved. The majority of platelets in these preparations were flattened, with nearly complete loss of morphologic integrity. An occasional platelet did retain a spherical shape. Ice crystal formation was extensive in these platelets and their hyaloplasm was disrupted (Figure 1). Some granules were preserved, and platelet limiting membranes were present.

Platelets Frozen and Fixed

Platelets frozen in isopentane, either with or without cryoprotective agents, and subsequently fixed, frequently lost their normal structures. These changes were especially noted in samples fixed in the absence of cryoprotective agents (Figure 2), and included the loss of platelet plasma membranes and organelles, the presence of numerous pseudopods and areas of vacuolization, although glycogen appeared to be retained. The structure of platelets frozen with cryoprotective agents and subsequently fixed was better preserved in some cases. For example, platelets frozen in the presence of DMSO-dextrose (Figure 3), had intact plasma membranes, glycogen and mitochondria. Platelet organelles were otherwise poorly preserved. Platelets preserved with DMAC-sodium glycerophosphate, frozen, and fixed showed only moderate evidence of structural damage (Figure 4). α-Granules again seemed to be lost and vacuoles were frequent. Glycogen appeared to be preserved, and platelet plasma membranes were intact. Some platelets retained their normal discoid structure. Platelets frozen at a rate of 1 degree/min with DMSO-dextrose followed by glutaraldehyde fixation, showed evidence of vacuolization, although basic platelet structures were retained. Platelet α-granules were present and platelet glycogen remained (Figure 5).

Platelets Mixed with Cryoprotective Agents and Subsequently Fixed

To study the structural effects of cryoprotective agents on platelets, without freezing, DMSO-dextrose, DMAC-dextrose, DMSO-sodium glycerophosphate and DMAC-sodium glycerophosphate were evaluated. Many platelets exposed to DMAC-sodium glycerophosphate retained their discoid appearance. Although vacuolization was increased, α-granules appeared to be well preserved, glycogen was intact and dense bodies as well as microtubules were seen (Figure 6). Similar changes were noted in platelets exposed to DMSO-dextrose (Figure 7), in which pseudopods were prominent. Microtubules were also present in those platelets.

Platelets Frozen With Cryoprotective Agents and Freeze-Dried

Platelets frozen in the presence of cryoprotective agents and freeze-dried developed pseudopods which extended to form interplatelet bridges. In some instances platelets appeared to have collapsed, but many platelets were well preserved, with intact plasma membranes,

α-granules and mitochondria (Figure 8). The exterior coat of the platelet appeared to be visualized, and contained organelle-like structures bounded by membranes which appeared to be external to the platelet plasma membrane (Figure 9). In some cases pseudopods which appeared to be membrane-bound and contained electron-dense material were seen. In a contiguous area, this material appeared to be released at the platelet surface, in an area of membrane discontinuity (Figure 10).

Platelets frozen in DMAC-sodium glycerophosphate (Figure 11) appeared similar to those frozen in DMSO-dextrose—limiting membranes were intact and organelles were seen throughout the platelet. In certain cases granule-like structures appeared exterior to an intact plasma membrane and within the platelet external coat (Figure 12); pseudopods were noted, which appeared to contain granule-like structures or electron-dense material. In other platelets, electron-dense material appeared to be released at the surface, directly into the surrounding plasma (Figure 13).

Pseudopods which extended from the platelets to produce interplatelet bridging contained electron-dense material, and occasionally were bounded by negatively stained structures similar to the plasma membrane and the membrane which surrounded platelet organelles (Figures 1, 14). Bridging also was noted between adjacent platelets, in which it appeared that platelets were bridged through the platelet external coat (Figure 15).

DMSO-dextrose was added to platelet-rich plasma containing EDTA. Morphology after freeze-drying was substantially similar to that observed with platelets prepared from acid citrate and frozen. Pseudopods connecting adjacent platelets were seen (Figure 14). Platelet bridging associated with freezing was not dependent upon the presence of plasma protein in the medium. Washed platelets collected in a button and frozen showed evidence that pseudopods fused in the platelet aggregate; electron-dense material also was noted at the surface of the platelet.

The morphology of platelets freeze-dried at 1 degree/min in the presence degree of DMSO-dextrose, a cryoprotective agent, was poorly preserved with most of the platelets collapsed. Ice crystal formation was extensive.

Discussion

Freeze-drying has been utilized to study the ultrastructure of cell membranes[15] and of influenza viruses.[16] Rabbit[17] and human[18] erythrocytes also have been observed in the electron microscope after freeze-drying. In red cell preparations, extensive ice crystal formation was present, similar to that observed in platelets frozen directly in isopentane (Figure 1). Nei[17] found that the temperature of freezing influenced morphology, because cells frozen at −30 C were distorted considerably but lacked ice crystal formation; those frozen at −150 C, retained their spherical shape, but had numerous intracellular cavities.

Ice crystal formation also depends on the rate at which the tissue is cooled.[19] If heat is removed at a sufficiently rapid rate, the transition of water to a vitreous state occurs almost completely without crystal formation. Theoretic considerations show that cooling at a rate of 5000 to 8000 cal/cu cm/sec causes minimal crystallization.[19] To remove heat at this rate the temperature must be reduced to −100 C, which approximates the transition temperature for water in tissue, in 15 to 30 mseconds. Cooling in isopentane at −155 C is of the order of 1500 cal/cu cm/sec. At that rate of cooling, the heat released by crystallization exceeds that removed by conduction before the temperature of vitrification is reached, and crystallization goes to completion. Immersion in liquid helium or nitrogen causes even slower cooling due to the formation of a gas interface at the surface of the specimen.[20]

Exact freezing rates in the platelet samples studied cannot be determined accurately because the theoretic rate of cooling varies with the inverse square of the least linear dimension of frozen tissue.[19] As expected from these theoretic considerations, platelet preservation was poor unless cryoprotective agents were used. Cryoprotective agents penetrate the cell membrane to exert a colligative action;[21] they do not contribute to osmotic support of the cell, but do increase the total solute concentration in the cell, thus diminishing the amount of ice formed at any subfreezing temperature. Reduction in the amount of ice formed in turn will reduce possible membrane damage due to increases in osmotic activity of electrolytes originally present in isotonic concentrations within the cell.

Platelets frozen in the presence of cryoprotective agents showed vacuolization and loss of structural detail when thawed and fixed, but their preservation was substantially improved when freeze-dried, compared to platelets frozen without cryoprotection. Freeze-dried platelets bore some resemblance to negatively stained whole mounts of human platelets,[22-23] but were observed in thin section, permitting improved definition of structure. Certain structures, such as microtubules, were not clearly observed in frozen platelets, in keeping with the observation that chilling causes depolymerization of the microtubules.[13] Frequently, pseudopods extended between, and formed bridges between, adjacent platelets. Bridging was not prevented by depleting calcium ions with EDTA, although aggregation by cold injury is calcium dependent.[24]

Fibrils have been described in pseudopods of whole mount preparations of normal platelets [22] and a role for submembrane filaments has been postulated in the extrusion and stabilization of pseudopods.[25] Submembrane filaments may also participate in the platelet contractile mechanism.[25] Although the appearance of filamentous material in frozen platelets was not observed, it is clear that electron-dense material appeared in spiky pseudopods, extending both into the interior of the platelet and into interplatelet bridges between adjacent platelets. This material was not identified in routinely fixed preparations exposed to cryoprotective agents. It was seen in freeze-dried platelets both in the presence and absence of cryoprotective agents. Thus, the electron-dense material appeared to be related to physical changes associated with freezing.

The site of origin of electron-dense material demonstrated in the present studies cannot be determined with certainty. This material could arise from submembrane microfilaments, from the dense tubular system, or on the platelet surface. Contractile protein has been localized on the platelet surface,[26] and if electron-dense material is formed from contractile protein, then it is clear that the material may extend between platelets within pseudopods, and into the platelet hyaloplasm. This observation could provide morphologic evidence for clot retraction based on contractile protein being found in interplatelet pseudopods. Such a hypothesis for the formation of actomyosin bridges between platelets has been proposed.[27] The extruded electron-dense material frequently was membrane-bound and also was observed in membrane-bound granule-like bodies, in spiky pseudopods, in the exterior coat of platelets, or was released directly from platelets. It is of interest that cold treatment of platelets causes a change in membrane permeability and extrusion of a C-thrombosthenin-rich platelet cytogel.[28] The exterior coat extending into spiky pseudopods was not membrane limited, however.

Granule-like electron-dense bodies in pseudopods may also be related to the appearance of microparticles of platelet origin. These bodies have been shown to contain much platelet factor 3-like activity,[29] and to have antigenic and chemical similarities to thrombosthenin.[30] The present observations are in accord with suggestions that these bodies originate in platelet cytomembrane structures and may result from extrusion through the surface membranes.[30] The chemical nature of these granule-like bodies, as seen in freeze-dried platelets, is being investigated.

References

1. Murphy S, Gardner F: Platelet preservation. Effect of storage temperature on maintenance of platelet viability. Deleterious effect of refrigerated storage. N Engl J Med 280:1094–1098, 1969
2. Roy A, Cavins J, Djerassi I: Circulation of concentrated one-day-old platelets *in vivo*. Transfusion 10:52–57, 1970
3. Handin RI, Valeri CR: Hemostatic effectiveness of platelets stored at 22°C. N Engl J Med 285:538–543, 1971
4. Djerassi I, Roy A: A method for preservation of viable platelets: combined effects of sugars and dimethylsulfoxide. Blood 22:703–717, 1963
5. Djerassi I, Farber S, Roy A, Cavins J: Preparation and *in vivo* circulation of human platelets preserved with combined dimethyl sulfoxide and dextrose. Transfusion 6:572–576, 1966
6. Djerassi I, Roy A, Alvarado J: Preservation of morphological integrity and clot retraction activity of human platelets after freezing. Thromb Diath Haemorrh 11:222–229, 1964
7. Djerassi I, Roy A, Kim J, Cavins J: Dimethylacetamide, a new cryoprotective agent for platelets. Transfusion 11:72–76, 1971
8. Pfisterer H, Weber F, Michlmayr G: *In vivo* survival of platelet concentrates following rapid freezing and thawing. Cryobiology 5:379–384, 1969
9. Streiff F, Alexandre P, Stoltz JF, Genetet B: Conservation et transfusion de concentres plaquettaires congeles a −80° en DMSO. Ann Biol Clin (Paris) 28:295–302, 1970
10. Greiff D, Mackey S: Cryobiology of platelets. II. Effects of freezing and storage at low temperatures on the survival of isolated human blood platelets as measured by assays for aminopeptidases. Cryobiology 7:9–13, 1970
11. Zucker MB, Borrelli, J: Reversible alterations in platelet morphology produced by anticoagulants and by cold. Blood 9:602–608, 1954
12. Bull BS, Zucker MB: Changes in platelet volume produced by temperature, metabolic inhibitors, and aggregating agents. Proc Soc Exp Biol Med 120:296–301, 1965
13. White JG, Krivit W: An ultrastructural basis for the shape changes induced in platelets by chilling. Blood 30:625–635, 1967
14. Sahud MA, Aggeler PM: Platelet dysfunction-differentiation of a newly recognized primary type from that produced by aspirin. N Engl J Med 280:453–460, 1969
15. Sjostrand FS, Elfin LG: The granular structure of mitochondrial membranes and of cytomembranes as demonstrated in frozen-dried tissue. J Ultrastruct Res 10:263–292, 1964
16. Nermut MV, Frank H: Fine structure of influenza A_2 (Singapore) as revealed by negative staining, freeze drying, and freeze etching. J Gen Virol 10:37–51, 1971
17. Nei T: Mechanism of haemolysis of erythrocytes by freezing, with special reference to freezing at near zero temperatures. The Frozen Cell. Edited by

GEW Wolstenholme and M O'Connor. London, J & A Churchill Ltd, 1970, pp 131–147

18. Luyet BJ: Attempt at correlating some of the extant data on low temperature preservation of various cells. Fed Proc 24 (Suppl 15): 315–322, 1965
19. Stephenson JL: Ice crystal growth during the rapid freezing of tissues. J Biophys Biochem Cytol (Suppl) 2:45–52, 1956
20. Bullivant S: Freeze substitution and supporting techniques. Lab Invest 14:1178–1195, 1965
21. Merryman HT: The exceeding of a minimum tolerable cell volume in hypertonic suspension as a cause of freezing injury.[17] pp 51–67
22. Bull BS: The ultrastructure of negatively stained platelets. Blood 28:901–912, 1966
23. White JG: The substructure of human platelet microtubules. Blood 32:638–648, 1968
24. Kattlove HE, Alexander B: The effect of cold on platelets. I. Cold induced platelet aggregation. Blood 38:39–48, 1971
25. White JG: The submembrane filaments of blood platelets. Am J Pathol 56:267–277, 1969
26. Booyse FM, Sternberger LA, Zschocke D, Rafelson ME: Ultrastructural localization of contractile protein (thrombosthenin) in human platelets using an unlabeled antibody-peroxidose staining technique. J Histochem Cytochem 19:540–550, 1971
27. Booyse FM, Rafelson M: Studies on human platelets III. A contractile protein model for platelet aggregation. Blood 33:100–103, 1969
28. Booyse FM, Rafelson M: Regulation and mechanism of platelet aggregation. Conference on Platelets and their Role in Hemostasis. NY Academy of Sciences, Oct 27, 1971 (abstr)
29. Wolf P: The nature and significance of platelet products in human plasma. Br J Haematol 13:269–288, 1967
30. Crawford N: The presence of contractile proteins in platelet microparticles isolated from human and animal platelet free plasma. Br J Haematol 21:53–68, 1971

Acknowledgments

The technical assistance of G. C. Holtz is greatly appreciated.

[*Illustrations follow*]

Legends for Figures

Fig 1—Freeze-dried human platelet-rich plasma. Plasma frozen in isopentane cooled to −155 C by liquid nitrogen. Ice crystal formation is extensive. Platelet pseudopods without internal structure *(lower)* and with electron-dense material *(upper arrow)* are noted (× 34,000).

Fig 2—Human platelets frozen in a button in isopentane cooled to −155 C. Platelets subsequently fixed in 3 percent glutaraldehyde followed by 1% osmium tetroxide. Poor preservation of platelet morphology is evident (× 19,000).

Fig 3—Human platelets frozen in a button in isopentane at −155 C. 5% DMSO and 5% dextrose added prior to freezing. Fixed in 3% glutaraldehyde and 1% osmium tetroxide after freezing. Platelets show loss of organelles, pseudopods, and vacuolization (× 24,000).

Fig 4—Human platelets frozen in a button in isopentane cooled to −155 C. 5% DMAC and 0.25 M sodium glycerophosphate added prior to freezing. Fixed in 3% glutaraldehyde and 1% osmium tetroxide after freezing. Vacuolization and loss of platelet hyaloplasm are seen (× 29,000).

Fig 5—Human platelets frozen in a button. 5% DMSO and 5% dextrose added prior to freezing. Frozen at 1°/min, and fixed with 3% glutaraldehyde followed by 1% osmium tetroxide. Platelet preservation is good but vacuoles and pseudopods are noted (× 22,000).

Fig 6—Human platelets. 5% DMAC and 0.25 M sodium glycerophosphate added to PRP before fixation in 3% glutaraldehyde followed by 1% osmium tetroxide. Large vacuoles are present. Microtubules are intact (× 24,000).

Fig 7—Human platelets. 5% DMSO and 5% dextrose added to platelet-rich plasma prior to fixation with 3% glutaraldehyde and 1% osmium tetroxide. Large vacuoles are present. Microtubules are noted (× 22,000).

Fig 8—Human platelets, frozen in a button after addition of 5% DMSO and 5% dextrose to platelet-rich plasma. Button frozen in isopentane at −155 C and freeze-dried. Platelet granules are intact. Cytoplasmic bridges extend between platelets (× 21,000). Granule-like structures appear in interplatelet bridges (*arrow*, and *insert* upper left) (× 70,000).

Fig 9—Human platelets, frozen in a button after addition of 5% DMSO and 5% dextrose to platelet rich plasma. Button frozen in isopentane at −155 C, and freeze dried. Areas of apparent ice crystal formation are noted. Granules have eccentric areas of electron density. Pseudopods are noted, both containing membrane-bound electron-dense material *(upper)* and lacking such material *(lower)* (× 81,000).

Fig 10—Human platelet, frozen in liquid N_2 at −196 C and freeze dried. 5% DMSO and 5% dextrose added to platelet rich plasma prior to freezing. Electron-dense material, apparently membrane bound, extends from within the platelet into a platelet pseudopod, and also is noted at the platelet surface, seemingly escaping into the surrounding medium *(arrow)* (× 166,000).

Fig 11—Human platelet, frozen in isopentane at −155 C, and freeze dried. 5% DMAC and 0.25 M sodium glycerophosphate added to platelet rich plasma prior to freezing. Good preservation of organelles is noted, some of which have eccentric electron-dense areas. Organelles are distributed diffusely throughout the platelet structure (× 69,000).

Fig 12—Human platelet, frozen in isopentane at −155 C, and freeze dried. 5% DMAC and 0.25 M sodium glycerophosphate added to platelet rich plasma prior to freezing. Projections at the platelet surface are seen containing electron-dense material appearing to be membrane bound, and external to the negatively stained platelet plasma membrane (× 160,000).

Fig 13—Human platelet, frozen in isopentane at −155 C and freeze dried. 5% DMAC and 5% dextrose added to platelet rich plasma prior to freezing. Electron dense material appears to be escaping into the surrounding medium through an area of discontinuity of negatively stained membrane type structure *(arrow)* (× 95,000).

Fig 14—Human platelets frozen in isopentane at −155 C and freeze-dried. Platelet-rich plasma collected in EDTA in the presence of 5% DMSO and 5% dextrose prior to freezing. Platelets are interconnected through pseudopod type bridging, similar to that observed in platelet-rich plasma collected in the presence of citrate (× 40,000).

Fig 15—Human platelets frozen in isopentane at −155 C and freeze-dried. 5% DMAC and 5% dextrose added to platelet-rich plasma prior to freezing. Two adjacent platelets are shown, joined by an amorphous material having no identifiable structures. Membrane-like structures are adjacent to the junction of the platelets, but do not appear to merge with each other (× 196,000).

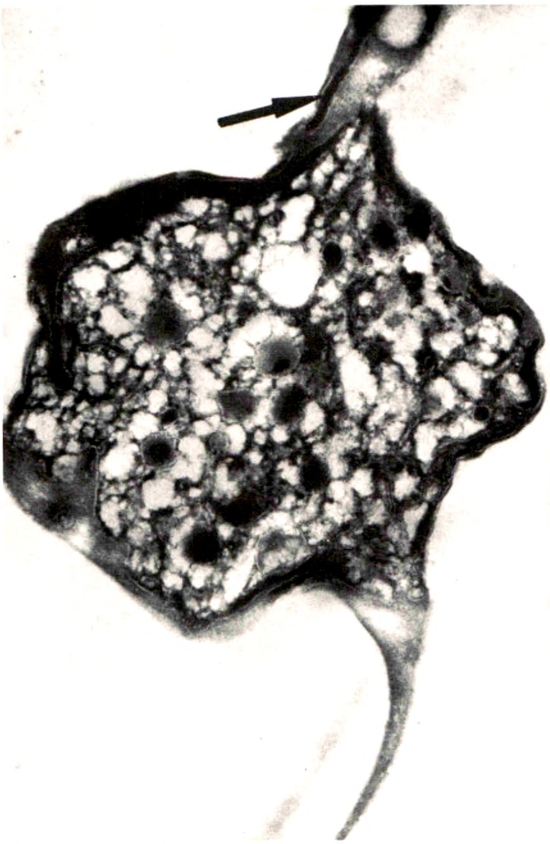

1

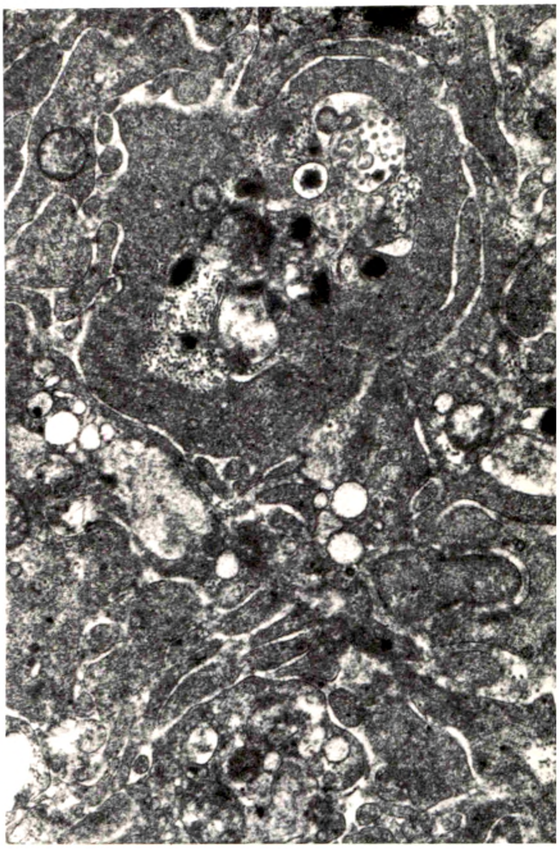

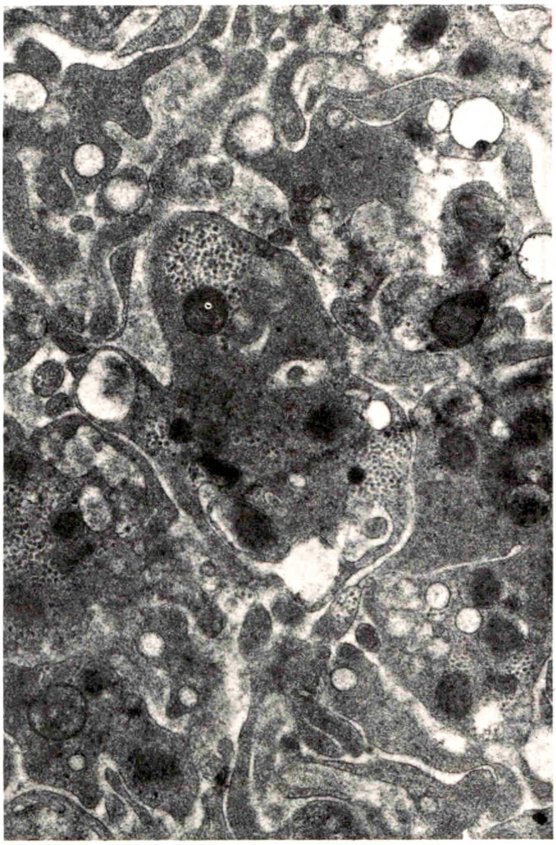

3

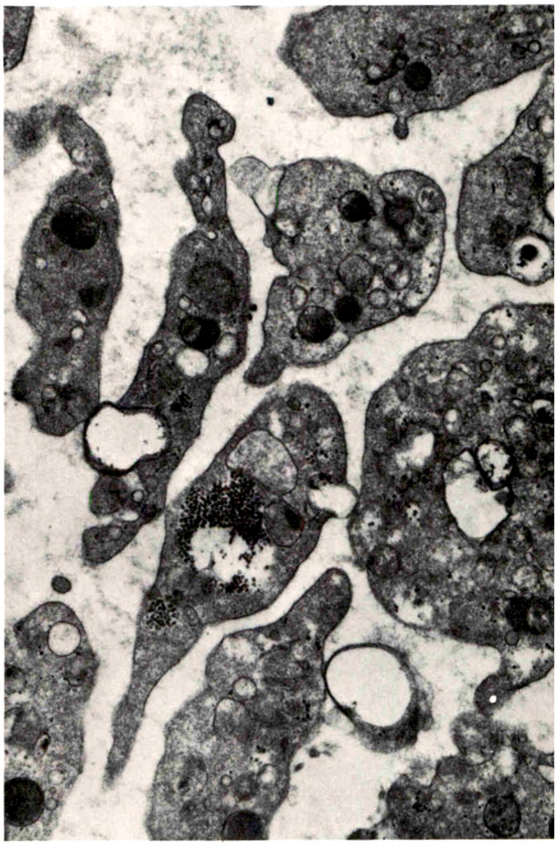

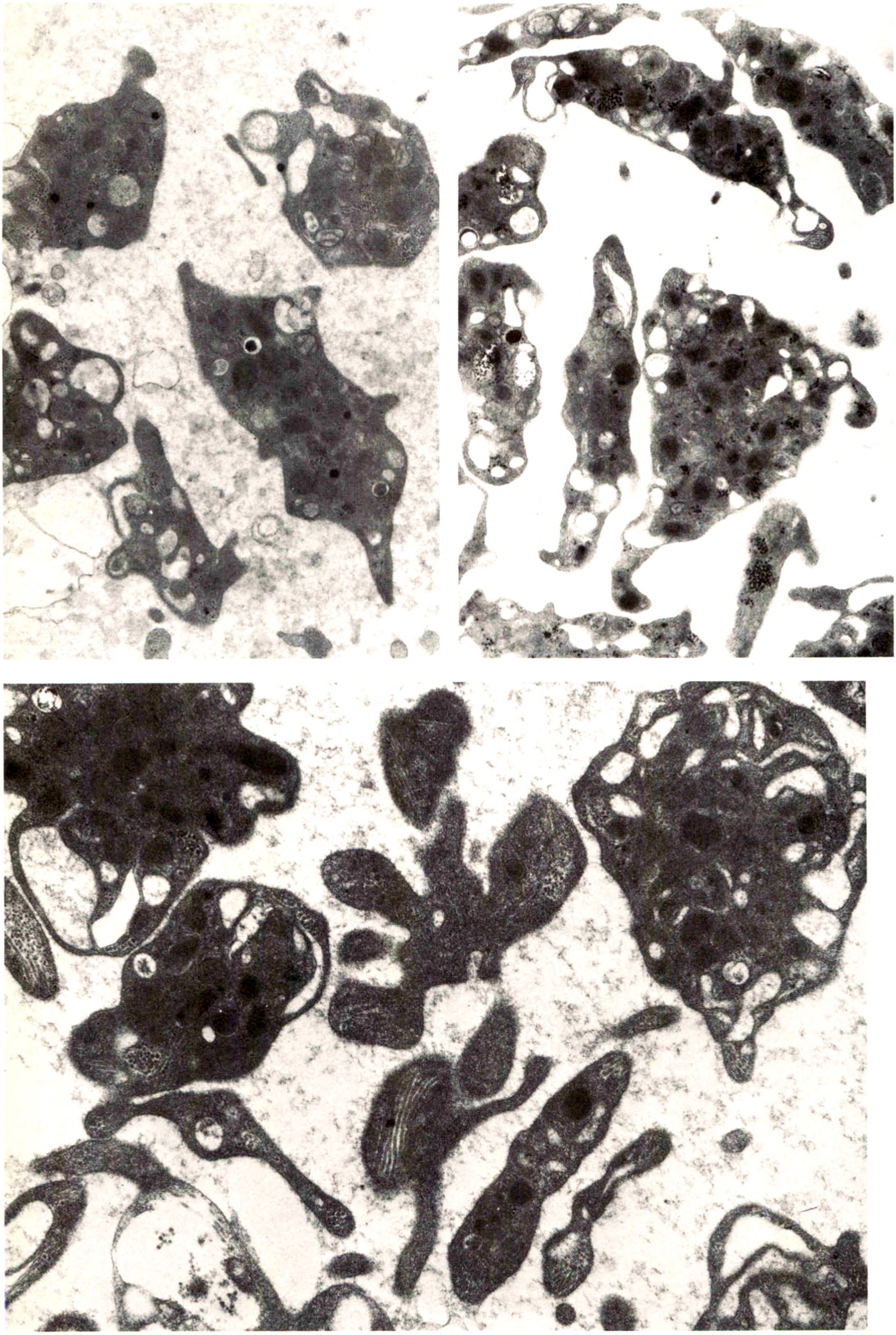

6

8

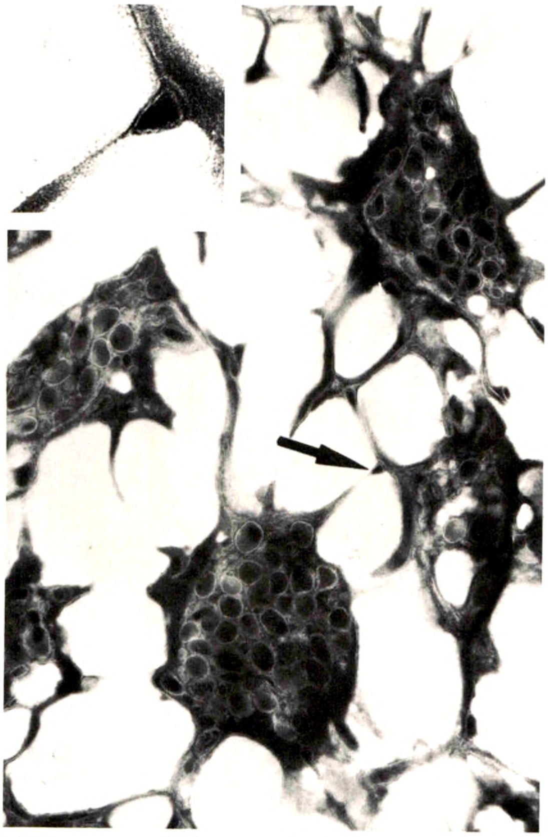

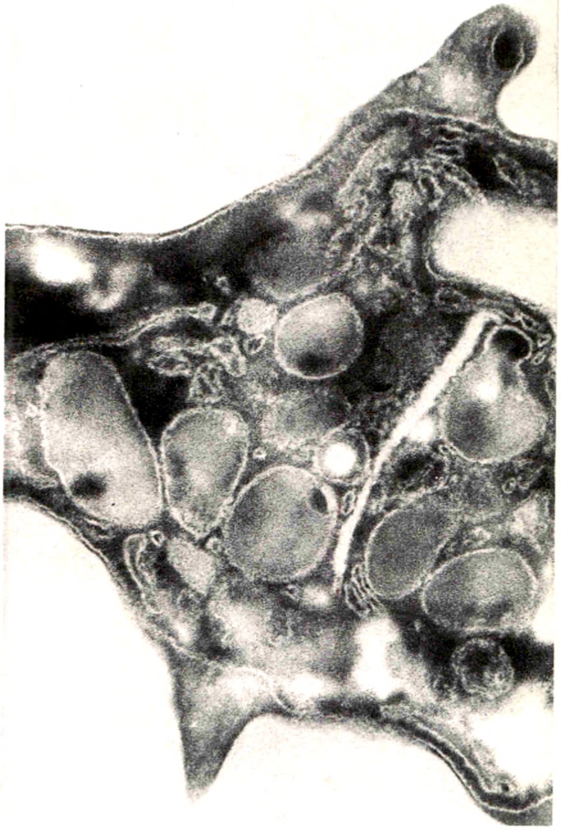

10

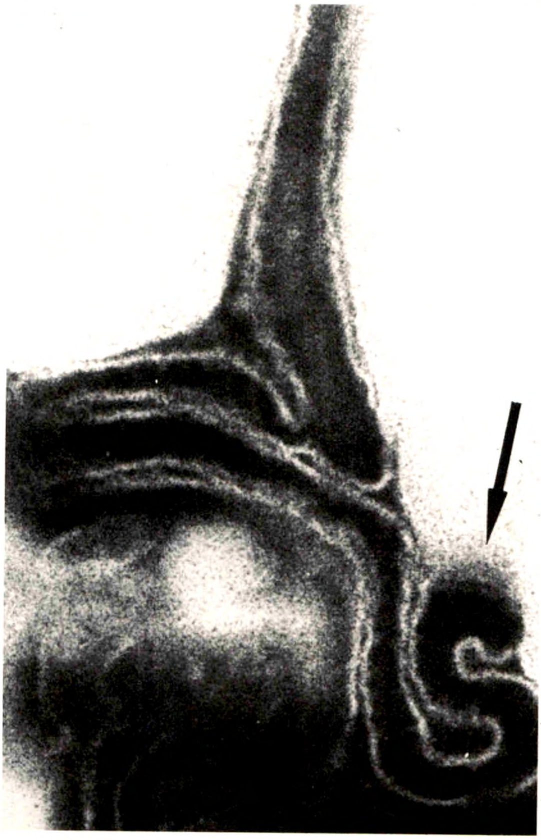

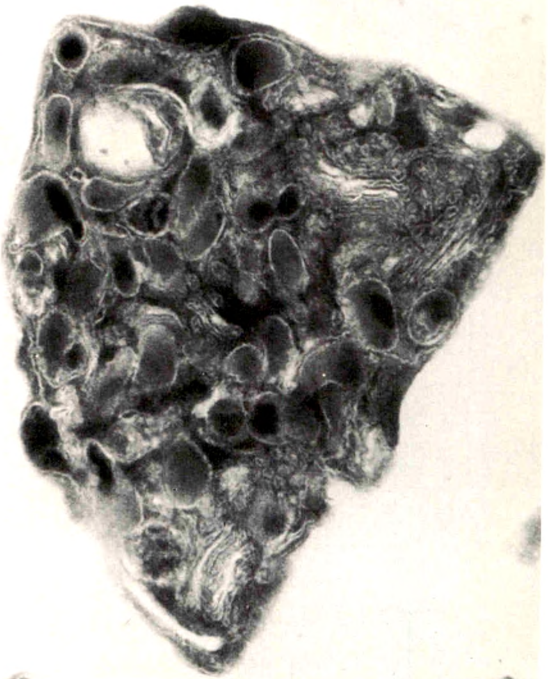

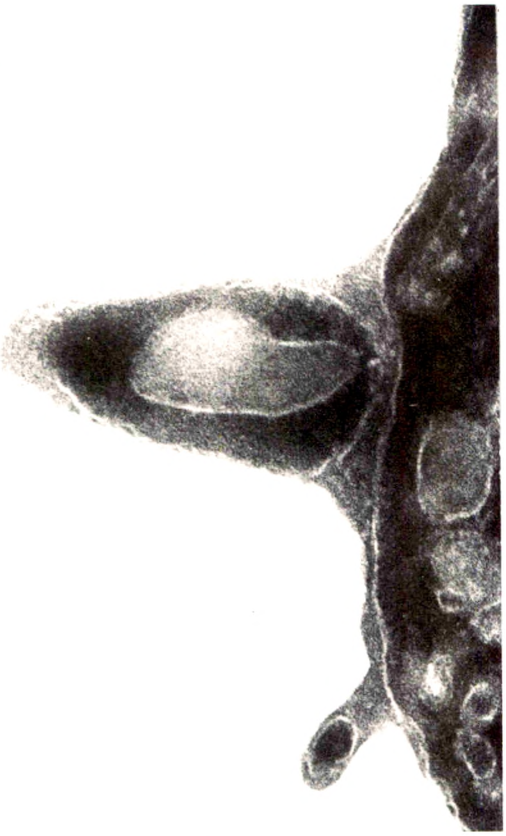
2

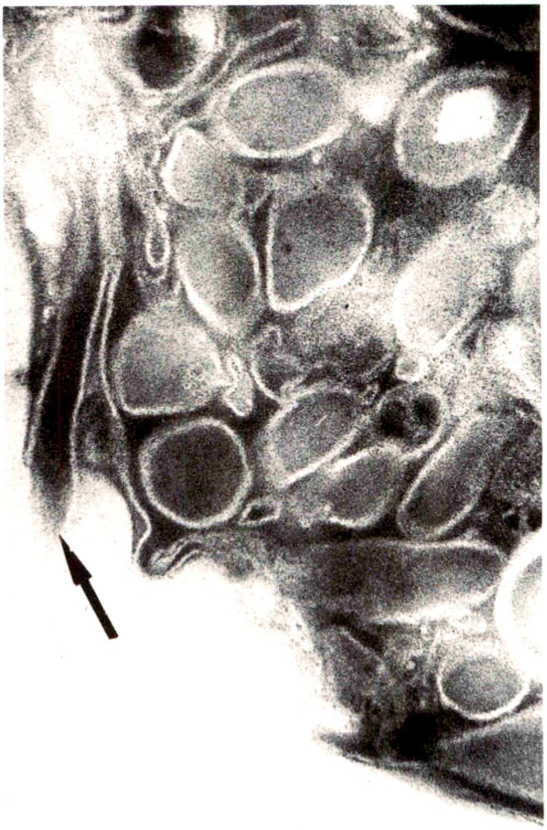
13

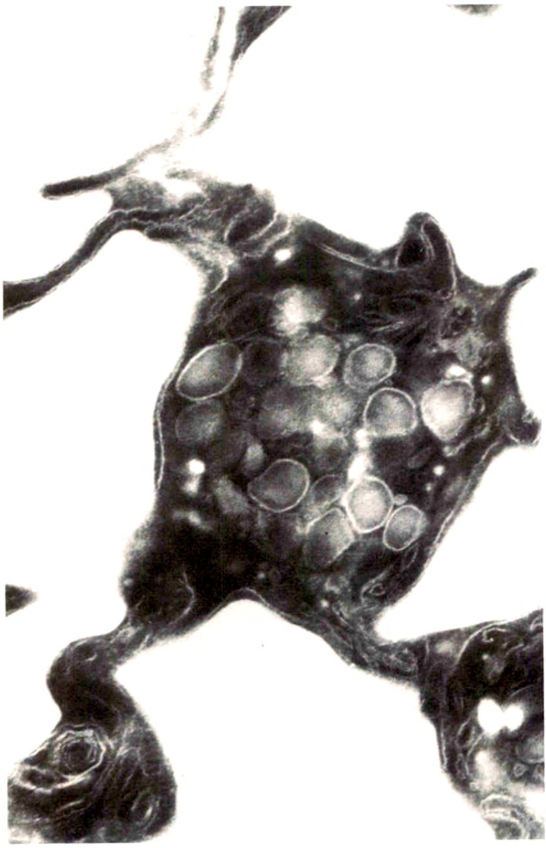
4

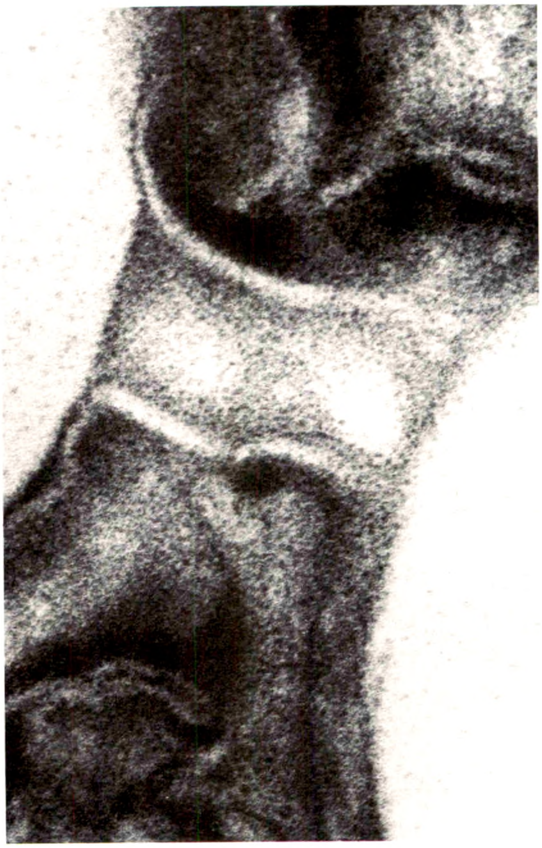
15

Alterations in Cell Proliferation in Mouse Lung Following Urethane Exposure

III. *Effects of Chronic Exposure on Type 2 Alveolar Epithelial Cell*

Shirley L. Kauffman, MD

The effect of chronic urethane exposure on proliferation of Type 2 alveolar epithelium was investigated by autoradiography. Control mice and mice exposed for 10 weeks to urethane in drinking water were injected with ^{3}H thymidine and killed at intervals for 7 days. Mean grain counts of Type 2 alveolar cells in the 2 groups showed that the cell cycle time of test mice was prolonged when compared with an estimated 22-hour cycle for controls; this was accompanied by a fivefold increase in labeling index in test animals (Am J Pathol 68:317–326, 1972).

Chronic exposure of mice to the carcinogen, urethane, in drinking water previously was shown to be associated with hyperplasia of bronchiolar epithelium [1] and a slowing of cell cycle time. Hyperplasia of Type 2 alveolar epithelium has also been noted prior to the appearance of Type 2 cell adenomas; [2] and hyperplasia of alveolar wall cells after a single injection of urethane has been described by some investigators,[3] but not by others.[4–6] The generalized increase in the number of cells in the alveolar wall [3] and the increase in labeling index of alveolar wall cells [4,5] have been regarded as a proliferative response to urethane. Whether this reflected an increased proportion of cells in cycle, a longer cycle, or both is not known. In the present experiment, the cell cycle of Type 2 alveolar epithelium in normal mice was estimated by a decline in the mean grain count after the injection of ^{3}H thymidine and compared with that of mice chronically exposed to urethane to see if changes in labeling index or cycle time could be detected.

Materials and Methods

Forty-two Swiss-Webster mice were divided into 2 groups: one that received 0.1% urethane (Ethyl Carbamate, Fisher Scientific) in their drinking water and

---

From the Department of Pathology, State University of New York, Downstate Medical Center, Brooklyn, NY.

Supported by The Council For Tobacco Research USA.

Accepted for publication Apr 10, 1972.

Address reprint requests to Dr. Shirley L. Kauffman, Department of Pathology, Downstate Medical Center, State University of New York, 450 Clarkson Ave, Brooklyn, NY 11203.

the second received tap water. Body weights and amounts of water consumed per cage were recorded weekly. To obtain an estimate of water consumption per animal the amount consumed was divided by the number of mice in the cage. After 10 weeks all animals were injected intraperitoneally with 1 μCi/g ^{3}H thymidine (3.0 Ci/mM, New England Nuclear) and killed in groups of 3 test and 3 experimental animals at intervals of 30 minutes, 24 hours and 2, 3, 4, 5 and 7 days. Lung sections for paraffin embedding were fixed in acetic alcohol for 1 hour and transferred to 10% formalin for 24 hours.

Additional 1 mm cubes of lung were fixed in osmium tetroxide for 1 hour, dehydrated and embedded in Epon. Slides were dipped in NTB_2 (Kodak) emulsion, exposed at 4 C for 3 (paraffin section) or 6 weeks (Epon sections), developed and stained with either methyl green thionine or toluidine blue. Grain counts were made over the labeled Type 2 alveolar epithelial cells and mean counts determined for each group by pooling the counts from the 3 animals and calculating the mean and standard deviation (Tables 1 and 2). These data were used to calculate cell cycle time. In addition, the mean grain count of each animals' Type 2 cells was determined so that the standard deviation and standard error of the control and experimental group at each interval could be compared.

Results

Water Consumed

Amount of water consumed by animals whose drinking water contained urethane decreased initially. The control animals drank an average of 50 to 55 ml/animal/week, whereas test animals drank 35 to 45 ml/animal/week until the sixth week, when water consumption was equal in both groups.

Amount of Urethane Consumed

For the first 6 weeks, the average amount of urethane consumed per animal was approximately 40 mg/wk. From 7 to 10 weeks, test animals consumed an average of 50 mg/wk.

Body Weight

Weekly body weights of control and test animals did not differ. These weights ranged between 26 to 32 g throughout the 11 weeks of the experiment.

Table 1—Pooled Grain Counts (Control)

Time after ^{3}H Thymidine	Grain counts/labeled cell: Mean (X)	Standard deviation (σ)	Coefficient of variation (CV = σ/X)
30 min	28.3	15.4	.544
24 hr	17.4	10.7	.615
2 days	14.1	10.2	.723
3 days	10.4	7.9	.760
4 days	7.8	5.5	.705

Table 2—Pooled Grain Counts (Urethane)

Time after ^{3}H Thymidine	Grain counts/labeled cell Mean (X)	Standard deviation (σ)	Coefficient of variation (CV = σ/X)
30 min	28.7	13.6	.474
24 hr	20.0	12.4	.620
2 days	16.4	9.9	.604
3 days	14.9	10.1	.678
4 days	14.3	9.4	.657
5 days	15.5	10.4	.671
7 days	14.4	10.6	.736

Histologic Findings in Lungs

All test animals had small tumors of Type 2 alveolar epithelial cells, as well as hyperplasia of the terminal bronchiolar epithelium. The number of Type 2 cells seemed to have increased; this will be the subject of a later quantitative study.

Labeling Index

A generalized increase in initial labeling index occurred throughout the lungs of test animals. Labeling indices of parenchymal cells, connective tissue and endothelial cells as well as circulating mononuclear cells and macrophages were all higher in the test group. Examples of labeled Type 2 cells and alveolar macrophages are shown in Figure 1.

The mean labeling index of Type 2 alveolar cells in the control group was 0.245% ± .030 30 minutes after the injection of ^{3}H thymidine and 0.499 ± .11 at 24 hours. In the experimental groups, the mean labeling index was 1.32 ± .113 at 30 minutes and 2.73 ± .548 at 24 hours.

Grain Counts

Mean grain counts with standard error for Type 2 epithelial cells in control mice at intervals after ^{3}H thymidine injection is shown in Text-figure 1. The mean grain count was 27.56 ± 1.10 in animals killed 30 minutes after injection with ^{3}H thymidine. This value decreased to 16.9 ± .49 within 24 hours then declined to 13.9 ± .07 on the second, 10.38 ± .27 on the third and 8.12 ± .03 on the fourth day. Labeled Type 2 cells were extremely rare in sections of lung taken from animals exposed to ^{3}H thymidine 5 and 7 days before sacrifice; therefore, mean grain counts could not be obtained for these points.

The mean grain count 30 minutes after ^{3}H thymidine injections in animals exposed to urethane was 28.40 ± .36 grains per labeled nucleus,

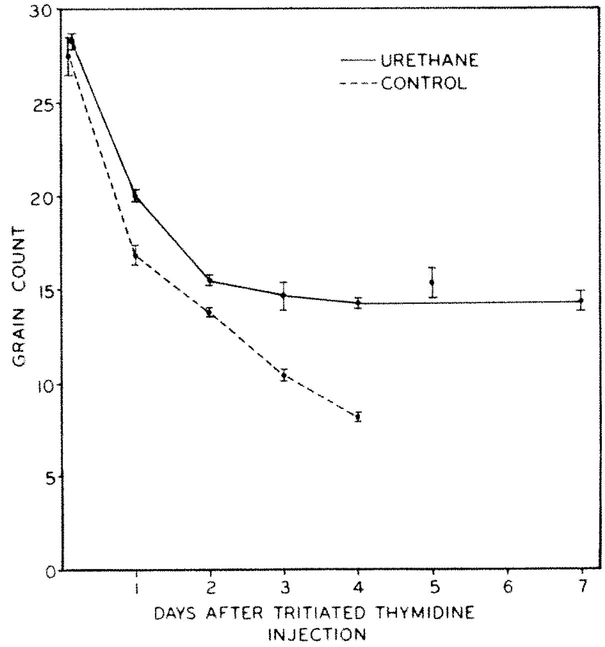

TEXT-FIG 1—Comparison of the mean grain counts of Type 2 alveolar cells in control mouse lung and in mouse lung exposed to urethane for 10 weeks. Abscissa—Days after ^{3}H thymidine injection (1 μCi/g body weight). Ordinate—Mean grain count with standard error indicated by vertical lines.

similar to control values. The count declined to 20.0 ± .29 at 24 hours, 15.5 ± .15 at 2 days and then remained in this range on days 3, 4, 5 and 7.

The mean for pooled grain counts from 3 animals, with its standard deviation, is shown for Type 2 cells in the control and test group in Tables 1 and 2.

Discussion

Cycle of Normal Type 2 Alveolar Cell

The cell cycle time was estimated by the time taken for the mean grain count to decrease to two-thirds of its 24-hour value, the method used in the analysis of bronchiolar epithelium.[1] This figure is based on the assumption that all cells initially labeled by ^{3}H thymidine would divide within 24 hours, reducing the mean grain count by half. Thereafter, only half, on the average, of labeled daughter cells would be expected to divide; identification of this completed division could give an estimate of the cycle time. The decline in mean grain count to 16.9 grains/labeled cell at 24 hours from an initial count of 27.6 grains/labeled cell is slightly less than that expected if all labeled cells divided. The failure of the mean grain count to decline by one-half in the first 24 hours was similar to that found in bronchiolar epithelium and is as yet unexplained. Assuming, for simplicity, a single population, and taking the 24-hour grain count as a reference point, the mean count should decrease to 11.3 grains/nucleus when the next division was completed. This figure was found 42 hours later (Text-figure 1); thus the mean cycle time of this labeled generation was approximately 21 hours.

Baserga, Tyler and Kisieleski [7] devised a method for determining the cell cycle time and the fraction of dividing cells in a population by mean grain counts at intervals after ^{3}H thymidine injection. This method, based on mean grain count and the coefficient of variation of the mean, is applicable to populations in which cell loss is negligible and the intervals of sampling are greater than one cycle time and less than 2 cycle times. Application of this method, using the pooled mean grain counts of 3 animals and coefficient of variation at 48 and 72 hours (Table 1), showed that .57 of the fraction of Type 2 cells divided once over this 24-hour period and .43 did not divide. The cell cycle time calculated from these data was 23.1 hours, a figure comparable to that obtained above. This result supports the assumption of a steady state, since approximately half of the labeled cells were shown to have not divided over the observation period.

Type 2 Cells of Animals Exposed to Urethane

Labeling Index

The increased labeling index of Type 2 cells (1.32% compared with 0.25% in controls) appears to reflect a real increase in the number of Type 2 cells in the division cycle. One alternative explanation—that the higher labeling index was due to an increase in the length of the S period—has been discussed in reference to bronchiolar epithelium,[1] where evidence from the low 24-hour labeling index seemed to support this. Urethane is a mitotic inhibitor [8] and does slow the cycle time, including the S period of embryonic neural tube cells *in vivo*, if presented during their rapid growth phase.[9] It is possible that the Type 2 cells were effected similarly in the S period, but this could not be shown as there was no discrepancy between the predicted and real labeling index at 24 hours.

Grain Counts

In the first 2 days after ^{3}H thymidine incorporation, mean grain counts in experimental and control Type 2 cells showed the same rate of decline, although mean counts were higher in the test animals. This finding suggests that cells incorporating ^{3}H-thymidine did progress through the DNA synthetic period, G_2 and division, but reduced the mean grain count by less than half at 24 hours. Labeled daughter cells must have entered the postmitotic (G_1) interphase and divided sometime over the next 24 hours as the mean count continued to decline. However, after 48 hours the grain count and coefficient of variation remained relatively constant until day 7 so that some of the daughter cells were unable to continue into the next division cycle.

This constant mean grain count from days 2 to 7 after an initial decline is markedly different from the data in control mice. Possibly, this curve reflects the presence of two populations of labeled cells, one dividing and one nondividing or slowly dividing. If a proportion of the population were dividing normally, the reduction in their grain count over the first 2 days would determine the initial part of the curve in Text-figure 1. As the number of labeled cells detectable was reduced by division (due to dilution of the label), persisting nondividing or slowly dividing labeled daughter cells would determine the shape of the latter part of the curve.

Thus it appears that the mean cycle time of Type 2 cells was prolonged in animals chronically exposed to urethane, an effect which could be produced either by slowing the cycle time of all or some of the cells, though the latter seems more probable. Since the portion of the cell cycle including S, G_2 and mitosis was not prolonged (judging from the decline in mean grain count over the first 24 hours), the significant lengthening of cycle time can be attributed to a slowed progression through the G_1 period.

The increased labeling index of Type 2 cells (1.32% compared with control valves of 0.25%) is subject to several interpretations. This may be a compensatory response, initiated by a decreased production of mature cells or cell products, or it may represent a pathologic disturbance in the control of cell numbers, associated with the emergence of lung tumors.

References

1. Kauffman SL: Alterations in cell proliferation in mouse lung following urethane exposure. II. Terminal bronchiolar epithelium. Am J Pathol 64:531–538, 1971
2. Mostofi FK, Larsen CD: The histopathogenesis of pulmonary tumors induced in strain A mice by urethane. J Natl Cancer Inst 11:1187–1222, 1951
3. Shimkin MB, Polissar MJ: Some quantitative observations on the induction and growth of primary pulmonary tumors in strain A mice receiving urethane. J Natl Cancer Inst 16:75–97, 1955
4. Foley WA, Cole LJ, Ingram BJ, Crocker TT: X-ray inhibition of urethane-

stimulated proliferation of lung cells of the mouse as estimated by incorporation of tritiated thymidine. Nature (Lond) 199:1267–1268, 1963

5. Kauffman SL: Alterations in cell proliferation in mouse lung following urethane exposure. I. The non-vacuolated alveolar cell. Am J Pathol 54:83–93, 1969
6. White MR, Grendon A, Jones HB: Tumor incidence and cellularity in lungs of mice given various dose schedules of urethane. Cancer Res 30:1030–1036, 1970
7. Baserga R, Tyler SA, Kisieleski WE: The kinetics of growth of the Ehrlich tumor. Arch Pathol 76:9–13, 1963
8. Cornman I: The properties of urethane considered in relation to its action on mitosis. Int Rev Cytol 3:113–130, 1954
9. Kauffman SL: Cell proliferation in embryonic mouse neural tube following urethane exposure. Dev Biol 20:146–157, 1969

Acknowledgments

The author wishes to acknowledge the excellent technical assistance of Mrs. Sudha Sulebele and Mr. Hiroshi Ozaki. The Text-figure was drawn by Mrs. Elizabeth Cuzzort and the photomicrographs were taken by Mr. Willy Kratel.

Legends for Figures

Fig 1—Comparative appearance of Type 2 alveolar epithelial cell, pulmonary macrophage and small mononuclear cell. **A**—The Type 2 cell is characteristically found between capillary loops, and its cytoplasm contains toluidine blue-positive lamellated bodies concentrically arranged around the nucleus. Pulmonary macrophage cytoplasm may be rounded up or flattened against the alveolar surface and contains a variety of ingested particles including lamellated bodies. Small mononuclear cell resembles macrophage except it has little surrounding cytoplasm (urethane 10 weeks, toluidine blue, × 900). **B**—Autoradiogram of lung of mouse drinking 0.1% urethane for 10 weeks and killed 24 hours after intraperitoneal injection of ^{3}H thymidine. Two labeled Type 2 alveolar cells are shown (toluidine blue, × 900). **C**—Autoradiogram of lung of control animal killed 30 minutes after ^{3}H thymidine injection. The nucleus of one pulmonary macrophage is labeled. Cytoplasm contains a moderate amount of ingested material.

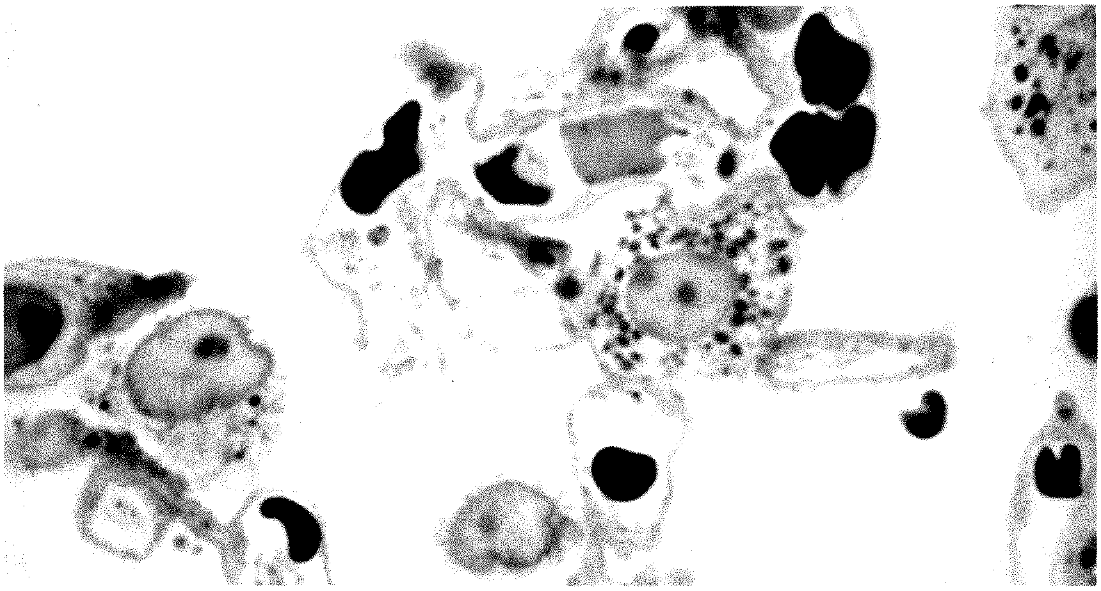

1

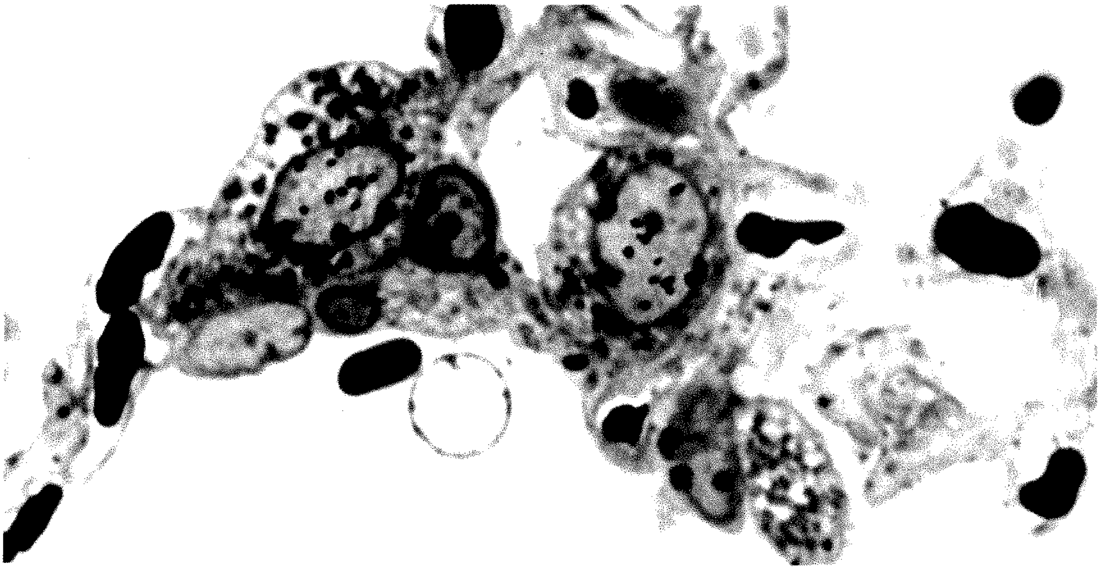

1

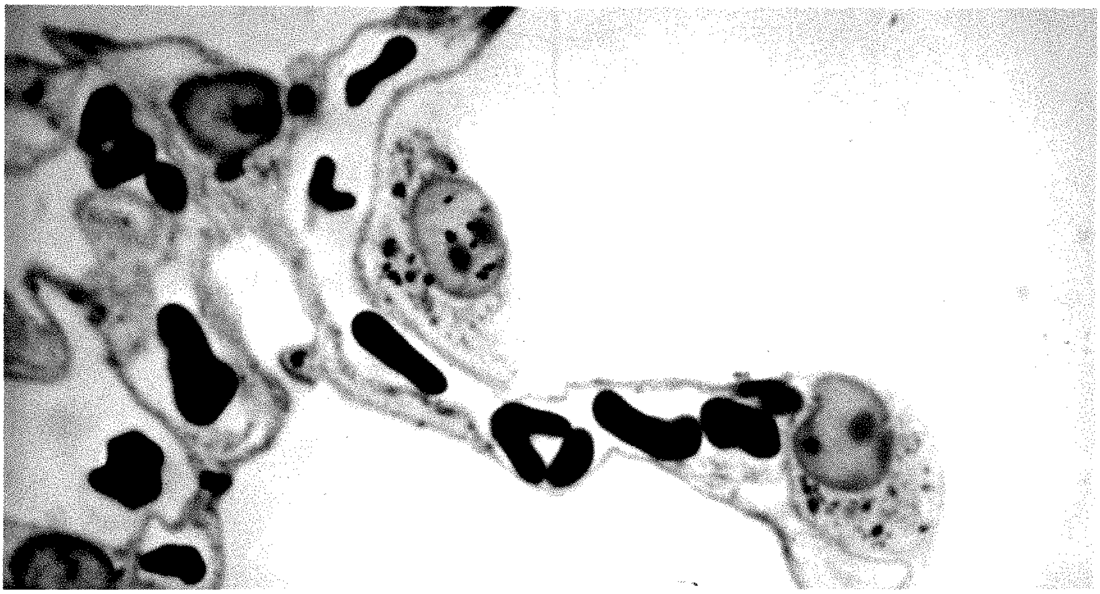

1

[End of Article]

In Vivo Quantitation of Local Anesthetic Suppression of Leukocyte Adherence

D. B. Giddon, DMD, PhD and J. Lindhe, Odont Dr

Using intravital microscopy, topically applied amide-type local anesthetics suppressed the adherence of leukocytes to the venular endothelium within surgical defects in the hamster cheek pouch. The response was reversible with physiologic saline and was localized to venules within the defect. Quantitation in terms of the percent of initially adhering leukocytes remaining in place on the venule wall at each minute following application of lidocaine and physiologic saline, respectively, revealed the suppression to be reliably related to the concentration, viz: 20.0 > 10.0 >5.0 >0.0 mg/ml of commercially available Xylocaine® (lidocaine) HCl (Am J Pathol 68:327–338, 1972).

ALTHOUGH SEVERAL WORKERS have identified substances which affect aggregation and adherence of leukocytes *in vitro*,[1-7] little success has been achieved in elucidating the mechanisms *in vivo*.[8] Recently, however, Thompson *et al*[9] reported that calcium plays a role in the adherence of leukocytes in the rabbit ear-chamber and rat mesentery.

The purpose of the present paper is to describe a quantitative method for studying leukocyte adherence *in vivo* and to report that local anesthetics suppress the adherence of leukocytes to the endothelial wall of venules in a hamster cheek pouch following injury. In preliminary experiments using intravital microscopy, it was noted that the direct application of several amide-type anesthetics (lidocaine, mepivacaine and prilocaine) on surgical defects within the cheek pouch caused adherent leukocytes to leave injured venular walls. The number of rolling and marginating leukocytes in the area was also markedly reduced. If physiologic saline was applied after several minutes, the leukocytes would again begin rolling, marginating and adhering to the same location on the vessel wall. This effect was not observed when the anesthetic was applied to an intact area of the cheek pouch or in defects adjacent to that on to which the anesthetic was applied. Moreover, there was no apparent relation-

---

From the Department of Periodontology, University of Gothenburg, Gothenburg, Sweden.

Supported in part by Astra Lakemedel AB, Södertalje, Sweden.

Accepted for publication Apr 14, 1972.

Address reprint requests to Dr. D. B. Giddon, Department of Dental Ecology, Harvard School of Dental Medicine, 188 Longwood Ave, Boston, Mass 02115.

ship between the reduction in leukocyte adherence and independent variation of pH or osmolarity or occasional changes in blood flow, vessel size or degree of hemolysis.

Materials and Methods

Based on these observations, the following experimental procedure was adopted for the quantitation of changes in leukocyte adherence. A total of 16 golden and albino hamsters weighing approximately 140 g were used for the exploratory and systematic studies to be reported here. The animals were anesthetized with Mebumal® (pentobarbital sodium), 100 mg/kg body weight, and the cheek pouch was everted over a glass plate. In an area exhibiting normal microvascular architecture and rheology, a defect of approximately 2 mm diameter was created by removing the epithelium and connective tissue in accordance with the method of Brånemark.[10] The entire cheek pouch was irrigated with physiologic saline at room temperature except during application of the test solution. The defect was then carefully examined intravitally under a water immersion lens (55 × 10) to locate a venule where 10 to 20 leukocytes could be seen adhering to the endothelium in a configuration convenient for counting (Figure 1A). The area selected was then depicted by hand, as illustrated in Text-figure 1 for reference during the counting procedure.

When the same leukocytes remained in place for approximately 8 minutes, coded test solutions were then applied in predetermined random order; 0.03 ml of the test solution was topically applied from a 1.0 ml disposable syringe by placement against the water immersion lens. The test solutions represented three concentrations of commercially available Xylocaine®, (lidocaine) HCl; namely: 5 mg/ml (0.018 M), 10 mg/ml (0.037 M), 20 mg/ml (0.074 M), and physiologic saline (control) at pH 6.5 to 7.0. Except for differences in con-

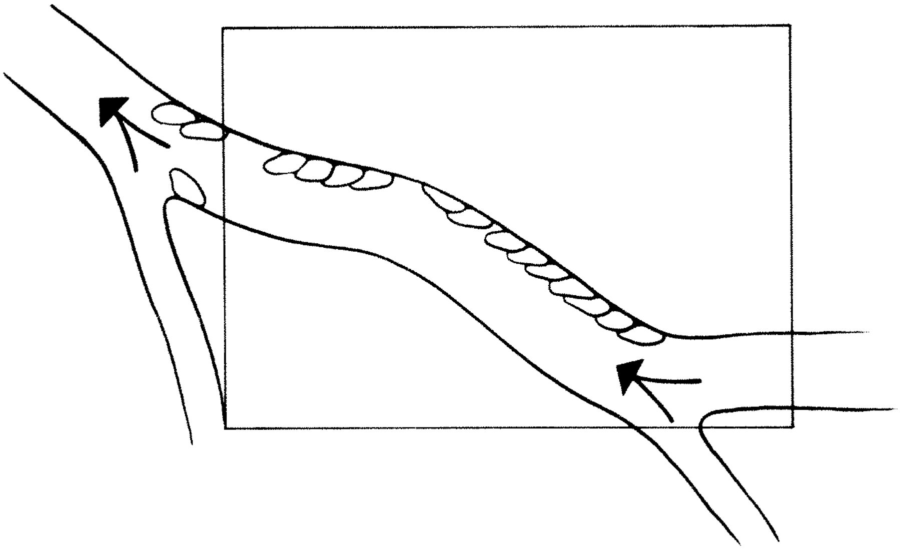

TEXT-FIG 1—Reference drawing for counting the number of adhering leukocytes shown in Figure 1.

centration of lidocaine and total sodium, the 3 test solutions were identical. The sodium content was 9, 8, 6 and 6 mg/ml for concentrations of 0 (saline), 5, 10 and 20 mg/ml lidocaine, respectively. These variations in sodium were independently determined not to be responsible for the results obtained with this system.

Two series of experiments were conducted, differing only in the number of minutes the test solutions were applied. The second series was performed to determine the effect on leukocyte adherence when the anesthetic was not replaced with saline after 8 minutes. For Series A, each of the concentrations was tested twice in 3 animals for a total of 6 observations/solution. The test solutions were left in place for 8 minutes, during which time the area was observed at 1 to 2-minute intervals. At each time interval the number of clearly visible leukocytes remaining in the original location was counted. Any changes in cell morphology, rheology or vessel size were also noted. After 8 minutes the test area was thoroughly washed with physiologic saline. The number of leukocytes was again recorded at 1 to 2 minute intervals through 16 minutes. For Series B, each of the concentrations was tested at least once in 3 animals for a total of 4 to 6 observations/solution—*ie*, animals × trials = 2 × 2 + 1 × 1 for 5 mg/ml, 2 × 1 + 1 × 2 for 10 mg/ml and 2 × 1 + 1 × 2 for 20 mg/ml. The same solutions remained on the defect for the entire test period of 16 minutes before washing with the saline. A summary of these procedures is shown in Table 1.

Results

The reduction in leukocyte adherence resulting from topical application of local anesthetic solutions can be seen by comparing the photomicrograph of the defect in Figure 1A during the pretest application of physiologic saline with the same area in Figure 1B, 3 minutes following application of lidocaine HCl 20 mg/ml. This reaction can also be graphically presented as shown in Text-figure 2 for a typical experiment. Here the number of leukocytes adhering to the

Table 1—Sequence of Procedures for Series A and B

Time (min)	Series A	Series B
−50	Mebumal® (pentobarbital sodium) 100 mg/kg	Same as for Series A
−30	Evert cheek pouch and prepare surgical defect	Same as for Series A
−13	Locate and depict adhering leukocytes on venular wall	Same as for Series A
−8	Isotonic saline applied	Same as for Series A
0	0.03 ml lidocaine applied	Same as for Series A
9	Isotonic saline applied Observe through 16 minutes or until to 50% level up through 24 minutes	0.03 ml lidocaine added —
17	—	Isotonic saline applied
24	—	Observe through 24 minutes or until return to 50% level up through 32 minutes

original site on the venular wall at each 1 to 2-minute interval following application of the lidocaine is compared with the number observed for the saline control.

Because of occasional manifestations of systemic toxicity or evidence of endothelial damage, it was not always possible to compare all concentrations of lidocaine with the saline control in all animals. Since the results were essentially similar for all studies, only those experiments in which all three concentrations of lidocaine and saline were tested in the same animal are presented here.

Differences in the number of initially adhering leukocytes necessitated the conversion of the data to the percentage of leukocytes on the venule wall immediately prior to the application of the test solution. The mean percentage of leukocytes remaining on the vessel wall at each time interval in Series A and B is presented in Text-figure 3. The method of least squares[11] revealed the data prior to saline intervention ('wash') to be best represented as exponential functions ($\%$ leukocytes $= ae^{-b(min)} + c$) with similar linear slopes ($-\log_{10} eb$). Using analysis of variance[12] (drugs $\times$ subject $\times$ time), the overall level (c) and acceleration ($b^2ae^{-b(min)}$) of the reduction of leukocyte adherence were found to differ significantly among the three concentrations of lidocaine and saline for both Series A and B ($P < .01$).

The rate at which leukocytes began to readhere following saline intervention was comparable for all 3 concentrations in both series.

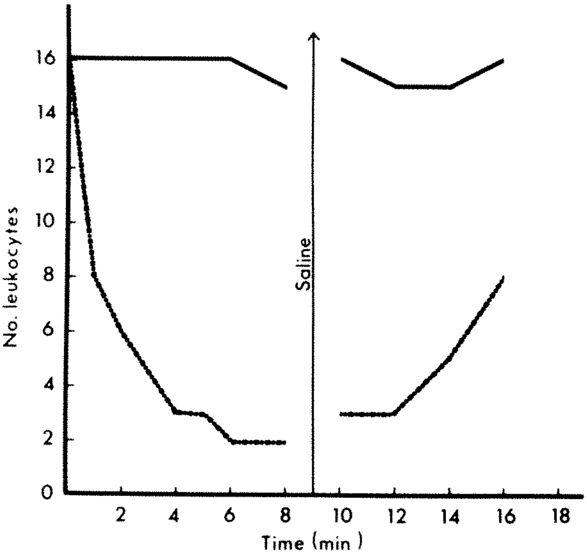

TEXT-FIG 2—Change in number of adhering leukocytes after application of lidocaine HCl 20 mg/ml and physiologic saline in typical experiment. 0 mg/ml (saline) (*solid line*), 20 mg/ml (*broken line*).

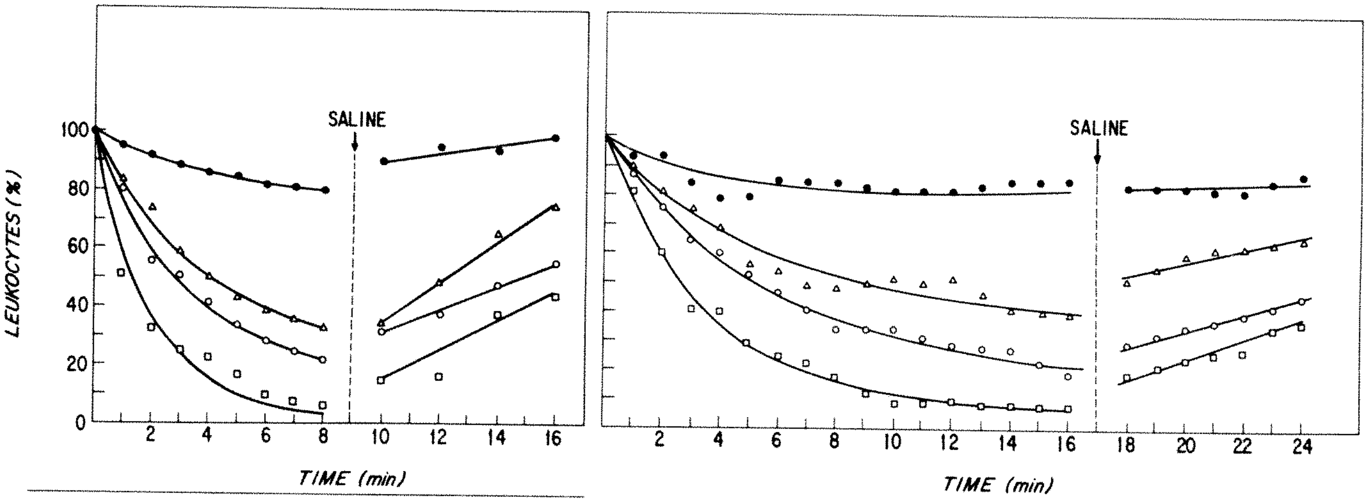

Text-fig 3—The average percent leukocytes remaining on venule wall × time for the 3 concentrations of lidocaine and saline. Left: Series A with 8 minutes lidocaine; Right: Series B with 16 minutes lidocaine. Control, 0 mg/ml (*solid circles*); lidocaine HCL, 5 mg/ml (*open triangles*); lidocaine HCl, 10 mg/ml (*open circles*); lidocaine HCl, 20 mg/ml (*open squares*).

Differences in overall recovery level were consistent with responses to the test solutions. The results can also be expressed as a variation of the ED_{50}; that is, in terms of the time required for a 50% reduction in adhering leukocytes. As shown in Text-figure 4, there was a linear dose response in the 50% reduction time for both series, as indicated by the slopes which are significantly different from 0 (Series A: $P <$ .01; Series B: $P < .02$). Although the slopes of the linear functions of the dose relationship of Series A and B are essentially identical, there is a statistically significant difference in overall level between the two series ($P < .01$). That is, because of probable greater endothelial damage with increased time of drug exposure referred to earlier, the reduction in leukocyte adherence for Series B (16 minutes) was less than for Series A (8 minutes) for each concentration of lidocaine.

Discussion

There are several possible explanations for the effects of lidocaine on leukocyte adherence. Although it is recognized that this response may not be specific to the amide-type anesthetics, a likely possibility is that the anesthetic reduces adherence by stabilizing the cell membranes of the endothelium and/or leukocytes. It is now well established that local anesthetics block propagation of the nerve impulse by altering the ionic conductance, thereby stabilizing the axon membrane.[13] There is also considerable support for an electrochemical

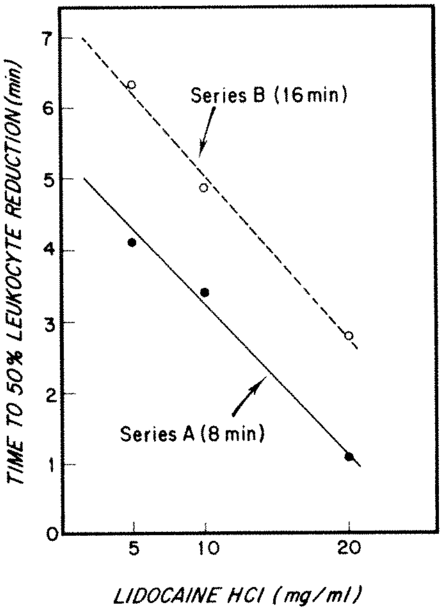

TEXT-FIG 4—Relation of lidocaine concentration to 50% reduction in adhering leukocytes in Series A (8 minute application) and Series B (16 minute application).

basis for increased adhesiveness of leukocytes to the venule wall following injury;[3] thus a state of relative membrane lability. Local anesthetics have, in fact, been shown to reduce the adhesiveness of other formed elements, such as platelets *in vitro*,[14] probably by affecting the cell membrane.[15] An increase in the stability of erythrocyte membrane by local anesthetics, as indicated by reduced osmotic fragility, has also been reported.[16]

Another related possibility of local anesthetic action is through interference with the metabolic pathways concluded by several authors to be essential to leukocyte adherence.[1,2,4–6]

The action of local anesthetics, however, is also dependent on a large number of physico-chemical factors—*eg*, pH, pK, osmolarity, temperature, various ions, interacting in complex ways with other cellular components and metabolites. For example, of the many ions which have been implicated in leukocyte adhesiveness,[1–4,7] calcium could be considered most important in that it interacts competitively with local anesthetics and stabilizes excitable membranes.[17] However, the results of experiments specifically designed to evaluate the role of calcium in leukocyte adherence have not been consistent. Following earlier *in vitro* demonstrations of the importance of calcium to leukocyte adhesiveness,[1,2] Thompson *et al*[9] reported that calcium was involved in the *in vivo* adherence of leukocytes. This is in contrast to more recent *in vitro* studies[3,4,7] in which magnesium was found to have a greater role than calcium in leukocyte adhesion.[1–4,7] Similarly, in our own exploratory studies the results with calcium have been equivocal.

It should be emphasized, however, that this is a report of an *in vivo* observation of the adherence of leukocytes to the endothelium, and that many of the possibilities suggested by other workers have evolved from *in vitro* studies of aggregation or adherence to artificial surfaces. Moreover, the mechanism responsible for adherence appears to be different from aggregation and may vary according to the type of cell.

The results of the present experiment may thus be significant in several ways: first, a reliable standardized method has been developed for quantifying the effects of pharmacologically active agents on the suppression of leukocyte adherence *in vivo*. Second, since leukocyte adherence is cardinal to acute inflammation, the technic might be used to evaluate antiinflammatory effects. Third, the observation that local anesthetics appear to mask the response to tissue injury may be of clinical significance. Fourth, the phenomena reported may provide an additional clue to the mechanism of leukocyte adherence.

References

1. Garvin JE: Factors affecting the adhesiveness of human leukocytes and platelets *in vitro*. J Exp Med 114:51–73, 1961
2. Allison F Jr, Lancaster MG, Crosthwaite JL: Studies on the pathogenesis of acute inflammation. Am J Pathol 43:775–795, 1963
3. Bryant RE, DesPrez RM, VanWay MH, Rogers DE: Studies on human leukocyte motility: I. Effects of alterations in pH, electrolyte concentration, and phagocytosis on leukocyte migration, adhesiveness, and aggregation. J Exp Med 124:483–499, 1966
4. Garvin JE: Effects of divalent cations on adhesiveness of rat polymorphonuclear neutrophils *in vitro*. J Cell Physiol 72:197–212, 1968
5. Baudisch W, Beckman A, Blank I, Jenssen HL: Klebrigkeit und Migrationsverhalten der Leukozyten unter Einwirkung von Stoffwechselhemmstoffen. [Adhesiveness and migration behavior of leukocytes under the action of metabolism inhibiting drugs.] Acta Biol Med Ger 23:265–270, 1969
6. Kvarstein B: Effect of some metabolic inhibitors on the adhesiveness of human leucocytes to glass beads. Scand J Clin Lab Invest 24:35–40, 1969
7. Kvarstein B: Effects of proteins and inorganic ions on the adhesiveness of human leucocytes to glass beads. Scand J Clin Lab Invest 24:41–48, 1969
8. Grant L: The sticking and emigration of white blood cells in inflammation. The Inflammatory Process, Chapter 5. Edited by BW Zweifach, L Grant, RT McCluskey. New York, Academic Press Inc, 1965, pp 197–244
9. Thompson PL, Papadimitriou JM, Walters M N-I: Suppression of leucocytic sticking and emigration by chelation of calcium. J Pathol Bacteriol 94:389–396, 1967
10. Brånemark P-I: Experimental biomicroscopy. Bibl Anat 5:51–55, 1964
11. Lewis D: Quantitative Methods in Psychology. New York, McGraw Hill Book Co, 1960, pp 24–28, 64–72
12. Lindquist EF: Design and Analysis of Experiments in Psychology and Education. Boston, Houghton Mifflin Co, 1956, pp 220–243
13. Ritchie JM, Greengard P: On the mode of action of local anesthetics. Ann Rev Pharmacol 6:405–430, 1965
14. O'Brien JR: Platelet aggregation: Part I. Some effects of the adenosine phosphates, thrombin, and cocaine upon platelet adhesiveness. J Clin Pathol 15:446–455, 1962
15. Mustard JF, Packham MA: Factors influencing platelet function: adhesion, release, and aggregation. Pharmacol Rev 22:97–187, 1970
16. Seeman P: II. Erythrocyte membrane stabilization by local anesthetics and tranquilizers. Biochem Pharmacol 15:1753–1766, 1966
17. Rothstein A: Membrane phenomena. Annu Rev Physiol 30:15–72, 1968

Acknowledgments

Dr. Giddon is on leave from Tufts University as Visiting Scientist and Honorary Fulbright Scholar in the Department of Periodontology, University of Gothenburg, Gothenburg, Sweden.

With the technical assistance of Maria G. Saretok and Dr. Hans Evers, and the statistical assistance of Dr. R. E. Clark, Tufts University, Boston, Mass.

[*Illustrations follow*]

Legends for Figures

Fig 1—Intravital photomicrographs ($1/50$ sec) of adhering leukocytes. **A**—Prior to application of lidocaine. Note the line of leukocytes lying along venular endothelium. **B**—Three minutes after topical application of 0.03 ml of 20 mg/ml lidocaine HCl. Only three of the leukocytes seen in **A** are still visible. *Calibration mark* = 50μ.

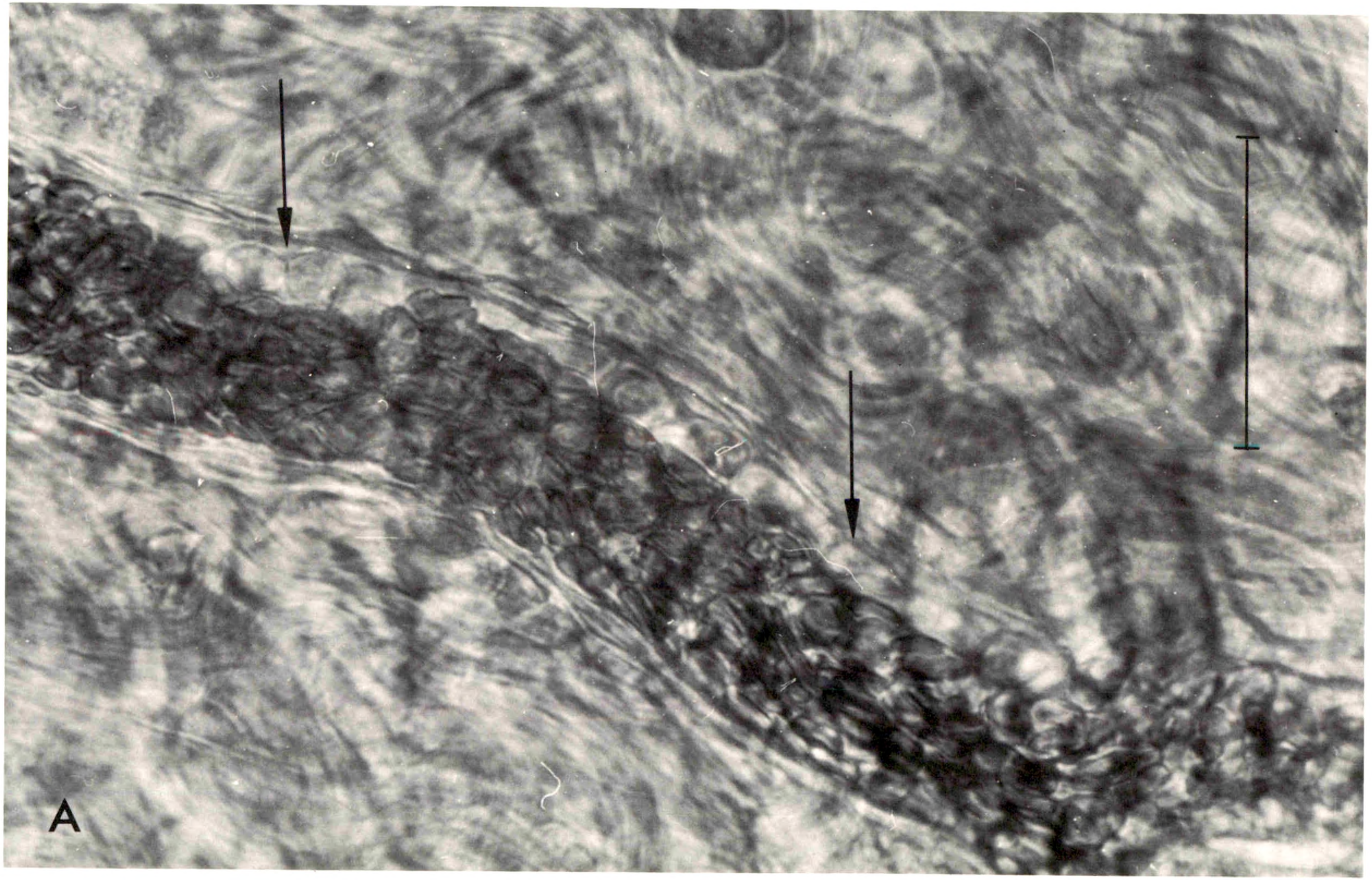
A

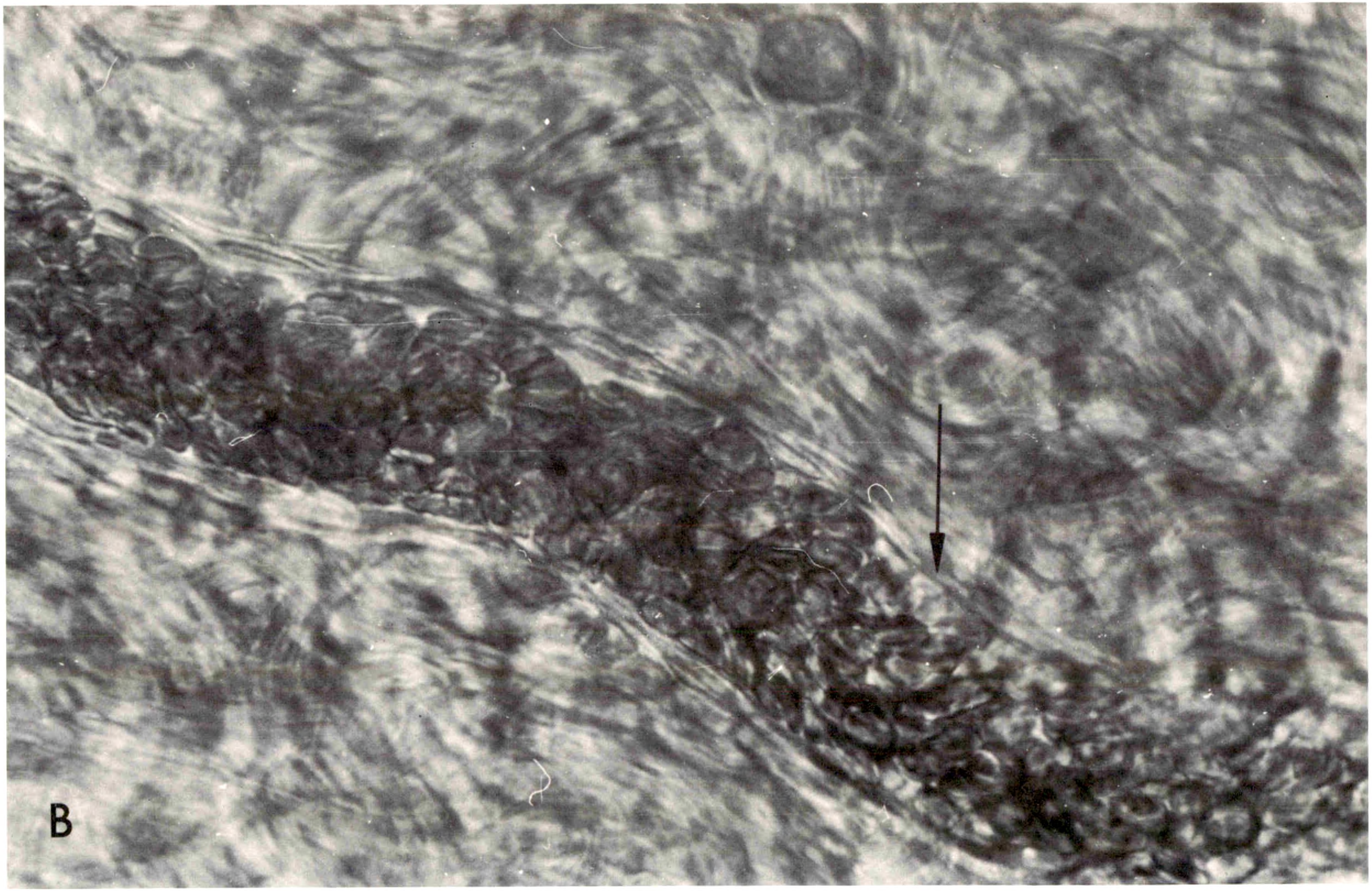
B

Glomerulonephritis Associated With Sarcoidosis

Ralph C. McCoy, MD and C. Craig Tisher, MD

Clinical findings and structural alterations in the kidneys of 6 patients with sarcoidosis and an associated glomerulonephritis are described. Five of the 6 patients manifested the nephrotic syndrome during some phase of their illness. Additional clinical evidence of renal disease included persistent microscopic hematuria (5 patients), hypertension (4 patients) and progressive renal failure (3 patients). Glomerular pathology varied and included proliferative glomerulonephritis (3 patients), membranous glomerulonephritis (1 patient), and chronic glomerulonephritis (2 patients). In 2 patients sequential examination of the kidney was possible, with renal biopsies preceding autopsy examination by 3 and 6 years, respectively. Glomerular pathology had progressed in severity in each case. Immunofluorescent studies in 2 patients revealed patterns of glomerular antibody localization consistent with immune complex disease. Electron microscopic studies of 1 revealed membranous changes characterized by electron-dense subepithelial and intramembranous deposits. Totally unexpected were virus-like intraendothelial structures in the glomeruli identical to those previously reported in systemic lupus erythematosus. Since current evidence suggests that the pathogenesis of both membranous and proliferative types of glomerulonephritis is immunologic, it should not be surprising that sarcoidosis, a disease which quite possibly results from an immune response to a disseminated antigen(s), should occasionally include glomerulonephritis as a part of its histologic expression (Am J Pathol 68:339–358, 1972).

IMPAIRED RENAL FUNCTION in patients with sarcoidosis has generally been attributed either to hypercalcemia with nephrocalcinosis and renal calculi [1-4] or to direct invasion of the renal parenchyma by the granulomatous process.[5-7] Primary glomerular alterations are not generally considered to be associated with systemic sarcoidosis, although a few isolated cases of glomerular disease have been reported.[8-11] Descriptions of the histopathology of the glomerular lesions have varied considerably. Membranous glomerulonephritis has been reported in 4 patients[8-10] and a proliferative glomerulonephritis characterized by glomerular hypercellularity and an increase in the mesangial matrix has been described in 2 patients.[10-11] Correa reported 1 patient with a progressive proliferative glomerulonephritis, demon-

---

From the Department of Pathology and the Department of Medicine, Division of Nephrology, Duke University Medical Center, Durham, NC.

Supported in part by Grants AM 13845 and 5-T02-GM00726 from the National Institute of General Medical Sciences of the US Public Health Service and Grant RR-30 from the General Clinical Research Centers Program of the Division of Research Sources of the National Institutes of Health; Dr. Tisher is the recipient of Research Career Development Award HL 440074 from the US Public Health Service.

Accepted for publication Apr 10, 1972.

Address reprint requests to Dr. Ralph McCoy, Department of Pathology, Box 3712, Duke University Medical Center, Durham, NC 27710.

strating epithelial crescent formation and neutrophilic infiltrates in glomerular tufts.[12] Early reports by Teilum emphasized the presence of hyaline and fibrinoid changes in glomerular capillaries and renal arterioles in a patient with sarcoidosis. He pointed out the similarity between that lesion and the renal lesion observed in systemic lupus erythematosus.[13,14]

Although proteinuria is occasional encountered in patients with sarcoidosis,[15,16] the nephrotic syndrome is exceedingly rare. To date this syndrome has been reported in 4 patients with sarcoidosis.[8-10] The present study describes the clinical and renal histologic features of 6 patients with sarcoidosis. In each there were significant renal glomerular alterations. In addition, 5 of the 6 patients developed the nephrotic syndrome during some phase of their illness.

Materials and Methods

The autopsy files at the Duke University Medical Center and the Durham Veterans Administration Hospital were reviewed for cases of systemic sarcoidosis. The diagnosis of sarcoidosis was based on histologic evidence of the disease in the absence of other demonstrated processes or etiologic agents known to cause granulomatous lesions. In addition, the surgical files of the two hospitals were reviewed for renal biopsies of patients with clinical and histologic evidence of systemic sarcoidosis. The clinical records of all patients identified were carefully evaluated for evidence of sarcoidosis.

Fifteen autopsy cases were identified in which adequate clinical and histopathologic evidence was available to support a diagnosis of systemic sarcoidosis. Of these 15, four had histologic evidence of associated renal glomerular disease. Two patients with glomerular disease underwent renal biopsy 3 and 6 years, respectively, before their deaths. In addition, biopsies with evidence of glomerular disease were available from an additional 2 patients with histologic diagnoses and clinical findings of sarcoidosis. Thus, a total of 8 specimens from 6 patients were available for evaluation.

Renal tissue for light microscopy was fixed in 10% buffered formalin and/or Zenker's solution, embedded in paraffin and stained with hematoxylin and eosin (H and E), periodic acid-Schiff (PAS), periodic acid-methanamine silver-Masson trichrome (PAMM) and von Kossa calcium stains.

Tissue obtained for electron microscopy was fixed in 4% glutaraldehyde buffered with 0.1 M sodium cacodylate, postfixed for 1 hour in 1% osmium tetroxide and embedded in Epon epoxy resin. Thin sections cut on a Porter-Blüm ultramicrotome were stained with lead citrate and uranyl acetate and studied and photographed with an Hitachi HS-8 electron microscope.

When tissue was available for immunofluorescent evaluation, the unfixed specimen was frozen at −70 C in a gelatin matrix. Sections for immunofluorescent evaluation were cut at 4 μ, fixed in acetone, washed in phosphate-buffered saline, incubated for 30 minutes with fluorescein-labeled antibody preparations, washed again in phosphate-buffered saline and mounted with glycerin. Sections were examined with a Leitz Ortholux microscope equipped with an HBO-200W mercury vapor light source, a UG-1 exciter filter and a K-490 barrier filter. Antibody preparations included goat or rabbit antihuman 7S globulin, IgG, IgM, IgA, β1C-globulin, fibrinogen and albumin. The antibody preparations were tested for specificity by immunoelectrophoresis. Sodium sulfate-precipitated immunoglobulin fractions were labeled with fluorescein isothiocyanate by the method of Marshall, Eveland and Smith.[17] Control preparations for immunofluorescent studies consisted of conjugates absorbed with specific antigen prior to incubation with tissue sections, and of tissue sections incubated first with unlabeled and then with labeled antibody preparations.

Clinical Material

Case 1

CM, a 47-year-old white male with sarcoidosis of 20 years' duration, initially diagnosed by lymph node and lung biopsy, first experienced recurrent nephrolithiasis and was found to be hypertensive 4 years after the onset of his disease. Fourteen years later, or 18 years after the onset of sarcoidosis, 3 to 4+ proteinuria and a 24-hour creatinine clearance of 54 ml/min were first noted. A few months before his death from progressive pulmonary insufficiency complicated by recurrent respiratory infections, the patient became nephrotic and developed peripheral edema, hypoalbuminemia, hypercholesterolemia and proteinuria of up to 4.0 g/24 hr. Microscopic hematuria was noted and the creatinine clearance fell to 25 ml/min shortly before death.

Case 2

LH, a 44-year-old black male with systemic sarcoidosis of 24 years' duration, initially diagnosed on lymph node biopsy, first manifested evidence of renal disease 13 years after the onset of his primary disease. Initially, signs and symptoms of renal involvement included microscopic hematuria, pyuria, proteinuria up to 1.5 g/24 hr and mild hypertension. Five years later, or 18 years after the onset of sarcoidosis, he became nephrotic, with hypoalbuminemia, hypercholestolemia and proteinuria up to 3.5 g/24 hr. Microscopic hematuria persisted while a 24-hour creatinine clearance was normal. A percutaneous renal biopsy was performed. During the 6 years preceding his death, the patient continued to manifest evidence of active renal disease with microscopic hematuria, proteinuria and a creatinine clearance severely reduced to 10 ml/min. The hypoalbuminemia (0.7 to 0.9 g/100 ml) persisted. At autopsy, noncaseating granulomata involved the lungs, lymph nodes, spleen, central nervous system and the right eye.

Case 3

AS, a 28-year-old black male, was found to have bilateral pulmonary infiltrates and right hilar adenopathy during an evaluation for severe headaches. A scalene lymph-node biopsy revealed a granulomatous lymphadenitis interpreted as compatible with sarcoidosis. Renal function was normal at the time. During the next 2 months the patient complained of a low-grade fever and night sweats followed by generalized mild arthralgias, ankle edema and orthopnea. There was no history of a preceding upper respiratory infection or a skin infection. Physical examination revealed mild hypertension and periorbital and ankle edema. Microscopic hematuria and red blood cell casts were noted. The patient excreted up to 3.5 g protein/24 hr and had evidence of hypoalbuminemia with a normal serum cholestrol. Blood urea nitrogen and serum creatinine remained normal. Extensive evaluation for a possible connective tissue or collagen-vascular disease was negative; a significant rise in ASO titer could not be documented. A percutaneous renal biopsy was performed. All signs and symptoms of renal disease cleared within 6 months. The patient was lost to further followup.

Case 4

DS, a 23-year-old black male was hospitalized for evaluation of asymptomatic hematuria and proteinuria of 2 years duration. The physical examination was unremarkable, but a chest x-ray revealed enlargement of the hilar and paratracheal lymph nodes and bilateral pulmonary infiltrates; these findings were interpreted as compatible with sarcoidosis. A percutaneous liver biopsy demonstrated noncaseating granulomata compatible with sarcoidosis. Urinalysis revealed both hematuria and proteinuria. The patient excreted up to 4.0 g protein/24 hr and manifested persistent hypoalbuminemia in the presence of a normal serum cholesterol. The blood urea nitrogen and creatinine clearance remained normal. Several LE cell preparations were negative and antinuclear antibodies could not be demonstrated. A percutaneous renal biopsy was performed. The patient was subsequently lost to followup.

Case 5

AA, a 30-year-old black male farm worker was initially evaluated for a foreign body in his right eye. Subsequently the eye was enucleated. At the time of hospitalization he was hypertensive and suffered from diabetes mellitus. He left the hospital against medical advice and received only sporadic medical care during the ensuing 4 years. He was then readmitted with malignant hypertension, azotemia, abdominal pain and severe dehydration. The admission chest x-ray revealed bilateral hilar and mediastinal adenopathy consistent with sarcoidosis. His total serum protein concentration was 4.1 to 4.5 g/100 ml with a serum albumin of 1.4 to 1.7 g/100 ml. With rehydration, pedal edema was noted. Urinalysis revealed 3+ proteinuria and microscopic hematuria with a fixed specific gravity. The patient developed staphylococcal septicemia and expired before more extensive renal evaluation could be completed. At autopsy, histologic changes in the hilar lymph nodes and lungs were compatible with sarcoidosis.

Case 6

EB, a 17-year-old black male was first suspected of having sarcoidosis on the basis of an abnormal chest x-ray, hypercalcemia, hypercalciuria and band keratopathy discovered during evaluation for congenital glaucoma. Qualitative proteinuria was evident at the time. One year later excisional biopsy of an anterior cervical lymph node revealed noncaseating granulomata consistent with sarcoidosis. Over the ensuing 2 years the patient developed progressive renal insufficiency with severe hypertension and continued to manifest hypercalcemia. Approximately 1 month before death, proteinuria increased to 4+, serum albumin fell to 1.6 g/100 ml and pedal and periorbital edema were present. The patient's blood urea nitrogen rose to levels greater than 200 mg/100 ml, and he underwent peritoneal dialysis. Shortly thereafter he died in terminal uremia and at autopsy generalized sarcoidosis involving the mediastinal lymph nodes, spleen, liver and lungs was found.

Results

Clinical Findings

The pertinent clinical findings in the 6 patients are presented in Table 1. All 6 were male; 5 were black and 1 was caucasian. The time relationship between the diagnosis of sarcoidosis and the diagnosis of

Table 1—Clinical Findings

Patient	Age Race Sex	Hyper-tension	Micro-hematuria	Urinary protein (g/24 hr)	Serum protein (g/100 ml) $\frac{\text{total}}{\text{albumin}}$	BUN	Creatinine clearance (cc/min)	Serum cholesterol (mg/100 ml)	Serum calcium (mg/100 ml)
CM	49 WM	—	+	4.0	$\frac{5.7}{2.3}$	120	25	420	9.6
LH	44 BM	+	+	3.5	$\frac{7.9}{2.4}$	15	115	312	9.6
AS	28 BM	+	+	3.5	$\frac{6.2}{2.6}$	15	ND†	170	ND
DS	23 BM	—	+	4.0	$\frac{7.8}{2.6}$	10	160	200	9.1
AA	30 BM	+	+	3+*	$\frac{4.5}{1.4}$	205	ND	226	4.7
EB	17 BM	+	—	2-4+*	$\frac{7.0\text{–}4.5}{2.8\text{–}1.4}$	200	8.3	410	11.9

* Semiquantitative determination only
† Not determined

renal disease varied considerably. In 2 patients (DS and AA) renal disease was noted when sarcoidosis was originally diagnosed, while in 1 patient (CM) the diagnosis of sarcoidosis preceded the onset of renal disease by 18 years. Four of the 6 patients (LH, AS, AA, and EB) were hypertensive, 5 had microscopic hematuria (CM, LH, AS, DS and AA), 3 (CM, AA and EB) eventually developed uremia and a fourth (LH) was mildly azotemic.

Five of the patients developed signs and symptoms of nephrotic syndrome during some phase of their clinical illness. The patients were edematous and had serum albumin levels below 3g/100 ml. Although the sixth patient (EB) may have been nephrotic terminally, as evidenced by hypoalbuminemia, hypercholesterolemia and qualitative proteinuria, other factors may have been at least partially responsible for the hypoalbuminemia; these factors include generalized sarcoid involvement of the liver, uremia with poor nutrition and peritoneal dialysis. In those patients in whom quantitative urinary protein determinations were obtained (CM, LH, AS and DS), all excreted 3.0 g or more protein/24 hr. In the 2 patients who did not have a quantitative urinary protein determination (AA and EB), qualitative values of 3 and 4+, respectively, were recorded. Three of the 6 patients (CM, LH and EB) had an elevated serum cholesterol. Four (LH, AS, DS and AA) did not receive steroid therapy, while 2 (CM and EB) were treated with prednisone; CM was treated intermittently for a period of 15 years and EB for 2 years. In the latter case, steroid therapy was initiated after the renal biopsy was performed.

Histopathology

Significant features of the renal histology in the 6 patients are summarized in Table 2; 3 of the 6 (CM, LH and AS) exhibited proliferative glomerulonephritis. The histologic features in Patient CM were characterized by a moderate increase in endocapillary cells and mesangial matrix material without prominent thickening of the glomerular capillary walls. Local accentuation of this proliferative process was marked in some glomeruli with segmental areas of sclerosis within individual glomerular tufts (Figure 1). Vascular lesions were characterized by mild to moderately severe intimal thickening and hyaline deposits in the small arteries and arterioles. The tubules and interstitium were normal except for small focal areas of calcium deposition in the medulla. Immunofluorescent studies in Patient CM revealed a diffuse linear localization of antihuman 7S globulin and IgG along the glomerular capillary walls and in the mesangial regions (Figure 2) with segmental linear localization of antihuman IgM. There was no significant glomerular localization of antihuman IgA, β1C-globulin, fibrinogen or albumin. In Patient LH a renal biopsy was taken 6 years before his death and autopsy. In the initial biopsy proliferation of glomerular endocapillary cells and an increase in mesangial matrix material were moderate. Local sclerotic lesions were seen within the tufts of some glomeruli (Figure 3). A small fraction of the glomeruli were completely sclerotic. Hyaline deposits were present in an apparent subendothelial location in some of the glomerular capillaries as well as in a few of the small arteries and arterioles. In addition, exudative or fibrin-cap lesions were observed in some glomerular capillaries. At autopsy, 6 years later, the severity of the glomerular disease had increased with endocapillary cell proliferation, an increase in mesangial matrix material, hyaline deposits in the glomerular capillaries and segmental as well as generalized sclerosis of many of the glomerular tufts (Figure 4). There was diffuse interstitial fibrosis with focal interstitial calcification and tubular atrophy were noted.

Patient AS had an acute proliferative glomerulonephritis with an increase in glomerular endocapillary cells, narrowing of capillary lumens and neutrophilic infiltrates in glomerular tufts (Figure 5). Interstitial edema was mild. The tubules and vasculature were unremarkable.

Patient DS had a membranous glomerulonephritis with diffuse and generalized thickening of the glomerular capillary walls. Special stains revealed silver-positive spikes projecting from the epithelial side of the capillary walls. There was mild proliferation of endocapillary cells of glomerular tufts and an associated mild increase in mesangial matrix material (Figure 6). In focal areas the tubules were atrophic, with thickening of the tubular basement membranes. The vessels were unremarkable. Immunofluorescent studies revealed that antihuman 7S globulin, IgG and β1C-globulin were localized in a diffuse granular pattern (Figure 9) and antihuman IgM in a segmental granular pattern along the glomerular capillary walls. Electron microscopy confirmed membranous alterations consisting of electron-dense deposits located on the subepithelial side of the basement membrane (Figure 7). There was villous transformation of the epithelial cells and loss of the epithelial foot processes with sheets of epithelial cytoplasm overlying the irregular external surface of the glomerular basement membrane. The mesangium was prominent: both the matrix material and the cytoplasmic processes were increased. In addition, microtubular or virus-like structures were present in rough surfaced endoplasmic reticulum of swollen endothelial cells (Figure 8). These

DS biopsy	MGN	+	subepithelial deposits silver-positive spikes	+	0	+	0	N	N	0
AA autopsy	CGN	++	+++ local subendothelial deposits	+++	++	++++	++	+++ intimal hyaline	D	0
EB biopsy	PGN	+	N	+	++	++	0	+ intimal proliferation	F	0
autopsy	CGN	++	+++ local subendothelial deposits	++	++	+++	0	++++ intimal proliferation and hyaline	D	0

* PGN = proliferative glomerulonephritis; MGN = membranous glomerulonephritis; CGN = chronic glomerulonephritis
F = focal; L = local or segmental; N = normal; 0 = absent; D = diffuse

structures were identical in appearance to those previously observed in systemic lupus erythematosus.

The 2 patients with clinical evidence of the most severe renal disease (AA and EB) had a chronic glomerulonephritis with complete sclerosis of most of the glomeruli. Those that were not completely sclerotic were hypercellular and contained increased numbers of endocapillary cells (Figure 10). In segmental areas, the glomerular capillary walls were markedly thickened by eosinophilic deposits (Figure 11), and occasional exudative or fibrin-cap lesions were found in both patients in the glomerular capillaries. Glomerular capsular adhesions were prominent as was pseudotubule formation within the parietal epithelium of Bowman's capsule. In neither of these cases were there nodular glomerular lesions of the type seen in diabetic glomerulosclerosis. Interstitial fibrosis and tubular atrophy were extensive in one patient and mild in the other. Arteries and arterioles from both patients revealed intimal thickening and hyaline deposits. The kidney of Patient TB had been biopsied 3 years before his death. Parenchymal alterations in that specimen were similar, though less severe, than those observed at autopsy.

Discussion

The occurrence of glomerulonephritis in patients with sarcoidosis immediately raises the question of whether the relationship between these conditions is causal or fortuitous. Although the etiologic agent(s) responsible for generalized sarcoidosis have not been identified, it is believed that this granulomatous reaction represents a type of immunologic hypersensitivity. Waksman[18] concluded that lesions of the sarcoid type are immunologic reactions to more or less widely disseminated antigens which either have a low solubility or cannot be metabolized. Scadding[19] suggested that the clinical findings of hyperglobulinemia, positive precipitins to certain antigens and positive tests for rheumatoid factor indicated that the normal immunologic mechanisms were altered in sarcoidosis. Since present evidence, drawn from studies of human disease as well as from experimental models, suggests that both membranous and proliferative types of glomerulonephritis have an immunologic or hypersensitivity pathogenesis, it should not be surprising to find that generalized sarcoidosis, a disease which quite possibly results from an immune response to a disseminated antigen, should occasionally include, as a part of its histologic expression, either a proliferative or membranous type of glomerulonephritis.

The type of glomerular lesions observed in both the autopsy material and the renal biopsies varied considerably. Similar observations have been made in the few scattered reports of glomerulonephritis associated with sarcoidosis (Table 3). This situation is not unlike that which prevails in systemic lupus erythematosus, the human prototype of immune complex nephritis. The nephritis associated with systemic lupus erythematosus may be either membranous, proliferative or a combination of both.[20] It may be either generalized and diffuse or focal and segmental. Teilum [13,14] emphasized the similarity between certain glomerular and renal arteriolar lesions in sarcoidosis and those observed in lupus nephritis. The results of the present study are very similar. Local and diffuse proliferative lesions, diffuse membranous alterations, and local as well as diffuse glomerular sclerosis were observed in the kidneys of patients included in this present study. Arteriolar hyaline deposits of the type described by Teilum were observed in the kidneys of 4 of the 6 patients. In addition, glomerular subendothelial deposits of the type often seen in lupus nephritis were noted in the same 4 patients. The histologic similarity between the two conditions was further evidenced by the findings in the kidney biopsy of Patient DS—the glomeruli exhibited a diffuse membranous glomerulonephritis, a lesion frequently seen in lupus nephritis. In addition, electron microscopy revealed microtubular or virus-like intraendothelial structures identical to those commonly observed in kidneys of patients with systemic lupus erythematosus.[21,22] Unfortunately, glomerular ultrastructure was not available in the other cases of sarcoidosis in the present study. However, glomerular ultrastructure in 2 additional patients with sarcoidosis but without clinical or histologic renal abnormalities who were not included in the present study revealed no such microtubular structures.

Table 3—Sarcoidosis with renal glomerular disease

Source	Description
Berkman **et al**[9]	Two cases of membranous glomerulonephritis with nephrotic syndrome
Falls **et al**[10]	One case of membranous glomerulonephritis with nephrotic syndrome; 1 case of proliferative glomerulonephritis
Laroche **et al**[8]	One case of membranous glomerulonephritis with nephrotic syndrome
Plattner **et al**[11]	One case of proliferative glomerulonephritis
Correa[12]	One case of rapidly progressive glomerulonephritis
Teilum[13]	One case with glomerular hyaline lesions

In those patients evaluated by immunofluorescence, the results differed. In Patient DS, a diffuse granular localization of antihuman immunoglobulins and β1C-globulin was similar to that usually observed in diffuse membranous glomerulonephritis. On the other hand, in Patient CM a diffuse linear localization of antihuman IgG was observed in the glomerular capillary walls, the exact significance of which is not apparent in this situation. Diffuse linear glomerular capillary localization of antihuman immunoglobulins is most often associated with antiglomerular basement membrane disease, such as is seen in Goodpasture's syndrome and other rare forms of rapidly progressive glomerulonephritis.[23,24] In Goodpasture's syndrome, antihuman β1C-globulin is also localized in an identical pattern. However, in the present case antihuman β1C-globulin localization was not observed. Diffuse linear localization of antihuman immunoglobulin without similar β1C-globulin localization has been observed in systemic lupus erythematosus,[25,26] as well as in rare cases of diabetes mellitus [26] and in certain unclassified forms of renal disease.[24] Thus, though the patterns of immunoglobulin localization in the two patients differed, both patterns have been associated with immune complex disease, specifically lupus nephritis.

Patient AA, in this series, had diabetes mellitus. The question must be raised as to whether clinical findings of the nephrotic syndrome—hypertension and renal failure—as well as the renal histologic alterations might be ascribed to diabetic glomerulosclerosis. Certainly many of the clinical findings could be explained on the basis of diabetic nephropathy. However, histologic evaluation failed to reveal the typical nodular lesions of diabetic glomerulosclerosis. Endothelial and mesangial hypercellularity of the extent seen in this patient is not characteristic of diabetic nephropathy, although some degree of cellular proliferation may accompany the less specific diffuse intercapillary type of glomerulosclerosis. The fibrin-cap lesion present in 3 patients in this report, though often associated with diabetic glomerulosclerosis, is not a specific lesion. It has been observed in arteriosclerotic kidneys, in various types of glomerulonephritis [27] and in animals treated with steroids.[28] In the present study 2 of the 3 patients whose kidneys contained this lesion did receive steroids. However, whether such a renal lesion occurs in humans treated with steroids is uncertain.[29]

The cases reported here should not be confused with Wegener's granulomatosis, although both conditions represent forms of granulomatous disease. Wegener's granulomatosis [30] is characterized by granulomatous lesions in the upper respiratory tract and lungs and by a florid form of glomerular disease. The upper respiratory symptoms are usually prominent and the progression of renal disease is usually rapid, with renal failure and uremia occurring in months. Histologically, the granulomatous inflammation has a necrotizing component which serves to distinguish it from sarcoidosis. In addition, there is frequently an associated polyarteritis in Wegener's granulomatosis which was not observed in any of the cases reported here. Furthermore, the glomerular lesions in Wegener's granulomatosis are usually characterized by a rapidly progressive process with prominent parietal epithelial cell proliferation (crescent formation) and fibrinoid necrosis involving the glomerular tufts. Such glomerular changes were not observed in any of the present cases.

This report of 6 patients with sarcoidosis and concommitant renal glomerular disease does not answer the question of causal relationship. Certainly the association of these conditions in 4 of 15 autopsies is greater than would be expected by chance alone. Considering the elusive nature of the inciting antigen, if indeed such exists in sarcoidosis as well as in most types of glomerulonephritis, the establishment of a causal relationship through an etiologic agent may not be imminent. However, awareness of the association may help to clarify the nature of this relationship.

References

1. Longcope WT, Freiman DG: A study of sarcoidosis based on a combined investigation of 160 cases including 30 autopsies from the Johns Hopkins Hospital and Massachusetts General Hospital. Medicine 31:1–132, 1952
2. Mayock RL, Bertrand P, Morrison CE, Scott JH: Manifestations of sarcoidosis. Analysis of 145 patients with a review of nine series selected from the literature. Am J Med 35:67–89, 1963
3. Klatskin C, Gordon M: Renal complications of sarcoidosis and their relationship to hypercalcemia. Am J Med 15:484–498, 1953
4. Scholtz DA, Keating FR: Renal insufficiency, renal calculi and nephrocalcinosis in sarcoidosis. Am J Med 21:75–84, 1956
5. Berger KW, Relman AS: Renal impairment due to sarcoid infiltration of the kidney. Report of a case proved by renal biopsies before and after treatment with cortisone. N Engl J Med 252:44–49, 1955
6. Ogilvie RI, Kaye M, Moore S: Granulomatous sarcoid disease of the kidney. Ann Intern Med 61:711–715, 1964
7. Coburn JW, Hobbs C, Johnston GS, Richert JH, Shinaberger JH, Rosen S: Granulomatous sarcoid nephritis. Am J Med 42:273–283, 1967
8. Laroche C, Merilion H, Morel-Maroger L, Turpin G, Uro J, Parrian F: Syndrome nephrotique and glomerulite extramembranuse associe a une sarcoidosis. J Urol Nephrol (Paris) 74:995–1001, 1968
9. Berkman JL, Bernstein SH: Membranous glomerulonephropathy in asso-

ciation with sarcoidosis. Proceedings of the Third International Congress of Nephrology, Washington, DC, 1966. Basel, S Karger A-G, 1967, p 156

10. Falls WF Jr, Stacy WK, Prazick JA, Abukurah AR, Still WJS, Randall RE Jr: Nonhypercalcemic nephropathy with sarcoidosis. Abstracts of the American Society of Nephrology. Washington, DC, 1970, p 24
11. Plattner HC, Nouskipel P, Morard JC: Nephropathie survenus au cours d'une sarcoidose de Besnier-Boeck-Schaumann. J Urol Med Chir 65:213–216, 1959
12. Correa Pelago: Sarcoidosis associated with glomerulonephritis. Arch Pathol 57:523–529, 1954
13. Teilum Gunnar: Glomerular lesions of the kidneys in sarcoidosis (Boeck's Sarcoid). Acta Pathol Microbiol Scand [A] 28:294–301, 1951
14. Teilum G: Morphogenesis and development of sarcoid lesions. Similarities to the group of collagenosis. Acta Med Scand 176: Suppl 425; 14–18, 1964
15. Freiman DG: Sarcoidosis. N Engl J Med 239:664–671, 1948
16. Leitner St J: Boeck's Sarcoidosis (chronic epitheloid-celled reticulo-endotheliosis or granulomatosis). Tubercle 31:174–183, 1950
17. Marshall JD, Eveland WC, Smith CW: Superiority of fluorescein isothiocyanate (Riggs) for fluorescent-antibody technic with a modification of its application. Proc Soc Exp Biol Med 98:898–900, 1958
18. Waksman B: Auto-immunization and the lesions of auto-immunity. Medicine 41:93–141, 1962
19. Scadding J: Sarcoidosis. London, Eyre and Spottiswoode, 1967, p 379
20. Baldwin DS, Lowenstein J, Rothfield NF, Galle G, McCluskey RT: The clinical course of the proliferative and membranous forms of lupus nephritis. Ann Intern Med 73:929–942, 1970
21. Tisher CC, Kelso HB, Robinson RR, Gunnells JC, Burkholder PM: Intraendothelial inclusions in kidneys of patients with systemic lupus erythematosus. Ann Intern Med 75:537–547, 1971
22. Kawano K, Miller L, Kimmelstiel P: Virus-like structures in lupus erythematosus. N Engl J Med 281:1228–1229, 1969
23. Lerner RA, Glassock RJ, Dixon FJ: The role of antiglomerular basement membrane antibody in the pathogenesis of human glomerulonephritis. J Exp Med 126:989–1004, 1967
24. McCluskey RT: The value of immunofluorescence in the study of human renal disease. J Exp Med 134:242s–245s, 1971
25. Koffler D, Angello V, Cass RI, Kunkel HG: Variable patterns of immunoglobulin and complement deposition in the kidneys of patients with systemic lupus erythematosus. Am J Pathol 56:305–316, 1969
26. Gallo G: Elution studies in kidneys with linear deposition of immunoglobulin in glomeruli. Am J Pathol 61:377–394, 1970
27. Heptinstall RH: Pathology of the Kidney. Boston, Little, Brown and Company, 1966, p 484
28. Moran TJ, Kurtz SM, Vazquez JJ: Diabetic and cortisone-induced renal lesions: A morphologic and immunohistochemical study. Lab Invest 11:240–254, 1962
29. Oppenheimer EH, Esterly J: Glomerular lesions in the nephrotic syndrome and their relation to cortisone therapy. Bull Johns Hopkins Hosp 113:158–172, 1963

30. Godman GC, Churg J: Wegener's granulomatosis: Pathology and review of the literature. Arch Pathol 58:533–553, 1954

Acknowledgments

The authors gratefully acknowledge the contributions of Dr. J. Caulie Gunnells, who kindly permitted the inclusion of patient DS in this study and of Dr. Peter M. Burkholder, who performed the immunohistochemical studies on patient DS.

[*Illustrations follow*]

Legends for Figures

Fig 1—Glomeruli from the kidney of patient CM revealing localized proliferation and sclerosis of a glomerular tuft. A capsular adhesion is present in the lower glomerulus (PAS, × 225).

Fig 2—Glomerulus from patient CM showing localization of antihuman IgG in a diffuse linear pattern along the capillary walls and in the mesangial regions (× 265).

Fig 3—Glomerulus from the biopsy of patient LH showing localized mesangial cell proliferation with segmental sclerosis of the glomerular tuft and a capsular adhesion (H&E, × 375).

Fig 4—Glomerulus from the autopsy kidney of patient LH obtained 6 years after the biopsy illustrated above. Note the subendothelial deposits and hyaline thrombi in the glomerular capillaries. A capsular adhesion with pseudotubule formation and a single exudative capsular drop lesion along the basement membrane of Bowman's capsule is demonstrated (H&E, × 375).

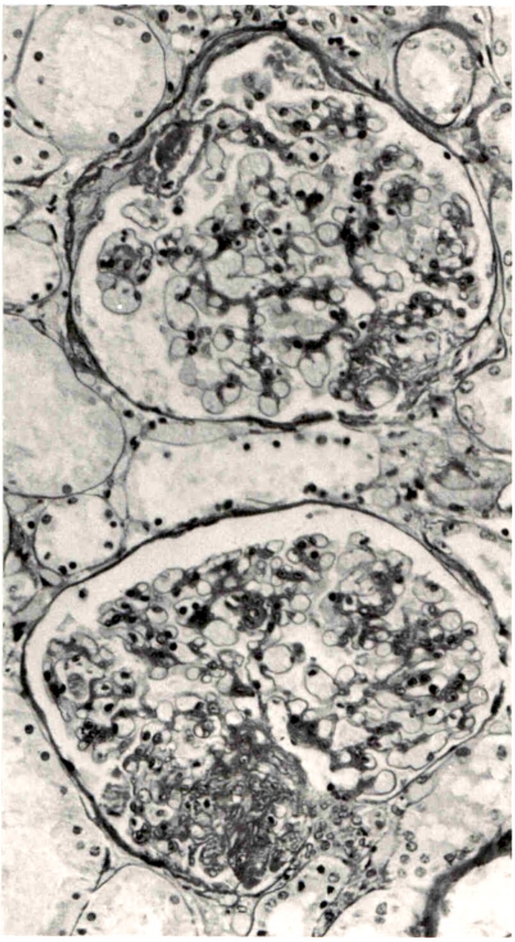

1

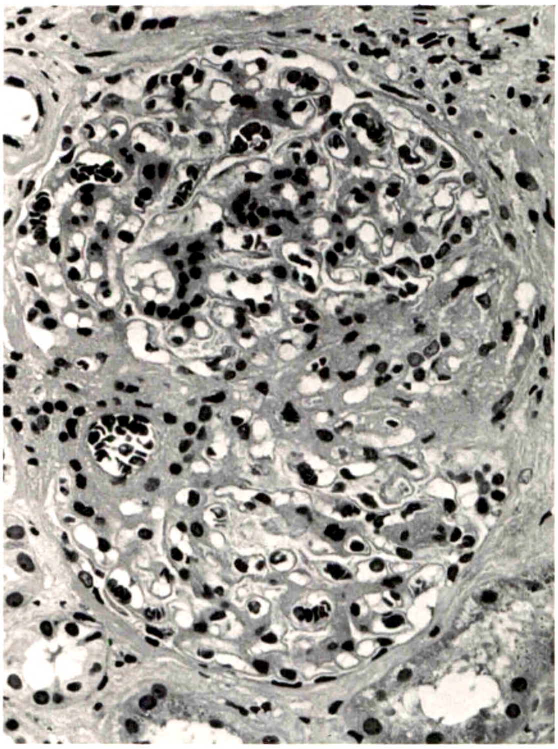

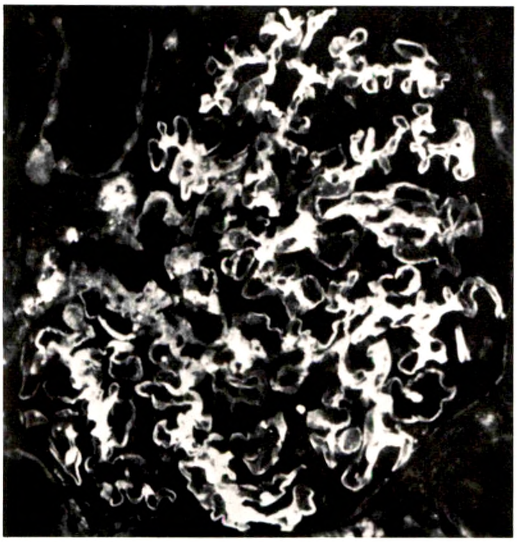

2

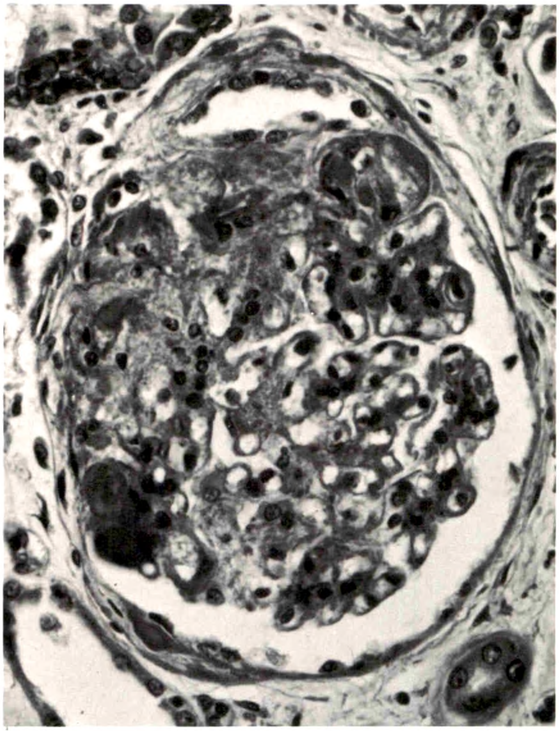

Fig 5—Glomerulus from the biopsy of patient AS revealing segmentally accentuated proliferation of endothelial and mesangial cells with neutrophilic infiltration of the glomerular tuft (H&E, × 315).

Fig 6—Glomerulus from the biopsy of patient DS revealing diffuse thickening of the glomerular capillary walls with marked segmental increase in the mesangial matrix and adhesion of the tuft to Bowman's capsule (PAMM, × 315).

Fig 7—Electron micrograph from a glomerulus of patient DS revealing subepithelial and intramembranous electron-dense deposits along the capillary basement membrane. Epithelial foot processes are retracted, leaving sheets of epithelial cytoplasm overlying the electron-dense deposits and basement membrane (× 11,980).

5

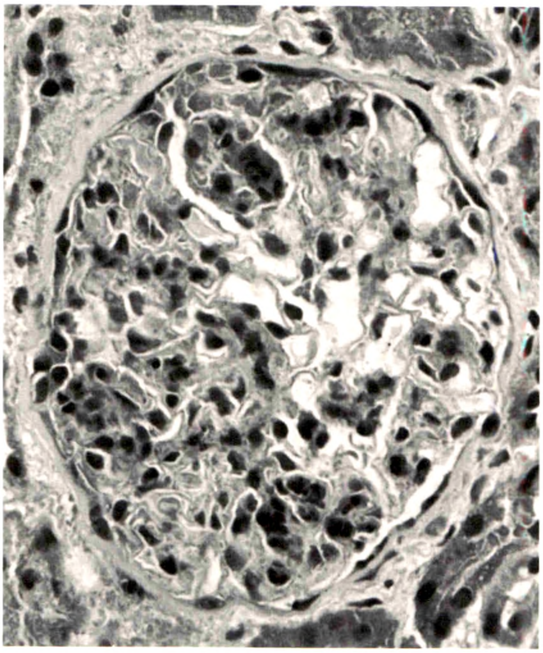

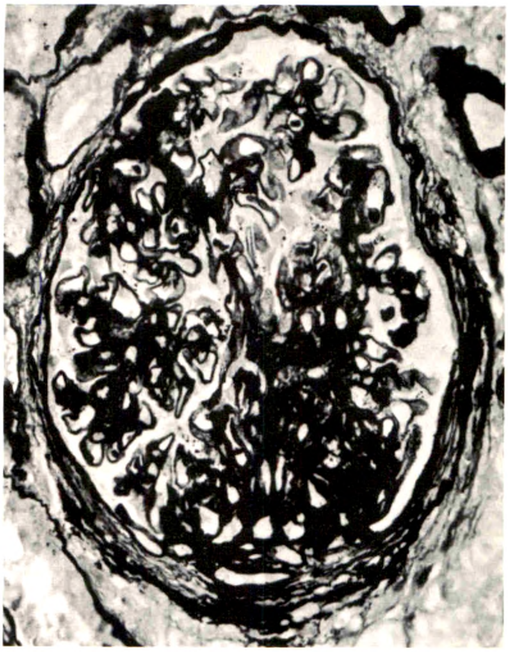

6

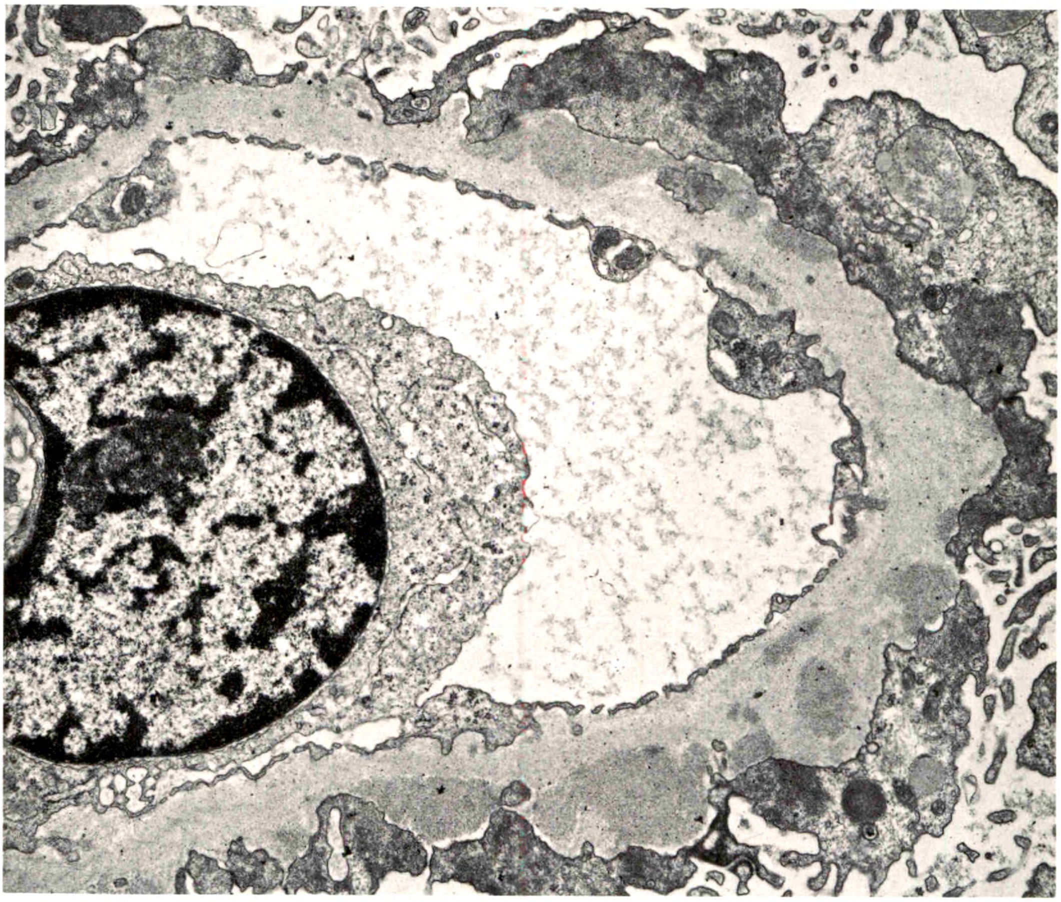

7

8

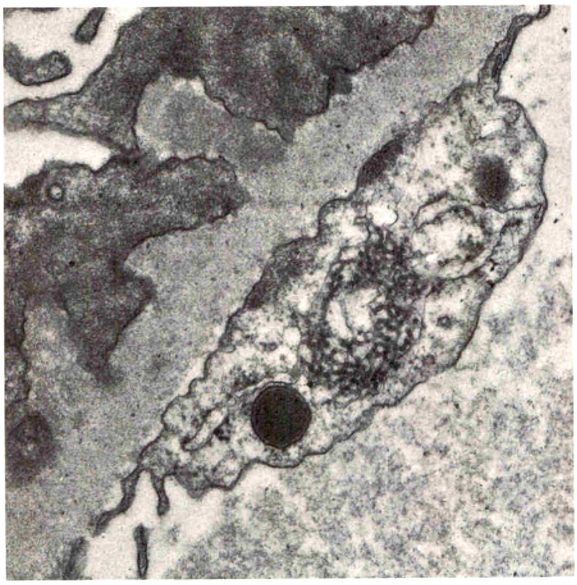

9

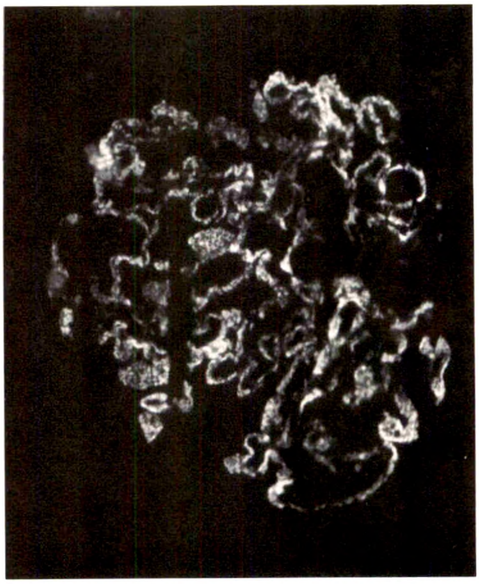

10

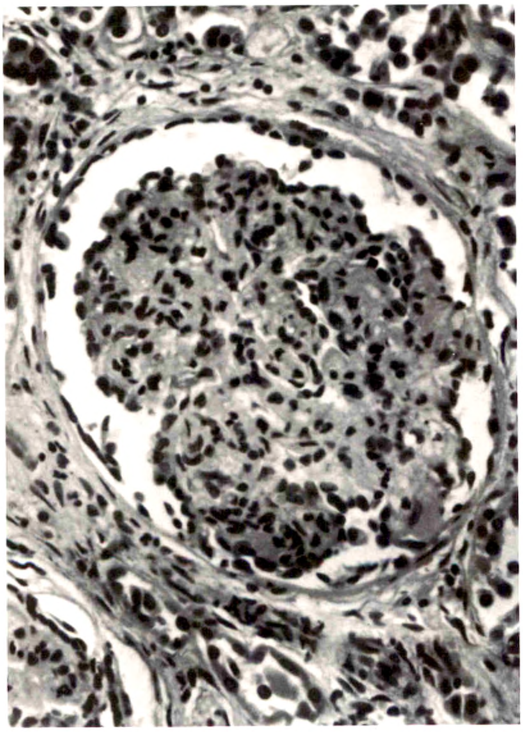

11

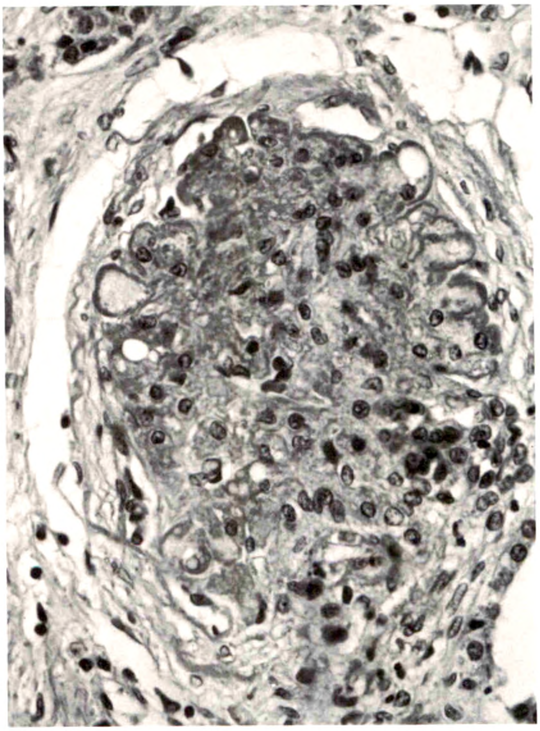

Fig 8—Electron micrograph from glomerulus of patient DS showing a collection of virus-like particles in the endoplasmic reticulum of a capillary endothelial cell. Subepithelial electron-dense deposits are present along the basement membrane (× 23,100). **Fig 9**—Glomerulus from patient DS showing localization of anti-human 7S globulin in a diffuse granular pattern along the glomerular capillary walls (× 265). **Fig 10**—Glomerulus from patient AA demonstrating endothelial and mesangial hypercellularity (H&E, × 375). **Fig 11**—Glomerulus from patient EB showing solidification of the glomerular tuft with marked thickening of several peripheral capillary walls (H&E, × 375).

Cell Proliferation in Rat Kidneys After Prolonged Treatment With Lead

David D. Choie, MS and Goetz W. Richter, MD

Effects of chronic lead intoxication on cellular proliferation in rat kidneys were investigated by autoradiography. The rats were given intraperitoneal injections of lead acetate in aqueous solution for 6 months. At the end of this period, the proliferative activity of proximal tubular epithelial cells was about 15 times greater in rats given lead than in untreated controls. In the leaded rats approximately 40% of the proximal tubular cells contained intranuclear inclusions, approximately 0.5% of proximal tubular epithelial cells were labeled and approximately 6% of labeled cells contained intranuclear inclusions. Thus, cells with intranuclear inclusions can replicate DNA. Effects of chronic lead poisoning on the replication of proximal tubular cells in rats subjected to left uninephretomy before inception of treatment with lead were substantially the same. No renal carcinomas were found after 6 months of treatment with lead, but there was epithelial hyperplasia in some proximal tubules, with occasional atypia. The presence of increased synthesis of DNA and epithelial hyperplasia in the kidneys of rats chronically poisoned with lead suggests that the renal carcinogenicity of lead, observed by others, is related to lead-induced stimulation of renal cell proliferation (Am J Pathol 68:359–370, 1972).

IN A VARIETY OF ANIMAL SPECIES, chronic treatment with lead results in the formation of intranuclear inclusion bodies in proximal tubular epithelial cells of the kidneys.[1-4] In rats and mice, administration of lead for more than a year often induces renal neoplasms.[5-8] Little consideration has been given, however, to possible effects of lead on cell replication. Recently, we have demonstrated that a single injection of lead markedly stimulates DNA synthesis in rat kidneys within 2 days.[9]

This paper deals with three questions about the effects of prolonged administration of lead on rat kidneys: What is the state of cell proliferation in the tubular epithelium after lead has been administered for 6 months? Do renal tubular cells that contain intranuclear inclusions display signs of nuclear activity? Does the absence of one kidney influence proliferative activity of the tubular epithelium in the remaining kidney after chronic poisoning with lead?

From the Department of Pathology, The University of Rochester Medical Center, Rochester, NY.

Supported by Research Grant ES–00474 and Training Grant GM–00133 from the National Institutes of Health.

Accepted for publication Apr 14, 1972.

Address reprint requests to Mr. David D. Choie, Department of Pathology, University of Rochester Medical Center, 260 Crittenden Blvd, Rochester, NY 14642.

We have found, by autoradiography, that the uptake of ^{3}H-thymidine is significantly greater in the proximal tubular epithelium of rats treated with lead for 6 months than it is in the proximal tubular epithelium of controls, and that renal epithelial cells with characteristic intranuclear inclusions can synthesize DNA. We have also noted the development of focal epithelial hyperplasia, sometimes atypical, in segments of proximal tubules.

Materials and Methods

Adult female Sprague-Dawley rats (Chordata Corp, Rochester, NY), weighing 210 to 240 g were used. The rats were housed individually in a room with 12-hour light–dark cycles, and given Purina rat chow and tap water *ad libitum*.

Experimental groups

Group A (Controls). Six control rats were not treated during the experimental period of 6 months.

Group B (Leaded Group). Eighteen rats were injected intraperitoneally once a week with lead acetate in sterile water, at doses of 1 to 7 mg lead per rat for 6 months. Injections were skipped when the rats appeared lethargic.

Group C (Uninephrectomized Group). The left kidney was removed from each of 12 rats at the beginning of the experimental period. The kidney was removed under ether anesthesia, through a dorsolateral subcostal incision. These rats were not treated further.

Group D (Uninephrectomized and Leaded Group). Twelve rats were uninephrectomized as was Group C, and were injected with lead acetate, as was Group B, for 6 months.

Labeling and Autoradiography

The rats in the four experimental groups were sacrificed after 6 months. One hour before sacrifice, all rats were injected intraperitoneally with ^{3}H-thymidine (Specific Activity 15.2 Ci/mM, Schwarz/Mann, Inc, Orangeburg, NY) in doses of 0.2 μCi/g body weight. Kidneys were excised and weighed after their capsules were removed. A central slice of each kidney, obtained by cutting through the long axis, was fixed in Carnoy's fluid, embedded in paraffin and sectioned at 4 μ. Deparaffinized sections mounted on slides were dipped into NTB2 nuclear track emulsion (Eastman Kodak Co, Rochester, NY), exposed for 2 weeks, developed in D-19 Kodak developer, fixed, washed and stained with hematoxylin and eosin.

Scoring of Cells

Epithelial cells in proximal tubules were classified as labeled, unlabeled and cells in mitosis. Each class of cells was further divided into cells with and without intranuclear inclusions. At least 10,000 cells were differentially scored for each animal, using an oil immersion objective.

Renal Lead Content

Renal tissue was weighed, rinsed in 0.9% NaCl solution and digested in a 3:2 mixture of concentrated nitric and perchloric acids on a Kjeldahl digestor. After appropriate dilution with a solution of 0.5% $LaCl_3$, lead content was determined in a Jarrel-Ash atomic absorption spectrophotometer.

Results

The results of differential scoring of the proximal tubular epithelial cells for each experimental group are given in Table 1 and Text-figure 1. The amounts of lead in the kidneys are shown in Text-figure 2. In the statistical analysis the 1% level ($P < 0.01$) in Student's t test was taken to indicate significant differences.

Effects of Prolonged Treatment with Lead on Renal Cell Proliferation

Nine of the 18 rats treated with lead survived for 6 months. At the time of sacrifice, blood smears showed basophilic stippling of some erythrocytes in all nine rats. The mean wet weight of kidneys was about 10% higher than that of kidneys from controls. After treatment with lead for 6 months, the mean labeling index of the epithelial cells in the proximal tubules was 45/10,000 cells (Text-figure 1). The uptake of ^{3}H-thymidine was approximately 15 times greater in the leaded rats than in controls ($P < 0.01$). ^{3}H-thymidine labels were found predominantly over cells without intranuclear inclusions. About 6% of the labeled cells also contained intranuclear inclusions (Table 1 and Figure 1A, B). A few cells in mitosis were suspected of containing intranuclear inclusions, but this has yet to be verified.

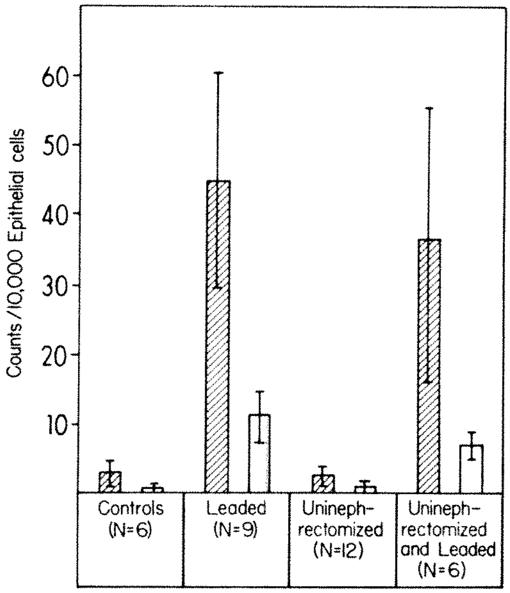

TEXT-FIG 1—Proliferative activities in epithelia of proximal tubules of kidneys in 4 experimental groups. The counts of labeled cells ±SD (*hatched columns*) and mitoses ±SD (*open columns*) are shown per 10000 epithelial cells.

Histologically, the nuclei of the epithelial cells in the proximal tubules were often enlarged and irregular in shape, but frequently exhibited prominent basophilic nucleoli even when they contained inclusions (Figure 2). About 40% of proximal tubular cells contained recognizable intranuclear inclusion bodies (Table 1) which were characteristically eosinophilic. Sometimes there were two or more inclusions in one nucleus. The epithelial cells of distal tubules contained no intranuclear inclusions but were labeled more frequently in leaded rats than in controls.

Occasionally, epithelial hyperplasia was found in segments of proximal tubules of rats treated with lead (Figure 3). These foci were easily distinguished from normal surroundings by the hyperbasophilic cytoplasm of the cells and by the increase in number of epithelial cells in the affected tubules. The nucleo-cytoplasmic ratio of the hyperplastic tubular cells was greater than normal. Some tubular cells in areas of hyperplasia were labeled, and some others contained intranuclear inclusions. Here and there, the hyperplasia of proximal tubular epithelial cells was distinctly atypical (Figure 4). Renal carcinomas were not found. In leaded rats, there was no evidence of frank renal necrosis, but desquamated cells were present in the lumen in some of the renal tubules. The renal content of lead was significantly ($P < 0.01$) higher in rats given lead than in controls (Text-figure 2).

Effects of Uninephrectomy on Cell Proliferation in the Remaining Kidney After 6 Months

All uninephrectomized rats survived for 6 months. At the time of sacrifice, the mean wet weight of the remaining kidney was approxi-

Table 1—Mean Labeling Indices of 4 Experimental Groups*

Experimental group	No. rats	No. kidneys	Labeled cells without inclusions†	SE	Labeled cells with inclusions†	SE	Cells with inclusions†	SE
Controls	6	12	3.0 ± 1.8	0.7	0	—	0	—
Leaded	9	17‡	42.1 ± 13.8	4.6	2.7 ± 2.2	0.7	4047 ± 273	91
Uninephrectomized	12	12	2.6 ± 1.5	0.4	0	—	0	—
Uninephrectomized and leaded	6	6	34.5 ± 20	8.1	2.2 ± 1.3	0.5	4216 ± 370	151

* All animals were labeled with ^{3}H-thymidine for 1 hour

† The counts are per 10,000 epithelial cells of the proximal tubules in the kidney ± SD

‡ Both kidneys were counted in all rats but one

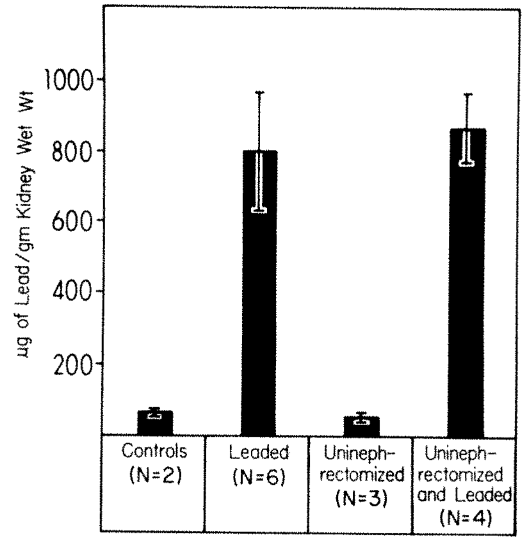

TEXT-FIG 2—Mean lead content of kidneys from 4 experimental groups, determined by atomic absorption analysis of acid digests. Amount of lead is expressed in µg lead/g wet kidney weight ± standard deviation.

mately 30% heavier than that of controls, presumably because of compensatory renal hyperplasia and hypertrophy.[9-11]

Six months after uninephrectomy, the mean labeling index of the proximal tubular cells in the remaining kidneys was not significantly different from that in control kidneys (Text-figure 1). The tubular lumina appeared somewhat enlarged compared with those in controls. The lead content of kidneys from uninephrectomized rats was about the same as that of kidneys from untreated controls (Text-figure 2).

Effects of Prolonged Treatment with Lead on Cell Proliferation in the Remaining Kidneys of Uninephrectomized Rats

Six of the 12 uninephrectomized rats that were treated with lead survived for 6 months. At autopsy the mean wet weight of the remaining kidneys was approximately 50% heavier than that of kidneys from untreated controls, and approximately 20% heavier than that of remaining kidneys from uninephrectomized unleaded rats. The mean labeling index in this group was 37/10,000 proximal tubular cells (Text-figure 1), and the labeling activity and the renal content of lead were significantly greater than in untreated controls and in uninephrectomized unleaded rats ($P < 0.01$). However, the proliferative activity of the proximal tubular epithelium in this group was not significantly different from that in the leaded group without uninephrectomy.

Approximately 6% of the labeled proximal tubular epithelial cells contained intranuclear inclusions (Table 1). Histologic changes in the remaining kidneys of this group were similar to those in kidneys of leaded rats without uninephrectomy. As in the case of leaded rats with both kidneys, epithelial cells of hyperplastic tubules showed hyperchromatic nuclei and hyperbasophilic cytoplasm. There were no renal carcinomas.

Discussion

The present study demonstrates that proliferation of proximal tubular epithelial cells was significantly greater in rats treated with lead for 6 months than in untreated controls. Moreover, the prominence of nucleoli in many cells of the tubular epithelium in the leaded rats may well be an indication of increased RNA metabolism associated with increased DNA replication.[12]

We have reported previously that a single dose of lead (0.04 mg lead/g body weight) stimulates DNA synthesis in rat kidneys within 2 days, without producing morphologically discernible cell damage.[9] This suggests that in chronic, as in acute, lead poisoning, renal tubular cell proliferation may be induced by lead. However, the proliferative activity in the course of chronic lead poisoning could in part be related to regeneration that follows shedding of damaged epithelial cells, although desquamated cells were only infrequently seen after 6 months of treatment with lead. It is unlikely that the increased uptake of ^{3}H-thymidine in the chronically leaded rats was related to repair of damaged DNA, because in the present experiments the mitotic indices of proximal tubular epithelial cells were comparable to the labeling indices (Text-figure 1) if one considers that the number of cells in mitosis is proportional to the duration of the mitotic phase and that in rat kidneys the mitotic phase is about a quarter of the synthetic phase.[13] Therefore, the increase in ^{3}H-thymidine uptake in the leaded rats appears to be a manifestation of genuine DNA replication involving cell division. The labeling activity in proximal tubular epithelium did not differ significantly between Group B (leaded) and Group D (uninephrectomized and leaded). This indicates that uninephrectomy had little or no effect on renal cell proliferation after 6 months. The mean labeling index of proximal tubular epithelial cells in control kidneys was low compared to the labeling index we have previously reported for 4-month-old rats, presumably because of the significantly greater age (approximately 10 months) of the controls in the experiments here reported.

An interesting finding of the present study was that in leaded rats a small number of proximal tubular cells with intranuclear inclusions was distinctly labeled by ^{3}H-thymidine (Table 1). This is evidence that cells with intranuclear inclusions can synthesize DNA. Yet the presence of intranuclear inclusions appears to be unfavorable for cell replication. In leaded rats approximately 40% of all proximal tubular epithelial cells contained intranuclear inclusions, whereas only 6% of labeled cells contained inclusion bodies. It should be noted, however, that small intranuclear inclusions may not be recognized by histologic examination. The intranuclear inclusion bodies have been reported to contain protein as well as lead.[3,14]

Zollinger[5] showed that lead is carcinogenic in rat kidneys. Others[6-8] have reported that ingestion of lead in the diet for a year or more induces renal neoplasm in rats and mice. Some have proposed that this carcinogenic effect of lead results from inhibition of mitosis in the kidney.[7] The findings presented here suggest strongly that it is not the inhibitory but the stimulatory potential of lead on renal cell replication which is related to renal carcinogenesis.

Chemical carcinogens, such as 2-acetylaminofluorene (2-AAF) and ethionine have been shown to stimulate proliferation of hepatocytes in rats and to produce hyperplastic nodules in the liver.[15-16] These reports, as well as other evidence,[17-19] suggest that increased cell proliferation in the target tissue during the latent period is an essential biologic feature of carcinogenesis. Therefore, the significant increase in proliferative activity of renal tubular epithelial cells after chronic treatment with lead is consistent with experimental data on the effects of other chemical carcinogens. Since a single injection of lead stimulates proliferation of renal tubular epithelial cells in rats,[9] it is likely that the increased proliferative activity observed in the chronically leaded rats lasted for the entire period of 6 months.

We did not find neoplasms in the kidneys of rats treated with lead for 6 months, presumably because the experimental period was not long enough for the production of neoplasia.[6-7] However, the spotty presence of epithelial hyperplasia in the proximal tubules, sometimes atypical, may be indicative of the development of a preneoplastic state. The concept of preneoplasia is supported by studies on hepatocarcinogenesis. Hyperplastic nodules in rat liver, induced by 2-AAF or by aflatoxin B, appear to be sites in which hepatomas originate.[15]

Perhaps sustained stimulation of mitosis in renal tubular cells by lead was the cause of the observed hyperplasia. If so, persistent interaction of lead with tubular epithelial cells may on occasion produce an enduring alteration in the regulation of cell replication that gives rise to neoplastic transformation.

References

1. Blackman SS Jr: Intranuclear inclusion bodies in the kidney and liver caused by lead poisoning. Bull Johns Hopkins Hosp 58:384–398, 1936
2. Beaver DL: The ultrastructure of the kidney in lead intoxication with particular reference to intranuclear inclusions. Am J Pathol 39:195–208, 1961
3. Richter GW, Kress Y, Cornwall CC: Another look at lead inclusion bodies. Am J Pathol 53:189–217, 1968
4. Goyer RA, Leonard DL, Moore JF, Rhyne B, Krigman MR: Lead dosage and the role of the intranuclear inclusion body. Arch Environ Health 20:705–711, 1970
5. Zollinger HU: Durch chronische Bleivergiftung erzeugte Nierenadenome und Carcinome bei Ratten und ihre Beziehungen zu den entsprechenden Neubildungen des Menschen. Virch Arch [Pathol Anat] 323:694–710, 1953
6. Boyland E, Dukes CE, Grover PL, Mitchley BCV: The induction of renal tumors by feeding lead acetate to rats. Br J Cancer 16:283–288, 1962
7. Van Esch GJ, Van Genderen H, Vink HH: The induction of renal tumors by feeding of basic lead acetate to rats. Br J Cancer 16:289–297, 1962
8. Van Esch GJ, Kroes R: The induction of renal tumors by feeding basic lead acetate to mice and hamsters. Br J Cancer 23:765–771, 1969
9. Choie DD, Richter GW: Cell proliferation in rat kidney induced by lead acetate and effects of uninephrectomy on the proliferation. Am J Pathol 66:265–275, 1972
10. Goss RJ, Rankin M: Physiological factors affecting compensatory renal hyperplasia in the rat. J Exp Zool 145:209–216, 1960
11. Johnson HA, Vera Roman JM: Compensatory renal enlargement: hypertrophy versus hyperplasia. Am J Pathol 49:1–13, 1966
12. Cooper HL: Biochemical alterations accompanying initiation of growth in resting cells. The Cell Cycle and Cancer. Edited by R Baserga. New York, Marcel Dekker, Inc, 1971, pp 197–226
13. Baserga R, Wiebel F: The cell cycle of mammalian cells. Int Rev Exp Pathol 7:1–30, 1969
14. Goyer RA, May P, Cates MM, Krigman MR: Lead and protein content of isolated intranuclear inclusion bodies from kidneys of lead-poisoned rats. Lab Invest 22:245–251, 1970
15. Slifkin M, Merkow LP, Pardo M, Epstein SM, Leighton J, Farber E: Growth in vitro of cells from hyperplastic nodules of liver induced by AAF or aflatoxin B. Science 167:285–287, 1970
16. Merkow LP, Epstein SM, Slifkin M, Farber E, Pardo M: Ultrastructural alterations within hyperplastic liver nodules induced by ethionine. Cancer Res 31:174–178, 1971
17. Ryser HJP: Chemical carcinogenesis. N Engl J Med 285:721–734, 1971

18. Becker FF: Cell function: its importance in chemical carcinogenesis. Fed Proc 30:1736–1741, 1971
19. Warwick GP: Effect of the cell cycle on carcinogenesis. Fed Proc 30: 1760–1765, 1971

Acknowledgments

We thank Miss Linda Cross and Mr. Lester Young for their able technical assistance.

[*Illustrations follow*]

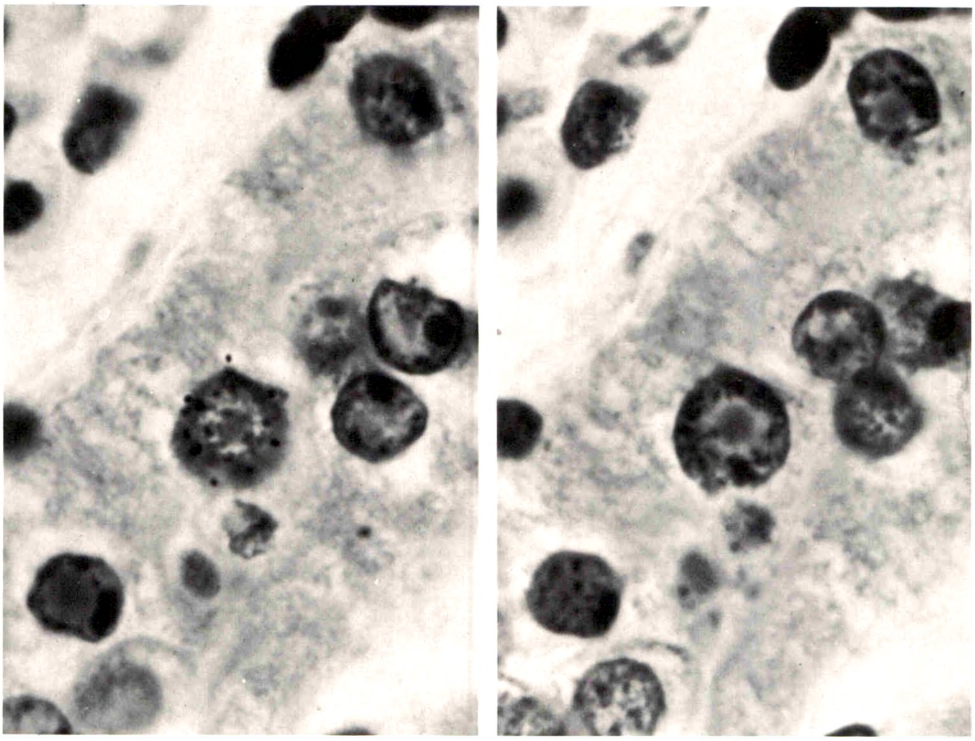

1B

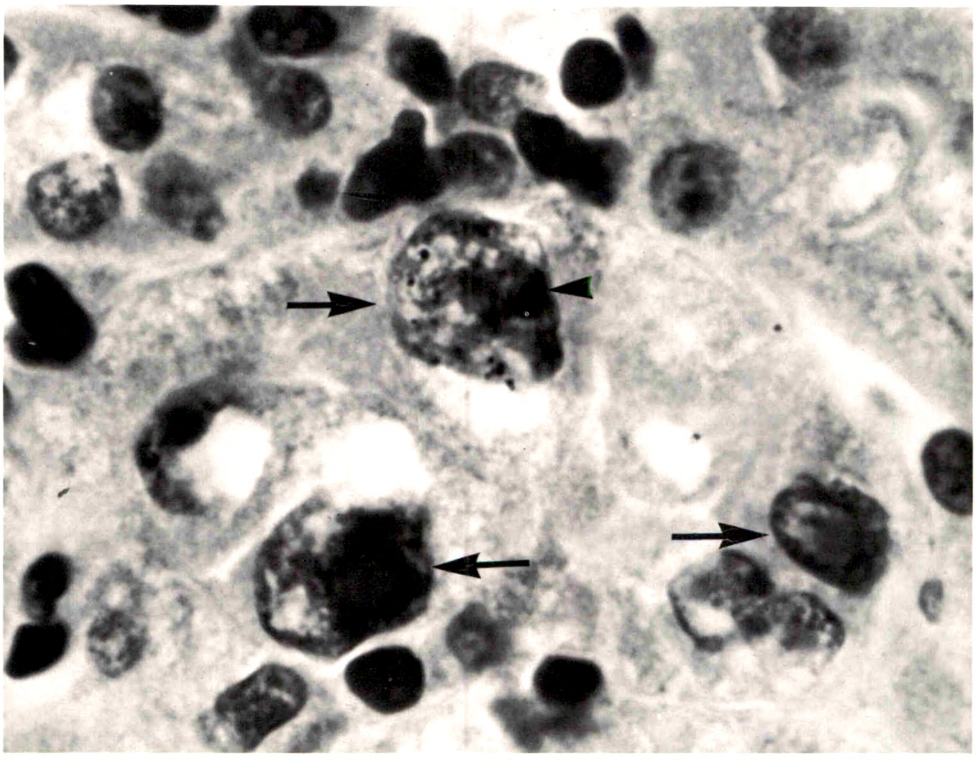

2

Fig 1—Proximal convoluted tubule of rat given lead during 6 months. Labeled nucleus of tubular epithelial cell with inclusion body, focused in **A** to show exposed silver grains of photographic emulsion, and in **B** to show intranuclear inclusion body (H&E, × 1700). **Fig 2**—From rat given lead for 6 months. Three proximal tubular epithelial cells (*arrows*) with intranuclear inclusion bodies. One of the nuclei is also labeled by ^{3}H-thymidine (*grains*). Note nucleolus (*arrowhead*) in the labeled nucleus (H&E, × 1700).

3

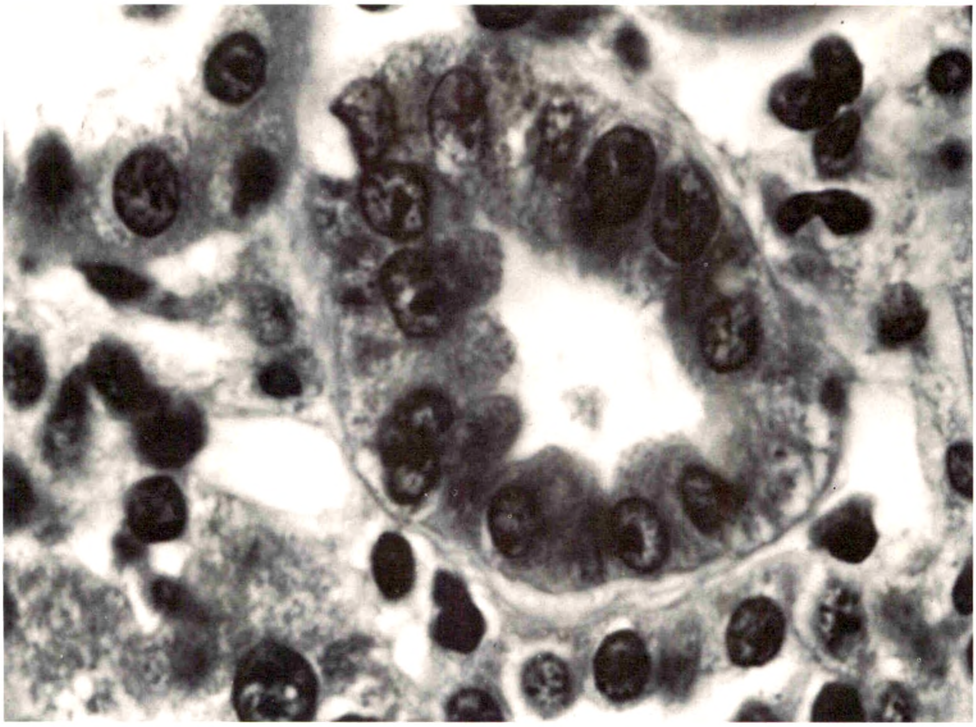

4

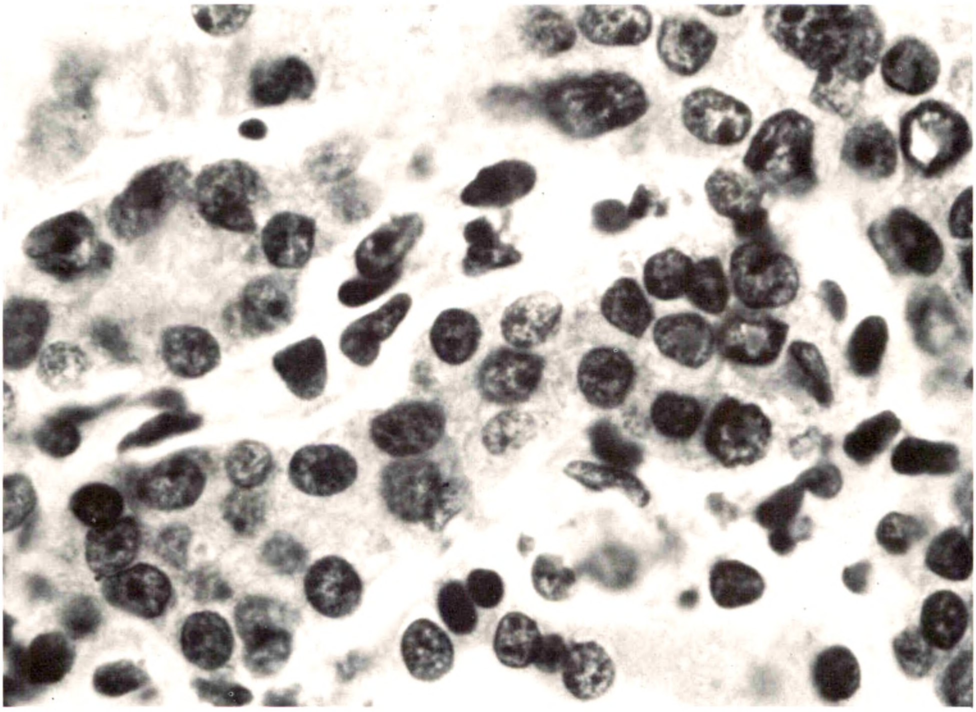

Fig 3—From rat given lead for 6 months. Hyperplasia of epithelial cells seen in cross section of proximal convoluted tubule. Several nuclei have abnormal, irregular shapes, appear to be larger than normal. Cells are more crowded than normally. Compare with cells near upper left corner, which line another segment of the proximal tubule (H&E, × 1700). **Fig 4**—From rat given lead for 6 months. Irregular hyperplasia of proximal tubular epithelium. Note inclusion bodies in several nuclei (H&E, × 1200).

Amyloidogenesis in Healing Wound

Electron Microscopic Studies of Biopsied Wounds in Macular Amyloidosis

Ken Hashimoto, MD and Martin H. Brownstein, MD

Clinically and histologically typical skin lesions of macular and lichenoid amyloidoses were biopsied. Rebiopsies were performed after 2 to 16 weeks, and the sequence of amyloid reproduction in granulation tissue was followed. Initially, medium electron-dense proteinaceous substance with fine filaments was produced within or in close relation to the rough-surfaced endoplasmic reticulum of fibroblasts and subsequently discharged. Typical amyloid filaments emerged within and in the vicinity of this substance. A significant number of collagen fibrils were admixed in the centers of some amyloid islands. Predominantly amorphous amyloid substance was seen in contact with the basal laminae. No plasma cells were observed in foci of amyloid regeneration. Phagocytes were present but did not phagocytose amyloid. Nonepithelialized wounds did not contain amyloid. It was suggested that, in the primary skin amyloidoses, abnormal dermal fibroblasts produce amyloid precursors under the influence of the epidermis (Am J Pathol 68: 371–390, 1972).

IN OUR PREVIOUS STUDIES on lichen amyloidosus [1,2] and its variant, macular amyloidosis,[3] skin lesions were shown to contain the same amyloid substance as that defined in other organs.[4,5] Most amyloid filaments in skin lesions of these conditions measured between 60 and 100 Å; differential staining with Congo red, crystal violet and thioflavin T exhibited tinctorial characteristics of amyloid.[1,2] The results of studies by other investigators on these skin amyloidoses [6–10] agreed with our findings.[1–3]

The origin of amyloid, in general, has not been settled. The concept that it is produced in the lesion by local tissue cells such as fibroblasts or reticulohistiocytes [1–4,6,8–10] was recently challenged by the finding that the amino acid sequence of purified amyloid is similar to the variable portion of the light chain of homogeneous immunoglobulin.[11,12] This

---

From the Memphis Veterans Administration Hospital and Division of Dermatology, Department of Medicine, The University of Tennessee, Memphis, Tennessee, and the Department of Dermatology and Pathology, New York Medical College–Metropolitan Hospital, New York City, NY.

Supported in part by a Medical Investigatorship Award of the Veterans Administration Career Development Program.

Accepted for publication Apr 10, 1972.

Address reprint requests to Dr. Ken Hashimoto, Medical Investigator, Veterans Administration Hospital, 1030 Jefferson Ave, Memphis, Tenn 38104.

new finding emphasizes the relationship between immunoglobulin and amyloid. However, from our previous observations,[1-3] this concept is not easily accepted for primary skin amyloidoses, such as the lichenoid and macular varieties, for the following reasons: a) in these conditions, patients are otherwise healthy and, by currently available methods, no immunologic abnormality can be detected; b) there are no plasma cells and lymphoid cells in the skin lesions. Perivascular spaces are devoid of amyloid, and large amyloid depositions are often avascular.

In this present study, typical lesions of macular amyloidosis[3,6] and lichen amyloidosus[1,2] were biopsied. After 2, 6, 12 and 16 weeks each lesion was biopsied again. The original biopsies were taken to confirm the diagnosis. Rebiopsies were taken from the sites of previous biopsies to determine: a) the rate at which amyloid reappears, b) whether fibroblasts that have migrated in from the surrounding lesion produce amyloid *de novo,* c) where the initial deposition of amyloid occurs and d) whether the epidermis is required for the new synthesis of amyloid. This experiment was thus designed for the *in vivo* cell culture of amyloid fibroblasts in an environment similar to the surrounding lesion and to observe the progression of amyloidogenesis from the very beginning.

Clinical Material

Patient 1

BM, a 55-year-old Puerto Rican man, had typical lesions of macular amyloidosis over the upper back, shoulders and extensor surfaces of the upper and lower extremities. He was in excellent health, and all laboratory studies, including plasma electrophoresis for serum proteins, were within normal limits. Two biopsies were taken from the upper and lower back on April 5, 1971. Two weeks later (April 19) the biopsy site of the upper back lesion, and 4 weeks later (May 3) the biopsy site of the lower back lesion were rebiopsied. In addition, scar formed in the site of diagnostic biopsy performed on January 25, 1971 was obtained on April 19, 1971. This specimen will be referred to as a 12-week specimen. All specimens were examined for amyloid with Congo red and crystal violet stains and with the electron microscope; the original biopsy of the 12-week specimen was not examined with the electron microscope.

Patient 2

MR, a 53-year-old Puerto Rican man with osteoarthritis and mild diabetes mellitus, had typical lesions of macular amyloidosis in the pretibial areas, lateral aspects of the legs and the lateral and anterior thighs. In addition, there were poorly defined pigmented macules on the lateral portions of the upper arms. All laboratory tests including plasma electrophoresis were normal. Two biopsies were taken from the left thigh on April 5, 1971. Two weeks later (April 19), one of the two biopsied lesions was rebiopsied. In 4 weeks (May 3), the other one was rebiopsied. In addition, a 16-week-old scar formed in the lesion originally biopsied for diagnostic purposes was rebiopsied. The original biopsy was examined with Congo red and crystal violet stains but not with the electron microscope. All other specimens were examined by both histochemical and electron microscopic methods.

Patient 3

AS, a 36-year-old Puerto Rican woman, was seen for pruritic eruptions of approximately 2 to 4 mm diameter that she had had for several years on her extremities. A dark brown pigmentation covered the involved area. The clinical picture was typical of lichen amyloidosus. The results of a physical examination and routine laboratory studies were within normal limits except for a slightly elevated serum IgM (Table 1). Punch biopsies of pretibial lesions on both legs on August 23, 1971 disclosed crystal violet-positive amyloid in the dermal papillae. On October 4, 1971, when the biopsy wounds had reepithelialized, each initial biopsy site was rebiopsied. These specimens will be referred to as 6-week specimens. Histologic examination disclosed granulation tissue and dermal fibrosis. Light microscopic examination with crystal violet stain did not demonstrate unequivocal deposits of amyloid in the healing wounds.

In all cases, the initial biopsies were taken with a 6 mm skin punch, and the subsequent rebiopsies were taken from the center of each wound using a 4 mm punch. Serum protein profiles of each patient, obtained with electrophoresis and radial immunodiffusion, are summarized in Table 1.

Results

Original Biopsies

Amyloid deposition was seen mainly in the papillary dermis, with some deposits in contact with the basal lamina of the epidermis (Figure 1). The deposits extended down to the upper reticular dermis (Figure 1). Amyloid was not diffusely infiltrating, rather, it formed islands similar to those of collagen (Figure 1). Some of the amyloid islands had electron-dense centers and relatively electron-light peripheries (Figures 2 and 3). Each island was composed of fine filaments measuring about 60 to 100 Å and of amorphous substance filling the

Table 1—Serum Protein Analysis

	Patient 1	Patient 2	Patient 3	Normal
Albumin	64	61	60	53–65
α_1	1	1	2	2.5–5.0
α_2	5	5	8	7–13
β	8	10	12	8–14
γ	19	21	17	12–22
IgG	950	630	500	900–1500
IgA	280	800	400	167–409
IgM	90	94	180	61–109

Values for albumin and its fractions expressed as per cent
Values for immunoglobulins expressed as mg%

spaces between the filaments (Figure 3). In some islands, relatively thin collagen fibrils were admixed (Figures 2 and 3); these fibrils were often surrounded with electron-lucent halos (Figure 3). Fibroblasts in the lesion showed dilated cisternae of rough endoplasmic reticulum, budding of peripheral cytoplasm and pinched off buds. No amyloid deposition was found in the perivascular spaces. Only a small number of elastic fibers were found. Elastotic fibers which are seen in actinic elastosis were not observed.

Rebiopsies at Two Weeks

Granulation contained numerous fibroblasts, macrophages and the other usual components of fresh granulation tissue. Collagen fibrils were irregular and smaller in size than normal. Amyloid deposits were seen only in completely reepithelialized wounds as small globular masses of moderate electron density lying in close association with fibroblasts (Figure 4). In many instances they were continuous with the basal lamina of the epidermis. On high magnification, these deposits were resolved into an admixture of variously sized filaments and electron-dense amorphous substances. They were found either independently or between collagen fibrils (Figure 5). Observing various degrees of development of amyloid islands, the following account of amyloid *maturation* seemed to be justified: Within the amorphous material, typical amyloid filaments measuring 60 to 100 Å emerge (Figure 5). As individual masses of initial amyloid islands grew, they often merged to produce larger masses. When the deposition was initiated between collagen fibrils, a growing mass of amyloid eventually embedded the collagen (Figure 6). The histologic changes were similar to those observed in the original biopsies, in which various numbers of collagen fibrils were admixed with amyloid (compare Figure 6 with Figure 3). Newly formed elastic fibers were often associated with amyloid (Figure 7). Fibroblasts in regenerating lesions showed accentuation of the characteristics observed in the original biopsies—*ie,* well-developed endoplasmic reticulum and pinching off of the peripheral cytoplasm. Amorphous, dense substance and fine filaments similar to those found in the presumed foci of extracellular amyloidogenesis were also found within or in close relation to the rough-surfaced endoplasmic reticulum of fibroblasts (Figure 8). Some of these accumulations were discharged into the extracellular spaces (Figure 8).

Perivascular spaces lacked precipitation of amyloid, although fine amorphous substances were increased in these spaces (Figure 9).

Nonepithelialized wounds contained active granulation tissue but no amyloid. The fibroblasts migrated very close to the fibrin-covered surface of the wound and contained amorphous material within the dilated rough-surfaced endoplasmic reticulum, but they were not associated with amyloid or its dense precursor material. No plasma cells were encountered in any specimen. Phagocytes contained melanosomes but no amyloid.

Rebiopsies at Four Weeks.

In completely epithelialized wounds, amyloid deposits were larger in size and number than those observed in the specimens taken at 2 weeks. Amorphous, dense matrix substances diminished, and filamentous components became more prominent. Admixture of collagen fibrils in amyloid islands was also observed. The nonepithelialized specimen did not contain any amyloid (Figure 10). In both epithelialized and nonepithelialized specimens, collagen fibrils became more mature; they were larger and more regular in size and stained more densely than those in the 2-week specimens. Elastic fibers were present, although their numbers were small. Active fibroblasts were still abundant, and no plasma cells were found. No increase of phagocytes was seen. Perivascular spaces were devoid of amyloid.

Rebiopsies at Six, Twelve and Sixteen Weeks.

All specimens were completely covered with regenerated epidermis. In the epithelialized specimens from Patients 1 and 2, the tendencies observed in 4-week-old specimens became more pronounced; amyloid islands became larger in size and number and the filamentous component increased at the expense of the amorphous component. Admixed collagen fibrils were observed. Thus, the observed states were close to those of the original biopsies of nonmanipulated lesions.

The 6-week specimens from Patient 3, the case of lichen amyloidosus, showed features described for 2-week biopsies from Patients 1 and 2 (macular amyloidosis). A small deposition of a chiefly amorphous component of amyloid was seen in the upper dermis and in connection with the basal lamina (Figure 11). Intracellular accumulations of amyloid precursor substances appeared similar to those described for Patients 1 and 2. In addition, some fibroblasts contained large accumulations of very fine filamentous material (Figure 11), some of which lay in close relation to the rough-surfaced endoplasmic reticulum (Figure 12). Actual discharge of this material, either by simple extrusion or concomitant with cellular disintegration, was observed in many fibroblasts (Figure 11). After discharge, this material seemed to admix with ground substance, but crystallization of amyloid filaments within such admixture had not occurred in the specimen examined.

Crystal violet-stain did not detect *intracellular amyloid* in any specimen studied.

Discussion

This investigation took advantage of easy access to the skin lesions of a well-established entity of cutaneous amyloidosis. Under direct observation, the second biopsies could be obtained from the exact sites of the initial biopsies. Since in our patients there is no known systemic involvement or immunologic abnormality, we observed a purely local phenomenon of amyloidogenesis limited to the skin. Three observations made in this investigation seem to be significant:

First, amyloid was reproduced in a close association with active fibroblasts in an absolute absence of plasma cells. The cell demonstrated in Figures 4, 10, 11 was the most common type found in the granulation tissue. It has elongated configuration, numerous peripheral villi and dilated, rough endoplasmic reticulum filled with medium electron-dense substances. By all criteria, this type of cell is identifiable as a dermal fibroblast [13] and referable to no other cell types, including the plasma cell. Plasma cells should have been recognized easily if present, since they have a round configuration, an eccentrically located round nucleus with cartwheel-like chromatin concentration along the periphery of the nucleus and numerous, but flat, rough endoplasmic reticulum.[14] It may be possible that these cells, which we called *fibroblasts* with all justification, produce γ-globulin or its precursors. γ-Globulin, however, is not commonly described as fibrous or filamentous, although it may be transformed into fibrous material after being processed in phagocytes.[12] In the granulation tissue, phagocytes were observed, but they mainly contained melanosomes.

The medium electron-dense substance of fibroblasts as shown in Figures 8 and 11 is present within or in close relation to the rough-surfaced endoplasmic reticulum. They may represent precursor proteins for amyloid.

Secondly, the very initial stage of amyloidogenesis could be observed. The rate of wound healing was so variable from one individual to another that the stage of amyloid maturation did not necessarily correlate with the time sequence; for example, in Patient 3, what we believed to be the first stage—*ie,* the discharge of proteinaceous material from fibroblasts could still be observed in the 6-week biopsy, whereas in the other 2 patients this phenomenon was already in progress in 2-week biopsies. However, when the time-sequenced biopsies from the same individuals were reviewed carefully, a sequence of events could be reconstructed as follows: a) production of medium electron-dense or proteinaceous material in the fibroblasts, b) discharge of the same material and c) precipitation of amorphous and filamentous amyloid substance within and in the vicinity of the discharged material. If one reviews Figures 8, 11, 4, 5 and 6 in this order, the sequence of amyloidogenesis as described above can be illustrated.

Admixture of collagen fibrils in certain amyloid islands may be the result of either nonspecific involvement of collagen in the amyloidogenesis, preferential (at least initially) precipitation of amyloid precursors on or as intercollagenous microfilaments (Figure 6) or *de novo* polymerization of collagen within the medium electron-dense substance discharged from fibroblasts. The third postulate presumes that this substance contains precursor proteins for collagen as well as for amyloid and emphasizes a close relationship between the two. In this respect, deposition of amyloid in islands very similar to collagen islands seems to be significant. This feature has been emphasized in our previous publications [1-3] and can be seen in Figure 1. Amyloid precipitation in the vicinity of newly developing elastic fibers is interesting in this respect because elastic fibers and collagen share certain precursor proteins.

Thirdly, the observation that amyloid was absent in the specimens which lacked the covering epidermis suggested the importance of the epidermal factor for the production of amyloid in purely cutaneous forms of amyloidoses. In the classic histopathology, lichen amyloidosus has been described by Lever: [15] "The amyloid deposits are much smaller in size than those found in primary systemic amyloidosis and are limited almost entirely to the subepidermal region of the dermis." This observation has been verified by electron microscopic observations: Small accumulation of amyloid is always present, not only in direct contact with the basal lamina (Figure 11) but often in the intercellular spaces of the epidermis.[2] The subepidermal region of the dermis is the site where the dermal–epidermal interaction occurs. In this region, relatively immature thin collagen fibrils—*ie, reticulum fibers,* and amorphous and microfilamentous intercollagenous material are abundant; collagenase activity is high;[16] and in actinic elastosis this region is spared. In lamprey skin, this region has 25 to 30 layers of special collagen in alternate lamellations, each lamella at 90 degrees to the adjacent one.[17] It may be postulated that collagen precursor excreted in this region by the fibroblasts mature under the influence of the epidermis into special fibrils, which may be constantly modulated by collagenase and other enzymes. In amyloid formation in the lichenoid and macular varieties of cutaneous amyloidoses, this modulating mechanism by the epidermis may also be necessary. Furthermore, the material contributed by the epidermis may be abnormal and induce abnormal fibrils—*ie*, amyloid. In the study of purified amyloid from spleens and livers of primary and secondary amyloidoses, Harada *et al*[17] reported recently that the amyloid proteins differed from patient to patient in molecular weight, in amino acid composition and in the presence or absence of specific tryptic peptides; amyloid proteins from the liver and spleen of the same individual were identical. They also noted occasional significant differences in the morphology of isolated amyloid filaments obtained from different patients. So far, no attempt has been made to analyze the amino acid composition of amyloid in lichenoid or macular amyloidoses. It is possible that amyloid in the purely cutaneous form of amyloidoses is different from that in the systemic amyloidoses.

The works of Harada *et al*[18] and Glenner *et al*[11,19] showed that there is a striking chemical similarity between amyloid proteins and the amino terminal variable fragment of the light and heavy chains of immunoglobulin proteins. These findings are interesting, but, as discussed in the introduction, are not necessarily compatible with the clinical and ultrastructural observations reported in our previous and the present studies. If an excess of light chain γ-globulin is produced by plasma cells[12] in the bone marrow, lymph nodes, spleen, etc, carried to the skin, and processed by phagocytes into amyloid,[12] the most likely site of amyloid deposition is the perivascular spaces where potential phagocytes—ie, perivascular histiocytes, abound. In cutaneous xanthoma, for example, the perivascular phagocytes first take up plasma lipid.[20] In Fabry's disease, deposition of the abnormal substance, ceramidetrihexoside, is predominantly in the vascular endothelial cells and perivascular phagocytes.[21] As demonstrated in our previous works[1-3] as well as in the present study, perivascular spaces of the old and reproduced lesions of the macular and lichenoid varieties of cutaneous amyloidoses are remarkably free from amyloid deposition. One may argue that in an old lesion the perivascular amyloid had been reabsorbed. Amyloid deposition in macular and lichenoid amyloidoses is, however, usually permanent.

References

1. Hashimoto K, Gross BG, Lever WF: Lichen amyloidosus. Histochemical and electron microscopic studies. J Invest Dermatol 45:204–219, 1965
2. Hashimoto K, Onn LLY: Lichen amyloidosus. Electron microscopic study of a typical case and a review. Arch Dermatol (In press)
3. Brownstein MH, Hashimoto K: Macular amyloidosis: Clinical, histochemical and electron microscopic features.
4. Cohen AS: Amyloidosis. N Engl J Med 277:522–530, 1967
5. Shirahama T, Cohen AS: Structure of amyloid fibrils after negative staining and high-resolution electron microscopy. Nature 206:737–738, 1965
6. Black MM, Wilson-Jones E: Macular amyloidosis: a study of 21 cases with special reference to the role of the epidermis in its histogenesis. Br J Dermatol 84:199–209, 1971
7. Ebner H: Licht-und elektronmikroskopische Untersuchungen uber das Amyloid der Haut. Z Haut Geschlechtskr 43:833–852, 1968
8. Rodermund OE, Klingmuller G: Zur submikroskopische Struktur des Amyloid. Arch Klin Exp Dermatol 236:147–160, 1970
9. Rodermund OE, Klingmuller G: Zur elektronenmikroskopischen Struktur des Lichen amyloidosus. Arch Klin Exp Dermatol 237:110–114, 1970
10. Schapiro L, Kurban AK, Azar HA: Lichen amyloidosus. Arch Pathol 90:499–508, 1970
11. Glenner GG, Terry W, Harada M, Isersky C, Page D: Amyloid fibril proteins: proof of homology with immunoglobulin light chains by sequence analyses. Science 172:1150–1151, 1971
12. Glenner GG, Ein D, Eanes ED, Bladen HA, Terry W, Page DL: Creation of "amyloid" fibrils from Bence Jones proteins *in vitro*. Science 174:712–714, 1971
13. Hashimoto K: Fibroblast, collagen and elastin. Ultrastructure of the Normal and Abnormal Skin. Edited by HS Zelickson. Philadelphia, Lea and Febiger, pp 228–260, 1967
14. Lentz TL: Cell Fine Structure. An Atlas of Drawings of Whole-Cell Structure. Philadelphia, W.B. Saunders Co, pp 50–51, 1971
15. Lever WF: Histopathology of the Skin. Fourth edition. Philadelphia, J.B. Lippincott Co, p 421, 1967
16. Eisen AZ: Human skin collagenase: localization and distribution in normal human skin. J Invest Derm 52:442, 1969
17. Porter KR: Cell fine structure and biosynthesis of intercellular macromolecules. Connective Tissue: Intercellular Macromolecules. Boston, Little, Brown and Company, pp 167–169, 1964
18. Harada M, Isersky C, Cuatrecasas P, Page D, Bladen HA, Eanes ED, Keiser HR, Glenner GG: Human Amyloid protein: chemical variability and homogeneity. J Histochem Cytochem 19:1–15, 1971
19. Glenner GG, Page D, Isersky C, Harada M, Cuatrecasas P, Eanes ED, Delellis RA, Bladen HA, Keiser HR: Murine amyloid fibril protein: isolation, purification and characterization. Science 19:16–27, 1971
20. Parker F, Short JM: Xanthomatosis associated with hyperlipoproteinemia. J Invest Dermatol 55:71–88, 1970
21. Hashimoto K, Lever WF: Angiokeratoma corporis diffusum (Fabry). Histochemical and electron microscopic studies. J Invest Dermatol 44:119–128, 1965

Fig 1—A low magnification view of the subepidermal deposition of amyloid in islands (**A**) similar to those of collagen (**C**). Contact of amyloid with the epidermal basal lamina indicated by *; *E* = epidermis, *f* = fibroblast (Patient 1, original biopsy, × 4250).

Fig 2—Three amyloid islands. Each island is composed of an electron-dense core (*A*) with admixed collagen fibrils (seen as electron-light dots) and a relatively electron-light periphery. Notice an increased amount of intercollagenous substance (c), some of which merge into the rims of amyloid islands (*arrows*). Scattered fragments (*) of fibroblasts are seen (Patient 1, original biopsy, × 9000).

Fig 3—Enlargement of amyloid islands. Dense core and light rim is shown on the left. In the right photograph, the electron-light rim is absent. The dense core portion contains numerous intact (*arrows*) and degenerated (*empty spaces*) collagen fibrils whose diameters are, on average, much smaller than those of the normal fibrils (*C*). Amyloid filaments (*arrowheads*) meausre 60 to 100 Å in width and are typically straight and nonanastomising. A cytoplastic process or debris from a fibroblast (*f*) is very closely associated with amyloid islands (Patient 2, original biopsy; left × 47,500, right ×74,450).

Fig 4—Rebiopsied lesion. Papillary dermis covered with regenerated epidermis (*E*) shows small islands of collagen which are less densely stained than those of the original biopsies (see Figure 1). There are several small depositions of amyloid (*). Four of them are found in close relation to the fibroblasts (*F*). *m* = melanocyte (Patient 1, 2-week specimen, × 6550). **Insert**—Enlargement of one of the fibroblast-associated amyloid islands. Arrow indicates half desmosome-like attachment of amyloid to the fibroblast (× 14, 800).

Fig 5—Various stages of amyloid formation are seen within an amorphous matrix of high electron density (Patient 2, 2-week specimen, × 57,500).

Fig 6—Various ratios of admixture of collagen and amyloid are seen in newly developing amyloid islands. Islands 1, 2 and 3 appear to be in early stages of development. As amyloid component increases (islands 4, 5 and 6), collagen fibrils become widely separated or degenerate. Islands 4, 5, and 6 thus resemble some of those of the original biopsy shown in Figure 3 (Patient 1, 2-week specimen, × 28,625).

Fig 7—Newly produced elastic fiber (*E*) in the granulation tissue is closely associated with amorphous (*A*) and filamentous (*) components of amyloid (Patient 1, 2-week specimen, × 62,500).

Fig 8—Intracellular accumulations of medium dense substance (*arrows*) are seen in close association with roughsurfaced endoplastic reticulum (*Er*) of three different fibroblasts. Discharge of this material is illustrated in the lower photograph. *C* = collagen fiber (Patient 1, 2-week specimen; upper, × 50,000, middle, × 79,600, lower, × 75,000).

Fig 9—An arteriole in the regenerating lesion is surrounded with a thick band of amorphous material (*), but no accumulation is seen. *C* = collagen, *E* = endothelial cell, *m* = smooth cell (Patient 1, 2-week specimen, × 3400).

Fig 10—Nonepithelialized surface of the wound is covered with fibrin (*), erythrocytes (*e*) and loosely knit collagen. A fibroblast (*F*) has well-developed, rough-surfaced endoplastic reticulum. No amyloid deposition is seen (Patient 2, 4-week specimen, × 6460).

Fig 11—In the upper dermis of the reepithelialized (*E*) lesion several fibroblasts are producing medium dense, proteinaceous substance within the rough endopasmic reticulum (*hollow arrow*). Some of the larger products are being excreted (*solid arrows*). Excreted materials are seen in the extracellular spaces (*). Chiefly amorphous amyloid substance (*a*) is being deposited in several places. One deposit is attached to the basal lamina (*b*), **Insert** shows enlargement of the deposit attached to the basal lamina (Patient 3, 16-week specimen. × 5000; Insert; × 75,000).

Fig 12—High magnification of medium electron-dense intracytoplasmic material reveals fine filaments in it (*arrows*). *Re* = rough-surfaced endoplasmic reticulum (Patient 3, 16-week specimen, × 140,000).

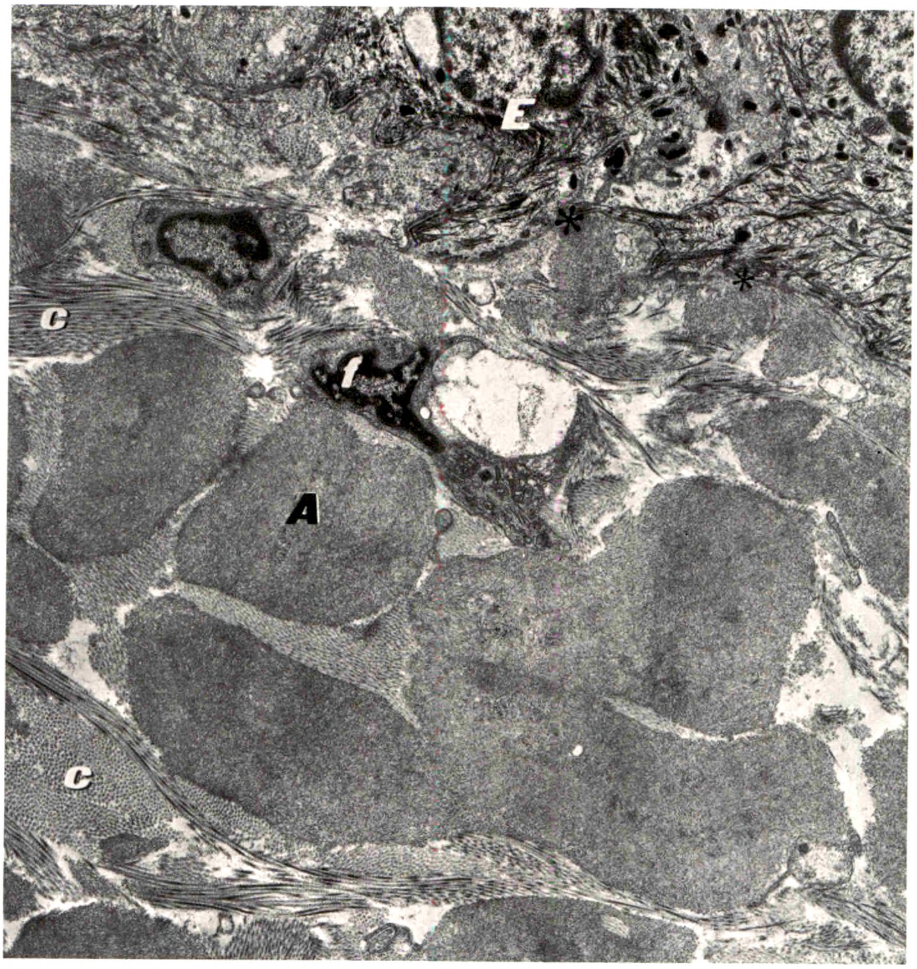

1

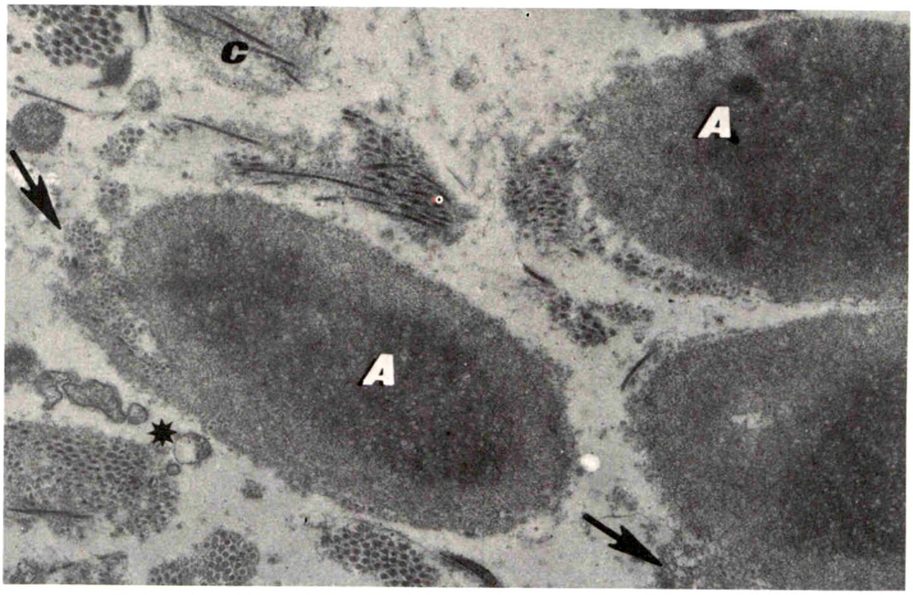

2

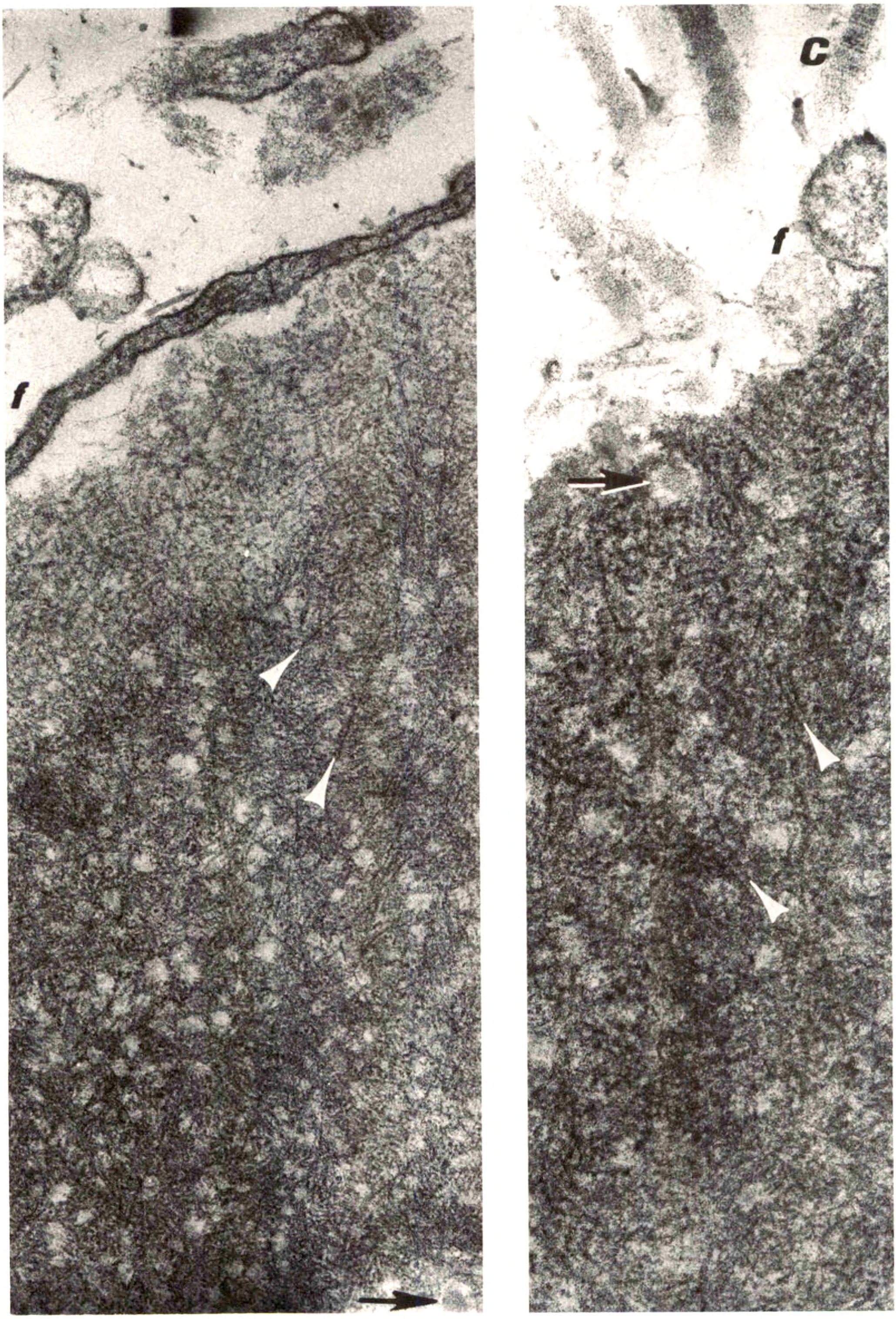
f
c
f

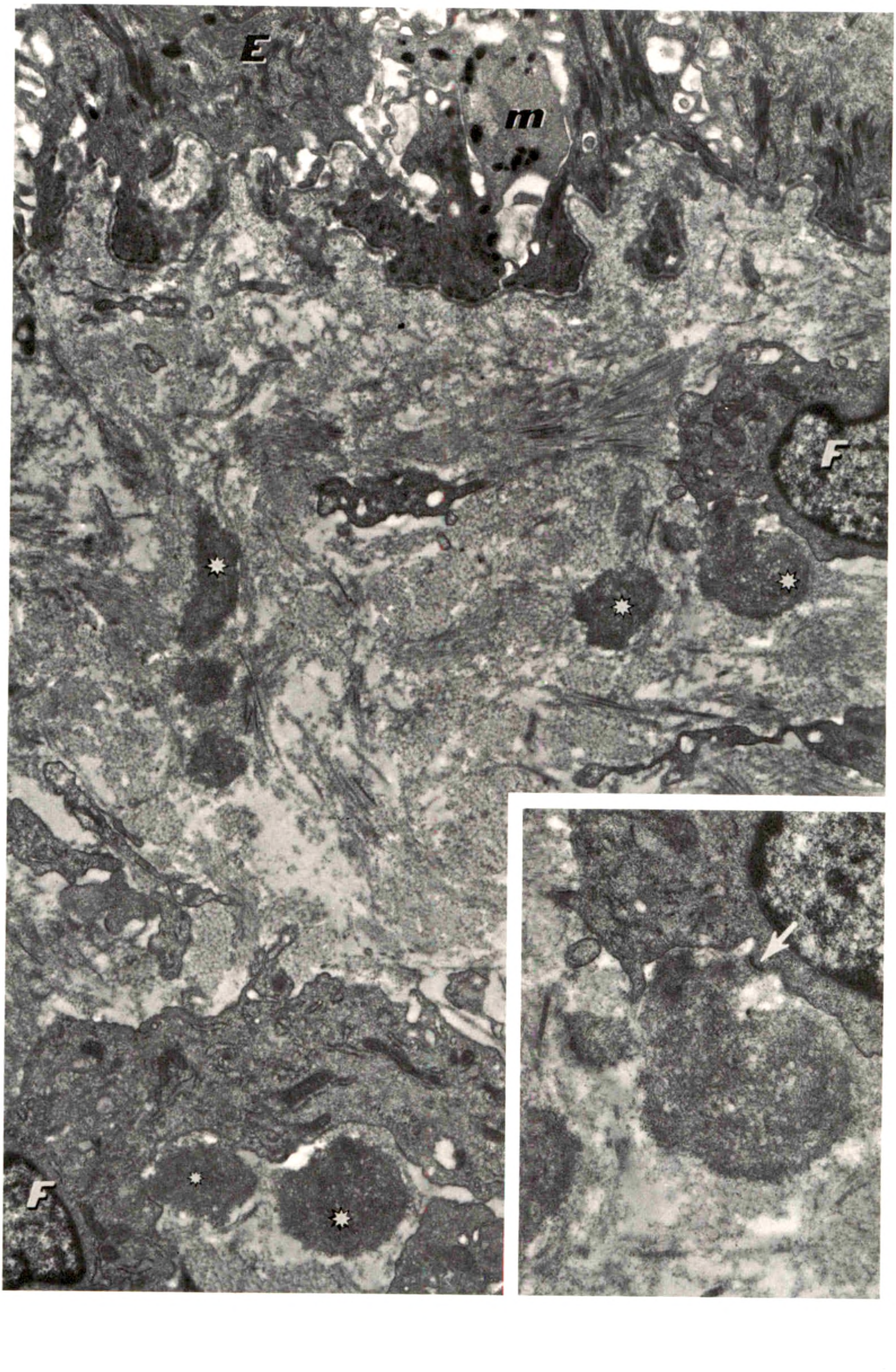

4

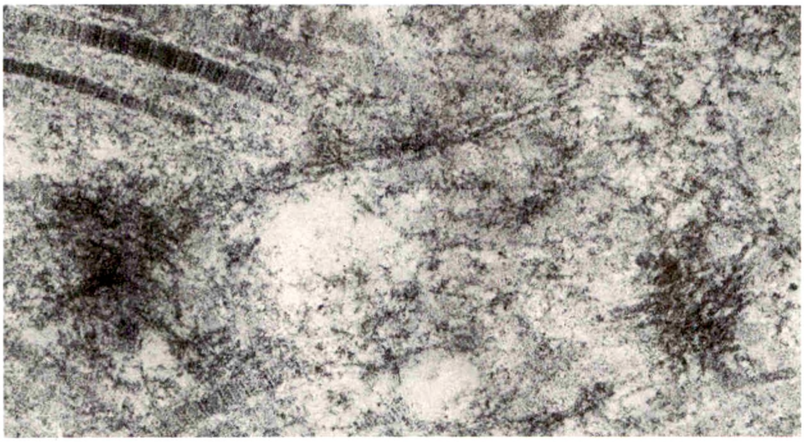

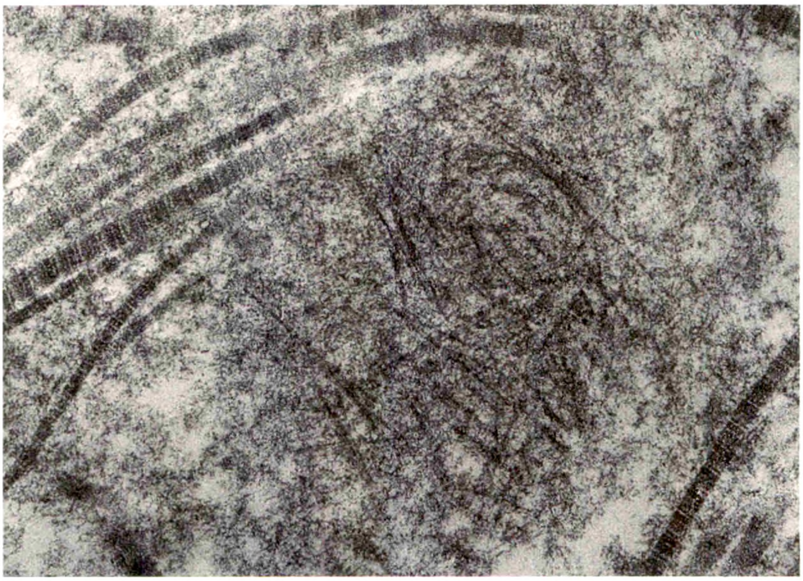

5

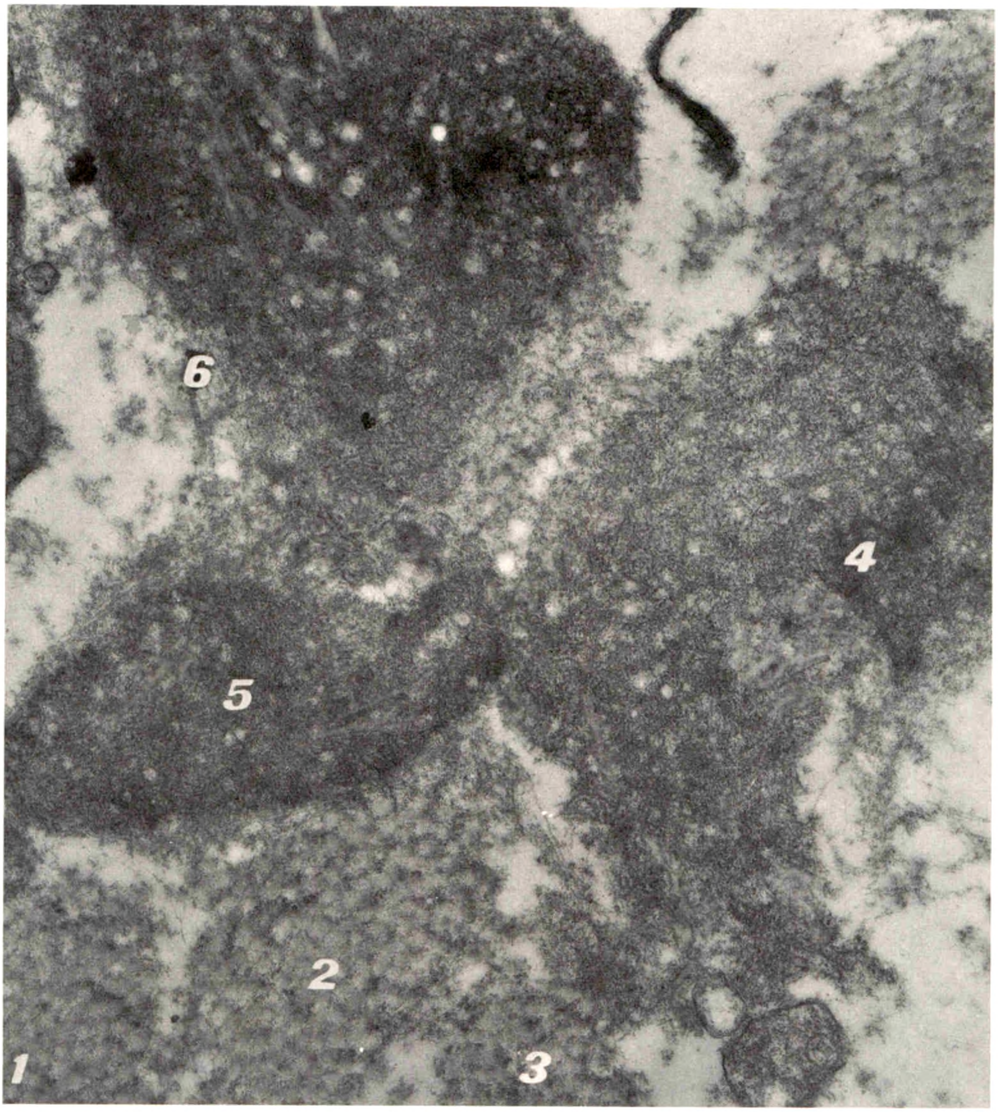

6

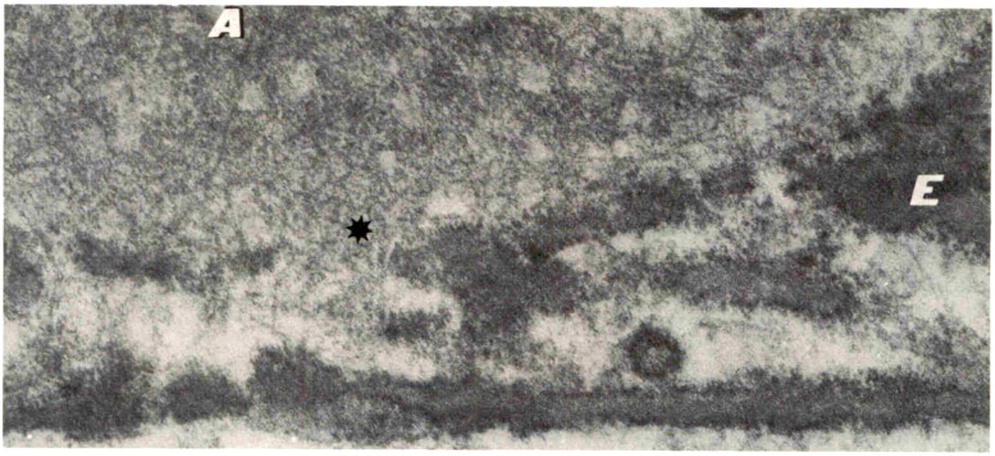

7

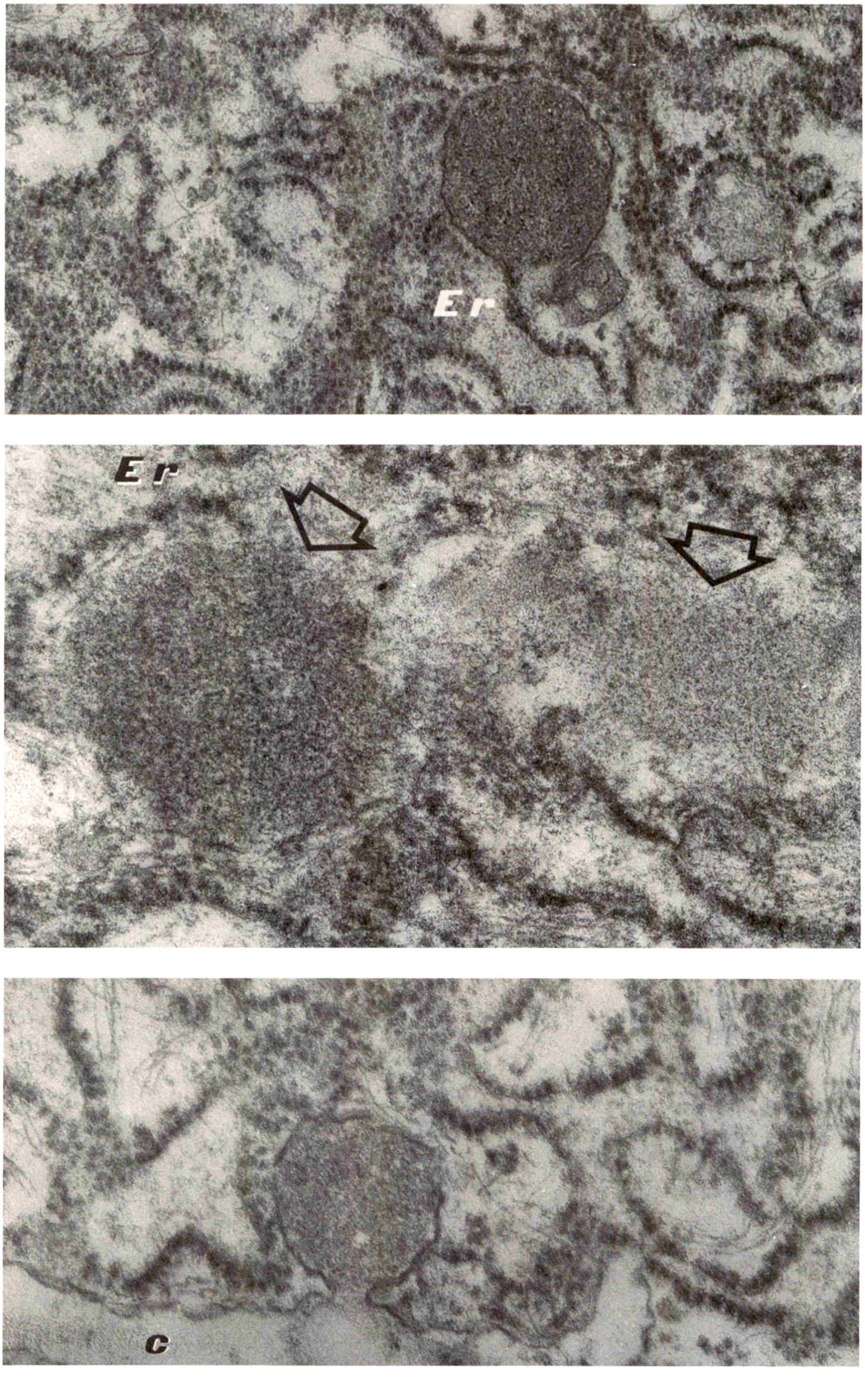

8

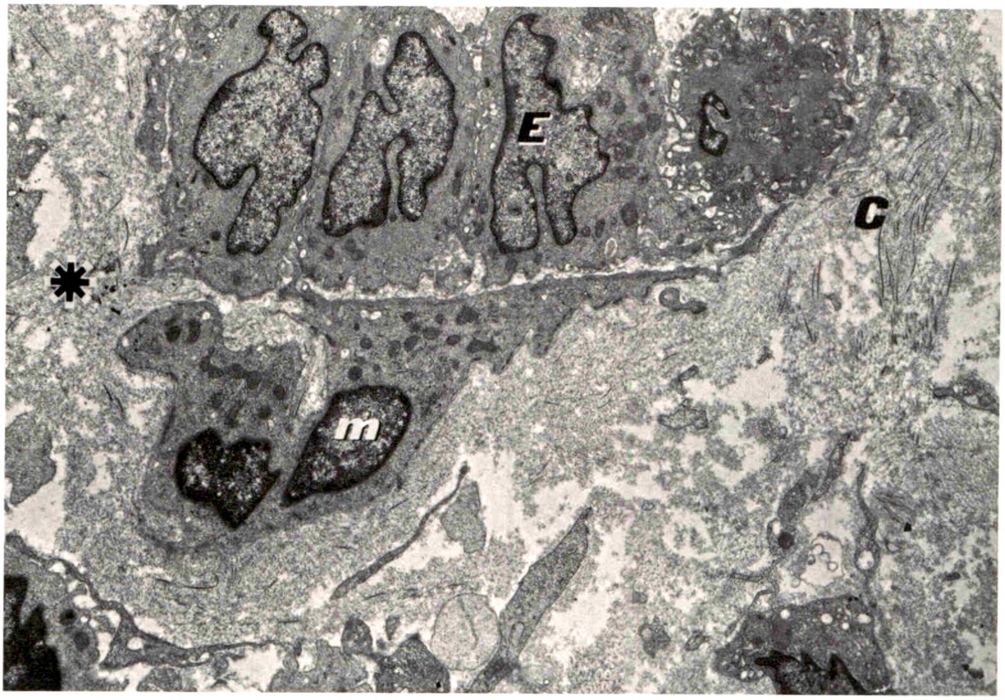

9

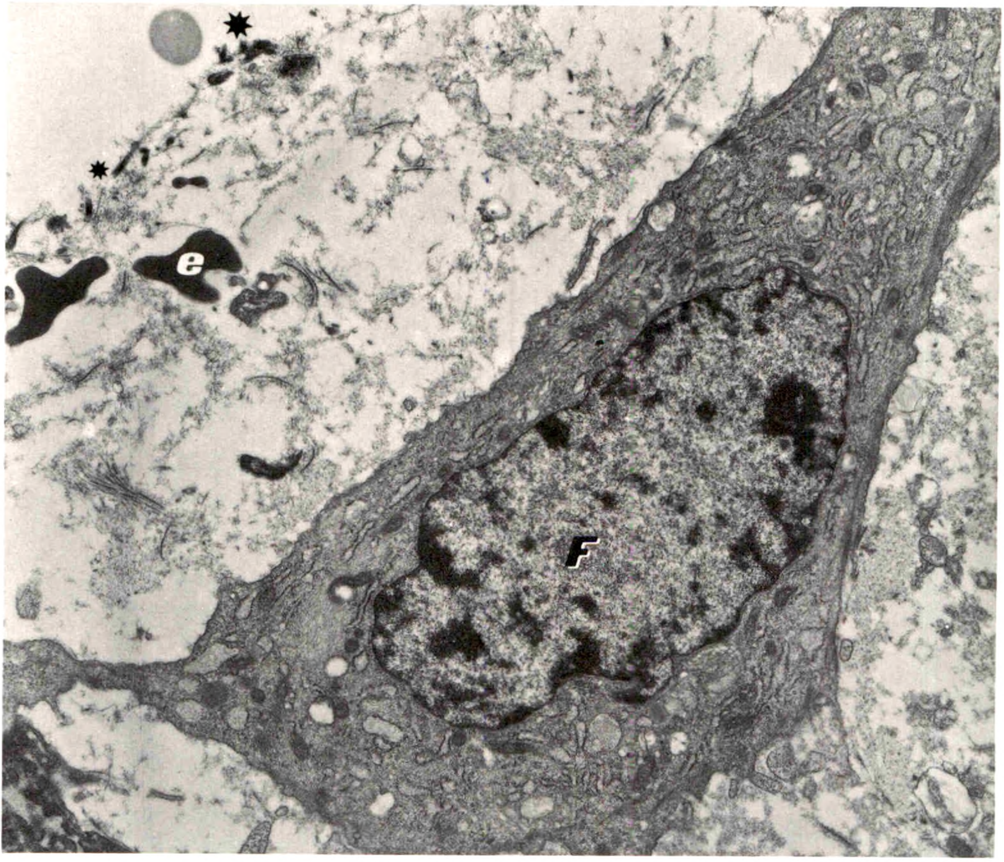

10

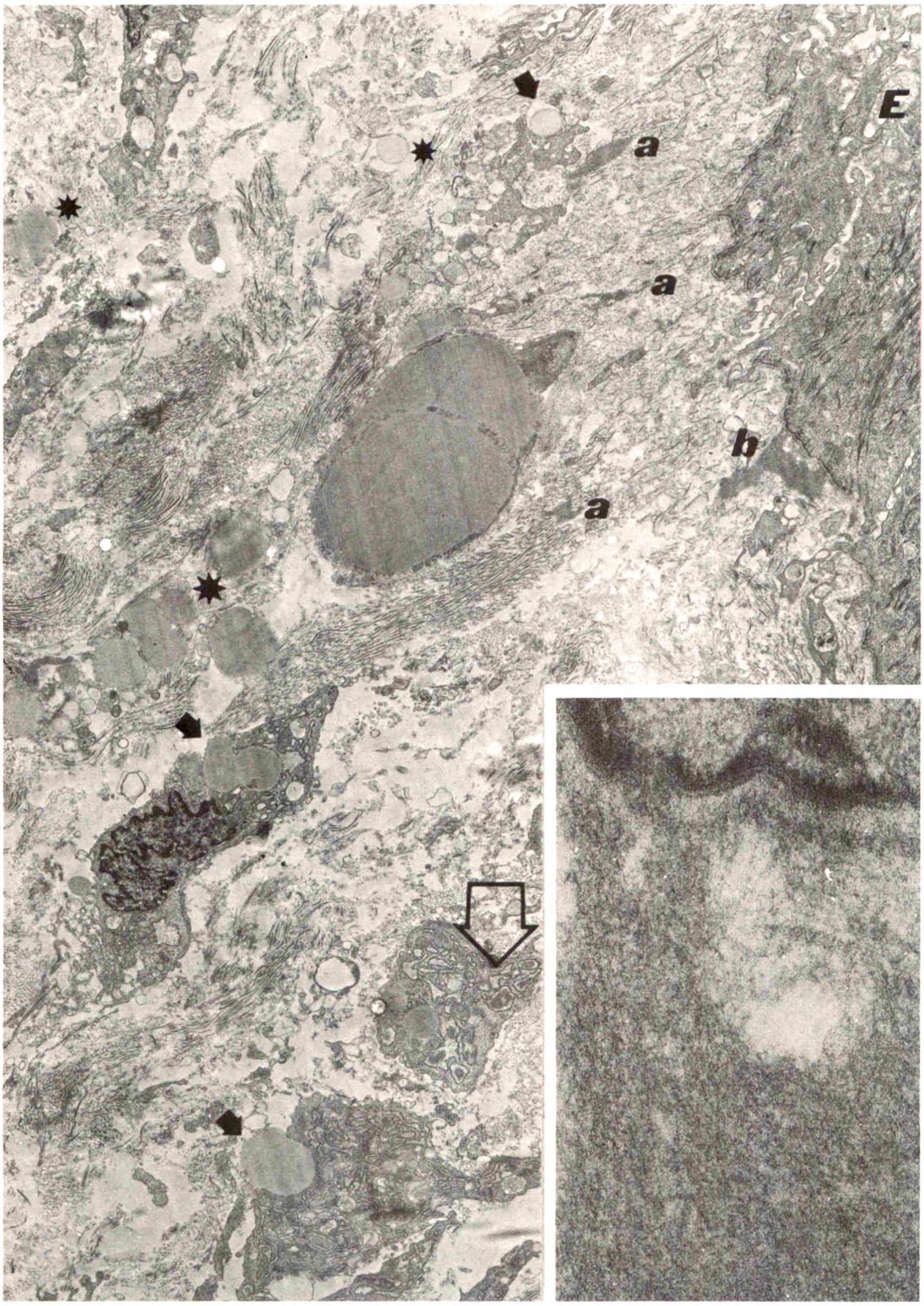
E
a
a
b
a

12

Chemical and Histochemical Studies of Glomerular Sialoprotein in Nephrotoxic Nephritis in Rats

Jane Chiu, MB and Keith N. Drummond, MD, CM, FRCP(C)

Glomerular sialoprotein (GSP) in nephrotoxic nephritis (NTN) rats was studied by chemical and histochemical methods at 1 to 2 hours, 48 hours, 10 days and 16 days after the induction of the disease by intravenous injection of rabbit antiserum to whole rat glomeruli. Histochemically, GSP was demonstrated by the CI and AB 8 GX stains. After the specimen was taken for histologic studies, the glomeruli from the kidneys of each rat were isolated by differential seiving and centrifugation. Quantitative determination of the glomerular sialic acid content from each rat was done using a combination of the chromatographic method of Svennerholm and the thiobarbituric acid assay of Warren. In normal rats the GSP is seen on the epithelial aspect of the glomerular basement membrane (GBM). Within 1 to 2 hours after induction of NTN, disruption of the normal membranous distribution of GSP and its dispersion into the mesangial space or the epithelial cytoplasm was noted. Reduction in the amount of staining was also observed after 48 hours. These changes increased in severity as the histologic lesions progressed. A quantitative decrease in glomerular sialic acid became apparent 10 days after the onset of NTN and was still observed at 16 days. Since GSP is situated at the filtration barrier site and is considered a major component of the glomerular antigenic structure, its changes in NTN suggest that it may play an important role in the pathogenesis of this disease and in the alteration of GBM permeability (Am J Pathol 68:391–406, 1972).

ALTHOUGH OVER A CENTURY has passed since Ludwig[1] suggested that the glomerular capillaries function as a mechanical filter in the formation of urine, the precise regulatory mechanisms of glomerular permeability remain as yet poorly understood. Hall[2] and Rhodin[3] suggested that the slit pores between the epithelial foot processes were the site of regulation for the filtration of small molecules; they also believed that the basement membrane—which they considered a hydrated gel-like substance—and the fenestrated endothelium played some role in the regulation of filtration. The studies of Farquhar *et al*[4] using ferritin (MW = 462,000) suggested that the basement membrane proper was the major barrier to filtration. Graham and Karnovsky,[5] using human myeloperoxidase, showed that

---

From the Department of Nephrology, McGill University—Children's Hospital Research Institute, Montreal, Quebec, Canada.

Supported by Term Grant MT-1579 from the Medical Research Council of Canada.
Accepted for publication Apr 10, 1972.

Address reprint requests to Dr. K. N. Drummond, Director, Department of Nephrology, McGill University—Montreal Children's Hospital Research Institute, 2300 Tupper St, Montreal 25, Quebec, Canada.

the barrier for substances of molecular weight from 160,000 to 180,000 was the site of the epithelial slit.

Recently, considerable interest has been focused on the polysaccharide-rich material, the so-called glycocalyx, which coats the surface of many cells from different sources in the animal kingdom.[6-8] In the renal glomerulus this material covers the foot processes of the visceral epithelial cells and fills the space between the podocytes.[9,10] Various names have been used for this carbohydrate-rich protein, including glomerular sialoprotein (GSP),[10] glomerular polyanion,[11] and glomerular mucosubstance.[9] The GSP contains sialic acid and its histochemical staining properties are believed to be directly related to the presence of sialic acid.[12] Insofar as can be shown by histochemical technics, the parietal epithelial cells and the endothelial cells contain only sparse amounts of GSP; none is present in the glomerular basement membrane (GBM) proper.[9,10] It should be noted, however, that most authors consider that the GBM does contain a certain amount of sialic acid; the failure to demonstrate sialic acid in the GBM by histochemical technics for GSP suggests that the sialic acid is in a different form here than is the case in the GSP. The demonstration of GSP [8-10] at the site of the filtration barrier proposed by Graham and Karnovsky raises the interesting possibility that this material may play a role in the regulation of membrane permeability. It has also been suggested [13] that GSP may have specific antigenetic properties which render it important in the pathogenesis of certain forms of immunologic injury to the kidney. In this regard it is of interest that we have observed by histochemical technics striking changes in the quantity and distribution of GSP in patients with acute poststreptococcal glomerulonephritis,[14] a condition which is generally accepted to be due to the deposition of antigen–antibody complexes along the glomerular capillary basement membrane.[15]

The present study was designed to investigate the changes in GSP at different stages of nephrotoxic serum nephritis (NTN) in rats. Histochemical studies of the quantity and distribution of GSP and chemical studies of the glomerular sialic acid content were done.

The results show reduction and redistribution of GSP at all stages studied and an absolute decrease in glomerular sialic acid content beginning at about the tenth day following induction of NTN.

Materials and Materials

Hooded male rats weighing 140 to 200 g were used. NTN was induced by the intravenous injection of 1.2 ml of rabbit antiserum against rat glomeruli.

The antiserum was prepared by injecting adult albino rabbits with an emulsion of equal parts of complete Freund's adjuvant (Difco Laboratories Inc, Detroit, Mich) and sonically vibrated whole rat glomeruli in a saline suspension. The rat glomerular suspension was prepared in the same manner as in the present study and the purity was over 95%. Prior to injection the antiserum was decomplemented by heating it at 56 C for 1 hour; it was then repeatedly adsorbed with rat red blood cells. Control animals received the same volume of normal rabbit serum similarly processed; normal animals who received no injections were also studied. Twenty-four hour urine collections from each rat were obtained for protein determination prior to the injection of antisera and again before sacrifice.

The following experimental groups and their respective controls were studied following injection of nephrotoxic serum at the times indicated:

Group 1: 1–2 hours—11 experimental and 5 control animals
Group 2: 48 hours—19 experimental and no control animals
Group 3: 10 days—23 experimental and 24 control animals
Group 4: 16 days—15 experimental and 8 control animals

Twenty normal animals were also studied. In some of the groups not all animals had a chemical determination of the glomerular sialic acid content as is indicated in Table 2. The animals were anesthetized by intraperitoneal injection of pentobarbital sodium; the kidneys were then perfused with cold normal saline until blanched, using a catheter placed in the aorta. A piece (2 × 5 mm) of 1 kidney from each rat was then taken for histochemical and histologic studies and the remaining kidney tissue was processed as described below for the quantitative determination of glomerular sialic acid.

The tissue specimen was fixed in precooled 2% buffered glutaraldehyde at pH 7.4 and imbedded in paraffin. Three μ sections were stained with hemalum phloxine saffron (HPS), periodic acid-Schiff (PAS), colloidal iron (CI) at pH 1.8,[12] and Alcian Blue 8 GX (AB) at pH 2.6[12] with 0.5% picric acid as counterstain. Specificity of the CI and AB staining for the sialic acid-containing moiety of the GSP was established by abolition of positive staining after prior incubation of the section with *Vibrio cholerae* neuraminidase. This method for confirming the specificity of the stain has been described by others.[9–11] A further control for the specificity of the stain was done by staining slides with potassium ferrocyanide without previously using CI; these sections were uniformly negative. Each of the specimen slides was coded and studied blindly by both authors. There were 50 to 100 glomeruli on each slide. The nature and extent of the pathologic changes were graded on a scale of 0 to 4+ (normal to severe); particular attention was paid in the histochemical studies to the intensity and amount of staining and to the distribution of the GSP within the glomerulus.

For sialic acid content determination, glomeruli were isolated using a modification of the method of Krakower and Greenspon.[16] The cortical tissue was minced into small pieces using a razor blade and gently buttered through a 150 mesh stainless steel sieve. The mash was collected and suspended in cold normal saline and centrifuged at 90*g* for 90 seconds. The supernatant was discarded and the sediment was gently washed through a 180 mesh stainless steel sieve with cold normal saline. The fluid collected was centrifuged at 90*g* for 90 seconds and the supernatant discarded. This was repeated 6 times; after the last centrifugation the infranatant was resuspended in cold distilled water and centrifuged at 1,150*g* for 10 minutes. The material obtained from this final centrifugation consisted of a very pure preparation of glomeruli: less than 5%

contamination by tubular fragments was noted when the glomeruli and the tubular fragments were counted under the light microscope. The glomerular preparation obtained from each rat was divided into 2 portions and each was vacuum dried and weighed. The glomerular sialic acid content was determined by a modification of the methods of Svennerholm [17] and Warren [18] following hydrolysis of the glomeruli with 0.1 N sulphuric acid at 80 C for 1 hour. Using this method, the recovery rate of chemically pure sialic acid in our hands was between 90 and 92%.

The 24-hour urine was obtained by placing the rat in a metabolic cage; water was provided *ad libitum* but food was withheld. The protein content of the urine was determined by a modified sulfosalicylic acid method.[19] In animals sacrificed at 1 to 2 hours after injection of nephrotoxic serum, the urine protein concentration was determined by a dipstick method wherever possible, using a specimen obtained by bladder puncture or voided at the time of sacrifice.

Results

Urinary Protein Excretion

The mean 24-hour urinary protein excretion in 78 normal rats was 2.11 mg (Table 1). In each of the experimental groups the 24-hour protein excretion was markedly elevated. Measurement of the 24-hour urine protein excretion was not possible in Group 1; however, in most of the animals in which urine was available at the time of sacrifice, the urine protein concentration was above 100 mg%. The diagnosis of nephritis was confirmed histologically in each of the animals even when documentation of proteinuria was not possible.

Glomerular Sialic Acid Content

There was no significant difference in glomerular sialic acid content between Groups 1 and 2 and their respective controls and the normal rats (Table 2). There was however a significant decrease in

Table 1—24-Hour Urine Protein (mg/24 hr)

		48 hours	10 days		16 days	
	Normal	Experimental group	Experimental group	Control group	Experimental group	Control group
No. animals	78*	10	18	21	14	8
Mean	2.1	55.1	59.0	2.77	40.5	3.8
SE	0.20	16.08	8.43	0.42	11.99	0.67
P†	—	<0.001	<0.001	>0.1	<0.001	0.02 > **P** > 0.01

* this includes the specimens obtained in the experimental groups before injection of serum

† using Student's **t** test each group was compared with the normal values

Table 2—Glomerular Sialic Acid Content

		1-2 hours		48 hours	10 days		16 days	
	Normal	Experimental group	Control group	Experimental group	Experimental group	Control group	Experimental group	Control group
No. animals	13	9	5	17	18	21	14	8
Mean	10.67	11.16	11.97	10.59	6.53	10.08	7.62	9.74
SE	0.69	0.30	0.30	0.25	0.64	0.36	0.25	0.51
P*	—	>0.6	>0.2	>0.9	<0.001	>0.4	<0.001	>0.3

* using Student's **t** test each group was compared with the normal values

glomerular sialic acid content in Groups 3 and 4 (the 10 and 16 day groups, respectively), when compared with their controls and with the normal animals. The mean values in the normal and control animals were 9.74 to 10.97 μg/mg dried glomeruli and the values in Groups 1 and 2 were 11.16 and 10.59 μg/mg. The values in the 10 and 16 day groups were 6.53 and 7.62 μg/mg, respectively; these differences from the normal and control animals are highly significant ($P < 0.001$). The 24-hour protein excretion was comparable in each of the experimental groups and no relation was seen between the 24-hour protein excretion and the reduction in glomerular sialic acid content, as shown in Text-figure 1.

Pathologic and Histochemical Findings

Using the CI stain in normal rat glomeruli, the GSP appears as a granular blue line distributed along the GBM with occasional staining of epithelial cytoplasm or mesangium. When AB was used the GSP appeared as an uninterrupted, smooth bluish green line with the same distribution. Although it was not possible by light microscopy to establish the precise location of the GSP within the glomerulus our observations about its localization are consistent with those reported by previous authors using both light and electron microscopy. By routine light microscopy the glomerular capillary loops in normal animals were open, the GBM was clearly seen and there were occasional islands of normal mesangial tissue (Figures 1–8).

Within 2 hours of induction of NTN (Group 1) routine light microscopy showed marked polymorphonuclear leukocyte infiltration with mesangial edema and reduction in the number of open capillary loops. Histochemical studies for GSP showed that the normal linear distribution was disrupted and the GSP was dispersed. We were

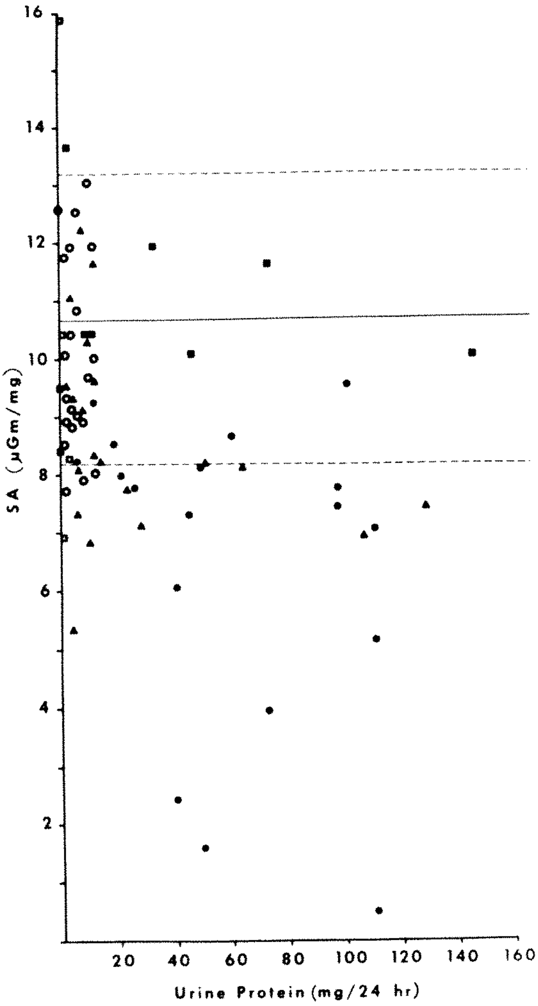

TEXT-FIG 1—Relation between glomerular sialoprotein content and 24-hour urine protein excretion in the period just prior to sacrifice. Note that there is no apparent relation between them. The horizontal lines indicate the mean normal glomerular sialoprotein content ±SD; note that the values for the 10 and 16 day experimental groups are low. Legend: Normal (*open square*); 48 hour experimental group (*solid square*); 10 day control group (*open circle*); 10 day experimental group (*solid circle*); 16 day control group (*open triangle*); 16 day experimental group (*solid triangle*).

unable by light microscopy to establish with certainty the exact location of this material however it seemed to be located in the mesangial region or in the epithelial cytoplasm. By 48 hours (Group 2) the polymorphonuclear leukocyte infiltration was less pronounced and mesangial tissue increase was present. Histochemically, there was, in addition to these changes, an apparent reduction in the total staining. By 10 days (Group 3) the HPS and PAS stains showed further increase in mesangial tissue with focal increase in the thickness of the GBM. An accentuation of the previously described findings for GSP was also seen in this group. Similar changes were also seen in Group 4. It should be pointed out that the reduction of staining for GSP was not confined to the areas of mesangial proliferation; there were numerous open capillary loops around whose periphery it was not possible to detect positive staining using either the CI or AB stains for GSP. In general there was a correlation between the severity of changes in glomerular morphology as shown by the routine HPS and PAS stains and the alteration in distribution and reduction in quantity of GSP as shown by the histochemical stains. The extent of glomerular damage was clearly more pronounced in Groups 3 and 4; it is in these groups that the histochemical changes were most abnormal as well. As mentioned above, these latter 2 groups also showed a significant reduction in total glomerular sialic acid content. However, it was not possible, in any particular animal, to correlate the severity of changes observed by routine and histochemical study with the total amount of sialic acid measured chemically in the glomeruli of that particular animal.

No changes in routine histology or histochemical staining for GSP from the normal were seen in any of the control animals.

Discussion

Because of the controversy concerning the contribution of cellular contamination to the sialic acid content of GBM[20] we decided to measure the total glomerular sialic acid content as an index of GSP, rather than separate the GBM from the other constituents of the glomerulus. Our study indicates that within several hours of induction of NTN there is a striking change in distribution of GSP within the glomerulus, which is followed by an apparent reduction, at least as measured by histochemical technics, in the total quantity of GSP. These changes were more pronounced in the later stages of the disease and correlated with the severity of changes seen by routine histologic studies. A reduction in total glomerular sialic acid content was not detected until 10 days following induction of NTN, by which time the mean levels had fallen from control values of 10.08 μg/mg to a mean value of 6.53 μg/mg of dried glomeruli. This reduction was still present 16 days following onset of nephritis.

It is of interest that changes in GSP have been seen in acute poststreptococcal glomerulonephritis;[14] there is a striking dispersion of GSP into epithelial cytoplasm during the acute inflammatory stages, with a loss of the normal linear pattern along the outer surface of the membrane. The extent of alteration from the normal GSP pattern correlated with the severity of the histologic changes detected by routine microscopic studies. By 6 weeks after the onset of acute poststreptococcal nephritis, the normal distribution of GSP along the capillary basement membrane has been reestablished. Michael and Blau, using the experimental model of aminonucleoside nephrosis in rats,[11] also showed a reduction in the histochemical staining for GSP and in total glomerular sialic acid content by the time the animals were nephrotic.

Thus it is apparent that changes in GSP may occur in both immunologic renal disease as demonstrated in acute poststreptococcal glomerulonephritis in humans and nephrotoxic serum nephritis in rats, and in aminonucleoside nephrosis which is not considered to result from an immunologic injury to the glomerulus.

There are several possible explanations for the changes observed in our study. It has been suggested that GSP is a major nephritogenic antigen; thus it is possible that nephrotoxic serum could contain specific antibodies to the antigenic determinants of GSP. The binding of the GSP with the antibodies contained in the nephrotoxic serum could lead to a neutralization of the negative charge of the GSP, which is presumably due to the carboxyl groups of the sialic acid; this could diminish the affinity of GSP for both CI and AB stains without affecting the total amount of sialic acid in the glomeruli. Alternatively, the binding of the GSP with antibody could block the binding sites for the AB and CI stains. This also could lead to decreased staining without an absolute reduction in the quantity of glomerular sialic acid. Antibodies to GSP may gain access to this compound on the epithelial side of the membrane by simple penetration of the GBM proper, since the molecular weight of γ-globulin is comparable to that of human myeloperoxidase; this may be facilitated by increased permeability of the GBM induced by the nephrotoxic serum.

As a result of the immunologic injury induced in nephrotoxic nephritis, possibly due to polymorphonuclear leukocyte infiltration, the GSP may be removed from its normal position and redistributed within the glomerulus. Loss of this material into the urine may also occur.

It is also possible that in NTN there is an alteration in the turnover rate of sialic acid which could eventually lead to a reduction in the total glomerular sialic acid content such as was observed in the 10 and 16 day groups, but which was not yet apparent in the earlier experimental groups.

Whether the changes we have observed in GSP and glomerular sialic acid content are of central importance in the pathogenesis of nephrotoxic serum nephritis is not at present clear. However the likelihood that GSP plays an important role in membrane permeability and in the antigenic characteristics of the membrane makes it probable that these findings are an integral part of the pathophysiology of the injury in this condition.

References

1. Ludwig K: Nieren und Harnbereitung. Handworterbuch der Physiologie. Edited by R Wagner. Brunswick, F Vieweg, 1844
2. Hall BV: The protoplasmic basis of glomerular ultrafiltration. Am Heart J 54:1–9, 1957
3. Rhodin J: Electron microscopy of the kidney. Am J Med 24:661–675, 1958
4. Farquhar MG, Wissig SL, Palade GE: Glomerular permeability. I. Ferritin transfer across the normal glomerular capillary wall. J Exp Med 113:47–65, 1961
5. Graham RC Jr, Karnovsky MJ: Glomerular permeability. Ultrastructural, cytochemical studies using peroxidases as protein tracers. J Exp Med 124: 1123–1134, 1966
6. Bennett HS: Morphological aspects of extracellular polysaccharides. J Histochem Cytochem 11:14–23, 1963
7. Ito S: Structure and function of the glycocalyx. Fed Proc 28:12–25, 1969
8. Rambourg A, LeBlond CP: Electron microscope observations on the carbohydrate-rich cell coat present at the surface of cells in the rat. J Cell Biol 32:27–53, 1967
9. Jones DB: Mucosubstances of the glomerulus. Lab Invest 21:119–125, 1969
10. Mohos SC, Skoza L: Glomerular sialoprotein. Science 164:1519–1521, 1969
11. Michael AF, Blau E, Vernier RL: Glomerular polyanion. Lab Invest 23:649–657, 1970
12. Mowry RW: The special value of methods that color both acidic and vicinal hydroxyl groups in the histochemical study of mucins. With revised directions for the colloidal iron stain, the use of Alcian Blue G8X and their combinations with the periodic acid-Schiff reaction. Ann NY Acad Sci 106:402–423, 1963
13. Skoza L, Mohos SC: Nephritogenic antigenicity of chromatographic fractions of trypsin and pronase glomerular digests. Proc Soc Exp Biol Med 131:1189–1193, 1969
14. Drummond KN, Chiu JM: Alterations in glomerular sialoprotein (GSP) during acute poststreptococcal glomerulonephritis (AGN). Presented at the Fourth Annual Meeting of the American Society of Nephrology, November 1970, Washington, DC, p 22 (Abstr)
15. Michael AF Jr, Drummond KN, Good RA, Vernier RL: Acute poststreptococcal glomerulonephritis: Immune deposit disease. J Clin Invest 45:237–248, 1966
16. Krakower CA, Greenspon SA: Localization of the nephrotoxic antigen within the isolated renal glomerulus. AMA Arch Pathol 51:629–639, 1951
17. Svennerholm L: Quantitative estimation of sialic acids. III. An anion exchange resin method. Acta Chemica Scand 12:547–554, 1958
18. Warren L: The thiobarbituric acid assay of sialic acids. J Biol Chem 234:1971–1975, 1959

19. Cipriani A, Brophy DA: Method for detecting cerebral spinal fluid protein by photoelectric colorimeter. J Lab Clin Med 28:1269–1272, 1943

20. Mohos SC, Skoza L: Variations in the sialic acid concentration of glomerular basement membrane preparations obtained by ultrasonic treatment. J Cell Biol 45:450–455, 1970

Acknowledgments

We wish to express our appreciation to Dr. Deirdre Walden-Edward and Dr. Sylvia Lui for their kind advice on methods for sialic acid determination, to Miss Marlyn Smith and Mrs. Jenny French for their expert technical assistance and to Mrs. Audrey Shannon without whose help this project could not have been completed.

Presented in part at the First International Conference on the Glomerular Basement Membrane, Cleveland, Ohio, Oct 1970.

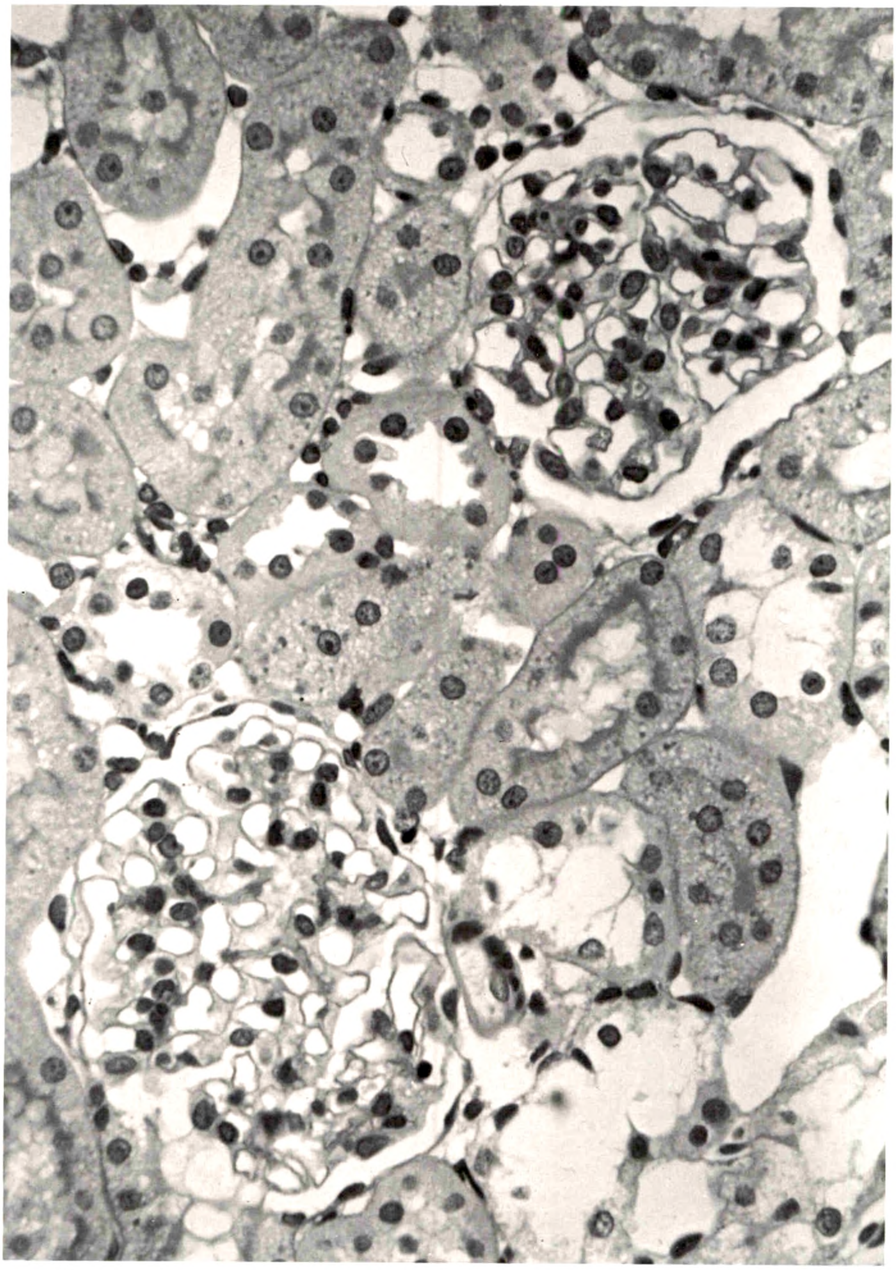

Fig 1—Normal rat glomeruli. Note the number of open capillary loops (PAS, × 700).

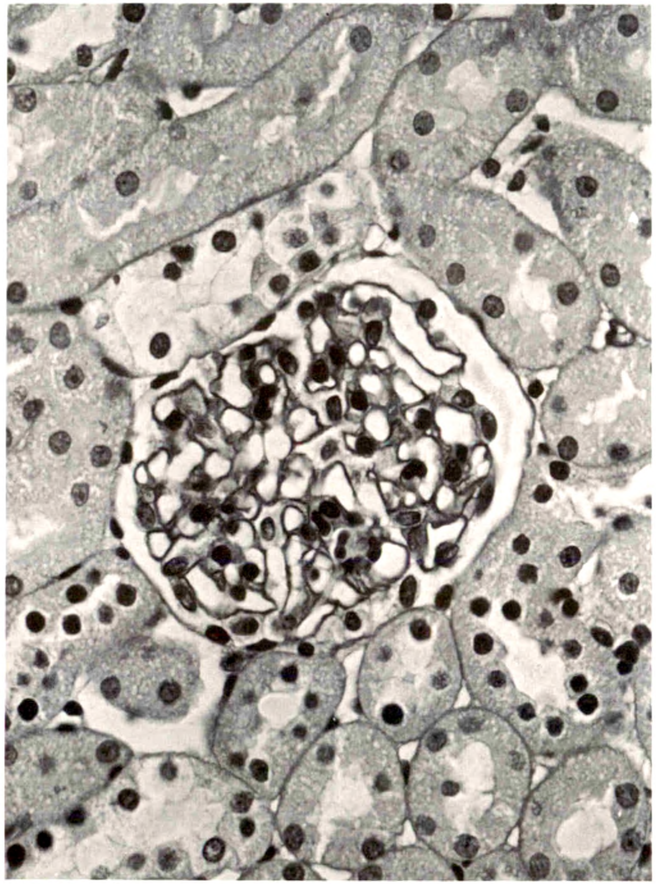

Fig 2—Alcian Blue stain of a normal rat glomerulus. The glomerular sialoprotein which stains greenish blue appears as a dark uninterrupted line along the glomerular basement membrane (× 500).

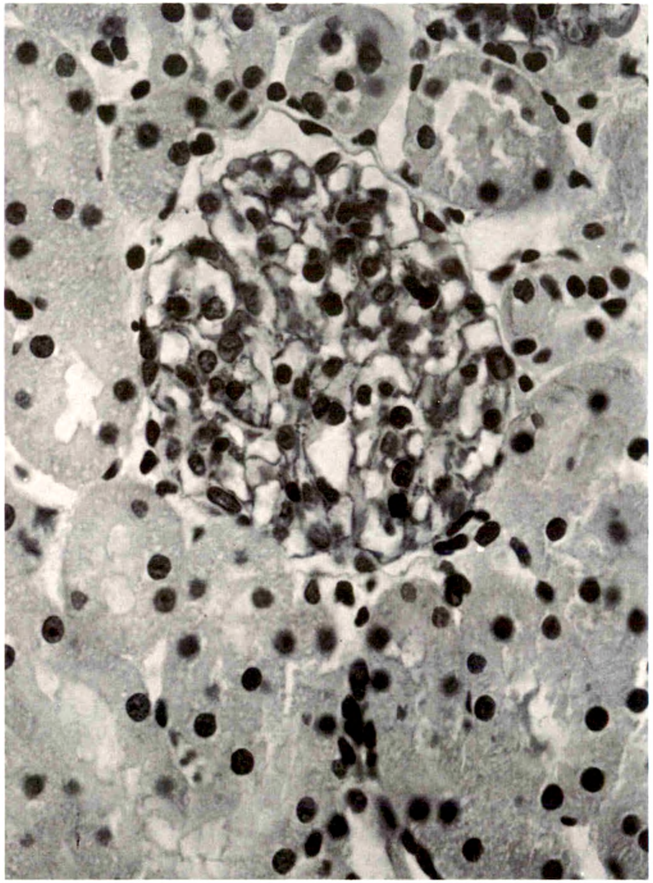

Fig 3—Colloidal iron stain of a normal rat glomerulus. The glomerular sialoprotein appears as a series of dark granular deposits along the glomerular basement membrane (× 600).

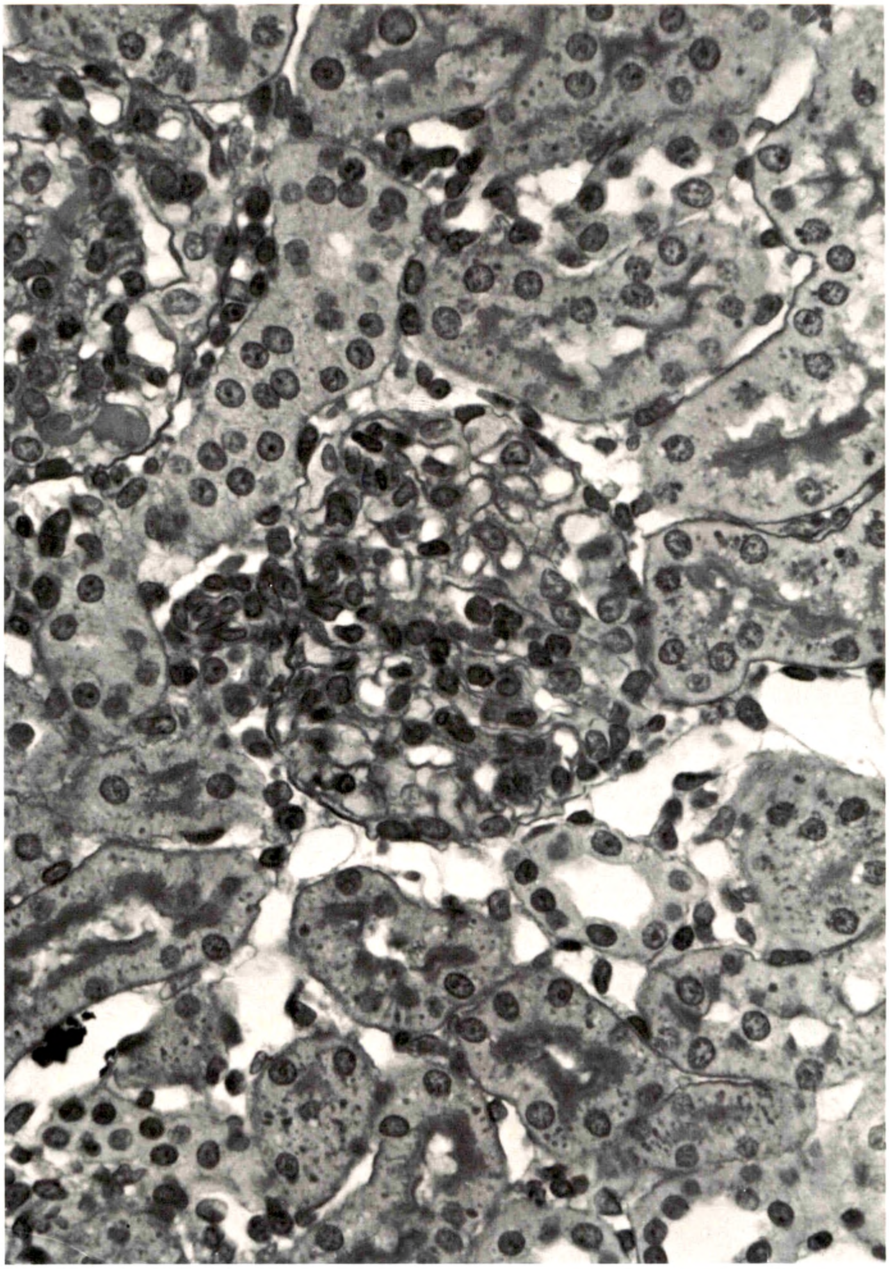

Fig 4—Glomerulus from a rat in the 48 hour experimental group. The number of open capillary loops is decreased and there is an increase in mesangial cells and matrix (PAS, × 700).

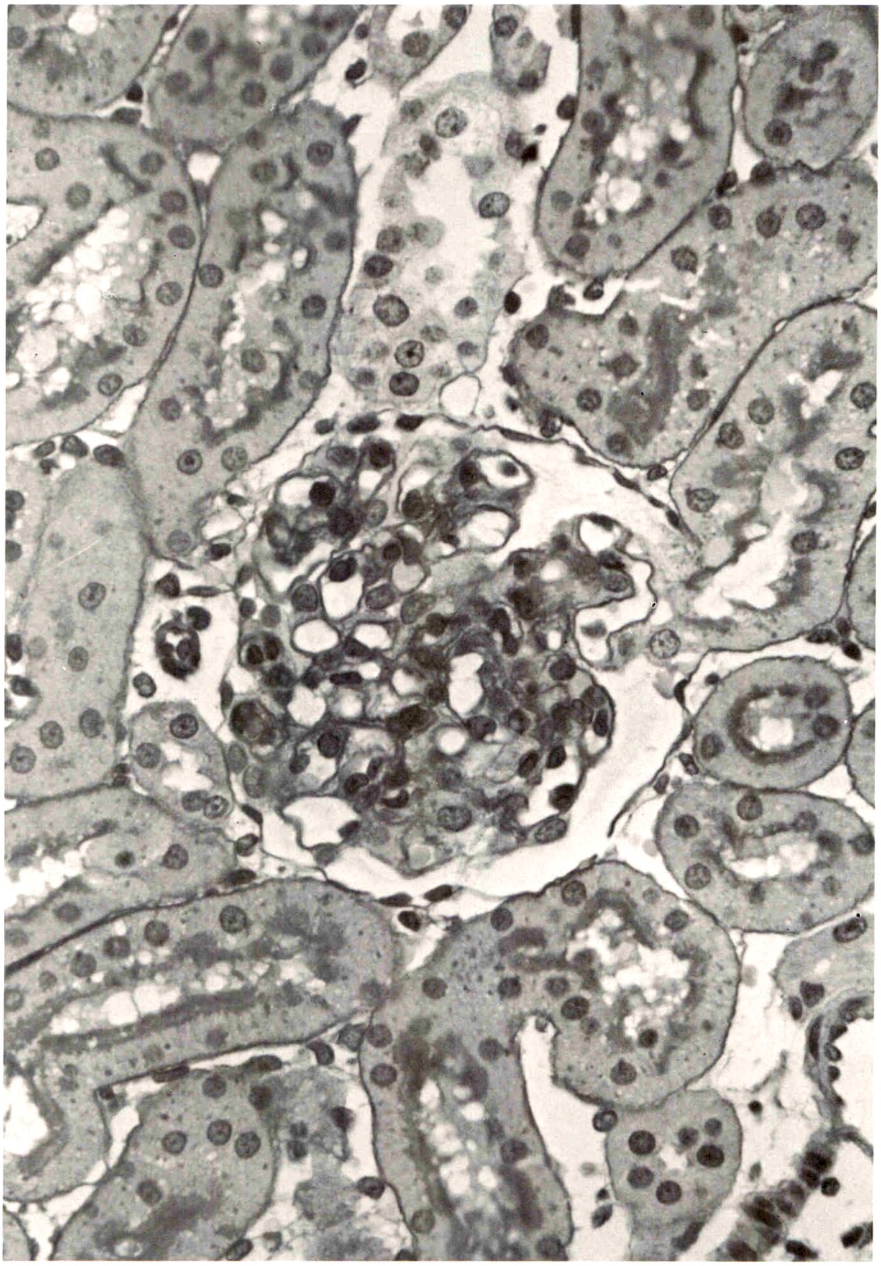

Fig 5—Glomerulus from a rat in the 10 day experimental group. Mesangial matrix is more prominent but the number of nuclei is less than in the 48 hour group. Focal thickening of the glomerular basement membrane is seen (PAS, × 700).

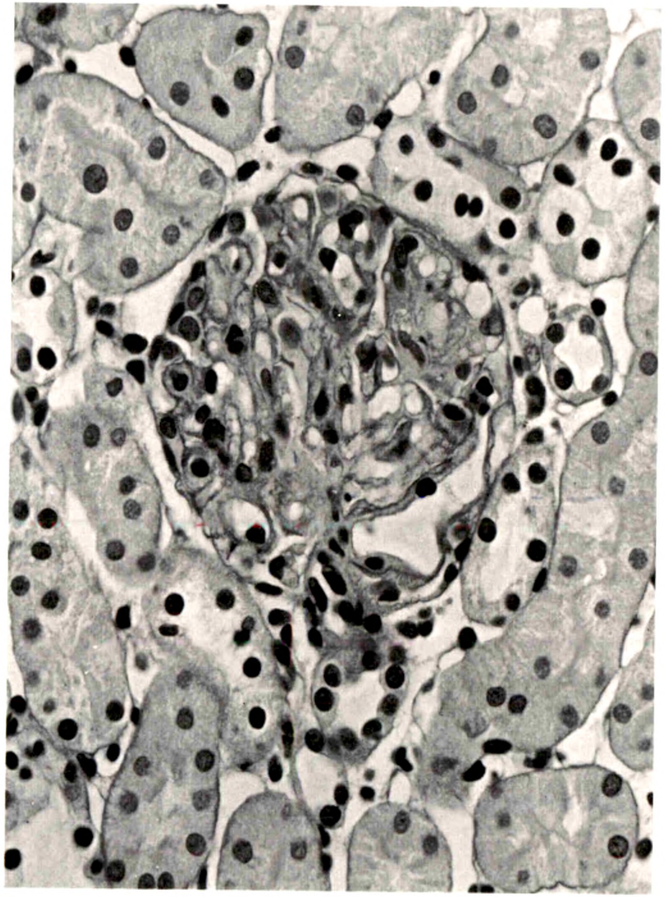

Fig 6—Alcian Blue stain of a glomerulus from a rat in the 10 day experimental group. Note the loss of the normal membrane pattern along most of the capillary loops. Some staining for glomerular sialoprotein is present in the mesangial regions or in the cytoplasm of the epithelial cells (× 500).

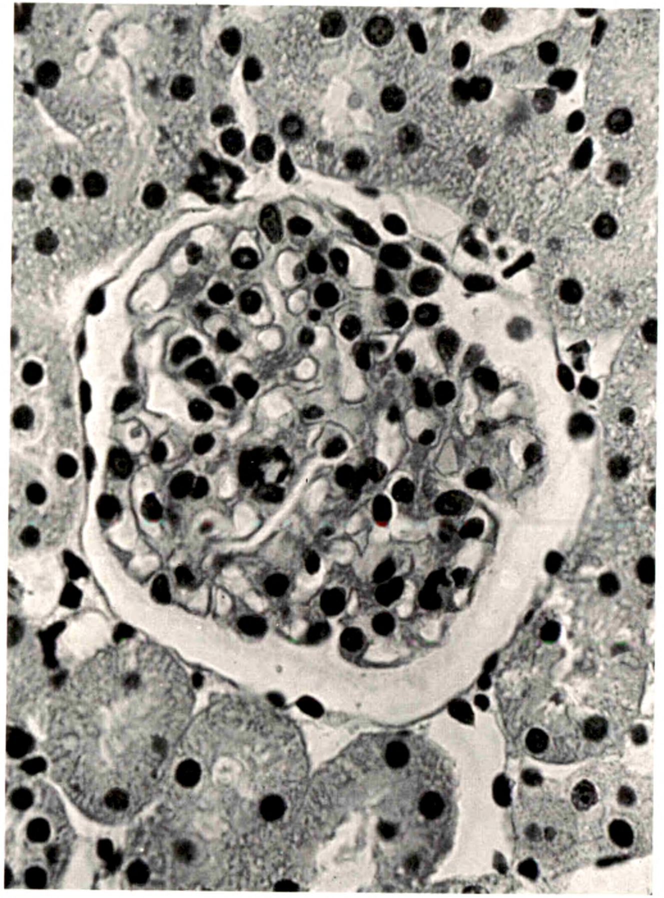

Fig 7—Colloidal iron stain of a glomerulus from a rat in the 10 day experimental group showing loss of the normal pattern of glomerular sialoprotein staining along the glomerular basement membrane. Occasional deposits within the mesangium or in the cytoplasm of the epithelial cells are seen (× 600).

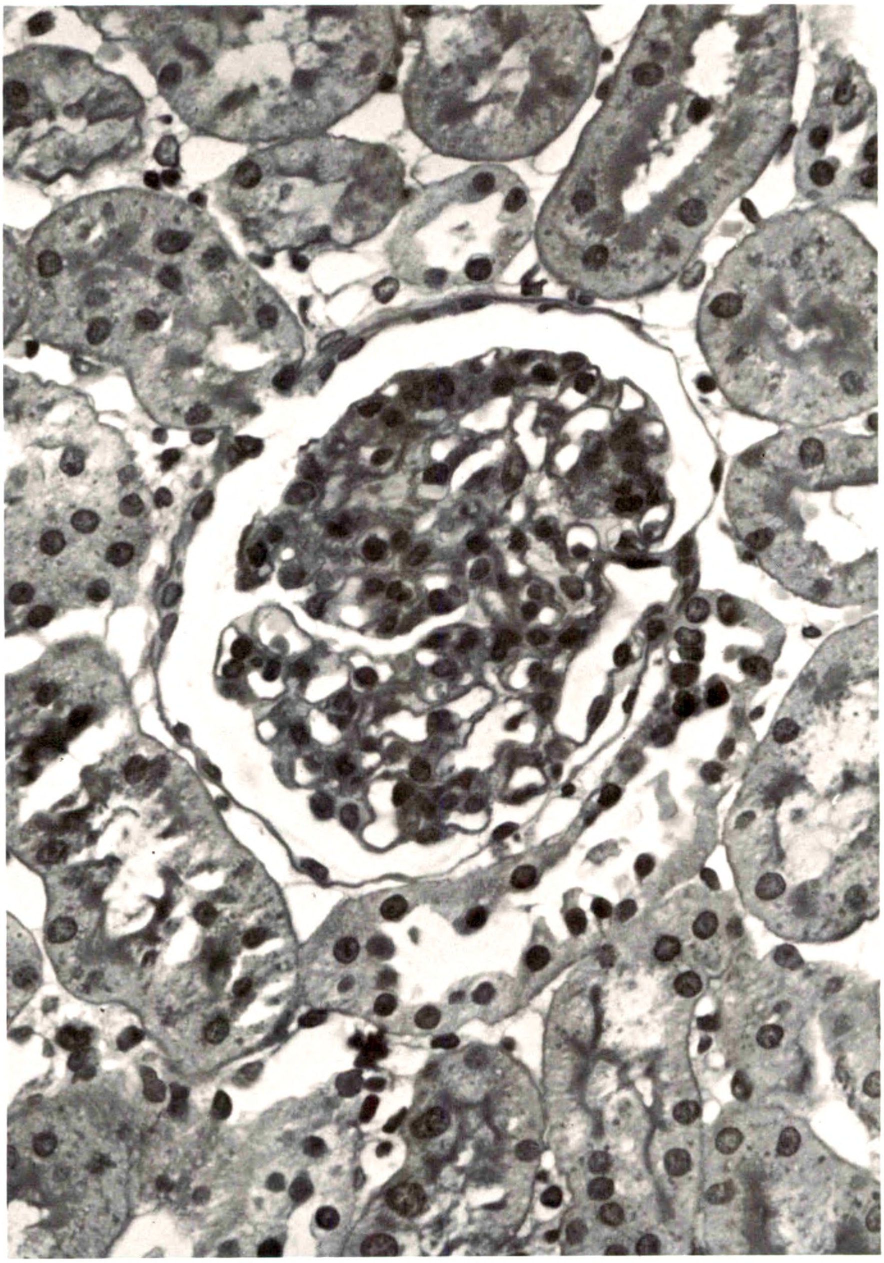

Fig 8—Glomerulus from a rat in the 16 day experimental group. There is a diffuse thickening of the glomerular basement membrane, mesangial proliferation, and reduction in the number of open capillary loops (PAS, × 700).

Mucous Hypersecretion Induced in Isolated Mucociliated Epithelial Cells by a Factor in Heated Serum

B. G. Bang, BA and F. B. Bang, MD

A factor in the serum of the marine coelomate, *Sipunculus nudus*, induced by injecting a mixture of a marine bacterial vibrio and a solution of dried cholera toxin, will, after heating to 85 to 90 C, cause intensive continuous hypersecretion of mucus in isolated free-swimming mucociliated cells from another Sipunculus. The factor, released from coleomic cells into the serum, is heat stable to 90 C, withstands several freeze-thawings, is induced only by specific stimuli, is rapidly released into the serum, persists for different time spans depending on the stimulus, and is not present in normal heated sera. It is proposed that in nature this factor is balanced by a heat labile inhibitory factor. Cholera toxin alone is a feeble stimulus. The marine vibrio alone is a powerful stimulus to mucus secretion but lethal for the host. In combination with cholera toxin, the vibrio is nonlethal (Am J Pathol 68:407–422, 1972).

The URN CELL of the marine coelomate *Sipunculus nudus* is a detached epithelial cell capable of producing excess mucus for defense against disease. The response is selective and seems to be set off by a factor which is released into the serum by the coelomic fluid (blood) cells. The present report describes a method by which hypersecretion of mucus can be consistently produced in urn cells cultured in their own coelomic fluid, in preparations free of all cells except those which produce the mucus.

The role of urn cells in normal and pathologic conditions was described in an extraordinary monograph by Jean Cantacuzène,[1] a Romanian physician whose primary interest was human infectious disease. Metchnikoff had sparked his interest in invertebrate immune responses, an interest which accelerated during successive summers at the Station Biologique at Roscoff; the Breton coast is one of the few places in the world where very low ebb tides allow *S nudus* to be collected in quantities sufficient for experimental study. Since the monograph is not widely available, three of Cantacuzène's experiments

---

From the Station Biologique, Roscoff, Finistère, France and The Johns Hopkins University School of Hygiene and Public Health Baltimore, Md.

Accepted for publication Apr 24, 1972.

Address reprint requests to Mrs. Betsy G. Bang, Research Associate, Department of Pathobiology, Johns Hopkins University School of Hygiene and Public Health, 615 N Wolfe St, Baltimore, Md 21205.

will be summarized, after a brief description of Sipunculus and the cells of its coelomic fluid.

Background

The experimental animal, *Sipunculus nudus*, is one of the few species in the family Sipunculoidea in which mucociliated epithelial cells detach from the coelomic cavity wall and become free-swimming in the fluid—*ie*, free urns as distinct from fixed urns of other sipunculids.[2] S *nudus*, which resembles a giant earthworm, is about 15 cm long and 2 cm in diameter when resting. Its muscular body wall encloses a long coiled gut, gonads, nerves, nephridia and ±20 ml of coelomic fluid in which hemocytes, amebocytes, sex cells, urn cells, and enigmatic vesicles mingle at random. The specific functions of the latter multinucleated vesicles are not known but they are clearly involved in a general process of cell agglutination during acute infection (see below).

Each free-swimming urn normally secretes a modest tail of mucus (Figure 1); dead cells and inert debris become stuck as the cells dart about in the fluid so that the urn normally acts as a scavenger. Even then the sticking of particles to urn mucus is selective—none of the animal's living blood cells stick to it; rather, they hit and bounce off. The hypersecretory response of which the urn is capable is also selective; the coelomic fluid of healthy Sipunculi is usually sterile, yet it may contain bacteria which have presumably worked their way through the gut wall into the coelom. Harmless bacteria are trapped in the mucus and are phagocytosed by amebocytes and do not induce hypersecretion; if certain vibrios or noxious organisms get into the fluid, urns are stimulated to produce great quantities of mucus in which the invaders become trapped. Such hypersecreting urns tend to agglutinate with one another and with collapsing enigmatic vesicles to form clots. Amebocytes spread over the surface of the clots, phagocytosis proceeds, and the resulting balls of compressed debris (brown bodies) are apparently eliminated periodically through a small sphincter-controlled orifice in the animal's posterior end.

Cantacuzène's Studies

Cantacuzène looked upon the hypersecretory response of urns as an immune response. To test whether hypersecretion could be porgressively induced, he gave individual Sipunculi successive injections of either sheep red blood cells, a marine bacterial vibrio, or macerated nematocysts from a sea anemone. As immunization with each substance proceeded, urns produced increasing amounts of viscous mucus at an increasing rate; the mucus of urns from Sipunculi injected with sheep red blood cells and bacteria then had the capacity to lyse these foreign cells, a property lacking in the urns of nonimmunized animals. In the case of the nematocysts, the vesicles of nonimmunized urns exploded when first exposed to their toxin, but in immunized Sipunculi the vesicles remained intact and the nematocysts were quickly trapped in hypersecreting urn mucus.

Cantacuzène proposed that these responses could be due not only to an altered quality of urn mucus but to selective electrostasis.

Previous Studies of Urn Hypersecretion

In previous studies at Roscoff, we found that: a) Each urn cell was in fact two cells, each with a nucleus: a fluid-containing cell of connective tissue origin[3] and a mucociliated cell of epithelial origin. The secretory portions of the latter cell stained metachromatically.[4] The two loosely attached cells fit together much in the manner of an acorn and its cup (Text-figure 1).[4] b) Urns could be kept alive in sterile cultures at room temperature for up to 21 days, at which time the rate of ciliation was retarded yet the cells were still capable of a distinct hypersecretory response.[5] c) When certain marine vibrios were added to cultured urns, great volumes of hypersecreted mucus were induced and continued to entrap bacteria for well over an hour, until the cells died. Normal urns were killed by methylene blue, but hypersecreting urns were not.[5] d) Some bacteria evoked no hypersecretion in urns cultured from healthy Sipunculi; such ineffective bacteria did evoke moderate hypersecretion in urns cultured from the same Sipunculus if the animal itself was first injected with a solution of cholera toxin. e) Such ineffective bacteria would also produce moderate excess secretion in cultured urns if the bacteria themselves were first mixed with filtered sera from an acutely bacteremic Sipunculus. f) If such filtered sera were heated to 85 to 90 C before the bacteria were added, the cultured urns rapidly produced prodigious amounts of secretion in which the bacteria were trapped and lysed.[6] g) The most unfailing and powerful stimulus was a vibrio which grew as a contaminant in a refrigerated preparation of cholera toxin solution. This was never injected *in vivo*, but one drop of the solution induced an immediate, vigorous and sustained response in

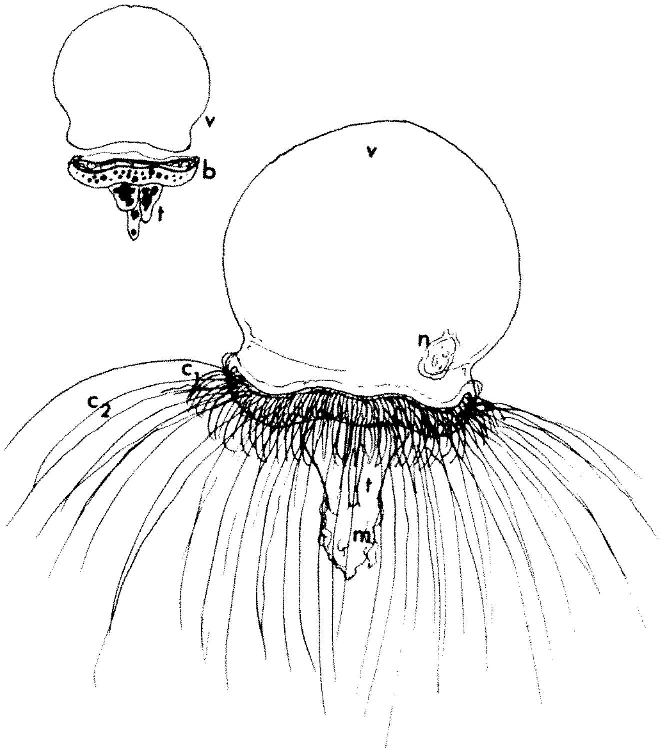

Text-fig 1—Diagram of urn, showing vesicle (*v*), its nucleus (*n*) and base cell (*b* on inset). Base has a central nucleus 2 rows of cilia (c_1, c_2) and secretory granules (*black spots* in inset) which stain vitally; secretions collect in the dependent central throat (*t*) and break through to form the tail of mucus (*m*). Cilia propel the cell and at the same time fling debris onto the mucus.

cultured urns. Agar plate cultures and subcultures of the vibrio failed to elicit response.[6]

Materials and Methods

Sipunculi were dug from the sand during the lowest monthly ebb tide and kept in large tanks of running seawater with beds of sand from their native area. For a given experiment, single Sipunculi were kept in individual, serially numbered, running-seawater aquaria, each provided with several inches of native sand.

The stock vibrio originated from the blood of an infected *Cancer pagurus* crab. A gram-negative rod with a flagellum at one pole, it induced vigorous hypersecretion in urns freshly removed from healthy sipunculus. It was cultured on seawater agar plates and pooled; pearly suspensions in cooled boiled seawater were divided into 1 ml lots and frozen for use as stock.

Eight percent solutions of cholera toxin were freshly prepared for each experiment from commercially prepared, dried material from human patients. The dried toxin was provided by Dr. Craig Wallace of the Johns Hopkins University Department of Medicine.

Populations of the ciliate Anophrys were taken from Cancer crabs infected with the ciliate. One milliliter of blood was drawn from an infected crab and injected directly into a Sipunculus.

Both injection and bleeding of Sipunculi were carried out by inserting a syringe needle into a small opening in the animal's posterior end; the opening gives direct access to the coelomic fluid and has no association whatever with the gut. Small samples of whole blood (or up to 10 ml for preparation of urn cultures) were withdrawn in this way. Sterile cultures were prepared by withdrawing 10 ml of whole blood by sterile procedures and placing 1 ml into each of 10 small sterile test tubes which were then stoppered with cork or cotton. The heavier blood cells settled in about an hour, leaving a clear supernatant in which hundreds of urns were swimming.

For each experiment in which cultured urns were used for testing the effects of a given substance, a few drops of supernatant containing urns were withdrawn by sterile procedure from the top of a test tube, one drop was put into a depression slide, and one drop of test material was then added. Effects on urns were viewed directly in a light or phase microscope. Urn preparations were checked frequently in the phase microscope for the presence of bacteria.

Heated sera of Sipunculi which had been injected with test substances (bacteria, Anophrys, etc) were obtained by withdrawing 3 ml of whole blood from an animal at given times after injection, centrifuging the blood at low speed for 3 to 5 minutes, filtering the supernatant to remove the urns, and placing the filtrate in a Pyrex® test tube marked with the animal's number. After testing and recording the response of cultured urns to one drop of unheated filtrate, the test tube containing the remaining filtrate was immersed for 5 minutes in water maintained at 85 to 90 C. Sera were then allowed to cool thoroughly, and one drop of the heated–cooled sera was added to one drop of cultured urn preparation. Effects of the drop of serum on urns over the next 15 to 30 minutes were recorded. When extraordinary (+++) hypersecretion was induced, the remaining filtrate was frozen. For each experimental series, tests were carried out on cultured urns from the same source animal if possible.

Results

For descriptive purposes the relative amount of secretion induced in cultured urns by particular stimuli will be expressed symbolically as 0, +, ++ or +++, as illustrated in Text-figure 2. It is understood that + and ++ responses designate true but moderate and short-lived output of excess mucus, while +++ specifically designates a continuing, usually rapid excretion in amounts ten or more times normal. The factor in heated sera which induces responses in cultured urns will be called the mucus-secretory stimulating (MSS) factor.

The degree of MSS factor in the heated sera of: a) normal Sipunculi, b) Sipunculi injected with stock marine vibrio, c) Sipunculi injected with the protozoan ciliate Anophrys, and d) Sipunculi injected with combined stock virbio and cholera toxin, was tested in cultured urns.

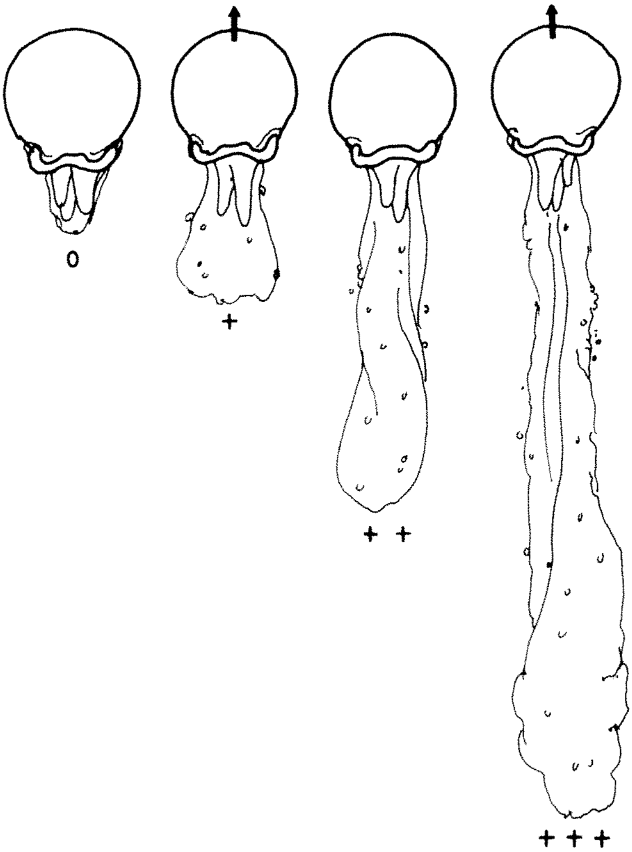

Text-fig 2—Diagram of amounts of secretion produced by particular stimuli. All grades between 0 and +++ may be produced: + and ++ production may be slow and steady, or brief temporary spurts; +++ production is rapid, may reach 10 to 15 times normal and stop, or may continue until cell death. Cell moves in direction of arrows.

Normal Sipunculi

In 4 sipunculus in apparently equal good health that were bled, the coelomic fluid of each was free of bacteria when examined in the phase microscope. Blood preparations were centrifuged and filtered and the filtered heated–cooled sera were tested on cultured urns. None of the four sera elicited excess mucous secretion.

Sipunculi Injected with Vibrio

Seven Sipunculi were each injected with 1 ml of a 1:200 dilution of freshly thawed stock vibrio. Blood was withdrawn from 2 at 15 and 30 minutes; when the heated–cooled sera were added to cultured urns, ++ and +++ responses were elicited. Sera from blood withdrawn from these and from the other 5 animals 24 and 48 hours after the original injection contained little or no MSS factor. By day 4 all seven were dead (Table 1). Thus there was vigorous early MSS response, the effect was not sustained, and the dose of bacteria was lethal.

Equal parts of a 1:100 solution of stock bacteria and an 8% peptone solution were mixed and 1 ml of the mixture was injected into each of 2 Sipunculi. Heated sera of both animals induced +++ amounts of mucus in cultured urns at 24 hours and essentially none thereafter; both animals were dead on day 4.

Injection of 1 ml of 1:200 solutions of killed bacteria or 8% peptone alone each into 2 individual Sipunculi, resulted in sera which elicited no response in cultured urns at 24 hours (Table 1).

Sipunculi Injected with Anophrys

The blood of Sipunculi injected with Anophrys produced a factor capable of rapid lysis of this protozoan ciliate on second challenge.[4] The factor was inactivated when sera were heated to 45 C. In order to determine whether there was any relationship between this factor and MSS factor, 2 Sipunculi were each injected with 1 ml of blood from a crab infected with the ciliate. Both were bled 15 minutes and 6 hours after injection; their heated sera induced

Table 1—Amount of MSS in Sera if Sipunculi Injected with Different Substances

	Time after injection				
Material injected	15-30 minutes	6 hours	24 hours	48 hours	4 days
Bacterial suspension	+++		+		D
	++		0		D
			0	0	D
			±	0	D
			0		D
			0	0	D
			0	0	D
Killed bacteria			0		
			0		
Bacteria in peptone			++	+	D
			+++	0	D
Peptone alone			0	0	
			0	0	
Anophrys	+++	+++	0		
	+++	+++	+		

D = death of injected Sipunculi

+++ hypersecretion at both time intervals. When tested at 24 hours there was little or no MSS factor in the sera (Table 1). Both Sipunculi remained active and healthy.

Thus, Anophrys induces release of at least two separate[7] factors into the sera of Sipunculi: one which is lytic and heat labile and one which is mucus-stimulatory and heat stable. Both responses are probably nonspecific.

Sipunculi Injected with Vibrio and Cholera Toxin

The most consistent means of inducing large amounts of MSS factor over the longest periods without killing the host Sipunculus was injection of 1 ml of equal parts of 1:100 dilution of stock vibrio and fresh 8% cholera toxin solution. Of 15 Sipunculi injected with this combination, or with 0.5 ml toxin followed 24 hours later with vibrio, the heated–cooled sera of all but one elicited +++ responses in cultured urns (Figure 2). As Table 2 shows, sera of most animals bled from 1 to 24 hours after injection induced +++ responses, 5 of 11 animals showed this degree of MSS factor at 48 hours, and half of those tested on day 4 still showed ++ amounts. Only 1 animal died.

In the light microscope, the mucus produced by urns stimulated with these latter sera was clear and granular (Figure 2); in the phase microscope it appeared agranular and homogenous as it continued to pour from the central portion of the base cell. The secretion was quite friable, and preparations were often littered with broken pieces of mucous tails.

Heated sera of 4 animals injected with 1 ml of 8% cholera toxin alone evoked no response in cultured urns (Table 2).

When the toxin solution itself was heated to 56 C for 30 minutes, then mixed with equal parts of a 1:100 solution of vibrio, the heated sera of 3 of the 4 injected animals elicited significant responses in cultured urns at 24 and 48 hours. The mucus was thick and rather dark; it was excreted slowly, reached quite a uniform length, and then tended to curl upon itself at the distal tip. Since the toxin produced by *Vibrio cholerae* is destroyed by heating at 56 C, it must be other components in the dried products which modify the effects of the stock vibrio. There may well be significant endotoxin in the crude preparation of dried toxin, yet, neither the cholera toxin solution alone nor killed bacteria alone, when injected into Sipunculi, released the heat stable factor into the sera.

Table 2—Amount of MSS in Sera of Sipunculi Injected with Different Substances

	Time after injection with toxin and bacteria					
Material injected	1 hour	5 hours	24 hours	48 hours	3 days	4 days
Toxin and bacteria mixed	+++	+++	+++	+++		
	+++	+++	++	+++		
			+++			
			+++	0	++	
			+++	++	++	++
			+++	++	+	++
			+++	++	++	+
			+++	+++	++	+
			+++	+++	D	
			0	0		
			+++	+++		
			+++			
			+++	++		
Toxin; bacteria 24 hours later			0	+++	+++	
			+++			
Heated toxin and bacteria			++	++		
			++	++		
			+++			
			0	0		
Toxin alone			0			
			0			
				0		
				0		

D = death of injected Sipunculi

Finally, two batches of frozen sera were thawed and refrozen successively. The capacity to stimulate excess secretion in cultured urns did not begin to diminish until about the sixth thawing. Diluting the sera in cooled, boiled seawater to 1:2 and 1:3 solutions significantly decreased the responses of urns to the serum factor; at 1:4 dilution the effect was eliminated.

Discussion

A factor which appears in the blood serum of an animal in response to a foreign stimulus, and which after heating will stimulate excess secretion in cultured mucous cells of a conspecific animal has been consistently induced. Six characteristics of the factor have been established: it is heat stable to at least 90 C; it withstands several successive freezings and thawings; it appears only in response to particular stimuli; it is released into the serum immediately after stimulus and may then gradually disappear or may persist several days, depending on the stimulus; the amount and quality of mucus which it provokes in cultured mucous cells is related to the stimulus which induced its release into the serum; it is not present in the sera of healthy Sipunculi.

In nature there would be no advantage, and much disadvantage, to the release of great amounts of MSS factor, unless there was an inhibitor which functioned to check hypersecretion when it was no longer needed. The accompanying diagram (Text-figure 3) shows a hypothesis of how a normal, balanced system would be unbalanced by heating the sera, if the factor was heat stable and the inhibitor heat labile; and how in nature an overwhelming bacterial infection might also stimulate the MSS factor to a degree which would overwhelm or destroy the inhibitor and kill the animal. Presumably both the MSS factor and the inhibitor are released into the serum from

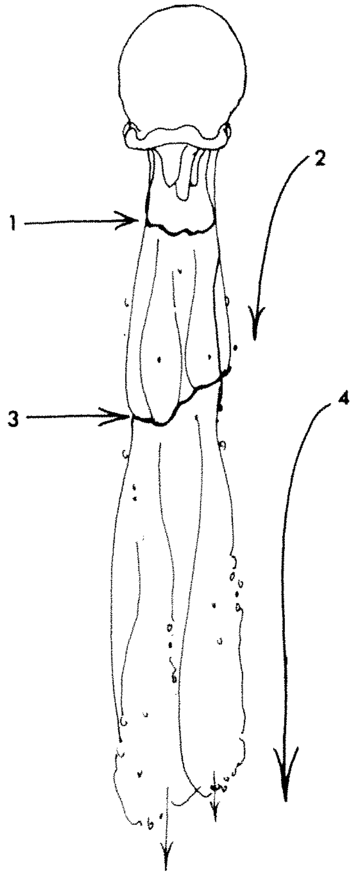

Text-fig 3—*1.* Mucous tail normally collects harmless organisms and inert debris from coelomic fluid; stimulus and inhibitor are in balance. *2.* Moderate hypersecretion is induced by certain foreign substances. *3.* Inhibitor functions when these are cleared from the fluid. *4.* Massive hypersecretion is induced *in vivo* by certain substances, or *in vitro* by heated sera of acutely infected host; if inhibitor is overwhelmed *in vivo,* animal dies. Experimentally, inhibitor is destroyed by heating sera and cultured urns hypersecrete until they die.

cells in the coelomic fluid. Specific cells involved in stimulus and inhibition remain to be investigated. Many mucous cell systems are known to hypersecrete prolifically in response to bacterial, mechanical, irritant and drug stimuli. However, the mechanism of production of abnormal secretions, such as the excess nasal secretions induced by the common cold and the profuse watery intestinal secretions of diarrhea and acute cholera are not known. The latter could result from rapid simultaneous synthesis and excretion of an abnormal mucus containing little or no mucoprotein. The urn base cell, which like the mammalian goblet cell has no CNS connection, may simultaneously secrete and excrete and does not respond to pilocarpine.[4]

Two of the most persistent blocks to the study of mucous secretion have been means of following the process *in vitro* in living secreting cells, and of harvesting the secretion without at the same time altering its properties. The cultured urn cell may be a model in which these methods can be developed.

References

1. Cantacuzène J: Recherches sur les réactions d'immunité chez les invertébrés. Arch Roumaines Pathol Exp Microbiol 1:7–80, 1928
2. Hyman LH: Smaller Coelomate Groups, Vol V, The Invertebrates. New York, McGraw-Hill Book Company, 1959 Ch XXII
3. Selenski W: Untersuchungen über die sogenannten Urnen der Sipunculiden. Z Wiss Zool 90:536–595, 1922.
4. Bang FB, BG Bang: Studies on Sipunculid blood: immunologic properties of coelomic fluid and morphology of "urn cells". Cahiers Biol Marine 3:363–374, 1962
5. Bang BG, FB Bang: Mucus hypersecretion in a normally isolated noninnervated cell. Cahiers Biol Marine 6:257–264, 1965
6. Bang BG, FB Bang: Hypersecretion of mucus induced in isolated noninnervated cells. Cahiers Biol Marine 12:1–10, 1971
7. Bang FB: Serologic response in a marine worm, *Sipunculus nudus*. J Immunol 96(6):960–972, 1966

[Illustrations follow]

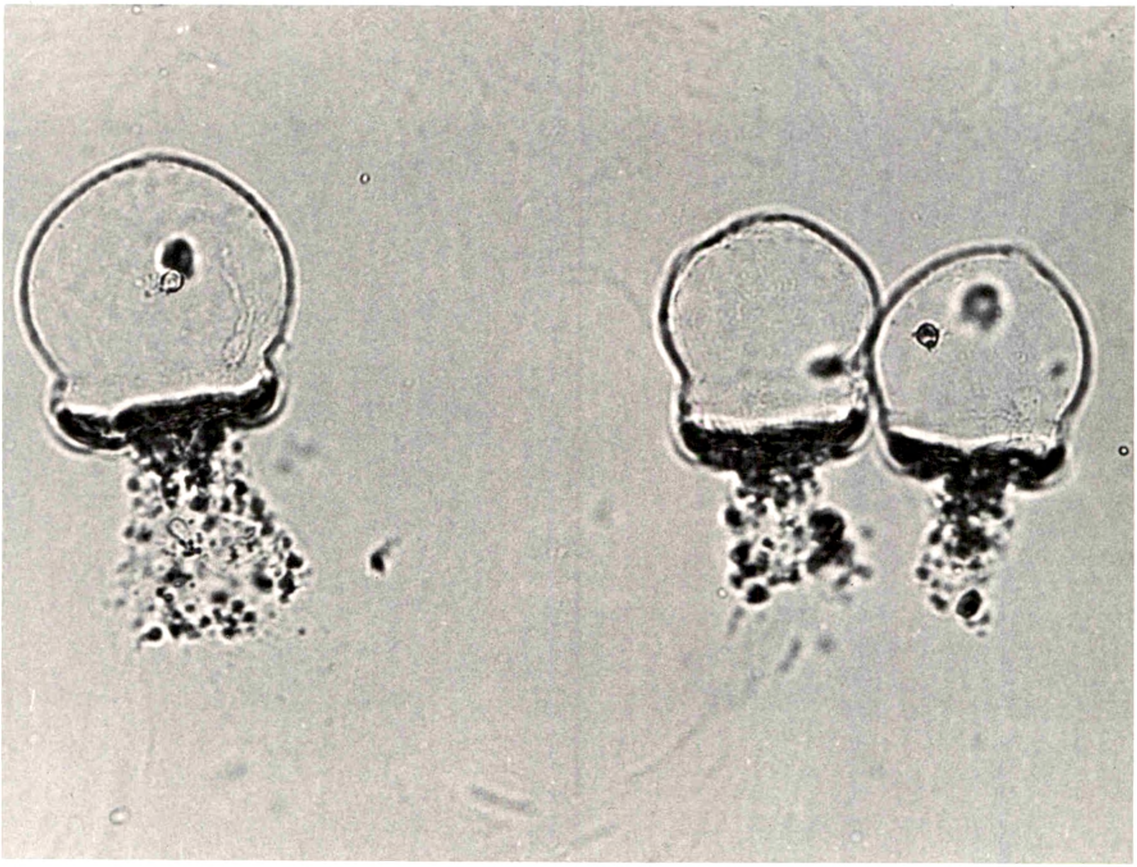

Fig 1—Three cultured urn cells, photographed while swimming *in vitro* so that cilia are not visible. Mucous tails show normal + amounts of secretion (Sizes average 30 μ).

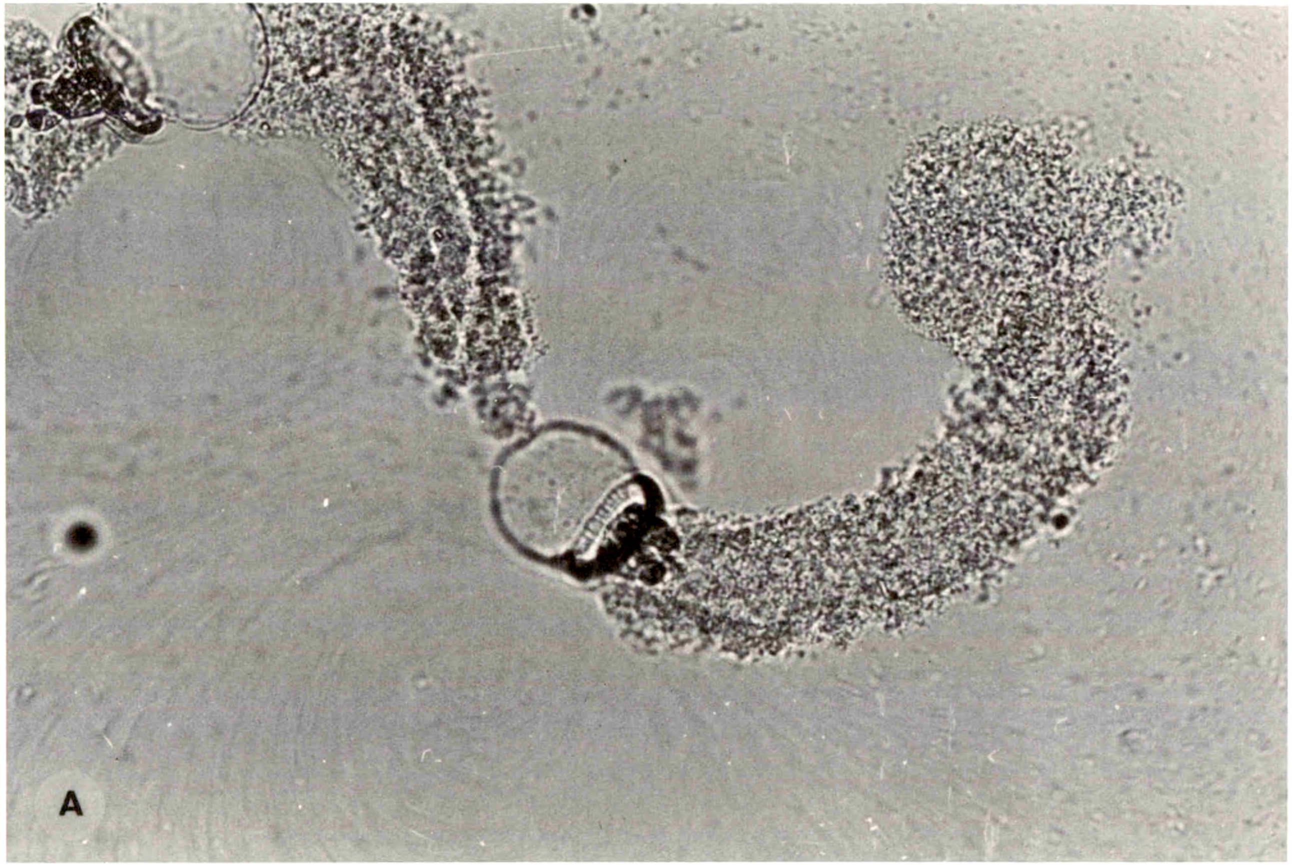

Fig 2A—Living 4-day cultured urn cell which has been stimulated to hypersecrete; one drop of heated (90 C) sera of a Sipunculi which had been injected 72 hours previously with mixture of marine vibrio and cholera toxin. Pieces of this mucous tail have broken away but the cell continues to secrete.

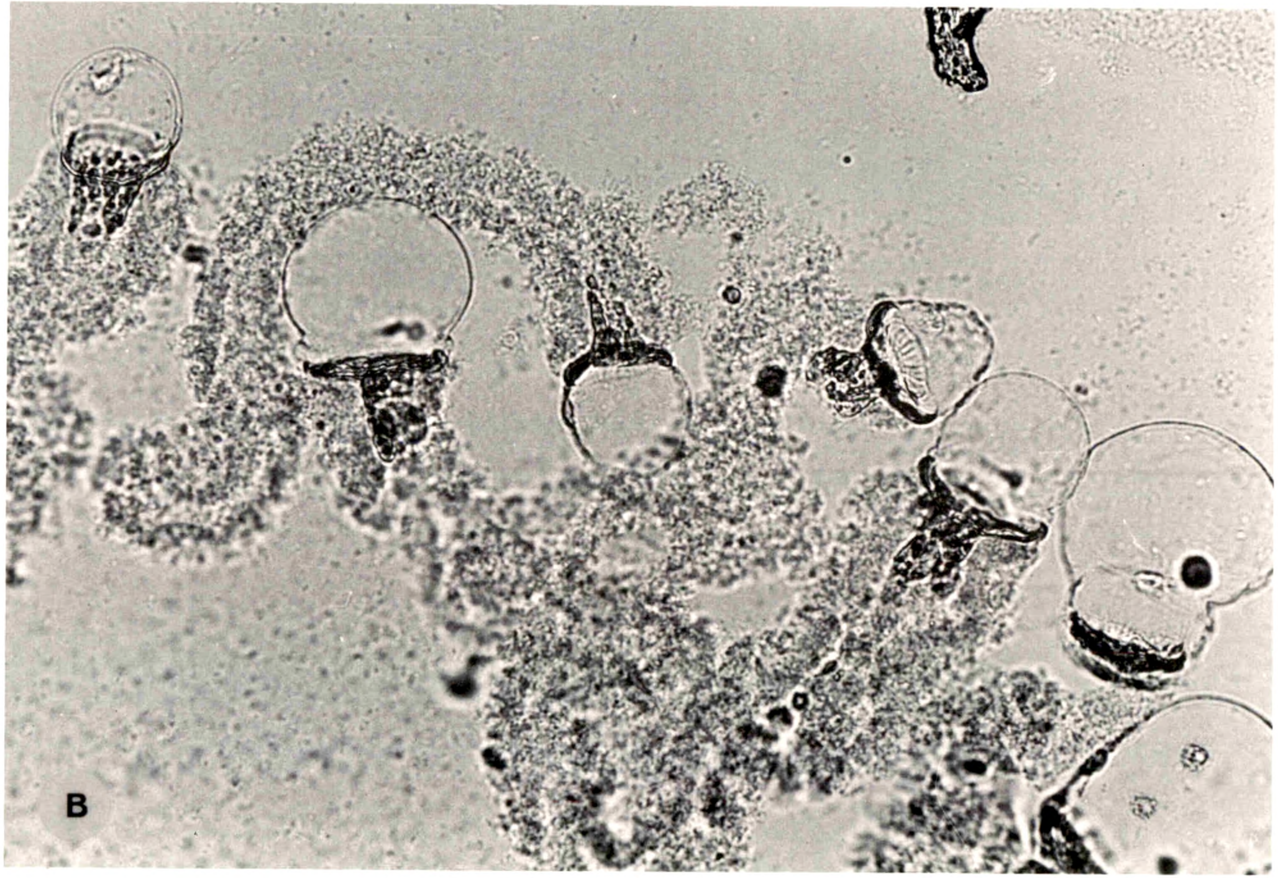

Fig 2B—Group of living 7-day cultured urn cells hypersecreting after stimulation with same mixture.

[*End of Article*]

The Variable Prevalence of Junctional-Complex-Associated Bodies in the Human Sweat Gland

S. S. Spicer, MD, B. J. Martin, PhD and J. P. Reynolds, PhD

Sweat gland biopsies have been examined for their content of junctional-complex-associated (JCA) bodies. These bodies have been observed at the lumen of the gland as well as the intercellular canaliculi. A JCA body was encountered in each of two dark cells with uncondensed secretory granules; one of these cells was from a specimen in which no other bodies could be found after an extensive search. All other JCA bodies occurred in either clear or undifferentiated cells. Junctional-complex-associated bodies occupied pairs of adjacent cells rather frequently, but no cell revealed more than one body. The prevalence of JCA bodies varied widely among specimens. Glands lacking morphologic abnormalities, and others with some atypical features, disclosed few or no such bodies. Some glands that contained JCA bodies also contained coil cells with extensive vacuolization, which occurred as a manifestation of Hurler's disease or on an unexplained basis. Glands from a patient with cystic fibrosis exhibited the highest prevalence of JCA bodies. Some of the coil profiles in glands near a scar in one specimen were composed of undifferentiated cells with rare mitotic figures and no identifiable clear or dark cells. Numerous JCA bodies, particularly at the lumen, were found in sweat glands in this and another specimen containing frequent undifferentiated cells (Am J Pathol 68:423–440, 1972).

ULTRASTRUCTURAL EXAMINATION of the human eccrine sweat gland disclosed a unique cytoplasmic structure lying near the intercellular canaliculus in clear cells and, more precisely, in close proximity to the zonula adherens of the junctional complex.[1] Because of its location and the morphologic similarity of its contents to that of the zonula adherens,[2] this newly observed organelle was designated the junctional-complex-associated (JCA) body. The purpose of the present investigation was to determine the prevalence of JCA bodies and, particularly, their possible variability in different clinical conditions, some of which are known to affect the sweat gland. The prevalence of JCA bodies was very low in some subjects but appeared to be increased in others, including several in whom the sweat glands deviated from the normal, morphologically[3] or functionally.[4] The

---

From the Department of Pathology, Medical University of South Carolina, Charleston, SC.

Supported by Grants AM–10956 and AM–11028 from the National Institutes of Health and a grant from the National Cystic Fibrosis Association.

Accepted for publication May 5, 1972.

Address reprint requests to Dr. S. S. Spicer, Department of Pathology, Medical University of South Carolina, 80 Barre St, Charleston, SC 29401.

investigation also disclosed JCA bodies associated with junctional complexes at the main lumen of the gland in addition to the bodies that were previously observed in association with junctional complexes at intercellular canaliculi. Those at the gland lumen frequently occurred in clear cells, but on rare occasions were observed in dark cells; in a number of instances they were encountered in undifferentiated cells which lacked the identifying characteristics of either clear or dark cells. Such undifferentiated cells, although not described previously in the sweat gland, were observed frequently in several of the specimens of this series and, in some subjects, their prevalence appeared to correlate with that of JCA bodies at the gland lumen.

Materials and Methods

Small skin ellipses were taken from the margin of abdominal or thoracic incisions at the time of surgery in 8 patients and by biopsy from the axilla in 1 patient (Patient 7). For the investigation of ultrastructural and cytochemical changes, the tissues were processed as described previously.[5] The specimen from Patient 11 was taken from the margin of an incision for the insertion of a dialysis catheter near a scar from a previous insertion. The subjects are listed by the same numbers assigned to them (Table 1) in the previous report. In addition, a specimen was obtained at surgery from a 53-year-old female (Patient 17), and by needle biopsy from 1- and 3-year-old females (Patients 18 and 19), as well as a 6-year-old (Patient 20), 25-year-old (Patient 21) and a 1-month-old (Patient 22) male.

For light microscopy, paraffin sections from a portion of the specimen fixed with formalin were stained with hematoxylin and eosin, Perl's ferrocyanide method for ferric iron[6] and methods for mucosubstance. For ultrastructural examination, specimens were fixed for 90 minutes in cacodylate-buffered, 3 to 6.25% glutaraldehyde at 4 C, and were postfixed for 60 minutes in collidine-buffered 2% osmium tetroxide prior to dehydration through graded alcohols and embedding in Epon. Thin sections were examined in an AEI-EM6B or Hitachi HS-8 electron microscope after staining by a uranyl acetate-lead citrate sequence. To determine the percent of junctional complexes or intercellular canaliculi which possess a JCA body, the sweat glands were mapped from the thick sections and structures of interest for each coil profile were counted in the electron microscope at one or at several well-separated levels in the block. Micrographs at low magnification were montaged for most of the coil profiles, and all JCA bodies were confirmed in prints at magnification of 12,000 or greater.

Results

Light Microscopy

The only distinct pathologic change found in the paraffin sections was seen in the specimen from Patient 11. In this specimen, the superficial corium contained a moderately inflamed scar with small suture granulomas. Mast cells and closely associated macrophages filled with Prussian blue reactive, and yellow pigment infiltrated the stroma within and between sweat glands. In epoxy sections, large, empty-appearing vacuoles filled many of the cells of the coil in the glands of Patient 9 and Patients 18 to 20;[3] lipid was increased in the glands of Patients 6 to 8,[5] as reported elsewhere.

Electron Microscopy

The sweat glands of patients in the present series disclosed the familiar cytologic structures [7–12] and certain pathologic features [3,5] demonstrated in previous ultrastructural studies of the human eccrine sweat gland. In addition, most of the specimens exhibited a number of JCA bodies bordering intercellular canaliculi (Figures 1–5) (Table 1). The bodies at canaliculi occurred usually in recognizable clear cells (Figure 1) and occasionally in unidentified, apparently undifferentiated cells; they were not observed in definite dark cells. Each of two adjacent cells contained a JCA body at two canaliculi (Figures 4 and 5).

In addition to the JCA bodies neighboring intercellular canaliculi, as previously described, a number were observed bordering the principal lumen of the gland in some specimens (Figures 6–12) (Table 1). The JCA bodies at the main lumen either lay laterally in the vicinity of the junctional complex (Figures 9 and 10) or, in cells with a narrow opening on the lumen, bridged most of the distance between the two junctional complexes (Figures 7 and 12). Two of the JCA bodies at the gland lumen were found in dark cells (Figures 11 and 12), and one of these occurred in the specimen from Patient 1 which disclosed no other bodies after an extensive search (Table 1). Both cells in four pairs of adjacent cells at the gland lumen contained JCA bodies (Figure 7, Table 1).

JCA bodies measured up to 1.8 μ in diameter and usually lay close to and sometimes in intimate contact with the lateral densification of the zonula adherens of the junctional complex (Figures 4 and 7–10), as previously noted.[1] Although lacking association with a zonula adherens in some profiles, a JCA body was often disclosed in contact with the zonula at an adjacent plane of section (Figure 8). Occasionally a body contacted the zonula with two projections from its surface (Figure 2), and in some profiles where they were not in close contact with the zonula adherens, the bodies were connected to it by tenuous extensions of their material (Figure 9C). The JCA bodies lacked a limiting membrane but were bordered, on some aspects of their surface away from the junctional complex or gland lumen, by profiles of endoplasmic reticulum with apparently enlarged ribosomes bound only to the membrane distal to the body (Figures 1, 2, 4 and 7–10). Usually free ribosomes and mitochondria were observed in this same region. Although profiles of JCA bodies were often round, they

Table 1—Prevalence of JCA Bodies in the Sweat Gland Secretory Coil in 14 Patients

			Intercellular canaliculi*				Central lumens*			
Patient	Primary diagnosis	Atypical ultrastructural features in the sweat coil	No. observed	No. with JCA bodies	Percent with JCA bodies	SE†	Junctional complexes observed	No. with JCA bodies	Per cent of junctional complexes with JCA bodies	SE†
1	Peptic ulcer	—	207	0	0	—	354	1‡	0.3	±0.29
6	Leaking abdominal aneurysm	Undifferentiated cells, increased lipid, nuclear lipid	161	16	10.0	±2.36	122	5	4.1	±1.80
7	Hypokalemia, hypertension	Increased lipid with associated mitochondria	206	0	0	—	233	0	0	—
8	Inguinal hernia, hypertension	Increased lipid	53	2	3.8	±2.63	48	0	0	—
9	Renal artery dysplasia, hypertension	Epithelial cell vacuolization	107	11	10.3	±2.93	167	4	2.4	±1.18
11	Uremia, hypertension	Undifferentiated cells, mitoses	168	10	6.0	±1.83	116	15§	12.9	±3.11
12	Renal artery stenosis, glomerulonepnritis, hypertension	—	60	2	3.3	±2.31	35	0	0	—
13	Hematuria, hypertension	—	63	2	3.2	±2.22	156	0	0	—
17	Cholelithiasis	Undifferentiated cells, uncondensed secretory granules	77	12§	15.6	±4.14	187	4‡	2.1	±1.05
18	Hurler's disease	Epithelial cell vacuolization	86	5	5.8	±2.52	120	0	0	—

19	Hurler's disease	Epithelial cell vacuolization	81	5	18.5	±4.31	54	0	0	—
20	Hunter's disease	Epithelial cell vacuolization	52	7	13.5	±4.73	72	1	1.4	±1.38
21	Cystic fibrosis	—	102	24§	23.5	±4.20	160	7§	4.4	±1.62
22	Hepato spleno-megaly undiagnosed	Absence of glycogen, condensed secretory granules	47	0	0	—	131	0	0	—
Total			1470	106	7.2		1955	37	1.9	

---

* Canaliculi or lumenal junctional complexes were counted more than once in a given coil only at levels more than 3 μ apart in the block. Consequently, individual bodies, although often observed at more than one level, were included only once in the tabulation, as these bodies were never larger than 1.8 μ.

† Standard error of the percentage.

‡ Includes one of the 2 JCA bodies observed in a dark cell.

§ In Patient 11, 3 pairs of adjacent cells at a lumen contained a JCA body; in Patient 21, one pair of cells at a lumen and another pair at an intercellular canaliculus contained a JCA body; and in Patient 17, a pair of adjacent cells at a canaliculus contained a JCA body.

were sometimes irregular, particularly in patients with Hurler's syndrome, and in a number of instances where they closely bordered a lumen, they appeared elongated in a direction parallel to the adjacent plasmalemma. A 65-mμ-thick band of material with hyaloplasmic density separated the JCA body from both the enveloping reticulum and the neighboring plasma membrane in profiles of bodies bordering the lumen closely. Except for more lucent enclosed foci or invaginations, JCA bodies consisted of material with the same density and texture as that of the zonula adherens.

Varying widely in prevalence, JCA bodies were absent or very infrequent in some specimens extensively surveyed but were relatively abundant in others (Table 1). Sweat glands in some specimens with infrequent bodies appeared normal ultrastructurally, whereas those in glands from other biopsies with few bodies exhibited certain unusual features (Table 1).

Some biopsies with abundant JCA bodies, in this series, revealed a pathologic change entailing the occurrence of numerous large vacuoles with a translucent flocculent content in the cytoplasm of many clear and dark cells (Figures 3 and 6). All specimens with such vacuolization contained relatively abundant JCA bodies but so did some other biopsies that lacked vacuoles. The patients exhibiting vacuolization included 3 in whom the vacuoles constituted a feature of Hurler's disease and 1 in whom they occurred in connection with renal hypertension secondary to fibromuscular dysplasia of the renal artery and consequent renal arterial stenosis.[3] The percent of luminal junctional complexes with a JCA body exceeded that of canaliculi with a body only in Patient 11 (Table 1).

The prevalence of JCA bodies in the sweat glands of a patient with cystic fibrosis exceeded that in other specimens (Table 1). One clear cell in this patient contained both a JCA body and numerous moderate-sized vacuoles which enclosed translucent material but which were smaller than the vacuoles in glands of patients with Hurler's disease (Figures 3 and 6). The other cells with JCA bodies, in this patient, lacked vacuoles and, on the other hand, were not of the undifferentiated type like some of the cells with JCA bodies in Patients 6 and 11. The hyaloplasm of clear cells containing JCA bodies in the patient with cystic fibrosis varied widely from very dense to very translucent (Figures 5 and 6), but, as a rule, the denser cells contained sparsely scattered particles of the glycogen, characteristic of clear cells. In this specimen, the glycogen occurred as sparse dense particles in the β-configuration or as extensive confluent accumulations and differed from that in other biopsies in which translucent areas apparently represented sites from which glycogen had been extracted (Figure 4).

Most of the cells which contained JCA bodies at the main lumen in Patients 6 and 11 appeared undifferentiated (Figure 9). The undifferentiated cells with JCA bodies lacked the secretory granules and bundles of microfilaments typical of dark cells and also lacked characteristic features of clear cells, such as abundant cytoplasmic glycogen, small Golgi complexes and multivesicular bodies near the intercellular canaliculus and elaborately folded lateral and basal plasma membranes. Instead, these undifferentiated cells usually possessed relatively dense, filamentous cytoplasm, a prominent supranuclear Golgi complex and mitochondria intermediate between those of clear and dark cells in size and compactness.

Sweat glands of Patient 11 had the most numerous JCA bodies at the main lumen and differed from glands previously illustrated as well as from most others of this study in that the profiles of the secretory coil were variable. Some full profiles, viewed at low magnification or in a montage, consisted, as usual, entirely of clear and dark cells in about equal numbers and of the encircling myoepithelial cells. Other full profiles of coil, identifiable by their cytoplasmic lipoid bodies and myoepithelial cells, were composed entirely of undifferentiated cells that lacked the identifying features of either dark or clear cells. The hyaloplasm in individual cells of the latter coil profiles varied from uniformly dense to uniformly translucent, and dense and lucent cells often alternated in the coil. Coil profiles, composed of undifferentiated cells, revealed infrequent mitotic cells in metaphase (Figure 13) or prophase together with neighboring cells, possibly in an early postmitotic stage since they possessed vesicular nuclei with dispersed chromatin and cytoplasm resembling that of mitotic cell in its numerous ribosomes, scattered small dense bodies and translucency. Junctional complex associated bodies were found in coils of this specimen containing clear and dark cells plus undifferentiated cells, but they were not encountered at the few intercellular canaliculi or junctional complexes seen in the coils with only undifferentiated cells or mitoses.

Glands from Patient 17 revealed a high prevalence of JCA bodies and appeared atypical in several features which presently have no established relationship to the frequency of the bodies seen in this specimen. Profiles of these glands often disclosed a dilated lumen lined by unusually low epithelial cells which, in some areas, varied markedly in density, some having translucent cytoplasm, numerous polysomes and no specialized identifying features. Virtually all of the dark cells in this specimen, including one cell that enclosed a JCA body, contained entirely uncondensed secretory granules that appeared to be empty or had a content of low density. Only two of the 43 dark-cell profiles with abundant secretory granules disclosed any very dense or fully condensed granules, and such granules comprised less than one-third of the granule population in these cells. In contrast, all 48 dark cells in the biopsy from Patient 22 that lacked JCA bodies contained a predominance of fully condensed granules—a few of moderate density and none of the translucent type. In 198 dark cells counted at random from patients of an earlier study,[5] the percentage of secretory granules with low, intermediate and high density averaged 19, 29 and 52, respectively.

Discussion

The physiologic significance of the JCA body remains undetermined, but its close association with the zonula adherens of the junctional complex and the remarkable similarity between content of the JCA body and that of the lateral densification of the zonula adherens strongly suggest a possible role in synthesis or replenishment of the lateral part of the zonula adherens. The granular reticulum enveloping part of a given body testifies moreover to the active protein synthesis that probably transpires in the genesis of these bodies. The JCA bodies seen at the gland lumen in this study further support the association of these bodies with the junctional complex, since they invariably lay apically near the zonula rather than elsewhere in the cytoplasm.

Present observations demonstrating the variable prevalence of JCA bodies provide a further basis for interpreting their significance. However, the normal prevalence of these bodies remains undertermined, both because sufficient specimens from "normal" controls were lacking and normal limits of sweat gland ultrastructure have not been defined with certainty. The virtual absence of JCA bodies from some specimens may reflect an abnormally low occurrence of these structures.

Patient 7, in whom an extensive search did not disclose JCA bodies for example, evidenced aberrant metabolism in the sweat gland, as indicated by the increased cytochemical activity of glucose-6-phosphate dehydrogenase, increased accumulation of atypically vesiculated and translucent lipid and increased association of lipid bodies with mitochondria.[5] The sweat glands of Patient 22, besides lacking JCA bodies appeared devoid of glycogen and almost entirely contained fully condensed secretory granules. Apparently the metabolism and physiologic activity in the sweat glands of these patients were such so as not to require a rapid turnover of junctional complex material or synthesis of new complexes. However, the extremely infrequent occurrence of JCA bodies in sweat glands of Patient 1 suggest that a low prevalence may be normal, since this gland conformed to normal as closely as any other in its ultrastructure and disclosed no undifferentiated cells. Lack of knowledge of the precise function of the zonula adherens impedes an understanding of the basis for the variable prevalence of bodies presumably concerned with its biogenesis. Present evidence indicates that the junctional complex facilitates cell-to-cell transport.[13] Thus in the sweat gland, in which junctional complexes possibly provide electrotonic coupling between cells, conditions altering transport activity might alter prevalence of JCA bodies.

On the other hand, the relatively high percentage of canaliculi or junctional complexes with JCA bodies in some specimens may manifest a pathologic state. Indeed, specimens with numerous JCA bodies exhibited several morphologic changes. All four of the biopies that revealed pathologic vacuolization of coil cells, for example, had JCA bodies in moderate abundance. An explanation for increased JCA bodies in glands with such vacuolization is not readily apparent but altered transport or synthesis of macromolecules in these specimens may be connected with increased need for junctional complex material.

Other glands with numerous bodies (Patients 6 and 11) lacked such vacuoles but contained a number of undifferentiated cells in the coil. Recognition of undifferentiated cells depended heavily on the occurrence of coil profiles composed entirely of such cells, especially in glands of Patient 11. Having been identified in coils such as these, however, the undifferentiated cells were distinguishable as occasional cells in coils otherwise populated by clear and dark cells.

These unidentifiable epithelial cells in the secretory coil could represent a phase in a cycle of cell activity wherein clear and dark cells are devoid of differential features or might constitute a stage in development of newly replicated cells preceding formation of specialized structures. The frequent occurrence of luminal JCA bodies in sweat glands of Patient 11, possibly relates to sweat gland repair or regeneration, since this biopsy was obtained from an area scarified by previous surgery. The scar, suture granulomas and infiltrate of siderophages and mast cells observed histologically in this biopsy testify that it came from an area of cell destruction and repair. The observations at the ultrastructural level that entire coil profiles in sweat glands of Patient 11 consisted of undifferentiated cells, and that these coils were the only ones in the present study to exhibit mitoses also favor interpreting the undifferentiated cells as a stage in replication. A relationship to cell turnover seems further indicated by the frequency of JCA bodies in adjacent cells.

One objection to relating JCA bodies to cell replication concerns the rarity with which they were observed in dark cells. The observed 60-fold greater prevalence of bodies in clear cells suggests they function in relation to activities of clear cells. However, many cells with JCA bodies at the gland lumen were undifferentiated and not classifiable as clear or dark cells. Moreover, since dark cells rarely abut on intercellular canaliculi, their content of JCA bodies would be restricted to those at the main gland lumen. In addition some JCA bodies may have been overlooked at the gland lumen in dark cells because of difficulty in differentiating these structures from secretory granules in the low magnification survey by which much of the search for bodies was conducted. The proportion of dark cells to clear cells with JCA bodies may then be less than at first apparent (Table 1). The two dark cells found with a JCA body at the gland lumen appeared somewhat atypical in containing only uncondensed secretory granules and could have been in an early developmental stage.

The abundance of JCA bodies in sweat glands from one patient with cystic fibrosis if confirmed on examination of more specimens might be considered related to the known abnormal function of these glands.[4] The increased number of bodies in the glands from this patient could result secondarily from altered electrolyte transport or might reflect cellular instability and increased cell turnover as suggested for other specimens in this study. If increased JCA bodies signify a pathologic response as the present results imply, the markedly increased prevalence of JCA bodies in the specimen from the cystic fibrosis patient provides evidence for an abnormality in the secretory coil of the sweat gland in this disease. Such evidence counters the prevailing opinion that the functional defect in cystic fibrosis is restricted to the sweat duct.[14-16]

References

1. Spicer SS, Martin BJ, Simson JV: The junctional complex associated body of the human eccrine sweat gland. J Cell Biol 53:582–586, 1972
2. Farquhar MG, Palade GE: Junctional complexes in various epithelia. J Cell Biol 17:375–412, 1963

3. Spicer SS, Wohltmann H, Wertelecki W: Ultrastructure and cytochemistry of the sweat gland in Hurler's disease. Abstract to be presented at the 47th Anniversary Congress of the PanAmerican Medical Association, Miami Beach, Florida, November 1972
4. di Sant 'Agnese PA, Darling RC, Perera GA, Shea E: Abnormal electrolyte composition of sweat in cystic fibrosis of pancreas; clinical significance and relationship to disease. Pediatrics 12:549–563, 1953
5. Spicer SS, Prioleau WH Jr: Ultrastructure of lipid inclusions and dense bodies in the human eccrine sweat gland. Lab Invest (In press)
6. Lillie RD: Histopathologic Technic and Practical Histochemistry. New York, The Blakiston Co, Inc, 1954, p 501
7. Hibbs RG: The fine structure of human eccrine sweat glands. Am J Anat 103:201–217, 1958
8. Charles A: An electron microscope study of the eccrine sweat gland. J Invest Dermatol 34:81–88, 1960
9. Munger BL: The ultrastructure and histophysiology of human eccrine sweat glands. J Biophys Biochem Cytol 11:385–402, 1961
10. Dobson RL: The correlation of structure and function in the human eccrine sweat gland. Advances in Biology of Skin, Vol 4. Edited by W Montagna, RA Ellis, AF Silver. New York, Pergamon Press, Inc, 1962, p 54
11. Ellis RA: The fine structure of eccrine sweat glands. Advances in Biology of Skin, Vol 3.[10] p 30
12. Ellis RA: Eccrine, sebaceous and apocrine glands. Ultrastructure of Normal and Abnormal Skin. Edited by AS Zelickson. Philadelphia, Lea & Febiger, 1967, p 132
13. Lowenstein WR: Permeability of membrane junctions. Ann NY Acad Sci 137:441–472, 1966
14. di Sant 'Agnese PA, Talamo RC: Pathogenesis and physiopathology of cystic fibrosis of the pancreas. Fibrocystic Disease of the Pancreas (Mucoviscidosis). N Engl J Med 277:1287–1295, 1343–1352, 1399–1408, 1967
15. Barbero GJ, Sibinga MS: Electrolyte abnormality in cystic fibrosis. Pediatr Clin North Am 11:983–1001, 1964
16. Schulz IJ, Peter G: Micropuncture studies of abnormality in sweat formation in cystic fibrosis (CF). Fed Proc 26:287, 1967

Acknowledgments

The authors are grateful to Ms. Joanne Wright and Fran Cameron for skilled technical and secretarial assistance and to Dr. R. C. Duncan for biometric consultation.

Legends for Figures

Figures 1 to 12 illustrate junctional complex associated (JCA) bodies in secretory coil cells from Patient 1 (Figure 12), 6 (Figures 1, 9, 10), 11 (Figures 2, 8), 17 (Figures 4, 11), 19 (Figure 3), and 21 (Figures 5, 6, 7); and Figure 13 depicts a mitotic cell in a coil from Patient 11. The cells with bodies are identifiable clear cells or undifferentiated cells except for those in Figures 11 and 12 which are dark cells. The JCA bodies border intercellular canaliculi in Figures 1–5 and the gland lumen in Figures 6–12. The specimens were fixed with a glutaraldehyde-osmium tetroxide sequence and the thin sections were stained with uranyl acetate followed by lead citrate.

Fig 1—The contour of this JCA body is flat where it abuts on an intercellular canaliculus. Collapsed ergastoplasmic cisternae (*arrow*) bordered by attached and free ribosomes conform closely to the more convex surface away from the canaliculus. The location of Golgi elements (G) near the canaliculus with a presumed multivesicular body (*M*) and the abundance of glycogen (extracted translucent areas) and the folded lateral plasmalemma identify this as a clear cell. Another clear cell and abundant glycogen lie at the left, and a dark cell at the upper right (× 12,500).

Fig 2—A JCA body, bordered below by a typical unit of agranular and granular reticulum and neighboring ribosomes and mitochondria, differs from most of these bodies in contacting at both ends a (similar appearing) zonula adherens. Small dense bodies (*arrows*) which may represent lysosomes lie nearby (× 14,000).

Fig 3—This unusually elongated JCA body (*arrow*) with a dense core in its less dense central area lies near a junctional complex in a presumed clear cell in a patient with Hurler's disease. Numerous large vacuoles with translucent flocculent content fill much of the cytoplasm in 4 cells here and most of the other cells in this secretory coil (3) (× 10,250).

Fig 4—Adjacent clear cells bordering an intercellular canaliculus (*IC*) each contain a JCA body. **A**—The cell with the upper body characteristically displays a Golgi complex (G) near the canaliculus. **B**—At an adjacent level the bodies (*arrows*) are tangentially sectioned and numerous small vacuoles populate the cytoplasm bordering the canaliculus (× 10,500).

Fig 5—JCA bodies occupy adjacent clear cells at a deep level in a gland from the patient with cystic fibrosis. The cells differ markedly in density but contain sparse glycogen deposits and no secretory granules, and the more lucent cell discloses a Golgi zone (G), and multivesicular bodies (*M*) in the region of the intercellular canaliculus (*IC*). Small, empty-appearing vacuoles and occasional membrane limited dense bodies (*arrows*) populate the cytoplasm of the denser cell. Glycogen lakes (*Gl*) fill cytoplasm above the myofilaments of the myoepithelial cell. The JCA body on the right differs from most in the large indentation by hyaloplasm devoid of organelles (× 7,000).

Fig 6—A JCA body neighbors a zonula adherens in a clear cell from a patient with cystic fibrosis. This and a neighboring clear cell disclose numerous empty appearing vacuoles in the apical lumen and moderately abundant glycogen (*Gl*) particles. The upper right cell shows a centriole and the dark cell (*lower right*) has uncondensed secretory granules (× 17,500).

Fig 7—Two adjacent clear cells from the same specimen as that of Figures 5 and 6 exhibit typical JCA bodies close beneath the gland lumen (*L*). The clear cells lining the lumen contain scattered dense particles and aggregates of glycogen which differ from the extracted appearing glycogen in other specimens (× 17,500).

Fig 8—A JCA body with bordering small cisternae of endoplasmic reticulum and a few ribosomes lies near the lumen (*L*) in an undifferentiated cell. The body lacks association with a junctional complex at the level of **A** but connects with the material similar to it in the lateral densification of the zonula adherens at the level of **B** (× 15,750).

Fig 9—The JCA body with its related structures shown here at three levels resembles the others observed close to a lumen in that it borders a junctional complex. **A**—

The cell with the JCA body (*arrow*) lacks the apical secretory granules such as those characteristically present in the two dark cells to the left. It also lacks the evidence of abundant glycogen deposition usually present in clear cells and shown here as translucent, extracted areas in two cells at the right. The cell with the JCA body differs from most clear cells in having a Golgi complex (G) above the nucleus and rather uniform, moderately dense filamentous cytoplasm. This cell and the similar cell on its left contain mitochondria intermediate in size and compactness between those of clear cells and dark cells and in general appear undifferentiated. This specimen and that from Patient 11, revealed an unusual number of these cells, and many of the JCA bodies at intercellular canaliculi or near the lumen occurred in such cells. The specimen also disclosed an abundance of large translucent vesiculated lipoid bodies in the cytoplasm and infrequent dense lipoid bodies in the nucleoplasm (5) (× 11,200). **B**—At an adjacent plane of section, a pocket of cytoplasm invaginates the JCA body indicating that the more lucent foci in the bodies represent extensions inward of surrounding hyaloplasm. The zonula adherens nearest the body appears largely devoid of its lateral densified area (× 23,750). **C**—The JCA body at a third level lies somewhat removed from the zonula adherens but connected with it by a tenuous band of dense material (× 23,750).

Fig 10—JCA bodies and their related structures are illustrated in three planes of section through their rather undifferentiated cells. **A**—Each JCA body (*arrows*) connects by a narrow extension with the zonula adherens of a luminal junctional complex. Note incidentally the pseudopod projecting into the coil lumen (*L*) from the surface of an intervening dark cell (× 8,750). **B**—The upper right JCA body of Figure 10A is observed at an adjacent level. The body is indented by cytoplasm containing several vesicles and contacts a zonula adherens (*arrows*). The JCA body is oriented at nearly a 90° different angle here to conserve space. Granular reticulum closely conforms to the surface of the body except where it is indented by cytoplasmic vesicles or is opposed to surface plasmalemma or the junctional complex (× 19,000). **C**—At a third level, the lower left JCA body of Figure 10A lacks the contact it had with the junctional complex above (*arrow*) and closely approximates the one toward the lower left, suggesting that this body may bridge between the two complexes. The cell containing this body has a narrow contact with the lumen apparently at the orifice of an intercellular canaliculus (× 14,250).

Fig 11—This is one of two JCA bodies observed in a dark cell. The secretory granules (*arrows*) like all of those observed in this specimen and those in the other dark cell with a JCA body (see Figure 12) have low density content and are apparently uncondensed (× 15,750).

Fig 12—This is the second of two JCA bodies found in a dark cell (See Figure 11) and the only one encountered in this specimen after extensive search (Table 1). **A**—The dark cell typically contains numerous bundles of tonofilaments (*T*) often inserting in desmosomes, but it differs from the usual dark cells like that on its right in disclosing, at least in this plane of section, only a few small uncondensed secretory granules (*arrows*) which presumably are in an early stage of granulogenesis. The cell rather atypically contains a centriole (c) close above the nucleus rather than near the central apical plasmalemma and lies above another dark cell. Clear cells at the far right characteristically contain abundant glycogen appearing as extracted lucent areas and larger, less dense mitochondria in orthodox configuration (× 9,225). **B**—The JCA body is seen at an adjacent level and lacks the translucent central area. It is bordered by uncondensed (immature) secretory granules with flocculent content (× 12,700).

Fig 13—Mitoses such as this were observed only in the secretory coil from patient 11. Small dense bodies (*arrows*) are scattered in the cytoplasm mostly in clusters. The cell is connected to a neighboring cell at the top by desmosomes and a junctional complex which apparently persisted after mitosis. This mitotic activity was associated with a high prevalence of undifferentiated coil cells not clearly identifiable as clear and dark cells. Some of these cells had translucent cytoplasm and numerous cytoplasmic ribosomes suggestive of a postmitotic state. The secretory coil also contained numerous JCA bodies particularly at the lumen (Table 1) and the specimen showed an inflamed scar with suture granulomas and an infiltrate of mast cells and siderophages (× 6000).

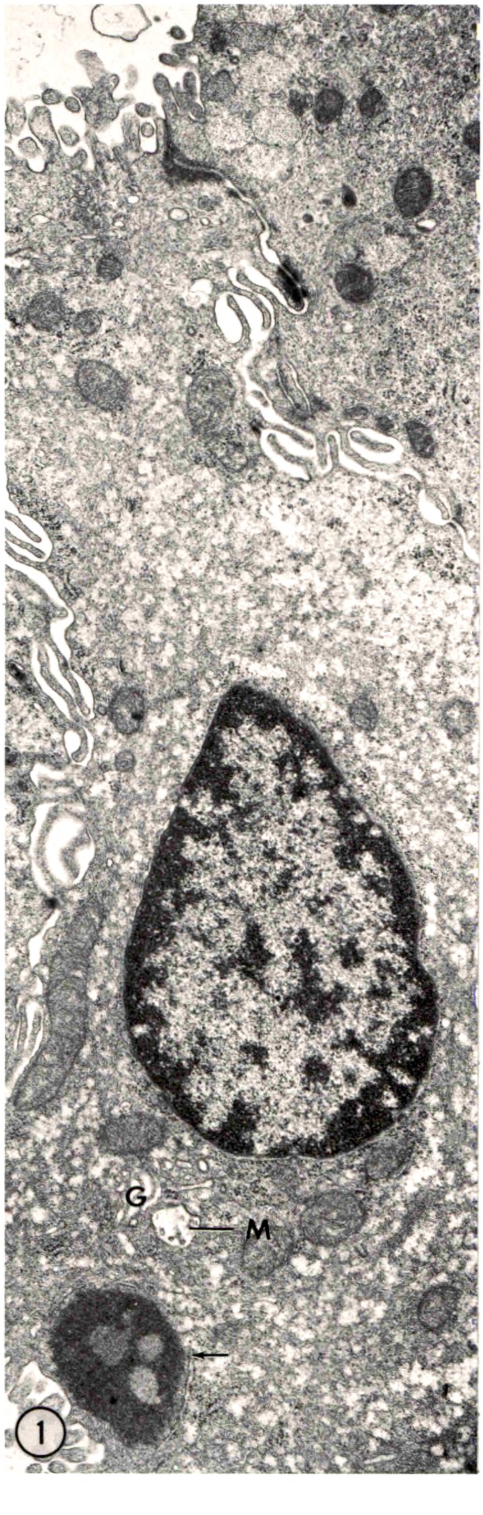

①

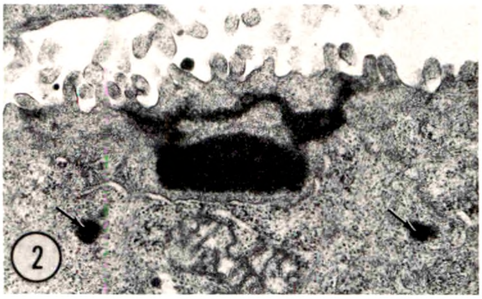

②

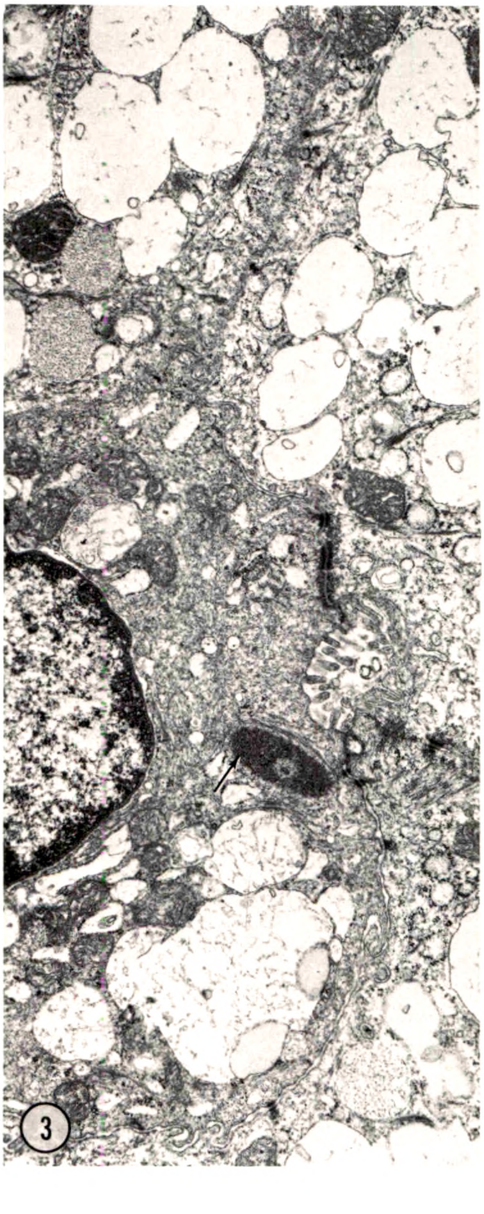

③

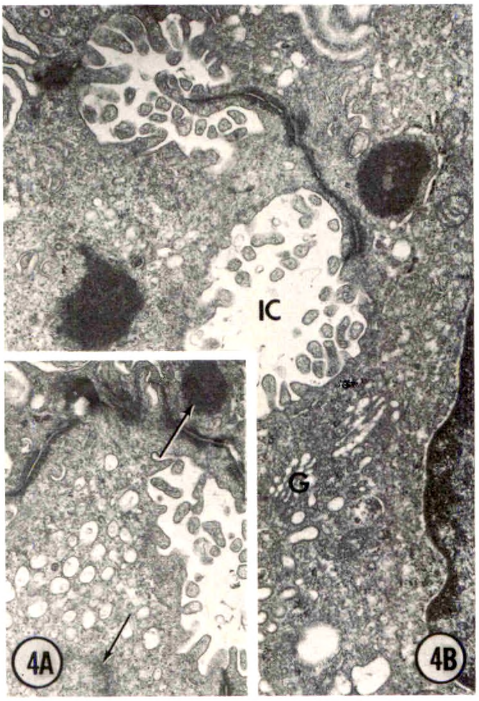
4A 4B

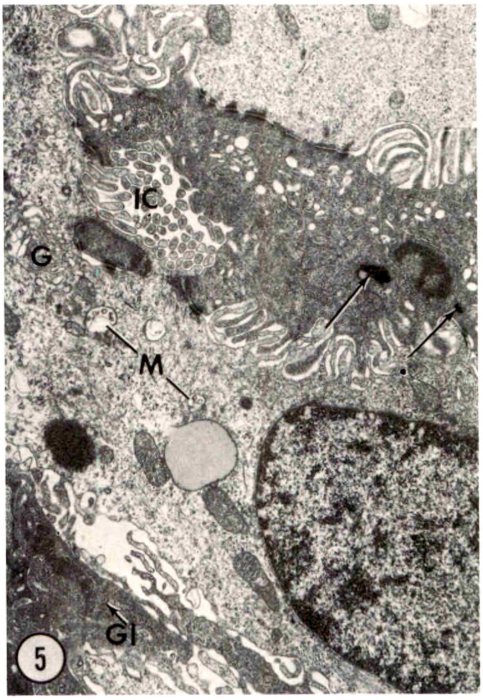
5

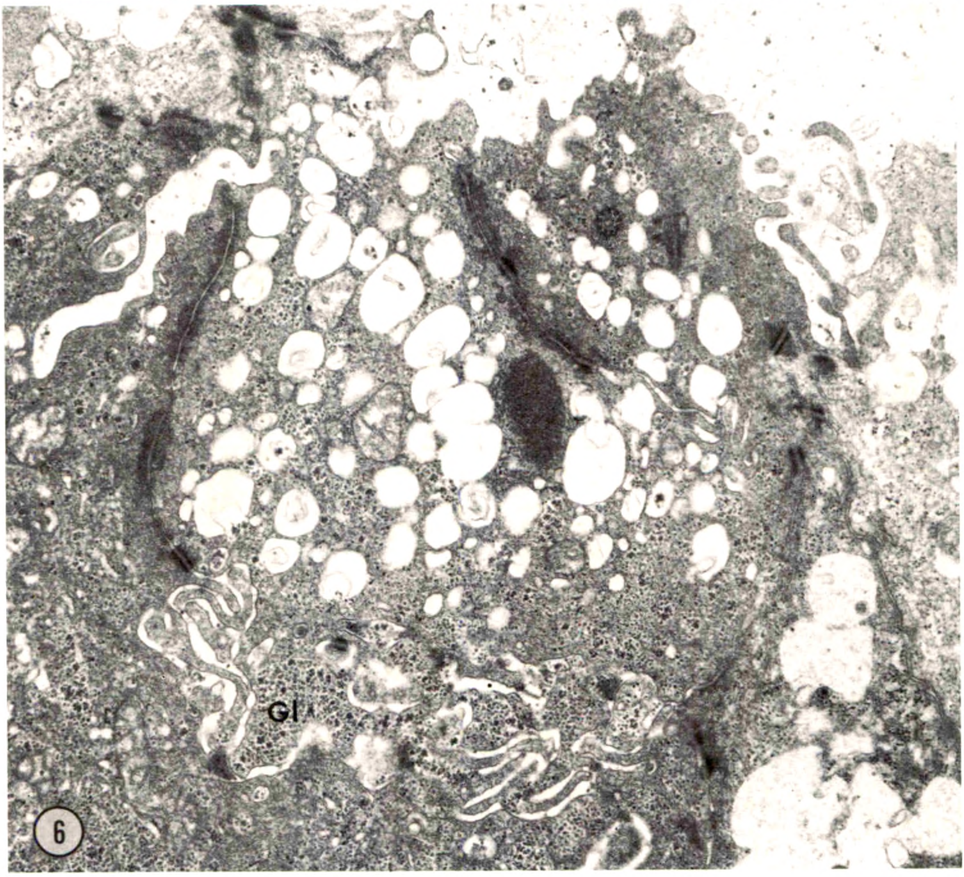
6

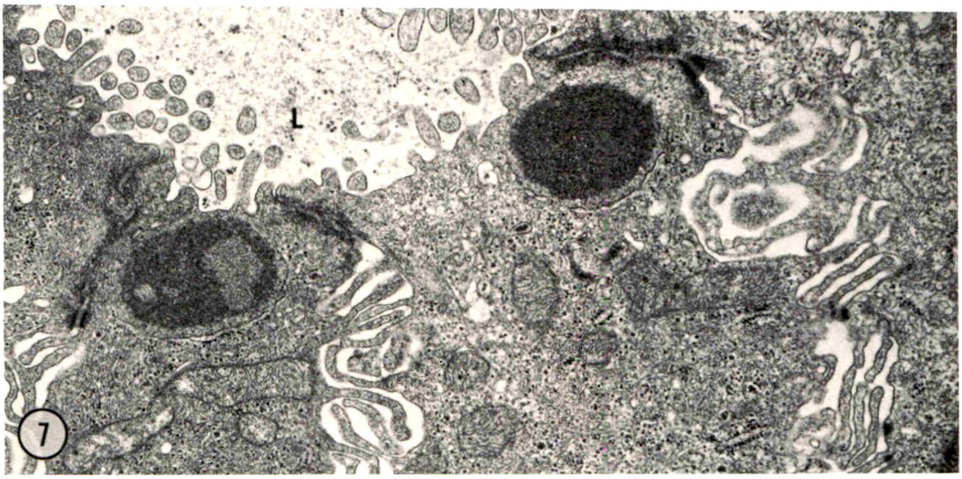
L
7

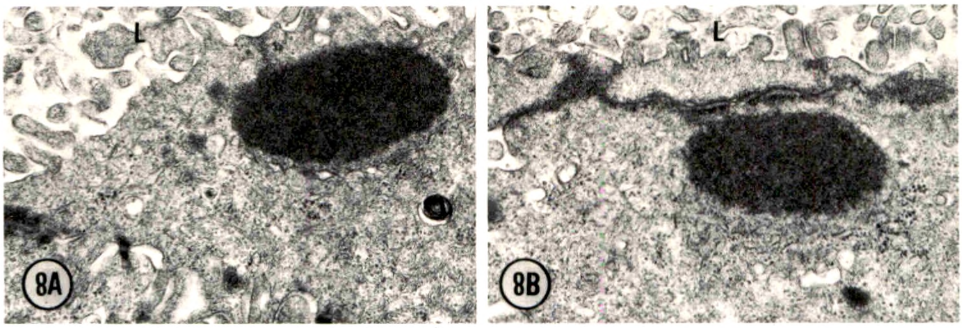
L
8A
L
8B

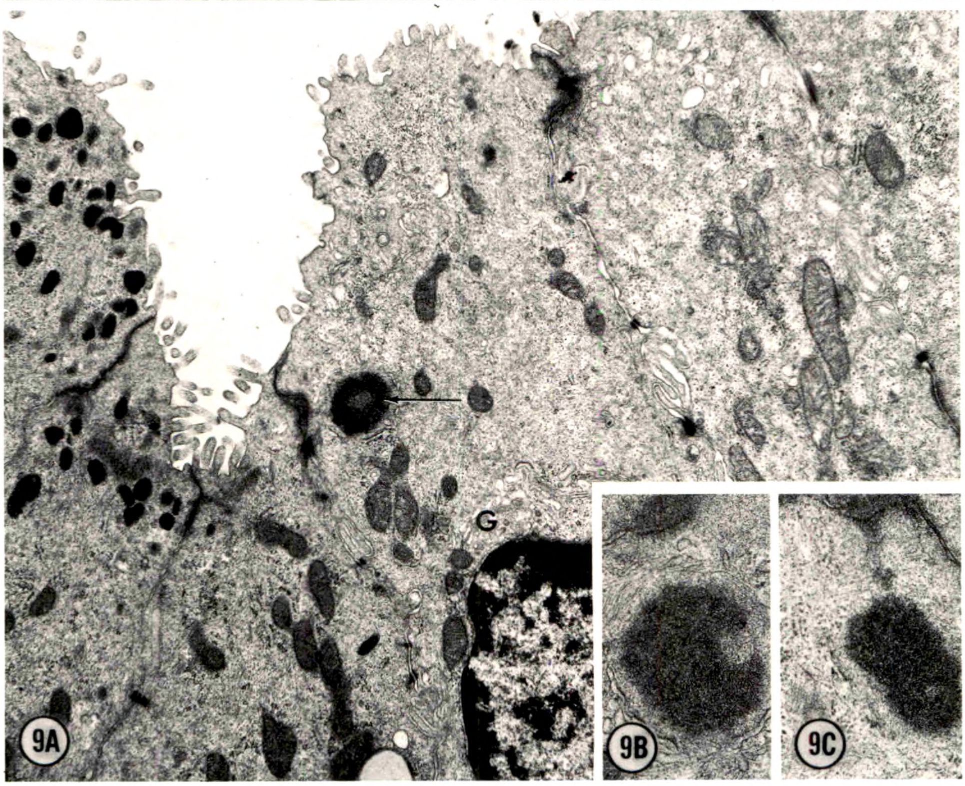
G
9A
9B
9C

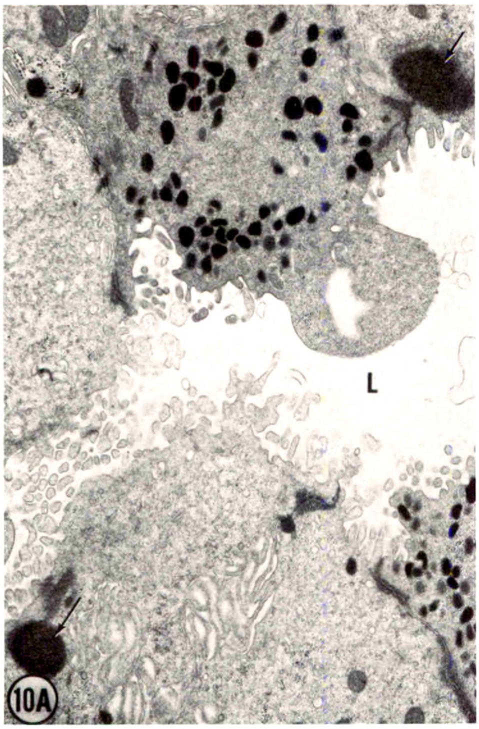
10A

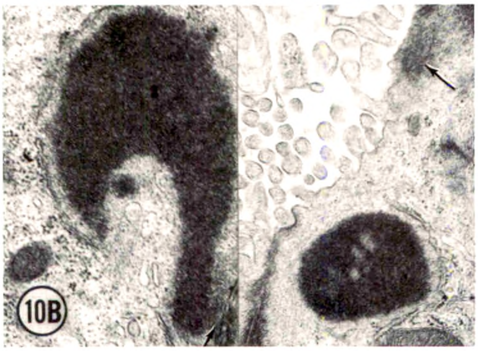
10B

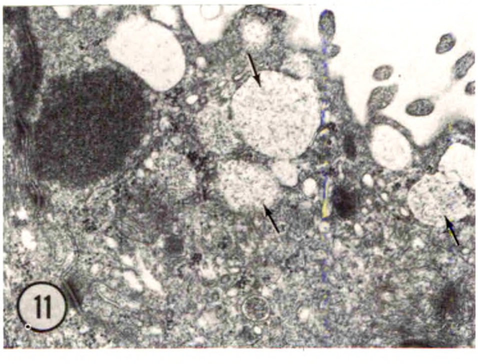
11

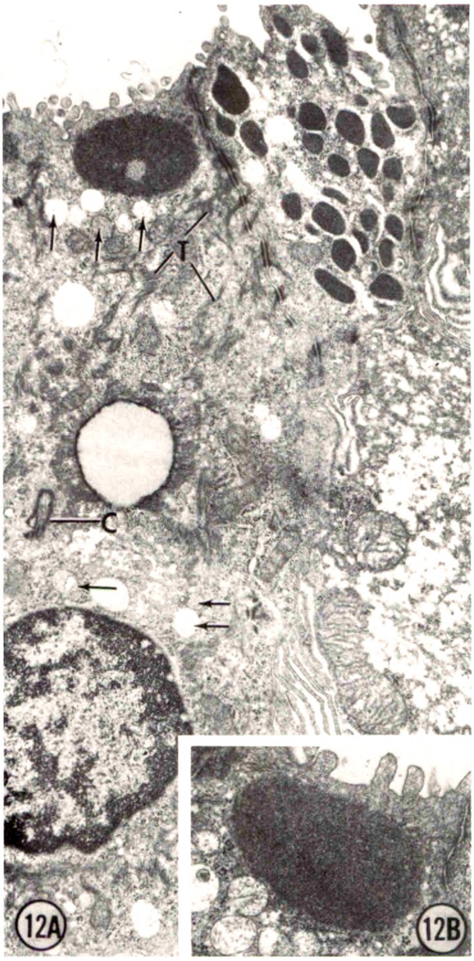
12A
12B

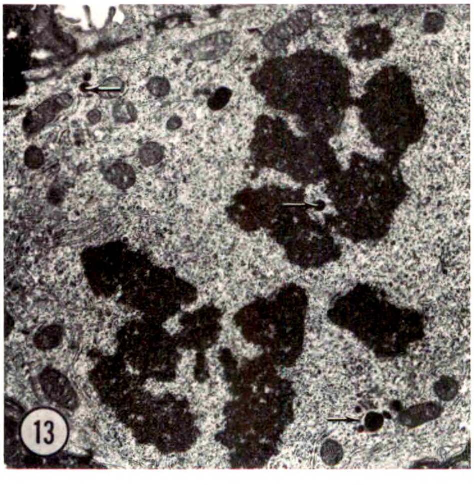
13

ANIMAL MODEL FOR HUMAN DISEASE

Amyloidosis

Animal Model: Spontaneous and Induced Amyloidosis

Contributed by: Alan S. Cohen, MD and Tsuranobu Shirahama, MD, Department of Medicine, Boston University Medical Center, Boston, Mass.

Biologic Features

Species Involved (Strains, Breeds, etc). Amyloid has been reported to occur spontaneously in a variety of animal species[1]—dogs,[2] cats,[3] mice,[4] birds[5] and many others. Several strains of mice (A/HeN, AALF, AL/N)[6] and the wild white Pekin ducks[7] are said to have a high spontaneous incidence.

Amyloidosis can be induced experimentally in many animal species—mice, hamsters, guinea pigs and rabbits, etc, although susceptibility to the amyloid-inducing regimen varies among species and strains.[6,8] Our present order of susceptibility to amyloid induction by casein injections in strains of mice is as follows: a) CBA/J, b) C57BL/6J, c) Swiss white (random bred from Charles River Laboratories), d) C_3H/Hej, e) Balb/cJ and f) SWR/J.

Clinical or Phenotypic Characteristics as Applicable. General weakness and loss of the body weight may occur, although there are no pathognomonic features. Animals may develop a nephrotic syndrome and associated illnesses; death from azotemia may occur.

Pathologic Features

Intercellular deposition of amyloid which by light microscopy has a hyalin eosinophilic appearance. It stains with Congo red and shows

---

Publication sponsored by the Registry of Comparative Pathology of the Armed Forces Institute of Pathology and supported by Public Health Service Grant RR-00301 from the Division of Research Resources, US Department of Health, Education and Welfare, under the auspices of Universities Associated for Research and Education in Pathology, Inc. Supported by Grants AM-04599 and TI-AM-5285 from the National Institute of Arthritis and Metabolic Diseases, US Public Health Service, and by the Massachusetts chapter of the Arthritis Foundation, The John A. Hartford Foundation and the Arthritis Foundation.

characteristic green birefringence under polarized light after such staining. It is PAS-positive and demonstrates crystal violet and methyl violet *metachromasia.*[1,9] In the electron microscope, amyloid *in situ* consists of characteristic fibrils approximately 100 A wide, indeterminate in length, rigid, nonbranching and often arranged in random array.[1,10] The deposition usually appears first in the perifollicular zone of the spleen, then in Disse's space in the liver and in the glomerular mesangial region in the kidney.[1,10]

When the animal is kept for a long period of time on an amyloid-inducing regimen, the deposition is wide-spread in a variety of organs, including the blood vessels.[10]

Essentials for Definitive Recognition. The recommended procedure for identification of amyloid deposits in tissue is: a) fixation of tissue in formalin, b) staining with alkaline Congo red, c) demonstration of the characteristic green birefringence for amyloid by polarizing microscopy and, if feasible d) demonstration of the characteristic amyloid fibrils by electron microscopy of osmium-fixed tissue sections (Figure 1).

Experimental Procedures used. A wide variety of methods for experimental induction of amyloidosis have been introduced.[1,4,10] At the present time, repeated injections of casein, as originated by Kuczynski in 1922,[11] seems to be an easily reproducible method. Generally, daily subcutaneous injections of 0.25 to 0.5 ml of 5 to 10% casein solution (which can be dissolved in approximately 0.05 N sodium hydroxide or 0.3 N sodium bicarbonate, with stirring and warming to 50 to 60 C) into mice usually produce amyloidosis in 3 to 4 weeks; 2 to 3 weekly injections of 1 to 2 ml of the casein solution into guinea pigs will induce amyloid within 2 to 4 months; while 2 to 3 weekly injections with 5 ml of the solution into rabbits will produce it within 3 to 5 months. These procedures, when established in a laboratory, are reproducible and induce amyloidosis in virtually 100% of the treated animals. Occasionally, longer periods of casein injection will be necessary before amyloid becomes apparent. However, the results are not always totally reproducible between laboratories; very subtle changes in the experimental conditions (for example, change of animal strains, change of the location of the laboratory, etc) can occasionally affect the induction of amyloid.[4]

Comparison with Human Disease

Differences From and Similarities with the Human Model. Experimentally induced amyloidosis in animals is comparable in virtually all respects with human amyloidosis[12] by histologic and electron microscopic standards.[1,4,10,12] It is likely that immunologic and biochemical differences will be discernible with future study.

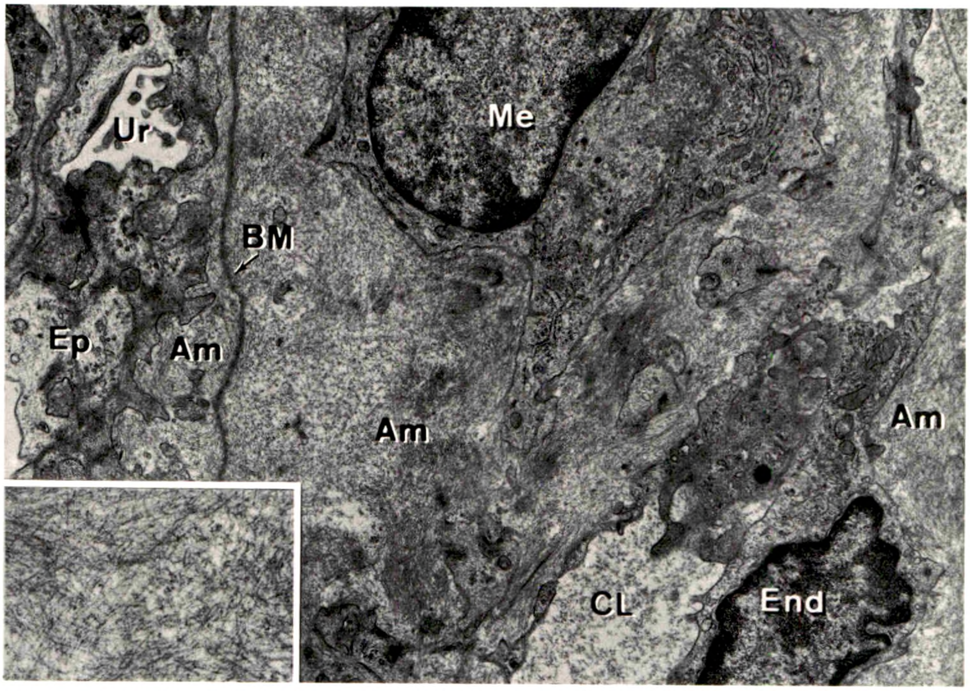

Fig 1—Amyloidosis experimentally induced by casein injections in a rabbit renal glomerulus. Am=amyloid fibrils, BM=basement membrane, CL=capillary lumen, End= endothelial cell, Ep=epithelial cell, Me=mesangial cell, Ur=urinary space (× 6000). **Inset**—A clearer demonstration of amyloid fibril structure (× 24,000).

Definitive Diagnosis. Recognition of amyloid deposition in the tissue, as defined by the appearance of green birefringence on polarization microscopy after Congo red staining.

Pathologic Features. As described above.

Problems Needing Solutions. More refined and faster methods for amyloid induction in reproducible fashion from laboratory to laboratory need to be established.

Usefulness and Availability of This Model

Since the model is quite comparable to human disease, it has been and can be used for studies of the course, pathogenesis and treatment of amyloid.

Animals (especially mice) suitable for experimental induction are readily available through commercial laboratories.

References

1. Cohen AS: The constitution and genesis of amyloid. International Review of

Erratum

McDowell, Elizabeth M: Light and electron microscopic studies of rat kidney after administration of inhibitors of the citric acid cycle *in vivo*. II. Effects of sodium malonate on proximal convoluted tubule. Am J Pathol 67:141–148, 1972.

Page 153 was inadvertently inverted in layout and Figures 9 and 10 are upside down, and numbered incorrectly. The entire page should be turned 180° and the numbers of the Figures switched.

The American Journal of
PATHOLOGY

is published by the Medical Department of Harper & Row, Publishers, under the auspices of The American Association of Pathologists and Bacteriologists and The American Society for Experimental Pathology, and is edited by a Board appointed by the Councils of the two Societies. It is devoted to the prompt publication of original observations and investigations in the field of pathology and microbiology and is published monthly in four volumes per year.

Information for Authors

ORIGINAL PAPERS will be considered for publication on condition that they are contributed solely to THE AMERICAN JOURNAL OF PATHOLOGY. Address manuscripts to the Editor-in-Chief: THOMAS D. KINNEY, MD, Department of Pathology, Duke University Medical Center, Durham, NC 27706.

MANUSCRIPTS must be typed **double-spaced** (including tables, references, and legends for figures), and all material should be submitted in duplicate. The literature should be summarized as concisely as is consistent with establishing the necessary basis for new material, and original observations should be presented in a clear, well-organized manner. Papers should rarely exceed 20 printed pages. Tables should be planned to suit the page size of THE JOURNAL. Excess tabular matter must be paid for by the contributor.

REFERENCES to the literature should be numbered in the order of citation in the text and should conform to the following style: names of all authors, complete title of article (including subtitle), abbreviated name of periodical (use *Index Medicus* style abbreviations), volume in Arabic numerals, inclusive pagination, and year (*eg*, 14:111–120, 1938). Titles are to be in the original language when they can be reproduced in the English alphabet. Translated titles should be enclosed in square brackets.

ILLUSTRATIONS must be planned to suit the page size of THE JOURNAL (**maximum plate size is 5¼ × 8 inches**) and should be submitted **unmounted,** with figure number, top, and author's name marked lightly on the back in soft pencil. Oversize illustrations should be avoided because handling of these delays publication. To be accepted, illustrations must reach a certain standard of excellence technically, present an attractive appearance, and add significantly to the value of the presentation. Marking lines and letters, if essential, must be kept at least ¼ inch inside all margins. If two or more illustrations are to appear on a page, they should be so trimmed that the edges may be butted and the outer margins squared. The legends for photomicrographs should state the staining method and the degree of magnification. Black and white illustrations will be furnished in moderate numbers. Excess illustrations, when accepted, and the cost of illustrations in color, must be paid for by the contributor.

REPRINTS: An order blank for reprints is sent with the proof.

Now, Automatic Quantitative Microscopic Image Analysis—from Zeiss!

We've added a unique precision scanning stage to our great optics, and the result is the most sophisticated system ever made for microphotometry. It's the Zeiss Scanning Microscope Photometer 05 for **all** types of photometric measurements in transmittance, absorbance, reflectance and fluorescence . . . and either on-line or off-line computer analysis. Cancer cytologists have already found it an invaluable tool . . . and other applications are developing daily in both the life sciences and industry.

Here's what this unusual system consists of:

A Zeiss Universal or Photomicroscope. Any analytical system that utilizes a microscope, no matter how sophisticated the electronics, cannot be any better than its optics allow. Information that's lost in the optical channels will not be retrieved in the electronic channels. That's why it's important to start with world-famous Zeiss optics.

A unique Zeiss precision scanning stage. The two available scanning stages allow, respectively, minimum increments of 0.5 and 10 microns, perform up to 200 steps per second, and travel 75mm and 25mm in the X and Y directions in several different scanning patterns, including meander, comb or line.

Much more. A modular electronic system that permits you to select components as you need them and as your budget permits. All the famous Zeiss accessories and photographic and analytical attachments—everything you might ever need for qualitative and quantitative microscopy—are, of course, available. We can even supply a PDP-12 computer with a number of programs prepared by well-known scientists. For the full story, write Carl Zeiss, Inc., 444 5th Ave., New York, N.Y. 10018. Or phone (212) 736-6070.

Nationwide Service.

ATLANTA, BOSTON, CHICAGO, COLUMBUS, DALLAS, DENVER, FORT LAUDERDALE, HOUSTON, KANSAS CITY, LOS ANGELES, PHILADELPHIA, PHOENIX, SAN FRANCISCO, SEATTLE, WASHINGTON, D.C.

digital PDP-12
ZEISS
THE GREAT NAME IN OPTICS
CARL ZEISS
WEST GERMANY

VOLUME 68 • NUMBER 3 / WHOLE NUMBER 364

The American Journal of PATHOLOGY

SEPTEMBER 1972

OFFICIAL PUBLICATION OF

THE AMERICAN ASSOCIATION OF PATHOLOGISTS AND BACTERIOLOGISTS • THE AMERICAN SOCIETY FOR EXPERIMENTAL PATHOLOGY

In this issue:

SUBACUTE SPONGIFORM VIRUS ENCEPHALOPATHIES: A review

BOARD OF EDITORS

Thomas D. Kinney, *Editor-in-Chief*
Donald B. Hackel, *Associate Editor*

Orville T. Bailey
Frederick F. Becker
Baruj Benacerraf
Kurt Benirschke
Kenneth M. Brinkhous
Joel G. Brunson
John R. Carter
Charles G. Cochrane
John M. Craig
Frank J. Dixon, Jr
John T. Ellis
Frank W. Fitch
Patrick J. Fitzgerald
David G. Freiman
Jack C. Geer
Gabriel Godman
John B. Hazard
Robert H. Heptinstall
Paul Kotin
Averill A. Liebow
Guido Majno
Donald G. McKay
Henry D. Moon
Councilman Morgan
Goetz W. Richter
David T. Rowlands, Jr
Edward A. Smuckler
Leon Sokoloff
Benjamin H. Spargo
Lewis Thomas
Jacinto J. Vazquez
F. Stephen Vogel

Editorial Assistant: Virginia Hotelling

MEDICAL DEPARTMENT • HARPER & ROW, PUBLISHERS

It takes time to refill, wash and replace animal watering bottles. Lots of time. You can save this time by switching to Hardco and eliminating your largest animal care nuisance and expense . . . bottles.

Small wonder that Hardco automatic watering systems have become so popular. Since 1963 over 500 organizations with animal facilities have switched. In fact, today Hardco equipment is installed in well over a million cages housing mice, rats, guinea pigs, hamsters, rabbits, primates and dogs.

There are two reasons for this acceptance. First, the Hardco dispensing valve is totally reliable. It's made entirely of stainless steel with only one moving part. This unique design is leakproof and seldom requires maintenance.

Secondly, you can be sure that a Hardco system will be ideally suited to your facility. Hardco staffs an engineering department that specializes in the design and installation of automatic watering systems — the only group of its kind in the country.

Isn't it time your organization kicked the bottle habit? Write for literature today.

hardco scientifi
division of fieldstone corporation
1709 Omni Drive, Cincinnati, Ohio 45245

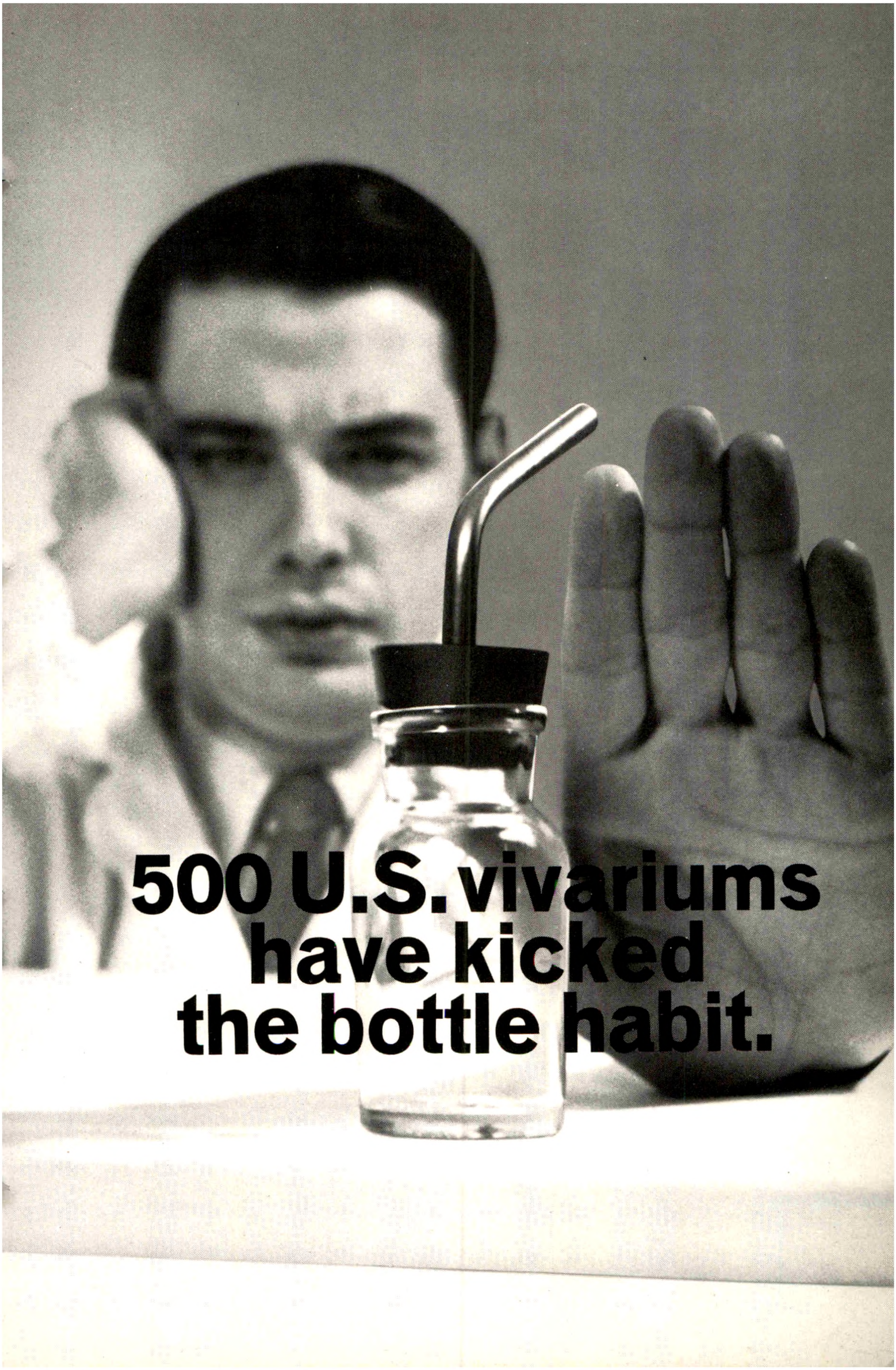
500 U.S. vivariums
have kicked
the bottle habit.

The new Reichert OmU3 Ultramicrotome:

exclusive darkfield alignment permits fast, one-pass positioning.

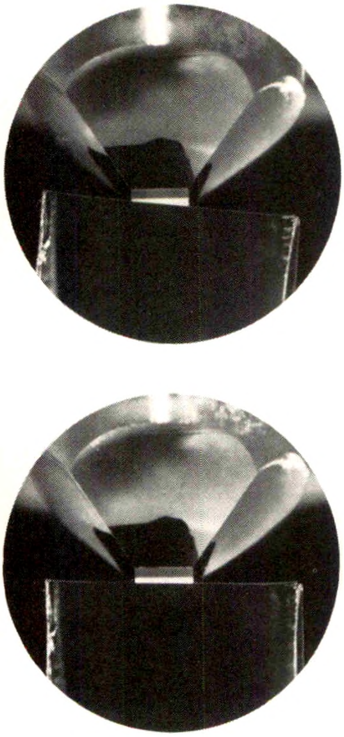

Through the microscope, the illuminated gap between specimen and knife is seen as a brilliant slit.

The new OmU3's unique darkfield alignment system enables the operator to position the knife in one pass, quickly and positively, without damaging specimen or knife. Its simple operation makes technician training easier, saves sectioning time, and greatly reduces the chance for error.

Another exclusive feature is instant start/stop thermal feed. Sectioning can be stopped and a section removed. Without delay or readjustment, sectioning may be resumed at the originally set thickness. Cutting and recycling speeds are controlled independently. Sections can be cut at slow speeds and recycled at a faster speed. The integral Reflexomat water pump allows filling the knife boat remotely to eliminate interruption of serial sections. For a convincing demonstration of the new Reichert OmU3, contact your American Optical representative and send for our new, detailed booklet.

AMERICAN OPTICAL
CORPORATION
SCIENTIFIC INSTRUMENT DIVISION • BUFFALO, N.Y. 14215

REICHERT
AUSTRIA

The American Journal of
PATHOLOGY

1971
1972

SEPTEMBER 1972 • Volume 68, Number 3

CONTENTS

447 Effects of Cationic Polypeptides on Thrombasthenic and Afibrinogenemic Blood Platelets
James G. White

461 Parathyroid Necrosis and Hypocalcemic Tetany Induced in Rabbits by L-Asparaginase
Francis V. Chisari, H. Donald Hochstein, Ruth L. Kirschstein and Edward B. Seligmann

469 Nuclear Localization of Immunoglobulins in Renal Biopsies of Patients with Lupus Nephritis
Ralph C. McCoy

479 Ultrastructural Changes in Muscular Dystrophy. I. Cardiac Tissue of Piglets Deprived of Vitamin E and Selenium
Phillip R. Sweeny and R. G. Brown

493 Ultrastructure of Muscular Dystrophy. II. A Comparative Study in Lambs and Chickens
Phillip R. Sweeny, J. G. Buchanan-Smith, F. deMille, J. R. Pettit and E. T. Moran

511 Scanning Electron Microscopy of Saccular Intracranial Aneurysms
O. Hassler

521 The Pulmonary Interstitial Cell as Immediate Precursor of the Alveolar Macrophage
Drummond H. Bowden and Ian Y. R. Adamson

SYMPOSIUM ON NEUTROPHIL PROTEASES AS MEDIATORS OF TISSUE INJURY

538 Introduction
Aaron Janoff

539 Leukocytic Proteases and the Immunologic Release of Lysosomal Enzymes
Gerald Weissmann, Robert B. Zurier and Sylvia Hoffstein

565 Role of Granulocyte Collagenase in Collagen Degradation
Gerald S. Lazarus, John R. Daniels, Jane Lian and Mary C. Burleigh

579 Human Granulocyte Elastase: Further Delineation of its Role in Connective Tissue Damage
Aaron Janoff

593 Pathologic Mechanisms in Neutrophil-Mediated Injury
Peter M. Henson

613 Leukocyte Kininogenases and Leukokinins from Normal and Malignant Cells
Lowell M. Greenbaum

625 REVIEW ARTICLE: Subacute Spongiform Virus Encephalopathies: Scrapie, Kuru and Creutzfeldt-Jakob Disease
Peter W. Lampert, D. Carleton Gajdusek and Clarence J. Gibbs, Jr

653 **Animal Model for Human Disease:** Adenocarcinoma
N. Baba and E. von Haam

---

657 Index of Subjects, Volume 68
661 Index of Authors, Volume 68

© 1972 by The American Association of Pathologists and Bacteriologists

The seal commemorates The Year of Pathology, being celebrated from October 1971 to October 1972 by the major national pathology societies. Special educational events will emphasize the expanding role of pathology and the medical laboratory in modern health care.

Medical Department • HARPER & ROW, PUBLISHERS

The American Journal of PATHOLOGY

GENERAL INFORMATION

Editorial Communications: All correspondence concerning editorial matters should be addressed to the Editor-in-Chief, DR. THOMAS D. KINNEY, Department of Pathology, Duke University Medical Center, Durham, N.C. 27706.

Business Communications: All subscriptions and advertising inquiries should be addressed to: MEDICAL DEPARTMENT, HARPER & ROW, PUBLISHERS, 2350 Virginia Ave, Hagerstown, Md. 21740.

Rates: THE AMERICAN JOURNAL OF PATHOLOGY is issued monthly, four volumes per year. Regular (individual) subscriptions: $27.50 per year in the U.S. and Possessions; $30.00 per year in Canada and countries of the Pan-American Postal Union; and $31.00 elsewhere. Special rate for Interns and Residents: $16.00 per year ($1.50 extra postage in Canada and countries of the Pan-American Postal Union; $2.50 extra postage elsewhere). Regular (individual) subscriptions and Resident and Intern subscriptions must be in the names of, and billed to, individuals. Institutional subscriptions, available to all libraries, schools, clinics, and hospitals, to all government agencies, local or national, and to all private or public institutions and organizations: $35.00 per year in the U.S. and Possessions; $37.50 per year in Canada and countries of the Pan-American Postal Union; $38.50 per year elsewhere. All subscriptions are payable in advance. Single copies, when available, $4.00.

Back Issues: Single issues and complete volumes of THE JOURNAL published prior to 1961 may be purchased from Walter J. Johnson, Inc., 111 Fifth Ave., New York, N.Y. 10003.

INDEX TO ADVERTISERS

American Optical Corporation 2
Dow Chemical Company, The . . . 10, 11
Hardco Scientific . . . . 2nd Cover, 1
Harper & Row, Publishers 12, 13, 14
The C. V. Mosby Company 6, 7
Nichols Institute for Endocrinology 9
Ortho Diagnostics 16
Sigma Chemical Company 15
Ivan Sorvall 5
Zeiss, Inc., Carl . . . . 4th Cover

MOVING?

To avoid interruption in your receipt of this Journal, we need to know your new address—six weeks in advance.

When writing us, be sure to type or print clearly your name and your new address—complete with zip code. It is *essential* that you also list your old address.

IMPORTANT: We publish a number of medical and scientific periodicals. Therefore, please be sure to give the name of THIS Journal when you write us.

Thank you for cooperating!

MEDICAL DEPARTMENT
Harper & Row, Publishers, Inc.
2350 Virginia Ave,
Hagerstown, Md. 21740.

(see page 8)

Published monthly by the Medical Department, Harper & Row, Publishers, Inc., 2350 Virginia Ave., Hagerstown, Md. 21740, and at 2901 Byrdhill Road, Richmond, Va. 23205. Second Class Postage paid at Hagerstown, Md., and additional mailing offices. Regular (individual) Rates: $27.50 per year in U.S. and Possessions, $30.00 in Canada and Pan-American Postal Union; and $31.00 elsewhere. Special Rates: Interns and Residents, $16.00 per year ($1.50 extra postage in Canada and countries of Pan-American Postal Union; $2.50 elsewhere). Institutional subscriptions; $35.00 per year in U.S. and Possessions, $37.50 per year in Canada and Pan-American Postal Unions; $38.50 elsewhere. Single copies, $4.00. Printed in U.S.A.

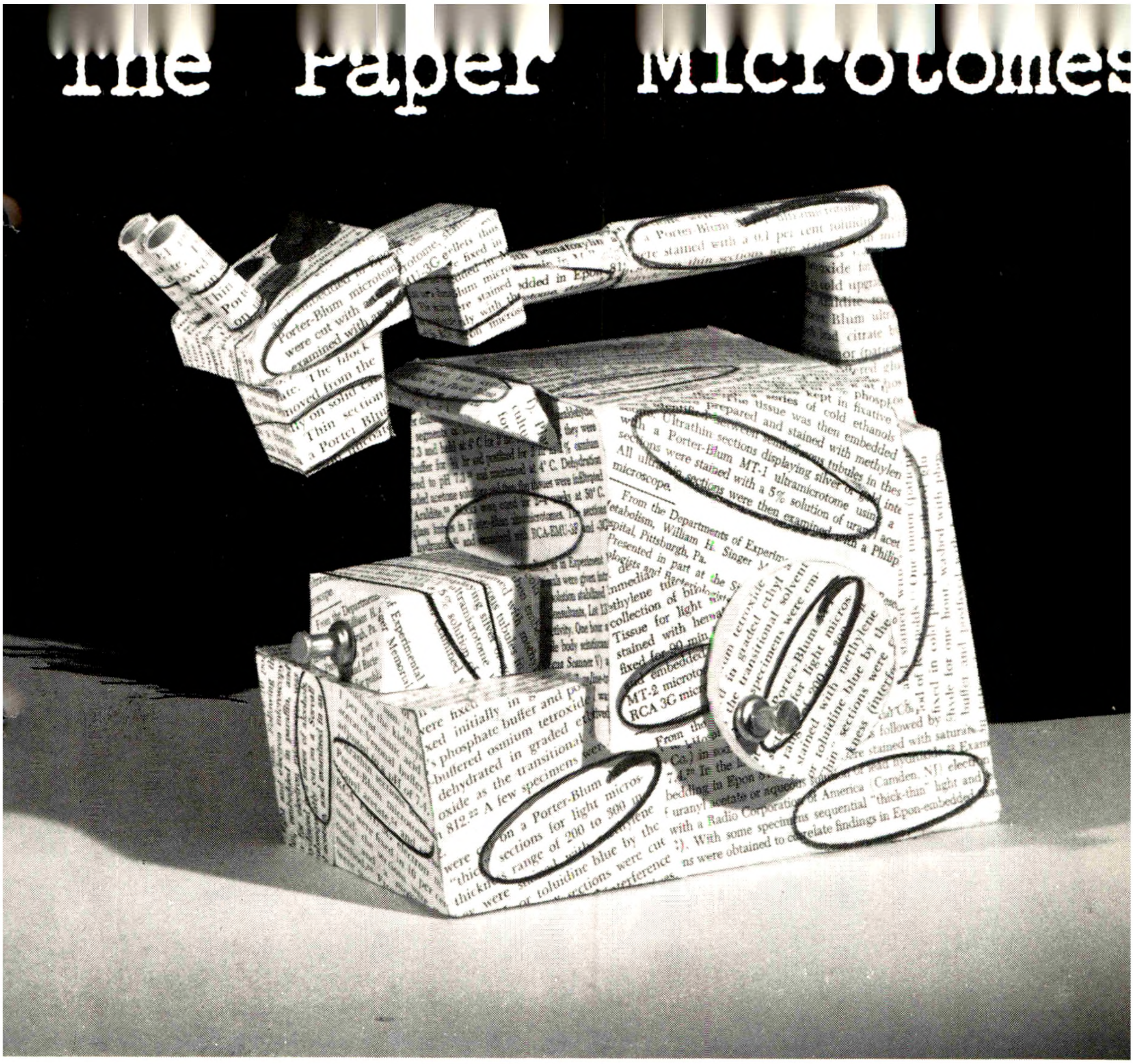

The "PORTER-BLUMS" are the "Paper" Microtomes

In scholarly paper after scholarly paper, where the "Materials & Methods" abstract discusses microtomy, you will find a "Porter-Blum" mentioned. The SORVALL "Porter-Blums" have earned a well-deserved reputation for reliability and accuracy that is unsurpassed by any other instrument in this field.

Also, ask for details on the "Smith & Farquhar" Tissue Sectioner for preparing fixed — and certain non-fixed — tissue; the FTS MT2-B (and older MT-2) Cryo-Sectioning Attachment; and the new JB-4 Microtome for clinical and research applications. Ivan SORVALL, Inc. Norwalk, Connecticut 06856.

SORVALL®

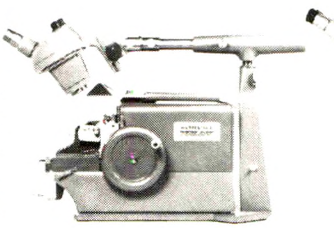

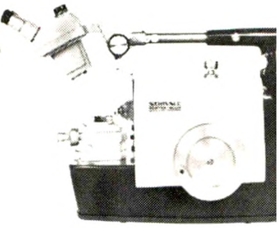

"PORTER-BLUM" MT-1, 25 mμ to ½ μ, is
ideal ultra-microtome for teaching and all rout
sectioning — and many of them have been in
forefront of important research advances o
many years.

"PORTER-BLUM" MT2-B, 10 Å to 4 μ, offers
highest precision sectioning in three operat
modes — automatic / semi-automatic / manu
The MT2-B is the most advanced instrument
ultra-microtomy available today.

Write for Bulletin JP-9F

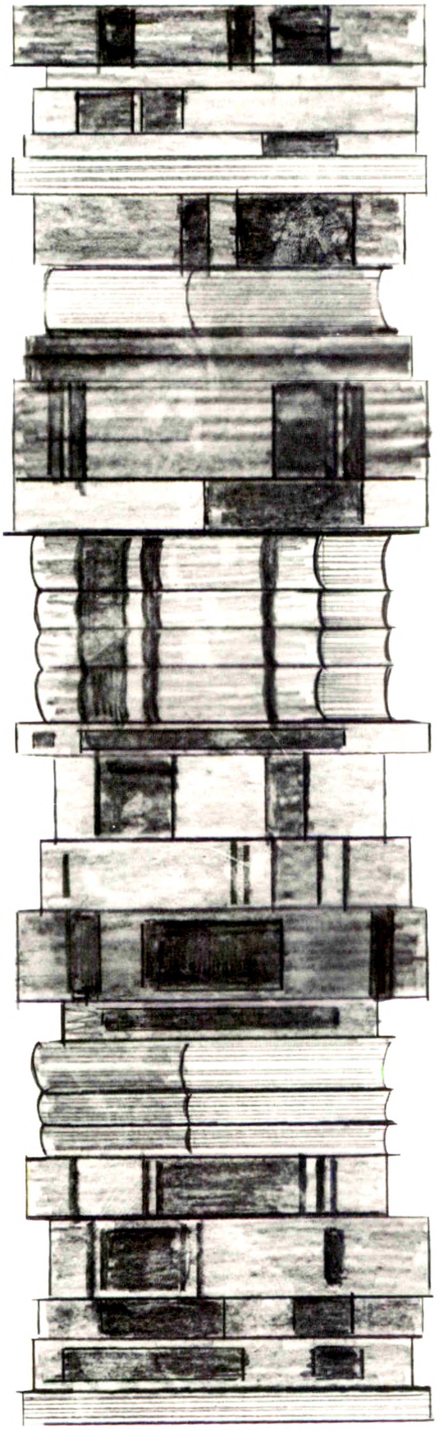

How does your library these new

New 8th Edition! **SYNOPSIS OF PATHOLOGY.** Thoroughly revised to incorporate recent advances in basic science and clinical medical knowledge, this survey clearly outlines general concepts of pathology, and examines each organ system. Topics include recent advances in histochemistry, enzymology, genetics, and immunology. *By W. A. D. Anderson, M.A., M.D., F.A.C.P., F.C.A.P.; and Thomas M. Scotti, A.B., M.D. July, 1972. 1,076 pages plus FMI-XII, 4⅞" x 7⅝", 430 illustrations and 3 color plates. Price $13.95.*

New 4th Edition! **BONE TUMORS.** This classic monograph stresses the need for precise diagnosis as the basis for effective treatment of bone tumors. Thoroughly revised discussions first examine general principles of pathologic classification and roentgenographic interpretation; the remaining chapters analyze 23 specific types of bone tumors and tumor-like lesions. *By Louis Lichtenstein, M.D. May, 1972. 441 pages plus FM I-XX, 6¾" x 9¾", 496 illustrations. Price, $24.50.*

A New Book! **PATHOLOGY OF THE CEREBRAL BLOOD VESSELS.** A comprehensive treatise on diseases of the blood vessels supplying the brain and spinal cord, this impressive new book reviews information from a wide and varied range of sources, appraises conflicting theories, and applies new information and concepts from general pathology and physiology to this specialized area. *By William E. Stehbens, M.D.(Syd.), D.Phil. (Oxon.), F.R.C.Path., F.R.C.P.A., M.R.A.C.P. May, 1972. 661 pages plus FM I-VIII, 7" x 10", 322 illustrations. Price $44.50.*

New 3rd Edition! **BLOOD DISEASES OF INFANCY AND CHILDHOOD.** This book, by an acknowledged giant in the field, supplies the practitioner with all the latest information on diagnosis, management and treatment of blood diseases in infants and children. Topics include transfusion, jaundice in newborns, Rh− incompatibility, sickle-cell anemia, etc. *By Carl H. Smith, M.A., M.D. September, 1972. Approx. 992 pages, 7" x 10", 175 illustrations, including 3 color plates. About $32.50.*

MOSBY

TIMES MIRROR

THE C. V. MOSBY COMPANY
11830 WESTLINE INDUSTRIAL DRIVE
ST. LOUIS, MISSOURI 63141 U.S.A.

stack up against Mosby references?

New 4th Edition! **LABORATORY MEDICINE: HEMATOLOGY.** Extensively revised, this exhaustive evaluation presents hematology from the standpoint of laboratory diagnosis and interpretation based on fundamental physiologic and pathologic mechanisms. The emphasis is placed on hematologic diagnosis rather than on treatment of blood diseases. *By John B. Miale, M.D. August, 1972. Approx. 1560 pages, 7¼" x 10½", 1399 illustrations and 37 plates, including 10 in color. About $26.50.*

New 2nd Edition! **PRACTICAL AUTOMATION FOR THE CLINICAL LABORATORY.** Expanded to almost twice the size of the first edition, this new revision now examines the automated systems used in every department of the clinical laboratory: blood banking, hematology, serology, microbiology, and cytology, as well as clinical chemistry. *By Wilma L. White, B.A., F.A.I.C.; Marilyn Erickson, B.S.; and Sue C. Stevens, B.A., M.A., Ph.D.; with 16 contributors. August, 1972. 591 pages plus FMI-XIV, 7" x 10", 387 illustrations. Price $22.50.*

A New Book! **TEXTBOOK FOR LABORATORY ASSISTANTS.** This introductory survey covers the essentials of the curriculum for Certified Laboratory Assistants. It provides full information on the nature of the assistant's responsibilities in easily understood terms, without unnecessary detail. Concise, simplified explanations and descriptions orient beginners to clinical laboratory organization, operation, and terminology. *By Irwin A. Oppenhein, M.D., F.C.A.P., F.A.S.C.P. March, 1972. 163 pages, 6" x 9", 79 illustrations. Price $4.90.*

A New Book! **AAOS SYMPOSIUM ON MYELOMENINGOCELE.** This volume presents a current overview of the treatment methods, techniques, and special problems of patients with this, and other related disorders. The viewpoints of 24 noted contributors are contained in this compendium, which also features a ten year follow up study of 267 myelomeningocele patients. *By the American Academy of Orthopaedic Surgeons; 24 contributors. September, 1972. Approx. 296 pages, 6¾" x 9¾", 216 illustrations. About $22.50.*

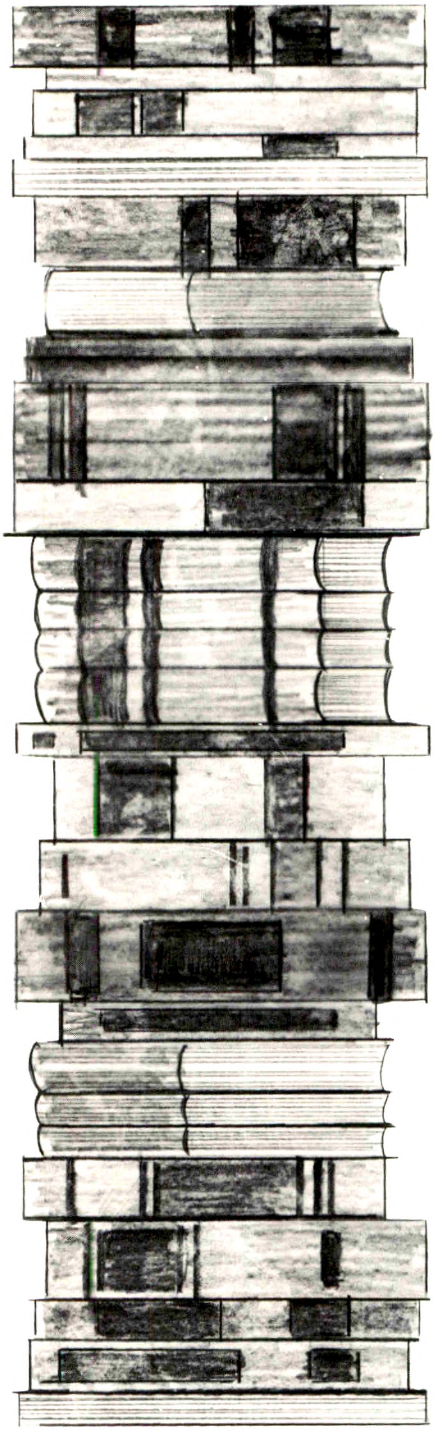

MOSBY

TIMES MIRROR

THE C. V. MOSBY COMPANY
11830 WESTLINE INDUSTRIAL DRIVE
ST. LOUIS, MISSOURI 63141 U.S.A.

Professional Opportunities

PHYSICIANS WANTED

STAFF PATHOLOGIST, DIVISION OF PATHOLOGY, Bureau of Foods, Food and Drug Administration, Washington, D.C. Applicant should have advanced training in pathology leading to a Ph.D., Masters Degree or Board Certification. Duties include collaborative studies in toxicologic experiments with food additives, contaminants, coloring agents and drugs. The incumbent will have the option to undertake independent (mission-oriented) research up to 50% of the time. An electron microscope is available in the Division. Starting salary range is $15,866 to $20,627 or higher depending on the applicant's qualifications. Major relocation expenses to Washington will be reimbursed. Send resume, including list of publications, or Federal application form, SF-171, to:

Morris A. Weinberger, M.D.
Director, Division of Pathology, BF-130
Food and Drug Administration
200 "C" Street, S.W.
Washington, D.C. 20204
OR TELEPHONE: AC (202) 962-3928

FDA—Where Equal Opportunity is the Rule

PHYSICIAN WANTED

WANTED—PATHOLOGIST QUALIFIED TO ASSUME full and sole responsibility in clinical and anatomic pathology for a small but enlarging department. Early partnership. Substantial fringe benefits with excellent non-contributory retirement program. Write or call Sam Packer, M.D., Medical Director, 11717 Euclid Avenue, Cleveland, Ohio 44106. Area Code 216, 795-4400.

CLASSIFIED ADVERTISING INFORMATION

RATES:

Non Display:	**1 Time**	**3 Times**	**6 Times or more**
20 words or less	$19.00	$16.00	$14.00
Each additional word	.50	.50	.50

Box Service—$2.00—First insertion only

Classified Display:	**1 Time**	**3 Times**	**6 Times or more**
	$35.00 per inch	$30.00 per inch	$25.00 per inch

Minimum Space—One (1) column inch

SEND ALL COPY,
AND BOX NUMBER INQUIRIES TO:

THE AMERICAN JOURNAL OF PATHOLOGY

Classified Dept.
P.O. Box 1510
617-A Cleveland Street
Clearwater, Florida 33517
Tele: 813-443-3047

CHANGING YOUR ADDRESS?

In order to receive your journal without interruption, please complete this Change of Address notice and forward to the Publisher, 60 days in advance, if possible.

Old Address: (PLEASE PRINT)

NAME____________________________

____

STREET____________________________

____

CITY____________________________

STATE (or Country)________________

ZIP CODE________________________

New Address: (PLEASE PRINT)

NAME____________________________

____

STREET____________________________

____

CITY____________________________

STATE (or Country)________________

ZIP CODE________________________

Date New Address Effective:____________

Name of Journal:____________________

NEW ADDRESS—MEDICAL DEPARTMENT

Harper & Row, Publishers, Inc.
Medical Department
2350 Virginia Avenue
Hagerstown, Maryland 21740

Academic researchers who pioneered many of the radioimmunoassays listed below are associated with the Nichols Institute for Endocrinology. They are not consultants. They are directly responsible for the correct performance of these tests.

T4-RIA (Total thyroxine)
T3-RIA (Triiodothyronine)
TBG Assessment (RT3U)
TBG-RIA
TSH-RIA (Thyroid stimulating hormone)
FT4 (Free Thyroxine-Dialysis)
Thyroid Screen -T4-RT3 Index (Adjusted T4) (T4 + TBG Assessment)
Hypothyroid Evaluation (T4 + TSH + TBG Assessment)
Hyperthyroid Evaluation (T4 + TBG Assessment + T3-RIA)
Aldosterone
Testosterone
Cortisol
Compound S (11-Desoxycortisol)
Metopirone Response (Cortisol + Compound S)
LH (Luteinizing Hormone)
LH + T (LH + Testosterone)
HGH (Human Growth Hormone)
Insulin
FSH (Follicle Stimulating Hormone)

The staff have also developed procedures that increase turnaround rate without compromising accuracy of results. For complete information, please contact Albert L. Nichols, M.D.

Nichols Institute for Endocrinology

250 East Pacific Coast Highway
Wilmington, California 90744
Tel: (213) 830-3870

Prepaid Air Mail:
P.O. Box 92797
World Way Postal Center
Los Angeles, California 90009

To protect her next baby…

Gamulin® Rh **$Rh_0(D)$ immune globulin (human)**

...complete with a disposable syringe
in a compact, space-saving package.

As a major producer of blood fractions, Dow now brings you a new source for $Rh_0(D)$ immune globulin to protect the Rh negative mother's next baby from probability of hemolytic disease.

Studies to demonstrate its safety and effectiveness show that Gamulin Rh is effective in suppressing the production of $Rh_0(D)$ antibodies.

And it comes in a space-saving, compact package that includes a vial, disposable syringe, lay literature, patient laboratory form, ID card, package insert and a crossmatch vial.

DESCRIPTION: GAMULIN Rh, $Rh_0(D)$ Immune Globulin (Human), is a sterile concentrated solution of gamma globulin derived from blood of human donors known to have antibodies to $Rh_0(D)$. It is standardized to contain 10.0 to 18.0 percent globulins with a level of antibody to $Rh_0(D)$ equal to or greater than that of the NIH Reference $Rh_0(D)$ Immune Globulin (Human). The final product contains 0.2 to 0.3 molar glycine as a stabilizer and 1:10,000 thimerosal as a preservative.

INDICATIONS: GAMULIN Rh suppresses the immune response of nonsensitized $Rh_0(D)$ negative mothers following Rh incompatible pregnancies. The criteria for an Rh incompatible pregnancy are: That the mother shall be $Rh_0(D)$ negative, D^u negative; and the infant shall be $Rh_0(D)$ positive or D^u positive.

CONTRAINDICATIONS: Gamulin Rh must not be given to the infant. Gamulin Rh also should not be administered to an $Rh_0(D)$ positive or D^u positive individual, to a recipient of an $Rh_0(D)$ positive blood transfusion, or to an $Rh_0(D)$ negative mother previously sensitized by an Rh incompatible pregnancy. Do not give intravenously.

PRECAUTIONS AND REACTIONS: It is essential that certain diagnostic and laboratory criteria be met before administering this product. (See package literature.) An occasional patient has shown a systemic reaction manifested by a low grade fever. Allergic reactions, although not expected, could occur.

ADMINISTRATION: Consult package insert for detailed instructions.

This product must be administered within 72 hours postpartum.

Gamulin® Rh
$Rh_0(D)$ immune globulin (human)

DOW

THE DOW CHEMICAL COMPANY
Rx Pharmaceuticals
Indianapolis

Laboratory

it's brand new now...
and
for years to come,
it will stay that way...

Medicine

Editor: George J. Race, M.D., M.S.P.H., Ph.D., Pathologist-in-Chief and Director of Laboratories, Baylor University Medical Center, Dallas, Texas.

Associate Editors: Clinical Pathology—Samih Y. Alami, M.D., Ph.D. Hematology—Eugene P. Frenkel, M.D. Chemistry—Robert J. Speer, Ph.D., Harold H. Varon, M.D., and Joel E. Young, Ph.D. Microbiology—Ralph Tompsett, M.D. With 100 Contributors.

In Four Volumes. **Here is a new exhaustive coverage presented for the first time as a loose-leaf reference. The dynamic loose-leaf concept means that your three volumes will always be new and updated through the ANNUAL SERVICE. *Volume 1* is entirely devoted to Clinical Chemistry, including the most modern automated techniques in use. *Volume 2* concerns Hematology, Blood Banking, Medical Microbiology, Virology, Serology, and Immunology. *Volume 3* covers Special Techniques (with modern methods and approaches to forensic pathology). *Volume 4* includes Body Fluids including Urine, Cytology and Cytogenetics, and Laboratory Management and Function. A separate annually revised index is included. *For all the future information coming out in the various fields covered in these volumes, it is a worthwhile investment for knowledge and practice.***

ANNUAL SERVICE includes:

"New pages for old." **Partially or completely rewritten monographs, addenda and chapters on new subjects supplied annually along with a completely revised index.**

HARPER & ROW, Publishers, Inc. *Medical Department*
2350 Virginia Avenue Hagerstown, Maryland 21740

☐ **Please send more information on LABORATORY MEDICINE**

LABORATORY MEDICINE (4 volumes, index volume & 1st yr. Annual Service): About $175.00.

About $27.50 a year thereafter for Annual Service. (Terms Available)

☐ **Bill me @ full price.** ☐ **Bill me @ $______a month *(minimum $10.00 a month)***

Name . . . .

Address . . . .

City . . . . **State** . . . . **Zip** . . . . AJP-9.

DERMAL PATHOLOGY

This new work presents current concepts of dermal pathology including related embryology, anatomy, histology, electron microscopy and histochemistry. The highly illustrated text is divided into five sections, with the first section providing basic information and defining the special language of dermal pathology. The other four sections consist of: inflammatory dermatoses; granulomatous dermatoses; nevi and neoplasms; and reticuloendothelial and alternative dermatoses.

The diseases are arranged according to histopathologic features, with disorders presenting similar histopathologic changes grouped together. This approach stresses the differential diagnosis and emphasizes the differentiating features between diseases. The discussion of each disease includes a brief description of gross pathology or clinical morphology, histopathologic characteristics, pertinent histochemistry, the differential diagnosis, and a short clinical description. This book should enable the reader to improve his ability to diagnose skin lesions and to understand the pathogenesis of the diseases discussed.

With 17 Contributors. Edited by **James H. Graham, M.D.,** Professor of Medicine (Dermatology), Department of Medicine; Chairman, Division of Dermatology; Professor of Pathology, Department of Pathology; and Director, Section of Dermal Pathology, University of California, Irvin; **Waine C. Johnson, M.D.,** Professor of Dermatology, Department of Dermatology; Associate Professor of Pathology, Department of Pathology, Temple University School of Medicine; Director of Laboratories, the Skin and Cancer Hospital of Philadelphia, Philadelphia; and **Elson B. Helwig, MD.,** Chief, Department of Pathology and Branch of Dermal Pathology, Armed Forces Institute of Pathology, Washington, D.C.

1,155 Illustrations, 77 in full color

Available in October. Advance orders now accepted.

HARPER & ROW, PUBLISHERS *Medical Department*

Mail Order Department, 2350 Virginia Avenue, Hagerstown, Maryland 21740

When published, please send me on approval: AJP9

GRAHAM, JOHNSON & HELWIG: Dermal Pathology $45.00

NAME ______________________

____

ADDRESS ______________________

____

CITY ______________ STATE ______________ ZIP ________

Available from SIGMA — manufactured by SIGMA

DPN-DIAPHORASE

(NAD-Diaphorase)

Technicon Reference No. 0193

For the Colorimetric determination of LDH per AutoAnalyzer®, AA-II®, and SMA® Procedures. Reconstitute with water to prepare "working solution".

Order: **Stock No. 940-3** 25 ml lyophilized vial $ 7.75
40 ml lyophilized vial 10.50
Larger quantities - Inquire - We guarantee the best prices.
CIF Destination Anywhere in the World via Air

For those laboratories that prefer to prepare their own blend, we offer the finest NAD and Diaphorase individually and at most competitive prices.

Also available from SIGMA — manufactured by SIGMA

MDH/NADH

(DPNH/MDH; NADH/MDH)

Technicon Reference No. 0444

For the Ultraviolet determination of SGOT per AA-II® and SMA® Procedures. Reconstitute with water to prepare "working solution".

Order: **Stock No. 936-3** 50 ml lyophilized vial 12 vials $37.50
Larger quantities - Inquire
CIF Destination Anywhere in the World via Air

If you prepare your own blend, call Sigma for the highest purity NADH (DPNH) and MDH (Malic Dehydrogenase).

® - Registered Trade Marks of Technicon Corporation

DON'T YOU BELIEVE the false rumors being circulated by a misguided competitor who claims that he is the only basic manufacturer of Diaphorase and certain other reagents.

SIGMA is the World's Foremost manufacturer of most of the important Enzymes and Substrates used in Automated and Manual Procedures. All of the above DIAPHORASE, DPN, DPNH, and MDH are produced by SIGMA.

Our Quality is guaranteed to be TOPS; our Prices are guaranteed to be BOTTOM!

It's a pleasure doing business with Sigma

ORDER DIRECT — TELEPHONE COLLECT from ANYWHERE in the WORLD
Day, **Station to Station, 314-771-5750** (Including Saturday and Sunday until 1 P.M.)
Night, **Person to Person**, Dan Broida, **314-993-6418**
TWX [Teletype] Day or Night: COLLECT 910-761-0593
TELEGRAM: SIGMACHEM, Saint Louis, Missouri

The Research Laboratories of
SIGMA® CHEMICAL COMPANY
P.O. BOX 14508 • SAINT LOUIS, MISSOURI 63178 U.S.A.
MANUFACTURERS OF THE FINEST BIOCHEMICALS AVAILABLE

Distributed through:
SIGMA LONDON Chem. Co. Ltd. • 12, Lettice St., London, S.W.6., England • Telephone: 01-736-5823 (Reverse Charges)
SIGMA ISRAEL Chem. Co. Ltd. • 28 Kaf-Gimel St., Givataim, Israel • Telephone: 03 760654 (Reverse Charges)

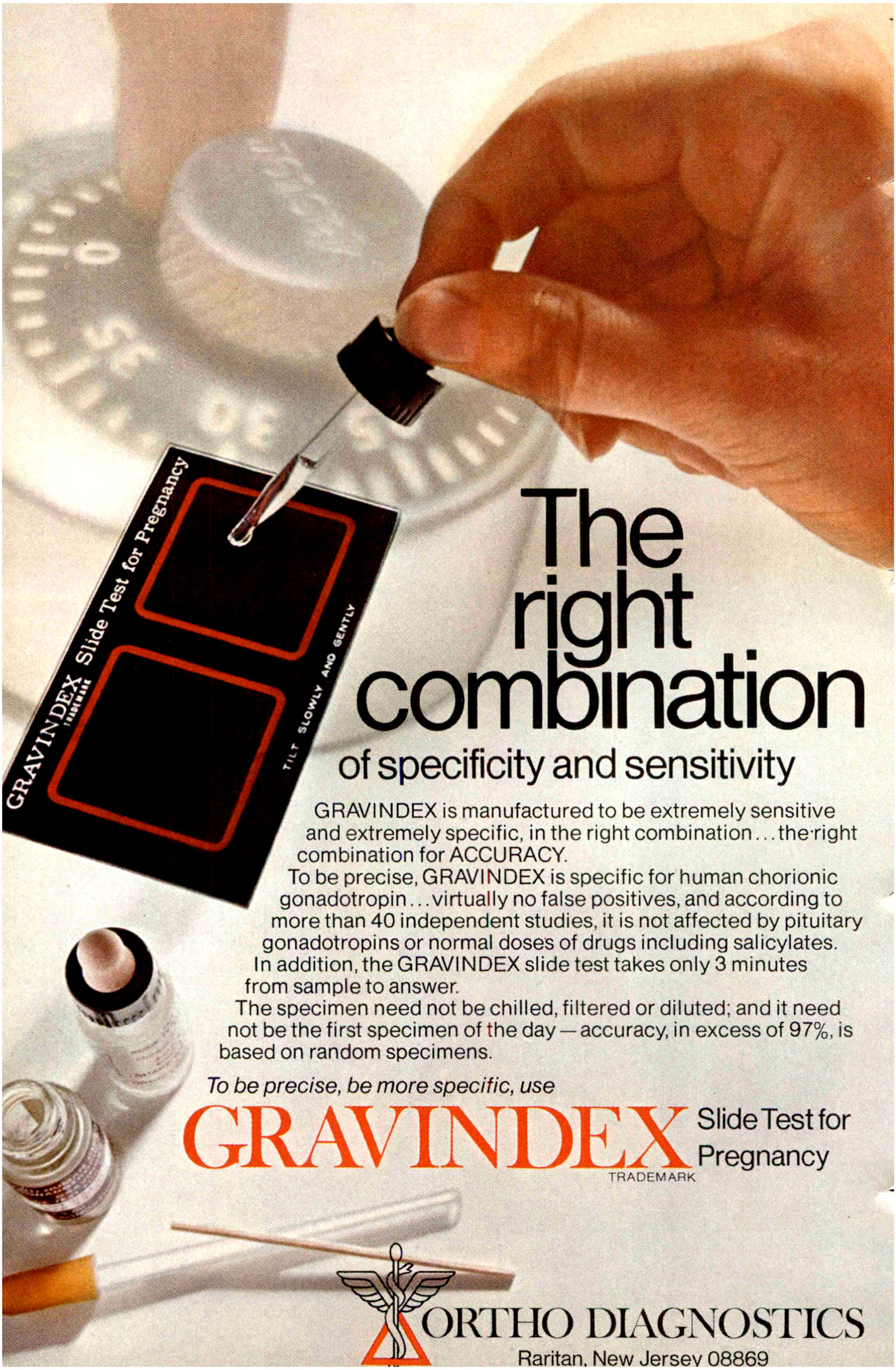

The right combination

of specificity and sensitivity

GRAVINDEX is manufactured to be extremely sensitive and extremely specific, in the right combination... the right combination for ACCURACY.

To be precise, GRAVINDEX is specific for human chorionic gonadotropin... virtually no false positives, and according to more than 40 independent studies, it is not affected by pituitary gonadotropins or normal doses of drugs including salicylates.

In addition, the GRAVINDEX slide test takes only 3 minutes from sample to answer.

The specimen need not be chilled, filtered or diluted; and it need not be the first specimen of the day — accuracy, in excess of 97%, is based on random specimens.

To be precise, be more specific, use

GRAVINDEX Slide Test for Pregnancy
TRADEMARK

ORTHO DIAGNOSTICS
Raritan, New Jersey 08869

The American Journal of
PATHOLOGY

SEPTEMBER 1972 • Volume 68, Number 3

Effects of Cationic Polypeptides on Thrombasthenic and Afibrinogenemic Blood Platelets

James G. White, MD

Cationic polypeptides are known to cause the conversion of fibrinogen to fibrin gel and the immediate aggregation of blood platelets. In the present study, the effects of the cationic polypeptides, polybrene and polylysine, on normal, afibrinogenemic and thrombasthenic platelets were examined by nephelometry and electron microscopy. Normal and afibrinogenemic platelets aggregated rapidly and irreversibly after exposure to either agent. Thus, fibrinogen was not an essential factor for the interaction, though it may facilitate the rate of clumping produced by polybrene or polylysine. Thrombasthenic platelets did not aggregate rapidly or irreversibly in the presence of either agent. Shape change and slight degrees of clumping were induced by the cationic substances, a response essentially identical to the reaction of thrombasthenic platelets to collagen. The failure of cationic polypeptides to cause immediate aggregation of thrombasthenic platelets was not due to a failure of the agents to interact with the abnormal cells. Electron microscopy revealed that normal, afibrinogenemic and thrombasthenic platelets all adsorbed polybrene and polylysine, and transferred the agents to intracellular organelles (Am J Pathol 68:447–460, 1972).

THE INHERITED BLEEDING DISORDERS, congenital afibrinogenemia and thrombasthenia, differ in pathogenesis and clinical manifestations, but share one unusual feature: a marked deficiency of platelet fibrinogen.[1-3] The reduced level of coagulant protein increases the amount of adenosine diphosphate (ADP) required to aggregate afibrinogenemic platelets, a defect which is corrected by small amounts of

---

From the Department of Pediatrics, University of Minnesota Medical Center, Minneapolis, Minn.

Supported by Grants HE-11880, AI-05153, CA-08832 from the US Public Health Service and the Cardiovascular Clinical Research Program Project.

Accepted for publication Feb 11, 1972.

Address reprint requests to Dr. James G. White, Department of Pediatrics, University of Minnesota, Box 284 Mayo Memorial Building, Minneapolis, Minn 55455.

fibrinogen.[4] Human fibrinogen does not correct the insensitivity of thrombasthenic platelets to aggregation by ADP, but the abnormal cells will aggregate in the presence of bovine fibrinogen.[5] These findings have suggested that the interaction of platelet surfaces with fibrinogen may be an important factor in the development of stickiness.[6]

The cationic polypeptides, polylysine, and polybrene, have been utilized in recent studies to cause non-thrombin-dependent polymerization of fibrinogen to fibrin gel [7] and to stimulate aggregation of blood platelets.[8-10] Just as in the case of collagen, free ε-amino groups on the polypeptides are required for their effect on platelet clumping, but the aggregating influence is not dependent on ADP, calcium, metabolic energy or the platelet release reaction.[11] It appeared from these studies that cationic polypeptides might be useful for evaluating the aggregation of abnormal platelets. The present report describes the action of polylysine and polybrene on afibrinogenemic and thrombasthenic platelets observed by nephelometry and electron microscopy.

Materials and Methods

This laboratory obtained blood samples by a two syringe technic; the samples were immediately mixed with 3.8% trisodium citrate or citrate citric acid anticoagulant, and the platelet-rich plasma (C-PRP) was separated by centrifugation at 100 g for 20 minutes at room temperature. Platelet-poor plasma (PPP) was prepared by sedimentation of C-PRP for an additional 20 minutes at 200 g; the platelet count of the C-PRP was adjusted to 3.0×10^5/cu mm by appropriate dilution with PPP.[12-15] A Chronolog model S 201 platelet aggregometer coupled to a Bausch and Lomb VOM-5 recorder was employed to study platelet aggregation. The baseline of the tracing was preset with C-PRP, and the maximum upward deflection of the recording pen with PPP. Samples of C-PRP were placed in a 37 C water bath for at least 5 minutes before being placed on the aggregometer, where they were stirred at a constant rate of 1200 rpm and maintained at 37 C. Aggregating agents in graded amounts were diluted in 0.1 ml buffered salt solution or distilled water and blown from a pipette directly into 0.9 ml samples of C-PRP on the aggregometer. The methods used for fixation of platelet samples in glutaraldehyde followed by osmic acid, dehydration in a graded series of alcohols and embedment in Epon 812 have been detailed previously.[12,16] Contrast of the thin sections was enhanced by staining with uranyl acetate and lead citrate. Observations were made in a Philips 200 electron microscope.

In the present study, blood was obtained from normal donors who had not taken drugs for at least 10 days before study, from 3 siblings with thrombasthenia, and 1 patient with congenital afibrinogenemia. Some clinical and laboratory data on the patients were reported previously,[17-19] and will be dealt with more extensively in a future publication. The platelets of the 3 children with thrombasthenia are typically unresponsive to ADP, but adhere normally to collagen. Clot retraction has been variable,[17] but with an improved method appears regularly absent or slight. The child with afibrinogenemia has been studied for the presence of platelet and plasma fibrinogen with several different methods.[18,19] By immunodiffusion and microimmunoelectrophoresis she has less than 1 mg% (10 μg/ml) of fibrinogen in her plasma and none detectable in her platelets; assays of all other clotting factors have been normal. Platelet counts and morphology have been normal in repeated studies on all 4 patients.

Polylysine and polybrene were diluted in Tris-buffered saline and added to samples of normal and patient C-PRP to final concentrations of 0.1, 0.5 and 1.0 mg/ml while the samples were stirred on the aggregometer. In other experiments the same amounts of polylysine and polybrene were layered on the surface of undisturbed samples of normal and patient C-PRP, and incubated at 37 C for 30 or 60 minutes. At the end of the incubation the samples were prepared for study in the electron microscope.

Results

Addition of polylysine and polybrene, at any of the three concentrations employed in this study, to samples of normal C-PRP resulted in a rapid increase in light transmission, indicating platelet aggregation, as previously described.[8–11] The aggregation produced by these agents was irreversible, unless heparin (10 units/ml C-PRP) was added to the system shortly after the occurrence of aggregation.

Platelets from the patient with afibrinogenemia did not develop a first or second wave of aggregation with epinephrine (5.5×10^{-6}M); underwent shape change but did not aggregate in response to serotonin (1×10^{-4}M); required 10 to 100 times the usual concentration of ADP (2.5×10^{-6}M) to produce irreversible platelet aggregation; and developed a single, irreversible wave of aggregation when collagen was added to the C-PRP (Text-figure 1). These findings are similar to those reported by Weiss and Rogers.[4]

Addition of polybrene and polylysine at concentrations of 0.1, 0.5 and 1.0 mg/ml of C-PRP caused aggregation in platelet samples from the afibrinogenemic patient (Text-figure 2). Onset of the increase in light transmission was slightly delayed and the slope of rise less abrupt in afibrinogenemic C-PRP than in samples of normal platelets exposed to the same amount of cationic polypeptide. As a result, the tracings from afibrinogenemic platelet samples resembled the pattern of reaction observed when collagen suspension was added to the abnormal cells. Despite these small differences, the two agents stimulated the same complete irreversible aggregation of afibrinogenemic cells that they produced in samples of normal C-PRP.

Samples of C-PRP from the patients with thrombasthenia did not develop a first or second wave of aggregation in response to epinephrine (5.5×10^{-6}M), but did undergo shape change; the samples aggregated only slightly, or not at all, in the presence of serotonin (1×10^{-5}M), ADP (10^{-6} to 10^{-3}M), thrombin (0.2 μ) and bacteria (S *aureus*

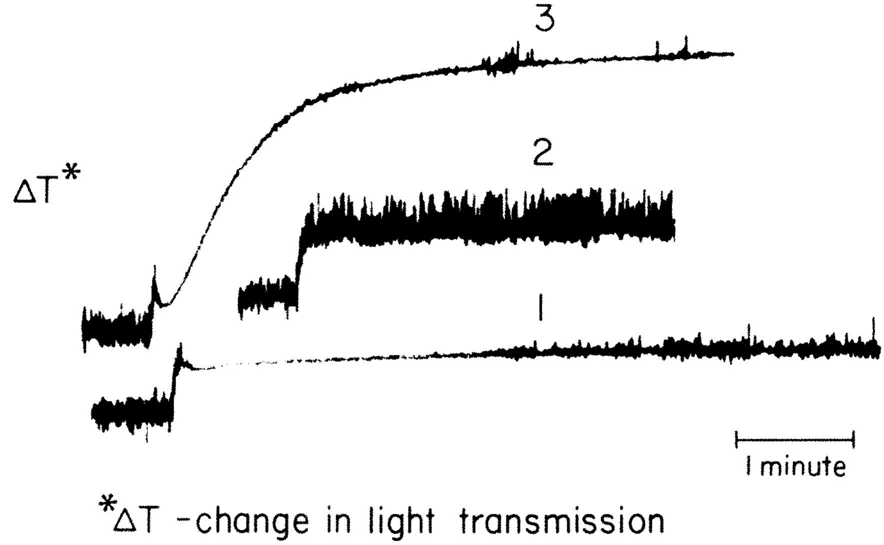

TEXT FIG 1—Tracings recorded after addition of various aggregating agents to samples of citrate platelet-rich plasma (C-PRP) from a patient with afibrinogenemia. The samples were stirred constantly at 37 C, and the maximum deflection of the recording pen preset with platelet-rich and platelet-poor plasma. Upward deflection of the pen indicates an increase in light transmission due to aggregation. Tracing one *(1)* was obtained following addition of serotonin at a final concentration of 1 × 10^{-4}M. The initial upward movement of the pen results from dilution of the sample when the agent is added. Serotonin caused a narrowing of the baseline indicating platelet shape change, but aggregation did not develop. The cells recovered their disc form within a few minutes, as indicated by restoration of the oscillating character of the baseline. The second tracing *(2)* was recorded after addition of epinephrine in a final concentration of 5.5 × 10^{-6}M to C-PRP from the patient. Epinephrine did not cause shape change or aggregation. Adenosine diphosphate (ADP) at a concentration of 1 × 10^{-4}M caused irreversible aggregation of the patient's C-PRP, but smaller amounts produced only a single wave which reversed completely.

502A 6 × 10^8). Collagen induced shape change and a slight increase in optical density, suggesting minimal aggregation on the aggregometer (Text-figure 3). These findings are characteristic of thrombasthenic platelets evaluated by nephelometry.[3]

Addition of polybrene or polylysine to samples of C-PRP from the 3 patients with thrombasthenia produced tracings resembling those produced by combining thrombin, ADP, or collagen with their platelets (Text-figure 4). The baseline of the tracing narrowed, indicating a shape change, and in some cases rose slightly, suggesting the formation of a few aggregates. However, the increase in light transmission was usually no greater than that produced by other potent aggregating agents added to platelet samples from the children with thrombasthenia.

Examination of samples of normal, afibrinogenemic and throm-

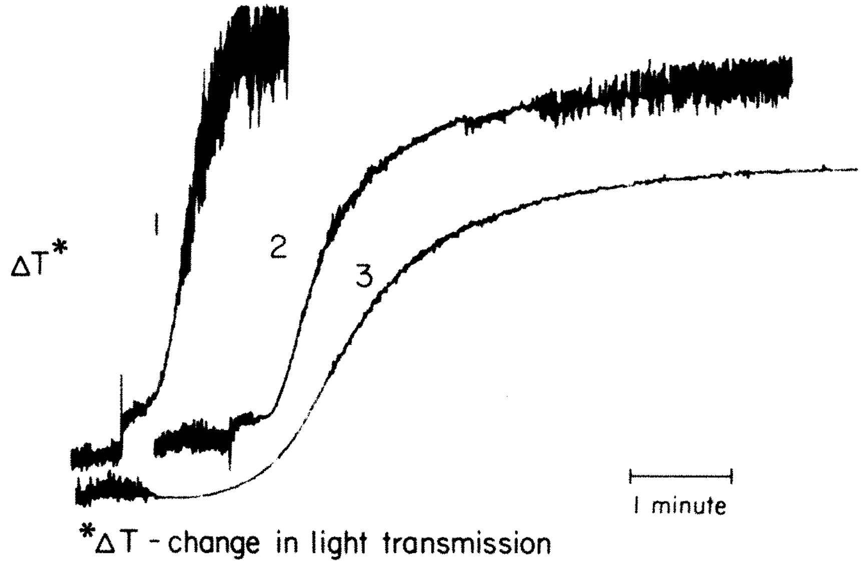

TEXT FIG 2—The first tracing *(1)* was obtained following addition of polylysine (0.1 mg) to a sample of normal C-PRP. An identical amount of polylysine added to C-PRP from the patient with afibrinogenemia produced the second tracing *(2)*. Aggregation began immediately in the normal sample and quickly reached a maximum. Clumping was delayed slightly in the afibrinogenemic sample, and took longer to reach the stage of maximum irreversible aggregation. The response of afibrinogenemic platelets to collagen *(3)* is similar to normal C-PRP, but slightly more collagen is frequently required to produce the typical reaction. A delay phase, followed by narrowing of the baseline, is characteristic of the collagen response before upward deflection takes place. The response of afibrinogenemic platelets to polylysine resembles the response to collagen, but is more rapid.

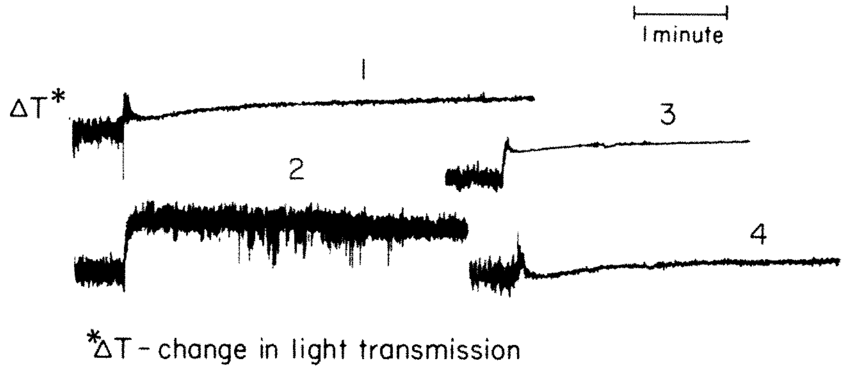

TEXT FIG 3—Recordings obtained from samples of thrombasthenic C-PRP after exposure to various aggregating agents. Epinephrine (5.5×10^{-6}M) failed to cause shape change or aggregation in Sample two (*2*). Thrombin (0.2μ) in Sample one (*1*), serotonin 1×10^{-5}M) in Sample three (*3*), and ADP (1×10^{-5}M) in Sample four (*4*) caused the thrombasthenic platelets to develop a shape change. Progressive, though slight upward deflection of the recording pen in these tracings suggested that minimal aggregation may have occurred.

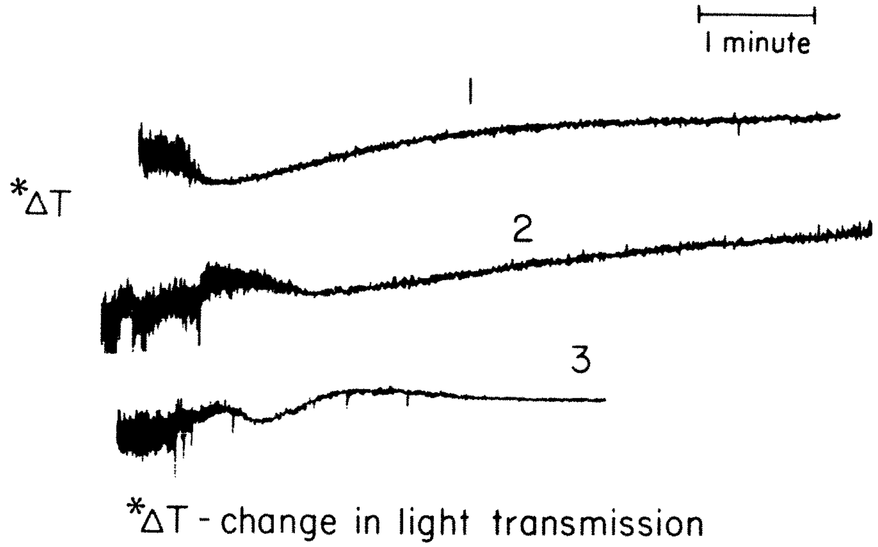

TEX FIG 4—The first tracing *(1)* was recorded following addition of collagen to C-PRP from a patient with thrombasthenia. Delay and shape change developed normally, but massive aggregation did not occur. The slow rise in optical density following shape change may indicate the formation of a few small aggregates. Polylysine (0.1 mg) produced an almost identical tracing in thrombasthenic C-PRP *(2)*. The third tracing *(3)* was obtained after adition of polybrene (0.1 mg) to C-PRP from a second patient with thrombasthenia. The cationic polypeptides cause shape change, but fail to stimulate immediate irreversible aggregation of thrombasthenic platelets.

basthenic C-PRP incubated with polylysine or polybrene for 30 to 60 minutes in the electron microscope revealed identical alterations in all three types (Figures 3A, 3B, 4A, 4B). The cationic polypeptides were taken up by the platelets and concentrated in granules and dense bodies. During this process the platelets developed the shape change and internal transformation usually observed following exposure of normal cells to thrombin or collagen, but did not aggregate. Formation of the dark coat on platelet surfaces described by others[11] was not prominent in this study, but the presence of cationic polypeptide in platelets was easily identified by a peculiar change in platelet internal structure. The agents caused swelling of the granules, formation of a lattice-like structure in the matrix of the organelles and increased staining of dense bodies. This type of effect on platelet granules and dense bodies has not been observed previously with other chemical agents. The influence on platelets was more marked at higher concentrations of polylysine and polybrene and increased on longer incubation. There were no apparent differences in the response of normal, afibrinogenemic or thrombasthenic platelets to incubation with the cationic polypeptides.

Discussion

Lalezari and Spaet[8] originally recognized the capacity of a cationic polypeptide, polybrene, to induce platelet clumping, and suggested that agglutination was probably due to neutralization of platelet surface charge and binding of cells by the long chain polymer. Subsequently, several other workers have evaluated the effects of polybrene and other polybases on blood platelets.[9-11] Their investigations indicate that cationic polypeptides reduce the electrophoretic mobility of platelets and cause aggregation which is independent of cations, occurs without platelet shape change or secretion of endogenous chemical constituents, and does not require metabolic energy from the cells. In a comprehensive study, Jenkins *et al*[11] noted that polylysine caused immediate, irreversible clumping, and that aggregated platelets formed a tight mosaic with electron-dense material between cells and coating surface membranes.

Zucker and her colleagues[20] were apparently the first to study effects of a cationic polypeptides on abnormal platelets. In their report on platelet function in thrombasthenia, they noted, without comment, that 0.5 mg polybrene/ml C-PRP caused 4+ aggregation of normal platelets, but failed to clump thrombasthenic cells. The French workers, Vainer, *et al*,[21] have recently examined the effects of cationic polypeptides on afibrinogenemic and thrombasthenic platelets. Their findings suggest that polylysine fails to aggregate afibrinogenemic platelets, but causes some clumping of the cells from patients with thrombasthenia.

The investigation described in this report was undertaken prior to publication of the French study, and differs from it sufficiently to warrant further discussion of the subject. Our patient with congenital afibrinogenemia has been followed since early childhood. Her levels of plasma and platelet fibrinogen have always been less than the smallest amount detectable by the most sensitive chemical and immunochemical methods available. The results of her platelet aggregation studies are consistent with the findings obtained in other patients profoundly deficient in fibrinogen.[4] Yet, in sharp contrast to the observations of the French workers,[21] the addition of small amounts of polylysine or polybrene to stirred samples of her C-PRP on the platelet aggregometer resulted in complete irreversible aggregation. The onset of aggregation was slightly delayed and the rate of change in optical density less rapid in afibrinogenemic platelet samples than in normal C-PRP combined with the same amount of polypeptide. It is possible, therefore, that the presence of fibrinogen facilitates the response of platelets to polybrene and polylysine, just as it increases the sensitivity of afibrinogenemic platelets to ADP and other agents. However, it is apparent that fibrinogen is not an essential cofactor for the aggregation of platelets from our patient with afibrinogenemia.

The only known biochemical defect in thrombasthenic platelets, aside from insensitivity to aggregation by ADP, is a marked reduction in their level of fibrinogen.[1-3] Since cationic polypeptides clump platelets in the absence of calcium, ADP, metabolic energy [11] and (as shown in this study) fibrinogen, it seemed worthwhile to examine the influence of polybrene and polylysine on thrombasthenic platelets. Addition of either cationic polyelectrolyte, at any of the three concentrations, chosen for study, to platelet samples from 3 patients with thrombasthenia failed to cause the complete irreversible aggregation observed in normal and afibrinogenemic C-PRP. Shape change developed following exposure to either agent. The baseline remained narrow and did not rise in most samples; in some a slight increase in light transmission developed, indicating formation of a few platelet aggregates. However, the change in optical density and rate of the rise were no greater or more rapid than with other potent aggregating agents capable of inducing the platelet release reaction stimulated in similar samples of thrombasthenic platelets. In fact, the tracings recorded in samples of thrombasthenic C-PRP, after adding one of the cationic polypeptides, were indistinguishable from those produced by collagen. These findings indicate that thrombasthenic platelets are insensitive to immediate aggregation by cationic polypeptides, just as the work of Zucker *et al* [20] indicated several years ago. In addition, our results reveal that polybrene and polylysine can cause platelet shape change and subsequent minimal aggregation identical to effects produced by collagen and thrombin in thrombasthenic C-PRP,[22] even though the cationic agents do not produce immediate clumping.

The evidence suggesting that cationic polypeptides interact with thrombasthenic platelets, even though they do not cause immediate aggregation, was supported by observations in the electron microscope. Normal, afibrinogenemic and thrombasthenic platelets incubated with various concentrations of polybrene and polylysine for 30 or 60 minutes revealed marked changes in form and internal structure. Polylysine and polybrene were taken up by the platelets and deposited in the matrix of granules and dense bodies. Granules became more swollen in appearance and developed an unusual lattice-like arrangement of their matrix. The darker zone of granules and the platelet dense bodies appeared more resistent to transmission of the electron beam after uptake of cationic polypeptides. Changes of this type have not been produced by other chemical substances and occur in only one platelet disorder, the carcinoid syndrome.[23] The alterations in platelet form and internal organization which developed during incubation, however, were similar to those caused by other agents capable of stimulating platelet release.[22] Incubation for 1 hour with the highest concentration of polyelectrolyte caused morphologic damage to some platelets, but the majority of cells appeared to remain intact despite marked alterations in form and and internal structure. No differences were apparent in the reaction of normal, afibrinogenemic or thrombasthenic platelets to incubation with cationic polypeptides in the unstirred system.

The nephelometric and ultrastructural findings in this investigation of the reaction of afibrinogenemic and thrombasthenic platelets to cationic polypeptides suggest that the drug–cell interaction, at least in plasma, may be more complex than has been indicated previously.[8–11] Polylysine does cause immediate irreversible aggregation of normal platelets, but the response of afibrinogenemic platelets, though ultimately complete and irreversible, is retarded slightly and develops at a less rapid rate. This pattern is typical of the decreased sensitivity of afibrinogenemic platelets to other aggregating agents[4] and suggests that fibrinogen, though not essential, may facilitate the immediate aggregation of normal platelets by cationic polypeptides.

Previous studies have shown that cationic polypeptides coat platelet surfaces with an electron-dense layer,[11] and have suggested that the agents promote aggregation by adhering to the negatively charged cells, reducing net negative charge and forming bridges between adjacent platelet membranes, thereby resulting in development of closely molded masses of cells.[8–11] The surface charge of thrombasthenic platelets, as measured by electrophoretic mobility, does not appear to differ significantly from that of normal cells.[24] Since the influence of cationic polypeptides on platelet clumping appears related to surface charge and is independent of ADP (to which thrombasthenic cells are refractory) it seemed, in theory, that polylysine and polybrene should cause immediate irreversible aggregation of thrombasthenic platelets. This was not the case; the two agents regularly failed to induce immediate clumping in C-PRP from patients with thrombasthenia, though they did cause slight rises in light transmission after the development of platelet shape change. Collagen and thrombin produce the identical sequence of changes as polylysine and polybrene in samples of thrombasthenic platelets, suggesting that the cationic polypeptides are capable of stimulating the same platelet reaction as the more potent aggregating agents. Thrombasthenic platelets adhere to collagen and undergo the release reaction, but aggregate only slightly, due to their insensitivity to secreted ADP.[3,20] Both collagen and cationic polypeptides interact with platelets through ε-amino groups on their surfaces; Massini and Luscher have shown that the cationic agents can stimulate the physiologic platelet release reaction.[25] The ultrastructural studies of this investigation have shown that thrombasthenic platelets take up cationic polypeptides in the same manner as normal and afibrinogenemic cells, and that the process of uptake is associated with the shape change and internal reorganization found in platelets after exposure to aggregating agents which stimulate the release reaction.[22] A subsequent report will demonstrate that cationic polypeptides cause the release of intact granules and dense bodies from normal and abnormal platelets.[26]

Immediate aggregation by neutralization of surface charge and formation of bridges between platelets by coating layers of polypeptide polymers may be involved in the rapid clumping of normal cells.[8-11] Yet the failure of thrombasthenic platelets to repond in the same manner as normal cells suggests that the proposed mechanism may be inadequate to explain the actual sequence of events occurring at the platelet surface. If the polypeptides did not adhere to thrombasthenic platelets, the explanation offered would still be plausible. However, the present study has demonstrated that cationic polypeptides not only stick to thrombasthenic platelets, but are deposited in intracellular organelles and cause the shape change and internal transformation which occurrs after exposure of normal or thrombasthenic platelets to agents which stimulate aggregation and the release reaction. Jenkins *et al* [11] have shown that inhibitors of release, such as aspirin, prostaglandin E_1 and adenosine monophosphate, do not affect aggregation of platelets by polylysine, and that polylysine-induced aggregation does not stimulate platelet release. The report of Massini and Luscher [25] and our results [26] indicate that polylysine can and does cause release of endogenous platelet constituents.

In the present study the effects of cationic polypeptides on afibrinogenemic and thrombasthenic platelets appeared identical to the influence of collagen. Whether or not the failure of cationic polypeptides to aggregate thrombasthenic platelets is due to the same defect which prevents their aggregation by collagen remains to be determined. The important consideration for the present is that cationic polypeptides fail to cause immediate aggregation of thrombasthenic platelets and can be used to probe the defect in the surface of these cells which makes them refractory to the influence of adenosine diphosphate. These studies are in progress.

References

1. Zucker MB: Platelet adhesion release, and aggregation. Thromb Diath Haemorrh 13 (Suppl):301–303, 1964
2. Hugues FB, Lapiere CM: Nouvelles rescherches sur l'accolement des plaquettes aux fibres de collagene. Thromb Diath Haemorrh 11:327–336, 1964
3. Cronberg S: Abnormal behavior of platelets. Platelet Aggregation. Edited by J Caen. Paris, Masson et Cie, 1971 pp 185–191
4. Weiss HJ, Rogers J: Fibrinogen and platelets in the primary arrest of bleeding: studies in two patients with congenital afibrinogenemia. N Engl J Med 285:369–374, 1971
5. Caen JP, Cronberg S, Levy-Toledano S, Kubisz P, Pinkhas J: New data in Glanzman's thrombasthenia. Proc Soc Exp Biol Med 136:1082–1086, 1971
6. Mason RG, Read MS, Brinkhous KM: The adhesion of platelets to glass: effect of fibrinogen concentration. Proc Soc Exp Biol Med 137:680–682, 1971
7. Biezunski N, Shafrir E, de Vries A, Katchalski E: The action of polylysine on the conversion of fibrinogen into fibrin by coagulase thrombin. Biochem J 59:55–64, 1955
8. Lalezari P, Spaet TH: Antiheparin and hemagglutinating activities of polybrene. J Lab Clin Med 57:868–873, 1961
9. Schneider W, Kubler W, Gross R: Induction of blood platelet aggregation by catonic polypeptides. Thromb Diath Haemorrh 19:307, 1968 (abstr)
10. Grottum KA: Platelet surface charge and aggregation: effects of polyelectrolytes. Thromb Diath Haemorrh 21:450–462, 1969
11. Jenkins CSP, Packham MA, Kinlough-Rathbone RL, Mustard JF: Interaction of polylysine with platelets. Blood 37:395–412, 1971
12. White JG: Effects of colchicine and vinca alkalaids on human platelets. III. Influence on primary internal contraction and secondary aggregation. Am J Pathol 54:467–478, 1969
13. White JG: A biphasic response of platelets to serotonin. Scand J Haematol 7:145–151, 1970
14. Clawson CC, White JG: Platelet interaction with bacteria. I. Reaction phases and effects of inhibitors. Am J Pathol 65:367–380, 1971
15. Clawson CC, White JG: Platelet interaction with bacteria. II. Fate of the bacteria. Am J Pathol 65:381–398, 1971
16. White JG: Fine structural alterations induced in platelets by adenosine diphosphate. Blood 31:604–622, 1968
17. White JG, Yunis E, Colliander M, Krivit W: The correction of prolonged bleeding times in two brothers by platelet transfusion despite normal *in vitro* platelet tests. Pediatrics 33:579–587, 1964

18. White JG, Krivit W: Platelet viscous metamorphosis in a child with total afibrinogenemia. Thromb Diath Haemorrh 13:4, 1964 (abstr)

19. Owen CH, Thompson, JH: Prothrombin utilization in congenital coagulation deficiency states. Thromb Diath Haemorrh 25:297–311, 1971

20. Zucker MB, Pert JH, Hilgartner MW: Platelet function in a patient with thrombasthenia. Blood 28:524–534, 1966

21. Vainer H, Jeanneau C, Booyse FM, Wassermann N: Platelet-polyelectrolyte interaction.[3] pp 137–146

22. White JG: Platelet morphology, The Circulating Platelet. Edited by SA Johnson. New York, Academic Press, Inc., 1971 pp 45–121

23. White JG, Davis RB: Alterations in platelet ultrastructure in patients with carcinoid syndrome. Am J Pathol 56:519–531, 1969

24. Zucker MB, Levine RU: Microelectrophoresis of washed and unwashed human blood platelets, with additional studies of platelets from patients with von Willebrand's disease and thrombasthenia. Thromb Diath Haemorrh 10:1–17, 1963

25. Massini P, Luscher EF: On the importance of close cell contact for initiation of the release reaction of blood platelets. Second International Congress on Thrombosis and Haemostasis, Oslo, 1971, p. 234 (abstr)

26. White JG: Exocytosis of secretory organelles from blood platelets incubated with cationic polypeptides. Am J Pathol 1972 (In press)

Fig 1—Platelet from a sample of afibrinogenemic C-PRP incubated with polylysine at a final concentration of 0.5 mg/ml for 30 minutes. The cell has lost its discoid form, and internal transformation is apparent. Granules *(G)* are swollen, and have an unusual organization of their matrix seen only after exposure to cationic polypeptides. The circumferential microtubules *(MT)* have shifted toward the cell center, but remain intact. Mitochondria *(M)* and other cell structures are altered slightly (× 41,500).

Fig 2—Platelet from afibrinogenemic C-PRP incubated with polybrene at a final concentration of 0.5 mg/ml. Most of the granules *(G)* are swollen due to concentration of polybrene in their matrix. The basis for lattice formation in granules is unknown. Dense portions of granules in platelets exposed to polylysine or polybrene appear more electron opaque than in untreated cells (× 39,400).

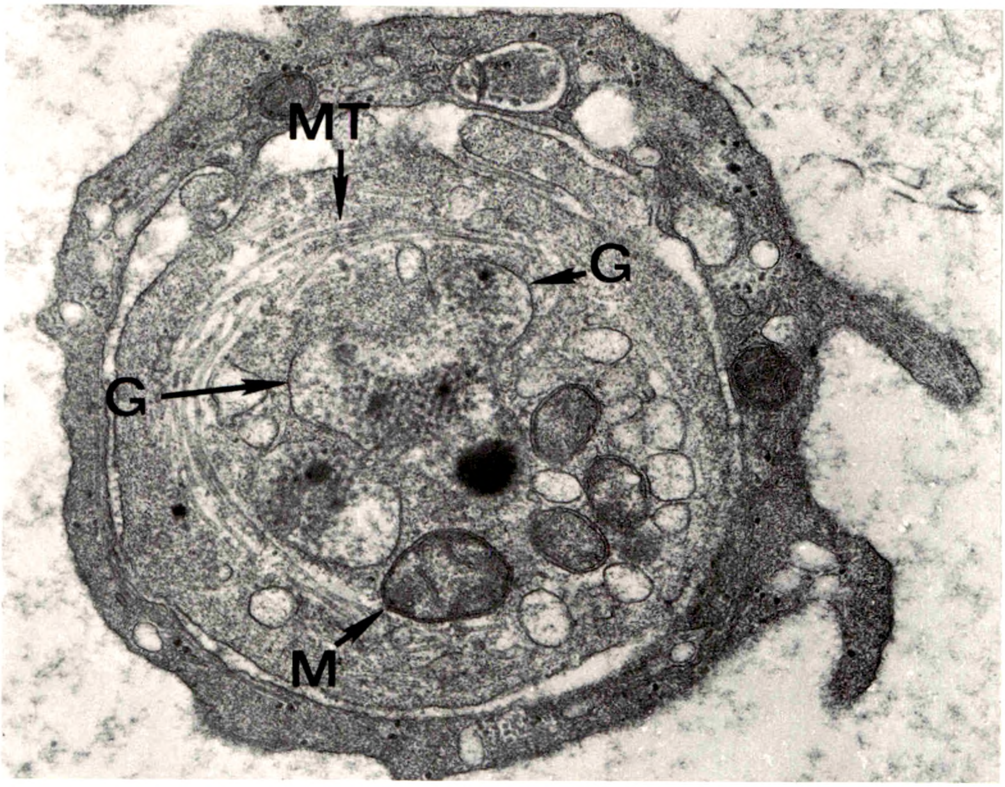

1

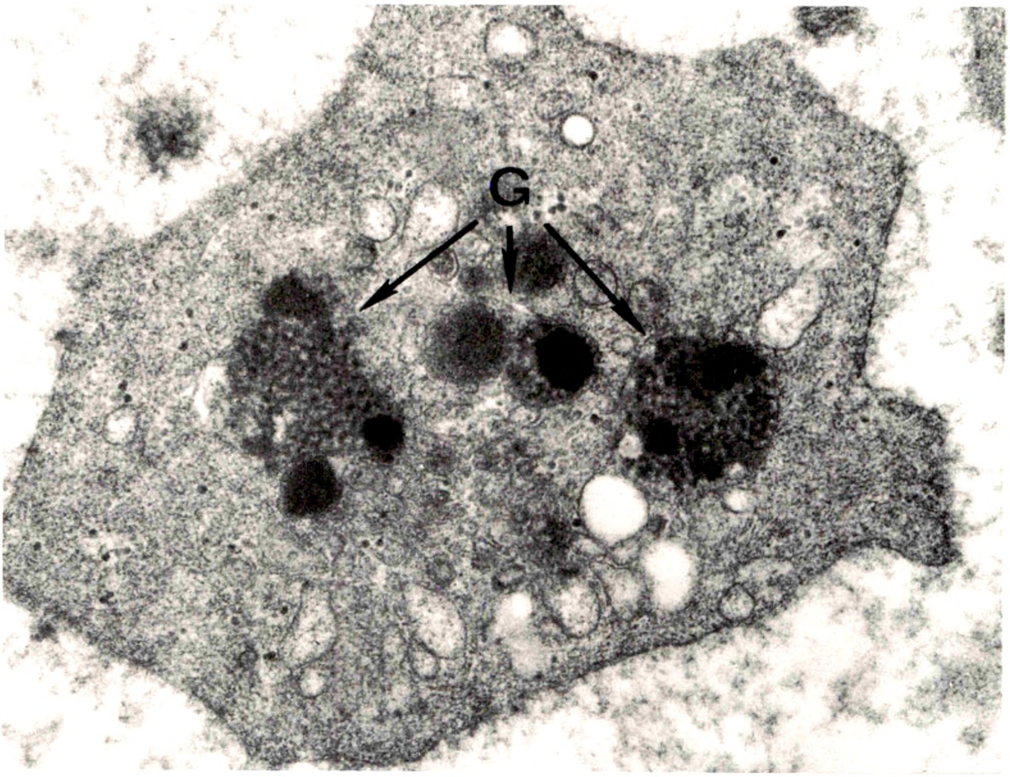

2

3

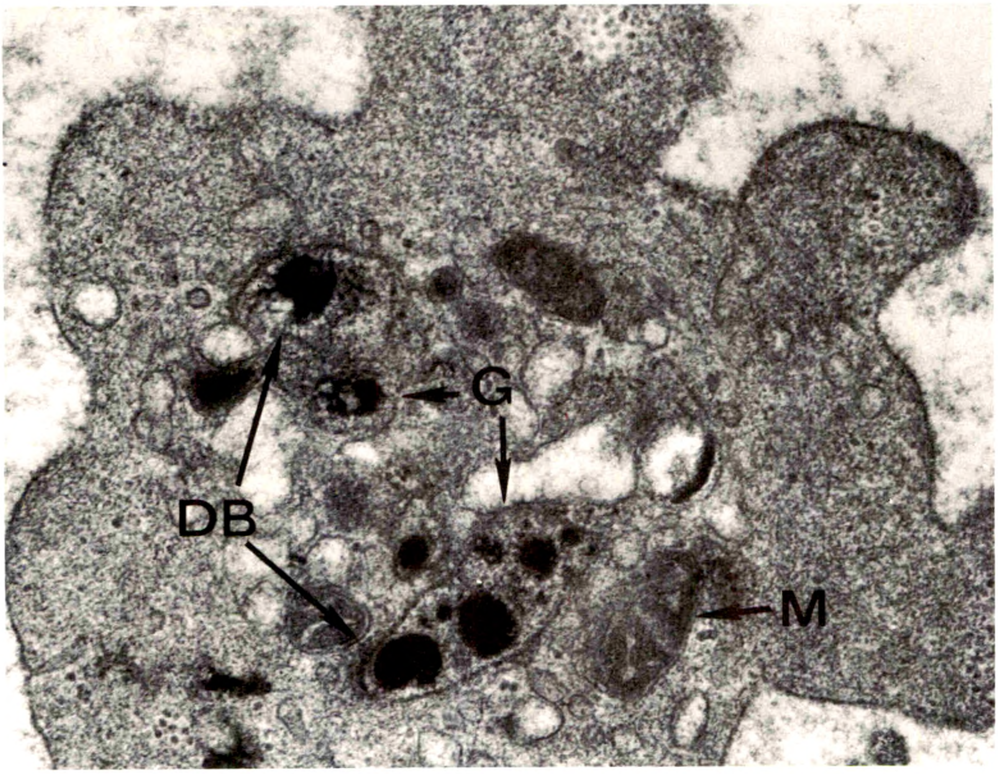

4

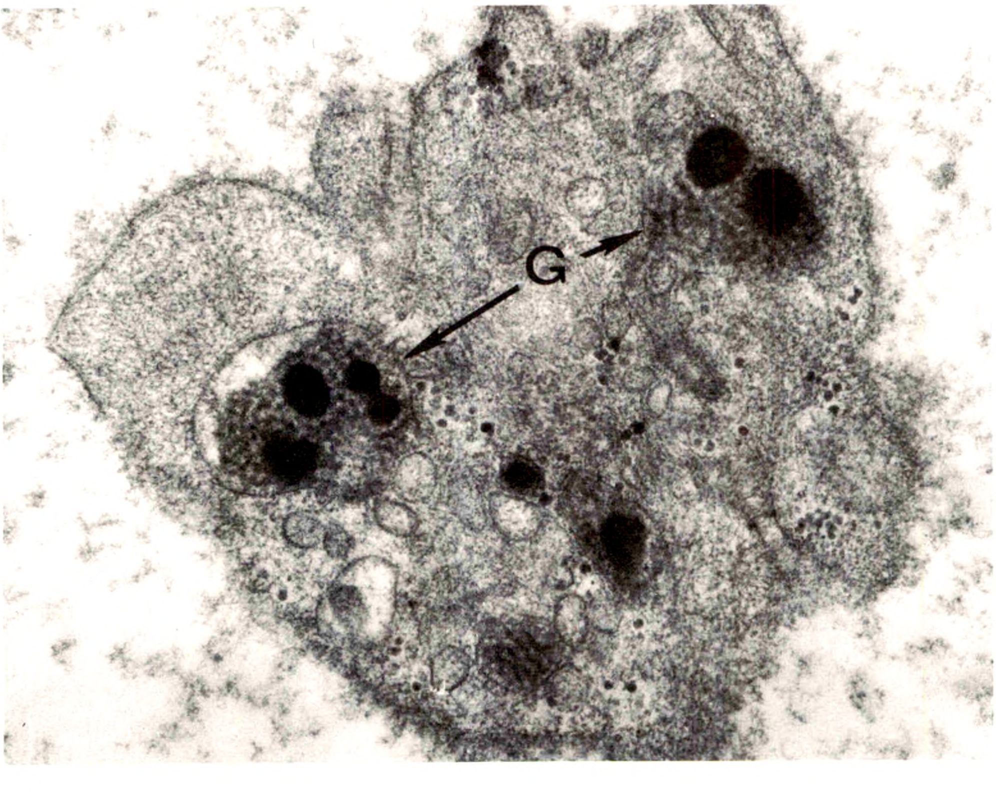

Fig 3—Afibrinogenemic platelet fixed after a 60 minute incubation with polybrene at 0.5 ml/ml of C-PRP. Shape change and internal transformation are well advanced. Dense bodies (*DB*) are affected by the agent, as are the dense zones of the granules (*G*) (× 42,100). **Fig 4**—Thrombasthenic platelets fixed after exposure to polylysine (0.5 mg) for 60 minutes. The agent causes fusion of the granules (*G*) and ultimately leads to their extrusion from the platelet (× 40,200).

Parathyroid Necrosis and Hypocalcemic Tetany Induced in Rabbits by L-Asparaginase

Francis V. Chisari, MD, H. Donald Hochstein, Dr PH, Ruth L. Kirschstein, MD and Edward B. Seligmann, PhD

Fifty percent of New Zealand white rabbits became profoundly weak, had generalized seizures and died between 22 and 47 hours after an intravenous injection of 1000 IU/kg of L-asparaginase. The biochemical correlate of this syndrome is severe hypocalcemia associated with marked, single cell, oxyphilic necrosis in the parathyroid glands. Although survivors remained clinically well, they also developed hypocalcemia and parathyroid necrosis but to a lesser degree. Rabbits given an equivolumetric amount of saline did not develop alterations in any of these parameters. L-Asparaginase, therefore, exerts a direct toxic effect on the parathyroid glands of rabbits. The implications of this finding for man are briefly discussed (Am J Pathol 68:461–468, 1972).

THE ANTILEUKEMIA DRUG, L-asparaginase, derived from *Escherichia coli* is a biologic product subject to regulation under the United States Public Health Service Act.[1] The Regulations state that any biologic product given intravenously to man must be free of pyrogens, as measured in rabbits.

While testing various lots of L-asparaginase for pyrogenicity, it was noted that although the material was uniformly nonpyrogenic, many of the rabbits died within 1 to 3 days after it was injected intravenously. Similar observations were reported by Oettgen *et al*,[2] who were unable to explain the nature of this lethal effect. Schein and his colleagues[3] did not observe this phenomenon in dogs, rats or monkeys; this drug has not caused excessive mortality in man.[2,4–9] The present study was undertaken to determine the pathogenesis of this delayed mortality in rabbits.

Materials and Methods

Rabbits

New Zealand white rabbits of both sexes were obtained from the Rodent and Rabbit Production Section, Laboratory Aids Branch, National Institutes of Health. The average weight of these rabbits was 2 kg.

From the Division of Biological Standards, National Institutes of Health, Bethesda, Md.

Accepted for publication May 16, 1972.

Address reprint requests to Dr. Francis V. Chisari, Department of Medicine, Dartmouth Medical School, Hanover, NH 03755.

L-Asparaginase

Eleven different lots of enzyme, produced by two different commercial manufacturers, were used. The drug was dissolved in normal saline at a concentration of 1000 IU/ml.

Injections

Fifty-three rabbits were injected intravenously with 1000 IU/ml/kg body weight of L-asparaginase from the 11 lots. Fourteen rabbits were injected intravenously with 1 ml/kg of normal saline. All animals were observed, as required by the test for pyrogenic substances,[1] and then hourly until death or until the study was discontinued 5 days after injection.

Biochemical Determinations

Determinations of serum levels of calcium, phosphorus, albumin, blood urea nitrogen (BUN) and creatinine were performed by Bionetics Research Laboratories, Inc. Serum was obtained prior to injection from 12 rabbits given L-asparaginase and 9 given saline. These values are considered normal for this study.

Twenty-two experimental animals were bled at varying intervals after injection, either when moribund or, if clinically well, at 30 or 47 hours after injection. Similar biochemical studies were performed on their sera. Eight of these animals died. Four of them had also been bled before L-asparaginase was injected, and their preinjection levels are included in the normal values. The remaining 14 survived, and 8 of these were also bled before L-asparaginase was injected, and their preinjection levels are included in the normal values.

Six of 14 control animals were bled at 30 or 48 hours after the injection of saline. These 6 and 3 others were also bled before saline was injected and their preinjection levels complete the normal values.

Autopsies

Complete autopsies were performed on all animals that died, on 8 of the animals injected with L-asparaginase and survived and on 2 animals injected with saline. The organs were examined grossly, removed, fixed in 10% neutral formalin or mercuric sublimate formalin (B–5), embedded in paraffin, stained with hematoxylin and eosin and examined by light microscopy.

Serial sections of either the thyroid glands or of the tracheal block containing thyroid tissue were prepared to search for the parathyroid glands.

Results

Clinical Observations

None of the 53 rabbits injected with L-asparaginase (1000 IU/kg) developed a pyrogenic response within 3 hours after the injections. Twenty-six died between 22 and 47 hours after injection. They developed varying degrees of salivation, weakness, inability to stand, tremulousness, opisthotonos and generalized convulsions, starting 2 to 6 hours before death. All were autopsied. Twenty-seven animals survived the injection of L-asparaginase without becoming clinically ill. Eight of these were autopsied: 6 at 3 days and 2 at 7 days after injection. None of the 14 animals injected with saline became ill or died. Two were autopsied 3 days after injection.

Biochemical Determinations

Serum levels of the various substances are shown in Table 1. As can be seen, in rabbits injected with L-asparaginase, the level of calcium fell while that of phosphorus, BUN, and creatinine rose. These values were more abnormal in animals that died than in those that survived, whereas, values in animals injected with saline remained virtually unchanged.

Histologic Findings

Complete autopsies were performed on all 26 animals that died after the injection of L-asparaginase. Pertinent findings are listed in Table 2. In all animals there was congestion and edema of many organs, including the heart, lungs, kidneys, liver, spleen, thymus and

Table 1—Biochemical Observations

	Normal*	L-Asparaginase (1000 IU/kg IV)		Saline control (1 ml/kg IV)
	Lived	Died	Lived	Lived
No. of rabbits	21	26	27	14
No. bled	21	8†	14‡	6§
Hour of bleeding	0	30.8	37.2	39.0
		(22.0–47.0)	(30.0–47.0)	(30.0–48.0)
Serum calcium (mg %)	14.7	7.2	11.4	14.0
	(12.7–15.3)	(6.1–11.4)	(7.2–14.5)	(12.9–15.5)
Serum phosphorus (mg %)	6.1	11.2	9.9	6.8
	(4.3–7.1)	(8.5–14.0)	(7.5–11.8)	(6.5–7.1)
Serum albumin (g %)	3.4	3.8	3.3	3.1
	(2.9–3.9)	(2.6–4.7)	(2.2–4.2)	(2.8–3.6)
Serum creatinine (mg %)	0.7	1.6	1.1	0.8
	(0.6–1.0)	(1.2–2.6)	(0.9–1.4)	(0.7–0.9)
BUN (mg %)	14.1	41.5	25.0	16.6
	(11.0–18.0)	(29.0–72.0)	(18.0–35.0)	(15.0–20.0)

* This group is comprised of 12 experimental and 9 control animals bled before injection.

† Four of these eight animals were also bled prior to L-asparaginase injection; their preinjection levels are included in the normal values.

‡ Eight of these fourteen animals were also bled prior to L-asparaginase injection; their preinjection levels are included in the normal values.

§ These 6 animals and 3 others were bled prior to saline injection; their preinjection levels are included in the normal values.

Range of values given in parentheses.

Table 2—Histopathologic Observations

	L-Asparaginase (1000 IU/kg IV)		Saline (1 ml/kg IV)
	Died	Lived	Lived
No. of rabbits	26	27	14
No. autopsied	26	8	2
Hours to death	32.8 (22–47)	72 + 168*	72
No. of rabbits in which parathyroids found	15	8	2
No. of oxyphil cells/1000 × field	18.9 (5–47)	1.1 (0–2.4)	0.3 (0.2–0.4)

* Six animals sacrificed at 72 hours, 2 at 168 hours; all clinically normal at time of sacrifice
Range of values given in parentheses

brain; of significance was the fact that the pancreas was normal in all cases. Parathyroid glands were identified in serial sections of either the thyroid gland or tracheal block of tissue in 15 of these animals. The striking, characteristic finding in all of these glands was the presence of numerous, small, shrunken cells with markedly oxyphilic cytoplasm and pyknotic nuclei (Figure 1) which were virtually absent from control glands (Figure 2). These oxyphilic cells were counted in each of 10 random 1000 × oil immersion fields and the average number of cells per field was computed. There was an average of 18.9 oxyphil cells per 1000 × field, with a range of 5 to 47 in this group.

Eight of the 27 survivors that received L-asparaginase were autopsied and the parathyroid glands were found in each case. Six of these 8 survivors were sacrificed 3 days after injection; their parathyroid glands contained an average of 1.3 oxyphil cells per 1000 × field (range 0.3 to 2.4). The remaining 2 of the 8 survivors autopsied were examined 1 week after L-asparaginase had been injected; their parathyroids contained none and 0.5 oxyphil cells per 1000 × field, respectively. No other abnormalities were noted.

Two of the 14 control animals were autopsied 72 hours after normal saline was injected. Parathyroid glands from these animals contained 0.2 and 0.4 oxyphil cells per 1000 × field and there were no other abnormalities.

Discussion

Tettenborn *et al*[10] reported similar findings in Chinchilla rabbits given 10,000 IU L-asparaginase/kg body weight. They found that a detectable fall in serum calcium and magnesium levels occurred as early as 5 hours after injection, reaching a low point at 29 hours and returning to normal (in the survivors) by 72 hours. Necrotic, oxyphil cells were also found in the parathyroids of those animals that died with essentially the same clinical syndrome as the rabbits reported herein.

In our study, 50% of the rabbits that received 1000 IU/kg of L-asparaginase, from several different lots provided by two manufacturers died between 22 and 47 hours after the intravenous injection. These animals manifested a syndrome characterized by profound weakness, tremulousness and opisthotonos strongly reminiscent of human tetany and associated with the classic biochemical alterations of hypoparathyroidism—*ie,* hypocalcemia and hyperphosphatemia. These findings correlate with the striking morphologic changes, in the parathyroid glands, of widespread oxyphilic necrosis of single cells. Rabbits that survived after the injection of L-asparaginase also had biochemical and morphologic changes similar to those in animals that died, but to a much lesser degree; the control animals were essentially normal. Thus, one may conclude that L-asparaginase exerts a variable but direct toxic effect on the parathyroid glands of rabbits. The effect results in cell death with concomitant hypocalcemia and tetany.

Several other factors (hypoalbuminemia, pancreatitis, and azotemia) known to cause hypocalcemia and associated with L-asparaginase therapy in humans,[2] do not appear to be implicated in this study. Serum albumin levels of rabbits that died were actually higher than those of survivors. The pancreas, in all cases, was entirely normal histologically. Finally, although L-asparaginase is known to cause azotemia in rabbits (Table 1), as well as in other species including man,[2] the acute onset and the severity of hypocalcemia induced in this study was much too marked to be caused by renal shutdown.

Therefore, it appears that the parathyroid glands of rabbits possibly are exquisitely sensitive to L-asparaginase, and that this system may provide a useful model for the study of hypoparathyroidism. In addition, the hypocalcemia seen in humans treated with L-asparaginase has been attributed largely to associated hypoalbuminemia. Although this finding is very well documented,[2] it also may be possible that L-asparaginase has some direct effect on human parathyroids as well. A study of the microscopic appearance of human parathyroid glands from patients treated with L-asparaginase is, therefore, now in progress.

References

1. United States Department of Health, Education and Welfare, Public Health Service Regulations, Biological Products. Washington, DC, US Government Printing Office, 1970 [PHS Title No. 42, Part 73, Section 73.740 (B)] p 13931
2. Oettgen HF, Stephenson PA, Schwartz MK, Leeper RD, Tallal L, Tan CC, Clarkson BD, Golbey RB, Krakoff IH, Karnofsky DA, Murphy ML, Burchenal JH: Toxicity of *E. coli* L-asparaginase in man. Cancer 25:253–278, 1970
3. Schein PS, Rakieten N, Gordon BM, Davis RD, Rall D: The toxicity of *E. coli* L-asparaginase. Cancer Res 29:426–433, 1969
4. Haskell CM, Canellos GP, Leventhal BG, Carbone PP, Block JB, Serpick AA, Selawry OS: L-Asparaginase: therapeutic and toxic effects in patients with neoplastic disease. N Engl J Med 281:1028–1034, 1969
5. Clarkson BD, Krakoff IH, Burchenal JH, Karnofsky DA, Golbey RB, Dowling M, Oettgen HF, Lipton A: Clinical results of treatment with *E. coli* L-asparaginase in adults with leukemia, lymphoma and solid tumors. Cancer 25:279–305, 1970
6. Tallal L, Tan C, Oettgen H, Wollner N, McCarthy M, Helson L, Burchenal J, Karnofsky D, Murphy ML: *E. coli* L-asparaginase in the treatment of leukemia and solid tumors in 131 children. Cancer 25:306–320, 1970
7. Dolowy WC, Henson D, Cornet J, Sellin H: Toxic and antineoplastic effects of L-asparaginase. Cancer 19:1813–1819, 1966
8. Capizzi RL, Bertino JR, Skeel RT, Creasey WA, Zanes R, Olayon C, Peterson RG, Handschumacher RE: L-Asparaginase: clinical, biochemical, pharmacological and immunological studies, Ann Intern Med 74:893–901, 1971
9. Whitecar JP, Bodey GP, Harris JE, Freireich EJ: L-Asparaginase. N Engl J Med 282:732–734, 1970
10. Tettenborn D, Hobik HP, Luckhaus G: Hypoparathyreoidismus beim Kaninchen nach Verabreichung von L-asparaginase. Arzneimittel Forsch 20:1753–1755, 1970

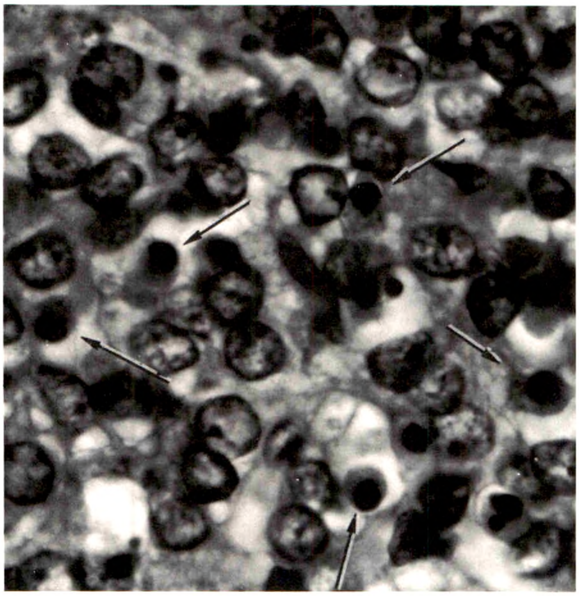

Fig 1—Parathyroid gland from a rabbit that died 32.5 hours after a single intravenous dose of *L*-asparaginase, 1000 IU/kg. Note the numerous shrunken cells with pyknotic nuclei and dense oxyphilic cytoplasm (*arrows*) (H&E, × 1000).

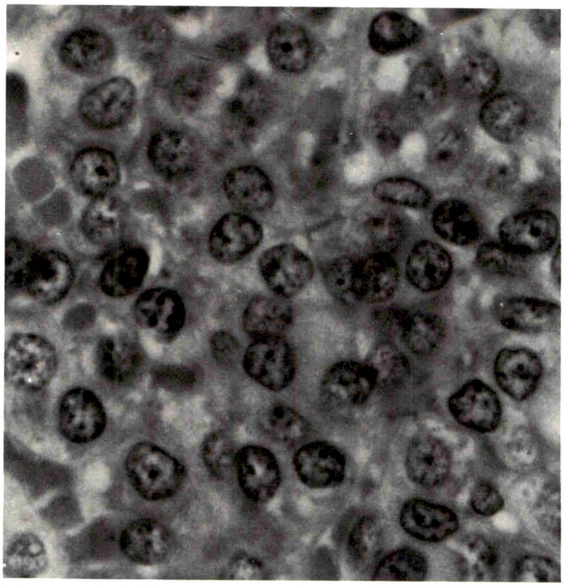

Fig 2—Parathyroid gland from a rabbit sacrificed 71 hours after the intravenous injection of saline. Note the absence of oxyphilic cells (H&E, × 1000).

[*End of Article*]

Nuclear Localization of Immunoglobulins in Renal Biopsies of Patients with Lupus Nephritis

Ralph C. McCoy, MD

Immunofluorescent evaluation of renal biopsies from 19 patients with lupus nephritis revealed nuclear localization of immunoglobulins (IgG and IgM) in 6 patients. Homogeneous, nuclear rim and speckled patterns of nuclear localization were observed. The extent of localization varied, with only occasional nuclei fluorescing in 1 case, whereas approximately 50% of the nuclei exhibited fluorescence in the most extreme case. The phenomenon of nuclear localization of immunoglobulins was not observed in immunofluorescent studies of 225 renal biopsies from patients with conditions other than lupus nephritis. The possibility that nuclear localization of immunoglobulins occurred artifactually in the 6 patients was considered and was discounted by determining antinuclear antibody titers on serum obtained concurrently with the renal biopsy Nuclear localization was not confined to areas of histologically evident parenchymal destruction, indicating that antinuclear antibodies do not react only with nuclear antigens after tissue breakdown, but may gain access to intracellular antigens prior to cell dissolution. (Am J Pathol 68:469–478, 1972).

INDIRECT IMMUNOFLUORESCENT TESTS employing tissue substrates as a source of nuclear antigen, patient's serum and antihuman immunoglobulins have become a well-recognized method for detecting antinuclear antibodies in patients with suspected systemic lupus erythematosus. Using this technic, three distinct patterns of nuclear localization (homogeneous, nuclear rim and speckled) have been characterized, and these patterns have been correlated with antibody activity to specific nuclear materials.[1,2] In spite of this characterization, the exact significance of these antibodies in the pathogenesis of systemic lupus erythematosus remains unclear.[3] Most studies in which direct immunofluorescent technics were used to evaluate immune complex lesions in renal tissue from patients with lupus nephritis have not described nuclear localization of immunoglobulins in the kidney.[4–8] Indeed, it is held that no such nuclear localization occurs in the kidney[9] or in other organs.[10,11] This negative find-

---

From the Department of Pathology, Duke University Medical Center, Durham, NC 27710.

Supported in part by US Public Health Service Grant 5-T02-GM00726 from the National Institute of General Medical Sciences.

Accepted for publication June 1, 1972.

Address reprint requests to Dr. Ralph McCoy, Department of Pathology, Box 3712, Duke University Medical Center, Durham, NC 27710.

ing has supported the concept that antinuclear antibodies do not bind *in vivo* with nuclear material of intact cells but only react with products of tissue breakdown to produce nuclear antigen-antibody complexes.[12]

The present report describes nuclear localization of immunoglobulins in renal biopsies from 6 of 19 patients with lupus nephritis studied by immunofluorescent technics at the Duke University Medical Center from August 1970 through January 1972. Serum from each of the patients, obtained concurrently with the biopsy, was evaluated for the presence and titer of antinuclear antibodies. The results were then correlated with nuclear localization of immunoglobulins in renal biopsies.

Materials and Methods

Immunofluorescent Studies of Renal Biopsies

Tissue from each of the 19 patients was obtained by percutaneous needle biopsy. The tissue specimens were divided into three portions: one for light microscopy, one for electron microscopy and one for immunofluorescent microscopy. Tissue for immunofluorescent microscopy was immediately frozen, unfixed, at −70 C in a gelatin matrix. Sections for immunofluorescent evaluation were cut at 4 μ on an International Harris cryostat. One set of slides was then air-dried, fixed for 5 minutes in acetone and washed twice in phosphate-buffered saline. These sections were then incubated for 30 minutes with fluorescein-labeled antibody preparations, washed again in phosphate-buffered saline and mounted under glass coverslips with 10% glycerin. A second set of sections was washed for 5 minutes in phosphate-buffered saline immediately after they had been cut and before they were fixed in acetone. This set was then incubated with antibody preparations and subsequently treated in the same manner as the first set. Sections were examined with a Zeiss Photoscope I equipped with an HBO-200W mercury vapor light source, UG-1 exciter filter and a K-490 barrier filter. Specimens were photographed with high speed Ektachrome film (ASA 160). The coordinates of photographed fields were recorded, and the coverslips floated from sections in phosphate-buffered saline. Sections were dehydrated in ether-alcohol, fixed in Zenker's solution and stained with hematoxylin and eosin. Nuclei were identified in the hematoxylin and eosin sections and compared with sites of labeled immunoglobulin localization in the same field.

Antibody preparations used in the immunofluorescent evaluations included goat or rabbit antihuman IgG, IgM, IgA, β1C-globulin, fibrinogen and albumin, which were tested for monospecificity by immunoelectrophoresis. Sodium sulfate-precipitated immunoglobulin fractions were labeled with fluorescein isothiocyanate by the method of Marshall *et al.*[13] Control preparations for the immunofluorescent studies consisted of: a) conjugated antibody preparations absorbed with specific antigen prior to incubation with tissue sections and b) tissue sections incubated with unlabeled antibodies before incubation with respective labeled antibody preparations. The former control procedure usually completely abolished, while the latter only moderately diminished specific fluorescence.

Serum Antinuclear Antibody Titers

The indirect immunofluorescent technic was used to determine antinuclear antibody titers on each patient's serum. Nuclear antigen substrate consisted of fresh rat kidney snap-frozen at −70 C and sectioned at 4 μ on an International Harris cryostat. Sections were fixed in acetone for 5 minutes, according to Tan's method[1] and then incubated for 30 minutes with serial dilutions of each patient's serum. Sections were washed in phosphate-buffered saline, incubated with goat antihuman IgG for 30 minutes, washed again in phosphate-buffered saline and mounted under glass coverslips with 10% glycerin. Specimens were examined and photographed with the equipment described above. The pattern of antinuclear antibody localization was recorded; the titer was reported as the highest dilution in which nuclear localization was observed.

Serum Anti-DNA Antibody Levels

Serum levels of antibody to DNA were determined by the nitrocellulose membrane filter method.[14]

Results

Features of the renal histopathology, pattern and class of nuclear immunoglobulin localization and results of serum antibody studies are given in Table 1, for each of the 6 patients in whom renal biopsy revealed nuclear localization of immunoglobulins.

Glomerular histopathology was varied. Membranous and proliferative glomerulonephritis, the latter in both a focal and diffused pattern, was observed in the 6 patients who exhibited nuclear localization of immunoglobulins. All biopsies contained some degree of parenchymal destruction, with either focal or diffuse interstitial inflammatory cell infiltrates, interstitial fibrosis and tubular destruction. Sites of nuclear localization of immunoglobulins did not always coincide with these areas of parenchymal destruction, however. In each of the 6 patients, the pattern of nuclear immunoglobulin localization in the biopsy was the same as the pattern observed by indirect immunofluorescent tests using patient's serum and rat kidney tissue as substrate. Speckled and homogenous patterns of nuclear antihuman immunoglobulin localization occurred most commonly in renal biopsies. In one case, however, a membranous or nuclear rim pattern was observed. Localization of antihuman immunoglobulins was observed in nuclei of glomerular visceral and parietal epithelium, tubular epithelium and interstitial cells (Figures 1–4). Antihuman IgG and IgM localized in the nuclei in 4 patients (CO, EE, AT, and BM), while 2 (LM and DH) demonstrated antihuman IgG localization only. There was no detectable localization of antihuman IgA, β1C-globulin, fibrinogen or albumin in nuclei of any of the 6 patients. The extent of nuclear localization in each case

Table 1—Features of the Renal Histopathology, Nuclear Immunoglobulin Localization, and Serum Antibody Studies

Patient	Age (yr) race sex	Type of glomerular lesion	Degree of parenchymal destruction*	Pattern of nuclear localization and class of immunoglobulin in renal biopsy	Pattern of indirect serum nuclear localization	Serum antinuclear antibody levels‡
CO	27 N F	Membranous glomerulonephritis	+ Focal	Speckled IgG, IgM	Speckled	2 μg/ml anti-DNA, 1:4 antinuclear antibody
EE	34 N F	Diffuse proliferative glomerulonephritis	+++ Focal	Homogenous and speckled IgG, IgM	Homogenous and speckled	0 μg/ml anti-DNA, 1:256 antinuclear antibody
AT	22 N F	Focal proliferative glomerulonephritis	++ Focal	Membranous IgG, IgM	Membranous	600 μg/ml anti-DNA, 1:1024 antinuclear antibody
BM	29 N F	Membranous glomerulonephritis	++ Diffuse	Speckled IgG, IgM	Speckled	10 μg/ml anti-DNA, 1:256 antinuclear antibody
LM	34 N F	Focal proliferative glomerulonephritis	+ Focal	Speckled and homogenous IgG	Speckled and homogenous	7.5 μg/ml anti-DNA, 1:128 antinuclear antibody
DH	39 W F	Membranous glomerulonephritis	+ Focal	Speckled IgG	Negative†	0 μg/ml anti-DNA, 0 antinuclear antibody†

* Graded 1–4 +

† Negative at biopsy, antinuclear antibody titer was 1:8; speckled pattern on followup 3 weeks postbiopsy

‡ Normal 0–6 μg/ml, see text

was variable. In 2 patients (CO and DH), only occasional nuclei in focal areas showed antihuman immunoglobulin localization (Figures 1, 4), while, at the other extreme, approximately half of all nuclei in the biopsy from patient EE revealed localization of antihuman IgG and IgM (Figures 2, 3).

Antinuclear antibody titers in patient's serum at the time of renal biopsy varied from 0 to 1:1024. Anti-DNA levels varied from 0 to 1400 μg/ml (normal level: 0 to 6 μg/ml). Negative tests for serum antibody were obtained in the sixth patient, DH, who presented with Raynaud's syndrome, proteinuria and hematuria. Lupus erythematosus cell preparations, antinuclear antibody determinations and anti-NDA determination were negative in initial tests. A renal biopsy revealed membranous glomerulonephritis with immunofluorescent findings of antihuman IgG and β1C-globulin localization in a granular pattern along glomerular capillary walls and antihuman IgG localization in a speckled pattern in nuclei. Subsequent examination of the renal biopsy by electron microscopy confirmed the membranous glomerular changes and revealed virus-like structures in the endoplasmic reticulum of glomerular endothelial cells identical to those described in lupus nephritis.[15-17] The antinuclear antibody titer, 3 weeks after the biopsy, was 1:8.

During the period in which these cases were observed (August 1970 through January 1972), immunofluorescent studies were performed on 225 renal biopsies from patients in whom there was no clinical diagnosis or suggestive evidence of systemic lupus erythematosus. Histopathologic diagnoses in that group included proliferative glomerulonephritis, membranous glomerulonephritis, membranoproliferative glomerulonephritis, focal glomerulonephritis, chronic glomerulonephritis, arteriolar nephrosclerosis, amyloidosis, diabetic glomerulosclerosis and chronic pyelonephritis. Nuclear localization of immunoglobulins was not observed in any of those cases which were processed with initial acetone fixation prior to washing with phosphate-buffered saline.

Discussion

Although localization of immunoglobulins has been observed in nuclei of nonkeratotic cells in skin biopsies from patients with systemic lupus erythematosus,[12] reports of nuclear immunoglobulin localization in kidney are almost nonexistent. In immunofluorescent studies utilizing autopsy kidney specimens, Paronetto and Koffler[18] reported nuclear localization in 3 of 16 patients with systemic lupus erythematosus.

Rapp,[19] on the other hand, working with HeLa cells in tissue culture, concluded that antinuclear antibodies did not penetrate the viable cell. The question thus arises, in the patients described by Paronetto and Koffler, whether nuclear localization may have occurred during the postmortem period, with antinuclear antibodies diffusing from serum and localizing in nuclei as autolysis occurred.

In the present study, biopsies from 4 patients exhibited nuclear localization of antihuman IgG and IgM, while nuclear localization of only antihuman IgG occurred in biopsies from 2 patients. Nuclear localization of other serum components, specifically IgA, β1C-globulin, fibrinogen or albumin was not observed in any of the biopsies. In each instance, the pattern of nuclear localization in the kidney was the same as that observed by indirect immunofluorescent antinuclear antibody tests using the patient's serum.

The possibility must be considered that nuclear localization observed in renal biopsies in this report was *artifactual*. It is conceivable that in patients possessing high titers of antinuclear antibodies, these might diffuse from the vascular compartment of the biopsy, during sectioning and washing procedures, and localize in nuclei artifactually at the time of processing. To evaluate this possibility, two methods of processing were used in each case. In the first method, sections were fixed in acetone for 5 minutes immediately after they were cut and before they were incubated with specific antibody preparations or washed. The initial acetone treatment in this technic was designed to fix serum proteins in the section and prevent leaching of nuclear antigens during subsequent rinsing procedures after incubation with antibody preparations. In the second method the cut sections were washed in phosphate-buffered saline for 5 minutes immediately after the tissue was sectioned before it was fixed in acetone or incubated with the specific antibody preparations. In this latter technic, the sections were rinsed in order to wash unbound γ-globulin from the specimen. Rinsing was confined to 5 minutes, as recommended by Tan,[1] to minimize leaching of saline-soluble components, such as DNA and phosphate-extractable Sm antigen from nuclei. There was no significant difference in localization with either method.

The strongest evidence that this nuclear staining represents true *in vivo* and not artifactual immunoglobulin localization which occurred during sectioning is derived from serum antinuclear antibody titers obtained at the time of renal biopsy. The antinuclear antibody titers varied from a low of 1:4 to a high of 1:1024 in 5 patients. However, in the sixth patient, DH, serum antinuclear antibody and anti-DNA antibody determinations were both negative at the time of renal biopsy. The latter finding would seem to suggest that nuclear localization did not occur during the processing procedure, since there was no measurable serum antibody to diffuse from the vascular compartment of the biopsy.

Since nuclear localization was not confined to areas of histologically evident parenchymal destruction, the above findings suggest that antinuclear antibodies not only react with nuclear antigens released during tissue breakdown, but may gain access to nuclei in the kidney before the cell disintegrates. The mechanism by which this phenomenon occurs remains to be elucidated. Since there is little evidence to suggest that immunoglobulins normally penetrate the intact cell, an alternate hypothesis is proposed. Nuclear localization of antinuclear immunoglobulins may occur in cells injured sublethally during the progressive parenchymal destruction which accompanies immune complex nephritis. This nuclear localization in injured cells could result either from antinuclear immunoglobulins which have been actively reabsorbed from the glomerular filtrate by epithelial cells or from immunoglobulins diffusing from the vascular and interstitial compartments through cell membranes that have lost their functional integrity.

Whatever the mechanism, the phenomenon of immunoglobulin nuclear localization in renal biopsies should be appreciated and anticipated by those performing immunofluorescent studies, since it might prove helpful in establishing the diagnosis of systemic lupus erythematosus in previously unconfirmed cases.

References

1. Tan EM: Relationship of nuclear staining patterns with precipitating antibodies in systemic lupus erythematosus. J Lab Clin Med 70:800–812, 1967
2. Beck JS: Variations in the morphologic patterns of "autoimmune" nuclear fluorescence. Lancet 1:1203–1204, 1961
3. Heptinstall RH: Pathology of the Kidney. Boston, Little, Brown and Co, 1966, p 554
4. Mellors RC, Ortega LG, Holman HR: Role of gamma globulins in pathogenesis of renal lesions in systemic lupus erythematosus and chronic membranous glomerulonephritis with an observation of the lupus erythematosus cell reaction. J Exp Med 106:191–202, 1957
5. Vazquez JJ, Dixon FJ: Immunohistochemical study of lesions in rheumatic fever, systemic lupus erythematosus and rheumatoid arthritis. Lab Invest 6:205–217, 1957
6. Burkholder PM: Complement fixation in diseased tissues. II. Fixation of

guinea pig complement in renal lesions of systemic lupus erythematosus. Am J Pathol 42:201–224, 1963

7. Paronetto F, Ludwig D, Tuchaman LR: Lupus erythematosus with fetal hemorrhage into the liver and lesions resembling those of periarteritis nodosa and malignant hypertension. Am J Med 36:948–955, 1964
8. Koffler D, Angello V, Carr RI, Kunkel HG: Variable patterns of immunoglobulin and complement deposition in the kidneys of patients with systemic lupus erythematosus. Am J Pathol 56:305–316, 1969
9. Burkholder PM: Immunology and immunohistopathology of renal disease, Structural Basis of Renal Disease. Edited by EL Becker. New York, Harper and Row, Publishers, Inc, 1968, p 206
10. Nairn RC: Fluorescent Protein Tracing. Baltimore, Williams and Wilkins Co, 1969, p 294
11. Holman HR: Systemic lupus erythematosus, Immunological Diseases, Second edition, Vol II. Edited by M Samter. Boston, Little, Brown and Co, 1971, p 998
12. Kunkel, HG, Tan EM: Autoantibodies and disease. Adv Immunol 4:351–395, 1964
13. Marshall JD, Eveland WC, Smith CW: Superiority of fluorescein isothiocyanate (Riggs) for fluorescent antibody technic with a modification of its application. Proc Soc Exp Biol 98:898–900, 1958
14. Kredich NM, Skyler JS, Batcelor LJ: Unpublished data
15. Gyorkey F, Min K-W, Sincovics JC, Gyorkey P: Systemic lupus erythematosus and myxovirus. N Engl J Med 280:333, 1969
16. Kawano K, Miller L, Kimmelsteil P: Virus-like structures in lupus erythematosus. N Engl J Med 281:1228–1229, 1969
17. Tisher CC, Kelso HB, Robinson RR, Gunnels JC, Burkholder PM: Intraendothelial inclusions in kidneys of patients with systemic lupus erythematosus. Ann Intern Med 75:537–547, 1971
18. Paronetto F, Koffler D: Immunofluorescent localization of immunoglobulins, complement, and fibrinogen in human disease. I. Systemic lupus erythematosus. J Clin Invest 44:1657–1664, 1965
19. Rapp F: Localization of antinuclear factors from lupus erythematosus sera in tissue culture. J Immunol 88:732–740, 1962

Acknowledgments

Appreciation is expressed to Dr. C. C. Tisher, who evaluated the light microscopic histopathology in many of these cases and to Dr. N. M. Kredich who performed the anti-DNA determinations.

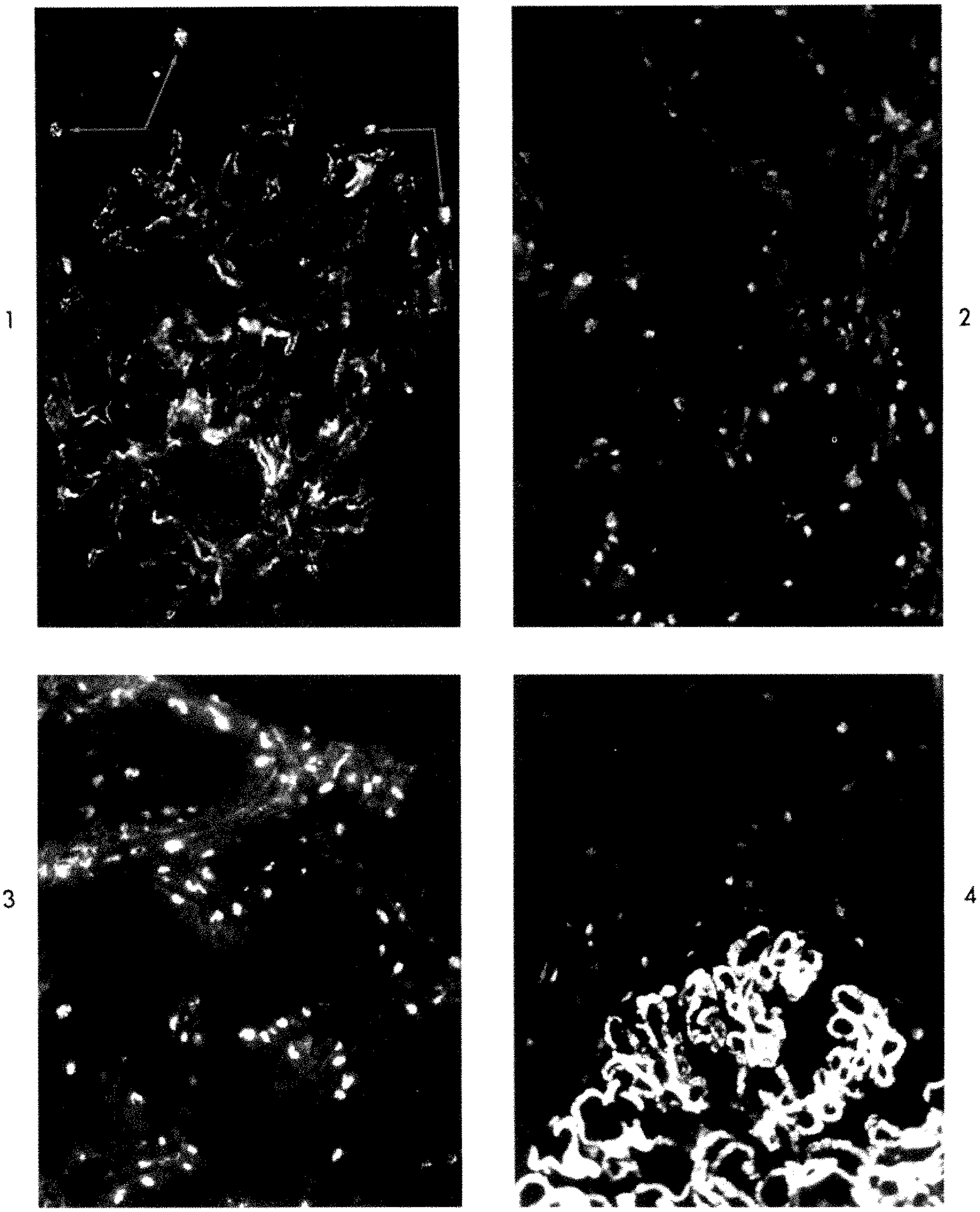

Fig 1—Biopsy from patient DH revealing antihuman IgG localization in a diffuse granular pattern along glomerular capillary walls, in a speckled pattern in two nuclei of proximal tubular epithelium (*arrows*, upper left) and in nuclei of visceral epithelial cells of the glomerulus (*arrows*, right) (× 475). **Fig 2**—Biopsy from patient EE revealing localization of antihuman IgG in a speckled and homogenous pattern in a large portion of tubular epithelial nuclei (× 315). **Fig 3**—Biopsy from patient EE showing localization of antihuman IgM in a speckled and homogenous pattern in tubular epithelial nuclei (× 315). **Fig 4**—Biopsy from patient CO revealing antihuman IgG localization in a diffuse, confluent granular pattern along the glomerular capillary walls and localization in a speckled pattern in occasional nuclei of tubular epithelial cells (× 315).

[*End of Article*]

Ultrastructural Changes in Muscular Dystrophy

I. Cardiac Tissue of Piglets Deprived of Vitamin E and Selenium

Phillip R. Sweeny, PhD and R. G. Brown, PhD

The ultrastructure of cardiac tissue from neonate, 3-, 6-, 8-, and 12-week-old piglets, born of vitamin E- and selenium-deprived sows was studied. A progression of lesions occurred in nonmuscular components of this tissue; the first lesion appeared in connective tissue elements. Fibroblasts and the extracellular compartment appeared most severely altered in the neonate, and progressive vascular damage was very evident from 3 to 12 weeks of age. Similarly, neuronal elements appear altered at 3 weeks and were almost nonevident in areas showing marked lesions at 8 and 12 weeks. Fairly extensive alterations were evident in all of these elements before any marked changes become evident in the muscle. The relevance of these observations is discussed in relation to the etiology of the disease (Am J Pathol 68:479–492, 1972).

NUMEROUS REPORTS ARE AVAILABLE on the production of cardiac muscular dystrophy in swine after nutritional deficiencies in vitamin E and selenium,[1-4] and the condition is commonly referred to as *mulberry heart* disease. Although numerous reports of histologic observations of this disorder are available, nothing has been published on ultrastructural changes in affected tissues.

Changes in the cardiac tissue of piglets born of vitamin E- and selenium-deficient sows were studied. Gross lesions were examined ultrastructurally but due to the complexities of observed cell alterations, an experiment was designed so that cardiac tissue from day 0 postnatally to 12 weeks of age could be collected and the sequence of changes established. This paper presents the ultrastructural changes observed during this investigation; primary consideration will be given to nonmuscular elements, since those appeared to be the first affected by the deficiency.

From the Department of Microbiology, College of Biological Science and the Department of Animal and Poultry Science, Ontario Agricultural College, University of Guelph, Guelph, Ontario, Canada.

Supported by grants from the National Research Council of Canada, Grant MA-4045 from the Medical Research Council of Canada and the Ontario Department of Agriculture and Food.

Accepted for publication May 25, 1972.

Address reprint requests to Dr. Phillip R. Sweeny, Department of Microbiology, College of Biological Science, University of Guelph, Guelph, Ontario, Canada.

Materials and Methods

All animals used in this study were piglets born to vitamin E- and selenium-deficient sows that had been maintained throughout gestation and lactation on a modified version of the Brown *et al*, diet [5]—vitamin E was not included and the soybean oil meal used was made from soybeans grown in selenium-poor soil. Analyses of the diet showed that it contained less than 0.05 ppm selenium. It was used as creep feed for the young from age 10 days to 3 weeks, after which time they were weaned and maintained solely on the diet. After weaning, half of the piglets received selenium as injected sodium selenate, 0.5 mg in sterile saline weekly, and vitamin E, 1000 IU in ethanol was given intramuscularly, weekly. Selected experimental animals were sacrificed at birth and at 3, 6, 8 and 12 weeks of age.

All cardiac tissues, normal or experimental, obtained for this study were collected from the right and left ventricles and the right atrium. They were immediately placed in appropriate fixative and cut into 0.75 mm cubes. Glutaraldehyde, in concentrations of 1.5, 2, 3 and 5% in 0.1, 0.15 and 0.2 M Sorensen's phosphate buffer at pH 7.2 to 7.3, was used as fixative. All samples were postfixed in 1% osmium tetroxide in phosphate buffer with 0.5% sucrose, pH 7.2 to 7.3. Other samples of all tissues were fixed only in 1% osmium tetroxide in phosphate buffer with 0.5% sucrose.[6] All fixations were performed at 4 C for 2 hours; subsequent to fixation, all tissues were dehydrated in acetone, (Baker analytical), and embedded in Epon.[7] Thick (1 μ) sections of all blocks were cut, stained with methylene blue [8] and examined by light microscopy for lesions or to confirm the presence of desired structures so that the proper areas of tissue would be thin-sectioned. All subsequent thin sections were cut on either a Porter Blum Ultramicrotome or a Reichert OMU2, using glass knives. The sections were placed on unsupported grids, stained with uranyl acetate and lead and examined in a Philips electron microscope, model 200.

Results

Electron microscopic examination revealed that normal cardiac tissue contained typical cardiac muscle cells with prominent intercalated discs and large quantities of mitochondria. The sarcoplasm contained ribosomes, the sarcoplasmic reticulum appeared normal, and the sarcomeres appeared to be in a state of contraction (Figure 1). In addition to mature contractile elements, myoblasts were seen on numerous occasions in specimens from animals up to 6 weeks of age; these are illustrated in Figure 2.

The noncontractile components of normal tissue include fibroblasts and small vessels (capillaries, arterioles and venules), as well as larger vessels, nonmyelinated neurons and extracellular collagen. In all ages examined, fibroblasts showed prominent dilations of ergastroplasmic cisternae containing an electron-dense, flocculent material (Figures 3, 4). The cytoplasm of these cells contained mitochondria, ribosomes and an occasional lipid-like droplet (Figure 4). The neurons contained all classic organelles: mictochondria, microtubules and neurosecretory granules. Occasional fibers contained electron-dense, lipid-like inclusions (Figure 5). The extracellular compartment contained relatively large quantities of collagen fibrils and, in some areas, an amorphous flocculent material was visible (Figures 3, 4, 5); the basal lamina was thin and distinct around muscles, vessels (Figure 3) and nerves (Figure 5).

Initial examination of those areas of cardiac tissue from deficient piglets, which visually appeared pathologic, revealed a complex array of degenerate muscle, nerves, vessels and fibroblasts (Figure 6). It was thus decided to study earlier stages of this disease in an effort to ascertain which tissue components were the first to show ultrastructural changes. At 3 to 6 weeks of age, the only major change visible in cardiac muscle cells was the appearance of lipid and evidence of mild mitochondrial degeneration (Figure 7). The most pronounced changes occurred in vessels and in the extracellular compartment. The predominant capillary changes involved varying degrees of endothelial degeneration, ranging from images showing slight loss of cytoplasmic density to excessive ballooning, with complete lack of all cytoplasmic organelles and organization (Figures 7–10). In addition to these alterations of the endothelium, electron-dense, lipid-like granules could be seen in vascular elements, degenerate neurons (Figures 7, 12) and fibroblasts; the latter appeared ruptured and degenerated (Figure 7). Numerous instances of major changes in neurons were seen wherein the axons appeared dilated and contained no discernable organelles (Figure 11); Schwann cells contained dilated endoplasmic reticulum as well as electron-dense inclusions (Figure 12).

The extracellular compartment of tissues at 6 and 8 weeks of age did not contain significant quantities of mature collagen bundles but did appear to contain a flocculent precipitate (Figures 6, 9, 11), 12). In addition, the basal lamina appeared thicker and more fibrous in nature in vessels which were most degenerate (Figure 10) and discontinuous in vessels with minimum alterations (Figures 8, 9). Thus, even at 3 weeks of age, significant alterations in most nonmuscular elements can be readily ascertained at the ultrastructural level. It should be emphasized that the above alterations in structure were not found throughout the tissue blocks examined, but only in restricted areas; they were most prevalent in the left ventricle.

It was then decided to examine tissues of newborn piglets of vitamin E- and selenium-deprived sows in the hope that perhaps only one of the above lesions would be observed. Light microscopic examination of these neonatal cardiac tissues revealed no apparent differences between them. Ultrastructural studies, however, revealed alterations in the capillaries and fibroblasts, as well as in connective tissues. The severity of lesions in the capillary endothelium progressed from normal endothelium to the mildest lesion at 6 weeks (compare Figures 13 and 7). No gross ballooning was seen at this stage with any fixation technic used. The most pronounced alterations were found in the fibroblasts, most of which appeared ruptured, with only scanty profiles of dilated endoplasmic reticulum (Figure 14). Normal fibroblasts were seen in certain areas and were similar to those at 3 to 6 weeks. In addition to these cellular changes, the extracellular compartment was almost devoid of the collagen bundles prevalent in controls. This compartment, however, contained large quantities of very fine filments which did not show axial periodicity, although they are found in close association with fibrils which do show the classic periodicity of collagen (Figure 15). These filaments were occasionally seen in controls but appeared to constitute the majority of extracellular filaments in the deficient piglet.

Discussion

In view of the above observations, it seems that there are two very early lesions in cardiac tissue of piglets from vitamin E- and selenium-deprived sows. These appear in connective tissue and capillaries and precede any apparent structural changes in muscle cells proper. Because the fibroblasts appear more degenerate than do the capillaries in newborns, it is felt that the deficiency has its most pronounced affect on this cell population and that capillary changes result from alterations in the connective tissue component of this organ.

The possibility that we are dealing with a connective tissue alteration is supported by the observations of King and Maplesdon [9] and Bourne and Golarz.[10] These authors suggest that changes occur in the polysaccharides of tissue; similar observations have been reported in muscle tissue of chickens suffering from genetic muscular dystrophy.[11] Brown *et al* [12] reported that avitaminosis E in rats increased the amounts of soluble collagen in the skin, decreased the rates of fibril formation *in vitro* and decreased the stability of fibrils *in vitro*. These data suggested that vitamin E was involved in normal fibril formation. Further studies [13–15] revealed that, although serum ascorbate remains relatively normal in these piglets, the ascorbate levels of cardiac tissue shows a continuous decline from birth. The role of this molecule in normal connective tissue metabolism is well known,[16] and its apparent loss from muscle would imply an alteration in connective tissue maturation, particularly fibrillogenesis. Our observations suggest an alteration in collagen fibril formation at early stages of the deficiency which could result from a decrease in available ascorbate. Indeed, Supplee[17] has shown that the feather abnormalities associated with nutritional muscular dystrophy in the chicken are partly protected by ascorbate.

It is apparent from our observations that myogenesis is still active up to 6 weeks postnatally and, therefore, differentiation of this organ is far from complete in the neonate. Thus full consideration must be given to developmental parameters in evaluating the effect of this deficiency on cardiac tissue. Recent evidence by Hauschka and Konigsberg[18] and Hauschka[19] has shown the influence of collagen on the *in vitro* differentiation of muscle. Their data show that the differentiation of cultured myoblasts is markedly enhanced if the cells are grown on a collagen substrate. The data of James[20] and Lieberman[21] also suggest the prominent role collagen development may have on the normal differentiation of the bundle of His and Purkinje fibers in the heart. There is thus ample evidence available in the literature to support the possibility that the primary site of action of the deficiency is the connective tissue compartment of the organ concerned, as suggested by our observations. If such were the case, capillary and nonmyelinated nerve damage would be secondary. Also relevant is the fact that in our experiments lesions appear first in the left ventricle, which postnatally is known to undergo a major burst of growth.[22] This rapid growth and its attendant activity would require effective tissue support system to maintain maximum cardiac output. In this regard, the effects of the deficiency are most pronounced on those muscle populations undergoing rapid growth with superimposed functional demands; this has been confirmed in studies on lamb and chickens.[23] Further studies are presently underway in an effort to elucidate early changes in tissues from other animals deprived of vitamin E and selenium.

References

1. Carpenter LE, Lundberg WO: Effect of tocopherols on viability of pigs in relation to baby pig disease. Ann NY Acad Sci 52:269–275, 1949
2. Lanneck K, Lindberg P, Nilsson G, Nostrom G, Orstadius K: Production of vitamin E deficiency and muscular dystrophy in pigs. Res Vet Sci 2:67–72, 1961
3. Ewan RC, Wastell NE, Bicknell EJ, Speer VC: Performance and deficiency symptoms of young pigs fed diets low in vitamin E and selenium. J Animal Sci 29:912–915, 1969

4. Sharp BA: Experimental induction of vitamin E and selenium responsive lesions in growing swine. MSc Thesis, University of Guelph, Guelph, Ontario, Canada, 1970

5. Brown RG, Sharma VD, Young LG: Ascrobic acid metabolism in swine. Interrelationships between the level of energy intake and serum ascorbate levels. Canad J Animal Sci 50:605–609, 1970

6. Millonig G: Advantages of a phosphate buffer for O_sO_4 solutions in fixation. J Appl Physiol 32:1637, 1961

7. Luft JH: Improvements in epoxy resin embedding techniques. Biochim Biophys Acta 9:409–414, 1961

8. Jeon KW: Simple method for staining and preserving epoxy resin embedded animal tissue sections for light microscopy. Life Sci 4:1839–1841, 1965

9. King JM, Maplesden DC: Nutritional muscular dystrophy in calves. III. Purkinje fiber degeneration in calves with experimentally produced nutritional muscular dystrophy. Canad Vet J 1:421–426, 1960

10. Bourne GH, Golarz MN: Histochemical evidence for a possible biochemical lesion in muscular dystrophy. J Histochem Cytochem 11:286–288, 1963

11. Cosmos E: Ontogeny of red and white muscles: the enzymatic profile and lipid distribution of immature and mature muscles of normal and dystrophic chickens, Physiology and Biochemistry of Muscle as a Food. Edited by EJ Briskey, RG Cassens, BB Marsh. University of Wisconsin Press, 1970, pp 193–207

12. Brown RG, Button GH, Smith JT: Effect of vitamin E deficiency on collagen metabolism in the rat's skin. J Nutr 91:99–106, 1967

13. Brown RG, Partridge IG, Sharp BA: Ascorbate in hepatosis dietetica and mulberry heart disease. J Animal Sci 33:1147 1971 (abstr)

14. Brown RG, Sharp BA, Young LG, Van Dreumel A: Serum ascorbate levels in swine with cardiac muscular dystrophy and hepatosis dietetica. Canad J Animal Sci 51:537–539, 1971

15. Brown RG, Sweeny PR: Ascorbate metabolism in swine changes in tissue ascorbate levels in vitamin E and selenium deficiency. Unpublished data

16. Robertson Wm Van B: The biochemical role of ascorbic acid in connective tissue. Ann NY Acad Sci 92:159–167, 1961

17. Supplee WC: Feather abnormality in poults fed a diet deficient in vitamin E and selenium. Poultry Sci 45:852–854, 1966

18. Hauschka SD, Konigsberg IR: The influence of collagen on the development of muscle colonies. Proc Nat Acad Sci 55:119–126, 1966

19. Hauschka SD: Clonal aspects of muscle development and the stability of the differentiated state, The Stability of the Differentiated State. Edited by H Ursprung. New York, Springer Verlag, Inc, 1968, pp 37–57

20. James RN: Cardiac conduction system: fetal and postnatal development. Am J Cardiol 25:213–226, 1970

21. Lieberman M: Physiologic development of impulse conduction in embryonic cardiac tissue. Am J Cardiol 25:279–284, 1970

22. Goss RJ: Adaptive growth of the heart, Cardiac Hypertrophy. New York Academic Press, Inc, 1971, pp 1–10

23. Sweeny PR, Buchanan-Smith J, deMille F, Pettit JR: Ultrastructural changes in muscular dystrophy. II. Comparative studies on lamb and chicken. Am J Pathol 68:493–510, 1972

Acknowledgments

We would like to thank Mrs. I. Hernandez and Barbara Atkinson for their technical assistance.

[*Illustrations follow*]

Fig 1—Electron micrograph of normal cardiac muscle cell showing myofilaments *(My)*, intercalated discs *(I)* and mitochondria *(M)*. Endothelium of a large vein can be seen at the top of the figure (Six weeks, osmium tetroxide uranyl acetate and lead stain, × 6300).

Fig 2—Electron micrograph of two myoblasts from normal tissue showing the immature myofilaments *(My)*, scattered mitochondria *(M)*, sarcoplasm *(S)*, collagen *(C)* and early phase of intercalated disc formation *(arrows)* (Six weeks, osmium tetroxide, uranyl acetate and lead stain, × 6300).

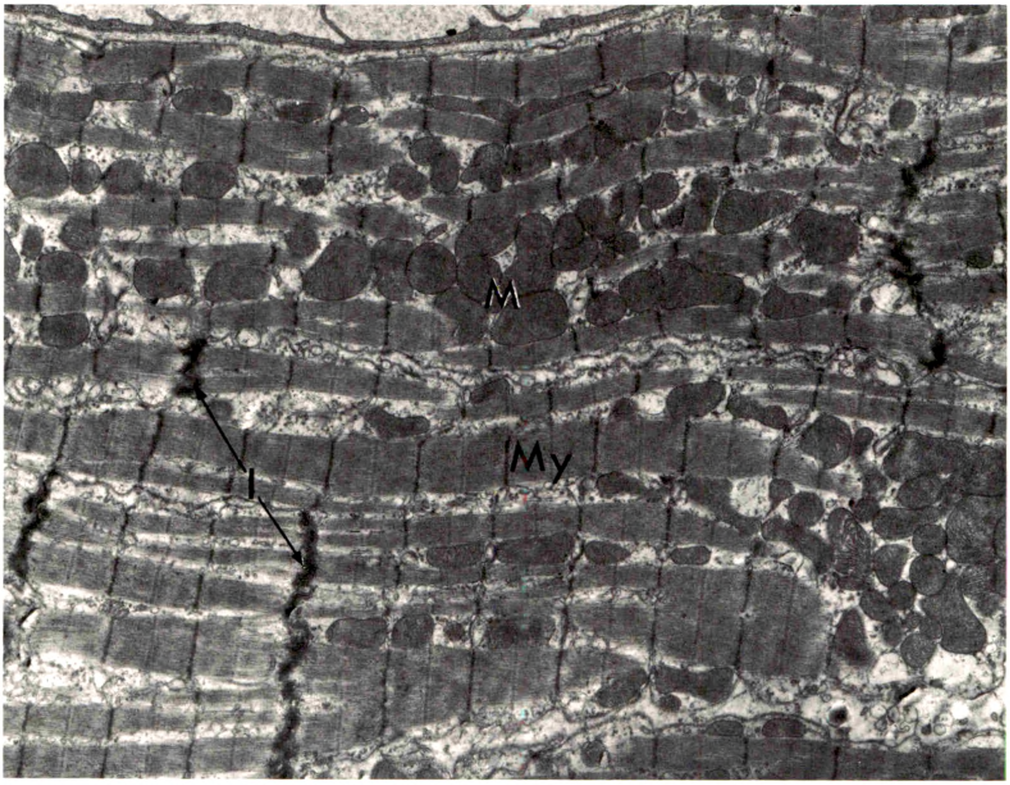

1

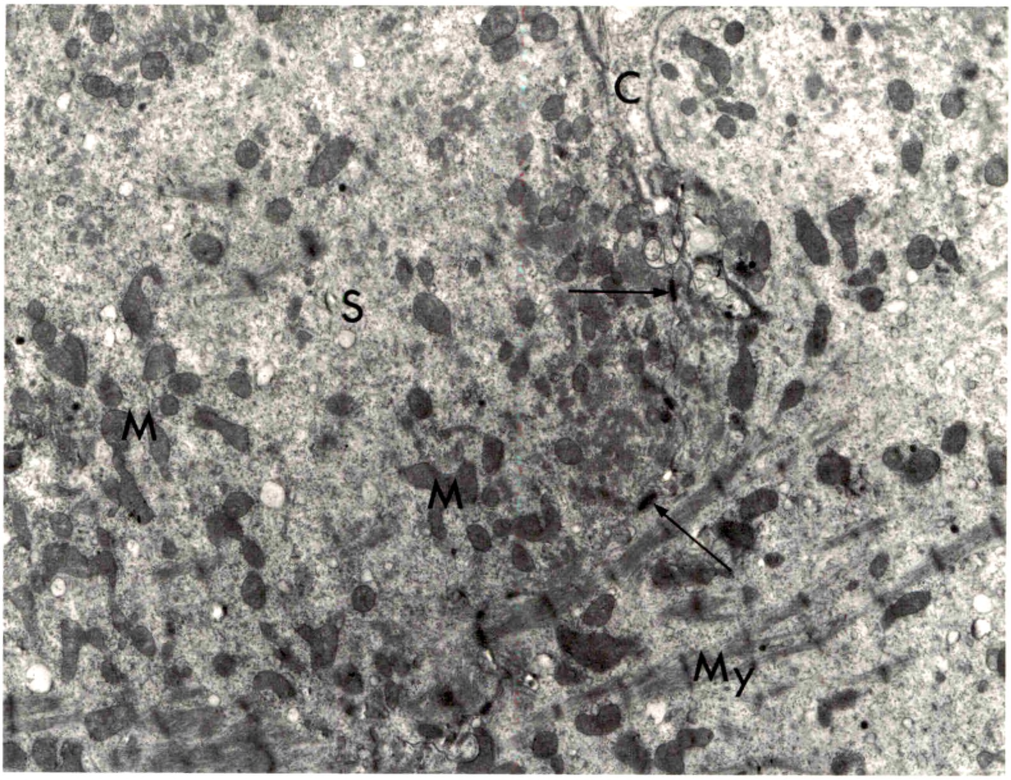

2

3

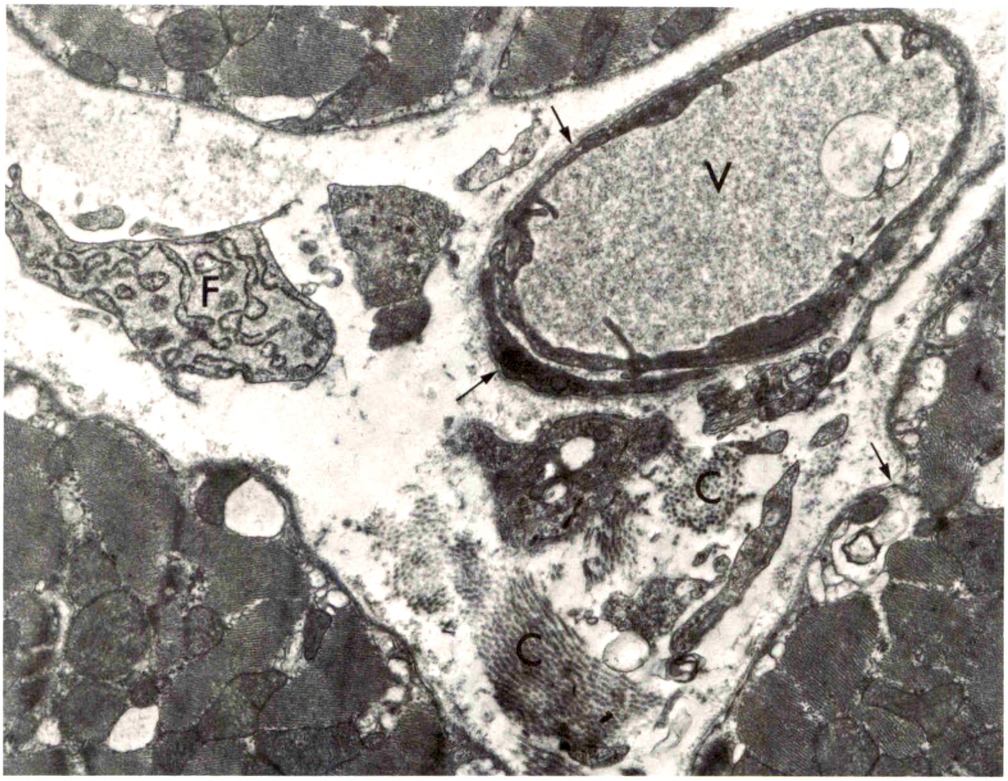

4

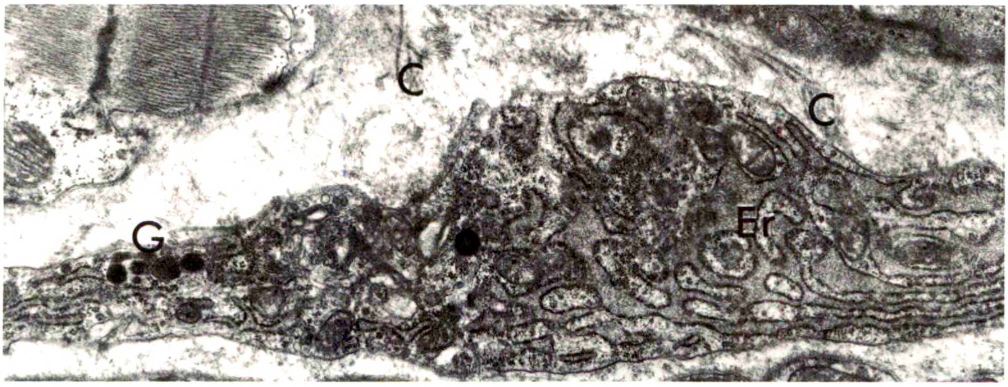

Fig 3—Electron micrograph of normal tissue showing a small vessel (*V*) fibroblast (*F*), collagen (*C*) and portions of three muscle cells. Also note basal lamina (*arrows*) (Six weeks, 3% isotonic glutaraldehyde and osmium tetroxide, uranyl acetate and lead stain, × 11,400). **Fig 4**—Electron micrograph of normal fibroblast showing the prominent ergastoplasmic cisternae (*Er*). Also evident are electron-dense granules (*G*) and extracellular collagen (*C*) (Six weeks, 3% isotonic glutaraldehyde and osmium tetroxide, uranyl acetate and lead stain, × 10,300).

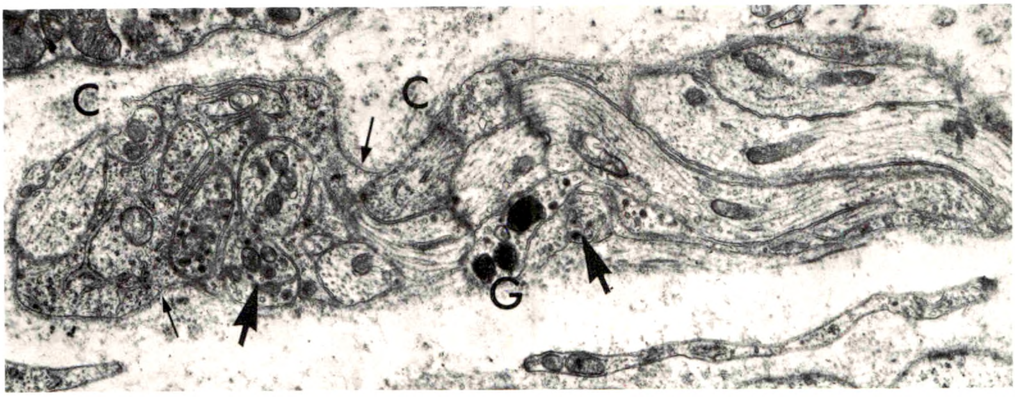

5

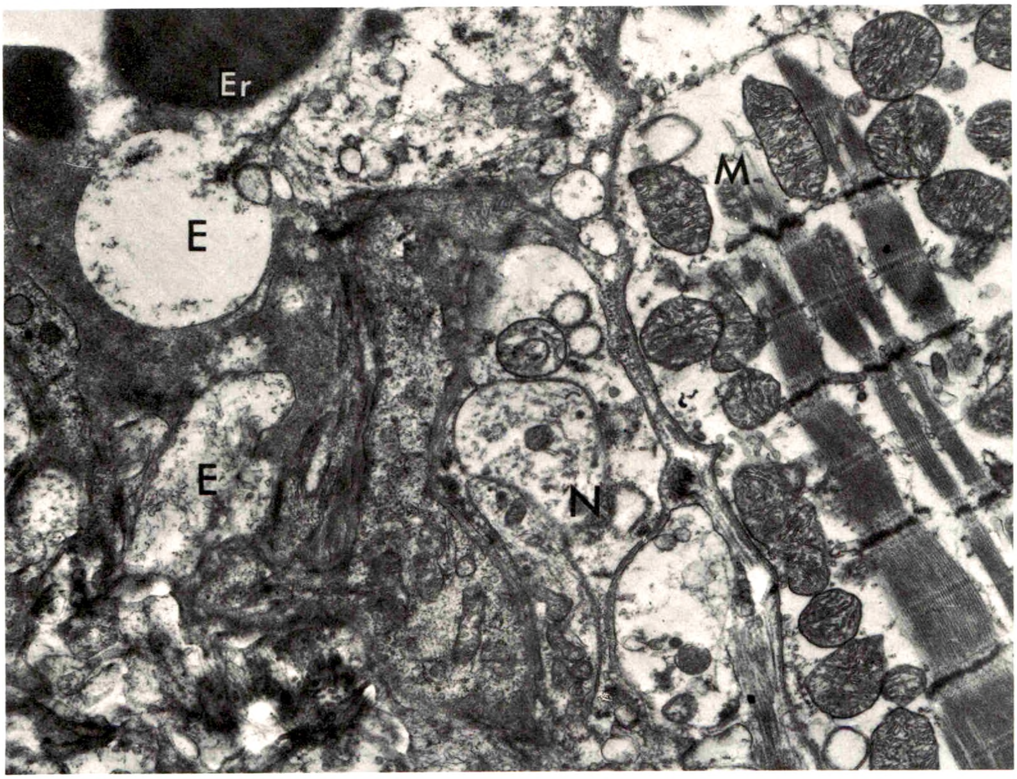

6

Fig 5—Electron micrograph of normal nonmyelinated nerve. Neurosecretory granules are evident (*large arrows*), as is collagen (*C*) and some electron-dense granules are also present (*G*). Note the thin basal lamina (*small arrows*) (Eight weeks, 3% isotonic glutaraldehyde and osmium tetroxide, uranyl acetate and lead stain, × 11,400). **Fig 6**—Electron micrograph of cardiac tissue showing gross alterations in cytologic elements. The muscle cells are degenerate (*M*). Also present are remnants of nerves (*N*), and capillary endothelium (*E*) with an erythrocyte (*Er*). Other unidentifiable elements are present. (Eight weeks, osmium tetroxide, uranyl acetate and lead stain, × 11,400).

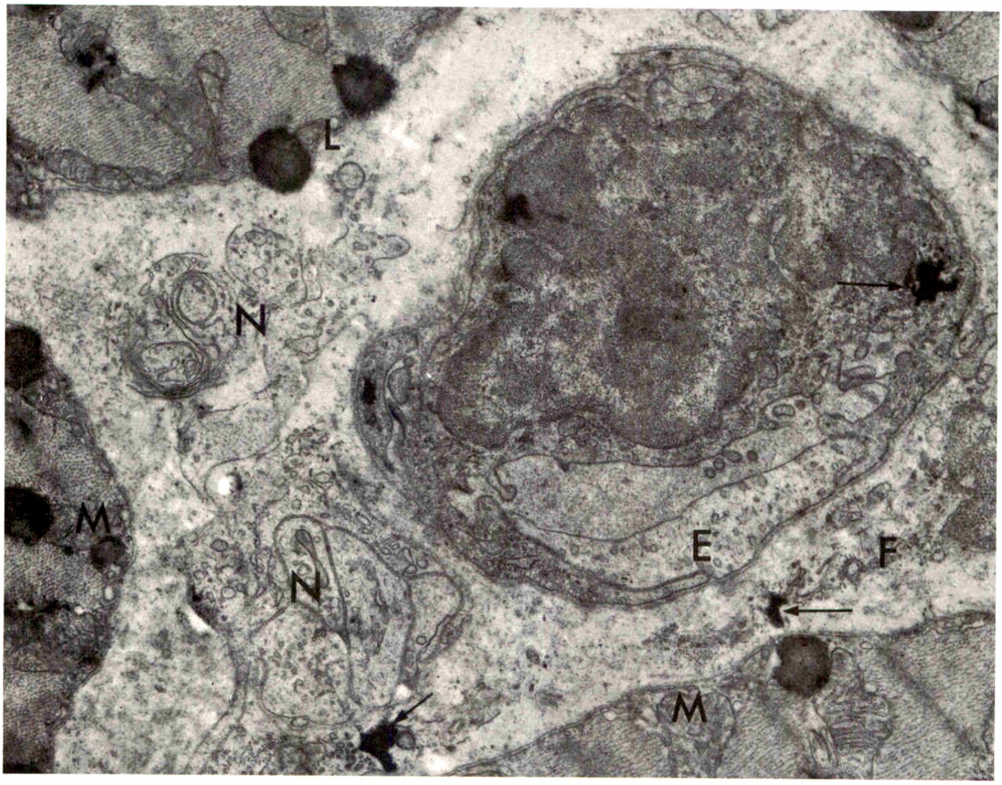

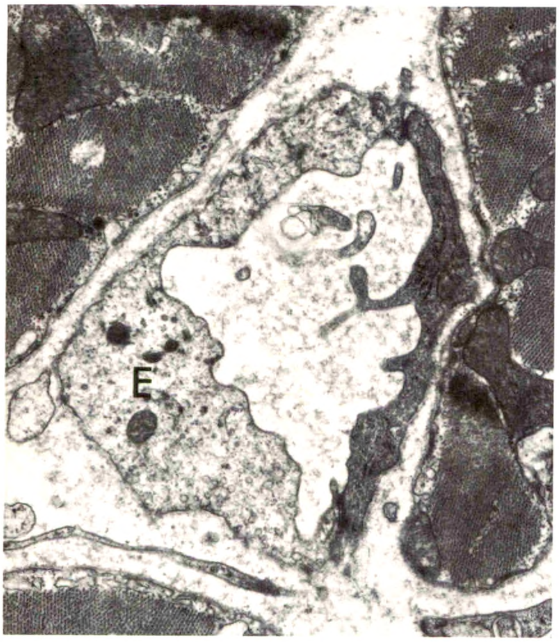

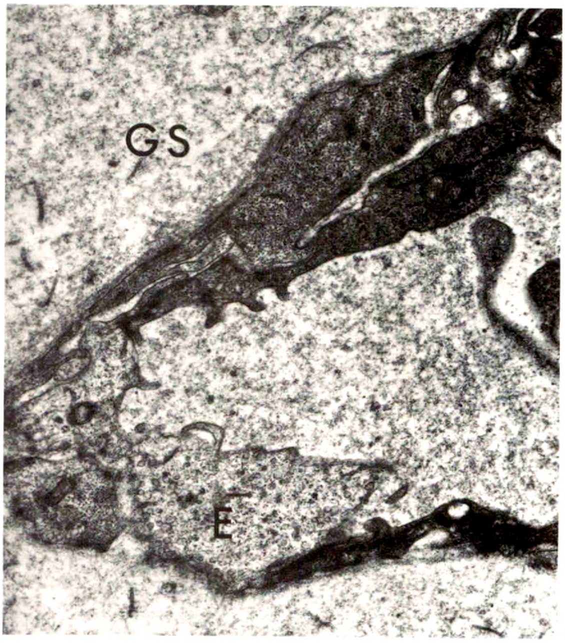

9

Fig 7—Electron micrograph of cardiac tissue from deficient piglet. Portions of three muscle fibers are present showing lipid droplets (*L*) and altered mitochondria (*M*). The capillary can be seen to contain an altered endothelial cell (*E*) and adjacent to this is a disrupted fibroblast (*F*) and nerve (*N*). All three elements contain electron-dense, lipid-like inclusions (*arrows*) (Six weeks, osmium tetroxide, uranyl acetate and lead stain, × 11,400). **Fig 8**—Electron micrograph of capillary showing degenerate endothelial cell (*E*). Portions of muscle cells are also present (Three weeks, 3% isotonic gutaraldehyde and osmium tetroxide, uranyl acetate and lead stain, × 12,400). **Fig 9**—Electron micrograph showing altered endothelial cell (*E*). Also note lack of extracellular collagen but prominent granular ground substance (*GS*) (Six weeks, 3% isotonic glutaraldehyde and osmium tetroxide, uranyl acetate and lead stain, × 11,400).

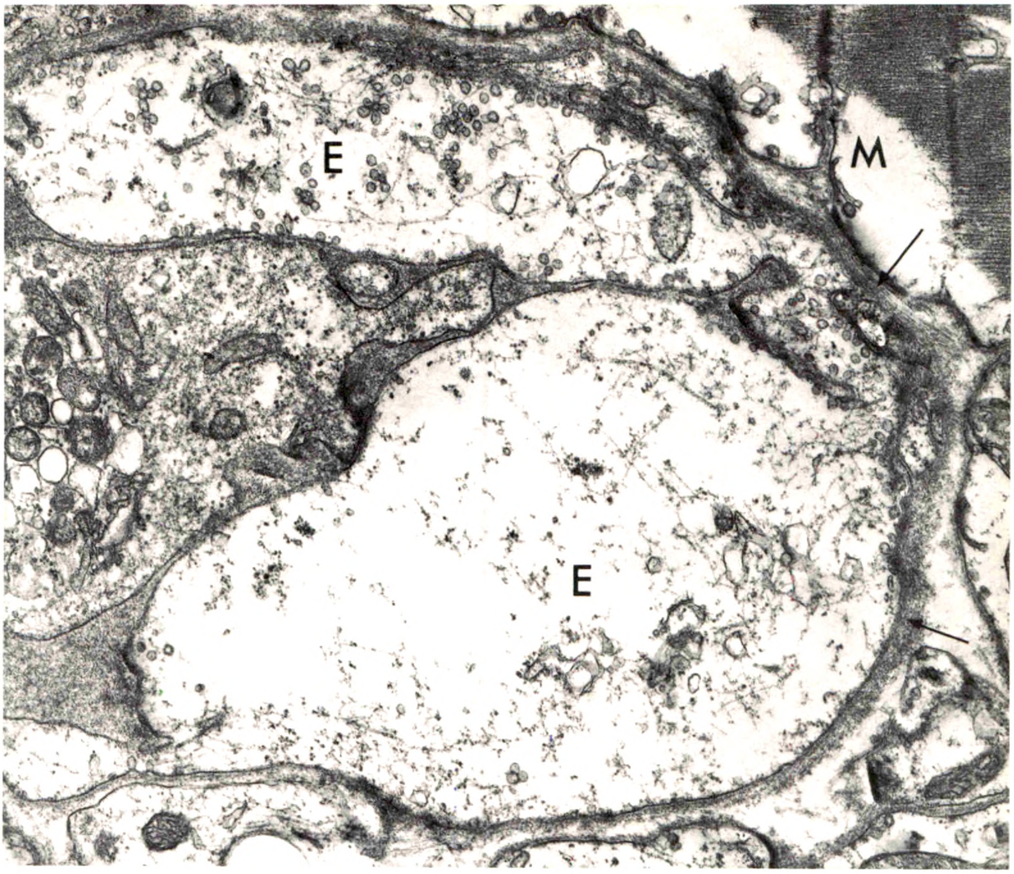

1

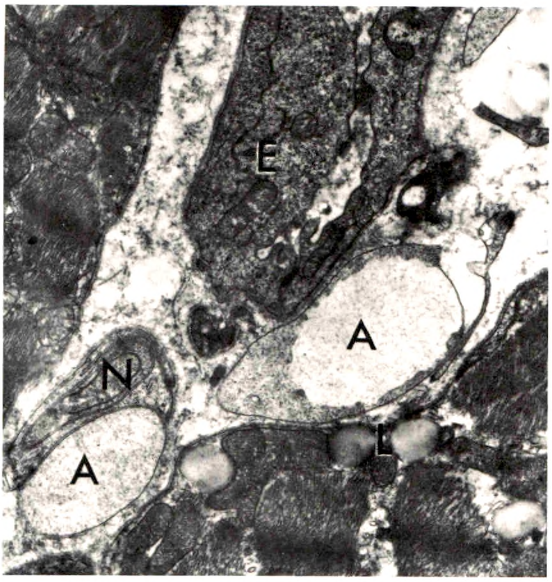

1

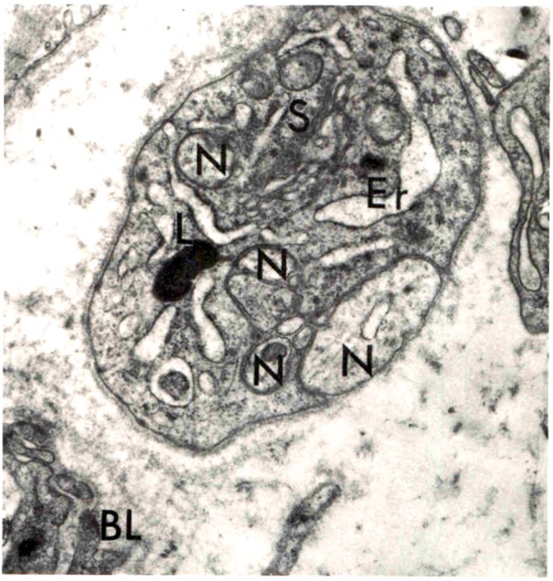

12

Fig 10—Electron micrograph showing major alterations of the endothelium at this stage (*E*). Also note prominent basal lamina (*arrows*), and adjacent abnormal muscle (*M*) (Six weeks, osmium tetroxide, uranyl acetate and lead stain, × 16,800). **Fig 11**—Electron micrograph of degenerate nerve. A portion of a neuron can be seen (*N*); swollen axon portions (*A*) devoid of structure. The only observable change in the muscle is the presence of lipid droplets (*L*); note the lack of extracellular collagen. Also present is a capillary with altered endothelium (*E*) (Three weeks, 3% isotonic glutaraldehyde and osmium tetroxide, uranyl acetate and lead stain, × 8,800). **Fig 12**—Electron micrograph showing a portion of a Schwann cell (*S*) enclosing four nerves (*N*). The former shows dilated ergastoplasmic profiles (*Er*) and a lipid droplet (*L*). Note the lack of definite collagenous fibrils and the basal lamina (*BL*) of nearby capillary (Three weeks, osmium tetroxide, uranyl acetate and lead stain, × 9,300).

3

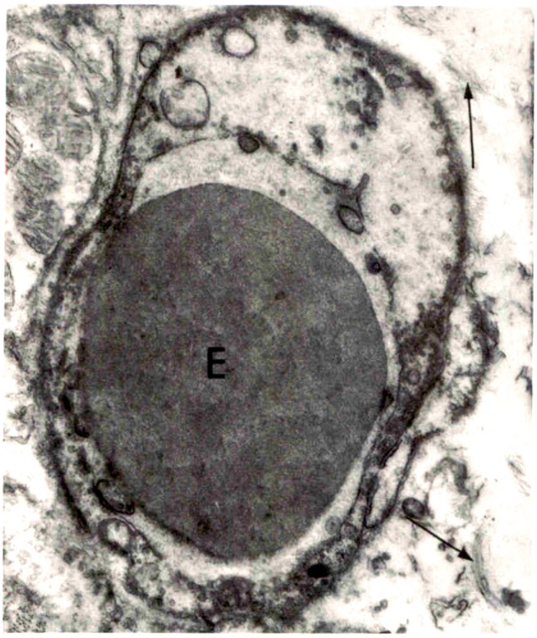

1

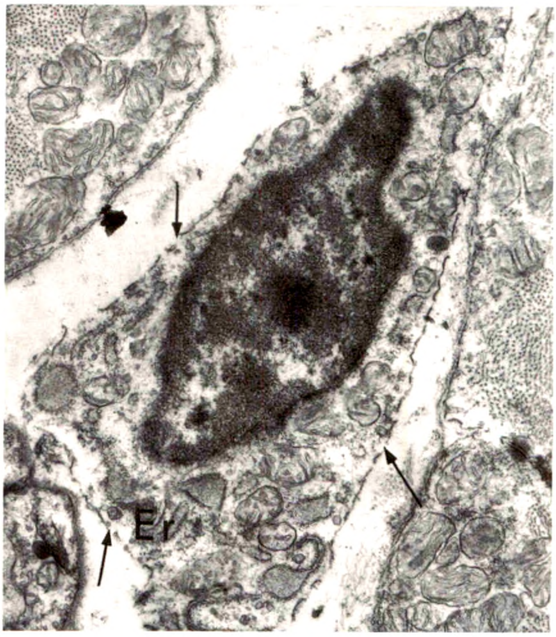

5

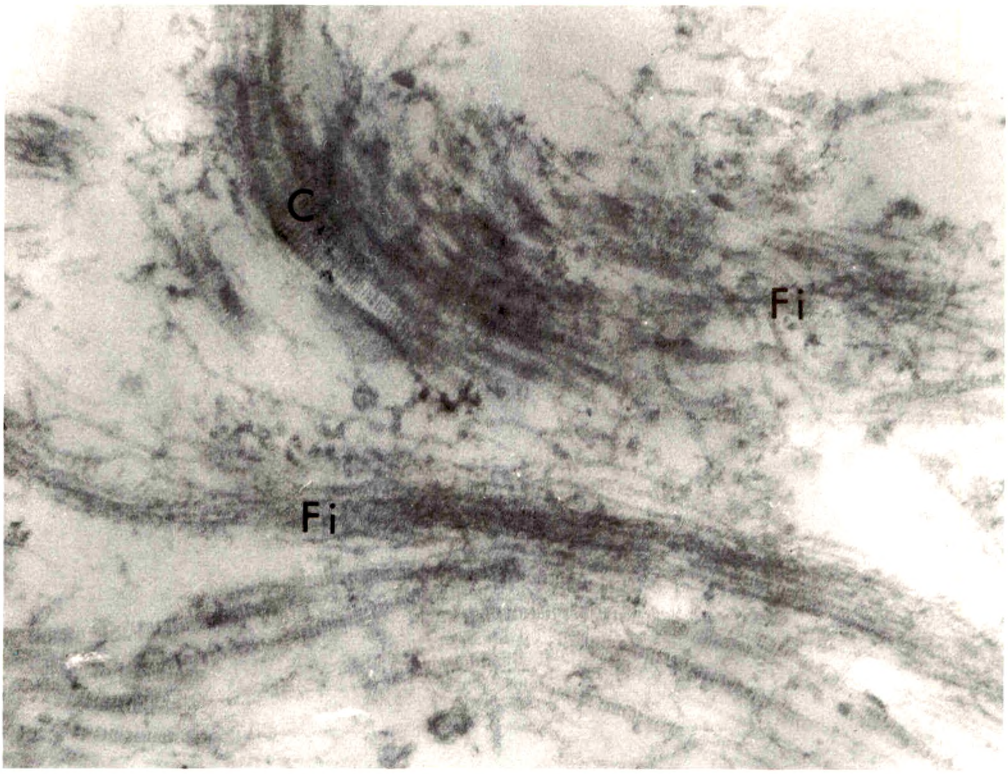

Fig 13—Electron micrograph showing a small degenerate capillary with enclosed erythrocyte (*E*) and fine extracellular filaments (*arrows*) (Newborn, osmium tetroxide, uranyl acetate and lead stain, × 13,800). **Fig 14**—Electron micrograph showing a degenerate fibroblast containing disorganized ergastoplasm (*Er*) and discontinuous plasma membrane (*arrows*). Also note the fine extracellular filaments (Newborn, osmium tetroxide, uranyl acetate and lead stain, × 15,600). **Fig 15**—Electron micrograph showing collagen fibrils (*C*) with an axial periodicity and associated filaments (*Fi*) (Newborn, osmium tetroxide, uranyl acetate and lead stain, × 70,300).

Ultrastructure of Muscular Dystrophy

II. A Comparative Study in Lambs and Chickens

Phillip R. Sweeny, PhD, J. G. Buchanan-Smith, PhD, F. deMille, MS,
J. R. Pettit, DVM and E. T. Moran, PhD

The ultrastructure of the semitendonosus muscle of lambs and the pectoralis major muscles of chickens suffering from nutritional muscular dystrophy were studied. Samples of tissue from histologically normal and mildly degenerate areas were examined. Ultrastructural examination of areas that appeared apparently normal histologically, revealed lesions in the small vessels, connective tissue elements and neuromuscular elements. The possible relationship of these findings to the etiology of this disease are discussed (Am J Pathol 68:493–510, 1972).

A LARGE BODY OF LITERATURE EXISTS describing changes in muscle tissue in both nutritional and genetic muscular dystrophies. Most of these studies involved light microscopic, histochemical and biochemical approaches,[1-5] though a few reports are available on the ultrastructural aspects of this disease.[6-12] It should be noted that few of the above papers dealt with early stages of degenerative processes; rather, all efforts seem to have been expended on visibly altered muscle areas.

In the avian species, considerable research has been done on nutritionally induced *white muscle* disease as well as on genetic muscular dystrophy.[13-19] Relatively few cases of muscular dystrophy in the ovine species have been reported in the literature, although these animals are known to show the classic symptoms, both clinical and histologic, of white muscle disease induced by vitamin E- and/or selenium-deficient diets.[20-26] Despite the existing literature on the histologic and biochemical alterations in muscles of animals with muscular dystrophy (avian or ovine), there are no detailed reports of the ultrastructural changes during early manifestations of this disease in these species.

From the Department of Microbiology, College of Biological Science, the Department of Animal and Poultry Science, Ontario Agricultural College, University of Guelph and Veterinary Services Branch, Ontario Department of Agriculture and Food, Guelph, Ontario, Canada.

Supported by grants from the National Research Council of Canada, the Medical Research Council of Canada and the Ontario Department of Agriculture and Food.

Accepted for publication May 25, 1972.

Address reprints requests to Dr. Phillip R. Sweeny, Department of Microbiology, College of Biological Science, University of Guelph, Guelph, Ontario, Canada.

Two years ago a detailed biochemical and ultrastructural study of vitamin E and selenium deficiency-induced white muscle disease in pigs was initiated.[24] During this study, it was decided that examinations of other species with similarly induced muscular alterations be examined for comparative purposes. This paper describes some of the ultrastructural changes in the pectoralis major muscle of the chick and semitendonosus muscle of the lamb after clinical evidence of nutritionally induced white muscle disease appeared.

This paper deals with nonmuscular lesions in areas that appeared normal or seemed to show early stages of degeneration under the light microscope. Observations on the vascular bed, connective tissues and neuromuscular junctions are included and relevance of the alterations in these tissue components are discussed with respect to the etiology of the disease.

Materials and Methods

Animals

The lambs utilized in these experiments were placed on a high fat diet deficient in vitamin E and selenium at 1 week of age.[26] The diet was modified to contain 50% torula yeast, 35.7% glucose and 10.0% lard. Biopsy specimens of semitendonosus muscle were collected at the onset of clinical symptoms. The birds utilized in this study were broiler chickens maintained on a ration based on a meal of corn and soy beans grown in selenium-deficient soil. All vitamins and minerals including vitamin E, 25 IU/ton, other than selenium were supplemented in adequate amounts. The diet, on analysis, contained 0.08 ppm selenium on a dry weight basis. The chickens (which had been diagnosed as muscular dystrophic on gross postmortem and histologic examination) were obtained from the Poultry Diagnostic Laboratory, Veterinary Services Branch, Ontario Department of Agriculture and Food, Guelph, and their protocol number was P3820/70. Only those muscles from birds showing minor visible lesions were collected.

Tissue Samples

The tissues, both normal and pathologic, obtained for ultrastructural studies on the lamb were removed from the semitendonosus muscle at 6 and 8 weeks after the diet was administered. All tissues from the chickens were removed after cervical dislocation, when muscle samples were taken from the pectoralis major; mildly pathologic, as well as normal, areas were prepared for examination. After they were removed from the animals, all tissues were fixed, as described in an earlier paper.[24]

Results

The structural changes, to be described, were observed in both lamb and avian muscle. The first tissue samples examined were from normal controls. Normal ultrastructural characteristics of muscle were observed in all tissue components; ultrastructurally, the fibers appeared normal. Most fibers were in the contracted state, and extensive examination was necessary to find satellite cells. In addition, both red and white types were present in the semitendinosus muscle of the lamb, whereas the white was the predominent fiber of the pectoralis muscle from the chicken.

After our survey of normal tissue components, areas showing minor lesions were examined and found to contain a complex array of cellular aggregates, showing all degrees of degeneration of fibroblasts, vessels, nerves and muscle fibers (Figure 1). The origin of these cellular aggregates could only be ascertained by observing other tissue samples which showed a progression from apparently normal to mildly degenerate conditions.

In areas which appeared histologically normal, the only morphologic alterations observed ultrastructurally involved the capillaries, fibroblasts, nonmyelinated nerves and, on very rare occasions, neuromuscular junctions. In areas showing minor signs of degeneration, the arterioles and neuromuscular junctions showed marked alterations, and muscle fibers in the early stages of degeneration could be found.

Capillary and small vessel changes were manifested by endothelial swelling and these cells lost all of their ultrastructural characteristics. The morphology of these cells was markedly changed, they appeared enlarged, contained remnants of degenerate mitochondria and, in some instances, they appeared devoid of all classic organelles (Figures 2, 3); the basal lamina appeared fibrous and thickened (Figure 3). Similar lesions were seen with all of the fixatives used but were never seen in the controls. Associated with these changes in the vascular bed, major alterations to the fibroblast populations was evident. The ergastoplasmic profiles often appeared dilated and the cytoplasm contained electron-dense granules. The mitochondria in some cells appeared normal and, in others, degenerate. The extracellular compartment could be seen to be rather amorphous, yet flocculent, and one had difficulty finding collagen fibrils (Figures 4, 5).

In areas with early definitive lesions, occluded vessels of varying sizes could be seen; endothelial cells often showed phagocytic characteristics. In large arterioles some of the endothelia and smooth muscles contained degenerate mitochondria, thus indicating minor alterations; these appeared to coincide with vascular occlusion (Figures 7, 8 and 9). It was first thought that these aggregates were muscular in origin, but remnants of tight junctions and erythrocytes precluded this. Endothelia of these vessels could be seen to contain electron-dense granules and degenerate mitochondria (Figure 7). Some cells within these aggregates appeared fibroblast-like and contained prominent ergastoplasmic profiles (Figures 8, 9). Some vessels also appeared to have withdrawn from the basal lamina, and their cells showed marked morphologic changes, especially in occluded vessels (Figures 8, 9); in some areas, glycogen could be seen within the cytoplasm of smooth muscle cells of small vessels (Figure 10). In all samples of tissue revealing minor or major degenerative changes, numerous aggregates of cells gave the appearance of dissociated endothelium still within the basal lamina (Figure 11); occasional mitotic figures were seen within this population. Since these cellular aggregates were seen in tissue areas with only minor muscle damage, as evidenced ultrastructurally, it is felt that they are of vascular origin, rather than derived from degenerate muscle cells.

Accompanying the early vascular changes were altered nerves and neuromuscular junctions. As mentioned earlier, altered fibroblasts, vascular endothelium and nerves were observed in areas showing minimal-to-no muscle fiber damage. In these tissue areas, all neuromuscular junctions, observed to date, have shown varying degrees of degeneration, none of which could be seen in routine histologic preparations. It is quite evident that these junctional complexes were no longer functional, as the whole foot pad was withdrawn from the muscle (Figures 12, 13). The terminals appeared to have undergone vacuolation, and contained degenerate mitochondria in addition to vesicles and myelin-like figures (Figures 12, 13). Occasionally, altered myelinated and nonmyelinated fibers were observed near neuromuscular junctions and both types contained vesicles and myelin-like dense bodies, thus inferring alterations to both sensory and motor endplates. In addition, electron-dense bodies often were seen in the Schwann-cell cytoplasm (Figure 12). In larger fibers, numerous perineural endothelial cells contained glycogen (Figure 14). In those tissues showing evidence of only minor muscle cell changes, the nonmyelinated fibers accompanying vessels could be seen to contain lipid-like droplets and some of the axons appeared empty and degenerate (Figure 6). Such alterations of nerves were never observed in the normal tissues examined, regardless of the fixation used.

A few major nerve fibers containing mixed nerves were examined, and some axons appeared degenerate. The number of altered nerve fibers and neuromuscular junctions appeared to be proportionate to the severity of lesions. In those areas with obvious muscle degeneration, no nonmyelinated fibers or neuromuscular junctions were ever observed, despite the appearance of relatively normal fibers.

In the lamb, a variety of degenerate muscle fiber types was observed. These ranged from fibers with small foci of degenerate sarcomeres through cells with complete disruption of sarcomeres, mitochondria and the tubular system (Figure 1). These degenerative fibers had withdrawn from their basal lamina which, although markedly folded, remained intact. Varying amounts of glycogen were seen throughout the sarcoplasm, the largest quantities being in the more degenerate fibers (Figure 1).

In normal areas of muscle, all fibers were in a state of partial-to-full contraction. In degenerate areas (minor or major), most normal fibers were in the relaxed state, thus inferring a lack of response to the fixative, and therefore, altered neuromuscular relationships. However, one type of cell in particular did not show normal contracture; in cells of this type some sarcomeres appeared fully contracted and some fully relaxed. In others, one I band was absent and, in still others, both I bands were absent (Figure 15). This finding was infrequent in more normal areas and common in areas showing obvious degeneration.

In addition to the above, degenerate fibers seemed to contain an inordinately large number of satellite cells. In normal muscle, these cells rarely were seen in any given section, whereas in degenerate tissue, many fibers in a given cross-sectional area contained at least a portion of a satellite cell. This was most obvious in the lamb and less so in the avian system. In abnormal cells, the cytoplasm of the satellite cell seemed increased, large quantities of organelles were present and the cell often bulged into the extracellular compartment (Figure 16). Although this seems to be most prevalent in those muscle cells in an advance state of degeneration, it is not uncommon in mildly altered muscle cells.

Discussion

The foregoing observations on nutritionally induced muscular dystrophy in lamb and chickens reveal that the earliest detectable lesions at the ultrastructural level are seen in the vascular bed, connective tissues and neuromuscular junctions.

Changes in the vascular bed, particularly the capillaries, have been described by Cheville [2] and Carlson [19] in vitamin-E-deprived chickens and by Pearce [6] in humans. Capillary changes have been investigated thoroughly by Ashmore [14] in chickens, and these authors believed that the primary lesion in muscular dystrophy lies in this compartment of the tissue. Numerous investigations have examined the nerves in this disease and suggest that the prime lesion is neuronal in origin and that one is dealing with a neuropathy.[10,16,18] None of the above investigations, however, dealt with ultrastructural changes in these tissues nor have they discussed in detail, developmental factors which may be affected in nutritional or genetic forms of muscular dystrophy. The nutritional deficiency undoubtedly leads to changes which become clinically manifest at the time the muscles of concern are undergoing major growth and differentiation.[5,24] There is ample evidence that in both nutritionally induced and genetic variations of muscular dystrophy, alterations are seen in various developmental parameters of muscle cells *per se.*[27-30] Previous investigators have shown that myosin,[27] lactic acid dehydrogenase isoenzymes[28] and acetyl cholinesterase patterns[18] do not follow normal developmental changes in genetic muscular dystrophies. Indeed, developmental parameters of a variety of muscle enzymes have been shown to be altered in genetic muscular dystrophy of chickens.[20,30] Similar observations have also been reported in muscles of lambs suffering from nutritionally induced muscular dystrophy.[22]

There is no doubt, from the above studies, that one is dealing with a change in the normal developmental sequences of affected muscles. It does, however, appear that, in deliberations to date, only a few observations have been made on connective tissue components of this tissue during the early development of the disease.[1,23]

It is well known that connective tissue elements, particularly collagen, appear to play an important role in the *in vitro* differentiation of muscle cells.[31,32] The significance of normal differentiation of connective tissues and its relationship to muscle differentiation has also been alluded to by James [33] and Lieberman [34] with regard to normal cardiac function. In addition to this, normal tendon insertions are known to play a prominent role in maintaining normal muscle tone, since muscular atrophy results when insertions are cut.[35] There can be no doubt that the normal differentiation of collagen and, probably, other connective tissue components in general are essential to the normal development of muscle. Indeed, normal connective tissue development is probably an essential factor for differentiation of the vascular bed and neural elements of this tissue.

The observations reported in this paper support the findings of Sweeny and Brown [24] on cardiac muscle in vitamin E- and selenium-deprived piglets. In that study there was no doubt that one of the first changes seen in the animals was fibroblast degeneration; collagen fibrillogenesis appeared abnormal. Similar observations have been made during the present study, in mildly degenerate areas of lamb and chicken muscles. The absence of gross lesions in this compartment, in these animals, as compared to the piglets, may well result from the fact that the piglet was deprived *in utero,* whereas the above animals were deprived either postnatally (lamb) or *ex ovo* (chicken). Thus, the probability of observing changes at the ultrastructural level would be higher in the former, as they would have had more time to become manifest.

It should be pointed out that vascular lesions in the pig and those described here strongly resemble changes seen in scurvy.[36] It is thus felt that the early lesion in muscular dystrophy is an alteration in the differentiation of the connective tissue compartment of the muscle. This has been inferred by Bourne and Golarz,[1] as well as by King and Maplesden,[23] both of whom suggest alterations in the polysaccharide fraction of this element. These observations are supported by the findings of Cosmos,[5] who reported polysaccharide changes in genetic muscular dystrophies in chickens. Other mainfestations in the tissue would result from the above in that, after vascular collapse, which is thought by us to be secondary to connective tissue alterations, physiologic anoxia would develop which would lead to changes in neuromuscular junctions and muscle atrophy. The red fibers would be least sensitive, as they are already well differentiated at birth, whereas the affect on white fiber differentiation would be detrimental.

Other lesions observed in the lamb and chicken (*ie,* vascular changes, neuromuscular degenerations and muscle changes) could conceivably result from a deterimental affect on connective tissue during differentiation and rapid growth. This could lead to alterations of differentiation in the pericapillary connective tissue compartment, failure of capillary permeability or expansion of the normal vascular network with a resultant hypoxia which would, in turn, lead to degeneration of neuromuscular junctions. Muscles thus deprived of innervation and oxygen could be expected to undergo structural changes which should be a combination of those expected to result from improper differentiation, or a lack of innervation and oxygen. Superimposed on these would be changes found after physiologic tenotomy, which would occur if connective tissue fibril formation were abnormal.

References

1. Bourne GH, Golarz MN: Histochemical evidence for a possible biochemical lesion in muscular dystrophy. J Histochem Cytochem 11:286–288, 1963
2. Cheville NF: The pathology of vitamin E deficiency in the chick. Pathol Vet 3:208–225, 1966
3. Nesheim MC, Leonard SL, Scott ML: Alberations in some biochemical constitutents of skeletal muscle of vitamin E deficient chicks. J Nutr 68: 359–370, 1959
4. Bunyan J, Green J, Diplock AT, Robinson D: Lysosomal enzymes and vitamin E deficiency. I. Muscular dystrophy, encephalomalacia and exudative diathesis in the chick. Br J Nutr 21:127–136, 1967
5. Cosmos E: Ontogeny of red and white muscles: the enzymatic profile and lipid distribution of immature and mature muscles of normal and dystrophic chickens, Physiology and Biochemistry of Muscle as a Food. Edited by EJ Briskey, RG Cassens, BB Marsh. University of Wisconsin Press, 1970 pp 193–207
6. Pearce GW: Electron microscopy on the study of muscular dystrophy, Muscular Dystrophy in Man and Animals. Edited by GH Bourne, M Golarz. New York, Hafner Publishers, 1963, pp 160–191
7. Nafstad I, Nafstad HJ: An electron microscopic study of blood and bone marrow in vitamin E deficient pigs. Pathol Vet 5:520–537, 1968
8. Ross MH, Pappas GD, Pinckney JH: Alterations in muscle fine structure in hereditary muscular dystrophy of mice. Lab Invest 9:388–403, 1960
9. Pelligrino C, Franzini C: An electron microscope study of denervation atrophy in red and white skeletal muscle fibers. J Cell Biol 17:327–349, 1963
10. Schapira G, Dreyfus Jean-Claude: Biochemistry of progressive muscular dystrophy.[6] pp 48–87
11. Van Breemen VL: Ultrastructure of human muscle. II. Observations on dystrophic striated muscle fibers. Am J Pathol 37:333–341, 1960
12. Van Vleet JF, Hall BV, Simon J: Vitamin E deficiency: a sequential light and electromicroscopic study of skeletal muscle degeneration in weanling rabbits. Am J Pathol 52:1067–1079, 1968
13. Cordy DR: Muscular dystrophy in cattle and sheep.[6] pp 500–514
14. Ashmore CR, Doerr L, Somes RG Jr: Microcirculation: loss of an enzyme activity in chickens with hereditary muscular dystrophy. Science 160:319–320, 1968
15. Erwin ES, Sterner W, Gordon RS, Machlin LJ, Tureen LL: Etiology of muscular dystrophy in the lamb and chick. J Nutr 75:45–50, 1961
16. McComas AS, Sica REP: Muscular dystrophy: myopathy or neuropathy? Lancet 1:1119, 1970
17. Holiday TA, Julian LM, Asmundson VS: Muscle growth in selected lines of muscular dystrophic chickens. Anat Rec 160:207–216, 1968
18. Wilson BW, Kaplan MA, Merhoff WC, Mori SS: Innervation and the regulation of acetylcholinesterase activity during the development of normal and dystrophic chick muscle. J Exp Zool 174:39–54, 1970
19. Carlson CW: Selenium vitamin E interrelationships in poultry nutrition. Thirty-first Annual Minnesota Nutritional Conference, 1970, pp 21–28

20. McGavin MD, Baynes ID: A congenital progressive ovine muscular dystrophy. Pathol Vet 6:513–524, 1962
21. Cristie B: Ovine muscular dystrophy in Victoria. Aust Vet J 38:392–394, 1962
22. Paulson GD, Pope AL, Baumann CA: Lactic dehydrogenase isoenzymes in tissues and serum of normal and dystrophic lambs. Proc Soc Exp Biol Med 122:321–324, 1966
23. King JM, Maplesden DC: Nutritional muscular dystrophy in calves III. Purkinje fiber degeneration in calves with experimentally produced nutritional dystrophy. Canad Vet J 1:421–426, 1960
24. Sweeny PR, Brown RG: Ultrastructural changes in muscular dystrophy. I. Cardiac tissue of piglets deprived of vitamin E and selenium. Am J Pathol 68:479–492, 1972
25. Buchanan-Smith JG, Nelson EC, Tillman AD: Effect of vitamin E and selenium deficiencies on lysosomal and cytoplasmic enzymes in sheep tissues. J Nutr 99:387–394, 1969
26. deMille F, Miller RB, Buchanan-Smith JG: Effects of vitamin E or ethoxyquin and rumen development upon muscular dystrophy in lambs. Canad J Animal Sci 1972, (In Press)
27. Oppenheimer H, Barany K, Milhorat AT: Myosin from mice with hereditary muscular dystrophy. Proc Soc Exp Biol Med 116:877–880, 1964
28. Kaplan NO, Cahn RD: Lactic dehydrogenase and muscular dystrophy in chicken. Proc Nat Acad Sci USA 48:2123–2130, 1962
29. Cosmos E: Enzymatic activity of differentiating muscle fibers. I. Development of phosphorylase of the domestic fowl. Dev Biol 13:163–181, 1966
30. Cosmos E, Butler J: Differentiation of fiber types in muscle of normal and dystrophic chickens, A Quantitative and Histochemical Study of the Ontogeny of Muscle Enzymes. Excerpta Medica International Congress, Series 147, Exploratory Concepts in Muscular Dystrophy and Related Disorders, 1966, pp 197–204.
31. Hauschka SD, Konigsberg IR: The influence of collagen on the development of muscle colonies. Proc Nat Acad Sci USA 55:119–126, 1966
32. Hauschka SD: Clonal aspects of muscle development and the stability of the differentiated state, The Stability of the Differentiated State. Edited by H Ursprung. New York, Springer-Verlag Inc, 1968, pp 37–57
33. James TN: Cardiac conduction system: fetal and postnatal development. Am J Cardiol 25:213–226, 1970
34. Lieberman M: Physiologic development of impulse conduction in embryonic cardiac tissue. Am J Cardiol 25:279–284, 1970
35. Shafiq SA, Gorycki MA, Asiedu SA, Milhorat AT: Tenotomy effect on fine structure of the soleus of the rat. Arch Neurol 20:625–633, 1969
36. Friederici HH-R, Taylor H, Rose R, Pirani CL: The fine structure of capillaries in experimental scurvey. Lab Invest 15: 1442–1448, 1966

Acknowledgments

We are grateful for the technical assistance of Mrs. I. Hernandez and Barbara Atkinson.

Legends for Figures

Fig 1—Electron micrograph of a mildly degenerate area from lamb. Four muscle fibers in varying stages of degeneration can be seen *(1–4)* and one of these contains a satellite cell(s), while all contain varying amounts of glycogen. Numerous portions of cells are visible at *arrows*, and a large central mass containing mitochondria *(M)*, a nucleus *(N)* and peripheral material is also visible (Lamb, 3% hypertonic glutaraldehyde and osmium tetroxide, uranyl acetate and lead stain, × 22,800).

Fig 2—Electron micrograph of a small vessel with an enclosed erthrocyte. The mitochondria *(M)* are degenerate and the nuclei appear degenerate *(N)* (Chicken, 3% hyertonic glutaraldehyde and osmium tetroxide, uranyl acetate and lead stain, × 10,400).

Fig 3—Electron micrograph of a small vein with a ballooning endothelial cell *(E)* and smooth muscle cell *(Sm)*. The basement membrane appears thickened and fibrous *(arrows)* (Chicken, 3% hypertonic glutaraldehyde and osmium tetroxide, uranyl acetate and lead stain, × 16,600).

Fig 4—Electron micrograph of a fibroblast showing dilated ergastoplasm *(Er)*, and electron-dense granules *(arrow)*. The muscle cells show dilated sarcoplasmic reticulum and the extracellular area contains flocculent materials as well as a degenerate vessel *(V)* (Lamb 3% hypertonic glutaraldehyde and osmium tetroxide, uranyl acetate and lead stain, × 8100).

Fig 5—Electron micrograph of a fibroblast showing dilation of the ergastoplasm *(Er)* and electron-dense granules *(arrows)*. Note prominent Golgi *(G)* and lack of collagen in the extracellular spaces (Lamb, 3% hypertonic glutaraldehyde and osmium tetroxide, uranyl acetate and lead stain, × 11,800).

Fig 6—Electron micrograph of an arteriole. E = endothelium, *El* = elastic lamina, S = smooth muscle, N = a nonmyelinated nerve. The mitochondria of the vessel appear degenerate *(arrows)* and lipid droplets *(L)* can be seen in the nerve. Collagen *(C)* can be seen around the latter (Chicken 3% isotonic glutaraldehyde and osimum tetroxide, uranyl acetate and lead stain, × 12,400).

Fig 7—Electron micrograph of an occluded vessel. Remnants of tight junctions can be seen at arrows and numerous electron-dense granules are visible throughout the cells *(G)* as are degenerated mitochondria *(M)* (Chicken, 3% hypertonic glutaraldehyde and osmium tetroxide, uranyl acetate and lead stain, × 9800).

Fig 8—Electron micrograph of an occluded vessel with enclosed erythrocyte *(E)*. One of the endothelial cells shows prominent endoplasmic reticulum *(Er)*, a large number of mitochondria *(M)* and the whole cellular aggregate appears withdrawn from the basal lamina *(BL)* (Lamb, 3% hypertonic glutaraldehyde and osmium tetroxide, uranyl acetate and lead stain, × 8900).

Fig 9—Electron micrograph of an occluded vessel showing alteration of cellular morphology, large vesicles *(V)* and basal lamina *(arrows)* as well as altered mitochondria *(M)*. Note extravascular erythrocyte *(EV)* and lack of collagen fibrils in the extracellular compartment (Lamb, 3% hypertonic glutaraldehyde and osmium tetroxide, uranyl acetate and lead stain, × 32,100).

Fig 10—Electron micrograph of a small vessel showing presence of glycogen *(arrow)* in the altered, smooth muscle cell. (Lamb, 3% hypertonic glutaraldehyde and osmium tetroxide, uranyl acetate and lead stain, × 43,900).

Fig 11—Electron micrograph of degenerate vessel. All cells appear altered morphologically and some contain classic organelles *(I)* while others seem to resemble macrophages *(Ma)*. The basal lamina is intact *(arrows)* and the extravascular space

contains no collagen fibers. (Lamb, 3% hypertonic glutaraldehyde and osmium tetroxide uranyl acetate and lead stain, × 8800).

Fig 12—Electron micrograph of a degenerate, sensory neuro-muscular junction *(NJ)*. The neuronal terminal, nerve and the Schwann cell contain vesicles *(V)* as well as electron-dense granules *(arrows)*. Collagen fibrils are prominent in this photomicrograph *(C)* (Lamb, 3% hypertonic glutaraldehyde and osmium tetroxide, uranyl and lead stain, × 10,400).

Fig 13—Electron micrograph of a degenerate motor neuromuscular junction. The nerve can be seen to contain vesicles *(V)* degenerate mitochondria *(M)* and myelin figures *(Mf)*. Similar changes can be seen in the footpad region. Note lack of collagen in the extra cellular compartment (Lamb, 3% hypertonic glutaraldehyde and osmium tetroxide, uranyl acetate and lead stain, × 12,400).

Fig 14—Electron micrograph of a nonmyelinated nerve and accompanying perineural endothelial cells. The former contains vesicles *(V)*, and glycogen aggregates can be seen in the latter *(G)*. Collagen fibrils can be seen throughout the photomicrograph *(C)* (Lamb, 3% hypertonic glutaraldehyde and osmium tetroxide, uranyl acetate and lead stain, × 20,200).

Fig 15—Electron micrograph of a degenerate muscle fiber showing adjacent sarcomeres, some normal *(1)*, others missing an I band *(2)*, while others appear fully contracted *(3)* (Lamb, osmium tetroxide, uranyl acetate and lead stain, × 10,400).

Fig 16—Electron micrograph of a satellite cell. Note the prominent ergastoplasm *(arrows)*, numerous mitochondria *(M)*, granules *(G)*, and cytoplasmic ribosomes (Lamb, 3% hypertonic glutaraldehyde and osmium tetroxide, uranyl acetate and lead stain, × 12,400).

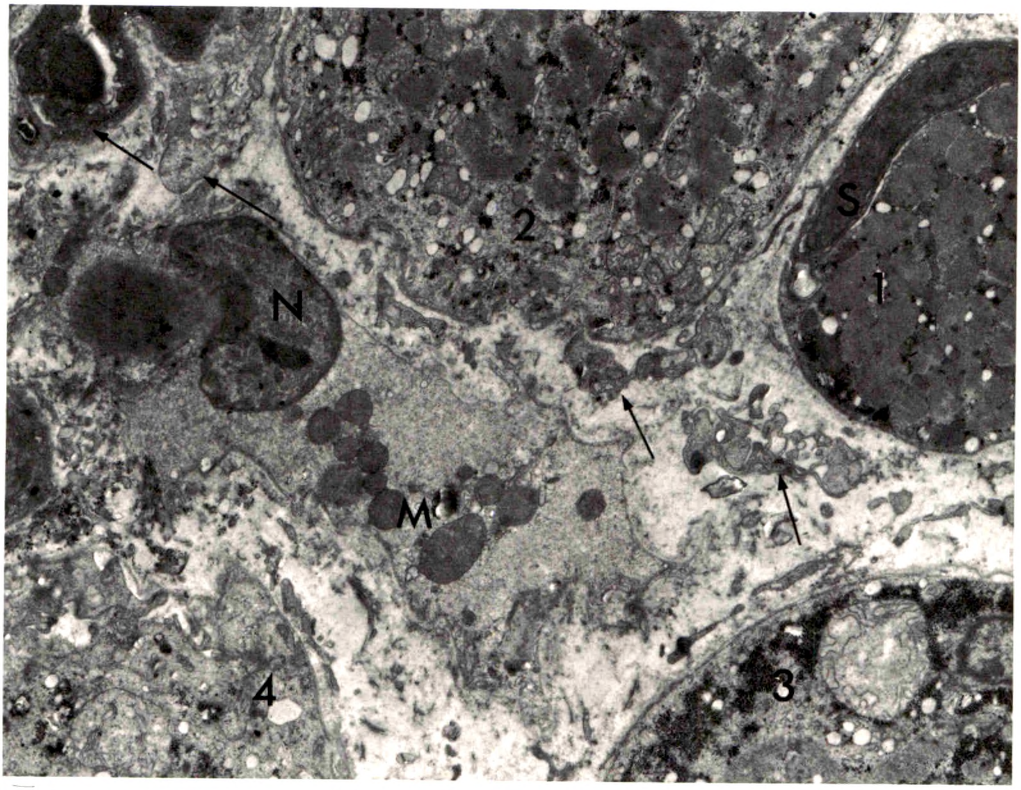

1

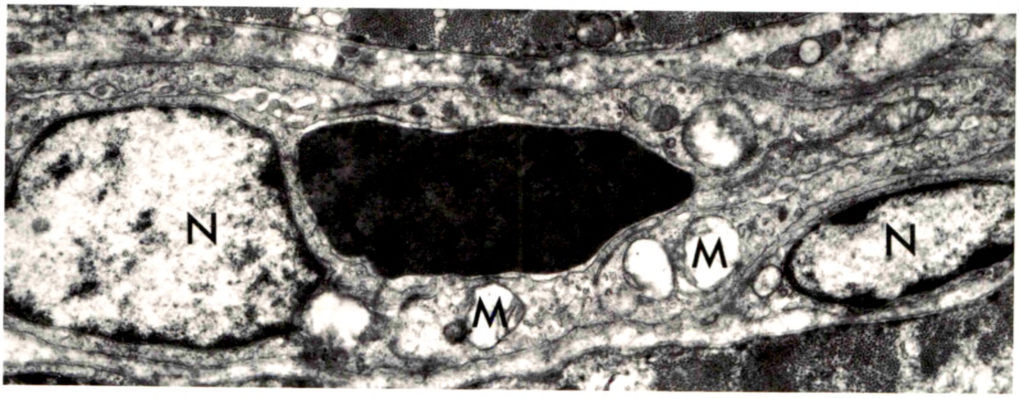

2

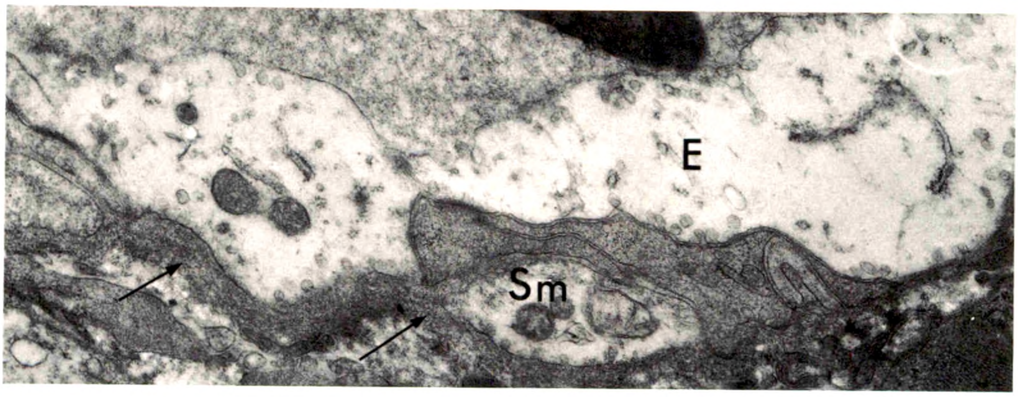

3

4

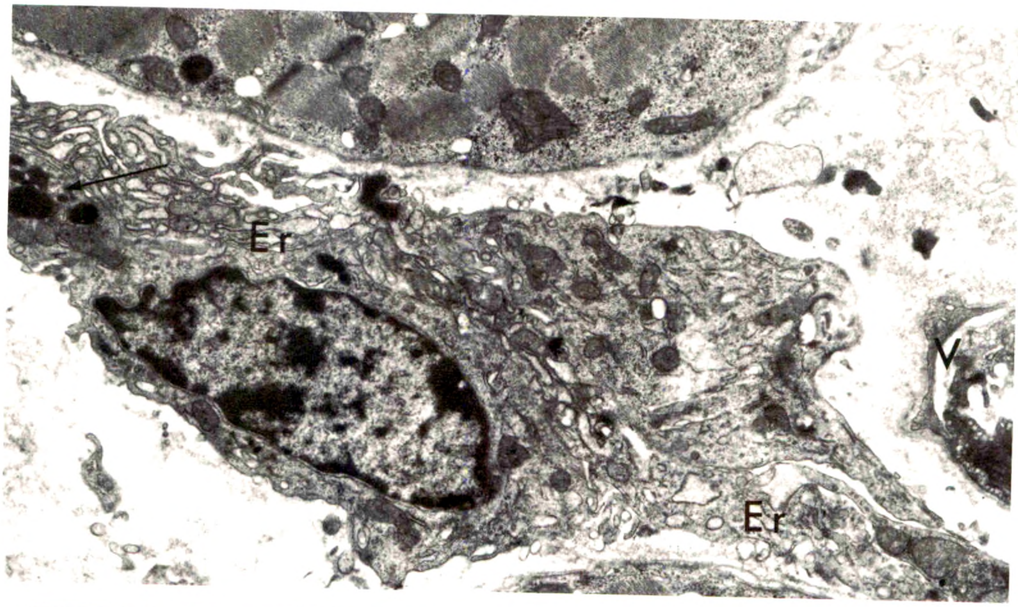

5

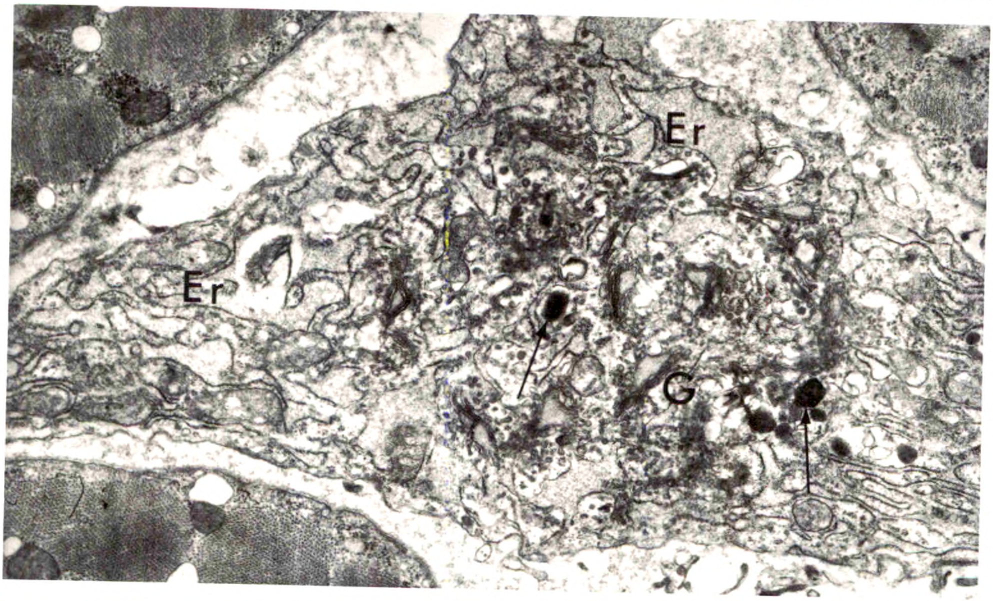

6

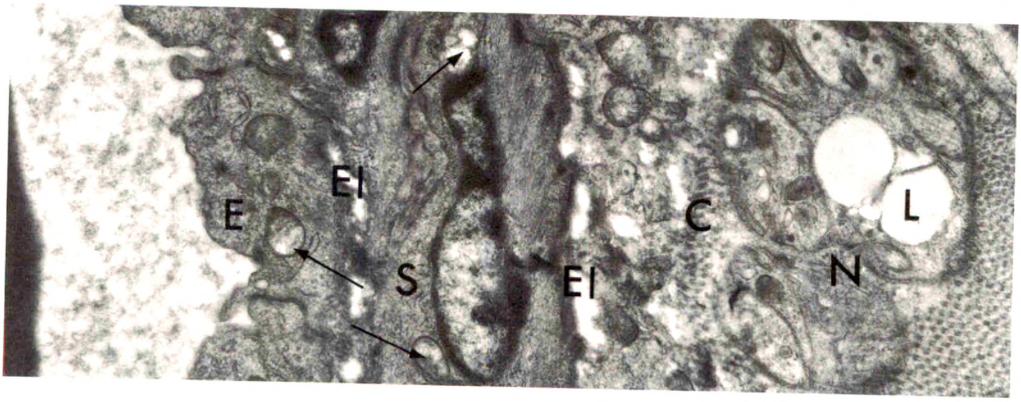

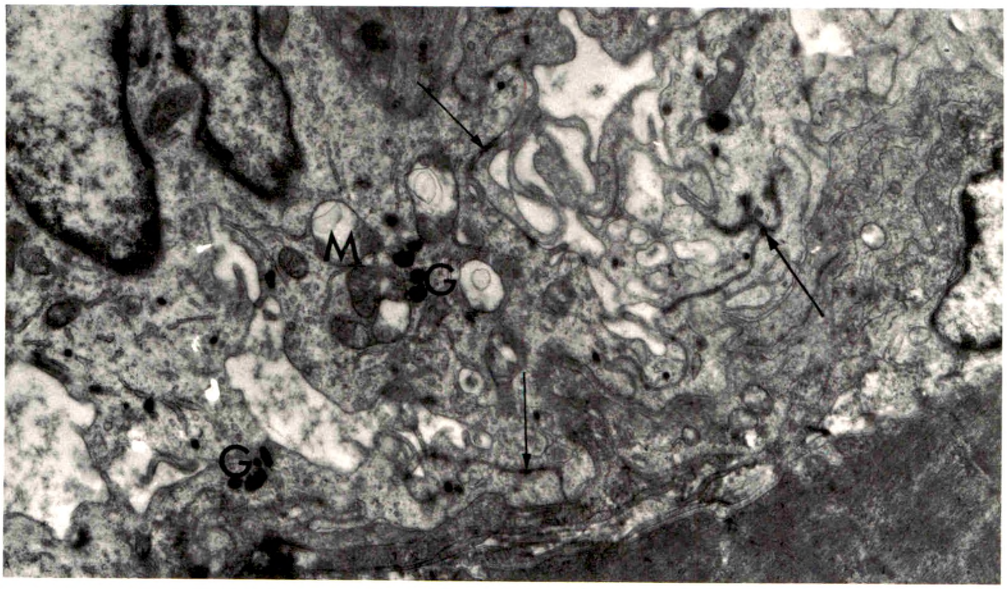

7

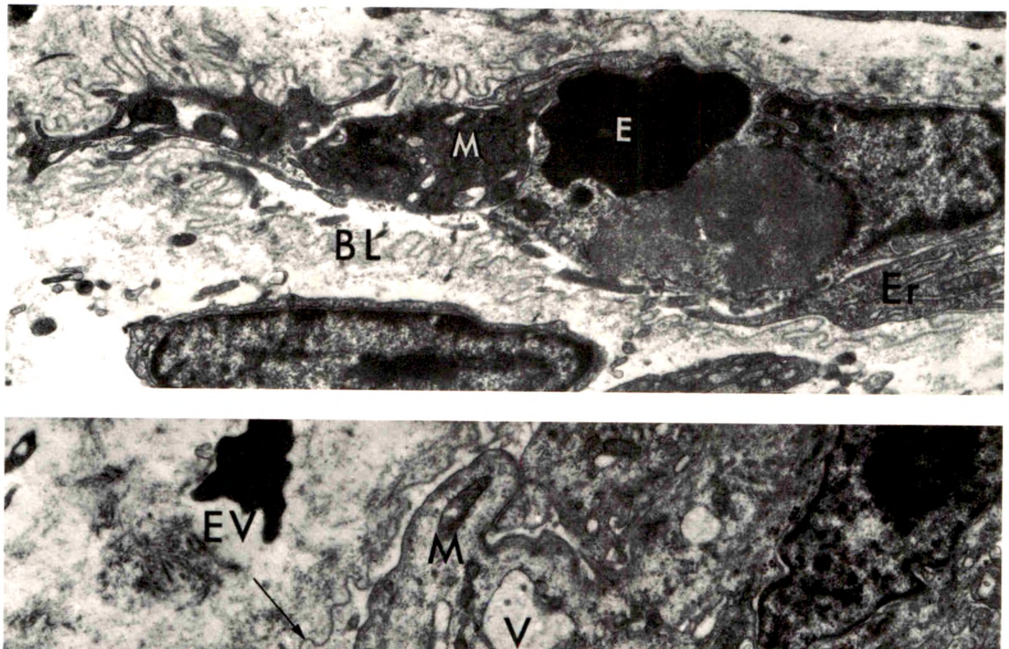

8

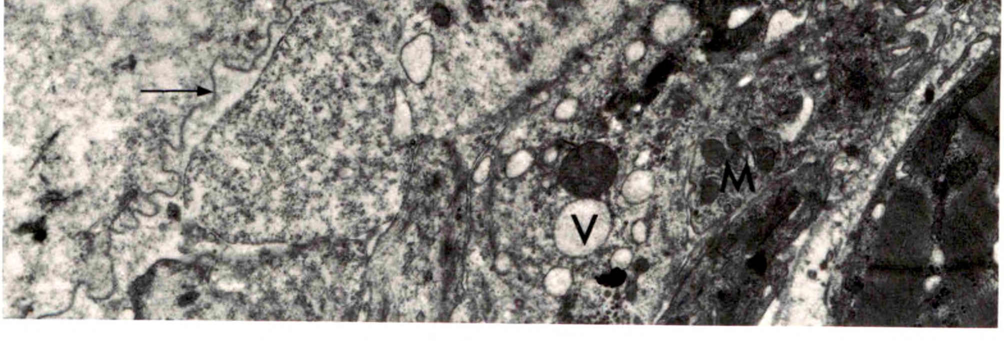

9

10

11

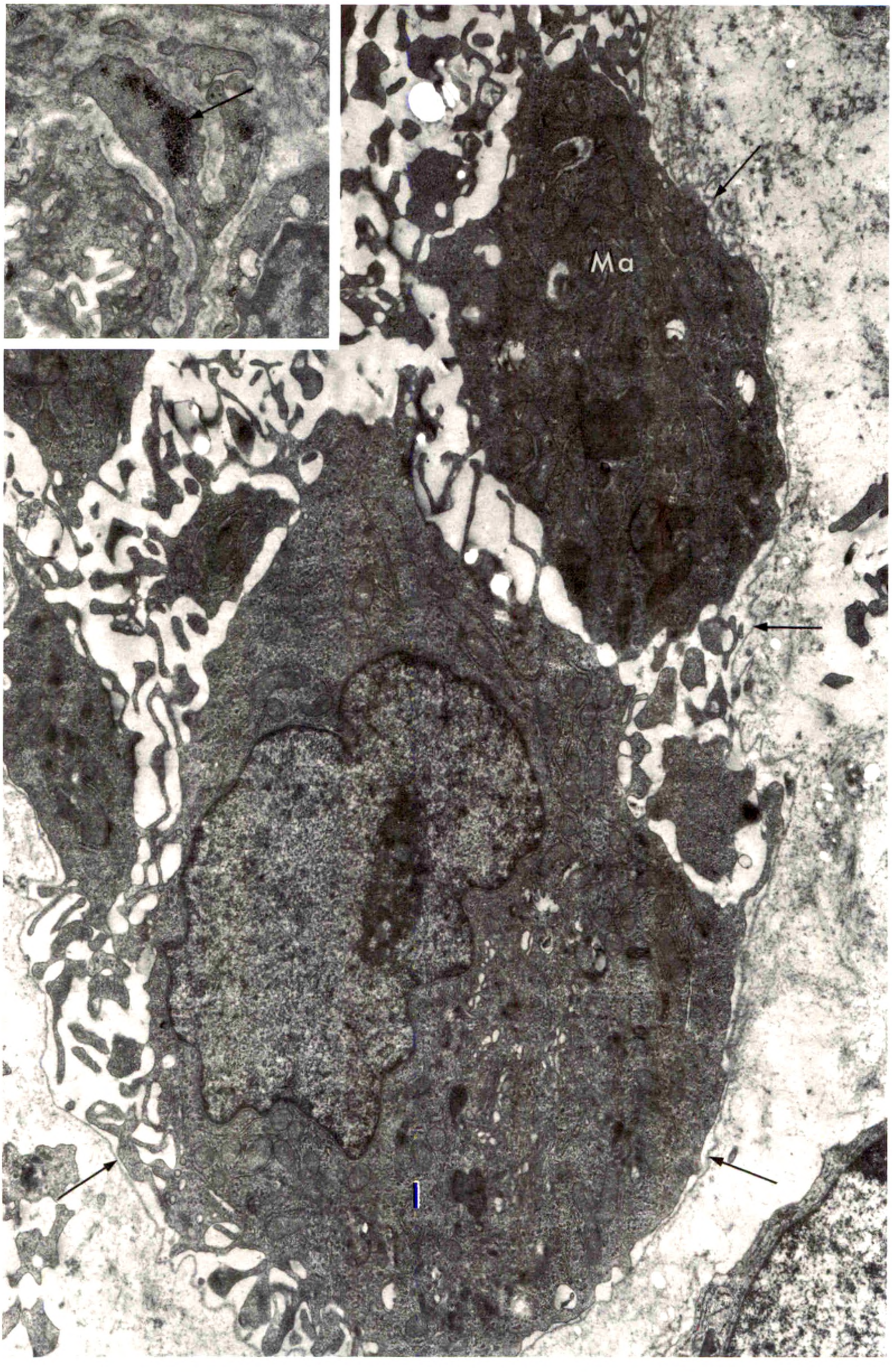

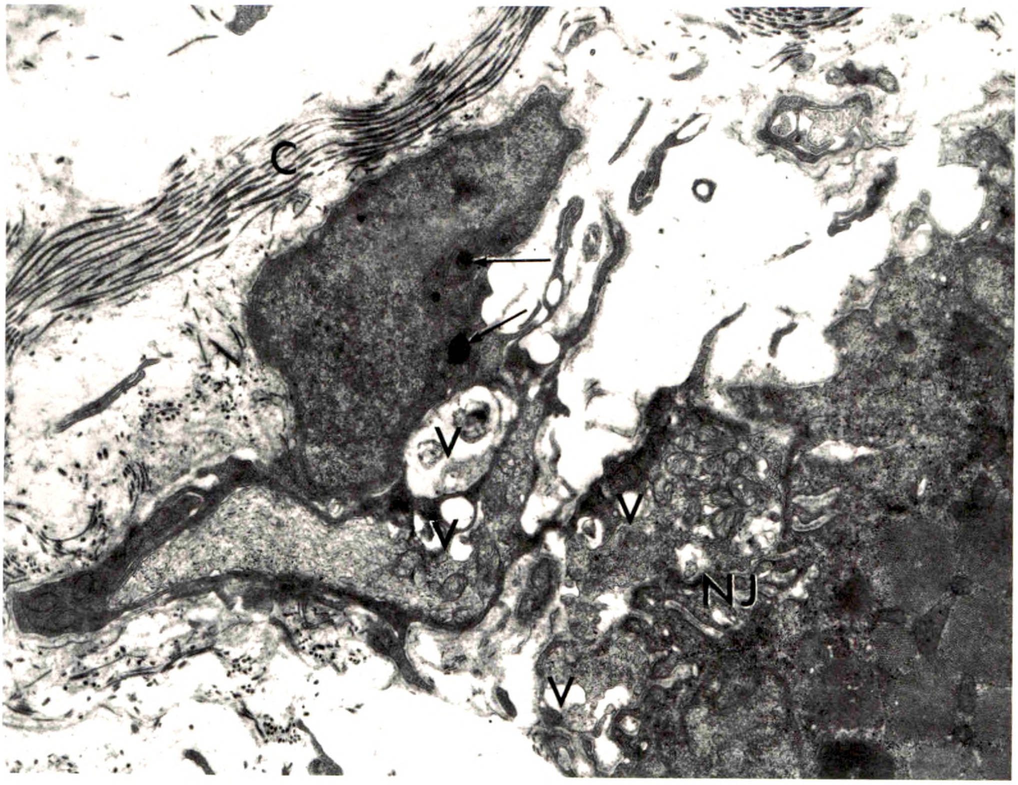

12

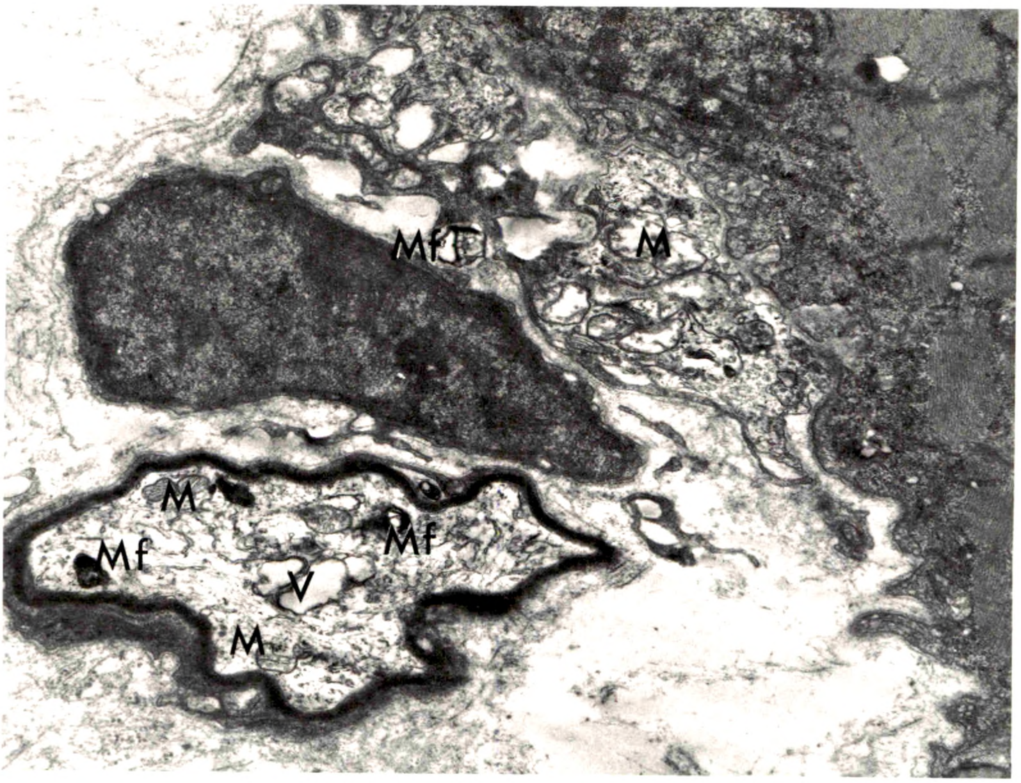
Mf
M
M
Mf
Mf
V
M

13

14

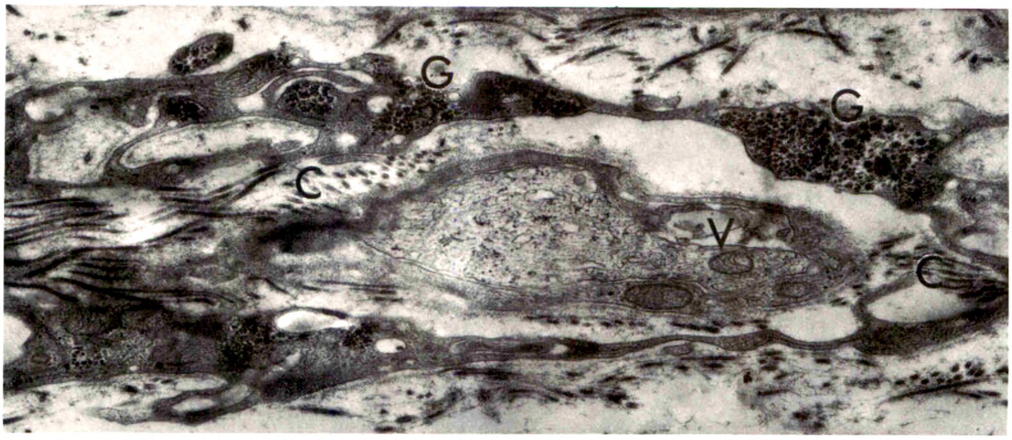

15

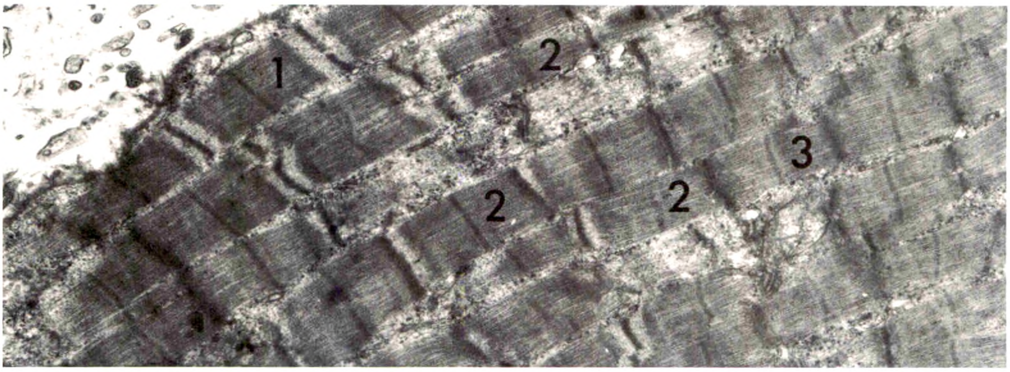

16

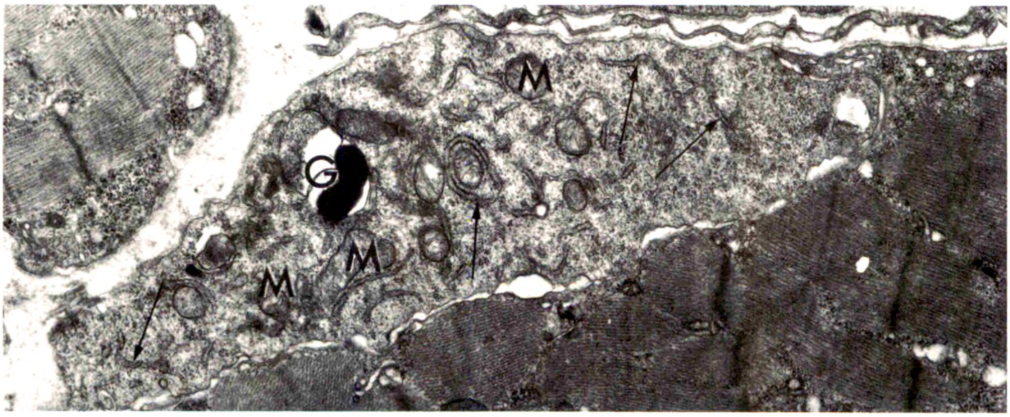

Scanning Electron Microscopy of Saccular Intracranial Aneurysms

O. Hassler, MD

Eight intracranial saccular aneurysms from 6 autopsies were studied with the scanning electron microscope and the cerebral arteries from control autopsies and rabbits were compared. The intima of the aneurysms had a more uneven and rugged surface than the surroundings. Only slight atherosclerotic changes were discovered in the immediate vicinity of the aneurysms. The windows of the internal elastic lamella were enlarged at the mouth of the aneurysms; the edge of the muscle layer was rounded and showed fibrosis. The structure of the walls of the aneurysms differed from that of the control arteries because they were composed of collagenous connective tissue. The adventitia of the aneurysms resembled that of control arteries. The findings are in accord with the assumption that saccular aneurysms develop at sites of developmental media defects. The internal elastic lamella over the area of the media defect shows primarily compensatory hypertrophy and later degeneration, extension and decay (Am J Pathol 68:511–520, 1972).

NORMAL ARTERIES AND ARTERIES from animals with experimental cholesterol atherosclerosis were studied by scanning electron microscopy.[1–3]

The morphology of intracranial saccular aneurysms under the light microscope is well known.[4] The transmission-electron-microscopic appearance of the aneurysms and media defects also have been studied.[5,6]

Many problems concerning the etiology, pathogenesis and treatment of saccular intracranial aneurysms are still unresolved. When an aneurysm is formed, the two normal main layers of the cerebral arterial wall—*ie*, the muscle coat and the internal elastic lamella, disappear and are replaced by collagenous connective tissue. It has been assumed, on good grounds,[4] that aneurysms develop at sites of developmental media defects, but this assumption has not been definitely proven. Knowledge of how the internal elastic lamella is destroyed is very incomplete. The possible connection between

---

From the Department of Pathology, University of Umeå, Umeå, Sweden.

Supported by grants from the Swedish Medical Research Council (Project No. B71-12X-561-07).

Accepted for publication May 9, 1972.

Address reprint requests to Dr. O. Hassler, Associate Professor, Department of Pathology, University of Umeå, 901 87 Umeå 6, Sweden.

aneurysms and atherosclerotic intimal thickening has been debated.[7] The rate at which an aneurysm grows is not known. The present study was started in the hope that the new morphologic method, scanning electron microscopy, would provide new information that could be of value for future attacks on these problems.

Material and Methods

Eight saccular intracranial aneurysms from 6 subjects were studied (Table 1). In those with multiple aneurysms, only the ruptured aneurysms and in 2 further cases one aneurysm were studied. The aneurysms were found on the anterior, middle cerebral internal carotid or basilar arteries. The specimens were taken 4 to 31 hours postmortem. Cadavers were kept at 3 to 6 C for most of the time. In one case, fixation was carried out by the injection of 10% formalin (buffered to pH 7 by a phosphate buffer) under a pressure of 30 mm Hg for 2 hours. In 3 cases, 2.5% glutaraldehyde buffered with 0.1 M of cacodylate at pH 7.3 was used instead of formalin. In one aneurysm that had ruptured recently, the blood clots of the aneurysm were removed by washing in physiologic saline. Fixation was then performed in 2.5% glutaraldehyde buffered with cacodylate. Three aneurysms were dehydrated intact; the others were cut with a pair of scissors or torn into pieces.

Control material was taken from the anterior and middle cerebral arteries of 8 subjects examined 6 to 43 hours postmortem (Table 1). In 3, the material was fixed in formalin and the remaining were fixed in glutaraldehyde as described above.

In addition, another kind of control material was taken from 4 young rabbits, weighing 1.4 to 1.6 kg. The animals were anesthetized with Mebumal® (ACO,

Table 1—Some Data on Subjects with Aneurysm and Control Subjects

Case	Age	Sex	Chief disease	No. of aneurysms	Enlargement of left side of heart (as reported at autopsy)	Weight of heart (g)
Subjects with aneurysms						
1	50	F	Subarachnoid hemorrhage	1	+	450
2	52	M	Subarachnoid hemorrhage	3	+	470
3	54	F	Subarachnoid hemorrhage	3	+	390
4	54	M	Subarachnoid hemorrhage	2	+	400
5	59	M	Subarachnoid hemorrhage	1	+	450
6	61	F	Subarachnoid hemorrhage; postoperative thrombosis with cerebral infarction	2	—	300
Control subjects						
7	4	M	Astrocytoma	—	—	70
8	32	F	Astrocytoma	—	—	290
9	47	M	Laennec's cirrhosis	—	+	420
10	49	M	Gastric carcinoma	—	—	330
11	53	M	Myocardial infarction	—	+	560
12	61	F	Carcinoma of breast	—	—	270
13	63	F	Carcinoma of colon	—	—	280
14	68	M	Myocardial infarction	—	+	460

Stockholm, Sweden) and killed by excising the heart and injecting 2.5% glutaraldehyde into the aorta under a pressure of 30 mm Hg. The two largest branching points of the cerebral, mesenteric and femoral arteries were excised, fixed for 2 hours in ice-cold 2.5% glutaraldehyde buffered with 0.1 M of cacodylate at pH 7.3.

After fixation, all of the specimens were washed in several changes of distilled water and freeze-dried. A conducting coat of approximately 100 to 200 Å of gold was deposited (Pirani Penning, model 4, Edwards, England). The specimens were studied with a scanning electron microscope (Cambridge Stereoscan S 4). The material was finally embedded in paraffin wax and sections, stained with Gomori's elastin stain combined with van Gieson's stain, were produced from several levels.

Results

The appearance of one of the intact aneurysms is shown in Figure 1. The perivascular net of arachnoidal fibers (Figure 1B) resembled that of the surroundings and of the control materials. The internal surface of the aneurysm (Figure 2A) was somewhat uneven and rugged, with an irregular pattern of small ridges and gullies. Thus, it differed from that of the autopsy control material (Figure 2B). The surface of the cut or torn wall of the aneurysm, consisting of collagenous connective tissue, had a finely granulated, compact appearance (Figure 3A) differing from that of the tunica media (Figures 3B, 4B), which was built up of fusiform, smooth-muscle cells. Similar, but less distinct, pictures of collagenous connective tissue were seen in the minimal media defects of the rabbit arteries. Photomicrographs of the site of the aneurysm rupture (Figure 2C) resembled those seen in Figure 3A.

The mouth of the aneurysms showed only very slight atheromatous changes of the intima. The surface of the cut or torn mouth of the aneurysm (Figure 3B) showed often dilated windows of the internal elastic lamella. No dilated windows could be discovered in the rabbit material. At the mouth of the aneurysm, there was a transition between the appearance of the aneurysm wall and the tunica media, due to fibrosis of the tunica media. The border of the muscle coat seemed to be rather smoothly rounded.

The intima cushions in the vicinity of the aneurysms (Figure 4) resembled other intima cushions in autopsy and rabbit arteries and consisted of elastic lamellae interspersed with layers of smooth-muscle cells (Figure 4B).

Photomicrographs of the paraffin sections showed typical saccular intracranial aneurysms occurring in all aneurysm cases. In seven branching points of the arteries of the rabbits, typical, but minute, media defects were observed.

Discussion

The intimal surfaces of the aneurysms were more irregular, with higher ridges and deeper gullies than those of the control material and those depicted in other works.[2] This may be due to the fact that the intima is newly formed and not particularly exposed to the forces of flowing blood. Only slight atherosclerotic changes were discovered in the neighborhood of the aneurysms, and they did not seem to have any relationship to the aneurysms. Thus, Carmichael's theory[7] of early atherosclerotic destruction of the vessel wall as the cause of aneurysm formation received no support.

The internal elastic lamella was thickened, with enlarged windows at the mouth of the aneurysms. This agrees with findings from other studies,[5,6] and agrees with the assumption that the elastic lamella becomes overstretched and hypertrophied.[4] No signs of degeneration of the elastic lamella could be demonstrated in the scanning-electron-microscope pictures.

The muscle coat showed a fibrosis and a rather soft border towards the aneurysms, a finding that confirms those of previous light-microscopic studies[4] and supports the assumption of a preexisting media defect formed by an error in development.

The adventitia resembled that of the normal cerebral artery. The growth of the aneurysms apparently is not more rapid than the rate at which adventitia of normal appearance is renewed. The adventitia showed no signs of external pressure, reinforcement or inflammation.

The rupture surfaces of the aneurysms resembled areas artificially torn or cut postmortem. They differed from similar areas of control arteries apparently because the aneurysms were composed of collagenous connective tissue, instead of the smooth muscle and elastic tissue of the control arteries.

It is obvious that autolytic changes occurred in the autopsy material. These changes resembled those observed by Shimamoto *et al*[2] and seem to be unavoidable in a study of aneurysms which, practically, only occur in man. The changes did not seem to be so important as to make other observations impossible. As a matter of fact, arteries are comparatively resistant to autolysis.[4]

References

1. Garbarsch C, Christensen BC: Scanning electron microscopy of aortic endothelial cell boundaries after staining with silver nitrate. Angiologica 7:365–373, 1970

2. Shimamoto T, Yamashita Y, Numano F, Sunaga T: Scanning and transmission electron microscopic observation of endothelial cells in the normal condition and in initial stages of atherosclerosis. Acta Pathol Jap 21:93–119, 1971
3. Weber G, Tosi P: Observations with the scanning electron microscope on the development of cholesterol aortic atherosclerosis in the guinea pig. Virchows Arch [Pathol Anat] 353:325–332, 1971
4. Hassler O: Morphological studies on the large cerebral arteries. With reference to the aetiology of subarachnoid haemorrhage. Acta Psychiat Neurol Scand 36 [Suppl 154] 1961
5. Boquist L, Hassler O: Media defects in arteries. An ultrastructural study on normal and hypertensive rabbits. Pathol Eur (In press), 1972
6. Nyström SHM: Development of intracranial aneurysms as revealed by electron microscopy. J Neurosurg XX:329–337, 1963
7. Carmichael R: The pathogenesis of noninflammatory cerebral aneurysms. J Pathol Bacteriol 62:1–19, 1950

[*Illustrations follow*]

Fig 1A—The scanning-electron-microscopic appearance of an unruptured saccular intracranial aneurysm *(arrow)* on the middle cerebral artery (Case 2, × 28). **B**—Detail enlargement of a part of the external wall of the same aneurysm. The surface appearance of the adventitia of the aneurysms did not differ from that of the normal arterial wall (× 7000).

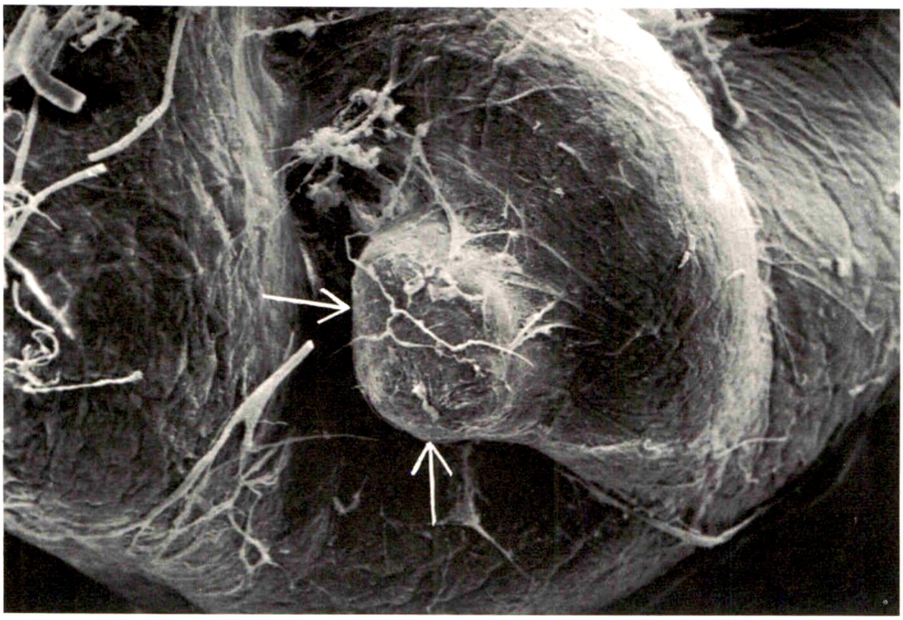

1A

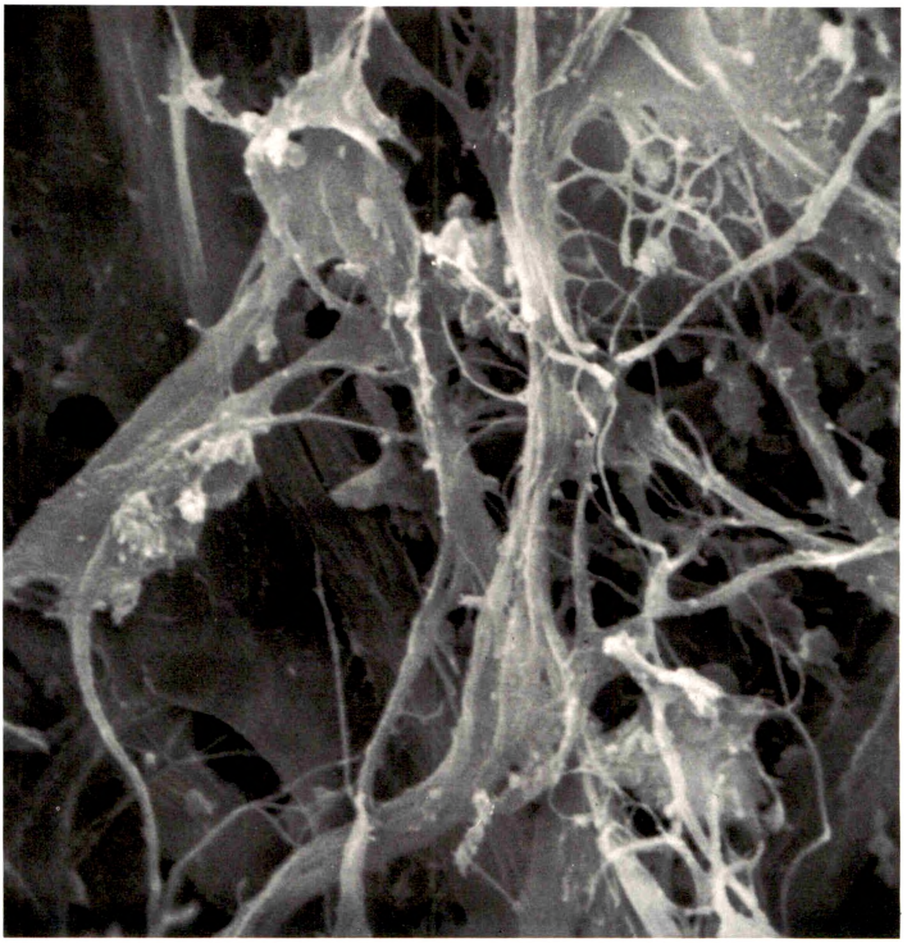

1B

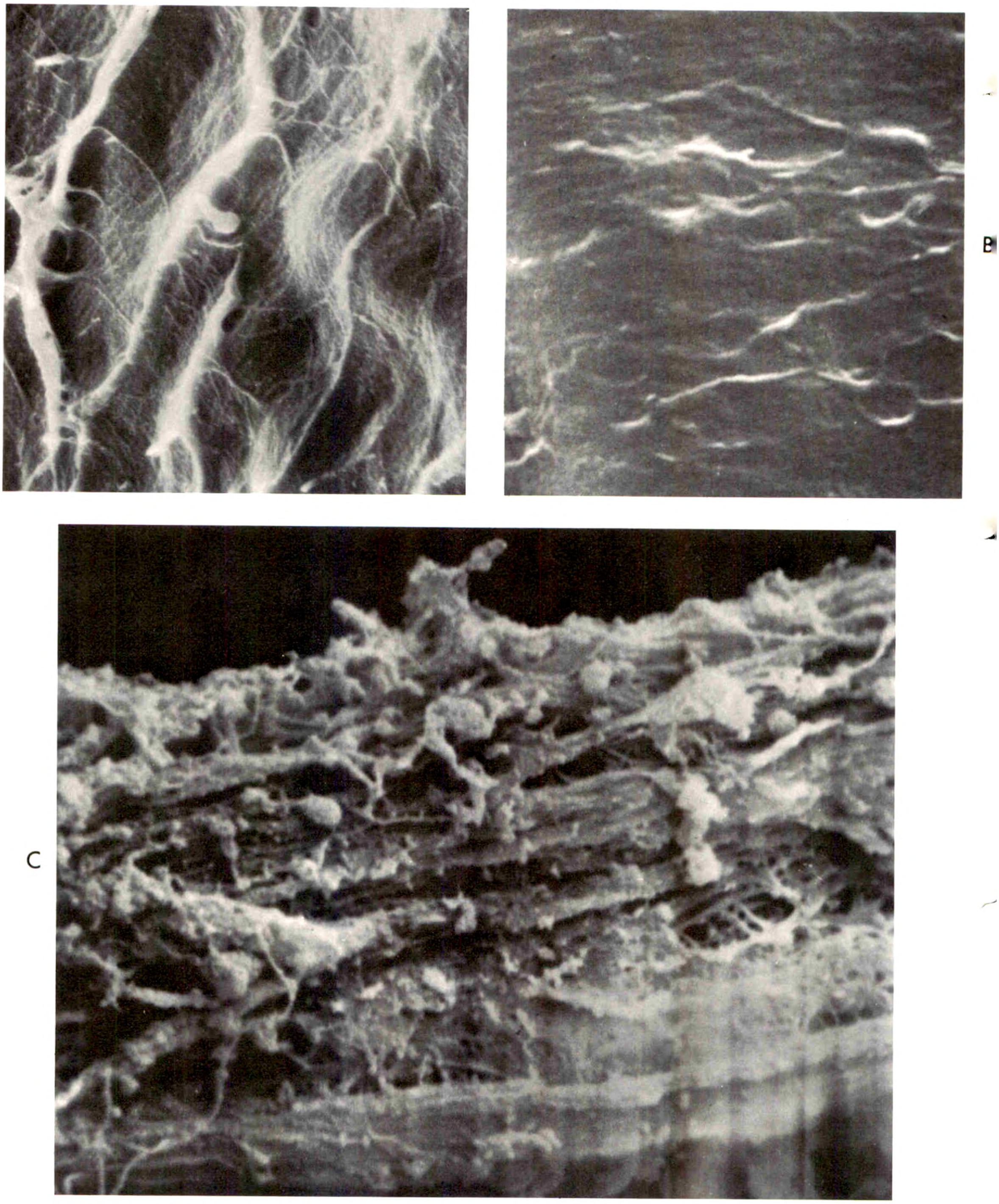

Fig 2A—Detail enlargement of the internal (intimal) surface of another aneurysm (Case 5). The intimal surface showed a rather irregular pattern, with small gullies and ridges (× 3400). **B**—Intimal surface of a control (middle cerebral artery of Case 10). The surface was smoother than that of the aneurysm (×3400). **C**—Rupture surface of an aneurysm (Case 4). Blood had to be washed away with a brush and physiologic saline. The surface resembles that in Figure 3A (× 6000).

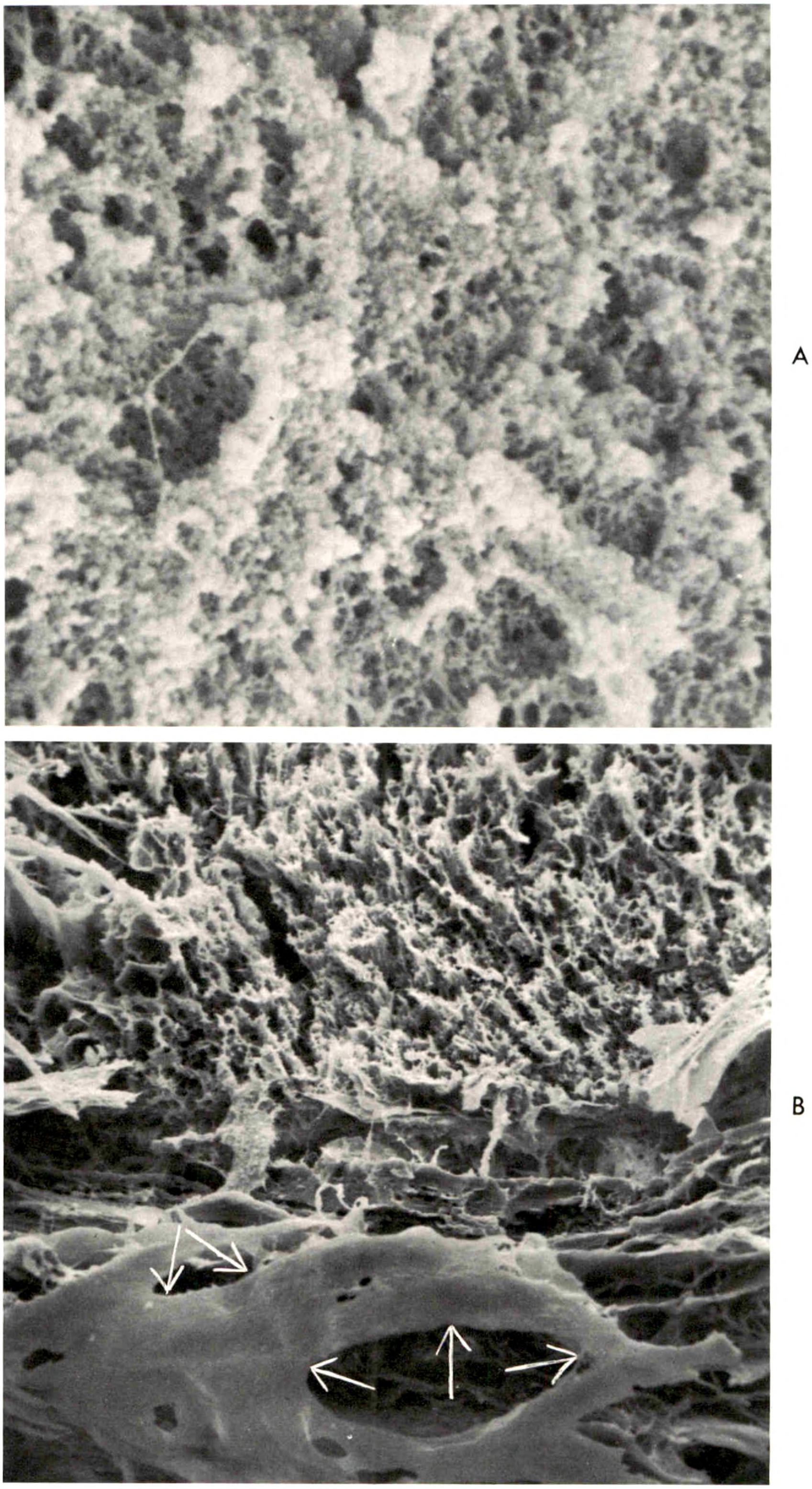

Fig 3A—The wall of an aneurysm sack. Surface of a torn portion which showed a compact, finely granulated appearance, apparently because it consisted mainly of collagenous connective tissue (compare with the smooth muscle of Figure 4B) (× 6000). **B**—Mouth of an aneurysm (Case 3). Surface of a cut portion of the wall which contains an internal elastic lamella (*bottom*) with enlarged windows (*arrows*) and smooth muscle (*top*) (× 1150).

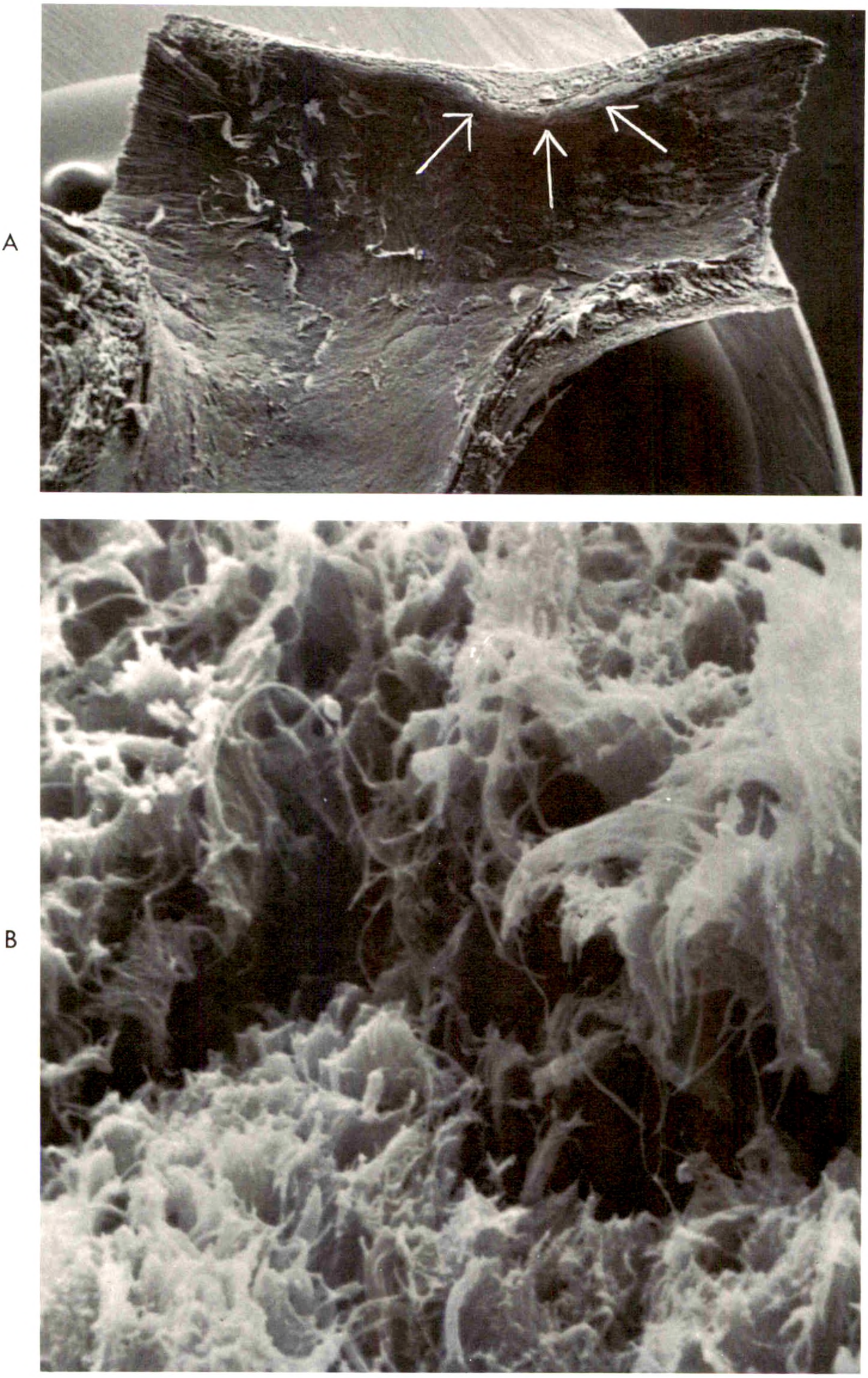

Fig 4A—Intima cushion (*arrow*) in the neighbourhood of an aneurysm. The lumen was opened by longitudinal incisions with a pair of scissors (× 28). **B**—Detail enlargement of a portion of the same cushion, showing smooth muscle and, in the middle of the figure, a dark empty area after the elastic lamella was torn away (× 6000).

The Pulmonary Interstitial Cell as Immediate Precursor of the Alveolar Macrophage

Drummond H. Bowden, MD and Ian Y. R. Adamson, PhD

The origin of the alveolar macrophage was studied in cultured explants of murine lung. In this system, which is free of circulating monocytes, a new population of alveolar macrophages was identified on the third day of culture; immediately preceding the appearance of these cells, proliferation of pulmonary interstitial cells was observed. A temporal relationship between interstitial cells and alveolar macrophages was established by autoradiographic studies; evidence is advanced which favors the direct migration of interstitial cells into alveoli. It is concluded that the pulmonary interstitium constitutes an intermediate compartment between the blood monocyte and the alveolar macrophage (Am J Pathol 68:521–536, 1972).

CYTOKINETIC STUDIES in a variety of animals, using different experimental models, have demonstrated conclusively that mononuclear phagocytes originate from precursor cells in the bone marrow, are transported in the blood as monocytes and eventually become tissue macrophages.[1] Cells of the mononuclear phagocyte system may, at any given moment depending on the stage of differentiation and geographic location, differ in their morphologic and functional characteristics. Such differences between the blood monocyte and alveolar macrophage, though compatible with the concept of a cell system, suggest a process of maturation before the macrophage reaches the air sac.[2] The pulmonary interstitial compartment has been advanced as the most likely site of this morphologic and functional maturation.[3]

In the experiments about to be described, the relationship of the pulmonary interstitial cell to the free alveolar macrophage was studied in cultured explants of murine lung, a system which eliminates the continuing supply of blood monocytes.

From the Department of Pathology, Faculty of Medicine, University of Manitoba, Winnipeg, Canada.

Supported by Grant MA 3878 from the Medical Research Council of Canada.

Presented at the Sixty-ninth Annual Meeting of the American Association of Pathologists and Bacteriologists, Cincinnati, Ohio, March 12, 1972.

Accepted for publication May 5, 1972.

Address reprint requests to Dr. Ian Y. R. Adamson, Department of Pathology, University of Manitoba Faculty of Medicine, 770 Bannatyne Ave, Winnipeg 3, Canada.

Materials and Methods

Male Wistar albino mice (25 g) were anesthetized by pentobarbital sodium, their chests opened and the lungs removed using aseptic technic. In some cases, vascular perfusion with warm medium was used to remove blood from the lungs prior to culture. Pieces of lung (1 cu mm) were cut and placed in the wells of a culture chamber[4] containing T8 medium[5] with 20% calf serum; no antibiotics were added. The chamber was placed in an incubator at 37 ± 1 C with a constant flow of a 95% oxygen and 5% carbon dioxide gas mixture. The cultures were maintained for intervals up to 6 days; the medium was changed on the third day. At the end of each experimental period, the explants were removed, rinsed in phosphate buffer and fixed in buffered formalin for light microscopy or in osmic acid for electron microscopy. In one experiment, 0.1 ml of a polystyrene latex suspension (1 μ particles) was added to 3-day organ cultures; the tissue was removed 1 hour later and processed for light and electron microscopy.

The system described above was utilized in a series of isotope labeling experiments:

Continuous Labeling

Tritiated thymidine (0.075 μCi) was added to each culture well; tissue from perfused and nonperfused lung was maintained in the labeled medium for intervals up to 6 days. Autoradiographs were prepared on 5 μ sections (Kodak NTB_2 emulsion, Feulgen stain) and the percentage of thymidine-labeled nuclei determined; bronchiolar cells were not included in the counts. The identification of labeled cells and the percentage of macrophages incorporating the isotope were determined on 0.5 μ sections (Kodak NTB_2 emulsion, toluidine blue stain); ultrastructural confirmation of cell type was made on ultrathin sections (Ilford L4 emulsion, double lead hydroxide stain).

Pulse Labeling

At daily intervals up to 6 days, 0.075 μCi of tritiated thymidine was added for the final 2 hours of culture before the explants were removed and fixed. Autoradiographs were prepared and counted as described above.

Interval Labeling

Explants were cultured in medium containing 0.075 μCi of tritiated thymidine; after 2 days the explants were rinsed and placed in unlabeled medium for further periods of up to 2 days. Autoradiographs were prepared, and differential counts of the labeled cells were taken, using 0.5 μ sections.

Mitotic Activity

In some cultures, 0.004 mg/ml colchicine was added 4 hours before fixation; the percentage of nuclei in metaphase was determined in 5 μ paraffin sections stained with hematoxylin and eosin or with Feulgen stains.

Results

Morphology

The cultural explants were examined serially by light and electron microscopy. Intravascular leukocytes disintegrated within a few days; otherwise, there were no notable differences between perfused and nonperfused lungs.

In the first 24 hours there was little evidence of cellular proliferation; some desquamated Type 2 alveolar epithelial cells and free membranous debris were found in the air sacs. The few alveolar macrophages observed at this time were large cells with indented nuclei and numerous phagosomes containing lamellar debris (Figure 1). After two days of culture the endothelial cells had swollen and almost filled the capillary lumens; the most prominent feature, however, was the increased cellularity of the interstitium (Figure 2). The 3-day cultures showed hyperplasia of bronchiolar and alveolar epithelium. At this time there was a pronounced increase in the number of free alveolar cells, particularly near the edges of the explanted tissue (Figure 3A, 3B); these cells, which resembled young macrophages, contained little ingested material (Figure 4) but readily phagocytosed latex beads added to the cultures (Figure 5).

Between 4 and 6 days, the alveoli became increasingly indistinct as epithelial overgrowth continued; the cultures were progressively encircled by fibroblasts and at 6 days were barely recognizable as lung tissue.

Autoradiography

In the continuous labeling experiments, the explants of perfused and nonperfused lung showed no differences in isotopic uptake at any of the observed time intervals (Text-figure 1); where intravascular leukocytes were seen, they had not incorporated the isotope. The percentage of labeled cells was low at day 1, increased sharply to 22% at day 3 and more slowly over the subsequent 3 days (Text-figure 1). Many free macrophages were observed on the third day; 50% of these cells showed nuclear incorporation of tritiated thymidine (Figure 6). The label was uniformly heavy (greater than 50 grains/nucleus) and there was no significant change in grain count or in the percentage of macrophages labeled over the next 3 days (Text-figure 2).

More precise information on ^{3}H thymidine uptake was provided by pulse labeling; maximal incorporation occurred between 2 and 4 days when 3 to 4% of the nuclei were labeled in a 2-hour period (Text-figure 3). Differential counts on 0.5 μ sections indicated that, at 2 days, mononuclear interstitial cells were predominantly labeled; the identity of these cells was confirmed by electron microscopy (Figure 7). No silver grains were observed over the free macrophages at this time but, on the third day, 15% of these cells incorporated

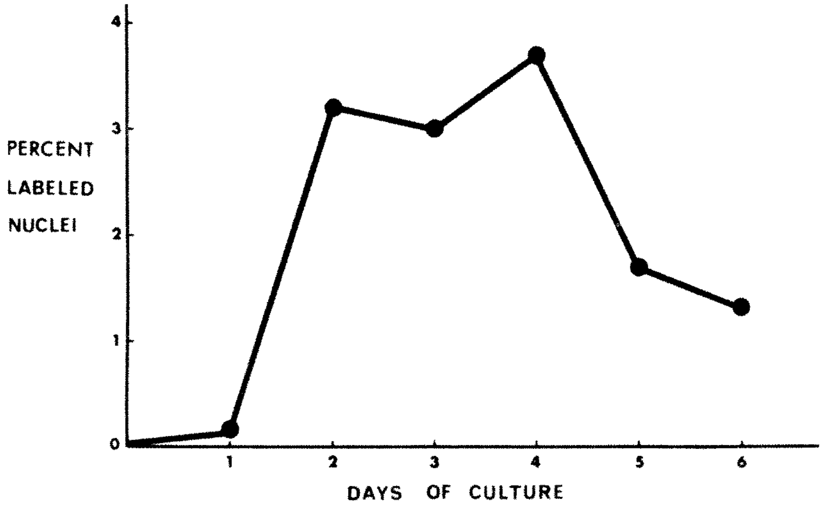

TEXT-FIG 1—Percentages of labeled nuclei in explants of perfused and nonperfused lung after continuous culture in ^{3}H thymidine-labeled media.

the isotope during the 2-hour pulse (Text-figure 2); in the subsequent 3 days very few macrophages were labeled.

The changing pattern of isotopic incorporation by interstitial and macrophagic cells between the second and third days was further investigated in the interval labeling experiment. The per-

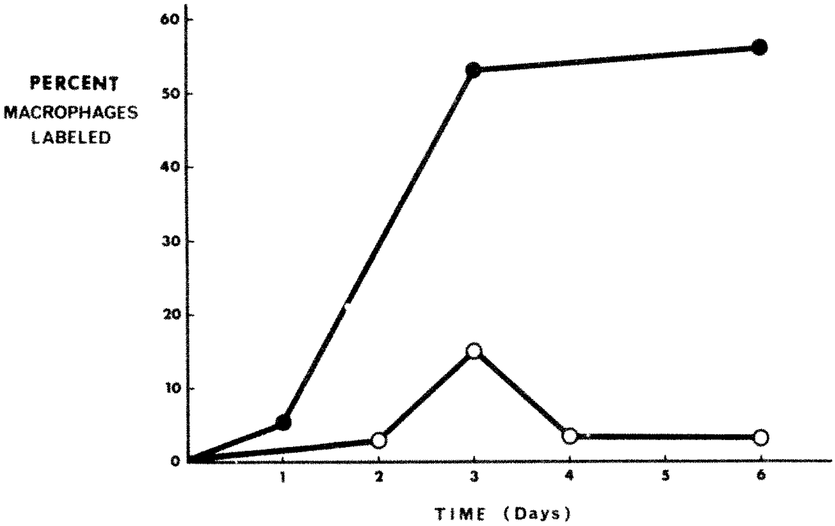

TEXT-FIG 2—Percentages of macrophages labeled at various times after continuous (*solid circles*) and pulse labeling (*open circles*).

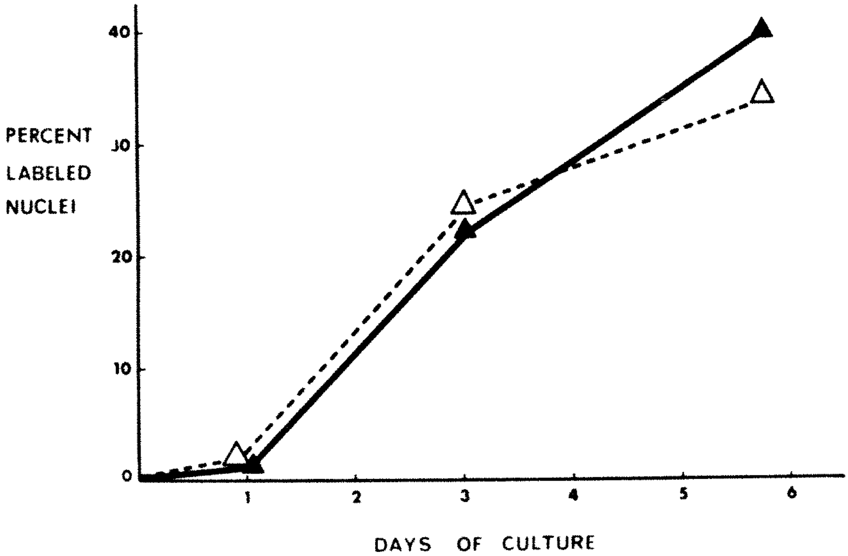

TEXT-FIG 3—Percentages of labeled nuclei after a final 2-hour pulse labeling by ^3H thymidine. Perfused lung (*open triangles*) and nonperfused lung (*solid triangles*).

centage of interstitial cells carrying the thymidine marker dropped from 73 to 11% in the 24 hours after removal from the isotope, whereas the value for free macrophages rose from 2 to 70% over the same period (Table 1). Grain counts in interstitial and macrophagic nuclei were uniformly heavy (greater than 50/nucleus) and there were no significant changes in labeling or grain counts in these cells over a further 24-hour period.

The mitotic activity of the explants, as measured by the colchicine technic, was much lower than the labeling index determined by the ^3H thymidine autoradiographs. The mitotic index was highest at 3 days, when 0.6% of nuclei were arrested in metaphase. No mitoses were seen in free macrophages.

Table 1—Differential Counts of Labeled Cells in the Interval Label Study; Explants Cultured for 2 Days in Media Containing ^3H Thymidine, then Transferred to Unlabeled Media

Time after 2 days of thymidine labeling (days)	Percent labeled cells			
	Interstitial	Free macrophages	Epithelial	Not identified
0	73	2	16	9
1	11	70	11	8
2	12	63	12	13

Discussion

Pulmonary explants maintained in nutrient medium exhibited DNA synthesis and cell division which were maximal on the third day. There was a discrepancy, however, between mitotic activity and the incorporation of tritiated thymidine, a finding previously reported by Simnett and Heppleston who calculated that the rate of entry into DNA synthesis in organ cultures of lung is 4 times the rate of entry into mitosis.[6] The reason for this divergence is not known, but it may be explained by the synthesis of metabolic DNA[7,8] or by a doubling of DNA without division.[6] Although the rate of DNA synthesis cannot be used as a precise measure of cellular multiplication in pulmonary explants, the identification of labeled cells in serial autoradiographs provides a useful technic for studying the derivation of alveolar macrophages in a blood-free system.

The origin of macrophages from marrow-derived monocytes has been established,[1,9] but the final steps in the delivery of a functional cell to the alveoli have not been determined.[2] Based on a previous study using whole body irradiation to suppress circulating monocytes, we proposed a pulmonary interstitial compartment intermediate between the blood monocyte and the functional free alveolar macrophage;[3] in this compartment the monocytes may undergo division and develop the biochemical characteristics that distinguish the alveolar macrophage from other mononuclear phagocytes. The present experiment clearly demonstrated that the elimination of peripheral blood from the system did not interfere with the continuing proliferation of macrophagic cells in the lung. The possibility that a few residual monocytes in the explant gave rise to new macrophages is also unlikely in view of the identical morphologic and labeling characteristics of perfused and nonperfused lung.

The structural and phagocytic properties of the free alveolar cells observed on day 3 characterize them as a population of young macrophages. It is unlikely that these cells were derived from preexisting macrophages because: a) the few alveolar macrophages observed on days 1 and 2 were effete cells with indented nuclei and many phagosomes; b) DNA synthesis by alveolar macrophages, as demonstrated by pulse labeling, occurred only on the third day, at which time the new population of macrophages was already established; c) DNA synthesis is not necessarily followed by cell division, and in fact no mitoses were seen in the alveolar macrophages; d) free macrophages showed heavy incorporation of isotope after 3 days continuous labeling and there was no significant change in this value or in the nuclear grain counts over the next 3 days. These findings suggest that free macrophages in pulmonary explants do not divide, a conclusion that supports the general tenet that alveolar macrophages do not proliferate in culture[10,11] unless a specific growth factor (MGF) is added.[12]

The increased number of free macrophages observed on day 3 was preceded by proliferation of interstitial cells, a temporal relationship that is strengthened by the results of the interval labeling study. The majority of labeled cells on day 2 were in the interstitium, whereas 24 hours after removal from the isotope, the macrophage was the predominantly labeled cell. The sharp fall in the number of labeled interstitial cells, the corresponding increase in labeled macrophages and the similarity in grain counts of both cell types suggests that the new population of alveolar macrophages was derived by migration of interstitial cells into the alveoli.

The interrelationships of blood monocytes, pulmonary interstitial cells and alveolar macrophages are pertinent to an understanding of cellular reactions in pulmonary granulomatous diseases. In the *in vitro* model described above, a population of proliferating interstitial cells has been delineated as the immediate source of alveolar macrophages; a similar genesis may be postulated for the *in vivo* situation. Proliferation of interstitial cells in response to viral infection and in granulomatous conditions such as sarcoidosis is well recognized, and in experimental animals the increased output of macrophages induced by BCG or Freund's adjuvant is preceded by division of interstitial cells.[13-15] The results of the present study provide further support for the concept of a pulmonary interstitial compartment as an essential link between the circulating monocyte and the functional alveolar macrophage.

References

1. van Furth R: The origin and turnover of promonocytes, monocytes and macrophages in normal mice. Mononuclear Phagocytes. Edited by R van Furth. Oxford and Edinburgh, Blackwell Scientific Publications, 1970, pp 151–165
2. Bowden DH: The alveolar macrophage. Current Topics in Pathology. Berlin, Springer Verlag, 1971, pp 1–36
3. Bowden DH, Adamson IYR, Grantham WG, Wyatt JP: Origin of the lung macrophage: evidence derived from radiation injury. Arch Pathol 88:540–546, 1969
4. Parsa I, Marsh WH, Fitzgerald PJ: Pancreas acinar cell differentiation. I. Morphologic and enzymatic comparisons of embryonic rat pancreas and pancreatic anlage grown in organ culture. Am J Pathol 57:457–487, 1969

5. Trowell OA: The culture of mature organs in a synthetic medium. Exp Cell Res 16:118–147, 1959
6. Simnett JD, Heppleston AG: Rates of DNA synthesis in organ cultures of lung and prostate as measured by tritiated thymidine autoradiography. Lab Invest 19:333–338, 1968
7. Roels H: "Metabolic" DNA: A cytochemical study. Int Rev Cytol 19: 1–34, 1966
8. Pelc SR: Biological implications of DNA turnover in higher organisms. Acta Histochem [Suppl] 8:41–52, 1968
9. van Furth R, Hirsch JG, Fedorko ME: Morphology and peroxidase cytochemistry of mouse promonocytes, monocytes and macrophages. J Exp Med 132:794–805, 1970
10. Myrvik QN, Leake ES, Fariss B: Studies on pulmonary alveolar macrophages from the normal rabbit. J Immunol 86:128–132, 1961
11. Maxwell KW, Dietz T, Marcus S: An *in situ* method for harvesting guinea pig alveolar macrophages. Am Rev Resp Dis 89:579–580, 1964
12. Virolainen M, Defendi V: Dependence of macrophage growth *in vitro* upon interaction with other cell types. Wistar Institute Symposium Monograph 7:67–83, 1967
13. Cohn ZA, Weiner E: The particulate hydrolases of macrophages. J Exp Med 118:991–1008, 1963
14. Heise ER, Myrvik QN, Leake ES: Effect of bacillus calmette-guerin on the levels of acid phosphatase, lysosyme and cathepsin in rabbit alveolar macrophages. J Immunol 95:125–130, 1965
15. Galindo B, Imalda T: Cellular response to Freund's adjuvant in the rabbit lung: an electron microscopic study. Lab Invest 15:1659–1681, 1966

[*Illustrations follow*]

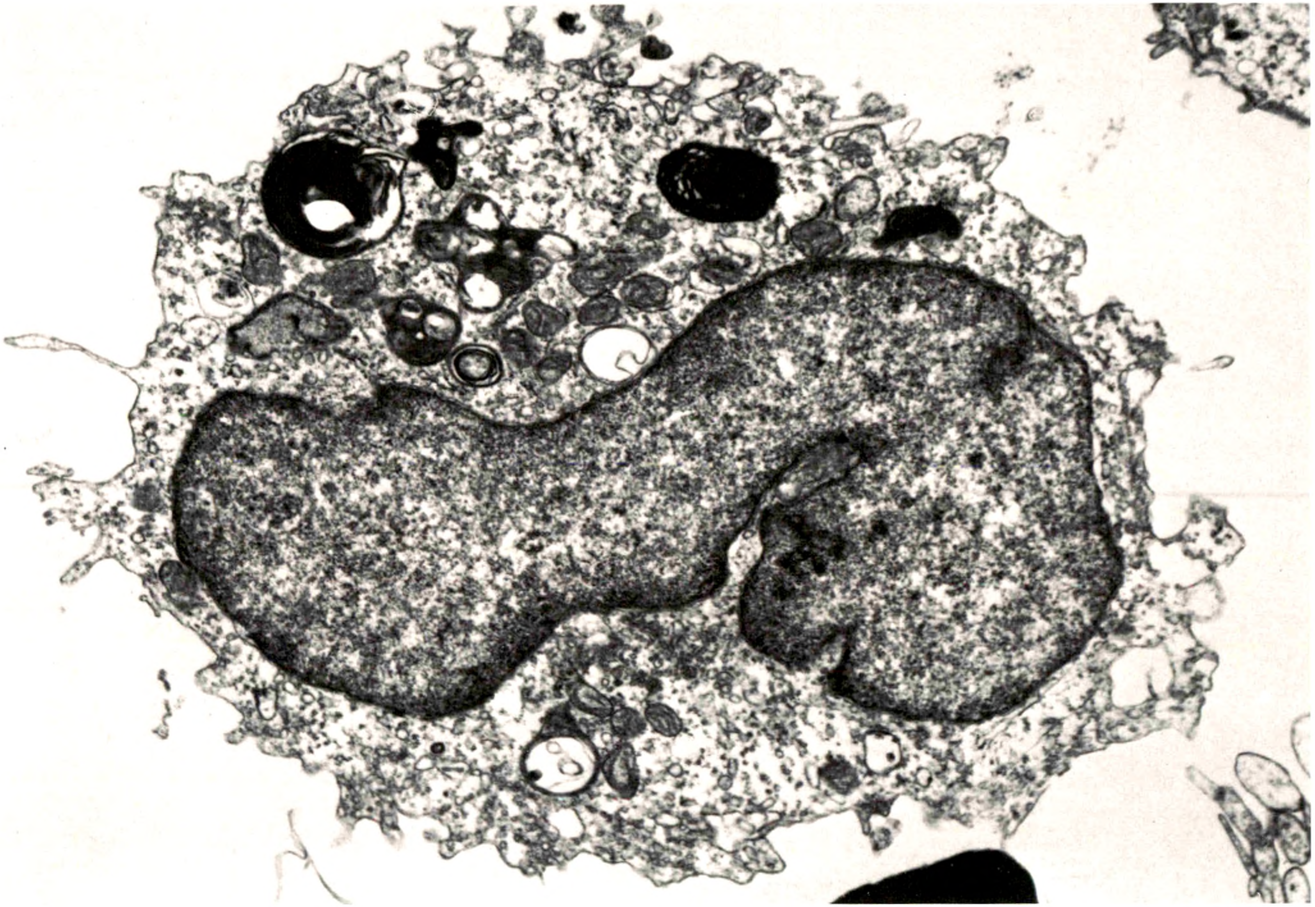

Fig 1—One-day explant. Typical alveolar macrophage with indented nucleus and ingested debris (× 8000).

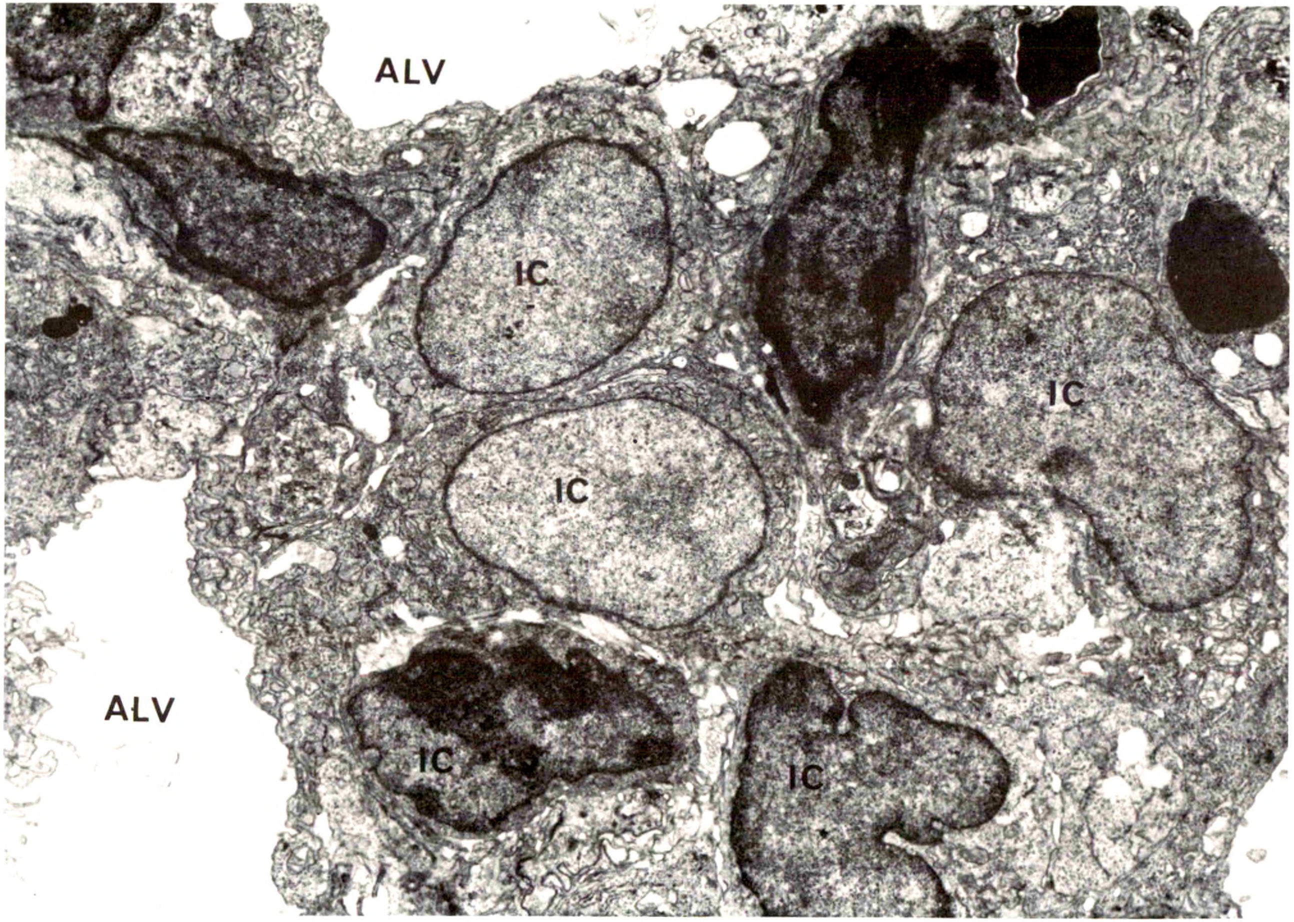
ALV
IC
IC
IC
ALV
IC
IC

Fig 2—Two-day explant showing increased cellularity of pulmonary interstitium. *IC* = interstitial cell, *ALV* = alveolus (× 3000).

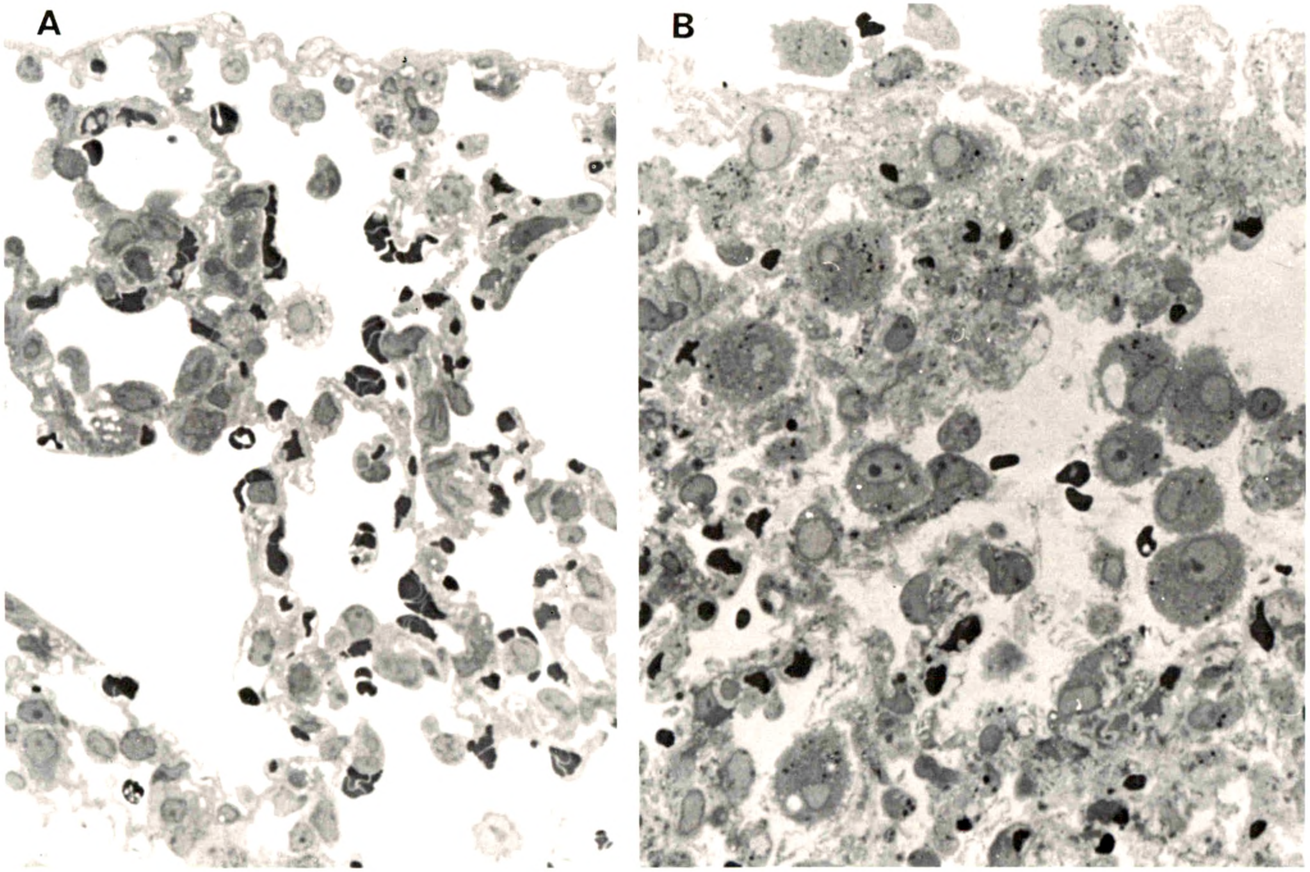

Fig 3A—One-day explant, 0.5 μ section. **B**—Three-day explant, 0.5 μ section. Many more free alveolar cells are seen in the 3-day explant than in the 1-day explant or in control (Toluidine blue, × 350).

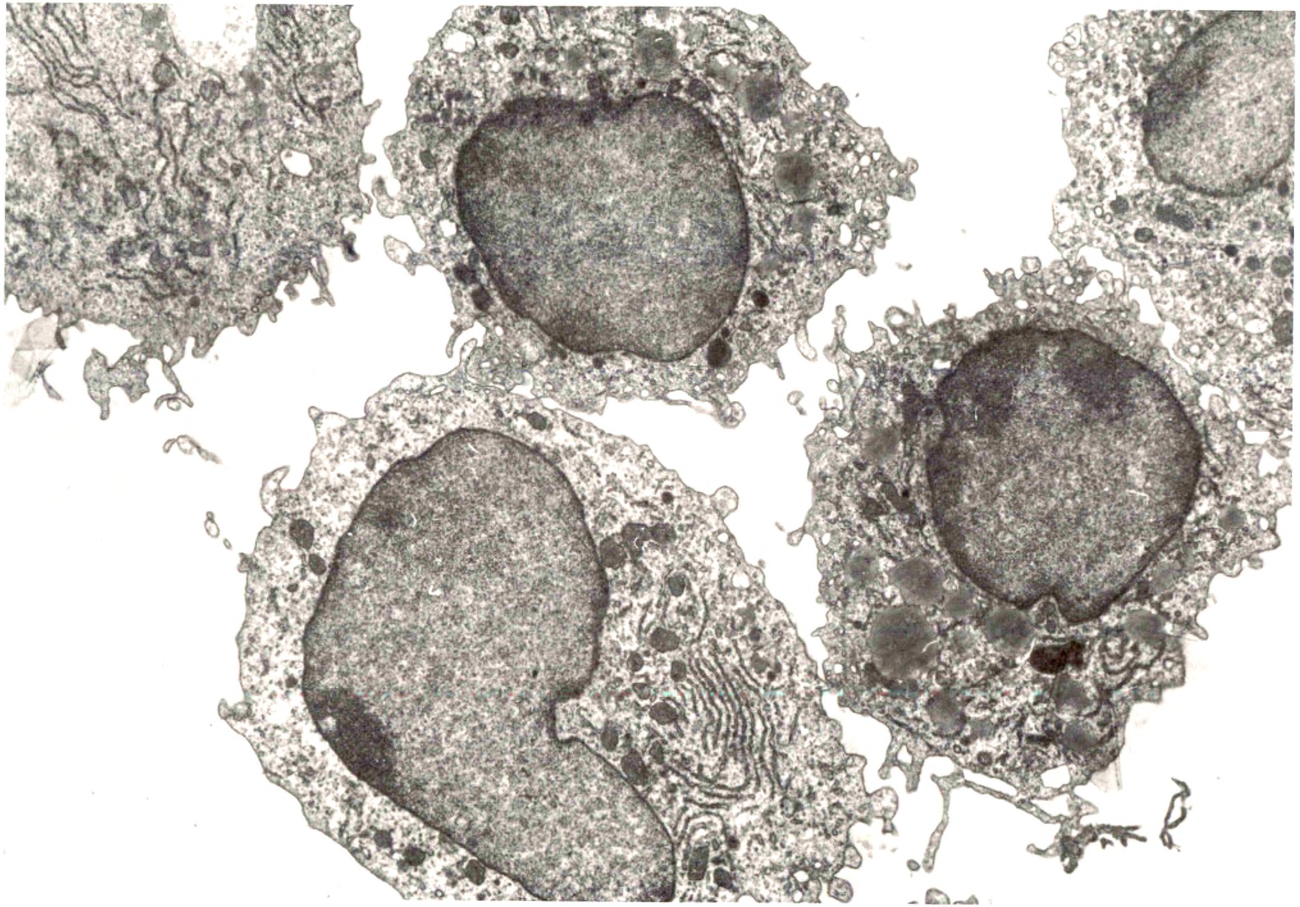

Fig 4—Three-day explant showing new population of alveolar macrophages; cells have round nuclei and contain little ingested debris (× 3000).

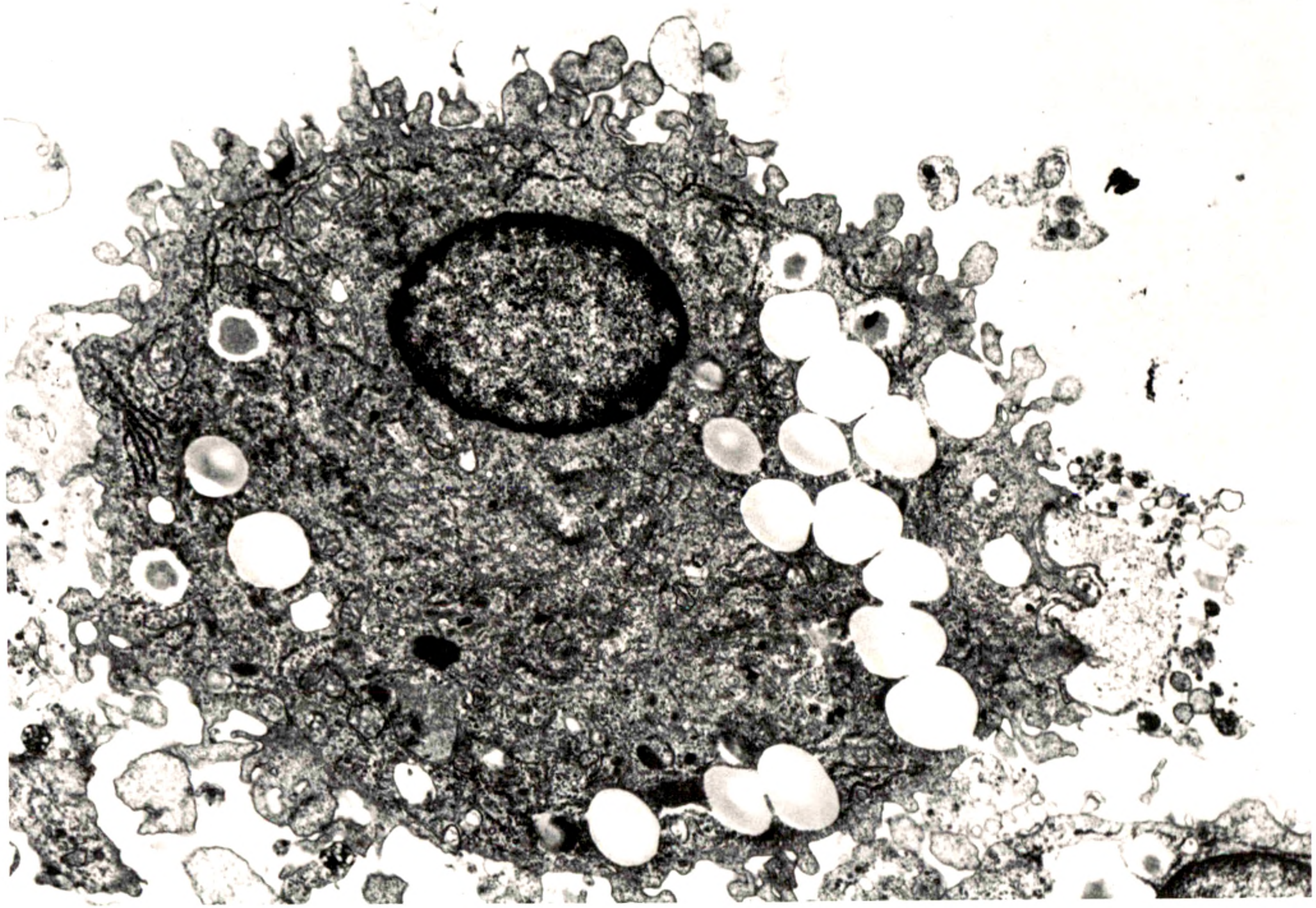

Fig 5—Alveolar macrophage in 3-day explant; phagocytic potential shown by ingestion of polystyrene spheres (× 11,000).

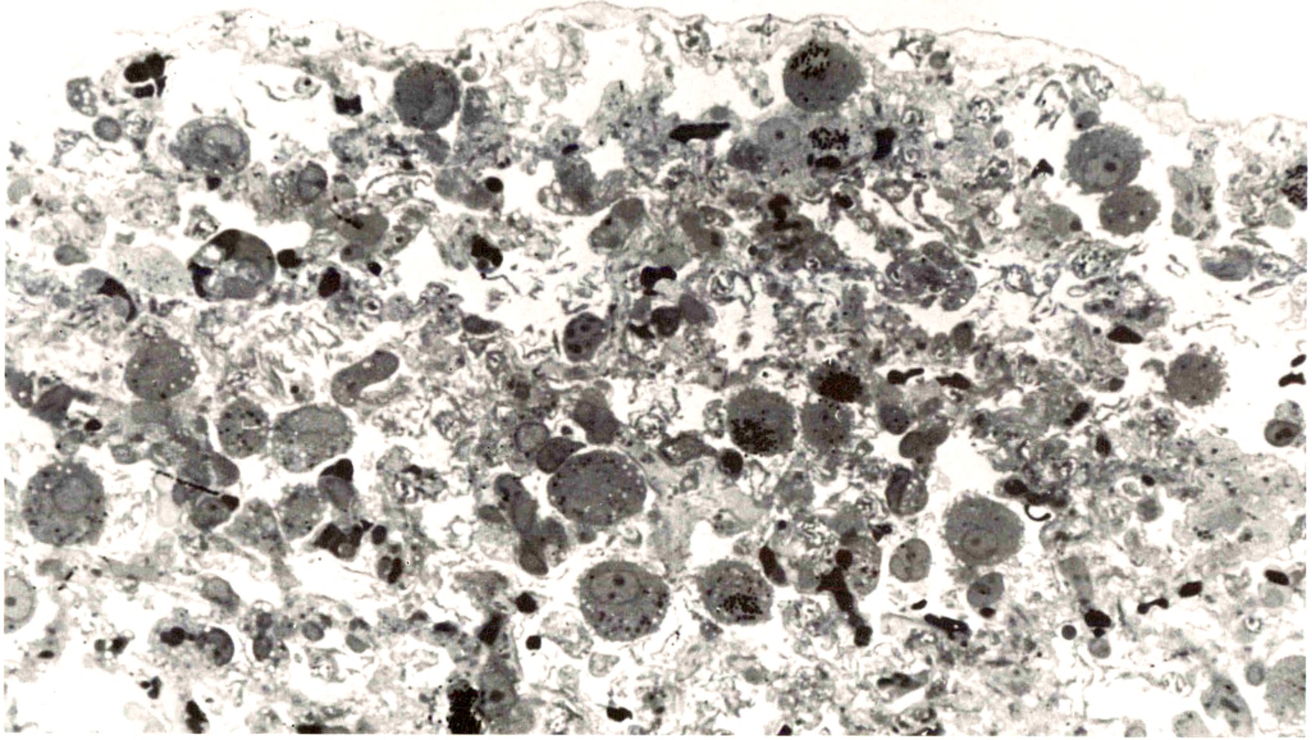

Fig 6—Three-day explant cultured in thymidine-labeled media, autoradiograph of 0.5 μ section. Many free alveolar macrophages incorporated the ³H thymidine (× 350).

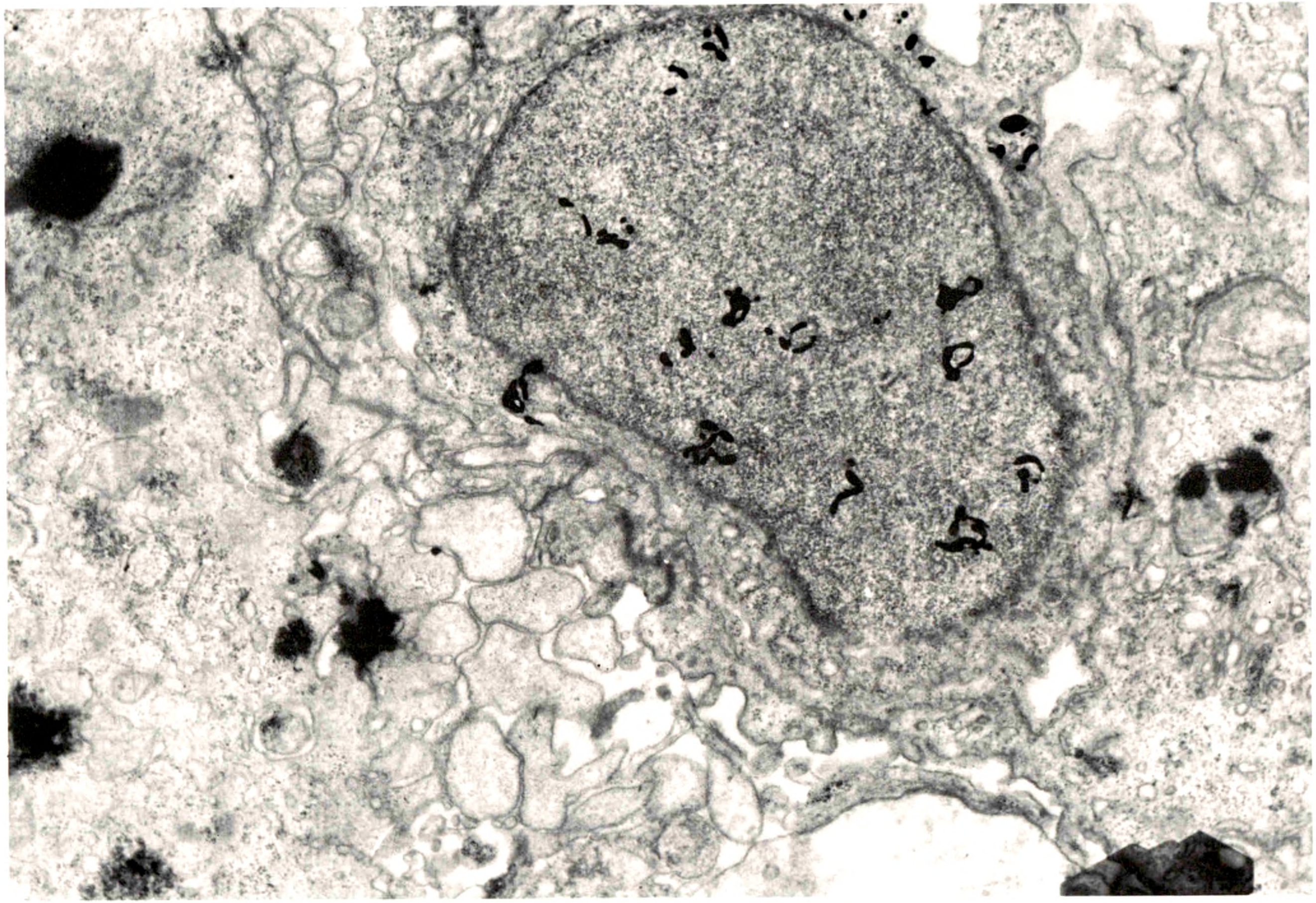

Fig 7—Two-day explant cultured in thymidine-labeled media, EM autoradiograph. Increased number of interstitial cells at this time were predominantly labeled (× 20,000).

[*End of Article*]

SYMPOSIUM

NEUTROPHIL PROTEASES AS MEDIATORS OF TISSUE INJURY

Sponsored by the American Society for Experimental Pathology. Papers presented at the Fifty-Sixth Annual Meeting of the Federation of the American Societies For Experimental Biology, Atlantic City, NJ, April 10, 1972.

Introduction

Considerable interest among experimental pathologists has been aroused by the fact that neutrophils function as a first line defense for the host threatened with infection and yet these cells are also capable of injuring the host during the course of their defensive role. Interest in the combined roles of neutrophils has not decreased in its intensity during the three score years since Metchnikoff's pioneering observations first called attention to the dual function of leukocytes in inflammation. During the past several years especially, our knowledge of the mediating role of neutrophilic leukocytes and their components in immunologically incited and nonspecific forms of inflammatory injury to host tissues has advanced rapidly. Of the various components of neutrophils implicated in tissue-injuring processes, proteolytic enzymes continue to attract the largest share of attention.

This Symposium is focused upon this latter subject, and has been organized around four principal themes: a) mechanisms of enzyme release from neutrophils, which will be discussed by Dr. Weissmann; b) mechanisms of interaction between neutrophils and their targets in connective tissues, to be discussed by Dr. Henson; c) studies on neutrophil proteases which attack the major fibrous proteins of connective tissues (collagen and elastin), to be presented by Dr. Lazarus and myself; and d) an example of a class of reactions in which soluble proteins in plasma are cleaved by neutrophil proteases with release of biologically active fragments capable of further modification of the inflammatory reaction. Several different systems are being actively studied in this last category; the one chosen for presentation involves kinin generation by leukocytes and will be discussed by Dr. Greenbaum. Obviously, under the limitations of a half-day symposium, it will be impossible to deal with all of the significant advances in these and related areas, and I appeal to the many workers whose meritorious contributions are not represented in the program to be sympathetic to this difficulty.

On behalf of our audience and certainly myself, for whom these presentations will prove especially instructive, I thank our speakers for their generous contributions to the program.

Aaron Janoff, PhD

Leukocytic Proteases and the Immunologic Release of Lysosomal Enzymes

Gerald Weissmann, MD, Robert B. Zurier, MD and
Sylvia Hoffstein, PhD

LYSOSOMES WERE INTRODUCED into the field of inflammation and connective tissue injury as a result of studies conducted at New York University and at the Strangeways Research Laboratory in Cambridge.[1-4] Shortly after it became clear that vitamin A acted to cause degradation of cartilage matrix both *in vitro* and *in vivo* by the release of proteases from cartilage lysosomes, it was hypothesized that lysosomal enzyme release in various forms of acute tissue injury could account for hydrolysis of connective tissue macromolecules.[5] Further studies in both laboratories have suggested the plausibility of this hypothesis. Thus, lysosomal proteases present in cartilage and in leukocytes have been shown capable of degrading cartilage matrix, isolated proteoglycans and simple chemical substrates.[6-8]

Leukocyte lysosomes of the rabbit contain at least two sorts of proteases capable of cleaving isolated cartilage proteoglycans: an enzyme or enzymes active at near neutral pH, and one enzyme active in the acid pH range.[7,8] When purified, high molecular-weight (10^6) proteoglycan of bovine nasal cartilage (PP-L) was exposed to extracts of leukocyte lysosomes (but not to other subcellular fractions), this substrate was readily cleaved, releasing polyanions of lower molecular weight which resembled those released by trypsin. This uronic acid-containing, readily diffusable material was nondialyzable and precipitated readily with hexamine cobaltic chloride. Thus, *in vitro* as *in vivo*, when proteoglycans are exposed to excess vitamin A, they could be degraded by lysosomal hydrolases to release anionic polysaccharides; degradation proceeded as readily at neutral as at acidic pH. Since it became clear that proteolytic activity in the acid pH range could be attributed to the cathepsin D in rabbit leukocyte granules, the identification of a neutral protease capable of cleaving extracellular materials became of considerable interest.

From the Department of Medicine, New York University School of Medicine, New York, NY.

Supported by Grant AM-11949 from the National Institutes of Health, and by The New York Heart Association, The Glenn B. and Gertrude P. Warren Foundation and The Whitehall Foundation.

Address reprint requests to Dr. Gerald Weissmann, Department of Medicine, New York University School of Medicine, 550 First Ave, New York, NY 10016.

Neutral proteolytic activity in *human* leukocytes has been studied extensively by several investigators and, indeed, the major portion of this sort of activity is usually attributed to the elastin-like enzymes studied extensively by Janoff and his associates.[9] We have investigated the subcellular distribution of a number of enzymes in *rabbit* polymorphonuclear leukocytes, and general results of these data can be seen in Table 1. Rabbit polymorphonuclear leukocytes clearly contain a neutral protease acting on calf thymus histone, using liberation of acid-soluble arginine or tyrosine as assay.[8] The enzyme has relatively little action upon hemoglobin. Its subcellular distribution differs considerably from that of enzymes acting in the neutral pH range on such substrates as acetyl-DL-phenylalanine β-naphthyl esters, on L-leucine-2-naphthyl amide and on N-CBZ-L-alanine *p*-nitrophenol esters.[10] Nor could orcein elastase be demonstrated in rabbit polymorphonuclear leukocytes. These data differ considerably from findings in human granulocytes. The enzyme was clearly shown to be associated with azurophil granules and was readily inhibited by a material present in the cytoplasm of these cells. Moreover, it could be activated by increasing the ionic strength of the medium—*eg*, in 2.5 M KCl, and by polyanions such as heparin and dextran sulfate. The enzyme, conveniently referred to as a *histonase*, was partially separated by Sephadex gel filtration and by isoelectric focusing, until the specific activity of the activated enzyme showed a 300-fold increase over that determined in whole cells. This relatively purified enzyme of rabbit polymorphonuclear leukocytes could be shown preferentially to hydrolyze substrates such as histones or

Table 1—Percentage Distribution of Protein, Histonase, Acid Cathepsin and β-Glucuronidase, in Subcellular Fractions of Rabbit Polymorphonuclear Leukocytes*

	Nuclear debris	Granule	Post granule supernatant
Protein	4.4 ± 0.9 (5)	33.0 ± 5.6 (5)	63.8 ± 5.3 (5)
Histonase (pH 7.2)			
Tyrosine	6.6 ± 5.5 (3)	87.0 ± 14.1 (3)	6.3 ± 11.0 (3)
Arginine	1.8 ± 2.3 (5)	97.2 ± 3.1 (5)	0.8 ± 1.8 (5)
Cathepsin (Hemoglobin pH 3.0)	7.0 ± 2.6 (4)	44.0 ± 17.1 (4)	48.5 ± 18.9 (4)
β-Glucuronidase (pH 4.5)	4.6 ± 3.9 (5)	77.4 ± 9.8 (5)	18.0 ± 6.4 (5)

* Mean ± SE, standard deviation in parentheses. From Davies P, Krakauer K, Rita GA, Weissmann G,[8] in which experimental details may be found.

Table 2—Specific Activity of Acid Hydrolases in Human Leukocyte Subfractions*

	Homogenate	Nuclei and debris	Granules	Postgranule fraction
β-Glucuronidase†	100.5	90.5	1095	12.3
Acid Proteases (pH 3.0)				
Hemoglobin‡	18.0	<1	26.2	6.1
Histone§	8.6	6.6	10.4	8.3
Neutral Proteases (pH 7.4)				
Hemoglobin‡	33.1	53.7	84.4	8.2
Histone§	16.6	17.1	19.3	5.3

* Human leukocytes fractionated in sucrose/heparin and differential centrifugation yielded: nuclei and debris (800**g**, 5 minutes) granules (15,000**g**, 10 minutes) and postgranule fractions. Mean of three determinations.

† μg of phenolphthalein/mg protein/hr

‡ μg of tyrosine/mg protein/hr

§ μg of arginine/mg protein/hr, determined in the presence of 2.5 M KCl

proteoglycans, but it displayed only modest activity on hemoglobin and lysozyme.

In direct contrast to this substrate-specificity in *rabbit* polymorphonuclear leukocytes, neutral proteases of *human* leukocytes are much more active upon hemoglobin. From data listed in Table 2, the specific activity of enzymes capable of cleaving both hemoglobin and histone is clearly greater at neutral than in the acid pH range. Moreover, the subcellular distribution of these proteolytic activities differs considerably from the relatively homogeneous distribution of the neutral protease in rabbit polymorphonuclear leukocytes. Thus, considerable proteolytic activity upon both hemoglobin and histone, in the acid pH range, remains in postgranule fractions; significant neutral proteolytic activity sediments with the nuclei. That the subcellular distribution of these enzymes truly reflects a difference from the distribution of a lysosomal (azurophile) marker enzyme may be seen from the subcellular distribution of β-glucuronidase in the same homogenates. These observations are in keeping with the morphologic heterogeneity of leukocyte lysosomes in the human, compared to those of the rabbit. Moreover, protease activity in the neutral and acid range in human leukocytes does not appear to be entirely confined to granules rich in β-glucuronidase.

What is the biologic function of these neutral proteases? We have been intrigued by the possibility that enzymes released from lysosomes within the cell, or perhaps taken up by other cells during inflammation, may provide one stimulus to alterations in transcription or translation.[13,14] In order to test this hypothesis, therefore, we turned to a system previously studied in relationship to mechanisms of lymphocyte transformation by phytohemagglutinin (PHA). The nucleus of the transformed lymphocyte may be characterized as containing excess of euchromatin over heterochromatin.[15] Moreover, the template activity of nuclei from stimulated lymphocytes for exogenous RNA polymerase exceeds that of unstimulated lymphocytes by severalfold. Indeed, the usual increments in template activity provoked by trypsin, an effect which has been attributed to hydrolysis of repressor materials and/or histone by the enzyme, are less easily demonstrated in nuclei from PHA-stimulated cells. These findings led us to suggest that nuclei of stimulated cells may have been exposed, preemptively, to an endogenous trypsin-like enzyme.[13] Subsequently it was found that, when isolated rabbit liver nuclei were incubated with increasing amounts of crystalline trypsin, their template activity for exogenous, bacterial, RNA polymerase was increasingly enhanced.[14] Were our hypothesis, that neutral proteases present in lysosomes could resemble trypsin in augmenting the template activity of isolated nuclei, correct, then it should be possible to incubate rabbit liver nuclei with fractions rich in neutral protease activity (rabbit leukocyte lysosomal lysates), in order to similarly increase their temperate activity for exogeneous RNA polymerase.

Data presented in Table 3 summarizes experiments in which nuclei from rabbit liver were incubated at 37 C, at neutral pH, with freeze-thawed lysates derived from rabbit polymorphonuclear leukocyte lysosomes, rich in neutral histonase. Template activity of nuclei exposed to histonase-rich fractions rose roughly fivefold when compared to nuclei incubated with buffer alone; exogenous RNA polymerase was added to both groups in order to test template activity. That these increments in RNA synthesis represented true

Table 3—Effect of Lysosomal Granules on Template Activity of Rabbit Liver Nuclei for Bacterial RNA Polymerase

Preparation	cpm*
RNA-Polymerase + nuclei + granules	2934
O + nuclei + granules	170
RNA-Polymerase + nuclei + O	634
O + nuclei + O	146
RNA-Polymerase + nuclei + granules + actinomycin	143
RNA-Polymerase + nuclei + O + actinomycin	154

* Assay: Results expressed as cpm of H_3GTP in RNA in 10 minutes. Assay with RNA-Polymerase = 50 units; Nuclei = 20 μg DNA; Granules = 7.1 μg protein; Actinomycin D = 25 μg; O = Glycerol solvent for RNA polymerase, 0.34 sucrose for granules.

DNA-dependent RNA synthesis was established by the finding that incorporation of H_3GTP into RNA was inhibited by appropriate levels of actinomycin-D. More exhaustive treatment of nuclei with granule preparations at neutral pH, or similar treatment at acid pH resulted in breakdown of DNA, RNA, and polymerase, effects which were attributable to lysosomal nucleases and cathepsins.

These data clearly suggest that neutral proteases derived from leukocyte lysosomes have the capacity to: a) degrade extracellular material such as the proteoglycans of cartilage matrix and b) expose sites in previously intact nuclei otherwise unavailable for transcription by RNA polymerase. Now it is clear that these experiments by no means indicate that such events take place in intact tissues or under pathologic circumstances. However, protease-sensitive steps in transcription have also been identified,[16] and it has recently become possible to suppress many of the inflammatory and proliferative events consequent to leukocyte accumulation in intact animals by administering appropriate protease inhibitors.[17] It will be important to determine whether, in pathologic states, materials extruded from leukocyte lysosomes can gain free access to the cytoplasm and/or the nuclei of, as yet, uninvolved cells.

Mechanisms of Enzyme Release from Phagocytic Cells

Since the description of *cytases* by Metchnikoff, which, he believed, escaped from phagocytic cells when these died, it was not appreciated that alternative means might exist whereby these enzymes might be released from phagocytes. Whereas a series of studies have clearly indicated that extracts of leukocyte lysosomes can provoke acute and chronic inflammation in experimental animals,[18] discrete mechanisms which account for the release of such materials from phagocytes were not clearly identified until recently. In Table 4 are listed four discrete situations under which lysosomal hydrolases and inflammatory substances, ordinarily sequestered in membrane-bounded granules, can gain access to the exterior of cells.

The *first* circumstance is indicated simply as *cell death* and is so readily appreciated that it may appear trivial. When a variety of toxins are added to phagocytic cells, injury to the cell membrane is an early consequence, and all intracellular materials are released *pari passu* from the injuried cell, including those ordinarily sequestered within lysosomes. In this regard we have studied the model amphipath melittin, which is a biologic *detergent* that causes primary lysis of the cell membrane and only subsequently disrupts

Table 4—Mechanisms of Lysosomal Enzyme Release in Tissue Injury

Mechanism	Model	Disease
Cell death	Melittin	Infection, toxins (animal, bacterial, chemical)
Perforation from within	MSU, silica	Gout, silicosis
Regurgitation after feeding	Bulk phase: AG/AB complexes, aggregated AB, zymosan, CPPD	Rheumatoid synovitis, pseudogout, immune complex nephritis
Reverse endocytosis	Surface: AG/AB complexes (? cytochalasin)	Vasculitis, SLE, nephrotoxic nephritis

intracellular lysosomes.[19,20] Similar rupture of the outer membranes of cells can be induced by a number of animal, bacterial and chemical toxins, as well as synthetic detergents such as Triton-X100, freezing and thawing, etc. Under these circumstances, cytoplasmic enzymes, potassium, and cellular constituents, in addition to lysosomal hydrolases, find their way into the surrounding tissues. The cell dies not because lysosomal hydrolyses are released into its cytoplasm but because injury to other parts of the cell, especially the cell membrane, cannot be reversed.

The *second*, albeit rare, circumstance more nearly conforms to the *suicide sac* hypothesis of DeDuve.[21] Under some circumstances, materials gain access to the inside of the lysosomal system wherein they cause membranes of the lysosomes to rupture from within. We have discussed elsewhere [22,23] reasons for believing that crystals of monosodium urate act in the same fashion as silica (elegantly demonstrated in the studies of Allison [24] and his coworkers). Both of these crystal types appear to be membrane-lytic, both for artificial and natural membrane systems, by virtue of their capacity to form hydrogen bonds with appropriately aligned phosphate ester groups, such as those of the internal lysosomal membrane. Damage to the organelle leads to the release of lysosomal enzymes concomitantly with the release of cytoplasmic enzymes and other intracellular contents as the cell dies by a kind of *perforation from within* of the cell's vacuolar system. This mechanism will not be discussed in detail.

The *third* mechanism is perhaps more common in pathology. Whenever cells engage in phagocytosis, they release a portion of their lysosomal hydrolases into the surrounding medium, unaccompanied by seepage of cytoplasmic marker enzymes.[22] This effect, now appreciated by many authors,[25-30] appears to be due to the extrusion of lysosomal materials from, as yet, incompletely closed phagosomes, open at their external border to tissue spaces but already joined at their internal border by lysosomes actively discharging their acid hydrolases into the vacuole. Pictures consistent with this mechanism have been published by Zucker-Franklin and Hirsch,[31] by Henson [27,29,30] and by several others. This mechanism is diagrammed in Text-figure 1. Under these circumstances, we have demonstrated that lysosomal acid phosphatase and β-glucuronidase are extruded into the surrounding medium without concomitant extrusion of lactate dehydrogenase. Trivial explanations could not account for these findings—*eg*, there was no consumption or degration of any of the enzymes during phagocytosis, nor was there selective absorption of LDH by granules or leukocytes after regurgitation. This sequence of events follows not only the uptake of immune complexes but accompanies ingestion of other inert particles such as zymosan or crystals of calcium pyrophosphate dihydrate.[22] When cells regurgitate their hydrolases after uptake of immune precipitates, they form the sort of inclusions found in the *RA* cells obtained from synovial fluids of patients with rheumatoid arthritis.

Indeed, it is the uptake of antigen-antibody complexes from the bulk phase of the circulation, tissue fluids or joint fluid that may account for the liberation of inflammatory materials from leukocytes in the many forms of tissue injury associated with circulating, large molecular-weight, aggregates.

We have studied the morphologic correlates of hydrolase extrusion, after the ingestion, by polymorphonuclear leukocytes, of inert particles such as zymosan, or of precipitates formed by the interaction of heat-aggregated immunoglobulin G (aIgG) with rheumatoid factor (IgM). In scanning electron photomicrographs (Figure 1), we see the appearance of a normal polymorphonuclear leukocyte, the ruffled leading edge of which is essentially free of cytoplasmic organelles (toward the upper right of the figure). The multilobed nucleus accounts for the snail-like appearance of the raised edge. When such a cell is exposed to zymosan particles (Figure 2) a striking surface rearrangement of the phagocyte is observed. In cell suspensions exposed to zymosan particles, all particles not engulfed by the cells are separated from the phagocyte during fixation and dehydration. The cells themselves undergo a series of internal gymnastics that result in the appearance at their surface of a series of phagocytic *cups* or invaginations presumably forming the residue of appendages designed to engulf the zymosan particles. These re-

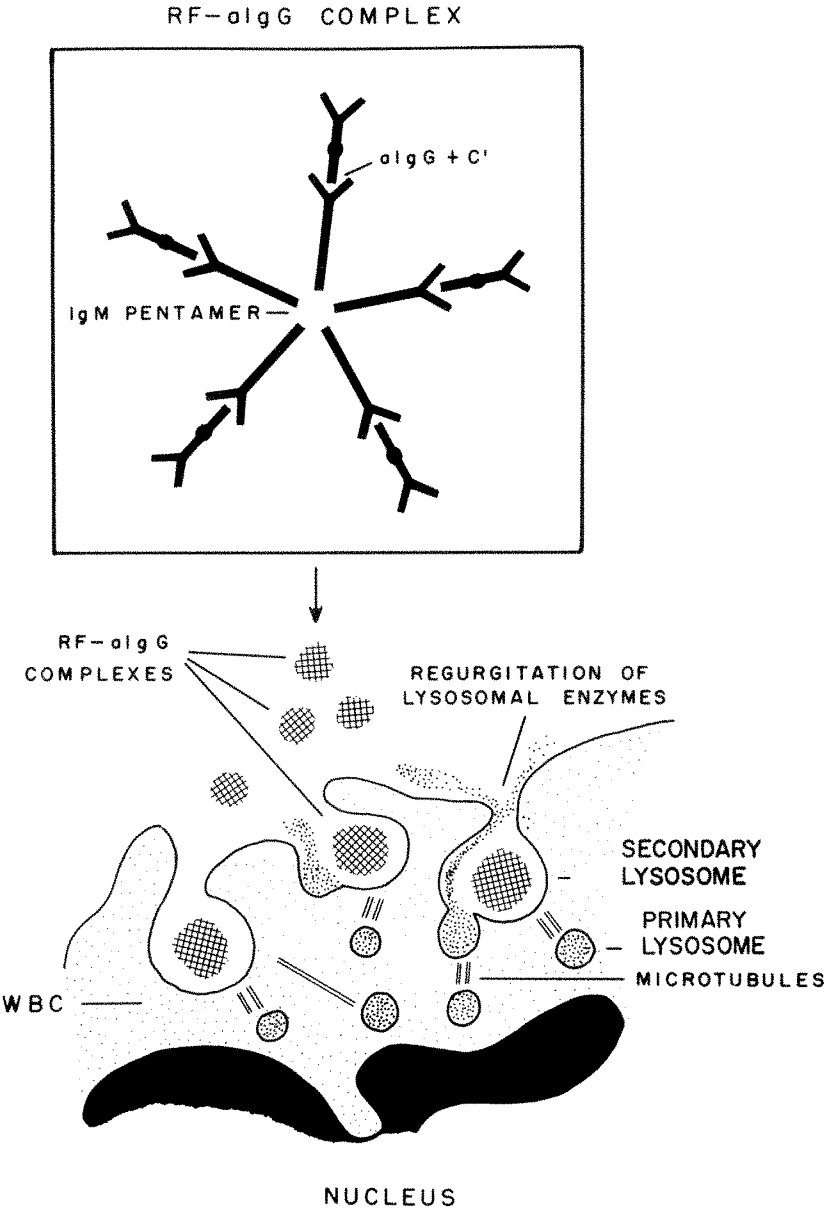
RF–aIgG COMPLEX
aIgG + C'
IgM PENTAMER
RF–aIgG COMPLEXES
REGURGITATION OF LYSOSOMAL ENZYMES
SECONDARY LYSOSOME
PRIMARY LYSOSOME
MICROTUBULES
WBC
NUCLEUS

TEXT-FIG 1—Lysosomal enzyme release from polymorphs exposed to RF-aIgG complexes.
]

markable invaginations, or cups, can be seen in over 90% of polymorphonuclear leukocytes from human peripheral blood exposed to zymosan. In direct contrast, when cells are exposed to immune precipitates formed by aggregated IgG and IgM, a different series of morphologic sequelae is observed (Figure 3). The cells become oriented towards one or two poles; at these poles the cells appear to erect a series of phagocytic projections or *tentacles* apparently designed to engulf the masses of immune precipitates still somewhat adherent to the cell. (In contrast to the behavior of zymosan, the immune complexes appear to be far more resistant to dissociation from the phagocyte by the process of fixation and dehydration.) The phagocytic tentacles, which appear almost squid-like in their morphology, do not arise uniformly over the surface of the phagocytic cell, but seem to be concentrated at one or another pole. Previously published results of transmission electron microscopy indicate that, at the base of such phagocytic projections, phagosomes may be seen merging with lysosomes which extrude their electron-opaque material into the still-open phagosome. Indeed, there may be discerned, by transmission microscopy, a phagocytic vacuole joined at its internal border by a lysosome.[22] The open vacuole is ringed by discrete cross-sections of cytoplasmic projections which have the same dimensions as the projections seen clearly in scanning electron photomicrographs (Figure 3).

In most cells, the kinds of intracellular rearrangements described above are accomplished by means of two systems of filamentous proteins: microtubules[32] and microfilaments.[33] The microtubule system, which is sensitive to colchicine,[32,34] has been shown to be responsible for granule movement in many cell types. These include the melanocyte,[35] the pancreatic islet cell,[36] the platelet,[37] the neuron,[38] the salivary gland cell and the basophil.[39] Therefore, it was reasonable to suppose that agents which influenced the state of aggregation of microtubules in such cell types might be used to influence the response of phagocytic cells to the ingestion of inert particles. Moreover, recent studies have suggested that the functional state of microtubules might be regulated by the intracellular level of cyclic AMP.[22,40,41] Consequently, we have exposed cells to a series of agents designed to raise the level of cyclic AMP within the leukocyte. Cells were treated with appropriate concentrations of cyclic AMP, with dibutyryl cyclic AMP and with these nucleotides, to which had been added agents capable of inhibiting the phosphodiesterase which degrades cyclic nucleotides (theophylline, 2-chloroadenosine). Furthermore, adenyl cyclase was stimulated in leukocytes by prostaglandins of E_1 and F, especially when added with theophylline. In studies described in detail elsewhere,[22] we have demonstrated that these agents have the capacity to retard the release of hydrolase from human peripheral blood polymorphonuclear leukocytes exposed either to particles of zymosan or to immune precipitates. Moreover, these effects could be mimicked by high concentrations of colchicine, a drug known to bind selectively to the tubulin subunits of the final microtubules.

It was therefore of considerable interest to determine the morphologic consequences of the action of these agents upon human white cells exposed to zymosan particles. Figure 4 is a scanning electron photomicrograph of a leukocyte, treated with prostaglandin E_1 and theophylline before challenge by zymosan particles. It may be seen that the phagocytic *cups* are still prominent—cup *formation* has not been inhibited—but within these cups (which indeed have now turned to *saucers*) the outlines of barely ingested zymosan particles may be identified still subjacent to the cell surface. These particles, which by virtue of their intercellular location, have not been washed from the cell during fixation and dehydration, can be seen only in outline. These data are compatible with the hypothesis that prostaglandin E_1 and theophylline inhibited the translocation of zymosan particles from loci near the periphery of the cell (the granule-poor, ruffled edge) to more central locations. It may, therefore, be inferred that lysosomal hydrolases still packaged within lysosomes concentrated at the granule-rich pole of the cell might have trouble gaining access to the peripheral phagocytic vacuoles. Indeed, recent studies in our laboratory have quantitatively documented the failure of leukocyte lysosomes to degranulate into phagocytic vacuoles of cells treated with prostaglandin E_1, mimicking, in this regard, the action of colchicine. These data would clearly suggest that at least one consequence of raising the level within cells of cyclic AMP is to impede the traffic of lysosomes to the phagocytic vacuoles. Consequently, extrusion of acid hydrolases into the surrounding medium by the *regurgitative* pathway would be significantly retarded.

Unfortunately for this simple scheme, detailed studies of the action of cyclic nucleotides (or agents which raise the levels within cells of cyclic AMP) have indicated that, at least for some particles, there is a significant retardation of uptake by phagocytic cells.[42] Thus it was found that concentrations of cyclic AMP above 10^{-4} M with theophylline, or prostaglandin and theophylline, have the capacity to retard phagocytosis of ^{125}I-labeled, heat-aggregated BSA by mouse peritoneal macrophages. Contrarywise, and perhaps more interestingly, very low concentrations of cyclic AMP itself (10^{-10} M) have the capacity to stimulate uptake of these particles. Therefore, it was difficult to decide whether inhibition of hydrolase extrusion in phagocytic cells was due to an intracellular event (interference with microtubule function) or due to inhibition of phagocytosis *per se*. Consequently, together with Dr. Peter Dukor, now of Basle, we studied the degradation of previously ingested ^{125}I-labeled BSA by mouse peritoneal macrophages.[42] In keeping with our previous results, we observed both effects. At low concentrations of cyclic AMP—$<10^{-8}$ M—translocation of previously ingested BSA to lysosomes was enhanced (judged by its subsequent degradation into TCA-soluble fragments). Contrarywise, at high concentrations of cyclic AMP—above 10^{-4} M, especially with theophylline—a colchicine-like effect was noted. Retardation of the breakdown of previously ingested aggregated ^{125}I-labeled BSA by the macrophage was observed. These data were entirely compatible with the hypothesis that cyclic nucleotides exert a biphasic effect intracellularly: acceleration of granule translocation by low concentrations and, retardation at high concentrations, the latter effect mimicking the effect of colchicine or incubation at 4 C. But data shown in Table 5 clearly indicate that when the metabolic response of human peripheral blood polymorphonuclear leukocytes to challenge by immune precipitates was measured, levels of prostaglandin and theophylline sufficient to inhibit hydrolase extrusion were also sufficient to inhibit the normal

Table 5—Glucose Oxidation in Human Polymorphs During Particle Uptake*

	Exposure of cells to RF-aIgG complex		
Compound added	Concentration (mM)	Difference resting vs phagocytic (cpm × 10^{-2})	% Inhibition
None	(Control)	96	00.0
PGE$_1$	0.28	48	50.0
Theophylline	1.0	61	36.5
PGE$_1$ + theophylline	0.28 1.0	24	75.0
Colchicine	1.0	28	70.6
	0.001	100	00.0

* C^1 oxidation of glucose, expressed in differences between resting and phagocytic cells.

metabolic accompaniment of phagocytosis, namely C-1 oxidation. Similarly, concentrations of colchicine sufficient to retard hydrolase release (1 mM) also inhibited C-1 oxidation of glucose. Consequently, in the human leukocyte system, it remained entirely possible that instead of interfering with the intracellular event we wished to study, we were interfering with the first part of the sequence of hydrolase extrusion, namely phagocytosis *per se*. Since in human leukocytes it was difficult to dissociate effects of phagocytosis *per se* from intracellular effects, another system was sought for.

Thus, we encountered the *fourth* mechanism of hydrolase release. Peter Henson [27,29,30] has been studying the effect of coating various solid surfaces with immune complexes and exposing these to polymorphonuclear leukocytes. When polymorphonuclear leukocytes make contact with such surfaces they discharge their hydrolases onto the surface by a mechanism that we have termed *reversed endocytosis* and Henson has called *frustrated phagocytosis*.[27] The former term may be preferable because superficially the process resembles protein extrusion from the salivary gland or from the pancreas and indeed, this process is basically one in which material previously stored within organelles is exported to the external milieu. Although in the leukocyte, this milieu is usually the phagocytic vacuole, under the special circumstances described above, stimulated by IgG in its antigen-reactive form, the granules appear to flow to the surface where their contents are directly discharged onto the filter.

In reverse endocytosis, phagocytosis *per se* does not take place. Therefore, it was of considerable interest to see whether agents which inhibited the export of acid hydrolases during uptake of immune precipitates from the bulk phase would have an effect upon extrusion of acid hydrolases onto the filters coated with immune complex. The scheme for such experiments is shown in Text-figure 2; from this diagram it will be clear that we postulate normal functioning of microtubules in order for granule extrusion to proceed. Data shown in Table 6 indicate that in this system, as well as in the previous system (regurgitation during feeding), release of acid hydrolases is significantly retarded by agents which elevate the level within the cells of cyclic AMP, as well as by colchicine. These data would indicate that the effect we have studied truly represents an *intracellular* effect of high levels of cyclic AMP rather than an indirect effect upon phagocytosis *per se*, since, in reverse endocytosis phagocytosis cannot proceed. Indeed, control experiments, in our laboratories and in that of Henson, have clearly shown that insufficient immunoglobulins are leeched off the filter paper during

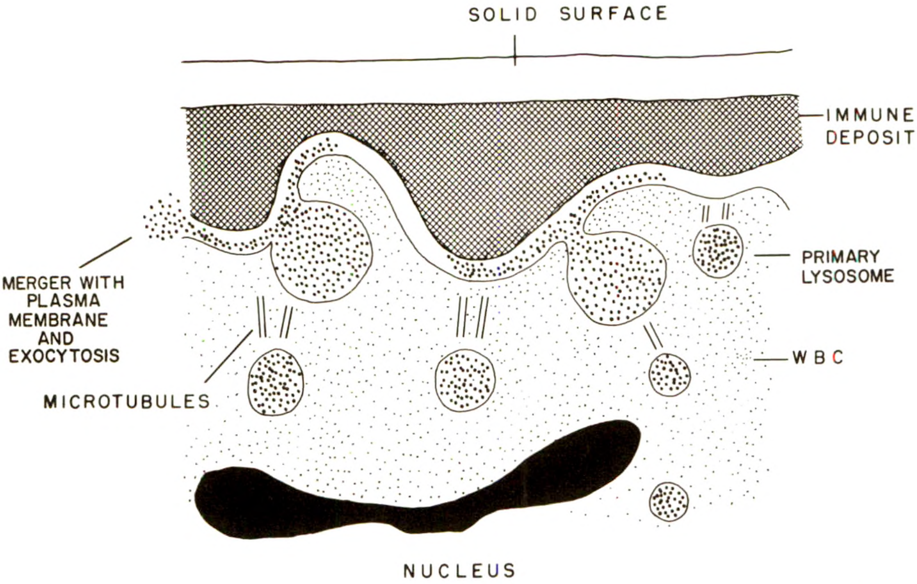

TEXT-FIG 2—Reverse endocytosis of lysosomal enzymes from white blood cells encountering immune deposits on a surface.

incubation (less than 10% of applied material) to cause enzyme extrusion were this small amount of immunoglobulin alone to be present in the bulk phase.

Not all immunoglobulins or precipitates *per se* will cause hydrolase extrusion. Thus, coating of the surface with IgM alone or of nonaggregated IgG does not cause extrusion of acid hydrolases.

Table 6—Inhibition of Enzyme Release from Human Leucocytes Exposed to Immune Complex on Nonphagocytosable Surface

Compound	Percent of control enzyme release	
	β-Glucuronidase	LDH
None (control)	100.0*	100.0*
Dibutyryl cAMP (10^{-3} M)	75.7	99.4
PGE$_1$ (2.8×10^{-4} M)	81.3	97.8
Theophylline (10^{-3} M)	83.1	101.4
2-Chloroadenosine (10^{-3} M)	73.0	97.8
PGE$_1$ + theophylline	55.9	96.6
PGE$_1$ + 2-chloroadenosine	62.9	99.0
Colchicine (10^{-6} M)	73.3	102.5

* Human WBC's exposed to aIgG + IgM (200 μg) on millipore filter released 16.5 ± 3.2% of total β-glucuronidase and 9.5 ± 3.7% of total LDH as opposed to resting cells, which released 3.2 ± 0.6% of total β-glucuronidase and 8.0 ± 4.4% of total LDH (N = 7). Drug-treated samples: N = mean of 4 determinations.

Nor is this process complement-dependent. Extrusion is unassociated with damage to the cells (as indicated by release of lactate dehydrogenase or other indexes of impaired cell viability). Nor is it likely that inhibition of enzyme release is due to some extraneous influence of cyclic AMP in combination with theophylline alone, since exhibition of prostaglandin E_1 and 2-chloroadenosine (another inhibitor of phosphodiesterase) is as effective as admixture of prostaglandin with the known inhibitor phosphodiesterase, theophylline.

Further support for this hypothesis has come from recent experiments in which cells have been pretreated with cytochalasin B, at concentrations ranging from 3 to 10 μg/ml. This agent, as Davies *et al*[43] and Malawista[44] have shown, inhibits phagocytosis of particles by polymorphonuclear leukocytes. After pretreatment with cytochalasin B, human leukocytes can be exposed to zymosan particles. The cells do not take up the particles, which aggregate onto the cell surface and cause the cells directly to extrude lysosomal hydrolases from organelles which discharge immediately subjacent to the adherent zymosan particles. What this experimental system accomplishes in effect, is to turn the regurgitation-during-feeding model into the reverse-endocytosis model. Biochemical studies of this event, to be published in detail elsewhere, indicate that when cells are treated with cytochalasin B and subsequently exposed to zymosan, hydrolase release is markedly enhanced compared to control cells fed zymosan alone. This explanation was appreciated from morphologic studies in which granules could be seen to merge with the cell membrane subjacent to the adherent zymosan particles.

Consequently, as background, we have studied the enhanced release of enzymes from cytochalasin B-treated cells exposed to zymosan. Such *relaxed* or *paralyzed* cells constitute another test for the hypothesis that agents which elevate the level of cyclic AMP within cells act via the microtubule system rather than by means of the microfilaments. While it is appreciated that cytochalasin B interferes with the function with microfilaments, indirect effects on microtubules have also been postulated. Consequently, we treated such cells with dibutyryl cyclic AMP, cyclic AMP and theophylline, prostaglandin and theophylline and with colchicine. When leukocytes were treated with each of these agents, inhibition of enhanced release was readily demonstrable. Such experiments tend to confirm the hypothesis that agents which raised the levels of cyclic AMP within cells acted at a site also sensitive to colchicine, probably the microtubules.

If cells relaxed by treatment with cytochalasin B could still respond with enhanced extrusion of lysosomal enzymes into the surrounding medium after contacting zymosan, and if translocation of granules to the cell surface was unimpaired (except when disrupted as above, by cAMP, etc), microtubules would be expected to be quite prominent in cytochalasin B-treated cells exposed to zymosan. Indeed, that is exactly what was found: cells treated in this fashion displayed an abundance of microtubules as regularly aligned as in control cells. Moreover, such cells treated with prostaglandin and theophylline also displayed intact microtubules. But, if anything, the microtubules were even longer and randomly arrayed throughout the cell. The possible significance of this observation will be discussed below.

A General Mechanism for Immunologically Induced Endocytosis

Since the observations of Lay and Nussenzweig,[45] it has been appreciated that peripheral blood leucocytes contain receptors for immunoglobulin G (but not immunoglobulin M). These receptors, which are not sensitive to trypsin, are discrete from the complement receptors present on the same cells, which are sensitive to trypsin. Moreover, Henson[27] has found that endocytosis and subsequent release of lysosomal hydrolases from polymorphonuclear leucotyes could be readily induced by aggregates of immunoglobulin G and of immunoglobulin A but not of immunoglobulin M or other classes. Immunoglobulins of the subgroups IgG_1 and IgG_3 were most effective in inducing release when ingested in the aggregated state, whereas native immunoglobulins induced little or no enzyme release. Therefore, it appears that immunoglobulins G (and perhaps A) in the antigen-reactive configuration have the property of interacting with nonprotein sites of the leukocyte membrane in order to provoke endocytosis (and hydrolase release). Recent studies in our laboratory by Mrs. Ann Brand have indeed shown that aggregated human IgG, but not native IgG, interacts with artificial lipid structures in the smectic mesophase (bilayer configuration). These structures (liposomes) undergo modest perturbation in contact with immunoglobulins in the antigen-reactive configuration. Studies of the association between immunoglobulins and liposomes by means of Sepharose chromatography on Sepharose 4B show both anionic (dicetyl phosphate) and cationic (stearylamine) liposomes capable of interacting with immunoglobulin G in the heat-aggregated stage. Moreover, the enhanced diffusion was demonstrated of previously sequestered marker anions from liposomes after their contact with these immunoglobulins.

Therefore, it is reasonable to suppose that the first stimulus to endocytosis of aggregated immune complexes from the bulk phase, or to extrusion of enzymes onto immunoglobulins in the antigen-reactive configuration when present on a filter paper, is the interaction of the Fc fragment of immunoglobulins with the lipid bilayers at the surface of leucocytes. This interaction (see above) would occur when IgG molecules become fixed in the antigen-reactive configuration by virtue of union of Fab with divalent antigen, antibody to Fab determinants, or by heat aggregation. Each of these can promote lattice formation of IgG monomers and would render available regularly arrayed, now hydrophobic, Fc ends for interaction with lipid bilayers (Text-figure 3).

What would be the consequences of this interaction between immunoglobulins and surface lipids? Membrane-perturbing agents such as digitonin, etc are capable of altering the reactivity of adenyl cyclase.[46] It would, therefore, be reasonable to suppose that it is membrane perturbation by Fc regions of immunoglobulins which stimulates leucocyte membrane adenyl cyclase to increase the level of cyclic AMP within cells.* Furthermore, in order for a phagocyte to respond to membrane perturbation by endocytosis and movement of lysosomes to phagocytic vacuoles or to the cell exterior (depending upon whether its task is to ingest from the bulk phase or to extrude onto a solid surface), the microtubule system must remain intact and under appropriate controls.

Within cells, microtubules are in a constant state of assembly and, disassembly. Monomers of tubulin are in equilibrium with the aggregated state in which intact microtubules exert their influence on cell form.[32,40,41] Goodman *et al*[41] have postulated that, in nervous tissue at least, microtubule protein can function as an appropriate substrate for phosphorylation by cyclic AMP-dependent protein kinases. Were this situation to hold in the case of the leukocyte, we would expect that cyclic AMP would activate a specific protein kinase in the leucocyte cytosol to phosphorylate microtubule subunits. It would therefore be expected that phosphorylation of tubulin subunits might promote

---

* Recent data[47] suggest that increments of cAMP in leukocytes after phagocytosis are found, not in polymorphs, but in mononuclear cells. This observation came from experiments using the cyclic AMP-binding assay. Since the protein kinase of human polymorphs has been found (by Dr. P-K. Tsung in our laboratory) to be stimulated equally well by *cyclic IMP*, assays of other cyclic nucleotides are required in phagocytic cells.

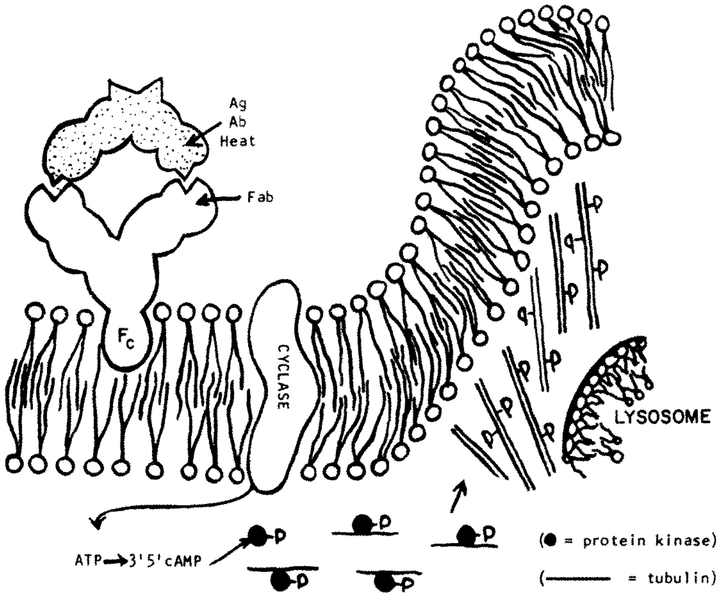

Text-fig 3—Relationship between immunoglobulins and endocytic rearrangement.

aggregation of microtubules and thus regulate their function. Indeed, Gillespie[40] has presented evidence (albeit in tubule-rich pancreatic strips), which suggests that cyclic AMP exerts a biphasic effect on microtubule protein, as judged by the affinity of the tubulin units for colchicine. Low concentrations of cAMP induced *aggregation* of microtubules (decreased colchicine-binding) whereas higher concentrations induced *disaggregation* (enhanced colchicine-binding by tubulin monomers).

For this hypothesis to have any validity in the leukocyte, it would be necessary to demonstrate that human polymorphonuclear leukocytes do indeed have a protein kinase which is activated by cyclic AMP. Recent experiments in our laboratory by Dr. Pi-Kwang Tsung have indeed identified such a protein kinase in purified preparations of human polymorphonuclear leucocytes. The protein kinase is maximally stimulated by 5×10^{-6} M cyclic AMP and demonstrates the usual requirements for absence of calcium and presence of magnesium. The protein kinase, which, as in other systems, consists of a regulatory and a catalytic subunit, could be purified approximately 400-fold over its content in the crude homogenate. On DEAE cellulose chromatography the protein kinase in its catalytic form could be shown to be specifically precipitable by vinblastine together with microtubule protein. Thus, the first step for suggesting that cyclic

AMP-dependent protein kinases can act to regulate tubule structure has been fulfilled, but it remains to be determined whether the tubulin subunits of human polymorphonuclear leukocytes can indeed serve as substrates for the protein kinase.

Were this hypothesis to be true, how can one explain the *inhibition* of granule extrusion by increasing the level of cyclic AMP within cells? This appears to be a paradox, since we would expect that cyclic AMP would *stimulate* endocytosis by promoting tubule function. We have previously shown (see above) that low levels of cyclic AMP *do* enhance translocation of lysosomes to phagosomes or the cell periphery (experiments with mouse macrophages done with Peter Dukor) and that high concentrations inhibit.[42] But high concentrations of cyclic AMP may have another interesting effect. We have noted before the polarity of endocytosis and phagocytosis. When cells are stimulated to endocytose foreign material they appear to rearrange their surfaces at specific sites rather than over the general cell periphery (Figure 3). This would imply that directed traffic of lysosomes to these locally perturbed areas is required and that a gradient of cAMP exists, which is highest in the perturbed region. Were cyclic AMP to be elevated uniformly throughout the cell, we would expect random aggregation of microtubules, thereby preemptively causing aggregation of tubulin into microtubules at areas not necessarily directed toward the cell surface or toward phagocytic vacuoles. A paraphrase of this process would be "if all tracks are open, train traffic cannot be directed where needed."

This series of events, it will be easily appreciated, is at the moment highly speculative. The actual data we have obtained indicate only that there may be an interaction between immunoglobulins and cell surfaces in general, specifically those of the polymorphonuclear leucocyte. Moreover, we have shown that agents which elevate the levels within cells of cyclic AMP have the capacity to interfere with the flow of lysosomes to the phagocytic vacuole or to the cell periphery. This effect is biphasic, as many effects of cyclic AMP are within cells (low concentrations appear to enhance and high concentrations appear to inhibit the flow and shuttle of granules). We have obtained evidence for the presence of a protein kinase (the catalytic unit of which is associated with microtubule protein) within human white cells. Much more experimentation will have to be done in order to verify the hypothesis presented above. It may well be, however, that phagocytic cells such as the polymorphonuclear leucocyte fall into a class of cells, the activities of which can be regulated by cyclic AMP, acting, as in other cells, via protein kinases to regulate the fully differentiated function of the cell.

References

1. Lucy JA, Dingle JT, Fell HB: Studies on the mode of action of excess of vitamin A. 2. Possible role of intracellular protease in the degradation of cartilage matrix. Biochem J 79:500–508, 1961
2. Thomas L, McCluskey RT, Potter JL, Weissman G: Comparison of the effects of papain and vitamin A on cartilage. I. The effects in rabbits. J Exp Med 111:705–718, 1960
3. Weissmann G, Dingle JT: Release of lysosomal protease by ultraviolet irradiation and inhibition by hydrocortisone. Exp Cell Res 25:207–210, 1961
4. Weissmann G, Fell HB: The effect of hydrocortisone on the response of fetal rat skin in culture to ultraviolet irradiation. J Exp Med 116:365–380, 1962
5. Fell HB, Dingle JT: Studies of the mode of action of excess of vitamin A. 6. Lysosomal protease and the degradation of cartilage matrix. Biochem J 87:403–408, 1962
6. Barret AJ, Dingle JT: Tissue Proteinases. Amsterdam, North Holland Publishing Company. 1971, pp 109–133
7. Weissmann G, Spilberg I: Breakdown of cartilage proteinpolysaccharide by lysosomes. Arthritis Rheum 11:162–169, 1968
8. Davies P, Krakauer K, Rita GA, Weissman G: Characterization of neutral protease from lysosomes of rabbit polymorphonuclear leucocytes. Biochem J 123:559–569, 1971
9. Janoff A: Alanine *p*-nitrophenyl esterase activity of human leucocyte granules. Biochem J 114:157–159, 1969
10. Davies P, Krakauer K, Weissmann G: Subcellular distribution of neutral protease and peptidases in rabbit polymorphonuclear leucocytes. Nature 228:761–762, 1970
11. Hirschhorn R, Weissmann G: Isolation and properties of human leukocyte lysosomes. Proc Soc Exp Med Biol 119:36–39, 1965
12. Chodirker WB, Bock GN, Vaughan JH: Isolation of human PMN leukocytes and granules: observations on early blood dilution and heparin. J Lab Clin Med 71:9–19, 1968
13. Hirschhorn R, Troll W, Brittinger G, Weissmann G: Template activity of nuclei from stimulated lymphocytes. Nature 222:1247–1250, 1969
14. Weissmann G, Hirschhorn R: Effect of trypsin and phytohemagglutinin on template capacity of mammalian nuclei for RNA polymerase. J Mt Sinai Hosp NY 37:192–205, 1970
15. Hirschhorn R, Decsy MI, Troll W: The effect of PHA stimulation of human peripheral blood lymphocytes upon cellular content of euchromatin and heterochromatin. Cell Immunol 2:696–701, 1971
16. Velez R, Farrell NL, Freedman M: Selective proteolytic dissociation of rabbit reticulocyte single ribosomes not attached to messenger RNA. Biochim Biophys Acta 228:719–727, 1971
17. Troll W, Klassen A, Janoff A: Tumorigenesis in mouse skin. Inhibition by synthetic inhibitors of proteases. Science 169:1211–1213, 1970
18. Weissmann G, Spilberg I, Krakauer K: Arthritis induced in rabbits by lysates of granulocyte lysosomes. Arthritis Rheum 12:103–116, 1969

19. Weissmann G, Hirschhorn R, Krakauer K: Effect of melittin upon cellular and lysosomal membranes. Biochem Pharmacol 18:1771–1775, 1969
20. Sessa G, Freer JH, Colacicco G, Weissmann G: Interaction of a lytic polypeptide, melittin, with lipid membrane systems. J Biol Chem 244:3575–3582, 1969
21. DeDuve C, Wattiaux R: Functions of lysosomes. Annu Rev Physiol 28:435–492, 1966
22. Weissmann G, Zurier RB, Spieler PJ, Goldstein IM: Mechanisms of lysosomal enzyme release from leucocytes exposed to immune complexes and other particles. J Exp Med 134:149s–165s, 1971
23. Weissmann G, Rita GA: The molecular basis of gouty inflammation: Interaction of monosodium urate crystals with lysosomes and liposomes. Nature (In press)
24. Allison AC, Harington JS, Birbeck M: An examination of the cytotoxic effects of silica on macrophages. J Exp Med 124:141–154, 1968
25. Baehner RL, Karnovsky MJ, Karnovsky ML: Degranulation of leukocyte in chronic granulomatous disease. J Clin Invest 48:187–192, 1969
26. Pruzansky JJ, Patterson R: Subcellular distribution of histamine in human leucocytes. Proc Soc Exp Biol Med 124:56–59, 1967
27. Henson P: Interaction of cells with immune complexes: Adherence, release of constituents, and tissue injury. J Exp Med 134(3, Pt. 2):114s, 1971
28. Hawkins D: Neutrophilic leucocytes in immunologic reactions: Evidence for the selective release of lysosomal constituents. J Immunol 108:310–318, 1972
29. Henson PM: The immunologic release of constituents from neutrophil leucocytes. I. The role of antibody and complement on nonphagocytosable surfaces or phagocytosable particles. J Immunol 107:1535–1546, 1971
30. Henson PM: The immunologic release of constituents from neutrophil leucocytes. II. Mechanisms of release during phagocytosis and adherence to nonphagocytosable surfaces. J Immunol 107:1547–1557, 1971
31. Zucker-Franklin D, Hirsch JG: Electron microscope studies on the degranulation of rabbit peritoneal leukocytes during phagocytosis. J Exp Med 120:569–575, 1964
32. Weisenberg RC, Borisy GG, Taylor EW: The colchicine-binding protein of mammalian brain and its relation to microtubules. Biochemistry 7:4466–4479, 1968
33. Wessells NK, Spooner BS, Ash JF, Bradley MO, Luduena MA, Taylor EL, Wrenn JT, Yamada KM: Microfilaments in cellular and developmental processes. Science 171:135–143, 1971
34. Malawista SE, Bensch KG: Human polymorphonuclear leucocytes: demonstration of microtubules and effect of colchicine. Science 156:521–523, 1967
35. Malawista SE: On the action of colchicine: the melanocyte model. J Exp Med 122:361–384, 1965
36. Lacy PE, Howell SL, Young DA, Fink CJ: New hypothesis of insulin secretion. Nature 219: 1177–1178, 1968
37. White JG: Effects of colchicine and vinca alkaloids on human platelets. III. Influence on primary internal contraction and secondary aggregation. Am J Pathol 54:467–478, 1969

38. Weiss PA: "Panta' Rhei"—and so flow our nerves. Proc Am Philo Soc 113:140–148, 1969
39. Levy DA, Carlton JA: Influence of temperature on the inhibition by colchicine of allergic histamine release. Proc Soc Exp Biol Med 130:1333–1336, 1969
40. Gillespie E: Colchicine binding in tissue slices. Decrease by calcium and biphasic effect of adenosine-3′, 5′-monophosphate. J Cell Biol 50:544–549, 1971
41. Goodman DB, Rasmussen H, DiBella F, Guthrow CE Jr: Cyclic adenosine 3′, 5′-monophosphate-stimulated phosphorylation of isolated microtubule subunits. Proc Natl Acad Sci USA 67:652–659, 1970
42. Weissmann G, Dukor P, Sessa G: Studies on lysosomes, mechanisms of enzyme release from endocytic cells and a model for latency *in vitro*. Immunopathology of Inflammation. Edited by B Forscher and JC Houck. Amsterdam, Excerpta Medica, 1971, p 107
43. Davis AT, Estensen R, Quie PG: Cytochalasin B. III. Inhibition of human polymorphonuclear leukocyte phagocytosis. Proc Soc Exp Biol Med 137:161–164, 1971
44. Malawista SE, Gee JBL, Bensch KG: Cytochalasin B reversibly inhibits phagocytosis: Functional, metabolic, and ultrastructural effects in human blood leukocytes and rabbit alveolar macrophages. Yale J Biol Med 44:286–300, 1971
45. Lay NW, Nussenzweig V: Receptor for complement on leukocytes. J Exp Med 128:991–1001, 1968
46. Bitensky MW, Gorman RE, Miller WH: Digitonin effects on photoreceptor adenylate cyclase. Science 175:1363–1364, 1972
47. Mangianello V, Evans WH, Stossel TP, Mason RJ, Vaughan M: The effect of polystyrene heads on cyclic 3′5′-adenosine monophosphate concentration in leucocytes. J Clin Invest 50:2741–2744, 1971

Acknowledgments

Portions of the experimental work quoted were performed by Drs. Rochelle Hirschhorn, Philip Davies, Peter Dukor, Gunter Brittinger, Daniel Weisberg, Giuseppe Rita, Paul Spieler and Ira Goldstein, to whom we owe a debt of gratitude.

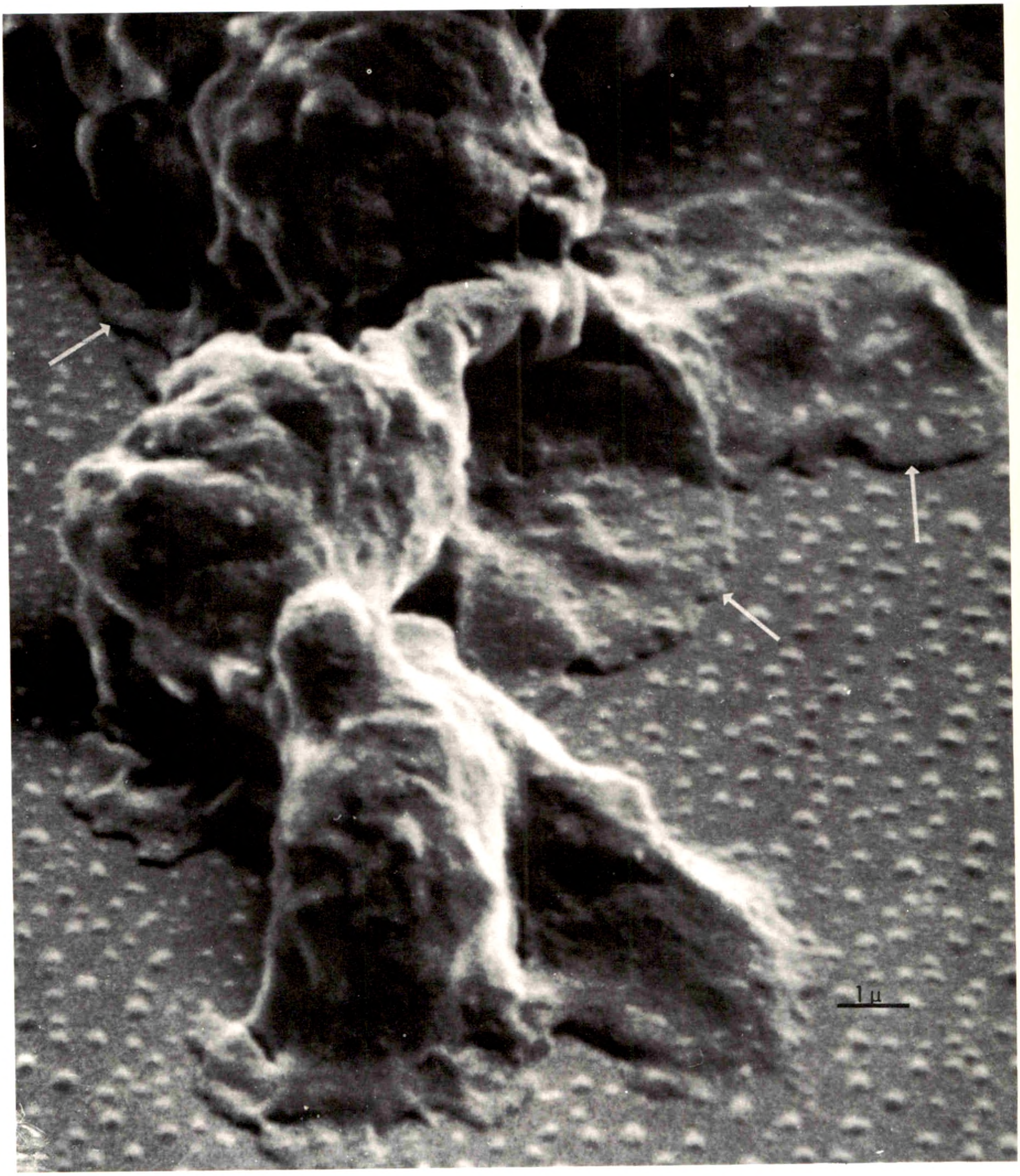

Fig 1—Human peripheral blood polymorphonuclear leucocytes, incubated for 1 hour in phosphate-buffered saline. The cells have flat ruffled extensions (*arrow*), less than 0.1 μ thick at the edge. The bulk of the cytoplasm is massed around the nuclear lobes.

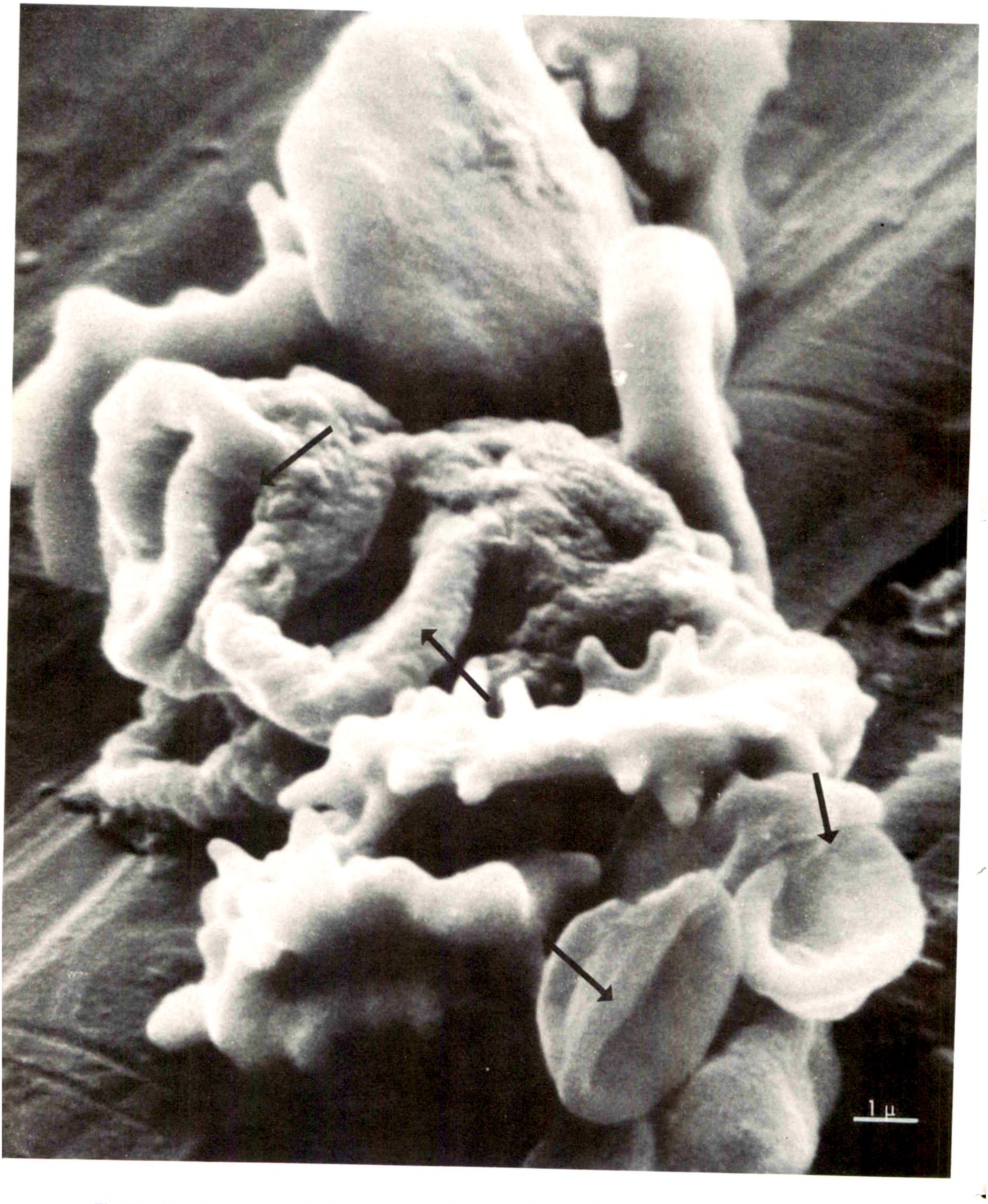

Fig 2—Human peripheral blood polymorphonuclear leucocyte, incubated for 1 hour with zymosan. *Arrows* indicate phagocytic cups. These cups have an inside diameter of approximately 2 μ and a wall thickness of 0.4 to 0.6 μ; each cell has several.

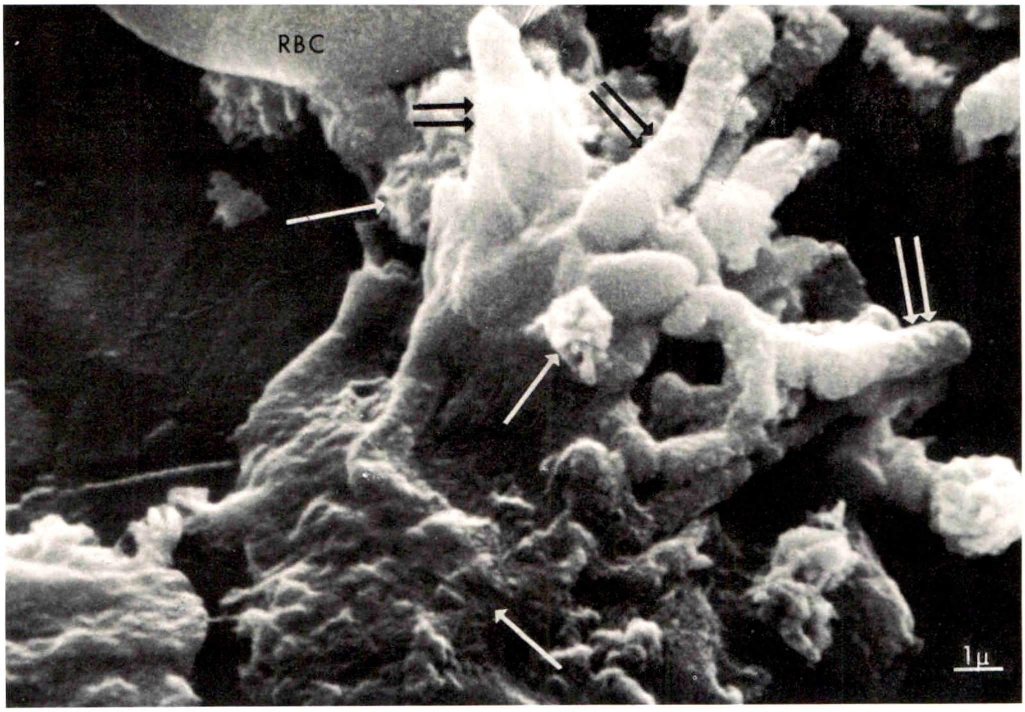

3

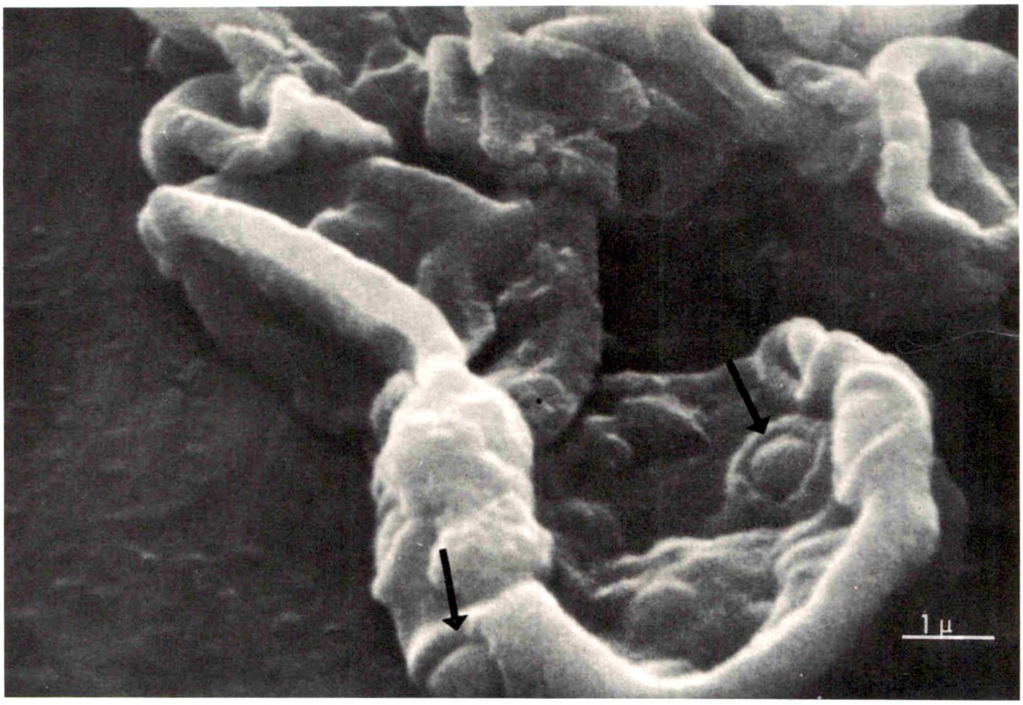

4

Fig 3—Human peripheral blood polymorphonuclear leucocyte, incubated for 1 hour with immune precipitates of IgG with rheumatoid factor. *Double arrows* indicate the multiple finger-like projections elaborated by these cells. The projections are approximately 1 μ in diameter with lengths of 2 to 5 μ. *Single arrows* indicate the amorphous precipitate of immune complex. **Fig 4**—Human peripheral blood polymorphonuclear leucocyte, incubated for 60 minutes with 2.8×10^{-4} M prostaglandin E_1 before exposure to zymosan (1 hour). The cup is transformed into a saucer and rounded projections (approximately 1 μ diameter) within these saucers indicate the presence of particles subjacent to the cell surface.

[*End of Article*]

Role of Granulocyte Collagenase in Collagen Degradation

Gerald S. Lazarus, MD, John R. Daniels, MD, Jane Lian, PhD and Mary C. Burleigh, PhD

INFILTRATION BY LEUKOCYTES in inflammatory conditions is frequently associated with collagen degradation. Resorption of collagen occurs during abcess formation, when large numbers of granulocytic leukocytes are present. Leukocytes have been shown to be responsible for the basement membrane degradation seen in such immunologic phenomenon as the arthus reaction and the arteritis of serum sickness.[1] Extracts of polymorphonuclear leukocytes are capable of digesting human renal basement membrane and causing damage to vessel walls in rabbit skin.[2] These observations imply that granulocytes have a mechanism for degrading collagen.

The mechanisms by which collagen is degraded have required elucidation, since collagen is quite resistant to degradation by most proteolytic enzymes. In 1962 Gross and Lapiere[3] described the first animal collagenase; this enzyme was found in the medium of tissue cultures of metamorphosing tadpole tails. Subsequently, collagenase was demonstrated in tissue culture fluids from: skin,[4-14] synovium from patients with rheumatoid arthritis,[15-19] synovial fluid from patients with rheumatoid arthritis,[20] involuting postpartum rat uterus,[21] bone of various species,[22-26] human gingiva,[27-29] crab hepatopancreas,[30] human middle ear cholesteotoma,[31] cornea[32-34] and carageenin granuloma.[35]

The study of collagenases requires some understanding of the biochemical characteristics of collagen. I will, therefore, review superficially some of the relevant aspects of collagen biochemistry. Tropocollagen molecules have a molecular weight of 300,000 and are 3000 Å in length and 15 Å in width.[36] These molecules are composed of three polypeptide chains, each of 100,000 molecular weight. The chains are referred to as α chains and they are characterized by the repeating glycine–X–Y triplet which is necessary for helix formation. There are

---

From the Strangeways Research Laboratory, Cambridge England, Department of Medicine, Albert Einstein College of Medicine, Bronx, NY, Department of Medicine, Stanford University Medical School, Stanford, Calif and the Department of Biochemistry, Boston University School of Medicine, Boston, Mass.

Dr. Lazarus is a Research Fellow of the Arthritis Foundation and Carl Herzog Fellow of the American Dermatological Association. His present address is: Section of Dermatology, Department of Medicine, Montefiore Medical Center, 210th St, Bronx, New York.

significant differences between constituent α chains, so that in most species at least two types are separable by chromatography.[36–38] These α chains may be covalently cross-linked through the lysyl residue at the fifth position from the A- or N-terminal end of the molecule, to form two-chain components (β), and three-chain components γ.[39] The cross-link area is further characterized by a lack of polyproline helix,[36] which makes this area especially susceptible to degradation by certain proteases which are not true collagenases.

Denaturation of collagen is the conversion of this rigid, tightly coiled, three-chain molecule to a random coil called *gelatin*. Collagen can be denatured by treating it with chemicals or by heating it to a sharply defined temperature. For solutions of salt-extracted rat skin collagen, this temperature is 37 C.[40] The possibility of denaturation of collagen solutions at physiologic temperature precludes their use in the study of collagenases. However, it is not generally appreciated that, even at temperatures as low as 25 C, collagen in solution is susceptible to degradation by several proteolytic enzymes.[41,42]

Individual collagen molecules secreted by fibroblasts aggregate into fibrils so that the molecules lie parallel to each other and overlap by one-quarter of their length. The organization into fibrils is governed by electrostatic forces, so that positive and negative charges on adjacent tropocollagen molecules neutralize each other.[43] Fibrils are stabilized further by intermolecular cross-links based on aldehydes derived from lysine and hydroxylysine.[44] Collagen fibrils are extremely stable; if they are not heated above their shrinkage temperature, constituent collagen molecules are degraded only by collagenases at 37 C.

Collagenases are enzymes capable of cleaving native collagen molecules through their characteristic helical portion. Almost all collagenases are also capable of degrading collagen molecules that have been stabilized into fibrils under physiologic conditions. Enzymes such as trypsin are not considered collagenases, since they only degrade an end of the native collagen molecule.[45] Finally, degradation of synthetic collagen peptides is not proof of collagenase activity; the purified collagenases do not degrade the synthetic collagen substrate, but associated peptidases are responsible for synthetic peptide hydrolysis.[46–48]

The enzyme found in the medium of tissue cultures of metamorphosing tadpole tails was the first collagenase described, and its mechanism of action has been extensively investigated.[3,47,49–53] Tadpole collagenase, under physiologic conditions of temperature and pH, cleaves the collagen molecule three-quarters of the way from the N-terminal end (Text-figure 1).[51] The resulting N-terminal three-quarter-length product is referred to as TC^A and the C-terminal one-quarter-length product is designated TC^B. These products maintain their helical conformation in solution at 28 C and, as a consequence, the reaction is characterized by a fall in relative viscosity and no change in optical rotation.[49] The products can be induced to form SLS aggregates and can be studied electron microscopically,[49] or they can be evaluated by acrylamide gel electrophoresis.[52] The tadpole collagenase requires calcium, is inhibited by EDTA and cysteine and is unaffected by diisopropylfluorophosphate. Using an antibody to highly purified tadpole collagenase, Harper *et al* [53] have detected immunologically reactive, but enzymologically inactive, collagenase zymogen in tadpole homogenates.[53] In homogenates of human skin, Eisen *et al* [14] demonstrated the presence of enzymologically inactive collagenase by immunologic methods. They were able to restore enzymatic activity to their immunologically detected collagenase by chromatographically separating the collagenase from serum collagenase inhibitors in tissue homogenates. These data demonstrate that collagenase is present *in vivo* and could be of significance in connective tissue catabolism.

In our initial studies with human leukocytes we employed the radioactive, reconstituted collagen fibril assay system.[54] In this technic,

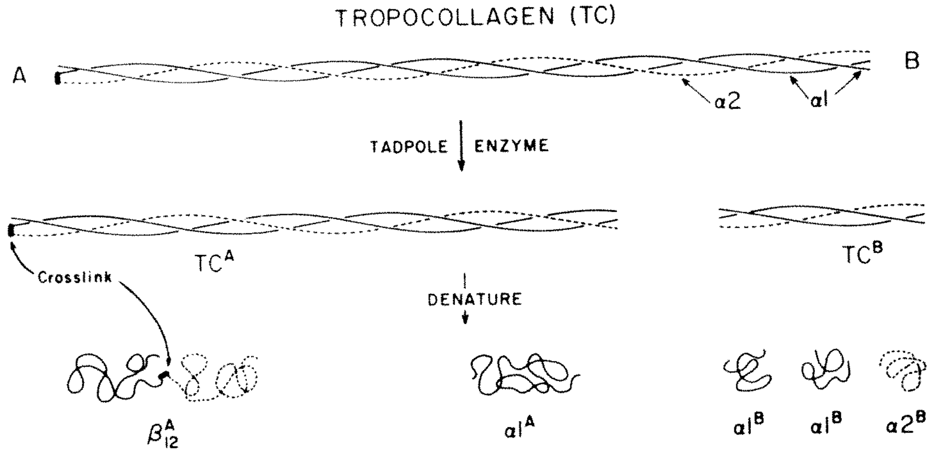

TEXT-FIG 1—Diagrammatic representation of the collagen molecule and the pieces resulting from digestion with tadpole collagenase. The minor helix of the individual chains is not shown; the major helix is not to scale. The letters A and B refer to the designations employed in electron microscopy to distinguish the ends of the molecule. In a sample of extractable collagen, some molecules would be crosslinked between $\alpha 1$ and $\alpha 2$, as shown; others between the two $\alpha 1$ chains and some not at all. The denatured products would than include $\alpha 2A$ and $\beta A11$ in addition to those shown (From Kang *et al*, 1966 [51]).

radioactive collagen fibrils are prepared from a solution of highly purified ^{14}C-glycine-labeled acid extracted native collagen.[51] These fibrils are then incubated with the material to be tested at 37 C. After a suitable period of time, the fibrils are removed by filtration or centrifugation;[12,49] the amount of radioactivity in the clarified solution reflects peptide reaction products and solubilized collagen molecules. All experiments include assays of buffer blanks and trypsin controls, which indicate the extent of nonspecific proteolytic breakdown of collagen fibrils. We found that human granulocytes, prepared according to the methods of Cohn and Hirsch,[55] were capable of degrading 21% of our collagen fibrils. Activity was found primarily in the granule fraction of the leukocytes. Similar results were obtained with 99% pure granulocyte preparations from patients with chronic granulocytic leukemia. Normal human lymphocytes or rabbit alveolar macrophages had little, if any, collagenase activity.[54,56] Since our enzyme preparation was exceedingly unstable, the collagenase had to be purified.

During purification, it became obvious that, although our collagenase was capable of specifically cleaving the collagen molecule into TC^A and TC^B fragments (Figure 1), it had lost its ability to cleave reconstituted collagen fibrils. As a consequence, Dr. Daniels designed an assay which directly measured the formation of TC^B products.[58,59] He incubated a solution of radioactive collagen with the enzyme preparation at 25 C and terminated the reaction by adding urea. The material was then separated by acrylamide gel electrophoresis and stained with Coomassie blue. The segment of gel containing the TC^B fragment was removed, solubilized in H_2O_2 and counted. All kinetic experiments measured initial velocity and were performed at saturating substrate conditions.

Leukocytes were separated from red cells by centrifugation, sedimentation in dextran and hypotonic hemolysis. From this point all procedures were carried out at 4 C. The white cells were then washed in 0.34 M sucrose, homogenized and a pellet containing both nuclei and granules was collected. This pellet was sonicated and the supernatant from a 78,000g 60-minute centrifugation was collected.[59] The enzyme preparation was applied to a diethylaminoethyl cellulose column, at pH 8.5, and eluted with a linear salt gradient.[57] The fractions containing activity were pooled, concentrated by ammonium sulfate precipitation, and applied to a column of Bio-Gel A-0.5M and eluted with Tris buffer, pH 7.8, containing 250 mM NaCl.[59] The active fractions were pooled and used for study. This partially purified material was able to hydrolyze 335 pmoles of collagen per milligram of enzyme protein at pH 7.8 and 25 C per hour. The exact purification of our enzyme was impossible to calculate, since the starting material was unstable during assay conditions. Its elution position from the agarose column, between bovine serum albumin and ovalbumin, suggested a Stokes radius compatible with a molecular weight of approximately 60,000. The enzyme preparation did not hydrolyze purified insulin A chain, insulin B chain or carboxymethylated bovine pancreatic ribonuclease.

The collagenase was able to effect a 65% reduction in relative viscosity without a detectable change in optical rotation.[57] This indicated that the overall helical structure of the TC^A and TC^B pieces had been maintained. Electron micrographs of SLS formed from reaction products revealed fragments of 2750 and 2150 Å which suggests that the electron microscopic site of cleavage was identical to that of the other human collagenase (Figure 2).[57] In addition, Bauer *et al*[10] have shown that there is a line of complete identity between granulocyte extracts and highly purified human skin collagenase when immunodiffusion is performed with an antiserum to purified human skin collagenase.

The enzyme showed maximal activity against native collagen between pH 7 and pH 8.[57] It was 50% inactivated after 80 minutes at 37 C. Hydrolysis was markedly effected by temperature, and there was a 50% increase in velocity when the temperature was raised from 21 to 25 C.[59] Compounds with free sulfhydryl groups, such as cysteine and D-penicillamine, were markedly inhibitory. The addition of 5,5′-dithiobis-2-nitrobenzoic acid (DTNB) or *p*-chloromercuribenzoate (PCMB) markedly activated collagenase activity.[59] In recent experiments with a 150-fold purified rabbit skin collagenase, 1 mM *p*-chloromercuribenzoate increased collagenase activity by a factor of 2.[60]

Incubation of denatured collagen or gelatin with partially purified granulocyte enzyme produced a complex pattern on acrylamide gel electrophoresis. The TC^B fragment was extremely prominent but multiple bands suggest that denaturation exposes new sites for enzyme action.[59]

There are several significant differences between granulocyte collagenase and other reported human collagenases. First, purification of the granulocyte enzyme results in loss of ability to degrade collagen fibrils (Figure 1); this implies that specific cleavage of the collagen molecule into TC^A and TC^B fragments does not guarantee dissolution of collagen fibrils. The mechanism by which granulocytes degrade collagen fibrils must therefore involve additional proteolytic activity. This impression is strengthened by observations with crude granulocyte extracts. Incubations with crude material result in extensive fibril lysis and complex patterns on acrylamide gel electrophoresis (Figure 1). The second, somewhat unique, property of the granulocyte enzyme is that it is not inhibited by human serum. The α2-macroglobulins and α1-antitrypsin inhibitor have been shown to be capable of inhibiting most collagenases,[61] with the exception of the heavy synovial fluid collagenase[20] and the granulocyte enzyme. The addition of serum to the crude granule preparation inhibits fibril lysis and simplifies the acrylamide gel electrophoresis pattern to that seen with partially purified granulocyte collagenase (Figure 1). Such a phenomenon suggests that serum is inhibiting the nonspecific proteases which work in association with collagenase to effect fibril lysis. Similar results can be obtained by adding the inactivated postgranule supernatant fraction from human polymorphonuclear leukocytes and 1 mM diisopropylfluorophosphate. There are, therefore, two distinctive systems involved in granulocyte-mediated collagenolysis (Table 1).

The specific collagenase, which cleaves collagen into TC^A and TC^B pieces, is inhibited by EDTA and cysteine. The nonspecific proteolytic system is inhibited by human serum inactivated postgranule supernatant or cytosol and DFP; it is partially inhibited, as judged by simplification of the acrylamide gel electrophoresis pattern towards

Table 1—Differentiation of Collagenolytic Systems in Human Granulocytes by the Use of Inhibitors*

	Specific collagenase inhibition		Nonspecific protease inhibition
Cysteine	10 mM	+	0
EDTA	10 mM	+	0
Human serum	7 %	0	+
Inactivated post-granule supernatant	400 μg	0	+
DFP	1 mM	0	+
Soya bean trypsin inhibitor	250 μg	0	partial
TLCK	0.3 mM	0	partial
TPCK	0.3 mM	0	partial
Pepstatin	25 μg	0	0

* Incubations included 800 μg of collagen, 400 μg crude granule protein, and listed final concentration of inhibitor in 600 μl of 50 mm Tris pH 7.0, containing 15 mM $CaCl_2$ + 325 mM NaCl, 20 hours at 25C. Effects studied by acrylamide gel electrophoresis.

that found with purified granulocyte collagenase, by soya bean trypsin inhibitor, tosylphenylalanyl chloromethylketone (TPCK) and tosyllysyl chloromethylketone (TLCK). Barrett and Dingle have shown that pepstatin is a potent new inhibitor of acid proteinases, including cathepsin D.[62,63] Complete inhibition of the 6 units[64] of cathepsin D/10^9 leukocytes, in our preparations, by pepstatin did not influence collagen degradation. This is explained by the data of Harris *et al*[65] and our own,[66] which demonstrate that cathepsin D is only capable of cleaving the cross-link area of denatured collagen and does not hydrolyze the peptide chain.

The leukocyte postgranule supernatant fraction or cytosol does not inhibit the specific collagenase. Although cytosol itself is incapable of degrading collagen fibrils, its addition (750 μg/ml final concentration) to a 150-fold, purified, rabbit-skin collagenase preparation caused fibril lysis to double from 40 to 80% (Table 2).[60] This facilitation could be prevented by the addition of 1 mM diisopropyl flourophosphate. The cytosol, therefore, contains an enzyme which assists collagenase in degrading collagen fibrils. If this cytosol helper-enzyme is inactivated by incubation with 1 mM diisorpropyl fluorophosphate, or by heating to 75 C for 20 minutes, the addition of cytosol to crude granule preparations inhibits the nonspecific protease system, and a pattern of specific TC^A and TC^B pieces is seen on acrylamide gel electrophoresis (Figure 1). The cytosol, therefore, contains an inhibitor of the nonspecific protease system found in, granules, as well as an enzyme capable of facilitating collagen-degradation by specific collagenase. The nonspecific granule protease system, therefore, has striking similarities to the granulocyte elastase system described by Janoff.[2,67,68] It also has some characteristics in

Table 2—Effect of Human Granulocyte Cytosol on the Fibril Degrading Activity of Partially Purified Rabbit Skin Collagenase

Preparation	Fibril lysis (%)
Cytosol	4
Skin collagenase	44
Skin collagenase + DFP 1 mM	44
Skin collagenase + cytosol	80
Skin collagenase + cytosol + DFP 1 mM	41
Trypsin 25 μg	4

Incubations included 200 μg of reconstituted collagen fibrils, 12.5 μg of skin collagenase protein, 7.5 μg of cytosol protein, 1 mM DFP final concentration, in 300 μl of 50 mM Tris buffer pH 7.4 containing 5 mM $CaCl_2$ and 100 mM NaCl, 20 hours at 37 C.

common with the neutral proteinase found in rabbit leukocytes by Davies *et al.*[69]

The specific collagenase, which hydrolyses collagen to TC^A and TC^B fragments, is an essential part of the mechanism by which granulocytes degrade collagen. When crude granulocyte preparations are incubated with 1 mM *p*-chloromercuribenzoate, the partially purified granulocyte collagenase is activated and collagen fibril lysis is increased by 50 to 100%. Inhibition of collagenase by the addition of 10 mM cysteine or 10 mM EDTA decreases fibril lysis by approximately 50%.

Recently, we have used very fresh granule preparations, washed to remove cytosol inhibitor. These preparations have been more active than previous ones, and they were capable of degrading over 30% of our collagen fibrils. The addition of cysteine and EDTA in quantities sufficient to totally inhibit granulocyte collagenase inhibited fibril lysis by only 50%. Furthermore, acrylamide gel electrophoresis patterns, obtained from incubations of collagen solution with crude granulocyte preparations in which collagenase had been inhibited by EDTA and cysteine (pH 7.0, 25 C), revealed β to α conversion and multiple bands. This pattern indicates that the nonspecific protease has cleaved the cross-link area and partially degraded the collagen chain. These data suggest that the nonspecific protease system might be capable of limited, independent collagen hydrolysis. Such a possibility is strengthened by Janoff's observation that the granulocyte elastase complex can solubilize bovine achilles tendon collagen.[2] Further studies with purified enzymes should clarify the role of the nonspecific system in collagen degradation.

The mechanisms by which leukocytes degrade collagen are quite complex. The granule fraction of granulocytes contain a specific collagenase which cleaves collagen in solution into the characteristic TC^A and TC^B fragments, but is unable to solubilize collagen fibrils. The specific granulocyte collagenase is inhibited by EDTA and cysteine, but not by serum, cytosol or diisopropyl fluorophosphate. Granulocytes also contain a protease system which is inhibited by serum, inactivated cytosol and diisopropyl fluorophosphate. This protease(s) is capable of degrading specific products of collagenase activity, the TC^A and TC^B fragments, and may also be capable of limited independent collagen hydrolysis. Both specific collagenase and nonspecific protease are necessary for maximal collagen degradation. In addition, noncollagenase granulocyte proteases, such as Cathepsin D, might facilitate collagen catabolism by degrading the matrix glycosaminoglycans and glycoproteins, thus expediting contact between the granulocyte collagenolytic system and collagen fibrils. The granulocyte, with its specific collagenase and its complement of other proteases, is admirably suited to the complex task of collagen catabolism.

Summary

The granule fraction of human granulocytes contains a specific collagenase which cleaves collagen molecules into characteristic TC^A and TC^B fragments. This specific collagenase is incapable of solubilizing collagen fibrils. Leukocyte granules also contain a second protease system capable of degrading specific products of collagenase activity and also may be capable of limited independent collagen hydrolysis. Both the specific collagenase and the nonspecific protease are necessary for maximal collagen fibril degradation.

References

1. Cochrane CG, Aikin BS: Polymorphonuclear leukocytes in immunologic reactions. The destruction of vascular basement membrane *in vivo* and *in vitro*. J Exp Med 124:733–752, 1966
2. Janoff A: Mediators of tissue damage in leukocyte lysosomes. X. Further studies on human granulocyte elastase. Lab Invest 22:228–236, 1970
3. Gross J, Lapiere CM: Collagenolytic activity in amphibian tissues: a tissue culture assay. Proc Nat Acad Sci USA 48:1014–1022, 1962
4. Fullmer HM, Lazarus GS, Gibson WA, Stam AC: Collagenolytic activity of the skin associated with neuromuscular disease. Lancet 1:1007–1009, 1966
5. Riley WB, Peacock EE: Identification, distribution and significance of collagenolytic enzymes in human tissues. Proc Soc Exp Biol Med 124:207–210, 1967
6. Eisen AZ, Jeffrey JJ, Gross J: Human skin collagenase. Isolation and mechanism of attack on the collagen molecule. Biochim Biophys Acta 151:637–645, 1968
7. Eisen AZ: Human skin collagenase: localization and distribution in normal human skin. J Invest Dermatol 52:442–448, 1969
8. Lazarus GS, Fullmer HM: Collagenase production by human dermis *in vitro*. J Invest Dermatol 52:545–547, 1969
9. Eisen AZ, Bauer EA, Jeffrey JJ: Animals and human collagenase. J Invest Dermatol 55:359–374, 1970
10. Bauer EA, Eisen AZ, Jeffrey JJ: Immunologic relationship of a purified human skin collagenase to other human and animal collagenases. Biochim Biophys Acta 206:152–160, 1970
11. Eisen AZ: Human skin collagenase: relationship to the pathogenesis of epidermolysis bullosa dystrophica. J Invest Dermatol 52:449–453, 1969
12. Lazarus GS: Collagenase and connective tissue metabolism in epidermolysis bullosa. J Invest Dermatol 58:242–248, 1972

13. Donoff RB, McLennan JE, Grillo HC: Preparation and properties of collagenases from epithelium and mesenchyme of healing mammalian wounds. Biochim Biophys Acta 227:639–656, 1971
14. Eisen AZ, Bauer EA, Jeffrey JJ: Human skin collagenase: the role of serum alpha globulins in the control of activity *in vivo* and *in vitro*. Proc Nat Acad Sci USA 68:248–251, 1971
15. Evanson JM, Jeffrey JJ, Krane SM: Human collagenase. Identification and characterization of enzyme from rheumatoid synovium in culture. Science 158:499–502, 1967
16. Evanson J, Jeffrey JJ, Krane SM: Studies on collagenase from rheumatoid synovium in tissue culture. J Clin Invest 47:2639–2651, 1968
17. Lazarus GS, Decker JL, Oliver CH, Daniels JR, Multz CV, Fullmer HM: Collagenolytic activity of synovium in rheumatoid arthritis. N Engl J Med 279:914–919, 1968
18. Harris JR, Evanson JM, Dibona DR, Krane SM: Collagenase and rheumatoid arthritis. Arthritis Rheum 13:83–94
19. Bauer EA, Eisen AZ, Jeffrey JJ: Studies on purified rheumatoid synovial collagenase *in vivo* and *in vitro*. J Clin Invest 50:2056–2064, 1971
20. Harris ED, Dibona DR, Krane SM: Collagenases in human synovial fluid. J Clin Invest 48:2104–2113, 1969
21. Jeffrey JJ, Gross JJ: Collagenase from rat uterus. Isolation and partial characterization. Biochemistry 9:268–273, 1970
22. Walker DG, Lapiere CM, Gross J: Collagenolytic factor in rat bone promoted by parathyroid extract. Biochem Biophys Res Commun 15:397–402, 1964
23. Kaufman EJ, Glimcher MJ, Mechanic GL, Goldhaber P: Collagenolytic activity during active bone resorption in tissue culture. Proc Soc Exp Biol Med 120:632–636, 1965
24. Fullmer HM, Lazarus GS: Collagenase in human, goat and rat bone. Israel J Med Sci 3:758–761, 1967
25. Fullmer HM, Lazarus GS: Collagenase in bone of man. J Histochem Cytochem 17:793–798, 1969
26. Shimizu M, Glimcher MJ, Travis D, Goldhaber P: Mouse bone collagenase: isolation, partial purification, and mechanism of action. Proc Soc Exp Biol Med 130:1175–1180, 1969
27. Fullmer HM, Gibson W: Collagenolytic activity in gingivae of man. Nature 209:728, 1966
28. Fullmer HM, Gibson WA, Lazarus GS, Bladen HA, Whedon KA: The origin of collagenase in periodontal tissues in man. J Dent Res 48:646–651, 1969
29. Fullmer HM: Metabolic hydrolysis of collagen, Metabolic Hydrolysis and Metabolic Conjugation. Vol 2. Edited by W Fishman. New York, Academic Press, Inc, pp 301–343, 1970
30. Eisen AZ, Jeffrey JJ: An extractable collagenase from crab hepatopancreas. Biochim Biophys Acta 191:517–525, 1969
31. Abramson M, Gross J: Further studies on a collagenase in middle ear cholesteotoma. Ann Otol Rhinol Laryngol 80:177–188, 1971
32. Itoi M, Gnädinger C, Slansky HH, Freeman MI, Dohlman CH: Collagenase in the cornea. Exp Eye Res 8:369–373, 1969

33. Slansky HH, Gnädinger MC, Itoi M, Dohlman CH: Collagenase in corneal ulcerations. Arch Opthalmol 82:108–111, 1969

34. Brown SI, Weller CA, Wasserman HE: Collagenolytic activity of alkalai-burned corneas. Arch Opthalmol 81:370–373, 1969

35. Perez-Tamayo R: Collagen resorbtion in carageenin granuloma. Lab Invest 22:137–159, 1970

36. Piez KA: Soluble collagen and denaturation components, Treatise on Collagen. Vol 1. Edited by GN Ramachandran. New York, Academic Press, Inc, pp 207–243, 1967

37. Miller EJ: Isolation and characterization of a collagen from chick cartilage containing three identical α chains. Biochemistry 10:1652–1660, 1971

38. Miller EJ, Epstein EH, Piez KA: Identification of three genetically distinct collagens by cyanogen bromide cleavage of insoluble human skin and cartilage collagen. Biochem Biophys Res Commun 42:1024–1029, 1971

39. Pinnell SR, Martin GA: The cross linking of collagen and elastin: enzymatic conversion of lysine in peptide linkage to alpha-aminoadipic delta-semialdehyde (allysine) by an extract from bone. Proc Nat Acad Sci USA 61:708–716, 1968

40. Kühn K, Zimmerman BK: Renaturation of soluble collagen. IV. Regeneration of native collagen molecules from α subunits. Arch Biochem Biophys 109:534–541, 1965

41. Martin GR, Mecca CE, Piez KA: Environmental Variables in Oral Disease. Edited by SJ Kreshover, FJ McLure. Washington, DC, American Association for the Advancement of Science, p 155, 1966

42. Drake MP, Davison PF, Bump S, Schmitt FO: Action of proteolytic enzymes on tropocollagen and insoluble collagen. Biochemistry 5:301–321, 1966

43. Kühn K, Braumer K, Zimmerman B, Pikkarainen J: The formation and structure of insoluble collagen, Chemistry and Biology of the Intercellular Matrix. Vol 1. Edited by EA Balazs. New York, Academic Press, Inc, 1970, pp 251–273

44. Bailey AJ, Peach CM, Fowler LJ: The biosynthesis of intermolecular cross-link in collagen.[43] pp 385–404, 1970

45. Seifter S, Harper E: The collagenases, The Enzymes. Vol 3. Edited by PD Boyer. New York, Academic Press, Inc, 1971, pp 649–698

46. Heidrich HG, Prokopova D, Hanning K: The use of synthetic substrates for the determination of mammalian collagenase. Is collagenolytic activity present in mitochondria. Hoppe-Seylers Z Physiol Chem. 350:1430–1436, 1969

47. Harper E, Gross J: Separation of collagenase and peptidase activities of tadpole tissue in culture. Biochem Biophys Acta 198:286–292, 1970

48. Evanson JM: Mammalian collagenases and their role in connective tissue breakdown, Tissue Proteinases. Edited by AJ Barrett, JT Dingle. Amsterdam, North Holland Publishing, 1971, pp 327–345

49. Gross J, Nagai Y: Specific degradation of the collagen molecule by tadpole collagenase. Proc Nat Acad Sci USA 54:1197–1204, 1965

50. Nagai Y, Lapiere CM, Gross J: Tadpole collagenase: preparation and purification. Biochemistry 5:3123–3130, 1966

51. Kang AH, Nagai Y, Piez KA, Gross J: Studies on the structure of collagen using collagenolytic enzyme from tadpole. Biochemistry 5:509–515, 1966

52. Sakai T, Gross J: Some properties of reaction of tadpole collagenase with collagen. Biochemistry 6:518–528, 1967
53. Harper E, Bloch KJ, Gross J: The zymogen of tadpole collagenase. Biochemistry 10:3035–3041, 1971
54. Lazarus GS, Brown RS, Daniels JR, Fullmer HM: Human granulocyte collagenase. Science 159:1483–1485, 1968
55. Cohn ZA, Hirsch JG: The isolation and properties of the specific cytoplasmic granules of rabbit polymorphonuclear leucocytes. J Exp Med 112:983–1022, 1960
56. Lazarus GS: Studies on the degradation of collagen by collagenases, The Lysosomes. Vol 3. Edited by JT Dingle. Amsterdam, North Holland Publishing Co (In press)
57. Lazarus GS, Daniels JR, Brown RS, Bladen HA, Fullmer HM: Degradation of collagen by a human granulocyte collagenolytic system. J Clin Invest 47:2622–2629, 1968
58. Daniels JR, Lian J, Lazarus GS: Granulocyte collagenase preparation and kinetic studies. Clin Res 17:154, 1969
59. Daniels JR, Lian J, Lazarus GS: Granulocyte collagenase purification and kinetic studies. J Biol Chem (In press)
60. Burleigh PCM, Lazarus GS, Reynolds JE: Physiological role of rabbit skin collagenase in collagen degradation. Unpublished data
61. Eisen AZ, Bloch KJ, Sakai T: Inhibition of human skin collagenase by human serum. J Lab Clin Med 75:258–263, 1970
62. Barrett AJ, Dingle JT: The inhibition of tissue acid proteinases by pepstatin. Biochem J (In press)
63. Dingle JT, Barrett AJ, Poole AR, Stovin P: Inhibition by pepstatin of human cartilage degradation. Biochem J (In press)
64. Barrett AJ: Cathepsin D. Purification of isoenzymes from human and chicken liver. Biochem J 117:601–607, 1970
65. Harris ED, Locke S, Lin TY: Limited degradation of gelatin substrate by Cathepsin D. Connective Tissue Research, Vol 1. (In press)
66. Burleigh PCM, Lazarus GS, Reynolds J, Barrett AJ: The effect of lysosomal proteinases on collagen and gelatin. Unpublished data
67. Janoff A, Scherer J: Mediators of inflammation in leukocyte lysosomes IX. Elastinolytic activity in granules of human polymorphonuclear leukocytes. J Exp Med 128:1137–1151, 1968
68. Janoff A, Blondin J: Further studies on an esterase inhibitor in human leukocyte cytosol. Lab Invest 25:565–571, 1971
69. Davies P, Rita GA, Krakauer K, Weissmann G: Characterization of a neutral protease from lysosomes of rabbit polymorphonuclear leukocytes. Biochem J 123:559–569, 1971

Acknowledgments

We gratefully acknowledge the support of the Medical Research Council for MCB. We also thank C. C. Entwistle, MB, ChB, MRC Pathol, of the East Anglia Regional Transfusion and Immunohematology Center for providing us with human granulocytes. Drs. J. J. Reynolds, J. T. Dingle and A. J. Barrett provided encouragement and much useful discussion.

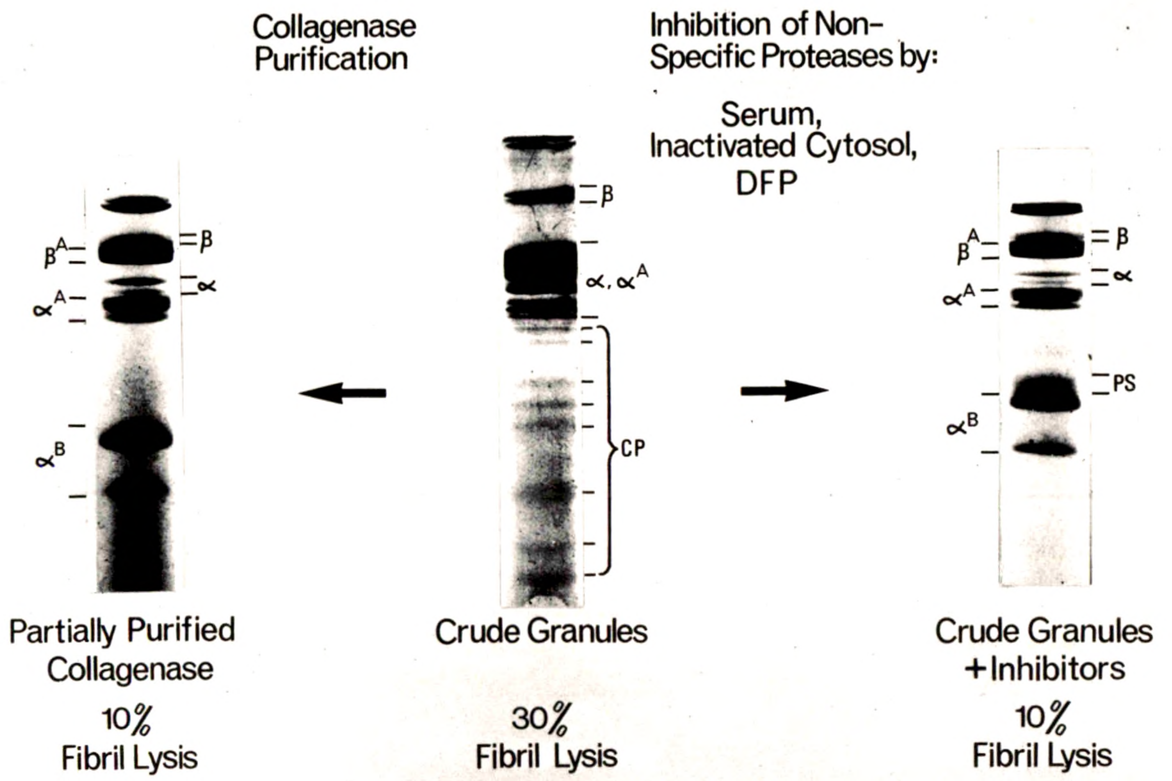
Collagenase Purification
Inhibition of Non-Specific Proteases by:
Serum, Inactivated Cytosol, DFP
β^A
α^A
α^B
β
α
α, α^A
CP
PS
Partially Purified Collagenase
10%
Fibril Lysis
Crude Granules
30%
Fibril Lysis
Crude Granules +Inhibitors
10%
Fibril Lysis

Fig 1—The mechanisms by which human leukocytes degrade collagen as studied by acrylamide gel electrophoresis and reconstituted collagen fibril assays. In the center is crude granulocyte extract, on the left partially purified granulocyte collagenase and on the right crude granule extract with either 7% human serum, 400 μg inactivated post-granule supernatant protein or 1 mM DFP. Percent fibril lysis is after 20 hours incubation at 37 C; the acrylamide gel electrophoresis patterns are after 20 hours at 25 C. α=monomeric chain; β=dimeric chain; *superscript A*=N-terminal three-quarters cleavage product; *superscript B*=C-terminal cleavage product; *PS*=protein smudge seen with serum and cytosol; *CP*=collagen peptides.

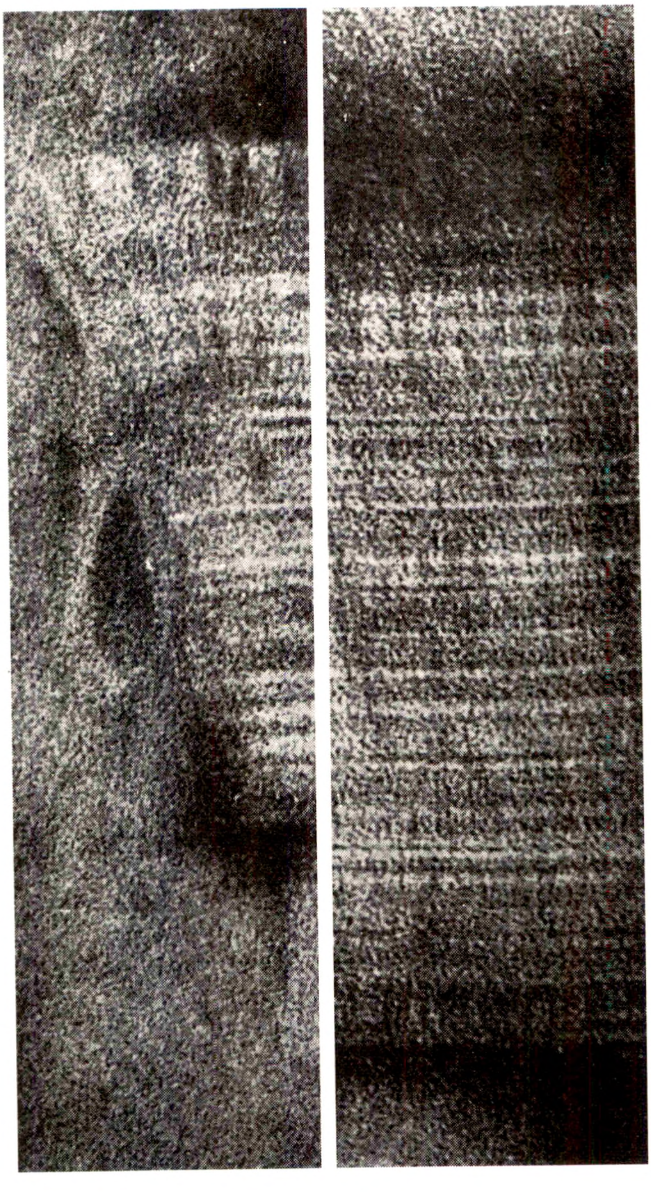

Fig 2—Comparison of SLS aggregates from collagen incubated with partially purified granulocyte collagenase (*left*) and heat-inactivated granulocyte collagenase (*right*). The SLS formed after incubation with active enzyme is missing the carboxy terminal one-quarter of the molecule (From Lazarus *et al*, 1968[57]).

Human Granulocyte Elastase

Further Delineation of its Role in Connective Tissue Damage

Aaron Janoff, PhD

THE PRECEDING PAPER by Dr. Lazarus and his colleagues[1] reviewed work on granulocyte collagenase and the collagen-degrading system of the neutrophil. A second fibrous protein of connective tissue, elastin, can be recognized as another potential target for neutrophil-mediated proteolysis, since it was found, in our laboratory, that human polymorphonuclear leukocytes (PMN) contain an elastase as well as the collagenase described before. The present paper deals with our studies of human granulocyte elastase. Initially, I will review, in summary fashion, some of the chief characteristics of the enzyme and its interaction with inhibitors. I will then present some previously unpublished preliminary findings which may offer an approach to further delineating the role of granulocyte elastase in connective tissue damage.

The first point to make is that the two known human granulocyte enzymatic activities (collagenase and elastase), directed against fibrous connective tissue proteins, can be separated by anion-exchange chromatography of leukocyte extracts, using methods previously described by Dr. Lazarus.[2] As he indicated, human leukocyte extract passed through diethylaminoethyl (DEAE)-cellulose in 0.01 M Tris-HCl buffer at pH 8.6 (4 C) separates cationic proteins, which elute from the resin with the starting buffer, from acidic proteins which, under these conditions, bind to the anion-exchanger. A subfraction of the bound proteins can be subsequently eluted with Tris buffer containing 0.045 to 0.075 M NaCl and 0.002 M $CaCl_2$, and was reported by Lazarus to contain the specific collagen-monomer cleaving enzyme of the starting extract.[2] This same fractionation step was utilized in our early experiments, except that discontinuous, rather than continuous, salt elution was employed. The resultant fractionation revealed hydrolytic activity directed against orcein-dyed and undyed bovine ligament elastin, *tert*-butyloxycarbonyl

---

From the Department of Pathology, State University of New York at Stony Brook, NY.

Supported in part by Grant HE-14262 from the National Institutes of Health.

Address reprint requests to Dr. Aaron Janoff, Department of Pathology, Health Sciences Center, State University of New York at Stony Brook, Stony Brook, NY 11790.

(t-BOC)-L-alanine-p-nitrophenyl ester (a moderately specific synthetic elastase substrate) and denatured hemoglobin in the cationic proteins of the leukocyte extract. None of these activities were detectable in the acidic proteins of the leukocyte extract eluted by increasing the concentration of NaCl. These results were reported earlier.[3,4]

Cationic elastase activity is first localized to PMN (as opposed to lymphocytes and monocytes) and then more specifically to the granule (lysosome-rich) fraction of the cells.[5] Table 1 summarizes the data from which these conclusions are drawn. Recently, other work has shown that human and rabbit alveolar macrophages[6] and human platelets[7] may be additional extrapancreatic sources of elastase-like enzymes in the body.

Enzymatic activity of PMN granules against dyed elastin is maximal at slightly alkaline pH,[5] decreases with increasing acidity but remains appreciable in the pH range associated with inflammatory exudates (gross measurements)—*ie*, at or slightly below neutrality.[8,9]

Human granulocyte elastin-digesting activity is partially suppressed by soybean inhibitor and salivary gland kallikrein-inactivator;[5] these properties readily distinguish it from porcine pancreatic elastase, which is not affected by these agents. Table 2 compares the inhibition profiles of the pig pancreatic enzyme and the human PMN agent and provides additional evidence of the nonidentity of these enzymes. The fact that 0.01 M Na_2EDTA does not inhibit the PMN agent is especially significant, since this further distinguishes granulocyte elastase from granulocyte collagenase and from porcine

Table 1—Demonstration of Elastase Activity in Human PMN

Enzyme source	Concentration protein tested (μg/ml)	Percent elastolysis
Trypsin	25	0
α-Chymotrypsin	25	0
Elastase	25	100
Human leukocyte homogenate		
Granules	500	100
Nuclei	500	15
Microsomes and cell sap	500	6
Human leukocyte homogenate previously depleted of PMN by nylon-wool extraction		
Granules	500	7

100% arbitrarily selected as the amount of dye released from orcein-impregnated elastin by 25 μg of pancreatopeptidase E (3.4.4.7) under standard incubation conditions. (Further details of methods are given in the primary references cited in the text.)

Table 2—Effects of Inhibitors on PMN and Pancreatic Elastases

		Percent inhibition of elastolysis* or esterolysis† by	
Agent	Concentration	PMN granules	Pancreatopeptidase E (EC 3.4.4.7)
NaCl (M)	0.15	0	70
Na_2EDTA (M)	0.01	0	54
SBTI (μg/ml)	500	50	0
Trasylol (u/ml)	2000	50	0
DPBB (M)†	0.00025	0	50
Human serum (%)	0.5	0	55
Human serum (%)	2	10	100
Human serum (%)	5	25	100
Human serum (%)	10	57	—

* Substrate was orcein-dyed ligament elastin (all agents except DPBB).

† Substrate was t-BOC-L-alanine-**p**-nitrophenol.

Amounts of each enzyme were selected to give approximately equivalent elastolysis or esterolysis in the absence of inhibitor. (Further details of methods are given in the primary references cited in the accompanying text.) SBTI = soybean trypsin inhibitor; trasylol = salivary gland kallikrein inactivator; DPBB = 1-bromo-4-(2, 4-dinitrophenyl)-butan-2-one.

elastase. Until quite recently, difficulties in purifying human pancreatic elastase-like enzymes made it impossible to carefully compare factors responsible for the elastolytic activities of PMN and pancreas in the same species. However, some of the properties of a human pancreatic elastase-like esterase have now been described,[10] and, while many of its characteristics are shared by the PMN agent, the two enzymes differ radically in their isoelectric points. As will be demonstrated shortly, the isoelectric pH of human granulocyte elastase-like esterase, like that of porcine pancreatic elastase, is highly alkaline, whereas human pancreatic elastase-like esterase is reported to have a much lower isoelectric point.[10] Thus, the elastase-like esterase activity of human PMN is not likely to result from contamination of leukocyte preparations with a circulating elastase-like esterase derived from human pancreas.

Table 2 also shows that human granulocyte elastase is inhibited by serum, although higher concentrations of the latter are needed than are required for comparable inhibition of porcine pancreatic elastase. We [11] and Ohlsson [12] have recently demonstrated that the serum or plasma inhibition of human granulocyte elastase is largely due to the α1-antitrypsin component. The data from my laboratory suggest that, at their relative molar concentrations in serum, α1-antitrypsin is an important inhibitor of granulocyte elastase, whereas

α2-macroglobulin (plasmin inhibitor) appears to be less important (Table 3). In interpreting the data in Table 3 based on the inhibition of esterolysis by the two plasma inhibitors, it is worth noting that complexes of α2-macroglobulin with *pancreatic* elastase have recently been reported to retain esterase activity against low molecular weight substrates.[13] The demonstration of an interaction between granulocyte elastase and α1-antitrypsin [11,12] supports the speculation that this protease, as well as other neutral leukocyte proteases which form complexes with this inhibitor,[12] plays a role in connective

Table 3—Inhibition of Human Polymorphonuclear Leukocyte Elastase by Serum and Serum Fractions

Elastolytic Activity of Polymorphonuclear Leukocyte Granules*

Serum type	TIC (mg/ml)	Concentration (%)	Elastolysis inhibition (%)
PiMM	1.47	3	50
		10	100
PiMM	1.25	5	50
		7.5	75, 100
PiZZ	0.15	3	0
		10	38
PiZZ	0.19	5	0
		7.5	0
PiZZ	0.26	7.5	24

Esterolytic Activity of Polymorphonuclear Granules†

Serum fraction	Concentration (mg/100 ml)	Esterolysis inhibition (%)
α1-Antitrypsin	38	88
α1-Antitrypsin	25	84
α1-Antitrypsin	13	30
α2-Macroglobulin	23	28
α2-Macroglobulin	15	12
α2-Macroglobulin	8	0

* Elastin-orcein substrate; 2-hour incubation, pH 8.7, 37 C, 240 μg/ml granule protein per assay. TIC = trypsin inhibiting capacity.

† **t**-BOC-L-alanine-**p**-nitrophenol substrate; 5-minute incubation, pH 6.5, 25 C, 12 μg granule protein/ml per assay.

PiZZ sera were kindly supplied by Dr. Morton Galdston, New York University School of Medicine, New York, NY. Purified human α1-antitrypsin (Behringwerke AG) was supplied by Dr. Fritz Beller, New York University School of Medicine, NY. Purified human α2-macroglobulin was supplied by Dr. Frederick Miller, Health Sciences Center, State University of New York at Stony Brook, NY.

Reprinted from Janoff A.[11]

tissue degenerations (*eg*, of elastic fibers) associated with genetic states leading to deficiencies in serum α1-antitrypsin. One such possibility, currently under investigation, is familial emphysema, in which inherited abnormalities in α1-antitrypsin occur with unusually high frequency. Preliminary evidence favors the view that granulocyte elastase levels may be a second determinant in the clinical course of this disease.[14]

An interesting feature of our inhibition studies with granulocyte elastase (although perhaps of less clinical relevance than those involving α1-antitrypsin) concerns the finding of an inhibitor of the enzyme in the cytosol fraction (microsome-free supernatant) of the same cells.[15,16] Inhibition is relatively specific, in that esterolytic activity of trypsin and pancreatic elastase is unaffected under identical conditions. This specificity suggests that the intracellular inhibitor is distinct from α1-antitrypsin of human serum. Ion-exchange chromatography on carboxymethyl cellulose at pH 6.0 reveals that the inhibitor is an acidic component of cytosol. RNA can be ruled out, since the incubation of yeast RNA (which also inhibits granulocyte elastase in high concentrations) with pancreatic ribonuclease and spleen phosphodiesterase results in nearly complete degradation of the RNA with a concomitant loss of inhibiting capacity; identical enzymatic treatment of cytosol followed by prolonged dialysis does not lead to loss of its inhibiting capacity. On the other hand, Pronase destroys most of the inhibitory activity, as does 0.4 M trichloroacetic acid. However, inhibitory activity is not diminished by heating to 80 C for 20 minutes. Some of these data are reviewed in Table 4. Molecular sieving through Sephadex and Agarose gels and Diaflo membranes suggests inhibitory activity is associated with high molecular weight components of cytosol. It is tempting to speculate that intracellular inhibitors, of the type affecting granulocyte elastase, function to protect the cell against leakage of lysosomal proteases active at neutral pH. Leakage may occur from secondary lysosomes (*eg*, phagolysosomes) and could be accelerated in leukocytes engaged in phagocytosis. On the other hand, for several reasons,[16] it seems unlikely that the intracellular inhibitor would constitute an effective extracellular antagonist of damage to connective tissue elastin by human leukocyte elastase. Instead, as indicated earlier, serum inhibitors may play the more significant protective role in the extracellular environment. Recently, a several-times more potent inhibitor of the neutrophil elastase, with physicochemical properties

Table 4—Effects of Various Treatments Upon Inhibitor Activity of Leukocyte Cytosol[*]

Material treated[†] (mg)	Treatment (concentration of agent)	Incubation time and temperature[‡]	Loss of inhibition (%)	Loss of starting material[§] (%)
Cytosol concentrate (0.85)	Pronase (10μg/ml)	3 hr 37 C	64	86
Cytosol concentrate (0.85)	Pronase (10μg/ml)	3 hr 37 C	58	83
Cytosol concentrate (0.85)	RNase (50μg/ml) and phosphodiesterase (0.34 U/ml)	3 hr 37 C	0	NT
Yeast RNA (1.0)	RNase (50μg/ml) and phosphodiesterase (0.34 U/ml)	3 hr 37 C	100	85
Cytosol concentrate (0.32)	Heat	20 min 80 C	0	NT
Cytosol concentrate (0.85)	TCA (0.4M)	1 hr 20 C	100	96

[*] Inhibition of **t**-BOC-L-alanine-**p**-nitrophenol esterolysis by leukocyte granules.

[†] Represents protein in the case of cytosol concentrate.

[‡] Except after heating, all treatments were followed by 48 hours of dialysis versus three changes of 0.01 M sodium phosphate-buffered saline (pH 7) at 20 C. In the case of trichloroacetic acid (TCA) treatment, the precipitate was first discarded and the supernatant was dialyzed.

[§] Loss of cytosol protein or yeast RNA to TCA precipitate or to dialysate after enzyme treatment.

NT = not tested.

Reprinted from Janoff A, Blondin J.[16]

essentially similar to those described above, was demonstrated in cytosol fractions from human alveolar macrophages.[17][*]

I now wish to shift the discussion to more recent observations which, although preliminary in nature, deal with a question of greater interest for this symposium—*ie*, delineating the role of human granulocyte elastase in connective tissue damage. If the cationic proteins of the leukocyte granule extract, separated by DEAE-chromatography as described earlier, are rechromatographed in phosphate-buffered saline (pH 7) on a 1.5 × 90 cm column of Sephadex G50, the proteins will be separated further into three fractions.[3] Hydrolytic activities at neutral pH against dyed-elastin (fivefold enrichment), denatured hemoglobin and *t*-BOC-L-alanine-*p*-nitrophenol are all restricted to the second (first retarded) peak. When this material is reconcentrated and again analyzed by isoelectric-focusing in polyacrylamide gel,[18] it becomes apparent that the activity against *t*-BOC-L-alanine-*p*-nitrophenol focuses at an alkaline isoelectric point (9.5), approximately that exhibited by porcine (but not human) pancreatic elastase. At the same time, it is also evident that at least three other protein species are present in the Sephadex fraction (see Text-figure 1, panel A). This degree of heterogeneity renders it impossible to ascribe specific forms of connective tissue damage, by the fraction enriched in elastase, to any single enzyme, except that granulocyte collagenase can probably be considered to have been eliminated by the earlier anion-exchange step. The elastase-enriched Sephadex fraction vigorously degrades human renal basement membrane[3] and cartilage matrix proteoglycan[19] (as does pancreatic elastase, in the latter case), but these actions cannot be unequivocally ascribed to the contained elastase. In addition, whole granule extracts attack arterial walls[3,5] and human lung elastin;[20] such activities would appear to be logical reflections of the presence of elastase, but proof that this assumption is valid is still lacking. Moreover, Ohlsson[12] demonstrated that α1-antitrypsin forms two distinctly separate complexes with components

---

[*] Folds JD, Welsh IRH, Spitznagel JK: Personal communication (and recent confirmatory data from our laboratory) suggest that the subcellular localization of the elastase inhibitor, which we found in PMN cytosol fractions, may in reality be the nucleus. This possibility is strengthened by virtue of the fact that many of the latter structures appear to be broken during homogenization of PMN by our technics.

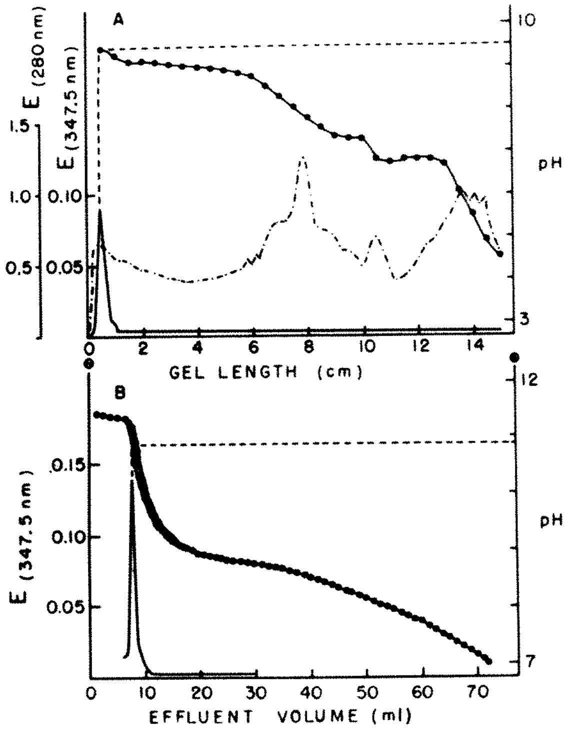

TEXT-FIG 1—Isoelectric focusing of leukocyte granule protein (Sephadex fraction) in acrylamide gel (*A*) and sucrose (*B*). Alanine *p*-nitrophenyl esterase activity measured as absorbance of free *p*-nitrophenol at 347.5 nm (——); protein measured as absorbance at 280 nm (- ● -); pH values in the gel or effluent fractions (●); cathode (−); anode (+). (Reprinted from Janoff A, Basch RS).[18]

of human PMN granules, one of which corresponds to a complex with elastase and the other to a complex with a second and different neutral protease. Ohlsson's elastase behaves as a strongly basic protein, while his second granulocyte neutral protease behaves as an acidic protein at pH 8.6 (and may be eliminated along with granulocyte collagenase in the DEAE-chromatography step we routinely employ). Other recent work[21] argues that neutral proteolytic activity against denatured hemoglobin and elastin and esterolytic activity against *t*-BOC-L-alanine-*p*-nitrophenol are present in a single class of human PMN granules and cannot be separated by several physicochemical technics. Distinctions can be made, however, on the basis that neutral proteolytic activity against denatured hemoglobin requires cysteine-activation, while activities against elastin and *t*-BOC-L-alanine-*p*-nitrophenol do not.[21]

In order to approach the question of the precise role of granulocyte elastase in tissue injury mediated by PMN lysosomes, we recently adopted the use of specific elastase inhibitors. These compounds are chloromethyl ketone derivatives of a highly specific synthetic elastase substrate, N-acetyl-L-alanyl-L-alanyl-L-alanine-methyl ester, first described for pancreatic elastase by Gertler and Hofmann[22] and then for human PMN granules in our laboratory.[18] Rates at which this substrate is hydrolyzed by PMN granules and pancreatic elastase are compared in Table 5. The chloromethyl ketone derivatives of polyalanine esters were synthesized by Drs. James C. Powers and

Table 5—Hydrolysis of N-Acetyl-L-alanyl-L-alanyl-L-alanine Methyl Ester by PMN Granules and Pancreatic Elastase

Enzyme	Amount tested (μg protein)	Hydrogen ion liberated* (μmoles/min)
Pancreatopeptidase E	2.5	0.28
	5.0	0.55
	7.5	0.81
	10.0	1.14
PMN granules	16.0	0.08
	32.0	0.21
	50.0	0.46
	75.0	0.81
	100.0	1.12

* Assay conditions: pH 8.0, 25 C, substrate concentration = 0.004 M, reaction volume = 3.0 ml. (Further details of methods and materials are provided in the primary references cited in the text)

Data recalculated from Janoff A, Basch RS.[18]

Table 6—Inhibition of Hydrolysis of Synthetic Ester Substrates by N-Acetyl-L-Alanyl-L-Alanyl-L-Alanine Chloromethyl Ketone*

Enzyme	Inhibitor concentration† (M)	Substrate	Percent inhibition
Trypsin	1.6×10^{-3}	BAPNA	0
Chymotrypsin	1.6×10^{-3}	GPAPNA	7
Pancreatic elastase	1.6×10^{-3}	**t**-BOC	100
Neutrophil granule extract	1.6×10^{-3}	**t**-BOC	85

* Inhibitor-enzyme mixtures were preincubated 2 hours at 25C in 0.01 M sodium-phosphate-buffered saline, pH 6.5 and then compared with control enzymes which were incubated alone

† In preincubation mixture

BAPNA = benzoyl-arginine-**p**-nitroanalide, GPAPNA = glutaryl-phenylalanine-**p**-nitroanalide, **t**-BOC = **t**-BOC-L-alanine-**p**-nitrophenol

Peter Tuhy of the Georgia Institute of Technology, and through their kindness the following experiments were made possible.

The inhibitor selected for our initial tests was N-acetyl-L-alanyl-L-alanyl-L-alanine-O-CH_2Cl. It inhibits slowly, but irreversibly, by binding to elastase and must be preincubated with preparations containing the latter for several hours at room temperature. Table 6 shows the inhibition of three pancreatic serine esteroproteases and of PMN granules after preincubation with this agent. Inhibition was measured using synthetic ester substrates; it is clear that the chloromethyl ketone derivative is highly effective against pancreatic elastase and the elastase-like esterolytic activity of PMN granules while remaining essentially ineffective against trypsin and α-chymotrypsin, the two homologous pancreatic serine esteroproteases.

Table 7 shows the results of a similar inhibition study with the peptide chloromethyl ketone, except that inhibition was assayed using a protein substrate (casein). Two significant features of the

Table 7—Inhibition of Proteolysis by N-Acetyl-L-Alanyl-L-Alanyl-L-Alanine-Chloromethyl Ketone*

Enzyme	Inhibitor concentration† (M)	Substrate	Percent inhibition
Trypsin	0.6×10^{-3}	Casein	0
Chymotrypsin	0.6×10^{-3}	Casein	6
Pancreatic elastase	0.6×10^{-3}	Casein	88
Neutrophil granule extract	0.6×10^{-3}	Casein	45

* Inhibitor-enzyme mixtures were preincubated as described in Table 6

† In preincubation mixture

results bear attention. First, as had occurred previously with synthetic substrates, trypsin and chymotrypsin essentially remained uninhibited by the agent at the concentrations employed, while pancreatic elastase and PMN granules were affected. Second, despite the marked inhibition of alanine-*p*-nitrophenyl esterase activity of PMN granules by the peptide chloromethyl ketone, as shown in Table 6, the degree to which caseinolysis was inhibited by PMN granules was less pronounced. On the other hand, as expected, caseinolysis by pancreatic elastase was almost completely inhibited. This observation suggests that several neutral proteases capable of digesting casein are present in human PMN granules and that only one of these (that accounting for approximately half the total caseinolytic activity of the granules) is the elastase or, at least, is susceptible to inhibition by the chloromethyl ketone derivative of a specific elastase substrate. An interpretation such as this is consonant with Ohlsson's finding[12] of two neutral proteases in human PMN granules, each of which attack casein but only one of which attacks elastin.

Table 8 summarizes our experience, to date, with several different connective tissue components, representing potential targets of neutrophil granule proteases in tissue damage. These observations constitute a preliminary effort to delineate the action of granulocyte elastase in tissue injury, using the peptide chloromethyl ketone inhibitor. As shown in this table, the attack by PMN granules upon cartilage matrix proteinpolysaccharides and renal basement membrane was not significantly affected by preincubating the granule extracts with the elastase inhibitor. In the same experiment, aliquots of granule extract, which had been preincubated with the chloromethyl ketone, were tested separately and shown to have essentially no alanine-*p*-nitrophenyl esterase activity. As expected, mixtures of trypsin and inhibitor retained full tryptic activity against synthetic substrate and against basement membrane. The activity of pancreatic elastase on the alanine-*p*-nitrophenyl ester and basement membrane was abolished by preincubation with the inhibitor. Thus, at the very least, these results suggest that another neutral protease and/or other lysosomal enzyme(s) of the neutrophil granule, distinct from the granulocyte elastase, play the dominant role in degrading basement membrane and cartilage matrix proteinpolysaccharide. However, elastases are capable of attacking such substrates, and the granulocyte elastase may normally participate in a supplementary fashion during a neutrophil-mediated attack upon them.

Table 8—Inhibition of Digestion of Connective Tissue Components by N-Acetyl-L-Alanyl-L-Alanyl-L-Alanine-CMK*

Enzyme	Amount (μg)	Inhibitor concentration† (M)	Substrate	Indices measured	Inhibition
Human PMN granule protein	200	1.2×10^{-3}	Rabbit articular cartilage	Loss of metrachromasia	None or slight
Trypsin	25	7.3×10^{-3}	Human renal basement membrane‡	Release of HO-proline and sialic acid-containing fragments; starch gel electropherograms of digestion supernatants	None
Pancreatic elastase	25	1.2×10^{-3}			Complete
Human PMN granule protein	400	7.3×10^{-3}			None
Pancreatic elastase	6	1.2×10^{-3}	Rat aorta (0.04 mm thick rings)	Loss of elastica staining	Complete
Human PMN granule protein	125	1.2×10^{-3}			Complete
Pancreatic elastase	25	1.6×10^{-3}	Human lung elastin-enriched fraction§	Solubilization of protein	Complete
Human PMN granule protein	500	5.0×10^{-3}			Complete

* Inhibitor-enzyme mixtures were preincubated as described in Table 6

† In preincubation mixture

‡ Kindly supplied by Dr. Charles G. Cochrane

§ Preparation described in Janoff A, Sandhaus RA, Hospelhorn VD, Rosenberg R.[30]

When elastin-rich connective tissues were studied, a completely different pattern was observed (Table 8). PMN granules were completely prevented from digesting arterial wall and a connective tissue fraction from lung by pretreating the granules with the peptide chloromethyl ketone elastase-inhibitor, suggesting that granulocyte elastase probably plays a dominant role in neutrophil-mediated attack upon these connective tissue elements.

A tentative working hypothesis could hold that granulocyte elastase is a critical mediator in those inflammatory diseases or other neutrophil-exacerbated degenerative processes which affect elastic fibers. Suggested relationships between neutrophil proteases and connective tissue targets are schematically summarized in Text-figure 2. This schema will obviously be subject to considerable modification as work proceeds in this area. Additional studies are clearly called for to properly delineate the roles of granulocyte elastase and other neutrophil enzymes in mediating tissue damage,

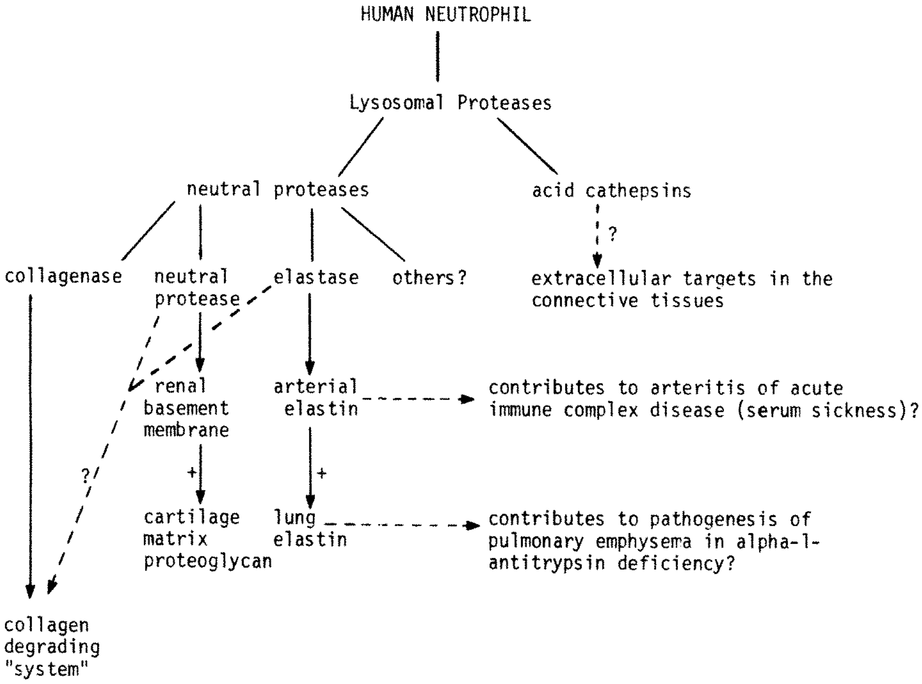
HUMAN NEUTROPHIL
Lysosomal Proteases
neutral proteases
acid cathepsins
?
collagenase
neutral protease
elastase
others?
extracellular targets in the connective tissues
renal basement membrane
arterial elastin
contributes to arteritis of acute immune complex disease (serum sickness)?
?
+
+
cartilage matrix proteoglycan
lung elastin
contributes to pathogenesis of pulmonary emphysema in alpha-1-antitrypsin deficiency?
collagen degrading "system"

TEXT-FIG 2—Possible interactions between human neutrophil proteases and selected connective tissue targets.

but until highly purified enzymes are available from human neutrophils, studies with specific inhibitors may provide one useful approach to the problem.

References

1. Lazarus GS, Daniels JR, Lian J: Granulocyte collagenase: Mechanism of collagen degradation. Am J Pathol 68:565–578, 1972
2. Lazarus GS, Daniels JR, Brown RS, Bladen HA, Fullmer HM: Degradation of collagen by a human granulocyte collagenolytic system. J Clin Invest 47:2622–2629, 1968
3. Janoff A: Mediators of tissue damage in leukocyte lysosomes. X. Further studies on human granulocyte elastase. Lab Invest 22:228–236, 1970
4. *Idem:* Alanine *p*-nitrophenyl esterase activity of human leucocyte granules. Biochem J 114:157–159, 1969
5. Janoff A, Scherer J: Mediators of inflammation in leukocyte lysosomes. IX. Elastinolytic activity in granules of human polymorphonuclear leukocytes. J Exp Med 128:1137–1155, 1968
6. Janoff A, Rosenberg R, Galdston M: Elastase-like, esteroprotease activity in human and rabbit alveolar macrophage granules. Proc Soc Exp Biol Med 136:1054–1058, 1971

7. Robert B, Legrand Y, Pignaud G, Caen J, Robert L: Activite elastinolytique associee aux plaquettes sanguines. Pathol Biol 17:615–622, 1969
8. Opie EL: Experimental pleurisy: resolution of a fibrinous exudate. J Exp Med 9:391–413, 1907
9. Menkin V: Studies on inflammation; cytological picture of inflammatory exudate in relation to its hydrogen ion concentration. Am J Pathol 10:193–210, 1934
10. Mallory P, Travis J: Properties of human pancreatic elastase. Fed Proc 31:883, 1972
11. Janoff A: Inhibition of human granulocyte elastase by serum alpha-l-antitrypsin. Am Rev Resp Dis 105:121–122, 1972
12. Ohlsson K: Neutral leucocyte proteases and elastase inhibited by plasma alpha-l-antitrypsin. Scand J Clin Lab Invest 28:251–253, 1971
13. Steinbuch M: Les antiproteases du plasma. Rev Franc Transf 14:61–76, 1971
14. Galdston M, Gottwalt C, Davis AL, Janoff A: Leucocyte lysosomal enzymes and alpha-l-antitrypsin: genetic determinants in chronic obstructive pulmonary disease. Fed Proc 31:282, 1972
15. Janoff A, Blondin J: Inhibition of the elastase-like esterase in human leukocyte granules by human leukocyte cell sap. Proc Soc Exp Biol Med 136:1050–1053, 1971
16. Janoff A, Blondin J: Further studies on an esterase inhibitor in human leukocyte cytosol. Lab Invest 25:565–571, 1971
17. Blondin J, Rosenberg R, Janoff A: An inhibitor in human lung macrophages active against human neutrophil elastase. Am Rev Resp Dis (In press)
18. Janoff A, Basch RS: Further studies on elastase-like esterase in human leukocyte granules. Proc Soc Exp Biol Med 136:1045–1049, 1971
19. Janoff A, Blondin J: Depletion of cartilage matrix by a neutral protease fraction of human leukocyte lysosomes. Proc Soc Exp Biol Med 135:302–306, 1970
20. Janoff A, Sandhaus RA, Hospelhorn VD, Rosenberg R: Digestion of lung proteins by human leukocyte granules *in vitro*. Proc Soc Exp Biol Med 140: 516–519, 1972
21. Folds JD, Welsh IRH, Spitznagel JK: Localization of proteases in a single granule fraction of human polymorphonuclear leukocytes. Fed Proc 31:282, 1972
22. Gertler A, Hofmann T: Acetyl-L-alanyl-L-alanyl-L-alanine methyl ester: a new highly specific elastase substrate. Canad J Biochem 48:384–386, 1970

Pathologic Mechanisms in Neutrophil-Mediated Injury

Peter M. Henson, PhD

TISSUE INJURY in acute inflammatory reactions is characteristically mediated by neutrophils. The pathogenetic mechanisms involved have been studied in some detail in immunologic models. Neutrophils accumulate at sites of antigen-antibody interaction, react with the complexes and release their injurious constituents; which then act on a variety of substrates to produce damage. In this discussion of the mediation processes, three areas will be considered: a) the substrates *in vitro* or *in vivo* upon which neutrophils act, directly or indirectly, to produce injury; b) the mechanisms by which neutrophils release injurious constituents; and c) the involvement of these and other neutrophil activities *in vivo*. These final studies employ models in which isolated neutrophils are infused intravenously into neutrophil-depleted animals, in order to reconstitute neutrophil-dependent immunologic reactions. The functions of neutrophils may then be altered *in vitro* and the effects followed *in vivo* after infusion.

Substrates

A host of potentially injurious constituents are contained within neutrophils, largely confined to the granules. A number of these have been considered by the other participants in this symposium. Under normal circumstances these materials are involved in the intracellular digestive functions of the neutrophil. However, if they escape from the cell, they may act on a variety of substrates in the body to produce tissue injury. A list of such substrates and effects is presented in Table 1 and is divided into two categories. Neutrophils may produce injury by enzymatically digesting tissue components, by generating cellular or humoral mediators or, perhaps, by acting directly on cellular or extracellular targets.

Digestion of Vascular Supporting and Connective Tissue Elements in the Arthus Reaction

Neutrophil enzymes have been shown to digest connective tissue elements, such as elastic tissue, collagen and basement membrane,

---

From the Department of Experimental Pathology, Scripps Clinic and Research Foundation, La Jolla, Calif.

Supported by Grant A1-07007 from the US Public Health Service and Grant in Aid 69 769 from the American Heart Association.

Address reprint requests to Dr. Peter M. Henson, Department of Experimental Pathology, Scripps Clinic and Research Foundation, 476 Prospect St, La Jolla, Calif 92037.

Table 1—Some Substrates Acted Upon by Neutrophils to Produce Tissue Injury

- Digestion
  - Elastic tissue
  - Collagen
  - Basement membranes
  - Cartilage
- Effect of Neutrophilic Mediators
  - Activation of mast cells to release vasoactive amines
  - Activation of platelets to release vasoactive amines
  - Cleavage of C5 to yield C5a
  - Initiation of clot formation
  - Generation of SRS-A
  - Generation of kinins
  - Increase of vascular permeability by means independent of histamine
  - Increase body temperature (endogenous pyrogen)

by releasing the proteases they contain.[1] This effect has been observed both in *vitro* and *in vivo*.[2-8] Two examples of these effects may be given. In Figure 1, two stages of an Arthus reaction are depicted. Release of enzymes from neutrophils phagocytosing the immune complexes leads to complete disruption of the vessel wall. Digestion of basement membrane ensues (Figure 1B). A similar situation results from the deposition of immune complexes in arteries in immune complex disease, wherein the internal elastic lamina is digested and disrupted.[9]

Digestion of Basement Membrane in Nephrotoxic Nephritis

In nephrotoxic nephritis, heterologous antiglomerular basement membrane antibody is injected into, for example, rabbits. Antibody and complement bind along the basement membrane, neutrophils accumulate and adhere to the immune reactants, apparently push aside the endothelial cell and come to lie in close apposition to the basement membrane (Figure 2A). Digestion of the basement membrane occurs and fragments can be detected antigenically in the urine,[8] along with neutrophil-derived catheptic enzymes.[5] That neutrophil cathepsins can indeed digest glomerular basement membrane *in vitro* is shown in Figure 3. Digestive enzymes are, therefore, released from the adherent neutrophils, even though the immune reactants are spread out upon the basement membrane surface and there is no phagocytosis. Nonselective proteinuria and severe necrotizing glomerulonephritis result. A similar accumulation of neutrophils occurs in human diseases such as poststreptococcal glomerulonephritis (Figure 2B).

Generation of Mediators and Direct Effects

Neutrophils, or their constituents, can induce the release of vasoactive amines from mast cells [10,11] and platelets [12] directly, or from mast cells indirectly by the generation of C5a (anaphylatoxin) from C5.[13] Other components of complement may also be cleaved by neutrophil proteases.[14] Clot-promoting activity has been reported,[15] and neutrophil-mediated inflammatory reactions are often accompanied by fibrin formation. This is true in both the Arthus reaction (Figure 1B) and in nephrotoxic nephritis. Release of slow reacting substance of anaphylaxis (SRS-A) in the rat peritoneum has been reported to require the presence of neutrophils,[16] and neutrophil enzymes are stated to possess kinin-generating properties.[17,18]

Rabbit neutrophil granules contain at least four cationic proteins which induce increased vascular permeability.[11] One of these acts by stimulating the release of histamine from mast cells. The other three act, by unknown mechanisms, to increase vascular permeability. Neutrophils also contain pyrogen, which is released during phagocytosis.[19] These few examples are by no means exhaustive, but they serve to illustrate some of the ways in which the constituents of neutrophils may mediate injury in inflammatory reactions.

Mechanisms of Release of Neutrophil Constituents

Since the substances contained within neutrophils play an essential role in the development of tissue injury, the mechanisms by which the constituents are released have recently received a great deal of experimental consideration. Although some lysis of the cells may be seen in many inflammatory reactions, this appears to be a secondary event and there is now ample evidence for the involvement of active secretory processes in liberating constituents of neutrophils to the exterior.[20]

Phagocytosis of particles by neutrophils results in the extrusion of neutrophilic granules into the phagocytic vacuoles.[21] Evidence has now accumulated which indicates that granule enzymes are also released to the outside of the cell.[22-26] In addition, if the neutrophils react with immune complexes, spread over a surface that is too large to be engulfed, the granule enzymes are discharged directly to the outside—*ie,* by exocytosis.[21,25-27] This process is probably of pathologic importance where immune reactants are oriented along surfaces in the body, as in nephrotoxic nephritis or poststreptococcal glomerulonephritis, and perhaps in other sites in the connective tissues, synovial surfaces, etc. For this reason, and because it provides a means of examining the degranulation process, the mechanism has been studied in our laboratory.

Materials and Methods

The preparation of pure populations of rabbit and human neutrophils has been described previously.[22] Nonphagocytosable surfaces consisted of micropore filters, or plastic petri dishes coated with aggregated γ-globulin or immune complexes.[22,28] Rabbit or human γ-globulin was aggregated[29] at a concentration of 2.5 mg/ml with 12 μg/ml bisdiazotized benzidine to yield soluble aggregates. The surfaces were soaked in these solutions and rinsed before use; approximately 30 μg of protein remained attached to the petri dishes. Controls consisted of surfaces coated with bovine serum albumin (BSA). Neutrophils were allowed to settle onto the petri dishes or were gently drawn onto the filters in Tris-buffered Tyrodes' solution with 0.25% BSA or egg albumin.[23,28] They were then incubated at 37C (30 minutes for human, 60 minutes for rabbit) and the supernatant assayed for release of the granule enzymes, (β-glucuronidase myeloperoxidase and lysozyme) or a cytoplasmic enzyme, (lactic dehydrogenase [LDH]) indicative of cell lysis. Experiments were performed in duplicate. Total enzyme content was assayed after lysis with Triton x100.[22]

Inhibitors used included: diiosopropylfluorophosphate (Boots Pure Drug Co, Nottingham, UK) dissolved in isopropyl alcohol; Prostaglandin E_1 (Kindly provided by Dr. J. Pike, Upjohn Co, Kalamazoo, Mich) in ethanol and Cytochalasin B (I.C.I. Research Laboratory, Cheshire, England) in dimethyl sulfoxide. Vincristine (Eli Lilly & Co, Indianapolis, Ind), colchicine (Sigma, St. Louis, Mo), theophylline (Sigma, St. Louis, Mo) and isoproterenol (Sigma, St. Louis, Mo) were dissolved in saline. Inhibitors (except where indicated) were incubated with neutrophils for 60 minutes at 37 C before the reaction with the surfaces, as well as being included in the reaction medium. They were shown not to interfere with enzyme assays, and the solvents were found to have no effect by themselves at the concentration used. Colchicine and vincristine experiments (and controls) were performed in Puck's saline G with added albumin, rather than in Tris-buffered medium, since Tris interferes with the action of colchicine. Inhibition of release of enzymes was calculated in percent. Electron microscopy was performed as described previously.[23] Release of enzymes from rabbit neutrophils during phagocytosis of zymosan particles coated with antibody was performed as described previously.[22]

Results

Exocytosis of Granules from Neutrophils on Nonphagocytosable Surfaces

Liberation of granule constituents from human neutrophils is shown in Text-figure 1. The cytoplasmic enzyme, LDH, was not released, indicating an absence of cell lysis. This was confirmed morphologically; Figure 4 depicts the mechanism of release—*ie,* by extrusion of granules along the membrane of the cell adhering to the immune reactants.[23] As described previously,[23] alkaline phosphatase was released but did not diffuse into the medium. It remained attached to the membrane of the cell and could be demonstrated there histochemically (Figure 4A). Among constituents released

TEXT-FIG 1—Release of lysosomal enzymes from human neutrophils adhering to aggregated IgG on nonphagocytosable surfaces. The percent release ±SE from 4 × 10^6 neutrophils reacting with aggregated IgG or BSA on petri dishes during 30 minutes incubation at 37 C is indicated.

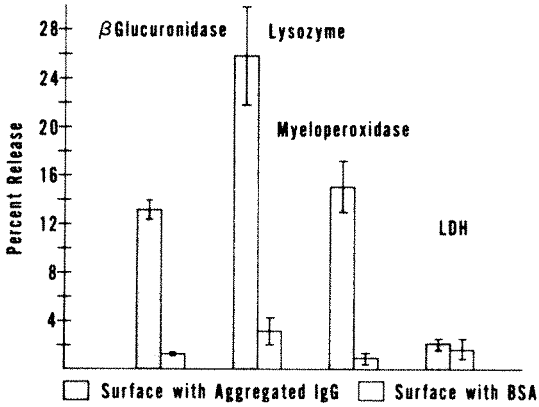

from rabbit neutrophils were acid cathepsins and cationic proteins, which, as described above, can be injurious. Neutral proteases could be detected in the medium after the reaction of human cells.

Studies on the Mechanism of Release of Granules from Neutrophils

Text-figures 2, 3 and 4 depict the effect of a variety of agents upon the release of β-glucuronidase (as a representative granule enzyme) from neutrophils. In each case, the amount of LDH released was determined and was found to be negligible. The liberation of granule enzymes was inhibited by removing calcium with Mg EGTA. However, it was found necessary to preincubate the chelating agent with human neutrophils, whereas simple addition of Mg EGTA sufficed to inhibit the release of β-glucuronidase from rabbit cells. Diisopropylfluorophosphate (DFP) was also inhibitory, indicating a possible role for serine esterases. Neutrophilic energy metabolism was required for release; iodoacetate was inhibitory

TEXT-FIG 2—Inhibition of release of β-glucuronidase from human neutrophils reacting with aggregated IgG on nonphagocytosable surfaces. The concentration of the inhibitors are indicated in M/l. EGTA and iodoacetate were incubated with the neutrophils for 1 hour before the reaction. Release of LDH was in every case assayed to check for cell lysis. Each point is the mean percent inhibition ±SE.

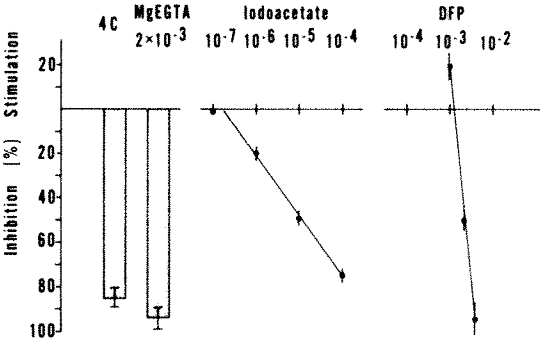

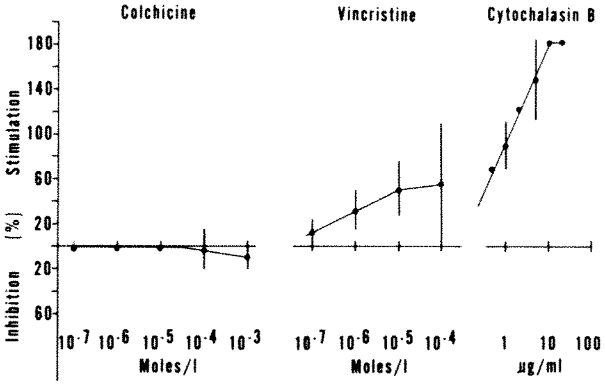

Text-fig 3—The effect of colchicine, vincristine and cytochalasin B on release of β-glucuronidase from human neutrophils reacting with aggregated IgG on non-phagocytosable surfaces. Colchicine and vincristine were incubated with the neutrophils for 1 hour before the reaction.

(Text–figure 2). Oxidation of glucose by the hexose monophosphate pathway was stimulated during this reaction but does not supply the energy required for granule exocytosis.[30] By contrast, glycolysis is required.[30]

A study of agents which affect contractile elements (microtubles and microfilaments) is shown in Text–figure 3. Colchicine was found to have little effect on release of β-glucuronidase. That the colchicine was active was ascertained by showing its inhibitory action on platelet release reactions.[20] These results are similar to those of Hawkins,[31] who, by employing a similar model, found that the release of granular constituents from neutrophils was only slightly inhibited. However, these data contrast with those of Weissmann and Zurier,[24] who noted that colchicine did inhibit the release of granular constituents. It should also be noted that colchicine has been reported

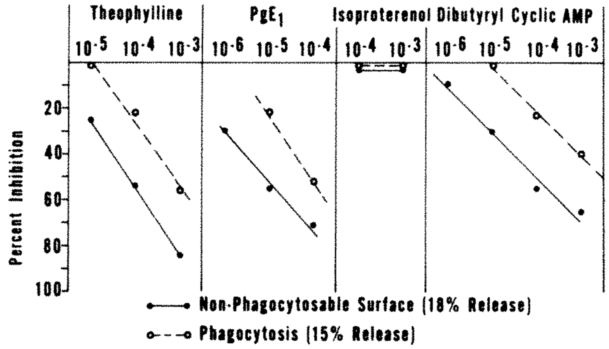

Text-fig 4—Inhibition, by agents increasing cyclic AMP, of release of β-glucuronidase from rabbit neutrophils. Neutrophils were reacted with immune complexes on micropore filters or were allowed to phagocytose zymosan particles coated with antibody. Agents were incubated with the neutrophils for 1 hour before the reaction. The results are representative of three similar experiments.

to reduce degranulation into vacuoles during phagocytosis.[32] Vincristine, on the other hand, mildly stimulated the release of granule enzymes, although there was considerable variation from experiment to experiment. Of great interest is the fact that cytochalasin B markedly enhanced release. This enhancement was reversible, it did not affect the amount of LDH liberated and did not occur if the neutrophils were adherent to petri dishes without the aggregated immunoglobulin stimulus.[28] Similar results have been reported by Hawkins [33] and Weissmann *et al.*[24] Morphologic observation indicated that the effect of cytochalasin was to increase the exocytosis of granules (Figure 4C). Interestingly, despite the increased release of lysosomal enzymes, stimulation of the hexose monophosphate pathway was inhibited. Thus, an inverse relationship was found between the release of granules to the outside of the cell and the activity of the hexose monophosphate pathway.

The effect on release of granular constituents by agents thought to increase intracellular levels of cyclic AMP is shown in Text–figure 4. Rabbit neutrophils were allowed to phagocytose zymosan particles (coated with rabbit antibody) or adhere to rabbit anti-BSA-BSA complexes on micropore filters. Prostaglandin E1 or theophylline inhibited release and have been shown by Bourne *et al* [34] to increase cyclic AMP in this type of cell. Both agents together had a mildly synergistic effect. Isoproterenol was inactive, perhaps indicating a paucity of β-adrenergic receptors on these cells, although Rivkind and Becker [35] have reported an inhibitory effect of epinephrine on neutrophil chemotoxis. Dibutyryl cyclic AMP itself was also inhibitory. Similar results have been recently obtained in other laboratories.[24,31,36] These findings suggest, but do not prove, that increased cellular cyclic AMP may inhibit the release of granule enzymes.

It may be seen from Text–figure 4 that ten times less inhibitor was required to prevent release of granular enzymes when the neutrophils reacted with nonphagocytosable surfaces than when they phagocytosed particles. Since less stimulation by immunoglobulin or complement is required for release in this former circumstance,[22] it may be possible *in vivo* to inhibit the exocytosis on surfaces while retaining the phagocytic and digestive properties of the neutrophils.

The Action of Neutrophils In Vivo

After mechanisms by which injurious constituents are released from neutrophils were demonstrated *in vitro,* it became necessary to show that similar processes were involved in neutrophil-mediated injury *in vivo*. Until now, most evidence has been obtained by observing neutrophils in the lesions and by showing that damage was alleviated by a depletion of circulating neutrophils.[1,3,9,37-39] Depletion of complement has generally prevented neutrophil accumulation in immunologic reactions, with a similar effect.[39-42]

Accordingly, two models of immunologic injury have been established in rabbits in which neutrophils depletion completely prevents damage and replacement of isolated neutrophils allows the injurious processes to be reconstituted. One of these, developed by Dr. C. De Shazo, is an acute arthritis.[43,44] The other model in which replacement has been achieved is nephrotoxic nephritis. These studies have been performed with Dr. C. G. Cochrane.

Replacement of Neutrophils in Nephrotoxic Nephritis

A dose of sheep antibasement membrane antiserum, which exhibited complete dependence on neutrophils for injury [8,42] over a 5-hour period, was injected intravenously into 1.3 kg rabbits which had been depleted of neutrophils by the injection of nitrogen mustard 3 days previously. After an hour, graded doses of purified rabbit peripheral neutrophils, prepared as for the *in vitro* experiments except that they were washed in plasma, were injected intravenously to reconstitute the injury. The animals were sacrificed at 4 hours, proteinuria was assessed, and the average number of neutrophils per glomerular section were counted.

Table 2 shows that the glomerular injury which occurred was directly dependent upon the number of neutrophils injected. This itself paralleled the number of these cells bound per section of glomerulus, directly demonstrating the requirement for neutrophils in this type of injury and confirming previous experiments.[41,42] Neutro-

Table 2—Glomerular Injury Induced by Replacement of Isolated Neutrophils into Neutrophil-Depleted Rabbits Given Nephrotoxic Antibody

Number of neutrophils injected/rabbit* × 10^8	Antibody†	Proteinuira (4 hrs) No. positive/total	Proteinuira (4 hrs) mg (average)	Neutrophils per glomerular section (average)
2.5	+	0/9	0.5	2.5
5.0-6.0	+	6/12	4.9	5.4
7.0-7.5	+	12/12	24.9	8.5
5.0-7.5	—	0/6	0.4	0.2
—	+	0/7	0.8	1.0

* Injected intravenously into 1.3 kg rabbits

† Sheep antirabbit GBM antiserum injected intravenously 1 hour before the neutrophils

phils injected without antibasement membrane antibody did not localize in the kidney and did not induce injury. Antibody injected without neutrophils resulted in no injury, and only a very few neutrophils entered the glomeruli, presumably those remaining after treatment with nitrogen mustard.

Figure 5 depicts a section of a glomerulus from such a replacement experiment and shows the neutrophils along the capillary loops. In the electron micrograph (Figure 6) these may be seen to occupy the same site in the glomerulus as those in conventional nephrotoxic nephritis in normal, neutrophil-sufficient animals (Figure 2).

Exocytosis of granules along the basement membrane has not been observed directly as yet. Nevertheless, Figure 6 demonstrates the presence of alkaline phosphatase activity on the external membrane of a neutrophil where it is in contact with the immune reactants along the basement membrane. From the *in vitro* experiments (Figure 4A),[23] this is a strong indication of exocytosis. This then appears to be one of the mechanisms by which digestive enzymes are released in nephrotoxic nephritis.

With this model system, neutrophils may be treated with inhibitors *in vitro* before replacement. Thus the effect of the substances studied *in vitro* (see above) can be compared with their effect on neutrophil-mediated injury *in vivo*. Preliminary experiments along these lines have shown that treatment with DFP or iodoacetate, both irreversible inhibitors of exocytosis, will prevent injury when the treated neutrophils are replaced. However the agents also prevent other neutrophil activities, such as chemotaxis. Interestingly, a concentration of iodoacetate (0.2 mM) which completely prevented the release on surfaces *in vitro* and the reconstituted nephrotoxic injury *in vivo* had no effect, in our hands, upon the phagocytosis of zymozan particles *in vitro*.

Replacement of Neutrophils in Arthritis

The tissue injury in a reversed passive Arthus reaction in the stifle joint of rabbits could be completely prevented by neutrophil depletion,[43,44] even though the immune complexes were still formed in the synovial vessel walls. As shown by De Shazo *et al*[44] in our laboratory, replacement of isolated neutrophils into the joint space reconstituted the injury. The neutrophils migrated a distance of at least 200 μ across the synovium to reach the immune complexes, presumably under the influence of chemotactic factors. That these were derived from complement was shown by preventing the migration (and injury) using complement-depleted or deficient rabbits. These experiments directly showed, for the first time *in vivo*, the involvement of chemotaxis and complement in bringing neutrophils to sites of injury. Once neutrophils accumulated, the complexes were phagocytosed and injurious constituents were released, inducing tissue injury (Figure 1).

Summary

The activation of complement by immune complexes at their sites of localization or deposition induces neutrophil accumulation; possibly by chemataxis, as in the Arthus reaction. Alternatively, adherence of neutrophils to bound C3 may initially localize the cells, perhaps as in nephrotoxic nephritis. Cell movement, chemotaxis and adherence may then all be involved in the penetration of neutrophils under the endothelial cells and adherence to the antibody and complement along the basement membrane.

Once adherent to the complexes, they may be phagocytosized by the neutrophils, which subsequently release their constituents. Alternatively, if attached to surfaces such as the basement membrane, the cells may release lysosomal constituents by direct exocytosis of granules. In either case, *in vitro* the models have shown that the release is an active secretory process, requiring environmental calcium and cell energy metabolism. It is inhibited by agents thought to increase cyclic AMP and stimulated by cytochalasin B.

Among the materials released are a variety of constituents which induce tissue injury by digesting tissue constituents or by generating mediators.

References

1. Cochrane CG: The functions of granulocytes, Principles of Hematology. Edited by WJ Williams, McGraw Hill, Philadelphia, 1972
2. Ziff M, Gribetz HJ, Lospalluto J: Effect of leukocyte and synovial membrane extracts on cartilage muco proteins. J Clin Invest 39:405, 1960
3. Cochrane CG: Immunologic tissue injury mediated by neutrophilic leukocytes. Advances in Immunology, Vol 9. Edited by FJ Dixon, HG Kunkel. New York, Academic Press, Inc, 1968, pp 97–162
4. Wasi S, Murray RK, Macmorine DRL, Movat HZ: The role of PMN-leukocyte lysosomes in tissue injury, inflammation and hypersensitivity. II. Studies on the proteolytic activity of PMN-leukocyte lysosomes of the rabbit. Br J Exp Pathol 47:411, 1966
5. Cochrane CG, Aikin BS: Polymorphonuclear leukocytes in immunologic reactions. The destruction of vascular basement membrane *in vivo* and *in vitro*. J Exp Med 124:733–753, 1966

6. Weissmann G, Spilberg I: Breakdown of cartilage protein polysacchoride by lysosomes. Arthritis Rheum 11:162, 1968
7. Liberman J, Gawad MA: Inhibitors and activators of leukocytic proteases in purulent sputum. Digestion of human lung and inhibition by alpha-antitrypsin. J Lab Clin Med 77:713, 1971
8. Hawkins D, Cochrane CG: Glomerular basement membrane damage in immunologic glomerulonephritis. Immunology 14:665, 1968
9. Kniker WT, Cochrane CG: Pathogenic factors in vascular lesions of experimental serum sickness. J Exp Med 122:83, 1965
10. Seegers W, Janoff A: Mediators of inflammation in leukocyte lysosomes. VI. Partial purification and characterization of a mast cell-rupturing component. J Exp Med 124:833, 1966
11. Ranadive NS, Cochrane CG: Isolation and characterization of permeability factors from rabbit neutrophil. J Exp Med 138:605, 1968
12. Henson PM: Mechanisms of release of constituents from rabbit platelets by antigen antibody complexes and complement. II. Interactions with neutrophils. J Immunol 105:490, 1970
13. Ward PA, Hill JH: C5 chemotactic fragments produced by an enzyme in lysosomal granules of neutrophils. J Immunol 104:535, 1970
14. Taubman SB, Lepoco IH: Cleavage of human Cls by human lysosomal enzymes, plasmin and trypsin. Immunochemistry 8:951, 1971
15. Rapaport SI, Hjort PF: The blood clotting properties of rabbit peritoneal leukocytes *in vitro*. Thromb Diath Haemorrh 17:222, 1967
16. Orange RP, Austen KF: Slow reacting substance of anaphylaxis. Adv Immunol 10:106, 1969
17. Greenbaum L: Leukocyte kininogenases and leukokinins from normal and malignant cells. Am J Pathol 68:613–624, 1972
18. Melmon KL, Cline MJ: Interaction of plasma kinins and granulocytes, Nature 213:90, 1967
19. Bodel P: Studies on the mechanism of pyrogen production. I. Investigation of new protein synthesis in stimulated human blood leukocytes. Yale J Biol Med 43:145, 1970
20. Becker EL, Henson PM: Immunologically stimulated *in vitro* mediator secretion and related phenomena. Advan Immunol (In Press)
21. Lockwood WR, Allison F: Electron micrographic studies of phagocytic cells. 1 Morphological changes of the cytoplasm and granules of rabbit granulocytes associated with ingestion of rough pneumococcus. Br J Exp Pathol 44:593–600, 1963
22. Henson PM: The immunologic release of constituents from neutrophil leukocytes. I. The role of antibody and complement on nonphagocytosable surfaces or phagocytosable particles. J Immunol 107:1535, 1971
23. Henson PM: The immunologic release of constituents from neutrophil leukocytes. II. Mechanisms of release during phagocytosis and adherence to nonphagocytosable surfaces. J Immunol 107:1547, 1971
24. Weissmann G, Zurier RB, Hoffstein S: Leukocytic proteases and the immunologic release of lysosomal enzymes. Am J Pathol 68:539–564, 1972
25. Hawkins D: Neutrophilic leukocytes in immunologic reactions: evidence for the selective release of lysosomal constituents. J Immunol 108:310, 1972

26. Henson PM: Interaction of cells with immune complexes, adherence, release of constituents and tissue injury. J Exp Med 134:114s, 1971
27. Hawkins D: Biopolymer membrane A model system for the study of polymorphonuclear leukocyte response to immune complexes. J Immunol 107:344, 1971
28. Henson PM, Oades ZG: Enhancement of immunologically induced granule exocytosis from neutrophils by cytohalasin B. Unpublished data
29. Ishizaka T, Ishizaka KS, Fudenberg H: Biologic activities of aggregated γ-globulin. VIII. Aggregated immunoglobulins of different classes. J Immunol 99:82, 1967
30. Henson PM, Oades ZG: Immunologically induced exocytosis of granules from neutrophils. The role of energy metabolism and the effect of increasing 3′, 5′ cyclic AMP. Unpublished data
31. Hawkins D: Inhibition of neutrophil lysosomal release. Fed Proc 31:748, 1972
32. Malawista SE, Bodel PT: The dissociation by colchicine of phagocytosis from increased oxygen consumption in human leukocytes. J Clin Invest 46:-786, 1967
33. Hawkins D: Unpublished data
34. Bourne HR, Lehrer RI, Cline MJ, Melmon KL: Cyclic 3′,5′-adenosine monophosphate in the human leukocyte: synthesis, degradation and effects on neutrophil candidacidal activity. J Clin Invest 50:920–929, 1971.
35. Rivkind I, Becker EL: Possible implications of 3′,5′-adenosine monophosphate in the chemotaxis of rabbit peritoneal polymorphonuclear leukocytes (PMN's). Fed Proc 31:657, 1972 (abstr)
36. Zurier RB, Weissmann G, Mitnick H: Effects of prostaglandins on enzyme release from human blood leukocytes. Fed Proc 31:254, 1972
37. Stetson CA: Similarities in the mechanism determining the Arthus and Schwartzman phenomena. J Exp Med 94:1347, 1951
38. Humphrey JH: The mechanisms of Arthus reactions. I. The role of polymorphonuclear leukocytes and other factors in reversed passive Arthus reactions in rabbits. Br J Exp Pathol 36:258, 1955
39. Cochrane CG, Weigle WO, Dixon FJ: The role of polymorphonuclear leukocytes in the initiation and cessation of the Arthus vasculitis. J Exp Med 110:481, 1959
40. Cochrane CG, Müller-Eberhard HJ, Aikin BS: Depletion of plasma complement *in vivo* by a protein of cobra venom: its effect on various immunologic reactions. J Immunol 105:55, 1970
41. Cochrane CG, Unanue E, Dixon FJ: A role of polymorphonuclear leukocytes and complement in nephrotoxic nephritis. J Exp Med 122:99–116, 1965
42. Henson PM: Release of biologically active constituents from blood cells and its role in antibody-mediated tissue injury, Progress Immunol. Edited by B Amos. New York, Academic Press, Inc, 1971, p 155
43. DeShazo CV, Henson PM, Cochrane CG: Acute immunologic arthritis in rabbits. J Clin Invest 51:50–57, 1971
44. DeShazo CV, McGrade MT, Henson PM, Cochrane CG: The effect of complement depletion on neutrophil migration in acute immunologic arthritis. J Immunol 108:1414–1419, 1972

Acknowledgment

The author wishes to thank Mrs. Z. G. Oades for expert assistance, Mrs. D. Durham for cutting the sections for electron microscopy and Mr. G. Sandford, Mrs. K. Prescott and Mrs. P. Wright for the illustrations.

Dr. Henson is a recipient of Research Career Development Award 5 K04 GM 42567-02 from the US Public Health Service.

[*Illustrations follow*]

Legend to Figures

Fig 1—Neutrophil-mediated tissue injury in the Arthus reaction. Reversed passive Arthus reaction in the rabbit bladder wall. **A**—Neutrophils *(N)* beneath the basement membrane *(BM)* of a small vessel. Phagocytic vacuoles containing immune complexes *(ppt)* are visible in this case because the antigen employed was ferritin.[26] There is little tissue damage as yet in this section. **B**—Arthus reaction after 6 hours. Disruption of the basement membrane is accompanied by deposition of fibrin *(fib)* in the interstitial space *(IS)*. The lumen *(L)* of the vessel is to the top.[5]

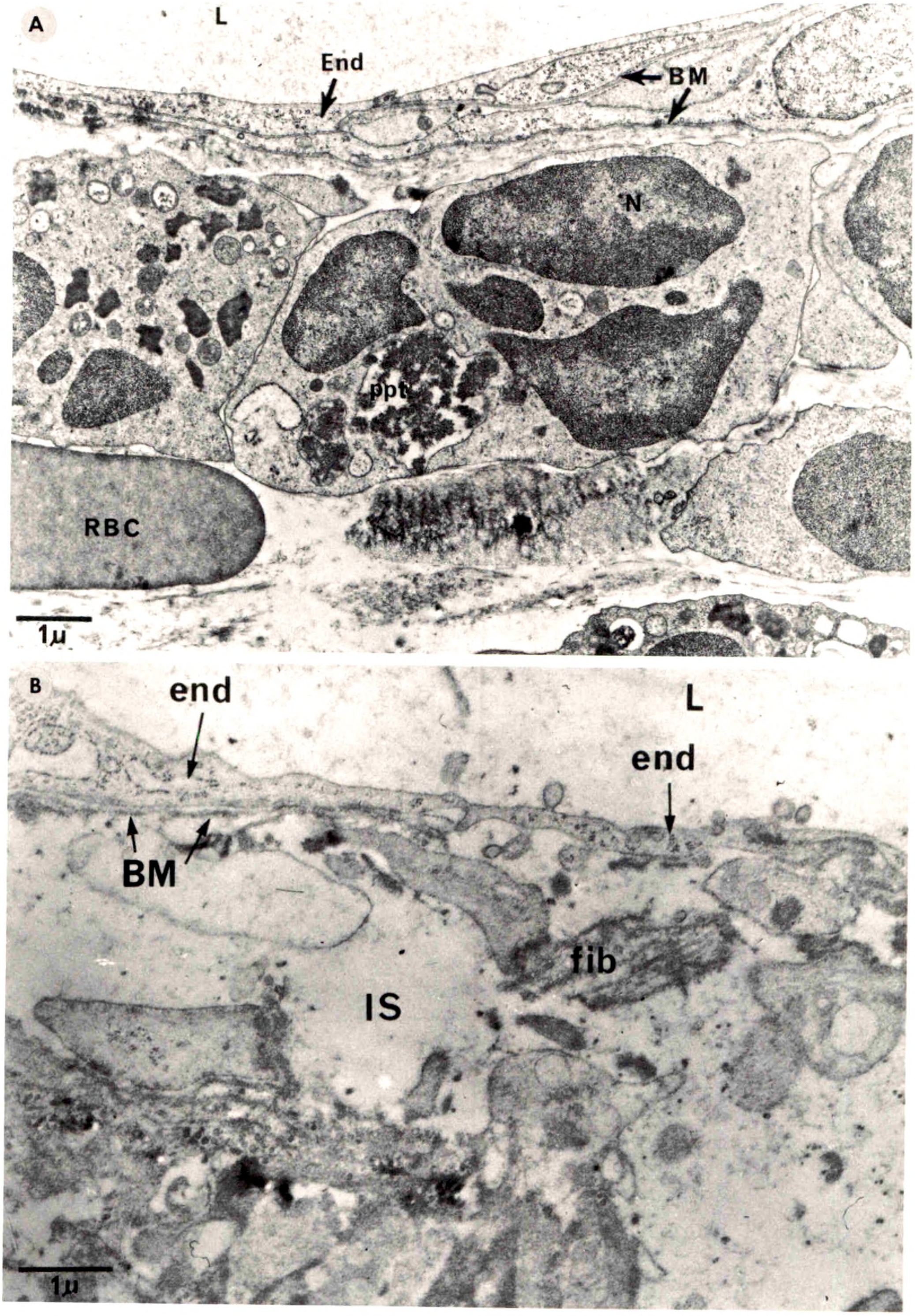
A
L
End
BM
N
ppt
RBC
1μ
B
end
L
end
BM
fib
IS
1μ

1

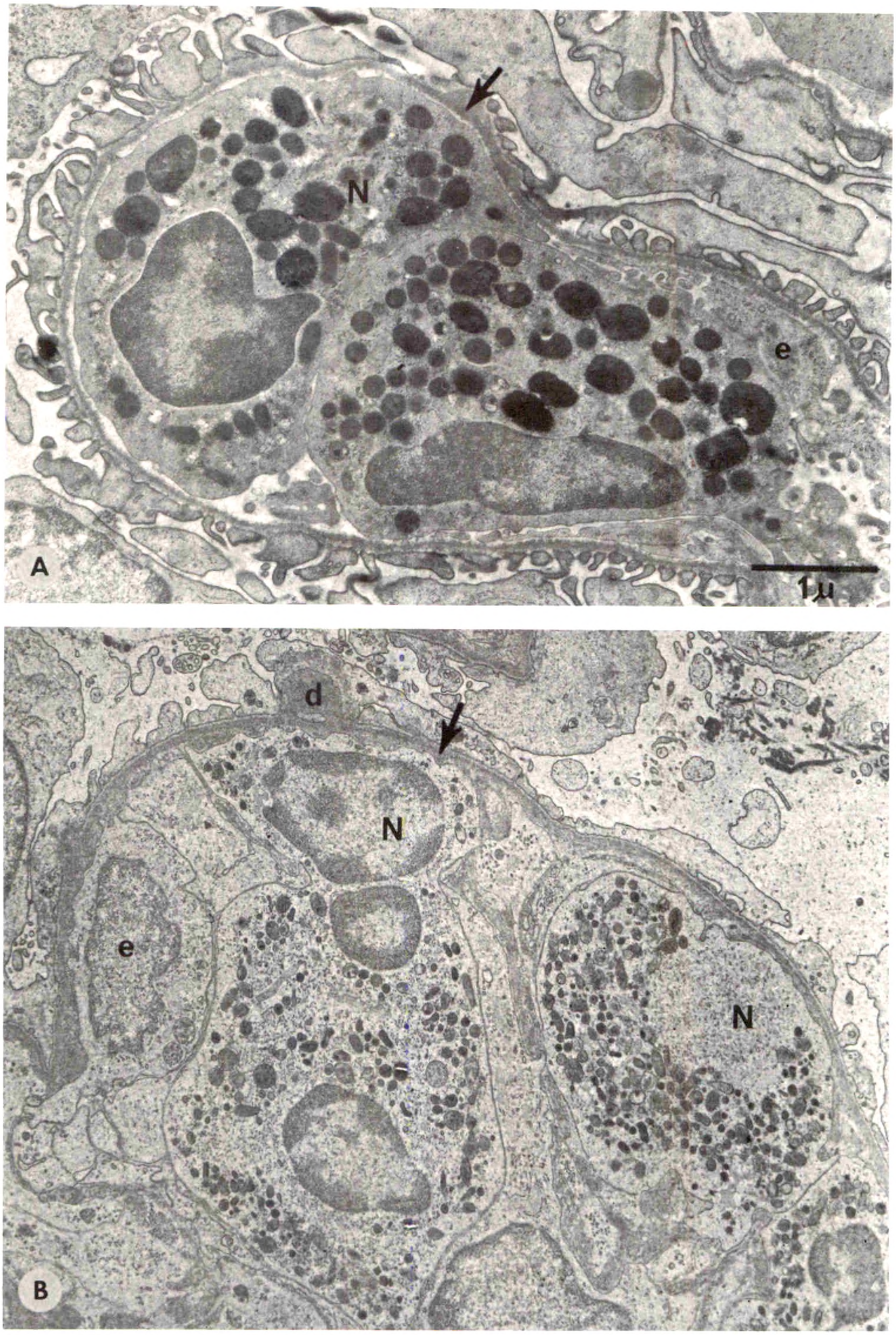

Fig 2—Neutrophils reacting with glomerular basement membrane *in vivo.* **A**—Electron micrograph of neutrophil in nephrotoxic nephritis in a rabbit. The endothelial cell (*e*) has been pushed aside and the neutrophil (*N*) is closely adherent to the antibody and complement on the basement membrane (*arrows*). **B**—Neutrophils adherent to the basement membrane in human acute post-streptococcal glomerulonephritis. *d*=deposits (immune complexes) along the basement membrane. Photograph courtesy of Dr. J. Feldman (× 12,000).

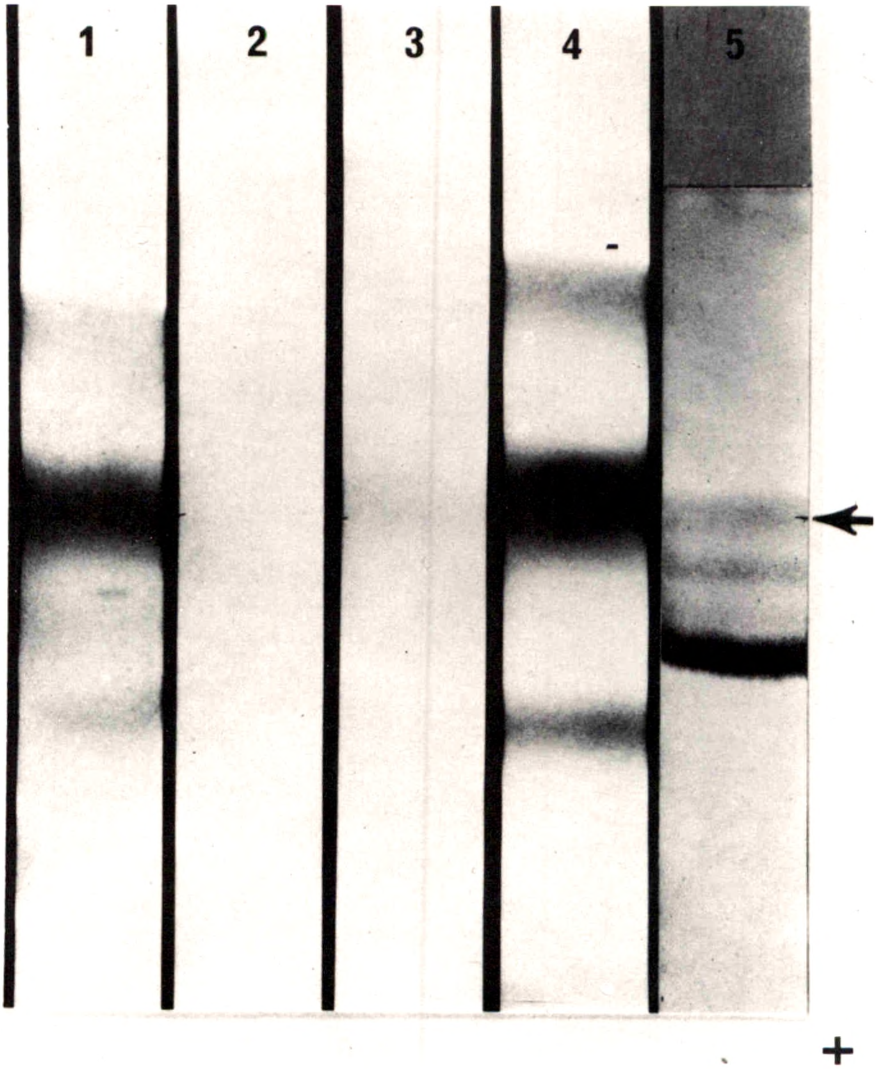

Fig 3—Digestion of basement membrane *in vitro.* Paper electrophoresis of supernatants after treatment of rabbit glomerular basement membrane with neutrophil lysate at pH 2.5 (**1**), distilled water at pH 2.5 (**3**), or trypsin (**4**). For comparison, the neutrophil extract alone (**2**) and normal serum (**5**) are included.[5]

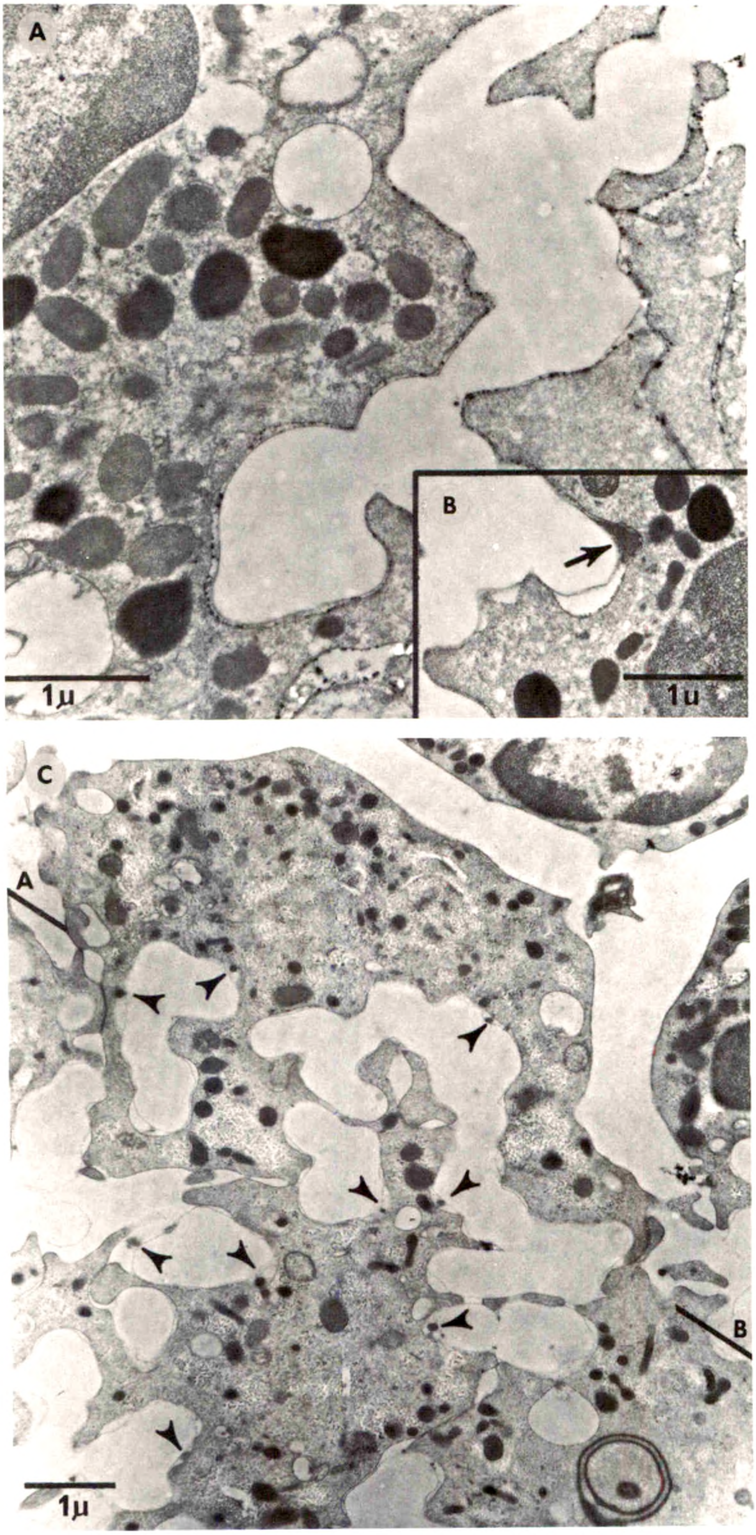

Fig 4—Exocytosis of granules from neutrophils reacting with aggregated immunoglobulin or immune complexes on nonphagocytosable surfaces. **A**—Alkaline phosphatase activity revealed histochemically[21] along the external membrane of a rabbit neutrophil closely adherent to the immune reactants on the micropore filter. This enzyme has been released from the secondary (less dense) granules. **B**—Extrusion of a secondary granule along the membrane of the neutrophil adherent to the nonphagocytosable surface. **C**—Human neutrophil adherent to aggregated IgG on a micropore filter in the presence of 5 μg/ml cytochalasin B. Numerous examples of granule exocytosis (*arrows*) are apparent along the adherent plasma membrane but not along the free membrane of the cell.

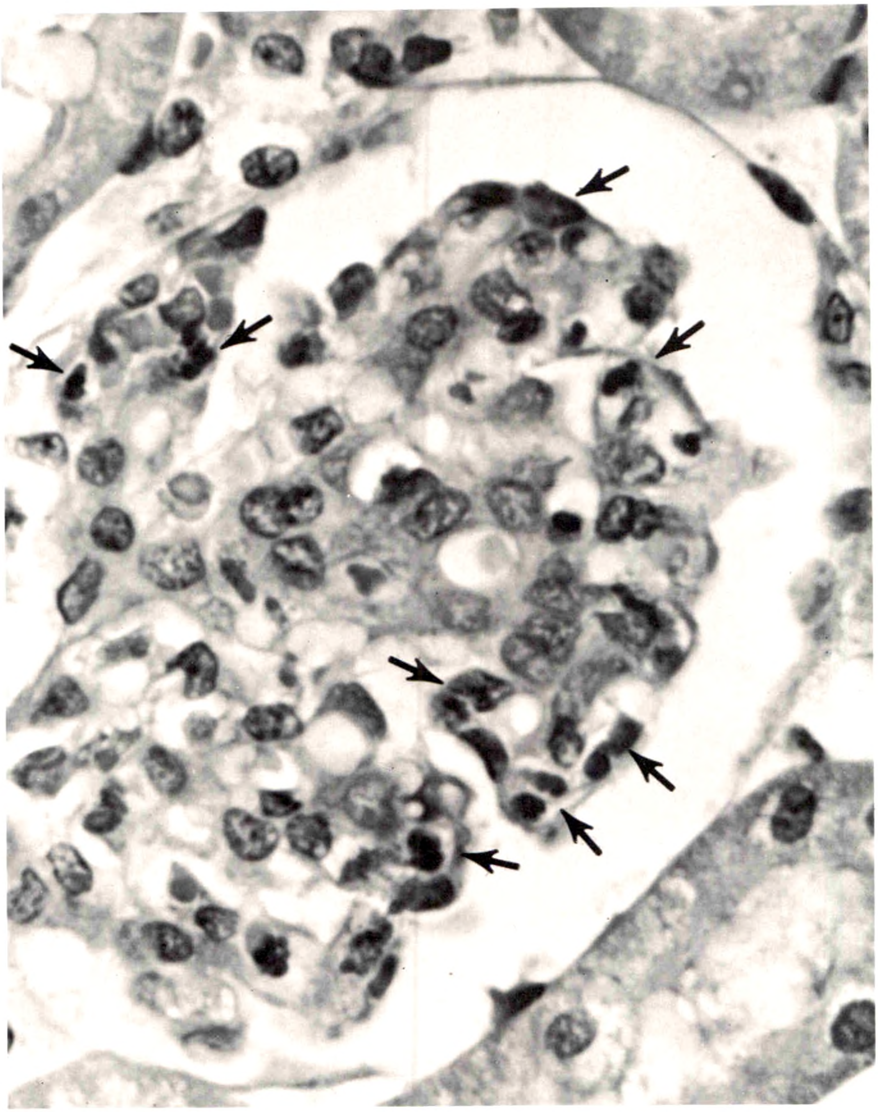

Fig 5—Section of a glomerulus from a rabbit with nephrotoxic nephritis, depleted of neutrophils with nitrogen mustard and injected with isolated neutrophils to reconstitute the injury. Neutrophils (*arrows*) have accumulated along the capillary loops (H&E, × 840).

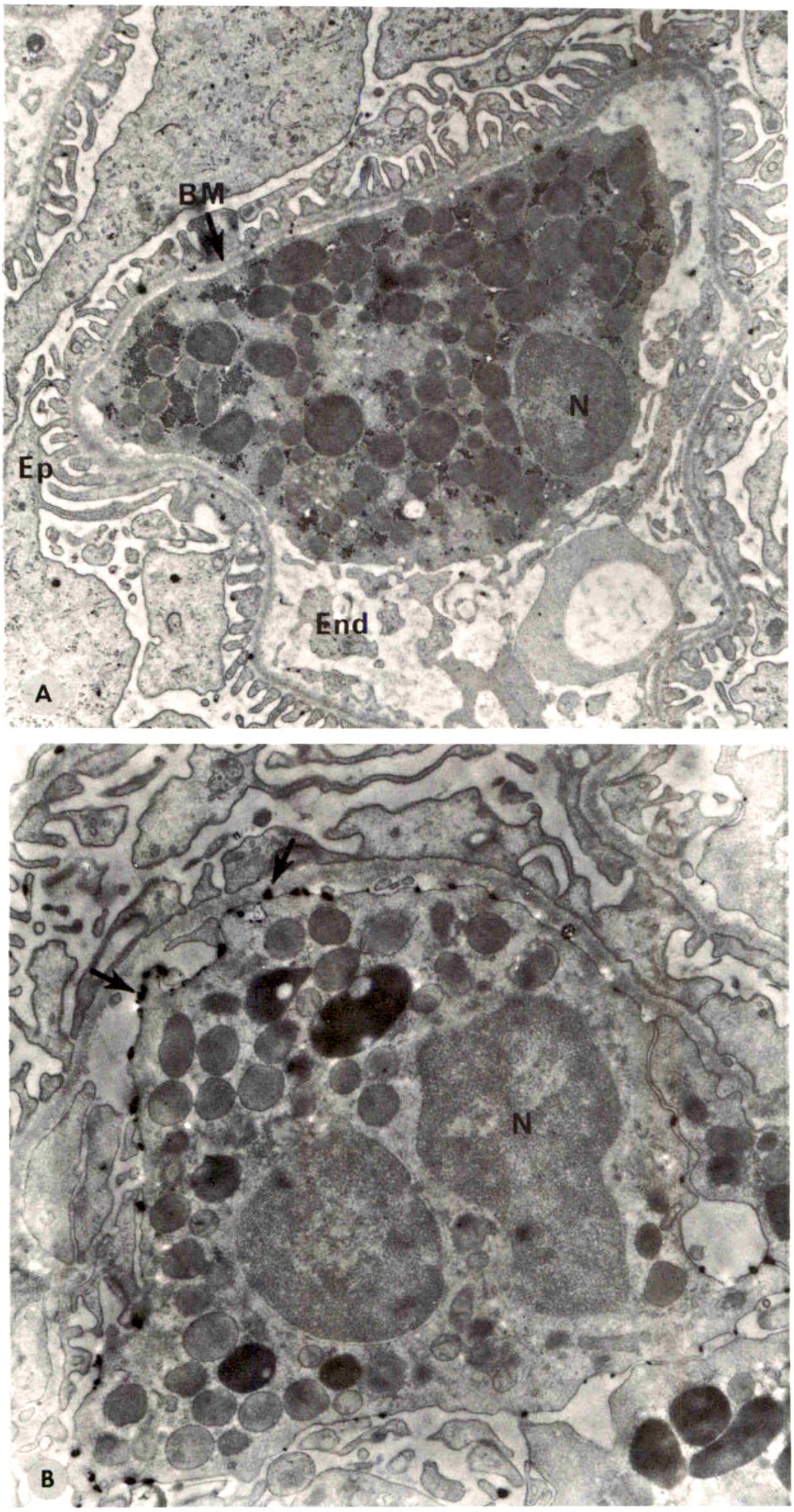

Fig 6—Electron micrograph of glomeruli from a rabbit with nephrotoxic nephritis, depleted of neutrophils and injected with isolated neutrophils to reconstitute the injury. **A**—The neutrophil (*N*) has become closely adherent to the basement membrane (*BM*) as was seen in the neutrophil-sufficient animal (Figure 2). The cell appears normal except for the large content of glycogen granules. *Ep*=epithelial cell; *End*=endothelial cell (× 4000). **B**—Neutrophil in a section strained histochemically for alkaline phosphatase.[21] The deposits of lead phosphate may be seen (*arrows*) along the external membrane of the neutrophil (× 5600).

Leukocyte Kininogenases and Leukokinins from Normal and Malignant Cells

Lowell M. Greenbaum, PhD

THIS PAPER REVIEWS our findings and ideas concerning acid proteases in white cells which catalyze the formation of pharmacologically active peptides. These peptides, which we term leukokinins,* may play an important role in some responses seen in inflammation, injury and allegic reactions. Since the leukokinins are also produced by enzymes in malignant cells and in ascitic fluids, they may play a role in malignancy as well.

One of the earliest investigations of polypeptide formation by white cells and conditions of acid pH was reported by Opie,[3] who noted acid protease activity in white cells (macrophages) and postulated that this activity aided digestion of ingested particles.

Menkin[4] is credited with observations that acid pH, proteases and polypeptides are part of the involvement of polymorphonuclear leukocytes in the inflammatory response. He postulated that a polypeptide, leukotaxine, produced by white cells and found in inflammatory exudates, may be an important chemotactic factor as well as an important permeability factor in inflammation.

Movat[5] made the significant observation that polypeptides or proteases capable of increasing vascular permeability are released from the interaction of leukocytes and immune precipitates, thus implicating polypeptides as a mediator of allergic inflammation.

Melmon and Cline[6] reported that intact granulocytes could activate the plasma kallikrein system to form bradykinin.

From the Department of Pharmacology, College of Physicians and Surgeons, Columbia University, New York, NY.

Supported by grants from the Health Research Council of New York and Training Grants GM-00438 and HL-12738-04 from the US Public Health Service.

Address reprint requests to Dr. Lowell M. Greenbaum, Department of Pharmacology, College of Physicians and Surgeons, Columbia University, New York, NY 10032.

* A few words concerning nomenclature: The term kinin has different meanings in different disciplines. As used here, the term leukokinin refers to a polypeptide produced by leukocyte proteases which has hypotensive properties and general pharmacologic properties similar to bradykinin. This name is in keeping with the recommendations of the International Committee on Nomenclature for Hypotensive Peptides.[1]

It should be noted, however, that a protein with chemotactic properties has been isolated and named leucokinin.[2] This name does not correspond with the recommendations of the International Committee.

The presence of catheptic enzymes, acid hydrolases, in PMN cells and macrophages has been described by several groups in recent times.[7-9] Drs. Yamafuji and Kim, of our laboratory, clearly demonstrated that the acid proteases of polymorphonuclear leukocyte (PMN) cells could act directly on plasma proteins to release pharmacologically active peptides.[10-12] Drs. Freer and Chang, also of our laboratory, isolated these peptides and found that, while they do have potent pharmacologic activity, their molecules do *not* contain bradykinin. Thus, the initial name PMN-kinin was given to the first such peptide isolated, since it was derived from enzymes of PMN cells.[13] After a second, somewhat different, peptide was isolated from the enzymatic activity of macrophages, the family of peptides was termed *leukokinins* with identifying initials (leukokinin-PMN and leukokinin-M).[14,15]

Comparison of White Cell and Plasma Kinin Systems

The white cell kinin-generating and kinin-metabolizing systems are quite different than the well-known bradykinin-generating system of plasma. Table 1 compares these two systems. The kininogenase (kinin-forming enzyme) of plasma, kallikrein, is a neutrally

Table 1—Comparison of Plasma Kinin and Leukokinin Systems

	Plasma	White Cell*
Kininogenases (kinin forming)	Kallikrein	Several (not kallikrein)
pH optimum	Neutral	Acid
Inhibitors	Soy bean trypsin	±
	Trasylol	—
	Plasma	Pepstatin
Presence	Prekallikrein	Active form
Synthetic substrates	BAEE	?
Product of kininogenase	Bradykinin	Leukokinin-M
	(Mol wt 1060)	Leukokinin-PMN
		(Mol wt 2416, 2826)
Substrate for Kininogenase	Plasma bradykininogen	Plasma leukokininogen
Kininases (kinin destroying)		
pH optimum	Neutral	Neutral
Inhibitors	Chelating agents	Copper
	Peptides	TPCK
		Trasylol
Lung inactivation	90–95%	80–90%

* Polymorphonuclear leukocytes, macrophages, lymphocytes, L-1210 cells (malignant) and mastocytoma cells

BAEE = benzoyl-L-arginine ethyl ester, TPCK = tosyl-L-phenylalanine chloromethyl ketone acting enzyme present in a zymogen-like form, prekallikrein. It is inhibited by soy bean trypsin inhibitor (SBTI), the polypeptide, Trasylol® and certain inhibitors in plasma. No such enzyme exists in the white cell or cancer cells we have tested. All of these cells, however, contain kininogenases (several) which are active at acid pH, are not inhibited by Trasylol, are not, or only partially, inhibited by SBTI and are probably present in active form, although sequestered in a cell particulate or in the membrane of the cells.

Characterizing these enzymes by their actions on synthetic substrates, kallikrein attacks benzoyl-L-arginine ethyl ester (BAEE). The leukokininogenases are difficult to characterize with small synthetic substrates, but seem to be true proteases (similar to cathepsins D or E).

The product of the action of kallikrein on its plasma substrate, bradykininogen, is the nonapeptide, bradykinin. The product of leukokininogenases of the white cell acting on plasma proteins are leukokinins, which contain 21 to 25 amino acids.[14,15] The leukokinins do not contain bradykinin in their molecules. The substrate(s) from which these peptides are released does not seem to be bradykininogen, and hence we have termed it leukokininogen.[16,17]

Kinin-destroying enzymes in plasma—so called kininases—are different than the kininases in white cells. Optimal pH for both is neutral, but chelating agents, such as hydroxyquinoline, EDTA and peptides, inhibit plasma kininase I and II,[18] while heavy metals, such as copper and agents like tosyl-L-phenylalanine chloromethyl ketone (TPCK), inhibit white cell kininases. Trasylol is also an inhibitor of white cell kininases.[13] Leukokinins like bradykinin are inactivated, as they pass through the circulation of the lung, but at a somewhat slower rate than bradykinin.[19]

In summary, the white cell system of kinin metabolism—the leukokinin system—seems to be quite different from the plasma-kinin system in terms of the: a) properties of kininogenases, b) product of the kininogenase action, c) substrate on which the kininogenase acts and d) kininase enzymes contained in the cell.

Properties, Structure and Formation of Leukokinins

Let us now consider the leukokinins—their formation, structure, and pharmacologic properties—and compare them with bradykinin. The leukokinins were first discovered when broken cell preparations of rabbit PMN cells were incubated with a partially purified plasma kininogen preparation. When the mixture was incubated at a pH range of 3 to 6, with appropriate blocking agents for kininases, pharmacologically active material was released.[10,11] Peptidases, such as chymotrypsin and carboxypeptidase B, destroyed the activity, indicating the peptide nature of the material.

While this material resembled bradykinin, chromatography and pharmacologic assay demonstrated that it differed from bradykinin. Using Sephadex A-50 the material moved off the column much earlier and was much more active on the rat uterus than bradykinin, in doses that induced comparable contractions of the guinea pig ileum.[13]

To purify this material, Drs. Freer and Chang incubated large quantities of human or rabbit plasma kininogen preparations with broken cell preparations of macrophages or granulocytes. The incubate was then extracted with hot alcohol, purified by carboxymethylcellulose (CMC) chromatography and analyzed. In Dr. Freer's earlier experiments, PMN cell enzyme produced one major peptide with an activity, termed *PMN-kinin*. In Dr. Chang's later experiments, using macrophage enzymes, an additional peptide was isolated; in the new nomenclature these are known as leukokinin-PMN and leukokinin-M. After establishing the purity of these peptides by end-group analysis, their amino acid content was determined.

Amino Acid Content

Table 2 compares the amino acid content of the leukokinins-PMN and M with bradykinin. It will be noted that the leukokinins are larger polypeptides than bradykinin. Molecules of leukokinins do not contain methionine and only one phenylalanine moiety, indicating that leukokinins do not contain bradykinin (which has two phenylalanine residues) or analogs of bradykinin, such as methionyl-lysl-bradykinin.

A partial sequencing of leukokinin-M has demonstrated that NH_2–Arg–Ala–Ser–?–?–Lys–. . . is the amino terminal sequence.

Pharmacologic Activity

Comparison of the pharmacologic properties of leukokinins and bradykinin is shown in Table 3. Bradykinin is a potent agent causing increased vascular permeability, hypotensive activity and smooth muscle contraction. Although leukokinin-M and bradykinin are equipotent in causing an hypotensive response, the former is almost 5 times more potent in its ability to increase vascular permeability.

Table 2—Amino Acid Composition of Leukokinins and Bradykinin

Amino acids	Number of residues Bradykinin	Leukokinin-M	Leukokinin-PMN
Alanine	0	2	1
Arginine	2	3	2
Aspartic acid	0	1	1
Cysteine	0	0	0
Glutamic acid	0	2	1
Glycine	1	2	2
Histidine	0	1	1
Isoleucine	0	0	0
Leucine	0	1	1
Lysine	0	3	2
Methionine	0	0	0
Phenylalanine	2	1	1
Proline	3	3	3
Serine	1	2	2
Threonine	0	1	1
Tyrosine	0	1	2
Valine	0	2	1
Total amino acids	9	25	21
Molecular weight	1060	2826.5	2416

Leukokinin-M is less active than bradykinin in smooth muscle assays. It has weak pain-producing property.

Leukokinins have two major properties which make them important in inflammation: a) their potency in increasing vascular permeability and b) their ability to cause changes in blood flow to an area, by relaxing arteriolar smooth muscle.

Table 3—Potency of Leukokinins Compared to Bradykinin*

	Leukokinin-M	Leukokinin-PMN
Blood pressure (depressor)		
Rabbit	1.0	3.5
Rat	—	10.4
Permeability		
Rabbit	4.6	1.30
Rat	—	1.30
Pain		
Dog	—	0.10
Uterus		
Rat (estrus)	0.23	0.80
Ileum		
Guinea pig	0.04	0.08
Duodenum		
Rat	0.04	0.32

* Bradykinin = 1.00 (molar basis)

Presence in Cells

Good sources of leukokinin-forming enzymes are listed in Table 4. It can be noted that in addition to their presence in normal cells, which include PMN-cells, macrophages and lymphocytes,[20] these enzymes are found in leukemic ascites (L-1210 cells), lymphosarcoma ascites cells (Meth-A) and mastocytoma cells (P815Y) of mice. Tissues, such as spleen and liver, also contain leukokinin-forming activity.

Cellular Location of Leukokininogenase Activity

The cellular location of these enzymes has been under study. After the cells were broken up, by freezing and thawing, homogenization or by a combination of these with changes in tonicity of the medium, the following pattern emerged. In most cells, the most stable leukokininogenase activity is found in the nuclear-membrane-debris fraction (low speed fraction). Since detergents, such as sodium dodecyl sulfate, solubilize the activity, we suspect that a good part of the cell activity may be membrane-bound. Activity is also found in lysosomal and extralysosomal fractions, these have proven unstable for purification. Kininase activity is also found in low speed and extralysosomal fractions. Kininase activity is *not* found in the lysosomal fraction.

pH Optimum

Studies on optimum pH of leukokinin-forming enzymes of various cells and fractions have demonstrated that major activity occurs in the acid pH range. When purified plasma protein fractions free of enzymatic activity are used as a substrate,[12] pH 4.0 is optimal.

Effect of Inhibitors

Antiinflammatory agents, such as salicylates, steroids, Trasylol, etc, have little inhibitory activity on the leukokininogenases. Pepstatin,[21]

Table 4—Some Sources of Leukokinin-Forming Enzymes

- White cells
  - Polymorphonuclear leukocytes (rabbit and human)
  - Macrophages (rabbit)
    - alveolar ± BCG
    - peritoneal
  - Lymphocytes ± PHA (human and rat)
- Cancer cells
  - Leukemic; L-1210 (mouse)
  - Lymphosarcoma; Meth-A (mouse)
  - Mastocytoma; P-815Y (mouse)
- Tissues
  - Spleen (bovine)
  - Liver (dog)

Table 5—Pepstatin Inhibition of Leukokinin Formation

Enzyme source	Concentration (μg/ml)	Percent inhibition
Macrophage	0.001	25
Macrophage	0.010	50
Macrophage	0.100	100
Mastocytoma	0.001	100

a polyepetide which inhibits pepsin and cathepsin D,[22] is a potent inhibitor of white cell and cancer cell leukokininogenases (Table 5). It has been reported to inhibit macrophage cathepsin D.[23]

Leukokininogen

Two major points should be noted concerning the substrate, leukokininogen, in human plasma: a) a variety of evidence, including chromatography and the use of pure bradykininogen, has shown that bradykininogen, the substrate for kallikrein, is distinct from leukokininogen[16,17] and b) in human plasma only small amounts of leukokininogen normally are available for leukokininogenase enzymes. However, after the action of a plasma protease, previously unavailable leukokininogen is converted into available leukokininogen. Warming plasma above 45 C for 15 minutes is one method we have used to activate the protease. The warming activation is blocked when it is carried out in the presence of SBTI or Trasylol (Table 6). Lima bean trypsin inhibitor (a plasmin inhibitor) does not block the warming activation. It would thus appear that kallikrein or a kallikrein-like enzyme is the converting protease, since SBTI and Trasylol are effective kallikrein inhibitors.

Our current concept of leukokininogen formation may be seen in Text-figure 1. A plasma protein (an unavailable substrate) is

Table 6—Effect of Agents on Leukokininogen Formation in Plasma

Agents	Percent leukokinin formation
No additions	100
Soy bean inhibitor (0.5 mg/ml)	0
Aprotinin (Trasylol; 2000 u/ml)	0
Lima bean inhibitor (5 mg/ml)	100
Polybrene (0.2 mg/ml)	100
EDTA (3×10^{-4} M)	150
o-Phenanthroline (1.5×10^{-3} M)	150
8-Hydroxyquinoline (3×10^{-3} M)	150

Plasma was warmed at 57 C for 2 hours in the presence of the agents. One milliliter of the warmed plasma was then incubated with 0.1 ml enzyme for 16 hours at pH 4.0. The reaction mixture was boiled, neutralized and assayed on the estrus rat uterus.

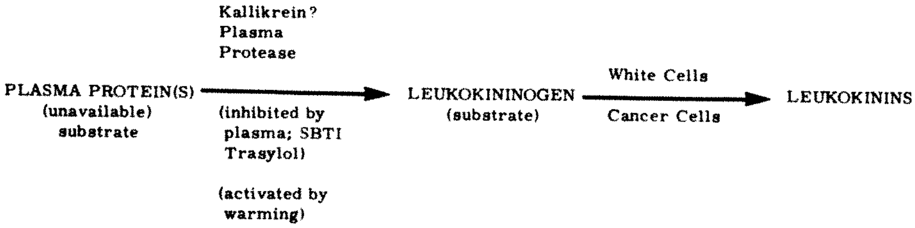

TEXT-FIG 1—Current concept of leukokininogen formation.

converted by a protease at neutral pH to leukokininogen, the substrate. The action of this protease may be blocked by SBTI or Trasylol. Normally, only a small amount of substrate is available in human plasma. After injury, the converting protease is activated (simulated by warming). The leukokininogen formed is then acted upon by enzymes from white cells and from cancer cells at acid pH to form the leukokinins.

Leukokininogen is readily available in the plasma of species such as the rabbit. Another readily available source of leukokininogen is the ascites fluid of murine mastocytoma cells; this was seen in experiments on mice with mastocytoma P-815Y ascites cells. Ascites fluid was aspirated from the peritoneal cavity, centrifuged to remove the cells, the fluid was brought to acid pH and within a few hours great quantities of leukokinins appeared. SBTI, Trasylol and heating had no effect on this system. Thus substrate and enzyme seem readily available in ascitic fluid for leukokinin formation (Table 7).

Role of the Leukokinin-Forming System

What is our concept of the role of the leukokinin system? What regulates it? Where does it fit into the scheme of mediators of inflammation?

Table 7—Leukokinin Formation in Ascites Fluid of Murine Mastocytoma 815Y Cells

Time (hr)	Kinin/ml fluid (ng)
0	0
2	500
4	1200
6	2000
11	5800
16	6200

Ascites fluid was aspirated from the peritoneal cavity. After centrifugation at 10,000g to remove the cells, the fluid was brought to pH 3.8 to 4.0 and kept at 37C. At the time intervals noted, a sample was boiled, neutralized and assayed on the estrus rat uterus. This experiment was carried out by M. Johnston of our laboratory.

As discussed above, leukokinins have been shown to be potent agents, causing increased vascular permeability and hypotensive changes in blood pressure. Such agents, produced by white cell enzymes and tissue enzymes, have to be considered as possible mediators of some or many of the responses seen in injury, inflammation, anaphylaxis and shock. Several lines of evidence can be cited to support this.

Steele and Wilhelm,[24] in their studies on the inflammatory reaction, concluded that mediators, such as leukokinins liberated from polymorphonuclear leukocytes, would account for changes in vascular permeability produced in the inflammatory response seen in their investigations. Van Arman [25] and Vinegar [26] agree that white cells are necessary for increased vascular permeability in the model inflammatory systems they employ. Berry *et al* [27] have pointed out that the acidic conditions of hemmorrhagic shock could promote kinin formation by proteases acting at acid pH. One might also consider that sensitized lymphocytes in the presence of antigen would release leukokinin-forming enzymes, which would contribute to the pathology seen in the inflammatory response of anaphylaxis.[20]

Finally, the existence of this system in extracellular fluid of ascites suggests that leukokinins may be important permeability factors in metastases of cells or in nutrition of cancer cells, because they promote extracellular fluid movement into the ascites area.

Regulation of the Leukokinin System

The leukokinin system, a pathologic one, has three major regulating mechanisms: a) The system is pH dependent since an acid pH is required for leukokinin formation; b) Circulating substrate is limiting, since the conversion of unavailable substrate to leukokininogen requires an enzymatic step (This enzyme may be activated, however, by blood clotting enzymes or other enzymatic systems activated in injury or allergy); c) Releasing mechanisms of leukokininogenases from within the cell or membrane would also regulate leukokinin formation.

Interrelationship of the Leukokinin System with Other Systems

Text-figure 2 summarizes our concept of the relationship of the leukokinin system to other systems of inflammation. The scheme reflects our interpretation of the interrelationships of six systems in inflammation: blood clotting, fibrinolysin, complement, antigen-antibody, kallikrein-bradykinin and leukokinin.

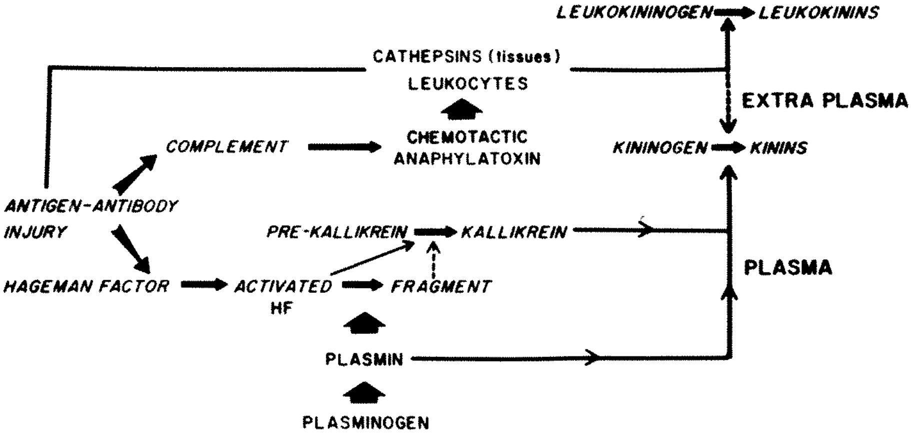
LEUKOKININOGEN → LEUKOKININS
CATHEPSINS (tissues)
LEUKOCYTES
EXTRA PLASMA
COMPLEMENT
CHEMOTACTIC ANAPHYLATOXIN
KININOGEN → KININS
ANTIGEN-ANTIBODY
INJURY
PRE-KALLIKREIN → KALLIKREIN
PLASMA
HAGEMAN FACTOR → ACTIVATED HF → FRAGMENT
PLASMIN
PLASMINOGEN

Text-fig 2—Summary of the relationship of the leukokinin system to other inflammation systems.

Injury causes activation of Hageman factor which is acted upon by plasmin to yield an activator of prekallikrein. Kallikrein acts on plasma kininogen to yield bradykinin. Antigen-antibody reactions fix complement. This is followed by the liberation of leukocyte chemotactic factors. Leukocytes emigrating to the sites of injury release leukokinin-forming enzymes which act on available leukokininogen substrate(s) in plasma or fluids to yield leukokinins.

References

1. Hypotensive Peptides. Edited by E Erdös, N Back, F Sicuteri. New York, Springer-Verlag, 1966, pp 648–652
2. Fidalgo BV, Najjar VA: The physiological role of the lymphoid system. Biochemistry 6:3386–3392, 1967
3. Opie EL: Intracellular digestion. Physiol Rev 2:552–585, 1922
4. Menkin V: Biochemical Mechanisms of Inflammation. Springfield, Ill, Charles C Thomas, Publishers, 1950
5. Movat HZ, Urihara T, Macmorine DL, Burke JS: A permeability factor released from leucocytes after phagocytosis of immune complexes. Life Sci 3:1025–1032, 1963
6. Melmon K, Cline MJ: Interraction of plasma kinins and granulocytes. Nature (Lond) 213:90–92, 1967
7. Cohn Z, Hirsch J: The isolation and properties of the specific cytoplasmic granules of rabbit polymorphonuclear leukocytes. J Exp Med 112:983–1004, 1960
8. Le Presle C, Webb T: The purification and properties of proteolytic enzymes E and D. Biochem J 84:455–462, 1962
9. Cochrane CG, Aikin BS: Polymorphonuclear leukocytes in immunological reactions. J Exp Med 124:733–752, 1966
10. Greenbaum LM, Yamafuji K: Role of cathepsins in the inactivation of

plasma kinins, Hypotensive Peptides. Edited by EG Erdös, N Back, F Sicuteri. New York, Springer Verlag Publishers, 1966, pp 252–262

11. Idem: The *in vitro* inactivation and formation of plasma kinins by spleen cathepsins. Br J Pharmacol 27:230–238, 1966
12. Greenbaum LM, Kim KS: The kinin forming and kininase activities of rabbit PMN cells. Br J Pharmacol 29:238–247, 1967
13. Greenbaum LM, Freer R, Chang J, Semente G, Yamafuji K: PMN-kinin and kinin metabolizing enzymes in normal and malignant leucocytes. Br J Pharmacol 36:623–635, 1969
14. Chang J, Freer R, Stella R, Greenbaum LM: Studies on leukokinins: formation and chemical properties. Biochem Pharmacol (In press)
15. Freer R, Chang J, Greenbaum LM: Studies on leukokinins: pharmacological properties. Biochem Pharmacol (In press)
16. Greenbaum LM, Nagasawa S: Studies on leukokininogen. Pharmacologist 13:214, 1971
17. Greenbaum LM, Prakash A, Semente G: Studies on leukokininogen in plasma. Fed Proc 31:534, 1972
18. Erdös E: Enzymes that inactivate peptides, Handbook of Experimental Pharmacology, Part 2. Edited by BB Brodie, JR Gillette. New York, Springer Verlag Publishers, 1971, pp 620–653
19. Stewart JM, Roblero J, Ryan JW: Response of the circulatory system to bradykinin and related peptides, Bradykinin and Related Kinins, Vol 8, Advances in Experimental Medicine and Biology. Edited by F Sicuteri, M Rocha e Silva, N Back. New York, Plenum Press Publishers, 1970, pp 175–181
20. Engleman EG, Greenbaum LM: Kinin forming activity of human lymphocytes. Biochem Pharmacol 20:922–924, 1971
21. Umezawa H, Aoyagi T, Morishima H, Matsuzaki M, Hamada M, Takeuchi T: Pepstatin, a new pepsin inhibitor produced by actinomycetes. J Antibiotics 23:259–262, 1970
22. Barrett AJ, Dingle JT: The inhibition of tissue acid proteinases by pepstatin. Biochem J 127:439–441, 1972
23. Dannenberg A Jr: Private communication
24. Steele RH, Wilhelm DL: The Inflammatory reaction in chemical injury. Br J Exp Pathol 51:265–279, 1970
25. Van Arman CG, Risley EA, Kling PJ: Correlation of white cell count and inflammatory swelling induced by carrageenin in the rat's foot. Pharmacologist 13:284, 1971
26. Vinegar R, Macklin AW, Truax JF, Selph JL: Histopathological and pharmacological study of carrageenin inflammation in the rat. Pharmacologist 13:284, 1971
27. Berry HE, Collier JG, Vane JR: The generation of kinins in the blood of dogs during hypotension due to hemorrhage. Clin Sci 39:349–365, 1970

Subacute Spongiform Virus Encephalopathies

Scrapie, Kuru and Creutzfeldt-Jakob Disease: A Review

Peter W. Lampert, MD, D. Carleton Gajdusek, MD and Clarence J. Gibbs, Jr, PhD

THE ENCEPHALOPATHIES to be reviewed here are often quoted as examples of *slow virus diseases.* This term was first used by Sigurdson,[1,2] who studied slowly evolving diseases of sheep in Iceland which, according to their predominant symptoms, are known as maedi (dyspnea), visna (wasting) and rida (trembling). The diseases have in common very long incubation periods, a protracted clinical course and pathologic changes restricted to only one organ—*ie,* the lungs in maedi and the brain in visna and rida. Striking differences exist, however, in regard to histopathology and pathogenesis of these diseases. Meningitis and leukoencephalitis with mononuclear cell infiltrates are characteristic of visna,[3] whereas vacuolar neuronal degeneration and gliosis without leukocytic infiltrates are the hallmark of rida, the Icelandic name for scrapie. Other real or suspected virus diseases with protracted clinical courses but varying pathology have been discussed under the heading *slow virus diseases,*[4,5] a term that would be more meaningful to pathologists if it were restricted to diseases with uniform pathogenesis. This report is confined to a group of encephalopathies with similar histopathology that are caused by infectious agents with unusual characteristics distinct from those of conventional viruses. Scrapie, kuru and Creutzfeldt-Jakob disease have in common: a) transmissibility by injection of infected organs; b) incubation time of several months to years; c) regular, protracted fatal clinical course and d) pathologic changes restricted to the brain and consisting of vacuolar neuronal degeneration and gliosis.

Scrapie

Natural scrapie is a disease of sheep that was already well known in England, Germany and France in the Eighteenth century.[6,7] In North America and Australia, outbreaks of scrapie have been of more

---

From the Department of Pathology, University of California San Diego, La Jolla, Calif and the National Institutes of Health, Bethesda, Md.

Supported by United States Public Health Research Grant NS 09053 from the National Institute of Neurological Diseases and Stroke.

recent date and in Australia were traced to imported Suffolk sheep.[5] The name is derived from the characteristic tendency of the sheep to rub or scratch their flanks against fixed objects. Other clinical signs are reflected in the names used in other countries; the disease is known in Iceland as rida (trembling), in France as la tremblante and in Germany as Wetz (rubbing), Zitter (trembling), Traber (trotting) or Knabber (nibbling) Krankheit. Sheep older than 2 years of age usually are affected; not all animals are equally susceptible. Increased excitability and nervousness are early signs, slowly followed by incoordination, tremor and ataxia. Constant rubbing, presumably due to pruritus, and impaired vision point to sensory disturbances. Nibbling, grinding of teeth and a high stepping gait (cuddy trot) are other outstanding clinical manifestations. Increased thirst, dysfunction of temperature control and cardiovascular instability suggest involvement of the hypothalamus or the autonomic nervous system. Blood and spinal fluid show no abnormalities. The fleece is worn away from constant rubbing; the animals become emaciated and die after an illness lasting for months.

Although it has long been established that the inoculation of brain tissue from affected animals will transfer the disease to other sheep,[9] it is still not clear how natural transmission occurs. Hereditary transmission by an autosomal recessive gene rather than contagion has been claimed on the basis of extensive breeding experiments,[10] but the disease also develops when sheep with normal ancestry are put on farms or pastures from which infected animals had been cleared.[1,8,11] Contact spread of scrapie among sheep is well documented,[12] but evidence of the infectivity of saliva, milk, urine or feces is still lacking.[13] Some reports indicate that blood [14] or serum [15,16] is infective, suggesting that natural transmission may occur after bites or through a vector, such as infected mice or other intermediate host.[12,17]

Experimentally, scrapie has been transmitted to goats,[18,19] mice,[20,21] rats,[22] hamsters,[23] garbils,[24] mink [25] and recently to monkeys.[26] Transfer is achieved by the parenteral injection of scrapie-infected brain emulsions, but can also be accomplished by injecting or feeding other tissues from infected animals. The incubation time varies from several months to years, depending on the species, route of injection and dose.[27] On serial passage in mice after intracerebral injection, the incubation period is reduced to 4 to 6 months, in contrast to the 2 to 5 years required in sheep. After peripheral injection, the scrapie agent can be demonstrated in the spleen and lymph nodes within weeks, but in the brain only after 3 months.[28] After intracerebral inoculation, the virus multiplies rapidly in the brain and after it is inoculated into the thigh, the agent is reported to invade the spinal cord before it spreads to the brain.[28] Variations in clinical course and incubation time also have been observed with particular strains of scrapie virus. *Drowsy* and *scratchy* scrapie have been distinguished in goats.[29] When injected into mice, these strains show differences in incubation time and distribution of lesions.[23] Differences of infectivity have been noted with tissue obtained from diseased Suffolk or Cheviot sheep.[30]

The agent responsible for transmissible mink encephalopathy most likely represents yet another strain of scrapie virus that has been modified after being passed through mink. Outbreaks of this disease, with pathologic changes identical to scrapie, have occurred on mink farms in Wisconsin, presumably after infected meat was fed.[31] The successful transmission of sheep scrapie to mink favors this interpretation.[25] The mink-adapted scrapie strain can be transferred to other species, but the host range differs from that of the mouse-adapted strain.[24,32,33,64]

Significant pathologic changes are always found in the brain in natural and experimental scrapie. Degeneration of skeletal muscle has been described,[34] though not consistently,[35,36] suggesting that this change develops subsequent to neuronal destruction. Adrenal enlargement and pituitary gland atrophy have been recorded in emaciated animals.[5,34] On gross inspection, the brains appear normal, except for some enlargement of the ventricles.[5] By light microscopy, vacuolated neurons within the central nervous system were recognized characteristic changes as early as 1898.[37] Such spongiform alterations in the gray matter associated with intense gliosis, but without leukocytic infiltrates, are pathognomonic for both natural and experimental scrapie.[13,19,23,38] It must be emphasized, however, that status spongiosus and reactive astrocytic proliferation occur in other diseases as well, and it is necessary to use the electron microscope to precisely define the origin of vacuoles in nervous tissue.[39] Astrocytic cytoplasmic swelling due to anoxia (recognized by light microscopy as perivascular and perineuronal vacuoles) may distort the histologic appearance. The presence of artifactitious vacuoles in white matter—*ie*, so called *Buscaino bodies* produced by the dissolution of myelin lamellae, must also be considered.[39]

In scrapie of sheep, the subcortical regions, particularly the medulla, are affected. Involvement of the cerebellum and hypothalamic nuclei has also been stressed.[40] Vacuolation of large nerve cells is an outstanding finding (Figure 1). Damaged neurons show chromatolysis and usually more than one large vacuole in their cytoplasm. Granular material has been detected inside the vacuoles.[41] In experimental scrapie, status spongiosus and gliosis are more pronounced, involving the cerebral cortex as well (Figure 2). The vacuoles, measuring up to 50μ in diameter, are located within the neuropil, within and around nerve cells, but rarely in perivascular regions—*ie*, areas occupied by astrocytes. This is best seen in tissue fixed by perfusion, which reduces the artifacts produced by postmortem anoxia and autolysis. Intense astrocytic gliosis is always present, particularly in advanced stages of the disease when neuronal loss is clearly evident. Astrocytic proliferation, however, has also been recorded as one of the earliest changes visible before neuronal degeneration or status spongiosus appear.[13,19,42] In this regard, the observations by Eklund *et al*[27] and by Field[43] are of particular interest. The authors claim that, after subcutaneous inoculation into the legs of mice, gliosis is first seen in the spinal cord and later in the brain. After injection into the forelimbs, astroglial activation develops first in the cervical region of the cord, whereas the lumbar cord is first involved after the hind limbs are inoculated.[43] Accumulation of lipochrome pigment in neurons and astrocytes, as observed in aging animals, is another feature of scrapie-infected brains. Stellate plaques of fibrillar material, similar to those seen in kuru (as described below), have been observed in the cerebellar cortex.[44,45] Gliosis and myelin digestion in macrophages, secondary to axonal degeneration are seen in the white matter. Primary demyelination does not occur. The absence of leukocytic infiltrates even in severely involved brains is emphasized.

Electron microscopic studies revealed that the status spongiosus corresponds to both swelling and vacuolation predominently of neurons.[46] The extracellular space is not enlarged. The swelling affects focal cytoplasmic areas in which organelles are replaced by finely granular material (Figure 3). The plasma membrane that surrounds the bulging cytoplasm is often ruptured.[46] Curled fragments of membranes accumulate at the sites where rupture occurs. Adjacent neuronal or glial processes, in contact with such altered plasma membranes, show similar cytoplasmic clearings. Fusion of adjacent swollen cells occurs after their respective plasma membranes rupture.[46] Membrane-bounded vacuoles are found in the perikaryal cytoplasm of nerve cells, and in axons and dendrites.[46,47] These vacuoles appear empty or are filled by finely granular material or fragments of membranes. In places, more than one membrane or only membrane fragments demarcate the vacuole from otherwise normal neuronal cytoplasm. Astrocytes occasionally show swelling and herniation of part of their cytoplasm, but vacuolation, as observed in neurons, does not develop in these cells which otherwise contain an increased number of glial filaments, ribosomes and mitochondria. Astrocytic changes of this kind are recognized as nonspecific reactions to injury. The additional finding of corpora amylacea and pigment granules in astrocytes has been interpreted as an aging phenomenon possibly accelerated by the disease.[5,48] Other nonspecific changes consist of axons with granular axoplasm or axonal enlargements filled with dense bodies and mitochondria;[49,50] such axoplasmic alterations are characteristic of degenerating axons.[51] Occasional microglial cells filled with layered arrays of membranes are spectacular findings,[52] but these changes are always seen in macrophages after phagocytosis of myelin debris.[53] Oligodendrocytes show no abnormalities. Except for an increased number of pinocytotic vesicles, the endothelial cells of vessels appear normal.

The search for virus particles thus far has failed to reveal structures that can be definitely identified as viruses. Virus-like particles, measuring about 35 to 40 nm in width, have been found in neuronal processes in experimental [46,54] and natural scrapie.[55] Aggregates of these vesicular and tubular structures are particularly common in dendrites. Visualization of the scrapie agent in explanted or trypsinized cultures of scrapie-infected tissues, in which virus multiplication has been reported,[56] has thus far also been unsuccessful. Filtration experiments indicate that the infectious agent passes filters with a pore size of 47 nm but not 27 nm.[24] An even smaller size has been calculated on the basis of inactivation studies by ionizing irradiation.[57] The agent is unusually resistant to heat.[58] Resistance to formalin,[59] acetylethyleneamine,[60] pepsin and trypsin digestion,[61] DNase, RNase [62] and ultraviolet radiation [63] has been recorded. The virus, however, is sensitive to 95% phenol, chloroethanol, ether, 6 to 8 M urea and periodate.[64] There is no evidence that interferon plays a role in the pathogenesis of scrapie. Interferon levels are unchanged, and responses to other stimuli in infected animals remain the same.[65] Prophylactic treatment of mice with high doses of potent mouse interferon, before and at intervals after exposure to scrapie virus, has no effect on the incubation period or clinical course in mice.[66,67] There is also no proof of any humoral or cellular immune response,[24,68–71] and no changes in the clinical course of scrapie can be demonstrated after immunosuppressive measures.[5,24]

On the basis of these unusual properties, a number of hypotheses concerning the nature of the scrapie virus have been proposed; a replicating agent without nucleic acid,[57] a small nucleic acid core with a large polysaccharide coat,[72] a provirus capable of binding to membranes in the presence of a linkage substance [5] or a replicating membrane.[73] The theories concerned with altered membrances [64] are further supported by observations that subcellular fractions containing membranes, particularly plasma membranes, reveal the highest infectivity.[74,75] The electron microscopic findings of focally altered plasma membranes of neurons and the accumulation of fragments of membranes within vacuolated neuronal processes are also relevant in this regard.[46] Alterations of plasma membranes with incorporation of viral antigen are not inconsistent with the concept of a classic virus, however, nor are some of the other unusual properties—*eg*, influenza virus is inactivated by periodate, polyoma and hepatitis virus can withstand brief exposures to 100 C and the virus of Venezuelan equine encephalomyelitis has remained viable after exposure to 4% formaldehyde.[66] All studies suggest that the genetic information of the scrapie virus is small in size and intimately bound to membranes, which could account for the many atypical properties of the virus.

Kuru

Kuru is a fatal disease found among the Fore and surrounding people in the eastern highlands of New Guinea. The name in Fore language means to shake or shiver from cold or fear. When the first detailed description of the disease by Gajdusek and Zigas[76] became known in 1957, kuru had reached epidemic proportions in some villages. Women, and children of both sexes, were predominately involved. Onset of the disease occurred as early as 4 and as late as 60 years of age. Only the Fore or the surrounding peoples with Fore ancestry were affected. Members of other peoples married to or in close contact with the Fore did not contact the disease. The incidence of kuru has been declining since the early 1960's and is now less than one-third of that during the early years of kuru investigation. Particularly striking is the complete disappearance of kuru among prepubertal children; the age of the youngest patients increases progressively each year.

On the average, the illness lasts about 1 year but may be as short as several months. The patients first become aware of kuru after noting unsteadiness of gait, which may be preceded by headaches and limb pains. Truncal instability, ataxia and tremor of the head and extremities aggravated by cold soon follow. Slurred speech, dysphagia, convergent strabismus, involuntary movements, emotional lability and mild dementia appear in most cases. European journalists were impressed by grin-like distortions of the face and called kuru the laughing disease, which does not at all reflect the native attitude and knowledge of impending death. Hyperactive reflexes with ankle and patellar clonus and disturbances in muscle tone are transient in all cases. Sensory disturbances are rare. Convulsions have not been observed. Blood and spinal fluid show no abnormalities. Terminally, the patients are totally incapacitated, incontinent, flaccid, mute and emaciated. Apparent remissions, while the patient adapts to slight physical disability, have been reported in very slowly evolving kuru, but recoveries have not been proven.[78] Hysterical mimicry of the kuru disease is not uncommon in the area.

No significant morphologic changes are found in organs other than the central nervous system. Grossly, the brains appear normal but in some the frontal lobes or cerebellum may show atrophy.[80] Microscopically there are widespread neuronal degeneration and gliosis.[79-81] The degenerating neurons may be swollen and vacuolated. Argentophilic axonal enlargements (torpedos) of degenerating Purkinje cells have been described.[81,82] Vacuoles around neurons and within the neuropil are not always prominent, but astrocytic proliferation is intense. Microglial clusters are noted about degenerating neurons. Although mild perivascular infiltrates of lymphocytes have been recorded, they are rare. The changes are found throughout the grey matter, without any well-defined pattern, and involve, most consistently, the cerebellum, pons, thalamus and basal ganglia; changes are also diffuse or patchy in the cerebral cortex (Figure 4) and anterior horns of the spinal cord.[81] Secondary axonal degeneration accompanied by a breakdown of myelin is noted in the cerebral white matter and in corticospinal and spinocerebellar tracts.

Stellate plaques with the histochemical and optical properties of amyloid have been described in many kuru brains, including those from children.[80-82] The plaques are most frequently found in the granular and Purkinje cell layer of the cerebellum (Figure 6) but they also occur in other regions of the brain.[83] By electron microscopy, the plaques consist of bundles of fibrils that radiate peripherally into tissue filled with glial processes (Figure 7). The fibrils measure about 10 nm in width and their microtubular nature is apparent at high resolution.[5,84] Granular densities and peculiar herringbone structures have been noted within the plaques.[5,85] These latter structures are suggestive of the Hirano bodies observed in Pick's disease,[86] the Parkinsonism-dementia complex and in amyotrophic lateral sclerosis on Guam.[87] Since the few published electron micrographs of kuru plaques have all been made on poorly preserved tissue, it is not possible, at present, to discuss the identity or differences between these plaques and the amyloid plaques that are prominent in senile dementia and Alzheimer's disease.[88]

The similarities of the histopathologic and clinical features of kuru to those of scrapie suggested the possibility of an infectious etiology.[89] Brain suspensions from kuru patients were inoculated into many species of subhuman primates and a wide variety of domestic and smaller laboratory animals.[90] After incubation periods varying from 18 to 38 months, the first 8 chimpanzees, each inoculated intracerebrally with a brain suspension from a different patient with kuru, came down with a kuru-like disease.[90,91] Second passages of brain tissue from afflicted to healthy chimpanzees reduced the incubation period to about 1 year.[92] The animals develop postural instability and ataxia. The gait becomes clumsy, hand movements dysmetric and falls are frequent. Soon they become unable to sit up without support and must be hand fed. The illness may last from 4 to 11 months. Kuru has now been transmitted to more than 40 chimpanzees and routes of inoculation other than intracerebral have produced disease.[66] Transfer of kuru to spider, capuchin, squirrel, marmoset and rhesus monkeys has also been successful.[93-95]

The pathology of experimental kuru differs from human kuru in that the status spongiosus of the cerebral cortex is more consistently severe (Figure 5), swollen neurons with argentophilic intracytoplasmic spheroids are present and stellate plaques absent.[96,97] Otherwise the resemblance is close. The brains show no gross abnormalities. Widespread status spongiosus and gliosis are present throughout the gray matter, involving, in order of decreasing severity, the cerebral cortex, basal ganglia, cerebellum, brain stem and spinal cord. In the most severely affected regions, an occasional vessel may contain a few lymphocytes in the perivascular space, but as a rule leukocytic infiltrates are absent. Gliosis of the white matter, secondary to axonal degeneration, is seen in advanced stages of the disease. No evidence of primary demyelination is recorded.

Electron microscopic studies show that the status spongiosus, like that in scrapie, corresponds to both neuronal swelling and vacuolation.[97] Nerve cells show focal cytoplasmic clearings or herniations of clear cytoplasm bounded by plasma membranes that may be ruptured in a few places. Membrane-bounded vacuoles containing fragments of curled membranes are observed within the perikaryal cytoplasm (Figure 8), dendrites (Figure 10) and axons. The fragments of membranes appear to be derived from the membrane that surrounds the intraneuronal vacuoles (Figure 9). Glial and neuronal processes in contact with plasma membranes of a focally swollen neuronal process are often similarly affected. Occasional swollen astrocytes are encountered, but as a rule these cells are filled with abundant filaments, ribosomes and mitochondria, which is consistent with the appearance of reactive astrocytes. Filaments with a helical ultrastructure have been observed in astrocytes in the cerebellum, but they have also been encountered in normal chimpanzees.[5] Increased amounts of lipochrome pigment, as well as myelin debris, are further noted within proliferated astrocytes. Degenerating axons characterized by granular axoplasmic disintegration or by enlargements filled with floccular dense bodies and mitochondria are numerous.

In the deeper layers of the cerebral cortex, nerve cells with swollen cytoplasm and eccentric displacement of the nucleus are easily seen (Figure 11). The cytoplasm of these cells is either diffusely argentophilic (Figure 12) or it contains a well-defined spheroid inclusion (Figure 13). The fine structure of these cells varies in regard to the number of randomly oriented tubules. Cells with few tubules contain abundant cisterns and vesicles of smooth endoplasmic reticulum which loosely aggregate in the center of swollen perikaryal cytoplasm that otherwise shows diffuse dispersion of the Nissl substance, consistent with the appearance of a nerve cell reacting to injury to its processes. Cells, which by light microscopy reveal an argentophilic spheroid inclusion in their cytoplasm, are filled with abundant, randomly oriented tubules that condense in the center of the perikaryl cytoplasm (Figure 14). The peripheral cytoplasmic rim contains normal neuronal organelles. The tubules are straight, about 20 to 25 nm wide and of indefinite length (Figure 15). Similar argentophilic spheroids formed by randomly oriented neurotubules are found in degenerating neurons in Pick's presenile dementia.[98] It has been suggested that these inclusions develop in nerve cells as a response to axonal or dendritic injury.[99] After axonal section, nerve cells swell, the endoplasmic reticulum disperses and proliferates, and, at later stages, tubules and filaments become prominent.[100] Injury to dendrites and, to a lesser degree, to axons, is certainly striking in experimental kuru, which could account for reactive changes in parent nerve cells.

Data on the nature of the kuru agent are slowly accumulating.[66] The virus has passed filters with a pore size of 450 to 220 nm. Chimpanzees inoculated with filtrates that passed through 100, 79 and 50 nm Millipore filters have not yet come down with kuru. The virus has survived freezing and lyophilization, storage at −70 C and heat treatment at 80 C for 30 minutes. The virus has been maintained for long periods of time *in vitro* in explant cultures of affected chimpanzee brains without losing its virulence for the chimpanzee.[101] The difficulty in finding a specific virus is best reflected by the observation that more than 100 different virus strains have thus far been isolated from organs of affected chimpanzees.[102–105]

Experimental kuru has been transferred to other chimpanzees by inoculating tissues other than the brain.[66] Peroral administration has thus far failed to induce disease in chimpanzees. Natural transmission is believed to be related to the mourning rituals of the Fore people, which consisted of cannibalistic consumption of their dead relatives.[77,106] Women and children who were engaged in the preparation of food could have become infected by selfinoculation through abrasions or cuts, or from nasal or conjunctival inoculation. In contrast to men, they also consumed the less well-cooked offal, including the brain; this could further account for the striking predominance of afflicted women and children of both sexes.[77,107] In addition to this mode of transmission, a genetic predisposition may exist.[108–109] Under pressure by Western civilization these mourning rituals have been abandoned, and kuru is now mainly a disease of adults who had become infected many years ago. If these transmission theories are correct, kuru should die out in New Guinea, and the current trend indicates that this is occurring.

Creutzfeldt-Jakob Disease

In 1920 Creutzfeldt[111] published the case of a 23-year-old girl who developed incoordination of gait, later followed by jerky movements, exaggerated reflexes, ankle clonus and abnormal behavior. Terminally, the girl was unable to stand and walk, showed nystagmus and myoclonic movements, spasticity of limbs, mental disturbances and finally coma. Histologic examination of the brain revealed widespread, patchy degeneration of nerve cells, neuronophagia and astrocytic proliferation. The changes were interpreted as a noninflammatory cell disease of the grey matter.

In 1921 Jakob[112] reported 4 middle-aged patients affected with a disease characterized by cortical dysfunction, pyramidal and extrapyramidal signs which terminated in death after a steadily progressive clinical course that averaged about 9 months. The histopathology of these cases was similar to the one described by Creutzfeldt, showing neuronal degeneration and gliosis in the cerebral cortex, basal ganglia, thalamus and the motor nuclei of cranial and spinal nerves.

Jakob recognized that these cases formed an entity that, on the basis of clinical and pathologic findings, could be separated from vascular, inflammatory, senile or other degenerative brain diseases.

In 1968, Kirschbaum[113] published a monograph with a detailed account of 150 cases. Roos *et al*[114] reported the clinical characteristics of another 47 patients, including cases whose inoculated brain tissue transmitted the same disease to primates. Most patients of both sexes are 40 to 60 years of age when they die after an illness that lasts approximately 1 year. Rare familial cases are recorded. The disease begins with vague complaints of anxiety, fatigue, inability to concentrate and speech and gait disturbances which are followed after several weeks by the classic triad of cortical, pyramidal and extrapyramidal dysfunctions. Myoclonic and epileptic seizures occur. Variations of the clinical symptomatology are described. The largest group of patients show diffuse involvement of the cerebral cortex and basal ganglia as well as changes in the thalamus, cerebellum, brain stem and spinal cord. Some patients show particular involvement of the occipitoparietal cortex (Heidenhain's agnostic visual type), some of the pyramidal system (Jakob's pseudosclerosis) and others of the cerebellum (ataxic type).[115] Examinations of blood, urine and serum are unrevealing. Spinal fluid studies are negative in the majority of patients but moderate increases in pressure and proteins are occasionally observed. Pneumoencephalography reveals air accumulation over the frontal and occipital lobes and dilatation of lateral ventricles. Electroencephalography shows periodic paroxysmal bursts of spike-wave discharges against a slow background, a valuable, though nonspecific, diagnostic aid. A brain biopsy of the cerebral cortex can confirm the diagnosis.

Except for slight atrophy, the gross appearance of the brain is unremarkable. Widespread status spongiosus in the grey matter (Figure 16) and intense gliosis (Figure 17) are characteristic light microscopic findings. Astrocytic proliferation may be seen in areas that show little or no neuronal degeneration. The vacuoles, occasionally as large as 50μ, are located within the neuropil, within and around neurons. The deeper layers of the cortex are usually involved more severely. Neuronal loss is often patchy. Microglial clusters about degenerating nerve cells are observed. Swollen neurons with eccentric nuclei—*ie*, cells reacting to axonal or dendritic injury—have been described in the original cases and later also in others,[116,117] but these changes are not always present. An excessive amount of lipochrome pigment, as demonstrated by the periodic acid-Schiff reaction, is observed in nerve cells and astrocytes. Loss of granule cells and degenerating Purkinje cells with axonal swellings are noted in the cerebellum. Gliosis, occasional swollen or vacuolated nerve cells and microglial clusters are found in the basal ganglia, brain stem and spinal cord. In exceptional cases, plaques, similar to those observed in the cortex in Alzheimer's disease and in the cerebellum in kuru, have been described.[118-120] Myelin breakdown in the white matter occurs secondary to axonal degeneration. There are no abnormal vessels or perivascular leukocytic infiltrates.

Electron microscopic studies on human biopsies contributed the following facts. The status spongiosus corresponds to swollen neuronal and atrocytic processes as well as membrane-bounded vacuoles within cells.[121-124] There is no enlargement of the extracellular space. Cytoplasmic clearings and herniation of focally swollen cytoplasm of both neurons and astrocytes, similar to those observed in experimental scrapie,[46] kuru [97] and mink encephalopathy,[25] are recognized as characteristic alterations.[121] Clusters of swollen neuronal and astrocytic processes [124] mimic precisely the changes seen in the experimental conditions.[46,125] Evidence suggestive of an accumulation of abnormal membranes in vacuolated processes has also been reported.[126] Astrocytic processes filled with glycogen granules, abundant filaments, mitochondria and pigment granules are numerous. These alterations are commonly seen in reactive astrocytes. An excessive amount of lipochrome pigment in both neurons and astrocytes are recorded. Axonal alterations, consisting of granular distintegration of axoplasmic organelles or of accumulations of mitochondria and floccular dense bodies, are other nonspecific changes indicative of axonal degeneration.[51] Virus-like particles of various size and shape have been described,[127,128] but their significance is questionable. Membrane-bounded particles, measuring 80 to 120 nm, are not uncommon in astrocytes; they have been described in a variety of other conditions.[129] Similar structures resembling papova viruses are easily confused with glycogen particles, and tubular structures, when observed in neuronal processes, must be distinguished from aggregates of neurotubules.[51]

In the original report on the histopathology of kuru, Klatzo *et al* [81] drew attention to the similarity between kuru and Creutzfeldt-Jakob disease. After the successful transmission of kuru to chimpanzees,[91,92] similar experiments were started using brain suspensions from patients with Creutzfeldt-Jakob disease. Thirteen months after intracerebral inoculation the first chimpanzee became increasingly somnolent and inactive. He developed ataxia, truncal titubation, intention tremor, myoclonus, hemiparesis and visual impairment. No abnormalities were detected in the blood or spinal fluid during th course of the illness. The moribund animal was sacrificed 2 months after the symptoms appeared. Changes in the brain of the chimpanzee closely resembled those seen in the patient from whom the inoculum was obtained.[117,130,131] Primary passage from 14 patients from England, France, Canada and the United States has now been established.[66,132] The major clinical features are somnolence, ataxia, tremor, myoclonus, fasciculation, visual disturbances and apparent dementia. In contrast to experimental kuru, in which incubation periods have ranged from 14 to 38 months and clinical disease from 3 to 11 months, experimental Creutzfeldt-Jakob disease develops after incubation periods of from 11 to 14 months, and the chimpanzees are moribund after an illness lasting from 1 to 2½ months. Secondary passage from chimpanzee to chimpanzee has been accomplished but without reduction of the incubation time.[131] Transmission of the disease to some species of New World monkeys after an incubation period of 23 to 29 months has also been achieved.[94] The experiments are conducted in different primate centers, widely separated from each other, in different parts of the USA, a fact which excludes the possibility of contact spread. Control animals that were simultaneously inoculated with brain suspensions from patients with other neurologic disease have not become ill.[66]

The pathology is essentially similar to that observed in chimpanzees afflicted with experimental kuru, except for less striking neuronal loss and status spongiosus in the cerebral cortex (Figure 18). In some animals the neurons of the basal ganglia, hypothalamus, brain stem and spinal cord show more prominent involvement (Figure 19). Astrocytic, as well as microglial, proliferation is observed throughout the damaged grey matter. An excessive amount of lipochrome pigment is seen in astrocytes and nerve cells. Swollen nerve cells with pale cytoplasm, sometimes containing an argentophilic spheroid inclusion, are found particularly in the deeper layers of the cortex.[117,125] These cells resemble those seen in man in Creutzfeldt-Jakob and Pick's disease and in experimental kuru in the chimpanzee (Figures 11–13). Such changes are nonspecific and known to develop in nerve cells in response to an injury to axons or dendrites.

Electron microscopic studies on the cerebral cortex of chimpanzees afflicted with Creutzfeldt-Jakob disease reveal the same findings as observed in scrapie and kuru.[125] The cytoplasm of neurons, in particular, their dendritic processes, and, to a lesser degree, astrocytes show focal clearings. Clusters of swollen neuronal and glial processes are observed. Plasma membranes that separate two adjacent swollen cells are frequently disrupted. Abnormal arrays of curled fragments of membranes accumulate at the sites of rupture. The altered membranes reveal the triple-layered structure of unit membranes, but they are more intensely osmiophilic when compared to normal plasma membranes. Membrane-bounded vacuoles are found predominently in dendrites. The vacuoles may be filled with finely granular material or with aggregates of curled membranes. Phagocytosis of swollen or vacuolated processes have been observed.[125] Vacuoles have, thus far, not been noted within astrocytes which, apart from focal swelling, reveal all of the features characteristic of reactive, proliferating cells. These findings suggest that the infectious agent damages the plasma membrane of both neurons and astrocytes, but in contrast to neurons which undergo vacuolar degeneration, astrocytes recover and respond by proliferation.

Little information is available, at present, regarding the properties of the virus causing Creutzfeldt-Jakob disease. It is known that the agent passes through a Millipore filter of 220 nm and that it remains stable when stored at −70 C. The virus also persists for many months *in vitro* in tissue cultures of human brain cells without losing its virulence in the chimpanzee.[101] No serologic relationship of the disease in man and animal could be demonstrated by complement-fixing antibody tests directed at a large spectrum of known viruses.[133] Studies are in progress to determine the presence and quantity of virus in brain and other organs of man and chimpanzees affected with Creutzfeldt-Jakob disease and to determine the size and stability of the virus.[66]

Summary

Scrapie, kuru and Creutzfeldt-Jakob disease are transmissible diseases caused by atypical viruses with unusual properties that implicate plasma membranes as essential structural components. After incubation periods lasting from months to years, a slowly progressive, always fatal disease develops that causes damage only in the brain, even though the infectious agent is present in other organs as well. The neuropathologic changes in man and animal in all three conditions are similar, differing only in the distribution and severity of lesions. The encephalopathies are characterized by widespread status spongiosus and gliosis of the grey matter. Neurons and astrocytes show focal clearing and herniation of swollen cytoplasm. Cells in contact with swollen neuronal processes show similar changes. Fu-

sion of the clear cytoplasmic portions of injured cells occurs after rupture of adjacent plasma membranes. Fragments of curled membranes accumulate at the points of rupture. Membrane-bounded vacuoles develop in neurons, particularly in dendrites. These vacuoles contain finely granular material or aggregates of curled membranes. Astrocytes react to the injury by proliferation, whereas neurons degenerate. The lack of leukocytic infiltrates, even in advanced stages of the disease, is remarkable, as is the failure to demonstrate evidence of an immune response.

References

1. Sigurdson B: Rida, a chronic encephalitis of sheep. With general remarks on infections which develop slowly and some of their special characteristics. Br Vet J 110:341–354, 1954
2. Sigurdson B, Palsson PA, Grimson H: Visna, a demyelinating transmissible disease of sheep. J Neuropathol 16:389–403, 1957
3. Sigurdson B, Palsson PH: Visna of sheep, a slow demyelinating infection. Br J Exp Pathol 39:519–528, 1958
4. Gajdusek DC, Gibbs CJ Jr, Alpers M: Slow, latent and temperate viruses. Washington, DC, US Government Printing Office, National Institute of Neurologic Disease and Blindness Monograph 2, Public Health Service Publication 1379, 1965
5. Field EJ: Slow virus infection of the nervous system. Int Rev Exp Pathol 8:129–239, 1969
6. Stockman S: Scrapie: An obscure disease of sheep. J Comp Pathol 26:317–327, 1913
7. M'Gowan JP: Investigations into the disease of sheep called scrapie. Edinburgh, Blackwood, 1914
8. Gordon WS: Transmission of scrapie and evidence of spread of infection in sheep on pasture. Scrapie Seminar, US Department of Agriculture Agricultural Research Service 91–53:8–18, 1966
9. Cuillé J, Chelle PL: La maladie dite tremblante du mouton est-elle inoculable? Compt Rend Acad Sci 203:1552–1554, 1936
10. Parry HB: Scrapie—natural and experimental, Virus Diseases of the Nervous System. Edited by JT Hughes, CWH Whitty, FO MacCallum. Oxford, Blackwell Scientific Publications, 1969, pp 99–105
11. Greig JR: Scrapie in sheep. J Comp Pathol 60:263–266, 1950
12. Brotherton JG, Renwick DG, Stamp JT, Zlotnik I, Pattison IH: Spread of scrapie by contact to goats and sheep. J Comp Pathol 78:9–17, 1968
13. Pattison IH: Experiments with scrapie with special reference to the nature of the scrapie agent and the pathology of the disease. Washington, DC, US Government Printing Office, National Institute of Neurologic Disease and Blindness Monograph 2, US Public Health Service Publication 1378, 1965, pp 249–251
14. Field EJ, Caspary EA, Joyce G: Scrapie agent in blood. Vet Rec 83:109–110, 1968

15. Clarke MC, Haig DA: Presence of the transmissible agent of scrapie in the serum of affected mice and rats. Vet Rec 80:504, 1967
16. Gibbs CJ Jr, Gajdusek DC, Morris JA: Viral characteristics of the scrapie agent in mice.[4] pp 195–222
17. Field EJ, Adams DH: Riley virus in wild mice. Lancet 1:868, 1968
18. Pattison IH, Gordon WS, Millson GC: Experimental production of scrapie in goats. J Comp Pathol 69:300–312, 1959
19. Hadlow WJ: The pathology of experimental scrapie in the dairy goat. Res Vet Sci 2:289–314, 1961
20. Chandler RL: Encephalopathy in mice produced by inoculation with scrapie brain material. Lancet 1:1378–1379, 1961
21. Morris JH, Gajdusek DC: Encephalopathy in mice following inoculation of scrapie sheep brain. Nature (Lond) 197:1084–1086, 1963
22. Chandler RL, Fisher J: Experimental transmission of scrapie to rats. Lancet 2:1165, 1963
23. Zlotnik I: The pathology of scrapie.[8] pp 213–224
24. Gibbs CJ Jr, Gajdusek DC: Characterization and nature of viruses causing subacute spongiform encephalopathies. Sixth International Congress of Neuropathology, Paris, Masson et Cie, 1970, pp. 779–817
25. Hanson RP, Eckroade RJ, Marsh RF, ZuRhein, GM, Kanitz CL, Gustafson DP: Susceptibility of mink to sheep scrapie. Science 172:859–861, 1971
26. Gibbs CJ Jr, Gajdusek DC: Transmission of scrapie to the cynomolgus monkey (*Macaca fascicularis*). Nature 236:73–74, 1972
27. Eklund CM, Hadlow WJ, Kennedy RC: Some properties of the scrapie agent and its behavior in mice. Proc Soc Exp Biol Med 112:974–979, 1963
28. Eklund CM, Kennedy RC, Hadlow WJ: Pathogenesis of scrapie virus in the mouse. J Infect Dis 117:15–22, 1967.
29. Pattison IH, Millson GC: Scrapie experimentally produced in goats with special reference to the clinical syndrome. J Comp Pathol 71:171–176, 1961
30. Zlotnik I, Rennie JC: Further observations on the experimental transmission of scrapie from sheep and goats to laboratory mice. J Comp Pathol 75:147–157, 1965
31. Hartsough GR, Burger D: Encephalopathy of mink. I. Epizoologic and clinical observations. J Infect Dis 115:387–392, 1965
32. Marsh RF: Studies on transmissible mink encephalopathy. PhD Thesis, University of Wisconsin, 1968
33. Marsh RF, Burger D, Eckroade R, ZuRhein GM, Hanson RP: A preliminary report on the experimental host range of the transmissible mink encephalopathy agent. J Infect Dis 120:713–719, 1969
34. Bosanquet FD, Daniel PM, Parry HB: Myopathy in sheep. Its relationship to scrapie and to dermatomyositis and muscular dystrophy. Lancet 27:737–745, 1956
35. Hulland TJ: The skeletal muscle of sheep affected with scrapie. J Comp Pathol 68:264–274, 1956
36. Beck E, Daniel PM, Parry HB: Natural (spontaneous) scrapie in sheep with particular reference to the neuromuscular system.[8] pp 108–117

37. Besnoit C, Morel C: Note sur les lesions nerveuses de la tremblante du mouton. Compt Rend Soc Biol 5:536–538, 1898
38. Bertrand I, Carre H, Lucam F: La tremblante du mouton (recherches histopathologiques). Ann Anat Pathol 14:565–586, 1937
39. Adornato B, Lampert P: Status spongiosus of nervous tissue. Electron miscroscopic studies. Acta Neuropathol 19:271–289, 1971
40. Beck E, Daniel PM, Parry HB: Hypothalamic and cerebellar system degeneration in sheep with "scrapie." Proceedings of the Fourth Internanational Congress of Neuropathology, Munich, 3:269–274, 1961
41. Holman HH, Pattison IH: Further evidence on the significance of vacuolated nerve cells in the medulla oblongata of sheep affected with scrapie. J Comp Pathol 53:231–236, 1943
42. Pattison IH, Smith I: Histologic observations on experimental scrapie in the mouse. Res Vet Science 4:269–275, 1963
43. Field EJ: Invasion of the nervous system by "slow" virus. A study with scrapie agent. Pathogenesis and etiology of demyelinating diseases. Edited by E Pette, O Westphal. New York, S. Karger, 1969, pp 568–573
44. Beck E, Daniel PM: Kuru and scrapie compared: are they examples of system degeneration? [4] pp 85–93
45. Beck E, Daniel PM: Observations on the pathology of experimentally produced scrapie.[4] pp 203–206
46. Lampert P, Hooks J, Gibbs CJ Jr, Gajdusek DC: Altered plasma membranes in experimental scrapie. Acta Neuropathol 19:81–93, 1971
47. Bignami A, Parry HB: Electron microscopic observations in slow virus infections of the central nervous system.[24] pp 933–934
48. Field EJ, Raine CS, Joyce G: Scrapie in the rat. An electron-microscopic study. I. Amyloid bodies and deposits. Acta Neuropathol 8:47–64, 1967
49. Chandler RL: Ultrastructural pathology of scrapie in the mouse. An electron microscopic study of the spinal cord and cerebellar areas. Br J Exp Pathol 49:52–59, 1968
50. Field EJ, Raine CS: An electron microscopic study of scrapie in mice. Acta Neuropathol 4:200–211, 1964
51. Lampert P: A comparative electron microscopic study of reactive degenerating, regenerating and dystrophic axons. J Neuropathol Exp Neurol 26:345–346, 1967
52. Field EJ, Raine CS, Joyce G: Scrapie in the rat. II. Glial inclusions. Acta Neuropathol 9:305–315, 1967
53. Lampert P, Cressman M: Fine structural changes of myelin sheaths after axonal degeneration in the spinal cord of rats. Am J Pathol 49:1139–1155, 1966
54. David-Ferreira JR, David-Ferreira KL, Gibbs CJ Jr, Morris JA: Scrapie in mice. Ultrastructural observations in the cerebral cortex. Proc Soc Exp Biol 127:313–320, 1968
55. Bignami A, Parry HB: Aggregations of 35 nanometer particles associated neuronal cytopathic changes in natural scrapie. Science 171:389–390, 1971
56. Haig DA, Clark ML: Multiplication of the scrapie agent. Nature 234: 106–107, 1971

57. Alper T, Haig DA, Clarke MC: The exceptionally small size of the scrapie agent. Biochem Biophys Res Commun 22:278–284, 1966
58. Hunter GD, Millson GC: Studies on the heat stability and chromatographic behaviour of the scrapie agent. J Gen Microbiol 37:251–258, 1964
59. Hunter GD: The size and intracellular location of the scrapie agent. Biochem J 114:22, 1969
60. Stamp JT, Brotherton JG, Zlotnik I, MacKay JMK, Smith W: Further studies on scrapie. J Comp Pathol 69:268–280, 1959
61. Haig DA, Clarke MC: Observations on the agent of scrapie.[13] pp. 215–219
62. Gibbs CJ Jr: Search for infectious etiology in chronic and subacute degenerative disease of the central nervous system, Current Topics in Microbiology and Immunology. Vol 40. New York, Springer Verlag. 1967, pp 44–48
63. Haig DA, Clarke MC, Blum E, Alper T: Further studies on the inactivation of the scrapie agent by ultraviolet light. J Gen Virol 5:455–460, 1969
64. Hunter GD: Biochemical properties and nature of the scrapie agent.[24] pp 802–817
65. Katz M, Koprowski H: Failure to demonstrate a relationship between scrapie and production of interferon in mice. Nature 219:639–640, 1968
66. Gibbs CJ Jr, Gajdusek DC: Transmission and characterization of spongiform virus encephalopathies: kuru, Creutzfeldt-Jakob disease, scrapie and mink encephalopathy, Immunological Diseases of the Nervous System. Res Publ Assoc Res Nerv Ment Dis 49:383–410, 1971
67. Gresser I, Pattison IH: An attempt to modify scrapie in mice by the administration of interferon. J Gen Virol 3:395–397, 1968
68. Chandler RL: Attempts to demonstrate antibodies in scrapie disease. Vet Rec 71:58–59, 1959
69. Clarke MC, Haig DA: Attempt to demonstrate neutralizing antibodies in the sera of scrapie-affected animals. Vet Rec 78:647–649, 1966
70. Gardiner AC: Gel diffusion reactions of tissues and sera from scrapie affected animal. Res Vet Science 7:190–195, 1965
71. Albrecht P: Immune status of the organism during experimental scrapie infection.[24] pp 833–834
72. Adams DH, Caspary EA: Nature of the scrapie virus. Br Med J 3:173, 1967
73. Gibbons RH, Hunter GD: Nature of the scrapie agent. Nature 215:1041–1043, 1967
74. Millson GC, Hunter GD, Kimberlin RH: An experimental examination of the scrapie agent in cell membrane mixtures. II. The association of scrapie activity with membrane fractions. J Comp Pathol 81:255–265, 1971
75. Kimberlin RH, Millson GC, Hunter GD: An experimental examination of the scrapie agent in cell membrane mixture. III. Studies on operational size. J Comp Pathol 81:383–391, 1971
76. Gajdusek DC, Zigas V: Degenerative disease of the central nervous system in New Guinea. The endemic occurrence of kuru in the native population. N Engl J Med 257:974–978, 1957
77. Alpers M: Kuru: Clinical and etiological aspects, Virus Diseases and the Nervous System.[10] pp 83–97

78. Hornabook RW: Kuru—a subacute cerebellar degeneration. The natural history and clinical features. Brain 9:53–74, 1968
79. Fowler M, Robertson EG: Observations on kuru. III. Pathological features in five cases. Aust Ann Med 8:16–26, 1959
80. Neuman M, Gajdusek DC, Zigas V: Neuropathologic findings in exotic neurologic disorders among natives of New Guinea. J Neuropathol Exp Neurol 23:486–507, 1964
81. Klatzo I, Gajdusek DC, Zigas V: Pathology of kuru. Lab Invest 8:799–847, 1959
82. Beck E, Daniel PM, Alpers M, Gajdusek DC, Gibbs CJ Jr: Neuropathological comparisons of experimental kuru in chimpanzees with human kuru: Pathogenesis and etiology of demyelinating diseases. Int Arch Allergy 36: 553–562, 1969
83. Kakulas BA, Lecours AR, Gajdusek DC: Further observations on pathology of kuru. J Neuropathol Exp Neurol 26:85–97, 1967
84. ZuRhein GM: Discussion: Pathogenesis and Etiology of Demyelinating Disease. Int Arch Allergy 36:604–606, 1969
85. Field EJ, Mathews JD, Raine CS: Electron microscopic observations on the cerebellar cortex in kuru. J Neurol Science 8:209–224, 1969
86. Schochet SS Jr, Lampert PW, Lindenberg R: Fine structure of the Pick and Hirano bodies in the case of Pick's disease. Acta Neuropathol 11:330–337, 1968
87. Hirano A, Dembitzer HE, Kurland LT, Zimmerman HM: The fine structure of some intraganglionic alterations. Neurofibrillary tangles, granulovacuolar bodies and "rod-like" structures as seen in Guam amyotrophic lateral sclerosis and Parkinsonism-dementia complex. J Neuropathol Exp Neurol 27:167–182, 1968
88. Terry RD, Gonatas NK, Weiss M: Ultrastructural studies in Alzheimer's presenile dementia. Am J Pathol 44:269–297, 1964
89. Hadlow WJ: Scrapie and kuru. Lancet 2:289–290, 1959
90. Gibbs CJ Jr, Alpers M, Gajdusek DC: Attempts to transmit subacute and chronic neurological disease to animals. With a progress report on the experimental transmission of kuru. Pathogenesis and etiology of demyelinating diseases. Int Arch Allergy 36:519–552, 1969
91. Gajdusek DC, Gibbs CJ Jr, Alpers M: Experimental transmission of a kuru-like syndrome to chimpanzees. Nature 209:794–796, 1966
92. Gajdusek DC, Gibbs, CJ Jr, Alpers M: Transmission and passage of experimental kuru to chimpanzees. Science 155:212–214, 1967
93. Gajdusek DC, Gibbs CJ Jr, Asher DM, David E: Transmission of experimental kuru to the spider monkey. Science 162:693–694, 1968
94. Gajdusek DC, Gibbs CJ Jr: Transmission of two subacute spongiform encephalopathies of man (kuru and Creutzfeldt-Jakob disease) to New World monkeys. Nature 230:588–581, 1971
95. Gajdusek DC, Gibbs CJ Jr: Primary transmission of kuru to the rhesus monkey. Unpublished data
96. Beck E, Daniel PM, Alpers M, Gajdusek DC, Gibbs CJ Jr: Experimental kuru in chimpanzees. A pathological report. Lancet 2:1056–1059, 1966
97. Lampert PW, Earle KM, Gibbs CJ Jr, Gajdusek DC: Experimental kuru

encephalopathy in chimpanzees and spider monkeys. J Neuropathol Exp Neurol 28:353–370, 1969

98. Wisniewski HM, Coblentz JM, Terry RD: Pick's disease, a clinical and ultrastructural study. Arch Neurol 26:97–108, 1972
99. Williams HW: The peculiar cells of Pick's disease. Arch Neurol Psychiat 34:508–519, 1935
100. Pannese E: Investigations on the ultrastructural changes of the spinal ganglion neurons in the course of axon regeneration and cell hypertrophy. Z Zellforsch Mikrosk Anat. 60:711–740, 1963
101. Gajdusek DC, Gibbs CJ Jr, Rogers NG, Basnight M, Hooks J: Persistence of viruses of kuru and Creutzfeldt-Jakob disease in tissue cultures of brain cells. Nature 235:104–105, 1972
102. Gajdusek DC, Rogers NG, Basnight M, Gibbs CJ Jr, Alpers M: Transmission experiments with kuru in chimpanzees and the isolation of latent viruses from the explanted tissue of affected animals. Ann NY Acad Sci 162: 529–550, 1969
103. Rogers NC, Basnight M, Gibbs CJ Jr, Gajdusek DC: Latent viruses in chimpanzees with experimental kuru. Nature 216:446–449, 1967
104. Basnight M, Rogers NG, Gibbs CJ Jr, Gajdusek DC: Characterization of four new adenovirus serotypes isolated from chimpanzee tissue explants. Am J Epidemiol 94:166–171, 1971
105. Hooks J, Gibbs CJ Jr, Cutchins EL, Rogers NG, Lampert P, Gajdusek DC: Characterization and distribution of two new foamy viruses isolated from chimpanzees. Arch Virusforsch, 1972 (In press)
106. Glasse RM: Cannibalism in the kuru region of New Guinea. Trans NY Acad Sci (Series 2) 29:748–754, 1967
107. Sorenson ER, Gajdusek DC: Nutrition in the kuru region. I. Gardening, food handling and diet of the Fore people. Acta Tropica Separatum 26: 281–330, 1969
108. Bennett JH, Rhodes FA, Robson HN: A possible genetic basis for kuru. Am J Hum Genet 11:169–187, 1959
109. Gajdusek DC, Alpers M: Genetic studies in relation to kuru. I. Cultural and historical background. Am J Hum Genet, 1972 (In press)
110. Wiesenfeld SL, Ferber RA, Gajdusek DC: Genetic studies in relation to kuru, VII. Genetic differentials among kuru and normal Fore. Unpublished data
111. Creutzfeldt HG: Uber eine eigenartige herdförmige Erkrankung des Zentralnervensystems. Z Gesamt Neurol Psychiat 57:1–18, 1920
112. Jakob A: Uber eigenartige Erkrankungen des Zentralnervensystem mit bemerkenswerten anatomischen Befunden. Z Gesamt Neurol Psychiat 64:147–228, 1921
113. Kirschbaum WR: Jakob-Creutzfeldt Disease. New York, American Elsevier Publishing Company, Inc, 1968
114. Roos R, Gajdusek DC, Gibbs CJ Jr: The clinical characteristics of transmissible Creutzfeldt-Jakob disease. Brain, 1972 (In press)
115. Brownwell B, Oppenheimer DR: An ataxic form of subacute presenile polioencephalopathy (Creutzfeldt-Jakob Disease). J Neurol Neurosurg Psychiat 28:350–361, 1965

116. Jansen J, Monrad-Krohn GH: Uber die Creutzfeldt-Jakobsche Krankheit. Z Neurol Psychiat 163:670–704, 1938
117. Beck E, Daniel PM, Matthews WB, Stevens DC, Alpers MP, Asher DM, Gajdusek DC, Gibbs CJ Jr: Creutzfeldt-Jakob disease. The neuropathology of a transmission experiment. Brain 92:699–716, 1969
118. Hirano A, Ghatak NR, Johnson AB, Partnow MJ, Gomori AJ: Argentophilic plaques in Creutzfeldt-Jakob disease. Arch Neurol 26:530–542, 1972
119. Chou SM, Martin JD: Kuru-plaques in a case of Creutzfeldt-Jakob disease. Acta Neuropathol 17:150–155, 1971
120. Beck E: Personal communication
121. Gonatas NK, Terry RD, Weiss M: Electron microscopy study in two cases of Jokob Creutzfeldt disease. J Neuropathol Exp Neurol 24:575–598, 1965
122. Kidd M: Some electron microscopical observations on status spongiosus. Acta Neuropathol Suppl 3:137–144, 1967
123. Foncin JF: Electron microscopic observations in Creutzfeldt-Jakob disease. Brain Edema. Edited by I Klatzo, F Seitelberger. New York, Springer. 1967, pp 171–177
124. Bignami A, Forno LS: Status spongiosus in Jakob-Creutzfeldt disease. Brain 93:89–94, 1970
125. Lampert PW, Gajdusek DC, Gibbs CJ Jr: Experimental spongiform encephalopathy (Creutzfeldt-Jakob disease) in chimpanzees. Electron microscopic observations. J Neuropathol Exp Neurol 30:20–32, 1971
126. Dumas JLR: Enroulements de fragments membranaires dans un cas de maladie de Creutzfeldt-Jakob. Acta Neuropathol 19:343–346, 1971
127. Vernon ML, Horta-Barbosa L, Fuccillo DA, Sever JL, Baringer JR, Birnbaum G: Virus-like particles and nucleoprotein type filaments in brain tissue from two patients with Creutzfeldt-Jakob disease. Lancet 1:964–966, 1970
128. Bots G: Virus-like particles in Creutzfeldt-Jakob disease. Acta Neuropathol 18:267–270, 1971
129. Gonatas NK, Martin J, Evangelista I: The osmiophilic particles of astrocytes. Viruses, lipid droplets or products of secretion? J Neuropathol Exp Neurol 26:369–376, 1967
130. Gibbs CJ Jr, Gajdusek DC, Asher DM, Alpers MP, Beck E, Daniel PM, Matthews WB: Creutzfeldt-Jakob disease (spongiform encephalopathy): Transmission to the chimpanzee. Science 161:388–389, 1968
131. Gibbs CJ Jr, Gajdusek DC: Infection as the etiology of spongiform encephalopathy (Creutzfeldt-Jakob disease). Science 165:1023–1025, 1969
132. Gajdusek DC: Subacute spongiform virus encephalopathies. Proceedings of the Symposium on Host-Virus Reactions with Special Reference to Persistent Agents. Roy Coll Pathologists (London) 1972 (In press)
133. Brown P, Hooks J, Roos R, Gajdusek DC, Gibbs CJ Jr: Attempt to identify the agent for Creutzfeldt-Jakob disease by CF antibody relationship to known viruses. Nature 235:149–152, 1972

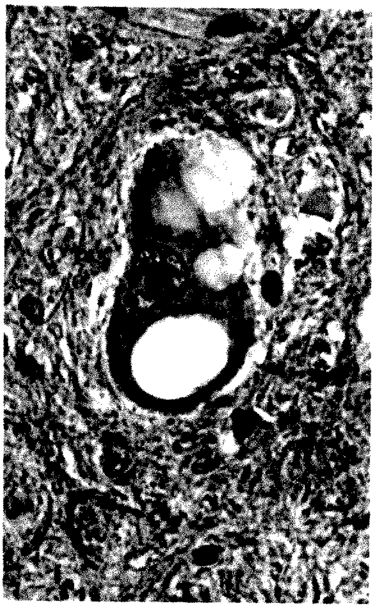

1

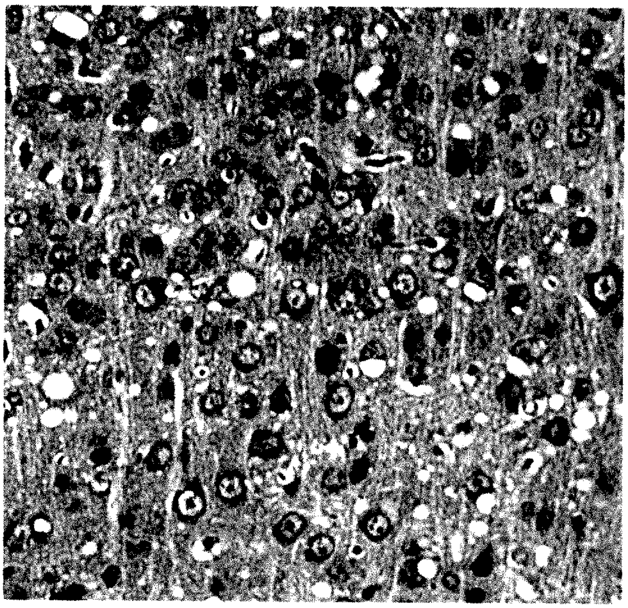

2

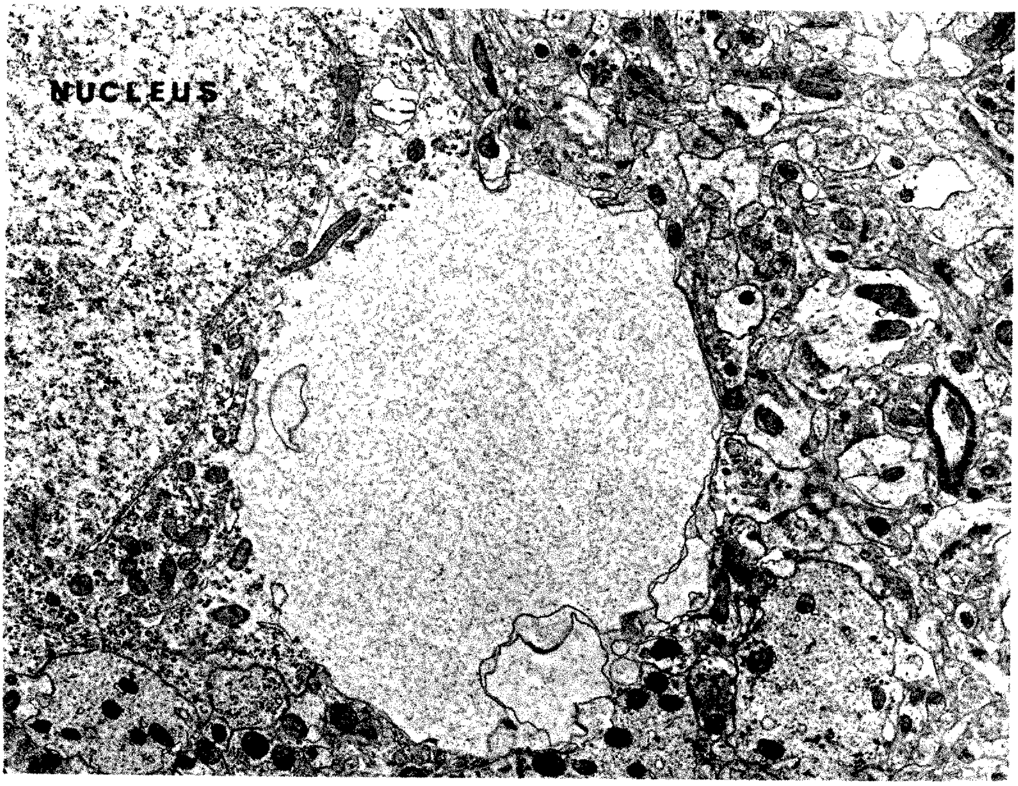

3

Fig 1—Vacuolated nerve cell in the medulla of a sheep with natural scrapie (H&E, × 575). **Fig 2**—Status spongiosus of the cerebral cortex of a mouse with experimental scrapie (H&E, × 300). **Fig 3**—Focal clearing and swelling of the perikaryal cytoplasm of a nerve cell in the cerebral cortex of a mouse with experimental scrapie (× 10,000).

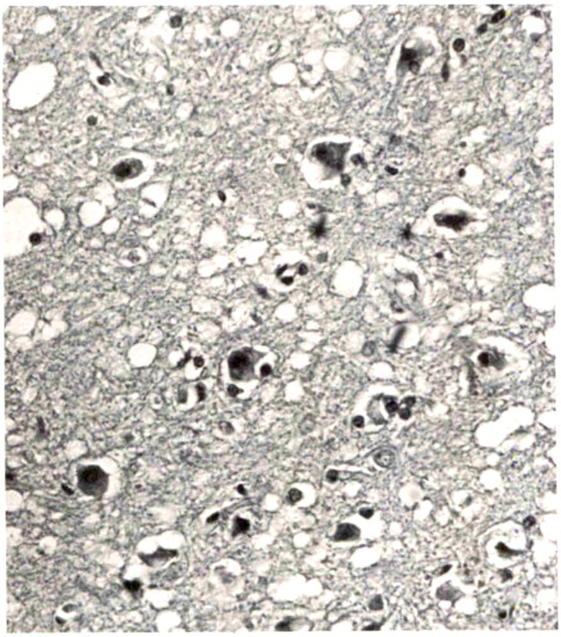

4

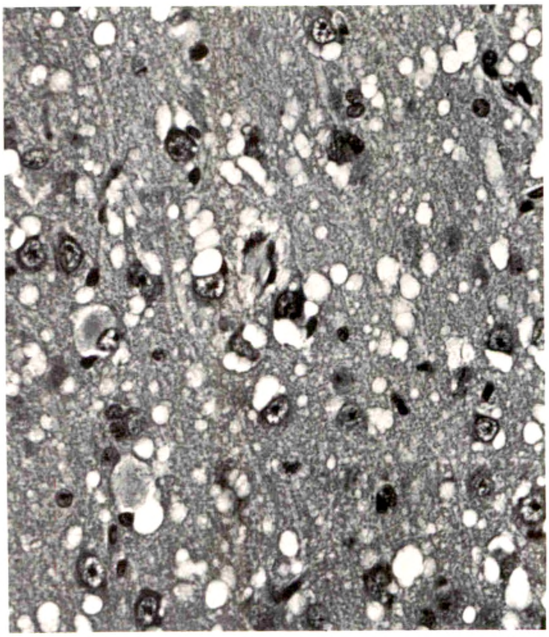

5

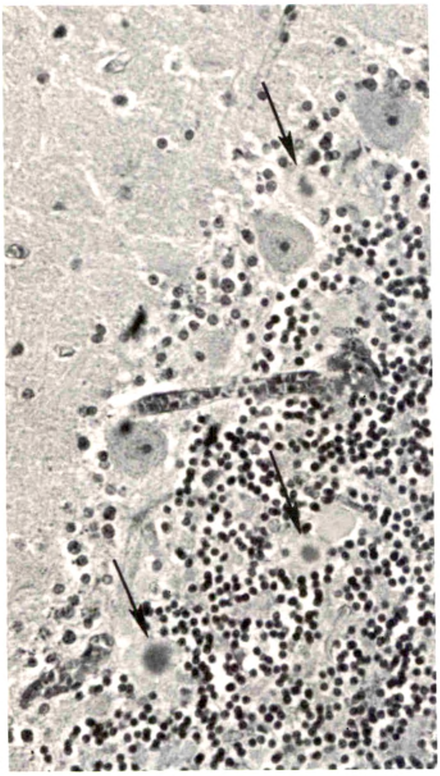

6

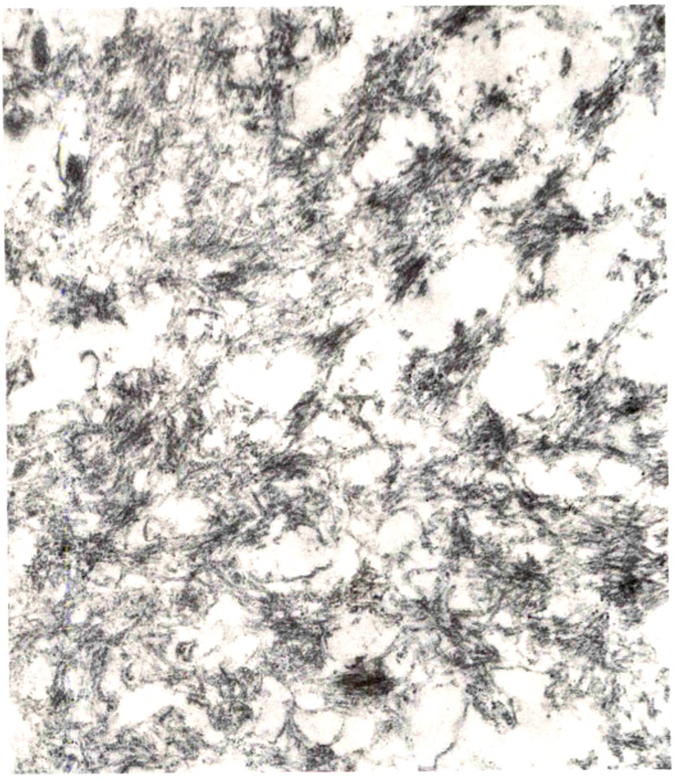

7

Fig 4—Status spongiosus of the cerebral cortex in human kuru (H&E, × 400). **Fig 5**—Spongiform changes in the cerebral cortex in experimental kuru (H&E, × 400). **Fig 6**—Cerebellar cortex in human kuru. *Arrows* indicate stellate, PAS-positive plaques (PAS, × 350). **Fig 7**—Ultrastructure of stellate plaque consisting of bundles of microtubules (× 60,000).

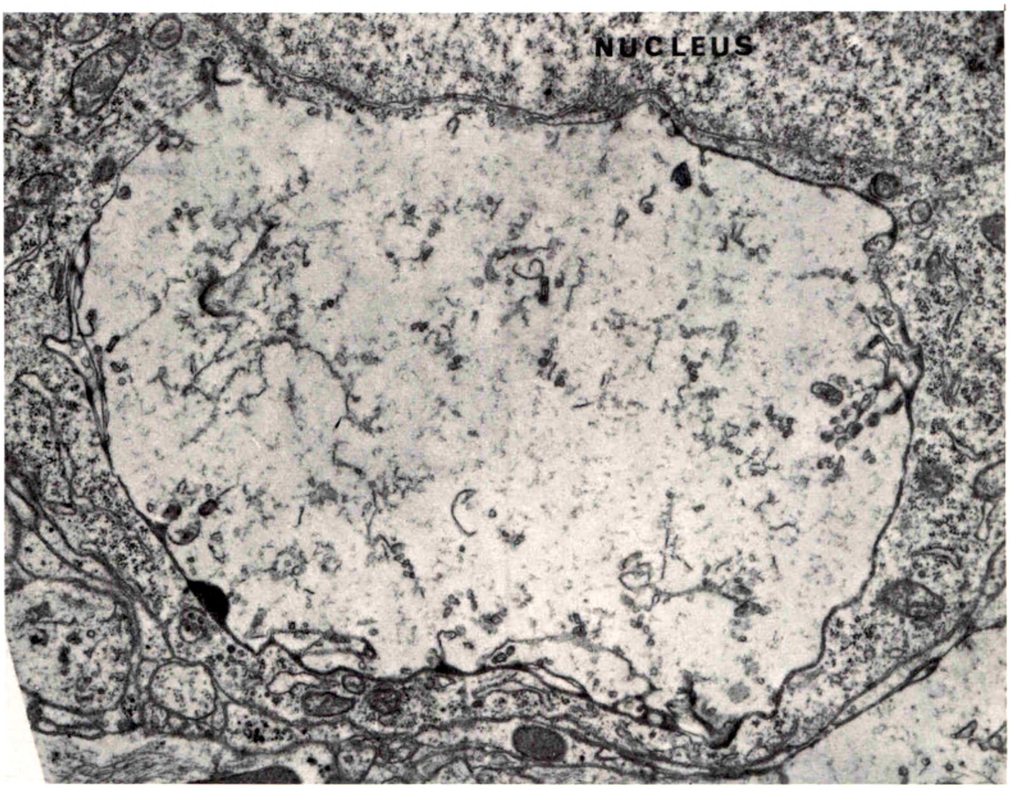

8

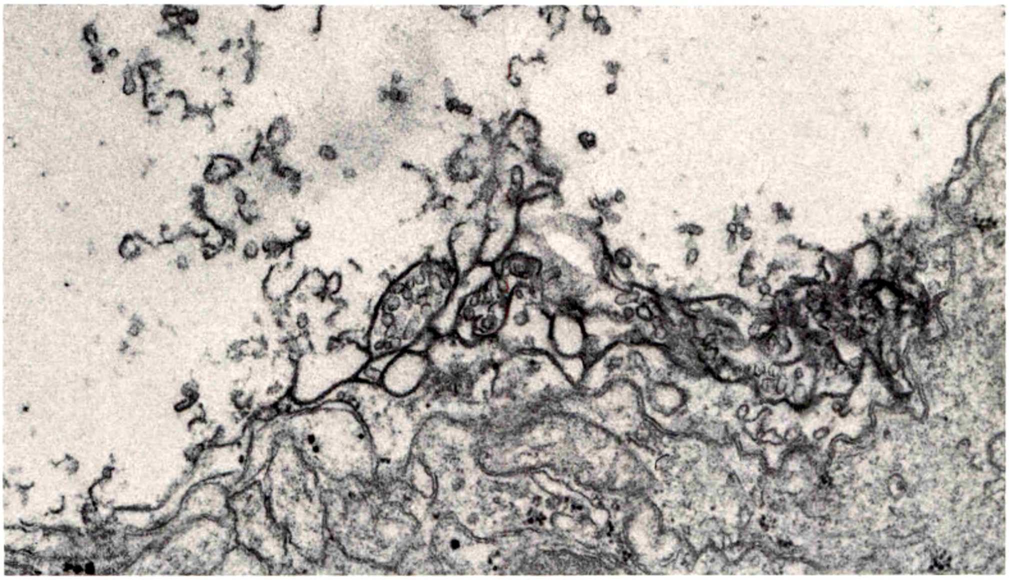

9

Fig 8—Membrane-bounded vacuole in the perikaryal cytoplasm of a nerve cell in experimental kuru. Note the accumulation of curled fragments of membranes (× 20,000).
Fig 9—Excessive aggregates of curled fragments of membranes at the margin of a vacuolated cytoplasmic process in the cerebral cortex in experimental kuru (× 30,000).

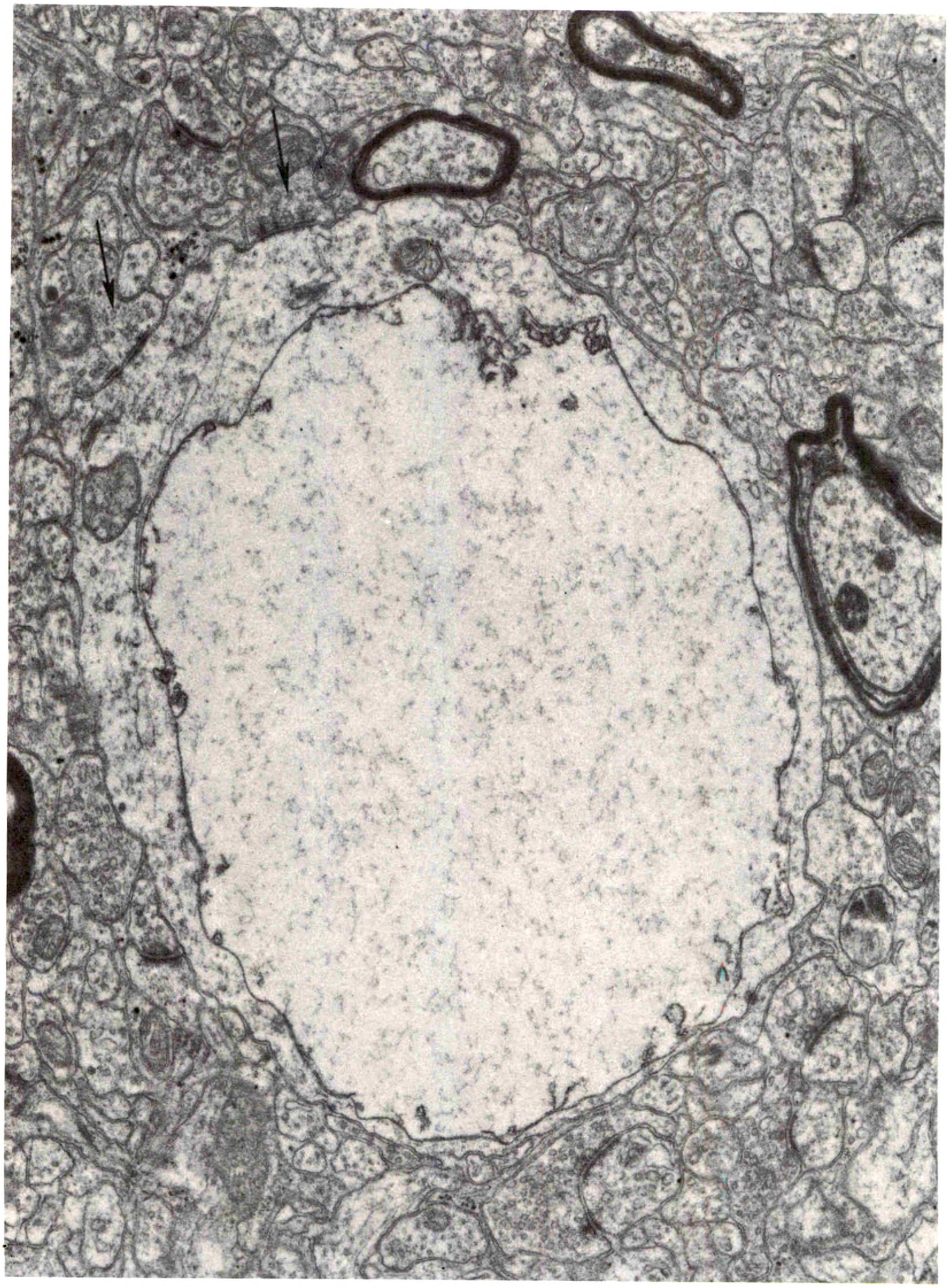

Fig 10—Membrane-bounded vacuole in a dendrite in experimental kuru. Fragments of membranes are noted at the margin of the vacuole. *Arrows* indicate intact synaptic junctions (× 20,000).

11

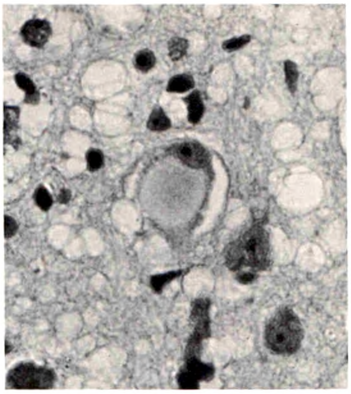

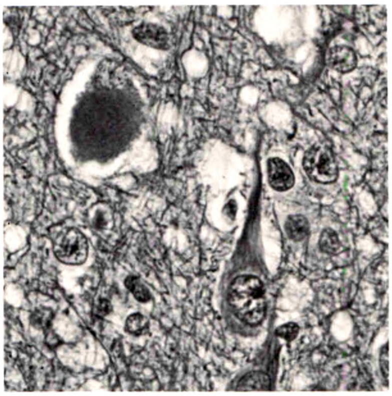

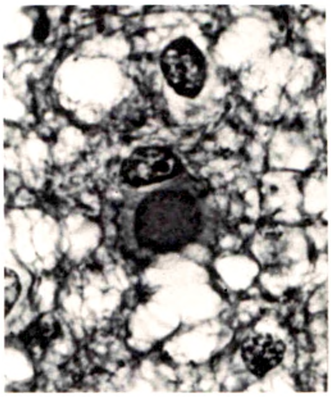

12

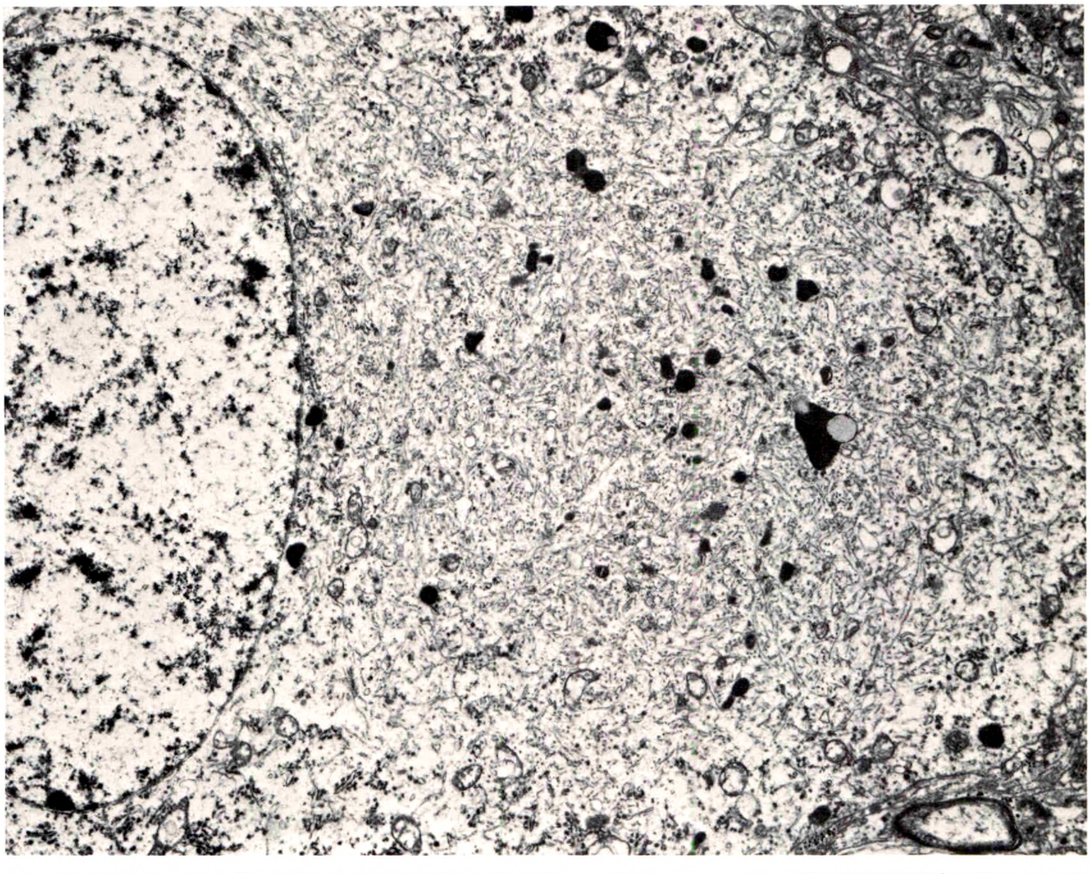

14

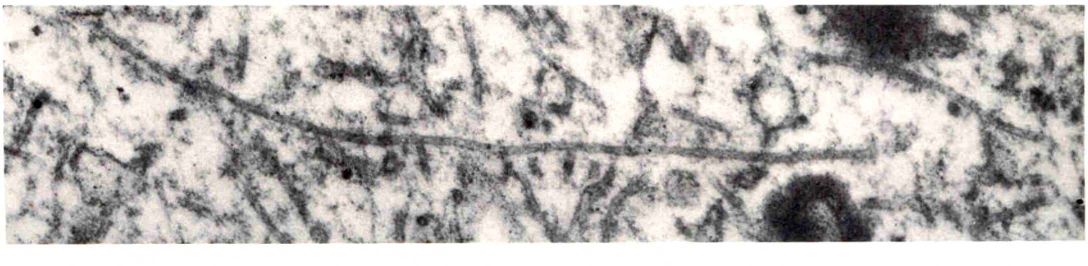

15

Fig 11—Swollen neuron showing chromatolysis in the cerebral cortex in experimental kuru (H&E, × 450). **Fig 12**—Swollen neuron with diffusely argentophilic cytoplasm in experimental kuru (Bielchowsky, × 500). **Fig 13**—Swollen neuron with an argentophilic spheroid intracytoplasmic inclusion in experimental kuru (Bielchowsky, × 600). **Fig 14**—Neuron containing an intracytoplasmic aggregate of randomly oriented tubules (× 20,000). **Fig 15**—Higher magnification of intraneuronal tubules as seen in Figure 14 (× 50,000).

6

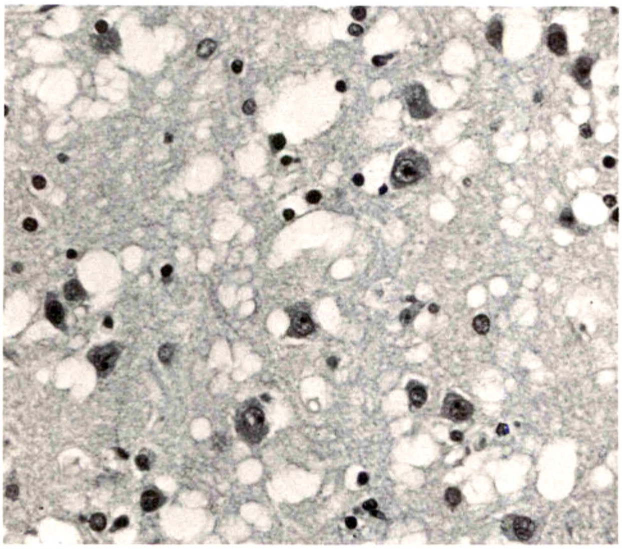

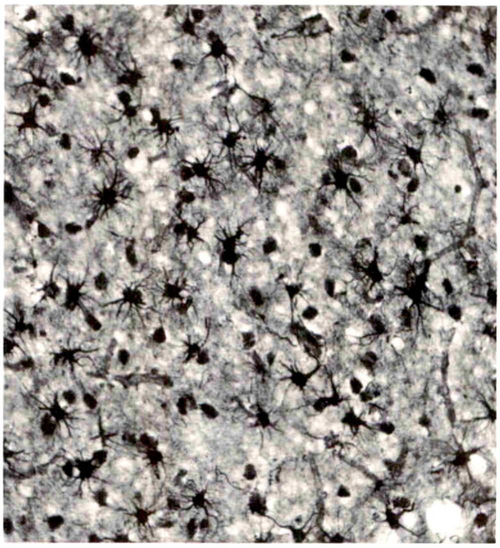

8

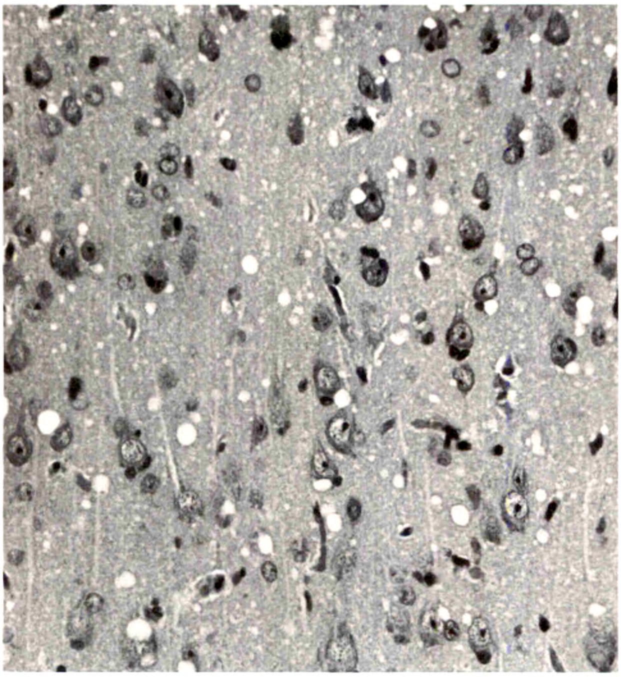

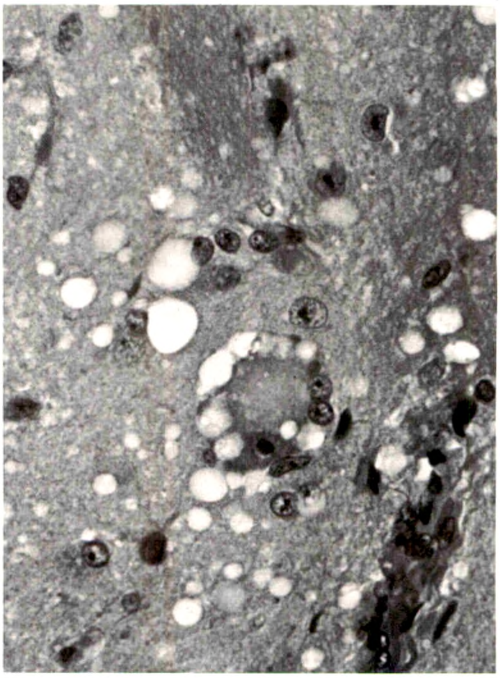

1

Fig 16—Status spongiosus in the cerebral cortex in human Creutzfeldt-Jakob disease (H&E, × 400). **Fig 17**—Intense astrocytic proliferation in the cerebral cortex in human Creutzfeldt-Jakob disease (Cajal, × 200). **Fig 18**—Status spongiosus in cerebral cortex in experimental Creutzfeldt-Jakob disease. Note the localization of the vacuoles within the neuropil but rarely around vessels (H&E, × 400). **Fig 19**—Status spongiosus in striatum in experimental Creutzfeldt-Jakob disease. Note vacuoles around the periphery of a swollen nerve cell (H&E, × 450).

Reprinted from Vol. 68, No. 3, September 1972
AMERICAN JOURNAL OF PATHOLOGY

ANIMAL MODEL FOR HUMAN DISEASE

Adenocarcinoma

Animal Model: Spontaneous Adenocarcinoma in Aged Rabbits

Contributed by: N. Baba, MD, PhD and E. von Haam, MD, Department of Pathology, The Ohio State University, College of Medicine, Columbus, Ohio 43210.

Biologic Features

Among various mammalian species investigated,[1,2] the incidence of spontaneous endometrial carcinoma was especially high in rabbits.[3] The most extensive study of these tumors was made by Greene *et al*,[4,5] who found 142 adenomas and adenocarcinomas in a colony of 849 rabbits observed for 9 years. Of the 14 breeds in this colony, the following showed appreciably higher incidences: Tan, 50%; French Silver (Champagne), 25%; Havana, 22%; and Dutch, 20%. Incidences in other breeds varied from 8 to 17%. Certain constitutional abnormalities and toxemia of pregnancy were associated with higher incidences of neoplasms.[6] Thirty-seven percent of tumor-bearing animals had second primary tumors elsewhere.[7] Ingalls *et al*[8] discovered 353 uterine tumors among 1735 rabbits of the Phipps colony, which was observed for 30 years. The incidence of tumors increased with age, reaching approximately 60% in animals over 4 years of age, in both colonies cited, and 79% in Greene's colony of 5-year-old animals.

We studied 117 Dutch rabbits for 30 months. This breed was chosen because it is available commercially in larger numbers than other breeds. The uteri of 83 rabbits were examined microscopically and 3 atypias (4%), 2 adenocarcinomas *in situ* (3%), 14 invasive adenocarcinomas (17%) and 1 leiomyosarcoma (1%) were found. Most of the tumor-bearing animals were 4 to 7 years old. The adenocarcinomas were often multicentric, involving both uterine horns. The tumors were polypous, with frequent central ulcerations (Figure 1). The uterine horns were distended with the tumor and hydro- and pyometra from neo-

---

Publication sponsored by the Registry of Comparative Pathology of the Armed Forces Institute of Pathology and supported by Public Health Service Grant RR 00301 from the Division of Research Resources, US Department of Health, Education and Welfare, under the auspices of Universities Associated for Research and Education in Pathology, Inc.

Published by Medical Department
HARPER & ROW, PUBLISHERS
© 1972 The American Association of Pathologists and Bacteriologists
Printed in the U.S.A.

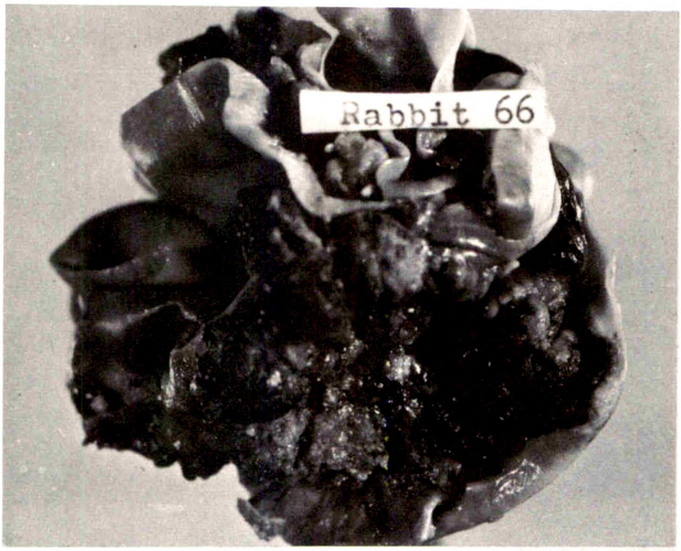

Fig 1—Gross appearance of an endometrial carcinoma. A markedly distended, thin-walled uterine horn contains a polypous tumor with central ulceration.

plastic obstruction of the lumen were observed. Carcinomatous dissemination on the peritoneal surface was observed in 3 animals. Pulmonary metastasis was noted from one carcinoma and one sarcoma. Histologically, the carcinoma was a well-differentiated adenocarcinoma (Figure 2) originating from the deeper glandular portion of the epithelium. Electron microscopically, the cells of the adenocarcinoma showed prominent nuclei and nucleoli, loss of secretory vesicles and cilia, and marked simplification of cytoplasmic organelles (Figure 3).[9] Histochemically, no alkaline or acid phosphatase activity could be demonstrated in either epithelial or stroma cells within adenocarcinomatous nodules.[10] Unlike normal endometrium, estrogens did not stimulate alkaline phosphatase actively in cancer cells but did elicit moderate acid phosphatase activity in malignant cells. Dysplasia and carcinomas *in situ* appeared in deeper portions of endometrial glands in association with severe senile atrophy of the endometrium. No association with glandular or cystic hyperplasia was recognized. Dysplasia and carcinoma *in situ* were not clearly differentiated, but many more atypical glands were present in the *in situ* stage. These lesions were characterized by irregularly distributed glands with advanced cellular atypia. Electron microscopic study of *in situ* carcinomas revealed lack of cilia and secretory vesicles, increased intercellular spaces and abundant lysosomes. Ultrastructurally, the cells of invasive and carcinomas *in situ* resembled those of severe senile atrophy of the endometrium in their loss of cilia and secretory vesicles and in the simplification of cytoplasmic structure. There was little ultrastructural resemblance between these lesions and glandular or cystic hyperplasia. Interestingly, estrogen, ad-

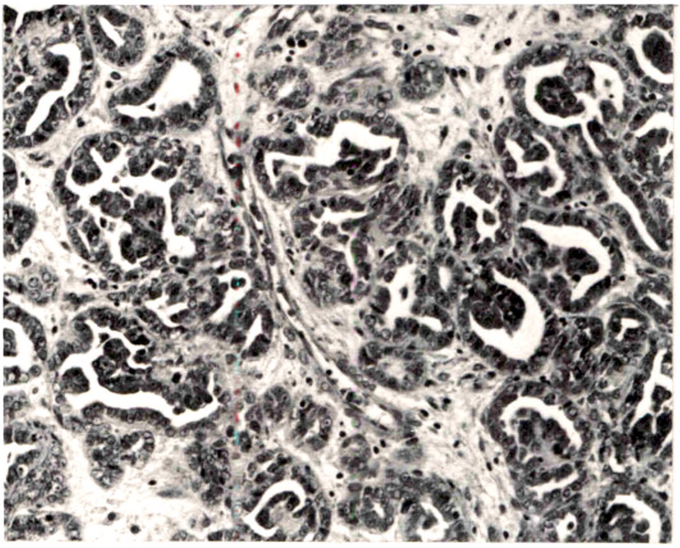

Fig 2—The carcinoma is a well-differentiated adenocarcinoma with infiltrating glands, often with papillary projections (X 170).

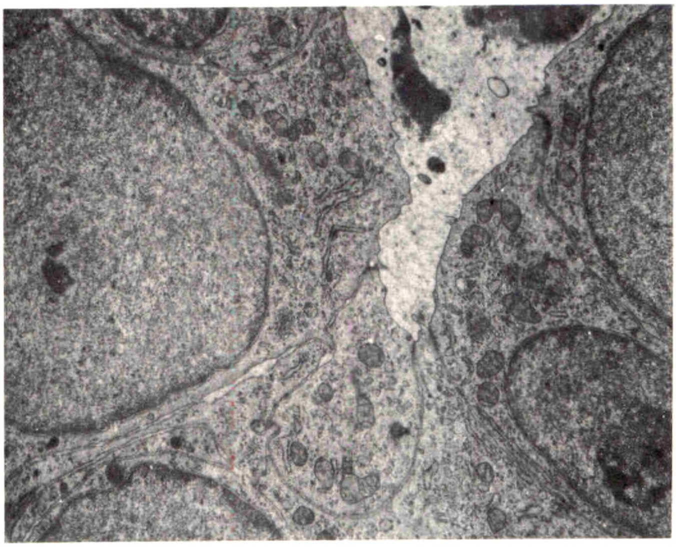

Fig 3—Electron micrograph of carcinoma cells which show large nuclei and a small amount of cytoplasm. The cilia and secretory vesicles seen in normal endometrial cells are absent. (X 10,000).

ministered to aged Dutch rabbits, reduced the incidence of endometrial carcinomas from 17 to 3%, Greene[11] transplanted the tumor into the anterior eye chamber of rabbits and commented that its neoplastic behavior was in no way related to the histologic appearance of the implants.

Comparison with Human Disease

Generally, human endometrial carcinoma is associated with glandular hyperplasia; rabbit carcinoma is associated with senile atrophy. Constitutional abnormalities, such as dwarfism and toxemia of pregnancy, were associated with endometrial carcinoma of the rabbit as often as diabetes, obesity and hypertension are associated with endometrial carcinoma of humans. While the relationship between hyperestrinism and human endometrial carcinoma remains controversial, senescence of the endometrium seemed important in spontaneous adenocarcinoma of the endometrium of rabbits; the administration of estrogens appeared to reduce the number of tumors. In humans, cessation of menstruation is related to the incidence of endometrial carcinoma and hormonal dysfunctions, such as the Stein-Leventhal syndrome, have been associated with endometrial carcinoma in young patients.

Potential Use

Further metabolic and endocrinologic studies on the carcinogenesis of endometrial carcinoma of rabbits will contribute greatly to the elucidation of the human counterpart.

Availability

The major rabbit colonies cited in this report were kept in the Departments of Pathology of Yale University,[4] The Ohio State University[3] and Henry Phipps Institute of the University of Pennsylvania;[8] however, the colonies are no longer being maintained. In our experience, female Dutch rabbits 2 to 3 years of age can be collected from commercial sources, and within 1 to 2 years investigators should obtain a number of spontaneous endometrial adenocarcinomas.

References

1. Montepellier JM, Samso A, Catanel J: Le cancer de l'útérus en pathologie vétérinaire. Bull Algér Carcinol 5: 45–56, 1952
2. Cotchin E: Spontaneous Uterine Cancer in Animals. Br J Cancer 18: 209–227, 1964
3. Baba N, von Haam E: Experimental carcinoma of the endometrium. Progr Exp Tumor Res 9: 192–260, 1967
4. Greene HSN, Saxton JA Jr: Uterine adenomata in the rabbit. I. Clinical history, pathology, and preliminary transplantation experiments. J Exp Med 67: 691–708, 1938
5. Greene HSN, Newton BL: Evolution of cancer of the uterine fundus in the rabbit. Cancer 1: 82–99, 1948
6. Greene HSN: Uterine adenomata in the rabbit. III. Susceptibility as a function of constitutional factors. J Exp Med 73: 273–292, 1941
7. Greene HSN, Strauss JS: Multiple primary tumors in the rabbit. Cancer 2: 673–691, 1949
8. Ingalls TH, Adams WH, Lurie MB, Ipsen J: Natural history of adenocarcinoma of the uterus in the Phipps rabbit colony. J Natl Cancer Inst 33: 799–806, 1964
9. Baba N, von Haam E: Ultramicroscopic changes in the endometrial cells of spontaneous adenocarcinoma of rabbits. J Natl Cancer Inst 38: 657–672, 1967
10. Baba N, Vidyarthi SC, von Haam E: Nonspecific phosphatases of rabbit endometrial carcinoma. Arch Pathol 90: 65–71, 1970
11. Greene HSN: Uterine adenomata in the rabbit. II. Homologous transplantation experiments. J Exp Med 69: 447–466, 1939

Index of Subjects

Volume 68, 1972

Acinar cells
  submaxillary, infected and normal, necrosis of during termination of cytomegalovirus infection, 183
Alopecia
  cyclophosphamide treatment induced (mice), 15
Alveolus
  changes in rats with biliary obstruction, 97
  macrophages, pulmonary interstitial cell as immediate precursor of, 521
Amyloidosis
  macular, amyloidogenesis in healing wound, electron microscopy of biopsied lesions, 371
  spontaneous and experimental, ANIMAL MODEL FOR HUMAN DISEASE, 441
Anesthetic
  local, *in vivo* quantitation of leukocyte suppression, 327
Aneurysms
  saccular intracranial, scanning electron microscopy of, 511
Animal Models
  adenocarcinoma, 653
  amyloidosis, spontaneous and induced, 441
  bluetongue virus induced nervous system malformations, 1, 15
  spina bifida, sacral dysgenesis, myelocele (Manx cats), 203
Antithymocyte serum
  effect of bluetongue virus infection in mice, 15
L-Asparaginase
  hypocalcemic tetany and parathyroid necrosis induced by, 461
Aspirin
  normal and platelets treated with, effects defective secondary aggregation in Hermansky-Pudlak syndrome, 57
Australia antigen
  immune complexes, tissue localization of in hepatitis and cirrhosis, 31

Basal lamina
  muscle capillary, in juvenile diabetes, incidence and thickness of, 67
Biliary obstruction
  pulmonary changes in rat, 97
Bluetongue virus infection
  in mice, effect of cyclophosphamide and antithymocyte serum on, 15
  nervous system malformations induced by, 1
Brain
  virus-induced morphologic changes in fetal mice, 1, 15

Capillary
  muscle, basal lamina thickening in juvenile diabetes, 67
  retinal, changes in hypertension, 81
Carbonic anhydrase
  histochemical distribution after pancreatic duct ligation, 23
Cardiac tissue
  ultrastructural changes in piglets deprived vitamin E and selenium, 479
Cell injury
  lysosome and phagosome stability in, morphologic tracer studies, 225
Cerebral malformation
  bluetongue virus induced in fetal mice, 1
Choline-deficiency
  lysosomes, role in pathogenesis of renal necrosis, 113
Cirrhosis
  liver, localization of Australia antigen immune complexes in, 31
Collagen
  degradation, granulocyte collagenase in, 565
Collagenase
  granulocyte, role in collagen degradation, 565
Connective tissue
  damage, role of granulocyte elastase, 579
Creutzfeldt–Jakob disease
  subacute, spongiform virus encephalopathies, REVIEW ARTICLE, 625
Cyclophosphamide
  effect on susceptibility of mice to bluetongue virus infection, 15
Cytolysis
  immune, energy metabolism and photosensitization, lethal cell injury due to, 255

Cytomegalovirus
  mouse, chronic infection, necrosis of infected and normal submaxillary gland acinar cells, 183

Degradation
  collagen, role of granulocyte collagenase, 565
Diabetes
  juvenile, muscle capillary basal lamina thickening in, 67
Discoid platelets
  degranulation of, 289

Elastase
  granulocyte, role in connective tissue damage, 579
Encephalopathies
  subacute spongiform viral, REVIEW ARTICLE, 625
Energy metabolism
  immune cytolysis, photosensitization and, lethal cell injury due to, 255
Enzymes
  carbonic anhydrase, distribution after pancreatic duct ligation, 23
  lysosomal, leukocytic proteases and immunologic release of, 539
Epithelial cells
  mucociliated, mucus hypersecretion induced by a factor in heated serum, 407

Glomerulonephritis
  sarcoidosis associated with, 339
Gold Headed Cane Award
  Esmond R. Long, 207
Granulocyte
  collagenase, role in collagen degradation, 565
  elastase, role in connective tissue damage, 579

Hepatitis
  tissue localization of Australia antigen, 31
Hepatocytes
  immunoglobulins and β1C globulin in Australia antigen-containing, 31
Hydrocortisone
  lysosome stabilizer, effect on renal necrosis in choline-deficient rats, 113
Hypertension
  experimental, cellular pathology of, changes in retinal vessels, 81
Hypocalcemia
  tetany, parathyroid necrosis and, induced by L-asparaginase, 461
Hypoxemia
  in liver disease, 97

Immune complexes
  Australia antigen, localization in hepatitis and cirrhosis, 31

Immunoglobulins
  complexes with Australia antigen in hepatitis and liver cirrhosis, 31
  nuclear localization of in lupus nephritis, 469
Injury
  neutrophil mediated, pathologic mechanisms, 593
Interalveolar septa
  thickening of in rats with biliary obstruction, 97
Intracranial aneurysms
  saccular, scanning electron microscopy of, 511
Intranasal epithelia
  atrophy in chickens fed vitamin A-deficient diets, 147

Junctional-complex-associated bodies
  prevalence in human sweat glands, 423

Kidneys
  Australia antigen immune complexes localized in, 31
  cell proliferation after prolonged lead treatment, 359
  necrosis, lysosomes in pathogenesis of in choline-deficient rats, 113
  nuclear localization of immunoglobulins in lupus nephritis, 469
  papillary necrosis, experimental, electron microscopy and histochemistry, 213
  papillary necrosis, effects of reserpine and other pharmacologic agents, 235
Kininogenases
  leukocyte, and leukokinins from normal and malignant cells, 613
Kuru
  subacute spongiform virus encephalopathies, REVIEW ARTICLE, 625

Leukocyte
  adherence, anesthetic suppression *in vivo*, 327
  kininogenases and leukokinins from normal and malignant cells, 613
  proteases and immunologic release of lysosomal enzymes, 539

Leukokinins
- leukocyte, kininogenases and, in normal and malignant cells, 613

Liver
- cirrhosis, tissue localization of Australia antigen immune complexes in, 31
- disease, changes in pulmonary ultrastructure in, 97

Local anesthetic
- suppression of leukocyte adherence, *in vivo* quantitation, 327

Lungs
- changes in biliary obstruction in rat, 97
- urethane exposure, changes in cell proliferation in mouse after, 317

Lupus nephritis
- nuclear localization of immunoglobulins in, 469

Lymph nodes
- Australia antigen immune complexes in, 31

Lymphocyte
- depression induced by vitamin A-deficient diet, 147
- role in terminating chronic cytomegalovirus infection in mice, 183
- separation from ascites myeloma cells and macrophages by zonal centrifugation, 163

Lysosomes
- enzyme release, immunologic, leukocytic proteases and, 539
- pathogenesis of renal necrosis in choline-deficient rats, 113
- phagosome and, stability, in lethal cell injury, 255

Macrophage
- alveolar, pulmonary interstitial cell as immediate precursor of, 521
- separation of ascites myeloma cells and lymphocytes from, by zonal centrifugation, 163

Malignancy
- leukocyte kininogenases and leukokinins from normal and malignant cells, 613

Microangiopathy
- diabetic, basal lamina thickness in early changes, 67

Mucociliated epithelial cells
- induced hypersecretion of mucus by factor in heated serum, 407

Muscular dystrophy
- ultrastructure, comparative study in lambs and chickens, 493
- ultrastructural changes in cardiac tissue of piglets deprived vitamin E and selenium, 479

Myelocele
- ANIMAL MODEL FOR HUMAN DISEASE (Manx cats), 203

Myeloma cells
- ascites, separation from lymphocytes and macrophages by zonal centrifugation, 163

Nasal mucociliated epithelia
- postsloughing hypoplasia induced by by feeding diets deficient in vitamin A and other components, 147

Nephritis
- lupus, nuclear localization of immunoglobulins in, 469
- nephrotoxic, glomerular sialoprotein in, chemical and histochemical studies, 391

Nervous system
- malformations of, bluetongue virus induced in mice, 1, 15

Neutrophil
- mediated injury, pathologic mechanisms, 593

Newcastle disease virus
- lymphocyte and plasma cell depression in birds fed deprived diets, 147

Nucleotides
- nonmetabolic, content in Hermansky-Pudlak platelets, 57

Neuroembryogenesis
- virus-induced malformations, 1

Pancreas
- duct ligation, histochemical distribution of carbonic anhydrase after, 23

Papillary necrosis
- kidney, electron microscope and histochemical studies of experimental, 213

Parathyroid
- necrosis and hypocalcemic tetany induced by L-asparaginase, 461

Phagosome stability
- lysosome and, in lethal cell injury, 255

Photosensitization
- energy metabolism, immune cytolysis and, lethal cell injury due to, 255

Plasma cell
- depleted populations in chickens fed vitamin A-deficient diets, 147

Platelets
discoid, degranulation of, 289
normal and aspirin, effects on secondary aggregation in Hermansky-Pudlak syndrome, 57
thromboasthenic and afibrinogenemic, effect of cationic polypeptides on, 447
ultrastructural characteristics of freeze-dried, 303
Proteases
leukocytic, immunologic release of lysosomal enzymes and, 539
Pulmonary interstitial cell
immediate precursor of alveolar macrophage, 521

Reserpine
and other pharmacologic agents, effects on papillary necrosis of kidney, 235
Retinopathy
hypertension, changes and in, 81
juvenile diabetes, significance of basal lamina changes in early diagnosis, 67
Review Article
Subacute spongiform virus encephalopathies: Scrapie, kuru and Creutzfeldt-Jakob disease, 625

Saccular intracranial aneurysms
scanning electron microscopy of, 511
Sacral dysgenesis
ANIMAL MODEL FOR HUMAN DISEASE (Manx cats), 203
Sarcoidosis
glomerulonephritis associated with, 339
Scrapie
subacute spongiform virus encephalopathies, 625
Selenium
cardiac tissue changes in piglets deprived of, 479
Serum
heated, mucus hypersecretion of isolated mucociliated epithelial cells by factor in, 407
Sialoprotein
glomerular, in nephrotoxic nephritis in rats, chemical and histochemical studies, 391
Spina bifida
ANIMAL MODEL FOR HUMAN DISEASE (Manx cats), 203
Spleen
Australia antigen immune complexes in, 31
Submaxillary gland
necrosis of cytomegalovirus-infected and normal acinar cells, 183
Surfactant
in rats with biliary obstruction, 97
Sweat gland
junctional-complex-associated bodies in, variable prevalence of, 423

Telencephalon
bluetongue virus-induced lesions in mice, 1
Tetany
hypocalcemic, parathyroid necrosis and induced by L-asparaginase, 461

Urethane
exposure, changes in cell proliferation in mouse lung after, 317

Vascular disease
diabetic, pathogenesis of, 67
Vascular system
Australia antigen immune complexes localized in, 31
Viruses
bluetongue, induced nervous system malformations, 1, 15
Vitamin A
deficiency, lymphocyte depression induced by, 147
lysosome labilizer, effect on renal necrosis in choline-deficient rats, 113
Vitamin E
cardiac changes in piglets deprived of, 479

Wounds
healing, amyloidogenesis in, electron microscopy of biopsied wounds in macular amyloidosis, 371

Zonal centrifugation
on isokinetic gradient, separation of ascites myeloma cells, lymphocytes and macrophages, 163

Index of Authors

Volume 68, 1972

Adamson IYR: *See* Bowden DH, Adamson IYR 521
Alzamora DB: *See* Pardo V, Perez-Stable E, Alzamora DB, Cleveland WW 67
Baba N, von Haam E: ANIMAL MODEL FOR HUMAN DISEASE: Adenocarcinoma (September) 653
Bang Betsy G, Bang FB, Foard Marie A: Lymphocyte depression induced in chickens on diets deficient in vitamin A and other components (July) 147
Bang Betsy G, Bang FB: Mucus hypersecretion induced in isolated mucociliated epithelial cells by a factor in heated serum (August) 407
Bang FB: *See* Bang Betsy G, Bang FB, Foard Marie A 147
Bang FB: *See* Bang BG, Bang FB 407
Biberfeld P: *See* Hawkins HK, Ericsson JLE, Biberfeld P, Trump BJ 255
Bowden DH, Adamson IYR: The pulmonary interstitial cell as immediate precursor of the alveolar macrophage (September) 521
Brown RG: *See* Sweeny PR, Brown RG 479
Brownstein MH: *See* Hashimoto K, Brownstein MH 371
Brzosko WJ: *See* Nowosławski A, Krawczyński K, Brzosko WJ, Madaliński K 31
Buchanan-Smith JG: *See* Sweeny PR, Buchanan-Smith JG, deMille F, Pettit JR, Moran ET 493
Burleigh Mary C: *See* Lazarus GS, Daniels JR, Lian Jane, Burleigh Mary C 565
Chisari FV, Hochstein HD, Kirschstein RL, Seligmann EB: Parathyroid necrosis and hypocalcemic tetany induced in rabbits by L-asparaginase (September) 461
Chiu Jane, Drummond KN: Chemical and histochemical studies of glomerular sialoprotein in nephrotoxic nephritis in rats (August) 391
Choie DD, Richter GW: Cell proliferation in rat kidneys after prolonged treatment with lead (August) 359
Churg A, Richter WR: Histochemical distribution of carbonic anhydrase after ligation of the pancreatic duct (July) 23
Cleveland WW: *See* Pardo V, Perez-Stable E, Alzamora DB, Cleveland WW 67
Cockrell Beverly Y: *See* Kitchen H, Murray RE, Cockrell Beverly Y 203
Cohen AS, Shirahama T: ANIMAL MODEL FOR HUMAN DISEASE: Spontaneous and experimental amyloidosis (August) 441
Daniels JR: *See* Lazarus GS, Daniels JR, Lian Jane, Burleigh Mary C 565
Davis RB: Ultrastructural characteristics of freeze-dried human blood platelets (August) 303
deMille F: *See* Sweeny PR, Buchanan-Smith JG, deMille F, Moran ET 493
Drummond KN: *See* Chiu Jane, Drummond KN 391
Ericsson JLE: *See* Hawkins HK, Ericsson JLE, Biberfeld P, Trump BJ 255
Estensen RD: *See* White JG, Estensen RD 289
Foard Marie A: *See* Bang Betsy G, Bang FB, Foard Marie A 147
Gajdusek DC: *See* Lampert PW, Gajdusek DC, Gibbs CJ Jr. 625
Ghoshal AK: *See* Monserrat AJ, Hamilton F, Ghoshal AK, Porta EA, Hartroft WS 113
Giacomelli F, Juechter KB, Wiener J: The cellular pathology of experimental hypertension. VI. Alterations in retinal vasculature (July) 81
Gibbs CJ Jr: *See* Lampert PW, Gajdusek DC, Gibbs CJ Jr. 625
Giddon DB, Lindhe J: *In vivo* quantitation of local anesthetic suppression of leukocyte adherence (August) 327
Greenbaum LM: Leukocyte kininogenases and leukokinins from normal and malignant cells (September) 613
Hamilton F: *See* Monserrat AJ, Hamilton F, Ghoshal AK, Porta EA, Hartroft WS 113
Hartroft WS: *See* Monserrat AJ, Hamilton F, Ghoshal AK, Porta EA, Hartroft WS 113

Hashimoto K, Brownstein MH: Amyloidogenesis in healing wound: Electron microscopic studies of biopsied wounds in macular amyloidosis (August) 371
Hassler O: Scanning electron microscopy of saccular intracranial aneurysms (September) 511
Hawkins HK, Ericsson JLE, Biberfeld P, Trump BJ: Lysosome and phagosome stability in lethal cell injury due to inhibition of energy metabolism, immune cytolysis and photosensitization (August) 255
Henson D, Strano AJ: Mouse cytomegalovirus: Necrosis of infected and morphologically normal submaxillary gland acinar cells during termination of chronic infection (July) 183
Henson PM: Pathologic mechanisms in neutrophil-mediated injury (September) 593
Heptinstall RH: *See* Hill GS, Wyllie RG, Miller M, Heptinstall RH 213
Heptinstall RH: *See* Wyllie RG, Hill GS, Murray G, Ramsden PW, Heptinstall RH 235
Hill GS, Wyllie RG, Miller M, Heptinstall RH: Experimental papillary necrosis of the kidney. II. Electron microscopic and histochemical studies (August) 213
Hill GS: *See* Wyllie RG, Hill GS, Murray G, Ramsden PW, Heptinstall RH 235
Hiramoto R: *See* Stewart MJ, Pretlow TG, Hiramoto R 163
Hochstein HD: *See* Chisari FV, Hochstein HD, Kirschstein RL, Seligmann EB 461
Hoffstein Sylvia: *See* Weissmann G, Zurier RB, Hoffstein Sylvia 539
Janoff A: Introduction: Symposium on Neutrophil Proteases as Mediators of Tissue Injury (September) 538
Janoff A: Human granulocyte elastase: Further delineation of its role in connective tissue damage (September) 579
Johnson RT: *See* Narayan O, McFarland HF, Johnson RT 15
Johnson RT: *See* Narayan O, Johnson RT 1
Juechter KB: *See* Giacomelli F, Juechter KB, Wiener J 67
Kauffman Shirley L: Alterations in cell proliferation in mouse lung following urethane exposure. III. Effects of cell exposure on Type 2 alveolar macrophage (August) 317
Kirschstein RL: *See* Chisari FV, Hochstein HD, Kirschstein RL, Seligmann EB 461
Kitchen H, Murray RE, Cockrell Beverly Y: ANIMAL MODEL FOR HUMAN DISEASE: Spina bifida, sacral dysgenesis and myelocele. Manx cats (July) 203
Krawczyński K: *See* Nowosławski A, Krawczyński K, Brzosko WJ, Madaliński K 31
Lampert PW, Gajdusek DC, Gibbs CJ Jr: REVIEW ARTICLE: Subacute spongiform virus encephalopathies: Scrapie, kuru and Creutzfeldt-Jakob disease (September) 625
Lazarus GS, Daniels JR, Lian Jane, Burleigh Mary C: Role of granulocyte collagen degradation (September) 565
Lian Jane: *See* Lazarus GS, Daniels JR, Lian Jane, Burleigh Mary C 565
Lindhe J: *See* Giddon DB, Lindhe J 327
Madaliński K: *See* Nowosławski A, Krawczyński K, Brosko WJ, Madaliński K 31
Martin BJ: *See* Spicer SS, Martin BJ, Reynolds JP 423
McCoy RC: Nuclear localization of immunoglobulins in renal biopsies of patients with lupus nephritis (September) 469
McCoy RC, Tisher CC: Glomerulonephritis associated with sarcoidosis (August) 339
McFarland HF: *See* Narayan O, McFarland HF, Johnson RT 15
Miller M: *See* Hill GS, Wyllie RG, Miller M, Heptinstall RH 213
Murray G: *See* Wyllie RG, Hill GS, Murray G, Ramsden PW, Heptinstall RH 235
Monserrat AJ, Hamilton F, Ghoshal AK, Porta EA, Hartroft WS: Lysosomes in the pathogenesis of the renal necrosis of choline-deficient rats (July) 113

Moran ET: *See* Sweeny PR, Buchanan-Smith JG, deMille F, Moran ET 493

Mullane JF: *See* Popovic NA, Mullane JF 97

Murray RE: *See* Kitchen H, Murray RE, Cockrell Beverly Y 203

Narayan O, Johnson RT: Effects of viral infection on nervous system development (July) 1

Narayan O, McFarland HF, Johnson RT: Effects of viral infection on nervous system development. II. Attempts to modify bluetongue virus-induced malformations with cyclophosphamide and antithymocyte serum (July) 15

Nowosławski A, Krawczyński K, Brzosko WJ, Madaliński K: Tissue localization of Australia antigen immune complexes in acute and chronic hepatitis and liver cirrhosis (July) 31

Pardo V, Perez-Stable E, Alzamora DB, Cleveland WW: Incidence and significance of muscle capillary basal lamina thickness in juvenile diabetes (July) 67

Perez-Stable: *See* Pardo V, Perez-Stable E, Alzamora DB, Cleveland WW 67

Popovic NA, Mullane JF: Effects of biliary obstruction on pulmonary ultrastructure in the rat (July) 97

Porta EA: *See* Monserrat AJ, Hamilton F, Ghoshal AK, Porta EA, Hartroft WS 113

Pretlow TG: *See* Stewart MJ, Pretlow TG, Hiramoto R 163

Ramsden PW: *See* Wyllie RG, Hill GS, Murray G, Ramsden PW, Heptinstall RH 235

Reynolds JP: *See* Spicer SS, Martin BJ, Reynolds JP 423

Richter GW: *See* Choie DD, Richter GW 359

Richter WR: *See* Churg A, Richter WR 23

Seligmann EB: *See* Chisari FV, Hochstein HD, Kirschstein RL, Seligmann EB 461

Shirahama T: *See* Cohen AS, Shirahama T 441

Spicer SS, Martin BJ, Reynolds JP: The variable prevalence of junctional-complex-associated bodies in the human sweat gland (August) 423

Stewart MJ, Pretlow TG, Hiramoto R: Separation of ascites myeloma cells, lymphocytes and macrophages by zonal centrifugation on an isokinetic gradient (July) 163

Stowell RE: Presentation of The Gold Headed Cane to Esmond R. Long (August) 207

Strano AJ: *See* Henson D, Strano AJ 183

Sweeny PR, Brown RG: Ultrastructural changes in muscular dystrophy. I. Cardiac tissue of piglets deprived of vitamin E and selenium (September) 479

Sweeny PR, Buchanan-Smith JG, deMille F, Pettit JR, Moran ET: Ultrastructure of muscular dystrophy. II. A comparative study in lambs and chickens (September) 493

Tisher CC: *See* McCoy RC, Tisher CC 339

Trump BJ: *See* Hawkins HK, Ericsson JLE, Biberfeld P, Trump BJ 255

von Haam E: *See* Baba N, von Haam E 653

Weissmann G, Zurier RB, Hoffstein Sylvia: Leukocyte proteases and the immunologic release of lysosomal enzymes (September) 539

White JG: Effects of cationic polypeptides on thromboasthenic and afibrinogenemic blood platelets (September) 447

White JG, Estensen RD: Degranulation of discoid platelets (August) 289

White JG, Witkop CJ: Effects of normal and aspirin platelets on defective secondary aggregation in the Hermansky-Pudlak syndrome: A test for storage pool deficient platelets (July) 57

Wiener J: *See* Giacomelli F, Juechter KB, Wiener J 81

Witkop CJ: *See* White JG, Witkop CJ 57

Wyllie RG, Hill GS, Murray G, Ramsden PW, Heptinstall RH: Experimental papillary necrosis of the kidney. III. Effects of reserpine and other pharmacologic agents on the lesion (August) 235

Wyllie RG: *See* Hill GS, Wyllie RG, Miller M, Heptinstall RH 213

Zurier RB: *See* Weissmann G, Zurier RB, Hoffstein Sylvia 539

The American Journal of
PATHOLOGY

OFFICIAL PUBLICATION OF
THE AMERICAN ASSOCIATION OF PATHOLOGISTS AND BACTERIOLOGISTS
THE AMERICAN SOCIETY FOR EXPERIMENTAL PATHOLOGY

Volume 68, 1972
(July through September)

BOARD OF EDITORS

Thomas D. Kinney, *Editor-in-Chief*
Donald B. Hackel, *Associate Editor*

Orville T. Bailey
Frederick F. Becker
Baruj Benacerraf
Kurt Benirschke
Kenneth M. Brinkhous
Joel G. Brunson
John R. Carter
Charles G. Cochrane
John M. Craig
Frank J. Dixon, Jr
John T. Ellis
Frank W. Fitch
Patrick J. Fitzgerald
David G. Freiman
Jack C. Geer
Gabriel Godman
John B. Hazard
Robert H. Heptinstall
Paul Kotin
Averill A. Liebow
Guido Majno
Donald G. McKay
Henry D. Moon
Councilman Morgan
Goetz W. Richter
David T. Rowlands, Jr
Edward A. Smuckler
Leon Sokoloff
Benjamin H. Spargo
Lewis Thomas
Jacinto J. Vazquez
F. Stephen Vogel

Editorial Assistant: Virginia Hotelling

MEDICAL DEPARTMENT HARPER & ROW, PUBLISHERS

COPYRIGHT © 1972

BY THE AMERICAN ASSOCIATION

OF PATHOLOGISTS AND BACTERIOLOGISTS

The American Journal of
PATHOLOGY

CONTENTS FOR VOLUME 68, 1972

July

1 Effects of Viral Infection on Nervous System Development. I. Pathogenesis of Bluetongue Virus Infection in Mice
Opendra Narayan and Richard T. Johnson

15 Effects of Viral Infection on Nervous System Development. II. Attempts to Modify Bluetongue-Virus-Induced Malformations with Cyclophosphamide and Antithymocyte Serum
Opendra Narayan, Henry F. McFarland and Richard T. Johnson

23 Histochemical Distribution of Carbonic Anhydrase After Ligation of the Pancreatic Duct
Andrew Churg and Ward R. Richter

31 Tissue Localization of Australia Antigen Immune Complexes in Acute and Chronic Hepatitis and Liver Cirrhosis
Adam Nowosławski, Krzysztof Krawczyński, Witold J. Brzosko and Kazimierz Madaliński

57 Effects of Normal and Aspirin Platelets on Defective Secondary Aggregation in the Hermansky-Pudlak Syndrome: A Test for Storage Pool Deficient Platelets
James G. White and Carl J. Witkop

67 Incidence and Significance of Muscle Capillary Basal Lamina Thickness in Juvenile Diabetes
Victoriano Pardo, Eliseo Perez-Stable, David B. Alzamora and William W. Cleveland

81 The Cellular Pathology of Experimental Hypertension. VI. Alterations in Retinal Vasculature
Filiberto Giacomelli, Kenneth B. Juechter and Joseph Wiener

97 Effects of Biliary Obstruction on Pulmonary Ultrastructure in the Rat
N. A. Popovic and J. F. Mullane

113 Lysosomes in the Pathogenesis of the Renal Necrosis of Choline-Deficient Rats
A. J. Monserrat, F. Hamilton, A. K. Ghoshal, E. A. Porta and W. S. Hartroft

147 Lymphocyte Depression Induced in Chickens on Diets Deficient in Vitamin A and Other Components
Betsy G. Bang, Frederik B. Bang and Marie A. Foard

163 Separation of Ascites Myeloma Cells, Lymphocytes and Macrophages by Zonal Centrifugation on an Isokinetic Gradient
M. J. Stewart, T. G. Pretlow II and Raymond Hiramoto

183 Mouse Cytomegalovirus: Necrosis of Infected and Morphologically Normal Submaxillary Gland Acinar Cells During Termination of Chronic Infection
Donald Henson and Alfonso J. Strano

203 **Animal Model for Human Disease:** Spinal Bifida, Sacral Dysgenesis and Myelocele
Hyram Kitchen, Ronald E. Murray and Beverly Y. Cockrell

August

207 Presentation of The Gold Headed Cane to Esmond R. Long
Robert E. Stowell

213 Experimental Papillary Necrosis of the Kidney. II. Electron Microscopic and Histochemical Studies
G. S. Hill, R. G. Wyllie, M. Miller and R. H. Heptinstall

235 Experimental Papillary Necrosis of the Kidney. III. Effects of Reserpine and Other Pharmacologic Agents on the Lesion
R. G. Wyllie, G. S. Hill, G. Murray, P. W. Ramsden and R. H. Heptinstall

255 Lysosome and Phagosome Stability in Lethal Cell Injury: Morphologic Tracer Studies in Cell Injury Due to Inhibition of Energy Metabolism, Immune Cytolysis and Photosensitization
Hal K. Hawkins, Jan L. E. Ericsson, Peter Biberfeld and Benjamin F. Trump

289 Degranulation of Discoid Platelets
James G. White and Richard D. Estensen

303 Ultrastructural Characteristics of Freeze-Dried Human Blood Platelets
Richard B. Davis

317 Alterations in Cell Proliferation in Mouse Lung Following Urethane Exposure. III. Effects of Cell Exposure on Type 2 Alveolar Epithelial Cell
Shirley L. Kauffman

327 *In Vivo* Quantitation of Local Anesthetic Suppression of Leukocyte Adherence
D. B. Giddon and J. Lindhe

339 Glomerulonephritis Associated with Sarcoidosis
Ralph C. McCoy and C. Craig Tisher

359 Cell Proliferation in Rat Kidneys After Prolonged Treatment With Lead
David D. Choie and Goetz W. Richter

371 Amyloidogenesis in Healing Wound: Electron Microscopic Studies of Biopsied Wounds in Macular Amyloidosis
Ken Hashimoto and Martin H. Brownstein

391 Chemical and Histochemical Studies of Glomerular Sialoprotein in Nephrotoxic Nephritis in Rats
Jane Chiu and Keith N. Drummond

407 Mucous Hypersecretion Induced in Isolated Mucociliated Epithelial Cells by a Factor in Heated Serum
B. G. Bang and F. B. Bang

423 The Variable Prevalence of Junctional-Complex-Associated Bodies in the Human Sweat Gland
S. S. Spicer, B. J. Martin and J. P. Reynolds

441 **Animal Model for Human Disease:** Spontaneous and Induced Amyloidosis
Alan S. Cohen and Tsuranobu Shirahama

September

447 Effects of Cationic Polypeptides on Thrombasthenic and Afibrinogenemic Blood Platelets
James G. White

461 Parathyroid Necrosis and Hypocalcemic Tetany Induced in Rabbits by L-Asparaginase
Francis V. Chisari, H. Donald Hochstein, Ruth L. Kirschstein and Edward B. Seligmann

469 Nuclear Localization of Immunoglobulins in Renal Biopsies of Patients with Lupus Nephritis
Ralph C. McCoy

479 Ultrastructural Changes in Muscular Dystrophy. I. Cardiac Tissue of Piglets Deprived of Vitamin E and Selenium
Phillip R. Sweeny and R. G. Brown

493 Ultrastructure of Muscular Dystrophy. II. A Comparative Study in Lambs and Chickens
Phillip R. Sweeny, J. G. Buchanan-Smith, F. deMille, J. R. Pettit and E. T. Moran

511 Scanning Electron Microscopy of Saccular Intracranial Aneurysms
O. Hassler

521 The Pulmonary Interstitial Cell as Immediate Precursor of the Alveolar Macrophage
Drummond H. Bowden and Ian Y. R. Adamson

SYMPOSIUM ON NEUTROPHIL PROTEASES AS MEDIATORS OF TISSUE INJURY

538 Introduction
Aaron Janoff

539 Leukocytic Proteases and the Immunologic Release of Lysosomal Enzymes
Gerald Weissmann, Robert B. Zurier and Sylvia Hoffstein

565 Role of Granulocyte Collagenase in Collagen Degradtion
Gerald S. Lazarus, John R. Daniels, Jane Lian and Mary C. Burleigh

579 Human Granulocyte Elastase: Further Delineation of its Role in Connective Tissue Damage
Aaron Janoff

593 Pathologic Mechanisms in Neutrophil-Mediated Injury
Peter M. Henson

613 Leukocyte Kininogenases and Leukokinins from Normal and Malignant Cells
Lowell M. Greenbaum

625 REVIEW ARTICLE: Subacute Spongiform Virus Encephalopathies: Scrapie, Kuru and Creutzfeldt-Jakob Disease
Peter W. Lampert, D. Carleton Gajdusek and Clarence J. Gibbs, Jr

653 **Animal Model for Human Disease:** Adenocarcinoma
N. Baba and E. von Haam

---

657 Index of Subjects, Volume 68
661 Index of Authors, Volume 68

The American Journal of PATHOLOGY

is published by the Medical Department of Harper & Row, Publishers, under the auspices of The American Association of Pathologists and Bacteriologists and The American Society for Experimental Pathology, and is edited by a Board appointed by the Councils of the two Societies. It is devoted to the prompt publication of original observations and investigations in the field of pathology and microbiology and is published monthly in four volumes per year.

Information for Authors

ORIGINAL PAPERS will be considered for publication on condition that they are contributed solely to THE AMERICAN JOURNAL OF PATHOLOGY. Address manuscripts to the Editor-in-Chief: THOMAS D. KINNEY, MD, Department of Pathology, Duke University Medical Center, Durham, NC 27706.

MANUSCRIPTS must be typed **double-spaced** (including tables, references, and legends for figures), and all material should be submitted in duplicate. The literature should be summarized as concisely as is consistent with establishing the necessary basis for new material, and original observations should be presented in a clear, well-organized manner. Papers should rarely exceed 20 printed pages. Tables should be planned to suit the page size of THE JOURNAL. Excess tabular matter must be paid for by the contributor.

REFERENCES to the literature should be numbered in the order of citation in the text and should conform to the following style: names of all authors, complete title of article (including subtitle), abbreviated name of periodical (use *Index Medicus* style abbreviations), volume in Arabic numerals, inclusive pagination, and year (*eg*, 14:111–120, 1938). Titles are to be in the original language when they can be reproduced in the English alphabet. Translated titles should be enclosed in square brackets.

ILLUSTRATIONS must be planned to suit the page size of THE JOURNAL (**maximum plate size is 5¼ × 8 inches**) and should be submitted **unmounted,** with figure number, top, and author's name marked lightly on the back in soft pencil. Oversize illustrations should be avoided because handling of these delays publication. To be accepted, illustrations must reach a certain standard of excellence technically, present an attractive appearance, and add significantly to the value of the presentation. Marking lines and letters, if essential, must be kept at least ¼ inch inside all margins. If two or more illustrations are to appear on a page, they should be so trimmed that the edges may be butted and the outer margins squared. The legends for photomicrographs should state the staining method and the degree of magnification. Black and white illustrations will be furnished in moderate numbers. Excess illustrations, when accepted, and the cost of illustrations in color, must be paid for by the contributor.

REPRINTS: An order blank for reprints is sent with the proof.

Now, Automatic Quantitative Microscopic Image Analysis—from Zeiss!

We've added a unique precision scanning stage to our great optics, and the result is the most sophisticated system ever made for microphotometry. It's the Zeiss Scanning Microscope Photometer 05 for **all** types of photometric measurements in transmittance, absorbance, reflectance and fluorescence . . . and either on-line or off-line computer analysis. Cancer cytologists have already found it an invaluable tool . . . and other applications are developing daily in both the life sciences and industry.

Here's what this unusual system consists of:

A Zeiss Universal or Photomicroscope. Any analytical system that utilizes a microscope, no matter how sophisticated the electronics, cannot be any better than its optics allow. Information that's lost in the optical channels will not be retrieved in the electronic channels. That's why it's important to start with world-famous Zeiss optics.

A unique Zeiss precision scanning stage. The two avai able scanning stages allow, respectively, minimum incremen of 0.5 and 10 microns, perform up to 200 steps per secon and travel 75mm and 25mm in the X and Y directions in seve different scanning patterns, including meander, comb or li

Much more. A modular electronic system that permi you to select components as you need them and as your budg permits. All the famous Zeiss accessories and photographic ar analytical attachments—everything you might ever need f qualitative and quantitative microscopy—are, of course, ava able. We can even supply a PDP-12 computer with a number programs prepared by well-known scientists. For the full sto write Carl Zeiss, Inc., 444 5th Ave., New York, N.Y. 10018. phone (212) 736-6070.

Nationwide Service.

ATLANTA, BOSTON, CHICAGO, COLUMBUS, DALLAS, DENVER, FORT LAUDERDALE, HOUSTON, KANSAS CITY, LOS ANGELES, PHILADELPHIA, PHOENIX, SAN FRANCISCO, SEATTLE, WASHINGTON, D.